CONTENTS

NUMBER 3, MAY, 1945

NUMBER 4, JULY, 1945

NUMBER 6, NOVEMBER, 1945

ERRATA

Volume 49, Number 4, July, 1945

Since figures 5 and 6 have been transposed, the corrections indicated below should be made:

Page 289: The legend under the second graph should read:
"Fig. 6. Binary system: goldenrod rubber and irradiated goldenrod rubber solutions."

Page 290: The legend under the first graph should read:
"Fig. 5. Binary system: hevea and irradiated hevea solutions."

.

.

.

PHYSICAL-CHEMICAL INVESTIGATIONS OF GOLDENROD RUBBER. IV

INCREASE IN VISCOSITY AND FORMATION OF PHOTOGELS BY IRRADIATION OF GOLDENROD RUBBER IN THE ABSENCE OF OXYGEN

MORRIS M. GRAFF AND EVALD L. SKAU

Southern Regional Research Laboratory,[1] New Orleans, Louisiana

When a benzene solution of raw Hevea rubber in an ordinary glass container is irradiated with sunlight in the absence of oxygen, its viscosity increases until finally a gel forms (1, 2, 3, 4, 5, 8, 9, 10, 11). This increase in viscosity is preceded by a slight decrease, which is attributed to oxidation by minute traces of oxygen. According to the accepted theory, the viscosity decreases until all the available oxygen has been used up in oxidation or depolymerization, and then polymerization causes it to increase until finally a gel forms. If depolymerization has progressed too far, that is, if the viscosity is too low, gelation does not take place.

The viscosity of goldenrod rubber is much lower than that of Hevea rubber; for a 0.175 per cent solution in benzene at 25°C. the absolute viscosity values are approximately 0.7 and 1.8 centipoises, respectively (7). It has been found, however, that photogels can be formed from goldenrod rubber, with, and sometimes without, added activators.

A benzene extract of acetone-extracted goldenrod (*Solidago leavenworthii*) leaves obtained in connection with the Emergency Rubber Project from the pilot plant in this Laboratory and containing no antioxidant was diluted to a concentration of about 3 per cent and clarified by slurrying with 3 g. of Merck's activated charcoal per 100 ml. and filtering, the whole procedure being carried out in an atmosphere of carbon dioxide. The exact concentration of the final solution, ascertained by a total-solids determination, was 2.91 g. per 100 ml.

In the following experiments 10-ml. aliquots of this solution were mixed with various activators and sealed off under vacuum in Pyrex-glass tubes. The weight of the activator was 5 per cent of the weight of the rubber, except in the experiments with chlorophyll and with carbon tetrachloride. In the latter case, 5 ml. of carbon tetrachloride was added to 5 ml. of the benzene solution. When chlorophyll was used, 1 mg. of chlorophyll was added for each 250 mg. of rubber (0.4 per cent). In all cases the samples were introduced into the Pyrex exposure tubes by a capillary-tipped funnel. The solutions were frozen solid in a slush of solid carbon dioxide and alcohol, evacuated to a pressure of about 0.2 mm., remelted, reëvacuated to eliminate most of the oxygen, and then sealed off.

A test run was made for a number of activators to determine the gelling time in sunlight. The results were as follows: benzophenone, less than 4.5 hr.; benzaldehyde, less than 4.5 hr.; carbon tetrachloride, 7 hr.; benzoyl peroxide, 8 hr.; maleic anhydride, 14 hr.; chlorophyll, 65 hr.; and quinone, 108 hr. A

TABLE 1

Irradiation of goldenrod rubber in absence of oxygen

ACTIVATOR	TIME EXPOSED	ABSOLUTE VISCOSITY OF 0.175 PER CENT SOLUTION IN BENZENE AT 25°C.	PRECIPITATION VALUE AT 25°C.
	hours	*centipoises*	*ml.*
Benzophenone........	0	0.700	4.45
	¼	0.681	4.75
	½	0.710	4.55
	¾	0.731 (incipient gelation)	4.55
	1	(gel)	
Carbon tetrachloride..	0	0.684	4.45
	½	0.679	4.45
	1	0.680	4.40
	2	0.674	4.30
	3	0.725	4.30
	4	0.728	4.30
	5	0.736	4.35
	6	0.765	4.30
	7	(gel)	
Benzoyl peroxide	0	0.665	5.05
	1	0.683	4.90
	2	0.685	4.85
	3	0.690	4.80
	4	0.685	4.75
	5	0.697	4.70
	6	0.691	4.70
	7	0.696	4.65
	8	0.716	4.70
	9	(gel)	
Maleic anhydride.........	0	0.694	4.40
	½	0.679	4.50
	1	0.689	4.65
	3	0.695	4.60
	5	0.710	4.65
	7	(gel)	
	10	0.771	4.70
	15	(gel)	

blank containing no activator did not gel after 108 hr. In a previous experiment, however, in which a different goldenrod rubber solution was used, a blank gelled in 10 hr. A similar inconsistency in the behavior of various goldenrod rubber solutions has been noted in the irradiation experiments in the presence

of oxygen. This inconsistency depended upon the active constituents that remained in the solution after the treatment with activated charcoal (6).

A series of tubes for each of a number of these activators was exposed to sunlight for different periods of time, one tube of each set being kept in the dark as a blank. After exposure the tubes were stored in the dark until they were opened and tested. Six milliliters of each of these solutions was diluted to 100 ml. to produce a 0.175 per cent solution of rubber. In the sample with carbon tetrachloride, 12 ml. was diluted to 100 ml., to give the correct final concentration. Aliquots were then used for the measurement of the absolute viscosity at 25°C. by means of a modified Ostwald viscometer, and also for determination of the precipitation value. The precipitation value (7) is a measure of the precipitability, being defined as the number of milliliters of absolute ethyl alcohol required at a given temperature to produce a cloud point in 10 ml. of a clarified benzene solution containing 0.0175 g. of rubber sample.

The results are given in table 1. The initial values for the viscosity and precipitation value of the different solutions differed slightly, either because of the mere presence of the activator in the solution or because of some change caused by the activator during storage in the dark.

In each case, continued irradiation caused an increase in the viscosity and resulted finally in gelation. With the exception of the benzoyl peroxide sample, this increase was preceded by an initial decrease in viscosity. In the latter case this initial decrease might actually have occurred during the first hour, at the end of which the first sample was taken. Since the gel which finally formed was practically insoluble in benzene, its viscosity and precipitation value could not be determined.

Formation of rubber hydrocarbon polymers of higher molecular weight by irradiation would be expected to result in a higher degree of precipitability; that is, the precipitation value would be expected to decrease as the viscosity increased. This seems to be the trend for the carbon tetrachloride and the benzoyl peroxide samples. In the case of maleic anhydride, however, the precipitation value actually increased, though the absolute viscosity increased from 0.694 to 0.771 centipoise. This corroborates the opinions of Stevens (11), Naunton (3), and Farmer (1) that the formation of photogels is not the result of a simple polymerization and that it may sometimes involve condensation with the activator.

SUMMARY

The viscosity of goldenrod rubber can be increased until gelation takes place by irradiation of its benzene solution in the presence of catalysts and in the absence of oxygen. Benzophenone, benzaldehyde, and carbon tetrachloride seem to be the best of the activators tested.

REFERENCES

(1) FARMER, E. H.: Trans. Faraday Soc. **38**, 340 (1942).
(2) MEYER, K. H., AND FERRI, C.: Helv. Chim. Acta **19**, 694 (1936).
(3) NAUNTON, W. J. S.: Trans. Faraday Soc. **38**, 332 (1942).
(4) PORRITT, B. D.: India Rubber J. **60**, 1161 (1920).
(5) PUMMERER, R., AND KEHLEN, H.: Ber. **66**, 1107 (1933).
(6) SKAU, E. L., KREEGER, F. B., AND RUNCKEL, W. J.: In press.
(7) SKAU, E. L., RUNCKEL, W. J., KREEGER, F. B., AND SULLIVAN, M. A.: In press.
(8) SMITH, W. H., AND SAYLOR, C. P.: J. Research Natl. Bur. Standards **13**, 453 (1934).
(9) SPENCE, D.: U. S. patent 2,234,743 (1941).
(10) SPENCE, D., AND FERRY, J. D.: J. Am. Chem. Soc. **59**, 1648 (1937).
(11) STEVENS, H. P.: Trans. Inst. Rubber Ind. **16**, 211 (1940).

THE TERNARY SYSTEM ISOBUTYL ALCOHOL–BENZENE–WATER AT 25°C.

ROBERT A. ALBERTY AND E. ROGER WASHBURN

Avery Laboratory of Chemistry, University of Nebraska, Lincoln, Nebraska

In continuation of the investigations of the solubility relationships for the ternary systems made up of benzene, water, and the lower alcohols (4), the system containing isobutyl alcohol has been studied.

MATERIALS

Redistilled water was used in all solubility measurements.

The benzene was dried with sodium ribbon and subjected to several slow recrystallizations, during which the material was constantly agitated. The benzene which was used in obtaining the recorded solubilities had a freezing point of 5.48°C., a refractive index, n_D^{20}, of 1.50124, and a specific gravity, d_4^{25}, of 0.87357.

Isobutyl alcohol from the Eastman Kodak Company was refluxed for over 24 hr. with active lime and then slowly fractionally distilled. Since measurements seemed to indicate that the alcohol still contained a little water, it was refluxed for an additional 4 hr. over metallic calcium and again fractionated. The best alcohol obtained had a refractive index, n_D^{20}, of 1.39615, and specific gravities, d_4^0, of 0.8172 and, d_4^{25}, of 0.79811. The latter value compares favorably with the values obtained by Timmermans and Martin (3) and Willard and Smith (5). The value at 0.0°C. is, however, appreciably lower than the 0.8197 obtained by Michels (2). We believe that this indicates that the alcohol used by Michels in his determination of the mutual solubility with water contained some water.

PROCEDURE AND RESULTS

With only a few exceptions, which will be mentioned, the experimental procedure was the same as that previously described (4). Fifty-milliliter volumetric flasks were used for the titrations, while 25.0-ml. volumetric flasks were employed in the study of conjugate solutions. Experiments indicated that the evaporation loss from the titration flasks was about 1 mg. per hour while they were shaken at 25°C. with their dry stoppers in place. When they were shaken without their stoppers, the loss was from 3 to 6 mg. in 10 min. Since the titrations were usually completed in 2 hr., and since the flasks were open only 2 or 3 min. during this time, losses due to evaporation were but a small fraction of the total weight of 15 g. employed. The long fine capillary tip from which water was added as a titrant was coated with bakelite lacquer so that very small drops could be added. The drops of water from the pipet weighed 5 to 7 mg. The alcohol and benzene drops from plain glass tips weighed 2 to 4 mg.

A set of ternary solubility determinations was run with second-quality alcohol and benzene before using the purified materials. On the basis of these titrations the compositions of the equilibrium mixtures could be closely approximated, and only five to twenty drops of titrant had to be added in a titration. As a check on evaporation losses the number of drops of titrant was counted, and the gain in the weight of the flask was compared with the sum of the drop weights. The difference between these values was usually less than 15 mg. When the differences were larger, the titration was repeated.

When the titrant, water, was added to the solutions rich in benzene, the water drops spread out on the bottom of the flask, displacing the benzene–alcohol solution. These drops held so tenaciously to the glass that the flasks had to be removed from the mechanical shaker and shaken by hand to break them up. The end point was a mist of water droplets in the solution. In the water-rich systems the end point was a mist of benzene droplets which floated up like little air bubbles. They could be distinguished from air bubbles by inspection through a magnifying glass because of their different index of refraction. The solubilities are recorded in table 1 and are plotted in figure 1.

An Abbe refractometer was used in determining the refractive indices of the saturated solutions, and these refractive indices were plotted *versus* the per cent alcohol, per cent benzene, and per cent water. The curves were of such a size that 1.0 mm. on the abscissa represented 0.0002 in refractive index, and 2.0 mm. on the ordinate represented 0.1 per cent. The refractive indices of the conjugate solutions were measured with the same refractometer, and the compositions were determined by reference to the curves. The sum of the percentages for any one liquid was always 100.00 per cent, within 0.07 per cent. The gross compositions of the tie-line mixtures were so chosen that approximately equal volumes of the two phases were formed, and the total volume was such that the 25-ml. flask was about half filled so that efficient agitation was possible. Evaporation losses in this part of the study were not over 5 mg. in the 4 hr. allowed for equilibrium to be reached. Concentrations of the conjugate solutions are recorded in table 2. The tie-lines are plotted in figure 1.

The solubilities of water in benzene and of benzene in water recorded in the literature (1) were employed.   New determinations, however, were made of the

TABLE 1

Ternary solubility data at 25.0°C.

ISOBUTYL ALCOHOL	BENZENE	REFRACTIVE INDEX	ISOBUTYL ALCOHOL	BENZENE	REFRACTIVE INDEX
weight per cent	*weight per cent*		*weight per cent*	*weight per cent*	
10.14	89.50	1.4844	67.85	23.24	1.4120
20.03	78.87	1.4719	73.94	15.09	1.4037
29.75	68.19	1.4597	79.22	7.06	1.3956
39.92	56.75	1.4471	6.10	0.17	1.3391
50.20	44.95	1.4343	4.02	0.26	1.3370
59.96	33.39	1.4222	2.05	0.23	1.3350

Isobutyl alcohol saturated with water   82.99 wt. % alcohol................   1.3880
Water saturated with isobutyl alcohol   91.99 wt. % water......... ....   1.3409
Benzene saturated with water   99.93 wt. % benzene (1)............   1.4978
Water saturated with benzene   99.85 wt. % water (1)..............   1.3330
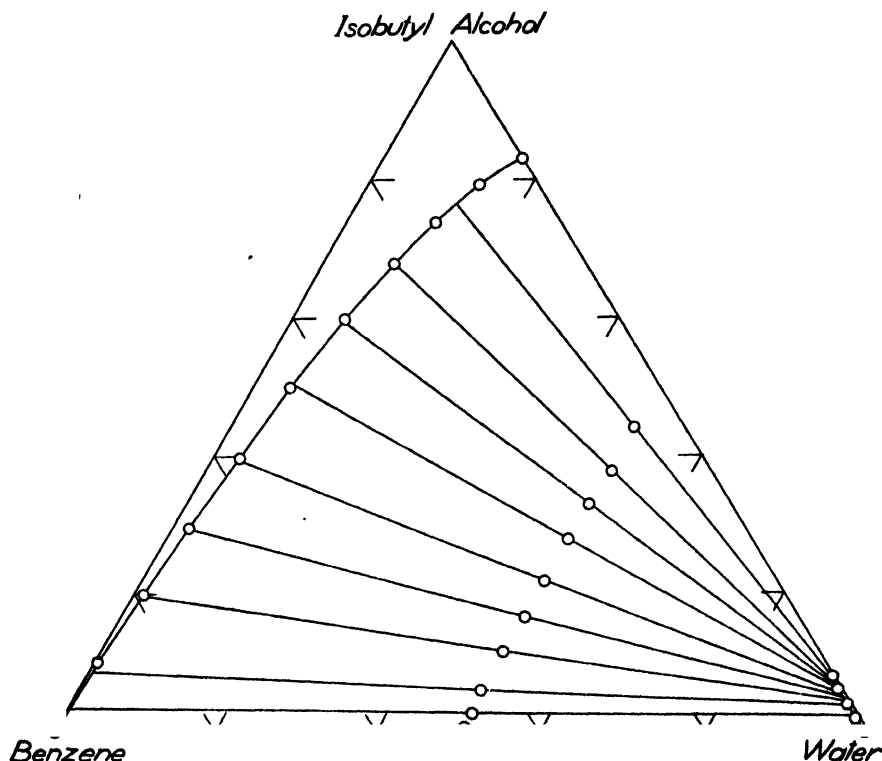
FIG. 1. The ternary system isobutyl alcohol–benzene–water at 25°C.

solubilities of isobutyl alcohol in water and of water in isobutyl alcohol.   Solutions of water in alcohol of approximately the equilibrium concentrations (at

23–26°C.) were made up by weight and sealed in drawn-out test tubes. The temperatures at which the water phases first appeared on cooling the homogeneous solutions were determined. The sealed tubes were rocked to and fro in the constant-temperature bath during the determination. These "cloud-points" could be reproduced to within ±0.07°C. The solubility at 25°C. was obtained by interpolation of the data recorded in table 3. The interpolated solubility ("x") at 25°C. is 17.01 per cent water, which agrees with the value obtained by titration and is higher than the value obtained by Michels (2) (16.66 per cent water, interpolated).

TABLE 2

Conjugate solutions at 25.0°C.

WATER LAYER			BENZENE LAYER		
Refractive index	Isobutyl alcohol	Water	Refractive index	Isobutyl alcohol	Benzene
	weight per cent	*weight per cent*		*weight per cent*	*weight per cent*
1.3339	0.93	98 87	1.4966	0 92	99.01
1 3353	2.33	97.39	1.4930	3.61	96.20
1.3366	3.62	96 11	1.4861	8.84	90.84
1.3373	4.30	95.44	1.4721	19.87	79.07
1.3378	4.82	94.98	1 4599	29 58	68.36
1.3382	5.23	94.59	1 4475	39.57	57.09
1.3387	5.73	94.13	1.4340	50.44	44 66
1.3390	6.04	93 83	1 4228	59.48	33.98
1.3394	6 43	93.46	1.4122	67.68	23.46
1.3403	7.32	92.64	1.4000	76.51	11.39

TABLE 3

Solubility of water in isobutyl alcohol

NO.	ALCOHOL	WATER	CLOUD POINT
	weight per cent	*weight per cent*	°C
1	82.85	17.15	26.51
2	82.93	17.07	26.14
"x"	82.99	17.01	25.00
3	83.12	16.88	23.33

The "cloud-points" for solutions of isobutyl alcohol in water were quite indistinct and not easily reproducible; accordingly, a different method was employed for this solubility. The refractive indices of several nearly saturated solutions were measured at 25.00°C. with an immersion refractometer. The curve for concentration *versus* refractive index was then plotted and extrapolated to the refractive index of a saturated solution, thus permitting the concentration of that solution ("y") to be determined. Extrapolation of the first four rows of the data in table 4 gave 8.02 per cent for the solubility of isobutyl alcohol in water ("y"). This is in agreement with the value obtained by titration and is lower than the value obtained by Michels (2), which is 8.15 per cent alcohol (interpolated). As mentioned under "materials", the density of Michels' alcohol

indicated that the alcohol was not completely dry, and this would explain why his solubility values are higher than those obtained in this study.

This system is very similar to the n-butyl alcohol–benzene–water system (4). n-Butyl alcohol is less soluble in water than isobutyl alcohol and shows a slightly greater tendency than isobutyl alcohol to concentrate in the benzene layer of a two-phase mixture. In the case of both alcohols, the tendency to concentrate in the benzene layer increases with increasing amounts of the alcohol. The ratio of the concentration of isobutyl alcohol in the benzene layer to the concentration in the water layer varies from 0.99 in the case of the first pair of conjugate solutions to 10.5 in the case of the last pair recorded.

TABLE 4

Solubility of isobutyl alcohol in water

NO.	ALCOHOL	WATER	REFRACTIVE INDEX
	weight per cent	*weight per cent*	
1	7.01	92.99	1.33996
2	7.57	92.43	1.34056
3	7.85	92.15	1.34082
4	7.94	92.06	1.34092
"y"	8.02	91.98	1.34100

SUMMARY

The ternary solubility curves and tie-lines for the system isobutyl alcohol, benzene, and water have been determined at 25°C. The solubility of water in isobutyl alcohol at 25°C. has been determined by the sealed-tube method, and the solubility of isobutyl alcohol in water has been determined by a refractive-index method.

REFERENCES

(1) *International Critical Tables of Numerical Data*, Vol. III, p. 389. The McGraw-Hill Book Company, Inc., New York (1926).
(2) MICHELS, A.: Arch. néerland. sci. (IIIA) **6**, 127 (1922).
(3) TIMMERMANNS, J., AND MARTIN, F.: J. chim. phys. **25**, 411 (1928).
(4) WASHBURN, E. ROGER, AND STRANDSKOV, CARL V.: J. Phys. Chem. **48**, 241 (1944).
(5) WILLARD, H. H., AND SMITH, G. F.: J. Am. Chem. Soc. **45**, 286 (1923).

NOTE ON THE RELATIONSHIP BETWEEN TIME OF DIALYSIS AND THE BURTON–BISHOP RULE

ELIZABETH F. TULLER[1] AND LAWRENCE P. EBLIN

Department of Chemistry, Ohio University, Athens, Ohio

The so-called Burton–Bishop rule (1), which relates the valency of the coagulating ion to the effect of sol dilution upon the coagulating value of an electrolyte, was found by Judd and Sorum (2) to hold for hydrous ferric oxide sols, provided that the sols are of extremely high purity. Since their results did not appear to agree with previous results, the authors have attempted to verify their conclusion and to determine whether there is a relationship between time of dialysis and the development of Burton–Bishop behavior in ferric oxide sols.

The sols were prepared according to the procedure of Sorum (3), as modified in a private communication. The modified procedure consists in dropping 40 ml. of a molal solution of ferric chloride into 1 liter of boiling distilled water. The sols were dialyzed for varying periods of time in order that the relationship between coagulation values and sol purity might be investigated.

Those sols which were dialyzed for sufficient periods of time were found by test to be chloride-free. The time required for this condition to be reached varied in different sols from $5\frac{1}{2}$ to 7 days.

Using sodium chloride and sodium sulfate as coagulating electrolytes, the authors have found that those sols which have been dialyzed until they are chloride-free conform to the Burton–Bishop rule. They have found also that sols may conform to the Burton–Bishop rule *before* they have become chloride-free, and that all sols exhibiting this unexpected combination of properties had been dialyzed for 96 hr. Sols which had been dialyzed for 90 hr. or 102 hr. did not show Burton–Bishop behavior.

It would be very difficult to determine the exact number of hours of dialysis required to develop either Burton–Bishop behavior or absence of chloride, since two sols that have been dialyzed the same length of time do not always exhibit precisely the same coagulation behavior. Such differences are presumably due to the impossibility of preparing two collodion bags of identical permeability. The difficulties to be overcome in making a quantitative study of the relationship between time of dialysis and the properties of the dialyzed sol seem to be very serious ones. The authors know of no prior attempt at such a study.

Further work is planned to determine the relationship of chloride-ion concentration to the Burton–Bishop rule. Additional electrolytes, as well as other sols, will be used.

REFERENCES

(1) BURTON AND BISHOP: J. Phys. Chem. **24**, 701 (1920).
(2) JUDD AND SORUM: J. Am. Chem. Soc. **52**, 2598 (1930).
(3) SORUM: J. Am. Chem. Soc. **50**, 1264 (1928).

[1] Present address: Department of Chemistry, Iowa State College, Ames, Iowa.

VAPOR PRESSURE OF THE TERNARY SYSTEM ACETIC ACID–BENZENE–CARBON TETRACHLORIDE

WILLIAM R. McMILLAN[1] AND HUGH J. McDONALD

Department of Chemistry, Illinois Institute of Technology, Chicago, Illinois

In continuation of the program of this laboratory in the study of liquid mixtures, the vapor pressure of the system acetic acid–benzene–carbon tetrachloride was investigated. The analytical data on the materials used in this study and the details of analysis have been discussed in a previous paper (1).

APPARATUS AND PROCEDURE

The apparatus used is shown in figure 1. A 250-cc. boiling flask was fitted with a side arm for a thermometer. Standard-taper ground-glass fittings were used. An ice-jacketed condenser gave efficient reflux, as shown by the fact that after several hours of use with many samples, only about 0.5 ml. was caught in the vapor trap. A hydrochloric acid–ice bath kept this trap at about $-16°C$. The manometer was carefully made and heated so as to expel any air which might be dissolved in the mercury or adsorbed on the surface of the glass. Air was admitted to the system by means of a regular stopcock. A calcium chloride tube extracted the greater part of the moisture from the air before it reached the pump. A Cenco Hyvac (with a slight change in design) was used for lowering the pressure in the system. Because of the large volume of air being pumped through the oil, some of it was splashed onto the under side of the plate covering the pump mechanism and was blown out in the form of a fine spray. To remedy this, a new plate was constructed with a 6-in. length of $\frac{3}{4}$-in. pipe in the center and flush with the under side of the plate. This outlet was large and long enough to prevent oil spray or bubbles from being blown out into the air. A large test tube inverted over the pipe prevented foreign matter from falling into the pump mechanism.

The use of a stopcock allowed the pressure to be set at the desired point with ease. After a few seconds, equilibrium was attained between the boiling liquid and its vapor. After a few minutes, the readings of pressure and temperature were made. The manometer was shut off and the temperature of the boiling liquid read simultaneously. The pressure could then be read at leisure with the cathetometer.

Superheating was avoided by the use of boiling chips. A slow leak immersed in the boiling liquid also prevented superheating but carried over so much vapor that it was abandoned. The effects of superheating became noticeable at pressures lower than one-third of an atmosphere.

The apparatus and experimental technique were tested by determining the boiling points of carbon tetrachloride at several different pressures. The vapor-

---

pressure values so obtained checked the best values reported in the literature within about 0.3 per cent, and were reproducible. In the case of the three-component system the accuracy was limited, not by the pressure measurement, which, in fact, was measured to a greater degree of accuracy than justified, but by the temperature measurement, which was read to somewhat better than one-tenth of a degree.

The boiling point of each sample was determined three times under different pressures. One determination was made at about atmospheric pressure, one at
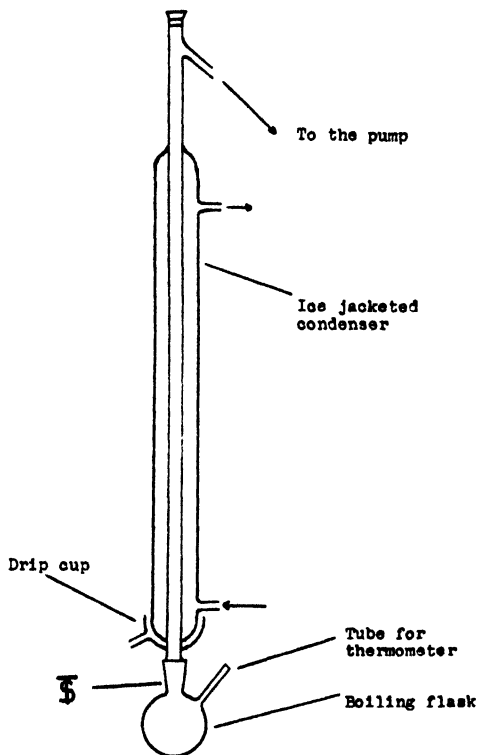
FIG. 1. Apparatus for determining boiling points under reduced pressure

a pressure about 10 cm. lower, and one at a pressure about 20 or 30 cm. lower. Three points were plotted for each sample, pressure against temperature.

The smooth curves drawn through the experimental points were extrapolated graphically so as to intersect the line representing 760 mm. pressure and the line representing a temperature of 60.0°C. In the first case, the boiling points of the system under normal atmospheric pressure were obtained. In the second case, the vapor pressures at 60°C. were obtained. These were plotted as isotherms and as isobars on the three-component diagram (see figure 2 and figure 3). In the graphical extrapolation the accuracy must necessarily have been reduced somewhat, from 0.3 to about 0.4 per cent. The normal boiling points and the vapor pressures at 60°C. are, therefore, not to be interpreted as being more
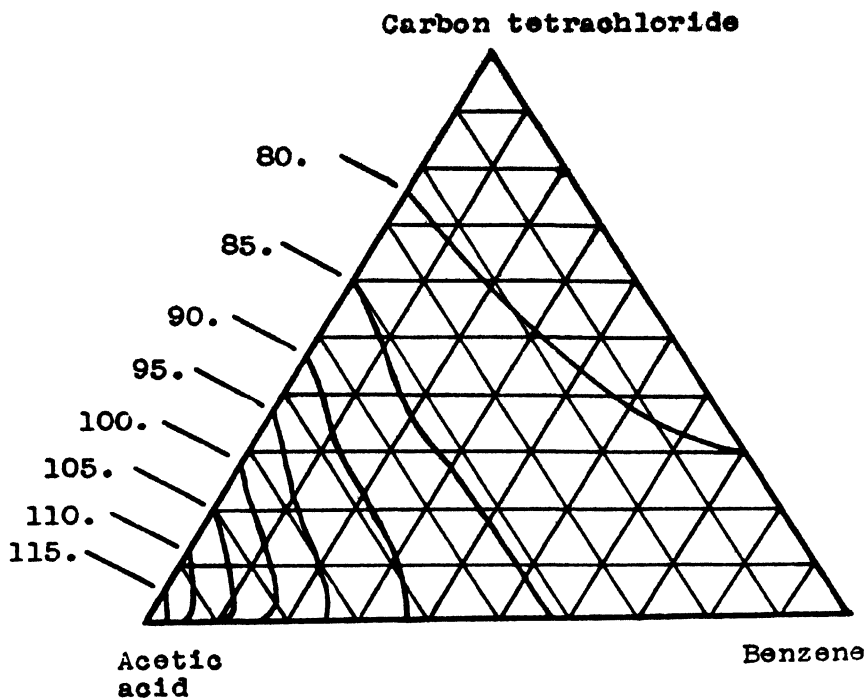
FIG. 2. Lines of constant-boiling point under atmospheric pressure for the ternary system.
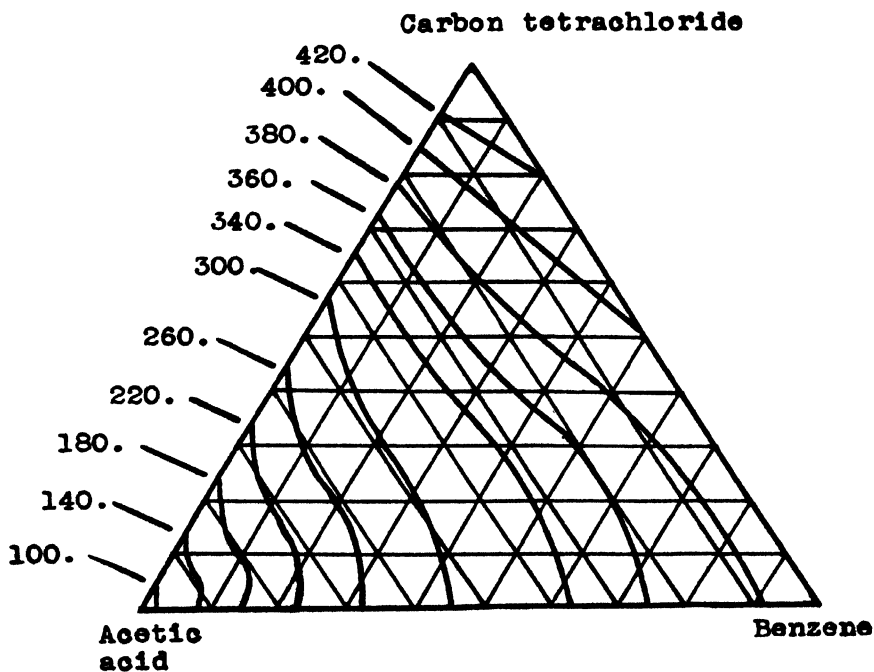
FIG. 3. Lines of constant vapor pressure at 60°C. for the ternary system. Pressures are given in millimeters of mercury.

12

TABLE 1

Vapor pressure of the ternary system

A, acetic acid; B, benzene; C, carbon tetrachloride

SAMPLE	BOILING TEMPERATURE	PRESSURE	WEIGHT PER CENT OF		
			A	B	C
	°C.	mm. Hg			
1	72.0	643.20	0	0	100.
	59.5	398.85			
	36.0	170.95			
	77.2*	760.00			
	60.0*	415.00			
2	74.0	677.10	11.6		
	60.5	413.30			
	43.0	213.35			
	76.8	760.00			
	60.0	410.00			
3	79.0	724.65	22.0		
	60.5	376.40			
	38.5	161.20			
	80.1	760.00			
	60.0	370.00			
4	80.6	688.90	31.6		
	66.6	424.30			
	42.4	171.65			
	82.9	760.00			
	60.0	338.00			
5	74.5	703.35	0	10	90.
	64.0	480.75			
	54.0	336.80			
	76.4	760.00			
	60.0	417.00			
6	78.0	717.70	20.5		
	70.0	547.05			
	54.0	306.95			
	80.2	760.00			
	60.0	398.00			
7	82.5	734.00	35.0		
	72.5	528.10			
	60.0	338.45			
	83.5	760.00			
	60.0	338.45			
8	88.0	704.50	54.0		
	77.0	488.80			
	56.0	229.20			
	90.4	760.00			
	60.0	273.00			

TABLE 1—*Continued*

SAMPLE	BOILING TEMPERATURE	PRESSURE	WEIGHT PER CENT OF		
			A	B	C
	°C.	mm. Hg			
9	74.6	693.95	0	20.0	80.0
	65.5	512.75			
	57.0	377.05			
	77.3	760.00			
	60.0	423.00			
10	81.2	713.65	34.0		
	69.1	499.25			
	59.8	346.40			
	83.7	760.00			
	60.0	351.00			
11	87.0	707.80	49.5		
	75.5	505.05			
	61.0	286.50			
	89.6	760.00			
	60.0	270.00			
12	90.0	715.75	64.6		
	81.0	498.40			
	64.2	282.95			
	91.2	760.00			
	60.0	255.00			
13	76.8	718.25	0	29.4	70.6
	69.6	575.20			
	58.8	388.70			
	78.7	760.00			
	60.0	410.00			
14	81.2	732.30	31.0		
	71.8	539.20			
	61.0	364.25			
	82.6	760.00			
	60.0	353.00			
15	84.5	727.10	44.6		
	76.6	563.50			
	59.8	314.05			
	86.0	760.00			
	60.0	318.00			
16	88.5	731.80	58.5		
	70.5	394.95			
	61.0	286.55			
	89.7	760.00			
	60.0	277.00			

TABLE 1—*Continued*

SAMPLE	BOILING TEMPERATURE	PRESSURE	WEIGHT PER CENT OF		
			A	B	C
	°C.	mm. Hg			
17	75.8	709.30	0	40.0	60.0
	69.4	579.05			
	59.5	404.10			
	78.0	760.00			
	60.0	413.00			
18	79.0	721.85	27.0		
	70.0	523.00			
	59.0	353.45			
	80.6	760.00			
	60.0	365.00			
19	82.1	724.95	38.8		
	72.0	510.80			
	58.5	307.45			
	83.4	760.00			
	60.0	330.00			
20	85.0	721.20	51.6		
	69.4	423.70			
	60 0	285.15			
	86.8	760.00			
	60.0	285.00			
21	77.0	730 70	0	49.0	51.0
	72.0	618.15			
	61.5	424.80			
	78.0	760 00			
	60.0	402.00			
22	79.2	716.20	21.4		
	73.7	603.95			
	53.5	291.40			
	81.2	760.00			
	60.0	376.00			
23	81.0	706.25	36.0		
	71.4	511.90			
	57.0	295.65			
	84.1	760.00			
	60.0	335.00			
24	84.0	701.25	53.0		
	73.5	493.55			
	60.5	303.85			
	86.6	760.00			
	60.0	299.00			

TABLE 1—*Continued*

SAMPLE	BOILING TEMPERATURE	PRESSURE	WEIGHT PER CENT OF		
			A	B	C
	°C.	mm. Hg			
25	78.0	732.95	0	59.5	40.5
	72.2	595.60			
	58.8	376.40			
	79.0	760.00			
	60.0	393.00			
26	79.8	734.20	19.6		
	71.0	550.30			
	55.5	308.90			
	80.8	760.00			
	60.0	360.00			
27	85.0	733.10	43.2		
	71.0	488.50			
	59.5	307.80			
	86.6	760.00			
	60.0	315.00			
28	86.7	730.05	53.0		
	70.0	415.65			
	59.0	281.65			
	86.8	760.00			
	60.0	295.00			
29	79.0	734.10	0	70.0	30.0
	72.0	579.30			
	58.9				
	80.0	760.00			
	60.0				
30	80.0	734.10	15.7		
	71.3	556.90			
	58.0	337.05			
	81.0	760.00			
	60.0	369.00			
31	83.0	736.15	36.5		
	72.1	504.10			
	61.0	340.60			
	84.0	760.00			
	60.0	330.00			
32	86.0	736.90	52.0		
	71.8	458.85			
	59.0	280.55			
	87.0	760.00			
	60.0	295.00			

TABLE 1—*Continued*

SAMPLE	BOILING TEMPERATURE	PRESSURE	WEIGHT PER CENT OF		
			A	B	C
	°C.	mm. Hg			
33	79.3	735.05	0	77.5	22.5
	70.0	537.30			
	58.0	353.75			
	80.4	760.00			
	60.0	380.00			
34	81.3	736.35	22.7		
	71.0	524.90			
	59.2	347.10			
	82.1	760.00			
	60.0	358.00			
35	82.8	736.30	37.6		
	70.0	471.40			
	60.0	323.70			
	83.5	760.00			
	60.0	323.70			
36	86.6	736.45	53.0		
	71.5	434.55			
	60.0	286.60			
	87.5	760.00			
	60.0	286.60			
37	79.4	732.65	0	89.5	10.5
	70.0	522.65			
	60.5	373.35			
	80.3	760.00			
	60.0	368.00			
38	80.9	736.50	16.5		
	70.1	521.25			
	58.5	336.10			
	81.8	760.00			
	60.0	358.00			
39	84.5	737.65	42.6		
	70.9	464.85			
	57.5	274.35			
	85.4	760.00			
	60.0	309.00			
40	86.0	737.00	51.0		
	72.5	446.05			
	59.5	266.25			
	86.8	760.00			
	60.0	275.00			

TABLE 1 (*Continued*)

SAMPLE	BOILING TEMPERATURE	PRESSURE	WEIGHT PER CENT OF		
			A	B	C
	°C.	mm. Hg			
41	79.0	723.90	0	100.0	0
	68.5	507.75			
	41.5	180.70			
	80.4	760.00			
	60.0	382.00			
42	80.0	695.65	26.3		
	71.5	534.35			
	43.0	181.15			
	82.5	760.00			
	60.0	369.00			
43	82.5	692.95	45.8		
	76.0	564.50			
	57.4	279.10			
	85.0	760.00			
	60.0	315.00			
44	84.8	689.00	58.5		
	73.0	463.75			
	59.4	280.40			
	87.4	760.00			
	60.0	288.00			
45	107.5	552.80	100.0	0	0
	91.5	312.75			
	79.0	193.45			
	118.5	760.00			
	60.0	89.00			
46	91.0	741.15	69.4	30.6	0
	79.0	488 85			
	66.8	322 35			
	91.6	760.00			
	60.0	251.00			
47	88.4	735.65	59.7	40.3	0
	72.4	429.40			
	61.5	294.50			
	89.3	760.00			
	60.0	279.00			
48	86.2	738.00	50.5	49.5	0
	70.0	418.85			
	57.4	272.25			
	87.2	760.00			
	60.0	300.00			

TABLE 1 (*Concluded*)

SAMPLE	BOILING TEMPERATURE	PRESSURE	WEIGHT PER CENT OF		
			A	B	C
	°C.	mm. Hg			
49	100.0	743.15	74.0	0	26.0
	78.0	364.55			
	69.0	245.45			
	100.8	760.00			
	60.0	138.00			
50	84.5	738.50	44.5	0	55.5
	74.5	515.75			
	60.5	311.25			
	85.4	760.00			
	60.0	304.00			
51	82.4	743 85	34.3	0	65.7
	70.8	498.65			
	58.6	326 15			
	83.3	760.00			
	60.0	344.00			

* The last two of the five values of temperature and pressure, for every sample, were obtained by extrapolation.

accurate than about 0.4 per cent. It is believed, however, that such data are of sufficient interest to be included in the tabulation of data. In table 1 the last two readings of temperature and pressure were obtained by extrapolation.

The solutions to be tested were made up in the following manner: Solutions were made of the binary system carbon tetrachloride and benzene at the approximate 10 per cent divisions. These solutions were then each treated in the same manner. First the vapor pressures at three different temperatures were determined, and a small sample withdrawn for analysis by refractive index. Acid was added two more times, and the same routine followed each time. To clarify the method of preparing and recording the samples of a given composition, consider sample 5 (table 1), which is 0 per cent A, 10 per cent B, and 90 per cent C, and sample 6 which is listed as 20.5 per cent A. Sample 6 was prepared by adding A to sample 5, so that the per cents of B and C are 10 per cent of 79.5, and 90 per cent of 79.5, respectively.

It was possible to analyze the first sample in each case by refractive index because it was only a binary system. When acid was added to any one of the eleven mixtures along the binary side, the composition of the resulting mixture varied along a straight line directly toward the acid vertex. The compositions of the other three mixtures could lie (if there was no great evaporation, and this seemed to be so, since little or no liquid was collected in the vapor trap) only on a straight line between the vertex and the given composition on the benzene–carbon tetrachloride side. The measurement of refractive index proved satisfactory for determining where the composition lay on that straight line (1).

The vapor pressures and boiling temperatures for the ternary mixtures are arranged in table 1.

SUMMARY

The vapor pressures of the system acetic acid–benzene–carbon tetrachloride were obtained by determining the boiling points at three different pressures of fifty-one samples covering the ternary diagram. The boiling points of the system at 1 atmosphere pressure and the vapor pressures at 60°C. are given.

REFERENCE

(1) McMILLAN, W. R., AND McDONALD, H. J.: Ind. Eng. Chem., Anal. Ed. **15**, 114 (1943).

HEATS OF COMBUSTION. III[1]

THE HEATS OF COMBUSTION OF SOME POLYNITROPARAFFINS

A. J. MILLER AND HERSCHEL HUNT

Department of Chemistry, Purdue University, Lafayette, Indiana

The combustion apparatus designed by Miles and Hunt (2) and Crog and Hunt (1) was modified so that a modern Parr oxygen bomb could be employed instead of the glass combustion chamber used with vapors. Essentially, the method is the so-called "ordinary" non-adiabatic calorimetric method, with proper corrections made for heat transfer, the energy involved in the firing of the iron wire, and energy liberated by the formation of nitric acid.

Uniform samples of iron wire were used to fire the sample. The energy liberated in firing the iron wire was 19.70 g-cal.$_{15°}$. The heat capacity of the calorimeter was determined by using benzoic acid as a standard. Its heat of combustion as furnished by the National Bureau of Standards is 6315.3 ± 1.7 g-cal.$_{15°}$ per gram. Nitric acid formed during the combustion was determined by titration with 0.01 N sodium hydroxide. Washburn's value of 14,621 g-cal.$_{15°}$ per mole was used as the heat of formation of nitric acid under these conditions. The volume of the calorimeter was 358.0 ml., so a sample of approximately 1 g. was used. This sample was made in the form of a pellet and was weighed with an accuracy of 0.05 mg. Five grams of water was placed in the bomb in order to saturate the air with water vapor before the combustion. The initial oxygen pressure in the bomb was 30 atmospheres.

The nitroparaffins were purified until they gave sharp melting points that did not change on recrystallization.

[1] This article is based upon a thesis submitted by A. J. Miller to the Faculty of Purdue University in partial fulfillment of the requirements for the degree of Doctor of Philosophy, August, 1943.

The heats of combustion given in the table below were found for the combustion of the solid nitroparaffins to form gaseous carbon dioxide, liquid water, and gaseous nitrogen in a bomb at constant volume and under a pressure of 30 atmospheres at 25°C.

NITROPARAFFIN	Δ_c
	kg-cal per mole
Dinitroneopentane........	-746.91 ± 0.77
2,3-Dimethyl-2,3-dinitrobutane....................	-292.0 ± 1.6
2-Methyl-2,3,3-trinitropentane....................... ...	-872.40 ± 0.44
2-Methyl-2,3,3-trinitrobutane..	-700.46 ± 0.72
2,2,3,3-Tetranitrobutane....	-586.13 ± 0.24

REFERENCES

(1) CROG AND HUNT: J. Phys. Chem. **46**, 1162 (1942).
(2) MILES AND HUNT: J. Phys. Chem. **45**, 1346 (1941).

COMPARISON OF THE PROPERTIES OF FRESHLY PRECIPITATED AND HEATED ALUMINOSILICATES AND ALUMINA AND SILICA GELS AND OF CLAY MINERALS

S. P. RAYCHAUDHURI AND N. B. DATTA

Chemical Laboratory, Dacca University, India

Raychaudhuri and Qudrat Ghani (13) have found that the uptake of base by pure gels of silica and alumina is comparatively small and that the uptake of base is greatest with aluminosilicate gel having a $SiO_2:Al_2O_3$ ratio of 8.0. They have shown that the buffer curves of the clay minerals do not correspond much in nature to the buffer curves of electrodialyzed precipitated aluminosilicate gels and of the same gels after treatment with hot 10 per cent aluminum chloride solution. Raychaudhuri and Hussain Miah (14) have shown that freshly prepared aluminosilicate gels possess much less buffer capacity than aged ones, and that the buffer capacity of freshly prepared materials passes through a maximum value with increasing $SiO_2:Al_2O_3$ ratios, whilst with aged ones, the buffer capacity continuously increases as the $SiO_2:Al_2O_3$ ratios of the precipitates increase, attaining a maximum value with pure silica gel. The maximum value of buffer capacity at a certain $SiO_2:Al_2O_3$ ratio of the freshly prepared gels is in agreement with the findings of Mattson (6, 7) and Wiegner (15). The continuous increase in buffer capacity with increase in $SiO_2:Al_2O_3$ ratio of the aged precipitate proves that aging brings about certain fundamental changes in the structure of the gels, such that the greater the proportion of silicic acid anions in the aged precipitates, the more open is the soil structure, pure

silicic acid gel having the maximum open structure. The work of Raychaudhuri and Hussain Miah suggests that aging of aluminosilicates favors the formation of clay mineral structure.

Chatterjee and Sen (4), working with synthetic mixtures of colloidal solutions of silicic acid and aluminum hydroxide, have shown that the pH and specific conductivity of the mixtures change with time, indicating the presence of a slow interaction between colloidal silicic acid and aluminum hydroxide. They have shown that the potentiometric titration curves of mixed gels with sodium hydroxide do not resemble those of either the silicic acid or aluminum hydroxide sols.

Noll (10) has synthesized a number of clay-forming minerals by heating amorphous silica and alumina with water or sodium hydroxide solution to 300–500°C. in a hydrothermal bulb. In the absence of alkali hydroxides, he obtained kaolin, but in their presence montmorillonite was produced. Noll has also shown that under the conditions of hydrothermal metamorphic mineral formation, up to 400°C., with SiO_2:Al_2O_3 ratio 2:1, kaolin is formed, and at 400–500°C. a pyrophillite mineral. He has also shown that no reaction takes place between alumina and silica in adsorption mixtures at room temperature, but that reaction is rapid under hydrothermal conditions.

It appears, however, that so far no systematic investigation has been carried out on the properties of aluminosilicates formed under different conditions. The approximate composition formulas of three important clay-forming minerals, kaolin, beidellite, and montmorillonite, are, respectively: $Al_2O_3 \cdot 2SiO_2 \cdot 2H_2O$, $Al_2O_3 \cdot 3SiO_2 \cdot nH_2O$ and $Al_2O_3 \cdot 4SiO_2 \cdot nH_2O$. It was felt desirable to mix the silicic acid and aluminum hydroxide sols in these molar ratios in different ways and to study the physicochemical properties of the precipitates. The aluminum hydroxide and silicic acid sols have been mixed in three different ways, viz.: (1) Silicic acid sol was added slowly, at a rate of about 120 drops per minute, to an aluminum hydroxide sol, in a beaker, with continuous stirring (precipitates 1, 2, and 3). (2) Aluminum hydroxide sol was added slowly, at a rate of about 120 drops per minute, from a buret to a silicic acid sol in a beaker, with continuous stirring (precipitates 4, 5, and 6). (3) Silicic acid and aluminum hydroxide sols were taken in two bottles and were allowed to come in contact with each other drop by drop (precipitates 7, 8, and 9).

The mixing molar ratios of silica to alumina of the sols were 2, 3, and 4 in each of the above three ways of mixing. The precipitated gels were purified by electrodialysis and the following properties were determined: (a) chemical composition (SiO_2:Al_2O_3 ratios); (b) electroösmotic charge; (c) base-saturation capacities; (d) moisture-holding capacity at 50 per cent relative humidity; (e) buffer curves. The above experiments were also carried out with electrodialyzed silica and alumina gels and clay-forming minerals,—viz., montmorillonite, halloysite, kaolin, quartz, and bauxite.

The nine precipitated aluminosilicates, the gels of silica and alumina, and the clay minerals were heated in a steam autoclave for a period of 12 hr. at 1 atmosphere pressure of steam. The substances were cooled and stored in wide-mouthed bottles and their physicochemical and electrical properties were studied.

Preparation of sols and precipitates

Silicic acid sol: Silicic acid sol was prepared by adding a 5 per cent solution of sodium silicate to an excess of dilute hydrochloric acid. The sol was purified by dialysis for 3 days in a parchment bag with running distilled water.

Aluminum hydroxide sol: A 6 per cent solution of aluminum chloride was heated to boiling and dilute ammonium hydroxide was added slightly in excess. The excess ammonia was boiled off, the precipitate was washed well with hot water, and transferred to a flask containing water—the actual proportions being 1 liter of water to every 6 g. of alumina. The mixture was heated and kept boiling and 0.05 N hydrochloric acid added from a buret. After each addition, water was added to replace that boiled off. An opalescent liquid that could be filtered unchanged was obtained. The colloidal solution of aluminum hydroxide thus prepared was then subjected to dialysis in a parchment bag for several days, the pH at the stage when dialysis was discontinued being 5.8.

Estimation of silica and alumina: Silica and alumina were estimated as given in A. E. O. C. (1).

Preparation of the precipitates: Alumina and silica sols were mixed in the different ways described previously, and nine precipitates were obtained.

Electrodialyzed gel of silicic acid: The silicic acid sol, on continued dialysis, set to a stiff gel, which was subjected to prolonged electrodialysis until the cathode was free from chloride.

Electrodialyzed gel of aluminum hydroxide: To a solution of aluminum chloride in water, ammonia was added. The precipitated aluminum hydroxide was washed with water, dialyzed in a parchment bag in running distilled water, and subsequently electrodialyzed.

Electroösmotic charge of precipitated gels and minerals

The electroösmotic experiments with the precipitates and minerals were carried out by the modified method of Briggs (3), as recommended by Mukherjee (8, 9).

Determination of saturation capacity at pH 7.0

The saturation capacities at pH 7.0 were determined by the barium acetate–ammonium chloride method of F. W. Parker (11).

Determination of moisture-holding capacity at 50 per cent relative humidity

The procedure adopted was that of Keen and Coutts (5).

Determination of the buffer curves of the precipitates and minerals

The procedure used was that devised by Schofield (1933).

RESULTS AND DISCUSSION

Table 1 shows the concentrations of the silicic acid and aluminum hydroxide sols.

Table 2 shows the moisture contents of the gels and minerals before and after heating in the autoclave in the presence of moisture. The moisture contents of the gels decrease after heating; the decrease in the moisture contents of the minerals after heating in the autoclave is only moderate.

Table 3 gives the molar silica–alumina ratios of the final precipitates obtained by different ways of mixing. The corresponding data for the minerals are also included. This table shows that when silicic acid sol is added to aluminum hydroxide sol the $SiO_2:Al_2O_3$ ratios of the precipitates are 2.49 and 2.96 with

TABLE 1

Silicic acid sol	1 gram-mole of SiO_2 in 4630 cc.
Aluminum hydroxide sol	1 gram-mole of Al_2O_3 in 19,680 cc.

TABLE 2

SUBSTANCE	$SiO_2:Al_2O_3$ RATIOS		MOISTURE CONTENT	
	Mixing ratio	Composition ratio	Before heating	After heating
			per cent	*per cent*
Precipitate 1	2.0	1.91	86.5	27.6
Precipitate 2	3.0	2.49	90.0	72.2
Precipitate 3	4.0	2.96	80.0	54.9
Precipitate 4	2.0	1.72	90.6	82.7
Precipitate 5	3.0	1.93	92.1	85.0
Precipitate 6	4.0	3.31	89.4	78.2
Precipitate 7	2.0	1.18	90.4	63.8
Precipitate 8	3.0	1.62	83.5	52.5
Precipitate 9	4.0	1.89	89.5	54.4
Silicic acid gel			86.5	34.9
Aluminum hydroxide gel			61.7	7.4
Montmorillonite		5.14	1.2	2.4
Halloysite		1.98	8.1	7.0
Kaolin		1.95	1.1	1.9
Quartz			0.4	2.2
Bauxite			1.4	1.9

precipitates 2 and 3. It is interesting to note that the composition ratios of precipitates 4 and 5, where the mixing ratios of $SiO_2:Al_2O_3$ are 2 and 3, are 1.72 and 1.93, respectively, both of which are lower than the corresponding composition ratios of the precipitates formed when silicic acid sol is added to aluminum hydroxide sol. With precipitate 6, however, where the mixing ratio is 4.0, the composition ratio is 3.31, which is higher than the corresponding figure when the precipitate is formed by adding silicic acid sol to aluminum hydroxide sol (2.96). On the other hand, when the precipitates are formed by mixing silicic acid and aluminum hydroxide sols dropwise, the $SiO_2:Al_2O_3$ ratios of the precipitates are always less

than 2.0. Thus when the mixing is done dropwise, there is a tendency for a greater proportion of aluminum to react with the silica. The conclusion may be drawn that the composition of a precipitate of an aluminosilicate depends on its mode of formation. In agreement with the work of Mattson (7), it is found that the $SiO_2:Al_2O_3$ ratios of the precipitates increase with increase in the ratio of silica to alumina. In the first method of mixing (precipitates 1, 2, and 3) silicic acid sol was added dropwise to aluminum hydroxide sol. It is probable there that some uncombined silica may have remained inside the cores of these precipitates. Hence with precipitates 1, 2, and 3, the composition ratios SiO_2: Al_2O_3 are comparatively high. The reverse may be the case with the precipitates obtained by the second method of mixing, where it is likely that some uncombined alumina may remain inside the cores of the precipitates, thereby lowering gener-

TABLE 3

SUBSTANCE	$SiO_2:Al_2O_3$ RATIOS	
	Mixing ratios	Composition ratios
Precipitate 1	2.0	1.91
Precipitate 2..	3.0	2.49
Precipitate 3 . .	4.0	2.96
Precipitate 4...	2.0	1.72
Precipitate 5	3.0	1.93
Precipitate 6	4.0	3.31
Precipitate 7..	2.0	1.18
Precipitate 8 . . .	3.0	1.62
Precipitate 9	4.0	1.89
Montmorillonite*		5.14
Halloysite		1.98
Kaolin		1.95

* Montmorillonite was found to be contaminated with a considerable amount of quartz.

ally the composition ratios. In mixing the sols dropwise, there is less likelihood of any alumina or silica remaining in the free state in the precipitates.

Electroösmotic experiments

The results of electroösmotic measurements of charge are shown in table 4. The data show that when silicic acid sol is added to aluminum hydroxide sol, the fresh precipitates are positively charged, and that the precipitates obtained in the other two modes of formation are negatively charged, except for precipitate 9. According to Mattson (7), the precipitates having $SiO_2:Al_2O_3$ molar ratios less than 3 should be electropositive and precipitates having $SiO_2:Al_2O_3$ molar ratios equal to 3 should bear no charge. In the present case, although the precipitation was carried out in hydrochloric acid medium, we found a noticeable exception to Mattson's generalization in the case of precipitates 4, 5, 6, 7,

and 8, which are negatively charged. The positive charge of precipitates **1, 2,** and **3** may be accounted for as being due to uncombined alumina on the surface of the precipitates which might have resulted from precipitation in an atmosphere of aluminum hydroxide to which silicic acid sol was added drop by drop. It appears from the data in table 4 that with precipitates formed in the same way of mixing, the electropositive character increases as the composition ratios $Si_2O:Al_2O_3$ of the precipitates increase.

The recent work of Chatterjee and Sen (4) shows that when the synthetic mixtures are prepared by adding increasing amounts of colloidal aluminum hydroxide to a definite volume of silicic acid sol, the precipitates having the

TABLE 4

SUBSTANCE	ELECTROÖSMOTIC MOVEMENT OF AIR BUBBLE IN CENTIMETERS PER 5 MIN., UNDER 110 VOLTS	
	Freshly precipitated	Heated
Precipitate 1........................	+2.41	−1.25
Precipitate 2.......	+2.66	−1.55
Precipitate 3........	+3.65	−1.80
Precipitate 4.	−2.54	−1.85
Precipitate 5.	−2.22	−1.72
Precipitate 6	−0.30	−1.65
Precipitate 7	−0.45	−2.65
Precipitate 8.	−0.31	−2.75
Precipitate 9.	+2.99	−2.35
Silica.	−1.12	−0.60
Alumina	+1.65	+1.18
Montmorillonite	−3.41	−3.25
Halloysite.	−1.28	−0.80
Kaolin	−2.19	−1.27
Quartz	−1.44	−1.18
Bauxite	+0.40	+0.30

mixed ratios of $SiO_2:Al_2O_3$ of 2:1, 1:1, and 1:2 are all electropositive. Similar results have also been obtained by Bradfield (2), who found that a mixture having a $SiO_2:Al_2O_3$ ratio of 1.85:1 was electropositive. The results in table 4, however, suggest that the electrical charges of freshly formed precipitates depend on their modes of formation and on their compositions.

The data in table 4 show that all the electropositive precipitates become electronegative on heating. Precipitates 6, 7, and 8, which possess only a small electronegative charge in the freshly precipitated condition, become appreciably more electronegative after heating. The naturally occurring silicate minerals are all electronegative. The suggestion may, therefore, be made that mineral structures are developed in the gels after heating in an atmosphere of moisture, the presence of which is necessary, as otherwise the minerals would be dehydrated.

The small decrease in the negative charges of the minerals montmorillonite, halloysite, kaolin, and quartz after heating is significant and suggests that with minerals whose structures have been fully developed, excess of heating causes destruction of the structures. It is interesting to note that the electropositive charges of both freshly precipitated alumina and bauxite decrease somewhat after heating, but still remain electropositive. On comparison of the electronegative charges of the heated precipitates and of the minerals, both before and after heating, it appears that with precipitates which have been formed by mixing the sols dropwise, the electroösmotic negative charge is of the same order as that of montmorillonite. On the other hand, the precipitates which have been

TABLE 5

SUBSTANCE	SATURATION CAPACITY IN MILLIEQUIVALENTS PER 100 G. OF OVEN-DRY MATERIALS	
	Freshly precipitated	Heated
Precipitate 1........	19.1	80.0
Precipitate 2	53.4	80.7
Precipitate 3	85.6	86.8
Precipitate 4	47.0	84.6
Precipitate 5	95.3	65.5
Precipitate 6	46.6	59.8
Precipitate 7 . . .	26.7	35.8
Precipitate 8	13.3	38.0
Precipitate 9	51.1	60.3
Silica.	41.4	110.0
Alumina.	5.9	4.2
Montmorillonite......	8.6	8.4
Halloysite...	9.2	4.1
Kaolin	4.5	2.4
Quartz	2.4	21.3
Bauxite	1.7	4.8

formed in the other two ways possess, after heating, electronegative charges of nearly the same order as that of kaolin (-1.27). The suggestion may, therefore, be made that substances having electrical charges of the order of montmorillonite tend to be formed when the precipitates are produced by mixing the silicic acid and aluminum hydroxide sols dropwise. On the other hand, when the precipitates of aluminosilicates are formed either by adding silicic acid sol to aluminum hydroxide sol or vice versa, the tendency is for the formation of substances having electrical charges of the order of kaolin.

Determination of base-saturation capacities

The results given in table 5 show that when silicic acid sol is added to aluminum hydroxide sol, the base-exchange capacities of the precipitates increase with

increase in the SiO₂:Al₂O₃ ratios. These observations are in agreement with the findings of Mattson (6, 7) and Wiegner (15). When alumina sol is added to silicic acid sol, however, a maximum value in base-exchange capacity is found (precipitate 5) with increasing SiO₂:Al₂O₃ ratios of the fresh precipitates, whilst with the heated ones, the base-saturation capacity decreases as the SiO₂:Al₂O₃ ratios of the precipitates increase. The observations with fresh precipitates 4, 5, and 6 are in agreement with the findings of Wiegner and Mattson: viz., that the base-combining capacity has a maximum value at a SiO₂:Al₂O₃ ratio of about 3.0. The decrease in base-combining capacity with further increase in the SiO₂:Al₂O₃ ratio of the precipitates has been explained as being due to the destruction of the silicate structure, and this probably explains the continuous decrease in the base-combining capacities of precipitates 4, 5, and 6 after heating. With precipitates formed by mixing silicic acid and aluminum hydroxide sols dropwise, there is a maximum value in base-combining capacity when the precipitates are fresh. When these precipitates are heated, however, the base-exchange capacities continually increase as the SiO₂:Al₂O₃ ratios increase.

A comparison of the data in tables 4 and 5 shows that the base-exchange capacity increases with increase in the negative charge of the heated precipitates 1, 2, and 3. With the fresh precipitates 1, 2, and 3, however, the positive charge increases with increase in the SiO₂:Al₂O₃ ratios and is attended with increase in base-combining capacities. This may be explained as being due to free alumina being present in the fresh precipitates; the free alumina, however, is transformed into aluminosilicates during the process of heating. With precipitates 4, 5, and 6, both fresh and heated, the base-exchange capacity generally decreases with decrease in the electric charge, except for the fresh precipitate 5. Also, for precipitates 7 and 8, both fresh and heated, it is found that as the electric charge decreases, the base-exchange capacity decreases. Precipitate 9, both fresh and heated, forms an exception to this rule.

All the precipitates show an increase in base-combining capacities after heating, except precipitate 5. With the silicate minerals, the base-exchange capacities decrease after heating, whilst with silica gel, quartz, and bauxite the base-exchange capacities increase after heating. It is rather significant that the base-combining capacities of the precipitates are all much higher than those of the minerals. The reason probably is that the precipitated substances are in a finer state of subdivision than the powdered minerals. The decrease in base-combining capacities of the minerals after heating is probably due to the loss in structure of some of the active materials.

Moisture contents at 50 per cent relative humidity

The results are shown in table 6. The moisture contents at 50 per cent relative humidity give a rough indication of the colloidal contents of the substances. With precipitates 1, 2, and 3, the moisture content at 50 per cent relative humidity increases with increase in the SiO₂:Al₂O₃ ratio, with the exception of the heated precipitate 3. With precipitates 4, 5, and 6, the moisture contents at 50 per cent relative humidity show a maximum value at an intermediate SiO₂:Al₂O₃ ratio, whilst with precipitates 7, 8, and 9 the moisture contents at 50

per cent relative humidity increase with increase in $SiO_2:Al_2O_3$ ratios, with the exception of the heated precipitate 7. The moisture contents at 50 per cent relative humidity of freshly precipitated and heated alumina and of the minerals are very low compared with those of the precipitates. The high moisture-holding capacities of the precipitates, as compared with those of the minerals, may be explained as being due to the highly dispersed characters of the precipitates. It is also significant that the moisture contents at 50 per cent relative humidity generally decrease after heating, the decrease being appreciable in some cases, particularly in the case of precipitates 3 and 4. This suggests that aging brings about certain fundamental changes in the structure of aluminosilicates; and, since the minerals are highly aged materials, the decrease in

TABLE 6

SUBSTANCE	MOISTURE CONTENT AT 50 PER CENT RELATIVE HUMIDITY (OVEN-DRY BASIS)	
	Fresh	Heated
	per cent	*per cent*
Precipitate 1......	18.8	15.7
Precipitate 2....	19.3	18.0
Precipitate 3.	22.7	13.8
Precipitate 4...	21.8	5.3
Precipitate 5..	23.5	18.1
Precipitate 6...	22.0	17.7
Precipitate 7..	15.5	17.2
Precipitate 8.	17.0	16.2
Precipitate 9.....	23.7	17.0
Silica..	17.7	15.8
Alumina.....	2.8	4.1
Montmorillonite.........	1.1	0.9
Halloysite...............	2.9	2.4
Kaolin........	0.9	0.7
Quartz..........	0.3	0.04
Bauxite......	0.4	0.1

moisture contents at 50 per cent relative humidity may be explained as being due to the changes in structure. It is interesting to note that with precipitate 7 and alumina gel, the moisture content at 50 per cent relative humidity increases after heating.

Buffer curves

Figure 1 shows the buffer curves of fresh and heated alumina and silica gels. It will be seen that the buffer curves of silicic acid gels rise fairly steeply up to pH 7.1 and then rise less steeply. Silica is negatively charged and it is found that as the pH increases, the base-combining capacity increases also. With alumina gel, however, it is observed that the base-combining capacity at pH 2.9 is less than the base-combining capacity at pH 1.3, for both the fresh and the

M.EQ. BASE UPTAKE PER 100 G. OVEN-DRY MATERIALS

FIG. 1. Buffer curves of fresh and heated alumina and silica gels
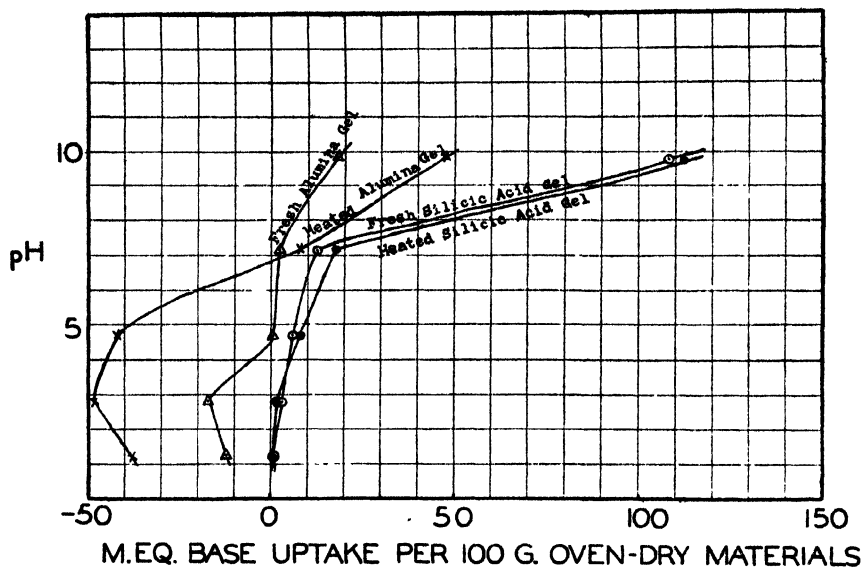
M.EQ. BASE UPTAKE PER 100 G.
OVEN-DRY MATERIALS
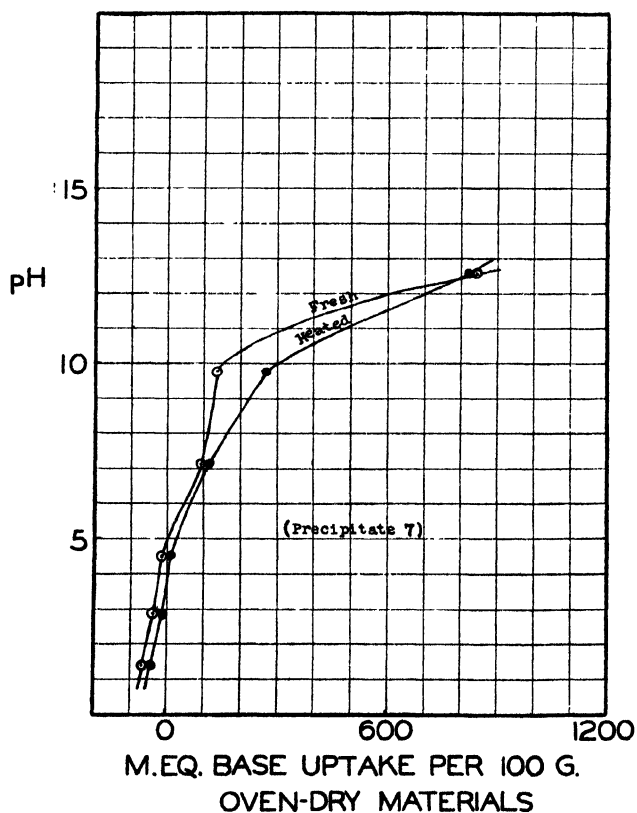
FIG. 2. Buffer curves of precipitate 7, both fresh and heated

30

heated precipitates. Similar observations have been made by Raychaudhuri and Basuraychaudhuri (12) with the mineral limonite. These observations are probably due to complex, sparingly soluble compounds being formed, whose solubility varies differently with variations in pH values. The buffer curves with fresh and heated precipitates were also drawn, but no striking differences in the buffer curves of the fresh and heated precipitates have been observed. Figure 2 shows the buffer curves of precipitate 7, fresh and heated. It will be observed that there is not much difference in the buffer curves of the fresh and heated precipitates. The buffer curves of the minerals kaolin, montmorillonite, bauxite, and halloysite have already been determined by Raychaudhuri and Basuraychaudhuri (12, p. 146).

CONCLUSIONS

To summarize, it may be said that the heating of precipitated aluminosilicates changes their structure in such a manner that their base-exchange capacities increase and their general properties tend to approach the properties of natural minerals. So far as the mode of precipitation is concerned, mixing the colloidal solutions of aluminum hydroxide and silicic acid dropwise seems to favor the formation of mineral structure.

SUMMARY

Nine kinds of aluminosilicate gels were prepared by mixing different proportions of silicic acid and aluminum hydroxide sols ($SiO_2:Al_2O_3$ ratios = 2:1, 3:1, and 4:1), in three different ways: viz., (1) by slowly adding aluminum hydroxide sol to an excess of silicic acid sol; (2) by slowly adding aluminum hydroxide sol to an excess of silicic acid sol; and (3) by mixing the two sols dropwise. The following properties of these precipitates have been determined: (a) chemical composition ($SiO_2:Al_2O_3$ ratios), (b) electroösmotic charge, (c) base-combining capacities, (d) moisture contents at 50 per cent relative humidity, and (e) buffer curves. These experiments were carried out also with electrodialyzed alumina and silica gels and with the minerals montmorillonite, halloysite, kaolin, quartz, and bauxite. All these substances were subsequently heated in a steam autoclave for 12 hr. at 1 atmosphere pressure, and the physicochemical and electrical properties of the heated substances were also determined. It was found that on heating the precipitated aluminosilicates tend to acquire the properties of naturally occurring aluminosilicates. It appears that mixing the colloidal solutions dropwise favors the formation of mineral structures.

REFERENCES

(1) A. E. O. C.: Methods of Analysis (1938).
(2) BRADFIELD, R.: Missouri Agr. Expt. Sta. Res. Bull. **60**, 60 pp. (1923).
(3) BRIGGS, L.: Nature **109** (December 2, 1922).
(4) CHATTERJEE, B., AND SEN, A.: Indian J. Agr. Sci. **13**, 59 (1943).
(5) KEEN, B. A., AND COUTTS, J. R. H.: J. Agr. Sci **18**, 740 (1928).
(6) MATTSON, S.: Soil Sci. **25**, 289 (1928).
(7) MATTSON, S.: Soil Sci. **30**, 459 (1930).
(8) MUKHERJEE, J. N.: Phil. Mag. **44**, 103 (1922).

(9) MUKHERJEE, J. N.: Nature **110**, 732 (1922).

(10) NOLL, W.: Ber. deut. keram. Gesell. **19**, 176 (1938).

(11) PARKER, F. W.: J. Agr. Soc. Agron. **21**, 1030 (1929).

(12) RAYCHAUDHURI, S. P., AND BASURAYCHAUDHURI, P. K.: Indian J. Agr. Sci. **12**, 137 (1942).

(13) RAYCHAUDHURI, S. P., AND GHANI, A. K. M. Q.: J. Indian Chem. Soc. **19**, 311 (1942).

(14) RAYCHAUDHURI, S. P., AND HUSSAIN MIAH, A.: J. Indian Chem. Soc. **20**, 195 (1943).

(15) WIEGNER, G.: J. Soc. Chem. Ind. **50**, 31, 65 (1931).

THERMAL TRANSITIONS OF THE ALKALI PALMITATES

ROBERT D. VOLD AND MARJORIE J. VOLD

Department of Chemistry, University of Southern California, Los Angeles, California

This paper presents the results of a study of the transitions of lithium, potassium, rubidium, and cesium palmitates at atmospheric pressure from room temperature (ca. 25°C.) to their melting points (to isotropic liquid). Results for sodium palmitate (1, 6) are included for comparison. From the appearance of the various forms and the magnitude of the heats of transition, an effort has been made to correlate the various transitions of the several palmitates with one another on the basis that the complete set corresponds to the same change of structure from crystal to liquid occurring in discrete steps as the temperature is raised. This research, varying the nature of the polar group as systematically as possible, parallels the study previously (5) made of the relations between transitions of sodium salts of normal fatty acids of varying chain length from C_6 (sodium caproate) to C_{26} (sodium cerotate).

MATERIALS

All of the soaps were prepared by neutralizing a solution of Eastman Kodak best-quality palmitic acid in 95 per cent ethyl alcohol with an alcoholic solution of the corresponding alkali hydroxide and drying the product to constant weight at 105°C. The palmitic acid had an equivalent weight of 257.0 (theory 256.3), and an iodine value of zero within experimental error.

PROCEDURE

Dilatometric measurements were made by observing the rise in level of mercury which had been flowed in to fill the residual space over a 0.6-g. sample of the soap being studied, which was contained in a small bulb sealed to a fine capillary. Operating details of the method have already been described (6).

Microscopic observations were made using the hot-wire technique (5), in which a thin film of material is subjected to a temperature gradient, boundaries between phases marking transition temperatures (which can be determined

from the magnitude of the gradient and the distance from the wire to the boundary, measured by means of the vernier scale attached to the mechanical stage of the microscope). Observations also were made of the behavior of samples sealed in glass capillary tubes and heated continuously in a small furnace mounted on the stage of a Spencer polarizing microscope (5). Temperatures were measured by means of a thermocouple. Finally, for all except sodium palmitate, single crystals were grown from 95 per cent ethyl alcohol and examined under the microscope as they were heated slowly. Magnifications of 40 to 100× were employed in the microscopic work.

Calorimetric observations were made in a differential calorimeter in which the sample and an inert material, each contained in a pear-shaped cell, are warmed together in the same environment. Transition temperatures in the sample are marked by large peaks in the time–differential temperature curve, from whose breadth and area a rough estimate can be made of the heat effect at the transitions. This procedure has also been described previously (4). Differential temperature–time curves were also obtained on cooling in order to observe whether or not undercooling occurred, and to what extent transition temperatures so found agreed with those found on heating.

<center>EXPERIMENTAL RESULTS</center>

Dilatometer curves for lithium, potassium, rubidium, and cesium palmitates are shown in figure 1. Curve A, for lithium palmitate, shows three transitions, at 93°, 189°, and 211°C. Curve B, for potassium palmitate, shows three transitions, at 67°, 174°, and 254°C., together with a small inflection at 130°C. This curve was not carried up to the melting temperature, which is above the boiling point of the dilatometer fluid used (mercury). Calorimetric evidence shows an additional transition at 152°C., which has apparently too small a volume change to be detected dilatometrically. Curves C and D, for rubidium and cesium palmitates, were carried only to 150°C. and show two transitions each, at 69° and 115°C. for rubidium palmitate and 61° and 95°C. for cesium palmitate.

Calorimeter curves (differential temperature *versus* time) are shown for the four soaps in figure 2. The three transitions of lithium palmitate (curve A) are conspicuous. The transition temperature is in each case the temperature of the system at the time when the temperature difference first begins to rise. Mean values for several runs are 103°, 190°, and 223°C. These values are more reliable than the dilatometric values, since the preparations used in the dilatometric studies were subsequently found to be contaminated with the corresponding alkali chlorides in considerable amount. Undercooling occurs at the top two transitions, initial solidification occurring on cooling at 199°C. and the next transition occurring at 164°C.

Curve B, for potassium palmitate, shows transitions at 57°, 131°, 152°, and 175°C. The transition from neat soap to the next lower form occurs on heating at about 246°C., with a very gradual rise in temperature difference between sample and reference cell. On cooling it begins sharply at 261°C., in close agree-

ment with microscopic observations.   Undercooling occurs at all the lower transitions.

Curve C, for rubidium palmitate, shows sharp peaks at 66°, 125°, and 256°C. There is also a somewhat rounded peak starting at 181°C.   Microscopic ob-
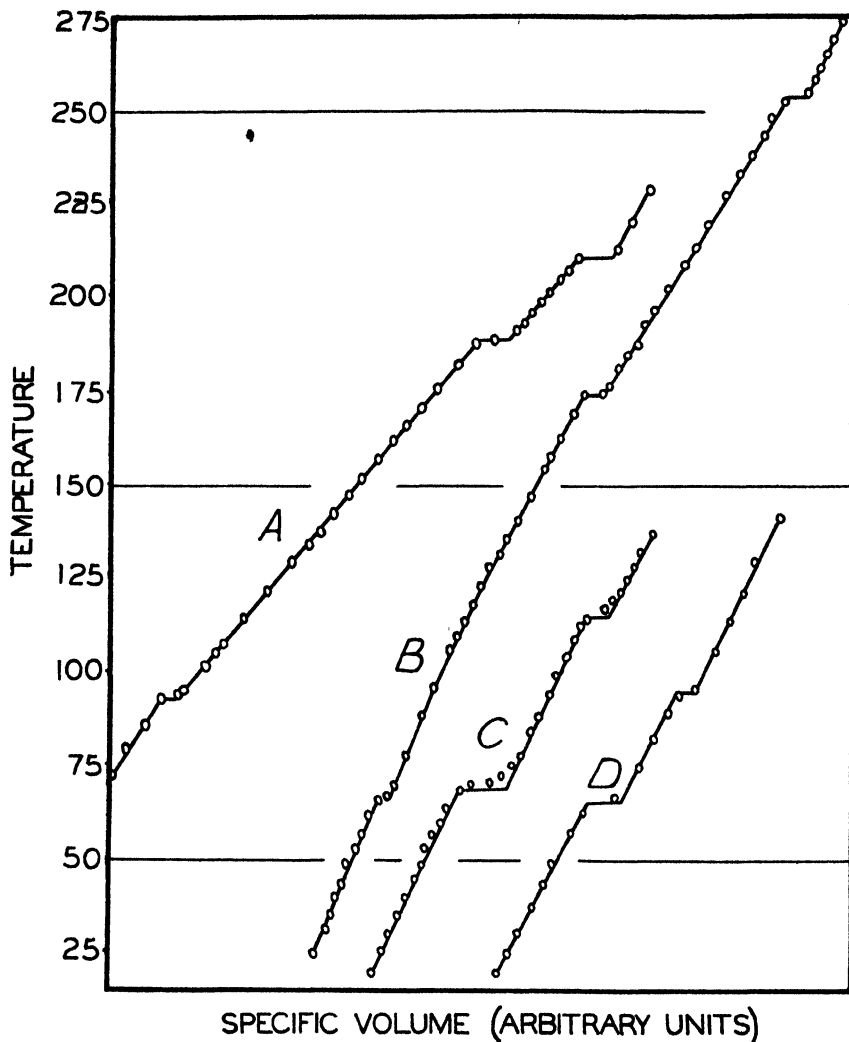
Fig. 1. Dialometric behavior of the alkali palmitates. Breaks in the curves show transition at the corresponding temperature. Curve A, lithium palmitate; curve B, potassium palmitate; curve C, rubidium palmitate; curve D, cesium palmitate.

servation seemed to show a transition at 215°C., but not at 181°C., and there is no separate peak in the calorimeter curve at 215°C. The cooling curve for rubidium palmitate showed transitions at 262°C. (corresponding to 256°C. on heating), at 192°C. (intermediate between the microscopically observed 215°C.

and the heating-curve rounded hump beginning at 181°C.), and at 117°C. and 63°C. (corresponding to the values of 125° and 66°C. obtained on heating).
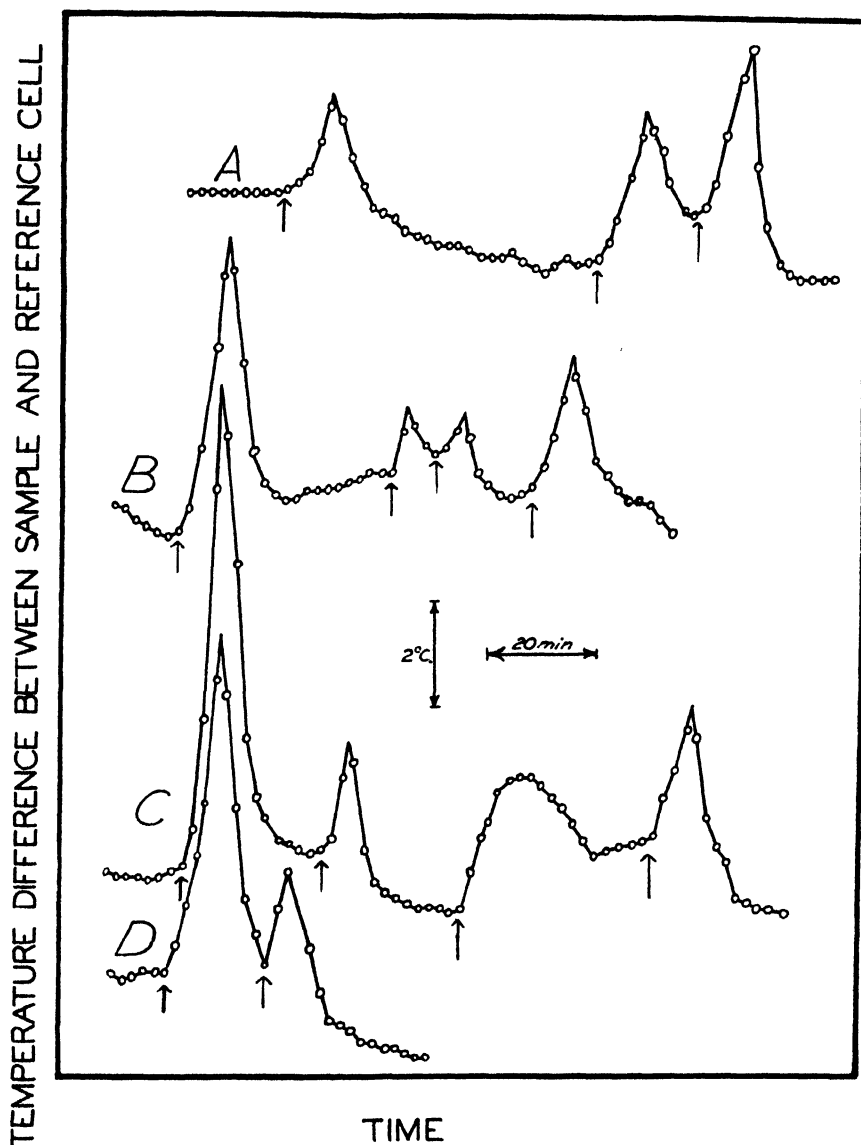
FIG. 2. Calorimetric behavior of the alkali palmitates. Peaks in the curves show transitions at the temperatures indicated, which are the temperatures at the times where the differential temperature begins to increase. Curve A, lithium palmitate; curve B, potassium palmitate; curve C, rubidium palmitate; curve D, cesium palmitate.

Curve D, for cesium palmitate, showed peaks only at 64° and 98°C. Higher transitions have heat effects too small to be detected with the present apparatus.

Table 1 records values of transition temperatures obtained by microscopic observation of samples sealed in flat glass capillaries heated in a small furnace on the stage of the microscope. The results for lithium palmitate are in fair agreement with the calorimetric data. In the case of potassium palmitate the transition at 131°C. was not seen. The transition at 265°C. is sharp and conspicuous. The transition was found calorimetrically also (though not shown on curve B of figure 2). Heat absorption begins to occur at about 246°C.; the calorimetric behavior is similar to that found for the analogous transition of sodium palmitate, where the dilatometric and microscopic values are consistently 20–30°C. higher than the calorimetric value. There is no doubt of the reality of this observation. Possible interpretations are discussed later in this paper. For rubidium palmitate, agreement between microscopic and calorimetric results is good except for the behavior between 181°C. and 215°C., which is also discussed later. For cesium palmitate a slight but reproducible change in appearance is recorded at 270°C., which may or may not be a real transition. The transition at 225°C. is sharp and conspicuous but apparently has too small a heat effect to be observed calorimetrically.

TABLE 1

Transition temperatures for the alkali palmitates observed microscopically

SOAP	OBSERVED TRANSITION TEMPERATURES
	°C
Lithium palmitate..........	102, 196, 223
Potassium palmitate.......	59, 152, 173, 265, 375
Rubidium palmitate	66, 122, 256, 380
Cesium palmitate	57, 94, 225 (270), 369

The hot-wire microscopic technique was used to confirm the order of the melting points of potassium, rubidium, and cesium palmitates as given in table 1 (RbP > KP > CsP) and to provide further information in the two cases cited above, where calorimetric and microscopic observations seem at variance. For potassium palmitate a visible transition occurs at 260°C., in good agreement with the microscopic value of 265°C., despite the fact that considerable heat absorption begins as much as 20°C. lower. For rubidium palmitate a transition is found at 216°C., much higher than the microscopic value of 197°C. and the calorimetric value of 181°C. Probably there are two separate transitions here, as is discussed later in the paper.

Values of the heats of the various transitions were calculated from the area and breadth of the peaks in the curves of differential temperature *versus* time, using the formula previously developed (4). These values are correct in order of magnitude only, being reproducible within 20 per cent. Relative values for the different transitions in the same sample are more reliable than the absolute values. The data are given in table 2. In this table the temperatures given are weighted mean values. The differences between these values and individual

values obtained by different experimental techniques, as cited in table 1 and throughout the description of experimental results, are not large except where real significant differences, discussed separately, appear to be inherent in the properties of the materials studied.

Crystals of the soaps were grown from ethyl alcohol (95 per cent) and observed under the microscope primarily to compare the changes in appearance at each transition from one soap to the next and thus gain some insight as to the nature of the transition. Satisfactory crystals of sodium palmitate were not obtained.

For lithium, potassium, rubidium, and cesium palmitates, the first transition observed on heating the crystals above room temperature is a rapidly reversible transformation from one crystal form to another. The orientation of the optic

TABLE 2

Heats of transition for alkali palmitates, in calories per mole

TRANSITION	LITHIUM PALMITATE		SODIUM PALMITATE		POTASSIUM PALMITATE		RUBIDIUM PALMITATE		CESIUM PALMITATE	
	$T°C.$	ΔH	$T°C.$	ΔH	$T°C.$	ΔH	$T°C.$	ΔH	$T°C$	ΔH
Inter-crystal........	101	3400	65	a	60	4900	67	7700	62	6500
Waxy group .	191	3900	117	4800	131	900	126	2700	95	3600
			134	3900	152	1000				
			172	a	174	1500				
Subneat and neat group	None	None	208	1900	259	2500	181	b	225	a
			253	1500			210	a		
							257	2290		
Melting point to iso-tropic liquid	223	5760	297	500	375	c	380	c	375	c

a. No heat of transition was observed.

b. In this case the experimental peak is so rounded as to make the calculated ΔH unreliable.

c. Calorimeter difficult to operate at these temperatures. Sometimes very large peaks were obtained, which the authors believe to be artifacts.

axis within the crystal changes; consequently, crystals oriented so as to be dark between crossed polaroids suddenly became light and *vice versa*. In the case of rubidium and cesium palmitates all semblance of crystallinity is lost at the second transition above room temperature. Individual crystals draw up to form elongated droplets. The first inter-crystal transition is not so apparent on cooling, since each single crystal has been broken up into a mass of randomly oriented submicroscopic crystallites. For potassium palmitate the loss of crystalline appearance is not observed until the transition at 174°C. is reached. For sodium stearate, and presumably therefore for sodium palmitate, the transition above which sharp plane external crystal faces no longer exist is that forming superwaxy soap. No analogous transition is found for lithium palmitate.

Correlation of the various transitions

The first part of this discussion is concerned with speculations concerning the relations between the sets of transitions for each of the alkali palmitates. At the two extremes of temperature represented by the melting point to isotropic liquid and room temperature the molecular arrangements are at least closely similar, though in the absence of crystal data, it cannot be said that the crystal forms at room temperature are identical. The set of intervening transitions taken together then corresponds to the same total change.

In the case of hydrogen palmitate (palmitic acid) the entire transformation occurs at one temperature, where palmitic acid melts from true crystal to true liquid. For the alkali metal palmitates, the change from crystal to liquid occurs in steps, which are similar, though not identical, for the different substances. Figure 3 shows the temperatures of transition side by side for the five soaps. Related transitions are connected by lines which are full or dotted according to the surety of the relation on the basis of available evidence. Where a single transition for one soap is joined to more than one for another, the interpretation is that in the former case, at least two distinct structural changes occur at one temperature, while in the latter the same changes occur at two successive temperatures.

For lithium palmitate there are three discrete steps in melting, with a total heat effect not much different from the heat of fusion of palmitic acid. The first of these (at 101°C.) occurs without loss of microscopic crystalline appearance. At the second (191°C.) a waxy form is produced. At the third (223°C.) complete melting occurs, with the absorption of considerable heat. Some measure of three-dimensional crystalline regularity of molecular arrangement probably exists in the waxy form, since the liquid form undercools easily. X-ray data of Bolduan, McBain, and Ross (1) for the waxy form of sodium palmitate support this hypothesis.

For potassium palmitate there are six discrete steps in transformation from the crystalline form at room temperature to the isotropic liquid at 375°C. The first of these (at 60°C.) is identical in microscopic appearance with the transition of lithium palmitate at 101°C. The next three (131°, 152°, and 174°C.) are closely related to one another and to three similar transitions for sodium palmitate (117°, 134°, and 172°C.). The form of potassium palmitate existing above 174°C. corresponds to the superwaxy form of sodium palmitate, since for the former single crystals cease to have sharp plane faces above this transition temperature, corresponding to the diffuseness in the *a* spacings observed by Bolduan, McBain, and Ross (1) for the superwaxy form of the latter. The fifth transition for potassium palmitate (259°C.) results in the formation of a true liquid crystal of the "smectic" type, which finally melts to true liquid at 375°C.

Whether or not the transition reported for sodium palmitate at 65–70°C. (1, 2, 6) corresponds to that of potassium palmitate at 60°C. and that of lithium palmitate at 101°C. has not been established. The next three transitions of

sodium palmitate (117°, 134°, and 172°C.) closely parallel the three corresponding changes in potassium palmitate, although total heat absorbed in the group is greater (3400 for potassium palmitate; 7300 for sodium palmitate) and it is distributed differently. Sodium palmitate forms a smectic liquid crystal at
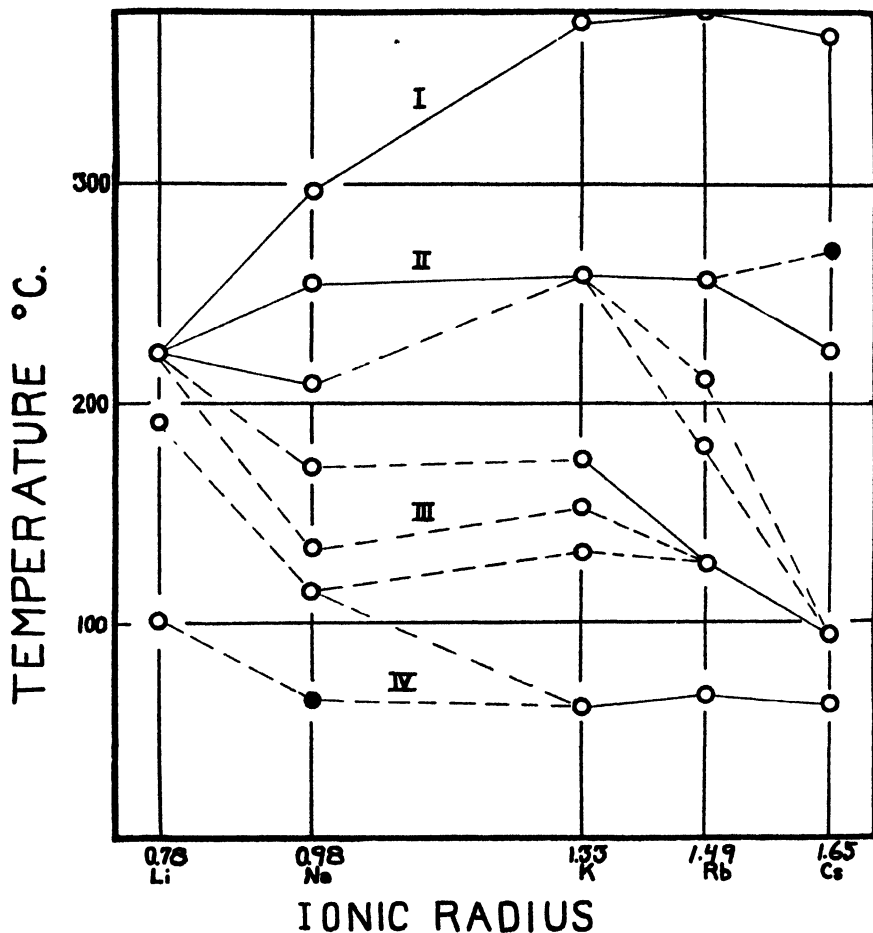
FIG. 3. Correlations between transitions of the alkali palmitates. Full lines indicate that the same structural changes occur at transitions so connected. Dotted lines indicate a similar, but less positively established, relation. The joining of a single point for one soap to two or more for another indicates that the same transitions occur at one temperature for the former as occur in discrete steps for the latter. The two solid points are transitions whose actual existence is in doubt.

253°C., similar to potassium palmitate at 259°C., but in reaching that structure from superwaxy soap an additional discrete step occurs,—namely, the formation of subneat soap at 208°C.

Consideration of the above facts leads to the hypothesis that the melting points of these three soaps should be connected by a line, since above those

temperatures all are isotropic liquid. Next, the transitions to neat soap at 257°C. for potassium palmitate and 253°C. for sodium palmitate should be connected by a line, which line should be further extended to the melting point of lithium palmitate, showing that neat soap has no finite temperature range of existence for this soap. The three transitions of the waxy group for sodium and potassium palmitates are connected by dotted lines, since, although the forms are similar, the different relative heat effects militate against any presumption of perfect correspondence. The lowest transition of the waxy group for both is connected to the transition of lithium palmitate at 196°C., while the upper two are connected with the melting point of the latter, since the high heat effect associated with this point indicates that the form between 196° and 223°C. is of the waxy group rather than being a liquid crystal of the subneat type. Since no transition of the character of the superwaxy-subneat type of sodium palmitate (208°C.) exists for potassium palmitate, this transition is presumed to occur simultaneously with neat soap formation. Finally, the transitions of lithium palmitate at 101°C. and potassium palmitate at 67°C. appear to be very similar, but that for sodium palmitate has so much smaller a heat effect that a portion of the structural change must not occur until the first of the waxy transition temperatures is reached (117°C.). These relations are all indicated by the appropriate connecting lines in figure 3.

Rubidium palmitate has an intercrystalline change at 67°C., paralleling that of potassium palmitate at 60°C. The subwaxy and waxy forms, however, have no separate stable existence over finite temperature intervals. Instead, superwaxy soap is formed in one step (126°C.), as is indicated by the large heat effect and by the physical resemblance between the transitions of potassium palmitate heated from room temperature to 174°C. and rubidium palmitate heated to 126°C., as observed microscopically on heating single crystals of the soaps.

Neat soap of rubidium palmitate forms at 257°C. There are two intervening transitions, as opposed to one for sodium palmitate and none for potassium palmitate. However, as pointed out earlier, the single transition for superwaxy soap to neat soap for potassium palmitate has peculiar properties. Although the microscopically visible change occurs at 259°C. or slightly higher, heat begins to be absorbed as much as 13°C. lower and the transition is thermally complete below 259°C., thus distinguishing the phenomenon from an exaggerated premelting effect. The same phenomenon was found for sodium palmitate (4) at the transition from subneat soap to neat soap. Preliminary measurements of electrical resistance (3) indicate that substantial conduction also begins where the heat absorption begins. It appears that the actual structural alterations occur over a finite range of temperature, with sharp changes in physical properties occurring at different temperatures in the interval. For rubidium palmitate heat is absorbed at 181°C. and at 246°C. (on heating; at 262°C. on cooling). Microscopic changes occur reversibly at 192° and 257°C.

On the basis of these facts, the melting point of rubidium palmitate is connected by a full line with that of potassium palmitate, and the transition to

neat soap (259°C.) is likewise connected to that of potassium palmitate. The two transitions at 181° and 215°C. seem to correspond to changes that occur with potassium palmitate at the single transition from superwaxy to neat, and are so correlated by the appropriate dotted lines of figure 3. Similarly, the three transformations of the waxy group for potassium palmitate occur at a single temperature (126°C.) for rubidium palmitate, as indicated. The transitions at 59° and 67°C. for the two soaps seem very similar.

For cesium palmitate the transition at 62°C. parallels that of rubidium palmitate at 67°C. The next transition, at 95°C., parallels that of rubidium palmitate at 126°C. but has a larger heat effect. Further, the formation of neat soap at 225°C. is free from the anomalies described above. Therefore it can be supposed that a portion of the changes associated with the transformation from the superwaxy structure to the neat structure occur for cesium palmitate simultaneously with other changes at 95°C.

The nature of the various transitions

Figure 3 shows that the melting point to isotropic liquid rises as the series is ascended from lithium palmitate to rubidium palmitate and drops only very slightly from rubidium palmitate to cesium palmitate. The temperature of formation of neat soap remains nearly constant throughout (250–260°C.), but is lower for lithium palmitate, where it occurs simultaneously with melting at 223°C., and for cesium palmitate where there are two changes, one at 225°C. and one at 270°C. The temperatures corresponding to the other transformations drop off as the series is ascended.

The essential constancy of the temperature of formation of neat soap on heating was observed also for variations in length of the hydrocarbon chain (4). This means that the characteristic structural change leading to its formation involves forces dependent neither on the length of the hydrocarbon chain, nor on the nature of the polar group (provided variation in these factors is not enough to change the whole nature of the set of transitions). It would seem of necessity to be concerned with interaction between chains.

The crystal transformation at 101°C. for lithium palmitate and at 60-70°C. for the other soaps is amenable to treatment by the standard procedures of x-ray crystallography. Speculations concerning it are therefore reserved until the x-ray study is complete.

It is noteworthy that the temperature of formation of superwaxy soap, which is accompanied by loss of crystalline character, diminishes as the series of palmitates is ascended from lithium to cesium. The same effect was found for increasing chain length. The melting temperature, however, increases, indicating that the strength of the network of carboxylate groups has been increased by increasing the size of the metal ion. This same increase in size has weakened the forces between chains, perhaps simply by inducing a somewhat greater average separation between them, although x-ray data are required to confirm this speculation.

Available data (5) for potassium and sodium stearates are compared with

those for the palmitates in table 3. Calorimetric data for potassium stearate are not available. The melting point of potassium stearate is high (345°C.) but lower than that for potassium palmitate, similar to the relation between the sodium salts. The transition at 265°C. has been shown to be the formation of neat soap, and like all cases of neat soap formation so far observed, occurs in the neighborhood of 260°C. Very likely the transition at 162°C. is the formation of superwaxy soap, comprising the same change as occurs in the sodium salts and potassium palmitate at three separate transitions. The transition in potassium stearate at 51°C. is doubtless similar to that of potassium palmitate at 60°C. There appear to be two transformations between 162° and 265°C., paralleling the behavior of rubidium palmitate rather than of sodium stearate.

TABLE 3

Comparison of transition temperatures for sodium and potassium palmitates and stearates

SODIUM PALMITATE	SODIUM STEARATE	POTASSIUM PALMITATE	POTASSIUM STEARATE
65	90	60	51
117	117		
		131	162
134	132	152	
172	167		
		174	⎰235
			⎱249
208	205		
253	257	259	265
295	288	375	345

SUMMARY

Transition temperatures are reported for the complete series of alkali palmitates between 25°C. and the melting points, together with their approximate heat effects. The sets of transitions are closely related, though not exactly parallel for the five substances. For all, one of the transitions can be identified as that at which microscopic external crystal form gives way to a measure of fluidity. For lithium palmitate this temperature is the melting point to isotropic liquid, 223°C.; for the remainder of the sequence, loss of microscopic crystallinity occurs at progressively lower temperatures and occurs before complete melting. The temperature of formation of neat soap, for all soaps having this form, is very nearly independent both of the nature of the cation and of the length of the fatty radical, and is therefore believed to involve a special spatial equilibrium of attractive and repulsive forces between the chains.

REFERENCES

(1) BOLDUAN, O. E. A., McBAIN, J. W., AND ROSS, S.: J. Phys. Chem. **47**, 528 (1943).
(2) CHESLEY, F. G.: J. Chem. Phys. **8**, 643 (1940).
(3) HELDMAN, M. J., AND VOLD, R. D.: Unpublished data.
(4) VOLD, R. D.: J. Am. Chem. Soc. **63**, 2915 (1941).
(5) VOLD, M. J., MACOMBER, M., AND VOLD, R. D.: J. Am. Chem. Soc. **63**, 168 (1941).
(6) VOLD, R. D., AND VOLD, M. J.: J. Am. Chem. Soc. **61**, 808 (1939).

NEW BOOKS

Cellulose and Cellulose Derivatives. Edited by EMIL OTT. 6 × 9¼ in.; xix + 1176 pp.
  New York: Interscience Publishers, Inc., 1943. Volume V of High Polymer Series.

At last, the book for which workers in the field of cellulose have been waiting has appeared. The need for a comprehensive, up-to-date treatise connecting the complex chemical and physical background of this highly important commercial raw material with its industrial treatment and use has been urgent. But no individual was qualified to discuss adequately and correctly the intricate details of the complex chemistry and physics of cellulose and at the same time to know the complicated industrial processes involved in the numerous commercial uses for which it is the fundamental raw material.

The task has been accomplished by a group of thirty-five experts under the able editorship of Dr. Emil Ott, Director of Research of the Hercules Powder Company. The well-known disadvantages usually apparent in collaborative works of this character have been largely circumvented by the able editing of Dr. Ott, and he is to be congratulated on having produced a smoothly flowing treatise with a minimum of useless repetition. Especially outstanding among the contributors is the work of Purves on chemical constitution, of Harris and his coworkers on degradation, of Mark, editor of the first three volumes of this series, on physical structure, and of Spurlin on the physical chemistry of cellulose.

The subject is presented in ten well-chosen chapters, five of which deal with the scientific knowledge and aspects of cellulose and the substances normally associated with it in nature and five with the occurrence, preparation, and industrial utilization of this increasingly mportant raw material. Dr. Purves has done an admirable job of presenting the modern picture of the cellulose molecule and of critically evaluating the enormous mass of chemical literature on which it is based. The only criticism that might be made, in the reviewer's opinion, is some lack of stress on the importance of the work of Hudson and his collaborators in developing the use of periodate oxidation as the final clear and convincing proof of the structure which the more laborious methods previously employed had evolved. The yet unsolved question of degree of polymerization of the building unit is excellently treated.

The important subject of the physical properties of this material, carrying almost equal weight to its chemical constitution in explanation of its treatment for industrial purposes, has been most excellently treated by a group of experts, most notably by H. M. Spurlin. Another notably important contribution is made by a different group of workers in the chapter on "Structure and Properties of Cellulose Fibers". The substances associated with cellulose have been given brief but adequate treatment. The reviewer appreciates the reasons which led to confining the selection of authors to the United States, but it does seem unfortunate to him that the book contains nothing from the pen of the greatest authority living on this continent who has contributed so much to the scientific aspects of the chemistry of cellulose and its related materials,—namely, Professor Harold Hibbert.

The occurrence and preparation of cellulose have received excellent and thorough treatment in two good chapters. Hatch gives an exhaustive treatment of bleaching and purification, which is a most important subject to workers in the technical field. To the academic ignorance of the reviewer, it seems that the comprehensive field of technical applications has been excellently, if of necessity somewhat briefly, treated by Dr. Gloor.

A very pleasing feature of the book is the liberal use of footnotes, so that the reader can trace almost any point back to the original sources. Another point of satisfaction is that the indices seem to be good. The format and technical details of the make-up are of high quality and the book seems to be on paper of better than average quality for these times of war restrictions. Here is a book which is a must for every scientific worker in the field of cellulose chemistry and technology and for every complete library whether in the commercial or the educational field.

RALPH E. MONTONNA.

Ten Lectures on Theoretical Rheology. By MARKUS REINER. 163 pp. Jerusalem: Rubin Mass. New York: Nordemann Publishing Company, Inc., 1943. Price: $4.50.

This book takes up the problem of the flow of matter from the classical continuum point of view as distinguished from the more recent atomic-molecular approach. This latter approach is dismissed as "metarheology". The book begins with the classical treatment of strain and stress. Various idealized behaviors are defined in terms of the tensor equations and are called after the men who first worked with them conspicuously. Examples are the "Euclid" and "Hooke" solids and the "Newtonian" and "Pascalian" liquids.

Chapter V deals with special problems—the simple pull of a rod, the bending of a beam, and various kinds of viscosimeters. This is followed by a chapter on creep and damping and then by one discussing the effects of structure such as arise when large particles are present in a viscous continuum.

Chapter VIII considers plastic flow and the dissipation of strain–energy. The next chapter considers the Mohr-Circle and Dimensional Analysis, while the final chapter seeks to lay the more general framework required for treating actual bodies as distinguished from the idealized behaviors called after the names of various investigators.

The book provides a sound introduction to the continuum theory of flow couched in no more mathematical language than the subject requires. A larger treatise is promised later which will probably allow space to consider flow also in its molecular and atomic aspects. The book will be a useful addition to the libraries of students of rheology.

HENRY EYRING.

Data on Chemicals for Ceramic Use. Compiled by ALEXANDER SILVERMAN, *Chairman*, GEORGE W. MOREY, AND FREDERICK D. ROSSINI, with the aid of Kuan-Han Sun, Librarian for the Committee. Bulletin National Research Council No. 107, June, 1943. Published by the National Research Council, National Academy of Sciences, Washington, D. C.

The title of this bulletin is misleading, in that the information contained in it is much more extensive than would be inferred from the title. The sub-title reads, "Formulas, molecular weights, colors, crystal forms, densities, refractive indices, melting points, boiling points, transition points, decomposition temperatures." These data are assembled for a large number of inorganic compounds, and the compilation is believed to be the most complete that has been made. It should be useful not only to ceramists but also to chemists, physicists, and geologists.

GEORGE W. MOREY.

Chemistry and Technology of Food and Food Products. M. B. JACOBS, *Editor*. 952 pp. New York: Interscience Publishers, Inc., 1944. Price: $10 50.

The scope of this volume extends beyond that suggested by the title, to the extent that it includes chapters on the general properties and classification of enzymes, hormones, and digestive processes. In addition to disclosing the quantity of various carbohydrates, lipids, and proteins in certain foods, there are chapters dealing with the detailed structure and chemical constitution of these food constituents.

Under the editorship of M. B. Jacobs, the chapters have each been written by a specialist or specialists. A chapter on the physical chemistry of foods by J. L. St. John is unique and singularly useful, since it defines the terms used to describe the common physical properties and outlines the methods and devices used in their measurement. This is followed by a chapter on the carbohydrates by E. F. Degering. A chapter on the lipids and another on amino acids and proteins were written by M. M. Baizer and Hugo Zahnd. Enzymes are discussed by Kurt G. Stern; vitamins, vitagens, and hormones by H. R. Rosenberg; and mineral matters and other inorganic food adjuncts by R. H. Carr. The chapter on coloring matters in foods, as presented by C. F. Jablonski, deals particularly with the art of coloring with coal-tar dyes and natural organic coloring matters rather than with the pigments found in natural, uncolored foods. A. E. Wilhelmi, in a chapter on the digestion and fate of foodstuffs, presents a very concise treatment of the digestive and assimilative processes. Food spoilage and food poisoning are surveyed briefly by H. O. Halvorson.

Part II of the book really deals with the chemistry of individual foods. The materials covered and the several authors include: Milk, Cream and Dairy Products by M. B. Jacobs; Meat and Meat Products by W. M. Urbain; Fish, Shellfish and Crustacea by M. E. Stansby; Poultry and Eggs by M. E. Pennington; Edible Oils and Fats by A. E. Bailey; Cereal Grains by W. F. Geddes; Baking and Bakery Products by W. H. Cathcart; Vegetables, Mushrooms, Nuts, and Fruits by F. A. Lee; Carbohydrates and Sugar Foods by E. F. Degering; Confectionery and Cacao Products by M. Schoen; Coffee and Tea by W. H. Ukers; and Flavors, Spices, and Condiments by Lee Worrell. A total of forty-nine pages is occupied by a convenient and detailed subject index.

There is a vast amount of useful information in these sections. In general, there appears to be more data and text discussion of the composition of the several foods than of the principles involved in or control of the processing treatments. The book would scarcely serve as a manual of the operations in which the food technologists might engage. The table of contents of Volume II suggests that it will be devoted quite largely to processes.

<div align="right">C. H. BAILEY.</div>

Soil and Plant Analysis. By C. S. PIPER. 368 pp. New York: Interscience Publishers, Inc., 1944. Price: $4.50.

This book comprises a description of methods for the analysis of soils at Waite Agricultural Institute (Australia). It includes detailed directions for the collection of samples and their preparation in the laboratory. The treatise is well organized and clearly and concisely written. The methods described are standard in the main and are as applicable in the United States as in Australia and New Zealand. The inclusion of procedures of calculations strengthens the book for student use. Weaknesses of methods are fully discussed.

As would be expected, there is a tendency to place emphasis on methods in use in the British Commonwealth, although many methods commonly in use in this country are included. This is a desirable feature, since it will give the American student a broad knowledge of applicable procedures This book constitutes a ready reference which soil scientists and chemists will be glad to have close at hand.

<div align="right">C. O. ROST.</div>

Contributions to Chemical Education. Number 3. More Acids and Bases. A Collection of Papers by D. DAVIDSON, W. F. LUDER (with W. S. McGUIRE and S. ZUFFANTI), L. F. AUDRIETH, AND T. MOELLER, and by R. GIWELL. 79 pp. Easton, Pennsylvania: The Journal of Chemical Education, 1943. Price: $1.00.

In the foreword, Dr N. W Rakestraw, *Editor*, states: "Since the publication of 'Acids and Bases' in 1941 (reviewed in J Phys. Chem. **46**, 1008 (1942)) several more articles on this same subject have appeared in the Journal of Chemical Education. The interest which many teachers and students of chemistry have shown in the earlier volume has led us to reprint these articles, with a few minor changes."

This addition to Volume I of the "Series" will be welcomed by many teachers, students, and other chemists interested in the subject. The appearance and print are attractive.

The seven papers reprinted in the volume all contain some original views and suggestions.

The reviewer anticipates that the emphasis on the relationship between an acid (electrophilic) and an oxidizing agent on the one hand and a base (electrodotic) and a reducing agent on the other hand (W. F. Luder, p. 39) may become the source of much confusion. For example, hydroquinone is an acid, but a reducing agent, whereas quinone is a base, but an oxidizing agent. As a base, then, quinone is electrodotic in the terminology of Luder, but as an oxidizing agent it is electrophilic.

In a recent article (J. Phys. Chem. **48**, 51 (1944)) the reviewer pointed out that the Lewis and Brönsted concepts are not contradictory and that both should be adopted (and taught). Fortunately, most of the authors of *More Acids and Bases* recognize both the Lewis and the Brönsted concepts. There is no justification in selecting one theory in preference to the other; there is a useful place for both. It would be desirable that a committee of the American Chemical Society express itself on this matter in an authoritative way.

<div align="right">I. M. KOLTHOFF.</div>

THE PHYSICAL CHEMISTRY OF MEMBRANES WITH PARTICULAR REFERENCE TO THE ELECTRICAL BEHAVIOR OF MEMBRANES OF POROUS CHARACTER. I

THE NATURE OF PHYSICOCHEMICAL MEMBRANES—MEMBRANES AS PHYSICO-CHEMICAL MACHINES; PREPARATION AND PROPERTIES OF MEMBRANES OF HIGHLY PRONOUNCED ELECTRICAL PROPERTIES[1]

KARL SOLLNER

The Department of Physiology, University of Minnesota, Minneapolis 14, Minnesota

I. MEMBRANES IN CLASSICAL PHYSICAL CHEMISTRY

Pfeffer's (20) measurement with "semipermeable" membranes of the osmotic pressure of sugar solutions has in the hands of van't Hoff become a corner stone of modern theory of dilute solutions.

The second instance in the history of physical chemistry in which membranes have played an important rôle was in connection with Donnan's work on membrane equilibria (9). Donnan and his collaborators tested this theory, using for their experimental work mostly the same kind of membranes as those used by Pfeffer, the copper ferrocyanide membrane, which originally had been developed by M. Traube (29).

van't Hoff's brilliant correlation of the osmotic pressure with the other thermodynamic properties of dilute solutions accounts for the fact that only a limited number of later investigators have made direct osmotic-pressure measurements with solutes of low molecular weight. The much more convenient methods of freezing- and boiling-point determinations have superseded the methods of osmotic-pressure measurement, except in the case of colloidal solutions.

On Pfeffer's and on Donnan's work are based the widely used osmotic methods for the determination of the molecular weight of high-molecular-weight substances and colloids. This method is today a physicochemical tool of great importance.

In all these instances the membranes were what is called conventionally "semipermeable."[2] Pfeffer's membranes were impermeable to the solute sugar

---

[1] Presented in abstract before the Division of Colloid Chemistry at the 108th Meeting of the American Chemical Society, New York City, September 14, 1944.

[2] The term "semipermeable" is used today in a sense wider than the literal meaning of the word. It can be taken to be literally correct only if applied to instances such as those originally treated by Pfeffer: namely, where only two species of particles are present, solute and solvent, and the one or the other of these molecular species (usually the solvent) penetrates the membrane freely, whereas the other molecular species cannot permeate through it. To avoid possible confusion it is advisable to qualify the term "semipermeable" by the addition: permeable to molecular species A, impermeable to molecular species B. Such a qualification would also indicate that semipermeability is not a universal property inherent in a membrane as such, but a quality which can be defined properly only with respect to a particular surrounding system. (See also the text below.)

In systems containing more than two molecular species, the term "semipermeable" loses

and permeable to water; Donnan membranes are impermeable to (at least) one ionic constituent, ordinarily referred to as the colloid ion, and permeable to the solvent and two or more kinds of ions in solution. These membranes, if considered to be perfect, can act as reversible physicochemical machines and therefore are highly useful in theoretical considerations; they are experimental realizations of the "semipermeable" walls and pistons which were so important in the early development of physical chemistry (19).

Ideal reversible membranes, however, represent only a very limited part of the membranes useful in chemical work and occurring in nature. Membranes of a somewhat imperfect character are used widely in the laboratory as dialyzing membranes, as ultrafilters, etc., and are used for similar purposes in industrial operations; likewise membranes of varying degrees of permeability and semipermeability occur universally in plant and animal organisms, constituting there one of the fundamental devices which regulate the exchange of material and thus the flux of life.

From a wider point of view "semipermeability" is only a limiting case of the possible properties of membranes, and the equilibrium state which can be observed with membranes becomes a limiting case of the dynamics of membrane systems.

It is therefore small wonder that literally thousands of papers deal with specific problems of the dynamics of membrane systems. Historically, interest has been focussed largely on the restrictive (barrier) action of membranes under various conditions, that is, on various aspects of simple membrane permeability and the underlying regularities.

II. NATURE AND DEFINITIONS OF MEMBRANES; MEMBRANES AS PHYSICOCHEMICAL MACHINES

Only rarely have investigators of membranes made an attempt to define the term "membrane". In most instances it is taken for granted that the reader possesses a sufficiently accurate concept of the meaning of this term, though the everyday usage of this word is anything but concisely circumscribed, as can readily be seen from the scientifically pointless definitions given in dictionaries. It seems to be impossible to find a universally acceptable definition for the term "membrane". A definition of this term which is useful for the mechanical engineer would be rather useless for the physiologist, and the latter's definition can be only of limited value to the physical chemist. A formal definition of the term "membrane" which would be useful from the physicochemical point of view has not yet come to the attention of the author.

---

its literal meaning. It might be advisable to substitute for it another term, such as "selectopermeable." In any case, in systems containing three or more species of molecules it is imperative to state specifically which molecular species are able to penetrate the membrane and which molecular species are prevented from doing so. A membrane ideal for the dialysis or the molecular-weight determination of a particular protein in solution, for instance, can be defined as a "selectopermeable" membrane which is impermeable to the protein under consideration and permeable to the solvent as well as to all other molecular species present in the system.

One characteristic feature of membranes, if considered from the physicochemical viewpoint, or as we may say of "physicochemical membranes", is the fact that they can be defined properly only in correlation to their surroundings. For example, a sheet of platinum separating oxygen and nitrogen does not show any characteristic membrane features; it is merely an inert separating wall. However, if the same sheet of platinum separates hydrogen from nitrogen, it assumes a typical membrane function. It completely prohibits diffusion of nitrogen across itself, whereas it is freely permeable to hydrogen (particularly if heated) (21). The same material, according to its surroundings, may or may not assume membrane functions (compare also footnote 2). A meaningful definition of physicochemical membranes therefore must necessarily stress the functional aspects of membranes.

Though membranes are usually thin flat sheets, the "main extension in two dimensions" which is frequently emphasized is not a necessary and essential characteristic of membranes. It has nothing to do with the quality of the processes which occur across membranes; it only enhances the quantitative efficiency by increasing the area which is available for the processes under consideration.

One may attempt to define a physicochemical membrane in the following manner: "A physicochemical membrane is a structure or phase, separating two other phases or compartments, which obstructs or prevents completely gross mass movement between the latter, but permits passage with various degrees of restriction of one or several species of particles from the one to the other or between the two adjacent phases or compartments, the passage of material across the membrane in some cases being due exclusively to molecular movement (diffusion) and in other cases to other forces, such as mechanical pressure, electric potential differences, etc."

In view of the different but very common biological usage of the term "membrane", it is worth while to keep in mind that the above definition includes tacitly the following addition: "A physicochemical membrane will not by expenditure of energy of its own bring about any transport of substances between the two phases or compartments separated by it." (Compare Krogh (14).)

The foregoing definition of the term "membrane", however, does not take into account explicitly some of the most important aspects of the functional characteristics and the behavior of membranes which give them their main scientific importance and interest.

Membranes, while regulating the movement of particles and the flow of energy, i.e., while being passively involved in various energetic processes occurring across their thickness, cause a great variety of effects such as movement of solute, the closely related development of (not necessarily static) hydrostatic pressures, and the partial or complete separation of solutes from the solvent. With electrolytes, in addition, numerous electrical effects may be observed, such as static or dynamic (23) membrane potentials, anomalous osmosis, movement of third ions against concentration gradients, electroösmosis, etc. In all these cases the membranes act as physicochemical machines, transforming by various mechanisms the free energy of the adjacent phases (or energy applied through them)

into other forms of energy (mechanical, concentration, electrical, etc.), sometimes in a reversible but ordinarily in an irreversible manner. Physicochemical membranes are in this respect strictly analogous to mechanical machines: they regulate energetic processes, essentially without thereby being changed, exhausted, or consumed.

Accordingly we may attempt now to define membranes in the following manner: "*A membrane is a phase or structure interposed between two phases or compartments which obstructs or completely prevents gross mass movement between the latter, but permits passage, with various degrees of restriction, of one or several species of particles from the one to the other or between the two adjacent phases or compartments, and which thereby acting as a physicochemical machine transforms with various degrees of efficiency according to its own nature and the nature and composition of the two adjacent phases or compartments the free energy of the adjacent phases or compartments, or energy applied from the outside to the latter, into other forms of energy.*"

As long as we consider only ideal "semipermeable" membranes and only reversible processes across them, as was done by the classical physical chemists, the special mechanisms by which the membranes act is of no importance whatsoever from the point of view of thermodynamic theory.[2]   As soon, however, as we consider the dynamics either of ideal semipermeable or of (non-ideal) membranes of various degrees of restricted permeability, the questions of mechanisms and membrane structure become of paramount importance.

One can hope to understand the dynamics of a membrane system only if the mechanism of the restricting action of the membrane under the given situation is known.   The machine function of membranes can be revealed fully only by model studies.   On account of their great importance one will have to pay particular attention to the simple and complex electrical machine actions of membranes. The construction of proper models constitutes, so to speak, a problem of membrane engineering which can be solved only by the use of membranes of carefully predetermined properties.

III. MEMBRANE MECHANISMS; COLLODION MEMBRANES AS EXAMPLES OF MEMBRANES OF POROUS CHARACTER

Conventionally one recognizes two main classes of membranes,—homogeneous phase ("oil") membranes and membranes of porous character.

Homogeneous phase membranes exert their typical membrane functions by means of selective differential solubility; particles, molecules, or ions which are soluble in an oil phase can penetrate and pass across.

Membranes of porous character act as sieves.   This is quite obvious with

---

[2] The attitude of many of the older classical physical chemists towards the problem of osmotic mechanisms can be characterized by van't Hoff's statement (Z. physik. Chem. **9,** 485 (1892): "Again we have the basically meaningless question: what exerts the osmotic pressure?   Indeed, as emphasized before, I care in the long run only about its magnitude. As it has been shown to be equal to gas pressure one is inclined to think of a similar mechanism of its origin as with gases.   Who, however, is led astray by this should rather cut out any thought of a mechanism."   Compare, however, the different attitude of Nernst (reference 19, page 138).

porous diaphragms and other microscopically porous structures, and has hardly ever been doubted for such membranes as parchment or collodion membranes of great water content. The *molecular sieve* character of the copper ferrocyanide membrane, already postulated by M. Traube (29), was verified by Collander (7), who also demonstrated the molecular sieve action of the "dried" collodion membrane (8), at least with solutions of non-electrolytes and weak electrolytes. The ion permeability of the latter membranes, according to Michaelis (17), must likewise be explained by sieve action.

Objections, however, have been raised against the concept of the "molecular sieve", the controversy centering around the "dried" collodion membrane. Some investigators prefer the view that the dried collodion membrane behaves more like a continuous phase, exerting its membrane function by means of a solubility mechanism (see, e.g., reference 3); some authors (30) attempt to reconcile the two antagonistic views. Some new experiments and considerations which prove that the electrolyte permeability of dried collodion membranes must be explained on the basis of a microheterogeneous structure of these membranes will be described in a subsequent paper.

Several years ago the author and his collaborators started work on membranes with the idea in mind of building physicochemical model systems involving membranes which would be helpful to the biologist in clarifying the structure and functions, in particular the electrical behavior, of microscopic and macroscopic membranes as they occur in living systems.

From the outset it was necessary to make a decision as to which class of membranes, those of "oil" or those of porous character, should be made the starting point of this work. We decided to start with membranes of the latter type. Membranes of porous character are at present much more suitable and convenient for experimental work, and also can be prepared with a great variety of characteristics. In addition, some effects of great interest to the biologist, such as (electrical) anomalous osmosis, electroösmosis, and (ultra) filtration cannot be obtained with membranes of the homogeneous-phase type.[4]

Collodion has for a long time been recognized to be a particularly desirable material for the preparation of membranes of porous character on account of its ready availability and the ease with which sturdy membranes of various degrees of porosity can be prepared. Collodion membranes, furthermore, can give rise to very pronounced electrical effects, such as membrane potentials and anomalous osmosis, and therefore seemed to be particularly desirable. They have the ad-

---

[4] The choice of membranes of porous character as the object of our work does not imply any decision as to whether membranes of homogeneous phase or of porous character are of greater importance in living systems. The question is probably not one which can be decided with a simple either-or. The available evidence indicates that in single cells as well as in macroscopic structures both types of membranes frequently are contained in some sort of complex mosaic. With individual cells, in most instances, the exchange of non-electrolytes is governed primarily by the solubility in the protoplasmic cell membrane, whereas electrolytes seem frequently to enter through some porous structure or its functional equivalent. The typical function of macroscopic biological membranes, such as the intestinal wall, the capillary blood vessels, and the filtering structures of the kidneys seems to be due primarily to a microheterogeneous porous structure.

ditional advantage that their use will allow linking further work closely to many of the best investigations on membranes, the majority of such investigations having made use of collodion membranes.

Collodion membranes, moreover, can be readily impregnated with foreign substances, such as proteins, dyestuffs, and alkaloids, which profoundly change the electrical characteristics of these membranes, transforming them from electronegative (preferentially cation-permeable) membranes into electropositive (preferentially anion-permeable) membranes.

For these reasons collodion membranes were chosen as the material of our studies; on account of their desirable properties we have been able to use them throughout all our work.

We do not suppose that collodion membranes are in themselves of particular scientific significance. Their real, wider scientific importance is based entirely on the fact that they can be used as convenient objects for the elucidation of the physicochemical nature and of the functional behavior of membranes of porous character in general.

IV. SOME METHODS OF CHARACTERIZATION OF THE ELECTROCHEMICAL BEHAVIOR OF MEMBRANES OF VARIOUS DEGREES OF POROSITY

The natural starting point of an extensive experimental investigation was the attempt to repeat outstanding work of earlier investigators, such as the classical experiments of Michaelis and collaborators (17), on membrane potentials ("concentration potentials") and the ionic selectivity of dried collodion membranes, and the studies on anomalous osmosis of Bartell (2), Loeb (15), and other investigators (10, 22).

Michaelis and collaborators (17) prepared flat and bag-shaped "dried" collodion membranes by allowing a layer of ether–alcoholic collodion solution to dry completely on a mercury surface or on the inside of a test tube. If such membranes are interposed between two solutions of different concentration of the same electrolyte, electromotive forces arise which are much higher than those observed on free diffusion. In certain cases these membrane potentials approach the value which theoretically could be obtained with reversible specific electrodes, the more dilute solution always being positive. The electromotive action of these membranes is due to the fact that they are nearly impermeable to anions but permeable to cations, the relative permeability of weakly adsorbable cations depending on their valency and ionic radius. Michaelis has characterized these membranes particularly by the measurement of the "characteristic concentration potential," the electromotive force which arises when $0.1\,M$ and $0.01\,M$ potassium chloride solutions are separated by a membrane. The values of the characteristic concentration potential with the best of his membranes vary between $+48$ and $+53$ mv., with occasional values slightly higher, the maximum thermodynamically possible values being $+55.1$ mv.

The term "anomalous osmosis" designates all those liquid movements across a membrane separating two solutions of different concentration which according to their rate or the pressures obtained would not be predicted on the basis of the van't Hoff osmotic theory. With (non-swelling) membranes of porous character

such anomalies are found only if an electrolyte diffuses through a membrane which allows its passage with fair ease. Anomalous effects are never found with strictly semipermeable membranes. The phenomenon of anomalous osmosis is entirely of a dynamic nature. After a sufficiently long time the electrolyte concentration on both sides of the membranes is the same, and hydrostatic heads which had developed intermediately have disappeared. The technique of Loeb (15) in his well-known experiments on anomalous osmosis, which we have followed with minor modifications, is as follows (25): Collodion bags are cast in 30 x 110 mm. test tubes and allowed to dry several minutes, the suitable drying time varying with different brands of collodion, even if the same solvent is used. Next the test tubes to which the membranes adhere are filled with water. The membranes loosen from the glass spontaneously and are tied to glass rings with thread while still filled with water. Following this, they are washed thoroughly with distilled water and are kept immersed in water continuously. For the osmotic experiments the membranes are fitted to rubber stoppers carrying long capillary glass tubes with an inner diameter of about 1.5 mm. Membranes are selected which when filled with 0.25 M sucrose solution and placed in 500 to 800 cc. of water for 20 min. yield without artificial stirring an osmotic rise of about 120 to 140 mm. of liquid in the capillary manometer. For the anomalous osmosis experiments the membrane bags are filled with solutions of varying concentrations of sucrose and various electrolytes,—potassium chloride, potassium sulfate, and potassium citrate being used as standard electrolytes. The rise of the meniscus in the manometer is read 20 min. after the bag is placed in water.

If the values read after 20 min. are plotted in a pressure–concentration diagram, sucrose and other non-electrolytes give flat, smooth curves lying very near to each other. With the electrolytes the curves have a characteristic N shape (see below, figure 1a). A pressure rise which deviates significantly from the results obtained with the non-electrolytes is considered to be due to "anomalous osmosis". In certain instances liquid may move from the side of the solution to the side of the solvent. This effect is called "anomalous negative osmosis" or "negative osmosis". Anomalous osmosis, according to the experiments of Loeb, Bartell, and others, is an electroösmotic phenomenon. The dynamic membrane potential which arises across the membrane in some peculiar way moves the charged liquid filling certain of the pores electroösmotically across the membranes. The physical theory of this phenomenon was developed several years ago by the author (24; see also 13), who based his consideration on the heteroporosity of the membranes. Loeb had found that the extent of anomalous osmosis is approximately proportional to the product of the electrokinetic (ζ) potential of the membrane times the membrane (ϵ) potential. According to the theory (13, 24, 28) this correlation is not quite so simple; nevertheless, anomalous osmosis under standardized conditions is an excellent method for the characterization of the electric behavior of collodion membranes of high porosity (28).

V. THE EXPERIMENTAL PROBLEM

When we originally tried to reproduce the electromotive and anomalous osmotic effects described by Michaelis and Loeb, the results were disappointing

(25). The ionic selectivity of the dried collodion membranes was poor, not at all comparable to that reported by Michaelis, the characteristic concentration potentials in many instances being only a small fraction of the thermodynamically possible value. Likewise, the anomalous osmotic effects described by Loeb could not be reproduced in an adequate manner (compare below, figures 1a and 1b).

This state of affairs indicated that some fundamental link in our understanding of the electrochemical nature of collodion membranes was missing, no difficulty having been found with respect to the reproduction of the behavior of such membranes towards solutions of non-electrolytes (25). We therefore were forced into an extensive physicochemical study of the nature and preparation of collodion membranes, with particular emphasis on their electrical properties and behavior.

One can classify membranes of porous character into four groups. On the one hand one has to distinguish electronegative membranes and electropositive membranes; on the other hand one must classify them according to the degree of porosity into membranes of high porosity, "porous" membranes, and molecular (ion) sieve membranes. The former are readily permeable, at least to solutes of low and medium molecular weight; in many instances they are permeable also to colloids. Molecular (ion) sieve membranes restrict partially or completely the permeation of low-molecular-weight solutes according to the molecular weight of the latter.

Negative "porous" (collodion) membranes with obviously satisfactory properties have been described many times, although we had been unable to reproduce them. "Dried" electronegative membranes with a fair or high degree of ionic selectivity have, as was said before, been described by Michaelis (12) and other investigators. For extensive work these latter membranes, however, show several shortcomings, foremost among them the fact that their degree of ionic selectivity from our point of view is only moderately satisfactory and moreover decreases quite appreciably on use, and that their absolute permeability is extremely small. On account of the great density of these membranes all the processes which occur across them are very slow, so slow indeed that days, in some instances weeks, must elapse before a quantity of material has crossed the membranes which can be measured by microanalytical methods.

Electropositive membranes of great porosity have been described repeatedly in the literature. The most satisfactory are the proteinized collodion membranes. The pore walls of highly porous collodion membranes are covered with suitable proteins by adsorption from solution. In the proper pH range—at the acid side of the isoelectric point of the protein used—such membranes are electropositive. The shortcomings of these membranes are the pH sensitivity of their characteristics and the fact that they can be used only in limited pH ranges, so far only at the acid side of the neutral point. Membranes showing a pronounced electropositive character over wide pH ranges at the acid as well as the alkali side of the neutral point have not been described in the literature.

Electropositive membranes of low porosity and high ionic selectivity analogous to the dried collodion membranes have been described repeatedly: for example, dried collodion membranes impregnated with dyestuffs and alkaloids. These

membranes have numerous shortcomings: Their ionic selectivity in most cases is not satisfactory even when they are freshly prepared and undergoes degradation fairly rapidly when the membranes are used.   In addition, the absolute permeability of these membranes is extremely low, similar to that of the abovementioned dried collodion membranes.

We have therefore proceeded with the development of methods for the preparation of electronegative (6, 12, 25, 27) and electropositive (1, 4, 12) membranes of porous character, for those of the "dried" type as well as for "porous" ones.   Our obvious goal was to produce membranes of somewhat extreme electrical characteristics, such as membranes which combine extreme ionic selectivity with great absolute permeability, as far as dried-type membranes are concerned, and membranes which show a very high degree of anomalous osmotic behavior in the case of the "porous" type.   The methods of preparation and characterization of such membranes can undoubtedly be applied with certain modifications to other membranes than those investigated so far.

VI. THE ORIGIN OF THE ELECTROCHEMICAL CHARACTER OF COLLODION

Collodion membranes of different porosity, prepared from various commercially available collodion solutions, all behaved alike and in normal fashion towards non-electrolyte solutions, but large differences, characteristic of the different preparations, appeared when the membranes were tested for their electrical behavior either with the anomalous osmosis or the concentration potential method (25, 26).   Considerable differences in the electrochemical behavior of various collodion preparations had already been found by Michaelis and Perlzweig (18) and by Wilbrandt (30).   The most characteristic electrical effects were obtained with certain brands of imported (Kahlbaum) preparations.

It has been assumed generally, though not universally, that the electrokinetic charge of collodion is due to ion adsorption (11, 16).   This, however, hardly seemed compatible with the fact that membranes prepared from different collodion preparations, though they behave exactly alike if tested with non-electrolytes, show profound differences in contact with electrolyte solutions (25, 26).

These differences, on the basis of the ion adsorption hypothesis, can be explained only by the assumption that indifferent, non-specific ions are adsorbed by the various collodion preparations to very different degrees.   Such an assumption, however, is not in harmony with the general experience on adsorption phenomena.[5]

The clarification of this controversial point could be achieved by comparison of several collodion preparations of different degrees of electrochemical "activity".   We were fortunate in securing at the time of the outbreak of the war a sufficient supply of the various electrochemically active German preparations, which had been used preferentially by previous investigators, to carry out such a

---

[5] Michaelis (L. Michaelis: Kolloid-Z. **62,** 2 (1933)) indicated that the purest collodion preparation seemed to show the most pronounced electrical properties, but left any decision on this question to the experts in nitrocellulose chemistry.   Wilbrandt (30) tried to explain the differences between different brands of collodion preparations by the assumption of differences in the number and distribution of polar groups (O—NO$_2$ groups).   His views were critically considered and cannot be accepted (26).

comparison.   It would mean too much of a deviation into the field of nitrocellu-
lose chemistry to give all the details.   Empirically we found with the various
preparations a very pronounced parallelism between ash content and activity,
sulfate content and activity, fluidity in solution and activity, and opacity in solu-
tion and activity.   The electrochemically active brands showed high ash and
high sulfate content and their solutions were of low viscosity and somewhat
turbid.   The electrochemical activity of collodion preparations therefore seemed
to go parallel with the impurities present and the degree of degradation of the
nitrocellulose molecules in solution (25, 26).

On the basis of further work it could be concluded that the electrochemical
activity of collodion membranes depends entirely upon the presence of impurities
of an acidic (anionic) nature contained in the collodion used for their preparation.

The active acidic impurities are largely due to partial oxidation which occurs
in the manufacturing process, and partially due to acidic groups which are present
in the native cellulose fiber (26).   It is easy to see that this view of the origin of
the electrochemical properties of collodion is compatible with the observation
that various collodion preparations may behave strictly similarly towards solu-
tions of non-electrolytes but very differently when tested with solutions of elec-
trolytes.

The impurities present in the collodion are high-molecular-weight organic
compounds of anionic, acidic character, such as "nitrocellulosic acids", i.e.,
nitrocellulose molecules carrying one or several carboxyl groups.   These
impurities must be assumed to act in the following manner: They constitute an
esential part of the membrane skeleton; some of them are located with
their acidic dissociable groups in the pore walls of the membrane.   Thus fixed,
dissociated or potentially dissociable units arise on the pore walls of the
membrane.   They are built permanently into the collodion structure, the cor-
responding counter-ions being actually or potentially dissociated off into the ad-
jacent solution which fills the pore.   The frequency of the occurrence of the
dissociable groups on the pore walls,—in other words, the charge density on the
structural elements of the membrane which are accessible to the solution,—deter-
mines the degree of electrochemical activity of a membrane.

Upon contact of the membrane with an electrolyte solution the counter-ions
of the fixed anionic groups exchange with the cations of the former.   This is
obviously the mechanism which determines the actual electrochemical activity
of a membrane in contact with various electrolyte solutions.   If the counter-ions
in solution are the cations of a strong inorganic base, complete or nearly complete
dissociation of the surface compounds can be assumed.   From this we can con-
clude that the base-exchange capacity of the pore surfaces of a membrane deter-
mines its electrochemical activity.[6]   It will be necessary to discuss this point
in greater detail later.

[6] This concept, of course, does not apply without restriction to all situations.   For
example, if any one of the ions present in solution is strongly adsorbable, it must strongly
influence the ionic structure of the interfacial layer.   In such cases we undoubtedly ap-
proach the situation formerly assumed also for strong electrolytes.

It is conceivable that with a membrane material which is completely or nearly completely

The above concept of the electrochemical nature of collodion membranes links them closely to the "proteinized" membranes of Loeb and others. In both cases the electrochemical character of the membrane is determined predominantly by the presence of high-molecular-weight dissociable compounds located in the microsurfaces of the membrane structure, not by non-specific ion adsorption. With the collodion membranes the electrochemically active compounds happen to be contained in the collodion itself; with the proteinized membranes the electrochemically active molecules cover the structural elements of the membrane in the adsorbed state—the end result from the electrochemical point of view is hardly distinguishable.

VII. THE ACTIVATION OF BULK COLLODION AND COLLODION MEMBRANES; MEGAPERMSELECTIVE COLLODION MEMBRANES

In the case of the electronegative membranes the immediate experimental problem was to increase by some method the surface concentration of fixed dissociable acidic groups present on the pore walls of collodion membranes, since the various collodion preparations which are commercially available at present in this country are too pure to yield membranes of pronounced electrochemical activity.[7]

Collodion can be activated by oxidation, for oxidation increases the number of dissociable anionic groups (carboxyl groups) in it (25,27). The oxidation method of activating collodion may be applied to fibrous collodion in bulk as well as to membranes. Oxidizing agents which were found to be satisfactory are sodium and calcium hypochlorites and sodium hypobromite in various concentrations and at various pH values. The most effective oxidizing agents, however, are solutions of sodium or potassium hydroxide. The alkalies cause a complicated decomposition of nitrocellulose with the formation of nitrites and probably other nitrous compounds. The nitrous compounds act upon the collodion, causing thorough oxidation. Detailed oxidation procedures have been worked out for bulk collodion and for highly porous and for dried membranes, the optimum conditions being different in the three cases.

---

void of any dissociable groups, even in solutions of strong electrolytes, preferential ion adsorption comes into play to a decisive extent. However, no case of this nature has so far been described for collodion membranes. Acetylcellulose membranes were found by Meyer and Sievers (K. H. Meyer and J.-F. Sievers: Helv. Chim. Acta **19**, 665 (1936)) to behave as electronegative membranes with dilute solutions of potassium chloride and lithium chloride, but as positive membranes in more concentrated solutions of these electrolytes (see also Wilbrandt (W. Wilbrandt: J. Gen. Physiol. **18**, 933 (1936)). This could be explained by the assumption of so low a surface concentration of acidic groups on the acetylcellulose particles that it is able to maintain the electronegative character of the membrane only if opposite influences are more or less absent. At higher electrolyte concentrations adsorption or the formation of an cationic surface compound—perhaps an oxonium salt—overcomes the influence of the acidic groups built into the acetylcellulose surfaces. Experiments with various electrolytes should be helpful in the clarification of this problem.

[7] Crude collodion, a product which is only partially purified and is known to contain a sizable number of acidic groups, shows considerable electrochemical activity, similar to that found with certain inferior grades of German collodion.

Collodion oxidized in bulk after thorough washing, drying, and dissolution in ether–alcohol yields very active membranes. Porous membranes prepared from properly oxidized collodion show a degree of electrochemical activity which substantially surpasses anything described for the most active collodion preparations in the past. Dried collodion membranes prepared from activated bulk collodion yield characteristic concentration potentials which are significantly higher than any previously reported, approaching the thermodynamically possible maximum closely. Whereas the purer commercial preparations show characteristic concentration potentials which vary between 10 and 40 mv., dried membranes prepared from activated collodion consistently show values of 52 to 54 mv., 55.1 mv. being the thermodynamically possible maximum value. Collodion activated in bulk by oxidation is therefore a superior substitute for the electrochemically active preparations which were formerly available.[8]

The oxidation of collodion membranes as such yields still more satisfactory results. Porous membranes after oxidation show an enormous magnification of the extent of anomalous osmosis, a great increase of the concentration potential across them, and likewise a considerable enhancement of electroösmosis through them. The behavior of the porous membranes towards non-electrolytes changes but little on oxidation. The volume of such membranes remains constant within the limits of experimental error, as does also their per cent water content; the rate of filtration is not much changed. From this it is concluded that the geometrical structure of membranes is but little changed on oxidation.

The enormous change in the electrochemical behavior of porous collodion membranes when subjected to oxidation can be seen in figures 1b and 1c, which show the extent of anomalous osmosis at various concentration levels for the same membrane specimen before and after oxidation. Figures 1b and 1c also show that the behavior of the membranes with non-electrolyte (sucrose) solutions is but little changed on oxidation.

Table 1 shows the rate of electroösmosis through a porous collodion membrane before and after oxidation.

In agreement with expectation, membranes prepared from different collodion preparations which behave rather uniformly towards non-electrolytes but very

[8] The collodion used for most of our work was "Collodion Cotton, Pyroxylin (Moistened with Denatured Alcohol)," as obtainable from the J. T. Baker Chemical Co. of Phillipsburg, New Jersey. All the samples used over a period of several years, with the exception of one, behaved very much alike and contained about the same quantities of impurities; they were all prepared from cotton. Of late a considerable part of the commercially available collodion is prepared from wood pulp. Information concerning the current manufacturing process is difficult to obtain. We wish to thank Mr. G. B. Hafer of the J. T. Baker Co., who has kindly given the following data concerning the collodion cotton obtainable from this company: "The conditions of nitration and extent of purification have changed only insofar as it is necessary to adapt conditions to the type of cellulose being used. The greater part of the nitrocellulose has been of 15–20 seconds. The ethyl alcohol used for dehydration has always been formula 2B, which contains no admixture other than approximately ¼% Benzol. The nitrogen content of the nitrocellulose is held reasonably close to 12%. The approximate molecular weight of this type of nitrocellulose is 118,500. This corresponds to a degree of polymerization of 450."

differently towards electrolyte solutions become similar in their behavior towards the latter after they are oxidized.

Table 2 can be taken as an additional proof for the earlier statement that the geometrical structure of membranes prepared from different collodion preparations seems to be essentially similar. The differences in their behavior towards
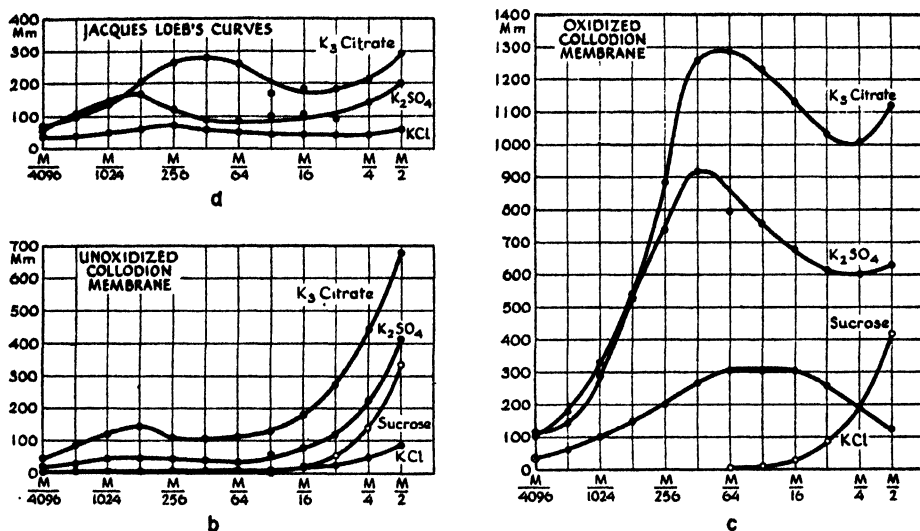
FIG. 1. A comparison of the extent of anomalous osmosis through various collodion membranes of about equal porosity.

TABLE 1

The influence of oxidation on electroösmosis through a porous collodion membrane

(Membrane area, about 100 cm.²; current, 10 milliamperes)

CONCENTRATION OF KCl SOLUTION	ELECTROÖSMOTIC FLOW PER HOUR	
	Before oxidation	After oxidation
moles per liter	*c.mm.*	*c.mm.*
0.001	2420	3750
0.005	730	2300
0.01	360	1210
0.05	0	490
0.1	0	360

electrolyte solutions are due to the electrical factor: namely, the frequency of the occurrence of dissociable groups in their pores at the collodion–water interface.

Dried collodion membranes may likewise be oxidized successfully. They give concentration potentials which approach the thermodynamically possible maximum still more closely than those prepared from "activated" collodion preparations; characteristic concentration potentials of 53 to 54 mv. can be obtained regularly. These oxidized dried membranes, however, in spite of their excellent

ionic selectivity, are not fully satisfactory from our point of view. Their resistance is too high to make them useful for extensive model studies.

Therefore we have developed a method of preparing dried-type membranes showing a combination of highest ionic selectivity with low resistance (6, 12). For the preparation of such membranes, porous membranes are oxidized with sodium hydroxide and dried over a mandrel.

Test tubes having a small hole which is sealed with sugar are rotated horizontally in a well-centered position. A 4 per cent solution of collodion cotton in absolute ether–alcohol (50:50) is poured slowly over the tubes while they are rotated. At the proper speed of rotation it is not difficult to cover the tubes evenly with collodion without the appearance of any ridges or thin spots.

TABLE 2

The influence of oxidation on the activity of porous collodion membranes prepared from various brands of collodion: anomalous osmosis

	a		b	
	BEFORE OXIDATION		AFTER OXIDATION	
BRAND OF COLLODION	Osmotic rise with 0.25 M sucrose	Anomalous osmosis with $M/512$ K_2SO_4[*]	Osmotic rise with 0.25 M sucrose	Anomalous osmosis with $M/512$ K_2SO_4[*]
	mm.	*mm.*	*mm.*	*mm.*
Mallinckrodt "Parlodion"............	124	43	142	332
Merck Collodion U.S.P...	128	54	140	290
Baker Collodion U.S.P.........	128	48	120	338
Schering-Kahlbaum Collodium "pro analysi"........................	125	32	140	320
Schering-Kahlbaum Collodium "zur Herstellung von Membranen"......	115	83	145	173
Schering-Kahlbaum "Celloidin" "for general use"......................	126	228	158	340
Schering-Kahlbaum Collodium DAB 6.......	124	195	Decomposes on oxidation	

* This concentration was chosen because it gives maximum effects with membranes of medium activity.

The tubes are next rotated for 3 min., another layer of collodion is added, and 3 min. later a third and final layer is put on. The tubes are now rotated for another 8 min. and then immersed in distilled water which is changed repeatedly. After 30 min. the membranes are ready for oxidation. The optimum duration of the various drying periods depends on the nature of the collodion solution and the room temperature. It is advisable to cast the membranes at a temperature below 22°C. (in a thermoconstant room if available), otherwise gas bubbles may readily appear in the membranes.

The porous membranes thus prepared are oxidized by placing the membranes still on the tubes in 1 M sodium hydroxide at controlled temperature for a measured length of time. The proper oxidizing time is found empirically; it varies

with the properties of the membranes desired. Increasing oxidation increases the absolute permeability of the membranes, but decreases their mechanical strength. After thorough washing with water, the membranes (still on the tubes) are dried in air of controlled humidity for several hours. While drying, the membranes undergo what amounts to a stretching in two dimensions, the whole volume loss being compensated for by a decrease in thickness. To remove these dried membranes from the tubes they are soaked in water for a few hours. The soaking swells the membranes slightly (5), makes them less brittle, and also provides a lubricant for their movement over the glass; the sugar is dissolved by the water, thus facilitating the removal of the membranes from the glass tubes. For easy handling the glass-clear, perfectly smooth membranes are tied with linen thread to glass rings which just fit inside the open end of the membrane. For further use they are kept in water to which thymol is added as a preservative. The thickness of the membranes is about 30 μ. The characteristic concentration

TABLE 3

Characteristic concentration potential and resistance of "megapermselective" collodion membranes

MEMBRANE	CHARACTERISTIC CONCENTRATION POTENTIAL 0.1 M KCl/0 01 M KCl ($\pm$ 0.1 mv.)	RESISTANCE IN 0.1 M KCl
	mv.	*Ω per cm.²*
a (3)............	54.5	550
b (4)............	54.5	525
c (1)............	54.6	125
d (1)...... ...	54.2	150
e (5).....	54.8	300
f (1)............	55.1	50
g (1)..	55.0	25
h (1).........	54.9	25

potential across these membranes is rarely below 54 mv. and in many instances approaches the thermodynamically possible maximum value of 55.1 mv., within the limits of experimental error. To obtain a quantitative measure of the absolute permeability of such membranes we have determined their resistance in 0.1 M potassium chloride solution. Data on the characteristic concentration potential and the resistance in 0.1 M potassium chloride solution per square centimeter are given in table 3. On account of the great absolute permeability and high ionic selectivity of these membranes they have been designated as "megapermselective" (or "permselective") collodion membranes.

Table 4 gives a comparison of the electromotive behavior and the resistance of several kinds of conventional-type dried and of megapermselective collodion membranes.

The megapermselective collodion membranes can at present be prepared with practically any desired resistance above 25 ohms per square centimeter in 0.1 M potassium chloride solution. Corresponding to the low resistance of these mem-

branes the exchange of cations across them is several orders of magnitude greater than that of previously described membranes.

VIII. ELECTROPOSITIVE MEMBRANES; POROUS AND MEGAPERMSELECTIVE PROTAMINE MEMBRANES

There is no simple and easy way to introduce basic (cationic) groups into collodion by means of a chemical reaction. Also, the incorporation of cationic material such as basic dyestuffs or alkaloids in the collodion solution from which membranes are prepared yields only unsatisfactory results. One therefore must

TABLE 4

A comparison of electromotive behavior and resistance of several kinds of conventional "dried" and of "megapermselective" collodion membranes

DESCRIPTION OF MEMBRANE	CHARACTERISTIC CONCENTRATION POTENTIAL 0.1 M KCl/0.01 M KCl	RESISTANCE IN 0.1 M KCl	REMARKS
	mv.	Ω *per cm.*^{2}	
Mallinckrodt "Parlodion," commercial preparation......	25–40	>500.000	
Baker collodion U.S.P., commercial preparation..........................	40–45	>500.000	
Schering-Kahlbaum "Celloidin"........	40–53	~75.000	
Crude Collodion..	45–50	~100.000	Resistance *can not* be adjusted at will
Oxidized collodion, Baker Collodion U.S.P., oxidized with sodium hypobromite.........	50–55	>500.000	
Oxidized collodion, Baker Collodion U.S.P., oxidized with sodium hydroxide.	50–55	>500.000	
"Oxidized" membranes, dried membranes oxidized with sodium hypobromite..........	51–53	~50.000	
"Megapermselective" membranes........	54–55	<25->5.000	Resistance *can* be adjusted at will

rely on the absorption method, using high-molecular-weight material of pronouncedly cationic (i.e., basic) character.

Electropositive membranes showing very satisfactory properties can be prepared by adsorption from solution of protamines on collodion membranes. Protamines are basic proteins with isoelectric points about pH 12 and of molecular weight around 3000.[9]

Porous protamine collodion membranes of great activity are prepared by immersing highly porous collodion membranes in solutions of protamine chloride or sulfate buffered with a borate buffer at a pH of about 10.5 (25). After several days' contact with the protamine solution, the membranes are washed and ready

[9] We are indebted to Eli Lilly and Company, Indianapolis, Indiana, for furnishing samples of protamine.

for further use.   The extent of positive anomalous osmosis obtained with such membranes is shown in figure 2.   Corresponding to the electropositive character of these membranes the differences in the behavior of various electrolytes depend on the valency of the cation (whereas the valency of anion was the determining factor with the electronegative collodion membranes).   Negative osmosis is very pronounced with these membranes, as can be seen from figure 3.
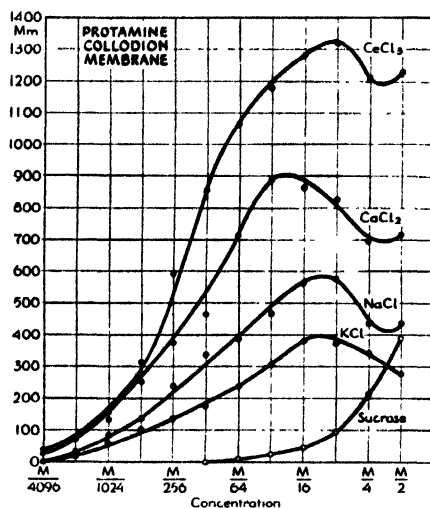
FIG. 2. The extent of anomalous osmosis through an (electropositive) protamine collodion membrane.
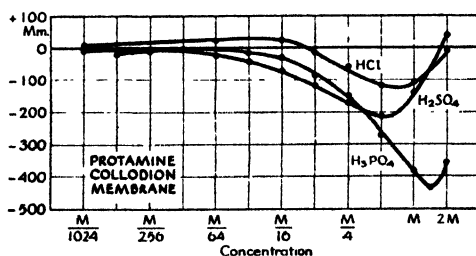
FIG. 3. The extent of negative osmosis through an (electropositive) protamine collodion membrane.

The pH range over which such membranes behave as strongly electropositive can be seen from figure 4, which for comparison gives also the behavior of an oxyhemoglobin membrane of Loeb.

Dried-type protamine collodion membranes can be obtained by drying porous protamine collodion membranes in air.   These membranes in all their properties —except their wrinkled shape—can be considered to be the electropositive analogue of conventional dried collodion membranes (1).   Their resistance is fairly high.

The preparation of really satisfactory, "megapermselective" protamine collodion membranes is carried out similarly to the preparation of the megapermselective collodion membranes (4). Three-layer collodion membranes of high porosity are cast as described before; after thorough washing they are immersed for several days, while still on the tubes, in protamine solution buffered at pH 10.5. Thereafter the membranes are washed and dried in air under controlled conditions, again still on the tubes. After this treatment they are removed from the tubes following lengthy immersion in water. In this state most of the mem-
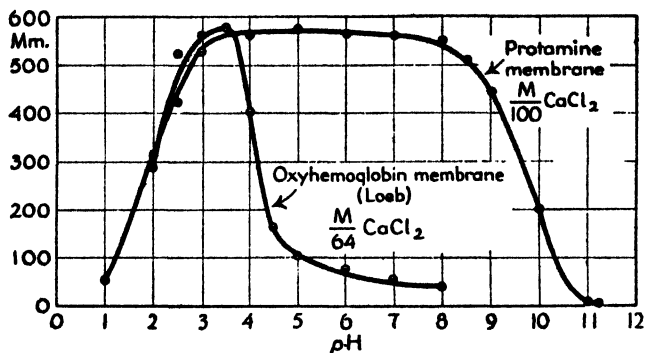
FIG. 4. A comparison of the pH ranges over which oxyhemoglobin and protamine membranes behave as electropositive membranes.

TABLE 5

Characteristic concentration potential and resistance of "megapermselective" protamine membranes

MEMBRANE	CHARACTERISTIC CONCENTRATION POTENTIAL 0.1 M KCl/0.01 M KCl	RESISTANCE IN 0.1 M KCl
	mv.	*Ω per cm.^{2}*
A............	−52.5	700
B............	−53.0	600
C............	−52.8	500
D............	−53.0	250
E............	−53.0	100
F............	−52.9	40
G............	−52.6	30

branes do not show satisfactory ionic selectivity. In order to acquire such selectivity they must in addition be dried in air without support for several hours, if possible at controlled humidity. The drying shrinks the membranes a little, giving them a perceptible waviness without causing them to lose their general shape and appearance.

The electromotive properties and the resistance of some megapermselective protamine collodion membranes are summarized in table 5. These membranes are mechanically strong and keep their electrochemical properties for at least a year when stored either dry or wet.

The thermodynamically possible maximum value has never been reached with the megapermselective protein membranes. This can be either due to the presence of a few anionic (i.e., acidic) groups carried inherently or as impurity by the protamine, or it may be that certain pores or parts of pores which are not covered by protamine carry no charges or perhaps even negative charges pertaining to the collodion matrix of the membrane. Only further work can decide whether it is possible to better the ionic selectivity of these membranes. The characteristic concentration potentials which have been obtained so far correspond to an anion leak of 2 to 3 per cent.

Except for this slight defect of the dried-type protamine collodion membranes, the porous as well as the megapermselective protamine collodion membranes constitute exact electropositive analogues of the activated porous and megapermselective collodion membranes.

SUMMARY

1. An attempt is made to circumscribe the meaning of the term "membrane" from the physicochemical viewpoint. Membranes are not only restrictive barriers but may also be the locus and the means of many diversified energetic processes. Accordingly the following definition is suggested for physicochemical membranes: "A membrane is a phase or structure interposed between two phases or compartments which obstructs or completely prevents gross movement between the latter, but permits passage, with various degrees of restriction, of one or several species of particles from the one to the other or between the two adjacent phases or compartments, and which thereby acting as a physicochemical machine transforms with various degrees of efficiency according to its own nature and the nature and composition of the two adjacent phases or compartments the free energy of the adjacent phases or compartments, or energy applied from the outside to the latter, into other forms of energy."

2. The investigation of the machine character and of the manifold machine actions of membranes in the past has been retarded greatly by the lack of membranes suitable for model studies, particularly for the study of the electrical membrane effects, the molecular mechanisms being responsible for these latter effects having been controversial. The characteristic electrochemical properties of collodion membranes are shown to be due to the presence of anionic (i.e., acidic) impurities (oxynitrocellulose, "nitrocellulosic acid") in the collodion.

3. The methods of electrochemical activation of collodion and collodion membranes developed by Sollner, Abrams, and Carr are briefly reviewed and new improvements of the technique are described. Dried-type collodion membranes may now be prepared which combine extreme ionic selectivity with very great permeability for the unrestricted ion. Over wide ranges of concentration such electronegative "megapermselective" collodion membranes prevent the penetration of anions while readily permitting the exchange of alkali (and certain other) cations across their thickness. The absolute permeability of megapermselective collodion membranes is three to four orders of magnitude greater than that of any previously described membranes of high ionic selectivity.

4. The method of Abrams and Sollner for the preparation of electropositive membranes by the adsorption of protamine on highly porous collodion membranes has been improved. The preparation of electropositive "megapermselective" protamine collodion membranes is described. These membranes—except for a small leak of cations—are in their properties strict electropositive analogues of the electronegative megapermselective collodion membranes.

REFERENCES

(1) ABRAMS, I., AND SOLLNER, K.: J. Gen. Physiol. **26**, 369 (1943).
(2) BARTELL, F. E.: "Membrane potentials and their relation to anomalous osmosis," Colloid Symposium Monograph **1**, 120 (1923); BARTELL, F. E., AND MADISON, O. E.: J. Phys. Chem. **24**, 444 (1920); BARTELL, F. E., AND CARPENTER, D. C.: J. Phys. Chem. **27**, 101, 252, 346 (1923); and many other publications.
(3) BEUTNER, R.: Arch. exptl. Zellforsch. **15**, 217 (1934).
(4) CARR, C. W., GREGOR, H. P., AND SOLLNER, K.: J. Gen. Physiol., in press.
(5) CARR, C. W., AND SOLLNER, K.: J. Gen. Physiol. **27**, 77 (1943).
(6) CARR, C. W., AND SOLLNER, K.: J. Gen. Physiol. **28**, 119 (1944).
(7) COLLANDER, R.: Kolloidchem. Beihefte **19**, 72 (1924); **20**, 273 (1925).
(8) COLLANDER, R.: Soc. Sci. Fennica, Commentationes Biol. **2**, 6 (1926).
(9) DONNAN, F. G.: London, Physiological Society, December, 1910; Z. Elektrochem. **17**, 572 (1911); Chem. Rev. **1**, 73 (1924); DONNAN, F. G., AND HARRIS, A. B.: J. Chem. Soc. **99**, 1554 (1911); DONNAN, F. G., AND ALLMAND, A. J.: J. Chem. Soc. **105**, 1941 (1914); DONNAN, F. G., AND GARNER, W. E.: J. Chem. Soc. **115**, 1313 (1919).
(10) GIRARD, P.: Compt. rend. **146**, 927 (1908).
(11) GORTNER, R. A.: *Outlines of Biochemistry*, 2nd edition, pp. 143-4. John Wiley and Sons, Inc., New York (1938).
(12) GREGOR, H. P.: Ph.D. Thesis, University of Minnesota; in preparation.
(13) GROLLMAN, A., AND SOLLNER, K.: Trans. Electrochem. Soc. **61**, 477, 487 (1932).
(14) KROGH, A.: Trans. Faraday Soc. **33**, 912 (1937).
(15) LOEB, J.: J. Gen. Physiol. **1**, 717 (1918-19); **2**, 173, 255, 387, 563, 577, 659, 673 (1919-20); and many other papers in the succeeding volumes of the same journal.
(16) MICHAELIS, L.: *The Effects of Ions in Colloidal Systems*. The Williams & Wilkins Company, Baltimore (1925).
(17) MICHAELIS, L., AND FUJITA, A.: Biochem. Z. **158**, 28 (1925); **161**, 47 (1925); **164**, 23 (1925); MICHAELIS, L., AND DOKAN, S.: Biochem Z. **162**, 258 (1925); MICHAELIS, L., AND HAYASHI, K.: Biochem. Z. **173**, 411 (1926); MICHAELIS, L., AND PERLZWEIG, W. A.: J. Gen. Physiol. **10**, 575 (1926-27); MICHAELIS, L., McELLSWORTH, R., AND WEECH, A. A.: J. Gen. Physiol. **10**, 671 (1926-27); MICHAELIS, L., WEECH, A. A., AND YAMATORI, A.: J. Gen. Physiol. **10**, 685 (1926-27); MICHAELIS, L.: Bull. Natl. Research Council, **No. 69**, 119 (1929); Kolloid-Z. **62**, 2 (1933), and other publications.
(18) MICHAELIS, L., AND PERLZWEIG, W. A.: J. Gen. Physiol. **10**, 575 (1927).
(19) NERNST, W.: *Theoretical Chemistry from the Standpoint of Avogadro's Rule and Thermodynamics*, revised in accordance with the eighth-tenth German edition by L. W. Codd, pp. 107, 109, 137, 780. Macmillan and Co., Ltd., London (1923).
(20) PFEFFER, W.: *Osmotische Untersuchungen*. Engelmann, Leipzig (1877).
(21) PLANCK, M.: *Vorlesungen über Thermodynamik*, 5th edition, pp. 218 ff. (§§235 and 236). Veit and Company, Leipzig (1917).
(22) PREUNER, G., AND RODER, O.: Z. Elektrochem. **29**, 54 (1923).
(23) SOLLNER, K.: Z. Elektrochem. **36**, 36 (1930).
(24) SOLLNER, K.: Z. Elektrochem. **36**, 36, 234 (1930); Kolloid-Z. **62**, 31 (1933). SOLLNER, K., AND GROLLMAN, A.: Z. Elektrochem. **38**, 274 (1932).
(25) SOLLNER, K., AND ABRAMS, I.: J. Gen. Physiol. **24**, 1 (1940).
(26) SOLLNER, K., ABRAMS, I., AND CARR, C. W.: J. Gen. Physiol. **24**, 467 (1941).

(27) Sollner, K., Abrams, I., and Carr, C. W.: J. Gen. Physiol. **25**, 7 (1941).
(28) Sollner, K., and Anderman, J.: J. Gen. Physiol. **37**, 433 (1944).
(29) Traube, M.: Arch. Anat. Physiol., p. 87 (1867); Gesammelte Abhandlungen, Meyer and Müller, Berlin (1899).
(30) Wilbrandt, W.: J. Gen. Physiol. **18**, 933 (1935).

THE SYSTEM ACETIC ACID–TRIETHYLAMINE

H. S. van KLOOSTER and WINSTON A. DOUGLAS

Department of Chemistry, Rensselaer Polytechnic Institute, Troy, New York

In contrast to the more than three thousand minimum azeotropes which have been recorded in the literature, there are only about two hundred and fifty maximum azeotropes. The best known of this type are systems having water as one component and an inorganic acid (hydrofluoric acid, hydrochloric acid, hydrobromic acid, hydriodic acid, nitric acid) as the second constituent. Less familiar are maximum azeotropes formed from acetic acid and organic bases (pyridine, picoline, triethylamine), first described by Gardner (2) in 1891, working in Victor Meyer's laboratory. On the assumption that definite compounds were formed, Gardner ascribed to one of his azeotropes the formula $4CH_3COOH \cdot N(C_2H_5)_3$ but admitted that in the vapor state, at the boiling point of thymol, this "compound" was completely dissociated into acetic acid and triethylamine molecules. Since no other information besides the boiling point (162°C.) of the "compound" was available, it was considered worthwhile to study the boiling point–vapor composition diagram for the acetic acid–triethylamine system at atmospheric pressure. In the course of this investigation it was discovered that the two components are not miscible in all proportions. In this respect the system resembles to some extent the water–hydrochloric acid and the water–hydrobromic acid systems, where there is little miscibility on the acid side in spite of the fact that considerable heat evolution and contraction occur when one of these acids is added to water.

EXPERIMENTAL

Glacial acetic acid (99.6 per cent) was purified by partially freezing the acid, decanting the liquid portion, and allowing the frozen acid to melt. The process was repeated, and the acid was finally distilled from chromic anhydride to remove traces of aldehyde. The density ($d_4^{25} = 1.045$) and refractive index ($n_D^{25} = 1.3722$) agreed with those given in the literature. Triethylamine obtained from Sharples Solvents Corporation was subjected to fractional distillation, and the fraction distilling over at 89.4°C. (corr.) at 760 mm. was collected. Its density, d_4^{25}, was 0.723, and the refractive index, n_D^{25}, was 1.3990.

In order to obtain the composition of the vapor phase in equilibrium with liquid

at various temperatures, a number of samples were prepared by weighing different quantities of both constituents in small tubes and determining their index of refraction at 25°C. with the Abbe refractometer. These data are recorded in table 1 and plotted as a dash-dash line in figure 1. On account of the small

TABLE 1

ACID	REFRACTIVE INDEX n_D^{25}	DENSITY d_4^{25}	ACID	REFRACTIVE INDEX n_D^{25}	DENSITY d_4^{25}
per cent			per cent		
100	1.3722	1.045	63.6	1.4275	1.009
95.3	1.3828	1.045+	57.65	1.4326	0.994
89.6	1.3950	1.045+	54.2	1.4338	0.976
86.5	1.3991	1.041	50.4	1.4332	0.952
76.75	1.4127	1.030	46.0	1.4304	0.936
74.0	1.4163	1.017	4.0	1.4009	
70.1	1.4208	1.017	0.0	1.3990	0.723
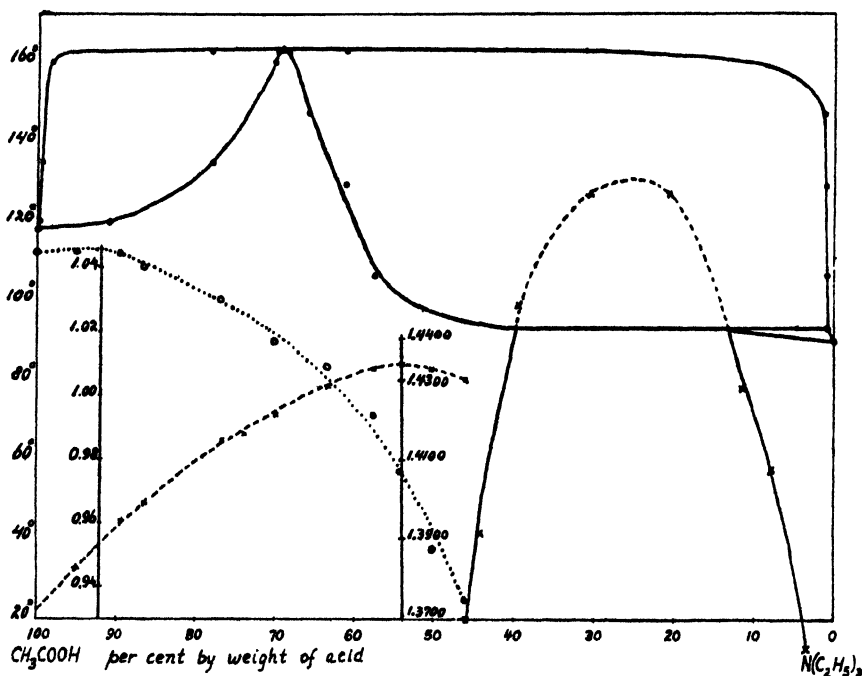
Fig. 1. The system acetic acid–triethylamine

amounts used (approximately 5 ml. each time), the densities (d_4^{25}) were determined in a small pyknometer (contents 0.615 ml.) built from a 1-ml. pipet. The results, accurate to within 0.2 per cent, are recorded in the same table and plotted as a dotted line in figure 1.

A number of solubility determinations were made. To this end weighed amounts of the components were placed in Pyrex test tubes narrowed in the center. The constricted part of each tube was sealed off after cooling in a mixture of ice and salt and removing the air by evacuation with a water pump. The tubes were heated in a glycerol bath and the two layers merged by vigorous shaking. The temperatures at which, on cooling, the clear solutions became clouded, were used to construct the solubility curve in figure 1. For mixtures containing 3.87, 7.91, 11.8, 20.8, 30.5, 39.5, 44.5, and 46.0 per cent acetic acid the corresponding temperatures of cloud formation were 13.5, 57.0, 77.6, 126.5, 126.5, 98.8, 42, and 20°C., respectively.

The pure components and mixtures of varying composition were heated (10 ml. each time) in a 50-ml. distilling flask, completely immersed up to the delivery tube in a 400-ml. beaker containing glycerol. The glycerol was stirred vigorously and the temperature of the bath recorded at regular intervals. The rate of heating was regulated, the beaker being covered with a thick layer of

TABLE 2

OVERALL COMPOSITION	EQUILIBRIUM TEMPERATURE	COMPOSITION OF LIQUID	COMPOSITION OF VAPOR
per cent acid	*°C.*	*per cent acid*	*per cent acid*
0	89.4	0.0	0.0
16	92.6	40 and 13	1.0
46	105.5	57.5	1.—
46	128.5	61	1.—
46	147	66	1.—
64	162.5	68.5	59
69	163	69	69
70	162.7	69.5	78
74	160	70	99
86.5	134.5	78	99.5
100	118.2	100	100

asbestos cement, and the temperature, if necessary, maintained to within 2°C. The temperature of the escaping vapor was read on a ground-in thermometer. Both thermometers used were calibrated against a U. S. Bureau of Standards thermometer for temperatures to 100°C. and for higher temperatures by determining the boiling points of pure acetic acid (118.2°C.) and bromobenzene 156.2°C.). The temperature of the bath was invariably a few degrees higher than that read on the inside (vapor) thermometer. The temperatures recorded in table 2 are those read on the latter and the readings were adjusted to 760 mm. pressure.

The temperature of the invariant liquid–liquid–vapor equilibrium was established by slowly heating, with constant shaking, a mixture containing 16 per cent acetic acid. The constant boiling point was located at 92.6°C. and the distillate contained 1 per cent acid. The composition of the two layers was derived from the intercepts on the horizontal line at 92.6°C. (40 and 13 per cent acetic acid).

Heating solutions of different compositions to definite temperatures and analyzing the distillate and residue refractometrically led to the data of table 2 and the corresponding vapor and liquid curves of figure 1.

RESULTS

Although the composition of the azeotrope (69 per cent acetic acid) is close to that required for a compound containing 4 moles of acetic acid plus 1 mole of triethylamine (70.4 per cent acetic acid), there is no direct evidence for the existence of such a compound. Attempts made by Zack (5) to establish its identity by means of freezing-point determinations failed, as no crystallization on cooling occurred beyond 75 per cent acid (f.p., $-19°C$.). Since considerable heat evolution and a slight contraction occurred on adding triethylamine to acetic acid, some kind of chemical action, possibly of ionic nature—to which conductance measurements might lend support—is indicated. Definite compound formation between acetic acid and amines has, however, been proven by O'Connor (4) and by Lucasse and coworkers (3). The presence of both dimers and monomers in acetic acid vapor naturally leads to the assumption of dimers (and polymers) in the liquid state, and it is possible that triethylamine, acting as a solvent, tends to break up the di(poly)mers, the resulting monomers being only slightly soluble in the amine. When the acid concentration is increased more dimers are present, which dissolve part of the amine and a two-layer system results. As pointed out by Ewell and coworkers (1), solubility is not necessarily governed by polarity (dipole moments). It seems premature, however, to make it largely a function of hydrogen bonding in view of the fact that even slight changes of temperature may greatly affect the solubility, as for the system triethylamine–water.

SUMMARY

The presence in the acetic acid–triethylamine system of a maximum azeotrope containing 69 per cent by weight of acetic acid at 163°C. was established. A non-variant equilibrium exists at 92.6°C., the coexisting phases containing 40, 13, and 1 per cent of acetic acid, respectively. The maximum critical solution temperature was located at 25 per cent acetic acid and 130°C. At room temperature (20°C.) the limits of miscibility are 46 and 4 per cent acetic acid.

REFERENCES

(1) EWELL, R. H., HARRISON, J. M., AND BERG, L.: Ind. Eng. Chem. **36**, 871 (1944).
(2) GARDNER, J. A.: Ber. **23**, 1587 (1891).
(3) LUCASSE, W. W., KOOB, R. P., AND MILLER, J. G.: J. Phys. Chem. **48**, 85 (1944).
(4) O'CONNOR, J.: J. Chem. Soc. **119**, 40 (1921); **125**, 1422 (1924).
(5) ZACK, H. S.: Thesis, Rensselaer Polytechnic Institute, August, 1944.

MINIMA IN SURFACE-TENSION AND INTERFACIAL-TENSION CURVES[1]

GILBERT D. MILES

Colgate-Palmolive-Peet Company, Jersey City, New Jersey

In a previous paper (1) evidence was presented which established the existence of minima in certain surface-tension–concentration curves as the result of the presence of at least two surface-active substances in the same solution. It was shown that the components could be either a mixture of sodium lauryl sulfate and unsulfated lauryl alcohol or sodium lauryl sulfate and a trace of a higher-molecular-weight homologue or analogue. In the latter case, it was postulated that the minima were due to a salt effect of the principal constituent, sodium lauryl sulfate, upon the traces of the higher-molecular-weight homologue or analogue.

At that time, it was suggested that a critical examination of all materials which have been reported to exhibit minima in surface tension might reveal that their "anomalous" behavior was the result of various impurities or hydrolysis products rather than the property of a single component.

The present paper deals with some of the data which have been obtained by means of experiments suggested by our previous concepts concerning the surface composition of solutions containing two or more surface-active electrolytes.

Specifically, the object of this work has been to obtain some information concerning the relative surface concentration of two component mixtures of surface-active materials as a function of bulk concentrations, which in turn could be related to the "anomalous" interfacial-tension data previously observed for these same solutions.

PROCEDURE

The experimental technique employed in determining the relationship between relative surface and bulk concentrations of these systems was based upon the interpretation of interfacial- or surface-tension data obtained before and after attempts at selective adsorption of one of the surface-active components.

The surface- and interfacial-tension measurements were made as previously described (1), using a du Noüy tensiometer. The precision of this method, while not the highest obtainable, is several times greater than is required to detect the effects observed. The materials used were highly purified. Details of their preparation appear elsewhere (2).

Selective adsorption of the surface-active materials was achieved by creating relatively large areas of either an air–liquid or benzene–liquid interface from relatively small volumes of the test solutions.

When this had been done, in a manner to be described, the solutions were brought to what was believed to be a steady state with respect to the newly

created interface by agitating the bulk liquid in contact with the interface for several minutes. At this point, samples of the bulk liquid were withdrawn from contact with the extended interface, and their surface or interfacial tensions were measured and compared with the values obtained for untreated solutions. Electrolytic conductance measurements were made on several occasions and established that the bulk concentration changes produced by the selective adsorption were less than ± 1 per cent, which is the limit of error of the resistance bridge used in the determination.

In the selective adsorption experiments at air–liquid interfaces, known volumes of foam of uniform bubble size were produced by passing clean air, at constant pressure, through a single glass orifice into 50 ml. of the test solution. The foam receptacle was a Pyrex-glass cylinder 32 cm. long and having an outside diameter of 7.0 cm. During the foam formation this cylinder was clamped in a vertical position. At the lower end, the bubbling orifice entered through a standard-taper, ground-glass joint, and the upper, open end of the cylinder was formed into a short narrow neck.

It was assumed that the interfacial area, in each experiment, was proportional to the foam column height, since the bubbles were of uniform size. In all the tests made, the foams produced were sufficiently stable to prevent any appreciable coalescence of the bubbles during the experiment. In each case, after the desired amount of foam had been formed, the air was shut off and the cylinder containing the foam was removed from the supporting clamps and gently rocked to and fro for several minutes to insure adequate mixing of the foam and bulk liquid. Samples of the bulk liquid which were to be tested were withdrawn from the cylinder by pouring from the upper end directly into clean Erlenmeyer flasks. The surface-tension measurements were made in these flasks. In preparing the Erlenmeyer flasks and the glass cylinder for use, they were cleansed with hot chromic and sulfuric acids cleaning solution, washed with distilled water, and paraffined inside and out, around the neck. This paraffin treatment has been found very useful in avoiding accidental contamination from handling.

The experiments on selective adsorption at benzene–liquid interfaces have been only qualitative. The solutions were prepared for interfacial-tension measurements by shaking 25 cc. of the solution with 15 cc. of benzene, thus forming a fine dispersion of the benzene.

These emulsions were permitted to cream, and the lower bulk liquid was withdrawn. This operation was repeated three times, after which the interfacial-tension measurements were made, using the clear aqueous phase. Obviously no exact knowledge of the relative interfacial areas was possible under these conditions. All of the experiments were carried out at room temperatures, which varied within ± 3°C.

RESULTS

The interfacial area in the foam experiments was approximately 2×10^4 cm.^{2} for a full cylinder of foam, as calculated from the bubble volume, which was estimated as 0.017 ml., and the cylinder volume of 1100 ml.

Curve 1 of figure 1 represents the surface-tension–concentration relationships for pure sodium lauryl sulfate which had been ether-extracted in the dry state for 36 hr. in a Soxhlet apparatus.   Curve 2 illustrates the minimum obtained when pure sodium lauryl sulfate is contaminated with 0.5 per cent lauryl alcohol, on the total solids basis.   Point A' is the value obtained after forming a full cylinder of foam from 50 ml. of solution of concentration A, 0.015 molal, and then diluting to 0.0075 molal.   Point B' is the value obtained when the same procedure is fol-
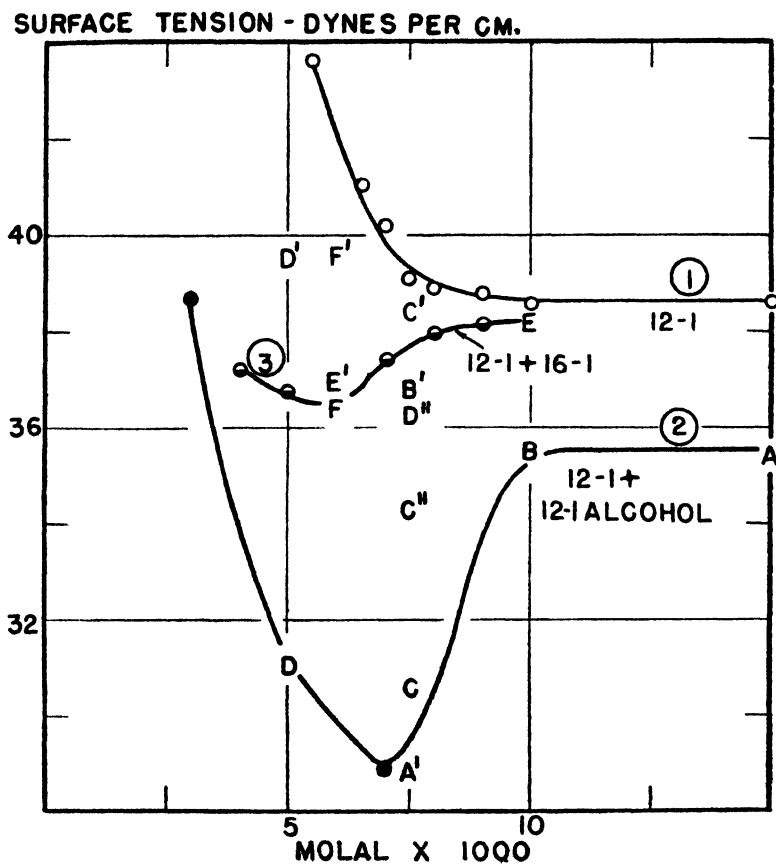
FIG. 1. Effect of foam extraction on surface tension of solutions

lowed starting with point B, 0.010 molal, and diluting to 0.0075 molal after selective adsorption.   Point C' was obtained by the same steps as points A' and B', except that the starting and final concentrations were 0.0075 molal.   Point C″ is like point C', except that one third the volume of foam was employed in obtaining C″ as compared to C'.   Point D' starts with 50 ml. of 0.005 molal solution, from which a full cylinder of foam was created and the surface tension of the bulk liquid measured.   On increasing the concentration to 0.0075 molal by the addition of pure sodium lauryl sulfate to solution D', point D″ is obtained.
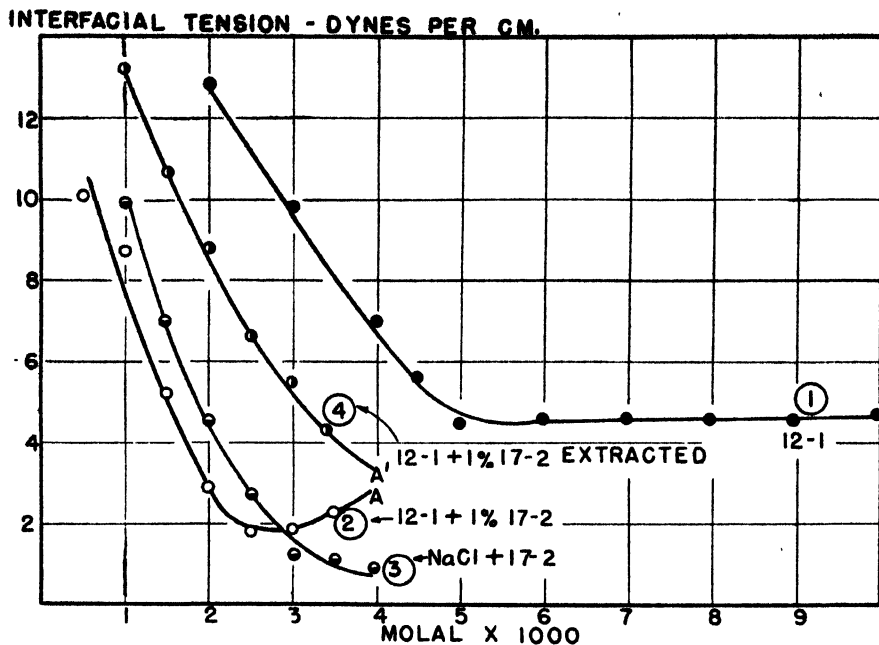
FIG. 2. Effect of benzene emulsion extraction on interfacial tension
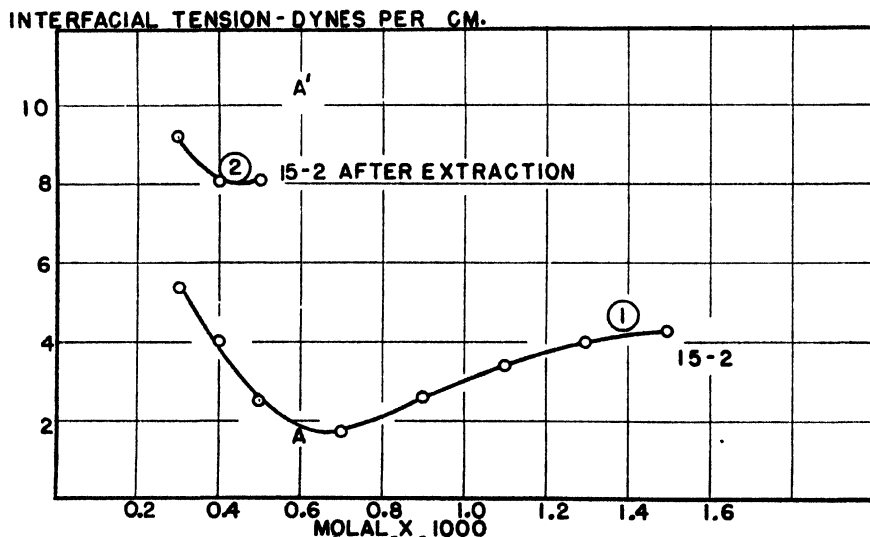
FIG. 3. Effect of benzene emulsion extraction on interfacial tension

Curve 3 of figure 1 was obtained from surface-tension measurements of solutions of sodium lauryl sulfate "contaminated" with 1 per cent of sodium cetyl sulfate, on the total solids basis. Point E′ was obtained by diluting 50 ml. of a 0.01 molal solution E to a 0.006 molal solution which had previously been used to

form a full cylinder of foam. Point F′ was obtained by the same adsorption procedure, starting from a 0.006 molal solution F.

Curve 1 of figure 2 represents the interfacial-tension data of pure sodium lauryl sulfate solutions against benzene. Curve 2 shows the interfacial tension of mixed sodium lauryl sulfate plus 1.0 per cent of sodium heptadecane-2-sulfate (17-2) on the total solids basis. Curve 3 was obtained for solutions of sodium chloride equivalent to the sodium lauryl sulfate in curve 2, plus the same amount of sodium heptadecane-2-sulfate used in solutions for curve 2. Curve 4 represents the interfacial-tension–concentration data obtained from a 0.004 molal solution of the composition described above, under curve 2, which had been shaken with benzene and extracted as described on page 72.

Curve 1 of figure 3 represents the interfacial-tension data for solutions of sodium pentadecane-2-sulfate against benzene, and is substantially the same as the curve obtained when the 17.5×10^{-4} molal stock solution is extracted with a benzene emulsion. Curve 2, point A′, was obtained by a threefold selective adsorption treatment with benzene of a solution corresponding to A. This was diluted further to give the other points on curve 2.

DISCUSSION AND CONCLUSIONS

In the cases studied it has been shown that minima in surface-tension–concentration curves can be attributed to the presence of two surface-active materials in the same solution. It has been demonstrated that at the concentrations which correspond to the minima in surface or interfacial tension, the relative concentration of one of the components is at a maximum. This confirms the interpretation previously suggested in which the "anomalies" in surface tension for solutions of mixed surface-active electrolytes were explained as special cases of the more general phenomena of "salt effects." Further evidence in support of this viewpoint is presented in figure 2 (curves 1, 2, and 3), where it is shown that the minimal values obtained in curve 2 are in close agreement with the values obtained where sodium chloride is substituted for sodium lauryl sulfate in the mixture (curve 3).

For bulk concentrations of sodium lauryl sulfate above 0.01 molal where the minimum in surface tension can be attributed to an ether-soluble, surface-active non-electrolyte (curve 2, figure 1), we might consider the possibility that the observed decrease in surface concentration of the lauryl alcohol may be explained as an effect of an increase in the solubilization of the lauryl alcohol by the sodium lauryl sulfate solutions.

One point which is worth mentioning is the possible relationship between these surface-active properties and the bulk properties of such solutions. The coincidence of a break in specific electrolytic conductance vs. concentration with the concentration for minimal surface or interfacial tension has been considered by some as evidence in support of the explanation for these minima on the basis of a "critical concentration for micelle formation."

In the case of sodium lauryl sulfate solution, no significant difference in conductance was observed between the solutions with or without lauryl alcohol in the concentration range where the minimum appeared in the surface-tension–concen-

tration curves. Both conductance curves showed the same break within the limit of error (± 1 per cent) of the conductance bridge. While this is only a fragmentary bit of evidence, it suggests that the discontinuities in the bulk properties of such solutions may not always be associated with "anomalous" surface behavior.

In an earlier paper (1) it was suggested that the purity of all solutions exhibiting minima in surface-tension–concentration curves was suspect. Here it has been demonstrated that by the application of a rather simple experimental technique, it can be established that certain solutions contain two surface-active components. By the application of these techniques, it may be possible to ascertain whether any solutions for which minima have been reported are composed of single surface-active species. Until it has been demonstrated that such minima exist for systems which contain one surface-active component, the theoretical significance previously attached to the appearance of minima in surface-tension–concentration curves must be considered as doubtful.

SUMMARY

1. The interfacial-tension–concentration curve for solutions of pure sodium lauryl sulfate against benzene shows no pronounced minimum.

2. A solution of a mixture of pure sodium lauryl sulfate and pure sodium heptadecane-2-sulfate, 100 moles to 1, does exhibit a pronounced minimum in interfacial-tension–concentration values against benzene.

3. The bulk concentration at which this minimum occurs and the actual interfacial-tension values observed for this mixture correspond to the bulk concentration where the greatest change in slope and the lowest interfacial tensions are observed for mixtures of pure sodium heptadecane-2-sulfate and sodium chloride equivalent to the previous mixture.

4. Minima in surface- or interfacial-tension–concentration curves have been produced by deliberate "contamination" of solutions of pure, surface-active primary or secondary alcohol sulfates with a second surface-active material. In all cases, attempts at selective adsorption at either an air–liquid or a benzene–liquid interface have shown these minima to occur at bulk concentrations where the relative surface concentration of the minor component is at a maximum.

5. It is suggested that the selective adsorption technique used in this work might be of value as a test in ascertaining whether or not any minima in surface- or interfacial-tension–concentration curves exist for systems supposedly containing only one surface-active component.

REFERENCES

(1) MILES, G. D., AND SHEDLOVSKY, L.: J. Phys. Chem. **48,** 57 (1944).
(2) DREGER, E. E., KEIM, G. I., MILES, G. D., SHEDLOVSKY, L., AND ROSS, J.: Ind. Eng. Chem. **36,** 610 (1944).

NOTE ON THE KINETICS OF SYSTEMS MANIFESTING SIMULTANEOUS POLYMERIZATION–DEPOLYMERIZATION PHENOMENA

P. J. BLATZ AND A. V. TOBOLSKY

Frick Chemical Laboratory, Princeton University, Princeton, New Jersey

Many substances form long-chain polymers of the type A—A—A—A—or A—B—A—B—A—B— from the monomeric units A or A plus B. The bond A—A or A—B may be electrostatic (hydrogen bonds as in hydrogen cyanide or in alcohols) or may be covalent as in the ester linkages of polyesters or the C—C linkage in vinyl polymers.

In many cases the polymerization process is reversible. In the case of polyesters or polyamides, hydrolysis can be effected by heating the polymer with water; in the case of polystyrene, the monomer can be distilled off at high temperatures; and finally, in the case of hydrogen bond association, as in hydrogen cyanide, the short polymeric molecules can be readily broken down into monomer at elevated temperatures. There is evidence that in many systems both polymerization and depolymerization are occurring simultaneously, leading at any given temperature to an equilibrium distribution in polymeric sizes.

In this paper we present the kinetics for a simple case of simultaneously occurring polymerization–depolymerization phenomena. We shall suppose that the polymerization process for the polymerization AAAA . . . is specified by a bimolecular rate constant, k_f, which is characteristic of the A—A bond but independent of the size of the reacting polymers. Similarly we shall suppose that the depolymerization process is specified by a unimolecular rate constant, k_b, which is also characteristic of each A—A bond. We shall assume that initially all the molecules are in the form of unreacted monomer. The following notation is used:

N_0 = total number of moles of monomer at time $t = 0$,

N = number of moles of unreacted monomer at any time t,

p = extent of reaction, or fraction of the total number of reacted groups, $\dfrac{N_0 - N}{N_0}$,

x = number of members of an individual chain molecule,

N_x = number of moles of x-mers at any time t,

$m_x = \dfrac{N_x}{N_0}$ = number fraction of x-mers,

k_f = rate constant of bimolecular addition, and

k_b = rate constant for unimolecular splitting.

The differential equations for this kinetic situation assume the following form:

$$\frac{dm_1}{dt} = -k_f m_1 \sum_{1}^{\infty} m_s + 2k_b \sum_{2}^{\infty} m_s \tag{1}$$

$$\frac{dm_x}{dt} = \frac{k_f}{2} \sum_{1}^{x-1} m_s \cdot m_{x-s} - k_f m_x \sum_{1}^{\infty} m_s - k_b(x-1)m_x + 2k_b \sum_{x+1}^{\infty} m_s \tag{2}$$

$(x = 2, 3, 4 \ldots)$

The first term in the first equation represents the disappearance of monomer by reaction with any other x-mer. The second term represents the formation of monomer by splitting of any x-mer, where the statistical factor 2 indicates that each x-mer can be split in two ways to give monomer. In the second equation the first term represents bimolecular formation of x-mer. (The division by 2 is necessary because $m_s \cdot m_{x-s}$ is equivalent to $m_{x-s} \cdot m_s$). The second term accounts for the disappearance of x-mer by bimolecular addition to any s-mer. The third term represents the unimolecular splitting of x-mer with a statistical factor of $x - 1$, since breaking can occur at any of the $x - 1$ bonds. The fourth term represents the unimolecular splitting of any polymer higher than x-mer to yield x-mer. The factor 2 occurs because x-mer can be split off from a higher polymer at both ends.

The solution of these equations is

$$m_x = p^{x-1}(1 - p)^2 \tag{3}$$

where

$$p = \frac{1}{K + (K^2 - 1)^{1/2} \coth \frac{k_f t}{2} (K^2 - 1)^{1/2}} \tag{4}$$

and where

$$K = 1 + k_b/k_f \tag{5}$$

It can be shown that

$$\lim_{k_b \to 0} p = \frac{k_f t}{2 + k_f t} \tag{6}$$

which is the equation deduced by Flory (3), Dostal (2), and Chalmers (1) for the condensation of linear polyesters in the case where the back reaction is eliminated.

When t approaches infinity, the limit of p becomes

$$p_\infty = \frac{1}{K + (K^2 - 1)^{1/2}} \tag{7}$$

This is the "equilibrium" extent of reaction and is of course always less than unity when $k_b > 0$.

In figure 1 p is plotted as a function of the logarithm of $k_f t$ for different values of K, i.e., for different ratios of k_b to k_f. It is seen from equation 7 that for large values of k_f/k_b, the extent of reaction p at infinite time is

$$p_\infty \cong \frac{1}{1 + \left(\frac{2k_b}{k_f}\right)^{1/2}} \tag{8}$$

It is to be further noted that the curves representing equation 4, shown in figure 1, exemplify a new type of kinetics which does not fall into the classical first, second, etc. order of reaction.
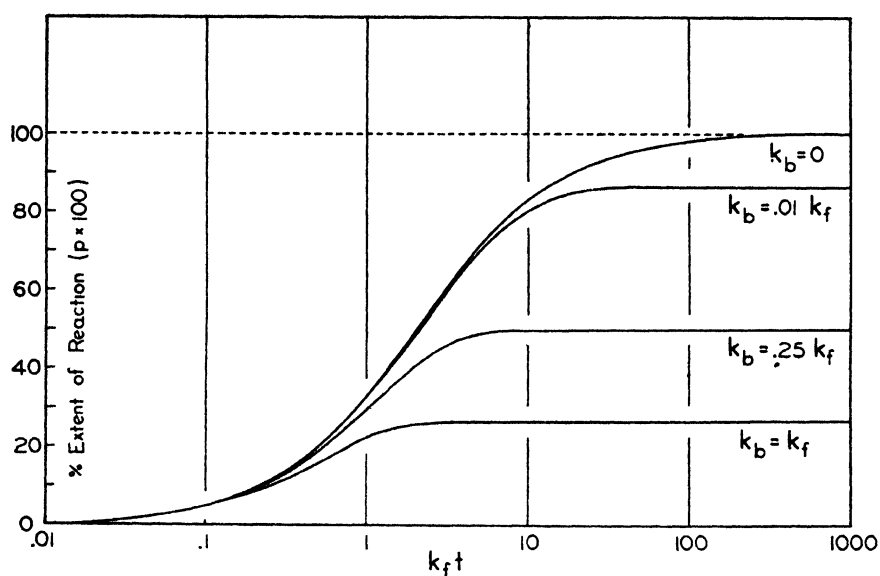
FIG. 1. Extent of reaction as a function of time
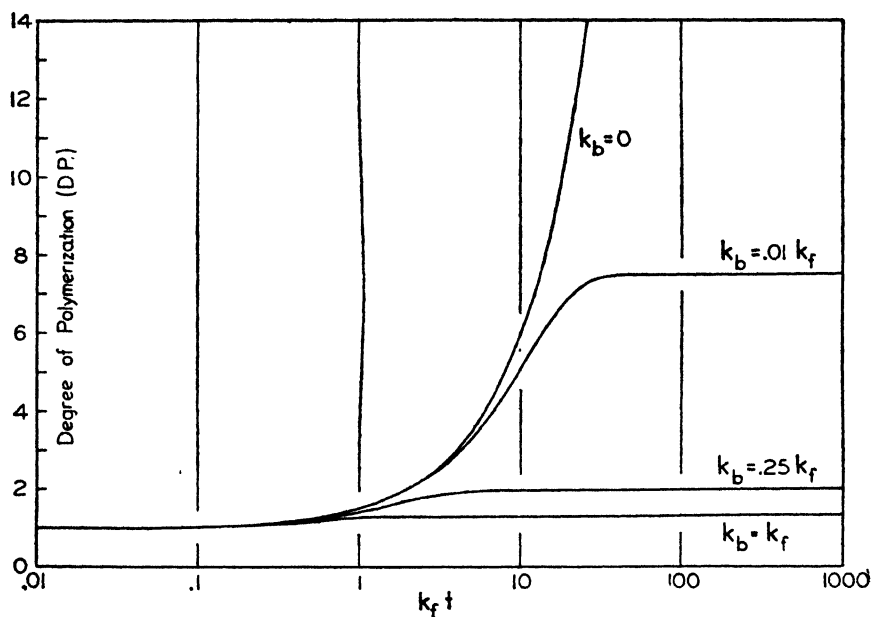
FIG. 2. Degree of polymerization as a function of time

In figure 2 $D.P.$ is plotted against the logarithm of $k_f t$. $D.P.$ is defined as the number average degree of polymerization.

$$D.P. = \frac{K + (K^2 - 1)^{1/2} \coth \frac{k_f t}{2} (K^2 - 1)^{1/2}}{K - 1 + (K^2 - 1)^{1/2} \coth \frac{k_f t}{2} (K^2 - 1)^{1/2}} = \frac{1}{1 - p} = \frac{\sum\limits_{}^{\infty} x N_x}{\sum\limits_{}^{\infty} N_x} \quad (9)$$

From equation 9 the value of $D.P.$ at infinite time becomes

$$D.P._{\infty} = \frac{K + (K^2 - 1)^{1/2}}{K - 1 + (K^2 - 1)^{1/2}} \quad (10)$$

For large values of k_f/k_b

$$D.P._{\infty} \cong 1 + \left(\frac{k_f}{2k_b}\right)^{1/2}$$

A comparison of the two functions p and $D.P.$ shows that both the extent of reaction and the number average chain length become appreciable only for large values of k_f/k_b. Thus, when k_f/k_b is only 4, corresponding to a p_{∞} of 50 per cent, the number average of monomeric units per chain is only 2. If k_f/k_b is 20,000, corresponding to a p_{∞} of 99 per cent, $D.P._{\infty}$ is then 101.

The bimolecular rate constant k_f and the unimolecular splitting constant k_b might be expected to depend only on the particular linkage involved in the polymeric bond. For example, in the case of polyesters, k_f and k_b are to a large extent determined by the ester linkage and independent of the size of the molecule. A thermodynamic equilibrium constant for the linkage may be defined as the ratio of k_f to k_b. Knowledge of k_b and k_f is sufficient to determine completely the functions p and $D.P.$, as seen from equations 4 and 9.

The kinetic scheme presented here can no doubt be extended to the case of condensation reactions and catalyzed polymerization–depolymerization reactions. Thus far there is insufficient experimental data on any reaction of this type to permit a detailed application or extension of our kinetic equations.

REFERENCES

(1) CHALMERS, W.: J. Am. Chem. Soc. **56**, 912 (1934).
(2) DOSTAL, H.: Monatsh. **68**, 188 (1936).
(3) FLORY, P. J.: J. Am. Chem. Soc. **58**, 1877 (1936); **61**, 3334, (1939); **62**, 1057, 1064, 1561, 2255, 2261 (1940).

THE ENERGETICS OF TRANSIENT AND STEADY STATES, WITH SPECIAL REFERENCE TO BIOLOGICAL SYSTEMS

J. M. REINER and S. SPIEGELMAN

Department of Physiology, University of Minnesota, Minneapolis, Minnesota, and Department of Bacteriology and Immunology, The School of Medicine, Washington University, St. Louis, Missouri

INTRODUCTION

Two characteristics of living systems vitiate the indiscriminate use of the elementary laws of physics and chemistry for the theoretical description of biological phenomena. One of them is the obvious structured nature of living cells. This unquestionably imposes geometrical constraints on the reactants; and so complicating factors are introduced into the interpretation of those physicochemical measurements (e.g., oxidation–reduction potential, equilibrium constants) which are usually taken to express tendencies of reactants in homogeneous systems (6).

The other characteristic, the one which the present paper will consider, is the "open" nature of living cells. The recent work of Schönheimer (10) and his collaborators has emphasized that the maintenance of structural integrity in most biological systems involves a continuous flow of matter and energy through them. Thus, the time-independent state in biological systems is a "steady state" rather than an equilibrium (the distinction will be made precise in what follows).

This fact has received increasing recognition in modern biological literature, but has as yet not been implemented by a sufficiently detailed analysis to be of much value to biological theory or experiment. For example, one would like to know what properties distinguish the steady state, and, if such exist, whether they present satisfactory models for the known properties of living tissue.

Some answers to these questions have been provided by the researches of Burton (3), who was able to show among other things that "overshoot" and "undershoot" phenomena, so commonly observed in stimulus–response curves, are derivable from very simple models of open systems approaching the steady state. Bertalanffy (1) has recently used essentially the same type of analysis to explain the relative independence from initial conditions reported in embryological and regeneration experiments. Both of these authors, however, confined their attention solely to the question of mass transport and its time variations.

A closer approach to biological reality would also consider the question of the energetics of such systems, and the properties which stem from the fact that their maintenance requires an energy flux as well as mass transport. Such an investigation, in addition to its greater generality, could also hope properly to delineate the rôle of thermodynamics in biology,—a question which has received much

attention of late. This branch of physics has been among the most frequently employed in biological theory. Thermodynamically derived laws of a special character, such as the law of mass action and the van't Hoff law, are in regular use. Among the most popular applications in recent years (5, 7) has been the calculation of free-energy changes in attempts to elucidate the mechanism of energy transport.

Unfortunately, thermodynamics and most of the associated field of statistical mechanics are governed implicitly and explicitly by the assumptions which denote the equilibrium state. It is true that thermodynamics takes cognizance of non-equilibrium states and of irreversible changes. But for these cases it has only inequalities to offer instead of equations. These inequalities are not sufficiently restricted to permit derivation of a host of special empirical laws such as those mentioned in the preceding paragraph, which are derived under the assumption of equilibrium and strictly reversible processes. Thus all the most usual applications of thermodynamics are strictly not available for non-equilibrium states or irreversible processes. Since, however, biological states and processes are almost always of this latter character, it follows that the usual laws and results of classical thermodynamics offer little hope to biological theory.

It is the aim of the present paper to render the needed formulations—at least the more important ones—explicit. The authors have worked out many consequences of this formulation, and these will appear in future communications. In what follows we propose to analyze the problem in as general a way as possible—to indicate the paths of detailed exploration which are made available by the fundamental formulae.

CHANGES OF STATE

Let us consider a system composed of elements such as molecules or ions. These elements are capable of existing in various states (e.g., those characterized by given energy values or a given kind of chemical combination). Let the states be numbered, and denote the number of particles in the ith state by N_i.

We know that in general a particle does not always remain in one state. Collisions, movement from one part of a force field to another, combination and dissociation produce changes of the states of the individual particles. As such changes occur, the set of numbers N_i may or may not change likewise. Denote the change in N_i during a given standard time interval by ΔN_i. Denote the number of particles leaving the state i for the state j in the unit of time by T_{ij}. Using the symbol Σ to denote summation over the possible values of j, we may
j
write:

$$\Delta N_i = \sum_j T_{ji} - \sum_j T_{ij} \tag{1}$$

That is, the increase in the number in state i is the number entering it from all other states less the number leaving it for any other state.

If the right side of equation 1 does not vanish, N_i is changing, and we have a *non-stationary state*. If the right side of equation 1 vanishes, N_i does not change. If this is true for every i, the system is in a *steady state*.

If for every value of i and j we have:

$$T_{ij} = T_{ji} \tag{2}$$

then also the right side of equation 1 will vanish. But this condition is much more special and restrictive than the vanishing of equation 1, and it is this condition which corresponds to an *equilibrium state*. This is what is usually known as the principle of detailed balancing.

Let us illustrate by a simple example which is closely related to the biological problems with which we shall be concerned. Suppose a system is characterized by the concentration of one or more substances, which may diffuse into or out of the system and which may undergo chemical reaction in the system. For any substance, with concentration n, the rate of change of the concentration is given by:

$$\frac{dn}{dt} = (R_c - R'_c) + (R_d - R'_d) = (R_c + R_d) - (R'_c + R'_d) \tag{3}$$

where R_c is the rate at which the substance is produced through chemical reaction, and R'_c the rate at which it disappears through chemical reaction; while R_d and R'_d have the corresponding significance for the rate of diffusion into and out of the system. The steady state would be characterized by the vanishing of the right side of equation 3; physically this would mean that the net rate at which the substance flows into the system equals the net rate at which it is consumed by chemical reaction, or that the net rate of production equals the net rate of outflow. The equilibrium state would demand that $R_c = R'_c$ and $R_d = R'_d$; that is, the chemical reaction is in equilibrium, and there is no diffusion. If there were more than one chemical reaction into which the substance could enter, each reaction must be in equilibrium separately: e.g., $R_{c1} = R'_{c1}$, $R_{c2} = R'_{c2}$, etc.

It is obvious from this that the steady state, as here defined, corresponds most closely to the characteristics of a biological system whenever it is not changing with time, while the equilibrium state is one which is likely to characterize such a system only when it is dead. A living system is marked by a continual chemical reactivity, and a continual diffusion of metabolites.

THE DYNAMICS OF PHYSICAL SYSTEMS

The systems in which we are interested may be characterized chiefly by specifying their chemical composition, their structure, and their motion. The first two may be treated together by giving the chemical composition at every point of space. By motion we shall understand every form from the slow motion of growth through protoplasmic streaming and local deformation and shape change to gross motion through space. This may likewise be dealt with by specifying the vector velocity of every point of the system.

Especially significant from the biological point of view are the energy relations of the system. An organism is the site of a continuous flow of energy, and of transformation of energy between its various forms,—thermal, chemical, mechanical, electrical, etc. Any treatment in physical terms must give some

account of this and indicate how it is related to the associated motions and chemical transformations.

A system of equations of the sort which is required may be found in the recent work of Eckart (4). However, the equations of Eckart are so expressed as to be most appropriate to a situation where no special distinction is made among the various constituents of the system, and where either no phase boundaries are observed, or such boundaries move on the average with *all* the constituents.

Now the experimental findings of the biologist reveal a somewhat different situation. He always finds a phase boundary. Moreover, he finds that one set of components does not diffuse through this boundary, so that the movement of the boundary is the average movement of these substances alone. These non-diffusible components are in a sense permanent, and the region within the boundary they determine is called the cell (or the organism).

Thus the equations of Eckart must be slightly rewritten to make them useful for our purposes. We shall divide the atomic and molecular species which make up our system into two groups: the first group consists of non-diffusible or permanent cell constituents, the second group is constituted of the diffusible constituents. We shall denote any property associated with the first group alone by a subscript 1, and any property associated with one species of the first group by a Greek letter subscript such as α. We denote a property of the entire second group by a subscript 2, a property of one of the species of the second group by a subscript $i, j, \ldots$. A property of any species of both groups will be denoted by a subscript $a, b, \ldots$.

Let the mass density of any species be m_a g.cm.$^{-3}$, and its average velocity $\overrightarrow{V_a}$ cm. sec.$^{-1}$ Then the average velocities of the two groups are defined by:

$$\sum_{\alpha} m_{\alpha} \overrightarrow{V_{\alpha}} = m_1 \overrightarrow{V_1}; \quad \sum_{i} m_i \overrightarrow{V_i} = m_2 \overrightarrow{V_2} \tag{4}$$

$$m_1 = \sum_{\alpha} m_{\alpha}; \quad m_2 = \sum_{i} m_i \tag{5}$$

Moreover:

$$m_1 \overrightarrow{V_1} + m_2 \overrightarrow{V_2} = m \overrightarrow{V}; \quad m = m_1 + m_2 \tag{6}$$

where $\overrightarrow{V}$ is the mean velocity of the entire system of molecules, and m the total mass density. It is to be remembered that in general all of the functions defined above vary from point to point of the system, and also vary with time; that is, they are functions of x, y, z, t.

We define the diffusion velocity of a species of molecules as the excess of its mean velocity over the mean velocity of the "cell" at the given point; that is:

$$\overrightarrow{U_a} = \overrightarrow{V_a} - \overrightarrow{V_1} \tag{7}$$

From this and equations 4–6 it follows that:

$$\sum_{\alpha} m_{\alpha} \overrightarrow{U_{\alpha}} = 0; \quad \sum_{i} m_i \overrightarrow{U_i} = m_2(\overrightarrow{V_2} - \overrightarrow{V_1}) = m(\overrightarrow{V} - \overrightarrow{V_1}) \tag{8}$$

We assume the usual notations of vector analysis, including the use of ∇ as a vector differential operator with components $\partial/\partial x$, $\partial/\partial y$, $\partial/\partial z$.

The time derivative $\partial/\partial t$ gives the rate of change of a function at a fixed point of space. We are interested, however, in the rate of change of a function at a given point in the cell, itself moving with velocity $\overrightarrow{V_1}$. This rate is made up of the ordinary change given by the partial derivative, together with the change due to the motion (passage from a point of space at which the function has one value to a neighboring point at which its value is slightly different). We therefore define the total rate of change, in the sense in which we are interested, by:

$$\frac{d}{dt} = \frac{\partial}{\partial t} + \overrightarrow{V_1}\cdot\nabla \qquad (9)$$

Following Eckart's notation, we define the net rate of chemical reaction of a species by Γ_a in moles g.$^{-1}$ sec.$^{-1}$ (positive if there is net production; negative if there is net consumption). We can also define the reaction rate in grams cm.$^{-3}$ sec.$^{-1}$ by the relation:

$$R_a = mM_a\Gamma_a \qquad (10)$$

where M_a is the molecular weight. It will also be convenient to have a notation for the overall reaction rates of the groups 1 and 2:

$$R_1 = \sum_a R_a; \quad R_2 = \sum_i R_i \qquad (11)$$

In the present case Eckart's equation 13 becomes

$$\frac{dm}{dt} = -m\nabla\cdot\overrightarrow{V_1} - \nabla\cdot\overrightarrow{J} \quad \text{or} \quad m\frac{dv}{dt} = \nabla\cdot\overrightarrow{V_1} + \frac{1}{m}\nabla\cdot\overrightarrow{J} \qquad (12)$$

while his equation 15 takes the form:

$$m\frac{dc_a}{dt} = m\Gamma_a - \nabla\cdot\overrightarrow{J_a} + c_a\nabla\cdot\overrightarrow{J} \qquad (13)$$

The quantity c_a, as in Eckart's case, is the concentration in moles per gram, related to m_a by:

$$m_a = mM_a c_a \qquad (14)$$

The $\overrightarrow{J_a}$ and $\overrightarrow{J}$ are defined by:

$$\overrightarrow{J_a} = mc_a\overrightarrow{U_a} \qquad (15)$$

$$\overrightarrow{J} = m\overrightarrow{U} = \sum_a M_a\overrightarrow{J_a} \qquad (16)$$

Equations 16 and 8 yield:

$$\overrightarrow{U} = \overrightarrow{V} - \overrightarrow{V_1} \qquad (17)$$

Equation 13 may also be written for certain purposes in the form:

$$\frac{dm_a}{dt} = R_a - \nabla \cdot (M_a \vec{J_a}) - m_a \nabla \cdot \vec{V_1} \tag{18}$$

If we sum equation 18 over the groups 1 and 2 respectively, we obtain:

$$\frac{dm_1}{dt} = R_1 - m_1 \nabla \cdot \vec{V_1}; \quad \frac{dm_2}{dt} = R_2 - m_2 \nabla \cdot \vec{V_1} - \nabla \cdot \vec{J} \tag{19}$$

taking account of equation 8.

We also require the hydrodynamical equation; but Eckart's single equation for $\vec{V}$ is replaced by:

$$m \frac{d\vec{V}}{dt} = \nabla \cdot P + \vec{F} - (\vec{J} \cdot \nabla)\vec{V}; \quad m_1 \frac{d\vec{V_1}}{dt} = \nabla \cdot P_1 + \vec{F_1} - R_1 \vec{V_1} \tag{20}$$

These are easily derived in the classical manner, and brought into the present convenient form with the help of equations 12 and 19. P is the stress tensor representing the stresses acting on all the material in unit volume, including the hydrostatic pressure; P_1 is the corresponding function for materials of group 1 only. $\vec{F}$ and $\vec{F_1}$ are the corresponding long-range plus external forces, which for simplicity were omitted in Eckart's derivation. They do not enter the energy equation, but they are necessary for the solution of equation 20.

If the total energy per unit volume is H, we define the internal energy per gram, ϵ, by:

$$m\epsilon = H - \tfrac{1}{2}mV^2 \tag{21}$$

We then obtain as in Eckart's case:

$$m \frac{d\epsilon}{dt} = (P \cdot \nabla) \cdot \vec{V} - \nabla \cdot \vec{q} - \sum \nabla \cdot (\mu_a \vec{J_a}) + \epsilon \nabla \cdot \vec{J} \tag{22}$$

where $\vec{q}$ is the vector of heat flow, and

$$\mu_a = \frac{\partial \epsilon}{\partial c_a} \tag{23}$$

is the well-known chemical potential of the species a.

Following Eckart's derivation, we can write the entropy equation:

$$m\theta \frac{d\eta}{dt} = (P \cdot \nabla) \cdot \vec{V_1} + (P \cdot \nabla) \cdot \vec{U} + p\nabla \cdot \vec{V_1} - \sum m\mu_a \Gamma_a$$
$$- \sum \vec{J_a} \cdot \nabla \mu_a + (\epsilon + pv - \sum \mu_a c_a) \nabla \cdot \vec{J} \tag{24}$$

where θ is the absolute temperature and η is the entropy per gram. Defining the Gibbs free energy as usual by

$$\Psi = \epsilon - \theta \eta \tag{25}$$

one can obtain after some elementary rearrangements the relation:

$$m \frac{d(\Psi/\theta)}{dt} = -\frac{m\epsilon}{\theta^2} \cdot \frac{d\theta}{dt} + \frac{1}{\theta}\left[-p\nabla \cdot \vec{V}_1 + \sum \mu_a \Gamma_a - \sum \mu_a \nabla \cdot \vec{J}_a \right.$$
$$\left. + (\sum \mu_a c_a - pv)\nabla \cdot \vec{J} \right] \quad (26)$$

The equations which we have obtained so far hold inside the cell; or, if we consider heterogeneities of the cell, equations of this form hold inside each phase. Outside the cell we have a similar set of equations; however, they involve only quantities pertaining to group 2, under our assumption that quantities of group 1 never leave the cell. However, in the case of cells of an organism, bathed by tissue fluids containing non-diffusible elements (serum proteins), there would be a similar group 1 for the exterior phase, but in general composed of different species of molecules.

At the surface of the cell (or, more generally, the surface of each distinct phase) certain boundary conditions must hold; these, together with initial conditions, will determine the solutions of the differential equations governing the system.

One such set constitutes the boundary conditions of the diffusion problem; they will have the form:

$$mc_1\vec{l'}_1 = \vec{J}_{1s}; \quad mc_\alpha\vec{l'}_\alpha = 0 \quad (27)$$

at the boundary, where $\vec{J}_{1s}$ is the flux of the ith species across unit area of the surface. This generally is of the form (9):

$$\vec{J}_{1s} = \vec{n}(a_1c_{1s} - a'_ic'_{is})m \quad (28)$$

the subscript s denoting the surface values, primes denoting the external medium, and $\vec{n}$ being the external normal to the surface.

There is a set of boundary conditions for the hydrodynamical equations also. The stresses P and P_1 are in general functions of $\vec{V}, \vec{V}_1$, and their space derivatives. The boundary conditions assert the equality of these functions, evaluated at the surface, with the externally imposed stresses at the surface; that is, they are of the form:

$$P(\vec{V}_1, \vec{V}_2, \nabla\vec{V}_1, \nabla\vec{V}_2) = P_s \quad (29)$$

at the boundary, and similarly for P_1.

It seems advisable, for the present, to treat $\vec{q}$ as an empirically given quantity; for the attempt, in the general case we are treating, to set up a heat conduction equation as for the simpler case usually treated leads to difficulties. These arise from the fact that increment of internal energy is in general not uniquely separable into increment of heat *content* and increment of potential energy—at least, not without making more detailed hypotheses of a molecular character, which in this discussion we shall eschew.

Another equation obtainable from the foregoing considerations is that of the surface of the phase.   Suppose that this surface were given by the equation:

$$S(x, y, z, t) = 0 \tag{30}$$

It would follow that:

$$\frac{\mathrm{d}S}{\mathrm{d}t} = \frac{\partial S}{\partial t} + \vec{V_1} \cdot \nabla S = 0 \tag{31}$$

This relates S to the solution of the two equations in 20.   Solving them simultaneously, we obtain a function which expresses the shape of the cell at every moment, and which, as is obvious from equation 20, depends on the forces acting and on the metabolic rate.

We can also write two equations which are of particular interest in connection with the problem of growth.   Consider any phase or region whose total mass is M and whose total volume is V_0.   We then obtain by the use of equations 9 and 12:

$$\frac{\mathrm{d}M}{\mathrm{d}t} = \frac{\mathrm{d}}{\mathrm{d}t} \int m \, \mathrm{d}\tau = - \int \vec{J} \cdot \vec{n} \, \mathrm{d}\sigma = - \int \nabla \cdot \vec{J} \, \mathrm{d}\tau \tag{32}$$

$$\frac{\mathrm{d}V_0}{\mathrm{d}t} = \frac{\mathrm{d}}{\mathrm{d}t} \int \mathrm{d}\tau = \int \vec{V_1} \cdot \vec{n} \, \mathrm{d}\sigma = \int \nabla \cdot \vec{V_1} \, \mathrm{d}\tau \tag{33}$$

In the above, $\mathrm{d}\tau$ denotes the element of volume and $\mathrm{d}\sigma$ the element of area of the bounding surface of the region; the integrals are taken over the volume and surface of the particular region being considered.   For the case of a region sufficiently small and homogeneous, these equations may be written in a special approximate form which will be of use:

$$\frac{\mathrm{d}M}{\mathrm{d}t} = -J_s S = -V_0 \nabla \cdot \vec{J} \tag{34}$$

$$\frac{\mathrm{d}V_0}{\mathrm{d}t} = V_{is} S = V_0 \nabla \cdot \vec{V_1} \tag{35}$$

Here S denotes the total surface area of the region, while J_s and V_{is} denote the magnitudes of the normal components of the corresponding vectors at the boundary of the region, assuming these values to be the same everywhere on the boundary.

DISCUSSION

Let us begin by considering the interpretation of some of the terms which appear in our fundamental equations.   The expression $\nabla \cdot \vec{V_1}$ receives an obvious interpretation in view of equation 35, as the fractional rate of volume change of any small region in which it has a constant value.   Similarly by equation 34 we may interpret $\nabla \cdot \vec{J}$ as proportional to the rate of increase of total mass in such a region.   The reader will easily satisfy himself that $\nabla \cdot \vec{J_a}$ has an analogous interpretation for the molecular species a.

Thus on the right side of equation 12 the first term represents the rate of decrease of density due to expansion without change of material content, while the second term represents the rate of increase of density due to material influx. Similarly we may interpret the terms of equation 13: the first term is the increase of moles per gram of species a due to chemical reaction; the second term is the rate of increase due to diffusion of species a molecules; the third term is the rate of decrease of the moles per gram due to total entry of material of all species, and represents a dilution effect, due to the dimensions of the quantity c_a.

Turning to equation 20, the first two terms of the right side are obvious as the forces due to the viscous stresses plus the long-range forces. In the first of these equations, the third term represents the effect of diffusion in bringing momentum into a given region of the cell.

Turning to equation 22, the first term represents the rate at which mechanical energy (i.e., kinetic energy $\frac{1}{2}mV^2$) is dissipated by the viscous forces. The last term again represents a dilution effect, the rate of decrease due to material influx.

In the entropy equation (equation 24), the first two terms on the right side correspond to the first term of equation 22; here the viscous dissipation is split up into the dissipation due to the mass motion of the cell and the dissipation due to diffusion. The third term represents the work done in volume expansion against the hydrostatic pressure p. The fifth term gives a diffusion contribution to entropy of a different kind from the second term; it represents the effect of equalization of concentrations or chemical potentials. The last term is again a dilution term. This is most readily seen if one defines the ζ potential of Gibbs as usual by:

$$\zeta = \epsilon + pv - \theta\eta \qquad (36)$$

The usual transformations of classical thermodynamics then yield:

$$\zeta = \Sigma\mu_a c_a \qquad (37)$$

Combining equations 36 and 37, we find that the coefficient of $\nabla \cdot \vec{J}$ is simply equal to $\theta\eta$. In a similar way the coefficient of $\nabla \cdot \vec{J}$ in equation 26 is shown to be equal to Ψ.

Eckart has given a discussion of equilibrium conditions in his paper. We may therefore go on to consider the nature of the steady state. A system is said to be in a steady state when the rates of change of the variables of state vanish. In our case this applies to the derivatives d/dt, not $\partial/\partial t$, since we are interested in the cell and its parts, not in arbitrary axes fixed in space. From the fundamental equations (equations 12, 13, 18–20, 22, 24, 26, 32, and 33) it is obvious that intermediate conditions are possible. That is, the time derivatives of some variables may vanish while those of others do not. Such conditions might be referred to as quasi-stationary, or stationary with respect to a given set of variables.

If ϵ is a function of state, obviously its rate of change must vanish when the variables of state are stationary. The converse, however, is not necessarily true: it is clearly possible to have a stationary value of the energy with non-stationary

variables of state, provided their variations are such as to cancel out in their effects upon the energy. However, in such a case a relation among the rates of change is imposed. For if in equation 22 we expand the third term on the right by the identity:

$$\nabla \cdot (\mu_a \vec{J}_a) = \vec{J}_a \cdot \nabla \mu_a + \mu_a \nabla \cdot \vec{J}_a \tag{38}$$

we may then introduce the rates of change of the molar concentrations by using equation 13. Setting the right side equal to zero now gives a relation between these rates and the other functions characterizing the system.

What it is customary to call weight growth and volume growth are easily defined in terms of equations 34 and 35, respectively. But if either of these expressions vanishes while the other is positive, and the results are applied to such equations as 18 and 19, it is evident that the conditions are not sufficiently restrictive to determine the remaining quantities, and only give rather general relations between them. Thus our analysis shows that the concept of weight growth and volume growth is not adequate to determine mechanism.

From equations 32 and 33 it is obvious that constant mass and constant volume are perfectly compatible with mass and volume changes in different parts of the cell or organism considered, the changes being merely restricted to compensate each other. A closer examination of the possibilities permitted by these restrictions should throw light upon the processes of differentiation, for this property is essentially definable in terms of the relative magnitudes of the densities of different components at different regions of the cell. It seems likely that similar considerations should permit a precise treatment of the concept of organization, in a rather more general way than that suggested by Rashevsky (8).

Another point worthy of note is that the right-hand sides of equations 32 and 33 are given by solutions of equation 20, which involve R_1. We thus obtain an implicit relation between growth rate and metabolic rate. In a similar way equation 31, together with equation 20, gives the change of cell shape in terms of metabolic rates and volume forces.

When we introduce the energy and entropy equations, further restrictions are found in addition to those obtainable from the mass equations alone. Thus any one of the special cases considered above introduces certain relations among the quantities appearing in equations 22 and 24.

In particular, it seems plausible to use equation 24 or 26 as a measure of degree of organization. It should be noted that, accepting the Second Law of Thermodynamics, it is still true that the entropy must increase or be stationary only for a closed system. The cell is not such a system, and it is not only plausible but almost necessary to assume that it may decrease its entropy at the expense of its environment (despite the objections made by Borsook (2), which are based on equilibrium thermodynamics). Moreover, since equation 24 holds for every element of volume of the cell, it is quite conceivable that the entropy of the cell as a whole may increase, and yet the entropy of certain portions of the cell may at the same time be decreasing.

It is of interest to consider a condition of the organism in which the entropy

is stationary or increasing, and to simplify by neglecting momentarily such factors as mass motion, diffusion, and heat flow. That is, in equation 24 we would have left essentially only the term $-\Sigma m\mu_\alpha\Gamma_\alpha$. Suppose now that a synthesis of structural components or of storage material takes place; this would give one or more terms with positive reaction rates and probably fairly large values of the chemical potentials. If the entropy is to remain stationary or increasing, it is then necessary that other terms shall enter representing the breakdown of some high-energy material at an appropriate rate. This would correspond precisely to the often-discussed energetic coupling of catabolism with synthesis, in which, for instance, the oxidation of carbohydrate would furnish energy for the synthesis of protein.

We may now consider some of the other terms. The term $-\nabla\cdot\vec{q}$ represents the net rate of heat influx into the system; evidently such a process might also compensate for the entropy decrease necessitated by certain syntheses. The fifth term of equation 24 may also contribute, for in general the vector $\vec{J}_a$ is in a direction not exceeding 90° from $-\nabla\mu_a$ (in the simple Fick's Law case the two are, in fact, in the same direction). Thus flow of material along the gradient of its chemical potential produces an increase of entropy. The limitation upon this as a compensation for synthetic reactions is imposed by the relative magnitude of diffusion velocities and potential gradients as compared with reaction rates. The reaction rates of certain protein syntheses, for instance, are sufficiently slow so that it may be possible for diffusion and heat flow alone to compensate for them. On the other hand, the relatively more rapid resynthesis of glycogen in muscle after a contraction may be too fast for such processes, and this may account for the accompanying oxidation processes.

The discussion of the energy and entropy equations suggests the solution of an exceedingly important aspect of the stationary state. Most of the reversible reactions in the cell proceed at a finite rate and are rarely, if ever, found at equilibrium. In terms of classical thermodynamics this would make no sense; the free-energy change of such a reaction, as calculated from the heat and entropy changes, does not agree with that which we would calculate from the concentrations if we assumed the existence of equilibrium. But from our fundamental equations it is clear that non-vanishing of any or all of the R_a is consistent with the stationary state, both materially and energetically. It is obvious also that this imposes certain definite restrictions on the other functions of the system; for any given case which one may choose to consider, these restrictions may be obtained from the fundamental equations.

Another important range of topics which can be treated comprises those phenomena often referred to under such names as "adaptation". Here we ask for the behavior of our system when a discontinuous change occurs in one or more of the parameters. Thus, we may investigate what happens when a new group of enzymes comes into play as at the fertilization of an ovum. Taking a preceding stationary state as the initial state, we study the variations of the functions of the system with time, and find in what manner the new stationary state is approached.

Even in the steady state, we have to solve a system of simultaneous partial differential equations before the system is completely determined; and the solution of the non-stationary forms presents a mathematical problem of great complexity. Approximate solutions have been found in a number of special cases which are of biological interest; the presentation of the details of these is reserved for succeeding communications.

SUMMARY

A mathematical description of the energetics as well as the mass transport of non-stationary systems of the kind encountered in biological phenomena has been formulated, including the stationary but non-equilibrium state as a special case. Those general properties of this formulation which are of biological interest are discussed.

REFERENCES

(1) BERTALANFFY, L. V.: Der Organismus als physikalisches System betrachtet. Naturwissenschaften **28**, 521–31 (1940).

(2) BORSOOK, H.: Reversible and reversed enzymatic reactions. Ergeb. Enzymforsch. **4**, 1–41 (1935).

(3) BURTON, ALAN C.: The properties of the steady state compared to those of equilibrium as shown in characteristic biological behavior. J. Cellular Comp. Physiol. **14**, 327–49 (1939).

(4) ECKART, CARL: The thermodynamics of irreversible processes. II. Fluid mixtures. Phys. Rev. **58**, 269–75 (1940).

(5) KALCKAR, H. M.: The nature of energetic coupling in biological syntheses. Chem. Rev. **28**, 71–178 (1941).

(6) KORR, I. M.: Oxidation-reductions in heterogeneous systems. Cold Spring Harbor Symposia Quant. Biol. **7**, 74–93 (1939).

(7) LIPMANN, FRITZ: Metabolic generation and utilization of phosphate bond energy. Advances in Enzymol. **1**, 99–162 (1941).

(8) RASHEVSKY, N.: On the origin of life. Bulletin of Mathematical Biophysics **5**, 165–9 (1943).

(9) REINER, JOHN M.: Diffusion and biological membrane permeability. II. Phil. Sci. **8**, 105–14 (1941).

(10) SCHÖNHEIMER, R.: *The Dynamic State of the Body Constituents.* Harvard University Press, Cambridge, Massachusetts (1940).

FOAM DRAINAGE[1]

GILBERT D. MILES, LEO SHEDLOVSKY, AND JOHN ROSS

Colgate-Palmolive-Peet Company, Jersey City, New Jersey

The rates of drainage of liquids through foams have been mentioned in several papers dealing with the measurement of foam properties (1, 2, 3, 5). Frequently, a relationship has been postulated between foam drainage rates and foam coalescence. In previous reports, the types of foams measured were often heterogeneous with respect to bubble size, and sufficiently unstable so that coalescence of bubbles occurred during the course of the experiments. In order to avoid such variables, we have studied some of the flow characteristics of liquids through foams of relatively uniform bubble size and of sufficient stability so that no appreciable coalescence occurred when the measurements were made.

Our present study has been restricted to the determination of rates of liquid flow through foams as a function of the amount of liquid held in the foam with the liquid uniformly distributed throughout a column of foam at constant temperatures, and to an investigation of some of the effects of varying temperatures, bulk and surface viscosity, and bubble size. Some typical measurements of drainage rates in homogeneous stable foams have also been made.

EXPERIMENTAL

Procedure

Rate of flow of liquid through foams of uniform liquid concentration: The drainage apparatus (figure 1) was filled with foam by passing filtered air which had been preheated to the temperature of the bath by a metal-coil heat exchanger, which is not shown in the diagram. As soon as the column was filled with foam, the solution at the same temperature was introduced at the top of the column at a fixed rate. This rate was measured directly by taking the time required to collect a known volume. The outlet tube (D) was adjusted to maintain the foam–liquid interface at a constant level. When this rate became constant, the volume of liquid in the foam was obtained by stopping the flow at the inlet tube and draining the column of foam.

In some cases the electrolytic conductivity through the foam was measured with a 60-cycle conductivity bridge[2] with a precision of ± 1 per cent. A linear relationship between the amount of liquid held and the conductance was found on calibrating solutions containing 1 per cent of sodium sulfate and the foam-stabilizing constituent. On this basis, the conductivity could be used to determine when the volume of liquid in the foam reached a steady state as well as the amount of liquid in the foam. The volume of the foam column was 295 cc.

---

[2] Industrial Instruments conductivity bridge, model RC.1B.

and the cell constant was 3.5.   When the volume of liquid in the foam was meas-
ured directly, no addition of sodium sulfate was made.
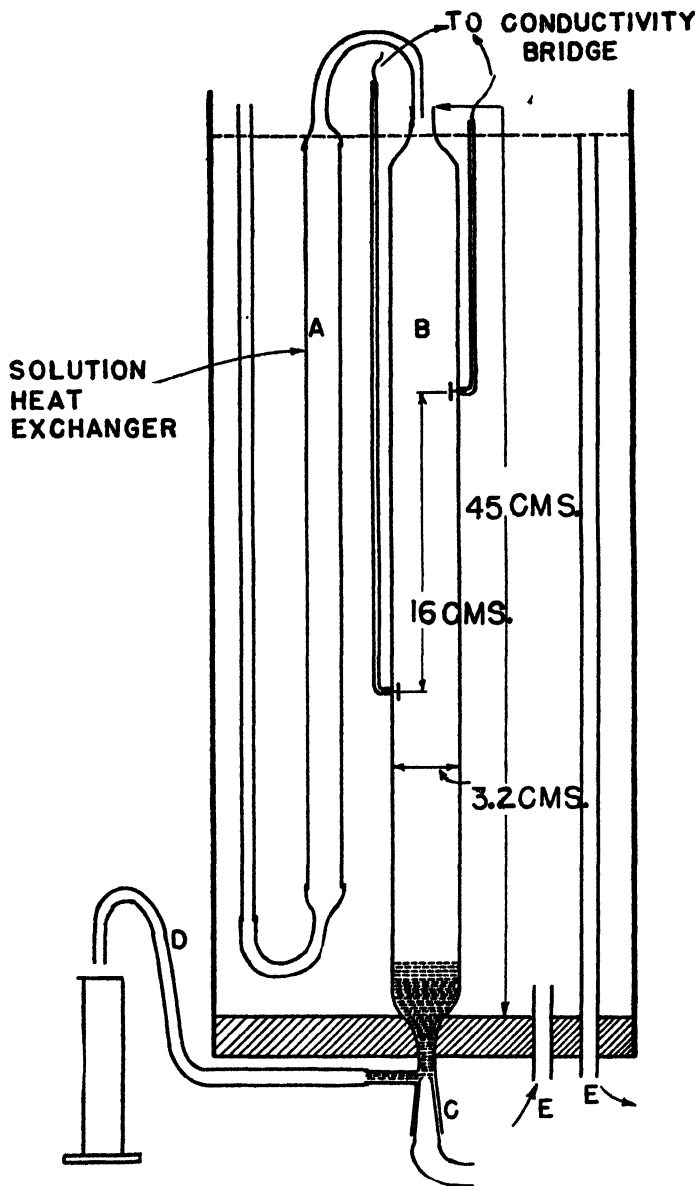
FIG. 1. Foam drainage apparatus

Rate of drainage of liquid from foams: The drainage of liquid from the foam
was started when the column contained a uniform concentration of liquid
throughout.   The flow of liquid into the foam was stopped, and the drainage

rate followed by weighing fixed increments of liquid on a torsion balance. Following these rates by weighing the liquid is more precise than by making volume measurements.

Measurement of bubble size

The rate of flow of air through the orifice (0.15 mm. diameter) was determined by measuring the time to fill the column with foam. As before, the volume of liquid in the foam was obtained by draining the foam. The difference between the volume of the column and the liquid held gives the gas volume. The volume of the bubbles was obtained by collecting bubbles made under the same conditions as above in a conical vessel containing the solution, for a short period of time. The bubbles at the surface of the liquid were collected within an inverted petri dish provided with an opening on the periphery. The petri dish was placed about $\frac{1}{8}$ in. below the liquid level. The bubbles could be slowly released through the opening and counted by tilting the petri dish.

MATERIALS

The sodium lauryl sulfate was prepared by a method previously described (4). The lauryl alcohol was purified by distillation. Syntex M is a commercial preparation consisting of the sodium salts of sulfated monoglyceride and sodium sulfate. Igepon T is a commercial preparation for which the following formula is given: $C_{17}H_{33}CON(CH_3)C_2H_4SO_3Na$. This product also contains sodium sulfate.

RESULTS

Rate of flow of liquid through foams: Figure 2 shows three typical curves for the rate of flow of liquid through the foam against the volume of liquid held in the foam. The solutions were chosen to cover a range of rates of flow for comparable amounts of liquid in the foam. The open and solid circles indicate two separate runs with 0.25 per cent Igepon T solution and indicate the extent of reproducibility which was obtained.

If the logarithms of the two variables of the above data are plotted against each other, the points fall on a straight line (figure 3) and this leads to a relationship of the form

$$y = \alpha x^n \tag{1}$$

where y = rate of flow of liquid through the foam (cubic centimeters per minute), x = volume of liquid in the foam (cubic centimeters), and "α" and "n" are constants. The following equations were obtained for three solutions tested:

0.25 per cent sodium lauryl sulfate	$y = 0.24x^{1.8}$
0.1 per cent sodium lauryl sulfate + lauryl alcohol . .	$y = 0.06x^{1.9}$
0.25 per cent Igepon T solution	$y = 0.42x^{1.6}$

Rate of drainage of liquid from foam: A series of curves for the rates of drainage of solutions of 0.25 per cent sodium lauryl sulfate and 0.1 per cent sodium lauryl

sulfate + lauryl alcohol were determined, starting with various fixed amounts of liquid in the foam. The data for a typical experiment for each solution are shown in figure 4, where the volumes of liquid left in the foam are plotted as a function of time.
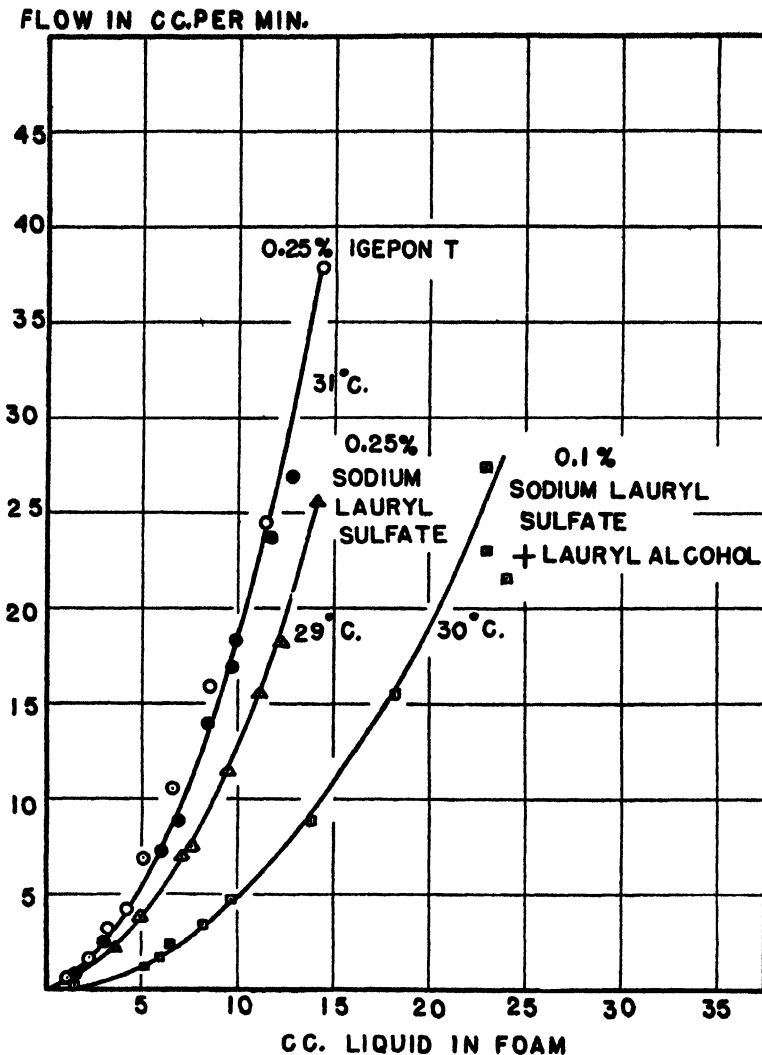
FIG. 2. Rate of flow of liquid through foam

As a much simplified approximation, let us consider the rates of flow in these drainage experiments analogous to the drainage of a liquid in a vertical capillary tube.

If L = the height of the liquid in the capillary at time t, and s the capillary rise due to surface tension, from Poiseuille's law we have:

$$\frac{dgr^2}{8\eta}\, \mathrm{d}t = \frac{L}{(L-s)}\, \mathrm{d}L \tag{2}$$

$$\int_0^t k\, \mathrm{d}t = \int_0^L \frac{L}{(L-s)}\, \mathrm{d}L \tag{3}$$

where

$$k = \frac{dgr^2}{8\eta}$$

$$kt = (L - L_0) + s \ln \frac{L-s}{L_0-s} \tag{4}$$

$$(L - L_0)\pi r^2 = v - v_0 = -V_d \tag{5}$$

where V = volume of liquid left in the foam at time t, V_0 = initial volume of liquid, and V_d = volume of liquid drained.
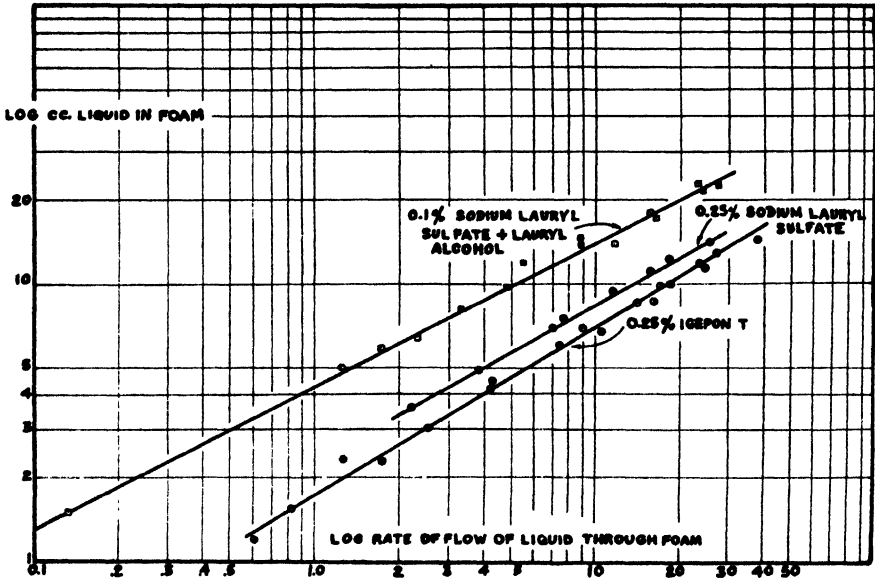
FIG. 3. Log cubic centimeters of liquid in foam *versus* log rate of flow of liquid through foam.

When s is small compared to L,

$$s \ln (L - s) = s \ln L \tag{6}$$

and $L_0 - s$ = constant.

Collecting all the constants in equation 4, this leads to an equation of the form

$$kt = V + a \log V + b \tag{7}$$

To test whether the data conform to such an approximate equation, a value of a was estimated from three points on the curve (figure 4) and then $(V + a \log V)$ plotted against t (figure 5). The points fall reasonably well on a straight line except for the lower and extreme upper portions of the curve. The data for
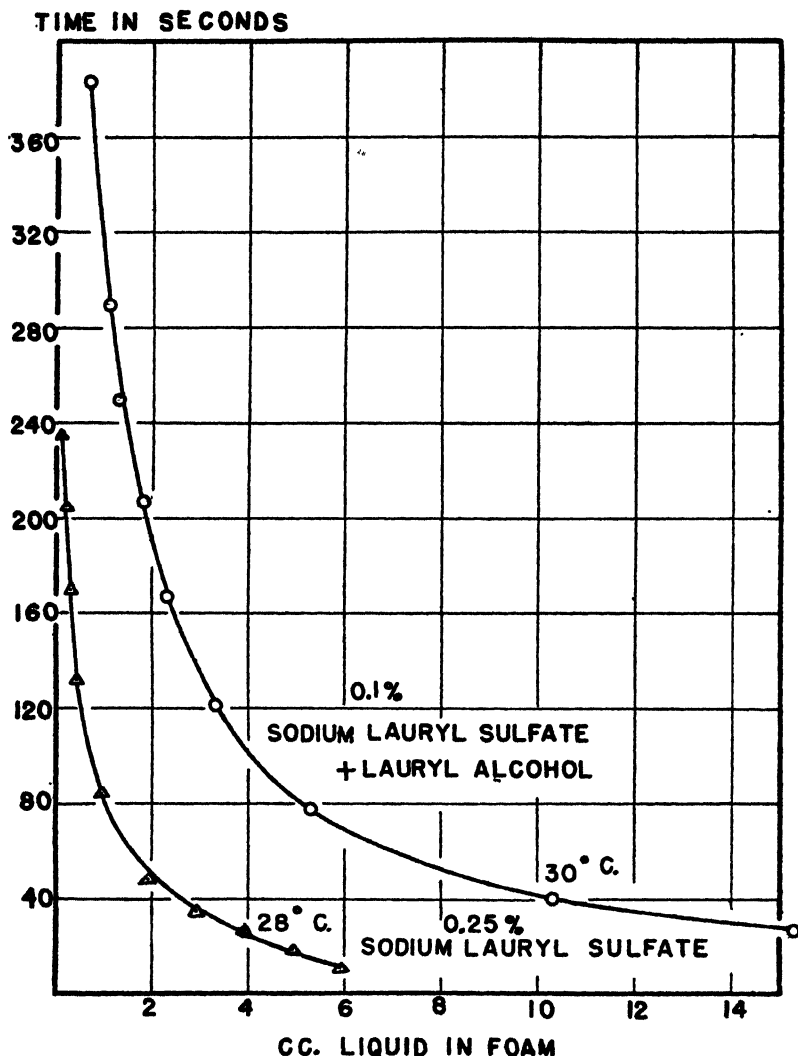
FIG. 4. Rate of drainage of liquid from foam

the two runs shown in figures 4 and 5 are typical of a series of ten experiments. This equation is merely a first step in considering the drainage characteristics of the foams tested, since the analogy to flow of a liquid in a tube would be expected to have limitations for foams.

From figure 5 the following equations are obtained for the curves shown in

figure 4: for the 0.25 per cent sodium lauryl sulfate solution where $V_0 = 6.9$ cc., $V - 21.7 \log V + 10.8 = 0.138t$; and for the 0.1 per cent sodium lauryl sulfate solution + lauryl alcohol, where $V_0 = 25.3$ cc., $V - 27.6 \log V + 18.2 = 0.057t$.

Electrolytic conductivity as a function of liquid in foam

In figure 6, the values of the electrolytic conductivity, $1/R$, corrected to 20°C., are shown against the volume of liquid in the foam for 0.25 per cent Igepon T solution + 1 per cent sodium sulfate. Each point on the line corresponds to a constant rate of flow and the direct measurement of the liquid held by the foam after stopping the flow of liquid into the column.
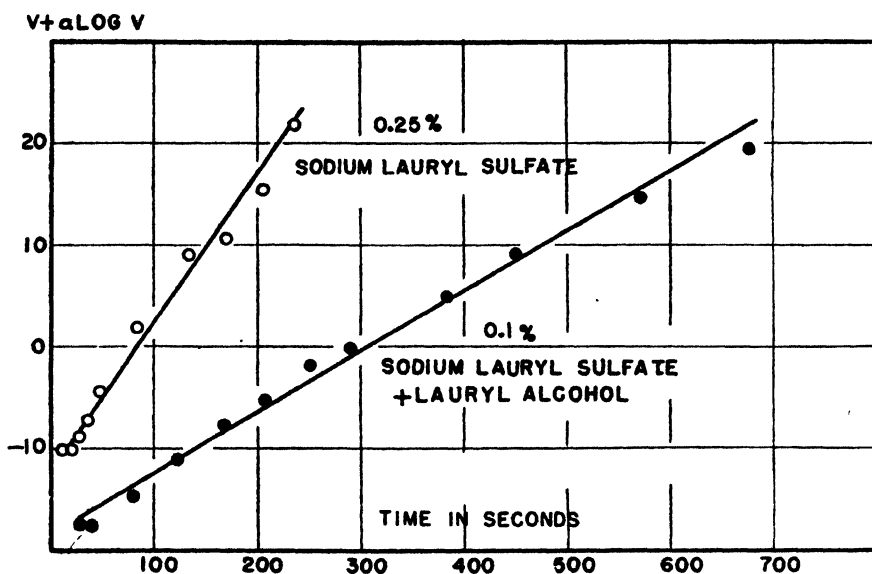
FIG. 5. $V + a \log V$ versus time (V = cubic centimeters of liquid in foam)

The bulk viscosities of the solutions used in the drainage and flow rate experiments with foams are given in table 1, as determined with an Ostwald viscometer.

Figure 7 shows sections of curves for the rate of flow of liquid as a function of the volume of liquid in the foam for 0.1 per cent sodium lauryl sulfate in 1 per cent sodium sulfate at 20°, 30°, and 40°C. and for 0.1 per cent sodium lauryl sulfate in 1 per cent sodium sulfate with glycerol added to make the bulk viscosity 1.78 centipoises at 25°C., and for 0.1 per cent sodium lauryl sulfate + lauryl alcohol at 25°C. The last solution has a bulk viscosity of 1.16 centipoises at 25°C., a value which is considerably lower than the solution containing glycerol, but the flow rates through the foam are as much as 30 per cent lower.

The rates of flow are shown in figure 8 for 0.25 per cent Igepon T at 10°, 20°, 30°, and 40°C. and for 0.25 per cent solutions of commercial sulfated coconut oil monoglyceride. The bulk viscosities of these two solutions are the same (within
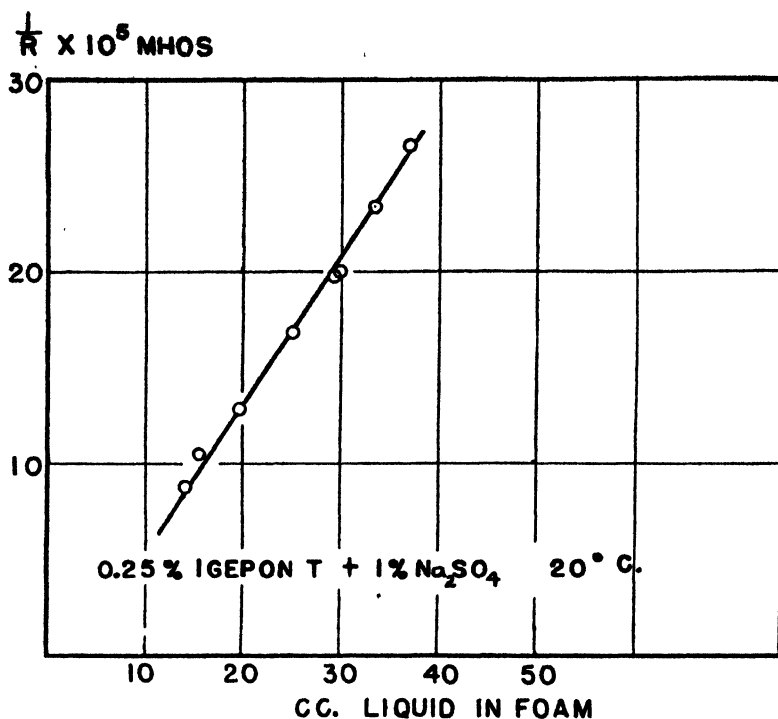
FIG. 6. Electrolytic conductivity *versus* volume of liquid in foam

TABLE 1

Bulk viscosities of solutions (in centipoises at temperatures given)

SOLUTION	10°C.	20°C.	25°C.	28°C.	29°C.	30°C.	31°C.	40°C.
0.25 per cent Igepon T (figures 2 and 3)...							0.81	
0.25 per cent sodium lauryl sulfate (figures 2 and 3)......				0.85	0.83			
0.1 per cent sodium lauryl sulfate + lauryl alcohol (figures 2, 3, 4) ...						1.42		
0.1 per cent sodium lauryl sulfate + lauryl alcohol (figure 7)........			1.16					
0.1 per cent sodium lauryl sulfate + 1 per cent sodium sulfate (figures 7 and 9)..	1.32	1.01				0.81		0.67
0.25 per cent Igepon T + 1 per cent sodium sulfate (figures 8 and 9). ..	1.31	1.01				0.82		0.67
0.25 per cent Syntex M + 1 per cent sodium sulfate (figures 8 and 9)..	1.32	1.02				0.82		0.67
Water*.............................	1.31	1.01	0.89	0.84	0.82	0.80	0.78	0.65

* International Critical Tables, Volume V, page 10.

1 per cent) at any given temperature (see table 1), but the rate of flow through the foam, for 30 cc. of liquid held in the foam at 20°C., is about 62 per cent lower for the Syntex M solution than for the Igepon T solution. In figures 7 and 8
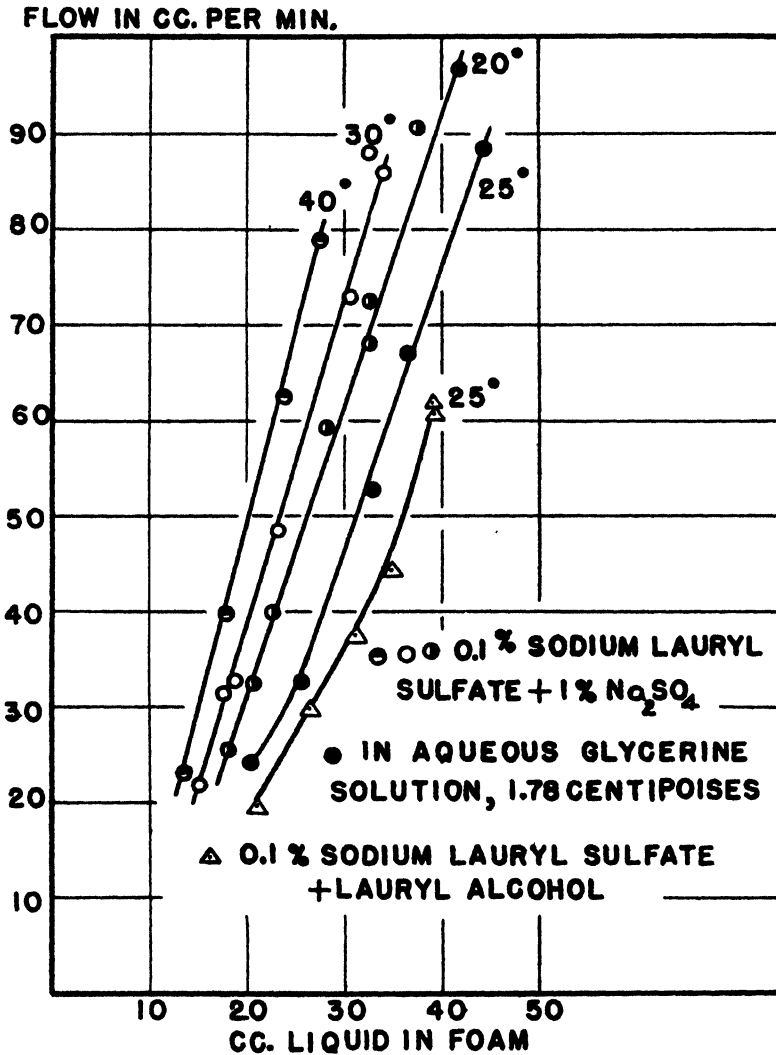
FIG. 7. Rate of flow of liquid through foam

only sections of the rate curves have been measured to show the greatest differences in flow rates.

Temperature effect on rate of flow of liquid through foam

Figure 9 indicates the rate of flow of liquid for several of the solutions at two fixed amounts of liquid held in the foam at temperatures from 10° to 40°C.
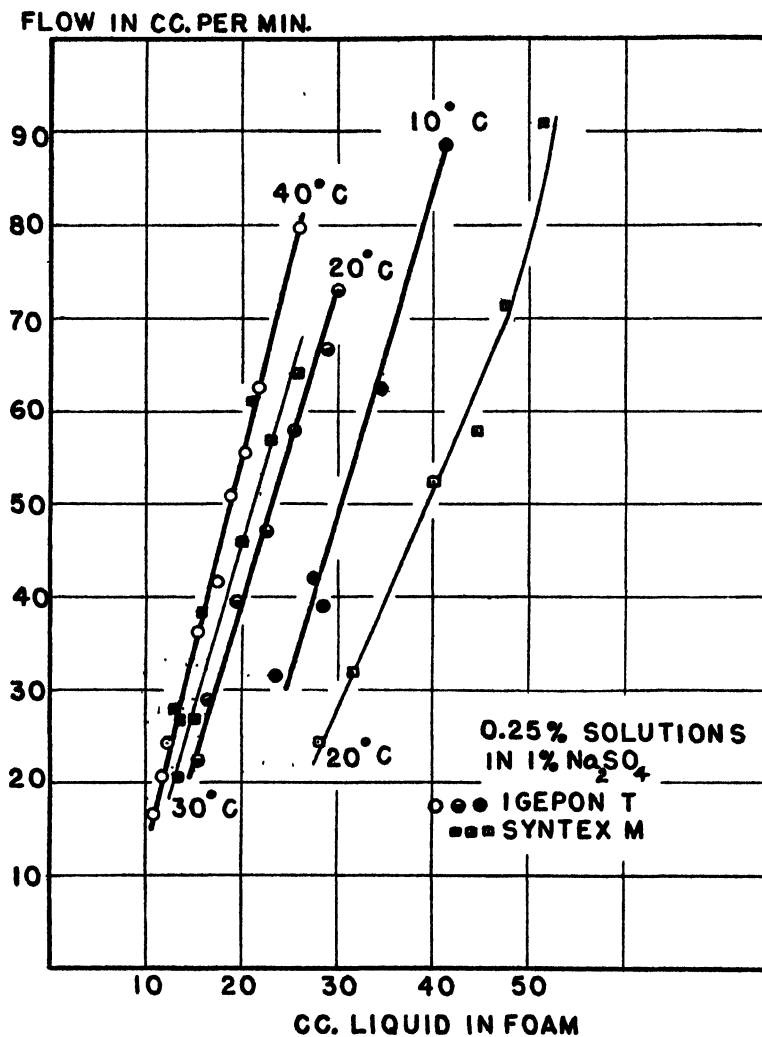
FIG. 8. Rate of flow of liquid through foam
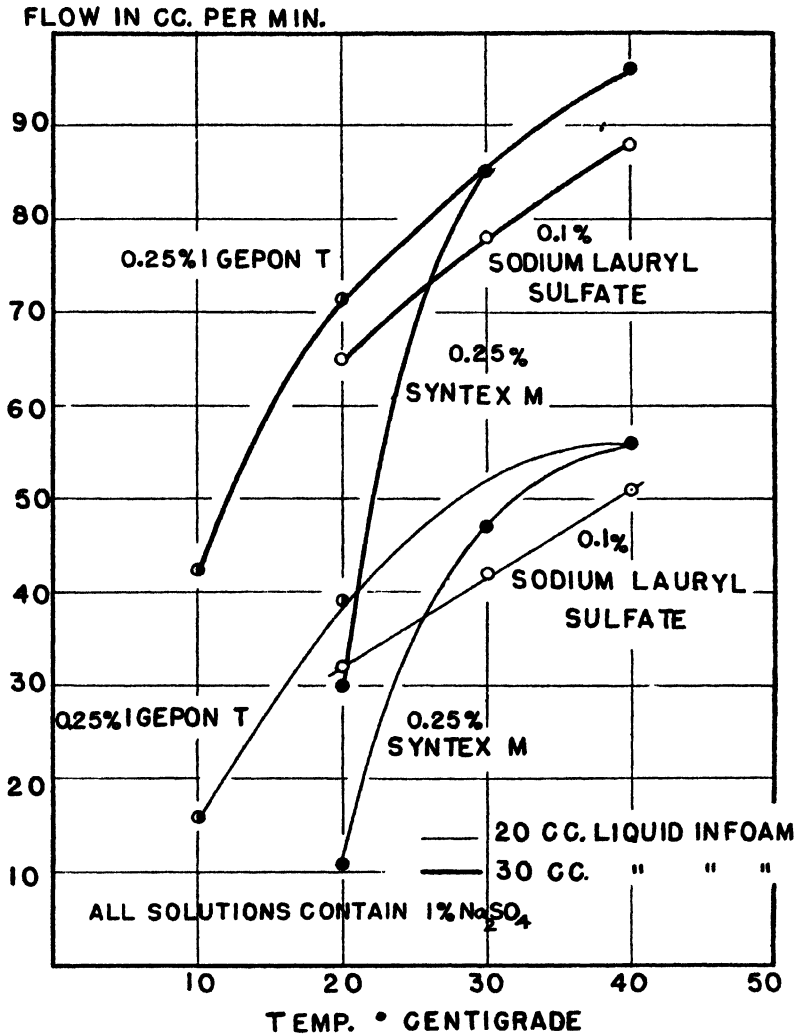
FIG. 9. Temperature effect on rate of flow of liquid through foam

Effect of bubble size on rate of flow of liquid through foam

An indication of the effect of changing the bubble size is shown by following the rate of flow of liquid through foams made with 0.1 per cent sodium lauryl sulfate + lauryl alcohol. This is shown in figure 10. The large bubbles which were made under the same conditions as in the other experiments referred to were made at a rate of flow of air of 45.9 cc. per minute and had a volume of 0.017 cc. per bubble. The smaller bubbles were prepared at a rate of air flow of 2.95 cc. per minute and had a volume of 0.0026 cc. per bubble.
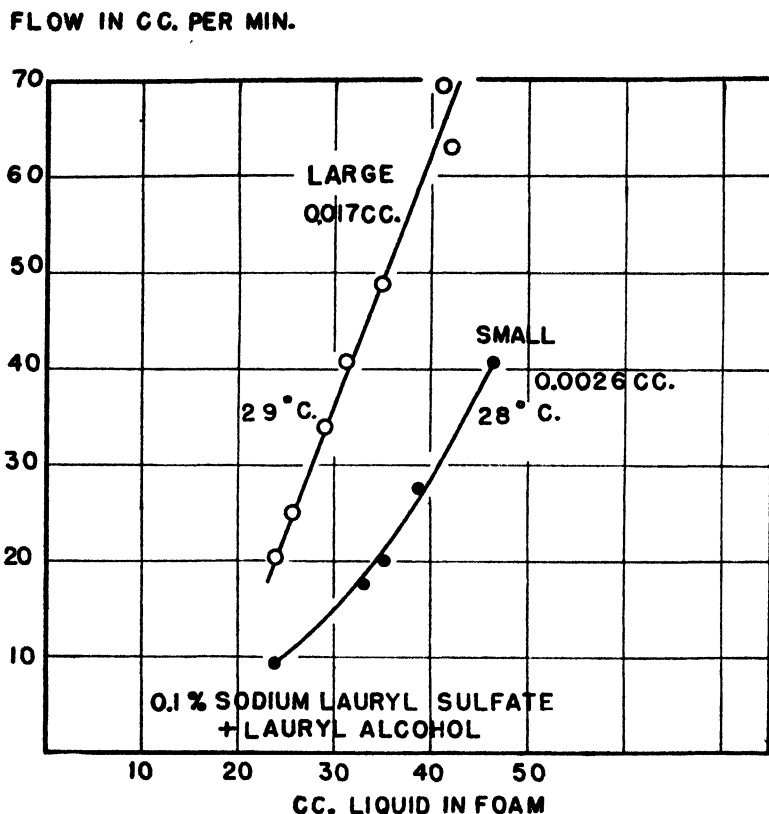
FIG. 10. Rate of flow of liquid through foam for two sizes of bubbles

DISCUSSION AND CONCLUSIONS

The rate of flow of liquid through foams of relatively uniform bubble size can be expressed by an equation of the form $y = \alpha x^n$, where y is the rate of flow of liquid through the foam, and x is the volume of liquid in the foam.

The rates of drainage of liquid through foams can be approximated by an equation of the type obtained from considering the analogous but much simplified flow of liquid in a vertical capillary. This type of equation holds fairly

well for a series of experiments starting with various amounts of liquid in the foam. The analogy is not to be considered rigorous, since for the flow of liquid through a foam there are limitations not involved in the flow through a single capillary of fixed dimensions. The foam network apparently is a series and parallel arrangement of flow channels. During foam drainage the effective radius of the flow channels changes, and such changes would be included in a change of the equivalent height of liquid in a capillary. We do not consider that the approximate equation gives a sufficient description of the drainage characteristics of the foams studied, but it may be useful as a first approach to such properties.

Differences in the rates of flow of liquid through a foam in figure 7 show a progressive decrease in the rate of flow for a solution of 0.1 per cent sodium lauryl sulfate containing 1 per cent sodium sulfate when the temperature is changed from 40° to 30° to 20°C. This may be explained by the higher bulk viscosity of the solution at the lower temperature (table 1). When the bulk viscosity is increased by using glycerol in the solution, a corresponding decrease in the rate of flow is obtained. On the other hand, when lauryl alcohol is added to the solution of sodium lauryl sulfate, the bulk viscosity of the solution (1.16 centipoises at 25°C.) is still less than that of the solution containing glycerol (1.78 centipoises at 25°C.), but the rate of flow of liquid through the foam is decreased. In this case the decreased flow is attributed to increased surface viscosity of the liquid at the interface.

The same kind of differences is indicated for solutions of Igepon T and Syntax M (figure 8), where the bulk viscosities are the same (within 1 per cent) at a particular temperature. The relatively slower flow for the Syntex M solution is again due to the higher surface viscosity for this solution.

When the other factors are the same, the position of the curves may be considered to be determined by both the surface as well as the bulk viscosity. Consequently, if two solutions with the same bulk viscosities have the same flow curves through the foam, the surface viscosities are probably the same.

The temperature effects on the flow rates (figure 9) have been shown to vary considerably for different solutions. In the range from 20° to 30°C., there is a sharp increase in the flow rate for the solution of Syntex M with added sodium sulfate where surface viscosity is relatively high, when compared to solutions of sodium lauryl sulfate and Igepon T with added sodium sulfate. It appears that differences in flow characteristics through foam are more pronounced at lower temperatures.

It has been seen that decrease in bubble size will decrease the rate of flow of liquid through the foam, and these changes become relatively greater at higher rates of flow or larger amounts of liquid in the foam. For two bubble sizes whose volume ratios were about 6.5 to 1, the rates of flow differed by as much as a ratio of 2.5 to 1. This emphasizes the importance of maintaining uniform bubble size.

From these data, it seems that methods of evaluating foam stability (1, 3, 5, 6) entirely from observations of relative foam drainage of liquid are not generally

valid and can be misleading for several reasons. The rate of flow of liquid through foam is influenced by the size of the bubbles and the bulk and surface viscosities, so that relative drainage rates do not evaluate foam stability under the same conditions, when the bubble size is not controlled or is changing in an unknown way, or if the surface and bulk viscosities vary. Foam drainage is analogous to the creaming of an emulsion, which is not a measure of emulsion stability. Similarly, drainage rates of liquids from foams cannot be considered as an indication of relative foam stability. Furthermore, in order to interpret relative foam drainage rates when breakdown occurs, it is desirable to know the flow characteristics of the foams when breakdown does not take place.

A number of foams drain completely to "black" films without breakdown, and these foams may be wetted again by allowing the solution from which they were formed to flow through them. Other foams show marked coalescence long before drainage is complete. Foam drainage can be a prerequisite, but is not necessarily sufficient to lead to foam breakdown.

In a recent paper, A. P. Brady and S. Ross (2) have mentioned some of these limitations which preclude the use of foam drainage data as a guide to foam stability. However, their treatment presumably does not include those cases where surface viscosity is an important factor.

From these considerations, it is evident that measurements of foam drainage alone cannot be interpreted in terms of foam stability. For example, if we know that two foams both break down on draining, then the drainage rates may be considered as a function of relative stability only providing the critical thickness for coalescence and collapse are the same in both cases. We do not agree with Arbuzov and with the earlier papers of S. Ross and others (1, 3, 5, 6) that the rate of foam drainage in general can be interpreted in terms of foam stability, unless other specific information concerning the stability of the foam is utilized.

SUMMARY

1. The flow characteristics have been studied of liquid in foams of relatively uniform bubble size and uniform liquid concentration without concomitant foam breakdown.

2. The rates of drainage of liquid from these foams have been measured and shown to approach an approximate simplified equation corresponding to liquid flow in a vertical capillary.

3. The rates of flow of liquid through these foams have been measured as a function of the liquid held in the foam. An empirical equation in accord with these data is given.

4. The rates of flow of liquid through foams decrease with increase in both surface and bulk viscosities as well as for smaller bubble sizes.

5. Differences in flow characteristics through stable foams are more pronounced at certain temperatures.

6. Attempts to evaluate foam stability from foam drainage rates which have been reported in the literature are not considered generally valid.

The writers wish to acknowledge and express their appreciation to George V. Scott for carefully carrying out a large number of the measurements reported.

REFERENCES

(1) ARBUZOV, K. N., AND GREBENSHCHIKOV, B. N.: J. Phys. Chem. (U.S.S.R.) **10**, 32 (1937).
(2) BRADY, A. P., AND ROSS, S.: J. Am. Chem. Soc. **66**, 1348 (1944).
(3) CLARK, G. L., AND ROSS, R.: Ind. Eng. Chem. **32**, 1594 (1940).
(4) DREGER, E. E., KEIM, J. I., MILES, G. D., SHEDLOVSKY, L., AND ROSS, J.: Ind. Eng. Chem. **36**, 610 (1944).
(5) ROSS, S.: J. Phys. Chem. **47**, 266 (1943).
(6) ROSS, S.: Ind. Eng. Chem., Anal. Ed. **15**, 329 (1943).

THE SIGNIFICANCE OF THE CONTACT ANGLE IN RELATION TO THE SOLID SURFACE   .

DANIEL C. PEASE

The Hopkins Marine Station of Stanford University, Pacific Grove, California

Contact-angle measurements have been a major experimental approach to many problems concerned with the solid–liquid interface. The well-known relation of contact angle to "work of adhesion" was developed by Dupré in 1869 (2), on the basis of the earlier work of Young in 1805 (4). Young put forward the relationship

$$W_{SL} = \gamma_{LA}(1 + \cos\theta)$$

where W_{SL} is the work of adhesion between solid and liquid, γ_{LA} is the surface tension of the liquid–air interface, and θ is the contact angle of the liquid and solid.

There are, however, three different contact angles which can be measured. Bartell and his group in recent years have developed particularly refined techniques for determining "advancing" and "receding" contact angles (for the literature, see reference 1). Fundamentally these are the same angles as are measured when the solid surface is very carefully advanced or removed from the fluid. Their reality has been established, and each is entirely specific for any system in question. In addition, there is the "equilibrium" contact angle, ordinarily having an intermediate value. Techniques for the measurement of the latter are less refined but, in the author's experience, measurements are reproducible within ±2°, using essentially the method of Nietz (3). In this procedure a coated plate is simply inclined until the air–liquid interface is perfectly plane, and the angle is recorded directly. Slight jarring or vibration is necessary to be sure that the air–liquid interface slips over the solid surface

(from the advancing or receding position) and assumes the equilibrium position. A little experience will convince anyone of the reality and specificity of such a measurement, which is also a constant of any given system.

The question at once arises as to the significance of these three measurable entities. How are they related to the work of adhesion and the wetting characteristics of the solid? Apparently no one has questioned the meaning of Young's equation, although there has been some debate about which angle should be used to calculate the work of adhesion. It is the author's thought that the real significance of contact-angle measurements has been overlooked, and that the overall mean work of adhesion cannot be calculated from any one of them.

It is perfectly legitimate for our purposes to regard most solid hydrophobic surfaces as being mosaics of polar and non-polar groups, arranged with regularity on a crystal face, and with a statistical distribution on an amorphous solid surface. The air–liquid interface in contact with the solid is very nearly a one-dimensional system. The junction is really a line of tension acting on the fluid surface. It is affected by the properties of the different groups of the solid surface which the line happens to cross. Any work of adhesion calculated from the contact angle will be a mean value of different tensions which are arranged linearly. The component parts of a simple system would include the works of adhesion of polar groups, W_p, and non-polar groups, W_{np}, applied over the relative linear distances or lengths each type of group occupies along the line of the three-phase junction, L_p and L_{np}, respectively, so that

$$W_{SL} = W_p L_p + W_{np} L_{np}$$

However, the three-phase line of junction might assume an infinite number of parallel positions on the solid surface. In so doing, it could ordinarily cross a varying number of polar and non-polar groups, depending upon the particular surface configuration of the solid. Varying mean works of adhesion would result from these different possible positions.

When the air–liquid interface is in equilibrium with the solid surface, the mean work of adhesion, W_e, must be an expression of a minimal energy value. The mean work of adhesion will then be as low as the configuration of the solid surface allows, and the contact angle will tend to be large. These conditions will be realized when the three-phase junction line passes across the largest possible number of non-polar groups, and avoids as many polar groups as possible. Then L_p/L_{np} is as small a fraction as can be in accordance with the distribution pattern of groups on the solid surface. Thus the application of Young's equation to the equilibrium contact angle is not at all a measure of the overall mean work of adhesion between solid and liquid. Instead, W_e is the smallest possible mean work of adhesion that can exist along any one of many possible parallel lines that might be drawn across the solid surface.

When considering the receding contact angle we are dealing with a wet surface that must be swept dry. Work must be applied to overcome the maximum mean work of adhesion, W_r, that can exist along any parallel line that the air–liquid interface can assume. When the work applied equals W_r, the interface begins to move. The same general relationship holds for W_r as for W_e

above, but with this fundamental difference,—that now L_p/L_{np} is as large a ratio as can exist in conformity with the configuration of the solid surface. As L_p/L_{np} is increased, so, of course, the mean work of adhesion is increased while the contact angle is decreased. We see that the application of Young's equation to the receding contact angle measures the largest possible mean work of adhesion along one of many possible parallel lines.

To advance the air–liquid interface, work must be applied to wet the solid surface unless the work of adhesion is at least equal to the work of cohesion (when the contact angle is 0°). The work applied will have to overcome the greatest possible mean resistance. The resistance to movement will equal the difference between the work of cohesion, W_{co}, and the work of adhesion. The resistance will be greatest when the mean work of adhesion is minimal, W_e. Thus the applied work must equal $W_{co} - W_e$. The application of Young's equation to the advancing contact angle would give the numerical value of this expression.

It is to be noted that when a mixed solid surface in contact with water is being dealt with, the hydrophobic groups of the solid surface play a major rôle in the determination of the equilibrium and advancing contact angles, while hydrophilic groups dominate the picture in considering the receding contact angle.

In actual practice, certain correction factors would be obvious. One would rarely, if ever, be dealing with as simple a solid surface as has been postulated. Also, we have considered the three-phase junction as a one-dimensional system, a procedure which is not strictly accurate. A complex correction would be necessary to take into account forces acting over molecular distances.

From these formulations one conclusion seems outstanding. The overall mean work of adhesion between liquid and solid cannot be determined by contact-angle measurements except, perhaps, in a few very special cases. The fundamental difficulty is that the line of junction of the three phases is essentially a one-dimensional system. The mean work of adhesion can and will vary with the various possible parallel positions of that line on the solid surface.

SUMMARY

Since "work of adhesion" values may be calculated from equilibrium, receding, and advancing contact angles of an air–liquid interface in contact with a solid, it has been deemed advisable to consider what these values really signify. It is emphasized that the junction of the air–liquid interface with the solid surface is fundamentally a one-dimensional system. This line of junction can occupy various possible parallel positions on the plane of the solid surface, and different positions allow different mean works of adhesion depending upon the configuration of the different groups exposed on the solid surface.

The equilibrium contact angle is related directly to the line of least possible mean work of adhesion that the three-phase junction can assume.

The receding contact angle is related directly to the line of greatest possible mean work of adhesion.

The advancing contact angle is dependent upon the greatest possible amount

of work necessary to wet the solid surface. This, in turn, is inversely related to the least possible mean work of adhesion.

REFERENCES

(1) BARTELL, F. E., AND HATCH, G. B.: J. Phys. Chem. **39,** 11 (1935).
(2) DUPRÉ: *La théorie méchanique de la chaleur* (1869).
(3) NIETZ, A. H.: J. Phys. Chem. **32,** 255 (1928).
(4) YOUNG, T.: Phil. Trans. Roy. Soc. **95,** 65 (1805).

A CLASSIFICATION OF STABLE NUCLEI[1]

J. D. KURBATOV

Department of Physics, The Ohio State University, Columbus 10, Ohio

INTRODUCTION

The classification of stable nuclei, that is, their division into sequences with common physical characteristics, has not been suggested for species throughout the entire range of mass numbers. Considerable work of this kind has, however, been done for nuclei of mass numbers less than 40, since the pertinent data are known mainly for light nuclei (12, 13, 70, 71).

The experimental material available for the present work, accordingly, remains deficient in desired data, particularly for heavy nuclei. Such a situation indicates that this classification will be subject to a succession of changes; improvements undoubtedly will follow with the appearance of new data. Nevertheless, the regularities in nuclear formation observed with the aid of this system give the whole project some justification and impetus for presentation.

Several authors have proposed, from various considerations, to picture the structure of light nuclei on the basis of the alpha-particle model (20). The common characteristics, such as binding energy, Coulomb forces, the statistics, and moments to some extent justify this application of the alpha-particle model to even-even-equal nuclei.

However, the attempt to present other light nuclei as

$$k\alpha + (\alpha \pm 1 \text{ or } 2p) \quad \text{or} \quad k\alpha + (\alpha \pm 1 \text{ or } 2n)$$

has not been successful in giving a picture of property regularities.

Building up nuclei by the addition of primary particles at the rate of one to form individual species by two methods:

$$v + H + v + H \quad \text{or} \quad v + v + H + H$$

in which v is a neutron and H is a proton, did not lead to continuity of formation because of the appearance and increase with mass number of extra neutrons (5).

The latter factor created a problem of the "disposal" of extra neutrons in some form, since no self-evident relation of isotopic number and mass number could be

traced. As a result, the possibility of considering extra neutrons as cementing material for clusters of particles has been rejected.

In general, it can be said that the process of building up nuclei by the addition of one particle to the previous species does not exhibit any valuable information on the periodicity in their properties. Consequently it has been admitted that some framework of heavy particles may exist. This is mainly from the consideration that such complicated systems as nuclei actually can be very much simplified if particle clusters are found to have some physical meaning (20). Therefore, the suggestion has been made to "dissolve" at least the unfilled part of the alpha particle with some of the extra neutrons. The simplest case, the $_3Li^7$ nucleus, has been tested as an alpha-triton (H^3) model (24). The last approach can be supported now by the fact that physical characteristics are common for large sequences of nuclei if built up of combinations of three and four mass units. Therefore, the preliminary division of all nuclei into series again became of some significance.

The known stable nuclei are usually listed as isotopes of elements in the consecutive order of their charge numbers (33, 34). In some cases, the nuclei are given in sequences of their isotopic numbers. The periodicity of nuclear properties, however, cannot be visualized well in either of the two forms, since the combination of protons and neutrons as a whole is the factor delineating the nuclei.

Hence, the problem in the classification of the stable nuclei is to reveal, simultaneously, the periodicity of common properties and the continuity of formation of nuclei. This can be accomplished by presenting the various combinations of protons and neutrons in some aggregated form.

PRIMARY COMBINATIONS OF NEUTRONS AND PROTONS

The proton–neutron composition of all the stable nuclei can be expressed as follows:

$$A \ \ = k(p2n) + l(2p2n) + q(n2p) \ ^2$$
$$A' \ = k'(p2n) + l'(2p2n)$$
$$A'' = k'' \ (p2n) + q''(n2p)$$

The aid of the groups of mass 3, in both their isobaric states, in addition to the group of mass 4 ($2p2n$), is significant in the classification as compared to other possible primary combinations.

Thus, up to mass 4, of eight possible proton–neutron combinations ($ap + bn$), three combinations can build up all the known species of stable nuclei, that is:

[2] The notation used throughout the paper is p for proton and n for neutron. In addition, no requirements were imposed to consider the existence of particles as alphas or tritons in the nucleus in "space separated" groups, since the classification is based on the periodicity of physical characteristics. For this reason the group of two protons and two neutrons is noted as ($2p2n$) in order to identify such a mass 4 combination and to distinguish it from the helium atom nucleus. Likewise, the two isobaric states of mass 3 in the nuclear structure are noted as ($p2n$) and ($n2p$) to distinguish them from atomic nuclei of $_1H^3$ and $_2He^3$. The mass number, charge, and mass are designated A, Z, and m, respectively. The isotopic number, that is, ($A - 2Z$) is noted as I, distinguishing it from the spin, I. The latter is given in $\hbar$ units. The magnetic moment in nuclear magnetons is designated as μ. The quadruple electric moment Q is given in 10^{-26} cm^2. The unconfirmed data of m, I μ, Q, and abundances are given in italics.

(1) $a = 0$, $b = 0$ leads to the even-even-equal series. These nuclei with their physical characteristics are given in Series 0, S_0.

(2) $a = 0$, $b = 1$ and (3) $a = 0$, $b = 2$. These two cases lead to the even-odd series, $(2k + 1)n + l(2p2n)$, in which $k = 0,1, \ldots 21$, and to the even-even-unequal series, $(2k + 2)n + l(2p2n)$, in which $k = 0,1,\ldots 21$. The first terms are isotopic numbers defining the separate groups in the series.

(4) $a = 1$, $b = 0$ does not form a series of stable nuclei. In the case in which $l = 0$, one stable nucleus, $_1H^1$, is known. However, this combination is represented by a number of radioactive nuclei.

(5) $a = 1$, $b = 1$ leads to four known odd-odd nuclei. Three of these are given as Series 1, S_1.

(6) $a = 1$, $b = 2$ leads to the odd-even series $(2k + 1)p2n + l(2p2n)$, given as Series 3, S_3, where the $(2k + 1)$ term is the isotopic number $k = 0,1, \ldots 21$; and to the even-even-unequal series, $(2k + 2)p2n + l(2p2n)$, S_2, where the $(2k + 2)$ term is the isotopic number $k = 0,1, \ldots 21$. Thus the third combination above is no longer required for the formation of the even-even-unequal series, S_2.

(7) $a = 2$, $b = 0$ represents no stable nuclei. One radioactive nucleus, $_6C^{10}$— $T = 8.8$ sec., is listed.

(8) $a = 2$, $b = 1$ does not form a series with groups of mass number 4 $(2p2n)$. When $l = 0$, one stable nucleus, $_2He^3$, is known. However, combination 8 together with combination 6 leads to the formation of: the odd-odd series (S_1) $(p2n + n2p) + l(2p2n)$, where $l = 0,1,2$; and the even-odd (S_4) series $(p2n + n2p) + (2k + 1)p2n + l(2p2n)$, where the $(2k + 1)$ term is the isotopic number $k = 0,1, \ldots 21$, and combinations 2 and 5 are no longer required.

The primary nuclear combinations and their characteristics are as follows:

	Z	0	1	2	
A		n	p		
1	m	$= 1.00897$ ($_0n^1$)	$= 1.00813$ (H^1)		
	μ	$= -1.935 \pm 0.02$	$= 2.790 \pm 0.002$	$I = 1/2$	(49, 38)
2			pn		
		$m = 2.01472 \pm 1$ (H^2)		$Q = 0.273$	(23, 38)
		$B.E. = 0.00237$		$I = 1$	
		$\mu = 0.8569$			(49)
3			$p2n$*	$n2p$	
		$m = 3.01705$ (H^3)	$= 3.01685 \pm 10$ (He^3)		
		$B.E. = 0.00902$	$= 0.00816$	$\Delta B.E. = 0.00086$	(35, 2)
		$\mu = 2.68$	$= -1.84$	$I = 3/2$	(52)
4				$2p2n$	
			$m = 4.00386 \pm 6$ (He^4)		
			$B.E. = 0.03034$		
			$\mu = 0$	$I = 0$	(34)

* Tritium, $_1H^3$, is radioactive with a half-life of 31 ± 8 yr., emitting electrons of 15 ± 3 kev. (47). The unstable nucleus $(p2n)$ of $_1H^3$ is converted to a stable nucleus $(n2p)$ of $_2He^3$ with a loss in binding energy of $= 0.00086$ m.u. It may be assumed that in heavier nuclei the $p2n$ group carries for stability the necessitated increase in binding energy. The mass given includes electrons of an atom.

PRINCIPLE OF CLASSIFICATION

The physical characteristics of nuclei, such as spin and magnetic moments, were taken as criteria for identification of the series.[3] The isotopic numbers of nuclei belonging to the same series are a continuous odd or even sequence. The nuclei of the same isotopic number of a series form a group which differ by and are built up by the addition of $2p2n$.

The following requirements, in addition, have been imposed in classification of nuclei: The first is that the mass number of the last nucleus of the group will not be higher than that of the first member of the following group. The second is that the differences in isotopic numbers between groups are equal and remain constant in a series. To fulfill the requirement in regard to the isotopic numbers and mass numbers it is necessary to separate Series 2 into four periods with $\Delta I = 8$ between adjoining groups of each period. The following division of nuclei results:

Protons and neutrons equal

SERIES 0 (S₀)	SERIES 1 (S₁)
Protons–neutrons even	Protons–neutrons odd
A single group with $I = 0, I = 0$ $\mu = 0$	A single group with $I = 0, I = 1$ μ is positive

Protons and neutrons unequal

SERIES 2 (S₂)	SERIES 3 (S₃)	SERIES 4 (S₄)
Protons–neutrons even–even	Proton–neutrons odd–even	Protons–neutrons even–odd
22 groups of consecutive even isotopic numbers $I = (2n + 2)$ $n = 0, 1, \dots 21$ $I =$ integer or 0	22 groups of consecutive odd isotopic numbers $I = (2n + 1)$ $n = 0, 1, \dots 21$ I is fractional μ mostly positive*	22 groups of consecutive odd isotopic numbers $I = (2n + 1)$ $n = 0, 1, \dots 21$ I is fractional μ negative and positive
Four periods: P2, P4, P6, P8	One period	One period

* $_{47}Ag^{107}$ and $_{47}Ag^{109}$ are listed with negative magnetic moments (26).

[3] The data on quadrupole electric moments remain insufficient in number to be used for identification of series.

Series O

Characteristics: even and equal number of protons and neutrons; consists of one group of eight nuclei; are most abundant species of respective elements with the exception of $_{18}A^{36}$; spin and magnetic moment are zero

MASS NUMBERS	NUCLEI	ISOTOPIC ABUN-DANCE	ABUN-DANCE RELATIVE TO EVEN-EVEN	NUMBER OF PARTICLES		CHARACTERISTICS OF NUCLEI	REFER-ENCE
				p	n		
		per cent	*per cent*				
12	$_6C^{12}$	98.9	100	6	6	$m = 12.00386 \pm 2$ B.E. $= 0.0987$ $\Delta B.E. = 0.0381$	(38)
16	$_8O^{16}$	99.76	99.80	8	8	$m = 16.00000$ B.E. $= 0.1368$ $\Delta B.E. = 0.0354$	
20	$_{10}Ne^{20}$	90.00	90.24	10	10	$m = 19.99881$ B.E. $= 0.1722$ $\Delta B.E. = 0.0411$	(B*, 48)
24	$_{12}Mg^{24}$	77.4	87.5	12	12	$m = 23.99189$ B.E. $= 0.2133$ $\Delta B.E. = 0.0397$	(48)
28	$_{14}Si^{28}$	89.6	95.5	14	14	$m = 27.98639$ B.E. $= 0.2530$ $\Delta B.E. = 0.0375$	(48)
32	$_{16}S^{32}$	95.1	95.7	16	16	$m = 31.98306$ B.E. $= 0.2905$ $\Delta B.E. = 0.0388$	(48)
36	$_{18}A^{36}$	0.31	0.31	18	18	$m = 35.97852$ B.E. $= 0.3293$ $\Delta B.E. = 0.0382$	(48)
40	$_{20}Ca^{40}$	96.97	97.11	20	20	$m = 39.9745$ B.E. $= 0.3675$	(48)

* Masses obtained by mass-spectrograph measurements are designated by letters in parentheses to signify the authors: (A) Aston, (B) Bainbridge, (D) Dempster, and (N) Nier. Otherwise the data are from transmutations. Isotopic abundances according to F. W. Aston (4).

All known stable nuclei, up to July, 1944, are included in the classification. However, since the purpose of the classification is to observe general regularities of properties and to note the deviation of species which do not fit the classification, there was no tendency to discard nuclei not fitting or to predict new ones to fill the gaps in groups.

Series 1

Characteristics: odd and equal number of protons and neutrons; consists of one group of three nuclei; spin is 1 and magnetic moment is positive

MASS NUMBER	NUCLEI	ISOTOPIC ABUNDANCE	NUMBER OF PARTICLES		CHARACTERISTICS OF NUCLEI	REFERENCE
			p	n		
		per cent				
6	$_3\text{Li}^6$	7.5	3	3	$m = 6.01684 \pm 11$	(2)
					$B.E. = 0.0345$	
					$\Delta B.E. = 0.0352$	
					$\mu = 0.8218$	(49)
					$I = 1$	
10	$_5\text{B}^{10}$	20.0	5	5	$m = 10.01579 \pm 22$	(1, 2)
					$B.E. = 0.0697$	
					$\Delta B.E. = 0.0425$	
					$\mu = 0.5977$	(49)
					$I = 1$	
14	$_7\text{N}^{14}$	99.62	7	7	$m = 14.00753 \pm 3$	(38)
					$B.E. = 0.1122$	
					$\mu = 0.4025$	(49)
					$I = 1$	

In Series 0, $_6\text{C}^{12}$ is listed as the first nucleus, since $_4\text{Be}^8$ has not been observed to the extent of 10^{-5} that of $_4\text{Be}^9$ and is unstable against alpha emission (69). In Series 1, $_3\text{Li}^6$ is given as the first nucleus. Thus, these two series differ from previous lists of the same nuclear sequences in the absence of $_2\text{He}^4$ and $_1\text{H}^2$, which are brought in here as primary combinations. The consecutive nuclei in Series 0 and 1 are built up by the addition of the group $2p2n$.[4]

ODD-EVEN AND EVEN-ODD NUCLEI

The physical characteristics of Series 3 and 4 are taken up here, in advance of Series 2, since the periodicity of the properties of Series 2 can be drawn up, with some advantage, on the basis of the regularities observed in the odd mass number nuclei. In addition, a comparative and simultaneous observation of the properties of Series 3 and 4 is found to be helpful in disclosing the deviations of some nuclei from the places where they are expected by the classification (see table 1).

As can be seen from Series 3 and 4, all consecutive mass numbers starting with 7 and ending with 209 are represented. Four stable isobars of these two series are known; therefore, the total number of species is 106 and of these, 51 are odd-even and 55 are even-odd.

The difference in mass number between the last nuclei of Groups 3, 4, 5, 7, 8, 10, 13, 18, 19, 21 and the first nuclei of the following groups in Series 3 is 2, corresponding to the difference in isotopic numbers. Likewise, the difference

----
[4] This does not impose the necessity of considering the nuclei of Series 0 as built up of "alpha particles" alone and those of Series 1 of "alpha particles" and "deuterium", since $(p2n\text{-}n2p)$ groups as models can be applied to the first nuclei, $_3\text{Li}^6$ and $_6\text{C}^{12}$, in these series.

TABLE 1

Series 3

Characteristics: odd number of protons and even number of neutrons; consists of 22 groups of consecutive odd isotopic numbers, the groups having from 1 to 43 extra neutrons; the known spins are fractional; the known magnetic moments are mainly positive

Group 1: $I = A - 2Z = 1$
Nine nuclei terminated by radioactive $_1H^3$ and $_{21}Sc^{43}$

Series 4

Characteristics: even number of protons and odd number of neutrons; consists of 22 groups of consecutive odd isotopic numbers, the groups having from 1 to 43 extra neutrons; the known spins are fractional; the known magnetic moments are negative and positive

Group 1: $I = A - 2Z = 1$
Seven nuclei terminated by radioactive $_{18}A^{37}$

MASS NUMBER	NUCLEI AND ISOTOPIC ABUNDANCE	NUMBER OF PROTONS AND NEUTRONS p	n	CHARACTERISTICS OF NUCLEI	NUCLEI AND ISOTOPIC ABUNDANCE	ABUNDANCE RELATIVE TO EVEN-ODD	NUMBER OF PROTONS AND NEUTRONS p	n	CHARACTERISTICS OF NUCLEI
	per cent				*per cent*	*per cent*			
7	$_3Li^7$　92.5	3	4	$m = 7.01814 \pm 11\ (2)^*$ $B.E. = 0.0421$ $\Delta B.E. = 0.0399$ $I = 3/2$ $\mu = 3.25\ (50,\ 37)$ $Q = -2.7\ (68)$					
9					$_4Be^9$　100	100	4	5	$m = 9.01494 \pm 13\ (2)$ $B.E. = 0.0625$ $\Delta B.E. = 0.0415$ $I = 3/2$ $\mu = -1.176\ (30)$ $Q = 3.4\ (68)$
11	$_5B^{11}$　80	5	6	$m = 11.01244 \pm 19\ (1)$ $B.E. = 0.0820$ $\Delta B.E. = 0.0418$ $I = 3/2$ $\mu = 2.682\ (42)$ $Q = 1.3\ (68)$					

13

15		$6C^{13}$			$m = 13.00761 \pm 15$ (35)
					$B.E. = 0.1040$
					$\Delta B.E. = 0.0373$
					$I = 3/2$ (1/2?)
					$\mu = 0.700 \pm 2$ (18)
					$Q = 0$ (68)

$_7N^{15}$ 0.38   8   7

$m = 15.00489 \pm 20$ (35)
$B.E. = 0.1238$
$\Delta B.E. = 0.0346$
$I = 1/2$
$\mu = 0.280 \pm 1$ (74)
$Q = 0$ (68)

7   6   100   1.1

17

$_8O^{17}$ 0.04   100   8   9

$m = 17.00450 \pm 7$ (35)
$B.E. = 0.1413$
$\Delta B.E. = 0.0385$

$_9F^{19}$ 100   10   9

$m = 19.00452 \pm 17$ (35)
$B.E. = 0.1584$
$\Delta B.E. = 0.0419$
$I = 1/2$
$\mu = 2.622$ (50)

19

$_{10}Ne^{21}$ 0.27   100   10   11

$m = 21.00018$ (48)
$B.E. = 0.1798$
$\Delta B.E. = 0.0416$

$_{11}Na^{23}$ 100   11   12

$m = 22.99680$
$B.E. = 0.2003$
$\Delta B.E. = 0.0414$
$I = 3/2$
$\mu = 2.216$ (31)

21

$_{12}Mg^{25}$ 11.5   100   12   13

$m = 24.99277$ (48)
$B.E. = 0.2214$
$\Delta B.E. = 0.0401$

23

25

TABLE 1—Continued

Group 1: I = A − 2Z = 1—Continued

MASS NUMBER	NUCLEI AND ISOTOPIC ABUNDANCE (per cent)	p	n	CHARACTERISTICS OF NUCLEI	NUCLEI AND ISOTOPIC ABUNDANCE (per cent)	ABUNDANCE RELATIVE TO EVEN-ODD (per cent)	p	n	CHARACTERISTICS OF NUCLEI
27	$_{13}Al^{27}$ 100	13	14	$m = 26.98960$ (48) $B.E. = 0.2417$ $\Delta B.E. = 0.0392$ $I = 5/2$ $\mu = 3.628$ (41)					
29					$_{14}Si^{29}$ 6.2	100	14	15	$m = 28.98685$ (48) $B.E. = 0.2615$ $\Delta B.E. = 0.0885$
31	$_{15}P^{31}$ 100	15	16	$m = 30.98457$ (48) $B.E. = 0.2809$ $\Delta B.E. = 0.0377$					
33					$_{16}S^{33}$ 0.74	100	16	17	$m = 32.98260$ (48) $B.E. = 0.3000$
35	$_{17}Cl^{35}$ 75.4	17	18	$m = 34.98107$ (48) $B.E. = 0.3186$ $\Delta B.E. = 0.0401$ $I = 5/2$ $\mu = 1.365 \pm 5$ (29)					
39	$_{19}K^{39}$ 93.4	19	20	$m = 38.97518$ (48) $B.E. = 0.3587$ $I = 3/2$ $\mu = 0.391$ (31)					

Group 2: I = 3

Three nuclei

37	$_{17}Cl^{37}$	24.6	17	20	$m = 36.97829$ (48) $B.E. = 0.3393$ $\Delta B.E. = 0.0386$ $I = 5/2$ (63) $\mu = 1.135$ (64)
39					
41	$_{19}K^{41}$	6.6	19	22	$m = 40.9739$ (48) $B.E. = 0.3779$ $\Delta B.E. = 0.0380$ $I = 3/2$ $\mu = 0.22$ (44)
43					
45	$_{21}Sc^{45}$	100.0	21	24	$m = 44.9701$ (48) $B.E. = 0.4159$ $I = 7/2$ $\mu = 4, 4, 4, 8$ (28)
47					

Group 3: I = 5

Four nuclei terminated by radioactive $_{21}Sc^{47}$ and $_{31}Ga^{67}$

49					

Group 2: I = 3

An incomplete group of two nuclei terminated by radioactive $_{16}S^{35}$ and $_{24}Cr^{51}$

39	$(_{18}A^{39})$	Unknown		18	21)
43	$_{20}Ca^{43}$	0.145	100	20	23
47	$_{22}Ti^{47}$	7.75	58.4	22	25	$m = 42.9723$ (48) $B.E. = 0.3966$

Group 3: I = 5

Four nuclei terminated by radioactive $_{20}Ca^{45}$ and $_{30}Zn^{65}$

49	$_{22}Ti^{49}$	5.52	41.6	22	27	$m = 48.9664$ (48) $B.E. = 0.4547$ $\Delta B.E. = 0.0434$

TABLE 1—Continued

MASS NUMBER	Group 3: I = 5—Continued				Group 3: I = 5—Continued				
	NUCLEI AND ISOTOPIC ABUNDANCE (per cent)	NUMBER OF PROTONS AND NEUTRONS p	n	CHARACTERISTICS OF NUCLEI	NUCLEI AND ISOTOPIC ABUNDANCE (per cent)	ABUNDANCE RELATIVE TO EVEN-ODD (per cent)	NUMBER OF PROTONS AND NEUTRONS p	n	CHARACTERISTICS OF NUCLEI
51	$_{23}V^{51}$ 100	23	28	$m = 50.9587$ (48) $B.E. = 0.4795$ $\Delta B.E. = 0.0276$					
53					$_{24}Cr^{53}$ 9.43	100	24	29	$m = 52.9572$ (48) $B.E. = 0.4981$ $\Delta B.E. = 0.0304$
55	$_{25}Mn^{55}$ 100	25	30	$m = 54.9653$ (D, 48) $B.E. = 0.5071$ $I = 5/2$ $\mu = 3$ (14)					
57					$_{26}Fe^{57}$ 2.1	100	26	31	$m = 56.9609$ (48) $B.E. = 0.5285$
59	$_{27}Co^{59}$ 100	27	32	$I = 7/2$ $\mu = 3.5$ (45)					
61					$_{28}Ni^{61}$ 1.2	100	28	33	
63	$_{29}Cu^{63}$ 68	29	34	$I = 3/2$ (58) $\mu = 2.43$ (66) $Q = -10$ (58, 26)					

Group 4: $I = 7$
Two nuclei terminated by radioactive $_{31}Ga^{73}$

65	$_{29}Cu^{65}$	32	29	36	$I = 3/2$ (58) $\mu = 2.54$ (66) $Q = -10$ (58, 26)
67					
69	$_{31}Ga^{69}$	61.2	31	38	$I = 3/2$ (55) $\mu = 2.11$ $Q = 20, = 100$ (55, 26)

Group 5: $I = 9$
Three nuclei

71	$_{31}Ga^{71}$	38.8	31	40	$I = 3/2$ (55) $\mu = 2.69$ (55) $Q = 13, = 50$ (51, 55)
73	$_{33}As^{75}$	100.0	33	42	$I = 3/2$ (57) $\mu = 1.5$ $Q = 30$ (26, 57)
75					
77					
79	$_{35}Br^{79}$	50.6	35	44	$I = 3/2$ $\mu = 2.61$ (21)

Group 4: $I = 7$
A single nucleus terminated by radioactive $_{28}Ni^{69}$ and $_{32}Ge^{71}$

$_{30}Zn^{67}$	3.9	100	30	37	$I = 5/2$ $\mu = 0.9$ (36)

Group 5: $I = 9$
Two nuclei terminated by radioactive $_{30}Zn^{69}$ and $_{36}Kr^{81}$

$_{32}Ge^{73}$	7.9	100	32	41
$_{34}Se^{77}$	8.3	100	34	43

TABLE 1—*Continued*

Group 6: I = 11

Four nuclei — **Five nuclei terminated by radioactive ₃₄Se⁷⁹**

MASS NUMBER	NUCLEI AND ISOTOPIC ABUNDANCE (per cent)		CHARACTERISTICS OF NUCLEI	NUMBER OF PROTONS AND NEUTRONS (p | n)		NUMBER OF PROTONS AND NEUTRONS (p | n)		ABUNDANCE RELATIVE TO EVEN-ODD (per cent)	NUCLEI AND ISOTOPIC ABUNDANCE (per cent)		CHARACTERISTICS OF NUCLEI
81	$_{35}$Br^{81}	49.4	$I = 3/2$ $\mu = 2.61$ (21)	35	46						
83						36	47	100	$_{36}$Kr^{83}	11.55	$I = 9/2$ $\mu = -1$ (7) $Q = 15$ (28, 57)
85	$_{37}$Rb^{85}	100.0	$I = 3/2$ (25, 40) $\mu = 1.345$ (29)	37	48						
87						38	49	100	$_{38}$Sr^{87}	7.02	$I = 9/2$ $\mu = -1.1$ (19)
89	$_{39}$Y^{89}	100.0		39	50						
91						40	51	100	$_{40}$Zr^{91}	11.5	
93	$_{41}$Cb^{93}	100.0		41	52						
95						42	53	62.5	$_{42}$Mo^{95}	16.1	
97	$(_{43}$Ma^{97}	Unknown		43	54)						
99						44	55	35.3	$_{44}$Ru^{99}	12	

Group 7: I = 13
Three nuclei terminated by radioactive $_{40}$Zr^{96} and $_{48}$Cd^{106}

Isotope			Z	N	I, μ
$_{42}$Mo^{97}	9.65	37.5	42	55	
$_{44}$Ru^{101}	22	64.7	44	57	
$_{46}$Pd^{105}	22.6	100	46	59	

Group 8: I = 15
Two nuclei terminated by radioactive $_{46}$Pd^{107}

Isotope			Z	N	I, μ
$_{48}$Cd^{111}	13	51.4	48	63	I = 1/2, μ = −0.65 (54)
$_{50}$Sn^{115}	0.4	2.1	50	65	

Group 9: I = 17
Two nuclei terminated by radioactive $_{46}$Pd^{109} and $_{52}$Te^{123}

Isotope			Z	N	I, μ
$_{48}$Cd^{113}	12.3	48.6	48	65	I = 1/2, μ = −0.65 (54)
$_{50}$Sn^{117}	9.1	47.1	50	67	I = 1/2, μ = −0.89 (59)

Group 7: I = 13
Two nuclei terminated by radioactive $_{43}$Ma^{99} and $_{49}$In^{111}

Isotope		Z	N	I, μ
$_{45}$Rh^{103}	100.0	45	58	
$_{47}$Ag^{107}	52.5	47	60	I = 1/2, μ = −0.10 (22)

Group 8: I = 15
Two nuclei terminated by radioactive $_{45}$Rh^{105}

Isotope		Z	N	I, μ
$_{47}$Ag^{109}	47.5	49	64	I = 1/2, μ = −0.19 (22)
$_{49}$In^{113}	4.5	49	64	I = 9/2 (17), μ = 5.43 (21)

Group 9: I = 17
A single nucleus terminated by radioactive $_{47}$Ag^{111}

Isotope		Z	N	I, μ, Q
$_{49}$In^{115}	95.5	49	66	I = 9/2 (17), μ = 5.49 (43), Q = 84 (58)

TABLE 1—*Continued*

Group 10: I = 19
A single nucleus terminated by radioactive $_{49}In^{117}$

MASS NUMBER	NUCLEI AND ISOTOPIC ABUNDANCE (per cent)	NUMBER OF PROTONS AND NEUTRONS — p	NUMBER OF PROTONS AND NEUTRONS — n	CHARACTERISTICS OF NUCLEI
119				
121	$_{51}Sb^{121}$ 56	51	70	$I = 5/2$ (8) $\mu = 3.7$ (61)
123				

Group 11: I = 21
Two nuclei

MASS NUMBER	NUCLEI AND ISOTOPIC ABUNDANCE (per cent)	NUMBER OF PROTONS AND NEUTRONS — p	NUMBER OF PROTONS AND NEUTRONS — n	CHARACTERISTICS OF NUCLEI
123	$_{51}Sb^{123}$ 44	51	72	$I = 7/2$ $\mu = 2.8$ (62)
125				
127	$_{53}I^{127}$ 100	53	74	$m = 126.948$ (A, 4) $I = 5/2$ $\mu = 2.8$ (62) $Q = -50$ (26, 57)
129				

Group 10: I = 19
Two nuclei terminated by radioactive $_{48}Cd^{115}$ and $_{54}Xe^{137}$

NUCLEI AND ISOTOPIC ABUNDANCE (per cent)	ABUNDANCE RELATIVE TO EVEN-ODD (per cent)	NUMBER OF PROTONS AND NEUTRONS — p	NUMBER OF PROTONS AND NEUTRONS — n	CHARACTERISTICS OF NUCLEI
$_{50}Sn^{119}$ 9.8	50.8	50	69	$I = 1/2$ $\mu = -0.89$ (59)
$_{52}Te^{123}$ 1.6	21.0	52	71	

Group 11: I = 21
Two nuclei terminated by radioactive $_{56}Ba^{133}$

NUCLEI AND ISOTOPIC ABUNDANCE (per cent)	ABUNDANCE RELATIVE TO EVEN-ODD (per cent)	NUMBER OF PROTONS AND NEUTRONS — p	NUMBER OF PROTONS AND NEUTRONS — n	CHARACTERISTICS OF NUCLEI
$_{52}Te^{125}$ 6.0	79.0	52	73	
$_{54}Xe^{129}$ 26.23	55.3	54	75	$m = 128.942 \pm 20$ (A, 4) $I = 1/2$ $\mu = -0.9$ (7)

Group 12: I = 23

Incomplete group of two nuclei

133	$_{55}\mathrm{Cs}^{133}$	100	55	78	$m = 132.9455$ (A, 4) $I = 7/2$ $\mu = 2.57$
137	$(_{57}\mathrm{La}^{137})$	Unknown	57	80)	
141	$_{59}\mathrm{Pr}^{141}$	100	59	62	$I = 5/2$

Incomplete group of four nuclei terminated by radioactive $_{52}\mathrm{Te}^{127}$

131	$_{54}\mathrm{Xe}^{131}$	21.17	44.7	54	77	$I = 3/2$ $\mu = 0.7$ (27) $Q = 10.$ (57)
135	$_{56}\mathrm{Ba}^{135}$	6.6	36.8	56	79	$I = 3/2$ (6) $\mu = 0.836 \pm 3$
139	$(_{58}\mathrm{Ce}^{139})$	Unknown		58	81)	
143	$_{60}\mathrm{Nd}^{143}$	13.0	58.6	60	83	
147	$_{62}\mathrm{Sm}^{147}$	17	53.1	62	85	

Group 13: I = 25

Incomplete group of two nuclei

137				
139	$_{57}\mathrm{La}^{139}$	100	57	82	$I = 7/2$ $\mu = 2.8$ (61)
141				

Incomplete group of three nuclei terminated by radioactive $_{54}\mathrm{Xe}^{133}$

137	$_{56}\mathrm{Ba}^{137}$	11.3	63.2	56	81	$I = 3/2$ (6) $\mu = 0.935 \pm 3$
141	$(_{58}\mathrm{Ce}^{141})$	Unknown		58	83)	

TABLE 1—Continued

Group 13: I = 25—Continued

MASS NUMBER	NUCLEI AND ISOTOPIC ABUNDANCE (per cent)	CHARACTERISTICS OF NUCLEI	NUMBER OF PROTONS AND NEUTRONS (p, n)
143	$_{59}Pr^{143}$ Unknown		59 84)
145			
147	$_{61}Il^{147}$ Unknown		61 86)
149			
151	$_{63}Eu^{151}$ 49.1	$I = 5/2$ $\mu = 3.4$ (39) $Q = 180$ (57, 26)	63 88

A single nucleus

Group 14: I = 27

MASS NUMBER	NUCLEI AND ISOTOPIC ABUNDANCE (per cent)	CHARACTERISTICS OF NUCLEI	NUMBER OF PROTONS AND NEUTRONS (p, n)
153	$_{63}Eu^{153}$ 50.9	$I = 5/2$ $\mu = 1.5$ (61) $Q = 250$ (57, 26)	63 90
155			

A single nucleus

Group 15: I = 29

MASS NUMBER	NUCLEI AND ISOTOPIC ABUNDANCE (per cent)	CHARACTERISTICS OF NUCLEI	NUMBER OF PROTONS AND NEUTRONS (p, n)
157			
159	$_{65}Tb^{159}$ 100		65 94
161			

Group 13: I = 25—Continued

NUCLEI AND ISOTOPIC ABUNDANCE (per cent)	ABUNDANCE RELATIVE TO EVEN-ODD (per cent)	NUMBER OF PROTONS AND NEUTRONS (p, n)	CHARACTERISTICS OF NUCLEI
$_{60}Nd^{145}$ 9.2	41.4	60 85	
$_{62}Sm^{149}$ 15	46.9	62 87	

Group 14: I = 27

A single nucleus terminated by radioactive $_{62}Sm^{151}$

NUCLEI AND ISOTOPIC ABUNDANCE (per cent)	ABUNDANCE RELATIVE TO EVEN-ODD (per cent)	NUMBER OF PROTONS AND NEUTRONS (p, n)	CHARACTERISTICS OF NUCLEI
$_{64}Gd^{153}$ 21	55.3	64 91	

Group 15: I = 29

Two nuclei terminated by radioactive $_{62}Sm^{151}$

NUCLEI AND ISOTOPIC ABUNDANCE (per cent)	ABUNDANCE RELATIVE TO EVEN-ODD (per cent)	NUMBER OF PROTONS AND NEUTRONS (p, n)	CHARACTERISTICS OF NUCLEI
$_{64}Gd^{157}$ 17	44.7	64 93	
$_{66}Dy^{161}$ 22	47.8	66 95	

Group 16: I = 31

Three nuclei terminated by radioactive $_{64}\underline{Gd}^{159}$

$_{65}Dy^{163}$	24	52.2	66 | 97
$_{68}Er^{167}$	24	100	68 | 99
$_{70}Yb^{171}$	9	34.6	70 | 101

$I = 1/2$
$\mu = 0.45$ (56)

Group 17: I = 33

Two nuclei terminated by radioactive $_{68}\underline{Er}^{169}$

$_{70}Yb^{173}$	17	65.4	70 | 103
$_{73}Hf^{177}$	19	51.3	72 | 105

$I = 5/2$ (57)
$\mu = -0.65$ (56)
$Q = 590$ (57)

Group 18: I = 35

Three nuclei terminated by radioactive $_{70}\underline{Yb}^{175}$

$_{72}Hf^{179}$	18	48.7	72 | 107

Two nuclei

Group 16: I = 31

$_{67}Ho^{165}$	100	67 | 98
$_{69}Tm^{169}$	100	69 | 100

A single nucleus

Group 17: I = 33

$_{71}Lu^{175}$	100	71 | 104

$I = 7/2$ (15)
$\mu = 2.6$ (15)
$Q = 590$ (57, 15)

Group 18: I = 35

Two nuclei terminated by radioactive $_{71}\underline{Lu}^{177}$

$_{73}Ta^{181}$	100	73 | 108

163
165
167
169
171
173
175
177
179
181

TABLE 1—Continued

Group 18: I = 35 —Continued

MASS NUMBER	NUCLEI AND ISOTOPIC ABUNDANCE (per cent)	NUMBER OF PROTONS AND NEUTRONS (p | n)	CHARACTERISTICS OF NUCLEI
183			
185	$_{75}$Re^{185} 38.2	75|110	$I = 5/2$ $\mu = 3.3$ (21) $Q = 2.80$ (57, 55)
187			

Group 19: I = 37

Two nuclei

MASS NUMBER	NUCLEI AND ISOTOPIC ABUNDANCE (per cent)	NUMBER OF PROTONS AND NEUTRONS (p | n)	CHARACTERISTICS OF NUCLEI
187	$_{75}$Re^{187} 61.8	75|112	$I = 5/2$ $\mu = 3.3$ (21) $Q = 2.80$ (57, 55)
189			
191	$_{77}$Ir^{191} 38.5	77|114	$I = 1/2$ (65)

Group 20: I = 39

Two nuclei

MASS NUMBER	NUCLEI AND ISOTOPIC ABUNDANCE (per cent)	NUMBER OF PROTONS AND NEUTRONS (p | n)	CHARACTERISTICS OF NUCLEI
193	$_{77}$Ir^{193} 61.5	77|116	$I = 3/2$ (65)
195			

Group 18: I = 35 —Continued

NUCLEI AND ISOTOPIC ABUNDANCE (per cent)	ABUNDANCE RELATIVE TO EVEN-ODD (per cent)	NUMBER OF PROTONS AND NEUTRONS (p | n)	CHARACTERISTICS OF NUCLEI
$_{74}$W^{183} 17.3	100	74|109	
$_{76}$Os^{187} 1.64	9.2	75|111	

Group 19: I = 37

A single nucleus terminated by radioactive $_{71}$W^{185}

NUCLEI AND ISOTOPIC ABUNDANCE (per cent)	ABUNDANCE RELATIVE TO EVEN-ODD (per cent)	NUMBER OF PROTONS AND NEUTRONS (p | n)	CHARACTERISTICS OF NUCLEI
$_{76}$Os^{189} 16.2	90.8	76|113	

Group 20: I = 39

Two nuclei terminated by radioactive $_{76}$Os^{191} and $_{82}$Pb^{208}

NUCLEI AND ISOTOPIC ABUNDANCE (per cent)	ABUNDANCE RELATIVE TO EVEN-ODD (per cent)	NUMBER OF PROTONS AND NEUTRONS (p | n)	CHARACTERISTICS OF NUCLEI
$_{78}$Pt^{195} 35.3	100	78|117	$I = 1/2$ $\mu = 0.6$ (60)

197	$_{79}Au^{197}$	100.0		79|118	$I = 3/2$ $\mu = 0.2$ (61)
199	$_{80}Hg^{199}$	17.03	56.4	80|119	$I = 1/2$ $\mu = 0.5$ (53) $Q = 50$ (53, 57)

Group 21: I = 41
A single nucleus terminated by radioactive $_{79}Au^{199}$ and $_{83}Bi^{207}$ | Group 21: I = 41
A single nucleus terminated by radioactive $_{78}Pt^{197}$ and $_{82}Pb^{205}$

201	$_{80}Hg^{201}$	13.17	43.6	80|121	$I = 3/2$ $\mu = -0.6$
203	$_{81}Tl^{203}$	29.1		81|122	$I = 1/2$ $\mu = 1.45$ (58)

Group 22: I = 43
Two nuclei | Group 22: I = 43
A single nucleus terminated by radioactive $_{80}Hg^{205}$ and $_{84}Po^{211}$

205	$_{81}Tl^{205}$	70.9		81|124	$I = 1/2$ $\mu = 1.45$ (58)
207	$_{82}Pb^{207}$	22.7	100	82|125	$I = 1/2$ $\mu = 0.6$ (7)
209	$_{83}Bi^{209}$	100		83|126	$I = 9/2$ $\mu = 4.0$ (39) $Q = -40$ (57, 58)

* References to the literature are given in parentheses. Underscored radioactive nuclei are not confirmed.

between the last nuclei of Groups 2, 9, 10, 11, 14, 15, 16, 17, 18, 20 and the first nuclei of the following groups in Series 4 is 2. A mass difference of 2 between adjoining groups is due to the existence of isotopic doublets in either S_3 or S_4. The mass difference between nuclei of adjoining groups which have no isotopic doublets is consequently expected to be 6.

Odd isobars distort these regularities in consecutive groups. This is due to the following nuclei:

<div align="center">

Series 3: Group 8 (G_8), $_{49}In^{113}$

Series 4: G_8, $_{50}Sn^{115}$; G_{10}, $_{52}Te^{123}$; G_{13}, $_{76}Os^{187}$

</div>

The non-existence of the stable nucleus $_{18}A^{39}$ in S_4–G_2 and the appearance of $_{19}K^{39}$ in S_3–G_1 results in irregularities of mass number differences in the respective groups.

The non-existence of the stable nucleus $_{21}Sc^{47}$ and the appearance of the nucleus $_{22}Ti^{47}$ result in exchange of position of an isotopic doublet from Series 3 to Series 4, with mass difference 2 in Series 4 instead of Series 3. This exchange involves the conversion of a neutron to a proton.

The non-existence of the stable nucleus $_{43}Ma^{97}$ in S_3–G_6 and the appearance of the nucleus $_{42}Mo^{97}$ in S_4 result in deviations in G_6 and G_7 of both series, the deviation being due to a conversion of a proton into a neutron.

A more complicated shift from nuclei expected by the classification to those actually existing occurs in Groups 12 and 13 of Series 3 and 4. These two pairs of groups are incomplete,—five nuclei are missing in the middle of the groups. In addition, the positions of some nuclei in both series are reversed with regard to charge numbers, i.e., a nucleus of lower charge number has a higher isotopic number than the nucleus of higher charge number:

<div align="center">

$_{57}La^{139}$ has I = 25	$_{56}Ba^{137}$ has I = 25
$_{59}Pr^{141}$ has I = 23	$_{60}Nd^{143}$ has I = 23

</div>

A reversed order likewise is observed in Groups 6 and 7 of Series 4, owing to the non-existence of $_{43}Ma^{97}$ in Group 6 of Series 3.

In table 2 are shown the proton–neutron combinations expected by the classification in G_{12} and G_{13} and the actually known nuclei. Isotopes expected but not existing are in parentheses and those existing but not expected are underscored.

Thus, four nuclei are expected in Series 3–Group 12 and five in Series 4–Group 12. In Group 13 of each series only a single species is expected. Actually the three nuclei, $_{57}La^{137}$, $_{58}Ce^{139}$, and $_{61}Il^{145}$ with the proton–neutron combinations 57–80, 58–81, and 61–84, respectively, are unknown as stable.[5] The shift toward stability takes place by the exchange of one proton for a neutron. This is a reversal of the conversion of one neutron into a proton which occurred in the light nuclei $_{18}A^{39}$ and $_{21}Sc^{47}$.

The groups of nuclei of S_3 and S_4 are very often terminated by known radioactive nuclei.

[5] The radioactive isotope of lanthanum of half-life 17 hr. has been assigned to nucleus $_{57}La^{137}$ (67).

TABLE 2

$S_3 - G_{12}$ I·23					$S_4 - G_{12}$ I·23			
A	Nuclei	p	n		Nuclei	p	n	
131					¹³¹₅₄Xe	54	77	
133	¹³³₅₅Cs	55	78					
135					¹³⁵₅₆Ba	56	79	
137	[¹³⁷₅₇La	57	80]	→	¹³⁷₅₆Ba	56	81	I·25
139	¹³⁹₅₇La	57	82	I·25 ←	[¹³⁹₅₈Ce	58	81]	
141	¹⁴¹₅₉Pr	59	82					
143					¹⁴³₆₀Nd	60	83	
145	[¹⁴⁵₆₁I1	61	84]	→	¹⁴⁵₆₀Nd	60	85	I·25
147					¹⁴⁷₆₂Sm	62	85	
$S_3 - G_{13}$ I·25					$S_4 - G_{13}$ I·25			
149					¹⁴⁹₆₂Sm	62	87	
151	¹⁵¹₆₃Eu	63	88					

Among several other questions arising from observing the classifying tables of Series 3 and 4 is that of whether elements of charge numbers 43 and 61 exist. The lack of stable isotopes of these charge numbers may be due merely to the coincidence that the proton–neutron combinations 43–54 and 61–84 are unstable.

EVEN-EVEN-UNEQUAL NUCLEI

All the nuclei of even-even-unequal number of protons and neutrons form twenty-two groups with consecutive even isotopic numbers:

$$I = 2k + 2, \text{ where } k = 0,1,\ldots 21$$

Each isotopic number is represented by a separate group of nuclei, the consecutive members of the group being built up by the addition of $2p2n$. Thus there is identity in the number of groups between the previously described series, S_3 and S_4, and Series 2.

However, the twenty-two groups of even-even nuclei are in some respects more complicated in the consecutive order of their formation than the nuclei of Series 3 and Series 4.

The requirement, followed in this classification, as to the interrelation of groups in regard to the isotopic and mass numbers, does not hold between consecutive isotopic number groups of the even-even-unequal species. The condition is fulfilled, however, after division of the series into periods.

The mass numbers and isotopic numbers of the species in the twenty-two groups can be regarded as comprising two separate sub-series defined as:

S_{2a} having $I = 4k + 2; k = 0,1,\ldots 10; A = 4k' + 18; k' = 0,1,\ldots 47$
S_{2b} having $I = 4k'' + 4; k'' = 0,1,\ldots 10; A = 4k''' + 36; k''' = 0,1,\ldots 43$

By division of the even-even-unequal isotopes into two sub-series, remarkable simplicity is apparent in the consequent formation of the groups and a connection is obtained with S_1. That is, the first nucleus of S_{2a} follows the last nucleus of S_1. The continuity between S_1 and S_{2a} can be seen from the following: the first nucleus, $_8O^{18}$, S_{2a}, is built up by the addition of $2p2n$ to $_7N^{14}$ and conversion of a proton to a neutron:

$$_7N^{14} + 2p2n \rightarrow {}_9F^{18} (R) \rightarrow {}_8O^{18} + \overset{+}{e}$$

The requirement that the mass number of the last member of a group be not higher than that of the first member of the succeeding group necessitates the further division of sub-series into two periods each. Sub-series S_{2a} has the periods:

P_2 having $I = 8k + 2; \quad k = 0,1,\ldots 5; A = 4k'' + 18; \quad k'' = 0,1,\ldots 47$
P_6 having $I = 8k' + 6; \quad k' = 0,1,\ldots 4; A = 4k''' + 46; \quad k''' = 0,1,\ldots 38$

Thus the nuclei of the two periods, P_2 and P_6, can have isobars in the mass number interval of 46 to 198.

The interrelation of the nuclear species of the two periods of Sub-series S_{2a} and the consecutive order of the nuclei in the adjoining groups is as follows:

Period 2 $I = 8k + 2$ $k = 0,1, \ldots 5$					Period 6 $I = 8k' + 6$ $k' = 0,1, \ldots 4$				
GROUP NO.	NUCLEI	I	ΔI	ΔA	GROUP NO.	NUCLEI	I	ΔI	ΔA
1	$_8O^{18}$ – $_{28}Ni^{68}$	2			3	$_{20}Ca^{40}$ – $_{36}Kr^{78}$	6		
			8	12				8	4
5	$_{30}Zn^{70}$ – $_{48}Cd^{106}$	10			7	$_{34}Se^{82}$ – $_{48}Sn^{114}$	14		
			8	4				8	8
9	$_{46}Pd^{110}$ – $_{56}Ba^{130}$	18			11	$_{50}Sn^{122}$ – $_{60}Nd^{142}$	22		
			8	0				8	8
13	$_{52}Te^{130}$ – $_{68}Er^{162}$	26			15	$_{60}Nd^{150}$ – $_{72}Hf^{174}$	30		
			8	8				8	12
17	$_{68}Er^{170}$ – $_{76}Os^{186}$	34			19	$_{74}W^{186}$ – $_{80}Hg^{198}$	38		
			8	12					
21	$_{78}Pt^{198}$ – $_{82}Pb^{206}$	42							

Thus the odd groups of even-even-unequal species make up Sub-series S_{2a} and the groups in P_2 and P_6 follow alternately.

The increase in the isotopic number between two successive groups is always 8, the nuclei in a group being built up consecutively by addition of $2p2n$.

The difference in mass number between the last nucleus of a group and the first nucleus of the following group might be expected to be equal to the difference in isotopic number, that is, to be 8. However, the last column shows that four cases are possible.

(1) $\Delta A = 0$, $_{56}Ba^{130}$ – $_{52}Te^{130}$ between G_9 and G_{13}. This leads to the appearance of six consecutive isobaric nuclei and one triode, $A = 130$, which actually are in existence.

(2) $\Delta A = 4$, $_{48}Cd^{106}$ – $_{46}Pd^{110}$ between G_5 and G_9 and $_{36}Kr^{78}$ – $_{34}Se^{82}$ between G_3 and G_7. This makes possible the existence of consecutive isobars for mass numbers 94 to 114 and 70 to 86 ($_{38}Sr^{90}$ is unknown).

(3) $\Delta A = 8$. This yields an intermediate single mass number species.

(4) $\Delta A = 12$. This leaves two intermediate single mass number species.

The groups of the Periods P_2 and P_6, with the exception of Group 7, are complete. Group 7 lacks the nucleus $_{38}Sr^{90}$.

Sub-series S_{2b} is divided into two periods in a manner similar to S_{2a}.

P_4 having $I = 8k + 4$; $k = 0,1, \ldots 5$; $A = 4k'' + 36$; $k'' = 0,1, \ldots 43$
P_8 having $I = 8k' + 8$; $k' = 0,1, \ldots 4$; $A = 4k''' + 48$; $k''' = 0,1, \ldots 39$

TABLE 3

Series 2

Characteristics: even number of protons and neutrons; consists of 22 groups of consecutive even isotopic numbers, the groups having from 2 to 44 extra neutrons

Period 2

$$I = 8k + 2; k = 0, 1, \ldots 5$$
$$\text{Group 1: } I = A - 2Z = 2$$

Eleven nuclei terminated by radioactive $_6C^{14}$

MASS NUMBER	NUCLEI AND RELATIVE ISOTOPIC ABUNDANCE	ABUNDANCE RELATIVE TO EVEN-EVEN	NUMBER OF PROTONS AND NEUTRONS		CHARACTERISTICS OF NUCLEI
			p	n	
	per cent	*per cent*			
18	$_8O^{18}$ 0.20	0.20	8	10	$m = 18.00369\ (35)^*$ $B.E. = 0.1511$ $\Delta B.E. = 0.0392$
22	$_{10}Ne^{22}$ 9.73	9.75	10	12	$m = 21.99864\ (B, 48)$ $B.E. = 0.1903$ $\Delta B.E. = 0.0422$
26	$_{12}Mg^{26}$ 11.1	12.5	12	14	$m = 25.99062\ (48)$ $B.E. = 0.2325$ $\Delta B.E. = 0.0419$
30	$_{14}Si^{30}$ 4.2	4.5	14	16	$m = 29.98294\ (48)$ $B.E. = 0.2744$ $\Delta B.E. = 0.0374$

Period 6

$I = 8k' + 6;\ k' = 0, 1, \ldots 4$

Group 3: $I = A - 2Z = 6$

Nine nuclei

NUCLEI AND RELATIVE ISOTOPIC ABUNDANCE	ABUNDANCE RELATIVE TO EVEN-EVEN	NUMBER OF PROTONS AND NEUTRONS		CHARACTERISTICS OF NUCLEI
per cent	per cent	p	n	
$_{20}Ca^{46}$ 0.0033	0.0033	20	26	
$_{22}Ti^{50}$ 5.34	6.15	22	28	$m = 49.9632$ (D, 48)
$_{24}Cr^{54}$ 2.30	2.54	24	30	$B.E. = 0.4668$
$_{26}Fe^{58}$ 0.28	.29	26	32	
$_{28}Ni^{62}$ 3.8	3.9	28	34	
$_{30}Zn^{66}$ 27.3	28.4	30	36	
$_{32}Ge^{70}$ 21.2	23.0	32	38	
$_{34}Se^{74}$ 0.9	1.0	34	40	$m = 77.9430 \pm 20$ (A)
$_{36}Kr^{78}$ 0.35	0.40	36	42	$B.E. = 0.7264$

	NUCLEI	abundance	abundance	p	n	CHARACTERISTICS
34	$_{16}S^{34}$	4.2	4.23	16	18	$m = 33.97974$ (48), $B.E. = 0.3118$, $\Delta B.E. = 0.0385$
38	$_{18}A^{38}$	0.06	0.06	18	20	$m = 37.97544$ (48), $B.E. = 0.3503$, $\Delta B.E. = 0.0385$
42	$_{20}Ca^{42}$	0.64	0.64	20	22	$m = 41.9711$ (48), $B.E. = 0.3888$, $\Delta B.E. = 0.0375$
46	$_{22}Ti^{46}$	7.94	9.15	22	24	$m = 45.9678$ (48), $B.E. = 0.4263$
50	$_{24}Cr^{50}$	4.49	4.95	24	26	
54	$_{26}Fe^{54}$	6.0	6.1	26	28	$m = 53.9601$ (D, 48), $B.E. = 0.5024$
58	$_{28}Ni^{58}$	67.4	68.1	28	30	
62						
66						

Group 5: $I = 10$

Ten nuclei

	NUCLEI	abundance	abundance	p	n
70	$_{30}Zn^{70}$	0.5	0.52	30	40
74	$_{32}Ge^{74}$	37.1	40.3	32	42
78	$_{34}Se^{78}$	24.0	26.2	34	44

TABLE 3—Continued

Group 5: I = 10—Continued

Ten nuclei

MASS NUMBER	NUCLEI AND RELATIVE ISOTOPIC ABUNDANCE (per cent)	ABUNDANCE RELATIVE TO EVEN-EVEN (per cent)	NUMBER OF PROTONS AND NEUTRONS p	n	CHARACTERISTICS OF NUCLEI
82	$_{36}Kr^{82}$ 11.53	13.03	36	46	$m = 81.9368 \pm 15\,(A,4)$ $B.E. = 0.7684$
86	$_{38}Sr^{86}$ 9.86	10.61	38	48	
90	$_{40}Zr^{90}$ 48	54.2	40	50	
94	$_{42}Mo^{94}$ 9.4	12.7	42	52	
98	$_{44}Ru^{98}$ Low undetermined abundance		44	54	
102	$_{46}Pd^{102}$ 0.8	1.0	46	56	
106	$_{48}Cd^{106}$ 1.4	1.9	48	58	

Group 9: I = 18

Six nuclei

MASS NUMBER	NUCLEI AND RELATIVE ISOTOPIC ABUNDANCE (per cent)	ABUNDANCE RELATIVE TO EVEN-EVEN (per cent)	p	n
110	$_{46}Pd^{110}$ 13.5	17.4	46	64
114	$_{48}Cd^{114}$ 28.0	37.5	48	66

Group 7: I = 14

An incomplete group of eight nuclei

NUCLEI AND RELATIVE ISOTOPIC ABUNDANCE (per cent)	ABUNDANCE RELATIVE TO EVEN-EVEN (per cent)	NUMBER OF PROTONS AND NEUTRONS p	n	CHARACTERISTICS OF NUCLEI
$_{34}Se^{82}$ 9.3	10.1	34	48	$m = 85.9363 \pm 15(A,4)$ $B.E. = 0.8049$
$_{36}Kr^{86}$ 17.47	19.75	36	50	
$(_{38}Sr^{90}$ Unknown		38	52)	
$_{40}Zr^{94}$ 17	19.2	40	54	
$_{42}Mo^{98}$ 24.1	32.5	42	56	
$_{44}Ru^{102}$ 30	45.4	44	58	
$_{46}Pd^{106}$ 27.2	35.0	46	60	
$_{48}Cd^{110}$ 12.8	17.1	48	62	
$_{50}Sn^{114}$ 0.8	1.0	50	64	

Group 11: I = 22

Six nuclei

$_{50}Sn^{112}$	5.5	6.8	50	72
$_{52}Te^{128}$	19.0	20.6	52	74
$_{54}Xe^{130}$	4.07	7.74	54	76
$_{56}Ba^{134}$	2.42	2.95	56	78
$_{58}Ce^{138}$	0.22		58	80
$_{60}Nd^{142}$	25.95	33.35	50	82

Group 15: I = 30

Seven nuclei

$_{60}Nd^{150}$	5.95	7.65	60	90
$_{62}Sm^{154}$	20	29.4	62	92
$_{64}Gd^{158}$	22	36	64	94
$_{66}Dy^{162}$	24	45	66	96
$_{68}Er^{166}$	35	46	68	98

Nine nuclei

$_{50}Sn^{118}$	22.5	27.9	50	68
$_{52}Te^{122}$	2.9	3.14	52	70
$_{54}Xe^{126}$	0.088	0.167	54	72
$_{56}Ba^{130}$	0.101	0.123	56	74

Group 13: I = 26

$_{52}Te^{130}$	33.1	35.9	52	78
$_{54}Xe^{134}$	10.54	20.04	54	80
$_{56}Ba^{138}$	71.7	87.3	56	82
$_{58}Ce^{142}$	11	11	58	84
$_{60}Nd^{146}$	16.5	21.2	60	86
$_{62}Sm^{150}$	5	7.4	62	88
$_{64}Gd^{154}$	1.5	2.4	64	90
$_{66}Dy^{158}$	0.1	0.2	66	92
$_{68}Er^{162}$	0.26	0.33	68	94

TABLE 3—Continued

Group 17: I = 34

Five nuclei

MASS NUMBER	NUCLEI AND RELATIVE ISOTOPIC ABUNDANCE (per cent)	ABUNDANCE RELATIVE TO EVEN-EVEN (per cent)	NUMBER OF PROTONS AND NEUTRONS (p)	(n)	CHARACTERISTICS OF NUCLEI
170	$_{68}$Er^{170} 10	13	68	102	
174	$_{70}$Yb^{174} 37	50	70	104	
178	$_{72}$Hf^{178} 28	44	72	106	
182	$_{74}$W^{182} 22.6	27.3	74	108	
186	$_{76}$Os^{186} 1.58	1.92	72	110	
190					
194					

Group 21: I = 42

Three nuclei terminated by radioactive $_{84}$Po^{210}

198	$_{78}$Pt^{198} 7.2	11.1	78	120	
202	$_{80}$Hg^{202} 29.56	42.35	80	122	
206	$_{82}$Pb^{206} 23.5	30.4	82	124	

Group 15: I = 30—Continued

Seven nuclei

NUCLEI AND RELATIVE ISOTOPIC ABUNDANCE (per cent)	ABUNDANCE RELATIVE TO EVEN-EVEN (per cent)	NUMBER OF PROTONS AND NEUTRONS (p)	(n)	CHARACTERISTICS OF NUCLEI
$_{70}$Yb^{170} 2	3	70	100	
$_{72}$Hf^{174} 0.3	0.5	72	102	

Group 19: I = 38

Four nuclei

$_{74}$W^{184} 29.8	36.0	47	112	
$_{76}$Os^{190} 26.4	32.1	76	114	
$_{78}$Pt^{194} 30.2	46.6	78	116	
$_{80}$Hg^{198} 10.11	14.48	80	118	

* References to the literature are given in parentheses.

The interrelation of groups is as follows:

	Period 4 $I = 8k + 4$ $k = 0, 1, \ldots 5$					Period 8 $I = 8k' + 8$ $k' = 0, 1, \ldots 4$			
GROUP NO.	NUCLEI	I	ΔI	ΔA	GROUP NO.	NUCLEI	I	ΔI	ΔA
2	$_{16}S^{36}$ – $_{30}Zn^{64}$	4			4	$_{20}Ca^{48}$ – $_{44}Ru^{96}$	8		
			8	12				8	0
6	$_{32}Ge^{76}$ – $_{50}Sn^{112}$	12			8	$_{40}Zr^{96}$ – $_{54}Xe^{124}$	16		
			8	4				8	0
10	$_{48}Cd^{116}$ – $_{62}Sm^{144}$	20			12	$_{50}Sn^{124}$ – $_{64}Gd^{152}$	24		
			8	–8(!)				8	8
14	$_{54}Xe^{136}$ – $_{70}Yb^{168}$	28			16	$_{64}Gd^{160}$ – $_{76}Os^{184}$	32		
			8	8				8	8
18	$_{70}Yb^{176}$ – $_{80}Hg^{196}$	36			20	$_{76}Os^{192}$ – $_{82}Pb^{204}$	40		
			8	8					
22	$_{80}Hg^{204}$ – $_{82}Pb^{208}$	44							

A deviation from the requirements imposed in the classification is observed in one case,—namely, in P_4 between G_{10} and G_{14},—on account of the existence of the nucleus $_{62}Sm^{144}$ of 3 per cent abundance (3, 46).[6]

In two cases there are no mass number differences between the last isotope of one group and the first of the succeeding group; in one case the mass difference is negative. All these may result, therefore, in the appearance of three triodes. These triodes actually exist for each of the mass numbers 96, 124, 136.[7]

A difference of four mass units between G_6 and G_{10} results in the longest sequence of isobars. A difference of eight mass units between adjoining groups corresponds to the existence of four single mass number species: they are $_{64}Gd^{156}$, $_{70}Yb^{172}$, $_{76}Os^{188}$, and $_{80}Hg^{200}$. A difference of twelve mass units brings two consecutive single mass number species, $_{30}Zn^{68}$ and $_{32}Ge^{72}$.

The Sub-series S_{2b} has seven complete groups. The incomplete groups are G_4, G_{10}, G_{12}, and G_{14}.

SUMMARY

It has already been indicated that the division of all known stable nuclei into groups of separate series according to their physical characteristics is lacking in continuity of species formation. However, with the aid of this division the ob-

---

[6] This deviation is rather significant; Sm^{144} may be looked upon as a product of the disintegration of $_{62}Sm^{148}$ and $_{60}Nd^{144}$. However, the radioactivity of $_{62}Sm^{148}$ has been clearly established, but that of $_{60}Nd^{144}$ remains in question. Some authors reported beta-radiation associated with an enriched fraction of Nd, making no definite isotopic assignment (32, 72).

[7] Thus, all four known triodes come at breaks between groups. A fifth triode, mass number 102, previously described is omitted here, since nucleus $_{42}Mo^{102}$ was not confirmed by recent analysis of the mass spectra. Should triode $A = 102$ exist, its position would not be in the location of a break between groups (9, 10).

TABLE 4

Series 2

Period 4

$I = 8k + 4; \; k = 0, 1, \ldots 5$

Group 2: $I = A - 2Z = 4$

Eight nuclei

MASS NUMBER	NUCLEI AND RELATIVE ISOTOPIC ABUNDANCE (per cent)	ABUNDANCE RELATIVE TO EVEN-EVEN (per cent)	NUMBER OF PROTONS AND NEUTRONS		CHARACTERISTICS OF NUCLEI
			p	n	
36	$_{16}S^{36}$ *0.016*	*0.016*	16	20	
40	$_{18}A^{40}$ 99.63	99.63	18	22	$m = 39.97504$ (B, 48)* $B.E. = 0.36864$
44	$_{20}Ca^{44}$ 2.06	2.06	20	24	
48	$_{22}Ti^{48}$ 73.45	84.69	22	26	$m = 47.9651$ (D, 48) $B.E. = 0.4470$ $\Delta B.E. = 0.0418$
52	$_{24}Cr^{52}$ 83.78	92.50	24	28	$m = 51.9575$ (A, 48) $B.E. = 0.4888$ $\Delta B.E. = 0.0309$
56	$_{26}Fe^{56}$ 91.6	93.6	26	30	$m = 55.9608$ (D, 48) $B.E. = 0.5197$
60	$_{28}Ni^{60}$ 26.7	27.0	28	32	

Period 8

$I = 8k' + 8; \; k' = 0, 1, \ldots 4$

Group 4: $I = A - 2Z = 8$

An incomplete group of nine nuclei

NUCLEI AND RELATIVE ISOTOPIC ABUNDANCE (per cent)	ABUNDANCE RELATIVE TO EVEN-EVEN (per cent)	NUMBER OF PROTONS AND NEUTRONS	
		p	n
$_{20}Ca^{48}$ 0.185	0.185	20	28
$(_{22}Ti^{52})$ Unknown		22	30
$(_{24}Cr^{56})$ Unknown		24	32
$(_{26}Fe^{60})$ Unknown		26	34

Group 6: I = 12

Ten nuclei

Nucleus			Z	N
$_{30}\text{Zn}^{64}$	50.9	53.0	30	34
$_{32}\text{Ge}^{76}$	6.5	7.1	32	44
$_{34}\text{Se}^{80}$	48.0	52.3	34	46
$_{36}\text{Kr}^{84}$	57.11	64.55	36	48
$_{38}\text{Sr}^{88}$	82.56	88.79	38	40
$_{40}\text{Zr}^{92}$	22	24.9	40	52
$_{42}\text{Mo}^{96}$	16.6	22.3	42	54
$_{44}\text{Ru}^{100}$	14	21.2	44	56
$_{46}\text{Pd}^{104}$	9.3	12.0	46	58
$_{48}\text{Cd}^{108}$	1.0	1.3	48	60
$_{50}\text{Sn}^{112}$	1.1	1.4	50	62

$$m = 83.9362 \pm 15 \ (A, 16)$$
$$B.E. = 0.7870$$

Group 8: I = 16

Eight nuclei

Nucleus			Z	N
$_{28}\text{Ni}^{64}$	0.88	0.89	28	36
$_{30}\text{Zn}^{68}$	17.4	18.1	30	38
$_{32}\text{Ge}^{72}$	27.3	29.6	32	40
$_{34}\text{Se}^{76}$	9.5	10.4	34	42
$_{36}\text{Kr}^{80}$	2.01	2.27	36	44
$_{38}\text{Sr}^{84}$	0.56	0.60	38	46
$(_{40}\text{Zr}^{88})$	Unknown		40	48)
$_{42}\text{Mo}^{92}$	14.9	20.1	42	50
$_{44}\text{Ru}^{96}$	5	7.6	44	52
$_{40}\text{Zr}^{96}$	1.5	1.7	40	56
$_{42}\text{Mo}^{100}$	9.25	12.5	42	58
$_{44}\text{Ru}^{104}$	17	25.8	44	60
$_{46}\text{Pd}^{108}$	26.8	34.5	46	62
$_{48}\text{Cd}^{112}$	24.2	32.4	48	64

TABLE 4—Continued

Group 10: I = 20
An incomplete group of seven nuclei terminated by radioactive $_{46}Pd^{112}$

MASS NUMBER	NUCLEI AND RELATIVE ISOTOPIC ABUNDANCE (per cent)	ABUNDANCE RELATIVE TO EVEN-EVEN (per cent)	CHARACTERISTICS OF NUCLEI	NUMBER OF PROTONS AND NEUTRONS p	m
116	$_{48}Cd^{116}$ 7.3	9.8		48	68
120	$_{50}Sn^{120}$ 28.5	35.3		50	70
124	$_{52}Te^{124}$ 4.5	4.87		52	72
128	$_{54}Xe^{128}$ 1.90	3.61		54	74 (46)
132	$_{56}Ba^{132}$ 0.097	0.118		56	76
136	$_{58}Ce^{136}$ 0.18			58	78 (D, 9)
140	$_{60}Nd^{140}$ Unknown			60	80)
144	$_{62}Sm^{144}$ 3	4.4		62	82 (A, 4)

An incomplete group of seven nuclei

Group 14: I = 28

136	$_{54}Xe^{136}$ 8.95	17.0		54	82
140	$_{56}Ba^{140}$ Unknown			56	84)
144	$_{58}Ce^{144}$ Unknown			58	86)

Group 8: I = 16—Continued
An incomplete group of seven nuclei

NUCLEI AND RELATIVE ISOTOPIC ABUNDANCE (per cent)	ABUNDANCE RELATIVE TO EVEN-EVEN (per cent)	NUMBER OF PROTONS AND NEUTRONS p	m
$_{50}Sn^{116}$ 15.5	19.2	50	66
$_{52}Te^{120}$ Low undetermined abundance		52	68
$_{54}Xe^{124}$ 0.094	0.179	54	70 (46)

Group 12: I = 24
An incomplete group of six nuclei

$_{50}Sn^{124}$ 6.8	8.4	50	74
$_{52}Te^{128}$ 32.8	35.5	52	76
$_{54}Xe^{132}$ 26.96	51.25	54	78 (46)
$_{56}Ba^{136}$ 7.8	9.5	56	80
$_{58}Ce^{140}$ 89	89	58	82
$_{60}Nd^{144}$ 22.6	29.1	60 (β-emitter (?))	84 (32)

Table 1

A	Nucleus			N	N
148	$_{60}\text{Nd}^{148}$	6.8	8.7	60	88
152	$_{62}\text{Sm}^{152}$	26	38	62	90
156	$_{64}\text{Gd}^{156}$	22	36	64	92
160	$_{66}\text{Dy}^{160}$	*1.5*	2.8	66	94 (D)
164	$_{68}\text{Er}^{164}$	*2*	2.6	68	96 (D)
168	$_{70}\text{Yb}^{168}$	*0.06*	0.08	70	98 (D)
172	Six nuclei		Group 18: I = 36		
176	$_{70}\text{Yb}^{176}$	12	16	70	106
180	$_{72}\text{Hf}^{180}$	30	47.5	72	108
184	$_{74}\text{W}^{184}$	30.1	36.4	74	110
188	$_{76}\text{Os}^{188}$	13.3	16.2	76	112
192	$_{78}\text{Pt}^{192}$	0.8	1.2	78	114
196	$_{80}\text{Hg}^{196}$	0.15	0.21	80	116
200	Group 22: I = 44 — Two nuclei terminated by radioactive $_{84}\text{Po}^{212}$				
204	$_{80}\text{Hg}^{204}$	6.72	9.63	80	124
208	$_{82}\text{Pb}^{208}$	52.3	67.7	82	126

Table 2

Nucleus			N	N
$(_{62}\text{Sm}^{148})$	14	20.6	62	86) Radioactive alpha-emitter (72)
$_{64}\text{Gd}^{152}$	0.2	0.3	64	88
Seven nuclei	Group 16: I = 32			
$_{64}\text{Gd}^{160}$	16	26	64	96
$_{66}\text{Dy}^{164}$	28	52	66	98
$_{68}\text{Er}^{168}$	29	38	68	100
$_{70}\text{Yb}^{172}$	23	31	70	102
$_{72}\text{Hf}^{176}$	5	8	72	104
$_{74}\text{W}^{180}$	0.2	0.24	74	106
$_{76}\text{Os}^{181}$	0.018	.022	76	108
Four nuclei	Group 20: I = 40			
$_{76}\text{Os}^{192}$	40.9	49.8	76	116
$_{78}\text{Pt}^{196}$	26.6	41.0	78	118
$_{80}\text{Hg}^{200}$	23.26	33.3	80	120
$_{82}\text{Pb}^{204}$	1.5	1.9	82	122

* References to the literature are given in parentheses.

TABLE 5

NUMBER OF PARTICLES OF MASS THREE (columns 0–16)

No. 2p2n	S_0 — 0	S_3 — 1	S_1 / S_2P_2 — 2	S_4 / S_3 — 3	S_2P_4 — 4	S_4 / S_3 — 5	S_2P_6 — 6	S_4 / S_3 — 7	S_4 / S_2P_8 — 8	S_4 / S_3 — 9	S_2P_2 — 10	S_4 / S_3 — 11	S_2P_4 — 12	S_4 / S_3 — 13	S_2P_6 — 14	S_4 / S_3 — 15	S_2P_8 — 16
0			$^{6}_{3}$Li	$^{9}_{4}$Be													
1		$^{7}_{3}$Li	$^{10}_{5}$B	$^{13}_{6}$C													
2		$^{11}_{5}$B	$^{14}_{7}$N	$^{17}_{8}$O													
3	$^{12}_{6}$C	$^{15}_{7}$N	$^{18}_{8}$O	$^{21}_{10}$Ne													
4	$^{16}_{8}$O	$^{19}_{9}$F	$^{22}_{10}$Ne	$^{25}_{12}$Mg													
5	$^{20}_{10}$Ne	$^{23}_{11}$Na	$^{26}_{12}$Mg	$^{29}_{14}$Si													
6	$^{24}_{12}$Mg	$^{27}_{13}$Al		$^{33}_{16}$S	$^{36}_{16}$S				$^{48}_{20}$Ca								
7	$^{28}_{14}$Si	$^{31}_{15}$P	$^{34}_{16}$S	$^{37}_{17}$Cl	$^{40}_{18}$A	$^{43}_{20}$Ca	$^{46}_{20}$Ca	$^{49}_{22}$Ti									
8	$^{32}_{16}$S	$^{35}_{17}$Cl	$^{38}_{18}$A	$^{41}_{19}$K	$^{44}_{20}$Ca	$^{47}_{22}$Ti	$^{50}_{22}$Ti	$^{53}_{24}$Cr									
9	$^{36}_{18}$A	$^{39}_{19}$K	$^{42}_{20}$Ca	$^{45}_{21}$Sc	$^{48}_{22}$Ti	$^{51}_{23}$V	$^{54}_{24}$Cr	$^{57}_{26}$Fe									

TABLE 5—Continued

Row	20 Ca	22 Ti	24 Cr	25 Mn	26 Fe	27 Co	28 Ni	29 Cu	30 Zn	31 Ga	32 Ge	33 As	34 Se	35 Br	36 Kr	37 Rb	38 Sr	39 Y	40 Zr	41 Cb	42 Mo	43 Tc	44 Ru	45 Rh	46 Pd	47 Ag	48 Cd	49 In	50 Sn	52 Te	54 Xe
10	40	46	52	55	58		64		70		76	—	82																		
11			50		56	59	62	65	68	71	74	—	80		86																
							61		67		73																				
12					54		60	63	66	69	72	75	78	81	84		—		96												
													77		83																
13							58		64		70		76	79	82	85	88		94	—	100										
																	87														
14													74		80		86	89	92		98	—	104								
																			91		97										
15															78		84		90	93	96	—	102		108						
																					95		101								
16																					94	—	100	103	106	109	112				
																							99		105						
17																					92	—	98		104	107	110	113	116		
18																							96		102		108		114	120	
19																											106		112		124

TABLE 6

PARTICLES OF MASS THREE

NO. 2p2n	S_4/S_3 17	S_2P_2 18	S_4/S_3 19	S_2P_4 20	S_4/S_3 21	S_2P_6 22	S_4/S_3 23	S_2P_8 24	S_4/S_3 25	S_2P_2 26	S_4/S_3 27	S_2P_4 28	S_4/S_3 29	S_2P_6 30	S_4/S_3 31	S_2P_8 32
13								$^{124}_{50}$Sn		$^{130}_{52}$Te		$^{136}_{54}$Xe				
14	—	$^{110}_{46}$Pd	$^{113}_{48}$Cd	$^{116}_{48}$Cd	$^{119}_{50}$Sn	$^{122}_{50}$Sn	$^{125}_{52}$Te	$^{128}_{52}$Te	$^{131}_{54}$Xe	$^{134}_{54}$Xe	$^{137}_{56}$Ba					
15	$^{111}_{48}$Cd	$^{114}_{48}$Cd	$^{117}_{50}$Sn	$^{120}_{50}$Sn	$^{123}_{51}$Sb	$^{126}_{52}$Te	$^{129}_{54}$Xe	$^{132}_{54}$Xe	$^{135}_{56}$Ba	$^{138}_{56}$Ba	—			$^{150}_{60}$Nd		
16	$^{115}_{49}$In	$^{118}_{50}$Sn	$^{121}_{51}$Sb	$^{124}_{52}$Te	$^{127}_{53}$I	$^{130}_{54}$Xe	$^{133}_{55}$Cs	$^{136}_{56}$Ba	$^{139}_{57}$La	$^{142}_{58}$Ce	$^{145}_{60}$Nd	$^{148}_{60}$Nd	—	$^{154}_{62}$Sm	$^{157}_{64}$Gd	$^{160}_{64}$Gd
17		$^{122}_{52}$Te		$^{128}_{54}$Xe		$^{134}_{56}$Ba	—	$^{140}_{58}$Ce	$^{143}_{60}$Nd	$^{146}_{60}$Nd	$^{149}_{62}$Sm	$^{152}_{62}$Sm	$^{155}_{64}$Gd	$^{158}_{64}$Gd	$^{161}_{66}$Dy	$^{164}_{66}$Dy
18		$^{126}_{54}$Xe		$^{132}_{56}$Ba		$^{138}_{58}$Ce	$^{141}_{59}$Pr	$^{144}_{60}$Nd	$^{147}_{62}$Sm	$^{150}_{62}$Sm	$^{153}_{63}$Eu	$^{156}_{64}$Gd	$^{159}_{65}$Tb	$^{162}_{66}$Dy	$^{165}_{67}$Ho	$^{168}_{68}$Er
19		$^{130}_{56}$Ba		$^{136}_{58}$Ce		$^{142}_{60}$Nd	—	—	$^{151}_{63}$Eu	$^{154}_{64}$Gd		$^{160}_{66}$Dy		$^{166}_{68}$Er	$^{169}_{69}$Tm	$^{172}_{70}$Yb
20				—				$^{152}_{64}$Gd		$^{158}_{66}$Dy		$^{164}_{68}$Er		$^{170}_{70}$Yb		$^{176}_{72}$Hf
21				$^{144}_{62}$Sm						$^{162}_{68}$Er		$^{168}_{70}$Yb		$^{174}_{72}$Hf		$^{180}_{74}$W
22																$^{184}_{76}$Os

TABLE 6—Continued

NO.	NO. PARTICLES OF MASS THREE												
	33	34	35	36	37	38	39	40	41	42	43	44	45
16	163 66Dy												
17	167 68Er	170 70Yb	173 70Yb	176 70Yb	179 72Hf								
18	171 70Yb	174 70Yb	177 72Hf	180 72Hf	183 74W	186 74W	189 76Os	192 76Os	195 78Pt	198 78Pt	201 80Hg	204 80Hg	207 82Pb
19	175 71Lu	178 72Hf	181 73Ta	184 74W	187 75Re	190 76Os	193 77Ir	196 78Pt	199 80Hg	202 80Hg	205 81Tl	208 82Pb	
20		182 74W	185 75Re	188 76Os	191 77Ir	194 78Pt	197 79Au	200 80Hg	203 81Tl	206 82Pb	209 83Bi		
21		186 76Os		192 78Pt		198 80Hg		204 82Pb					
22				196 80Hg									

NO. PARTICLES of M·3

	2p2n		
	17	21	37
15		123 52Te	
16	115 50Sn		
19			187 76Os

servation has been made that the groups of Series 4 always precede the groups of nuclei of Series 3 with a difference of four mass units. The isotopic number of a sequence of Series 4 is always two units lower than the following sequence of Series 3.

With this observation it was possible to connect stable nuclei in the order of their mass numbers while maintaining sequences of identical characteristics. Tables 5 and 6 are arranged in a form so that the series appear periodically and coincide with consecutive numbers of particles of three mass units. The number of particles of mass 3, except for Series 4, also represent the isotopic numbers of respective groups of nuclei. The number of particles of mass 3 in Series 4 is two units higher than the isotopic number of the corresponding group. This connection of Series 4 and three species can be regarded as a change of an $n2p$ group into a $p2n$. Identically the nuclei of Series 1 (S_1) precede the nuclei of Series 2, Period 2. The connection likewise, can be regarded as a change of $n2p$ into $p2n$. Vertically are given the number of particles of four mass units ($2p2n$).

CLASSIFICATION OF STABLE NUCLEI WITH THE AID OF THREE AND FOUR MASS UNITS
(TABLES 5 AND 6)

Series 0 remains separated from the other series. However, the nucleus $_6C^{12}$ could be as well regarded as the first nucleus of a sequence with four particles of three mass units.

The shifted position of the nucleus of mass number 39, $_{19}K^{39}$ described above, is found to be adapted to the summarized classification.

The shifts described in Group 6, I = 11, of Series 3 and Group 7, I = 13, of Series 4, and in Groups 12 and 13 of Series 3 and 4, I = 23 and 25, suggest that sixty-one protons may not form a stable nucleus with any combination of neutrons.

In the even-even series all charge numbers are represented; however, there are gaps in Periods 4, 6, and 8, due to non-observance of stable nuclei $_{40}Zr^{88}$, $_{38}Sr^{90}$, $_{56}Ba^{140}$, $_{58}Ce^{144}$. The radioactive species of these mass numbers are not yet established.

The position of $_{57}La^{139}$ remains unique, since it is a nucleus of Series 3 located in the middle of a sequence of Series 4.

Only three nuclei, odd isobars, the stability of which is debated, could not be placed in the summarized classification. These three nuclei are shown separately on the tables. On the other hand both the isobars $_{48}Cd^{113}$ and $_{49}In^{113}$ are properly placed in the classification.

Four nuclei of known even-even triodes, A = 96, 124, 130, 136, have the species $_{40}Zr^{96}$, $_{50}Sn^{124}$, $_{52}Te^{130}$, and $_{54}Xe^{136}$ occupying positions out of line.

It is reasonable to assume some future corrections of presently known stable isotopes, especially in the rare earth region.

REFERENCES

(1) ALLISON, S. K.: Phys. Rev. **55**, 624 (1939).
(2) ALLISON, S. K., MILLER, L. C., PERLOW, G. J., SKAGGS, L. S., AND SMITH, N. U., JR.:
     Phys. Rev. **58**, 178 (1940).

(3) Aston, F. W.: Proc. Roy. Soc. (London) A146, 46 (1934).
(4) Aston, F. W.: *Mass Spectra and Isotopes*. Edward Arnold Company, London (1942).
(5) Barkas, W. H.: Phys. Rev. 55, 691 (1939).
(6) Benson, A., and Sawyer, R. A.: Phys. Rev. 49, 867 (1936).
(7) Bethe, H. A., and Backer, R. F.: Rev. Modern Phys. 8, 82 (1936).
(8) Crawford, M. F., and Bateson, S.: Can. J. Research 10, 693 (1934).
(9) Cohen, A. A.: Phys. Rev. 63, 219 (1943).
(10) Dempster, A. J.: Phys. Rev. 49, 947 (1936).
(11) Elliott, A.: Proc. Roy. Soc. (London) 127, 638 (1930).
(12) Feenberg, E., and Phillips, M.: Phys. Rev. 51, 597 (1937).
(13) Feenberg, E., and Wigner, E.: Phys. Rev. 51, 95 (1937).
(14) Fisher, R. A., and Peck, E. R.: Phys. Rev. 55, 270 (1939).
(15) Gollnow, H.: Z. Physik 103, 443 (1936).
(16) Hamilton, D. R.: Phys. Rev. 56, 30 (1939).
(17) Hardy, T. C., and Millman, S.: Phys. Rev. 61, 459 (1942).
(18) Hay, R. H.: Phys. Rev. 58, 180 (1940); 60, 75 (1941).
(19) Heyden, M., and Kopfermann, H.: Z. Physik 108, 232 (1938).
(20) Inglis, D. R.: Phys. Rev. 60, 837 (1941); and references given therein.
(21) Inglis, D. R.: Phys. Rev. 60, 843 (1941).
(22) Jackson, D. A., and Kuhn, H.: Proc. Roy. Soc. (London) 158, 372 (1937).
(23) Kellogg, J. M. B., Rabi, I. I., Ramsey, N. F., Jr., and Zacharias, J. R.: Phys. Rev. 57, 677 (1940).
(24) Kittel, C.: Phys. Rev. 62, 109 (1942).
(25) Kopfermann, H.: Z. Physik 83, 417 (1933).
(26) Kopfermann, H.: *Kernmoments*. Akademische Verlagsgesellschaft, Leipzig (1940).
(27) Kopfermann, H., and Rindal, E.: Z. Physik 87, 460 (1934).
(28) Kopfermann, H., and Wittke, H.: Z. Physik 105, 16 (1937).
(29) Kusch, P., and Millman, S.: Phys. Rev. 56, 527 (1939).
(30) Kusch, P., Millman, S., and Rabi, I. I.: Phys. Rev. 55, 666 (1939).
(31) Kusch, P., Millman, S., and Rabi, I. I.: Phys. Rev. 55, 1176 (1939).
(32) Libby, W. F.: Phys. Rev. 45, 845 (1934); 46, 196 (1934).
(33) Livingood, J. J., and Seaborg, G. T.: Rev. Modern Phys. 12, 30 (1940).
(34) Livingston, M. S., and Bethe, H. A.: Rev. Modern Phys. 9, 380 (1937).
(35) Livingston, M. S., and Bethe, H. A.: Rev. Modern Phys. 9, 373 (1937).
(36) Lyshede, J. M., and Rasmussen, E.: Z. Physik 104, 434 (1937).
(37) Margenau, H., and Wigner, E.: Phys. Rev. 58, 103 (1940).
(38) Mattauch, J.: Phys. Rev. 57, 1155 (1940).
(39) McLay, A. B., and Crawford, M. F.: Phys. Rev. 44, 986 (1933).
(40) Millman, S., and Fox, M.: Phys. Rev. 50, 220 (1936).
(41) Millman, S., and Kusch, P.: Phys. Rev. 56, 303 (1939).
(42) Millman, S., Kusch, P., and Rabi, I. I.: Phys. Rev. 56, 165 (1939).
(43) Millman, S., Rabi, I. I., and Zacharias, J. R.: Phys. Rev. 53, 384 (1939).
(44) Manley, J. H.: Phys. Rev. 49, 921 (1936).
(45) More, K. R.: Phys. Rev. 46, 470 (1934).
(46) Nier, A. O.: Phys. Rev. 52, 933 (1937).
(47) O'Neal, R. D., and Goldhaber, M.: Phys. Rev. 58, 574 (1940).
(48) Pollard, E.: Phys. Rev. 57, 1186 (1940).
(49) Rabi, I. I.: *The Moments of the Light Nuclei, Nuclear Physics*. University of Pennsylvania Press (1941).
(50) Rabi, I. I., Millman, S., Kusch, P., and Zacharias, J. R.: Phys. Rev. 55, 526 (1939).
(51) Renzetti, N. A., and Hamilton, D. R.: Phys. Rev. 57, 570 (1940).
(52) Sachs, R. G., and Schwinger, J.: Phys. Rev. 61, 732 (1942).
(53) Schüler, H., and Jones, E. G.: Z. Physik 74, 631 (1932).
(54) Schüler, H., and Keyston, J. E.: Z. Physik 71, 413 (1931).

(55) Schüler, H. and Korsching, H.: Z. Physik **103**, 434 (1936).
(56) Schüler, H., and Korsching, H.: Z. Physik **111**, 386 (1939).
(57) Schüler, H., Roig, J., and Korsching, H.: Z. Physik **111**, 165 (1939).
(58) Schüler, H., and Schmidt, Th.: Z. Physik **104**, 468 (1937).
(59) Schüler, H., and Westmeyer, H.: Naturwissenschaften **21**, 660 (1933).
(60) Schmidt, Th.: Z. Physik **101**, 486 (1936).
(61) Schmidt, Th.: Z. Physik **108**, 408 (1938).
(62) Schmidt, Th.: Z. Physik **112**, 199 (1939).
(63) Shrader, E. F.: Phys. Rev. **58**, 475 (1940).
(64) Shrader, E. F., Millman, S., and Kusch, P.: Phys. Rev. **58**, 925 (1940).
(65) Sibaiya, L.: Phys. Rev. **56**, 768 (1939).
(66) Tolansky, S., and Forester, G. O.: Proc. Roy. Soc. (London) **50**, 826 (1938).
(67) Weimer, K. E., Pool, M. L., and Kurbatov, J. D.: Phys. Rev. **63**, 67 (1943).
(68) Welles, S. B.: Phys. Rev. **62**, 197 (1942).
(69) Wheeler, J. A.: Phys. Rev. **59**, 108 (1941).
(70) Wigner, E.: Phys. Rev. **51**, 106 (1937).
(71) Wigner, E.: Phys. Rev. **51**, 947 (1937).
(72) Wilkins, T. R., and Dempster, A. J.: Phys. Rev. **54**, 315 (1938).
(73) Wood, R. W., and Dieke, G. H.: Phys. Rev. **55**, 1120 (1939).
(74) Zacharias, J. R., and Kellogg, J. M. B.: Phys. Rev. **57**, 570 (1940).

THE MERCURY–PHOTOSENSITIZED REACTIONS OF ISOBUTANE

B. de B. DARWENT[1] and C. A. WINKLER

Physical Chemistry Laboratory, McGill University, Montreal, Canada

INTRODUCTION

Investigations of the mercury–photosensitized reactions of the lower paraffin hydrocarbons have shown that with ethane (12, 14, 19), which contains only primary hydrogen atoms, considerable C—C bond splitting occurs at some stage of the process, whereas with propane (15) and butane (4), both of which contain secondary C—H bonds, reaction proceeds almost entirely by a C—H split. The behavior of isobutane under similar conditions is of interest, since either the shielding of the tertiary bond or the 9:1 statistical factor in favor of the primary C—H bonds conceivably could make the reaction occur preferentially on one of the primary bonds, in which case the nature of the products should indicate a reaction of the same type as with ethane, if the anomalous behavior of ethane is due to the absence of secondary or tertiary C—H bonds.

The mercury–photosensitized reactions of isobutane have therefore been investigated with the results recorded in the present paper.

Isobutane was obtained from the Ohio Chemical Co.   It was stated to be at least 99 per cent pure, the only impurity being n-butane.   Since no impurity could be detected by the analytical methods employed, the isobutane was used after a simple bulb-to-bulb distillation.

The essential features of the apparatus are shown in the accompanying diagram (figure 1).   The lamp-reactor unit L-R, of the type described by Steacie and Phillips (18), was connected in a closed circuit with three traps, T-1, T-2, and T-3, a set of mercury valves (V) to ensure unidirectional flow of the gas, a circulating pump (P), and a mercury saturator (S).   The volume of the reactor was about 870 ml.   The lamp was filled with 3 mm. of neon as carrier gas and a drop of mercury.   The electrodes were surrounded by copper coils through which water could be circulated to cool or heat the chambers.   The pump (P) was made from
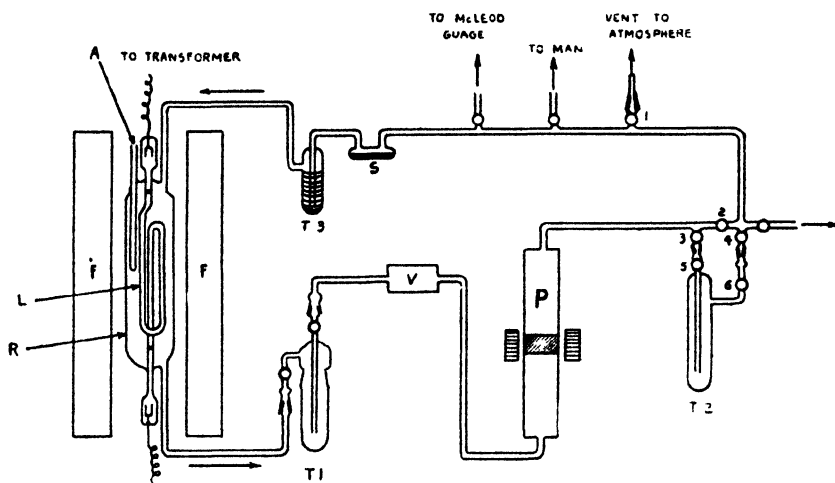
FIG. 1. The apparatus

a brass tube 4 cm. in diameter and 35 cm. long; it was fitted with a steel piston which was drawn in reciprocating motion by an external electromagnet attached to an eccentric on a $\frac{1}{4}$ H.P. motor.   The displacement was about 440 ml. per stroke.

Before each experiment the temperature of the reactor was raised to about 350° C. and the vessel evacuated overnight to remove any high-boiling polymers that might have been produced in previous experiments.   Absence of these polymers was assumed when no pressure rise was observed (McLeod gauge) after 30 min. illumination of the evacuated system.

A measured volume of isobutane was introduced, and trap T-2 was cooled with solid carbon dioxide–acetone to a temperature such that the isobutane condensed and provided the requisite working pressure of the gas.   Trap T-1 was then cooled to a temperature slightly higher than that of T-2 to condense the high-boiling products of the reaction.   The circulating pump was started and the

stopcocks arranged so that the gases passed through the traps. The lamp was turned on and regulated by adjusting the current to the primary of the transformer. The gases were illuminated for a measured time, after which the pressure of the volatile products of the reaction and the residual isobutane was measured by placing T-1 in ice water and then in liquid air. (The gases were circulated to constant pressure in each case.) The permanent gas fraction was removed in a Toepler pump and analyzed by low-temperature distillation, followed by combustion of the hydrogen–methane fraction. The combustion was carried out in a large excess of oxygen, and the carbon dioxide produced was absorbed in standard alkali to which a drop of 1-butanol had been added as a neutral foaming agent. The condensed gases in T-1 were also analyzed by low-temperature fractional distillation, and the higher boiling products of the reaction removed from the trap and weighed.

The heavy products were found to consist mainly of octanes and dodecanes. From the results of previous work on similar reactions it might be inferred that only three octanes,—namely, 2,5-dimethylhexane, 2,2,4-trimethylpentane, and 2,2,3,3-tetramethylbutane,—would be produced in the reaction. These octanes form a continuous series of solid solutions (11), so that the 2,2,3,3-tetramethylbutane could not be separated from the others by freezing. The analysis of the octane fraction was further complicated by the proximity of the boiling points of the isomers and the small difference between the melting and boiling points of 2,2,3,3-tetramethylbutane. A reasonably precise analysis of the octane fraction was obtained, however, by the partial fractionation of the mixture with an efficient semi-micro column (twenty-two plates) provided with a modified Stedman type wire gauze packing, as recommended by Bower and Cooke (1), and run with intermittent draw-off of 0.5-ml. samples. The fractions thus obtained were weighed, and their melting and boiling points determined in the usual manner. The composition of each fraction was determined, assuming each to consist of 2,2,3,3-tetramethylbutane and one of the other two possible octanes, by determination of the refractive indices of solutions containing known percentages of the fraction in n-hexane.

The nature of the reaction was investigated at 80°, 150°, and 250°C. and under various working pressures of isobutane. In all experiments the current to the lamp was kept constant on the assumption that the output of λ2537 was independent of the operating temperature within the limits covered.

<center>RESULTS</center>

Details of the operating conditions are given in table 1. The quantum output of the lamp was determined by the use of a monochloroacetic acid actinometer with the corrections proposed by Smith, Leighton, and Leighton (10) for the effect of temperature on the ratio of the dark to the photochemical reaction instead of the value of unity given by Rudberg (8) for the quantum yield of this reaction. Accordingly, the values for the quantum yield reported here should be altered by a factor of 0.4 for comparison with most of the past work on similar reactions.

The amount of liquid product obtained in the individual experiments was too

small for independent analysis; accordingly, the products from several experiments at the same temperature were combined for analysis.   Details of the

TABLE 1

Experimental conditions

Volume of reactor, 870 ml.; volume of system, 1985 ml.; arc current, 89 milliamperes; circulation rate, 2.67 liters per minute; resonance radiation absorbed, 1.19×10^{-5} einsteins per second

RUN NO.	AVERAGE TIME OF RUN	INITIAL PRESSURE OF BUTANE	WORKING PRESSURE OF BUTANE	FINAL PRESSURE		LIQUID PRODUCTS
				Total products	Hydrogen and methane	
Series A: runs at 80°C.						
	min.	*cm.* Hg	*cm.* Hg	*cm.* Hg	*cm.* Hg	*grams*
A1	120	30.5	6.4	26.2	5.2	
A2	120	50.5	9.2	45.0	5.3	0.4
A3	540	60.0	10.7	44.6	18.0	1.90
A4	593	50.5	11.4	33.1	19.0	2.15
A5	120	51.3	21.8	44.8	6.3	0.55
A6	180	60.0	30.6	50.5	10.3	0.95
Series B: runs at 150°C.						
B1	180	.50.2	5.0	34.0	16.6	1.53
B2	300	50.0	10.0	29.8	24.0	
B3	150	50.1	11.0	36.9	14.1	1.51
B4	150	60.3	11.0	42.4	14.6	1.27
B5	240	51.3	11.0	27.8	24.5	2.20
B6	90	60.2	31.7	55.3	8.9	
Series C: runs at 250°C.						
C1	300	50.5	6.0	40.6	11.0	1.12
C2	150	49.8	10.0	35.5	14.4	1.13
C3	210	70.2	10.8	45.2	21.7	2.12
C4	180	69.9	12.6	51.0	23.7	1.40
C5	120	60.8	19.0	49.0	10.5	0.92
C6	120	60.5	23.8	50.4	11.6	1.10
C7	90	50.0	27.0	45.3	6.8	
C8	120	58.9	27.8	48.0	10.6	
C9	150	70.0	32.9	54.3	13.2	1.26
C10*	120	56.9	41.8	48.9	7.9	1.23
C11*	210	54.4	51.4	43.5	11.3	1.81
C12*	120	65.0	61.0	56.0	8.3	1.19

* Volume of system = 3190 ml.

fractionation of the liquid products, and of the properties of the fractions so obtained are shown in table 2.

The compositions of the products, based on the results of the gas and liquid analyses, are given in table 3.   The composition of the liquid products follows from the characteristics of the individual fractions given in table 2.   In all cases

the first fraction was arbitrarily assigned a composition of 60 per cent 2,2,4-tri-methylpentane and 40 per cent lower paraffins.   It must be admitted that this procedure is unsound but, with the exception of Series B runs, the boiling points and refractive indices of the first fractions indicate that they contained 2,2,4-tri-methylpentane; the nature of the other components is unknown.   In view of the

TABLE 2

Fractionation of liquid products and properties of fractions

Series A: runs at 80°C.

Charge to distillation......	9.70 g., 100% of charge
Distillate.......	5.83 g., 60% of charge
Residue..........	1.67 g., 17% of charge
Loss on distillation.....	2.20 g., 23% of charge

FRACTION NO.	PER CENT OF DISTILLATE	BOILING POINT	MELTING RANGE	REFRACTIVE INDEX n_D^{20}	HEXANE SOLUTION	
					C_8	n_D^{20}
		°C.	°C.		per cent	
1	10.3	73.6	−78	1.3860	49.7	1.3851
2	10.3	92.1	−78	1.3925		
3	10.1	95.1		1.3962	61.2	1.3899
4	10.0	100.0		1.4000	45.9	1.3881
5	9.2	103.3	0 to 62	1.4015	48.6	1.3888
6	8.5	105.2	20 to 69		28.1	1.3842
7	9.9	104.6	50 to 89		38.0	1.3860
8	9.7	104.8	50 to 90		31.3	1.3840
9	12.8	105.2	30 to 85		47.0	1.3890
10	9.2	106.6	−10 to 68			

Series B: runs at 150°C.

Charge to distillation	7.99 g., 100% of charge
Distillate...................................	4.75 g., 59% of charge
Residue.............................	0.92 g., 12% of charge
Loss on distillation......	2.32 g., 29% of charge

FRACTION NO.	PER CENT OF DISTILLATE	BOILING POINT	MELTING RANGE	REFRACTIVE INDEX n_D^{20}	HEXANE SOLUTION	
					C_8	n_D^{20}
		°C.	°C.		per cent	
1	9.9	101.5	? to −78	1.3954	61.8	1.3884
2	10.5	105.0	−10 to 45		49.4	1.3878
3	7.0	105.0	−10 to 82		56.4	1.3904
4	11.2	106.0	5 to 91		53.4	1.3901
5	9.3	106.0	65 to 95		44.6	1.3881
6	8.0	106.2	75 to 98		52.8	1.3906
7	8.2	106.1	92 to 100		50.0	1.3899
8	8.6	106.5	93 to 100		48.6	1.3891
9	9.5	106.7	25 to 88		61.6	1.3951
10	7.3	115.4	5 to 30			
11	10.5					

TABLE 2—*Concluded*

Series C: runs at 250°C.

Charge to distillation...... .... 7.80 g., 100% of charge
Distillate.................................. ... . 5.52 g., 70.9% of charge
Residue... .... 0.34 g., 4.4% of charge
Loss on distillation.......................................•.. 1.94 g., 24.7% of charge

FRACTION NO.	PER CENT OF DISTILLATE	BOILING POINT	MELTING RANGE	REFRACTIVE INDEX n_D^{20}	HEXANE SOLUTION	
					C_8	n_D^{20}
		°C.	°C.		per cent	
1	11.1	79.0	−78	1.3885	63.9	1.3880
2	10.5	98.0	? to −78	1.3969	61.7	1.3906
3	9.2	102.5	0 to 15	1.4000	49.0	1.3890
4	14.6	101.0	20 to 49		40.9	1.3874
5	9.6	105.7	80 to 93			
6	12.7	103.6	96 to 100			
7	10.9	105.0	98 to 100		41.1	1.3874
8	9.1	103.8	55 to 92		50.4	1.3904
9	8.5	104.4	10 to 54		31.1	1.3846
10	3.8					

attendant uncertainties only a rough estimate of the composition was possible, but an error of 20 per cent in the assigned composition could affect the analysis of the total liquid product by only 2 per cent.

Fractions after the first may be assumed to contain not more than two components, both octanes.   The analysis of these fractions is based on the refractive

TABLE 3

Analysis of products

(1) Product from runs at 80°C.

(a) *Liquid:*

FRACTION NO.	PER CENT OF TOTAL DISTILLATE	HEXAMETHYL-ETHANE	2,2,4-TRI-METHYLPEN-TANE	2,5-DIMETHYL-HEXANE	HYDROCARBONS LOWER THAN OCTANES
1	10.3	0.0	60.0*	0.0	40.0*
2	10.3	23.0	77.0	0.0	0.0
3	10.1	34.0	66.0	0.0	0.0
4	10.0	45.1	54.9	0.0	0.0
5	9.2	71.4	28.6	0.0	0.0
6	8.5	70.9	29.1	0.0	0.0
7	9.9	96.5	3.5	0.0	0.0
8	9.7	72.0	0.0	18.0	0.0
9	12.8	61.1	0.0	38.9	0.0
10	9.2	76.9	0.0	23.1	0.0
Total distillate..	100.0	55.4	29.7	9.8	5.1

(b) *Gas:* Per cent CH_4 = 5.8; per cent H_2 = 94.2

TABLE 3—*Concluded*

(2) Product from runs at 150°C.

(a) *Liquid:*

FRACTION NO.	PER CENT OF TOTAL DISTILLATE	HEXAMETHYL-ETHANE	2,2,4-TRI-METHYLPEN-TANE	2,5-DIMETHYL-HEXANE	HYDROCARBONS LOWER THAN OCTANES
1	9.9	0.0	60.0*	0.0	40.0*
2	10.5	31.4	68.6	0.0	0.0
3	7.0	56.0	44.0	0.0	0.0
4	11.2	63.4	34.6	0.0	0.0
5	9.3	69.1	30.9	0.0	0.0
6	8.0	76.4	23.6	0.0	0.0
7	8.2	76.4	11.8	11.8	0.0
8	8.6	79.4	0.0	20.6	0.0
9	9.5	74.0	0.0	26.0	0.0
10	7.3	95.6	0.0	4.4	0.0
10 (a)	10.5	100.0	0.0	0.0	0.0
Total..................	100.0	64.6	25.8	5.6	4.0

(b) *Gas:* Per cent CH_4 = 4.0; per cent H_2 = 96.0

(3) Product from runs at 250°C.

(a) *Liquid:*

FRACTION NO.	PER CENT OF TOTAL DISTILLATE	HEXAMETHYL-ETHANE	2,2,4-TRI-METHYLPEN-TANE	2,5-DIMETHYL-HEXANE	HYDROCARBONS LOWER THAN OCTANES
1	11.1	0.0	60.0*	0.0	40.0*
2	10.5	24.1	75.9	0.0	0.0
3	9.2	52.4	47.6	0.0	0.0
4	14.6	72.1	27.9	0.0	0.0
5	9.6	85.2	17.5	0.0	0.0
6	12.7	100.0	0.0	0.0	0.0
7	10.9	100.0	0.0	0.0	0.0
8	9.1	81.8	0.0	18.2	0.0
9	8.5	83.1	0.0	16.9	0.0
10	3.8	85.2	7.4	7.4	0.0
Total..................	100.0	67.7	25.9	3.1	3.3

(b) *Gas:* Per cent CH_4 = 8.9; per cent H_2 = 91.1

* Estimated values.

indices of solutions containing known proportions of the mixed octanes in *n*-hexane.

Details of the rate, quantum yield, and products of the reaction are given in table 4. The reaction rate was based on the number of moles of isobutane reacted and the quantum yield was derived accordingly from the known output of the lamp.

TABLE 4

The mercury-photosensitized decomposition of isobutane—results

(Conditions as in table 1)

RUN NO.	AVERAGE WORKING PRESSURE	REACTION RATE MOLES C₄H₁₀ REACTED SEC.⁻¹	QUANTUM YIELD	PRODUCTS MOLES OF PRODUCT PER 100 MOLES C₄H₁₀ REACTED			
				H_2	CH_4	C_8H_{18}	$C_{12}H_{26}$
	cm. Hg						
A1	6.4	1.6×10^{-6}	0.14	49.5			
A2	9.2	1.8×10^{-6}	0.15	45.0		24.0	3.1
A3	10.7	1.1×10^{-6}	0.09	50.5	2.6	40.5	5.6
A4	11.4	1.1×10^{-6}	0.0	49.0	2.6	42.0	5.9
A5	21.8	2.1×10^{-6}	0.18	45.7		26.7	4.0
A6	30.6	2.1×10^{-6}	0.18	49.4		30.5	4.5
Average		1.6×10^{-6}	0.14	49.8	2.6	32.7	4.6
B1	5.0	2.9×10^{-6}	0.24	46.6	1.9	36.9	3.4
B2	10.0	2.3×10^{-6}	0.17	51.7	2.3		
B3	11.0	2.6×10^{-6}	0.22	51.9	2.6	50.1	4.3
B4	11.0	3.2×10^{-6}	0.27	46.0	1.7	33.9	3.1
B5	11.0	3.1×10^{-6}	0.26	48.4	2.0	38.1	3.3
B6	31.7	2.3×10^{-6}	0.19	60.0			
Average		2.7×10^{-6}	0.23	48.9	2.1	39.8	3.5
C1	6.0	1.0×10^{-6}	0.09	49.0	4.8	50.6	1.7
C2	10.0	2.5×10^{-6}	0.22	43.9	7.4	40.9	1.3
C3	10.8	3.1×10^{-6}	0.27	40.9	3.1	45.4	1.5
C4	12.6	3.2×10^{-6}	0.27	47.9	5.9	33.1	1.1
C5	19.0	2.6×10^{-6}	0.22	45.0		41.9	1.1
C6	23.8	2.6×10^{-6}	0.22	50.9		50.1	1.6
C7	27.0	1.8×10^{-6}	0.15	54.4			
C8	27.8	2.5×10^{-6}	0.21	47.0			
C9	32.9	2.6×10^{-6}	0.22	40.5	4.3	45.4	1.3
C10	41.8	3.1×10^{-6}	0.26	43.7	2.8	50.8	1.4
C11	51.4	2.3×10^{-6}	0.19	42.8	3.6	52.6	1.7
C12	61.0	3.6×10^{-6}	0.30	41.0		38.6	1.2
Average ..		2.6×10^{-6}	0.22	42.9	4.6	45.0	1.4

TABLE 5

Yield of products

PRODUCT	MOLES OF PRODUCT PER 100 MOLES OF ISOBUTANE REACTED		
	80°C.	150°C.	250°C.
Hydrogen....................................	49.8	48.9	42.9
Methane......................................	2.6	2.1	4.6
Heptanes and lower...........	1.7	1.6	1.4
Hexamethylethane..........	18.2	25.7	30.4
2,2,4-Trimethylpentane...............	9.7	10.3	11.6
2,5-Dimethylhexane.........	3.2	2.2	1.4
Dodecanes.....................................	4.6	3.5	1.4

More precise details of the effect of temperature on the average yields of the individual products are given in table 5. The values are averages for the three series of runs and are based on the average values shown in tables 3 and 4.

DISCUSSION

The following characteristics of the reaction merit discussion:

(1) The products of the reaction are almost entirely hydrogen, octanes, dodecanes, and higher paraffin hydrocarbons.

(2) Only small amounts of methane and hydrocarbons lighter than octane were detected in the products.

(3) The rate of the reaction and the nature of the products are independent of the working pressure of the hydrocarbon at all temperatures investigated.

(4) The reaction temperature has little influence on the reaction rate but does affect the nature of the products. With increase of temperature the production of hexamethylethane increases while the production of dodecanes decreases.

(5) The material balance shows a loss of material at low temperatures. It improves with increasing temperature and is almost perfect at 250°C.

The effect of working pressure of isobutane on the course of the reaction is shown in table 4. It is seen that, at constant temperature, neither the nature of the products nor the rate of the reaction is influenced to any appreciable extent by a wide variation in the working pressure. In the type of system used it is known that quenching was essentially complete at the lowest pressure (6 cm.). Since the emission line is very narrow and the concentration of mercury vapor in the reactor relatively high, it would appear that pressure broadening could have little or no effect on the course or rate of the reaction. Hence the absence of pressure effect shows that none of the major reactions were significantly affected by the dreierstoss restriction, and that the relative proportions of isobutane and hydrogen, within the limits covered, in the reaction mixture do not affect the course of the reaction. This independence of the reaction on the proportions of hydrogen and paraffin is in agreement with the results obtained by Steacie and Dewar (15), who found that addition of hydrogen in the mercury-photosensitized reactions of propane did not change either the rate of the reaction or the nature of the products.

The effect of temperature on the reaction is shown in tables 4 and 5. It is seen that the rate is increased by increasing the temperature from 80° to 150°C. but that further increase from 150° to 250°C. causes no alteration of reaction rate. The following changes in the products of the reaction with increasing temperature are considered significant:

(a) *Hydrogen:* the yield decreases with increasing temperature above 150°C.

(b) *Methane:* the yield increases with increasing temperature above 150°C.

(c) *Dodecanes:* the yield decreases with temperature above 150°C.

(d) *Octanes:* The variation in the production of the individual octanes with temperature shows that the initial C—H split apparently occurs on the primary C—H as well as at the tertiary C—H bonds and that the extent of the latter split increases relative to the former with increasing temperature.

The most significant result of the investigation was the fact that the products of the reaction consisted almost entirely of octanes (and dodecanes) and hydrogen. Very little methane was found. This indicates clearly that the primary reaction of the isobutane molecule is the production of the corresponding radical:

$$i\text{-}C_4H_{10} + Hg(6^3P_1) = C_4H_9 + HgH \qquad (1)$$

followed by

$$HgH = H + Hg(6^1S_0) \qquad (2)$$
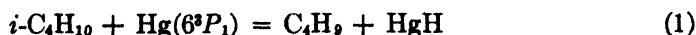
The production of the radical as the initial act is in complete accord with the mechanisms postulated for the photosensitized and hydrogen atom reactions of the lower paraffin hydrocarbons.

In the early stages of the reaction the hydrogen atom produced in reaction 2 will certainly enter into collision with an isobutane molecule, and the reaction

$$H + i\text{-}C_4H_{10} = C_4H_9 + H_2 \qquad (3)$$

has been shown by White, Winkler, and Kenalty (20) to occur readily.

As the reaction proceeds and as hydrogen accumulates in the system, the reaction

$$H_2 + Hg(6^3P_1) = H + HgH \qquad (4)$$

will assume increasing importance and, owing to the high efficiency with which hydrogen is known to quench $Hg(6^3P_1)$ atoms, will eventually be the major source of hydrogen atoms. In the later stages of a run it is evident that reaction 3 will be the main source of butyl radicals.

The production of hydrogen atoms by a reaction between butyl radicals and hydrogen molecules

$$C_4H_9 + H_2 = C_4H_{10} + H \qquad (5)$$
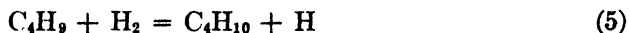
might be considered as probable in the later stages of a run, but the indications (5) are that reactions of this type do not occur readily below 160°C. and, as the hydrogen atom produced would probably react by reaction 3, the reaction can have little significance in the present investigation. The production of hydrogen molecules by recombination

$$H + H + M = H_2 + M \qquad (6)$$

cannot be regarded as important because of the dreierstoss restriction, the small probability of collision, and the fact that the rate of reaction in the present type of system is independent of the relative concentrations of paraffin and of hydrogen. The production of octanes is most easily accounted for as the result of recombination of the butyl radicals:

$$2C_4H_9 = C_8H_{18} \qquad (7)$$

These reactions are known to occur with little or no real activation energy (3) and have been postulated as responsible for the major products of photosensitized reactions. The only reasonable alternative to this reaction would be:

$$C_4H_9 + C_4H_{10} = C_8H_{18} + H \tag{8}$$
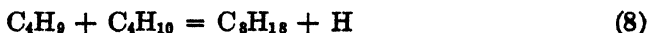
Reactions of this type have been estimated (16) to have an activation energy of 40 to 50 kcal., so that reaction 8 would be improbable and, in any case, could not be postulated from any of the results obtained in the present investigation.

The dodecanes probably are formed by the combination of butyl and octyl radicals, these latter bodies being produced by reactions similar to those given in equation 1 or 3 involving octane instead of butane molecules. By analogy with the results of Smith and Taylor (9), the octyl radicals may be produced also by the reaction

$$C_4H_9 + C_8H_{18} = C_4H_{10} + C_8H_{17} \tag{8'}$$
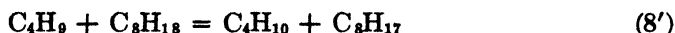
since these authors consider that the activation energy of this type of reaction is less than 10 kcal. The reaction

$$C_4H_9 + C_8H_{18} = C_{12}H_{26} + H$$
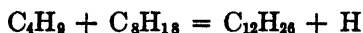
must be discounted for the same reasons as was reaction 8 and so cannot be regarded as a source of dodecane.

The presence of small amounts of methane in the products requires some explanation. In past work on similar photosensitized reactions (4, 15), as well as in the reactions between paraffins and hydrogen atoms produced by the discharge-tube method (13, 17, 21), the methane was accounted for as the result of "atomic cracking" reactions. In the present case these reactions would be:

$$H + C_4H_9 = CH_3 + C_3H_7 \tag{9a}$$

$$H + C_3H_7 = CH_3 + C_2H_5 \tag{9b}$$

$$H + C_2H_5 = 2CH_3 \tag{9c}$$
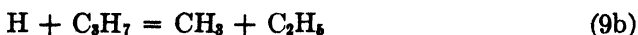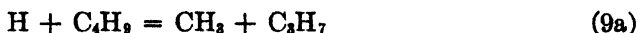
The methane would then be formed by the combination of methyl radicals and hydrogen atoms in the presence of a third body:

$$H + CH_3 + M = CH_4 + M \tag{10}$$
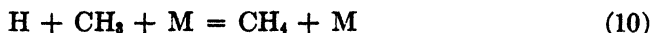
The activation energies of reactions of the type of equations 9a, 9b, and 9c is low (about 5 kcal.) compared with that of the reaction of hydrogen atoms with isobutane (3), which probably is about 10 kcal. However, the much higher concentration of isobutane should tend to counteract the disparity in activation energies and could account for the fact that only a small amount of methane was obtained. If the chance of a butyl radical colliding with a hydrogen atom is small, then the propyl and ethyl radicals produced in reactions 9a and 9b, which would be present in even smaller concentrations, should have progressively smaller opportunity for colliding with hydrogen atoms, so that the probability of the "atomic cracking" chain of reactions reaching completion must be slight.

It seems likely, from a consideration of the products of the reaction as well as by analogy with other similar reactions, that the fate of the propyl radical is to combine with butyl radicals to form heptanes, which were probably present in the liquid products, and the fate of the methyl radical is to react either with butane

$$CH_3 + C_4H_{10} = CH_4 + C_4H_9$$
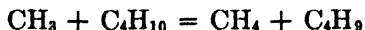
or with hydrogen atoms in the presence of a third body. These reactions account satisfactorily for the composition of the products. The logical extension of the above series of reactions would be the combination of methyl and butyl radicals, since methyl and propyl radicals were probably present in approximately equivalent amounts. Such a reaction would lead to the production of neopentane which, because of its boiling point, should have been readily detectable in the products. In spite of diligent search, no trace of neopentane could be found. Hence, if the above series of reactions do represent the course by which methane and heptanes are formed, it must be concluded either that methyl radicals are more easily hydrogenated than are propyl, or that butyl radicals combine with propyl radicals more readily than with methyl. A consideration of the activation energies of the following reactions

$$CH_3 + H_2 = CH_4 + H \qquad E \approx \ 8 \ kcal.$$

$$C_2H_5 + H_2 = C_2H_6 + H \qquad E \approx 12 \ kcal.$$

indicates that the greater velocity of hydrogenation of methyl as compared with ethyl radicals could account for the absence of neopentane in the products.

At high temperatures (250°C.) it is probable that the propyl radicals also decompose thermally:

$$C_3H_7 = C_2H_4 + CH_3 \qquad\qquad (11)$$

The ethylene would then combine with a hydrogen atom to form an ethyl radical

$$C_2H_4 + H = C_2H_5{}^* \qquad\qquad (11a)$$

which may be expected to contain a surplus of energy, as recognized by Rabinovitch, Davis, and Winkler (6), and should therefore be even more liable to thermal decomposition than would be the normal radical at these temperatures. The decomposition of this "hot" radical

$$C_2H_5{}^* = CH_3 + CH_2 \qquad\qquad (11b)$$

would then account for the increased production of methane at 250°C. A similar instability of the butyl radicals at 250°C. is also likely and would also account for the increased production of methane. This series of reactions is not subject to the same objections as were raised previously to the "atomic cracking" series, since the postulated decomposition of the intermediate radicals is not second order and since the chance of survival of the "hot" radicals produced as intermediates, and their subsequent reaction with the butyl radicals present, is probably very small. Hence the fact that the production of heptanes does not

increase and that neither ethane nor propane appears in the products at this temperature is not surprising.

The apparent increase in the relative extent of the tertiary C—H split in the primary act is surprising at first sight, since all estimates show that the tertiary C—H bond is significantly weaker than the primary. It might have been expected that the extent of the primary split relative to that of the tertiary should have increased with increasing temperature. On the basis of the evidence presented, it is therefore necessary to postulate some secondary act whereby the amount of hexamethylethane in the products, relative to that of the other octanes, is increased with rise in temperature. An explanation may be offered on the basis of the negative temperature coefficient of the production of dodecanes.

Working with n-butane, Hay and Winkler (7) found a large amount of dodecane in their product at low temperatures and the production of dodecanes relative to octanes to decrease with increasing temperature. They explained their results by assuming that the octyl radicals were unstable at higher temperatures and decomposed, not by splitting off a methyl radical, but at the middle of the carbon chain with the production of a butyl radical and a molecule butene:

$$C_8H_{17} = C_4H_8 + C_4H_9$$

The butene produced is then hydrogenated to a butyl radical. This appears to be the only mechanism which will account for the behavior observed in their work.

Steacie and Dewar (15) found that only small amounts of nonanes were formed in the mercury-photosensitized reactions of propane and that the production of nonanes increased with temperature. However, we understand that in those experiments the reactor was placed horizontally, a fact which may have allowed a significant percentage of the nonane (and higher hydrocarbons) to remain in the reactor at low temperatures instead of accumulating in the trap together with the lighter products of the reaction.

In the isobutane reaction only three octanes are formed. In producing the corresponding radicals it may be assumed that in any one molecule tertiary C—H bonds are broken more easily than the secondary or the primary. This assumption is in accord with the reported strengths of the bonds in question, and with the results obtained in the present study. Hence the following are the only octyl radicals that are likely to be formed in significant amounts:

$(CH_3)_3C \vdots C(CH_3)_2CH_2—$ from hexamethylethane

$(CH_3)_3C \vdots CH_2C(CH_3)_2—$ from 2,2,4-trimethylpentane

$(CH_3)_2CHCH_2 \vdots CH_2C(CH_3)_2—$ from 2,5-dimethylhexane
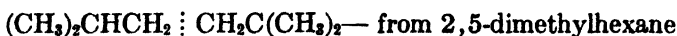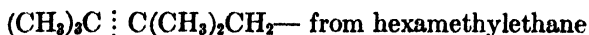
The increased production of hexamethylethane with temperature found in the present study can be explained by a C—C split in these radicals at the point indicated by a broken line, to form 2-methylpropene ("isobutene") in all cases and

either a primary or a tertiary butyl radical. These modes of decomposition are in agreement with the assumptions that the free bond in a radical confers unsaturation character to bonds involving the unsatisfied carbon atom and that a carbon chain breaks preferentially near the middle (2, 7). Since the most likely point of addition of a hydrogen atom to an olefin is at the most highly hydrogenated carbon atom, hydrogenation of 2-methylpropene would lead to the further production of tertiary butyl radicals. Increasing temperature increases the extent of the decomposition of the octyl radicals and consequently increases the production of tertiary butyl radicals. Since some of the octanes were produced originally from $(CH_3)_2CHCH_2$—, the net effect of increasing temperature is to increase the apparent extent of the initial tertiary C—H split.

The improvement in the material balance obtained with increased temperature, shown in table 5, may also be explained by an argument similar to that used above. If we assume that at low temperatures there is little decomposition of the octyl radicals, there will then be a large production of dodecanes. It is reasonable to suppose that these compounds will then react further to produce the dodecyl radical, which will then react with butyl radicals to produce C_{16} paraffins. These paraffins have sufficiently high boiling points to condense on the walls of the reactor where, under the influence of excited mercury atoms, they would probably be converted to unsaturated high polymers with production of hydrogen. The excess of hydrogen in the products at low temperatures tends to confirm this suggestion. The deficiency of hydrogen at 250°C. is probably due to an increase at these temperatures in the amount of radical decomposition, such as in equation 11, with accompanying increase in the production of methane.

REFERENCES

(1) BOWER, J. R., AND COOKE, L. M.: Ind. Eng. Chem., Anal. Ed. **15**, 290–3 (1943).
(2) FREY, F. E., AND HEPP, H. J.: Ind. Eng. Chem. **25**, 441–9 (1933).
(3) GORIN, E., KAUZMANN, W., WALTER, J., AND EYRING, H.: J. Chem. Phys. **7**, 633–45 (1939).
(4) HAY, A. W., AND WINKLER, C. A.: Can. J. Research **B21**, 149–55 (1943).
(5) MOORE, W. J., AND TAYLOR, H. S.: J. Chem. Phys. **8**, 396–403 (1940).
(6) RABINOVITCH, B. S., DAVIS, S. G., AND WINKLER, C. A.: Can. J. Research **B21**, 251–7 (1943).
(7) RICE, F. O.: J. Am. Chem. Soc. **53**, 1959–72 (1931).
(8) RUDBERG, E.: Z. Physik **24**, 247–63 (1924).
(9) SMITH, J. O., AND TAYLOR, H. S.: J. Chem. Phys. **7**, 390–6 (1939).
(10) SMITH, R. N., LEIGHTON, P. A., AND LEIGHTON, W. G.: J. Am. Chem. Soc. **61**, 2299–2301 (1939).
(11) SMITTENBERG, J., HOOG, H., AND HENKES, R. A.: J. Am. Chem. Soc. **60**, 17–22 (1938).
(12) STEACIE, E. W. R., ALEXANDER, W. A., AND PHILLIPS, N. W. F.: Can. J. Research **B16**, 314–18 (1938).
(13) STEACIE, E. W. R., AND BROWN, E. A.. J. Chem. Phys. **8**, 734–8 (1940).
(14) STEACIE, E. W. R., AND CUNNINGHAM, R. L.: J. Chem. Phys. **8**, 800–4 (1940).

(15) STEACIE, E. W. R., AND DEWAR, D. J.: J. Chem. Phys. **8**, 571-6 (1940).

(16) STEACIE, E. W. R., LE ROY, D. J., AND POTVIN, R.: J. Chem. Phys. **9**, 306-14 (1941).

(17) STEACIE, E. W. R., AND PARLEE, N. A. D.: Trans. Faraday Soc. **35**, 854-60 (1939).

(18) STEACIE, E. W. R., AND PHILLIPS, N. W. F.: Can. J. Research **B16**, 219-21 (1938).

(19) STEACIE, E. W. R., AND PHILLIPS, N. W. F.: J. Chem. Phys. **4**, 461-8 (1936); Can. J. Research **B16**, 303-13 (1938).

(20) WHITE, W. H., WINKLER, C. A., AND KENALTY, B. J.: Can. J. Research **B20**, 255-64 (1942).

COMMUNICATION TO THE EDITOR

Sir:

Professor I. M. Kolthoff in a book review of *More Acids and Bases* (printed in the January issue of This Journal) has made a criticism which gives an entirely misleading impression of the contents of my portion of the book. He states that my terminology (using electrophilic to describe both acids and oxidizing agents and electrodotic to describe both bases and reducing agents) "may become the source of much confusion. For example, hydroquinone is an acid, but a reducing agent, whereas quinone is a base, but an oxidizing agent. As a base, then, quinone is electrodotic in the terminology of Luder, but as an oxidizing agent it is electrophilic."

I do not see how anyone who had read the paper carefully could fall into such a trap—especially any chemist already so familiar with *amphoteric behavior* as Professor Kolthoff. I had already used water as an illustration of the necessity of retaining the idea of relativity expressed by the word "amphoteric". The following paragraph quoted from the paper under criticism demonstrates the unfairness of the criticism:

"It is an experimental fact that the same substance may under properly chosen conditions act as an acid, a base, an oxidizing agent, or a reducing agent. For example, water acts as an acid toward ammonia, as a base toward hydrogen chloride, as an oxidizing agent toward active metals, and as a reducing agent toward fluorine. Water is not only amphoteric but is both an oxidizing agent and a reducing agent. This is true of many other substances besides water. Most reagents cannot be arbitrarily classified as acid or base, oxidizing or reducing agent. Their behavior depends upon the specific circumstances of a particular reaction. Therefore, the words electrophilic and electrodotic are relative terms, depending upon conditions. They refer to the behavior of a substance as it acts in the particular reaction under consideration."

W. F. LUDER.

Northeastern University
Boston, Massachusetts
February, 1945

COMMUNICATION TO THE EDITOR

THE RARITY OF ZERO CONTACT ANGLES[1]

When a liquid is found to wet a solid, it is common practice to assign the value 0° to the contact angle between the liquid and the solid. This unfortunate habit of speech is still bringing confusion into the literature on contact angles.

When two fluid phases A and B form a line of contact on a solid S, the magnitude of the contact angle θ is determined by the relative values of the free interfacial energies γ_{AB}, γ_{AS}, and γ_{BS}. The interface between A and B will assume

$$\gamma_{AB} \qquad A \qquad B \qquad \theta \qquad \gamma_{AS} \qquad \gamma_{BS} \qquad S$$
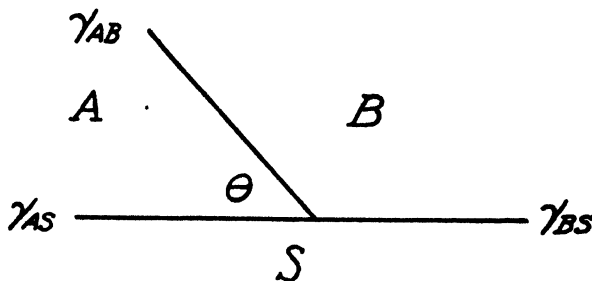
that position relative to the solid surface for which the resultant of γ_{AB} (considered as an interfacial tension) along this surface balances the difference between γ_{AS} and γ_{BS}. The establishment of contact equilibrium and a finite contact angle thus requires that γ_{AB} exceed the difference between γ_{AS} and γ_{BS}, that is,

$$\gamma_{AB} > |\gamma_{BS} - \gamma_{AS}| \qquad (1)$$

in which case θ will be determined as

$$\gamma_{AB} \cos \theta = |\gamma_{BS} - \gamma_{AS}| \qquad (2)$$

In the borderline case where γ_{AB} precisely equals the difference between γ_{AS} and γ_{BS}, γ_{AB} will ally itself fully with either γ_{AS} or γ_{BS}, whichever is the smaller, and a contact angle of 0° in A or in B will exist. It must be expected that only fortuitously will the energy relations at three independent interfaces balance so nicely as to result in a contact angle of 0°.

In many instances either γ_{AS} or γ_{BS} exceeds the sum of its two associates, and the one liquid spreads over the solid to the exclusion of the other. While the spread layer in this instance may be difficult to distinguish geometrically from the infrequent case in which θ is actually 0°, nevertheless the spread layer does not form a contact angle of 0° with the solid—in fact, it forms no contact angle at all, since no equilibrium line of contact can under these conditions be maintained. Nearly all if not all of the systems reported as instances of zero contact angle are undoubtedly cases of no contact angle. This holds for two liquids against air as well as for two fluids against a solid.

It is disconcerting that even recently these simple relationships are ignored

in discussions concerning contact angles, adhesion tensions, the wetting of solids, "Antonoff's rule", etc. When a liquid A is found to displace a second liquid B in contact with a solid S (or with air), it has been asserted that the contact angle is thereby established as 0°, and that the valid equilibrium relationship

$$\gamma_{BS} = \gamma_{AS} + \gamma_{AB} \cos \theta \tag{3}$$

therefore (since cos "0°" = 1) becomes

$$\gamma_{BS} = \gamma_{AS} + \gamma_{AB} \tag{?} \tag{4}$$

as a demonstration of Antonoff's rule, notwithstanding accurate measurements of γ_{BS}, γ_{AS}, and γ_{AB} (where S is air) to the contrary.

Such predicaments will be avoided if we forego the use of the phrase "zero contact angle" except in those rare instances for which θ actually is 0°. Water on clean glass shows no contact angle. "No contact angle" and "zero contact angle" are not synonymous.

Interchemical Corporation   DAVID M. GANS.
New York 11, New York
September 27, 1944.

NEW BOOKS

Valency, Classical and Modern. By W. G. PALMER. 242 pp. Cambridge: The University Press, 1944. New York: The Macmillan Company, 1944. Price: $2.50.

This little book is addressed primarily to students preparing for comprehensive examinations in chemistry, although it might be profitably read by many others. The author presents material which is included for the most part in the basic chemical courses in a different organization, leading the student at the same time to review the subjects and to see new relationships which were obscured in the conventional organization of courses.

This book is organized primarily on a historical basis, which makes it an interesting account of the human factors in the development of ideas. The first chapter gives the early history through Mendeléeff, and the second describes later developments up to the rise of electronic theories. The third chapter develops the classical chemical valence theory to the ultimate. Therein one naturally finds certain phenomena which are unexplainable without arbitrary additional postulates. In this development modern structural data are introduced; in fact, this represents a deviation from historical order. The fourth chapter then introduces modern electronic concepts and completes the discussion of typical cases chosen from light elements.

The two remaining chapters consider the additional aspects of electronic theory with particular regard for heavier elements, including magnetic properties. Also, numerous recent developments, some still controversial, are included.

The author's presentation is excellent; his style is clear and easily read. Fact is clearly distinguishable from fancy. No typographical errors of consequence were noted. The reviewer was pleased with the full use made of structural data. As might be expected, there are a few controversial points where the reviewer does not agree with the view presented. Nevertheless he does not hesitate to recommend the book heartily.

KENNETH S. PITZER.

The Photography of the Reciprocal Lattice. By M. J. BUERGER. American Society for X-Ray and Electron Diffraction Monograph Series, No. 1. 6 x 9¼ in.; x + 37 pp.; 18 fig. Cambridge, Massachusetts: The Murray Printing Company, 1944. Price: $1.50.

The purpose of the ASXRED Monograph Series is to take care of the publication of contributions within the sphere of interest of the American Society for X-Ray and Electron Diffraction which are too long to be acceptable in the ordinary scientific journals.

Modern single-crystal x-ray diffraction techniques are based on the reciprocal lattice. This monograph discusses briefly the theory of photographing the reciprocal lattice without distortion, and describes a new instrument, the precession instrument, for taking such photographs. The interpretation of precession photographs is comparatively simple, since they are scaled photographs of the reciprocal lattice levels. Details of the technique, including the orientation of crystals, the accurate measurement of spacings, and the form of the Lorentz factor for the method, are given. The precession method possesses important advantages over other methods for crystals with large cell dimensions. The exposures required are very short, the photographs are readily interpreted by inspection, and the method requires a less perfect crystal than other methods. The reviewer can foresee that this method in the future may well assume the importance which the Weissenberg method now enjoys in single-crystal technique.

The printing, reproduction, and binding have been well done with the exception of Fig. 12, which unfortunately appears to have lost considerable detail from the original.

HAROLD P. KLUG.

General Sessions of the Academy of Sciences, U. S. S. R., September, 1943. 242 pp.

A volume containing twenty-two papers (in Russian) presented at the meeting and biographical sketches of the members of the Academy and of its sponsors, Marshall Stalin and Secretary Molatov.

S. C. LIND.

The Chemical Industry. By JOSEPHINE PERRY. 123 pp. New York: Longmans, Green and Co., Inc., 1944. Price: $1.75.

This volume is one of the series of *America at Work* written by this author, and is presented in popular style for the layman. In an attempt to cover the whole field, much of the material is too abbreviated and the language oversimplified, so that in many instances there is a lack of accuracy both in material and in terminology. The book is very readable and has many excellent photographic illustrations. It may give the uninitiated a fair picture of this very broad field. It would have been much better to have tried to cover a few related industries and to have written several books on the whole field of chemical industry.

CHARLES A. MANN.

Quantum Chemistry. By HENRY EYRING, JOHN WALTER, AND GEORGE E. KIMBALL. vi + 394 pp. New York: John Wiley and Sons, Inc., 1944.

The purpose of the authors, as stated in their preface, has been to present in a single unified treatment the basic principles of quantum mechanics and its applications to chemical problems, in a reasonably complete fashion so that a serious student could acquire a solid foundation on which to build. The topics included are indicated in the list of chapter headings: Introduction (largely historical); Principles of Classical Mechanics; Principles of Quantum Mechanics; Differential Equations of Quantum Mechanics; Quantum Mechanics of Some Simple Systems; The Hydrogen Atom; Approximate Methods; Time-Dependent Perturbations and Radiation Theory; Atomic Structure; Group Theory; Electronic States of Diatomic Molecules; The Covalent Bond; Resonance and the Structure of Complex Molecules; Principles of Molecular Spectroscopy; Elements of Quantum Statistical Mechanics; Quantum Mechanical Theory of Reaction Rates; Electric and Magnetic Phenomena; and Special Topics (van der Waals forces, the virial theorem, the restricted rotator).

It will be seen from this list that considerably more topics are included than in other introductory texts. The result has been, inevitably, that the book is written in a somewhat

severe mathematical style, with very few illustrations of practical applications` of the topics discussed. Now it seems to us that in teaching quantum mechanics to chemistry students the dilemma has for one horn the deep penetration into the subject required to reach the chemical applications, which lie in an advanced region, and for the other horn the step-by-step introduction required by most chemistry students, who come to the subject without much helpful background in mathematical physics. We believe that the average graduate student in chemistry would profit from this text only in connection with a course of lectures designed to expand and illustrate the material studied. However, once "led into" the subject in such fashion, the student would, we believe, find this book most valuable, for it would provide him with an introduction to almost all the quantum applications of interest to chemists—a thorough introduction from which he could go on intelligently. In this respect we might compare the book to Joos's well-known *Theoretical Physics*, except for the omission of any problems.

To comment on a few particulars: We were pleased to find an early introduction and free use of group theory. This mathematical tool is of great value in molecular problems, and gives generous dividends on the little effort required to master its application. Actually it is less subtle than the calculus—and, like that tool, can be easily applied to physical problems even without an understanding of the mathematical foundations.

The chapter on reaction rate theory is not concerned with the application of the theory of absolute reaction rates to concrete reactions; it presents a rather careful derivation of the expression for the reaction rate together with quantum-mechanical investigation of its validity, particularly with regard to the transmission coefficient. The same approach is to be found in the chapter on statistical mechanics. It is, of course, consistent with the general purpose of the volume.

On the other hand, the treatments of molecular energies (by both the molecular orbital and the Heitler–London methods) and of molecular spectra, while compact, are quite complete.

To summarize, we feel that the authors have produced a book which will be a valuable and welcome addition to the bookshelves of physical chemists, and which, when supplemented by illustrative lectures and problems, should make a sound text for a thorough course in quantum chemistry.

BRYCE L. CRAWFORD, JR.

Hydrogen Ions, Their Determination and Importance in Pure and Industrial Chemistry. By H. T. S. BRITTON. Third edition. Two volumes (420 and 443 pp.). New York: D. Van Nostrand Company, Inc., 1943. Price: $16.00.

From the thermodynamic and physical-chemical point of view W. M. Clark's classic treatise, *The Determination of Hydrogen Ions*, is still the most exact one among the many texts which have been written on the subject. Britton's well-known book is of a somewhat different nature. Although the first volume deals mainly with the theory and methods of determining hydrogen-ion concentration, the main emphasis is placed on the part played by hydrogen ions in chemistry and in numerous technical processes (Volume II). The author's viewpoint is reflected in the Preface: "As much of the fundamental work on hydrogen ions was carried out before the activity theory of electrolytes had gained wide acceptance, and as the electrometric determinations of pH are usually made with cells in which liquid junctions exist and to which the modern theory is not strictly applicable, the theoretical interpretation of the E.M.F. of such cells, given in the earlier editions, has been retained. To some, this procedure might appear unjustifiable, but the fact must not be lost sight of that the activity theory can only be rigidly applied to cells without transport, i.e., without a liquid junction, which type of cell is scarcely ever used for ordinary pH determinations. Whatever may be the true meaning of the pH value, there is no doubt that pH values will remain an invaluable means of accurately assessing the extent of the acidity or the alkalinity of a solution." Granting that the exact value of the hydrogen-ion activity of a solution will be forever unknown, it may be stressed that in many instances this value can

he measured with a close approximation, even though the two half-cells containing different electrolytes are connected by a salt bridge.

Most of the data in the first volume are based on the out-dated assumption that conductivity data in hydrochloric acid solutions yield the true concentration of hydrogen ions, although later in the same volume (pp. 253–294) the activity theory of solutions is discussed. It seems to the reviewer that it would be preferable to base the entire discussion on the modern theory of electrolytes and to interpret the older data in the light of the modern views. A more critical presentation of standard potentials of standard half-cells would also be desirable (compare, e.g., Table 4, p. 29; Table 7, p. 36; and Table 48, p. 263). The values of K_w given in Table 9 (p. 53) are no longer accepted as accurate; they could be replaced by more modern data.

In the above the reviewer has emphasized what he considers to be the most outstanding weakness of Britton's extremely valuable book. It is admitted that every author of a book on the determination of the hydrogen-ion (or any other ion) activity exposes himself to criticism, since its *exact* determination is a physical impossibility. An *approximate* determination is possible, and the approximate value obtained is of such importance in pure and industrial chemistry that a compromise between exact theory and approximate measurements is more than justified.

The previous editions of Britton's book are so well known and have served so many people engaged in "pure" and "industrial" research that the new edition hardly needs a recommendation. The present two-volume edition is even more valuable than its predecessors; it is not only brought up to date but it also contains several new chapters not found in previous editions. The inorganic chemist will be well pleased with the various chapters in Volume II dealing with the fundamental importance of pH in inorganic chemistry. (The chapter on sulfides could be made more complete.) Chapters dealing with the importance of pH in leather manufacture, tanning, sugar manufacture, brewing, milk, hen's eggs, baking, water, soils, ceramics, and textile and dye industries conclude the second volume. In connection with the chapters on milk, eggs, baking, etc., the introduction of a few concise chapters dealing with the significance of pH in enzymology (and in biochemistry in general), physiology, and bacteriology would make this important book still more useful to a wider circle of scientists.

<div align="right">I. M. KOLTHOFF.</div>

THE PHYSICAL CHEMISTRY OF MEMBRANES WITH PARTICULAR REFERENCE TO THE ELECTRICAL BEHAVIOR OF MEMBRANES OF POROUS CHARACTER. II

THE NATURE OF THE "DRIED" COLLODION MEMBRANE. SOME CURRENT MEMBRANE THEORIES AND THEIR LIMITATION[1]

KARL SOLLNER

Department of Physiology, University of Minnesota, Minneapolis 14, Minnesota

I. INTRODUCTION

Current theories concerning the nature of membranes are primarily "permeability theories" focussed on the question of the penetration of various solutes through membranes. Much less attention has been paid to the solvent in contact with membranes, to its state in the latter, and to its fate during various membrane processes.[2]

It is impossible to obtain a really clear picture of the nature and the function of a membrane without some insight into the latter questions; nevertheless, it is necessary at present to start investigations concerning the applicability of the various membrane theories to specific cases, beginning with the conventional concepts.

In the subsequent sections of this paper various physicochemical approaches are used to elucidate the nature of collodion membranes in general, particular attention being paid to the much-investigated though still highly controversial dried collodion membrane. These studies were originally undertaken in order to be able to answer a number of specific questions concerning the functional behavior of collodion membranes. The present treatment attempts to put the several isolated facts together in a comprehensive manner.

In the past, membrane phenomena have too frequently been treated in the abstract without considering their exact structural and kinetic bases. The ex-

---

[1] Presented in abstract before the Division of Colloid Chemistry at the 108th Meeting of the American Chemical Society, New York City, September 14, 1944.

[2] One can easily conceive of membranes of homogeneous-phase type which are permeable to the solute but impermeable to the solvent. The osmotic phenomena to be expected under these conditions have never been discussed in a systematic manner, though this would obviously be desirable.

A satisfactory kinetic theory of the osmotic processes which occur across membranes of porous character must coördinate the general concept of the activities of solvent and solute in solution and the influence of hydrostatic pressure on these activities with the following fact: With "semipermeable" membranes the hydrostatic pressure (under equilibrium conditions) compensates the osmotic pressure of the solution, in the case of membranes of relatively high porosity in the pores of which the normal hydrodynamic laws seem to hold true, as well as with membranes the pores of which are of molecular size and thus outside the range of the normal hydrodynamic laws. The author hopes to be able to present a discussion of this matter in the near future jointly with Dr. M. B. Visscher.

perimental results reported will, it is hoped, demonstrate that it is possible to
investigate such phenomena as specific physicochemical problems and to estab-
lish or eliminate the possibility of one or another mechanism operating to bring
about observed effects.

II. INDIVIDUAL DIFFERENCES IN "DRIED" COLLODION MEMBRANES

In a preceding paper (12) it was indicated that the majority of investigators '
seem to be inclined to the view that dried collodion membranes owe their charac-
teristic properties to their microheterogeneous structure, i.e., to their porous
character, though other prominent investigators prefer the view that dried col-
lodion membranes should be considered to be closely similar to, if not identical
with, oil phases. Experiments which could throw decisive light on this question
were therefore highly desirable.

There is one well-known observation which can throw considerable light on the
mechanism of the electrolyte permeability of dried collodion membranes (16).
Dried collodion membranes cast in the conventional way from the same solution
give widely varying concentration potentials. This effect is particularly pro-
nounced with membranes prepared from electrochemically inactive preparations.
Though they are of fairly uniform thickness, different membranes may show con-
centration potentials which vary by more than 100 per cent, the potentials across
the individual membranes being very constant and easily reproducible over long
periods. It can be shown readily that this effect is not due to any cracks or other
imperfections of some of the membranes.

The homogeneous-phase theory cannot conceivably account for this variability
in electromotive behavior. All specimens of a homogeneous phase must of
necessity have the same properties. The homogeneous-phase theory must
assume equivalence or at least statistical equivalence of all actual or virtual
molecular interstices (the only ones which exist in a homogeneous phase) and
likewise equivalence of all the characteristic groups which determine the electro-
chemical behavior of the membrane. A structural theory, however, can easily
explain the observed facts; differences in aggregation and orientation of molecules
and micelles could easily account for the uncontrollable variation in the prepara-
tion of the individual membranes. According to such a theory one must think
of the membranes as having a "micellar-structural" constitution as opposed to
the molecular-structural constitution of a perfect crystal or a liquid, the emphasis
being more on the nature of the interstices than of the structure-forming physical
elements.

III. EXPERIMENTS TO APPRAISE THE RELATIVE MERITS OF THE HOMOGENEOUS-PHASE THEORY AND THE STRUCTURAL THEORY AS APPLIED TO DRIED COLLODION MEMBRANES

The following line of reasoning has also served as a basis for experiments de-
signed to be helpful in a decision between the homogeneous-phase theory and the
micellar-structural theory as applied to the dried collodion membrane (16). A
number of dried collodion membranes are prepared under standardized conditions

in the conventional manner on the inside of test tubes from the same solution of electrochemically inactive collodion (state I). The mean characteristic concentration potential across a representative group of these membranes is determined. Next, the membranes are "activated" by oxidation (state II), as described previously (12, 13), and the mean concentration potential of a representative number of these membranes is determined. The remaining majority of the membranes in state II is dissolved in the same solvent mixture as used originally. Dried collodion membranes are prepared from this solution (state III); as before, the concentration potentials across these membranes are measured and the mean value noted as in the former cases. The concentration potentials across the membranes in states I, II, and III are compared.

The homogeneous-phase theory would predict that the properties of the membranes in state II and state III are substantially identical, since the properties of an interphase which behaves like a homogeneous phase should be independent of its history. No rearrangement of molecules or micelles, brought about by any means, should be able to alter the properties of membranes prepared from the same material.

The micellar-structural theory would predict a distinct difference between state II and state III. According to this view, the dissociable groups which are introduced by oxidation are mainly confined to certain more accessible structural elements, i.e., the surfaces of those particles which form the pore walls. When the membrane is dissolved, the elements which are the cause of the characteristic properties of state II are mixed with the whole mass of the membrane material. If new membranes are now prepared from this solution (state III), the concentration of the active groups at the accessible points is necessarily reduced as compared with state II.

In order to demonstrate the anticipated effect most clearly, the activation should be stopped just at the time when maximum or nearly maximum concentration potentials are obtained. Too thorough oxidation must necessarily lead to diminution in the expected effect.

In two series of experiments seventy membranes were cast (state I): the characteristic concentration potentials across ten of them, selected at random, were measured, the mean being 27.5 and 30.4 mv., respectively. The two batches of seventy membranes each were oxidized to a different degree (state II). Twenty of these membranes were selected at random from each batch, and the mean characteristic concentration potential across them was determined: with the one series it was 49.9, with the other series 51.3 mv. The fifty remaining membranes of each batch were dissolved in the same solvent mixture which had been used for preparation of the original membranes, and dried collodion membranes were prepared in exactly the same manner as originally (state III). In the one series thirteen such membranes were obtained, in the other series twenty. The mean characteristic concentration potential of the membranes in state III was 26 mv. in the series which had undergone less oxidation, and 37.7 mv. in the more highly oxidized series. In the first series the characteristic concentration potentials in state I and state II are identical within the limits of experimental and statistical

error; in the case of the more highly oxidized series the concentration potential in state III, though significantly higher than in state I, is much lower than in state II.

In an analogous third series the membranes were oxidized very strongly. In agreement with expectation, the average concentration potential of the membranes in state III in this series was rather high, about 49 mv.

Since the properties of a homogeneous phase should not be influenced by a rearrangement of its constituent particles, these results strongly indicate that the homogeneous-phase theory cannot hold true in the case of the dried collodion membrane. The experimental results agree excellently with the predictions of the micellar-structural theory and seem to provide clear evidence that the characteristic behavior of dried collodion membranes in solutions of strong inorganic electrolytes is due to the micellar character of its electrochemically important interstices.

FIG. 1   FIG. 2
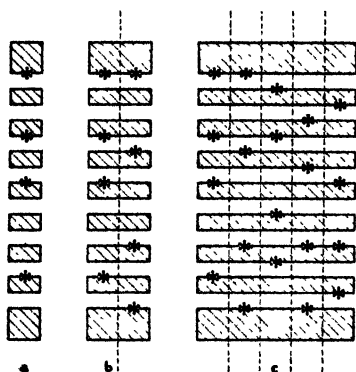
Two simple membrane structures; highly schematized
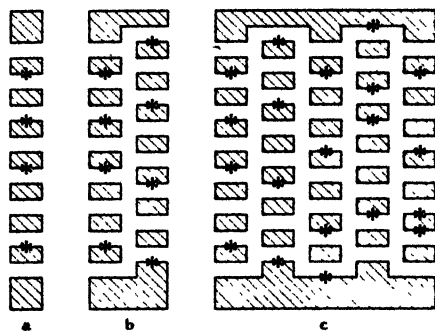
IV. THE THICKNESS EFFECT

Prior investigators have always made the assumption, tacitly or explicitly, that thicker membranes show the same characteristic behavior as thinner membranes of the same general character, all processes across them, of course, occurring more slowly. Thus it has been generally assumed that the characteristic concentration potential across dried collodion membranes must be independent of the thickness of the membrane (20). Since, as we shall see below, the concentration of the electrically important dissociable groups is very small, the question arose whether there is a sufficient number of active groups available to supply each of the possible pathways across the membrane with at least one such active group. If the critical groups are really scarce, the chance of this latter occurrence, generally speaking, should diminish with decreasing thickness of the membrane, though this need not necessarily be the case (17).

Figures 1 and 2 present in highly schematic manner two possible ways of visualizing the distribution of the active groups and the thickness effect. We as-

sume, in agreement with the best available information, that a dissociable group in a narrow pore prevents the passage of an ion of the same sign, but allows the passage of oppositely charged ions; pores of proper dimensions having no such charged groups allow the passage of both anions and cations. In the figures the membrane substance is indicated by striation; spots which carry a fixed charge and thus prevent the passage of ions of the opposite sign are denoted by asterisks.

Figure 1 shows the simplest conceivable structure of a porous membrane. Figure 1a, representing a unit thickness of membrane, shows every other pore blocked for the passage of ions, the ratio of the free to the geometrically possible pathways thus being 0.5. It is easy to see that the number of pathways free to the permeation of ions of the same sign as that of the fixed dissociable groups decreases in a geometrical series as the thickness of the membrane increases in an arithmetical series. The theoretically possible maximum value of the concentration potential could be reached with such membranes if they are sufficiently thick.

However, this kind of very simple behavior is by no means necessarily inherent in membranes which have a structure; another possibility is shown in figure 2.

Figure 2a represents a unit layer of membrane, 50 per cent of the pores being blocked; figure 2b shows a possible assembly of two such layers which allow a free cross connection of the pores between two adjacent membrane layers. If an electrolyte diffuses through such a membrane, this space will soon be filled with an electrolyte solution, the concentration of which is somewhere between the concentrations of the solutions on the two sides of the membrane. It is easy to see, and we have also developed the idea in detail (17), that the potential across a membrane of this character is independent of the number of unit layers from which the membrane is built up, i.e., it is independent of the thickness of the membrane.

Thus we see that the cross connections between different pores influence the behavior of membranes profoundly. According to the micellar-structural theory, therefore, the relative frequency of the blocking groups and of the branchings of the pores should be the paramount factors determining the electrochemical behavior of dried collodion membranes.

The membrane structures represented in figures 1 and 2 may be considered in some respects as the two possible limiting cases of an infinite variety of possibilities. The micellar-structural theory must therefore be considered to be compatible with dependence or independence of the concentration potential upon membrane thickness. The homogeneous-phase theory would under all circumstances predict independence of the concentration potential of the thickness of the membrane.

Since, as said above, the concentration potential across dried collodion membranes of identical thickness varies greatly, the question of the existence of a thickness effect could only be decided by the use of statistically significant numbers of membranes. We therefore have used, as required by the circumstances, up to twenty membranes to determine the average characteristic concentration potential arising across membranes of different thickness prepared from collodion of various electrochemical activities.

Bag-shaped membranes were prepared in the conventional manner on the inside of test tubes.   In order to obtain membranes of different thickness, collodion solutions of various concentrations (2, 4, 6, 8, and 10 per cent) in the same solvent mixture were used.   To obtain very thick membranes we have in a few instances superimposed several layers of collodion on top of one another.   Figure 3 gives the mean characteristic concentration potentials obtained with the various membranes.

The results of the experiments represented in figure 3 may be summarized as follows: The concentration potential is a function of the membrane thickness with all the collodion preparations which were investigated.   With membranes prepared from electrochemically active collodion, membranes of 15 to 20 μ thickness give potential values which closely approach the thermodynamically possible maximum.   With inactive collodion preparations the potential values obtained
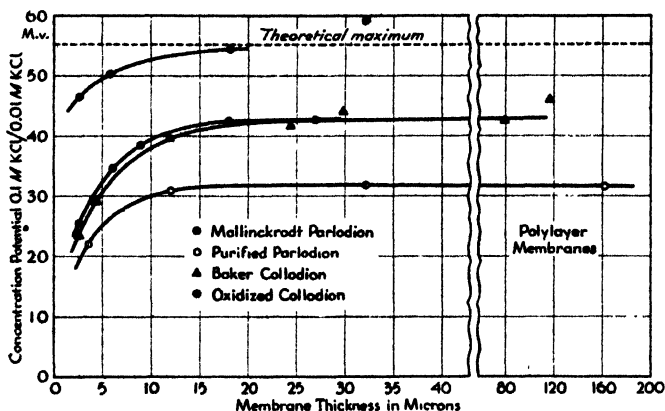
FIG. 3. The correlation between the thickness of various dried collodion membranes and the characteristic concentration potential 0.1 N potassium chloride–0.01 N potassium chloride across them.

with thin membranes are low; they increase with increasing thickness of the membranes and reach constant values well below the thermodynamically possible maximum when 20 to 30 μ thick; still thicker membranes do not yield significantly higher concentration potentials; there is no indication that the thermodynamically possible maximum value could be obtained with membranes of any thickness.

The assumption that the concentration potential is independent of membrane thickness does not therefore hold true in the case of the dried collodion membranes.   These results are incompatible with the predictions of the homogeneous-phase theory; they are compatible with the micellar-structural theory.   However, neither of the two simple pictures of membrane structure represented in figures 1 and 2 fully agrees with the results.

Though with active collodion preparations the thermodynamically possible maximum value can be approached with increasing membrane thickness, the shape of the thickness–potential curve does not fit the predictions of the theory.

With inactive preparations there is first an increase in the potential with increasing membrane thickness qualitatively (though not quantitatively), as can be predicted on the basis of figure 1. With still thicker membranes, however, a constant potential value is reached, as predicted in a qualitative manner by the assumptions which underlie figure 2. The real situation is obviously more complicated, somewhat in between the two extremes represented by figures 1 and 2. In a tentative way one may explain the observed facts on the basis of the assumption of highly active surface layers which with thicker membranes enclose zones of low specific activity. This picture, however, has not yet been proven experimentally; it must therefore be considered to be of an entirely hypothetical nature (17).

V. WATER UPTAKE AND SWELLING OF COLLODION MEMBRANES

It is impossible to have a clear picture of the structure of a membrane if it is unknown whether it is permanent and rigid or whether it undergoes changes when it is immersed in different solutions. Water and aqueous solutions of inorganic and organic compounds are generally believed to exert no specific influence on collodion membranes, but this point has never been proven definitely. Concentrated solutions of most organic compounds are known to swell collodion membranes appreciably. Michaelis (9, 20) assumes that the dried collodion membrane behaves as a rigid porous structure which shows no trace of swelling; water and aqueous solutions are supposed to enter the membrane by filling preformed pores. Manegold (6), who has carried out extensive physical investigations on collodion membranes, states specifically that dried collodion is non-swelling in water. Experimental proof for this statement, however, could not be found; it seems to be questionable in view of the well-known hygroscopicity of collodion, which was investigated by Northrop (11) for the specific case of the dried collodion membrane.

The questions which need an answer under these circumstances are: (1) How much water does a completely dried collodion membrane take up when placed in water? (2) Does this water uptake cause any detectable change in the volume of the membrane? (3) Do dried collodion membranes swell or shrink when transferred from water to solutions of strong electrolytes? (4) Do "porous" collodion membranes swell or shrink when transferred from water to solutions of strong electrolytes? (1)

For this work the conventional thin bag-shaped collodion membranes were useless; fairly thick flat sheets had to be used in order to be able to make the necessary measurements. The membranes were prepared by pouring collodion solution on glass plates which floated on mercury. To obtain dried membranes the solvent was allowed to evaporate completely; to obtain porous membranes of 50 to 60 volume per cent water content, the drying was interrupted after 90 min. The dried membranes, 0.10 to 0.15 mm. thick, after being cut to standard size are kept in a desiccator; the porous membranes are kept in water.

The volume of the membranes was determined with a pycnometer filled with

mercury, the only liquid we know that would not wet the membranes. The weight determinations were carried out in weighing bottles. First, the volume and the weight of a dehydrated dried membrane were measured; next, the membrane was placed in water or the solution under investigation. After a measured length of time it was removed from the liquid, blotted free of surface liquid, and weight and volume determinations were carried out. This process was repeated at intervals till equilibrium was obtained.

It became apparent immediately that the behavior of dried collodion membranes is less simple than is generally supposed. The membranes in equilibrium with water showed a volume increase of 5 to 11 per cent, depending on the brand of collodion used.
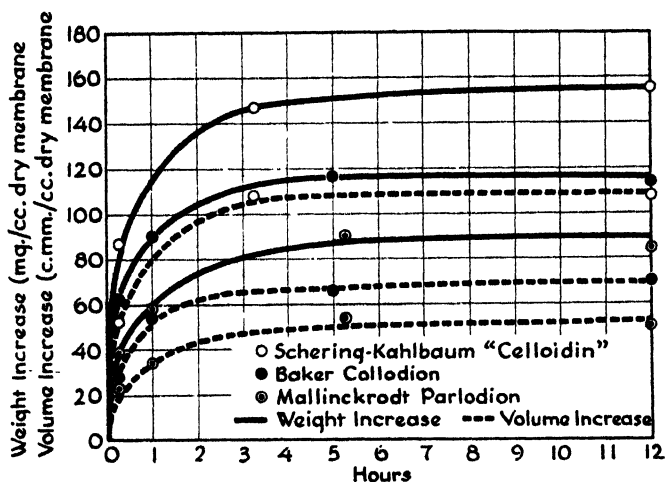
FIG. 4. Weight and volume increases of dried collodion membranes prepared from various collodion preparations on contact with water.

In order to visualize the quantitative meaning of the observed weight and volume increases, they were reduced to the standard unit of 1 cc. of dry membrane. The weight and volume increases are expressed in milligrams and cubic millimeters, respectively, for 1 cc. of dry collodion.

In figure 4 are plotted the weight and volume increases against the immersion time obtained with membranes prepared under very similar conditions from several brands of collodion. Membranes prepared from the same collodion but under different conditions show small though significant differences in weight and volume increase. Unoxidized and oxidized (activated) collodion (not shown in the figure) of the same origin show identical water uptake and swelling when prepared under identical conditions.

If a dried collodion membrane is transferred from water to a solution of an inorganic electrolyte, no weight or volume changes can be determined with certainty, nor can any be determined when the membranes are transferred back to water.

"Porous" collodion membranes do not exist in an air-dry state; one can measure only the weight and volume change on transfer from water to electrolyte solution and back into water. There is no change of volume under these conditions, and the observed weight changes are quantitatively accounted for by the differences in specific gravity of water and solution filling the pores.

The following conclusions can be drawn from these experiments: Contrary to the general assumption, dried collodion membranes swell on wetting with water, the extent of the swelling varying with different brands of collodion.

On wetting with water, dehydrated dried collodion membranes undergo fundamental changes; the air-free and the water-wetted dried membranes are structurally different entities. Once wetted with water the dried collodion membranes, as well as the always water-wet porous membranes, do not undergo significant structural changes when transferred from water to solutions of strong inorganic electrolytes. They can be considered under these conditions as rigid structures which do not show a specific swelling effect in aqueous solutions of the typical strong inorganic electrolytes.

In all cases the water uptake is in excess of the volume increase. This difference (34 to 46 cmm. per cubic centimeter of dry collodion) could be taken as a measure of the true porosity of these membranes, if one did not have to take into account the compression of water and other minor effects. An evaluation of the known factors indicates that a substantial fraction, probably the greater part, of the difference between the weight and volume increases can be taken as a measure of the pore space. How much, however, of this pore space is available for the typical membrane functions cannot be evaluated on the basis of the data presented. We hope to carry out such studies at a later date with megapermselective membranes (12).

When studying the swelling of dried collodion membranes in solutions of organic substances it was found that the behavior of collodion membranes under these conditions is much less simple (15). The swelling of dried collodion membranes in solutions of organic electrolytes and non-electrolytes is not uniform, as in the case of water and the strong inorganic electrolytes, but depends on the nature and concentration of the solute, as can be seen in figure 5.

The solutions of typically "hydrophilic" substances, e.g., glycerol, glucose, and citric acid, swell collodion membranes only to the same extent as water and solutions of strong electrolytes. In solutions of typically carbophilic substances (e.g., butyric acid, valeric acid, isobutyl alcohol, valeramide, phenol, and m-nitrophenol), the swelling of the membranes is much stronger than in water, depending on the concentration of the solute. For the brand of collodion used (Baker Collodion U.S.P.) the swelling in 0.5 M solution was in some cases as high as 26 per cent of the original volume, as compared to 6 per cent in water. Therefore, in these solutions the "water-wetted dried" collodion membrane is not rigid, inert, and non-swelling, but behaves as a swelling membrane.

The solutes which cause an increased swelling of the membranes are accumulated in the latter, the degree of accumulation being markedly parallel with the degree of their specific swelling action (15).

The anomalously high permeabilities of certain carbophilic organic solutes reported by Michaelis (10), Collander (3), and Höber (5) find an explanation in the specific interaction of these substances with collodion.

The investigation of swelling and water uptake of collodion membranes defines the range of conditions within which collodion membranes may be used as models of ideal non-swelling membranes of porous character. They can be used as such models only in those instances in which no specific interaction occurs between the solute and the collodion.
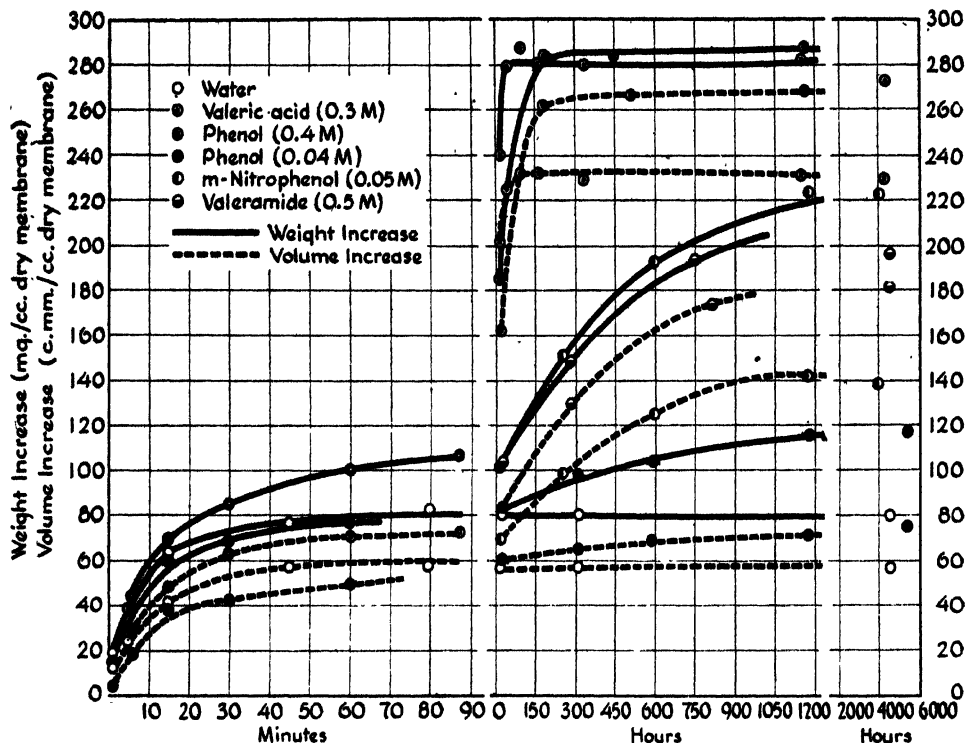
Fig. 5. Weight and volume increases of dried collodion membranes on contact with aqueous solutions of various organic substances.

VI. THE NATURE OF THE PERMEABILITY OF DRIED COLLODION MEMBRANES

In the foregoing sections the assumption was made tacitly, in the conventional manner, that the interstices of a membrane of porous character are accessible to the solvent, and that correspondingly the solute molecules within the pores are present in an aqueous medium. The water in the pores may be somewhat changed by the forces emanating from the pore walls; nevertheless, it is generally assumed essentially to retain its material properties.

There is little reason to doubt the correctness of this picture in the case of the collodion membrane. Water molecules are small, actually smaller than nearly all possible solutes; moreover, collodion is wetted by water. From the work of

Collander (3), Michaelis (9), and others we know that, at least with non-electrolytes, the size of the molecules is the factor which determines their chances to penetrate dried collodion and similar membranes.[3]

Membranes having a fixed structure must not, however, necessarily behave like collodion membranes. Glass membranes, e.g., undoubtedly do not contain preformed channels which can be filled with water and through which certain hydrated ions may move. The mechanism of the transportation of material particles in such membranes is apparently an anhydrous process. Ions moving through the solid, amorphous, or crystalline structure of such a phase are not hydrated.[4]

That the movement of ions in dried collodion membranes is a process in which the aqueous medium which fills the pores is strongly involved is also indicated by the following consideration: The unhydrated Li^+ ion is much smaller than the unhydrated Na^+ or K^+ ion, the ionic diameters of the unhydrated ions being 0.60, 0.95, and 1.33 Å., respectively. In aqueous solutions, i.e., in the hydrated form, the Li^+ ion is the largest and the K^+ ion the smallest, with the Na^+ ion taking an intermediate position; this is evident from the equivalent conductances of these ions: 33.4, 43.5, and 64.6 for Li^+, Na^+, and K^+, respectively (at 18°C.).

Thus one might expect that the Li^+ ion would penetrate an anhydrous interphase easiest and fastest on account of its smaller size, and Na^+ ion more easily than K^+ ion. However, the opposite is true with collodion membranes. Li^+ ions penetrate through collodion membranes more slowly than Na^+ ions, and Na^+ ions more slowly than K^+ ions, as was shown conclusively by Michaelis and collaborators (9). The differences in the rates of penetration of the three ions are actually much greater than those found in aqueous solutions. This finds its obvious explanation in the fact that many pores which are large enough to allow the penetration of those ions which are smallest in the hydrated state, i.e., K^+ ions, are not accessible to larger ions, such as the hydrated Na^+ ions or the still larger Li^+ ions. Gregor (4) has lately furnished very clear evidence that the relative ease of penetration of the different ions can be changed by changing slightly the porosity of dried-type collodion membranes. One therefore must conclude that collodion membranes in contact with aqueous solutions of salts of the strong inorganic bases allow the penetration of the cations in the hydrated form, i.e., by means of an aqueous mechanism, the hydration of the ions determining their effective size.

VII. BASE-EXCHANGE CAPACITY AND ACID NUMBER OF COLLODION

In a preceding paper (12) it was pointed out that—aside from the pore structure—the charge density at the collodion–solution interface is the ultimate factor

---

[3] Experiments on the rate of diffusion of DHO, "heavy water," through such membranes would be highly desirable.

[4] Whether or not ions moving through glasses or solid crystalline phases like silver iodide move with equal ease across all the possible points in such phases or along preformed lines of irregularities is immaterial for our further discussion. The second of the two possibilities mentioned undoubtedly is realized with crystalline materials.

determining the electrochemical behavior of membranes of porous character. This general concept was actually used some time ago by Teorell (19) and Meyer and Sievers (7, 8) in some very interesting attempts to put the theory of electrochemical membrane behavior on a quantitative basis.

The charge density of a given surface is identical with its exchange capacity per unit area. The base-exchange capacity of collodion in the fibrous state and of collodion membranes under various conditions was studied, in order to see how far the general concept of what one may call the "fixed-charge theory" is supported by the facts (18), and how far the Teorell, Meyer–Sievers theoretical concepts hold true (17a). The inherent acidity—the "acid number"—of different collodion preparations, i.e., the equivalent weight of these preparations, was also studied in this connection (14).

Base-exchange experiments are usually carried out in the following manner: First the material to be investigated for its base-exchange properties is brought into a well-defined chemical state by saturating it with cations of a single kind. For experimental reasons it is advisable to bring the material into the state of free acidity, either by treatment with hydrochloric acid or by electrodialysis. Known quantities of such material are brought into contact with a neutral salt solution. The hydrogen ions from the exchange body are replaced by the other cations in the solution, and the latter becomes acid. The quantity of titratable hydrogen ions in the supernatant solution represents the actual base exchange, if no complicating reactions occur. If a relatively concentrated electrolyte solution is used for this exchange, it is complete within the limits of experimental error on the first treatment of the exchange body with the neutral salt solution. The free acid in solution can be determined either by titration or electrometrically. The difficulties and limitations of this method when it is applied to very small quantities, as in the case of collodion, have been discussed critically elsewhere (14, 18) and therefore need not be considered here in detail. The base-exchange values in table 1 are given in milliliters of 0.01 N sodium hydroxide per gram of dry collodion; the lowest of these values must be considered to be fictitiously high (14, 18).

The acid number, and therefore also the mean equivalent weight, of a collodion preparation can be determined by bringing it into the state of free acidity, as discussed before, and titrating samples of this material dissolved in a suitable organic solvent (alcohol–acetone) with alcoholic potassium hydroxide solution (14). The corresponding values are given in table 1 under the heading "acid number" and are expressed in milliliters of 0.01 N potassium hydroxide per gram of dry collodion.

The last two columns of table 1 give a measure of the electrochemical activity of the various collodion preparations.

The results of the experiments listed in table 1 and the conclusions based on these experimental data can be summarized briefly as follows: High base-exchange capacity is always found with preparations of great "electrochemical activity"; medium and low base-exchange capacities occur with electrochemically active as well as with inactive preparations. The acid numbers, expressed in

milliliters of 0.01 N potassium hydroxide per gram of dry collodion, vary from 1.0 for a highly purified collodion preparation of very low electrochemical activity to 3.3 for a highly oxidized sample of very high activity. Acid numbers of about 1.5 (corresponding to an equivalent weight of about 67,000) are found both with inactive commercial and with fairly active oxidized preparations. The

TABLE 1

Acid number, base exchange, and activity of various collodion preparations

(1)	(2)	(3)	(4)	(5)	(6)
		ACID NUMBER (CORRECTED FOR ASH) ML. 0.01 N KOH PER GRAM OF DRY COLLODION	BASE EX-CHANGE (48 HR.) ML. 0.01 N NaOH PER GRAM OF DRY COLLODION (CALCULATED FROM pH VALUES)	ELECTROCHEMICAL ACTIVITY	
NO.	BRAND OF COLLODION AND PRETREATMENT (ALL PREPARATIONS WERE PRECIPITATED FROM ETHER–ALCOHOL SOLUTIONS AND DRIED)			Osmotic rise with 0.25 M sucrose	Anomalous osmotic rise with M/512 K_2SO_4
				mm.	*mm.*
1	Mallinckrodt "Parlodion," commercial preparation	1.2	0.0016	110 120 127	36 40 45
2	Mallinckrodt "Parlodion," boiled 8 hr. in 90% alcohol (two alcohol changes)	1.0	0.0013	108 110 114	28 18 22
3	Baker Collodion U.S.P., commercial preparation	1.5	0.004	115 121 130	52 40 60
4	Oxidized collodion; (Baker Collodion Cotton, "Pyroxylin") oxidized 48 hr. with 1 M NaOBr and boiled several times with water	3.3	0.26	130 140 158	145 138 178
5	Oxidized collodion (No. 4), washed eight times with 95% alcohol	2.9	0.11	135 144 158	180 145 172
6	Oxidized collodion (No. 4), washed sixteen times with 95% alcohol	2.8	0.0066	122 138 148	137 145 155
7	Oxidized collodion (No. 4), boiled 3 hr. with 90% alcohol	1.6	0.0066	135 140 150	125 134 120

base-exchange capacity of the same preparations in the fibrous state (as measured after 48 hr. of exchange time) varies from 0.0013 ml. of 0.01 N sodium hydroxide per gram of dry collodion for the most inactive preparation up to 0.26 ml. of 0.01 N sodium hydroxide per gram for the most active preparations. Thus the acid numbers over the whole range investigated differ only in the ratio of 1:3.3, whereas the base-exchange values differ in the range of 1:200.

In the inactive preparation only one in 770 acid groups is available for base exchange, in the most active collodion one group in 13; values between these extremes are found with commercial and alcohol-purified oxidized preparations.

The high base-exchange capacity of the electrochemically active preparations is not so much due to their higher acid number as to their more open structure. This difference in structure can be ascribed to the presence of a small fraction of low-molecular-weight material, which inhibits normal formation and arrangement of the collodion micelles.

So far we have considered the base-exchange data which correspond to the base exchange as obtained after prolonged contact of the electrolyte solution with the various collodion preparations. The base exchange which is obtained on short contact of the collodion with the electrolyte solution is much lower (14, 18), owing to the fact that fibrous collodion has not only easily accessible outer surfaces but also inner surfaces which are accessible only with difficulty; in addition, there may be also some slow base exchange from the interior of the micelles. Since the electrochemical properties of the collodion membranes are usually established after short contact of the membranes with electrolyte solutions, we are actually more interested in the magnitude of the short-time base exchanges than in final, long-time base-exchange values. Unfortunately, short-time base-exchange studies yield rather poorly defined and somewhat arbitrary base-exchange values. Nevertheless, this much can be said: short-time base-exchange experiments with fibrous collodion indicate that the number of acid groups which in membranes would be available for the typical electrochemical membrane functions may be estimated to be about 50 to 1000 times less numerous than those found in the 48-hr. base-exchange experiments discussed before. On the basis of these experiments with collodion in the fibrous state it can be estimated that even with the most active collodion preparations not more than one in 500 acid groups may be available for the typical membrane functions; with the less active preparations, this ratio can be estimated to be only one in 1,000,000 or more.

It may be added parenthetically that these figures can be taken as a measure of the discrepancy between the real situation and a fundamental postulate of the homogeneous-phase theory as applied to the dried collodion membrane,— namely, equivalence of all critical groups.

VIII. AN EXPERIMENTAL TEST OF SOME ASPECTS OF THE TEORELL, MEYER–SIEVERS THEORY OF ELECTROCHEMICAL MEMBRANE BEHAVIOR

The experimental results which have been discussed in the foregoing section were in many respects contrary to the original expectation and, more important, seemed to be incompatible with the Teorell and Meyer–Sievers theories. An attempt was therefore made to clarify the situation on a quantitative basis. The base exchange of membranes was compared with what should be an identical or at least a similar value calculated according to the Teorell (19) and Meyer–Sievers (7, 8) theories on the basis of potentiometric measurements.

A short exposition of these theories must be given. In essence the two concepts are identical. The Teorell, Meyer–Sievers theory is today the outstanding

example of an attempt to put on a rational basis the most important electro-chemical function of membranes,—namely, their electromotive action. Since this theory is highly involved, it is preferable to give a short outline of it as presented by Meyer (7) in a condensed form stripped of everything that is not of primary importance here.

" . . . Consider a membrane consisting of an acid high-molecular substance, for instance of pectin chains, of which the carboxyl groups have been neutralized with metallic cations, *e.g.*, potassium ions. The membrane then possesses fixed anions and mobile cations. The cations may therefore be displaced if a supply of others is maintained from one side: the membrane is cation permeable. The concentration of the fixed anions, calculated in gram equivalents per litre of the imbibed liquid, is a quantity characteristic for each membrane which we will call the 'selectivity constant,' A. If now the membrane be immersed in a salt solution, both ions of the salt will penetrate into it; the equilibria then obtaining may be calculated from the Donnan equation: the actual membrane behaves like a solution bounded by two ideal Donnan membranes through which the fixed ions cannot pass. . . . "

". . . If a current is passed across the membrane, the transport of the electricity will be divided between the two kinds of mobile ions in accordance with the relative numbers of ions passing through the membrane. The ratio, n_C/n_A between the numbers of cations and of anions traversing the membrane, which we will call the ratio of the transport or 'traversal' numbers, may be determined by the same methods as those used for the determination of transport numbers in a solution. n_C/n_A depends on the rates of migration of the mobile ions and on their number; as mentioned above, the latter is dependent on the concentration of the ions in the surrounding liquid. We then obtain

$$\frac{n_C}{n_A} = \frac{U_C \cdot (y + A)}{U_A \cdot y} = \frac{U_C}{U_A} \cdot \frac{\sqrt{4c^2 + A^2} + A}{\sqrt{4c^2 + A^2} - A} = \frac{U_C}{U_A} \cdot R,$$

where U_C and U_A are the rates of migration, c the molar concentration of the salt in the surrounding liquid, and A the selectivity constant . . . " y is the concentration of mobile anions in the membrane.

The quotient U_C/U_A and the selectivity constant of a membrane "can be determined by measuring the traversal numbers at different concentrations. The potentiometric method is the best; the potential set up when the membrane separates two solutions of the same salt, but of different concentrations is measured, the absolute concentrations being varied in such a way that their ratio is kept constant. When there is no ionic selectivity the potential is determined only by the quantity U_C/U_A, which is dependent on the absolute concentration; the greater the value of A as compared with the external concentration, the more marked will be the ionic selectivity.

A, the selectivity constant, and U_C/U_A . . . can be quantitatively determined . . . graphically. . . .

Curves are constructed plotting as ordinates the potential differences ("E") measured between two solutions of the same binary electrolyte, the concentrations (c_1, c_2) of which are always as 1:2, and as abscissae the quantity $\log \frac{A \cdot}{c_1}$. For an electrolyte, the two ions of which have equal mobilities in the membrane (i.e., $U_C/U_A = 1$), a certain curve will then be obtained, while other values of U_C/U_A will result in other curves . . . ." (The calculated curve for $U_C/U_A = 1$ is given below in figures 6 and 7.)

" . . . To determine A and U_C/U_A for an unknown membrane it will then only be necessary to determine several values of E for different absolute vales of c_1, the concentration c_2 being always kept equal to $2c_1$. The observed values of E are then plotted against c_1 (ordinates) using the same co-ordinates as before, and then the experimental curve is displaced sideways (parallel to the abscissae) until it has been successfully brought into co-

incidence with one of the curves already drawn; interpolation may be necessary in this procedure. In this way U_C/U_A is determined, the value depending only on the shape of the curve. The amount of the displacement as read off on the abscissa gives log A, and therefore A. . . . "

The quantity A, according to Meyer and Sievers, can thus be determined on the basis of potentiometric measurements. Values obtained in this manner are designated as A_p.

On the other hand, A by definition is the concentration of the fixed ions in the aqueous part (pore space) of the membrane, or more correctly the concentration calculated from the number of equivalents of anions (or anionic groups) fixed immovably to the pore walls, divided by the pore space (in liters) of the same membrane.

Electrically these anions are compensated for by an equivalent quantity of cations. These cations—potassium ions in the example given by Meyer—can be replaced by other cations if the membrane is brought into a suitable electrolyte solution.

If one is able to determine the base-exchange capacity of all the pore walls in a membrane, i.e., the base-exchange capacity of the membrane, and if one knows its pore space, one is able to calculate the A value of the Meyer and Sievers theory, A being the base-exchange capacity in equivalents divided by the pore volume in liters. The A values which are calculated from base-exchange studies are denoted A_b.

If the theoretical assumptions on which the theory is based are correct, A_p derived from potential measurements must be identical with A_b derived from base-exchange studies.

The main question which one can hope to decide by the comparison of the two selectivity constants is whether the Teorell, Meyer–Sievers theory is inherently a correct representation of the physical facts which lie behind the observable potential–concentration relationships, or whether it is only a formal way of bringing the latter relations into a fictitious, formally correct framework.

Two kinds of measurements were performed with the same membranes: First, the potentiometric studies were made; then the base exchange of the same membranes was determined, and in order to obtain the water content, the wet and dry weights of the membranes were measured. From these data the selectivity constants, A_p and A_b, were obtained as explained in principle above. Since the de-

---

[5] The water content of collodion membranes represents only a maximum value for the available pore space. Some water, undoubtedly, is "bound" to the collodion and not available for the typical membrane functions. With "porous" membranes of high water content the fraction of "bound" water is negligibly small; with dried membranes the "bound" water may be a sizable fraction of the total water content (see C. W. Carr and K. Sollner: J. Gen. Physiol. **27**, 77 (1943)). In the calculations reported below, which involve the pore water content of the membranes, the assumption is made that the total water content is pore water. If we make the exaggerated assumption that 50 per cent of the water content of the "dried" membranes is "bound" water, the figures for cases No. 1–4 in column 3 of table 2 would be twice as large as given, and the figures in column 6 would be half of the present values. This, however, would in no way affect the essence of the conclusions which will be drawn below from these figures.

tails of the experimental work involved and of the calculation methods used will
be published shortly elsewhere (17a), not many details need to be given here.
Figures 6 and 7 show in a graphical manner the results of experiments with mem-
branes prepared from various collodion preparations and also indicate how in a
graphical manner the selectivity constant, A_p, is obtained. A_b is determined
from the base-exchange capacity of the membranes and their known water con-
tent.[5] Tables 2 and 3 contain these magnitudes together with the ratio A_p/A_b.
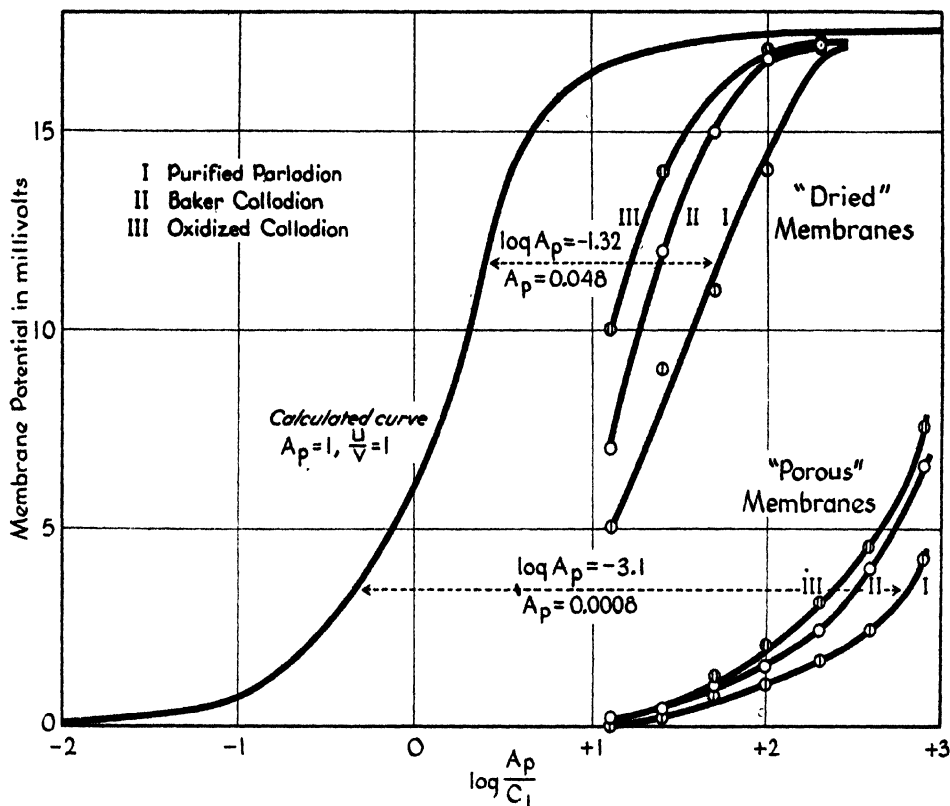
FIG. 6. Potential-log $\frac{A_p}{c_1}$ curves of "dried" and "porous" membranes prepared from various collodion
preparations.

According to the Teorell, Meyer–Sievers theory, A_p/A_b should be 1, or, con-
sidering the uncertainties of the theory, this ratio should not deviate too strongly
from unity.   A glance at the last column of tables 2 and 3 shows that this ratio
is spread over three orders of magnitude, varying from 0.08 to 107; in the ma-
jority of the cases it is greater than 30.

In evaluating the meaning of the A_p/A_b ratio, two facts must be considered.
It was shown repeatedly (14, 18) that the long-time base-exchange values, as
they are used in tables 2 and 3, are much higher than those obtainable after the

shorter periods which it takes the membranes to assume their final electro-
chemical properties. Therefore one may estimate that the A_b values which
determine the functional behavior of the membranes are only 5 to 20 per cent of
those given in tables 2 and 3. Correspondingly, the A_p/A_b values would be
about ten times greater. In addition there is another factor which tends to in-
crease this discrepancy in the case of the membranes having only a very low
base-exchange capacity. In these cases the A_b values are fictitiously high; the
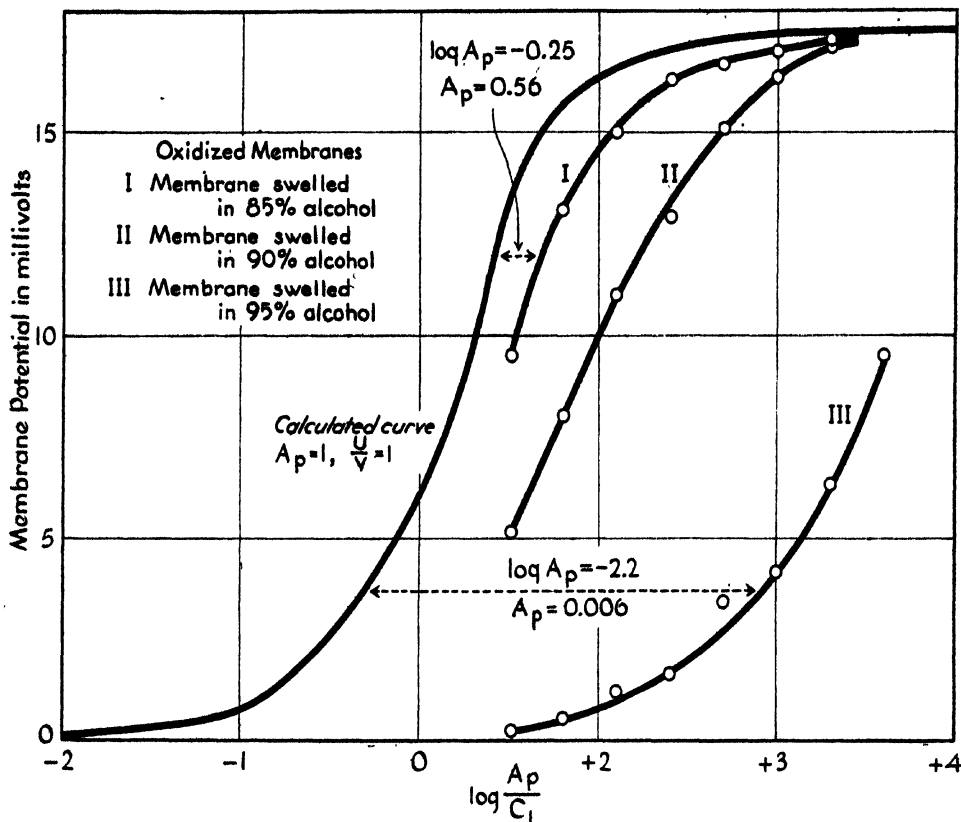
FIG. 7. Potential-log $\frac{A_p}{c_1}$ curves of "oxidized membranes" of various porosities

true base exchange cannot be determined accurately with the available methods
on account of difficulties discussed elsewhere (14, 17a, 18). For this reason alone,
A_b values may easily be 10 or even 100 times lower than those given in table 2.
   It is therefore a conservative estimate that the A_p/A_b ratio in the case of the
membranes having low base-exchange capacity is two, probably three, orders of
magnitude smaller than given in the table; in the case of the membranes with
high base-exchange capacity the A_p/A_b ratio is probably not much less than one

order of magnitude smaller than represented in the table.   Considering this, we find that a reasonable agreement between the A_p and the A_b values exists only

TABLE 2

A_b and A_p values of membranes prepared from various collodion preparations

(1) NO.	(2) BRAND OF COLLODION AND TYPE OF MEMBRANES	(3) WATER CONTENT OF MEMBRANES	(4) A_b CALCULATEED FROM BASE- EXCHANGE DATA	(5) A_p OBTAINED FROM EXPERIMENTAL POTENTIAL CURVES OF FIGURE 6	(6) $\dfrac{A_p}{A_b}$
		volume per cent	*equivalents per liter ×10³*	*equivalents per liter ×10³*	
1	Purified "Parlodion"; dried membranes....	8.2*	<1.4*	48	> 34*
2	Baker Collodion U.S.P.; dried membranes.... . ..	10.5*	<1.5*	100	>67*
3	Oxidized collodion; dried membranes...	10.5*	<1.4*	150	>107*
4	Oxidized collodion, purified; dried membranes . . .	10.5*	<1.6*	100	>62*
5	Purified "Parlodion"; porous membranes.... .	80	<0.05	0.8	>16
6	Baker Collodion U.S.P.; porous membranes .	75	<0.02	1.5	>75
7	Oxidized collodion; porous membranes...	79	0.3	2.0	6.7
8	Oxidized collodion, purified; porous membranes. .	77	<0.045	1.5	>33

* Compare footnote 5.

TABLE 3

A_b and A_p values of various "oxidized membranes"

(1) NO.	(2) CONCENTRATION OF ALCOHOL USED FOR SWELLING OF MEM- BRANES BEFORE OXIDATION	(3) WATER CONTENT OF MEMBRANES	(4) A_b CALCULATED FROM BASE-EXCHANGE DATA	(5) A_p OBTAINED FROM EXPERIMENTAL POTENTIAL CURVES OF FIGURE 7	(6) $\dfrac{A_p}{A_b}$
	per cent	*volume per cent*	*equivalents per liter ×10³*	*equivalents per liter ×10³*	
1	85	17	330	560	1.8
2	90	24	220	170	0.77
3	95	62	78	6	0.08

in one case, No. 3 of table 3.   In all other cases the disagreement varies between relatively low figures and figures as high as 10,000 or more.

It does not seem to be without significance that the disagreement between the

A_p and A_b values is the smaller the greater the porosity of the membranes and the higher their base-exchange capacity.

The attempt to verify the Teorell, Meyer–Sievers theory as applied to a variety of collodion membranes by the comparison of selectivity constants arrived at on the basis of two different, experimentally independent methods has failed completely. We shall discuss in a subsequent paper the probable significance of this disagreement.

SUMMARY

1. Various new experimental approaches furnish proof that the characteristic behavior of "dried" collodion membranes with solutions of inorganic electrolytes and those non-electrolytes which are not strongly adsorbable must be explained on the basis of the porous, micellar-structural character of these membranes. The homogeneous-phase theory of membrane permeability cannot be applied to dried collodion membranes.

2. Air-dried "dried" collodion membranes swell slightly when immersed in water. No specific swelling effect is observed with solutions of strong inorganic electrolytes and those organic compounds which are but weakly adsorba le; within these limits water-wetted dried collodion membranes behave as rigid non-swelling structures. Adsorbable solutes in many instances cause pronounced specific swelling. The behavior of highly porous collodion membranes towards the solutions of the various solutes is analogous to that of the dried membranes.

3. The dissociable groups located in the interstices of the membranes which determine the electrochemical behavior ("activity") of collodion membranes can be determined by base-exchange measurements. The base-exchange capacity of various collodion preparations in the fibrous state, as measured after 48 hr. of exchange time, varies from 0.0013 ml. of 0.01 N sodium hydroxide per gram of dry collodion for the most inactive preparation up to 0.26 ml. of 0.01 N sodium hydroxide per gram for the most active preparation. High base-exchange capacity is always found with preparations of great "electrochemical activity"; medium and low base-exchange capacities occur with electrochemically active as well as with inactive preparations.

4. The inherent acidity of various collodion preparations, their "acid number," was determined by electrometric titration. Collodion in the acidic state was titrated in an organic solvent mixture with alcoholic potassium hydroxide, using a quinhydrone electrode. The acid numbers, expressed in milliliters of 0.01 N potassium hydroxide per gram of dry collodion, vary from 1.0 for a highly purified collodion preparation of very low electrochemical activity to 3.3 for a highly oxidized sample of very high activity. Thus the acid numbers over the whole range investigated differ only in the ratio of 1:3.3, whereas the base-exchange values differ in the range of 1:200.

5. The high base-exchange capacity of the electrochemically active preparations is due not so much to their higher acid number as to their more open structure.

6. Short-time base-exchange experiments indicate that in membranes prepared even from the most active collodion not more than one in 500 acid groups may be available for the typical membrane functions; with the less active preparations this ratio is estimated to be as high as one in 1,000,000 or more.

7. The Teorell, Meyer–Sievers theory characterizes the electrochemical behavior of membranes by their selectivity constant A_p, which is derived conventionally from concentration potential measurements at various concentration levels. The selectivity constant may, however, be derived also from entirely independent, different experimental data,—namely, base-exchange studies. The constants arrived at in this second way are designated as A_b. The selectivity constants derived by these two methods must be in reasonable, at least semiquantitative agreement if the basic assumptions of the theory are correct. The selectivity constants A_p and A_b were determined for eleven different sets of membranes of different electrochemical activity and of different (8.2 to 80 volume per cent) water content. The potentiometric selectivity constants A_p are in most cases several orders of magnitude greater than the corresponding A_b values. With membranes of great porosity and high electrochemical activity the A_b values approach at least in order of magnitude the A_p values. The cause of the unexpectedly large discrepancy between the A_p and A_b values will be discussed in a subsequent paper.

REFERENCES

(1) CARR, C. W., AND SOLLNER, K.: J. Gen. Physiol. **27**, 77 (1943).
(2) CARR, C. W., AND SOLLNER, K.: J. Gen. Physiol. **28**, 119 (1944).
(3) COLLANDER, R.: Soc. Sci. Fennica, Commentationes Biol. **2**, 6 (1926).
(4) GREGOR, H. P.: Ph. D. Thesis, University of Minnesota, 1945.
(5) HÖBER, R.: J. Cellular Comp. Physiol. **7**, 367 (1936).
(6) MANEGOLD, E.: Kolloid-Z. **61**, 140 (1932).
(7) MEYER, K. H.: Trans. Faraday Soc. **33**, 1073 (1937).
(8) MEYER, K. H., AND SIEVERS, J.-F.: Helv. Chim. Acta **19**, 649 (1936).
(9) MICHAELIS, L.: Bull. Natl. Research Council, No. 69 (1929).
(10) MICHAELIS, L., AND FUJITA, A.: Biochem. Z. **161**, 47 (1925).
(11) NORTHROP, J. H.: J. Gen. Physiol. **12**, 435 (1929).
(12) SOLLNER, K.: J. Phys. Chem. **49**, 47 (1945).
(13) SOLLNER, K., ABRAMS, I., AND CARR, C. W.: J. Gen. Physiol. **25**, 7 (1941).
(14) SOLLNER, K., AND ANDERMAN, J.: J. Gen. Physiol. **27**, 433 (1943).
(15) SOLLNER, K., AND BECK, P. W.: J. Gen. Physiol. **27**, 451 (1944).
(16) SOLLNER, K., AND CARR, C. W.: J. Gen. Physiol. **26**, 17 (1942).
(17) SOLLNER, K., AND CARR, C. W.: J. Gen. Physiol. **26**, 309 (1943).
(17a) SOLLNER, K., AND CARR, C. W.: J. Gen. Physiol. **28**, 1 (1944).
(18) SOLLNER, K., CARR, C. W., AND ABRAMS, I.: J. Gen. Physiol. **25**, 411 (1942).
(19) TEORELL, T.: Proc. Soc. Exptl. Biol. Med. **33**, 282 (1935); Proc. Natl. Acad. Sci. (U. S.) **21**, 152 (1935).
(20) WEECH, A. A., AND MICHAELIS, L.: J. Gen. Physiol. **12**, 221 (1928).

FIBROUS FROM GLOBULAR PROTEINS[1]

F. R. SENTI, M. J. COPLEY, AND G. C. NUTTING

Eastern Regional Research Laboratory,[2] Philadelphia, Pennsylvania

Most proteins of current or potential industrial importance are in the molecular sense compact, almost globular structures as they occur in nature or as they are isolated by laboratory or commercial procedures. While the structure of none of the proteins is known in detail, it is a widely held view that, fundamentally, the molecules are chainlike (1, 12, 25) but are normally maintained in a coiled configuration by interaction among the numerous polar groups. Opportunity for interaction between molecules is thus minimal. If the molecules were uncoiled and fixed in a linear form, the number of intermolecular bonds would be far greater, and the mechanical properties of objects such as fibers, films, and plastics made from the altered proteins should be much improved. This is not merely conjectural, for filaments of the natural fibrous proteins, silk and collagen, are far stronger and tougher than filaments of unoriented globular proteins. Casein fiber is now in commercial production, and experimentation is being conducted in several laboratories on the preparation of fiber from soybean and peanut proteins, zein, and other globular proteins. Fiber prepared in the conventional way from an alkaline dispersion has in general been somewhat deficient in dry and wet strength and gives no evidence of molecular orientation in its diffraction pattern. It is the purpose of this paper to describe experiments by which conversion of several globular proteins to the fibrous form has been accomplished and to give some of the properties of filaments made of the converted protein.

Observations of Carothers and Hill (9), Sookne and Harris (27), Mark (19), and others indicate that the length of an extended linear polymer molecule, as measured by the average degree of polymerization (D. P.) or molecular weight (M. W.), must exceed a critical minimum if fibers of usable pliability and strength are to be prepared. For the polyester of ω-hydroxydecanoic acid, Carothers and van Natta (10) found the limit to be between M. W. 10,000 and 15,000 or D. P. about 60 to 90. This corresponds to a length of 800 to 1200 Å. For cellulose and for polyamides the figures are roughly the same, while for hydrocarbons the D. P. for corresponding tensile strength is considerably higher because of the weakness of the interaction between non-polar groups. In all these linear polymer molecules, side groups are either completely absent or, if present, are small, are alike, and are spaced at regular intervals along the chain. On stretching, the molecules are readily oriented and form quasi-crystalline arrays in which segments of adjacent molecules match one another rather perfectly. Within

these crystalline regions the potential energy tends toward a minimum, and intermolecular cohesion is correspondingly increased.

The molecular weight of globular proteins ranges from about 15,000 to several million (29). As measured, it indicates the weight of the effective kinetic units in sedimentation, osmosis, or diffusion, or the weight of crystallographically equivalent constituents in the unit cell as determined by x-ray analysis. It does not necessarily give any indication of the molecular weight, the degree of polymerization, and the maximum length of the polypeptide chain or chains contained in the molecule, and for our purposes these are the significant quantities. For example, the molecular weight of hemoglobin is about 68,000. Of this, 2500 units are due to the four associated haems. On treatment even with as mild a reagent as aqueous urea, hemoglobin splits into halves of molecular weight approximately 34,000. From a partial structure analysis, Boyes-Watson and Perutz (8) have proposed that the hemoglobin molecule consists of four substantially equal and parallel layers of polypeptide chains, with the main chains folded in the plane of the layers and the side chains extending at right angles to them. The position of the haem groups is unknown. If this model is correct, it is evident that the upper and lower pairs of layers are not joined by a peptide or other strong bond. Whether the paired layers are themselves linked by a strong covalent bond is not certain. If they are not, one would expect to be able to split the pairs into halves of molecular weight 17,000. Thus far, there is no report that hemoglobin from the higher animals has been dissociated into fragments of this size, but the hemoglobin of the cyclostomata, containing one haem per molecule, has a normal weight of 17,000 (28).

Molecular-weight measurements of globin derived from normal (68,000 M. W.) hemoglobin are not helpful, because globin readily forms loose association complexes and apparently it is the weight of the complex rather than the weight of the individual molecule that is usually found (24). Chibnall (11) has recently presented what seems to be good evidence that hemoglobin (68,000 M. W.) contains sixteen peptide chains. These may or may not be of similar size and constitution. From what has been said above, it is probable that not more than eight chains are firmly bonded together. If eight chains were joined by strong bonds adjacent to terminal amino groups to make a continuous chain of weight 34,000, the latter would have a D. P. of about 320, and if extended would be 1050 Å. long.[3] This should make a satisfactorily strong, tough fiber. It is important to note that in globular proteins about half the total weight is in the side chains, so that a fully extended 34,000 M. W. molecule would be much shorter than a molecule of rubber, 6-6 nylon, or polyvinyl alcohol of equal molecular weight, but would be comparable in length to cellulose. The effect of smaller D. P. and chain length on intermolecular cohesion may, however, be partly or fully compensated for by the large proportion of polar groups in both the main

[3] The average residue weight for globin is 106 (Chibnall (11)). Dividing 34,000 by 106 gives for the D.P. a rough value of 320. The length of the extended chain is computed by multiplying D.P. by 3.3 Å., the fiber repeat distance found in β-keratin and in globular proteins converted to the fibrous form.

and the side chains. If the chains pack regularly, as they do in collagen, a strong structure results.

Should the eight polypeptide chains in the hemoglobin half-molecule be linked, not end-to-end, but through cross-bonds, the length of fully extended chains would be correspondingly shorter, and conceivably no usably strong fiber could be made from hemoglobin regardless of how perfectly the chains might be oriented and packed. Taking an extreme case of sixteen equal polypeptide chains without covalent links, the D. P. and maximum length of each chain would be about 40 and 120 Å., respectively. These values are much smaller than the minimum values for usable fibers quoted earlier.

Chibnall (11) has concluded similarly that molecules of edestin (M. W. 310,000), insulin (35,000), ovalbumin (43,000), and lactoglobulin (42,000) are systems of six, eighteen,[4] about four, and nine peptide chains, respectively. It is well known that edestin in urea solution splits into fragments having a molecular weight of about 50,000. Apparently, then, edestin contains single peptide chains having a weight of 50,000, amply long for our purposes if they are not cross-bonded or degraded.[5] For the other proteins listed, no reliable estimates of the effective D. P. can be made, since the mode of linking of the constituent peptide chains is unknown. It is clear, however, that for these globular proteins, which may probably be regarded as typical, the highest possible D. P. does not greatly exceed the permissible minimum for forming fibers of good quality. As a corollary it follows that the process of unfolding and orienting the chains, and all other procedures applied to the protein, may have to be mild if ruinous chain degradation is to be avoided.

Astbury, Dickinson, and Bailey (2), working with edestin, first described the conversion of a globular protein to the fibrous form. By a different method Palmer and Galvin (22) and Lundgren and O'Connell (18) produced the same result with ovalbumin. Through work done in this laboratory still other means have been developed for converting globular proteins to a fibrous form in which the peptide chains are unfolded, oriented, and regularly arranged in space. One such means (21, 26) involves, essentially, heating the protein in the presence of water,[6] followed by mechanical treatment such as stretching to extend and orient

---

[4] Chibnall, taking 35,000 for the molecular weight of insulin, computed that there are eighteen chains in the molecule. The recent work of Miller and Anderson (J. Biol. Chem. **144,** 459 (1942)) indicates that the molecular weight of insulin is actually about 46,000. By using this value rather than 35,000, the number of polypeptide chains per molecule is raised to twenty-four.

[5] Adair and Adair (Biochem. J. **28,** 199 (1934)) suggest from measurements of membrane potentials that edestin on mild acid hydrolysis is split into fragments of molecular weight approximately 17,000. Bailey (Biochem. J. **36,** 140 (1942)) has found the sedimentation constant of a similar edestin preparation to be 2.6×10^{-13}. Correction for electroviscosity would raise this value and would indicate that the molecular weight of the sedimenting particles is roughly 40,000 to 50,000. If the molecular weight were 17,000, the sedimentation constant would be about 1.8×10^{-13}, or less if there were appreciable electroviscosity. It appears to us that there is no conclusive evidence that the edestin submolecule of M. W. 50,000 breaks down into 17,000 M. W. fragments.

[6] It has been found that heat as an agent in effecting the transformation from the globular to the fibrous state may be supplanted by a variety of chemical agents. A brief report of

the chains. Primary evidence that the conversion has been accomplished is provided by x-ray observations. The processed protein gives a typical "fiber diffraction pattern" which is remarkable in its similarity to the fiber pattern of the β-keratin of feathers and stretched hair. Among the globular proteins which we have thus converted to the oriented fibrous form giving the β-keratin diffraction pattern are casein, lactoglobulin, zein, hemoglobin, soybean protein, peanut protein, ovalbumin, edestin, tobacco-seed globulin, pumpkin-seed globulin, gliadin, and the albumin, globulin, and mixed proteins of horse serum.

PREPARATION OF SPECIMENS

Coarse fibers or bristles made by extrusion were convenient specimens for orientation. Suitable mixtures for extrusion were made from the more soluble proteins by mixing the powdered material with approximately half its weight of water. Pumpkin-seed globulin and other water-insoluble native proteins were tackified by incorporating about 1 per cent of sodium chloride with the protein-water mixture. Casein filaments were extruded at 95°C. from a briefly heated mixture of casein and water. Zein and gliadin were precipitated from alcoholic solution by addition of water. After washing with water, they were readily extrudable.

Thin sheets, plates, and small rods formed by conventional methods were also used as specimens. In making the plates, forming and heat treating were done simultaneously in a press. The heat treatment was usually given close to 100°C. Filaments of readily denaturable proteins such as lactoglobulin, serum albumin, the oil-seed globulins, and ovalbumin were simply kept in boiling water for 5 to 30 min. Filaments of casein, zein, and gliadin were conditioned in water vapor at 0.5–1.0 atmosphere pressure for several hours. During the heat treatment the filaments become tough and rubbery and so coherent that they may in general be stretched a considerable amount before fracture occurs. Changes in molecular structure that take place simultaneously will be discussed in the section on diffraction effects. Since the heat-conditioned proteins are decidedly viscous, application of shear stress provides the most obvious means of producing molecular orientation. Stretching has been utilized almost exclusively, because it is a convenient technique and because it is possible without undue difficulty to

---

initial observations has already been made (21). Of the several proteins thus far examined, ovalbumin has been outstanding in the variety of reagents found that may substitute the thermal treatment. As judged by several tests, the mode of interaction of protein with both heat and the chemicals is similar. Ovalbumin filaments soaked in, for example, 75 per cent ethanol, or in boiling water become insoluble, elastic, and structurally so composed that they can be stretched to several times their initial length. The stretched filaments have much increased tensile strength and are pliable when dry. They are positive-birefringent and give β-keratin fiber patterns.

A specimen of ovalbumin surface denatured in a Waring Blendor, when stretched, gave the β-keratin diffraction pattern. An unusual feature of this pattern was the occurrence on the equator of a reflection at about 23 Å.

Ovalbumin, dispersed in phenol and spun into a precipitating bath such as ethanol, also gave a fiber pattern after stretching.

prepare specimens sufficiently cohesive to permit stretching. Stretching was usually done slowly in steam or in air approximately saturated with water vapor at about 100°C. Draw ratios (D. R.) or ratios of final to initial lengths of five or more were commonly obtained. In general, molecular orientation, as revealed by the diffraction pattern, increased with the draw ratio under comparable conditions. When specimens were drawn at room temperature or at an elevated temperature with a low pressure of water vapor, a small draw ratio produced the same diffraction effects as a much higher draw ratio when the specimens were more highly plasticized. On stretching in an alkaline solution or in the vapor of a boiling saturated solution of cresol, draw ratios as high as 25 have been obtained without any comparable increase in orientation.

Attempts to produce orientation in the absence of water have uniformly failed. Specimens prepared, for example, from intensively dried ovalbumin and cresol were stretched in cresol vapor at temperatures up to 150°C. or more. The diffraction pattern of the stretched material consisted of two full, diffuse rings.

Since the orientation process appears to be rather generally applicable to globular proteins, it is perhaps not surprising that proteins of various degrees of purity and from various sources should when oriented give comparable diffraction effects.[7] In our experience there is, however, a marked variation in the ease with which the different proteins and protein preparations may be crystallized and oriented. (The word crystallized is used in the restricted sense that the x-ray reflections sharpen and become more numerous, indicating increased regularity or order in the spatial arrangement of the scattering matter.) Generally speaking, the proteins ordinarily classed as heat-denaturable are most readily converted to the oriented fibrous form by the thermal process. Examples of readily convertible proteins are lactoglobulin, serum albumin, ovalbumin, and the globulins of tobacco and pumpkin seeds, provided that these are in the native state. If the proteins are denatured, as by heating, prolonged drying, chemical agents, or other means, the conversion becomes more difficult and less complete. The increased difficulty probably arises largely from insolubilization and loss of tack, making it hard to form filaments or other objects suitable for stretching. We have not yet sought to determine the feasibility of producing an oriented fibrous protein from a denatured protein powder by other shear processes, such as rolling, or flowing, or extruding under high pressure. Casein, zein, gliadin, and commercial soybean protein have proved considerably more difficult to crystallize and orient than the native, heat-denaturable proteins listed above.

DIFFRACTION EFFECTS

In our experiments, we have been concerned with the conversion of the globular protein molecule to an extended polypeptide chain in filaments (or other

formed objects). That is, the filaments as extruded are composed of native protein, and denaturation or unfolding of the molecules occurs in subsequent operations. X-ray diffraction measurements provide the best method of following the change in molecular configuration that takes place during these operations.

The diffraction pattern of most protein filaments as extruded and dried at room conditions without further treatment is characterized by two diffuse reflections, corresponding to interplanar spacings of about 10 Å. and 4.6 Å. The breadth of these reflections, the fact that only two reflections are observed, and the general scattering on the pattern indicate that the size of any crystalline regions in the sample must be very small. The spacings 10 Å. and 4.6 Å. must correspond to frequently occurring interatomic distances, and by comparison with x-ray patterns of disoriented keratin have been identified as the "side-chain" and "backbone" spacings between adjacent polypeptide chains (3). That is, considerable portions of the polypeptide chains form mesomorphic regions in which a number of chain segments lie parallel over a distance corresponding to several amino acid residues. This does not necessarily imply that the chains are unfolded; adjacent segments in a given region may be part of one more or less regularly folded protein molecule. The pronounced broadening of the two observed reflections is probably best interpreted as due to imperfect side-by-side packing of the amino acid residues rather than to extremely small perfect crystallites.

When a globular protein is heated with water, the diffraction pattern improves considerably. The 10 Å. and 4.6 Å. reflections sharpen, and at least one additional reflection (3.7 Å.) appears. Astbury and Lomax (3) have observed this change in the patterns of serum albumin and egg white upon heat denaturation and have attributed the pattern to regular bundles or crystallites composed of fully extended parallel polypeptide chains. We have found that filaments of many globular proteins heated to give the pattern characterized by three or more well-defined reflections can, in general, be stretched when plasticized with water to give a diffraction pattern nearly identical with that of β-keratin. On stretching, the existing crystallites are oriented with their longest axis parallel to the direction of stretch, and possibly new crystallites are formed by the action of the stress in extending and parallelizing polypeptide chains. The formation of crystallites or ordered regions of extended chains from curled or folded chains in the protein filaments is analogous to the ordering that occurs in the cold-drawing of polyamide fibers (20).

The rate of transformation of the protein from the mesomorphic state to the more ordered state under the influence of heat and water depends on the particular protein. Thus proteins readily denatured by heat, such as ovalbumin, lactoglobulin, and hemoglobin, are converted to the ordered state after a few minutes in boiling water. Since insolubilization of these proteins occurs rapidly on contact with the boiling water, there is no disintegration or dissolution of the filaments. Filaments of casein, on the other hand, are not readily heat-denatured, and if immersed in boiling water after extrusion, they rapidly disintegrate before they are insolubilized in the conversion to the ordered state. Consequently,

protein filaments of this type must be treated by a different method, and it has been our practice to heat them in atmospheres of controlled humidity. For example, casein fibers are conditioned at 100°C. over a 5 per cent solution of sodium chloride. There is a progressive change in the diffraction pattern of casein filaments with increasing conditioning time. The 4.6 Å. reflection becomes sharper, and a new reflection at 3.7 Å. is resolved. At later stages, two weak reflections at 2.2 and 2.0 Å. appear.

Although the x-ray pattern generally shows continuous improvements with increased time of heat-conditioning, mechanical properties of fibers may be impaired by long heating. Casein bristles, for example, show a decline in tensile strength if heat-conditioned for more than 50 hr. under the conditions described above. This may be due to chain degradation, which would not hinder the ordering process but would reduce the tensile strength.

We have observed that the water content of the protein filament has an effect on the x-ray pattern. As an illustration, wet casein gives sharper reflections than does bone-dry casein. To study this effect in greater detail, two series of freshly extruded casein filaments were equilibrated at 27°C. in air of 0, 25, 50, 75, and 100 per cent relative humidity. In one series, equilibrium was approached from the dry side and in the other series from the wet side. The equilibrated filaments were mounted in a closed chamber which maintained the proper humidity during exposure to the x-ray beam. In each series, equilibrating the filaments at 50 per cent relative humidity or greater sharpened the reflections, but there was little or no effect below 50 per cent relative humidity. Most of our patterns have been obtained from filaments equilibrated at room conditions, which correspond to 15 to 30 per cent relative humidity. Moreover, the sharpening of the pattern due to water alone is much less than the corresponding change resulting from heat-conditioning, so there is no doubt that heat-conditioning has a real effect on the crystallinity of the protein.

The action of heat in rearranging the mesomorphic structure in quenched polyamides (13) and cellulose triesters (6) to give a crystalline structure indicates that there is high mobility of chains or chain segments in these substances in the solid state. The crystallinity of quenched cellulose derivatives (6) which contain unsubstituted hydroxyl groups cannot be improved by annealing at temperatures below the softening point. The reduced mobility of the chains in these derivatives has been attributed to the presence of hydrogen bonds between residual hydroxyl groups. If such derivatives are annealed in water at 100°C., however, the strong hydrogen-bonding agent, water, splits the interchain hydrogen bonds and permits chain motion and crystallization.

Proteins contain a high concentration of hydrogen-bonding and other polar groups which contribute to a high interaction between adjacent chains. One might predict that there would be little tendency for chain rearrangement upon the application of heat alone, and that it would be necessary to introduce some polar solvent to increase mobility. This is borne out by the observations of Barker (7) that ovalbumin dried over phosphorus pentoxide is denatured, as measured by solubility, only at 160–170°C., while ovalbumin in the presence of excess water is denatured at 56°C. We have tried to crystallize and orient

globular proteins by our usual techniques, substituting for water other representative hydrogen-bonding liquids such as ethanol, cresol, and formamide. Our attempts have been uniformly unsuccessful.

TABLE 1

Observed spacings and intensities in the fiber diagram of lactoglobulin, ovalbumin, and β-keratin

INDEX	LACTOGLOBULIN		OVALBUMIN		β-KERATIN*	
	A.		A		A.	
001	9 7	S	9.8	S	9.7	S+
200	4.6₄	S+	4.6₃	S+	4.65	S+
400			2.3	W	2.4	W
600			1 6	W		
111	4.7	M	4 7	M	4.7	M
210	3 7₂	M+	3 7₃	M	3.75	S
410			2 2	W	2.2	W
020	3 2₆	M+	3 3₃	M+	3.33	S
220	2.7₁	W	2 7₃	W	2.7	W
030					2.2	W
130	2.1₆	W	2.1₄	W		
230	2 0₃	W+	2 0₃	W+	2 0	W

* From reference 4.
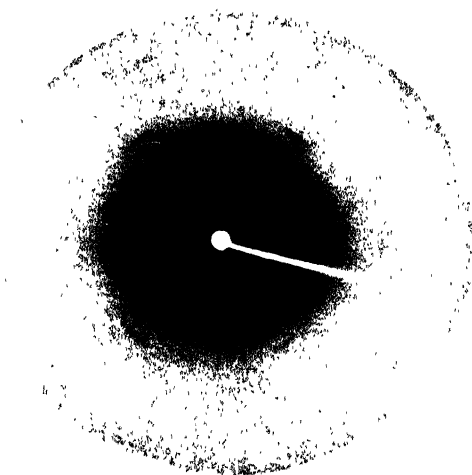
FIG. 1. X-ray diffraction pattern of a highly oriented ovalbumin filament. The fiber axis is vertical.

Protein filaments, annealed and stretched, give x-ray fiber patterns very nearly identical with the pattern of oriented β-keratin. Patterns showing the greatest number of reflections have been obtained from β-lactoglobulin and ovalbumin. Data on these proteins are summarized in table 1, together with indices and corresponding data for β-keratin given by Astbury and Street (4). The diffraction pattern of a highly oriented ovalbumin filament is shown in figure 1.

The 2.2 Å. reflection indexed by Astbury and Street as (030) is resolved into two near-meridian reflections which we have designated as (130). Thus, both (010) and (030) are absent, and the b-axis is probably a twofold screw axis. This is consistent with the packing of extended chains, with side chains projecting on alternate sides of the main chain, in successive amino acid residues. Such a structure is required by a fully extended polypeptide chain of amino acid residues having the same configuration (14). Meridian reflections at distances greater than 3.3 Å., such as are observed in feather keratin, do not occur in any of our preparations and, so far as we are aware, have not been found in the β-keratin of stretched wool and hair.

Comparison of the lattice spacings of β-lactoglobulin, ovalbumin, and β-keratin in table 1 shows only small variations, which are probably within the experimental error of measurement. Our data on oriented filaments of casein, pumpkin-seed globulin, hemoglobin, serum albumin, zein, gliadin, tobacco-seed globulin, edestin, soybean and peanut protein, while not as extensive as those for
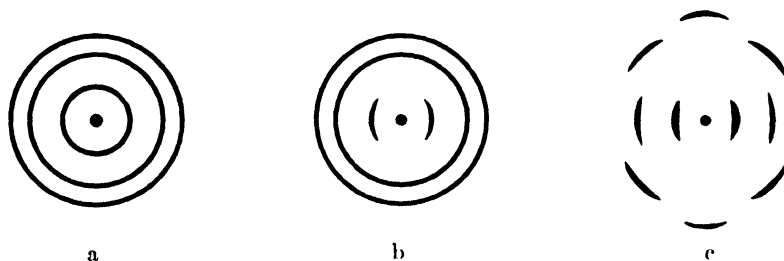
Fig. 2. Change of the diffraction pattern of a heat-conditioned globular protein during orientation by stretching: (a) no stretch; random orientation of crystallites, (b) low stretch; uniplanar orientation; (c) high stretch; uniaxial orientation.

ovalbumin and β-lactoglobulin, also show that the lattice spacings of these proteins are close to those of β-keratin.

Starting with an unstretched filament of denatured[5] protein which gives an x-ray pattern corresponding to random orientation of crystallites, there is a particular sequence in which the three strongest x-ray reflections are as stretching proceeds. This sequence is illustrated in figure 2. At low elongations, the innermost reflection (10 Å.) shows a concentration of intensity on the equator of the pattern, while the other reflections appear to have a uniform distribution of intensity. At higher elongations the 4.6 Å. reflection shows an intensity maximum on the equator, and the 3.7 Å. reflection shows four intensity maxima at about 45°. This phenomenon must be related to the shape of the crystallites or ordered regions which are being oriented by the stretching of the fibers.

A model which seems to account well for the observed phenomena may be described as follows: We may consider the crystallites to be plates of dimensions x, y, and z, where $x > y >> z$. The polypeptide chains are assumed to be parallel to x; the 10 Å. spacing is approximately along z; the 4.6 Å. spacing, approximately along y; and the 3.7 Å. spacing, a diagonal spacing perpendicular to the direction z. In unstretched filaments the platelets have random orientation

(figure 3a).   Upon application of stress the first tendency will be for the plane
xy to orient in the direction of stress, that is, the fiber axis, but with no preferen-
tial orientation of *x* or *y* of the various platelets (figure 3b).   Orientation of the
planes *xy* in the direction of stress requires the lattice planes with the 10 Å.
spacing to be parallel to the fiber axis and hence to reflect on the equator.   Since
the planes *xy* have random orientations around a perpendicular to the fiber axis,
the lattice planes of spacing 4.6 Å. and 3.7 Å. will reflect with uniform intensity
through 360° on the x-ray photograph.   Upon further stretching (figure 3c), the
longest axis *x* of the platelets will turn toward the direction of stress, orienting
the 4.6 Å. planes parallel to the fiber axis, and causing the corresponding reflection
on the x-ray photograph to be arced on the equator.   Similarly, the diagonal
planes of 3.7 Å. spacing will give four intensity maxima at approximately 45°.
    According to the structural scheme proposed by Astbury and Woods (5), the
10 and 4.6 Å. spacings are lateral spacings of the polypeptide chains and are ap-
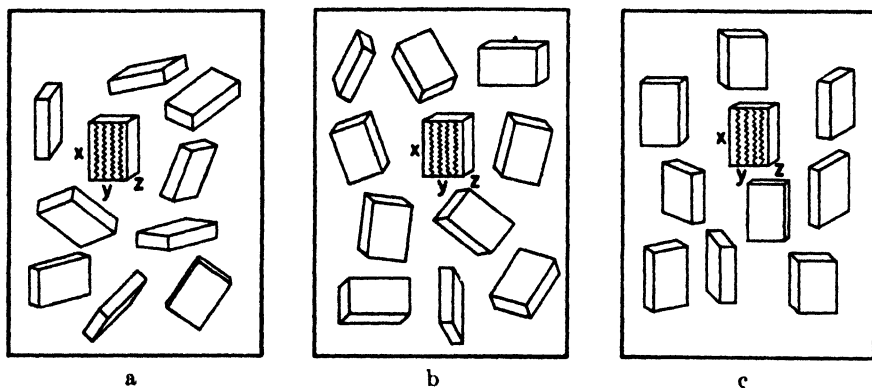
Fig. 3. Orientation of crystallites during stretching: (a) initial random orientation; (b)
uniplanar orientation; (c) uniaxial orientation.

proximately at right angles to each other.   From changes observed on swelling,
Astbury and Lomax (3) concluded that the 10 Å. spacings are in the direction of
the side chains, while the 4.6 Å. spacing represents the separation of the chains in
the plane of the zigzag of the main chain, as illustrated in figure 4.
    From the orientation sequence, then, the crystallites must be much longer in
the direction of the backbone spacing than in the direction of the side-chain
spacing.   This conclusion is supported by the breadth of the corresponding
reflections, the 10 Å. reflection being much broader than the 4.6 Å. reflection.
Assuming equal lattice perfection in the two directions, this indicates that the
crystallite is much smaller in the 10 Å. or *z* direction.   Additional evidence is
supplied by specimens which have been rolled to give biaxial orientation of the
crystallites.   X-ray patterns of such specimens taken with the beam parallel and
at right angles to the plane of rolling are shown in figure 5.
    It is seen that the crystallites orient so that the planes with the 10 Å. spacing
are parallel to the plane of rolling, that is, the *z* direction of the crystallites is per-
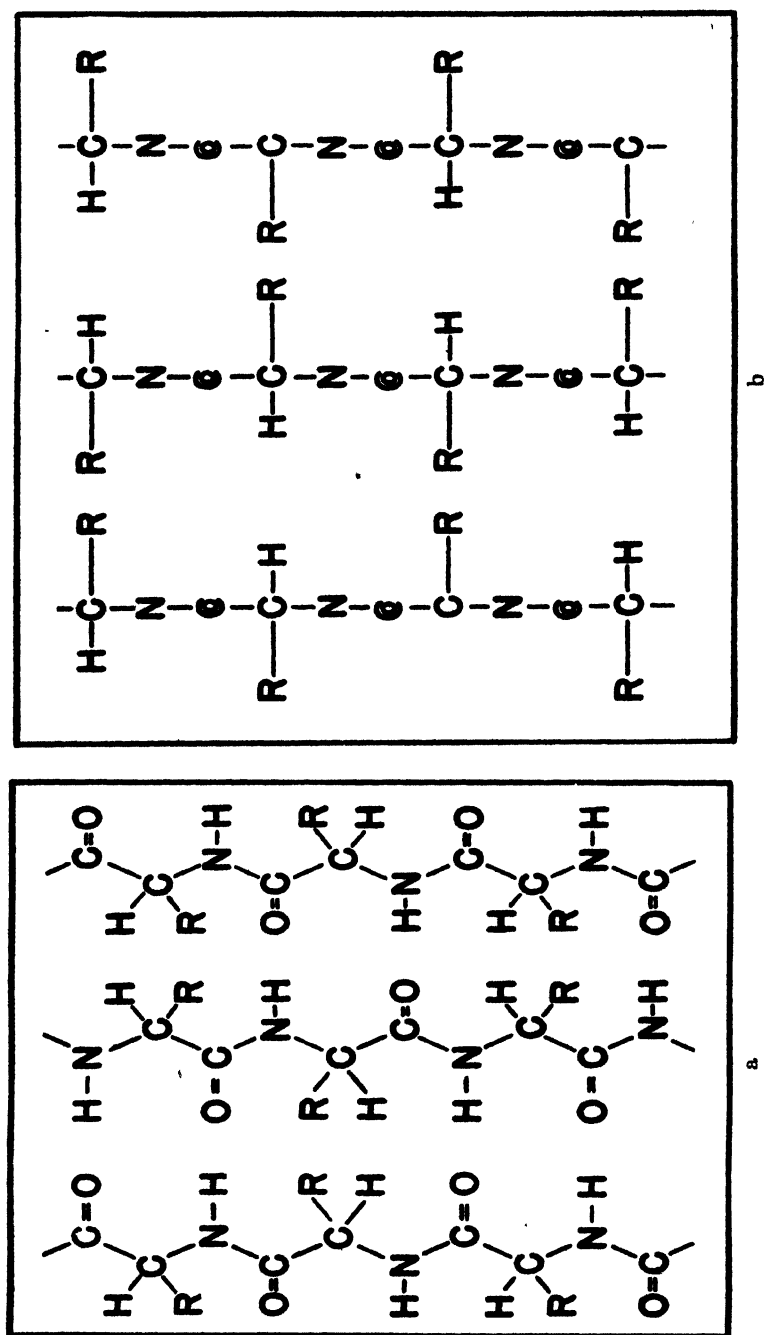
FIG. 4. Packing of extended peptide chains in the direction of (a) the 4.6 Å. "backbone" spacing, and (b) the 10 Å. "side-chain" spacing. Hydrogen atoms attached to nitrogen atoms are not shown.

pendicular to the plane of rolling, while the x and y directions lie in this plane. This, again, is consistent with the relative lengths $x > y >> z$. The crystallites thus have a pronounced tendency to grow in the direction in which the polypeptide chains are bonded laterally by hydrogen bridges between $\diagdown\mathrm{C}{=}\mathrm{O}$ and $\diagdown\mathrm{N{-}H}$ groups of adjacent chains. The regular occurrence of these groups along the chain gives opportunity for regular packing of chains in the direction of the hydrogen bridges. On the other hand, the packing in the direction of the side chains will be influenced by the variable length and nature of the side chain
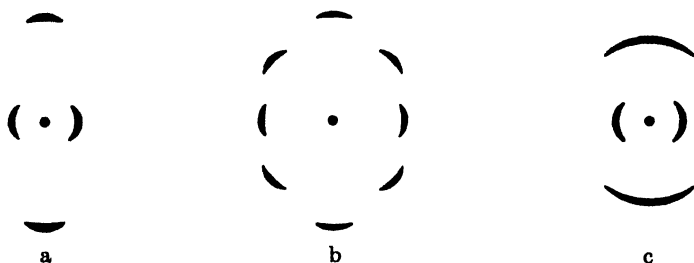
FIG. 5. Diffraction patterns of biaxially oriented ovalbumin. (a) X-ray beam perpendicular to the fiber axis, parallel to the plane of rolling; (b) beam perpendicular to both fiber axis and plane of rolling; (c) beam parallel to fiber axis. Plane of rolling is vertical.
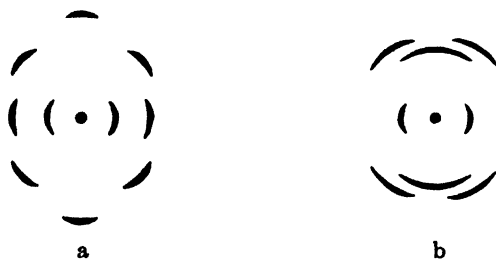
FIG. 6. The two types of fiber pattern exhibited by oriented globular proteins: (a) the "β-keratin" patterns; (b) the "egg-white" pattern.

from the different amino acid residues, and consequently the order will be much less perfect and will extend a shorter distance. The 3.3 Å. "fiber repeat" reflection is normally weak. It becomes prominent only in rather well-oriented specimens, even though the repeating units lie in the direction of the longest dimension of the crystallites.

The tendency of the crystallites to grow in the y direction may explain another type of diffraction pattern frequently observed in drawn protein filaments. This pattern, illustrated in figure 6, was first observed by Astbury, Dickinson, and Bailey (2) in stretched films of poached egg white. The distinguishing feature of this pattern is that the 4.6 Å. reflection is arced on the meridian rather than on the equator, the interplanar spacings of the three principal reflections being the same as in the β-keratin type. Astbury, Dickinson, and Bailey (2)

report a faint reflection of 3.3 Å. spacing on the equator, corresponding to the repeat distance along the polypeptide chain, but we have never observed this although we have examined dozens of photographs showing this egg-white pattern. The simplest explanation of this photograph is that the crystallites have developed such that $y > x > z$. Hence, upon stretching, y will orient along the fiber axis, causing the 4.6 Å. reflections to fall on the meridian, while the 10 Å. reflection occurs on the equator as before.

This pattern has been obtained from ovalbumin, casein, zein, peanut protein, hemoglobin, and edestin. It usually occurs if a fiber is given relatively low extension after a relatively short period of heat-conditioning. For example, it appears when ovalbumin filaments are immersed in boiling water for 2 to 5 min. and are then stretched 50 to 85 per cent. At greater elongations this pattern is transformed to the β-keratin pattern. The reverse transformation of the β-keratin pattern into the egg-white pattern has never been observed. Although many oriented protein filaments have been contracted in hot water or steam to give disoriented β-keratin, an intermediate form giving the egg-white pattern has not occurred.

<div align="center">BIREFRINGENCE</div>

X-ray diffraction provides the best method of gaining information about the orientation and packing of the molecules in the crystalline regions of a fiber, but it gives little direct information concerning the alignment of chains in the less-ordered regions. Optical and swelling anisotropy do, however, provide a rough measure of orientation of intercrystallite chains.

The refractive index of a substance for plane polarized light depends on the polarizability of the atomic groups in the direction of the plane of the electric vector. When a high polymeric substance is stretched, there is an alignment of molecular groups which usually results in greater polarizability along the direction of stretch than at right angles to it, with a consequent difference in refractive index in these two directions. Birefringence has the advantage that it can detect orientation in substances which do not produce any easily observable x-ray diffraction effect and are thus seemingly amorphous. On the other hand, calculations by Treloar (30) indicate that the birefringence is insensitive to small departures from perfect orientation of crystallites along a given direction.

A comparative study of birefringence and diffraction effects has been made on ovalbumin fibers heat-denatured and stretched in steam. Birefringence was computed from the retardation and the diameter of the fibers. The retardation was measured by means of an uncalibrated quartz wedge. Birefringence changes with draw ratio, as shown in figure 7. At D. R. = 2, diffraction patterns of the same fibers show marked arcing of the 10 Å. reflection, but only very slight arcing of the 4.6 Å. reflection. This corresponds to approximately uniplanar orientation of crystallites, as suggested above, and judging from the x-ray pattern alone the filaments should be optically nearly isotropic. The birefringence is 6×10^{-3}, however, suggesting that there is preferred orientation of polypeptide chains in the direction of stretch. Treloar (30) predicts that in this region of low

orientation the birefringence will change most rapidly.   Part of the birefringence may be contributed by preferentially oriented intercrystallite chains that do not appreciably affect the diffraction pattern.   This would be analogous to the behavior of polymerized methyl methylacrylate when stretched.   The polymer molecules are evidently linear, but it is difficult or impossible to pack them into regular arrays in space.   Although when stretched the material becomes birefringent, the diffraction pattern shows very little asymmetry (15, 23).   Similarly, a number of samples of casein textile fiber prepared in this laboratory by precipitation from an alkaline dispersion, followed by stretching and formaldehyde hardening, had birefringence ranging from 1 to 10 $\times$ 10^{-3} without any indication of arcing on the diffraction patterns.
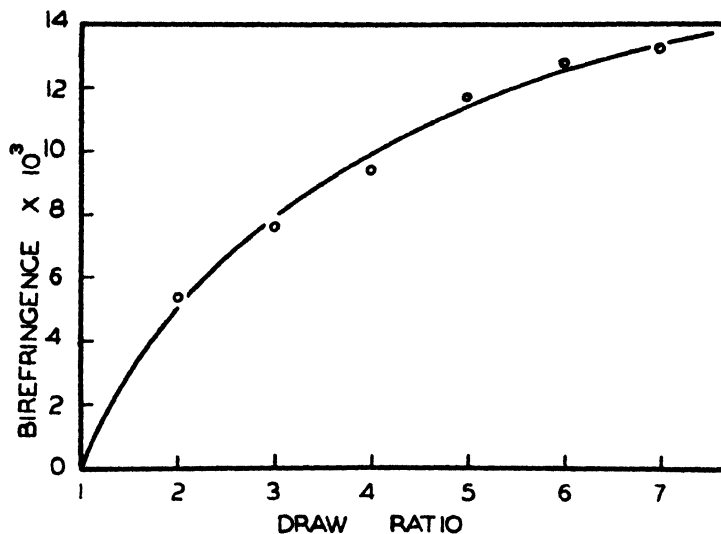
Fig. 7. Change of birefringence of ovalbumin with draw ratio

With increasing stretch, the birefringence of ovalbulin increases, while the arcs on the x-ray pattern decrease in angular width and increase in intensity.   At D. R. = 7 the birefringence is 14 $\times$ 10^{-3}, and the slope of the curve of figure 7 indicates that it has not yet attained its maximum value.

It might be supposed that protein preparations giving the egg-white type of fiber pattern would be negative-birefringent.   The refractive index is greatest along the direction of the extended peptide chains, and this direction in the crystallites from which the fiber pattern arises is perpendicular to the fiber axis.   Actually the birefringence of all the several specimens examined was positive, and of the order of 10^{-3}.   The following may be offered in explanation of this anomaly: By simple visual comparison of the intensity of arcs and rings, it is clear that the proportion of crystalline matter is not high.   Furthermore, the diffraction pattern obtained with the beam parallel to the fiber axis has full rings of comparable intensity at 4.6 and 10 Å.   In the diffraction pattern of the crystallites alone, the 4.6 Å. ring would be missing.   Consequently, the negative birefringence con-

tributed to the total birefringence by the crystallites is small and is apparently overweighed by the positive contribution of the non-crystalline chains oriented parallel to the fiber axis.

High optical anisotropy without corresponding x-ray effects has also been found in fibers drawn from surface films. At a water–air interface, soluble globular proteins in general unfold to form a monolayer. This, on compression between parallel barriers, is anisotropic, and from it filaments may usually be drawn (17). Accepting the view of Langmuir (16) that protein monolayers are composed principally of long polypeptide chains, it might be expected that filaments pulled from such monolayers would contain the chains in a linearly extended parallel array. We have prepared fibers suitable for examination from monolayers of casein and ovalbumin spread on a 0.003 M citric acid–phosphate buffer at pH 4.7. At a pressure of approximately 25 dynes per centimeter, fibers were formed by slowly withdrawing a 0.5-mm. platinum wire from the film-covered surface. When maintained taut until air dry, many of the fibers had high positive birefringence, a maximum value of 7 $\times$ 10^{-2} being recorded. A bundle of fine ovalbumin fibers having a rather uniform birefringence of about 2 $\times$ 10^{-2} was examined in a micro-diffraction camera. The diffraction pattern consisted of full rings, with no suggestion of arcing. The combined evidence of birefringence and x-ray diffraction would seem to indicate that in the fibers there is a high degree of preferred orientation of chain molecules which are imperfectly packed. Because of the extreme smallness of the fibers, no attempt was made either to improve the spatial order by an annealing process or to measure the tensile strength.

SWELLING MEASUREMENTS

A stretched protein fiber dried under tension generally contracts in length when immersed in water, and contracts further upon drying. If the fiber is again immersed in water, both length and diameter increase. The contraction in length and the increase in diameter upon the first immersion in water diminish as the stretch given the fiber increases. For example at D. R. = 2 an unhardened ovalbumin fiber contracted 14 per cent in length and increased 33 per cent in diameter, while at D. R. = 8 the corresponding values were 3 per cent and 19 per cent.[8] Similarly, the reversible dimensional changes in a completely relaxed fiber decrease with elongation. At D. R. = 2 a relaxed fiber on wetting swelled 12 per cent in length and 20 per cent in diameter, while at D. R. = 8 the values were 4 and 13 per cent.

The fiber thus appears to be stabilized toward water by stretching. If stretching affected only the orientation of existing crystallites, we should expect that lateral swelling would increase and longitudinal swelling decrease. Instead, both longitudinal and lateral swelling decrease. This suggests that the molecular packing is improved by stretching, that is, crystalline areas are produced.

Swelling anisotropy is defined as the ratio of the increase in diameter to the increase in length of a fiber on immersion in a swelling liquid. For the ovalbumin

---

[8] These values refer to the wet fibers; on drying, further dimensional changes occur.

fibers of D. R. = 8 mentioned above, its value is slightly greater than 3. For cotton, wool, and silk, the value is about 10, whereas for regenerated cellulose it is about 6 to 8 (31).

TENSILE STRENGTH

As expected, tensile strength is increased upon conversion of globular proteins to the oriented fibrous form. Tensile measurements have been made for the most part on coarse filaments, approximately 150–300 microns in diameter. Single-filament breaking loads were measured on a Scott Type I-P-2 inclined-plane testing machine. Specimens were kept in the testing room at 70°F. and 65 per cent relative humidity at least 16 hr. before breaking. Initial diameters were used in the computations. Strengths reported are in general the average strength of ten or more fibers.

Air-dried extruded filaments of all the proteins were so weak and brittle that tensile measurements were impracticable, but after the heat treatment the strength[9] was 4.5 to 6.7 kg. per mm.^{2} Upon orientation, strengths were raised to the following values: casein, 18.6 kg. per mm.^{2}; pumpkin-seed globulin, 16.2; hemoglobin, 11.6; lactoglobulin, 12.8; zein, 17.6; ovalbumin, 20.9. Individual filament strengths as high as 30 and 34 kg. per mm.^{2} have been measured on specimens of casein and ovalbumin, respectively. All the oriented preparations gave β-keratin-like fiber patterns. It seems clear, however, that by no means all the protein even in our best specimens is in the form of oriented crystallites, although we know of no experiment by which the proportions of crystalline and non-crystalline material may be precisely judged.

On immersion in water, dimensional changes and changes in birefringence suggest that part of the protein in stretched filaments is unfolded and oriented but is not crystallized, and thus seems amorphous to x-rays. We are unable to estimate the proportion of molecules which have substantially the same configuration as in the original protein.

If the protein chain is 1000 Å. or so long when fully extended, two or more portions of the chain could pack in orderly arrays with matching segments of other protein molecules to form crystallites of a not improbable size—let us say 100–200 Å. Intercrystallite regions, although composed from the same chains forming the crystallites, may be incapable of forming a regular network in space. This may be caused by chain flexibility, variable chain length between crystallites, or other factors. On application of tensile stress to the system, the composite of crystallites and non-crystalline connecting matter tends to align itself parallel to the tension direction. Intercrystallite chains trend in the same direction. The chains are thus oriented, and in such a way as to increase the tensile strength of the whole structure, but there is no corresponding diffraction effect of discernible magnitude.

Protein filaments, crystallized and oriented by heat and stretching, contract

---

[9] Assuming the density of the protein filaments to be 1.29, the relationship between the common tensile strength units is as follows: 1 gram per denier = 11.6 kg. per mm.^{2} = 16,500 lb. per in.^{2}.

considerably in water. This property has been studied in some detail on ovalbumin, because high orientation can be produced more readily in it than in any other protein available in quantity with which we have worked. The crystallites in a highly oriented ovalbumin filament are rather stable structures, since the β-keratin diffraction pattern persisted even after the filament was boiled for 8 hr. in distilled water. During boiling, the crystallites are disoriented to a significant extent, as is evidenced by an increase in the angular width of the diffraction spots. The radial dimension and the sharpness of the spots are practically unchanged, however, indicating that the size of the crystallites and the perfection of atomic arrangement within them are largely unaltered.

On the other hand, oriented intercrystallite chains, being imperfectly packed, are readily penetrated by swelling agents such as water and forced apart, causing the specimen as a whole to contract unless it is clamped so that contraction is impossible. A fixing treatment, designed to minimize swelling by cross-linking chains or diminishing their hydrophilic character, should heighten the dimensional stability of the oriented fiber and increase its strength after swelling. Accordingly, oriented ovalbumin filaments were treated with acetic anhydride, with formaldehyde, and with benzoquinone.

In the acetylation experiments, filaments stretched in steam to the draw ratio 10.5 were heated with acetic anhydride at 100°C. for 1 hr. Residual acetic anhydride and acetic acid were removed by acetone in a Soxhlet extraction. To harden with formaldehyde, filaments with a draw ratio of 6.0 were soaked, while clamped, for 16 hr. at 25°C. in a solution containing 5 per cent formaldehyde and 30 per cent sodium acetate at pH 5.8. The filaments were washed thoroughly with water and dried for 1 hr. at 40°C. To harden with quinone, filaments with a draw ratio of 10.5 were soaked, while clamped for 40 hr. at 25°C. in a 1 per cent benzoquinone solution at pH 4.7 maintained by a 0.05 M acetic acid–acetate buffer. The hardened filaments were washed with water and dried at 40°C.

Tensile and retraction data on the treated and untreated oriented filaments are assembled in table 2. It is apparent that all three treatments markedly diminish dimensional change and reduction in strength on soaking in water, although the effect of formaldehyde is destroyed rather rapidly at 100°C. The fiber diagrams of acetylated and quinone-hardened filaments changed remarkably little, even on boiling for 4 or 8 hr. There is a small increase in the length of the arcs, corresponding to a slight disorientation of the crystallites, but otherwise the pattern is not altered. After corresponding treatment of formaldehyde-hardened oriented ovalbumin, the diffraction pattern was much like that of the unhardened protein. The principal reflections of the β-keratin structure were present, and the width and sharpness of the spots were about the same as they were initially, but the length was increased several fold.

Wet and dry strengths have been determined for a series of oriented coarse filaments. Before testing, the filaments were relaxed in water at 25°C. for 6 hr., dried at 40°C. for 1 hr., and stored at 70°F. and 65 per cent relative humidity for 16 hr. In addition, filaments used for wet-strength determinations were soaked in distilled water at 70°F. for at least 30 min. immediately before the tests were made. Table 3 gives the results of the tests. The data show that, while

TABLE 2

Effect of hardening by acetylation, formaldehyde, or quinone on the tensile strength and retraction in water of oriented ovalbumin filaments

(Measurements made on air-dry material)

Acetylation-hardened filaments soaked in water at 100°C.

	RETRACTION IN WATER, PER CENT				TENSILE STRENGTH, KG. PER MM.²				
	1 hr.	2 hr.	4 hr.	8 hr.	0	1 hr.	2 hr.	4 hr.	8 hr.
Hardened....	10	11	12	16	21	14	13	12	9
Untreated..........	29	31	31	33					

Formaldehyde-hardened filaments soaked in water at 25°C.

	RETRACTION IN WATER, PER CENT			TENSILE STRENGTH, KG. PER MM.²			
	10 min.	1 hr.	24 hr.	0	10 min.	1 hr.	24 hr.
Hardened	5	6	6	16	16	15	16
Untreated.....	13	13	16	14	13	12	12

Formaldehyde-hardened filaments soaked in water at 100°C.

	RETRACTION IN WATER, PER CENT					TENSILE STRENGTH, KG. PER MM.²					
	10 min.	30 min.	2 hr.	4 hr.	8 hr.	0	10 min.	30 min.	2 hr.	4 hr.	8 hr.
Hardened	16	29	34	40	40	16	14	9	9	8	7
Untreated.....	36	39	40	44	46	14	7	7	7	7	7

Quinone-hardened filaments soaked in water at 25°C.

RETRACTION IN WATER, PER CENT			TENSILE STRENGTH, KG. PER MM.²			
10 min.	1 hr.	24 hr.	0	10 min.	1 hr.	24 hr.
0	0	2	16	19	17	19

Quinone-hardened filaments soaked in water at 100°C.

RETRACTION IN WATER, PER CENT				TENSILE STRENGTH, KG. PER MM.²				
10 min.	30 min.	2 hr.	4 hr.	0	10 min.	30 min.	2 hr.	4 hr.
5	5	7	9	16	16	15	16	13

TABLE 3

Tensile strength of relaxed oriented ovalbumin filaments

TREATMENT	DRY	WET	RATIO OF WET TO DRY STRENGTHS
	kg. per mm.²	*kg. per mm ²*	
Untreated........	18.9	10.4	0.55
Acetylation-hardened........	17.2	10.3	0.60
Formaldehyde-hardened.	16.5	15.2	0.92
Quinone-hardened..	17.8	14.9	0.84

the wet strength of oriented but unhardened filaments was only a little more than half the dry strength, the ratio for quinone- and formaldehyde-hardened filaments was increased to more than 0.8 and 0.9, respectively. On acetylation, the gain was slight.

SUMMARY

1. By means of heat, water, and mechanical shear, several globular proteins have been converted into a fibrous form giving an x-ray diffraction pattern nearly identical with that of β-keratin of stretched hair and wool. Among the proteins thus converted are lactoglobulin, ovalbumin, casein, zein, peanut protein, soybean protein, gliadin, hemoglobin, serum albumin, edestin, and tobacco-seed globulin. The process is most effective when applied to native, typically heat-denaturable proteins.

2. Under similar but milder conditions most of the proteins have given a second type of fiber pattern, characterized by the appearance of the 4.6 Å. "backbone" reflection on the meridian and the 10 Å. "side-chain" reflection on the equator.

3. When a protein is heated in the presence of water the diffraction pattern sharpens and new lines appear, indicating ordering of chains analogous to that occurring in the annealing of cellulose ester and polyamides.

4. Relative dimensions of the crystallites giving the fiber patterns are deduced from the sequence in which the x-ray reflections arc when a protein filament is stretched.

5. Comparative data on birefringence, x-ray diffraction, and swelling anisotropy as measures of molecular orientation are presented.

6. Tensile strength is increased by conversion of the globular protein to the oriented fibrous form. Wet strength after treatment with boiling water and dimensional stability of oriented ovalbumin filaments are improved by acetylation and hardening with formaldehyde or quinone.

REFERENCES

(1) ASTBURY: Advances in Enzymol. **3**, 63. Interscience Publishers, Inc., New York (1943).
(2) ASTBURY, DICKINSON, AND BAILEY: Biochem. J. **29**, 2351 (1935).
(3) ASTBURY AND LOMAX: J. Chem. Soc. **1935**, 846.
(4) ASTBURY AND STREET: Trans. Roy. Soc. (London) **A230**, 75 (1931).
(5) ASTBURY AND WOODS: Trans. Roy. Soc. (London) **A232**, 333 (1933).
(6) BAKER, FULLER, AND PAPE: J. Am. Chem. Soc. **64**, 776 (1942).
(7) BARKER: J. Gen. Physiol. **17**, 21 (1933).
(8) BOYES-WATSON AND PERUTZ: Nature **151**, 714 (1943).
(9) CAROTHERS AND HILL: J. Am. Chem. Soc. **54**, 1579 (1932).
(10) CAROTHERS AND VAN NATTA: J. Am. Chem. Soc. **55**, 4714 (1933).
(11) CHIBNALL: Proc. Roy. Soc. (London) **B131**, 136 (1942).
(12) COHN AND EDSALL: *Proteins, Amino Acids, and Peptides*, p. 333. Reinhold Publishing Corporation, New York (1943).
(13) FULLER, BAKER, AND PAPE: J. Am. Chem. Soc. **62**, 3275 (1940).
(14) HUGGINS: Chem. Rev. **32**, 195 (1943).

(15) Kolsky and Shearman: Proc. Phys. Soc. **55**, 383 (1943).
(16) Langmuir: Cold Spring Harbor Symposia Quant. Biol. **6**, 171 (1938).
(17) Langmuir and Schaefer: Chem. Rev. **24**, 181 (1939).
(18) Lundgren and O'Connell: Ind. Eng. Chem. **36**, 370 (1944).
(19) Mark: *Cellulose and Its Derivatives* (edited by Emil Ott), p. 1008. Interscience Publishers, Inc., New York (1943).
(20) Mark: *The Chemistry of Large Molecules*, p. 44. Interscience Publishers, Inc., New York (1943).
(21) Nutting, Senti, and Copley: Science **99**, 328 (1944).
(22) Palmer and Galvin: J. Am. Chem. Soc. **65**, 2187 (1943).
(23) Robinson, Ruggy, and Slantz: J. Applied Phys. **15**, 343 (1944).
(24) Roche and Adair: Biochem. J. **26**, 1811 (1932).
(25) Schmidt: *The Chemistry of the Amino Acids and Proteins*, 2nd Edition, Chapter 7. Charles C. Thomas, Springfield, Illinois (1944).
(26) Senti, Eddy, and Nutting: J. Am. Chem. Soc. **65**, 2473 (1943).
(27) Sookne and Harris: J. Research Natl. Bur. Standards **30**, 1 (1943).
(28) Svedberg and Hedenius: Biol. Bull. **66**, 191 (1934).
(29) Svedberg and Pedersen: *The Ultracentrifuge*. Oxford University Press, London (1944).
(30) Treloar: Trans. Faraday Soc. **37**, 84 (1941).
(31) Valco: *Cellulose and Cellulose Derivatives* (edited by Emil Ott), p. 412. Interscience Publishers, Inc., New York (1943).

POLYMERIZATION OF STYRENE UNDER VARIOUS EXPERIMENTAL CONDITIONS[1]

J. ABERE, G. GOLDFINGER, H. NAIDUS, and H. MARK

Queens College and Polytechnic Institute of Brooklyn, Brooklyn, New York

Various authors (compare particularly 1, 6, 7, 20, 24, 25, 26, 27, 30, 36, 37) have recently studied the rate of styrene polymerization with the aim of establishing the kinetics of this reaction by resolving it into its individual elementary steps, such as activation, propagation, termination, etc. In general, each of these investigations was undertaken in order to study the influence of one or two of the principal variables of the system under consideration, such as monomer concentration, catalyst concentration, temperature, nature of catalyst, type of solvent, etc. As a consequence of these measurements several mechanisms have been proposed for the peroxide-catalyzed styrene polymerization in bulk or homogeneous solution (1, 2, 6, 7, 10, 15, 18, 20, 24, 25, 26, 27, 30, 36, 37). The present article attempts to contribute to our knowledge of this reaction by presenting rate measurements in the course of which *all* quantities mentioned above have been varied systematically over a not too small range, using the same equipment and identical materials in all runs.

---

[1] Some results of this paper were presented in a lecture given at a meeting of the New York Academy of Sciences in New York City, January 8 and 9, 1943.

Materials

The solvents used were toluene, methanol, ethyl methyl ketone, and carbon tetrachloride. All were of C.P. grade, and with the exception of the carbon tetrachloride were used without further purification. The carbon tetrachloride was further purified by shaking in succession with alkaline alcohol, water, concentrated sulfuric acid, and again with water, after which it was dried over calcium chloride and distilled.

The monostyrene was the C. P. Monsanto grade. Distillation does not seem to remove the traces of inhibitors in this substance, but keeping it at −10°C. when not in use assured a more or less constant starting material. Frequent tests for the presence of oxygenated compounds and polymers were invariably negative.

Procedure

The molar compositions of the solutions studied were varied systematically from 0 to 40 mole per cent of monomer and 0 to 0.32 per cent of catalyst with respect to monomer. The solutions were prepared using microburets reading to ±0.01 ml. Solvent, monomer, and catalyst were added in that order to 20-ml. glass capsules, cooled, the ampoules sealed and then kept at −10°C.

To carry out an experiment the charged ampoules were transferred to a 60°C. ± 0.1° or a 100°C. ± 0.2° thermostat. After a measured interval of time they were plunged into an ice–salt–water bath. After a few moments the chilled contents were poured into a tared beaker containing an excess of methanol and a little hydroquinone. If any precipitate was formed and retained in the ampoule, this was rinsed into the beaker. When the polymer had coagulated and the supernatant liquid appeared completely clear, the latter was decanted. The remaining polymer was washed thrice with methanol, then dried for 3 to 5 hr. in a vacuum oven to constant weight, and stored for future use. The reproducibility of the weight obtained was about ±5 per cent.

For the determination of the intrinsic viscosity, samples of the polymer produced under various experimental conditions were dissolved in toluene and their viscosities measured at 25°C., using ordinary Ostwalt-type viscometers according to the methods described by Staudinger (31) and Kraemer and Lansing (14).

RESULTS AND DISCUSSION

Two quantities have been determined as functions of time of reaction: (a) the total amount of monomer polymerized, and (b) the viscosity average polymerization degree of the polymer. These measurements permit the representation of both quantities as functions of monomer and catalyst concentration (1). Figures 1, 2, and 3 show typical curves for the polymerization of styrene in toluene at 100°C. for 20 min., in carbon tetrachloride at 100°C. for 30 min., and in methanol at 60°C. for 3 hr.

Figure 1 represents five curves expressing the total amount of polymer in per

cent of initial monomer formed in toluene at 100°C. as a function of the initial monomer concentration at different catalyst concentrations after the system had polymerized for 20 min. It can be seen that the polymer formed at that time increases with monomer and catalyst concentration. Corresponding graphs were made for 10, 30, and 40 min., and the initial rate of polymerization was established as a function of the monomer and catalyst concentration (compare the discussion on pages 216 and 217).
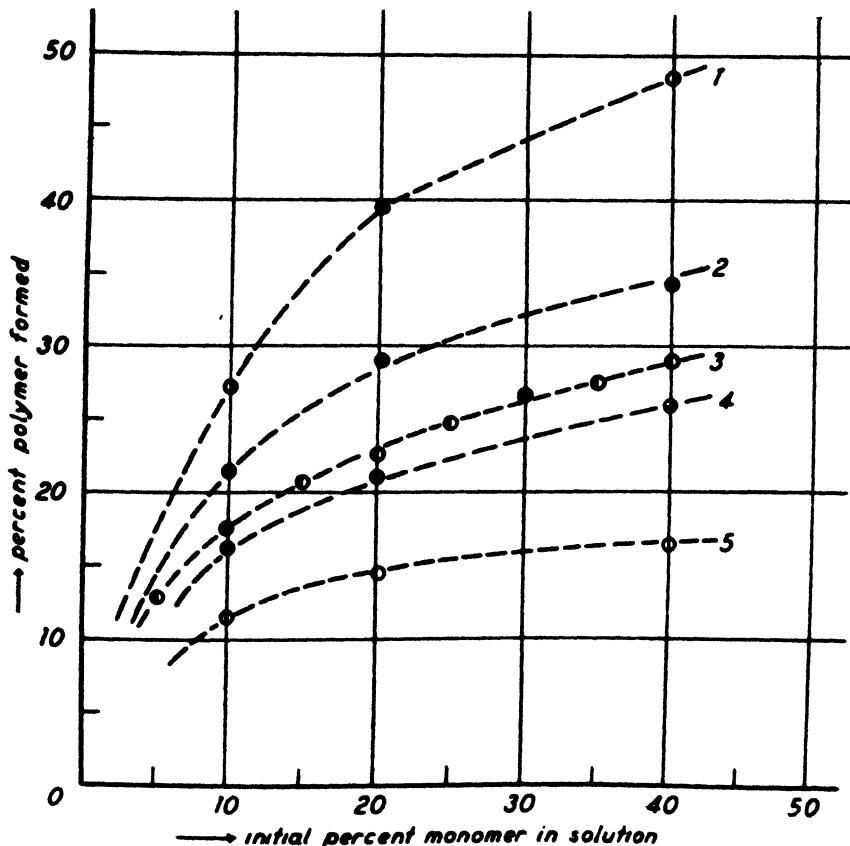
FIG. 1. Total amount of polymer (in per cent of initial monomer) formed after 20 min. in toluene at 100°C. plotted against initial monomer concentration. Curves 1 to 5 correspond to initial catalyst concentrations of 0.32, 0.16, 0.10, 0.08, and 0.04 per cent.

Figure 2 shows five corresponding curves for the polymerization of styrene in carbon tetrachloride at 100°C. after 30 min., with five different benzoyl peroxide concentrations. Again it can be seen that the polymer formed after this period increases continuously with both concentrations. This has already been observed by Price (23, 24, 25, 26), Schulz (28), and Suess *et al.* (36) in various solvents, and is nothing but a confirmation of their results. Again, curves

corresponding to those of figure 2 have been worked out for 10 and 30 min. and the initial rate of polymer formation established as a function of monomer and catalyst concentration (compare the discussion on pages 216 and 217).
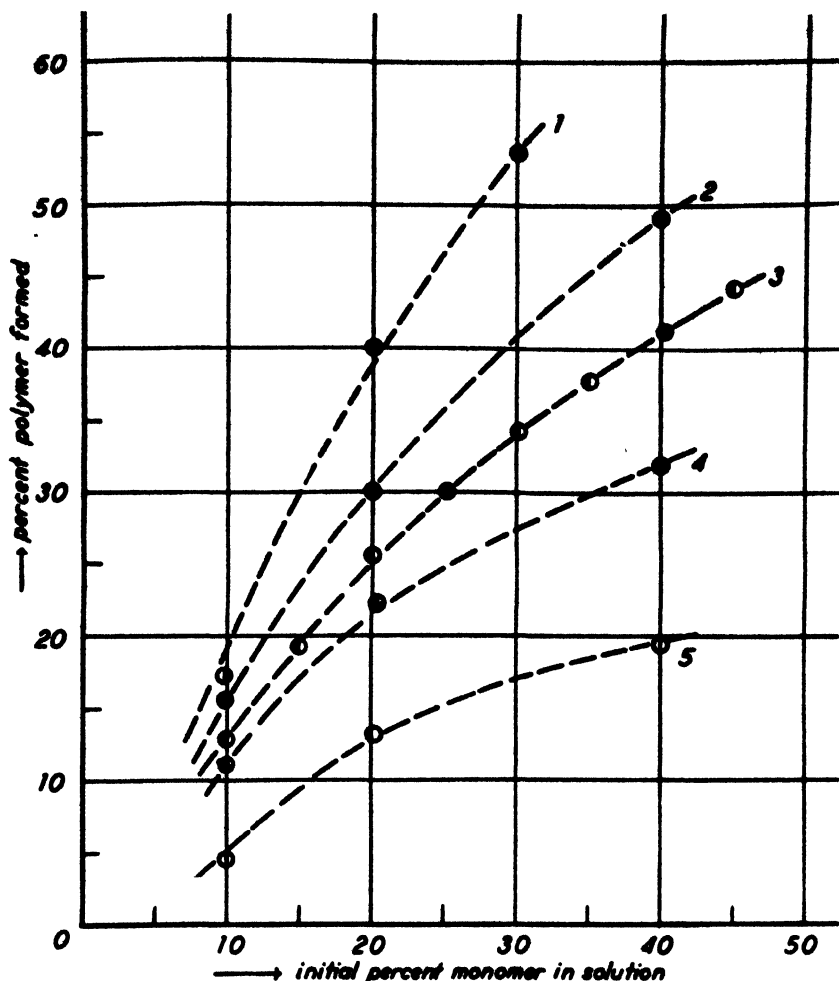
FIG. 2. Total amount of polymer (in per cent of initial monomer) formed after 30 min. in carbon tetrachloride at 100°C. plotted against initial monomer concentration. The five curves (1 to 5) correspond to catalyst concentrations of 0.32, 0.16, 0.10, 0.08, and 0.04 per cent.

Figure 3 represents five curves which give the corresponding results for the polymerization of styrene in methanol at 60°C. after a period of 3 hr. They show a significant difference from those in figures 1 and 2, inasmuch as the amount of polymer formed does not simply increase with monomer and catalyst concentration as it did in toluene and carbon tetrachloride. Presently it can be seen that in the range of relatively higher conversions (above 2.5 per cent polymer formed)

more polymer is formed after 3 hr. at 10 per cent initial monomer concentration than after the same time at 20 per cent. This is a startling anomaly, which called for further experimental investigation. Therefore, graphs corresponding to that of figure 3 were made for 2, 4, and 5 hr., and it was found without exception that in methanol at low monomer concentrations and relatively high conversions the rate of polymer formation is distinctly higher, as demonstrated in the rest of the diagrams and from the behavior in other solvents.

The explanation seems to be as follows: While toluene and carbon tetrachloride are solvents for *both* mono- *and* poly-styrene, methanol dissolves only mono-styrene and is a non-solvent for the polystyrene. If one starts a polymerization
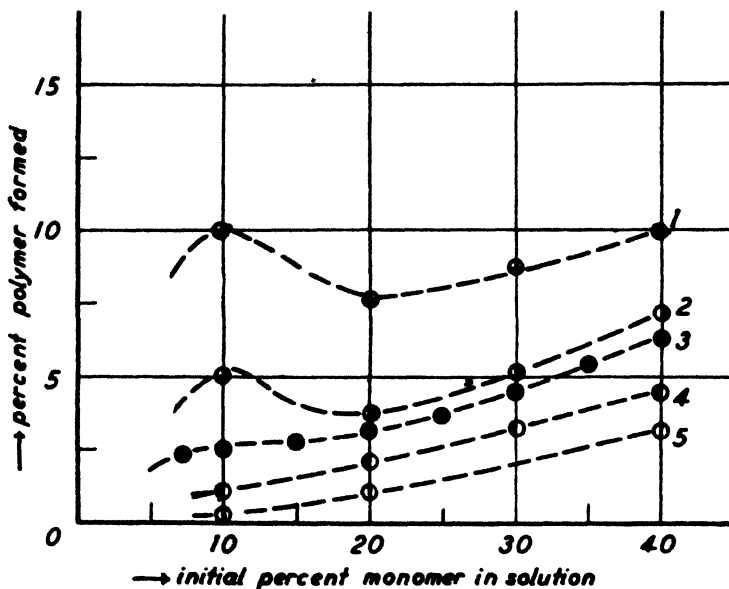
Fig. 3. Total amount of polymer (in per cent of initial monomer) formed after 3 hr. in methanol at 60°C. plotted against initial monomer concentration. The five curves (1 to 5) correspond to catalyst concentrations of 0.32, 0.16, 0.10, 0.08, and 0.04 per cent.

in methanol at low monostyrene concentrations (say 10 per cent monomer), the first amount of polystyrene formed (say the first 2 per cent) will remain dissolved in the system, because there is still enough monomer left to act as a very good solvent and keep the polymer in solution (see curves 4 and 5 in figure 3). However, as soon as more monomer is converted into polymer (curves 1, 2, and 3 in figure 3) at low initial monomer concentration, the polymer is no longer soluble and a gelatinous precipitate is formed. This is highly swollen in monomer, while the supernatant liquid is a solution of monomer in methanol. In fact, we have observed that in all cases in which the rate of polymerization was abnormally high, the solution contained a hazy, gelatinous precipitate. In the range of higher initial monomer concentration (right-hand side of all curves of figure 3) no precipitation was observed, because the mixture methanol–monomer is rich enough

in respect to the good solvent to keep the polymer in homogeneous solution. No rate anomalies were found in this concentration range.

Such an increased rate of polymer formation under certain conditions has already been observed by Norrish and his collaborators (21, 22) for the polymerization of methacrylic esters in various solvents. It seems that the curves of figure 3 represent the same phenomenon for styrene polymerization. If one adopts the usual aspect, that a polymerization reaction of this type is characterized by the interference of activation, propagation, and termination, one arrives at three possibilities for an increased overall rate of the reaction: (a) increased rate of activation; (b) increased rate of propagation; (c) decreased rate of termination.

The first possibility must be excluded because increase in rate of initiation, all other conditions being the same, would lead to decrease in the average molecular weight. Experimentally the opposite was found. Furthermore, we have shown that the energy of activation for the initiation reaction is essentially the same in all solvents. This is an indication of similarity in mechanism. The values obtained are:

$$E \doteq 24,000 \text{ cal. per mole in toluene}$$
$$E = 21,000 \text{ cal. per mole in carbon tetrachloride}$$
$$E = 23,000 \text{ cal. per mole in methanol}$$

It is not easy to see how the rate of *propagation* should be affected by the solvent in order to produce the above behavior and it appears, therefore, that the accelerated rate and increased molecular weight of the polymer formed in the gelatinous phase indicate a *slowing down of the termination* step. This may be due to the increased monomer concentration inside of the gelatinous phase, or to the decreased accessibility of the activated chain ends for any kind of terminating agent, such as solvent or impurities in the case that polymerization takes place in a polymer phase, which is swollen in a mixture of monomer and solvent.

It seems that the present experimental data are not yet sufficient to distinguish between these two effects. It may be that they both contribute.

The curves of figures 1, 2, and 3 and the corresponding data obtained at shorter times of polymerization allow the correlation of the initial rate of styrene polymerization with the concentrations of monomer and catalyst, respectively. The influence of monomer and of peroxide catalyst concentration has already been studied by Schulz (27 *et seq.*) and Price (23 *et seq.*), and our results confirm their findings. If one omits the cases in which gelation takes place during polymerization in methanol and plots the initial rate of monomer consumption *versus* monomer concentration, one obtains a curve which approximates a straight line over a certain range of monomer concentration. In a previous paper (1) an equation was derived for the influence of monomer concentration upon the initial rate which includes a number of different activation and termination processes. This is only valid as long as a stationary concentration of active centers exists. According to Ginell and Simha (10) such a stationary concentration is reasonably well maintained over a longer period of time if the rate constants of activation, propagation, and termination are in the proportion of 1 to

10^4–10^6 to 10^2–10^4. It seems that in the case of styrene polymerization under the conditions referred to in this paper, a steady state of active centers is reached after a few minutes and is maintained up to 25 or 30 per cent monomer conversion. In this range the initial rate of the peroxide-catalyzed reaction is given by (compare equation 18 on page 386 of reference 1):

$$-\frac{dm_1}{dt} \text{ (initial, catalyzed)} = k_1 m_1 c^* + \frac{k_{2o} m_1}{2k_3} [\sqrt{k_3^2 c^{*2} + 4k_1 k_3 m_1 c^*} - k_3 c^*] \quad (1)$$

where k_1 and k_3 = rate constants for activation and termination, respectively, and c^* = concentration (activity) of the catalyst.

At very low monomer concentrations the second term under the square root can be neglected as compared with the first. Expression 1 reduces to $k_1 m_1 c^*$ and the initial rate becomes proportional to monomer and catalyst concentration. At larger values of m_1, the first term under the square root can be neglected and one obtains

$$-\frac{dm_1}{dt} \text{ (initial, catalyzed)} = k_1 m_1 c^* + k_{2o} \sqrt{\frac{k_1}{k_3}} m_1^{3/2} c^{*1/2} \quad (2)$$

The first term represents the monomer consumption due to the conversion of inactive styrene molecules into activated nuclei, while the second accounts for the monomer molecules which are consumed during chain growth. If long chains are produced in the course of the reaction (polymerization degrees above 100), the first term will be negligible and the overall rate of the reaction becomes proportional to $m_1^{3/2}$. In fact, from figures 1, 2, and 3 it follows that the initial rate of monomer consumption increases with monomer concentration somewhat faster than proportionally (compare figure 2 on page 386 in reference 1). Experiments to investigate more thoroughly the influence of monomer concentration will be presented in another article.

Equation 2 also shows that the initial rate of monomer consumption should be proportional to the square root of the active catalyst concentration, as found previously by several authors and also as can be deduced from the results given in figures 1, 2, and 3 (compare figure 3 on page 386 in reference 1).

The next question was to investigate how the average degree of polymerization of the initially formed polymer depends upon the different variables, such as monomer and catalyst concentration, temperature, and nature of solvent, and to bring this dependence into correlation with the kinetics of the different elementary steps of the polymerization reaction.

It has recently been demonstrated (3, 4, 5, 9, 12, 13, 19, 32–35) that the viscosity of polymer solutions may be related to molecular weight by the following equation:

$$[\eta] = KM^a \quad (3)$$

For polystyrene formed at 60°C., $K = 1.22 \times 10^{-4}$ and $a = 0.70$; at 120°C. $K = 5.44 \times 10^{-5}$ and $a = 0.80$. We have evaluated the viscosity molecular weights of our samples by means of these two equations. It has to be kept in mind, however, that: (a) The experiments referred to in this article were carried

out at 60°C. and 100°C. in toluene and carbon tetrachloride, conditions which deviate somewhat from those in the previous paper (3). Nevertheless, we have used the constants given above because they seem to lead to the comparatively most reliable values for M and P in our case. Experiments for the direct determination of K and a for the exact conditions are under way and will be communicated in a later article. (b) The kinetic considerations lead to the *number average* polymerization degree, while intrinsic viscosity measurements evaluated by equation 3 give the *viscosity average* molecular weights. If a is 1, the viscosity average is equal to the weight average (14). The relation between weight and number average polymerization degree depends upon the shape of the chain-length distribution curve. Flory (8), Schulz (29), Ginell and Simha (10), Raff (17), and Herington and Robertson (11) have shown that the weight average molecular weight is just twice the number average, if the distribution curve is normal.

The shape of a normal differential weight distribution curve can be obtained by statistical considerations concerning the competition between propagation and termination and has the general shape:

$$W(x)\mathrm{d}x = (1 - p)^2 x p^{x-1}\mathrm{d}x \qquad (4)$$

where x is the degree of polymerization, $W(x)$ the weight fraction between x and $x + \mathrm{d}x$, and p a function of the ratio of the rate constants of propagation and termination (2, 10, 15, 18, 23).

In order to pass from the viscosity average, as determined by experiment with the aid of equation 3, to the number average, which is connected with the reaction mechanism, one has to know explicitly the general shape of the distribution curves of the polymers. It has already been found (16, 17, 29) that polystyrenes formed in a solution of toluene and the pure monomer exhibit distribution curves of the general types expressed in equation 4. We have carried out several fractionations of polymer produced in the undiluted monomer and toluene at various temperatures, using the technique described in a previous paper (3). The shape of these curves was in fair agreement with the shape predicted by the statistical considerations.

In order to convert viscosity average polymerization degrees into number average polymerization degrees $\bar{P}_N$, we first write equation 3 for $\bar{P}_V$ instead of M and get:

$$[\eta] = K'\bar{P}_V^a \qquad (5)$$

The constants in this equation for polystyrene prepared in the undiluted monomer are

$$\left.\begin{array}{l} [\eta] = 4.0 \times 10^{-3}\bar{P}_V^{0.70} \\ \bar{P}_V = 2.7 \times 10^3[\eta]^{1.43} \end{array}\right\} \cdots \cdots \text{ 60°C.}$$

$$\left.\begin{array}{l} [\eta] = 2.7 \times 10^{-3}\bar{P}_V^{0.80} \\ \bar{P}_V = 1.6 \times 10^3[\eta]^{1.25} \end{array}\right\} \cdots \cdots 120\text{°C.}$$

$$(6)$$

If one has a polymer with a distribution function (equation 4), the specific viscosity $d\eta_{sp}$ contributed by the species of chains having polymerization degrees between x and $x + dx$, will be given by

$$d\eta_{sp} = K'x^a dc \tag{7}$$

where K' and a are the constants of equation 5 and dc is the volume fraction of this species of long-chain molecules in the solution.[2] According to equation 4 dc is given by

$$dc = \frac{g}{100\rho} \cdot W(x)\, dx \tag{8}$$

where g is the number of grams of polymer with the density ρ dissolved in 100 cc. of solvent. Hence the viscosity contribution of the species under consideration is

$$d\eta_{sp} = \frac{K' \cdot g}{100\rho} (1 - p)^2 x^{1+a} p^{x-1} dx \tag{9}$$

and the contribution to the intrinsic viscosity becomes

$$d[\eta] = \frac{100\rho\, d\eta_{sp}}{g} = K'(1 - p)^2 x^{1+a} p^{x-1} dx \tag{10}$$

The intrinsic viscosity of the solution containing g grams of a polymer with the characteristic constants (equation 6) and the distribution curve (equation 4) in 100 cc. will therefore be expressed by

$$[\eta] = \int_0^\infty d[\eta] = K'(1 - p)^2 \int_0^\infty x^{1+a} p^{x-1} dx = \frac{K'(1 - p)^2 \Gamma(a + 2)}{p(-\ln p)^{a+2}} \tag{11}$$

In the range of real polymers (average degrees of polymerization around and above 50) p deviates only slightly from unity (its value is between 0.98 and unity) and $\ln p$ can be replaced by $(1 - p)/p$ without committing an appreciable error. With this approximation we get

$$[\eta] = \frac{K'\Gamma(a + 2)p^{1+a}}{(1 - p)^a} = K'\overline{P}_V^a \tag{12}$$

and the viscosity average polymerization degree becomes

$$\overline{P}_V = \frac{[\Gamma(a + 2)p^{1+a}]^{1/a}}{(1 - p)} \tag{13}$$

On the other hand, the number average polymerization degree of a polymer having the same distribution curve as given (16, 17) by

$$\overline{P}_N = \frac{1}{(1 - p)^2 \int_0^\infty p^{x-1} dx} = \frac{1}{1 - p} \tag{14}$$

[2] The values for K' and a as given in reference 28 hold for this choice of units. If one prefers to express the concentration of the polymer in grams per 100 cc. of solution, one has to use a correspondingly changed numerical value for K'.

From equations 13 and 14 follows

$$\bar{P}_N = \bar{P}_V \frac{1}{[\Gamma(a+2)p^{1+a}]^{1/a}} = \left[\frac{[\eta]}{K'\Gamma(a+2)p^{1+a}}\right]^{1/a} \qquad (15)$$

This equation was used to compute the number average polymerization degrees of our samples from the experimental $[\eta]$ values with the aid of the three parameters a, K', and p. The first two were taken from equation 6 for the samples polymerized at 60° and 100°C., respectively; p is very near to unity and was therefore approximated by 1.00. Using these numerical values and expressing
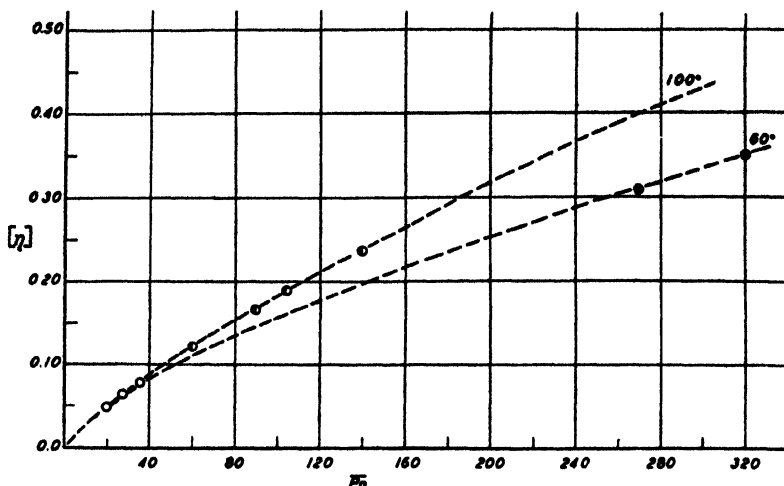
FIG. 4. Intrinsic viscosities of toluene solutions of polystyrenes prepared at 60° and 100°C. plotted against the number average polymerization degrees. The points on the two curves represent a few actual measurements. The open circles (O) correspond to a polymer formed at 100°C. in carbon tetrachloride, ◐ to a polymer prepared at 100°C. in toluene, and ◖ to a polymer formed in toluene at 60°C.

the intrinsic viscosities as specific viscosities divided by the concentration in grams of solute per 100 cc. of solution, one gets for the measurements carried out at 60°C.:

$$\bar{P}_N = 0.535 \, \bar{P}_V = 1450 \, [\eta]^{1.43} \qquad (16)$$

and for the measurements carried out at 100°C.:

$$\bar{P}_N = 0.532 \bar{P}_V = 850[\eta]^{1.25} \qquad (17)$$

Figure 4 shows the two curves corresponding to equations 16 and 17, with the aid of which the experimental $[\eta]$ values were converted in $\bar{P}_N$. On each curve are a few representative points, referring to actually measured values of $[\eta]$ for certain samples. The intrinsic viscosities were determined by measuring the specific viscosity at four or five different volume concentrations of the solute (between 0.1 and 0.5 per cent) and extrapolating the η_{sp}/c straight line to zero concentration.

Table 1 contains the number average polymerization degrees as computed from the intrinsic viscosities for the polymer formed in toluene at 100°C., and table 2 the corresponding values for 100°C. in carbon tetrachloride. It can be seen that the latter values are considerably smaller than the former, as already observed by Schulz (27, 30) and Suess and his collaborators (36).

TABLE 1

Initial number average polymerization degrees of the polymer formed in toluene at 100°C.

c	$m_1 = 10$ per cent	$m_1 = 20$ per cent	$m_1 = 40$ per cent
per cent			
0.04	45	75	140
0.08	40	60	105
0.16	30	40	85
0.32	20	30	50

TABLE 2

Initial number average polymerization degrees of the polymer formed in carbon tetrachloride at 100°C.

c	$m_1 = 10$ per cent	$m_1 = 20$ per cent	$m_1 = 40$ per cent
per cent			
0.04	33	36	38
0.08	20	26	32
0.16	16	22	29
0.32	12	18	25

In a previous article (compare equation (16) on page 385 of reference 1), the initial number average polymerization degree for a peroxide-catalyzed styrene polymer has been represented as

$$\bar{P}_n \text{ (initial, catalyzed)} = \frac{k_{3c} c^* + k_{2g} m_1}{k_{3c} c^* + k_{2t} m_1} \tag{18}$$

where m_1 = concentration of the monomer,

c^* = concentration of the active catalyst,

k_{2g} = rate constant of normal growth,

k_{2t} = rate constant of chain transfer, and

k_{3c} = rate constant of termination by collision of the growing chain with another growing chain or a catalyst radical.

In order to check the significance of this equation, which already involves certain simplifications (compare the discussion on pages 384, 385, and 386 of reference 1), it is appropriate to discuss the value of $1/\bar{P}_n$ rather than $\bar{P}_n$ itself as a function of the quantities involved:

$$1/\bar{P}_n = \frac{k_{3c} c^* + k_{2t} m_1}{k_{3c} c^* + k_{2g} m_1} \tag{19}$$

In a solvent which catalyzes chain transfer, such as carbon tetrachloride, at low catalyst concentrations, $k_{3c}c^*$ can be considered as small compared with both $k_{2t}m_1$ and $k_{2g}m_1$, and equation 19 reduces to

$$1/P_n = \frac{k_{2t}}{k_{2g}} \tag{20}$$

The number average degree of polymerization becomes independent of monomer concentration and is given by the ratio of the probability for chain propaga-
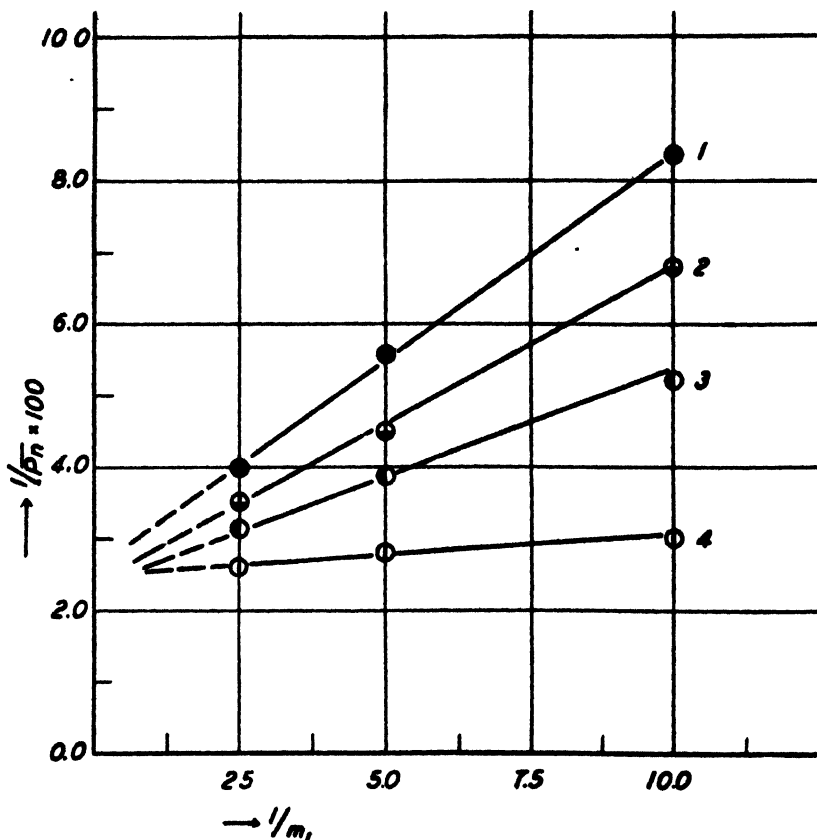
FIG. 5. Reciprocal number average polymerization degree plotted against reciprocal monomer concentration. The four curves (1 to 4) correspond to catalyst concentrations of 0.32, 0.16, 0.08, and 0.04 per cent. Runs are in carbon tetrachloride.

tion and chain transfer. In this case termination plays only a minor rôle; one produces short chains, but produces them at a high rate. Suess and his collaborators (compare the lowest curve in Figure 2 on page 369 of reference 36) have already found indications for this behavior, and Majo (18) has studied it more thoroughly recently. Curve 4 in figure 5 shows that these conditions are apparently approached (although not exactly fulfilled) during the runs at 100°C.

in carbon tetrachloride with 0.04 per cent catalyst concentration. The rate of propagation, k_{2g}, is about 45 times as great as the rate of chain transfer.

As the catalyst concentration increases, $k_{3c}c^*$ cannot be neglected any more in comparison with $k_{2g}m_1$, although it still can be neglected as compared with $k_{2g}m_1$. In this case equation 19 reduces to

$$1/\overline{P}_n = \frac{k_{2t}}{k_{2g}} + \frac{k_{3c}c^*}{k_{2g}m_1} \qquad (21)$$

Plotting $1/\overline{P}_n$ versus $1/m_1$, as represented in figure 5, one has to expect a straight line for each catalyst concentration. This is not exactly true in the figure, but it is not too badly fulfilled either. All interpolated straight lines converge at high monomer concentrations to a point in the neighborhood of $\overline{P}_n = 45$, as required by equations 20 and 21.

If, on the other hand, the solvent does not favor chain transfer (toluene, ethylbenzene, xylene), $k_{2t}m_1$ in equation 19 can be neglected as compared with $k_{3c}c^*$ and one obtains

$$1/\overline{P}_n = \frac{k_{3c}c^*}{k_{3c}c^* + k_{2g}m_1} \qquad (22)$$

If k_{2t} is very small (very unfavorable conditions for chain transfer), this will even be permissible at low catalyst concentrations (or high monomer concentrations), in which case $k_{3c}c^*$ is small as compared with $k_{2g}m_1$. Hence we obtain

$$1/\overline{P}_n = \frac{k_{3c}c^*}{k_{2g}m_1} \qquad (23)$$

which expresses the fact that under such conditions the initial number average polymerization degree is produced by competition of propagation k_{2g} and termination k_{3c}. Plotting again $1/\overline{P}_n$ versus $1/m_1$, one has to expect straight lines. Figure 6 shows a plot of our measurements at 100°C. in toluene at different monomer and catalyst concentrations. The curves seem to emerge from the origin as straight lines, the slope of which leads to an approximate ratio of around 5 for $k_{2g}/k_{3c}c^*$. Assuming

$$c^* \cong \frac{1}{20}\sqrt{c_K} \quad \text{to} \quad \frac{1}{50}\sqrt{c_K}$$

we see that the probability for propagation is about 100-250 times as great as for termination, which permits use of the steady state as derived by Ginell and Simha (10).

It can be clearly seen from figure 6 that the curves bend towards the abscissae as the monomer concentration decreases. This follows from equation 19 if one neglects $k_{2t}m_1$ in comparison with $k_{3c}c^*$, but not $k_{3c}c^*$ as compared with $k_{2g}m_1$. One obtains

$$1/\overline{P}_n = \frac{k_{3c}c^*}{k_{3c}c^* + k_{2g}m_1} \qquad (24)$$

which in the plot of figure 6 represents a curve of the type of a Langmuir adsorption isotherm.

We do not feel that the number of our observed points is great enough to draw further conclusions as to the exact numerical relationships between the three rate constants k_{2g}, k_{2t}, and k_{2c} at various temperatures, but it seems that the above discussion contributes at least semiquantitatively to the problem of how a solvent
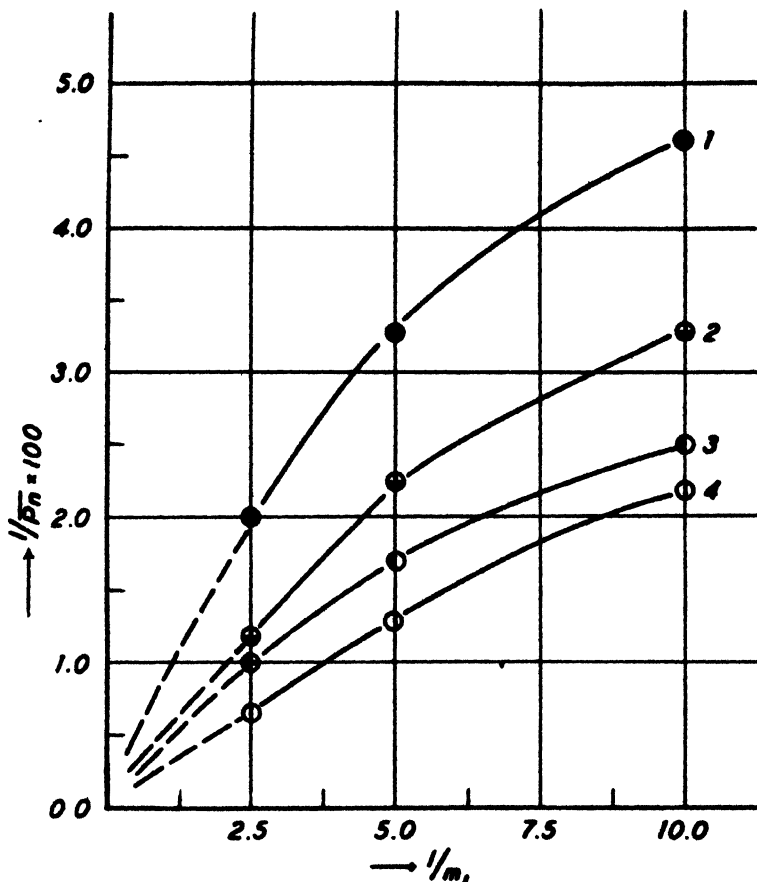
FIG. 6. Reciprocal number average polymerization degree plotted against reciprocal monomer concentration, for the polymerization in toluene at 100°C. The four curves (1 to 4) correspond to catalyst concentrations of 0.32, 0.16, 0.08, and 0.04 per cent.

can affect the degree up to which polymerization takes place by influencing the probability for chain transfer. It is intended to improve and expand the observations of this kind in a later article.

SUMMARY

1. Polymerization of styrene has been carried out in various solvents (particularly toluene, methanol, and carbon tetrachloride) with various amounts of ben-

zoyl peroxide as catalyst at 60° and 100°C. in various concentrations of the monomer.

2. It is found that the polymerization in methanol shows certain irregularities, which are presumably due to the formation of a gelatinous phase during polymerization.

3. The initial overall rate of the polymerization increases with monomer concentration somewhat faster than simple proportionality would require.

4. A method is indicated to show how intrinsic viscosities of the polystyrene samples obtained can be used to estimate the number average polymerization degree.

5. The initial number average polymerization degree can be expressed in terms of three rate constants: rate of propagation, termination, and chain transfer. The influence of the solvent on the last of these is discussed.

REFERENCES

(1) ABERE, J., GOLDFINGER, G., NAIDUS, II., AND MARK, II.: J. Chem. Phys. **11**, 379 (1943).
(2) ABERE, J., GOLDFINGER, G., NAIDUS, II., AND MARK, II.: "Mechanism of High Polymeric Reactions," paper presented at a meeting of the New York Academy of Sciences, January 8 and 9, 1943.
(3) ALFREY, T., BARTOVICS, A., AND MARK, H.: J. Am. Chem. Soc. **65**, 2319 (1943).
(4) BAKER, W. O., FULLER, C. S., AND HEISS, J. H.: J. Am. Chem. Soc. **63**, 3316 (1941).
(5) BARTOVICS, A., AND MARK, II.: J. Am. Chem. Soc. **65**, 1901 (1943).
(6) BREITENBACH, J. W., AND RUDORFER, H.: Monatsh. **70**, 37 (1937); **71**, 275 (1938).
(7) DOSTAL, H., MARK, H., AND RAFF, R.: Z. physik. Chem. **B29**, 299 (1935); **B32**, 117 (1936).
(8) FLORY, P. J.: J. Am. Chem. Soc. **58**, 1877 (1936).
(9) FLORY, P. J.: J. Am. Chem. Soc. **65**, 372 (1943).
(10) GINELL, R., AND SIMHA, R.: J. Am. Chem. Soc. **65**, 706–15 (1943).
(11) HERINGTON, E. F. G., AND ROBERTSON, A.: Trans. Faraday Soc. **38**, 490 (1942).
(12) KERN, W., AND FERNOW, H.· J. prakt. Chem. [2] **160**, 307 (1942).
(13) KERN, W., AND KAEMERER, H.: J. prakt. Chem. [2] **161**, 100 (1942).
(14) KRAEMER, E. O., AND LANSING, W. D.: J. Phys. Chem. **39**, 153 (1935).
(15) MAGEE, J. L., SHAND, W., AND EYRING, H.: J. Am. Chem. Soc. **63**, 677 (1941).
(16) MARK, H.: Paper Trade J. **113**, 34 (1941).
(17) MARK, H., AND RAFF, R.: *High Polymeric Reactions*, pp. 47–63, particularly figure 8 on page 54. Interscience Publishers, New York (1941).
(18) MAJO, R.: J. Am. Chem. Soc. **65**, 2324 (1943).
(19) MATTHES, A.: J. prakt. Chem. [2] **162**, 245 (1943).
(20) MOORE, J. K., BURK, R. E., AND LANKELMA, H. P.: J. Am. Chem. Soc. **63**, 2954 (1941).
(21) NORRISH, R. W. G.: Trans. Faraday Soc. **35**, 1087 (1939).
(22) NORRISH, R. W. G., AND SMITH, R. R.: Nature **150**, 336 (1942).
(23) PRICE, C. C.: "Mechanism of Vinyl Polymerization," paper presented at a meeting of the New York Academy of Sciences, January 8 and 9, 1943.
(24) PRICE, C. C., AND KELL, R. W.: J. Am. Chem. Soc. **63**, 2798 (1941).
(25) PRICE, C. C., KELL, R. W., AND KREBS, E.: J. Am. Chem. Soc. **64**, 1103 (1942).
(26) PRICE, C. C., AND MEISTER, M.: J. Am. Chem. Soc. **61**, 1595 (1939).
(27) SCHULZ, G. V.: Z. physik. Chem. **B30**, 379 (1935); **B32**, 27 (1936).
(28) SCHULZ, G. V.: Z. physik. Chem. **B39**, 246 (1938).
(29) SCHULZ, G. V.: Z. physik. Chem. **B30**, 379 (1935); **B44**, 227 (1939).
(30) SCHULZ, G. V., AND HUSEMANN, E.: Z. physik. Chem. **B34**, 187 (1936); **B36**, 184 (1937); **B39**, 246 (1938).

(31) STAUDINGER, H.: *Die hochmolekularen organischen Verbindungen.* J. Springer, Berlin (1932).

(32) STAUDINGER, H., AND JORDER, E.: J. prakt. Chem. [2] 160, 176 (1942).

(33) STAUDINGER, H., AND SCHNEIDER, H.: Ann. 541, 155 (1939).

(34) Reference 33, p. 161.

(35) STAUDINGER, H., AND WARTH, W.: J. prakt. Chem. [2] 155, 278 (1940).

(36) SUESS, H., PILCH, K., RUDORFER, H., AND SPRINGER, A.: Z. physik. Chem. A179, 361 (1937); A181, 81 (1937).

(37) WHITBY, G. S.: Trans. Faraday Soc. 32, 315 (1936).

STUDIES ON ADSORPTION IN RELATION TO CONSTITUTION. V

ADSORPTION OF ALCOHOLS, ESTERS, AND KETONES ON SILICA GEL[1]

B. P. GYANI AND P. B. GANGULY

Chemistry Department, Science College, Patna, India

INTRODUCTION

In the previous series of papers, attempts have been made to study adsorption in relation to the constitution of the molecule adsorbed (11, 12, 13, 14). It has been found that the adsorption of alkaloids, organic acids, carbohydrates, and hydrocarbons of both the aliphatic and the aromatic series is considerably dependent on the constitution of the molecule. Definite evidence for particular orientations of the adsorbed molecules has been obtained. The present paper deals with the adsorption of some more organic compounds in the vapor phase.

No systematic attempt has been made by previous authors to study the adsorption of members of different homologous series. Anderson (2) studied the adsorption of alcohol on silica gel. The isotherms obtained showed a hysteresis loop. The appearance of the loop might be due to the presence of residual air inside the gel, as Lambert and Clark (5), using carefully evacuated gel, obtained a series of smooth isotherms, no hysteresis effect being noted. Traube and St. Birutowitsch (29) measured the adsorption of some alcohols, esters, and ketones on both charcoal and silica gel. They considered the adsorbed layer to be monomolecular in nature. Others who have generally depended on the dynamic method for the measurement of such compounds on silica gel include Holmes and Weide (17), Patrick and Opdycke (23), Okatov (20), Jones and Outridge (19), von Putnoky and Szélenyi (26), and Schmidt and Hinteller (28).

In the present experiments, the adsorption of different homologues of alcohols esters, and ketones on silica gel has been measured. A static method of investigation has been used, in which the gel has been thoroughly degassed. The complications arising from the presence of residual gases are thus absent.

---

[1] Abridged from Doctoral Thesis of B. P. Gyani, Patna, 1944.

The apparatus employed is shown in figure 1. The amount of adsorption was determined by direct weighing of the gel. About 5 g. of the gel was weighed out in the bulb B, which was then sealed to the tap T_1 carrying the ground joint J at the other end. The stopper G served to connect or disconnect the reservoir L, containing the experimental liquid, with the rest of the apparatus. The pressure of the vapor inside the apparatus was recorded on the manometer M, which was
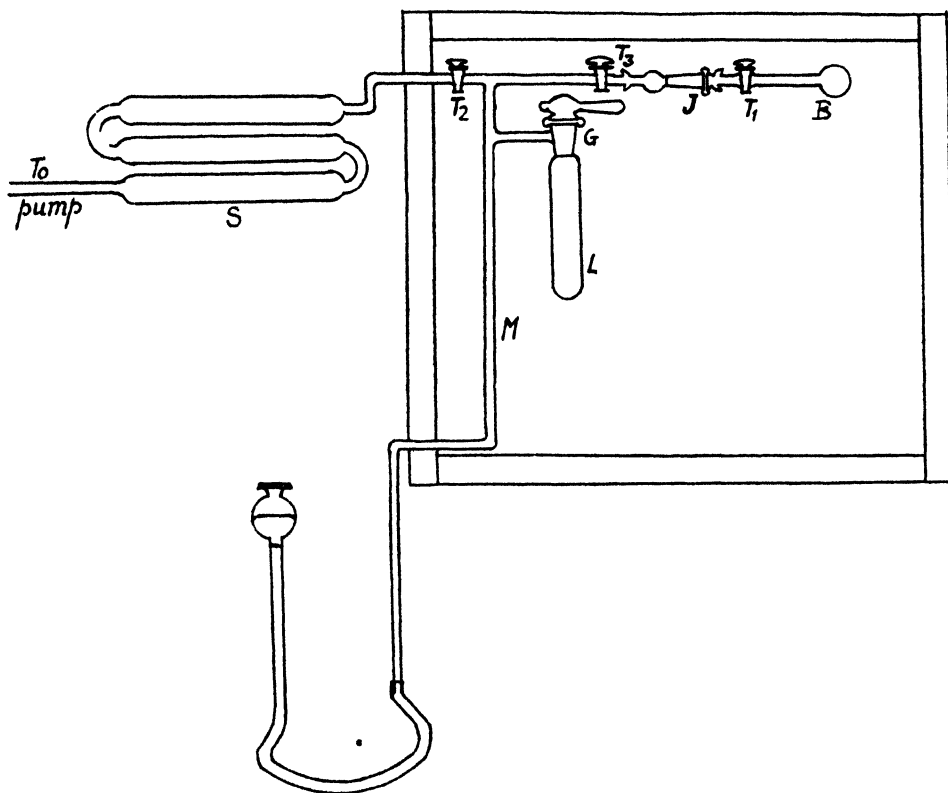
FIG. 1. The adsorption apparatus

read by means of a cathetometer. The whole apparatus, including part of the manometer, was enclosed inside an electrically regulated air thermostat. The measurements were thus extended nearly up to the vapor pressure of the liquid at the temperature of the thermostat.

The pump system consisted of a two-stage mercury diffusion pump backed by a Cenco-Hyvac oil pump. To protect the pumps from vapor a series of adsorbers (3) was used. Evacuation was started with the tap G closed and all the other taps open. The gel was simultaneously heated to about 250°C. When the gel had been completely degassed, taps T_1 and T_3 were closed. The liquid in the reservoir L was freed from air by repeated evacuation, till it recorded the vapor

pressure of the pure compound on attaining the temperature of the thermostat. To sweep out the last traces of impurities from the gel, it was allowed to attain the maximum adsorption at saturation pressure, and then degassed by continuous evacuation and heating. All the liquids employed in these measurements

TABLE 1

Adsorption of ethyl alcohol on silica gel

p	p/p_s	x/m	$\dfrac{p}{x/m}$	p	p/p_s	x/m	$\dfrac{p}{x/m}$
87.0	0.8683	78.85	1.1035	31.0	0.3144	40.59	0.7760
84.7	0.8454	77.18	1.0972	25.0	0.2495	37.29	0.6703
81.0 ·	0.8086	73.81	1.0971	18.5	0.1846	34.12	0.5421
68.5	0.6838	70.12	0.9774	13.0	0.1297	31.49	0.4129
62.9	0.6279	68.40	0.9197	10.0	0.0999	30.43	0.3286
57.0	0.5690	66.70	0.8545	7.0	0.0699	28.78	0.2432
52.0	0.5190	63.08	0.8246	4.3	0.0429	27.01	0.1592
48.0	0.4791	49.98	0.9603	3.0	0.0299	25.43	0.1180
44.0	0.4392	45.60	0.9650	1.5	0.0149	23.67	0.0633
37.0	0.3693	44.71	0.8276				

TABLE 2

Adsorption of methyl alcohol on silica gel

p	p/p_s	x/m	$\dfrac{p}{x/m}$	p	p/p_s	x/m	$\dfrac{p}{x/m}$
161.5	0.8075	111.62	1.4470	63.0	0.3150	54.70	1.1515
152.0	0.7600	107.93	1.4086	56.5	0.2875	52.05	1.0852
143.0	0.7150	104.72	1.3660	50.2	0.2510	49.60	1.0122
136.0	0.6800	102.58	1.3256	42.5	0.2125	46.84	0.9075
128.0	0.6400	99.72	1.2835	35.5	0.1775	45.04	0.7882
122.0	0.6100	93.98	1.2978	28.0	0.1400	42.20	0.6636
113.0	0.5650	84.10	1.3436	21.0	0.1050	39.91	0.5261
105.0	0.5254	77.83	1.3490	16.2	0.0810	37.35	0.4337
96.0	0.4800	74.20	1.2936	8.0	0.0400	31.97	0.2503
91.0	0.4550	69.64	1.3067	5.2	0.0260	29.74	0.1749
88.5	0.4425	68.90	1.2218	3.5	0.0175	27.38	0.1278
70.0	0.3500	58.42	1.1983	2.0	0.0100	25.72	0.0778

were of the purest available quality, and were freshly distilled before use. The data refer to a temperature of 35°C. ± 0.05° except where otherwise stated.

RESULTS

The experimental results are recorded in tables 1 to 14. The first column gives the equilibrium pressure, p, in millimeters of mercury. The second column gives the relative pressures p/p_s, where p_s = saturation pressure of the liquid at 35°C.

TABLE 3
Adsorption of methyl formate on silica gel (31°C.)

p	p/p_0	x/m	$\dfrac{p}{x/m}$	p	p/p_0	x/m	$\dfrac{p}{x/m}$
246.0	0.2911	47.87	5.1390	40.0	0.0474	25.97	1.5403
156.0	0.1846	39.20	3.9790	30.0	0.0355	24.70	1.2143
120.0	0.1420	38.56	3.1115	25.0	0.0295	23.83	1.0490
100.0	0.1184	33.40	2.9940	18.0	0.0213	22.22	0.8100
72.0	0.0853	29.87	2.4175	10.0	0.0118	20.10	0.4975
49.0	0.0579	27.11	1.8073	7.0	0.0083	18.13	0.3861

TABLE 4
Adsorption of methyl formate on silica gel (35°C.)

p	p/p_0	x/m	$\dfrac{p}{x/m}$	p	p/p_0	x/m	$\dfrac{p}{x/m}$
252.0	0.2982	44.13	5.7110	65.0	0.0769	28.07	2.3155
230.0	0.2721	42.20	5.4500	53.0	0.0627	26.70	1.9850
199.0	0.2355	39.47	5.0420	41.0	0.0485	25.40	1.6145
168.0	0.1988	36.83	4.5610	31.0	0.0444	23.73	1.3067
132.0	0.1563	34.12	3.8680	25.0	0.0367	22.39	1.2260
102.0	0.1207	31.55	3.2330	15.0	0.0296	20.13	0.7452
83.0	0.0982	29.90	2.7760	8.0	0.0093	17.93	0.4462
75.0	0.0888	29.03	2.5840				

TABLE 5
Adsorption of ethyl formate on silica gel

p	p/p_0	x/m	$\dfrac{p}{x/m}$	p	p/p_0	x/m	$\dfrac{p}{x/m}$
260.0	0.7328	52.03	4.9971	80.0	0.2204	32.85	2.4729
230.0	0.6334	51.27	4.4860	65.0	0.1790	29.85	2.1708
192.0	0.5288	49.00	3.9184	53.0	0.1460	28.16	1.8821
162.0	0.4462	47.11	3.4387	38.0	0.1047	25.92	1.4661
147.0	0.4053	42.73	3.4402	20.0	0.0551	21.99	0.9091
120.0	0.3306	37.99	3.1579	15.0	0.0413	20.97	0.7153
115.0	0.3167	35.82	3.2105	7.0	0.0193	19.86	0.3525

TABLE 6
Adsorption of methyl acetate on silica gel

p	p/p_0	x/m	$\dfrac{p}{x/m}$	p	p/p_0	x/m	$\dfrac{p}{x/m}$
174.0	0.5385	51.30	3.3890	54.0	0.1672	31.94	1.6900
141.0	0.4365	48.86	2.8860	45.0	0.1393	30.24	1.4880
137.0	0.4241	47.80	2.8650	30.0	0.0927	27.23	1.1020
124.0	0.3839	47.13	2.6310	25.0	0.0773	25.81	0.9685
120.0	0.3715	46.22	2.5960	10.0	0.0310	23.72	0.4217
112.0	0.3467	43.59	2.5690	8.9	0.0275	21.22	0.4195
96.0	0.2973	39.53	2.4290	5.0	0.0152	17.58	0.2845
70.0	0.2167	34.80	2.0110				

TABLE 7
Adsorption of n-propyl acetate on silica gel

p	p/p_0	x/m	$\dfrac{p}{x/m}$	p	p/p_0	x/m	$\dfrac{p}{x/m}$
48.0	0.8888	35.16	1.3653	24.0	0.4444	32.84	0.7479
45.0	0.8334	35.11	1.2815	13.0	0.2408	29.61	0.4390
40.0	0.7408	35.09	1.1400	10.0	0.1852	28.17	0.3550
35.0	0.6482	34.84	1.0005	5.0	0.0926	23.73	0.2157
31.0	0.5741	34.42	0.9009				

TABLE 8
Adsorption of acetone on silica gel

p	p/p_0	x/m	$\dfrac{p}{x/m}$	p	p/p_0	x/m	$\dfrac{p}{x/m}$
278.0	0.8150	63.39	4.3850	64.0	0.1877	35.05	1.7854
222.0	0.6505	61.80	3.5890	55.0	0.1613	33.41	1.6460
213.0	0.6246	59.87	3.5580	41.0	0.1202	30.82	1.3300
186.0	0.5454	57.31	3.2450	31.0	0.0909	29.65	1.0458
157.0	0.4603	55.05	2.8520	23.0	0.0674	27.29	0.6624
146.0	0.4282	51.32	2.8450	14.0	0.0411	25.00	0.5600
120.0	0.3519	47.21	2.5425	4.0	0.0117	21.21	0.1886
107.0	0.3138	42.73	2.5045	2.0	0.0059	18.88	0.1069
75.0	0.2199	36.73	2.0420				

TABLE 9
Adsorption of ethyl acetate on silica gel

p	p/p_0	x/m	$\dfrac{p}{x/m}$	p	p/p_0	x/m	$\dfrac{p}{x/m}$
112.0	0.7619	43.40	2.5805	43.5	0.2926	31.84	1.3508
102.0	0.6939	42.86	2.3800	36.5	0.2483	29.11	1.2540
88.5	0.6020	42.16	2.0990	28.0	0.1905	27.90	1.0039
83.0	0.5647	41.53	1.9991	24.0	0.1633	24.17	0.9933
77.0	0.5239	40.38	1.9115	18.0	0.1225	22.09	0.9797
64.5	0.4388	38.35	1.6860	10.0	0.0680	19.29	0.5185
55.0	0.3744	36.13	1.5225	7.0	0.0476	17.62	0.3974
53.7	0.3653	35.73	1.5033	3.6	0.0245	16.03	0.2246
47.5	0.3197	33.40	1.4078	2.5	0.0170	14.79	0.1690

TABLE 10
Adsorption of n-propyl alcohol on silica gel

p	p/p_0	x/m	$\dfrac{p}{x/m}$	p	p/p_0	x/m	$\dfrac{p}{x/m}$
30.0	0.8180	60.00	0.5000	13.0	0.3513	39.42	0.3297
25.0	0.6756	58.98	0.4239	10.0	0.2838	35.98	0.2918
23.0	0.6216	55.86	0.4139	8.0	0.2162	33.75	0.2372
21.0	0.5675	50.42	0.4165	6.0	0.1622	31.81	0.1887
17.0	0.4594	44.20	0.3856	4.6	0.1244	30.50	0.1509

TABLE 11
Adsorption of n-propyl formate on silica gel

p	p/p_0	x/m	$\frac{p}{x/m}$	p	p/p_0	x/m	$\frac{p}{x/m}$
128.0	0.9622	44.01	2.9081	35.0	0.2631	30.12	1.1480
107.0	0.8044	42.50	2.5176	20.0	0.1504	25.00	0.8000
83.4	0.6270	41.72	2.0000	16.5	0.1241	24.07	0.6850
66.0	0.4961	39.69	1.6634	14.0	0.1052	23.30	0.6009
56.0	0.4210	38.82	1.4433	10.0	0.0752	21.39	0.4706
51.0	0.3834	36.94	1.3821	8.0	0.0601	20.50	0.3902
43.0	0.3233	33.08	1.2991	4.0	0.0301	18.39	0.2174

TABLE 12
Adsorption of n-butyl alcohol on silica gel

p	p/p_0	x/m	$\frac{p}{x/m}$	p	p/p_0	x/m	$\frac{p}{x/m}$
10.0	0.7478	47.10	0.2124	2.0	0.1481	37.08	0.0539
7.0	0.5186	45.62	0.1534	1.0	0.0741	31.42	0.0318
4.0	0.2964	42.38	0.0944				

TABLE 13
Adsorption of methyl sec-butyl ketone on silica gel

p	x/m	$\frac{p}{x/m}$	p	x/m	$\frac{p}{x/m}$
25.5	33.20	0.7680	10.0	30.31	0.3300
21.5	33.16	0.6483	8.0	28.51	0.2806
16.0	33.00	0.4849	6.0	26.35	0.2277
13.0	32.11	0.4048	4.0	20.67	0.1933

TABLE 14
Adsorption of diethyl ketone on silica gel

p	x/m	$\frac{p}{x/m}$	p	x/m	$\frac{p}{x/m}$
44.0	43.62	1.0092	16.5	36.61	0.4508
41.5	42.48	0.9765	15.0	33.91	0.4425
35.5	41.95	0.8462	8.5	26.98	0.3148
31.5	41.77	0.7536	6.2	25.54	0.2427
27.0	40.98	0.6591	4.5	24.16	0.1863
24.5	40.67	0.6024	2.0	20.91	0.0957
20.5	38.64	0.5305			

The third column records the maximum amounts adsorbed in gram-moles ($\times$ 10⁴) per gram of the gel, obtained as described elsewhere.

DISCUSSION

In the experiments recorded in the previous pages, values for the adsorption of methyl, ethyl, n-propyl, and n-butyl alcohols, of methyl, ethyl, and n-propyl formates and acetates, and of acetone and diethyl ketone on activated silica gel have been determined. An examination of the data shows that silica gel is a powerful adsorbent for the vapors of all these substances. The amount of adsorption in all the cases, when saturation has been reached, is about one-third the weight of the gel. It would be interesting to compare some of the present values with those obtained for active charcoal by previous authors.

SUBSTANCE	x/m FOR SILICA GEL	x/m FOR CHARCOAL	OBSERVER
Ethyl formate	0.394 g.	0.430 g.	Coolidge (6)
Methyl acetate	0.436 g.	0.470 g.	Coolidge (6)
Methyl alcohol	0.358 g.	0.365 g.	Coolidge (6)
n-Pentane	0.304 g.	0.312 g.	Polanyi and Goldmann (4)

It is evident that adsorption in both cases is practically the same. In this comparison, it must be remembered that all the data regarding active charcoal refer to 0°C., while the data of the present authors refer to 35°C. As the temperature coefficients of adsorption for the vapors is generally negative, the amounts of adsorption for silica gel when referred to 0°C. would be distinctly increased. One is thus led to think that the special capillary structure sometimes ascribed to silica gel, even if it represents a true picture, does not make it less efficient as compared to charcoal.

It is usual to analyze experimental data on adsorption in the light of the parabolic equation:

$$x/m = \alpha p^{1/n}$$

In the present case, as the saturation pressures of the various liquids are widely different, it would be more reasonable to compare the amount of adsorption at the same relative pressures, i.e., at the same values of p/p_s. Consequently, the values of x/m in gram-moles ($\times 10^4$) have been plotted against the relative pressures, p/p_s, and the curves are given in figure 2. This figure has also been utilized to determine the values of maximum x/m by extrapolating the curves to $p/p_s = 1$.

It has often been considered that the amount of adsorption varies regularly with increasing molecular weight of the adsorbate. Some authors have recorded an increase in adsorption, among whom may be mentioned Griffin, Richardson, and Robertson (9), Hayashi (15), and Bhatnagar, Kapur, and Bhatnagar (3). Others, for example, Heymann and Boye (16), Tsuruta (30), and Bhatnagar, Kapur, and Bhatnagar (4), observed the reverse effect, which has been variously ascribed to the presence of impurities (30), inverse orientation of the adsorbed molecules (18), and reduced size of the ultra-pores (7, 25).

An examination of the curves in figure 2 shows that the amount of adsorption at high relative pressures is always in the inverse order of the molecular weight of

the vapors. It must be pointed out that if a comparison is made at comparatively low relative pressures, or if the adsorption data be plotted as x/m against p, different results are obtained. This aspect must be borne in mind in considering the effect of molecular weight on adsorption. This is clear from a comparison
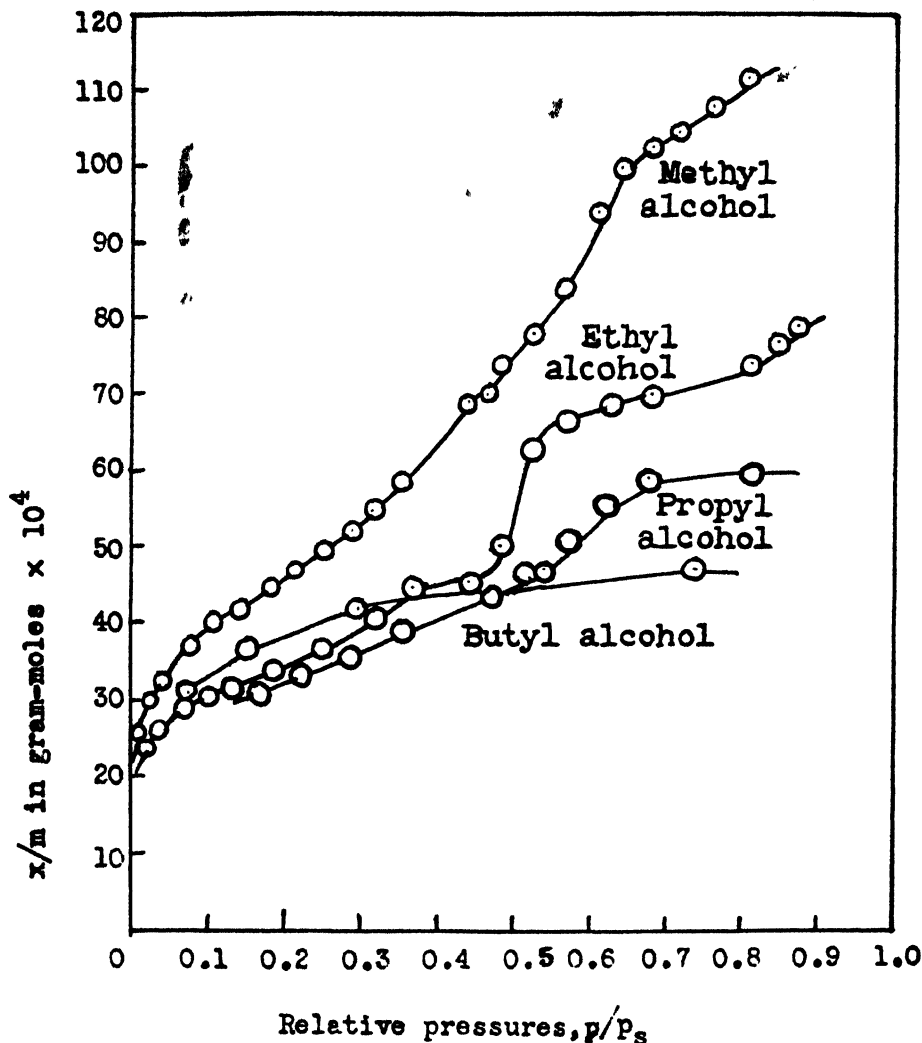
FIG. 2a. Adsorption isotherms of alcohols: x/m plotted against p/p_s

of the isotherms of alcohols in figures 2 and 3. The order in the former instance is methyl > butyl > ethyl > propyl, which becomes butyl > propyl > ethyl > methyl in the latter. The order of the curves in the upper portions, however, remains unaltered.

Adsorption on silica gel has often been considered to be in accordance with the
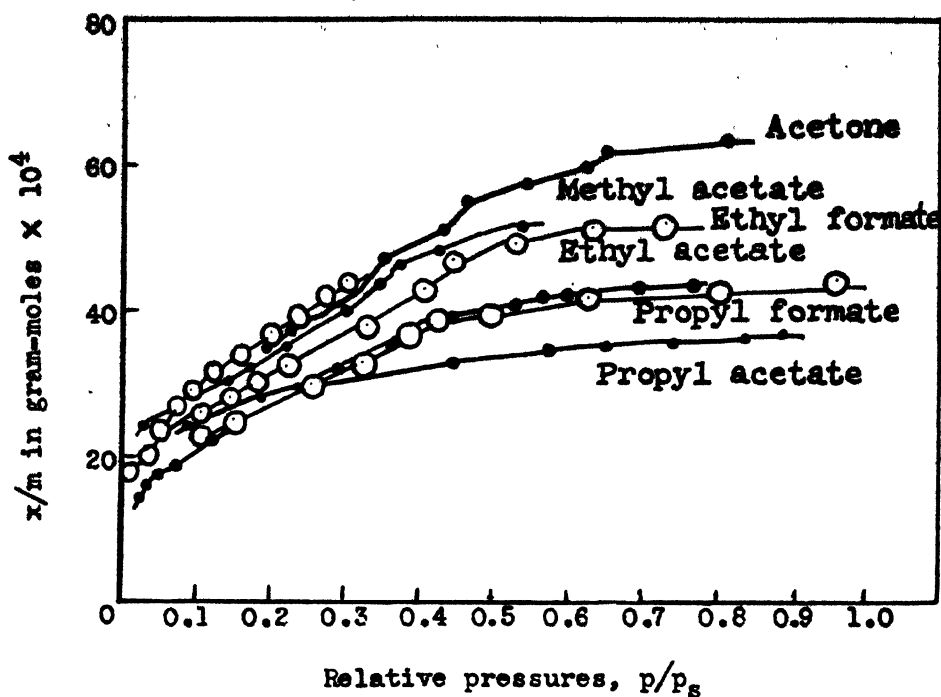
FIG. 2b. Adsorption isotherms of esters and acetone: x/m plotted against p/p_s
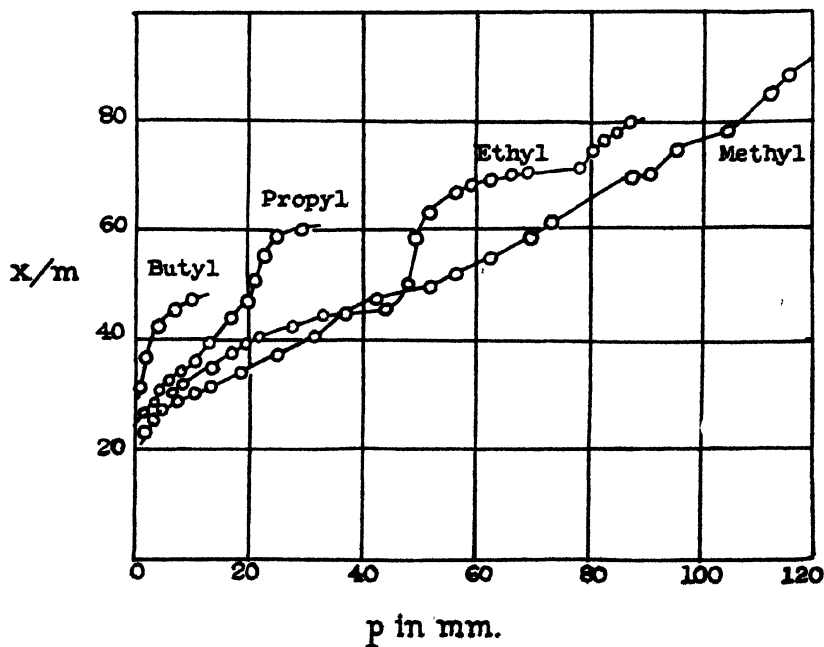
FIG. 3. Adsorption isotherms of alcohols: x/m plotted against p

capillary condensation theory (21, 31). According to this theory, the amount of adsorption should be inversely proportional to the molecular volumes of the liquids. To examine the present data in the light of the capillary condensation theory, the value of the product (maximum adsorption × parachor) for each of the compounds has been calculated. Parachor values are preferred to molecular volumes, for the data in the former case are easily available and do not require any correction due to differences in surface tension. The values of this product are recorded in column 3 of table 15, whence it is evident that they cannot be regarded as satisfactory constants. Thus, there is no strict proportionality between adsorption and the inverse molecular volumes of the liquids.

TABLE 15

N = maximum number of gram-moles adsorbed ($\times 10^4$)

SUBSTANCE	N	$N \times$ PARACHOR
Methyl alcohol.	120.0	1102.8
Ethyl alcohol	80.0	1048.2
n-Propyl alcohol	61.2	1048.5
n-Butyl alcohol	48.4	1018.0
Methyl formate	70.3	972.7
Ethyl formate	54.0	956.0
Propyl formate	44.7	965.6
Methyl acetate	54.0	954.2
Ethyl acetate	44.0	955.5
Propyl acetate	37.0	947.7
Acetone	64.7	1037.0
Diethyl ketone	45.0	1072.0

The present experimental data may be examined in the light of the monomolecular theory. Langmuir's formula, with slight transformations, may be written as

$$\frac{p}{x/m} = \frac{1}{ab} + \frac{p}{b}$$

It is clear that the plot of $\frac{p}{x/m}$ against p should be a straight line, having a slope $1/b$ and an intercept $1/ab$. The present data have been plotted in the above manner in figure 4. The ketones and esters show a marked tendency toward being linear, and the adsorption of these compounds may be considered as being limited to a monomolecular layer. In the case of alcohols, however, the graphs based on the Langmuir equation are not linear and exhibit points of inflexion. Up to a pressure of about 40 mm., a more or less linear curve for all the alcohols is obtained. As the pressure increases the curves bend, and several points of inflexion appear. At still higher pressures, the curves again exhibit a rough tendency toward being linear. The second and subsequent branches slope at a distinctly smaller angle. The peculiarities cannot be put down as being due to inaccuracies in experimental measurements. In the case of alcohols, the experi-

mental data have been checked by careful duplicate experiments, the equilibrium being attained from both sides.

It is possible to interpret the behavior of the alcohols in several ways. It might be considered that adsorption in the initial stages is strictly monomolecular, but as the pressure increases and a greater crowding of the molecules on the surface sets in, a second layer may begin to be formed. A careful examination of the curves in figure 2, however, brings out a difficulty. The surface valencies should be considered to be satisfied to a large extent in the first layer, and only a weak field of force would be available for building up a second layer. Thus, the rate at which the second layer will be formed will be definitely slower. Consequently, the slope of the curve corresponding to the formation of the second layer
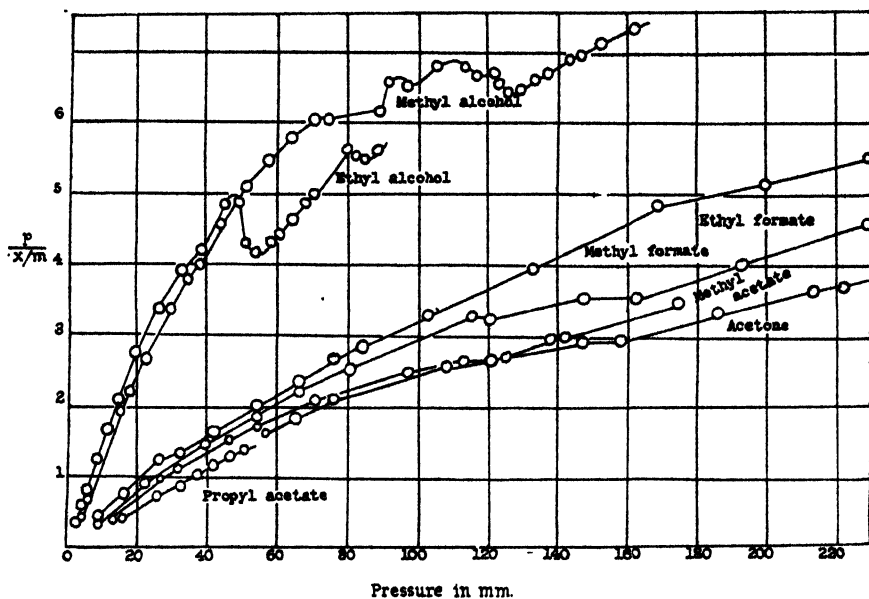
FIG. 4. $\frac{x/m}{p}$ plotted against p

should be less steep. This is just the opposite of what is seen from figure 2. Apparently, the adsorption process corresponding to the second branch proceeds at a somewhat higher rate, and it is difficult to reconcile this behavior with the theory of the second layer.

The case of the alcohols may be considered from a second point of view. The presence of different groups of elementary spaces, which will become operative at different stages of adsorption, has often been considered. Thus, the adsorption curves obtained by Gustaver (10) showed different branches which correspond to different sets of active patches. Such a postulate regarding the active surface would not satisfactorily explain the peculiarities met with in the case of alcohols. The other vapors studied in the present experiments have failed to reveal any

tendency towards stepwise isotherms.   There is no reason why these should not be revealed in the adsorption of vapors other than the alcohols, the adsorbing surface remaining the same in all cases.

In the view of the authors, the behavior of the alcohols might be sufficiently explained on the basis of a chemical theory.   It is assumed that the adsorbing material enters into a loose chemical combination with the alcohols, giving rise to alcoholates, somewhat analogous to hydrates of salts.   The combination envisaged in the present hypothesis should not be considered as a compound which separates out as a new phase from the bulk of the adsorbing material.   Evidence for this point of view is obtained from an analysis of the curves in figure 2.   The values of x/m at the points where the first distinct changes in the slopes of the curves occur is approximately 48×10^{-4} gram-moles per gram of the gel for all the alcohols studied.   Considering the gel as pure silica, this corresponds to the ratio 48 molecules of alcohol to 166 of silica.   Obviously there is no simple stoichiometric ratio between the adsorbing and adsorbed materials.   This is to be expected, since the gross weight of the gel does not enter into the combination. It is only the molecules at the surface which operate in the formation of the alcoholates.   If we similarly consider the amount of adsorption corresponding to the second break in the case of alcohols which exhibit a pronounced second discontinuity, it corresponds to about 72×10^{-4} gram-moles.   Thus the ratio between the molecules of alcohol corresponding to the first and second breaks is roughly 2:3.   This simple integral ratio between the number of alcohol molecules for a fixed amount of surface silica definitely suggests the formation of alcoholates between which the same ratio applies.   Patrick and Greider (22) found that a certain sample of silica gel took up 36.1 per cent water, which corresponds to $1SiO_2:1H_2O$.   The corresponding maximum adsorption obtained by Ray and Ganguly (27) was 37.5 per cent which, owing to some error in calculation, they take for the formation of the hydrate $SiO_2 \cdot 2H_2O$.   Alcohols, being nearest to the water molecule in constitution, might easily form definite alcoholates.   In the view of the present authors, this is the most important factor in so far as the peculiarities in the cases of ethyl and propyl alcohols are concerned.   The case of butyl alcohol is, however, slightly different.

A very important set of observations, which has a bearing on the foregoing discussion, is due to Allmand and others (1).   They have shown that a number of adsorption processes are discontinuous.   The discontinuities, though small, are quite distinct.   In fact, the adsorption isotherm rises in a series of regular steps from the beginning to the end.   The explanation given by Allmand is that the adsorption process "starts from active centres on the adsorbent, and the molecules spread out in a series of concentric rings to form a two-dimensional pool or island of adsorbed molecules."   Evidently, this theory would not meet the case of the alcohols, where, for quite a large portion of the isotherms, the course is smooth.   In the absence, however, of further experimental verification and a more precise enunciation of the nature of forces operative in filling up the concentric rings, further comments are difficult.

SUMMARY

1. The adsorption of the lower members of the series of alcohols, esters, and ketones on active silica gel has been measured by a static method, the gel being completely freed from residual gases.

2. Silica gel is a powerful adsorbent for all the vapors studied. The maximum capacity is as good as that of the charcoals used by Coolidge or Polanyi and Goldmann.

3. At high relative pressures the amounts of adsorption are always in the inverse order of the molecular weights in the same series of compounds. These orders are not maintained at lower relative pressures, and may further change according to the mode of plotting adopted.

4. Esters and ketones give smooth isotherms; those for the alcohols reveal multiple branches. The peculiarities in the curves for alcohols have been explained on the basis of formation of surface compounds.

5. The capillary condensation theory has been examined afresh with the help of the parachors of the compounds studied, and is not found to apply satisfactorily as far as the present data are concerned.

REFERENCES

(1) ALLMAND *et al.*: Trans. Faraday Soc. **28**, 218 (1932); *cf.* BENTON AND WHITE: J. Am. Chem. Soc. **52**, 2325 (1930).
(2) ANDERSON: Z. physik. Chem. **88**, 212 (1914).
(3) BHATNAGAR, KAPUR, AND BHATNAGAR: J. Indian Chem. Soc. **16**, 261 (1939).
(4) BHATNAGAR, KAPUR, AND BHATNAGAR: J. Indian Chem. Soc. **17**, 361 (1940).
(5) CLARK AND LAMBERT: Proc. Roy. Soc. (London) **A122**, 511 (1929).
(6) COOLIDGE: J. Am. Chem. Soc. **46**, 596 (1924).
(7) DUBININ: Z. physik. Chem. **140A**, 81 (1929).
(8) FREUNDLICH: *Colloid and Capillary Chemistry*, p. 195. London (1922).
(9) GRIFFIN, RICHARDSON, AND ROBERTSON: J. Chem. Soc. **1928**, 2705.
(10) GUSTAVER: Kolloid-Beihefte **15**, 185 (1922); *cf.* CHAPLIN: J. Phys. Chem. **36**, 909 (1932).
(11) GYANI: J. Indian Chem. Soc. **21**, 79 (1944).
(12) GYANI AND GANGULY: J. Indian Chem. Soc. **19**, 453 (1942).
(13) GYANI AND GANGULY: J. Indian Chem. Soc. **20**, 331 (1943).
(14) GYANI AND GANGULY: Communicated to National Academy of Sciences (India), 1944.
(15) HAYASHI: J. Biochem. (Japan) **16**, 1 (1932).
(16) HEYMANN AND BOYE: Kolloid-Z. **53**, 153 (1932).
(17) HOLMES AND WEIDE: Science **60**, 596 (1924).
(18) ILYIN: Z. physik. Chem. **155**, 403 (1931).
(19) JONES AND OUTRIDGE: J. Chem. Soc. **1930**, 1574.
(20) OKATOV: Zhur. Priklad. Khim. **2**, 121 (1929).
(21) PATRICK: Dissertation, Göttingen, 1914, *et seq.*
(22) PATRICK AND GREIDER: J. Phys. Chem. **29**, 1035 (1925).
(23) PATRICK AND OPDYCKE: J. Phys. Chem. **29**, 596 (1925).
(24) POLANYI AND GOLDMANN: Z. physik. Chem. **91**, 120 (1916).
(25) POSPELOVA: J. Russ. Phys. Chem. Soc. **11**, 99 (1938).
(26) VON PUTNOKY AND SZÉLENYI: Z. Elektrochem. **34**, 805 (1928).
(27) RAY AND GANGULY: Trans. Faraday Soc. **30**, 997 (1934).
(28) SCHMIDT AND HINTELLER: Z. physik. Chem. **91**, 120 (1916).
(29) TRAUBE AND ST. BIRUTOVITSCH: Kolloid-Z. **44**, 233 (1928).
(30) TSURUTA: J. Soc. Chem. Ind. Japan **41**, 129B (1938).
(31) ZSIGMONDY: Z. anorg. Chem. **71**, 356 (1911).

THE EQUILIBRIUM SPREADING COEFFICIENT OF AMPHIPATHIC ORGANIC LIQUIDS ON WATER

E. HEYMANN AND A. YOFFE

Chemistry Department, University of Melbourne, Melbourne, Australia

I

The equilibrium spreading coefficient on water

$$F'_s = \gamma'_w - \gamma'_o - \gamma'_{wo} = W'_A - W'_C \tag{1}$$

(where γ'_m and γ'_o are the surface tensions of water and organic liquid, respectively, and γ'_{wo} is the interfacial tension, all quantities, as well as W'_A and W'_C (*cf.* later), referring to mutually saturated phases and surfaces) is always zero, according to Antonoff (2, 3). A number of other investigators, however, have found small negative values in the case of many amphipathic organic compounds. Some results are shown in table 1.

It is seen that the compounds of group A are incapable of hydrogen-bond formation and approach fairly closely a zero value for F'_s, irrespective of the polar or non-polar nature of the molecule in question. On the other hand, the compounds listed under group B, which are all amphipathic and in which the polar group is capable of hydrogen-bond formation and thus possesses strong attraction for water, exhibit appreciably negative values for F'_s, except for the results obtained by Antonoff and coworkers. Antonoff is of the opinion that the experiments of all workers who obtained a value of F'_s differing from zero are invalidated mainly by non-attainment of equilibrium with regard to all bulk phases and surfaces. Further experimental research will have to show whether this claim can be upheld.

Langmuir (14), Harkins (9). and Miller (15) have put forward theoretical considerations in favor of the reality of a finite negative equilibrium spreading coefficient. Miller has interpreted the negative spreading coefficient in terms of the work of orientation.

We have pointed out recently (19) that, *if a lens of an amphipathic compound is considered in equilibrium with the monolayer on water, the work of cohesion of the organic liquid in bulk* (W'_C) *is greater than the work of separation of the organic bulk phase from the interfacial layer of the amphipathic substance which is oriented* (W'_A), because the first process involves the formation of *two* oriented layers, whereas the second involves the formation of only *one* newly oriented layer. As a consequence, F'_s is negative.

H. L. Cupples (6) considers that it should be impossible (by our reasoning) to predict whether W'_A is greater or smaller than W'_C, because, while W'_C depends only on γ'_o, W'_A depends on all three tensions, which he apparently assumes to be independent of each other. In our opinion, this assumption is erroneous, because γ'_{wo} depends on both γ'_w and γ'_o, its magnitude being determined by the forces between the organic molecules and those between the water molecules, as well

as the mutual forces between organic and water molecules. Further, Cupples considers that the free-energy changes associated with orientation may only be small fractions of W'_A and W'_C. However, as will be shown in Section III (table 2), the work of orientation may amount to more than 20 per cent of W_C. Even if it were considerably smaller than this estimate, this would not impair our

TABLE 1

Values of equilibrium spreading coefficient on water

	F'_s	TEM-PERATURE	REFERENCE
	ergs × cm.⁻²	°C.	
Group A:			
Cyclohexane	−1.0	25	Carter and Jones (5)
Benzene	−0.2	25	Carter and Jones (5)
Benzene	0	19	Fox (8)
Benzene	−1.5	20	Harkins (9)
Carbon tetrachloride	−0.4	23	Miller (15)
Carbon tetrachloride	0	17	Fox (8)
Nitrobenzene	+0.14	25	Carter and Jones (5)
Nitrobenzene	0	18	Fox (8)
Nitrobenzene	−0.21	25	Bartell and coworkers (4)
Chloroform	0	18	Fox (8)
Chloroform	+0.1	18	Reynolds (17)
o-Nitrotoluene	−0.2	23	Miller (15)
Group B:			
Aniline	−2.7	22	Fox (8)
Aniline	−0.6	20	Reynolds (17)
n-Butyl alcohol	−3.4	25	Carter and Jones (5)
sec-Butyl alcohol	0	25	Antonoff and coworkers (2)
Isoamyl alcohol	−2.6	25	Harkins (9)
Isoamyl alcohol	0	25	Antonoff and coworkers (2)
n-Heptyl alcohol	−5.9	20	Harkins (9)
n-Heptyl alcohol	−5.6	25	Carter and Jones (5)
m-Cresol	−4.1	25	Carter and Jones (5)
Isobutyric acid	0	25	Antonoff and coworkers (2)
n-Caproic acid	−3.7	25	Carter and Jones (5)
Nonylic acid	−2.4	25	Carter and Jones (5)
Oleic acid	−4.0	23	Miller (15)
Oleic acid	−3.0	18	Heymann and Yoffe (11)
Linoleic acid	−1.4	23	Miller (15)
n-Amyl phthalate	−3.1	23	Miller (15)

argument, because $-F'_s$ is usually of the order of 1.5–5 ergs × cm.⁻² for amphipathic compounds, and hence only a small fraction of W'_A and W'_C.

II

Our conclusion that $W'_A < W'_C$ receives further support from an analysis of the forces that are involved. On separating a column of a liquid hydrocarbon, the work of cohesion of the hydrocarbon W^H_C is required, its magnitude being determined by the van der Waals forces between the hydrocarbon molecules.

Figure 1 shows a column of an *amphipathic* organic liquid in equilibrium with an aqueous phase having a layer of oriented amphipathic molecules in the interface and surface.[1] If separation is effected at the cross-section AA', the work of cohesion of the organic phase is required. W'_C will be greater than W^H_C because separation in *this* case involves work against the dipole and hydrogen-bond forces between the polar groups as well as against the van der Waals forces between the hydrocarbon chains. Many experimental findings support this conclusion. Firstly, the work of cohesion, calculated from the surface tension, of amphipathic compounds is markedly greater ($\sim$ 20 per cent for alcohols, and up to 30 per cent for fatty acids, of medium chain length) than that of the corresponding hydrocarbons (*cf.* table 2). Secondly, the so-called molar cohesions of various groups and radicals, calculated by Dunkel (7) from the heats of vaporization (though extrapolated rather crudely to absolute zero), are as follows: CH_2, 990; CH_3,
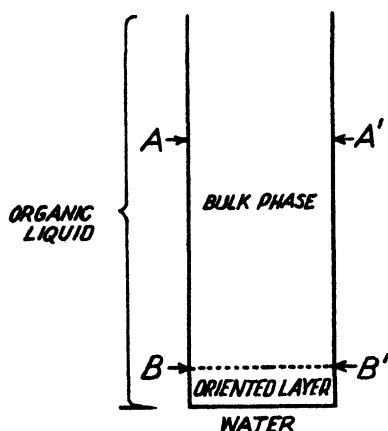
FIG. 1. A column of an amphipathic organic liquid in equilibrium with an aqueous phase having a layer of oriented amphipathic molecules in the interface and surface.

1780; OH, 7250; and COOH, 8970 cal. per mole. From these figures we obtain for the molar cohesion of hexadecane 17,420, cetyl alcohol 23,880 and palmitic acid 24,610 cal. per mole, again showing greater cohesion of the amphipathic compound than of the corresponding hydrocarbon.

If separation is effected at the cross-section BB' (in figure 1), W'_A, the work of separation of the organic liquid phase in bulk from the oriented interfacial layer, is required. This involves a very much smaller number of polar groups than separation across AA', because the molecules of the oriented layer have their hydrocarbon chains turned towards the bulk phase; this point was clearly recognized by Harkins (9) in the system heptyl alcohol–water. As a consequence, the work of separation at BB' is smaller than at AA', i.e., $W'_A < W'_C$, and thus F'_s is negative. Actually, W'_A will have a value between W'_C and W^H_C.

[1] The surface film is not shown in figure 1.

III

As mentioned above, fatty alcohols and fatty acids have a higher work of cohesion (W_C) than the corresponding hydrocarbons (W_C^z). Hence we may write

$$W_C = W_C^z + W_P \qquad (2)$$

where W_P is due to the contribution of the polar groups to the work of cohesion of amphipathic liquids. However, equation 2 admits of a more detailed interpretation. When an amphipathic liquid is pulled apart, the two newly created surfaces contain the molecules with their hydrocarbon chains oriented outwards, although the chains will not be strictly parallel as a consequence of thermal agitation which produces a certain amount of "disorientation." The configuration of the surface of a hydrocarbon is probably not very much different from that of an amphipathic liquid, according to Adam's (1) discussion of the temperature coefficient of the surface tension of both classes of liquids. For thermodynamic reasoning, the process of pulling an amphipathic liquid apart may be considered to consist of bringing the molecules in the cross-section concerned to a degree of orientation corresponding to that of the surface, and then pulling apart the somewhat oriented layers of hydrocarbon chains thus formed. The same process may also be visualized for the hydrocarbon.

The work of orientation of the amphipathic liquid involves rotation of a considerable fraction (statistically about one-fourth) of the molecules in the cross-section concerned, whereby the polar groups are immersed in the bulk of the liquid. This work of orientation will be contained in a large measure by W_P (equation 2). It would be equal to W_P if we were justified in assuming that the work required to pull apart the somewhat oriented layers of hydrocarbon chains were virtually equal to W_C^z (cf. equation 2), i.e., if the work of orientation of the hydrocarbon,[2] which is actually included in W_C^z, were small compared with W_P and W_C^z. There are reasons in favor of such an assumption. Orientation of *normal hydrocarbon molecules* having identical groups at both ends and possessing a symmetrical field of force will involve smaller potential barriers and a less far-reaching geometrical rearrangement than the orientation of *amphipathic molecules* with one polar group possessing a strongly asymmetrical field of force, and involving rotation of about a quarter of all molecules concerned. We may therefore assume that, as a first approximation, W_P represents a minimum value of the work of orientation of the amphipathic liquid which is probably not far below its actual value. From equation 2 it is obvious that W_P concerns two layers of molecules at unit cross-section.

Values for W_P calculated from equation 2 are shown in table 2 (for experimental data cf. references 13, 16, 18).

From this somewhat limited experimental material, it is seen that W_P decreases markedly with increasing chain length. This at first sight surprising result may be due to the fact that W_P (like W_C) is defined per cm.[2], and the number of amphipathic molecules, and hence of polar groups involved, will decrease

---

[2] It would be interesting to estimate the work of orientation of a hydrocarbon from the difference between the work of cohesion of a disordered and that of an ordered hydrocarbon liquid. At present, we hardly possess the data necessary for such a calculation.

with increasing chain length provided there is a certain amount of disorientation in the surface due to thermal agitation, as mentioned above. An additional reason may be connected with the amount of orientation already existing in the amphipathic liquid (cybotaxis), which is probably more pronounced with the higher homologues than with the lower ones, although opinion regarding the interpretation of x-ray data on this point appears to be divided.[3]

TABLE 2

NUMBER OF CARBON ATOMS	W_C^{H}	W_C	W_P
Normal alcohol at 25°C.:			
5	30.8	50.6	19.8
6	35.8	51.6	15.8
7	39.6	54.2	14.6
9	44.8	56.2	11.4
10	47.0	56.2	10.2
11	48.6	57.8	9.2
12	50.0	59.2	9.2
Normal saturated fatty acids at 20°C.:			
5	32.0	54.8	22.8
7	40.6	56.6	16.0
8	43.6	57.3	13.7
Normal saturated fatty acids at 50°C.:			
6	30.4	50.2	19.8
8	37.6	51.2	13.6
10	42.2	54.0	11.8
12	45.4	56.0	10.6

IV

On separating the liquid column at AA' (figure 1) (corresponding to W_C'), two oriented surfaces are formed, whereas on separating at BB' (corresponding to W_A') only one newly oriented surface is formed. Hence the work of orientation at the interface (W_{PI}'), which is included in W_A', may, as a first approximation, be assumed to be one-half of W_P', the work of orientation on separating the bulk phase which is included in W_C'. Thus we have, besides

$$W_C' = W_C^{\text{H}} + W_P' \tag{2a}$$

$$W_{PI}' \cong \tfrac{1}{2}W_P' \tag{3}$$

and

$$W_A' = W_C^{\text{H}} + W_{PI}' \cong W_C^{\text{H}} + \tfrac{1}{2}W_P' \tag{4}[4]$$

Hence

$$F_s' = W_A' - W_C' = W_{PI}' - W_P' = -\tfrac{1}{2}W_P' \tag{5}$$

[3] Discussions on anisotropic liquids in Transactions of the Faraday Society **29** (1933), and on structure and molecular forces in liquids in Transactions of the Faraday Society **33** (1937).

[4] Strictly speaking, a quantity $W_C'^{\text{H}}$, the work of cohesion of hydrocarbon saturated with water, should be introduced instead of W_C^{H}. However, the difference in surface tension of a pure hydrocarbon and of a hydrocarbon saturated with water is inappreciable (*cf.* later).

In this reasoning, the work of orientation of hydrocarbon, which is probably small compared with W_C^a and W'_P (cf. Section III) is neglected. Should this not be permissible, it can be shown easily that $-F'_s$ would be somewhat greater than $\frac{1}{2}W'_P$.

Further, according to equations 2, 2a, and 5

$$\frac{1}{2}W'_P = \frac{1}{2}W_P - \Delta \tag{6}$$

where

$$\Delta = \frac{W_C - W'_C}{2} = \gamma_o - \gamma'_o$$

γ_o being the surface tension of the pure organic liquid and γ'_o that of the organic liquid saturated with water. Δ is usually positive, e.g., for n-heptyl alcohol 0.98, isoamyl alcohol 0.34, aniline 0.2, benzene 0.08 ergs $\times$ cm.$^{-2}$ at 20°C.; in other cases it is negative, e.g., for m-cresol 0.88 ergs $\times$ cm.$^{-2}$ (8, 9, 10); for the higher homologues of amphipathic compounds, and for all hydrocarbons, it is very small because of the low solubility of water in these compounds. Hence we obtain

$$-F'_s \cong \frac{1}{2}W'_P \cong \frac{1}{2}W_P - \Delta \tag{7}$$

where Δ may be positive or negative, but not greater than about 1 erg $\times$ cm.$^{-2}$, and hence does not amount to more than about 10 per cent of $\frac{1}{2}W_P$.

The experimental results show that $-F'_s$ is almost invariably smaller than indicated by equation 7. This is probably due to the fact that the reasoning leading to

$$W'_{PI} \cong \frac{1}{2}W'_P \tag{3}$$

is too simplified. The interfacial layer (at BB') is probably somewhat disoriented, and less well oriented than the surface film on water[5] resulting from separation at BB'. Hence, separation involves more work than that of orientation of only one layer, i.e., $W'_{PI} > \frac{1}{2}W'_P$, and, by equation 5,

$$-F'_s < \frac{1}{2}W'_P \tag{8}$$

which is in agreement with experimental results.

SUMMARY

A theoretical discussion concerning the equilibrium spreading coefficient of amphipathic organic compounds on water is given, with particular reference to intermolecular forces and the work of orientation. The experimental material is briefly reviewed.

[5] Interfacial films tend to be more expanded and less well oriented than the corresponding surface films (1, 19), owing to the reduction of the lateral adhesion between the hydrocarbon chains when in contact with an organic bulk phase.

REFERENCES

(1) ADAM, N. K.: *Physics and Chemistry of Surfaces*, 3rd edition, pp. 100, 163. Oxford University Press, London (1942).
(2) ANTONOFF, G., CHANIN, M., AND HECHT, M.: J. Phys. Chem. **46**, 492 (1942).
(3) ANTONOFF, G.: J. Phys. Chem. **46**, 497 (1942); **47**, 709 (1943).
(4) BARTELL, F. E., CASE, L. O., AND BROWN, H.: J. Am. Chem. Soc. **55**, 2774 (1933).
(5) CARTER, E. G., AND JONES, D. C.: Trans. Faraday Soc. **30**, 1027 (1934).
(6) CUPPLES, H. L.: J. Phys. Chem. **48**, 75 (1944).
(7) DUNKEL, M.: Z. physik. Chem. **A138**, 42 (1928).
(8) FOX, W.: J. Chem. Phys. **10**, 623 (1942).
(9) HARKINS, W. D.: J. Chem. Phys. **9**, 552 (1941).
(10) HARKINS, W. D.: *International Critical Tables*, Vol. IV. McGraw-Hill Book Company, Inc., New York (1928).
(11) HEYMANN, E., AND YOFFE, A.: Trans. Faraday Soc. **38**, 408 (1942).
(12) HEYMANN, E., AND YOFFE, A.: Trans. Faraday Soc. **39**, 217 (1943).
(13) LANDOLT-BÖRNSTEIN: *Physikalisch-chemische Tabellen*, Erganzungsband IIa, p. 155.
(14) LANGMUIR, I.: J. Chem. Phys. **1**, 775 (1933).
(15) MILLER, N. F.: J. Phys. Chem. **45**, 1025 (1941).
(16) QUAYLE, O. R., DAY, R. A., AND BROWN, G. M.: J. Am. Chem. Soc. **66**, 938 (1944).
(17) REYNOLDS, W. C.: J. Chem. Soc. **119**, 466 (1921).
(18) SMITH, G. W., AND SORG, L.: J. Phys. Chem. **45**, 671 (1941).
(19) YOFFE, A., AND HEYMANN, E.: J. Phys. Chem. **47**, 409 (1943).

THE SOLUBILITY OF SILVER ACETATE IN MIXTURES OF ETHYL ALCOHOL AND WATER

THE FORMATION OF COMPLEX IONS[1]

F. H. MacDOUGALL AND MARTIN ALLEN

School of Chemistry, Institute of Technology, University of Minnesota, Minneapolis 14, Minnesota

INTRODUCTION

Previous investigations carried out in this laboratory dealing with the effect of added strong electrolytes on the solubility of silver acetate in water and in mixed solvents may be classified in two groups: (*1*) those in which the added electrolyte contained no ion common to those supplied by the silver acetate (5, 8, 9, 10); (*2*) those in which the added electrolyte furnished either silver ion or acetate ion (6, 7).   For our present purpose, the results obtained in the investigations of the first group may be summarized in the statement that the effect of the added electrolytes on the solubility of silver acetate could be accounted for, with a considerable degree of accuracy, in solutions of low and moderately high ionic

---

[1] This paper is based on a thesis presented by Martin Allen to the Graduate School of the University of Minnesota in partial fulfillment of the requirements for the degree of Doctor of Philosophy, August, 1944.

strength, by the changes in the activity coefficients of the ions predicted by the Debye equation in which an ionic-diameter parameter of reasonable magnitude is employed. The assumption was tacitly made that the strong electrolytes were completely ionized and that no complex ions were formed.

On the other hand, the Debye equation seemed to fail when applied to the solubility of silver acetate in water when the added electrolyte was sodium acetate, potassium acetate, silver nitrate, or silver perchlorate. This happened even in the case of moderately dilute solutions. Assuming that the departure of the ions from ideal behavior is due mainly to the magnitude of the ionic strength of their environment, we found it difficult to believe that a silver or acetate ion could distinguish clearly between sodium and silver ions in their neighborhood or between nitrate and acetate ions. We decided therefore to test the hypothesis that, when sodium or potassium acetate is the added electrolyte, appreciable amounts of the diacetatoargentate ion, $Ag(C_2H_3O_2)_2^-$, are formed and that when silver nitrate or perchlorate is the added electrolyte, appreciable quantities of the acetatodisilver ion, $Ag_2C_2H_3O_2^+$, exist in the solution.

If this hypothesis is correct, it is easy to show that, in saturated solutions of silver acetate containing a strong electrolyte with a common ion, the *apparent* solubility product of silver acetate will be greater than in an analogous solution of equal ionic strength in which the added electrolyte does not furnish a common ion; moreover, the difference between the two solubility products will increase with the ionic strength. In other words, in solutions in which the added electrolyte is sodium acetate, the amount of diacetatoargentate ion will constitute an increasing fraction of the total silver in the solution as the concentration of added sodium acetate is increased. If our hypothesis is correct, complex ions will exist even in solutions of silver acetate containing no other electrolyte or containing an added electrolyte without an ion in common. But in this case the quantities of the complex ions will not only be small but will also be approximately *constant* fractions of the total silver acetate.

In previous papers (6, 7) we produced evidence indicating the formation of AgA_2^- and Ag_2A^+ ($A = C_2H_3O_2$) in aqueous solutions and obtained values for the dissociation constants of these complex ions, as well as more exact values for the true activity product of Ag^+ and A^-. In the present paper we publish analogous results obtained when the solvents were 10, 20, and 30 per cent ethyl alcohol, respectively.

EXPERIMENTAL DETAILS

Materials used

We report here only on materials not described in a previous paper (7).

The silver nitrate, C.P. grade, manufactured by the Goldsmith Bros. Refining Co., was pre-dried at 120°C. and then fused at 220–240°C. over a sand bath. It was then ground in an agate mortar and stored in a dark bottle.

Anhydrous silver perchlorate of reagent quality was obtained from the G. F. Smith Co. It was first stored in a vacuum desiccator containing magnesium perchlorate and then dried in a vacuum oven for several days at 120°C. and 40 mm. (11).

Experimental procedures and analytical methods

The general experimental procedure has been described previously (5).

The composition of the alcohol–water mixtures used as "solvents" was found by determining their densities and using the data given in the *International Critical Tables* (3). As a check on this procedure, the density of an approximately 10 per cent mixture which had been prepared from known weights of alcohol and water was determined at 25°C. A Gay-Lussac type of specific gravity bottle with thermometer attached was used. The density so obtained agreed to within one part in ten thousand with that given by the *International Critical Tables*.

The dielectric constants of the alcohol–water mixtures were obtained by linear interpolation from the data of Åkerlöf (1).

Stock solutions of sodium acetate, potassium acetate, silver nitrate, and silver perchlorate were made by weighing out appropriate amounts of the "solvent" and of the dried salt. The concentrations of the acetate solutions were also checked by a gravimetric method in which a known weight of solution is evaporated to dryness after the addition of hydrochloric acid. The silver nitrate and perchlorate solutions were analyzed volumetrically by a Volhard titration, as outlined by Kolthoff and Sandell (4).

This same Volhard method was used in determining the concentration of silver acetate in solvents saturated with silver acetate and containing in addition sodium or potassium acetate on the one hand or silver nitrate or perchlorate on the other hand. In the first case, no serious difficulties are encountered until the concentration of dissolved silver acetate becomes so small that the method is no longer accurate. In the second case (addition of silver salt), the concentration of dissolved silver acetate must be obtained by difference; hence the concentration of added silver nitrate or perchlorate must not exceed about 0.3 molar. In general, quadruplicate determinations of the solubility of silver acetate agreed to within three or four parts per thousand.

MEANING OF SYMBOLS

The letters c, m, and x denote moles per liter of solution, moles per kilogram of solvent, and mole-fraction, respectively.

Values of ionic molarity, molality, mole-fraction, ionic strength, or solubility product calculated on the assumption of complete ionization of the dissolved salts and no complex-ion formation will be called apparent values. Thus c_1, m_1, and x_1 are the apparent molarity, molality, and mole-fraction of silver ion, whereas c_2, m_2, and x_2 refer in a similar manner to the acetate ion. $L^x = x_1 x_2$, $L^m = m_1 m_2$, $L^c = c_1 c_2$ are apparent solubility products; $x_\pm$ is defined as equal to $(x_1 x_2)^{1/2}$ and is therefore called the apparent mean mole-fraction of AgA. The actual (or true) concentrations of ions will be represented by such symbols as c_{Ag^+} or x_{A^-}. A true solubility product would be $x_{Ag^+} x_{A^-}$. D is the dielectric constant, and d_0 the density of a "solvent"; d is the density of a solution.

The (true) ionic strength, S, is defined by the equation

$$S = \tfrac{1}{2} \Sigma\, z_i^2 c_i$$

where c_i is the true molarity of a species and $z_i\epsilon$ is its electrical charge, ϵ being the charge on a proton. The apparent ionic strength, $S_{app.}$, is defined by a similar equation, except that the molarity of a species is calculated on the assumption of complete ionization of the electrolytes with no formation of complex ions.

TABLE 1

Solubility of silver acetate in the presence of sodium acetate at 25°C. in 10.17 per cent alcohol

$D = 72.71$; $d_0 = 0.9802$

m NaA	c NaA	d (SATURATED SOLUTION)	m AgA	c AgA	$\frac{10^3 x_+}{AgA}$	$S_{app.}$
0.0	0.0	0.9875	0.04960	0.04858	0.9508	0.04858
0.01159	0.01135	0.9879	0.04470	0.04379	0.9613	0.05514
0.05028	0.04920	0.9879	0.03318	0.03247	1.007	0.08167
0.09923	0.09687	0.9884	0.02562	0.02501	1.081	0.1219
0.1970	0.1918	0.9924	0.01907	0.01856	1.223	0.2104
0.4931	0.4747	1.0040	0.01411	0.01359	1.594	0.4883
0.6633	0.6347	1.0110	0.01331	0.01273	1.776	0.6474
0.9837	0.9296	1.0234	0.01273	0.01203	2.083	0.9416

TABLE 2

Solubility of silver acetate in the presence of potassium acetate at 25°C. in 10.17 per cent alcohol

$D = 72.71$; $d_0 = 0.9802$

m KA	c KA	d (SATURATED SOLUTION)	m AgA	c AgA	$\frac{10^3 x_+}{AgA}$	$S_{app.}$
0.0	0.0	0.9875	0.04960	0.04858	0.9508	0.04858
0.01073	0.01051	0.9878	0.04517	0.04424	0.9630	0.05475
0.05007	0.04898	0.9882	0.03347	0.03273	1.012	0.08171
0.1005	0.09803	0.9889	0.02525	0.02489	1.077	0.1229
0.2003	0.1946	0.9938	0.01913	0.01859	1.234	0.2132
0.5071	0.4855	1.0071	0.01419	0.01359	1.619	0.4991
0.6981	0.6622	1.0157	0.01338	0.01269	1.824	0.6749
0.8642	0.8134	1.0231	0.01307	0.01230	1.990	0.8257

EXPERIMENTAL RESULTS

Tables 1 to 12 give for three different solvents (10.17, 20.03, and 30.01 per cent alcohol) the solubility of silver acetate in the presence of each of the following electrolytes: sodium acetate, potassium acetate, silver nitrate, and silver perchlorate. For each saturated solution the density and the apparent ionic strength are given.

In figures 1 to 3 the logarithm of the apparent solubility product, $L^z = x_1 x_2$, is plotted against the square root of the apparent ionic strength for the three solvents, 10, 20, and 30 per cent alcohol. Each figure contains three curves. Curve I describes the relation between L^z and $S_{app.}^{1/2}$ when sodium nitrate is the added electrolyte; curve II and curve III refer to sodium acetate and silver

TABLE 3

Solubility of silver acetate in the presence of silver nitrate at 25°C. in 10.17 per cent alcohol

$D = 72.71$; $d_0 = 0.9802$

m AgNO₃	c AgNO₃	d (SATURATED SOLUTION)	m AgA	c AgA	$10^3 x_{\pm}$ AgA	$S_{app.}$
0.0	0.0	0.9875	0.04960	0.04858	0.9508	0.04858
0.01013	0.00993	0.9891	0.04567	0.04475	0.9675	0.05468
0.05025	0.04916	0.9921	0.03394	0.03320	1.023	0.08236
0.1052	0.1028	0.9985	0.02639	0.02578	1.126	0.1286
0.2021	0.1969	1.0110	0.02058	0.02005	1.289	0.2170
0.3005	0.2920	1.0242	0.11844	0.01791	1.455	0.3099

TABLE 4

Solubility of silver acetate in the presence of silver perchlorate at 25°C. in 10.17 per cent alcohol

$D = 72.71$; $d_0 = 0.9802$

m AgClO₄	c AgClO₄	d (SATURATED SOLUTION)	m AgA	c AgA	$10^3 x_{\pm}$ AgA	$S_{app.}$
0.0	0.0	0.9875	0.04960	0.04858	0.9508	0.04858
0.01168	0.01144	0.9892	0.04460	0.04369	0.9601	0.05513
0.04920	0.04814	0.9937	0.03342	0.03269	1.006	0.08083
0.09618	0.09392	1.0002	0.02613	0.02552	1.081	0.1194
0.1880	0.1829	1.0141	0.01991	0.01937	1.226	0.2023
0.2841	0.2755	1.0297	0.01714	0.01662	1.364	0.2921

TABLE 5

Solubility of silver acetate in the presence of sodium acetate at 25°C. in 20.03 per cent alcohol

$D = 66.97$; $d_0 = 0.9664$

m NaA	c NaA	d (SATURATED SOLUTION)	m AgA	c AgA	$10^3 x_{\pm}$ AgA	$S_{app.}$
0.0	0.0	0.9716	0.03601	0.03478	0.7378	0.03478
0.01018	0.00981	0.9707	0.03190	0.03073	0.7505	0.04054
0.04957	0.04780	0.9717	0.02194	0.02116	0.8104	0.06896
0.1006	0.09683	0.9732	0.01668	0.01605	0.9032	0.1129
0.1987	0.1906	0.9768	0.01316	0.01262	1.074	0.2032
0.5014	0.4754	0.9888	0.01008	0.01032	1.500	0.4857
0.6991	0.6574	0.9962	0.01077	0.01013	1.713	0.6675
1.002	0.9306	1.0068	0.01101	0.01023	2.081	0.9408

TABLE 6

Solubility of silver acetate in the presence of potassium acetate at 25°C. in 20.03 per cent alcohol

$D = 66.97$; $d_0 = 0.9664$

m KA	c KA	d (SATURATED SOLUTION)	m AgA	c AgA	$10^3 x_{\pm}$ AgA	$S_{app.}$
0.0	0.0	0.9716	0.03601	0.03478	0.7378	0.03478
0.01053	0.01017	0.9717	0.03199	0.03089	0.7554	0.04106
0.05067	0.04885	0.9724	0.02207	0.02128	0.8197	0.07013
0.1027	0.09870	0.9734	0.01662	0.01597	0.9093	0.1147
0.2099	0.2009	0.9787	0.01290	0.01235	1.090	0.2133
0.4961	0.4685	0.9918	0.01095	0.01035	1.498	0.4789
0.6953	0.6503	1.0007	0.01083	0.01013	1.744	0.6604
1.004	0.9242	1.0132	0.01115	0.01026	2.096	0.9345

TABLE 7
Solubility of silver acetate in the presence of silver nitrate at 25°C. in 20.03 per cent alcohol
$$D = 66.97; \ d_0 = 0.9664$$

$\frac{m}{AgNO_3}$	$\frac{c}{AgNO_3}$	d (SATURATED SOLUTION)	$\frac{m}{AgA}$	$\frac{c}{AgA}$	$\frac{10^2 x_\pm}{AgA}$	$S_{app.}$
0.0	0.0	0.9716	0.03601	0.03478	0.7378	0.03478
0.01029	0.00993	0.9718	0.03202	0.03090	0.7539	0.04083
0.05064	0.04880	0.9756	0.02228	0.02147	0.8246	0.07027
0.09996	0.09627	0.9822	0.01730	0.01666	0.9197	0.1129
0.2049	0.1968	0.9957	0.01415	0.01358	1.132	0.2104
0.2972	0.2845	1.0080	0.01339	0.01282	1.307	0.2973

TABLE 8
Solubility of silver acetate in the presence of silver perchlorate at 25°C. in 20.03 per cent alcohol
$$D = 66.97; \ d_0 = 0.9664$$

$\frac{m}{AgClO_4}$	$\frac{c}{AgClO_4}$	d (SATURATED SOLUTION)	$\frac{m}{AgA}$	$\frac{c}{AgA}$	$\frac{10^2 x_\pm}{AgA}$	$S_{app.}$
0.0	0.0	0.9716	0.03601	0.03478	0.7378	0.03478
0.01028	0.0093	0.9726	0.03185	0.03075	0.7504	0.04068
0.05216	0.05027	0.9777	0.02146	0.02069	0.8131	0.07096
0.1023	0.09840	0.9853	0.01647	0.01584	0.9031	0.1142
0.2007	0.1924	1.0005	0.01272	0.01220	1.060	0.2046
0.3060	0.2919	1.0162	0.01123	0.01071	1.209	0.3026

TABLE 9
Solubility of silver acetate in the presence of sodium acetate at 25°C. in 30.01 per cent alcohol
$$D = 61.04; \ d_0 = 0.9507$$

$\frac{m}{NaA}$	$\frac{c}{NaA}$	d (SATURATED SOLUTION)	$\frac{m}{AgA}$	$\frac{c}{AgA}$	$\frac{10^2 x_\pm}{AgA}$	$S_{app.}$
0.0	0.0	0.9538	0.02625	0.02493	0.5780	0.02493
0.01045	0.00992	0.9536	0.02215	0.02103	0.5915	0.03095
0.05632	0.05340	0.9547	0.01389	0.01317	0.6863	0.06657
0.1004	0.09501	0.9559	0.01126	0.01066	0.7778	0.1057
0.2063	0.1944	0.9596	0.00946	0.00891	0.9865	0.2033
0.5009	0.4664	0.9708	0.00910	0.00847	1.469	0.4749
0.6691	0.6190	0.9774	0.00941	0.00871	1.710	0.6277
1.019	0.9284	0.9890	0.01021	0.00931	2.161	0.9377

TABLE 10
Solubility of silver acetate in the presence of potassium acetate at 25°C. in 30.01 per cent alcohol
$$D = 61.04; \ d_0 = 0.9507$$

$\frac{m}{KA}$	$\frac{c}{KA}$	d (SATURATED SOLUTION)	$\frac{m}{AgA}$	$\frac{c}{AgA}$	$\frac{10^2 x_\pm}{AgA}$	$S_{app.}$
0.0	0.0	0.9538	0.02625	0.02493	0.5780	0.02493
0.01045	0.00991	0.9523	0.02191	0.02076	0.5861	0.03067
0.05107	0.04835	0.9538	0.01418	0.01342	0.6686	0.06177
0.1044	0.09867	0.9558	0.01111	0.01049	0.7857	0.1092
0.2024	0.1903	0.9606	0.00945	0.00889	0.9772	0.1992
0.5062	0.4690	0.9740	0.00915	0.00848	1.480	0.4775
0.6994	0.6416	0.9819	0.00956	0.00877	1.760	0.6504
1.008	0.9100	0.9941	0.01032	0.00832	2.162	0.9193

nitrate, respectively, as added electrolytes.   The experimental data reproduced in curve I in each of the three figures are taken from the results of a previous investigation (8).

TABLE 11

Solubility of silver acetate in the presence of silver nitrate at 25°C. in 30.01 per cent alcohol

$D = 61.04;$ $d_0 = 0.9507$

m AgNO$_3$	c AgNO$_3$	d (SATURATED SOLUTION)	m AgA	c AgA	$10^3 x_2$ AgA	$S_{app.}$
0.0	0.0	0.9538	0.02625	0.02493	0.5780	0.02493
0.00995	0.00945	0.9550	0.02249	0.02136	0.5945	0.03081
0.04998	0.04644	0.9595	0.01484	0.01408	0.6817	0.06152
0.1002	0.09500	0.9658	0.01178	0.01116	0.7967	0.1062
0.1974	0.1864	0.9776	0.00990	0.00935	0.9896	0.1958
0.3002	0.2826	0.9915	0.00930	0.00876	1.165	0.2914

TABLE 12

Solubility of silver acetate in the presence of silver perchlorate at 25°C. in 30.01 per cent alcohol

$D = 61.04;$ $d_0 = 0.9507$

m AgClO$_4$	c AgClO$_4$	d (SATURATED SOLUTION)	m AgA	c AgA	$10^3 x_2$ AgA	$S_{app.}$
0.0	0.0	0.9538	0.02625	0.02493	0.5780	0.02493
0.01014	0.00964	0.9552	0.02228	0.02116	0.5916	0.03080
0.05296	0.05021	0.9607	0.01398	0.01326	0.6724	0.06347
0.1014	0.09598	0.9680	0.01112	0.01053	0.7759	0.1065
0.2001	0.1885	0.9827	0.00922	0.00868	0.9596	0.1972
0.2974	0.2789	0.9970	0.00881	0.00826	1.130	0.2872

THEORETICAL CONSIDERATIONS

The equilibria that we assume to exist are represented, along with the corresponding equilibrium constants, in equations 1, 2, and 3.

$$\text{I} \quad \text{AgA(s)} = \text{Ag}^+ + \text{A}^-; \quad K_1^x = a_{\text{Ag}^+} a_{\text{A}^-} \tag{1}$$

$$\text{II} \quad \text{AgA}_2^- = \text{Ag}^+ + 2\text{A}^-; \quad K_2^x = \frac{a_{\text{Ag}^+} a_{\text{A}^-}^2}{a_{\text{AgA}_2^-}} \tag{2}$$

$$\text{III} \quad \text{Ag}_2\text{A}^+ = 2\text{Ag}^+ + \text{A}^-; \quad K_3^x = \frac{a_{\text{Ag}^+}^2 a_{\text{A}^-}}{a_{\text{Ag}_2\text{A}^+}} \tag{3}$$
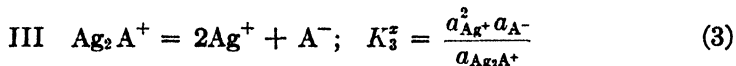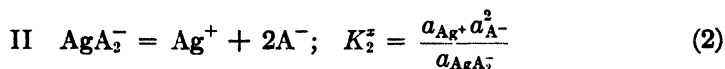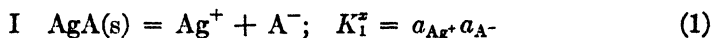
We relate K_2^x and K_3^x to the activity product K_1^x by the equations

$$K_2^x = K_1^x \cdot \frac{a_{\text{A}^-}}{a_{\text{AgA}_2^-}}; \quad K_3^x = K_1^x \cdot \frac{a_{\text{Ag}^+}}{a_{\text{Ag}_2\text{A}^+}} \tag{4}$$

If we make the approximately valid assumption that in a given solution all univalent ions have equal activity coefficients, we can replace the constant activity

ratios of equation 4 by the corresponding concentration ratios. The constants u_1 and u_2 are defined by the equations

$$\frac{u_2}{1 - 2u_2} = \frac{c_{Ag_2A_2^-}}{c_{A^-}}; \quad \frac{u_1}{1 - 2u_1} = \frac{c_{Ag_2A^+}}{c_{Ag^+}} \tag{5}$$

We used, without any essential changes, the method previously reported (6) in applying the theory to our experimental results.[2] Certain numerical changes
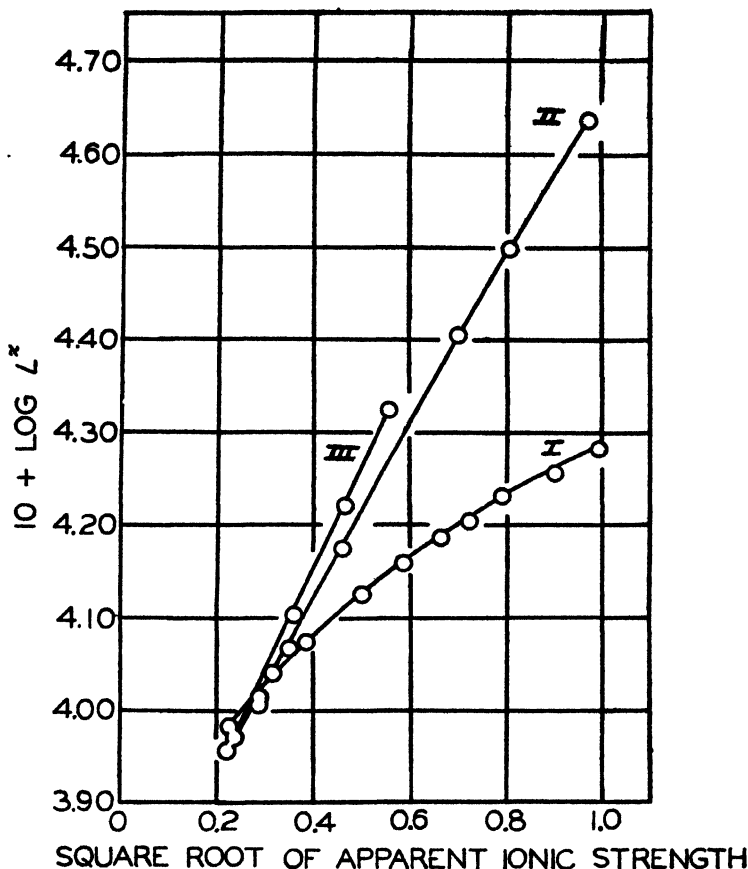
FIG. 1. Logarithm of the apparent solubility product of silver and acetate ions against the square root of the apparent ionic strength. Curve I, sodium nitrate—9.17 per cent alcohol; curve II, sodium acetate—10.17 per cent alcohol; curve III, silver nitrate—10.17 per cent alcohol.

in the Debye equation were necessary; in place of 1.0184 in equation 23, we used $2B$, where for 25°C. B is given by the equation

$$B = 354.37/D^{3/2} \tag{6}$$

[2] We take this opportunity of making the following corrections in the previous paper (6). In equation 14 on page 741 substitute "$c_1 u_1 u_2$" for "$c_2 u_1 u_2$"; in equations 24 to 28 on pages 742 and 743 substitute "$(1 - u_1 u_2)^2$" for "$1 - u_1 u_2$."

and the parameter A is related to the "ionic-diameter" a by the equation

$$A = 2.9124 \times 10^8 \, a/D^{1/2} \tag{7}$$

For the parameter A we adopted an average of the empirical values previously reported (8, 10).
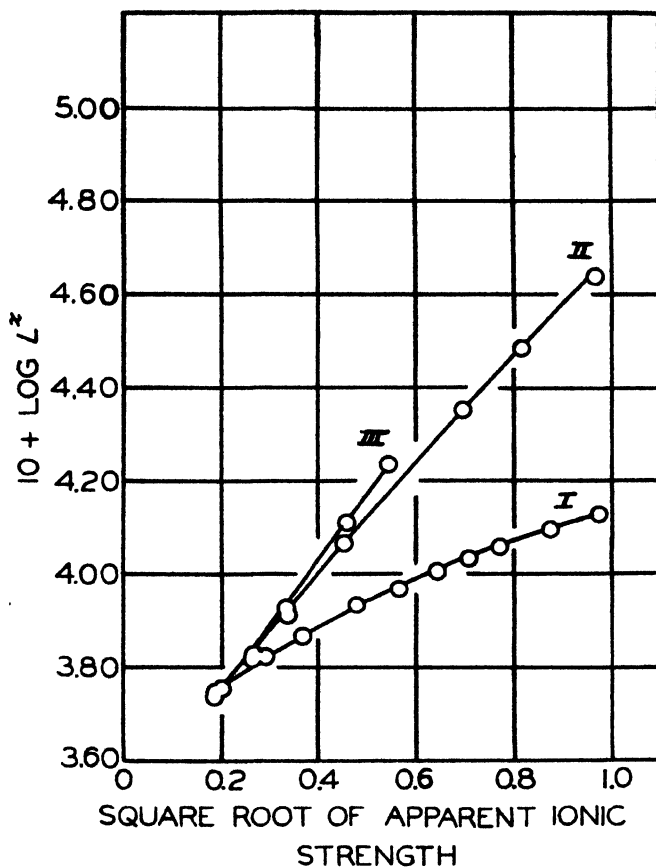
FIG. 2. Logarithm of the apparent solubility product of silver and acetate ions against the square root of the apparent ionic strength. Curve I, sodium nitrate—20.37 per cent alcohol; curve II, sodium acetate—20.02 per cent alcohol; curve III, silver nitrate—20.03 per cent alcohol.

Table 13 summarizes the values of u_1 and u_2 obtained for the various solvents, including from a previous paper (6) the case in which water is the solvent. Values of K_1^x, K_2^x, and K_3^x will be presented in a later section.

The values of u_1 and u_2 given in table 13 were derived using only the data from solutions in which the added electrolytes were sodium nitrate, sodium acetate, and silver nitrate. From our experiments in which potassium acetate and silver perchlorate were the added electrolytes, we might, in a similar manner, have derived a new set of values of u_1 and u_2. However, it seemed to us to be sufficient

(and certainly a great deal easier) to test our fundamental hypothesis by using the tabulated values of u_1 and u_2 in equations 24 and 25 of our previous paper (6) and, by applying these equations to our data for potassium acetate and silver perchlorate, to calculate therefrom values of K_1^a. We even used the same value of A (*viz.*, 1. 3) as was employed in our previous calculations. The results so obtained are found in tables 14, 15, and 16, which include also applications of
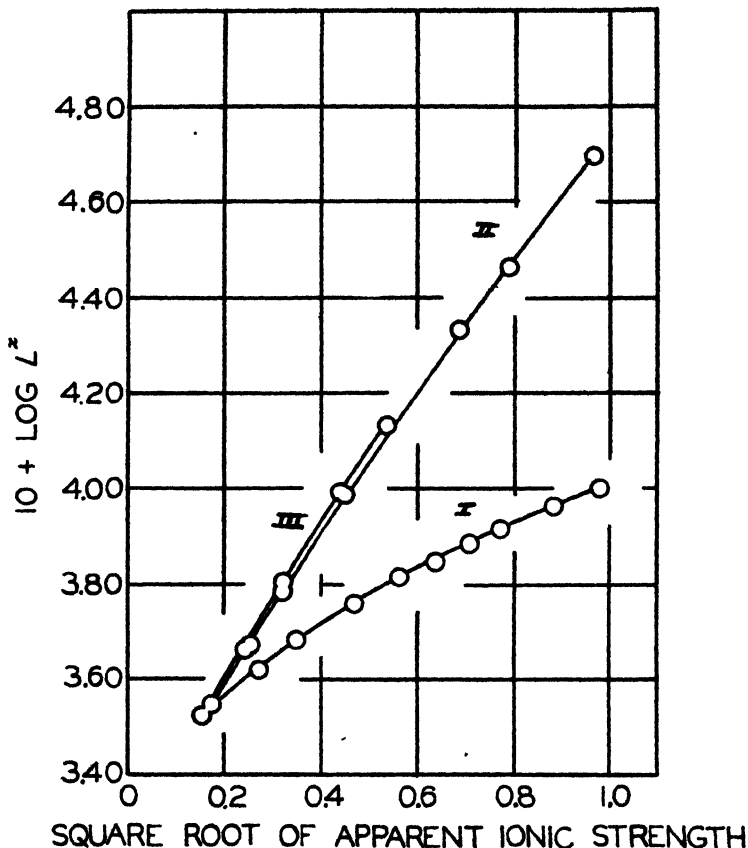
FIG. 3. Logarithm of the apparent solubility product of silver and acetate ions against the square root of the apparent ionic strength. Curve I, sodium nitrate—30.02 per cent alcohol; curve II, sodium acetate—30.01 per cent alcohol; curve III, silver nitrate—30.01 per cent alcohol.

equation 24 or 25 to the individual solutions in which the added electrolytes were sodium acetate and silver nitrate. We give also in each of these tables a grand average of log K_1^a for each of the three solvents employed in this investigation. The calculated values of log K_1^a that have been excluded in forming the mean are enclosed in parentheses.

This procedure of excluding some of our calculated values in forming the mean should certainly be justified. We proceed to offer the following justification.

An examination of tables 14, 15, and 16 will show that the calculated values of $-\log K_1^x$ show a satisfactory degree of constancy at the lower ionic strengths,. but that these values increase systematically at higher ionic strengths; furthermore, this systematic increase begins at lower concentrations when silver nitrate or silver perchlorate is the added salt than when the added electrolyte is sodium or potassium acetate.

We make the following statements:

(1) The experimental evidence presented in this and a preceding paper proves conclusively, in our opinion, the existence of complex ions in our solution. We

TABLE 13

Values of u_1 and u_2 in various solvents

ALCOHOL	u_1	u_2
per cent		
0	0.0317	0.0105
10.17	0.0252	0.0114
20.03	0.0234	0.0130
30.01	0.0234	0.0158

TABLE 14

Values of $\log K_1^x$ in 10.17 per cent alcohol

$u_1 = 0.0252;\ u_2 = 0.0114$

MOLARITY NaA	$-\log K_1^x$	MOLARITY KA	$-\log K_1^x$	MOLARITY AgNO₃	$-\log K_1^x$	MOLARITY AgClO₄	$-\log K_1^x$
0.01135	6.285	0.01051	6.283	0.00993	6.281	0.01144	6.288
0.04920	6.279	0.04898	6.275	0.04916	6.279	0.04814	6.292
0.09687	6.265	0.09803	6.269	0.1028	6.265	0.09392	6.290
0.1918	6.246	0.1946	6.240	0.1964	6.279	0.1829	6.310
0.4747	6.274	0.4855	6.269	0.2920	6.322	0.2755	6.377
0.6347	6.358	0.6622	6.368				
0.9296	(6.852)	0.8134	(6.539)				
Average. .	6.285		6.284		6.285	.	6.295

Grand average: $-\log K_1^x = 6.291$

have represented these ions by AgA_2^- and Ag_2A^+, but we do not exclude the possibility that ions of higher complexity, such as AgA_3^{--} and Ag_3A^{++} may also exist.

(2) The postulate that ions of equal valence in a given solution have equal activity coefficients becomes more nearly exact the lower the ionic strength.

(3) Since the concentration of a complex ion of a given type increases with the concentration of the corresponding added salt, the deviations from "normal behavior" will be greater and more readily detected at the higher ionic strengths.

(4) Combining statements (2) and (3), we see that the error in calculating the concentration of a complex ion will probably be greater for high and for very low concentrations of added salt than for intermediate values.   Tables 14, 15, and 16

show that the concentrations of added salt which we employed were not so low as to involve a serious error; the appreciable errors occur at higher concentrations. Our procedure is in practice equivalent to an extrapolation to zero ionic strength, which gives great weight to the values for low or moderate ionic strengths and little or no weight to those for high ionic strengths.

TABLE 15

Values of log K_1^z in 20.03 per cent alcohol

$u_1 = 0.0234; u_2 = 0.0130$

MOLARITY NaA	$-\log K_1^z$	MOLARITY KA	$-\log K_1^z$	MOLARITY AgNO₃	$-\log K_1^z$	MOLARITY AgClO₄	$-\log K_1^z$
0.00981	6.500	0.01017	6.496	0.00993	6.500	0.00993	6.503
0.04870	6.488	0.04885	6.480	0.04880	6.488	0.05027	6.503
0.09783	6.474	0.09870	6.461	0.09627	6.480	0.09840	6.503
0.1906	6.438	0.2009	6.440	0.1968	6.489	0.1924	6.564
0.4754	6.562	0.4685	6.551	0.2845	6.550	0.2919	(6.749)
0.6574	(6.904)	0.6503	(6.876)				
0.9306		0.9242					
Average....	6.493	....	6.485	....	6.501	....	6.518

Grand average: $-\log K_1^z = 6.499$

TABLE 16

Values of log K_1^z in 30.01 per cent alcohol

$u_1 = 0.0234; u_2 = 0.0158$

MOLARITY NaA	$-\log K_1^z$	MOLARITY KA	$-\log K_1^z$	MOLARITY AgNO₃	$-\log K_1^z$	MOLARITY AgClO₄	$-\log K_1^z$
0.00992	6.718	0.00991	6.725	0.00945	6.715	0.00964	6.720
0.05340	6.685	0.04835	6.696	0.04744	6.692	0.05021	6.711
0.09501	6.665	0.09867	6.664	0.09500	6.679	0.09598	6.710
0.1944	6.661	0.1903	6.662	0.1864	6.751	0.1885	(6.815)
0.4664	(7.180)	0.4690	(7.191)	0.2826	(7.020)	0.2789	(7.124)
0.6190		0.6416					
0.9284		0.9100					
Average....	6.682	.. ..	6.687	....	6.709	....	6.714

Grand average: $-\log K_1^z = 6.698$

(5) We come now to the difference between the effects of silver nitrate or silver perchlorate on the one hand and sodium acetate or potassium acetate on the other. This difference can be readily accounted for if we suppose (a) that complex ions (such as AgA_3^{--} and Ag_2A^{++}) are also formed to some extent; (b) that the dissociation constant of Ag_3A^{++} into $Ag^+ + Ag_2A^+$ is smaller than the corresponding dissociation constant of AgA_3^{--} into $A^- + AgA_2^-$. Examination of table 17 shows that K_3 (the dissociation constant of Ag_2A^+) is appreciably smaller than

K_2 (the dissociation constant of AgA_2^-). If Ag_2A^+ is a stabler structure than AgA_2^-, it is probable that Ag_3A^{++} is stabler than the corresponding AgA_3^{--}. Note that the concentrations of Ag_3A^{++} and of AgA_3^{--} will be proportional to $(c_{Ag^+})^2$ and $(c_{A^-})^2$, respectively. A mathematical treatment leads to the conclusion that if higher complex ions are also present, the values of u_1 and u_2 defined by equation 5 and calculated on the assumption that the only complex ions present are Ag_2A^+ and AgA_2^- will be larger than the true values. The deviation will increase with the concentration of the added salt and will increase more rapidly for u_1 than for u_2. Turning now to equation 28 in a previous paper (6), which gives a relation between K_1^x, K_{st}^x, u_1, and u_2, we see that on the basis of the preceding discussion we should expect the following behavior: (a) for low and moderate concentrations of added salt, the calculated values of u_1 and u_2 should be close to their true values and hence constant values of K_1^x should be obtained; (b) at greater concentrations of added salt, the calculated values of K_1^x will be less than the true value; (c) the decrease in the calculated value of K_1^x should occur at a lower concentration when silver nitrate or silver perchlorate is the added salt than when the solution investigated contains sodium acetate or potassium

TABLE 17

Final values of various equilibrium constants

SOLVENT	$K_{st}^m \times 10^3$	$K_1^x \times 10^7$	$K_1^m \times 10^3$	$K_2^x \times 10^5$	K_2^m	$K_3^x \times 10^5$	K_3^m
Water....	2.83	8.08	2.49	7.5	0.23	2.4	0.073
10.17% Alcohol .	1.55	5.12	1.39	4.4	0.12	1.9	0.052
20.03% Alcohol .	0.841	3.17	0.753	2.4	0.056	1.3	0.031
30.01% Alcohol.	0.465	2.01	0.412	1.2	0.025	0.82	0.017

acetate as added electrolyte. Of course, a decrease in K_1^x means an increase in $-\log K_1^x$.

Following table 16 we give in table 17 our final values for the various equilibrium constants in water and the three alcoholic solvents. They are expressed in terms of molal activities (as in K_1^m), as well as in terms of mole-fraction activities (as in K_1^x). We include also values of K_{st}^m, the stoichiometric activity product of silver acetate in each of the four solvents. The values of K_1^x, K_1^m, and K_{st}^m are believed to have an uncertainty of less than 3 or 4 per cent; those of K_2 and K_3 may be uncertain by as much as 10 per cent.

VARIATION OF EQUILIBRIUM CONSTANT WITH DIELECTRIC CONSTANT OF SOLVENT

An equation developed by Born (2) enables one to compare equilibrium constants for a given reaction in different solvents. If we adopt the simple hypothesis that a given ion of charge z_i remains essentially identical in the various solvents concerned and hence that it can be characterized by the same effective radius r_i in the various solvents, we obtain the following equation:

$$\ln K^x = \text{constant} - \frac{N\epsilon^2}{2DRT} \sum \frac{\nu_i z_i^2}{r_i} \tag{8}$$

For a temperature of 25°C. this equation becomes

$$\log K^z = \text{constant} - \frac{121.6}{D} \sum \frac{\nu_i z_i^2}{r_i} \tag{9}$$

where r_i is to be expressed in Ångström units.

In figure 4 we have plotted $-\log K_1^z$, $-\log K_2^z$, and $-\log K_3^z$ against $1/D$ for the four solvents we have employed. The four points, in each case, fall pretty
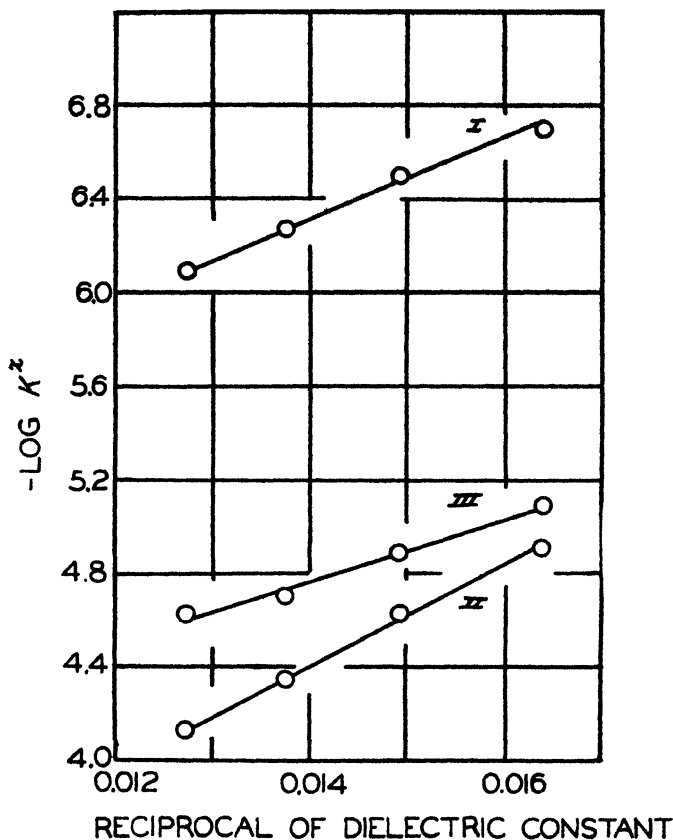
Fig. 4. Logarithm of equilibrium constants against the reciprocal of the dielectric constant. Curve I, K_1^z; curve II, K_2^z; curve III, K_3^z.

well on a straight line, in agreement with the requirements of equation 9. The equations for the three straight lines, obtained by the method of least squares, are as follows:

$$\log K_1^z = \bar{5}.985 - \frac{164.7}{D} \tag{10}$$

$$\log K_2^z = \bar{2}.630 - \frac{217}{D} \tag{11}$$

$$\log K_3^z = \bar{3}.036 - \frac{129}{D} \tag{12}$$

Comparing equations 10, 11, 12 with equation 9, we find:

$$\frac{1}{r_{Ag^+}} + \frac{1}{r_{A^-}} = 1.35 \qquad (13)$$

$$\frac{1}{r_{Ag^+}} + \frac{2}{r_{A^-}} - \frac{1}{r_{AgA_2^-}} = 1.8 \qquad (14)$$

$$\frac{2}{r_{Ag^+}} + \frac{1}{r_{A^-}} - \frac{1}{r_{Ag_2A^+}} = 1.1 \qquad (15)$$

Since there are four different ionic radii, the three equations (13, 14, and 15) do not suffice for their determination. In any case, even if the Born theory were unobjectionable, we do not consider that the experimental data, especially with respect to K_2 and K_3, are accurate enough to warrant drawing quantitative inferences from equations 13, 14, and 15. Nevertheless, if we were to define a mean radius r of Ag^+ and A^- by the equation

$$\frac{2}{r} = \frac{1}{r_{Ag^+}} + \frac{1}{r_{A^-}}$$

we should obtain from equation 13 a value of r equal to 1.5 Å., which is certainly of the correct order of magnitude. On the whole, then, we think we are justified in saying that the application of the Born theory to our experimental data leads to results that are not incompatible with what we know from other evidence about ionic dimensions.

STABILITY AND STRUCTURE OF THE COMPLEX IONS

The structures of AgA_2^- and Ag_2A^+ have been discussed in a previous paper (6) and need not be examined here.

From equations 4 we can obtain the relation

$$\frac{a_{Ag_2A^+}}{a_{AgA_2^-}} = \frac{a_{Ag^+}}{a_{A^-}} \cdot \frac{K_2^z}{K_3^z} \qquad (16)$$

It follows then from the values of K_2 and K_3 given in table 17 that if, in each of the four solvents we have employed, Ag^+ and A^- are present at equal concentrations, the ratio of Ag_2A^+ to AgA_2^- will be about 3 in an aqueous solution and will drop to about 1.5 in 30 per cent alcohol. These conclusions may be expressed in the statement that at 25°C. and in the four solvents studied the complex ion Ag_2A^+ is more stable than AgA_2^-.

SUMMARY

1. Measurements have been made of the solubility at 25°C. of silver acetate in the presence of sodium acetate, potassium acetate, silver nitrate, and silver perchlorate in 10, 20, and 30 per cent ethyl alcohol.

2. The apparent solubility product of silver acetate in the presence of any one of the four electrolytes mentioned is greater, for a given apparent ionic strength, than when the added electrolyte has no ion in common with silver acetate.

3. The apparent inapplicability of the theory of Debye can be accounted for quantitatively by assuming the formation of the complex ions Ag_2A^+ and AgA_2^-.

4. The activity product of Ag^+ and A^- and the dissociation constants of AgA_2^- and of Ag_2A^+ in various solvents have been determined.

5. The acetatodisilver ion is more stable than the diacetatoargentate ion.

6. The Born equation leads to values of the ionic radii which are of the right order of magnitude.

REFERENCES

(1) ÅKERLÖF, G.: J. Am. Chem. Soc. **54**, 4125 (1932).
(2) BORN, M.: Z. Physik **1**, 45 (1920).
(3) *International Critical Tables*, Vol. III, p. 116. McGraw-Hill Book Company, Inc., New York (1929).
(4) KOLTHOFF, I. M., AND SANDELL, E. B.: *Textbook of Inorganic Quantitative Analysis.* The Macmillan Company, New York (1937).
(5) MacDOUGALL, F. H.: J. Am. Chem. Soc. **52**, 1390 (1930).
(6) MacDOUGALL, F. H.: J. Phys. Chem. **46**, 737 (1942).
(7) MacDOUGALL, F. H., AND ALLEN, MARTIN: J. Phys. Chem. **46**, 730 (1942).
(8) MacDOUGALL, F. H., AND BARTSCH, C. E.: J. Phys. Chem. **40**, 649 (1936).
(9) MacDOUGALL, F. H., AND LARSON, W. D.: J. Phys. Chem. **41**, 417 (1937).
(10) MacDOUGALL, F. H., AND REHNER, JOHN, JR.: J. Am. Chem. Soc. **56**, 368 (1934).
(11) SMITH, G. F., AND RING, F.: J. Am. Chem. Soc. **59**, 1889 (1937).

NEW BOOKS

Isomerization of Pure Hydrocarbons. BY GUSTAV EGLOFF, GEORGE HULLA, AND V. I. KOMAREWSKY. 499 pp. New York: Reinhold Publishing Corporation, 1944. Price: $9.00.

This monograph is an exhaustive treatment of the important subject of hydrocarbon isomerization. Upon examining the book, it becomes clear that the authors have expended considerable effort in preparing the volume, especially the tabulations. Many of the items covered would not be easily found in the literature, so the book should prove to be a time-saver for those interested in the field.

The monograph consists of three main parts, namely: six chapters of discussion, extensive tables of isomerizations, and a section of appendices. In addition it contains a complete bibliography (681 references) as well as author and subject indexes.

As stated in the summary, isomerizations are discussed for "alkanes, alkenes, allenic alkadienes, . . . bicyclodienes with saturated side chains, tricyclenes, . . . [etc.],"—a total of forty-six different headings. This is done in the six chapters of textual material, each of which is frequently interspersed with conclusions. Numerous theories and mechanisms of the isomerization reactions appear in the discussion, with several alternatives given for many of the reactions. It is clear from reading the book that isomerizations are quite specific reactions, with the result that the reader does not learn many generalizations. This is no fault of the book, of course, but is a result of the complex nature of the subject treated.

The tables of isomerization data, which comprise about one-third of the entire volume, should prove to be most useful. These tables provide, in convenient form, the following information about isomerizations: reactants (including catalysts), conditions of reaction, products of reaction, and appropriate references to the literature.

On the whole the book provides an excellent summary of the vast literature concerning isomerization of hydrocarbons and it should find a useful place in the libraries of those interested in hydrocarbons and their reactions. Although some of the data are necessarily meagre, the monograph is nevertheless complete up to the time of publication.

F. T. WALL.

Chemistry and Technology of Food and Food Products, Vol. II. M. B. JACOBS, *Editor.* 890 pp. New York: Interscience Publishers, Inc., 1944. Price: $10.50.

This is the second of the two volumes in this series, the first of which was reviewed in this Journal (Volume 49, page 44). The several parts of the extended series of contributions are numbered serially through the two volumes. Thus Volume II comprises: Part III. Unit Operations and Processes; Part IV. Sanitary and Quality Control; Part V. Preservation; and Part VI. Production. Each part in turn is divided into several chapters.

Under "Unit Operations and Processes", the author, Kenneth M. Gaver, discusses the types of equipment and physical or other manipulations involved in handling raw materials, and in general and typical processing. Part IV includes the following contributions: "Food Supervision by Government Agencies", by Jerome Trichter and Sol Pincus; "Food Grading", by T. A. Samuelson; "Food Machines", by A. E. Abrahamson; "Washing, Detergency, Sanitation and Plant Housekeeping", by John L. Wilson; "Insect Control", by H. H. Shepard; "Prevention and Control of Rodent Life" by B. E. Holsendorf.

Part V, "Preservation", is divided into chapters on dehydration, temperature control, hermetically sealed containers, microörganisms, chemicals, and packaging as food-preserving practices.

Part VI, "Production", occupies nearly one-half of this volume and contains chapters on groups of commodities, including production and/or processing of cereal grains; bread and bakery products; fruit juices; jams, jellies, and preserves; milk and milk products; meat and meat products; oils and fats; non-alcoholic beverages; and alcoholic beverages. There is also a chapter on industrial waters, and their uses in various departments of food processing.

It follows, perforce, that the limitations of space in a single volume devoted to so many subjects have resulted in reducing many sections to small proportions. Thus Chapter XX, on milk and milk products, covers only 32 pages, and would hardly serve as an adequate textbook for students of milk technology. The same might be said of several other special fields that are covered briefly in this book. Moreover, the description of a process and of the resulting products may appear in Volume II, while the data on the composition of these or related products may be recorded in Volume I. The interests of the student might have been served better had the chemistry of the processing described in the present volume been traced, together with the discussion of the mechanics of the treatments that are described.

For a general overview of the broad general field of food technology, this book and its companion volume should prove very useful. They cover a wide range of plant engineering, biological, and biochemical interests. So far as the reviewer's knowledge justifies a judgment in this very inclusive area, the material presented appears to be adequate and up-to-date.

C. H. BAILEY.

Thomas Jefferson and the Scientific Trends of his Time. BY CHARLES A. BROWNE. Excerpt of 65 pages from the Chronica Botanica (Vol. 8, No. 3), Waltham, Massachusetts, 1944. Price: $1.25.

Few if any public men of the present have so much contact with and knowledge of the sciences and of agriculture as had Jefferson, Franklin, Washington, and some of the other founders of our Republic. Dr. Browne has given an excellent account of Jefferson's widely diversified interests in science, which by intention were rather strictly confined to utili-

tarian ends. It was perhaps his conservatism which prevented his carrying through the plan he began so well for the adoption of the metric system in the United States. Had he persevered to success in this it would have been a contribution of equal merit to his support of the Lewis–Clark expedition or to the founding of the University of Virginia. What statesman of the future will be equal to the task, which has now become truly Herculean?

Dr. Browne's long services to the Department of Agriculture have especially fitted him to appreciate Jefferson's ideas applicable to agriculture, horticulture, animal husbandry, soil conservation, botany, etc. It is noteworthy that, although he lived through the period in which Lavoisier revolutionized chemistry and overthrew the phlogiston theory, Jefferson never adopted the new ideas nor terminology, again evidence of his conservatism in science.

S. C. LIND.

The Svedberg, 1884–1944. Uppsala: Almquist and Wiksells Boktryckeri, 1944.

In honor of The Svedberg's sixtieth birthday (August 30), the Institute of Physical Chemistry of the University of Uppsala has issued a volume of 730 pages, containing fifty-six contributions from seventy alumni and members of the staff of the Institute: thirty-seven papers in English, twelve in German, five in Swedish, and two in French.

The subjects treated cover an extraordinarily wide range, extending outside the fields in which Professor Svedberg is so well and favorably known in the United States. The biological and industrial applications of Svedberg's work are proving their importance for Sweden's technological future.

S. C. LIND.

Advances in Enzymology and Related Subjects of Biochemistry, Vol. IV. F. F. NORD AND C. H. WERKMAN, *Editors.* 332 pp.: 45 illustrations. New York: Interscience Publishers, Inc., 1944. Price: $5.50.

Ten authors have contributed to the fourth volume of this series of independent monographs.

The direct and explicit aid rendered by chemistry to the understanding of genetics and biological evolution has been rather limited. A chemical formulation of gene structure and gene action, which depends closely upon the structural picture we make at present of the protein molecule, is discussed by Addison Gulick. An analogy exists between genes and viruses; both catalyze their own synthesis and therefore constitute units of heredity. An assumption is proposed that each gene has one enzymatic function which may explain defect mutations of a metabolic nature.

The specificity and mechanism of action of the glycosidases are reviewed and a provisional classification of the carbohydrases is suggested in the article by William Ward Pigman. The investigations on the action of enzymes on glycosides and various derivatives provide one of the most extensive studies made of the influence of structure on the rate of a chemical reaction.

The transamination reaction, transfer of amino groups from α-amino acids to α-keto acids, is discussed by Robert M. Herbst. Model systems are·considered briefly, while a more detailed account of enzyme-catalyzed transaminations is given, indicating the significance of the reaction in metabolic processes of animal and plant cells.

J. M. Nelson and C. R. Dawson present an interpretation of the physical nature and action of tyrosinase, supplemented by numerous experiments from their laboratory.

An excellent review by Rollin D. Hotchkiss deals with antagonistic effects of gramicidin, tyrocidine, and tyrothricin on the growth of susceptible microörganisms. The crystalline substances gramicidin and tyrocidine have been studied chemically and biochemically, with the aim of relating their chemical and physical natures to the mechanism of their antibacterial action.

Biological energy transformations and their possible relations to cancer problems are discussed by V. R. Potter.

The results of various investigations concerning the influence of hormones on enzymatic

reactions are summarized by H. Jensen and Leon E. Tenenbaum. A close physiological interrelationship seems to exist between hormones, enzymes and vitamins. However, our present knowledge of the mechanism by which the various endocrine principles may affect enzymatic reactions is rather meager and does not permit any definite conclusions.

The use of absorption spectra in the study of vitamins, hormones, and coenzymes has become an important tool for determining the concentration, structure, and identity of these compounds. The fundamentals underlying the absorption phenomenon as well as its numerous applications are discussed by Wallace R. Brode.

ERWIN HAAS.

Colorimetric Determination of Traces of Metals. BY E. B. SANDELL. New York: Interscience Publishers, Inc., 1944.

Dr. Sandell has earned signal applause for this new book on quantitative analysis. He has lifted the term "trace" from a limbo of ambiguity and attempted to furbish it to a degree which will justify its use in scientific language. A trace has often been an expression of the analytical chemist's limitations, or the *deus ex machina* by which vagaries of catalytic or medicinal properties, reaction rates, or the fundamental properties of color, taste, odor, etc. could be plausibly explained. When one considers the many vast fields—metallurgy, agriculture, nutrition, etc.—in which it is imperative to give precision to the meaning of "trace", one can realize what a wide welcome this book deserves.

The discussion of the first two chapters on trace analysis and its general method are not duplicated elsewhere in the chemical literature and possess great value apart from the rest of the book. We are inclined by conventionalities of thought to underestimate the importance of so-called "traces". If we take, as a lower limit, 0.000,01 per per cent for spectrographic analysis, a spectroscopically pure gram-atom containing 6.06×10^{23} atoms, may still contain 6.06×10^{16} atoms of one or many other elements! If we discuss the purity of water, we give the concentration of traces in terms of parts per million, but, if we deal with iron, another high-tonnage product, we speak in ten thousandths of a per cent for corresponding concentrations. With water, "parts per million" is the common term for discussing its quality, but how seldom is commercial iron assessed in terms of impurities present in only a ten thousandth of a per cent. Yet we cannot be sure that they are less important to the latter than the former. In fact, evidence suggests otherwise. Dr. Sandell points out the desirability of speaking of concentration in terms of a logarithmic scale which would improve our perspective. A change of 0.01 per cent in the absolute amount of an impurity is more significant when it constitutes only 0.05 per cent of the total than when it comprises 50 per cent, and this significance is more apparent on a logarithmic scale.

The third chapter deals with the general problem of colorimetry and spectrophotometry. There is no room for the adequate treatment of instruments available for this work, but there is an original and valuable discussion of error in colorimetry which transcends the former in importance because of its neglect by other authors. Although Dr. Sandell has not exhausted the subject, particularly with respect to psychological factors which are hard to assess, he has provided an important and original approach. The hue, as well as the density (the only factor controlled by Beer's Law), often enters into visual estimations, as in the dithizone procedure referred to at the top of page 85. Similarly, volumes of a colored lake, not readily measured by a photometer, may, as in the aurin method for aluminum (page 116), be compared reliably by the eye when matching unknowns with standards.

This chapter is marked by the inclusion of many excellent tables such as are used throughout the book for summarizing and surveying. It is interesting to note from Table 4 that one may generally increase the sensitivity of measurement about ten times by the use of a spectrophotometer instead of visual comparison.

On page 53 the author fails to point out that in working with solutions of high transmittancy, above 80 per cent, the error in the measurement may be reduced by the use of longer or deeper cells.

On page 62 a further procedure may be added in Table 7 under B to minimize interference. A large excess of the interfering ion may be added until its concentration becomes so great that small variations in the interfering ion no longer interfere with the color. For example, this method has been used to eliminate the interference of phosphates in the determination of titanium and to minimize the effect of hydrogen-ion concentration on the determination of phosphate by the method of Misson.

On page 45, in mentioning the use of colored glasses as standards, the work of Mellon and his associates on the preparation of stable solutions for permanent standards spectro-photometrically matched with evanescent colors, such as the silicomolybdate complex, has not been mentioned. No mention is made here or elsewhere of the "grey solution" methods of A. Thiel, which have not so far attained importance in this country.

No mention is made in this chapter that the precision of instruments is often limited by their optical quality, by reflections, and by other mechanical considerations. This is important to keep in mind, as there is a popular tendency to minimize the sensitivity of the eye and to believe that all the problems of photometry are solved by the use of a photo-electric cell in one form or another.

One valuable achievement of Dr. Sandell has been to make plain in this book avenues of investigation which will further the extent and accuracy of application of colorimetric methods. Beyond the service that the statement of these problems renders the practicing analyst, is the assistance it lends the cause of analytical chemistry by emphasizing to students fertile areas of activity and by dispelling the suspicion wherever it may still exist that analytical chemistry is not a living subject.

The fourth chapter, devoted to general colorimetric reagents, provides valuable information on the chemistry of many commonly used reagents and will be welcome to any chemist attempting to use these substances intelligently. The treatment of dithizone is especially thorough, and correspondingly useful.

The remainder of the book is devoted to the methods useful for individual metals. One of the greatest virtues of the book is that the treatment is eclectic and not encyclopedic, as the author makes clear in the Introduction. Dr. Sandell's experience in the determination of trace metals is shared with the reader in a knowledgeable selection of methods clearly described. Evidences of thoughtful selection in the methods given are everywhere plain, and the user of the book will look forward to a similar treatment of boron, sulfur, phosphorus, nitrogen, and other elements classed as non-metals and hence not included in the present work.

The publishers have earned the gratitude of analytical chemists by their establishment of this series of monographs. It is to be hoped that their venture will receive the continued support of readers and authors which will insure its permanent success.

S. E. Q. ASHLEY.

THE PHYSICAL CHEMISTRY OF MEMBRANES WITH PARTICULAR REFERENCE TO THE ELECTRICAL BEHAVIOR OF MEMBRANES OF POROUS CHARACTER. III

THE GEOMETRICAL AND ELECTRICAL STRUCTURE OF MEMBRANES OF POROUS CHARACTER; SOME EXAMPLES OF THE MACHINE ACTION OF MEMBRANES[1]

KARL SOLLNER

Department of Physiology, University of Minnesota, Minneapolis, Minnesota

I. THE HETEROPOROUS CHARACTER OF REAL MEMBRANES

In this and following sections an attempt will be made to integrate the experimental results reported in preceding papers (15, 16) and many older observations into a tentative picture of the geometrical and electrical structure of membranes of porous character.

The work of Collander (6), Michaelis (11), and other investigators provides sufficient experimental proof that real membranes are not homoporous but heteroporous, having pores of many different sizes, the relative frequency of various pore sizes being distributed, one must assume, according to the Gauss distribution curves characteristic of different kinds of membranes. The empirical permeability characteristics of real membranes can hardly be explained without emphasis upon their heteroporous character.[2] The heteroporosity of membranes has been stressed also by investigators who try to elucidate membrane structures primarily from the geometrical-mathematical point of view, foremost among them Manegold (9). This line of approach, however, has yielded limited success. It ordinarily suffers still from the fatal fallacy of assuming a fictitious mean pore size, in other words, an unreal homoporous structure.

The correlation of the heteroporous character of membranes with electrolyte permeability has been touched upon by Michaelis and collaborators; some of its consequences were discussed several years ago by the author (8, 14, 20). An extensive and thoroughgoing discussion of this problem has never appeared.

If a heteroporous membrane which is not strictly impermeable to ions of the same charge separates two solutions with differing concentrations of the same electrolyte, the various pores of the membrane yield different potentials according to their widths and electrical characteristics. The measurable membrane potential is, so to speak, the overall resultant of the several individual pore potentials. The different pores act upon one another, and thereby set up local

---

[1] Presented in abstract form before the Division of Colloid Chemistry at the 108th Meeting of the American Chemical Society, New York City, September 14, 1944.

[2] It is only the difficulty of providing a sufficient number of experimental data which prevents the evaluation of apparent or effective pore size distribution curves from permeability data obtained with non-electrolytes. If sufficient data were available, this would be relatively easy; the theoretical difficulties are relatively small.

electrical circuits.[3] The electrical heterogeneity of pores may be due either to differences in effective width, or to differences in the distribution of the dissociable groups in similar pores, or to a combination of these two factors.[4] The singular cases of strictly anion or cation impermeable membranes with which (geometrical) heteroporosity can lose its electrical significance will be mentioned below.

The heteroporous character of collodion and other real membranes could be anticipated when one considers their formation.[5] For instance, in the formation of a collodion film the nitrocellulose molecules become aggregated to form micelles of various sizes and various degrees of regularity, and the micelles align themselves more or less in a random manner, at least in two dimensions, to form the membrane (a two-dimensional orienting effect upon the micelles being exerted at the surfaces of the membrane). This picture of the collodion membrane is similar to the concept of the "brush heap" structure of gels. A plate of compressed straw or hay or a cocoanut fibre door mat may be taken as a macroscopic analogy of the collodion membrane.

In the more or less random aggregation of irregular micelles the interstices must of necessity be heterogeneous in character, and (except if the membrane is extremely thin) many cross connections between the various interstices and many dead-end cavities must exist. This complex structure of the membranes makes it impossible to distinguish well-defined individual pores. When discussing the penetration of a solute through such a membrane it seems advantageous to consider rather the possible pathways which are open differentially to various solute molecules according to the size of the latter. The availability of any particular pathway for non-electrolytes of a given molecular size is obviously determined by its narrowest spot; with electrolytes, or more correctly with ions, the availability of a pathway is dependent upon a combination of this geometrical factor and an electrical factor, the repelling action exerted on ions of the same sign of charge by the fixed charged groups on the pore walls.

II. THE GEOMETRICAL AND ELECTRICAL STRUCTURE OF REAL MEMBRANES

In the discussion of the electrical factor which governs (in combination with a purely geometrical factor) the behavior of membranes towards electrolyte

---

[3] The situation in this respect is analogous to the situation frequently found with metals immersed in electrolyte solutions. Here for various reasons, such as the presence of impurities, mechanical stress, differences in crystal size, etc., electrical potential differences arise which cause local electrical circuits. Such local circuits are known to be one of the main causes of metallic corrosion.

[4] The theory of anomalous osmosis put forward by the author (K. Sollner: Z. Elektrochem. **36**, 36, 234 (1930)) takes into account only differences in pore width. It would not be difficult to expand this theory to cases of differences in charge distribution.

[5] Attempts to build up artificially homoporous membranes have so far been unsuccessful. Certain crystalline substances, if free from imperfections, conceivably could behave as homoporous membranes. The clay membranes of Marshall and collaborators (C. E. Marshall and W. E. Bergman: J. Am. Chem. Soc. **63**, 1911 (1941); J. Phys. Chem. **46**, 52, 325 (1942); C. E. Marshall and C. A. Krinbill: J. Am. Chem. Soc. **64**, 1814 (1942)) are of the greatest interest in this connection.

solutions one must recall the results of the studies of the base-exchange capacity and the acid number of collodion which were reported in a preceding paper (16). These studies have indicated that the acidic groups which cause the characteristic electrochemical behavior of collodion are distributed sparsely, and that no simple relationship could be found between the base-exchange capacity of a given collodion preparation or its acid number and the electrochemical activity of the membranes prepared therefrom (17, 18, 19). It is on account of the scarcity of the dissociable groups that the problem of their distribution arises. If they were so numerous as to be present in every geometrically possible spot on the pore walls of the membranes, i.e., if they were closely packed like fatty acid molecules in a condensed film, the problem of their distribution would not arise. The relative scarcity of the dissociable groups gives rise to such situations as were indicated in figure 1 (on page 174) of a preceding paper (16). The chances that a dissociable group is present in a short pore are small. It is easy to see that their distribution becomes critical to membrane behavior if every non-branching part of a pore does not contain at least one dissociable group which completely blocks the pore for ions of the same sign. One may add that the water content in volumes per cent and the charge density of the three membranes represented in figure 1 (page 174) in a preceding paper (16) is the same; nevertheless, the electrical effects are entirely different, as has been pointed out previously (16). With pores which are wider than those indicated in this figure the situation is more complicated: the problem of the simultaneous action of two (or more) groups arises, which obviously is determined by their relative position. The schematic figures given below are helpful in clarifying this problem.

Figure 1 indicates in a rough way how the ionic selectivity of pores carrying fixed charges on their pore walls may be visualized, the plus and minus signs indicating the cations and anions, respectively. The continuous circles around the plus or minus signs represent the size of the ions (or ionized groups, respectively) including their effective shell of hydration, the outer dotted circles indicating the effective range of the electrical force of repulsion acting between the fixed charges situated on the pore walls and ions of identical signs in the solution. According to the best information available, the size of the hydrated ions changes but little with changing concentration. However, the distance over which the repulsive forces of the charges are effective changes greatly with the concentration or, more correctly, with the ionic strength.[6]

It is quite easy to see how under proper conditions a single charge in a given pore may block it completely for the passage of ions of the same sign. This occurrence is indicated in figure 1. In this and subsequent figures an arrow indicates how far the ions identical in sign with the charged wall groups may penetrate (from the left side) into the pores; an arrow across the whole length of the pore indicates that these ions are able to pass through the pore.

---

[6] In a qualitative way this picture explains the concentration effect as well. It could be used as the basis of a quantitative theory of electromotive membrane behavior which would present marked analogies with the Gouy theory of the electrical double layer. However, it should be realized that at the present time little is known about such matters as the relative efficiency of the mechanical and the electrical blocking of pores.

In wider pores the situation may easily arise that a single charge at any given spot of the pore would be unable to effect complete blockage to the passage of ions of the same sign. Even if several charged groups are located in a pore, the situation is not much different, provided the dissociable groups are so far apart that they cannot act simultaneously on an ion of the same sign in solution (compare figure 2). If, however, two (or more) charges should coincide fairly closely in their position in the pore, as indicated in figure 3, then even a fairly wide pore may become completely impermeable for ions carrying the same charge as the fixed charges on the pore walls.

It was indicated previously that there is no reason to assume that the pores in any real membrane are as simple and homogeneous as those indicated in the schematic figures 1, 2, and 3. With pores having a width which varies from point to point, the situation is less simple. Figures 4 and 5 indicate how in geometrically identical pores of this type the location of the fixed charged groups determines the electric characteristics of the pore. If a fixed charge is located
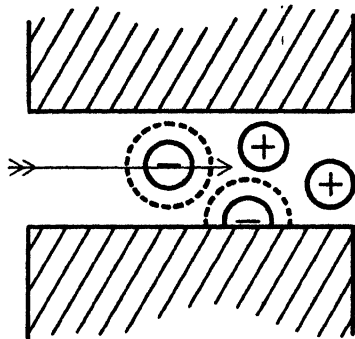
FIG. 1. The blockage of the passage of ions by one fixed charged group of the same sign in a narrow pore.

at a fairly wide spot, it is rather ineffective (figure 4) and does not block the pore completely for the passage of ions of the same sign; however, if located at a narrow spot, it can completely block the pore for ions of the same sign (figure 5).

In the case of the more complex pores, their length, the charge density, and distribution determine their electrical behavior in a similar manner as with the highly schematized cylindrical pores. With membranes of a given water content and a given charge density on the pore walls, the chance that an electrically effective group will be present at a narrow spot is greater the more irregular the pores, provided the membrane is thick compared with the average distance between two charged groups. This means that the more irregular are the micelles which form the pore walls, the higher will be the electrical efficiency of the average pore in a membrane formed from collodion of a given acid number.

So far only individual pores or parts of pores which do not branch have been discussed. However, it was indicated before that this situation cannot be expected to prevail with collodion or similar membranes. Branching of pores as well as dead-end cavities must occur, as indicated in figure 6. It is easy to

visualize the effect of different locations in the same geometrical structure of an identical number of charged groups. A few suitably located fixed charges may completely block such a heteroporous system of pathways for ions carrying the same sign of charge; a higher average charge density with the groups less favorably located may still allow the passage of some such ions.

The picture of the collodion membrane which has been sketched is as yet by no means completely worked out; many details are still missing. Further experimental work is needed on such problems as the correlation between non-
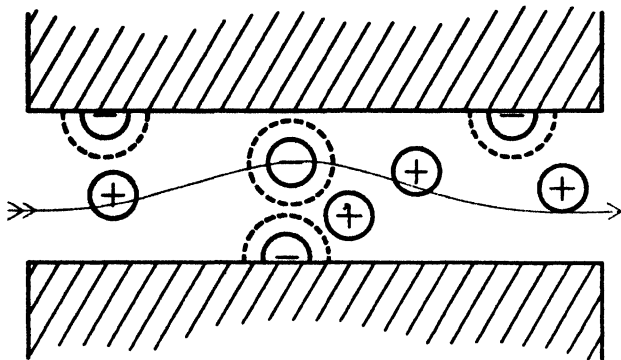
Fig. 2
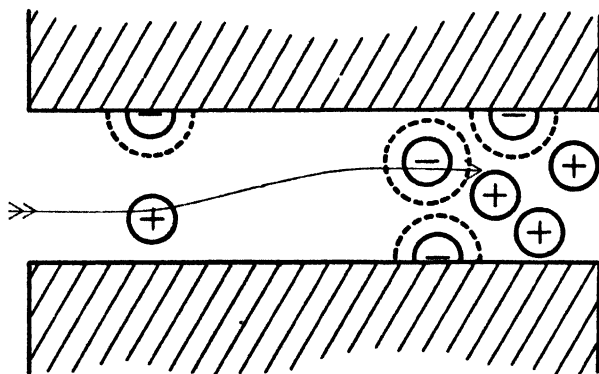
Fig. 3

Fig. 2, 3. The influence of the relative location of fixed charged groups in a moderately wide pore upon the blockage of ions of the same sign (see text).

electrolyte and ion permeability, the electromotive behavior and the conductance of a variety of membranes with different electrolytes at different concentrations, the electromotive effects when different electrolyte solutions are separated by the membrane, etc. (5).

III. THE HETEROPOROUS CHARACTER OF REAL MEMBRANES AND ITS BEARING UPON THE TEORELL AND MEYER–SIEVERS THEORY

In this section we shall discuss briefly the bearing of the heteroporosity of membranes of porous character in general on the Teorell (21) and Meyer–Sievers

(10) theory which was discussed in a preceding paper (16). One must recall on the one hand that the selectivity constants A_p and A_b, which should be
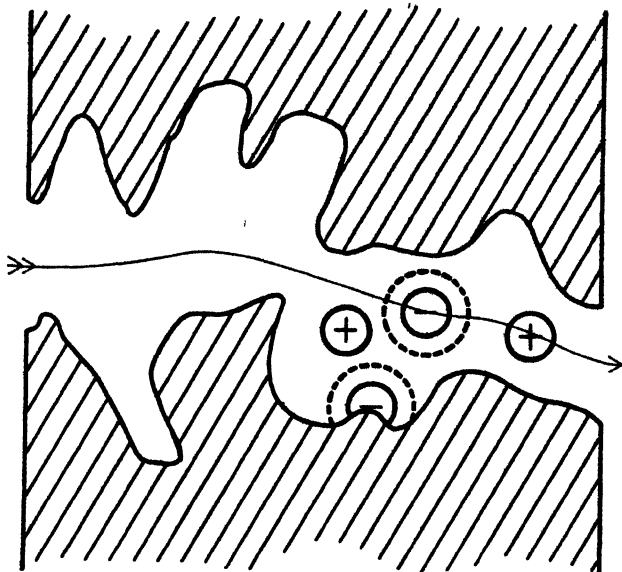
FIG. 4
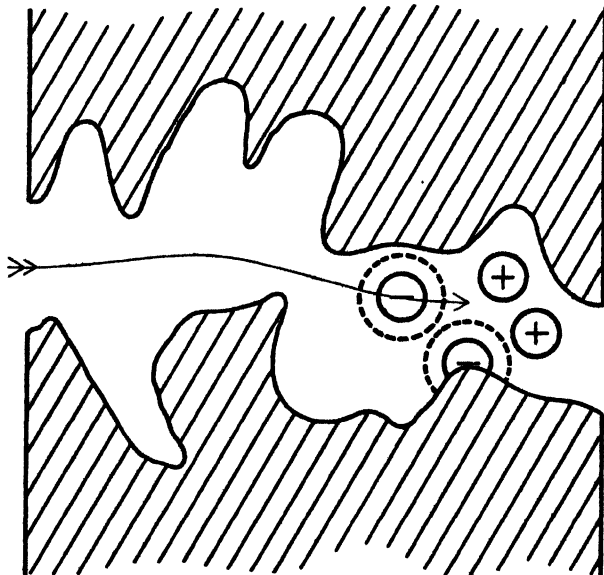
FIG. 5

FIG. 4, 5. The influence of the location of a fixed charged group in a heterogeneous pore upon the blockage of ions of the same sign (see text).

identical according to the theory, do not show any regular or reasonable agreement; the A_p values derived from potentiometric measurement are in nearly all

instances several orders of magnitude higher than the A_b values derived from base-exchange data.   On the other hand, the theory predicts rather accurately in a semiquantitative way the shape of the potential–concentration curves on the basis of clear and well-defined assumptions.   This situation can indicate one of several possibilities, foremost among them that the attempt to measure
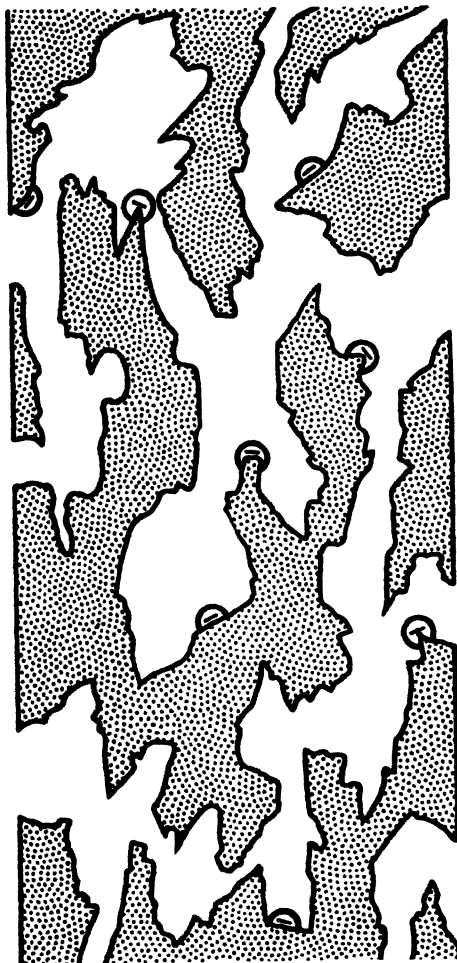
FIG. 6. The branching of pores and the random distribution of fixed charged groups in a real membrane.

A_b values is basically erroneous; or that the theory is basically erroneous; or that the theory, though at least formally correct in some respects (as far as formal A_p values are concerned), is based not on a true but on an inadequate, fictitious picture of the physical facts, in which case it may not in its present form permit any application which goes beyond the establishment of formal A_p values.

The first of these three possibilities seems least likely, for the theory is founded

on the very assumptions which coincide with the definition of the A_b selectivity constant. For the reasons given above one is reluctant to accept the second possibility: namely, that the theory is basically erroneous throughout. The greatest inherent probability seems to be with the third of the above-mentioned possibilities: namely, that the theory is built on a basis which, though partially correct, neglects some essential features of the real physical situation.

The discussion of the heterogeneous character of the pore system of real membranes makes it appear likely that the weakness of the Teorell and Meyer–Sievers theory is basically connected with its rather ideal character; it does not take into account any real structural factors. The electromotive properties of membranes, as we have seen previously (15, 16), are determined essentially by the fixed charged groups located in narrow spots of the geometrically possible pathways across the membrane. The A_p values on the basis of this picture are determined by one or a few critically located charges along each possible pathway across the membrane; the A_b values are a mean concentration defined by the number of fixed charged groups divided by the pore volume. This situation becomes clearly evident from a comparison of figures 4 and 5. The base-exchange selectivity constant A_b is identical for the two cases sketched in these figures; A_b as a mean concentration is not influenced by the location of the fixed dissociable group on the pore wall. The ionic selectivities of the two pores represented in figures 4 and 5, however, which according to the Teorell and Meyer–Sievers theory are measured quantitatively by the A_p values, are entirely different. The electrical efficiency of a fixed dissociable group—as shown in these figures—is determined by its location in the heterogeneous pore, in other words, the electrical characteristics of the pore are determined by the geometrical structure of the immediate vicinity of the fixed dissociable group; the rest of the pore is actually ineffective and insignificant, provided it does not mechanically block out ions of different size. A fixed dissociable group must be thought of as being surrounded by a sphere of action extending into the solution according to the prevailing conditions of ionic strength, etc., as indicated by the dotted lines in the figures. Therefore, a suitably located dissociable group must give rise to a high degree of ionic selectivity, i.e., to a high A_p value in terms of the Teorell and Meyer–Sievers theory.

If there is only one charged group in a pore, A_p describes the electromotive properties of that part of the pore which contains the dissociable group. If there are several dissociable groups in a pore, the electromotive properties of the latter will be determined primarily by that group (or combination of groups) which is located so as to be electromotively most effective. The A_b value in this case will generally be lower than A_p according to the heterogeneity of the pore.[7]

---

[7] The A_b values would become as high as the A_p values if the following set of conditions were realized: homoporosity of all parts of all possible pathways across the membrane; a spacing of the dissociable groups on the pore walls which coincides with the diameter of the sphere of action surrounding the individual charged groups; and the absence of branching

The discrepancy between the A_p and the A_b values, which is a necessary consequence of the heteroporosity–fixed-charge theory is found experimentally, as was mentioned before. In the preceding paper (16) it was demonstrated that the A_p values in most instances are several orders of magnitude higher than the corresponding A_b values; in agreement with the predictions of the heteroporosity–fixed-charge theory the disagreement between the two selectivity constants is less pronounced with membranes which carry an unusually high surface concentration of dissociable groups in their pores,—namely, with membranes which were oxidized in the formed state.[8]

Thus it becomes evident that the basic weakness of the Teorell and Meyer–Sievers theory lies in the neglect of the structural factor. The theory is built upon oversimplified assumptions. This, however, does not mean that the theory is valueless or should be abandoned. On the contrary, it should be used as a foundation for further theoretical work. Whether it will ultimately be advisable to split up the observed membrane potential into three parts, as was done by Teorell and Meyer–Sievers,—namely, two Donnan potentials and one diffusion potential,—or whether it may not be preferable to consider statistically the probability that individual ions will pass critical spots, cannot yet be decided. The former method of approach, which has the advantage of being based on rather fully developed concepts, will be applicable to the actual physical situation only after considerable modification. The latter method of approach,—namely, by a consideration of molecular processes occurring at individual spots,—would be much closer to the physical facts but could not be based quite as conveniently on prior theoretical work.[9]

IV. SOME EXAMPLES OF MACHINE ACTIONS OF MEMBRANES

In a preceding paper (15) it was pointed out that much of the interest in membranes is due to their machine character. The machine actions of mem-

parts of the pores which are too short to carry that number of dissociable groups which would give the same electrical characteristics as those of much longer pores.

[8] It does not seem advisable to use the experimental values of A_p and A_b given previously (16) for a discussion which goes much farther than that already given. The experimental data are too uncertain. The low base-exchange values, as was pointed out previously, are still fictitiously high, and the high base-exchange values which can be measured experimentally with a satisfactory degree of accuracy are likewise high. Many groups which contribute to the measured (long time) base exchange are undoubtedly located in the interior of micelles or in micro dead-end cavities where they cannot contribute to the electromotive action of the membrane.

[9] The latter approach stresses several important facts. The function behavior of any real membrane is the result of the action and interaction of discrete (generally not equivalent) spots in the various pathways across the membrane which are separated from each other by the framework of the membrane. A number of dissociable groups located in the pores, which is far too small to yield a condensed monomolecular film of the same area as the membrane, may easily determine the behavior of even fairly thick membranes of porous character.

It is tempting to expand this argument to a speculation concerning the nature, the mode of action, and the extreme sensitivity towards chemical changes of the very thin membranes frequently found in cells and tissues.

branes which do not involve electrical forces are ordinarily rather simple. Their electrical machine actions are numerous; some of them are simple, others rather complex. On account of the great variety of the electrical machine actions of membranes and their importance in living systems, they command unusual interest.

Membrane phenomena in the past have been discussed in most instances from the phenomenological point of view; only in rare instances have the machine action aspects of these phenomena—their energetics—been considered, and never in a comprehensive manner. The present statement represents a program and an outline more than a report on finished accomplishments.

After a brief mention of some machine actions of membranes which do not involve-electric forces, some of the characteristic electrical machine actions will be discussed.

Semipermeable membranes may act under suitable conditions as perfect machines in reversible processes, transforming concentration energy into mechanical work by moving a piston against pressure (15). The best-known case of this type is represented by Pfeffer's measurement of the osmotic pressure of sugar solutions. Conversely, mechanical pressure may be used to separate by filtration pure solvent from a solution, in which case mechanical energy may be transformed in a reversible manner into concentration energy.

"Leaky" membranes which are not completely impermeable to the solute likewise may be used for the mutual transformation of mechanical and concentration energy, though, of course, only in an irreversible manner.

Another non-electrical machine action of membranes of some interest occurs in systems of the following character: A membrane separates two solutions of different osmotic concentrations of two different solutes both of which are unable to penetrate the membrane, while the solvent may readily pass through it. In such systems the osmotically more concentrated solution will do concentration work on the more dilute solution, increasing the concentration of the solute in the latter. Even with semipermeable ("selectopermeable" (15)) membranes such processes are not reversible unless very special circumstances prevail. With "leaky" membranes analogous effects can be produced, though, of course, in the long run the system moves towards equilibration of concentration and pressure on the two sides of the membranes. This list of non-electrical membrane phenomena could be greatly expanded by the discussion of similar, more complicated systems involving three or more species of molecules in solution and membranes of various degrees of permeability for various of these molecular species (compare the work of Schreinemakers (12)).

For the following presentation it is convenient to distinguish two groups of electric machine actions of membranes: phenomena or aspects of such phenomena which theoretically could occur with homoporous membranes which, in other words, do not need the assumption of heteroporosity for their explanation; and phenomena which are inherently based on a heteroporous or otherwise complex character of real membranes.

The electromotive action of membranes is an effect which does not require for its explanation the assumption of heteroporosity. This effect can be under-

stood as the summation of the parallel action of identical pores which may or may be not strictly impermeable to the one or the other species of ions.

With real membranes which are strictly impermeable to one kind of ions, all the pores behave electrically alike. The other physical differences of the pores on account of their electrical perfection are without significance. The observable effect with such membranes is the sum of the identical and parallel effects caused by all the pores. Such membranes can act as reversible electrochemical machines; their overall efficiency is strictly comparable to that of reversible metallic electrodes, though the mechanism of their electromotive action is entirely different. The reader may recall that the previously discussed megapermselective membranes (15) act to a remarkable degree as nearly perfect machines over fairly wide concentration ranges.[10]

"Leaky" membranes give rise to electromotive forces which are below the theoretically possible maximum values obtainable with ideal reversible membranes, the observable effects depending on pore size and charge density as discussed in a preceding section of this paper. The electromotive behavior of "leaky" membranes which only partially restrict the penetration of one kind of ions could likewise be understood as the summation of the identical electromotive action of their pores. "Leaky" membranes as they exist in reality, however, combine a variety of pores with varying degrees of ionic selectivity; at least some of the pores in such membranes are too wide or too void of fixed charged groups to act as perfect ion sieves.

The observable electrical effects on real "leaky" membranes are, of course, the result of the interplay of the various heterogeneous pores of the membrane. Viewed superficially, however, the electromotive effect can be looked upon as originating from the summation of identical electrical effects arising in an equivalent homogeneous pore system. Such leaky membranes are able to transform only a part of the free concentration energy of the surrounding solutions into electrical energy; they are imperfect electrochemical machines.[11]

Another interesting machine action of selectively ion-permeable membranes is the Donnan effect.[12]

---

[10] Membranes of this type therefore may be used for the potentiometric determination of ion activities. The (electronegative) megapermselective collodion membranes may be used as non-specific "electrodes" for the determination of alkali ions and NH_4^+; the (electropositive) megapermselective protamine membranes as non-specific "electrodes" for the titration of most inorganic monovalent anions, such as NO_3^-, ClO_3^-, F^-, etc. (K. Sollner: J. Am. Chem. Soc. **65**, 2260 (1943)). Electronegative clay membranes which may show a considerable degree of specificity have been studied extensively by Marshall and collaborators (C. E. Marshall and W. E. Bergman: J. Am. Chem. Soc. **63**, 1911 (1941); J. Phys. Chem. **46**, 52, 325 (1942); C. E. Marshall and C. A. Krinbill: J. Am. Chem. Soc. **64**, 1814 (1942)).

[11] Such membranes occur nearly universally in living systems; the question which has not yet been decided is under what conditions the electromotive forces arising at these membranes are utilized to bring about specific useful processes, and in what situations the electrical energy is dissipated in an unorganized manner.

[12] For a fairly comprehensive treatment of this effect compare T. R. Bolam, *The Donnan Equilibria and their Application to Chemical, Physiological and Technical Processes*, G. Bell and Sons, London (1932).

Experiments on the Donnan effect in which the non-diffusible ion is not of colloidal or semicolloidal size but of low molecular weight have been described in rare instances only and with not altogether satisfactory results.

We have recently been able to investigate systems which allow the establishment of membrane equilibria involving only the ions of strong low-molecular-weight inorganic electrolytes (7). With the negative megapermselective collodion membranes, the anions take the place of the non-diffusible "colloid" ions; with the electropositive megapermselective protamine membranes, the cations represent the non-diffusible ions. Table 1 shows Donnan equilibria obtained with megapermselective collodion membranes.

TABLE 1

Donnan equilibria across megapermselective collodion membranes

Identical volumes of solution on the two sides of the membrane

Vol.$_{In}$ = Vol.$_{Out}$

NO.	SOLUTE	ORIGINAL STATE		EQUILIBRIUM STATE				RATIO $\frac{IN}{OUT}$	
				Experimental		Calculated		Experimental	Calculated
		In	Out	In	Out	In	Out		
		millimoles per liter	*millimoles per liter*	*millimoles per liter*	*millimoles per liter*	*milli-moles per liter*	*milli-moles per liter*		
A	NH_4^+	30.0		22.4	7.5	22.5	7.5	2.99	3.00
	K^+		10.0	7.5	2.5	7.5	2.5	3.00	3.00
	Cl^-	30.0	10.0	29.8	10.1	30.0	10.0	2.95	3.00
	Sucrose*		33		(33)		(33)		
B	Na^+	30.0		22.5	7.5	22.5	7.5	3.00	3.00
	NH_4^+		10.0	7.4	2.5	7.5	2.5	2.95	3.00
	$C_2O_4^{--}$	15.0	5.0	14.9	5.0	15.0	5.0	2.98	3.00
	Sucrose*		19		(19)		(19)		

* Sucrose is added in the proper concentration to establish osmotic equilibrium.

The Donnan effect is without doubt of great importance in biological processes; it also could assume industrial importance if use were made of "megapermselective" membranes.

With suitable leaky membranes an analogous, though temporary, electrical machine effect can be observed.

The electrical machine actions of membranes which have been discussed so far are all due to energy which is stored in the solutions which are separated by the membrane. We shall now consider also some effects which are due to the application of energy from the outside to liquid–membrane–liquid systems.

The simplest electrical effect due to the application of mechanical pressure is the "streaming potential". The phenomenological as well as the theoretical aspects of this effect have been treated repeatedly in an adequate manner and therefore do not require further discussion here (3, 13).

Of great interest are the electrical machine actions of membranes which are

observed when a current is passed through a system electrolyte solution–membrane–electrolyte solution. The best known of these effects is electroösmosis, the movement of liquid under the influence of an outside electric field through the membrane in such systems (3, 13). The primary observable effect is the transportation of liquid, which can occur against hydrostatic pressure. In this case electrical energy may be transformed—in a rather inefficient manner—into mechanical energy. The phenomenology and general theory of this effect have been dealt with rather adequately in the literature and therefore do not need further discussion here. The purely energetic and efficiency aspects of this problem, however, have never been dealt with adequately and will require in the future further experimental study.

While electroösmosis occurs, certain changes in the composition of the solutions adjacent to the membrane are observed rather universally. Practical use is made of these concentration changes in electrodialysis, when under suitable conditions electrolyte solution (and ions) are removed from a solution containing colloidal material. The energetics of this process are still unsolved.

Of great basic interest are the very considerable concentration changes which occur with dense membranes in contact on both sides with the solution of an electrolyte. If a current is passed through such a system, there are not only changes in the concentration of this electrolyte but free acid appears on the one side of the membrane and free base on the other. This is due to the fact that within the membrane the H^+ or OH^- ions contribute substantially towards the transportation of current. The basic theory of this effect was worked out in some detail by Bethe and Toropoff (4) nearly thirty years ago. Unfortunately, however, this line of work, in spite of its great importance, has never been continued. Many aspects of the Bethe–Toropoff effect, particularly the problems connected with its energetic efficiency, are still in a state of obscurity. Parenthetically it may be added that many physiologists are inclined to look to the Bethe–Toropoff effect for an explanation of many biological membrane actions.

Some of the electrical machine actions of membranes described in the preceding paragraphs can be explained fully and others can be understood at least in a superficial manner without taking into account the heteroporous character of real membranes. For a complete understanding of the latter cases, however, it would be necessary to consider the interaction of the various non-equivalent pores. Such detailed considerations are desirable, e.g., when considering the electromotive action of leaky membranes or the liquid movement and back-movement (and the corresponding mixing of the solutions at the two sides of the membranes) in electroösmosis.

There are, however, some electrical machine actions of membranes the mechanisms of which are essentially due to the heteroporous or otherwise complex character of real membranes. Such effects, therefore, can be understood only if this character of real membranes is taken into account.

The best-investigated effect which is due entirely to the electrically heterogeneous character of real membranes is the phenomenon known as anomalous osmosis. Under this heading one designates all those liquid movements across

membranes separating two solutions of different concentration which, according to their rate or the pressures obtained, would not be predicted on the basis of the van't Hoff osmotic theory. With (non-swelling) membranes of porous character such anomalies are found only if an electrolyte diffuses through a leaky membrane; they are never found with membranes which are strictly impermeable to the one or the other species of ions. The theory of this effect has been discussed in previous papers (8, 14, 20); therefore only an outline of the basic idea of this theory needs to be given here.

Since membranes are heteroporous, different pores may give rise to pore potentials of different magnitude. Pores or parts of the membrane which give rise to different pore potentials or local dynamic membrane potentials act upon each other. Local electric circuits are thereby set up, some of the pores (or parts of the membrane) acting as sources of electric energy, while through other pores the current is driven passively. While the current flows through the latter pores, it brings about electroösmosis. This electroösmotic translocation of liquids across the membrane is the anomalous osmotic liquid movement observed with suitable porous membranes when an electrolyte dialyzes through them.

Though these considerations were based only on the assumption of pores of different width and constant charge density (the converse situation and intermediate cases having been neglected), it was possible to deduce rules from a few simple premises which, in agreement with all known experimental facts, seem to govern the occurrence of anomalous osmosis. This is the outstanding case in which the assumption of heteroporosity in membranes has led with inherent necessity to the solution of a long controversial problem.

Anomalous osmosis is thought by many investigators to furnish a possible explanation for many complicated actions in living membrane systems. In this connection it is of interest to note that using the previously (2, 15, 16) described types of electrochemically active membranes, we demonstrated that anomalous osmosis is able to drive appreciable quantities of liquid through a membrane, even against considerable concentration gradients (1). Under favorable conditions liquid transports up to 1 cc. per cm.^{2} per hour could be observed. We have not yet measured the energetic efficiency of this process under various conditions. It undoubtedly is very low. In spite of this low efficiency, however, it seems that anomalous osmosis may play an important part in the translocation of liquids in living systems in which concentration energy of metabolic waste products is available in sufficient quantity.

In naturally occurring membranes there is reason to believe that heterogeneity of properties beyond simple variations of pore size and charge distribution exists. There is evidence that different areas in the surfaces of single cells or multicellular membranes may have oppositely charged pores. One area may have electropositively and another electronegatively charged channels. Such mosaic structures offer numerous interesting possibilities for the operation of useful machine actions. The further investigation of such mosaic membranes, their properties, and their functional behavior is now possible and the author hopes to undertake this in the near future.

V. SUMMARY

1. The empirical permeability characteristics of membranes of porous character for solutes of different molecular weight generally cannot be explained without the assumption of a heteroporous structure of these membranes. Likewise, anomalous osmosis, which is frequently observed when an electrolyte solution diffuses through a porous membrane, cannot be understood without the assumption of geometrical and electrical heteroporosity of such membranes, the mechanism which brings about anomalous osmosis essentially being a result of the electrical interaction of these inhomogeneities. Membranes of porous character therefore must be assumed in general to be heteroporous. The heteroporosity of collodion and similar membranes is due to the more or less random aggregation of the macromolecules and micelles which form the membrane skeleton.

2. The pore systems of real membranes can be visualized as a sequence of narrow channels and wider cavities which, interconnected at random, traverse the membrane. The electrical behavior of these pore systems is governed by two factors: the ability or inability of the ions of an electrolyte to enter purely on the basis of size into the various parts of the pore system, and an electrical factor, the repelling forces emanating from fixed dissociable groups on the pore walls. The frequency and distribution of these dissociable groups which restrict or prevent the penetration of ions carrying the same charge seem to be the main factor which governs the ion permeability of membranes of porous character. A tentative picture of this electrical screening effect is given in the text.

3. In a previous paper it was shown that the selectivity constant of the Teorell and Meyer–Sievers theory of electrical membrane behavior can be determined in two independent ways,—namely, from electromotive measurements and from base-exchange studies. It was then found that the electromotive selectivity constant A_p is universally higher, in many instances by several orders of magnitude, than the selectivity constant A_b of the same membrane which is derived from base-exchange data. The assumption of heteroporosity affords at least qualitatively a satisfactory explanation of this discrepancy. The electromotive properties of a membrane are determined by the fixed dissociable groups located in the narrowest part of each possible pathway across the membrane; A_p therefore must necessarily be higher than the corresponding A_b value, which is based on the assumptions of averages. The weakness of the Teorell and Meyer–Sievers theory is the neglect of any real structural factors.

4. Several membrane phenomena, such as electromotive action, osmotic action, Donnan equilibria, electroösmosis, the Bethe–Toropoff effect, anomalous osmosis, etc., are considered from the point of view of the machine character of membranes.

These discussions have contributed in no small measure to the clarification of many of the general problems touched upon in this and foregoing papers.

He also wishes to take this opportunity to thank heartily his faithful collaborators Dr. Irving Abrams, Dr. John Anderman, Mr. Paul W. Beck, Dr. Charles W. Carr, and Dr. Harry P. Gregor, without whose ceaseless efforts and valuable contributions the experimental work described in these papers could not have been carried out.

The author also wishes to express his sincerest thanks to the Rockefeller Foundation for generous grants which have enabled him to carry out these investigations.

The author is indebted to the editors and to the publisher of the *Journal of General Physiology* for the permission to utilize data published therein and to reproduce a number of figures.

REFERENCES

(1) ABRAMS, I., AND SOLLNER, K.: Am. J. Physiol. (Proceedings) **133**, 189 (1941).
    ABRAMS, I.: Ph. D. Thesis, University of Minnesota, 1942.
(2) ABRAMS, I., AND SOLLNER, K.: J. Gen. Physiol. **26**, 369 (1943).
(3) ABRAMSON, H.: *Electrokinetic Phenomena and their Application to Biology and Medicine.* The Chemical Catalog Company, Inc., New York (1934).
(4) BETHE, A., AND TOROPOFF, TH.: Z. physik. Chem. **88**, 686 (1914); **89**, 597 (1915).
(5) CARR, C. W.: Ph. D. Thesis, University of Minnesota, 1943.
(6) COLLANDER, R.: Soc. Sci. Fennica Commentationes Biol. **2**, 6 (1926).
(7) GREGOR, H. P.: Ph. D. Thesis, University of Minnesota, 1945.
(8) GROLLMAN, A., AND SOLLNER, K.: Trans. Electrochem. Soc. **61**, 477, 487 (1932).
(9) MANEGOLD, E.: Kolloid-Z. **61**, 140 (1932) and many other publications in the same journal.
(10) MEYER, K. H., AND SIEVERS, J.-F.: Helv. Chim. Acta **19**, 649 (1936).
     MEYER, K. H.: Trans. Faraday Soc. **33**, 1073 (1937).
(11) MICHAELIS, L., AND WEECH, A. A.: J. Gen. Physiol. **12**, 55 (1928).
     MICHAELIS, L.: Bull. Natl. Research Council. **No. 69** (1929).
(12) SCHREINEMAKERS, F. A. H.: *Lectures on Osmosis.* G. Nafft, The Hague (1938).
(13) SMOLUCHOWSKI, M. S.: "Elektrische Endosmose und Strömungsströme," in Graetz's *Handbuch der Elektrizität und des Magnetismus*, Vol. 2, pp. 366–428 (1921).
(14) SOLLNER, K.: Z. Elektrochem. **36**, 36, 234 (1930); Kolloid-Z. **62**, 31 (1933).
(15) SOLLNER, K.: J. Phys. Chem. **49**, 47 (1945).
(16) SOLLNER, K.: J. Phys. Chem. **49**, 171 (1945).
(17) SOLLNER, K., ABRAMS, I., AND CARR, C. W.: J. Gen. Physiol. **25**, 7 (1941).
(18) SOLLNER, K., AND ANDERMAN, J.: J. Gen. Physiol. **27**, 433 (1944).
(19) SOLLNER, K., AND CARR, C. W.: J. Gen. Physiol., in press.
(20) SOLLNER, K., AND GROLLMAN, A.: Z. Elektrochem. **38**, 274 (1932).
(21) TEORELL, T.: Proc. Soc. Exptl. Biol. Med. **33**, 282 (1935); Proc. Natl. Acad. Sci. (U. S.) **21**, 152 (1935).

PHYSICAL CHEMICAL INVESTIGATIONS OF GOLDENROD RUBBER. I

"PRECIPITATION VALUE" AND ITS SIGNIFICANCE IN CHARACTERIZATION AND EVALUATION OF NATURAL RUBBERS

EVALD L. SKAU, WILLIAM J. RUNCKEL, FLORENCE B. KREEGER, AND MARY A. SULLIVAN

Southern Regional Research Laboratory,[1] *New Orleans, Louisiana*

The solubility of a polymer is a function of the degree of polymerization; in general, it decreases with an increase in molecular weight. The direct determination of solubility for such a substance is usually very difficult and cumbersome (2). When a non-solvent is added gradually with thorough mixing to a dilute solution of a polymer, a mixture of non-solvent and solvent in definite proportions is eventually obtained in which the polymer is no longer completely soluble. At this point a turbidity appears, owing to incipient precipitation. Jirgensons (2) used this simple method of titrating to the cloud point in order to determine relative degrees of polymerization in such substances as nitrocellulose, starch triacetates, and polystyrene polymers.

In the case of rubber, Midgley *et al.* (3, 4) distinguished between fractions of different molecular weight by means of their solubilities in mixed solvents and in this connection used the "standard precipitation point" as a characterizing property. This point was defined as the temperature at which a slowly cooled mixture of 0.85 per cent of the rubber, 28.55 per cent of absolute alcohol, and 70.60 per cent of benzene shows a sudden increase of turbidity.

In the course of the evaluation or characterization of rubber recovered on a pilot-plant scale from the leaves of goldenrod (*Solidago leavenworthii*) in this laboratory by a two-stage extraction process in which the leaves are extracted with acetone prior to extraction of the rubber with benzene, a simple titration method has been developed for estimating the relative solubilities or "precipitation value" of rubber samples. This method might be modified for use in characterizing polymers other than those of isoprene. The "precipitation value" as used for rubber is defined as the number of milliliters of absolute ethyl alcohol required to produce a cloud point in 10 ml. of a clarified benzene solution containing 0.0175 g. of sample. The larger the volume of alcohol required, the greater is the solubility of the rubber. Unless stated to be otherwise, all precipitation values are corrected to 25°C.

Experiments have been performed which show that, in general, treatments such as mastication, heating, and exposure to light, which are known to cause a decrease in the viscosity (average molecular weight) of rubber, cause an increase in the precipitation value. Information has been obtained concerning the

significance of the precipitation value and therefore of solubility data, and concerning the limits of their applicability in the characterization of rubber.

EXPERIMENTAL METHODS

Preparation of the rubber solution

One gram of the rubber sample is dissolved in 200 ml. of reagent-grade benzene in a stoppered flask by allowing it to stand in the dark overnight or until solution is complete. To clarify the solution 1 g. of Merck's activated charcoal is added and the solution is slurried and allowed to settle at least 15 min. The slurry is then filtered through a filter paper on a Buchner funnel previously prepared by filtering a small benzene slurry of activated charcoal and a filter aid (Hyflo Super-cel) and washing with benzene. The rubber solution is not added until the benzene comes through clear. No washing is necessary.

Total solids are determined on the clarified solutions by evaporating an aliquot in an impinging stream of nitrogen under a bell jar. The solution is then diluted with benzene to such a concentration that 100 ml. contains 0.175 g. of total solids.

Other methods were tried for making the solutions clear enough to be titrated. Aluminum oxide columns similar to chromatographic columns were employed; though effective, they were too slow to be practicable. The precipitation value obtained seems to be independent of the method of clarification used; a sample of hevea smoked sheet gave the same value whether clarified by slurrying with activated carbon, by filtering through cotton, or by passing through a column of activated alumina.

Titration

Ten milliliters of this solution is titrated with absolute ethyl alcohol with continuous shaking in a 30-mm. test tube until the cloud point is reached. The cloud point is observed against a black background with illumination by a fluorescent lamp. The temperature of the solution is then measured, and the precipitation value at 25°C. is obtained by applying a slight temperature correction as described below.

The reproducibility of the end point is 0.05 ml. for precipitation values up to about 6 ml. and is less satisfactory for higher values. End points above 25 ml. cannot be determined because of the high degree of dilution.

The precipitation value is not very sensitive to errors in the rubber concentration. Solutions of hevea smoked sheet and goldenrod rubber of various concentrations were titrated; for hevea, it was difficult to obtain good cloud points for concentrations above 0.3 g. per 100 ml., owing to the tendency of the rubber to precipitate in the form of agglomerates. The results, shown graphically in figure 1, indicate that for hevea and goldenrod the measured precipitation values do not change within the limit of error, 0.05 ml., for any concentration between 0.150 and 0.200 g. per 100 ml. of solution.

The effect of temperature on the precipitation values of hevea smoked sheet and goldenrod rubber was determined by performing the titration at various

temperatures between 20° and 50°C.   The data obtained (figure 2) can in each case be represented by a straight line within the limits of error through the range
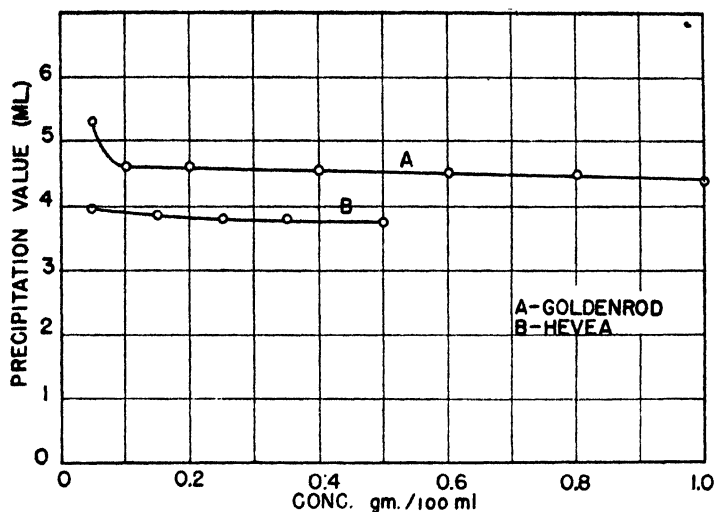
FIG. 1. Effect of concentration on the measured precipitation value
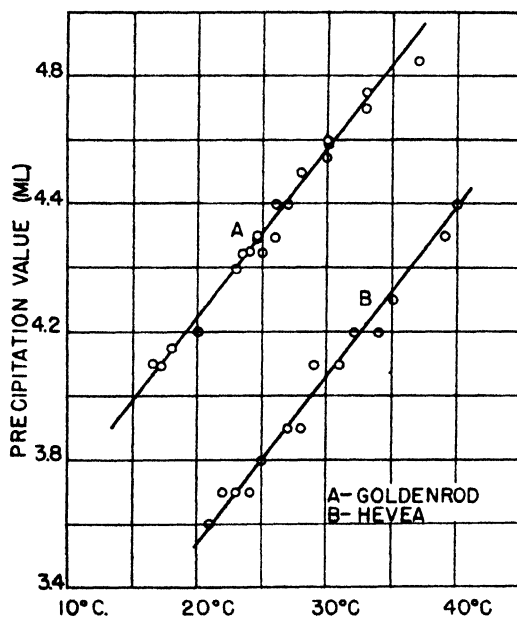
FIG. 2. Variation of precipitation value with temperature

considered, each having a slope of about 0.05 ml. per degree C.   Thus to correct precipitation values to 25°C., 0.05 ml. is subtracted for each degree above that

temperature or added for each degree below it. This value has been assumed to be applicable to all types of rubber in the present investigation for temperature corrections of a few degrees.

Viscosity measurements

Viscosities were measured by means of Ostwald viscometers as modified by Zeitfuchs (6), using the technique of Craxton (1). They were determined at 25°C. in benzene solutions containing 0.175 g. per 100 ml. The same rubber solutions can be used for these determinations as are used for the determinations of precipitation value if special precautions are taken to obtain the correct concentration. The viscometers were calibrated with benzene and checked against water. The results were calculated as absolute viscosities, η_a, in centipoises at 25°C. The absolute viscosity of benzene at 25°C. was taken as 0.608 centipoise.

Throughout the experiments precautions were taken to expose rubber solutions to light as little as possible.

RESULTS AND DISCUSSION

Data for various samples of rubber

Precipitation values and viscosities were determined for benzene extracts of goldenrod rubber obtained from the various pilot-plant runs in this laboratory and also for specimens of different types of natural rubber. The results are tabulated in tables 1 and 2, respectively. Leaving gutta percha out of consideration, as an exception, the precipitation values varied from 3.80 ml. for hevea smoked sheet to 5.30 ml. for the poorest goldenrod rubber, Pilot Plant Run No. 2. In general, the lower the precipitation value, the greater is the viscosity of the rubber sample. No simple relationship exists, however, nor, in view of the results on binary mixtures to be discussed later, would it be expected.

The average results for precipitation value and viscosity of rubbers obtained in the various pilot-plant extractions of goldenrod are 4.52 ml. and 0.681 centipoise, respectively. A poor grade of rubber gives a very high precipitation value and a low viscosity. Pilot Plant Run No. 2 gave the highest precipitation value, 5.30 ml., and a very low viscosity, 0.649 centipoise. This sample resulted from the extraction of goldenrod leaves from dead and field-dried stems and was very much degraded, judging (1) from fractionation data given in a separate publication and (2) from the fact that the sample was extremely sticky and semiliquid. On the other hand, Pilot Plant Run No. 17 (acetone precipitated), probably the best goldenrod rubber obtained direct from the pilot plant, gave a precipitation value of 4.30 ml. and a viscosity of 0.728 centipoise. This sample was in a sense partially purified, since the acetone used in the preliminary extraction of the leaves contained some 20 per cent of benzene; it has been shown that a mixture of acetone and benzene dissolves some of the lower-molecular-weight fractions of rubber. The sample was fairly hard and practically nonsticky. The relationship between the precipitation value and viscosity will be further discussed below in connection with additional data.

Inspection of table 1 shows that all the goldenrod rubber samples having

TABLE 1

Precipitation values and absolute viscosities of pilot-plant goldenrod rubbers

PILOT PLANT RUN NO.	PRECIPITATION VALUE	η_a AT 25°C. IN BENZENE (0.175 G. PER 100 ML.)
	ml.	centipoises
10	4.25	0.692
9	4.30	0.689
17 (acetone precipitated)	4.30	0.728
30 (1st 12 hr.)*	4.35	0.716
19	4.35	0.698
18 (acetone precipitated)	4.35	0.693
14	4.35	0.692
e	4.35	0.685
17 (1st 10 hr.)	4.40	0.722
11	4.40	0.698
31	4.40	0.695
26 (1st 12 hr.)	4.45	0.703
13 (4th to 6th hr.)	4.45	0.695
18	4.45	0.692
34	4.45	0.687
30 (2nd 12 hr.)	4.45	0.685
29	4.45	0.683
35	4.45	0.682
a	4.45	0.676
21	4.45	0.665
12	4.50	0.697
32	4.50	0.681
25	4.50	0.680
27 (1st 12 hr.)	4.55	0.692
23	4.55	0.680
27 (2nd 12 hr.)	4.55	0.666
24	4.55	0 663
13 (7th to 24th hr.)	4.55	0.655
33	4.60	0.690
26 (2nd 12 hr.)	4.60	0.672
20	4.60	0.663
22	4.60	0.652
17 (2nd 12 hr.)	4.65	0.677
15	4.75	0.644
28	4.80	0.670
16	5.00	0.648
15 (no antioxidant)	5.00	0 644
2	5 30	0.649
Average	4.52	0.681

* Time indicated is period of benzene extraction of the goldenrod leaves.

precipitation values below 4.45 ml. have relatively high viscosities (above 0.685 centipoise). For the samples having precipitation values above 4.80 ml. the viscosities are relatively low, below 0.650 centipoise. When the precipitation

values lie between 4.45 and 4.80 ml., however, there seems to be no definite correlation between the precipitation value and the viscosity of a sample; that is, the corresponding viscosities vary inconsistently between 0.650 and 0.720 centipoise. A possible explanation for this inconsistency will be mentioned in connection with the discussion of the significance of the precipitation value.

TABLE 2

*Precipitation values and absolute viscosities of various natural rubber specimens**

SAMPLE	PRECIPITATION VALUE	η_a AT 25°C. IN BENZENE (0.175 G. PER 100 ML.)
	ml.	*centipoises*
Hevea (purified crepe sheet)	3.90	2.4
Cryptostegia (smoked sheet)	3.95	1.9
Castilla (smoked sheet)	4.00	1.8
Hevea (smoked sheet)	3.80	1.8
Hevea (yellow crepe)	3.90	1.2
Kok-saghyz	4.15	1.1
Guayule	3.90	0.98
Chilte (commercial)	4.05	0.98
Guayule (Mexican resinous)	4.10	0.97
Guayule (Domestic deresinated)	4.15	0.92
Guayule (Mexican deresinated)	4.20	0.97
Guayule (Domestic resinous)	4.20	0.85
Gutta percha	3.65	0.73
Gutta percha (old sample)	4.15	0.66
Goldenrod (average)	4.52	0.68

* These values can be considered as characteristic only of the particular specimen and not necessarily of the variety of rubber.

TABLE 3

Effect of aging of sample of guayule on precipitation value and viscosity

TIME	PRECIPITATION VALUE	η_a AT 25°C. IN BENZENE (0.175 G. IN 100 ML.)
days	*ml.*	*centipoises*
0	3.90	0.98
280	4.25	0.82
302	4.50	0.75
307	4.45	0.75
362		0.73

It is well known that rubber may undergo degradation on aging owing, for example, to oxidation or exposure to light. This is illustrated by the data given in table 3 for a sample of guayule rubber after various periods of time. The sample, which was rather spongy in appearance, was in the form of a large lump and was kept protected from light in a laboratory drawer. In ten months the precipitation value had risen from 3.90 to about 4.50 ml., the viscosity had

decreased from 0.98 to 0.73 centipoise, and the sample had become very sticky. It should be mentioned that this behavior is not typical of all the guayule samples studied.   Since the properties of a given sample depend upon its history, the values in table 2 can be considered characteristic only of the particular specimen tested and not necessarily of the variety of rubber.

Effect of mastication

A sample of hevea smoked sheet was extensively masticated by a stepwise process in a mill by setting the rolls successively closer and closer together. Samples were taken off after treatment at each setting.   The precipitation value changed progressively from the original value, 3.80 ml., as follows: 4.25, 4.60, 4.80, 4.85 ml.   The viscosity of the final product was 0.68 centipoise, as compared to 1.84 for the original unmasticated sample.
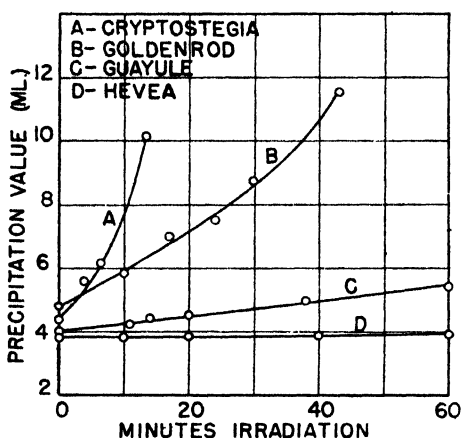
Fig. 3. Irradiation of solutions of rubber specimens

In another experiment the mastication was carried to the extent estimated to be approximately that usually attained for compounding.   The viscosity had decreased from 1.84 to 0.73 centipoise and the precipitation value had increased from 3.80 to 4.45 ml.   This change in precipitation value, indicating increased solubility due to depolymerization, corroborates the finding of Midgley, Henne, and Renoll (5), that their "standard precipitation point" (temperature of precipitation) for a pale crepe rubber was reduced by milling.

Effect of heat

The precipitation value of hevea smoked sheet was changed from 3.80 to 4.00 ml. by heating the solid for 6 hr. at 120°C. in an air oven.

Effect of irradiation

· Exposure to light also causes an increase in the precipitation value.   Figure 3 gives a graphical representation of the results obtained in a preliminary experi-

ment. The rubber samples were dissolved, clarified, and diluted to a concentration of 0.175 g. per 100 ml. of benzene solution by the usual procedure. Ten-milliliter aliquots were then exposed in Pyrex test tubes at a distance of 12 cm. from a 100-watt Mazda bulb, removed at the intervals indicated, and titrated. As shown by the figure, the rate of degradation increased rapidly in the order: hevea, guayule, goldenrod, cryptostegia. It was found that Agerite, Flectol H, and other antioxidants inhibited this reaction, while the presence of chlorophyll and other activators enhanced the rate of the reaction. When a trace of chlorophyll was added to the original hevea solution, for example, a 60-min. exposure caused the precipitation value to change from 3.80 to 9.30 ml., while without the chlorophyll the change was only from 3.80 to 3.90 ml. This affords a possible explanation of the different rates of degradation in figure 3, since the rates increased in the same order as the depth of green color in the clarified solutions. The hevea solution was almost water-white and the cryptostegia, which was a benzene extract of the leaves, was quite green. It was observed that different goldenrod solutions give different rates according to the degree of removal of coloring matter.

The rate of change of the precipitation value during irradiation is greater at higher temperatures. Aliquot samples of a benzene solution of the goldenrod rubber, 0.175 g. per 100 ml. of solution, were placed in Pyrex test tubes 6 cm. from a Mazda lamp and irradiated for 1 hr. The original solution had a precipitation value of 4.40 ml. In the case of two sets of duplicates cooled by an electric fan (temperature of the solution 31°C.), the precipitation values at 25°C. were 7.6 and 7.4 ml.; the corresponding values for two other sets of duplicates without fan cooling (55°C.) were 8.6 and 8.2 ml.

The following experiment was performed in the study of the relationship between the change in viscosity and precipitation value during irradiation. A large batch of a benzene solution of goldenrod rubber was clarified with activated carbon and diluted to a concentration of 0.175 g. per 100 ml. in the usual way. Twelve 50-ml. portions of this solution were measured into 125-ml. Pyrex Erlenmeyer flasks and placed in direct sunlight. As the irradiation progressed, they were removed one by one and placed in the dark; their properties were then determined and the results plotted as in figure 4. Within the first 30 min. of irradiation, the precipitation value had risen to more than 25 ml., the maximum significant value determinable. The viscosity had decreased from 0.682 to 0.661 after 30 min. of irradiation and was still falling after 60 min., when it had reached 0.646 centipoise.

Investigation of binary mixtures of rubber solutions

Benzene solutions of various kinds of rubber were prepared by clarifying with activated carbon and making up to a concentration of 0.175 g. per 100 ml. in large batches. Considerable volumes of some of these solutions were then irradiated in sunlight to cause degradation, as indicated by the decrease in viscosity and increase in precipitation value.

Pairs of the irradiated and unirradiated solutions were then mixed in varying

proportions, and the precipitation values and viscosities of the mixtures were determined. For example, 1, 2, 3, etc. ml. of the first solution were pipetted into different test tubes and 9, 8, 7, etc., ml., respectively, of the second solution were then added to make the total volume 10 ml. in each case. The results
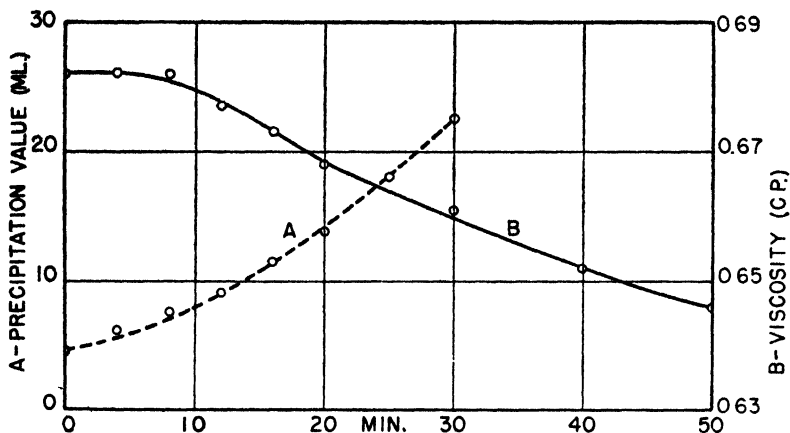
Fig. 4. Irradiation of goldenrod rubber solution
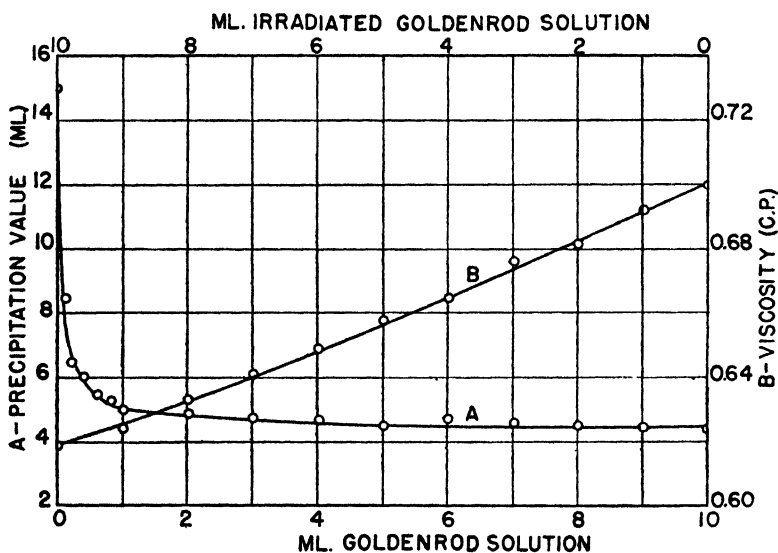
Fig. 5. Binary system: hevea and irradiated hevea solutions

are shown graphically in figures 5 to 9. Figure 10, showing the precipitation values for mixtures of a 0.175 per cent solution of gutta percha with pure benzene instead of with another rubber solution of the same concentration, is included for consideration with the others. It is really a concentration curve of the type shown in figure 1.
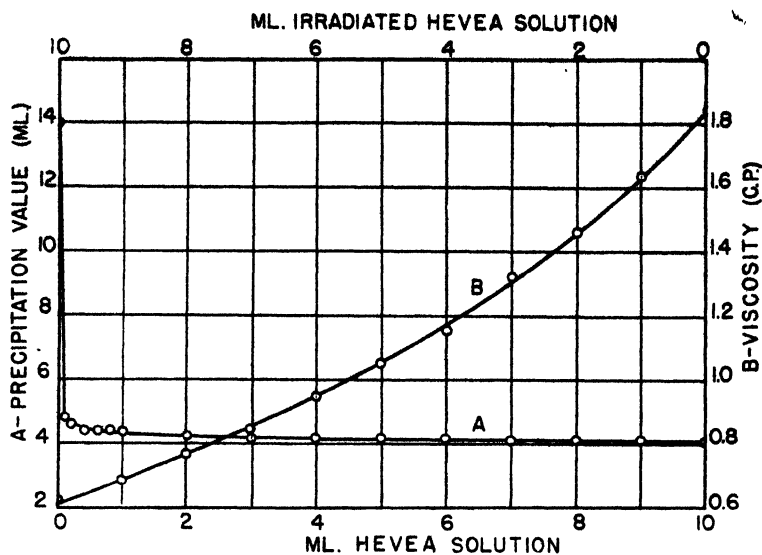
FIG. 6. Binary system: goldenrod rubber and irradiated goldenrod rubber solutions
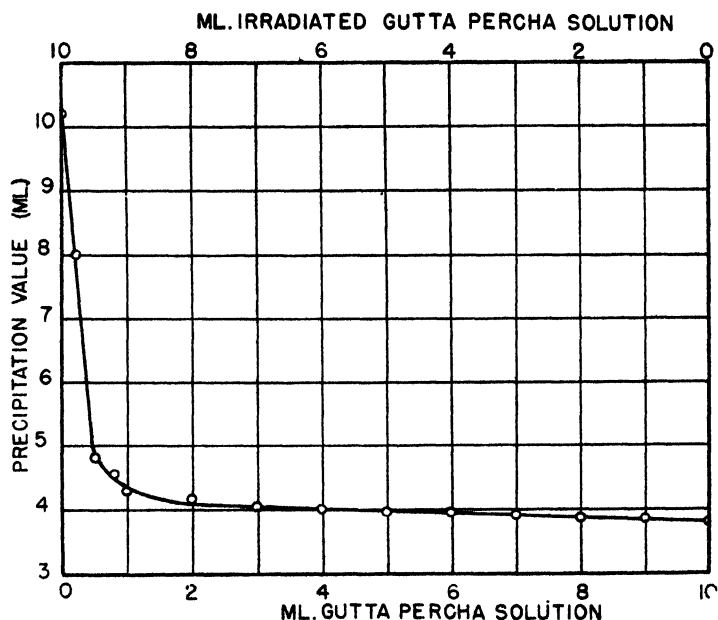
FIG. 7. Binary system: gutta percha and irradiated gutta percha solutions

In another experiment a clarified benzene solution containing 0.175 g. of hevea per 100 ml. was exposed in a Pyrex flask to the light of a Sunlamp, and

samples were removed after various periods. The precipitation value was
determined for each sample and also for a mixture of 1 ml. of each sample with
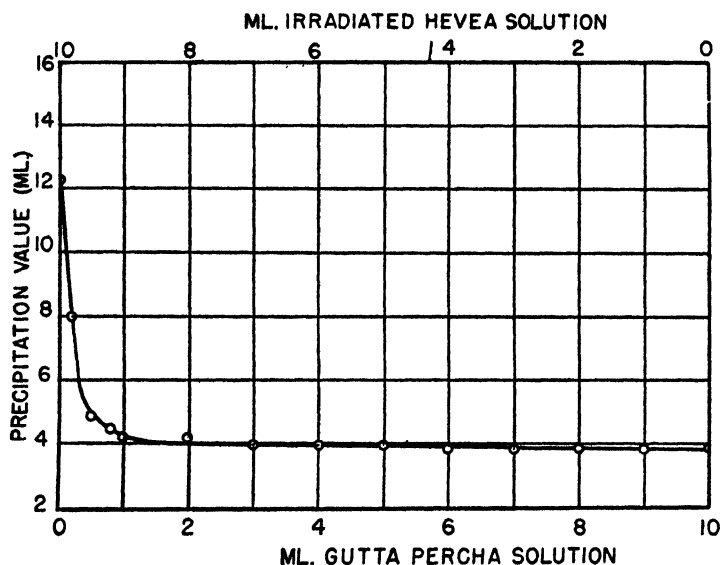
FIG. 8. Binary system: gutta percha and irradiated hevea solutions
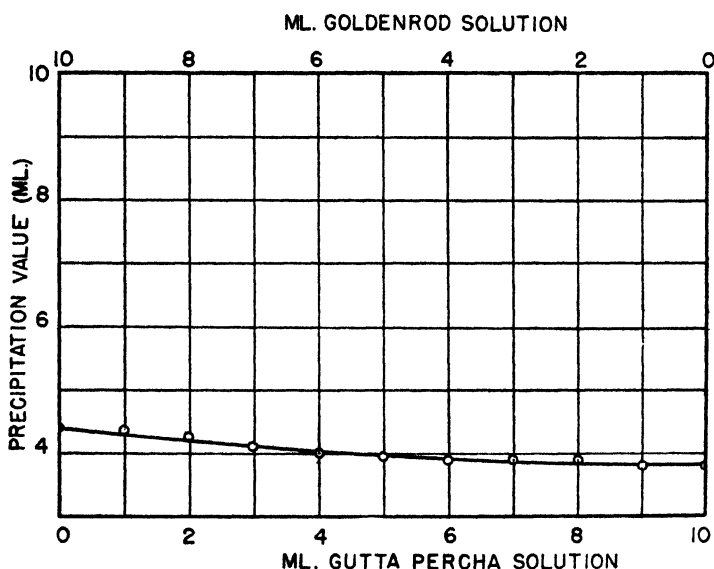
FIG. 9. Binary system: gutta percha and goldenrod rubber solutions

9 ml. of the end product, which had a precipitation value of 10.5 ml. The
results are given in table 4.

Significance of the precipitation value

Curves 5 to 10 show quite clearly that while viscosity is roughly an additive property the precipitation value is not. The viscosity is known to be a function of the average molecular weight. From these curves the precipitation value seems to be a measure of the largest molecular weight present in the rubber in an appreciable amount and is more or less independent of the average molecular weight.

Consider the case of a 0.175 per cent solution of hevea rubber irradiated so as tò change its viscosity from 1.84 to 0.620 centipoise and its precipitation value from 4.05 to 14.0 ml. The addition of four volumes of the irradiated sample to
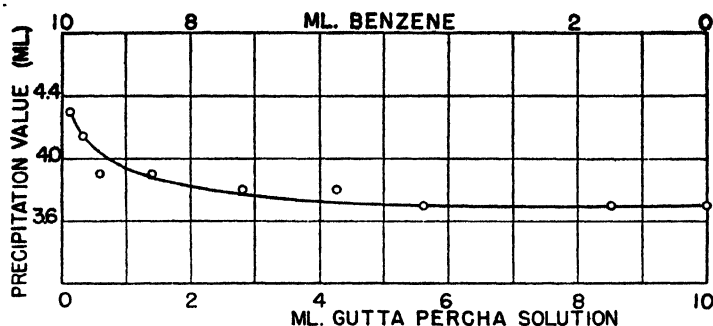
FIG. 10. Effect of concentration on measured precipitation value of gutta percha

TABLE 4

Effect of light on precipitation value of hevea solutions in benzene

SAMPLE NO.	EXPOSURE TIME	PRECIPITATION VALUE	PRECIPITATION VALUE OF 1:9 MIXTURE WITH SAMPLE 6
	hours	*ml.*	*ml.*
1......................	1	4.00	4.10
2.......	5	4.10	4.25
3......................	15	5.50	6.10
4......................	19	7.7	9.1
5.........	21	8.7	10.4
6......................	24	10.5	

one volume of the untreated sample lowers the viscosity by about 1.1 centipoises, while the corresponding change in precipitation value is only 0.15 ml. (see figure 5). It is thus apparent that from these two hevea rubber solutions it would be possible to prepare samples having a precipitation value of 4.10 ± 0.10 ml. and any desired viscosity (average molecular weight) between 1.84 and 0.77 centipoise.

Samples having the same precipitation value may, in fact, differ markedly in their behavior depending on their history. This is illustrated by sample 3 in table 4. A 1:9 mixture of this sample (precipitation value 5.50 ml.) and the end product (precipitation value 10.5 ml.) had a precipitation value of 6.10 ml.

Consider, on the other hand, the mixture of hevea rubber having a precipitation value of 5.50 in figure 5. From this curve, it is obvious that a mixture with nine volumes of a solution having a precipitation value of 10.5 ml. would have a precipitation value of about 10 ml. Thus precipitation value (solubility) alone cannot be used to characterize a rubber sample.

This behavior also affords a basis for a possible explanation of the inconsistencies mentioned above in connection with table 1. In the case of the various pilot-plant goldenrod rubbers, when the precipitation values were between 4.40 and 4.80 ml., the corresponding viscosities varied inconsistently between 0.650 and 0.720 centipoise. This can now be accounted for by assuming slight differences in molecular-weight distribution in the pilot-plant products.

Further, on the basis of this behavior, it might perhaps be anticipated that the relative changes of viscosity and precipitation value caused by irradiation would depend upon the thickness of the layers irradiated and thus upon the size of the sample being irradiated and upon the degree of natural or mechanical agitation. One might expect the precipitation value to increase more for a given fall in viscosity if a thin layer or a small batch were irradiated. In the case of a large batch, that part of the solution on the opposite side of the vessel from the light source might receive less intense irradiation and thus tend to lower greatly the precipitation value of the final mixed product, the viscosity of which might be very low. This would explain the difference between the relationship of precipitation value and viscosity for the goldenrod irradiation product shown in figure 4 and that for the large-batch irradiated solution used to obtain the results of figure 6. In the former case a precipitation value of 25 ml. was reached when the viscosity had fallen to about 0.66 centipoise, while in the latter the precipitation value had risen to only 15.0 ml., though the viscosity had fallen to 0.62 centipoise.

The existence of inconsistency between the relative values of the viscosity and precipitation value for different rubber samples has a bearing on the application of the "standard precipitation point" of Midgley and coworkers. The underlying cause of the inconsistency is the fact that the precipitation value is not very sensitive to changes in the concentration of the rubber solution used, while the viscosity is. This is illustrated by a comparison of figure 1 with figure 6, and figures 7, 8, and 9 with figure 10. The data of Midgley, Henne, and Renoll (4) seem to show that this holds also for the concentration used in the determination of the "standard precipitation point". It therefore follows that neither the precipitation value nor the "standard precipitation point" alone can be satisfactorily used to characterize a rubber. Both may prove of value, however, when considered in conjunction with the viscosity. For example, if two goldenrod samples gave the same viscosity, it could be concluded that the one with the lower precipitation value contained an appreciable amount of a higher-molecular-weight fraction and that it must therefore contain a larger portion of a lower-molecular-weight fraction as a counterbalance.

From the values for the precipitation value and absolute viscosity of hevea smoked sheet, 3.80 ml. and 1.9 centipoises, respectively, and the corresponding average values for goldenrod rubber, 4.52 ml. and 0.68 centipoise, it is apparent

that hevea has a much higher average molecular weight. Attention is called to the fact that this very high molecular weight is not necessary for the preparation of vulcanizates having good tensile strength and elongation; in fact, before compounding and vulcanization, hevea rubber is first broken down by mastication to a condition very close to that of goldenrod rubber. This is shown by the precipitation value and viscosity of masticated hevea, 4.45 ml. and 0.73 centipoise. The corresponding values obtained for rubber from Pilot Plant Run No. 17 are 4.40 ml. and 0.722 centipoise. Goldenrod rubber gum stock vulcanizates have been obtained in this laboratory[2] which have a tensile strength of 2900 to 3600 pounds per square inch and an ultimate elongation of 750 per cent.

SUMMARY

A simple titration method has been developed for determining the "precipitation value" of a sample of rubber. This constant is defined as the number of milliliters of absolute alcohol required at a given temperature to produce a cloud point in 10 ml. of a clarified benzene solution containing 0.0175 g. of the sample. The precipitation value, which depends fundamentally on solubility, is shown to be relatively insensitive to errors in concentration; that is, it changes relatively little over a considerable range of rubber concentrations. It increases progressively when the sample is degraded by treatments which decrease the viscosity, such as mastication, heating, and irradiation. Precipitation values and viscosities have been determined on goldenrod rubber from various pilot-plant runs, on a number of different kinds of natural rubber, and on various binary mixtures of these and other samples of rubber partially degraded by irradiation. It is indicated that the precipitation value—and therefore the solubility—of a rubber specimen is determined by the fraction of highest molecular weight that is present in appreciable quantity. It thus differs from viscosity, which is generally considered to be a function of the average molecular weight. If used in conjunction with viscosity for the same solution, the precipitation value may be expected to give information concerning the relative molecular-weight distributions in different rubber samples.

REFERENCES

(1) CRAXTON, F. C.: Ind. Eng. Chem., Anal. Ed. 14, 593 (1942).
(2) JIRGENSONS, J.: J. prakt. Chem. [N.F.] 161, 30 (1942)
(3) MIDGLEY, T., JR., AND HENNE, A. L.: J. Phys. Chem. 36, 2880 (1932).
(4) MIDGLEY, T., JR., HENNE, A. L., AND RENOLL, M. W.: J. Am. Chem. Soc. 53, 2733 (1931).
(5) MIDGLEY, T., JR., HENNE, A. L., AND RENOLL, M. W.: J. Am. Chem. Soc. 54, 3381 (1932).
(6) ZEITFUCHS, E. H.: Natl. Petroleum News 31, 109 (1914); Proc. 9th Midyear Meeting Am. Petroleum Inst., Sect. III, Refining, 20, 104 (1939).

[2] Private communication.

PHYSICAL CHEMICAL INVESTIGATIONS OF GOLDENROD RUBBER. II

THE PRECIPITATION VALUE AS AFFECTED BY IRRADIATION IN THE PRESENCE OF VARIOUS RUBBER ANTIOXIDANTS AND OTHER REAGENTS

EVALD L. SKAU, FLORENCE B. KREEGER, AND WILLIAM J. RUNCKEL

Southern Regional Research Laboratory,[1] *New Orleans, Louisiana*

In connection with the Emergency Rubber Project, goldenrod rubber has been recovered on a pilot-plant scale from the leaves of the goldenrod (*Solidago leavenworthii*) at the Southern Regional Research Laboratory by a two-stage extraction process in which the leaves were first extracted with acetone to remove resins and then with benzene to recover the rubber.   The present publication is the outgrowth of an investigation of the effectiveness of various rubber anti-oxidants when added to the benzene extracts so obtained.   The results may find application to extracts of other natural rubbers that are obtained from leafy material and may contain chlorophyll.

It has been shown previously (11) that when a benzene solution of goldenrod rubber is irradiated in a Pyrex vessel in the presence of oxygen the precipitation value increases, the viscosity decreases, and the rubber undergoes degradation to a more liquid and sticky product.   The precipitation value was defined as the number of milliliters of absolute ethyl alcohol required to produce a cloud point at 25°C. in 10 ml. of a clarified benzene solution containing 0.0175 g. of sample.   The exact nature of this degradation is uncertain, but for hevea rubber it is generally considered that it involves some kind of oxidation (1, 3, 4, 5, 9).   Also, as in the case of hevea, it may be inhibited by antioxidants and accelerated by activators.

In the present investigation the precipitation value has been used to investigate the light degradation of goldenrod rubber in benzene solution and especially to compare the effects of various commercial[2] rubber antioxidants and other reagents on the rate of such degradation.

EXPERIMENTAL

That goldenrod rubber takes up oxygen on irradiation was shown by the following experiment: A benzene solution of about 1 per cent concentration was clarified with Merck's activated charcoal (11) and put into two stoppered Pyrex Erlenmeyer flasks.   One flask was kept in the dark, and the other was exposed to sunlight for 6 hr.   Aliquots of these solutions were brought to a concentration of 0.175 g. of total solids per 100 ml. of benzene solution, and 10-ml. portions

were then titrated to a cloud point with absolute alcohol to determine the precipitation value. This value was found to be 4.40 ml. for the non-irradiated sample, the same as the original, while that for the irradiated sample had changed to 21 ml. Both irradiated and non-irradiated solutions were evaporated to dryness; benzene was removed in a nitrogen atmosphere and then in high vacuum; and the samples were subjected to combustion analysis. Empirical formulas were calculated from the data, five carbon atoms being assumed in the goldenrod isoprene unit and a trace of nitrogen disregarded. The results are tabulated below:

SAMPLE	C	H	UNIT FORMULA ISOPRENE $= (C_5H_8)_n$	AVERAGE FORMULA
	per cent	*per cent*		
Non-irradiated..........	86.0	11.48	$C_5H_{8.02}O_{0.11}$	$(C_5H_{7.98}O_{0.11})_n$
	86.1	11.40	$C_5H_{7.95}O_{0.11}$	
Irradiated...............	78.6	10.46	$C_5H_{8.00}O_{0.52}$	$(C_5H_{7.92}O_{0.53})_n$
	78.4	10.25	$C_5H_{7.85}O_{0.54}$	

These data show that a total of about 9 per cent of its weight of oxygen was taken up by the goldenrod rubber during the irradiation, that the sum of the percentages of carbon and hydrogen was changed by irradiation from 98 per cent to 89 per cent, and that the calculated formula had changed from $(C_5H_{7.98}O_{0.11})_n$ to $(C_5H_{7.92}O_{0.53})_n$. Thus, 6 hr. of irradiation resulted in an increase of oxygen content corresponding to 0.4 atom of oxygen per isoprene unit.

Procedure for comparing antioxidants

Several common antioxidants and other reagents were tested by adding them to clarified goldenrod rubber solutions, irradiating the solutions, and comparing the precipitation values obtained after irradiation. The solutions were benzene extracts of acetone-extracted goldenrod leaves and were prepared from benzene extracts obtained in the pilot plant. As these extracts were very highly pigmented, it was necessary to clarify them. They were first brought to a concentration of about 1 g. of total solids per 100 ml., and an amount of Merck's activated charcoal equal to the weight of the rubber was added. The mixture was stirred well and allowed to settle. It was then filtered through a layer of the charcoal and a filter aid (Hyflo Super-cel) on a Buchner funnel, brought to a concentration of 0.175 g. per 100 ml., and stored in the dark. During the preparation of the solution exposure to light was avoided as much as possible. This is the standard procedure and concentration used in the determination of precipitation value (11).

Ten-milliliter aliquots of this stock solution were pipetted into the required number of 30-mm. test tubes. Each tube contained a 5-mg. portion of a specific antioxidant. After solution was complete all the tubes were exposed simultaneously to direct sunlight. Complete sets were removed at definite intervals and placed in the dark. Each set included duplicate blanks containing no anti-

oxidant.   The precipitation value was then determined for each tube by titrating to the cloud point with absolute alcohol, and the temperature at the end point was noted.   The precipitation values were corrected to 25°C. by subtracting (or adding) 0.05 ml. for each degree above (or below) that temperature.   Precipitation values above 25 ml. are not measurable because of the high dilution involved.   The presence of the added reagents did not affect the precipitation value of the stock solution appreciably.

Table 1 shows the results of such an experiment.   Irradiation of the blank (the stock solution) for 60 min. changed its precipitation value from 4.45 ml. to 9.6 ml.   On the other hand, no change in the precipitation value was noted after a 60-min. irradiation of the blank in low-actinic Pyrex glass that had approximately the following transmission characteristics: 0 per cent at 3000 Å.; 1 per

TABLE 1

Sunlight irradiation for 60 min.; 5 mg. of reagent in 10 ml. of benzene solution containing 0.0175 g. of goldenrod rubber; precipitation value of original sample = 4.45 ml.

REAGENT ADDED	PRECIPITATION VALUE AFTER 60 MIN. IRRADIATION
	ml.
JZF	5.6
Flectol H (Sample 1)	7.0
Agerite Resin D	8.0
β-Naphthylamine	8.3
Pyrogallol	8.7
Catechol... .	8.9
Hydroquinone	9.3
None (blank)	*9.6*
Quinone	12.0
Phenyl-β-naphthylamine	15.0
Benzophenone	Over 25.0

After 60 min. irradiation in low-actinic red Pyrex glass tube, the titration value was unchanged, 4.45 ml.

cent at 4000 Å.; 4 per cent at 5000 Å.; and 12 per cent at 6000 Å.   It is apparent that this special glass filters out, for the most part, the wave lengths of light that are effective in the photochemical reaction involved.

JZF, Flectol H (Sample 1), Agerite Resin D, β-naphthylamine, pyrogallol, catechol, and hydroquinone inhibited the light reaction in lesser and lesser degree in the order named, while quinone, phenyl-β-naphthylamine, and benzophenone increased the rate of the reaction.   Since 25 ml. is the highest precipitation value measurable, it is apparent that the benzophenone sample may have reached that value in considerably less than 60 min.

In general, the lower the precipitation value after irradiation, the greater is the antioxidant or inhibiting effect of the reagent added.   If the precipitation value after irradiation is higher than that of the irradiated blank, the added reagent can be said to enhance or activate rather than inhibit the light reaction.

In table 1 and in all other tables, the reagents tested are arranged in the order of their apparent efficiencies as inhibitors; all above the blank are inhibitors, all below are activators.

The results of a similar experiment including additional commercial antioxidants are recorded in table 2. A number of apparent anomalies are disclosed by a comparison of these results with those of table 1. The commercial antioxidants, JZF, Flectol H (Sample 1), and Agerite Resin D, show quite definite inhibiting effects on the reaction (table 1). Table 2, however, shows that JZF

TABLE 2

Sunlight irradiation; 5 mg. of reagent in 10 ml. of benzene solution containing 0.0175 g. of goldenrod rubber; precipitation value of original sample = 4.45 ml.

REAGENT ADDED	PRECIPITATION VALUE AFTER IRRADIATION FOR			
	40 min.	70 min.	100 min.	125 min.
	ml.	*ml.*	*ml.*	*ml.*
p-Aminophenol........................	5.10	6.0	6.50	6.7
Stabilite Alba........................	6.4	7.1	7.8	9.5
P.C.P. No. 5.........................	5.7	6.9	8.5	10.5
Methylumbelliferone.................	6.7	7.5	9.3	10.6
JZF................................	6.3	7.7	10.0	11.8
BLE Powder......	6.7	8.5	10.5	12.5
Agerite Resin D.....................	6.2	8.5	11.0	
None (blank)........................	*6.4*	*8.3*	*11.0*	*13.0*
Chlorocarvacrol (crude).............	7.0	10.0	12.5	13.0
Flectol H (Sample 2)..............	6.7	9.0	12.5	13.5
Diphenylamine......................	8.3	11.3	15.5	24.
Albasan............................	7.7	11.0	20.0	25+
Agerite powder.....................	9.7	16.0	25+	25+
1,4-Naphthaquinone.................	11.0	16.0	24.	25+
Phenyl-β-naphthylamine.............	11.0	19.0	25+	25+
MUF	12.5	20.0	25+	25+
Stabilite............................	23.0	25+	25+	25+
Chlorothymol N.F. VII..............	25+	25+	25+	25+
BLE................................	25+	25+	25+	25+
Carvacrol C.P.......................	25+	25+	25+	25+

was less effective, Agerite Resin D had no effect, and Flectol H (Sample 2) had a slight activating effect. Furthermore, phenyl-β-naphthylamine, Agerite powder, and other commercial rubber antioxidants favored the light reaction strongly.

The results of other similar irradiation experiments, for example those given in table 3, verified the effectiveness of Flectol H (Sample 1) and p-aminophenol as inhibitors. In this particular case, as shown by the behavior of the blank, the stock solution used was obviously very much more sensitive to light than that used to obtain the results shown in tables 1 and 2. Examination of the stock solution revealed that it still contained considerable pigment, which indicated that the charcoal treatment for clarification had probably not been as effective as usual.

The discrepancy between Flectol H (Sample 1) and Flectol H (Sample 2) might be due either to a difference between the two samples or to a difference in the two stock solutions of goldenrod rubber used.   The results given in table 4 were obtained to determine the relative efficacy of Flectol H (Sample 1) and Flectol H (Sample 2), and to determine the effect of residual pigmentation on the

TABLE 3

Sunlight irradiation; 5 mg. of reagent per 10 ml. of benzene solution containing 0.0175 g. of goldenrod rubber (sample still slightly pigmented)

REAGENT ADDED	PRECIPITATION VALUE AFTER IRRADIATION FOR			
	0 min.	40 min.	60 min.	80 min.
	ml.	*ml.*	*ml.*	*ml.*
Flectol H (Sample 1)...............	4.45	9.5	23.0	25+
	4.45	9.7	23.0	25+
p-Aminophenol......................	4.45	10.0	22.0	25+
	4.45	10.0	22.5	25+
None (blank)........................	*4.45*	*25+*	*25+*	*25+*

TABLE 4

Sunlight irradiation; 5 mg. of Flectol H per 10 ml. of benzene solution containing 0.0175 g. of goldenrod rubber; rubber solution C was least colored

RUBBER SOLUTION	REAGENT ADDED	PRECIPITATION VALUE AFTER IRRADIATION FOR		
		0 min.	30 min.	70 min.
		ml.	*ml*	*ml.*
A...........	Flectol H (Sample 1)	4.60	8.5	15.0
	Flectol H (Sample 2)	4.50	8.5	14.0
	None (blank)	*4.60*	*25+*	*25+*
B..........	Flectol H (Sample 1)	4.80	9.2	17.5
	Flectol H (Sample 2)	4.90	9.0	15.0
	None (blank)	*4.80*	*25+*	*25+*
C..........	Flectol H (Sample 1)	4.40	6.00	8.6
	Flectol H (Sample 2)	4.50	6.00	8.5
	None (blank)	*4.35*	*6.5*	*10.2*

results obtained.   Three stock solutions, A, B, and C, prepared from different pilot-plant benzene extracts, were so selected as to cover a range of degrees of pigmentation.   Rubber solution A was slightly green; B, slightly yellow; and C, almost colorless.   The results show definitely that the two samples of Flectol H behaved essentially the same; they also indicate that the apparent effectiveness of Flectol H as an inhibitor of the light reaction depends upon the amount of pigment left in the stock solution.   In the case of rubber solution A, for example,

after 30 min. irradiation the Flectol H sample had reached a precipitation value
of only 8.5 ml. when the value for the blank exceeded 25 ml. In the case of
solution C, on the other hand, when the value for the sample in the Flectol H
had reached 8.5 ml., that for the blank had reached only 10.2 ml. Thus the
Flectol H apparently acted more efficiently as an inhibitor in a colored solution
than it did in a colorless solution.

TABLE 5

*Sunlight irradiation; 5 mg. of reagent per 10 ml. of benzene solution containing 0.0175 g. of
goldenrod rubber treated three times with carbon and practically colorless; precipitation
value of original solution = 4.45 ml.*

REAGENT ADDED	PRECIPITATION VALUE AFTER IRRADIATION FOR			
	13 min.	23 min.	33 min.	43 min.
	ml.	*ml.*	*ml.*	*ml.*
p-Aminophenol......................	4.40	4.45	4.50	4.70
	4.50	4.50	4.50	4.70
None (blank).......................	*4.60*	*4.70*	*4.90*	*5.05*
	4.50	*4.70*	*4.90*	*5.10*
P.C.P. No. 5.........................	4.55	4.80	4.95	5.05
	4.55	4.85	4.95	5.05
Stabilite Alba.......................	4.70	4.80	5.10	5.20
	4.60	4.70	5.20	5.30
Methylumbelliferone.................	4.65	4.85	5.00	5.20
	4.65	4.85	5.05	5.25
JZF................................	4.70	4.90	5.20	5.30
	4.70	4.90	5.20	5.30
Agerite Resin D.....................	5.00	5.40	6.70	7.25
	4.80		6.60	7.35
Flectol H (Sample 1)................	5.00	5.95	7.65	8.30
	5.10	5.80	7.75	8.35
Phenyl-*β*-naphthylamine.............	5.10	6.50	8.9	11.0
	5.00	6.60	8.9	11.4

A stock solution of goldenrod rubber that was practically colorless was then
prepared. This was accomplished by three successive treatments, each with a
fresh portion of Merck's activated charcoal. The various reagents that had
shown good antioxidant or inhibiting effects (tables 1, 2, and 3) were added to
10-ml. portions of this solution, and the irradiation was carried out. A sample
with phenyl-*β*-naphthylamine was included. The results, given in table 5,
bring out a number of interesting facts.

Of the antioxidants tested, only *p*-aminophenol inhibited the light reaction.

P.C.P. No. 5, Stabilite Alba, and methylumbelliferone had little or no effect, and JZF, Agerite Resin D, and Flectol H (Sample 1) definitely activated the light reaction. Thus, by removal of the color from the rubber solution by successive treatments with activated charcoal the inhibiting effect of some of the antioxidants was nullified, and in some cases it was changed to an activating effect. This exhaustive charcoal treatment also made the goldenrod rubber solution itself, with no reagent added, much less sensitive to light than were the solutions used in the previous experiments. This is shown by the fact that a 43-min. irradiation of the blank had increased its precipitation value to only 5.10 ml. as compared, for example, to an increase to more than 25 ml. for the corresponding blank in table 3, indicating that the charcoal treatment removes some constituent, or constituents, that activate the light reaction.

TABLE 6

Irradiation of benzene solution containing 0.0175 g. of goldenrod rubber per 10 ml. with added reagents

RUBBER STOCK SOLUTION	REAGENTS ADDED PER 10 ML. SOLUTION	PRECIPITATION VALUE AFTER IRRADIATION FOR		
		0 min.	40 min.	80 min.
		ml.	*ml.*	*ml.*
D.........	None	4.70	5.20	5.90
D.........	5 mg. Flectol H	4.75	6.00	9.1
E.... .. .	0.035 mg. chlorophyll	4.60	25+	25+
E.........	0.035 mg. chlorophyll and 5 mg. Flectol H	4.60	9.2	25+
F....... .	0.14 mg. chlorophyll	4.70	25+	ppt
F.........	0.14 mg. chlorophyll and 5 mg. Flectol H	4.70	25+	25+

It is quite possible that the activating constituents in question are the pigments themselves. Chlorophyll and carotenoids are present in appreciable quantities in goldenrod rubber obtained by benzene extraction of acetone-extracted goldenrod leaves, and these pigments can be completely removed by exhaustive treatment with activated charcoal (10). Chlorophyll is recognized as a catalyst in the photoöxidation of such widely different substances as oleic acid (5, 7), ergosterol (13), benzidine (8), and citronellal (6). It has already been shown that small quantities of chlorophyll speed up the light reaction in the case of hevea rubber (11). On exposure to sunlight for 20 min., for example, a hevea rubber solution in benzene retained its original precipitation value, 3.90 ml., while another portion of the same solution containing a trace of chlorophyll under the same conditions gave a precipitation value of 6.00 ml.

A final experiment was therefore made to determine whether the anomalous behavior of rubber antioxidants in the light reaction under consideration could be explained by the presence or absence of chlorophyll. A colorless solution of goldenrod rubber similar to that used to obtain the results shown in table 5 was prepared by three treatments with activated charcoal. This solution was used to make up three different stock solutions, labelled D, E, and F. Stock solution

D was the original colorless solution; stock solution E contained 0.035 mg. of chlorophyll per 10 ml. and was greenish yellow; and stock solution F contained 0.14 mg. of chlorophyll per 10 ml. and was green.   Ten-milliliter aliquots of these three solutions, with and without 5 mg. of Flectol H added, were then irradiated as before and the changes in precipitation value determined.

The results, shown in table 6, prove (1) that chlorophyll activates the light reaction, (2) that if chlorophyll is present in small quantities Flectol H inhibits the light reaction, and (3) that if no chlorophyll is present Flectol H activates the light reaction.   In all cases the chlorophyll was bleached by irradiation.

When rubber stock solution F was irradiated for 80 min., a slight flocculent precipitate formed and further irradiation for 2 hr. caused the entire rubber sample to separate out on the sides of the tube.   This formation of insoluble rubber by continued irradiation of a solution has already been noted in the literature for hevea rubber (1, 3, 5, 12).

DISCUSSION

It is apparent from this investigation that the relative inhibiting effect of anti-oxidants as estimated by the method described is not a measure of the effectiveness of rubber antioxidants as used in the trade.   p-Aminophenol acted as an inhibitor of the light reaction in all cases where it was tested; on the other hand, phenyl-β-naphthylamine, which is known to be a good rubber antioxidant in the ordinary sense, behaved very definitely as an activator in all the experiments tried.

It is interesting to note that Blake and Bruce (2) reported a similar anomaly. They found that "materials used commercially as antioxidants and which are used regularly in vulcanized rubber are active agents in accelerating the development of tackiness" (stickiness) when milled into hevea pale crepe rubber and irradiated.   They also found that p-aminophenol and hydroquinone acted as inhibitors in this reaction.

In general, the order of the antioxidants and other reagents tested is the same in all the tables.   However, the relative position of the blank, which gives the demarcation between inhibitors and activators, rises in the list as the color in the stock solution decreases.

It has been shown that an antioxidant such as Flectol H activates the light reaction when the rubber solution is colorless and inhibits it when a small amount of chlorophyll is present.   There should be some very small critical concentration of chlorophyll where Flectol H would have no effect.   At this concentration the irradiated sample containing Flectol H should give the same precipitation value as the irradiated blank.   That this critical concentration is slightly different for each antioxidant is indicated by the fact that the position of the blank in the series of antioxidants differs in the tables.

SUMMARY

The precipitation value has been used to investigate the light degradation of goldenrod rubber in benzene solution as affected by the presence of rubber

antioxidants and other reagents. The results indicate: (a) that the reaction of sunlight transmitted by Pyrex glass on a benzene solution of goldenrod rubber may involve the absorption of at least 9 per cent of its weight of oxygen, corresponding to 0.4 atom of oxygen per isoprene unit; (b) that this reaction is activated or accelerated by some substance or substances present in the pilot-plant benzene extracts, but which can be removed by treatment with activated charcoal; (c) that these activating substances include chlorophyll; (d) that certain commercial rubber antioxidants may inhibit this light reaction if the rubber solution used contains a small amount of chlorophyll; (e) that these same antioxidants may, on the other hand, activate the light reaction if the rubber solution used is first exhaustively treated with activated charcoal until colorless; and (f) that the light reaction in question is brought about by wave lengths that pass through ordinary Pyrex glass but are held back for the most part by low-actinic red Pyrex glass. Of the antioxidants tested, p-aminophenol was the most effective in inhibiting the light reaction. Phenyl-β-naphthylamine behaved consistently as an activator. It is apparent that the inhibiting effect of antioxidants as estimated by this method is not a measure of the effectiveness of rubber antioxidants in the ordinary sense.

The authors are indebted to Mary A. Sullivan for assisting in obtaining the results of table 6 and to C. L. Hoffpauir for making the combustion analyses cited.

REFERENCES

(1) ASANO, K.: India-Rubber J. **70**, 307, 347, 389 (1925).
(2) BLAKE, J. T., AND BRUCE, P. L.: Rubber Techn. Conf. (London), Paper 21, p. 736 (1938).
(3) DUFRAISSE, C.: Rubber Chem. Tech. **6**, 157 (1933).
(4) DUFRAISSE, C., AND DRISCH, N.: Rev. gén. caoutchou **8**, No. 71, 9 (1931).
(5) HOUWINK, R.: India Rubber World **107**, 369 (1943).
(6) MEYER, K.: J. Biol Chem. **103**, 597 (1933).
(7) MEYER, K.: Cold Spring Harbor Symposia Quant. Biol. **3**, 341 (1935).
(8) NOACK, K.: Biochem. Z. **183**, 153 (1927).
(9) PORRITT, B. D.: India Rubber World **60**, 1159 (1920).
(10) SKAU, E. L., GRAFF, M. M., AND O'CONNOR, R. T.: Unpublished data.
(11) SKAU, E. L., RUNCKEL, W. J., KREEGER, F. B., AND SULLIVAN, M. A.: J. Phys. Chem. **49**, 281 (1945).
(12) STAUDINGER, H.: Rubber Techn. Conf. (London), Paper 98, p. 253 (1938).
(13) WINDAUS, A., AND BRUNKEN, J.: Ann. **460**, 225 (1928).

PHYSICAL CHEMICAL INVESTIGATIONS OF GOLDENROD RUBBER. III

The Fractionation of Goldenrod and Other Natural Rubbers

EVALD L. SKAU, WILLIAM J. RUNCKEL, FLORENCE B. KREEGER, AND MARY A. SULLIVAN

Southern Regional Research Laboratory[1], New Orleans, Louisiana

It is generally accepted that natural rubber consists essentially of a mixture of homologous polymeric polyprenes differing widely in molecular weight. It was shown by Fol (3) in 1909 that the more readily soluble parts have a lower viscosity than have the more difficultly soluble parts. This difference in solubility has been used by a number of investigators in the past fifteen years as a basis for methods of separating rubber into a number of fractions of different ranges of molecular weights (1, 7, 9, 10, 11, 12, 13, 14, 15, 16, 17, 20). Intrinsic viscosity can be used as a measure of the molecular weight; the higher the intrinsic viscosity, the higher is the average molecular weight (4, 7, 19).

The techniques of fractionation may be classified roughly as either dissolution (diffusion) methods, in which successive fractions are leached out of the rubber by different solvents or solvent mixtures, or precipitation methods, in which the successive fractions are precipitated from solution by increasing amounts of a non-solvent. Fractionation of rubber by these procedures does not result in a sharp separation of polymers of definite molecular weight; on the contrary, each fraction consists of a mixture of polymers over a wide range of molecular weights, as can be shown by its refractionation (5, 7, 8, 11, 12, 13).

In the course of the investigation of rubber obtained from goldenrod leaves (*Solidago leavenworthii*) on a pilot-plant scale by a two-stage extraction process, as part of the Emergency Rubber Project, fractionation was employed as a means of characterization and evaluation of the rubber obtained and also of comparing it with other natural rubbers.

EXPERIMENTAL

Procedure

The method of fractionation employed in the present investigation is a slightly modified form of that used by Johnson (6). In brief it involves the following steps: a sample of about 3 g. of rubber is partially freed from resins by standing in reagent-grade acetone in the dark for 18 to 24 hr. The acetone is decanted, and the rubber is dried *in vacuo*. Two grams of this sample is weighed into a tared 500-ml. glass-stoppered flask with 2 per cent of its weight of antioxidant (Flectol H); 200 ml. of reagent-grade benzene is added, and the flask is allowed to stand in the dark for from 4 to 12 hr., or until solution of the rubber is com-

plete. (In some cases it is necessary to clarify the solution as described in connection with the fractionation of other natural rubbers.) The solution is then brought to 25°C. in a constant-temperature bath, and successive definite quantities of methyl alcohol are added slowly with swirling to precipitate a small portion of the rubber. The temperature is raised until the turbidity disappears, and then the solution is allowed to stand in the 25°C. bath with gentle swirling while the gelatinous precipitate gradually forms. This precipitate is allowed to settle, and the supernatant liquid is then decanted, brought to 25°C. again, and treated with an additional portion of methyl alcohol, as before, to get a second precipitate. This procedure is continued until a total of about 200 ml. of alcohol has been added, after which no precipitate is formed on further addition. The time necessary for settling is short for the first precipitate, and it increases as the fractionation progresses. The last precipitate, which in the case of goldenrod is fluid, is allowed to settle overnight. The size of the fractions obtained depends upon the amount of methyl alcohol added and is influenced somewhat by the rates of precipitation, the amount of agitation, the time allowed for settling, and perhaps by other variables in the technique.

Each successive precipitate is dried *in vacuo*, weighed, and redissolved in benzene to make a 0.2 to 0.4 per cent solution. The concentration of this solution is accurately determined by a total-solids determination on an aliquot. Its relative viscosity is then measured at 25°C. by means of an Ostwald viscometer, as modified by Zeitfuchs (21), the technique of Craxton being used (2). The intrinsic viscosity of the fraction, η_i, is then calculated from the formula

$$\eta_i = \frac{2.303 \log \eta_r}{c}$$

where η_r is the relative viscosity (with respect to pure benzene), and c is the concentration in grams per 100 ml. of solution. The higher the values of the intrinsic viscosity, the higher is the average molecular weight of the sample. The successive volumes of methyl alcohol added to precipitate the various fractions depend on the type of rubber being fractionated and sometimes must be determined by a preliminary experiment. The whole procedure, after the first precipitation is begun, usually requires 2 days, and it must be carried out as rapidly and with as little exposure to light and oxygen as possible during the handling of the sample and of the separate fractions so as to avoid degradation. As the precipitates probably contain only traces of antioxidant, they may be very sensitive to light and oxygen. The intrinsic viscosity is very susceptible to concentration error, and therefore the total solids of the solutions involved must be determined with accuracy.

Typical data

The results of experiment 1, for a sample of goldenrod rubber from Pilot Plant Run No. 17, are given in table 1. These are typical data obtained by the technique described.

Choice of method of graphical representation

As mentioned below, it has been found that these data can best be represented as a form of histogram. The intrinsic viscosity of each successive fraction precipitated is plotted as ordinate against the cumulative percentages precipitated as abscissa. The histogram corresponding to table 1 is shown in figure 1, experiment 1.

TABLE 1

Fractionation data for goldenrod rubber from Pilot Plant Run No. 17

(All viscosities at 25°C.)

METHANOL ADDED, CUMULATIVE	FRACTION NO.	PRECIPITATED	PRECIPITATED, CUMULATIVE	η_a	η_r	CONCENTRATION	η_i	$\eta_i \times$ FRACTION PRECIPITATED
ml.		per cent	per cent			grams per 100 ml.		
53	1	14.25	14.25	1.145	1.883	0.251	2.522	35.93
57	2	17.98	32.23	0.865	1.422	0.330	1.068	19.20
62	3	21.10	53.33	0.808	1.329	0.410	0.694	14.64
70	4	15.24	68.57	0.698	1.149	0.277	0.500	7.62
90	5	14.60	83.17	0.674	1.108	0.272	0.379	5.52
135	6	5.40	88.57	0.646	1.063	0.188	0.325	1.76
185	7	6.99	95.56	0.642	1.056	0.198	0.274	1.92
Unprecipitated....4.18		(99.74)						
Antioxidant added......		2.00						86.60
Accounted for.........		97.74						

$100(\eta_i$ of original sample$) = 87.2$.

Area of histogram a measure of the average molecular weight

It is already known that for rubber polymer mixtures intrinsic viscosity is an additive property and that therefore the intrinsic viscosity of a mixture is the weighted average of the intrinsic viscosities of the constituents (17). That this additivity of intrinsic viscosities is valid for mixtures of goldenrod rubber polymers was confirmed by measurements of the intrinsic viscosities of binary mixtures of two fractions obtained from a fractionation. It thus follows that the total area under the histogram should be independent of the size and number of the individual fractions. That is, $\Sigma[\eta_i$(per cent precipitated)$]$, the sum of the values in the last column of table 1, should be equal to 100 times the intrinsic viscosity of the original sample. In the case of the fractionation data of table 1, these two values, 86.6 and 87.2, are in excellent agreement. Since the intrinsic viscosity is a function of the average molecular weight, it follows that the larger the area of the histogram the larger the average molecular weight of the rubber sample.

The difference between the histogram area and the area calculated from the intrinsic viscosity of the original sample can be taken as a measure of the experimental error in a fractionation. One source of error in obtaining the area of the

histogram is the fact that the total amount precipitated does not add up exactly to the original sample weight.   This is caused (1) by experimental error in estimating the weight of the fractions and (2) by the fact that all of the sample is not precipitated by an excess of the methyl alcohol, as shown by the unprecipitated fraction of 4.18 per cent in table 1.   The first of these errors usually amounts to less than 2 per cent and may be positive or negative.   The second source of error varies with the sample.   The small portion unprecipitated would, if it could be isolated, have a lower intrinsic viscosity than fraction 7, and therefore the area involved in this error, the product (η_i × per cent precipitated), would usually be very small.   This error would always be negative.   The combined effect of both these errors would thus be expected to favor a slightly low value for the experimental   area.

Differences between the histogram areas for duplicate fractionations indicate the reproducibility of the fractionation data.

RESULTS AND DISCUSSION

Experimental results obtained by the fractionation of a number of rubber samples are summarized in table 2, and they are represented graphically for some typical samples in figure 1.   Column 3 of table 2 lists the areas of the histograms. The values in column 4 were obtained by multiplying the intrinsic viscosities of the original samples by 100, and the deviations from these calculated values are given in column 5.

Table 3 shows the differences between the histogram areas for duplicate experiments on a number of rubber samples.

The shape of the histogram

In general, the histogram is a stepwise curve descending from left to right. Experiments 13 and 14 in figure 1 are typical duplicate histograms for a goldenrod rubber sample.   In this case the determinations were run under identical conditions with the same volumes of methyl alcohol added for corresponding fractions.   Experiments 15 and 16 in figure 1, on the other hand, show the histograms for duplicate samples where the sizes of the corresponding fractions were varied by using different amounts of methyl alcohol in their precipitation. As would be expected, the first step of the histogram is higher when the first fraction is small.   Although the histograms for experiments 15 and 16 are quite different, their areas are essentially the same, 60.1 and 59.6, respectively (see table 2).   This further corroborates the general applicability of the additivity of intrinsic viscosity.

Removal of resins

Experiments were made to determine whether it is necessary to remove the resins from the goldenrod rubber by soaking with acetone for 18 to 24 hr. in preparing the sample for fractionation.   Duplicate runs were made on goldenrod rubber PP32 (resin content 15 per cent) in which the sample was prepared for fractionation (a) by the usual procedure as above (experiments 9 and 10); (b)

by acetone precipitation (experiments 11 and 12); and (c) by omitting the removal of resins and taking enough sample to give 2 g. of rubber, excluding resins, calculated on the basis of the resin content previously determined by analysis (experiments 13 and 14).   The areas of the histograms obtained are shown in
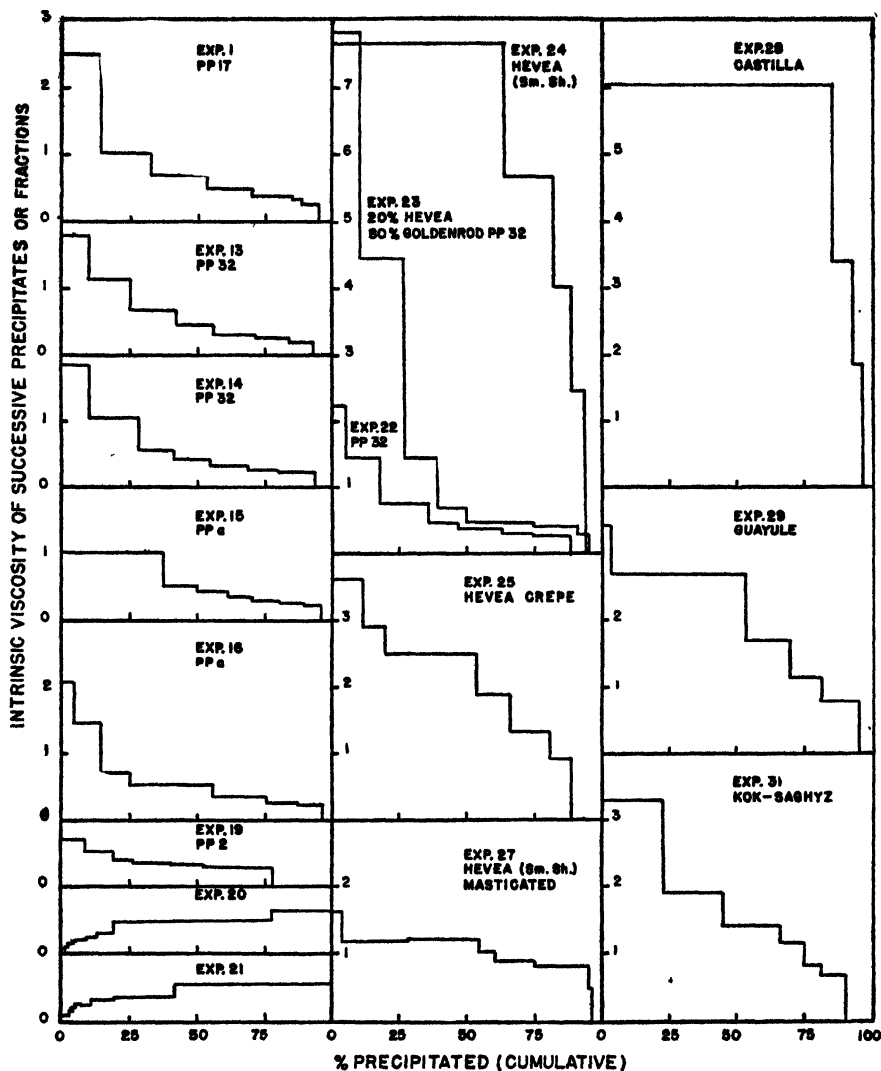
FIG. 1. Histograms corresponding to experiments in table 2

table 2.   The areas for the acetone-precipitated sample, 65.2 and 63.8, as compared to the acetone-soaked sample, 59.9 and 62.2, indicate that precipitation of the goldenrod rubber from the benzene extract with an excess of acetone results in a slightly larger histogram area.   On the other hand, the areas for the sample in which removal of resins was omitted, 62.7 and 61.8, are the same,

TABLE 2

Summary of fractionation data for goldenrod and other natural rubber samples

EXPERIMENT NO.	SAMPLE	AREA (EXPERI-MENTAL)	AREA (CALCU-LATED)	Δ AREA
1*......	Goldenrod PP17†	86.6	87.2	−0.6
2......	Goldenrod PP18	71.8	73.7	−1.9
3......	Goldenrod PPe	69.0	67.2	+1.8
4......	Goldenrod PPc	68.8	67.3	+1.5
5......	Goldenrod PP26	68.8	68.8	0.0
6......	Goldenrod PPd	64.1	71.5	−7.4
7......	Goldenrod PP29	62.6	63.6	−1.0
8......	Goldenrod PPb	62.5	62.1	+0.4
9......	Goldenrod PP32	59.9	63.6	−3.7
10......	Goldenrod PP32	62.2	63.6	−1.4
11......	Goldenrod PP32‡	65.2	63.6	+1.6
12......	Goldenrod PP32‡	63.8	63.6	+0.2
13*......	Goldenrod PP32§	62.7	63.6	−0.9
14*......	Goldenrod PP32§	61.8	63.6	−1.8
15*......	Goldenrod PPa	60.1	59.4	+0.7
16*......	Goldenrod PPa	59.6	59.4	+0.2
17......	Goldenrod PP28	53.0	55.5	−3.0
18.....	Goldenrod PP2¶	34.6	37.3	−2.7
19*......	Goldenrod PP2¶	30.6	37.3	−6.7
20*......	Goldenrod PP4‖	44.7	(58.4)	
21*......	Goldenrod PP4‖	44.7		
22*......	Goldenrod PP32	62.2	63.6	−1.4
23*......	20% hevea smoked sheet–80% goldenrod PP32	198.5		+27.5
24*......	Hevea smoked sheet	626.2	600	+26.2
25*......	Hevea crepe	199.3	205	−5.3
26......	Hevea crepe	213.3	205	+8.3
27*.. ..	Hevea smoked sheet masticated	104.5	102.5	+2.0
28*......	Castilla	550.7	565.0	−14.3
29*......	Guayule (Sample 1)	199.1		
30......	Guayule (Sample 2)	126.8	120	+6.8
31*......	Kok-saghyz	166.3	171.5	−5.2

* Represented graphically in figure 1.
† Sample hard and almost non-sticky.
‡ Acetone-precipitated sample.
§ Resins not removed.
¶ Sample very soft and sticky.
‖ Fractionated by dissolution method.

TABLE 3

Reproducibility of histogram areas

EXPERIMENT NO.	AREAS Σ[ηᵢ(per cent precipitated)]	DIFFERENCE Δ	DIFFERENCE
			per cent
9, 10.................	59.9, 62.2	2.3	3.7
11, 12.................	65.2, 63.8	1.4	2.2
13, 14.................	62.7, 61.8	0.9	1.4
15, 16.................	60.1, 59.6	0.5	0.8
18, 19.................	34.6, 30.6	4.0	12.2
25, 26.................	199.3, 213.3	14.0	6.8

within the probable experimental error, as those for the samples prepared by extracting with acetone.   It can be concluded, therefore, that if the resin content of the golden rod rubber sample is known, the fractionation may be carried out without removal of the resins.   In the experiments reported in table 2, however, unless otherwise indicated, the resins were first removed by standing in acetone for 18 to 24 hr.

Comparison of pilot-plant goldenrod rubber samples

The various samples of goldenrod rubber obtained from the pilot plant have been arranged in table 2 roughly in the decreasing order of the magnitude of their histograms (experiments 1 to 19).   Most of these areas fall between 60 and 70.   Excluding PP17 (experiment 1) and PP2 (experiments 18 and 19), which are exceptional samples, the average area found for goldenrod rubber in these and other experiments made in connection with this investigation is about 63. The average for goldenrod rubber PP2 (32.4) indicates a much lower average molecular weight than usual.   This sample resulted from the extraction of "goldenrod leaves from dead and field-dried stems" and was very much degraded, judging from the fact that it was very sticky and semi-liquid.   On the other hand, the large area (87.2) found for goldenrod rubber PP17 showed that it had an abnormally high average molecular weight.   In fact, this was in a sense a partially fractionated rubber, since the acetone used for the initial extraction of resins from the leaves contained some 20 per cent of benzene, and it had been shown in previous experiments that a mixture of acetone and benzene will extract some of the lower molecular fractions from the rubber, leaving behind a rubber of higher average molecular weight.   This fact is also discussed in connection with experiments 20 and 21.   Goldenrod rubber PP17 obviously had more body and practically no stickiness.

Comparison of hevea rubber samples

A comparison of the areas for experiments 22, 23, 24, 25, and 27 in table 2 and an inspection of the corresponding histograms in figure 1 indicate a marked difference between the various hevea samples and afford an interesting comparison with goldenrod rubber.   The histogram for hevea smoked sheet, experiment 24, shows that hevea rubber in this form has the highest average molecular weight (area = 626).   The duplicate histograms for the sample of crepe rubber investigated, experiments 25 and 26, indicate that hevea in this form has a much lower average molecular weight, as shown by the average area, 206, than hevea in the form of smoked sheet.   The figure for experiment 27, with an area of 104.5, shows the extent to which the hevea smoked sheet was broken down by mastication.   It was estimated that this sample had been masticated roughly to the extent necessary for compounding.   This histogram differs from the others obtained in the present investigation by being nearly horizontal, thus indicating that the sample was made up for the most part of rubber of approximately uniform molecular weight.

Experiment 23, figure 1, is the histogram of a binary mixture of 20 per cent

hevea smoked sheet (experiment 24) and 80 per cent of goldenrod rubber PP32 (experiment 22) made by mixing appropriate volumes of benzene solutions of these two samples of rubber. The histograms obtained in all three of these experiments are plotted together on the same coördinates in figure 1 for comparison. The presence of hevea in the goldenrod rubber sample is apparent by inspection.

It is interesting to note that since intrinsic viscosity is an additive property it is possible to estimate the percentage of hevea rubber in the hevea–goldenrod rubber mixture from the histogram areas. Thus, from the values given in table 2 for the areas of histograms of the hevea and goldenrod rubber samples, 626.2 and 62.2, respectively, and for the 20 per cent hevea mixture, 198.5, the following equation can be written:

$$626.2 \frac{(x)}{100} + 62.2 \frac{(100 - x)}{100} = 198.5$$

where x is the percentage of hevea in the mixture. Solution of this equation gives $x = 24.1$ per cent hevea rubber.

Comparison of samples of various natural rubbers

Several different varieties of natural rubber were subjected to the fractionation procedure. In order to make the benzene solutions, the samples extracted with acetone and dried in the usual way were allowed to stand in benzene for several days with occasional gentle swirling and then clarified. For clarification the solution was filtered through glass wool or cotton, or, if not too viscous, through filter paper. That this procedure is adequate to dissolve the high-molecular-weight polymers is evidenced by the results obtained for hevea smoked sheet (experiment 24) and castilla (experiment 28). The procedure also gives reproducible results. This is shown by the results for duplicate samples of hevea crepe (experiments 25 and 26 in table 2), and by the agreement between the experimental areas of the histograms and their areas calculated from the intrinsic viscosity of the original sample usually determined independently.

The conclusions that can be drawn from these fractionation results are, however, necessarily limited. In the first place, the history of the various specimens is unknown, and secondly, the samples were sometimes not completely soluble in benzene. Though the insoluble residue appeared to be foreign non-rubbery material, it may have consisted partially of rubber that had become insoluble owing to oxidation or some other transformation in the original sample. For this reason the results obtained and summarized in table 2, experiments 24 to 31, and plotted in figure 1 are for the particular specimens of rubber, and may be considered as only roughly representative of the variety of rubber.

Weight distribution curves

Differential weight distribution curves were plotted for the above fractionation data but were found less satisfactory and significant than the histograms in figure 1, because data for only seven fractions were available in each case. The

differential weight distribution curve is obtained by first plotting the integral
weight distribution curve (cumulative per cent precipitated as ordinate against
η_i of the successive precipitates as abscissa) and then plotting the slope of this
curve at various values of η_i against these values of η_i. A smooth integral
weight distribution curve can be drawn accurately only if data for a large number
of small fractions have been obtained. Errors in this plot are of course reflected
in the differential weight distribution curve. This becomes particularly appar-
ent in experiment 23, table 2 and figure 1, a case in which the complete integral
weight distribution curve could be drawn from the given data only arbitrarily.
From the histogram areas, on the other hand, it was even possible to estimate the
percentage of hevea present.

Fractionation and the precipitation value

The various fractions obtained in some of the above experiments were brought
to the appropriate concentration in benzene and titrated with alcohol to deter-

TABLE 4

Precipitation values of successive fractions obtained in fractionation experiments

η_i = intrinsic viscosity at 25°C.; P.V. = precipitation value at 25°C. in milliliters
of alcohol

FRACTION	EXPERIMENT 14		EXPERIMENT 15		EXPERIMENT 19		EXPERIMENT 27	
	η_i	P.V.	η_i	P.V.	η_i	P.V.	η_i	P.V.
		ml.		*ml.*		*ml.*		*ml.*
1..................	1.860	4.20	1.034	4.40	0.713	4.90	1.587	4.40
2..................	1.052	4.40	0.512	5.20	0.540	5.00	1.136	
3............. ...	0.547	4.60	0.453	5.85	0.403	5.25	1.158	4.40
4......	0.413	5.15	0.328	6.70	0.326	5.65	1.010	4.45
5......	0.334	5.70	0.286	7.45	0.304	6.25	0.880	4.50
6..................	0.256	6.35	0.274	8.00	0.292	6.65	0.806	4.60
7..................	0.244	6.95	0.215	9.80			0.483	
Original sample..	0.636	4.50	0.594	4.50	0.373	5.30	1.025	

mine their precipitation values at 25°C. (18); i.e., the number of milliliters of
absolute ethyl alcohol necessary to produce a cloud point in 10 ml. of a clarified
benzene solution containing 0.0175 g. of rubber sample. Typical results are
listed in table 4, which gives the intrinsic viscosities and precipitation values
of the separate fractions obtained in experiments 14, 15, 19, and 27, thus cor-
responding to the successive steps in these histograms in figure 1.

It is evident that the precipitation value is always lowest for the first fraction
and that it increases, while the intrinsic viscosity decreases with each successive
fraction; thus, for experiment 14 it increases from 4.20 to 6.95 ml. from fraction
1 to fraction 7.

The first fraction usually has a lower precipitation value than that of the
original sample, and the difference is more marked if the first fraction is small.
For example, in experiments 14 and 15 the precipitation values of the original

goldenrod rubber samples were identical, 4.50 ml.   As can be seen by referring to figure 1, the first fraction in experiment 15 was very large (37.7 per cent); still it had a precipitation value of 4.40 ml., which was lower than that of the original sample.   The first fraction in experiment 14, on the other hand, was relatively small (10.3 per cent), and it had a much lower precipitation value, 4.20 ml.   The second fraction (17.0 per cent) had a precipitation value of 4.40 ml., which was also lower than that of the original sample.   These differences are significant; with the fact that the precipitation value increases rapidly for successive fractions, they indicate that the fractionation-by-precipitation technique used is fairly efficient for goldenrod rubber.   Since the presence of only a small amount of a higher polymer is effective in lowering the precipitation value (18), it can be concluded that very little of the high-polymer portion of the sample is included in the later fractions.

Fractionation by dissolution

Some of the first fractionations of rubber performed in this laboratory were by the so-called dissolution method with mixed solvents, essentially as described by Bloomfield and Farmer (1).   This method is probably not so reliable as the precipitation method, since considerable degradation may take place before the fractions are separated and characterized.   For example, it involves long periods of standing under solvents, evaporation of quantities of solvent, and considerable handling of the separate fractions before they can be evaluated.   Complete fractionation takes 2 to 3 weeks as compared to 2 or 3 days by the precipitation method.

For comparison the results of two fractionations of a sample of goldenrod rubber by the dissolution method are given graphically in figure 1, experiments 20 and 21.

Briefly the procedure for experiment 20 was as follows: A 20-g. goldenrod rubber sample was weighed into a stoppered 5-liter Erlenmeyer flask.   It was covered with 1 liter of a mixture of 97 per cent acetone–3 per cent benzene and allowed to stand at 25°C. in the dark under an atmosphere of nitrogen, being gently swirled twice daily.   After 48–72 hr. an equilibrium seemed to be reached, as shown by occasional total-solids determinations on 10-ml. aliquots.   The solvent was then decanted carefully, and the residue was reëxtracted in the same way with 1 liter of a mixture of 95 per cent acetone and 5 per cent benzene.   Each successive extraction was with a solvent mixture richer in benzene (3, 5, 10, 20, 25, 30, 35, 40, 50, and 60 per cent, respectively).   When a mixture of 40 per cent acetone and 60 per cent benzene was finally used, no undissolved material remained.

The various decanted solutions were evaporated to dryness in an atmosphere of nitrogen, precautions being taken against undue exposure to light.   Each residue or fraction so obtained was dried in vacuo, weighed, and redissolved in benzene to determine its intrinsic viscosity.

A similar extraction using acetone and petroleum ether (boiling point, 35–60°C.) mixtures is designated as experiment 21.

The results of experiments 20 and 21 have been plotted in figure 1.   In the

case of fractionation by dissolution the first, more soluble, fractions contain the "oxide" portion and the polymers of lower molecular weight. Thus, in this case, the intrinsic viscosities of the first fractions are very low (less than 0.1) and for successive fractions are higher and higher. The precipitation values of the first two fractions in these two experiments were greater than 25 ml., which was additional proof of the absence of appreciable amounts of high-molecular-weight constituents in these fractions.

As shown in table 2, the areas of the histograms for experiments 20 and 21, plotted in figure 1, are identical (44.7). They are, however, much lower than the area (58.4) obtained for this sample by a preliminary form of the technique for fractionation by precipitation. This large difference in area indicates that considerable degradation of the sample had occurred during the fractionation by the dissolution method.

SUMMARY

A method for fractionation of rubber by successive precipitations from a benzene solution has been investigated and applied to various samples of goldenrod and other varieties of natural rubbers. The size of each successive fraction and its intrinsic viscosity are determined. These factors give an indication of the weight distribution. The data can best be presented in the form of a histogram, the shape of which depends upon the number and size of the fractions, but which for the natural rubbers investigated is always a series of descending steps. The area of each histogram, however, is independent of the number and size of the fractions and is characteristic of the particular sample of rubber. The higher the average molecular weight, the larger is the area. This area is shown to be 100 times the intrinsic viscosity of the original sample. It might therefore be concluded that as a control method, or for the evaluation of different samples of goldenrod rubber, fractionation has no advantage over the relatively simple determination of the intrinsic viscosity of the original sample, unless the information revealed by distribution of the components of variable viscosity warrants the considerable amount of work involved in obtaining the results.

Comparison has been made of the histogram areas obtained for (1) various samples of goldenrod rubber from pilot-plant runs, (2) various hevea rubber samples, and (3) specimens of various other natural rubbers.

Evidence is given to show that histogram areas obtained from fractionation data can be used to estimate the percentage of hevea rubber in hevea–goldenrod rubber mixtures.

Fractionations by the dissolution method were found to be less satisfactory, owing perhaps to degradation of the sample.

REFERENCES

(1) BLOOMFIELD, G. F., AND FARMER, E. H.: Trans. Inst. Rubber Ind. 16, 69 (1940).
(2) CRAXTON, F. C.: Ind. Eng. Chem., Anal. Ed. 14, 593 (1942).

(3) Fol, J. G.: Kolloid-Z. **12**, 145 (1913).
(4) Gee, G.: Trans. Faraday Soc. **36**, 1162, 1171 (1940).
(5) Gee, G., and Treloar, L. R. G.: Trans. Inst. Rubber Ind. **16**, 184 (1940); Rubber Chem. Tech. **14**, 580 (1941).
(6) Johnson, B. L.: Private communication from Dr. J. N. Street, Firestone Tire and Rubber Co.
(7) Kemp, A. R., and Peters, H.: Ind. Eng. Chem. **33**, 1391 (1941).
(8) Mark, H.: Paper Trade J. **113**, No. 3, 34 (1941).
(9) Midgley, T., Jr., and Henne, A. L.: J. Phys. Chem. **36**, 2880 (1932).
(10) Midgley, T., Jr., and Henne, A. L.: J. Am. Chem. Soc. **59**, 706 (1937).
(11) Midgley, T., Jr., Henne, A. L., and Renoll, M. W.: J. Am. Chem. Soc. **53**, 2733 (1931).
(12) Midgley, T., Jr., Henne, A. L., and Renoll, M. W.: J. Am. Chem. Soc. **54**, 3343 (1932).
(13) Midgley, T., Jr., Henne, A. L., and Renoll, M. W.: J. Am. Chem. Soc. **54**, 3381 (1932).
(14) Pummerer, R.: Kautschuk **3**, 233 (1927).
(15) Pummerer, R., Andriessen, A., and Gundel, W.: Ber. **61B**, 1583 (1928).
(16) Pummerer, R., and Miedel, H.: Ber. **60B**, 2148 (1927).
(17) Sebrell, L. B.: Ind. Eng. Chem. **35**, 735 (1943).
(18) Skau, E. L., Runckel, W. J., Kreeger, F. B., and Sullivan, M. A.: J. Phys. Chem. **49**, 281 (1945).
(19) Staudinger, H., and Bondy, H. F.: Ann. **488**, 153 (1931); Rubber Chem. Tech. **5**, 278 (1932).
(20) Titani, T., and Yosida, T.: Proc. Imp. Acad. (Tokyo) **16**, 33 (1940).
(21) Zeitfuchs, E. H.: Natl. Petroleum News **31**, 109 (1914); Proc. 9th Midyear Meeting Am. Petroleum Inst., Sect. III., Refining, **20**, 104 (1939).

THE POLYMORPHISM AND TRANSITIONS OF ANHYDROUS AND HYDROUS SODIUM STEARATE

ROBERT D. VOLD

Department of Chemistry, The University of Southern California, Los Angeles, California

This paper presents the results of a study of the transitions occurring in dry and hydrous sodium stearate (2.5 per cent water), based on dilatometric, microscopic, and calorimetric measurements. The work is of importance with respect to the question of how many modifications of soap can be realized at room temperature, the conditions for preparing each form, and the reversibility of the various transitions.

The results, together with previous work, lead to the transformation scheme shown below. Full lines indicate thermal transitions at the temperature given. Dotted lines indicate that one form is convertible to the other in various ways, to be discussed later in the paper. All are properly referred to as forms or modifications of soap, irrespective of whether they are true polymorphs (different molecular arrangements of the same composition), distinct phases in the

soap-water system or even, as is probably true of beta and lambda, modifications differing from each other merely by a transition of the second kind.

```
GAMMA         ◄─────────────────────────┐
(dry or hydrous)                         │
                                         │
    ▲                                    │ 90°C.
    ┊                                    │
    ┊                                    ▼
         71°C.
BETA  ◄══════════► LAMBDA  ◄─ ─ ─ ─►  SUPERCURD
   ┊▲▲             (hydrous)   90°    (dry or hydrous)
   ┊┊┊│
   ┊┊┊│ 52°C.
   ▼┊┊│
   ┊┊
ALPHA
(C₁₇H₃₅COONa·½H₂O)
```

$$\text{ALPHA} \quad (C_{17}H_{35}COONa \cdot \tfrac{1}{2}H_2O)$$
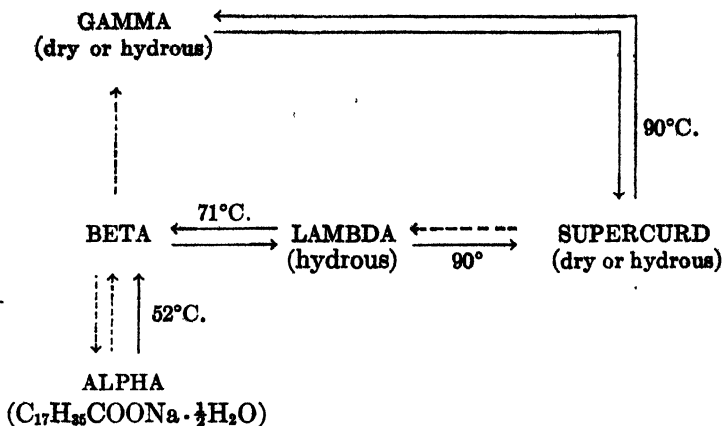
The nomenclature of soap phases is rather confused, owing to the recent independent developments in several laboratories. The "high-temperature curd" of earlier work (14) is now referred to as "supercurd", in accord with the suggestion of McBain and Lee (7). "Beta" was first used by Thiessen and co-workers (12) to describe the form resulting from heating the alpha phase of a single pure soap to its transition temperature. The same symbol has also been used to describe crystalline soap forms at room temperature obtained in various other ways (spontaneous fiber growth (6), slow cooling of soap boiler's neat soap (4), grinding (2), and room-temperature dehydration of alpha). Some or all of these may be very different from the "beta" formed by heating "alpha". The author has suggested (15) the use of the term *Thiessen's beta* or simply *beta* alone to refer to the nearly anhydrous phase formed on heating alpha, and *hydrous beta* for the phase formed by cooling soap boiler's neat soap. Mills (10) independently described an "omega" form which has been shown to be identical with gamma. Although Ferguson (4) prefers to retain the term "omega", it seems more useful to conform to the original designation of McBain and de Bretteville (3). Ferguson (5) has also described a "delta" phase of unknown hydration. Finally, we find it necessary to introduce the term "lambda", since the form produced by cooling supercurd is not always gamma.

EXPERIMENTAL METHODS AND MATERIALS

Since it is relatively difficult to prepare perfectly pure stearic acid, most work on sodium stearate systems has been done with slightly impure preparations. It is consequently a result of some importance that the number of transitions, their reversibility, and to some extent their temperatures are not critically dependent on the purity of the stearic acid, provided a fairly pure preparation is used, or on the precision of its neutralization.

This is shown by the results in table 1, giving the values obtained for the transition temperatures of five independent preparations of anhydrous sodium stearate,

all of which had been previously melted (in sealed glass containers) and cooled slowly. Sample A is neutral. Sample I-b, in addition to being made from an

TABLE 1

Transition temperatures of various anhydrous sodium stearates

SAMPLE NO.	SOURCE OF ACID	IODINE NUMBER OF ACID	EQUIVALENT WEIGHT OF ACID	MELTING POINT OF ACID °C	SOAP PREPARATION
A	Kahlbaum's best		284 3	69	Neutralized in 95% alcohol; dried at 105°C.
I-b.	Eastman Kodak best	2 3	285 2	68 9	Neutralized; recrystallized from 75% aqueous alcohol
II	L. L Lyon*	0.1	282 5	68 5	4% excess NaOH added; soap then recrystallized from 85% aqueous alcohol
III	L. L. Lyon*	0 1	282.5	68 5	Same as II, except exactly neutral
IV	L. L. Lyon*	0 1	282.5	68 5	Neutralized, recrystallized from 85% aqueous alcohol with a trace of urea
E	Eastman Kodak Practical	2.9	284.3	63–66	Neutralized in 95% alcohol, dried at 105°C.

Transition temperature (calorimetric)†

TRANSITION	SAMPLE A	SAMPLE I b	SAMPLE II	SAMPLE IV	SAMPLE E
Formation of supercurd	89	91	93	94	Present
Supercurd–subwaxy	114	116	116	118	108
Subwaxy–waxy	134	139	132	135	129
Superwaxy–subneat	208	204	209	204	209
Subneat–neat	238	232	226	235	233

* This acid was prepared from Sample E by Mr. Luther L. Lyon of this laboratory by double recrystallization of the lead salts from alcohol and vacuum distillation of the methyl esters. Later work has shown its low equivalent weight, and presumably also its low melting point, to be due to a small content of residual methyl stearate. Since this would be saponified and the alcohol driven off during the neutralization of the stearic acid, the resulting soap would be purer than indicated by the constants of this acid.

† The waxy superwaxy transition has too small a heat effect to be observed in the calorimeter used. Sample E exhibited a small heat absorption at 180°C., possibly due to its content of oleate.

inferior acid, undoubtedly contains some free stearic acid, owing to having been crystallized from an aqueous medium in the absence of excess alkali to repress hydrolysis. Sample II is probably the closest to pure sodium stearate of the

present preparations. Sample IV, though from the same acid, contains some free stearic acid for the same reason given above, and also a trace of urea, which Thiessen (12) found useful in promoting the growth of alpha crystals.

Experimental technique

The general features of the dilatometric technique have already been described (13, 16). The sample is packed into a small glass tube which is then sealed to a calibrated capillary and filled with mercury by means of a three-way stopcock connecting the dilatometer alternatively with a vacuum line or a mercury reservoir. Care was taken to avoid mechanical damage to the soap crystals,

A   B
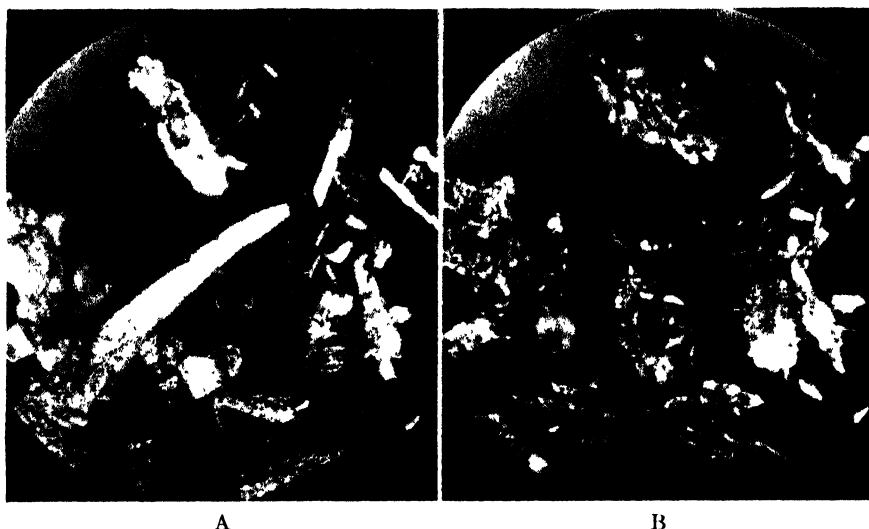
Fig. 1. Mechanical disintegration accompanying the alpha–beta transition of sodium stearate. Plate a was taken at 25°, plate b at 65°, of the same field of view. (Crossed polaroids; 40 fold magnification.)

heating the sample, or prolonged evacuation. Heating and cooling rates were uniformly 0.2–0.3°C. per minute.

Microscopic observations were made to determine the occurrence or non-occurrence of the alpha–beta transition. Alpha sodium stearate forms well-defined crystals whose external form is retained on drying, although the ability to transform to beta at 52°C. is thereby lost. The transition is marked by violent mechanical disintegration of the crystals, as is illustrated in figure 1. These photographs were taken between crossed polaroid plates at a magnification of 40×. The sample was placed on a glass cover slip supported above a heating element of parallel wires. It was then observed while heating to a temperature (62°C., determined by the melting of a reference crystal of palmitic acid) above the alpha–beta transition but below other transitions of sodium stearate.

No apparent change in microscopic appearance at the transformation beta ⇆ lambda was detectable with the same apparatus.

The calorimetric procedure was essentially that previously described (14). The sample was filled into a pear-shaped cell having a thermocouple well as core of the pear, with due precautions to avoid grinding or powdering of the crystals, and heating of the sample in the sealing operation. This cell and a reference cell containing inert material (Nujol) were heated in the same environment, and the temperature difference between them recorded accurately at intervals of 1 or 2 min. by means of a thermocouple, type K2 potentiometer, and H. S. galvanometer.

In previous work good thermal contact was achieved between the sample and the wall of the thermocouple well by melting the sample against the glass, which it wets. This expedient was impossible in the present work, since certain of the transitions are not thermally reversible. The effect of having the sample present as a loose powder is to slow down heat transfer. This was found to be of insufficient magnitude to affect the results obtained for transition temperatures at the rate of heating employed (1.5°C. per minute), although the sizes of the peaks for each transition were larger than in premelted samples (i.e., the temperature of the sample fell further below that of the reference cell and remained lower longer for a given heat absorption because of the lowered transfer rate). Relative values of heats of transition can be obtained from the size of the peaks, however, even though the physical state of the sample makes any calculation of absolute values of doubtful validity.

Before and after calorimetric experiments the samples were always cooled at the same rate to minimize the effect of possible difference in phase composition resulting from unequal degrees of reversal of certain transitions. The selected rate, that of natural cooling of the entire calorimeter in the laboratory, whose temperature seldom varies 5°C., ranged from 10°C. per minute at 300°C. through 6°C. per minute at 200°C. to 1°C. per minute below 100°C. A few samples were cooled more rapidly than this without apparent effect on the transition temperatures found on subsequent reheating. No differences were found between samples re-run immediately after cooling and those re-run after standing at room temperature for three months.

Dry soap samples were prepared for this work by heating the loose powder to constant weight at 105°C. Aqueous samples were prepared by exposing samples crystallized from aqueous media in a desiccator for varying lengths of time. The water content was then determined by drying to constant weight at 105°C. (16).

<center>RESULTS AND DISCUSSION</center>

<center>*Alpha → beta sodium stearate*</center>

Alpha sodium stearate was prepared by crystallization of the soap at room temperature from many solvents including alcohol, pyridine, *n*-amyl alcohol, and 1,4-dioxane, none being specially dried. Buerger, Smith, and coworkers (2) report that it has the constitution $C_{17}H_{35}COONa \cdot \frac{1}{2}H_2O$. This composition requires 2.86 per cent water, whereas all the present samples had considerably less water and would thus be mixtures of alpha and one or more less hydrous phases. Confirmatively, though all recognizable crystals had the alpha shape,

only a portion underwent the alpha–beta transition, as determined by micro-scropic examination. For the least hydrous sample, containing 0.75 per cent water, no microscopically visible transition occurred, showing that no alpha was present.

The transition from alpha to beta occurring at 52°C. is not generally reversed on cooling, as is demonstrated by its failure to recur on second heating. These results are illustrated by the curves shown in figures 2 and 3. Dilatometric
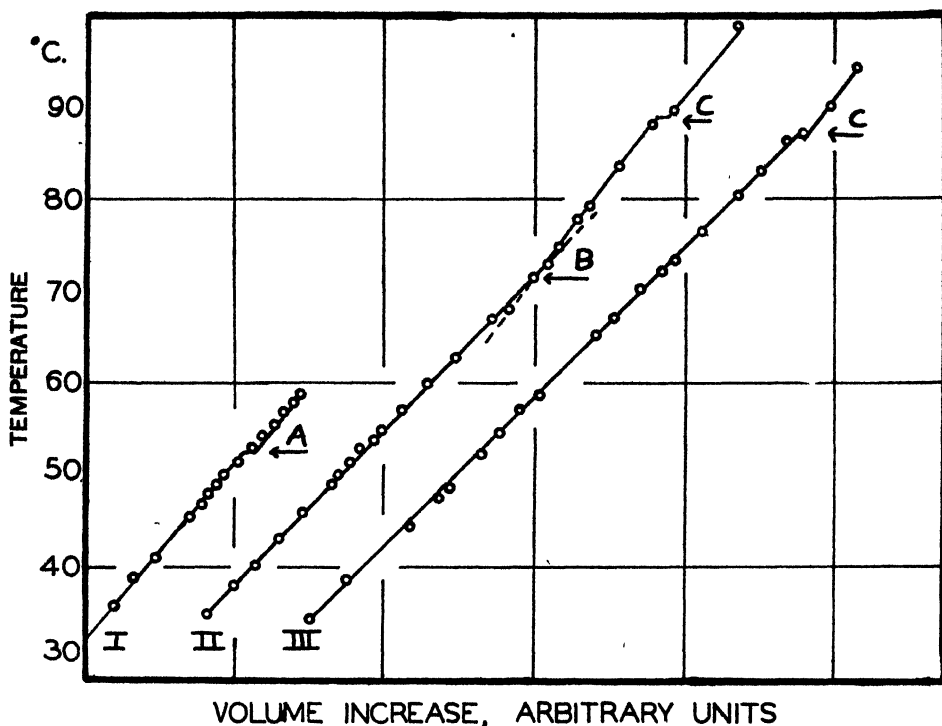
FIG. 2. Dilatometric behavior of sodium stearate between room temperature and 100°C. Curve I, sodium stearate with 1.47 per cent water, first heating; curve II, the same sample after cooling from 57°C.; curve III, the same sample after cooling from 99°C.

curve I of figure 2, obtained on first heating of crystalline sodium stearate, shows a small but definite break at 52°C. On second heating of this same sample (curve II), this break is absent. Similar results were obtained when these experiments were repeated on a fresh sample. Calorimetric curve I of figure 3, obtained on first heating of a preparation containing alpha sodium stearate, shows a large peak due to the heat of decomposition of the hemihydrate. This peak is generally missing on reheating, as seen in curves II and III of this same figure. Similar results were obtained on five other crystalline preparations, only a sample containing 0.75 per cent water failing to show this peak on first heating. It seems likely that this sample had undergone room-temperature dehydration sufficient to convert it completely to beta or some less hydrous form.
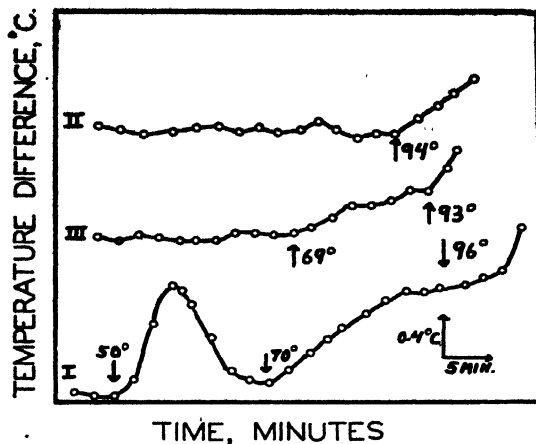
FIG. 3. Calorimetric behavior of sodium stearate between room temperature and 100°C. Curve I: sodium stearate with 1.88 per cent water, containing some alpha form; first heating; transitions present are alpha–beta, genotypic, and lambda–supercurd. Curve II: the same sample after heating to 167°C. and cooling; only transition present is to super-curd. Curve III: the same sample dehydrated to 0.75 per cent moisture over phosphorus pentoxide at room temperature; first heating; transitions present are genotypic and lambda–supercurd.

TABLE 2

Dilatometric data for figure 2

Weight of sodium stearate, 0.1582 g.; dilatometer calibration, 1 mm. is 2.24×10^{-4} cc. $= 1.42 \times 10^{-3}$ cc. per gram of soap

RUN NO. 1		RUN NO. 2		RUN NO. 3	
Temperature	Reading	Temperature	Reading	Temperature	Reading
°C.	mm.	°C.	mm.	°C.	mm
36.0	332.0	23.5	365.0	26.0	399.0
39.0	326.2	27.2	356.5	29.0	392.0
41.1	321.2	35.2	337.0	33.5	382.0
45.5	311.5	38.0	330.0	38.0	371.0
47.0	308.0	40.2	324.0	44.5	353.5
48.0	306.5	43.5	318.0	47.5	345.0
49.0	304.5	46.0	313.0	48.6	342.2
50.0	302.5	49.0	304.0	52.2	334.5
51.5	299.0	50.0	302.0	54.5	329.0
54.0	292.0	51.5	298.8	57.0	324.0
55.5	289.5	53.0	296.5	58.7	318.5
57.0	286.9	54.0	293.5	65.0	303.5
58.0	284.0	55.0	291.0	67.0	298.5
59.0	282.5	57.0	286.0	70.0	291.8
		60.0	278.5	72.0	286.0
		63.2	271.2	73:0	282.5
		67.0	261.5	76.5	275.0
		69.0	256.5	80.5	265.0
		71.5	250.5	83.0	259.5
		73.0	247.0	85.8	252.5
		75.0	243.5	87.0	247.5
		77.5	238.5		
		79.0	236.0		
		83.5	227.0		
		88.0	219.0		
		89.5	212.5		
		98.6	196.0		

These observations are in accord with Thiessen's (12) earlier conclusion that the transition from alpha to beta is monotropic and with the x-ray work of Mc-Bain and coworkers (3), who found that after alpha had been heated above 54°C. only beta was present in the cooled sample. Recently, however, Buerger *et al.* (2) found that beta sodium stearate when heated in a sealed tube at 47°C. with a drop of water reverts to alpha. We find that beta will dissolve and alpha grow when both are in contact with the same saturated solution of sodium stearate in
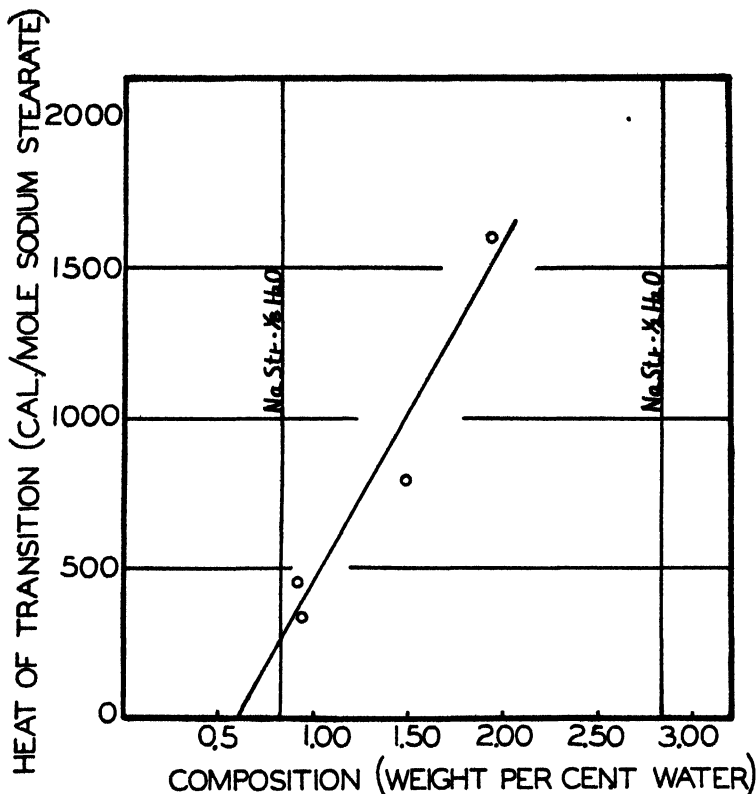
FIG. 4. Dependence of the heat effect at the alpha–beta transition upon water content of the sample.

70 per cent ethyl alcohol and water at room temperature. In one isolated instance a small amount of alpha was re-formed in a calorimeter cell after heating above the temperature of the alpha–beta transition and cooling to room temperature. Thus it appears that another variable, the relative humidity of the atmosphere, must be considered in connection with the reversibility of transitions amongst these hydrous soap phases.

Also, according to Buerger (2), alpha is transformed to beta by grinding or dehydration at room temperature. Calorimetric and dilatometric results confirm the conclusion that alpha is destroyed by these treatments, although it

seems likely from x-ray results (11) that other phases than beta may also be formed.

The heat of transformation at 52°C. of samples containing alpha varies with the water content of the sample and, in particular, extrapolates to zero at a water content of *ca.* 0.6 per cent. Data illustrating this point are shown in figure 4. This result might be taken to indicate that the phase produced by room-temperature dehydration of alpha contains about 0.6 per cent water, which is not far from the 0.74 per cent required for the compound $C_{17}H_{35}COONa \cdot \frac{1}{8}H_2O$ reported for beta by Buerger (2), using a xylene distillation method to determine water. However, neither observation suffices to prove that a true stoichiometric hydrate of this composition is formed.

The genotypic transition: beta ⇆ lambda

Thiessen (12) was the first to report the existence of a transition in soaps at or near the melting point of the corresponding fatty acids (hence the name "genotypic"). According to our present evidence this transition seems to be of the second kind, i.e., finite discontinuities occur only in derivative properties. No change occurs in microscopic appearance. The curve of volume *versus* temperature shows only a change in slope, as is seen at point B in curve II of figure 2. Likewise the curve of differential temperature *versus* time shows a change in slope, but not a peak, as is seen in curves I and III of figure 3 at the points marked 70°C. and 69°C., respectively. This effect, while not pronounced, is clearly identifiable by contrast with curve II obtained on a sample in which this transition did not occur. Above this temperature the heat capacity of the soap increases so that it heats more slowly in relation to the reference cell than it did below that temperature, at constant rate of heat input.

Table 3 summarizes the results of calorimetric studies of this transition. All samples were made from Lyon's stearic acid and the soap then recrystallized from aqueous alcohol (see table 1) except those with 1.88 per cent water, which were from Eastman Kodak best-quality stearic acid. The samples were heated in sealed glass containers to the temperatures shown in column 2 and then cooled slowly to room temperature before running in the calorimeter. Column 3 gives the phases probably present (judging from current literature and the known transition temperatures) at the maximum temperature, while column 1 gives the water content. Column 4 gives the temperature of the genotypic point, if any, as determined calorimetrically.

The temperature of the genotypic transition shows no systematic variation with water content. The transition is reversible, i.e., is found repeatedly on reheating the same sample, if the system has not been heated hot enough to form supercurd before cooling. In some cases it is reversible even after the sample has been heated above the lambda → supercurd transition temperature, particularly with samples containing less than 1.5 per cent water. However, it is generally not found on reheating samples which have been heated beyond the supercurd–subwaxy transition point.

If the beta ⇆ lambda change is reversible but is not shown by some samples

heated into the supercurd phase, it follows that the lambda → supercurd transition is not always reversible, gamma sometimes being formed when supercurd is cooled.

The apparent dependence of the occurrence or non-occurrence of the genotypic transition on the temperature to which the sample has been heated previously

TABLE 3

Calorimetric data for the genotypic transition

COMPOSITION	MAXIMUM PREVIOUS TEMPERATURE	PHASE AT MAXIMUM PREVIOUS TEMPERATURE	TRANSITION TEMPERATURE
weight per cent water	°C.		°C.
0.94	35	α and β (or some other phase less hydrous than α)	71
1.47	35	α and β (or some other phase less hydrous than α)	76
1.50	35	α and β (or some other phase less hydrous than α)	76
1.88?	35	α and β (or some other phase less hydrous than α)	70
1.88	35	α and β (or some other phase less hydrous than α)	76
0.75	66	β (or some other phase less hydrous than α)	70
0.75	80	λ	69
0.94	84	λ	75
0.75	98	Supercurd	77
0.75	106	Supercurd	69?
0.94	101	Supercurd	80?
1.47	89	Supercurd	Absent
1.47	99	Supercurd	Absent
1.88	89.5	Supercurd	Absent
0.75	129	Subwaxy	Absent
0.94	127	Subwaxy	(70), 80?
1.47	124	Subwaxy	Absent
0.75	290	Isotropic liquid	Absent
1.47	290	Isotropic liquid	Absent
1.50	290	Isotropic liquid	Absent
1.88	290	Isotropic liquid	Absent
1.88	167	Superwaxy	73?

strongly suggests that it is related in some way to the degree of hydration of the soap rather than necessarily being characteristic of the absolutely anhydrous material. This speculation is difficult to reconcile with the absence of a heat of transition, unless the change is attributed to a gradual loss of adsorbed water commencing at this temperature rather than to decomposition of a stoichiometric hydrate.

The transition to supercurd: lambda (or gamma) ⇆ supercurd

Any sample of reasonably pure sodium stearate will show a reversible transition close to 90°C. On cooling, gamma is almost always formed, as shown by the subsequent non-occurrence of the genotypic transition. It appears as a coincidence that both lambda and gamma transform to supercurd at nearly the same temperature (within a few degrees).

Taking no cognizance of the genotypic point, Buerger and coworkers (2) report that beta transforms to gamma at 103°C. in an open but not in a closed system, basing their conclusion on x-ray diffraction patterns of cooled systems. A reinterpretation of these results is not that transformation does not occur in closed systems, where no loss of water can occur, but that it is reversible under these conditions. As seen in table 3, samples containing less than 1.5 per cent water re-form beta after cooling from temperatures around 103°C., since reheating gives rise to the genotypic transition. Of course, in an open system at 103°C., water is lost and the supercurd present at 103°C. forms gamma on cooling to room temperature.

The effect of water on the high-temperature transitions

The effect of water on the high-temperature transitions (gamma or lambda ⇆ supercurd and above) is given in table 4. Since three independent preparations of sodium stearate were used in this particular series of observations, the transition temperatures of the anhydrous soaps are included for comparison. In using the table to ascertain the effect of progressive increase in the amount of water, only results on the same soap preparation should be compared directly, the conclusions from the three different series being in qualitative agreement.

Typical differential temperature–time curves are shown in figure 5. Curve A is for anhydrous sodium stearate. There are five distinct peaks, each marking a transition at the point where sample and reference cell begin to heat at different rates owing to heat absorbed in the transition. The size of a peak is a rough measure of the heat of transition. Curve B is for a sample of sodium stearate containing 0.75 per cent water. The single peak of curve A at 225°C. here appears as two or perhaps three smaller peaks at (189°), 202°, and 225°C. The striking change, however, is in the first group of transitions. The change from gamma to supercurd occurs at nearly the same temperature as the water content increases but with a much smaller heat effect. The lowered heat of transition is paralleled by a decrease in the change of specific volume from 0.007 cc. per gram for the anhydrous soap to 0.003 cc. per gram for a sample with 1.47 per cent water. The change from supercurd to subwaxy is lowered in temperature and very greatly in magnitude of heat effect. That from subwaxy to waxy is unchanged in temperature but has a greatly increased heat effect in the hydrous system.

Curve C, for a sample containing 1.47 per cent water, shows the same trends in the first three peaks but shows only one broad low peak in the region of formation of neat or subneat soap.

TABLE 4

TABLE 4

The effect of water on the calorimetric transition temperatures of sodium stearate

SOAP PREPARATION..................... WEIGHT PER CENT H₂O............	IV 0.00	IV 0.75	IV 1.47	II 0.00	III* 1.50	I-b 0.00	I-b 1.58
Gamma–supercurd.................	94	91	95–99	93	95	91	93
Supercurd–subwaxy...............	118	116	109	118	104	116	107
Subwaxy–waxy....................	135	133	135	132	134	139	134
Waxy–superwaxy†........	—	—	—	—	—	—	—
Superwaxy–subneat..	204	202	205	209	209	204	195
Subneat–neat....................	235	225		226		232	

* Preparations II and III were both made from the same stearic acid.

† In anhydrous soap this transition has too small a heat effect to be detected by the calorimetric method. Hydrous systems usually show a small peak in this region of temperature but rather higher than would be expected for the superwaxy–waxy transition (184–193°C. *versus* 167°C.)
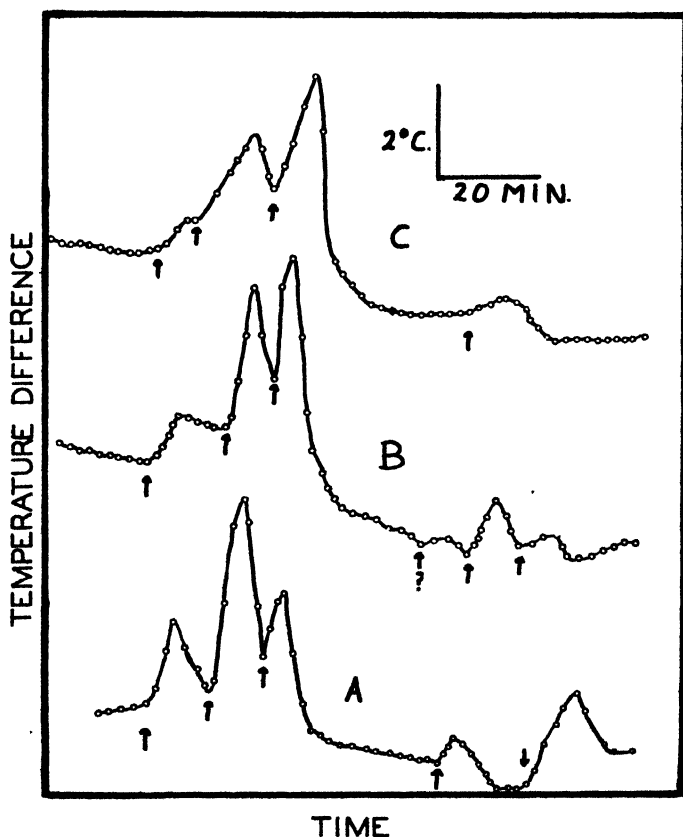
Fig. 5. The effect of water on the thermal transitions of sodium stearate. The different curves have been somewhat transposed on the time axis. A, anhydrous sodium stearate; transitions marked at 94°, 118°, 135°, 204°, and 235°C. B, sodium stearate with 0.75 per cent water; transitions marked at 91°, 116°, 133°, 189°?, 202°, and 225°C. C, sodium stearate with 1.47 per cent water; transitions marked at 99°, 109°, 135°, and 205°C. The heat of a transition is roughly proportional to the height and breadth of the corresponding peak.

The behavior at the gamma–supercurd transition is what one might expect of a eutectoid, in which case three phases coexist at a single temperature over a range of composition. The decrease in temperature and simultaneous decrease in apparent heat of transition of supercurd to subwaxy is in accord with the hypothesis that subwaxy scap is a phase of continuously varying composition projecting like a tongue into the phase diagram of sodium stearate and water (9). The constancy of the transition temperature from subwaxy to waxy soap with increasing moisture content is not explained by any of the published phase diagrams for sodium stearate–water (8, 9), although here again the inference is that three phases must be simultaneously present.

Possibly some of the variations between results reported using different techniques to determine the phase diagram of soap and water are due to inadequate control of experimental conditions, particularly relative humidity and mechanical working (1, 5).

SUMMARY

A calorimetric method, supplemented by dilatometric and microscopic observations, has been used to study the transitions of anhydrous and slightly hydrous samples of sodium stearate. Alpha sodium stearate can be taken to be a hemihydrate and beta sodium stearate a less hydrous form but not necessarily a hydrate. Transition from alpha to beta occurs at 52°C. on heating and is usually not reversed on cooling. The genotypic point appears to be a transition of the second kind, occurring reversibly at about 71°C. The name lambda sodium stearate has been suggested for the form existing between 71° and 90°C., which reverts to beta on cooling below 71°C. Ordinarily cooling supercurd below 90°C. results in the fomation of gamma sodium stearate, particularly for samples containing more than 1.5 per cent water. The transition from supercurd to subwaxy appears to be entirely reversible and always occurs regardless of the initial form of the soap at room temperature. The same is true of all the higher temperature transitions.

The following facts are established which any correct phase diagram of the system will have to explain: (1) The transition temperature from gamma to supercurd is independent of composition up to 1.9 per cent water but its heat effect decreases. (2) Temperature and heat effect of the transition from supercurd to subwaxy both diminish with increasing water content. (3) The temperature of the transition from subwaxy to waxy sodium stearate remains constant independent of increasing moisture content, but the heat effect increases very markedly over the range from 0.0 to 2 per cent water.

REFERENCES

(1) BODMAN, J. W.: U. S. patent 2,215,539 (1940).
(2) BUERGER, M. J., SMITH, L. B., DE BRETTEVILLE, A., JR., AND RYER, F. V.: Proc. Natl. Acad. Sci. U. S. 28, 526 (1942).
(3) DE BRETTEVILLE, A., JR. AND MCBAIN, J. W.: Science 96, 470 (1942).
    MCBAIN, J. W., DE BRETTEVILLE, A., JR., AND ROSS, S.: J. Chem. Phys. 11, 179 (1943).

(4) FERGUSON, R. H.: Oil & Soap **21**, 6 (1944).
(5) FERGUSON, R. H., ROSEVEAR, F. B., AND STILLMAN, R. C.: Ind. Eng. Chem. **35**, 1005 (1943).
(6) McBAIN, J. W., BOLDUAN, O. E. A., AND ROSS, S.: J. Am. Chem. Soc. **65**, 1873 (1943).
(7) McBAIN, J. W., AND LEE, W. W.: Ind. Eng. Chem. **35**, 784 (1943).
(8) McBAIN, J. W., AND LEE, W. W.: Oil & Soap **20**, 17 (1943).
(9) McBAIN, J. W., VOLD, R. D., AND FRICK, M.: J. Phys. Chem. **44**, 1013 (1940).
(10) MILLS, V.: U. S. patent 2,295,594 (September 15, 1942).
(11) ROSS, S.: Private communication.
(12) THIESSEN, P. A., AND EHRLICH, E.: Z. physik. Chem. **A165**, 453 (1933).
THIESSEN, P. A., AND SPYCHALSKI, R.: Z. physik. Chem. **A156**, 435 (1931).
THIESSEN, P. A., v. KLENCK, J., GOCKOWIACK, H., AND STAUFF, V.: Z. physik. Chem. **A174**, 335 (1935).
(13) VOLD, M. J.: J. Am. Chem. Soc. **63**, 1427 (1941).
(14) VOLD, R. D.: J. Am. Chem. Soc. **63**, 2915 (1941).
(15) VOLD, R. D., AND LYON, LUTHER L.: Ind. Eng. Chem. **37**, 497 (1945).
(16) VOLD, R. D., AND VOLD, M. J.: J. Am. Chem. Soc. **61**, 808 (1939).

THE ACID BEHAVIOR OF PECTINIC ACIDS

R. SPEISER, C. H. HILLS, AND C. R. EDDY

Eastern Regional Research Laboratory[1], Philadelphia, Pennsylvania

INTRODUCTION

Some time ago there was initiated in this laboratory an investigation of methods for producing pectinic acids of low ester content from apple pomace for use in preparing calcium pectinate jellies of low sugar content (14). These pectinic acids were made by two methods—acid deësterification and enzyme deësterification. Acid deësterification requires treatment of pectinic acid of high ester content for 1 to 2 days at 40–50°C. at a pH less than 1, whereas enzyme deësterification requires only a few minutes at 40°C. and pH 6. The economic advantages of the enzyme method are obvious.

Unfortunately 65 per cent sugar jellies and 35 per cent sugar–calcium pectinate jellies prepared from enzyme-deësterified pectinic acids were not so strong as those prepared from acid-deësterified pectinic acids. This was true even for pectinic acid samples of the same ester content and viscosity (in water solutions) prepared by the above two methods. Table 1 and figure 1 illustrate this point.

It was thought that if the factors governing the behavior of pectinic acids were determined, improved strength of enzyme-deësterified pectinate jellies could be obtained and the anomalies in the physicochemical behavior of pectinic acids could also be satisfactorily explained. Therefore, the following studies

---

[1] One of the laboratories of the Bureau of Agricultural and Industrial Chemistry, Agricultural Research Administration, United States Department of Agriculture.

have been made upon pectinic acids prepared by the two methods: acid behavior; kinetics of deësterification; electrophoretic behavior; viscosity, molecular weight, and molecular-weight distribution; and properties of pectin jellies.

The strength and other mechanical properties of pectinic acid jellies of high sugar content are very sensitive to the pH (1, 30) of the jelly and the degree of

TABLE 1

Strength of pectin jellies as a function of method of deësterification

SAMPLE	METHOD OF DEËSTERIFICATION	ESTER CONTENT	JELLY STRENGTH*	
			65 per cent sugar jellies	35 per cent sugar-calcium pectinate jellies
		per cent CH₂O	*cm.*	*cm.*
H59	Acid	4.53	72	56
H74	Enzyme	4.48	24	4

* The jelly strength, as measured by the Delaware jelly tester (39), is the number of centimeters of water pressure that a jelly can support without rupture. The maximum jelly strength (14) was obtained by varying the pH and calcium concentration.
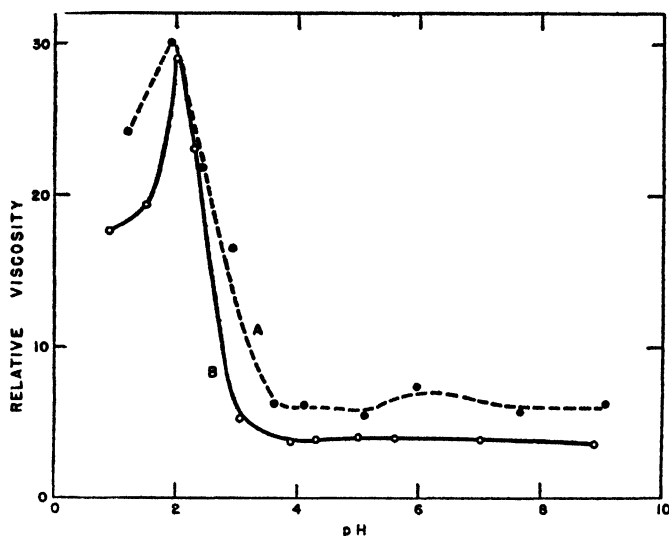
Fig. 1. Viscosity as a function of pH for 0.6 per cent pectinic acid solutions. (A) H-59, acid deësterified, CH₂O = 4.53 per cent; (B) H-74, enzyme deësterified, CH₂O = 4.48 per cent.

dissociation (15) of the pectinic acid. Evidence has been obtained in this laboratory that the three-dimensional elastic structure of the jelly is built up through extensive hydrogen bonding between the sugar and pectinic acid molecules. Calcium pectinate gel structures are built up through a system of both hydrogen bonds and ionic bonds (1). The stability of these structures is a function of the ionic equilibria involved, as well as of the dissociation of the pectinic acid.

Viscosity, osmotic pressure, and solubility are also greatly influenced by the acid behavior of the pectinic acid. Furthermore, changes in the electrolytic properties of the carboxyl group in passing from the monomer to the polymer molecule are of fundamental interest in the general theory of the behavior of high polymers. For these reasons, a study of the acid behavior of pectinic acid was undertaken.

Constitution of the pectinic acid molecule[2]

In order to explain the behavior of pectin, it is necessary to have a clear understanding of the constitution and structure of the pectinic acid molecule. Unfortunately, the literature is not in entire agreement even upon this fundamental point (32), a state of affairs not uncommon in the realm of naturally occurring high polymers.

The pectinic acid complex extracted from apple pomace consists of a long straight-chain skeleton of partially methyl-esterified polygalacturonic acid to which are attached side groups of araban (a branched-chain polyarabinose) and galactan (a straight-chain polygalactose) (2, 3, 17, 25, 26, 27, 34, 35, 38). Pre-
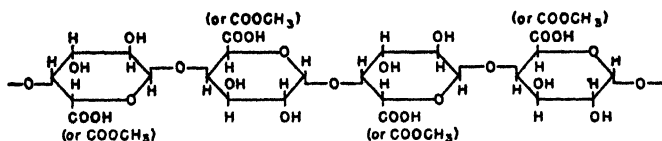
FIG. 2. Backbone chain of the pectinic acid molecule

viously proposed ring structures (9, 28) have been abandoned in the light of conclusive evidence (from x-ray (40), optical (40), viscosity (35), ultracentrifugal sedimentation (33), and osmotic pressure (35) studies) that the pectinic acid skeleton is essentially linear, resembling that of cellulose to a high degree. Data in the literature (29, 32) and data obtained in this laboratory show that pectinic acid is not homogeneous and that the methyl ester, araban, and galactan contents of a sample vary with the source, method of extraction, and subsequent treatment. The molecular weight ranges from relatively low values to approximately 300,000 (25, 33, 34). The methyl ester, araban, and galactan contents range from approximately 0 to 11 per cent, 0 to 30 per cent, and 0 to 40 per cent, respectively. It has been suggested (18, 29, 34, 36) that the araban and galactan are attached to the main chain by purely physical forces (that is, secondary valence forces), instead of primary valence bonds. However, rate measurements to be reported in a later paper indicate that a substantial portion of this polysaccharide material requires an activation energy of at least 18,000 cal. for its removal from the main chain.

According to this conception of the pectinic acid molecule, figure 2 represents the main skeleton to which are attached, at undetermined points, the electrolytically inert araban and galactan.

[2] The nomenclature used here is that agreed upon by the American Chemical Society Committee for Revision of the Nomenclature of Pectic Substances (22).

Titration curves were obtained according to the method of Briggs (4). For example, approximately 1 g. of pectinic acid was dried to constant weight in a vacuum oven at 80°C. The sample was moistened with about 1 ml. of alcohol and made up to 100 ml. with water. Measured quantities of 0.01 N sodium hydroxide were added to 5-ml. portions of this solution and then diluted to 25 ml. The pH of each solution was measured with a Cambridge electron-ray pH meter to ±0.005 pH unit. By this procedure the pH as a function of degree of neutralization was measured at constant pectinic acid concentration. The same procedure was used with carefully purified d-galacturonic acid.

Preparation of acid-deësterified pectinic acids

A commercial 200-grade apple pectin was reprecipitated from water solution with alcohol several times and washed repeatedly with 70 per cent alcohol. A 6.75-kg. portion of the pressed alcohol precipitate was dissolved in 38 liters of distilled water. After the pectin had been stirred for 3 hr. and had completely dissolved, the volume of the solution was made up to 50 liters with distilled water. The temperature was adjusted to the desired point before the final adjustment to volume. Enough concentrated hydrochloric acid was added to the pectinic acid solution to make the mixture 0.872 N in hydrochloric acid. The mixture was then placed in a thermostat at 40°C., and deësterification was allowed to proceed for several days. Portions were removed from time to time, and pectinic acids of various degrees of deësterification were recovered in the following manner:

About 2 volumes of 80 per cent alcohol was added to the reaction mixture, which was then strongly stirred to break up the lumps of gel. To remove the ash-forming constituents, the alcohol was filtered off, and the precipitate was washed repeatedly with 80 per cent alcohol until the filtrate showed a negative test for chloride ion. The pectinic acid was then washed with absolute alcohol to facilitate dehydration. After the alcohol was pressed out, the pectinic acid was dried for 1 day at room temperature and then for 1 or 2 days at 60°C. in a mechanical convection oven. Finally, the dried pectinic acid was ground to pass a 40-mesh screen and analyzed for ash, carboxyl, and methyl ester content.

Preparation of enzyme-deësterified pectinic acid

Enzyme deësterification was carried out on another portion of the same pressed alcohol precipitate from which the raw material for the acid deësterification had been taken. A 6.75-kg. portion of this precipitate was dissolved in distilled water, and the volume was made up to 57 liters. A separate 9-kg. portion of this solution was used for each of the enzyme deësterifications. The solution was placed in a thermostat maintained at 40°C. and was carefully adjusted to pH 6.0, after which the enzyme catalyst (tomato pectase) was added. As the deësterification proceeded, 2 N sodium hydroxide was added slowly and with rapid stirring to maintain the pH at 6.0. When the desired degree of deësterification was attained, the reaction was stopped by immediately lowering the pH to about 3.0,

thereby inactivating the enzyme. The pectase was then destroyed by heating the solution to 65°C. for 20 min., after which the product was purified as above.

Preparation of the enzyme catalyst

The pectase enzyme was extracted from firm, ripe tomatoes. The tomatoes were ground to a pulp; sufficient alkali was added to adjust the pH to 6.0; and then the juice was expressed from the pulp. Suspended material and pigment were removed by decantation and filtration. The clear, yellow solution containing the pectase was then stored at 0°C. under a layer of xylene, added as a preservative. This pectase preparation could be stored under such conditions for several months, although its activity was always checked before use.

Analysis of the pectinic acid

Ash was determined in the usual manner. The methoxyl content was determined by a Zeisel procedure (6) upon samples of pectinic acid which had been treated with water vapor at low pressures to remove all adsorbed alcohol. This precaution is necessary to avoid erroneous results in the analysis for methoxyl content (13).

Calculations

N, the total concentration of carboxyl groups in equivalents per liter, was determined from the titration curve of pH *versus* volume of base added at constant pectinic acid concentration. A pH of 7.5 was accepted as the point of equivalence, since complete titration curves have shown this to be the inflection point for concentrations used in this study. Theoretical considerations show that the point of true equivalence occurs at a pH somewhat higher than that of the inflection point, but the pH of this true equivalence point is a complicated function of N and of the dissociation constants, and the error in using the inflection point is not large.

(COO^-), the concentration of dissociated carboxyl groups, was calculated from the relation

$$(COO^-) = (B^+) + (H^+) - (OH^-)$$

in accordance with the requirement of electrical neutrality of the solution. (B^+) represents the concentration of base in equivalents per liter, corrected for the alkalinity of the ash associated with the pectinic acid. (H^+) and (OH^-) represent the concentrations of hydrogen and hydroxyl ions, respectively, calculated from the measured pH values on the assumption that activity coefficients are unity.

α, the degree of dissociation, was calculated as the ratio of (COO^-) to N.

G, the titration constant, was calculated from its defining equation

$$G = \frac{(H^+)\alpha}{1 - \alpha} = \frac{(H^+)(COO^-)}{N - (COO^-)} \tag{1}$$

pG is defined as the negative logarithm of G, by analogy with pH.

Γ, the ratio of the number of carboxyl groups in the system to the total number of galacturonide residues, was calculated from the relation:

$$\Gamma = \frac{COOH}{COOH + COOCH_3} = \frac{N/c}{N/c + CH_3O/3100} \tag{2}$$

where c is the concentration of pectinic acid in grams per liter, CH_3O is the methoxyl content as customarily expressed in per cent by weight of solid, and 31 is the molecular weight of the CH_3O residue. The ratio Γ is the significant quantity in comparing and characterizing pectinic acids of different ester contents and neutralization equivalents, because Γ is independent of extraneous materials, such as araban and galactan, which do not contribute directly to the electrolytic behavior but affect the ester content and neutralization equivalent calculated from the total weight of material.

Accuracy

Estimates of the probable accuracy of the calculated values reveal that the error in α is of the order of ± 1 per cent and that the error in pG varies, with the degree of neutralization, from ± 0.02 pG unit for low values of α to ± 0.05 at $\alpha = 0.9$, and increases rapidly without limit as α increases from 0.9 to 1.0. Hence, the conclusions we have drawn are based entirely on the region of α less than 0.9.

The importance of errors inherent in the method of calculating pG seems to have been overlooked by most of the workers dealing with dissociation phenomena. It should be emphasized that the mathematical nature of the calculations causes small, fixed errors to introduce spurious trends in G, which can be of serious magnitude for high values of α and lead to erroneous conclusions about the nature of the dissociating system. It is therefore essential to evaluate these errors.

RESULTS

Titration data have been obtained on a wide variety of different pectinic acids of various ester contents, both acid- and enzyme-deësterified. Representative examples are given in tables 2, 3, 4, and 5 and in figure 3, which show the variation of pH with degree of neutralization. Table 3 and figure 4 give a typical example of the effect of concentration. For comparison, table 6 and figure 3 also show the behavior of d-galacturonic acid, which can be considered the monomer on which the pectinic acid main chain is based.

From these figures it is seen that the behavior of pectinic acid resembles qualitatively that of a monobasic acid, in that it has only a single buffer range. The resemblance is only superficial, however, as can be seen by comparison with the curve for galacturonic acid in figure 3 and with the two theoretical curves in figure 4 calculated from the monobasic acid equation

$$K = \frac{(H^+)\alpha}{1 - \alpha} \tag{3}$$

TABLE 2

Titration data for acid-deësterified pectinic acid

Sample H91B: CH_3O content, 6.80 per cent; $\Gamma = 0.56$; ash content, 0.24 per cent; ash alkalinity, 0.034 milliequivalent per gram of pectinic acid. Concentration = 1.94 g. per liter; $N = 5.19 \times 10^{-3}$ equivalents per liter; temperature = 27°C.

α	pH	pG	α	pH	pG
0.233	2.937	3.455	0.566	4.116	4.001
0.258	3.059	3.522	0.637	4.280	4.036
0.289	3.196	3.587	0.710	4.486	4.098
0.328	3.359	3.671	0.860	4.941	4.196
0.377	3.532	3.751	0.935	5.545	4.390
0.435	3.695	3.808	0.991	6.596	4.563
0.499	3.879	3.881	0.995	6.990	4.657
			0.997	7.220	4.108

TABLE 3

Titration data for acid-deësterified pectinic acid

Sample H91E: CH_3O content = 1.70 per cent; $\Gamma = 0.90$; ash content = 0.53 per cent; ash alkalinity = 0.064 milliequivalent per gram of pectinic acid

α	pH	pG	α	pH	pG
Concentration = 1.00 g. per liter; $N = 4.15 \times 10^{-3}$ equivalents per liter; temperature = 27°C.					
0.204	3.105	3.695	0.594	4.571	4.405
0.237	3.280	3.787	0.780	5.145	4.594
0.282	3.503	3.909	0.874	5.523	4.679
0.342	3.778	4.063	0.969	6.411	4.908
0.419	4.038	4.180	0.988	6.980	5.045
Concentration = 2.00 g. per liter; $N = 8.35 \times 10^{-3}$ equivalents per liter; temperature = 27°C.					
0.172	2.882	3.563	0.683	4.613	4.280
0.212	3.071	3.641	0.776	4.899	4.359
0.259	3.349	3.806	0.870	5.310	4.486
0.328	3.642	3.955	0.964	6.188	4.759
0.411	3.894	4.052	0.988	6.951	5.034
Concentration = 4.00 g. per liter; $N = 16.82 \times 10^{-3}$ equivalents per liter; temperature = 27°C.					
0.164	2.772	3.481	0.499	3.932	3.934
0.186	2.897	3.538	0.907	5.221	4.160
0.215	3.021	3.584	0.969	6.351	4.858
0.247	3.160	3.643			

The behavior of pectinic acid more closely resembles that of citric acid, saccharic acid, and other polybasic acids whose buffer ranges are so close together that they overlap and produce only one composite buffer range, as illustrated in figure 5.

As shown in figure 4, an increase in concentration increases the degree of dissociation for a given value of pH. This is typical of the behavior which we have found for apple pectinic acids of high and low ester content, deësterified by either acid or enzyme treatment. The same effect has been observed by Hinton (15) for orange, currant, and strawberry pectinic acids, and also by Kern (21) for polyacrylic acid and Briggs (4) for arabic acid. In contrast, d-galacturonic acid,

TABLE 4

Titration data for enzyme-deësterified pectinic acid

Sample H91H: CH_3O content = 4.48 per cent; Γ = 0.67; ash content = 0.55 per cent; ash alkalinity = 0.089 milliequivalent per gram of pectinic acid. Concentration = 1.98 g. per liter; N = 5.64 × 10^{-3} equivalents per liter; temperature = 27°C.

α	pH	pG	α	pH	pG
0.248	3.085	3.568	0.953	5.973	4.664
0.280	3.221	3.632	0.989	6.650	4.710
0.319	3.376	3.707	0.994	7.144	4.901
0.365	3.555	3.796	0.996	7.479	5.110
0.608	4.298	4.107	0.997	6.910	4.364
0.744	4.690	4.227	0.999	7.787	4.939
0.883	5.269	4.391			

TABLE 5

Titration data for enzyme-deësterified pectinic acid

Sample H91J: CH_3O content = 2.04 per cent; Γ = 0.86; ash content = 1.01 per cent; ash alkalinity = 0.184 milliequivalent per gram of pectinic acid. Concentration = 1.83 g. per liter; N = 6.98 × 10^{-3} equivalents per liter; temperature = 27°C.

α	pH	pG	α	pH	pG
0.216	3.111	3.671	0.569	4.298	4.178
0.243	3.250	3.745	0.619	4.456	4.235
0.275	3.409	3.830	0.682	4.604	4.274
0.315	3.585	3.922	0.736	4.757	4.311
0.361	3.741	3.990	0.849	5.158	4.408
0.410	3.881	4.039	0.906	5.449	4.467
0.464	4.013	4.079	0.962	5.938	4.536
0.517	4.159	4.129			

like all monobasic acids, shows no change in α as concentration is changed at constant pH.

The effect of ester content, as can be seen from figure 3, is to decrease the degree of dissociation with increasing Γ at a given concentration and pH. Unexpectedly, bringing the carboxyls closer together in solution by increasing the concentration causes α to increase, whereas bringing the carboxyls closer together by increasing the number of carboxyls per unit length of chain causes α to decrease.

From measurements on a large number of pectinic acids with widely different

molecular weights, we have found no detectable variation in acid behavior with changes in molecular weight. This is similar to the findings of Kern (21) for polyacrylic acid.
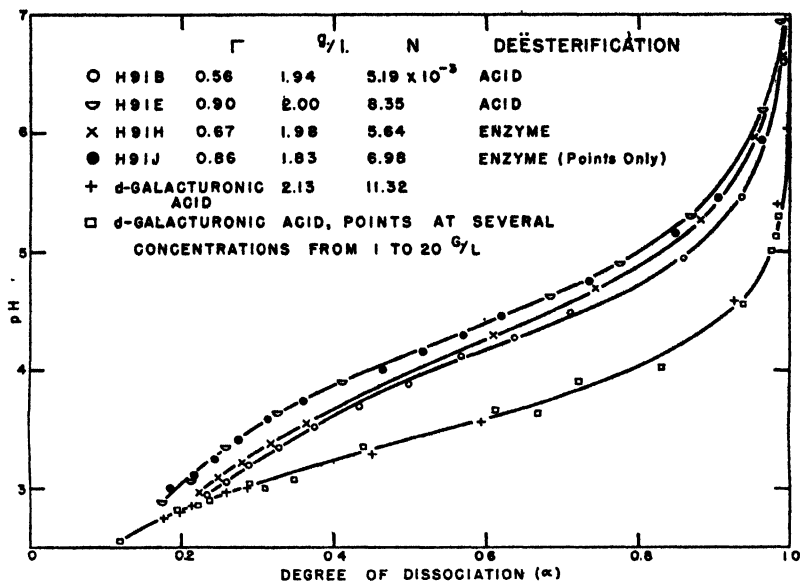
FIG. 3. Titration curves of pectinic and galacturonic acids

TABLE 6

Titration data for d-galacturonic acid

α-d-Galacturonic acid, recrystallized three times: ash content, 0.161 per cent; ash alkalinity, 0.018 milliequivalent per gram of acid; equilibrium rotation, $[\alpha]_D^{25} = 51.7°*$. Concentration $= 2.13$ g. per liter; $N = 11.32 \times 10^{-3}$ equivalents per liter; temperature $= 27°C$.

α	pH	pK	α	pH	pK
0.176	2.749	3.418	0.431	3.302	3.423
0.197	2.798	3.412	0.596	3.570	3.400
0.212	2.864	3.434	0.927	4.589	3.485
0.234	2.919	3.433	0.982	5.404	3.653
0.259	2.969	3.426	0.996	6.040	3.630
0.287	3.014	3.410			

Average pK $= 3.419 \pm 0.009$ ($K = 3.81 \times 10^{-4}$) for the range $0 < \alpha < 0.6$

* Compare this value with the following:

$[\alpha]_D^{20} = 50.9°$ (F. Ehrlich and F. Schubert (10))
$[\alpha]_D^{20} = 51.5°$ (W. W. Pigman (31))
$[\alpha]_D^{20} = 51.9°$ (H. S. Isbell and·H. L. Frush (19))

Also, from the data so far obtained, there seems to be no appreciable difference between pectinic acids demethylated to comparable values of Γ by acid treatment and by enzymes. Representative curves are shown in figure 3.
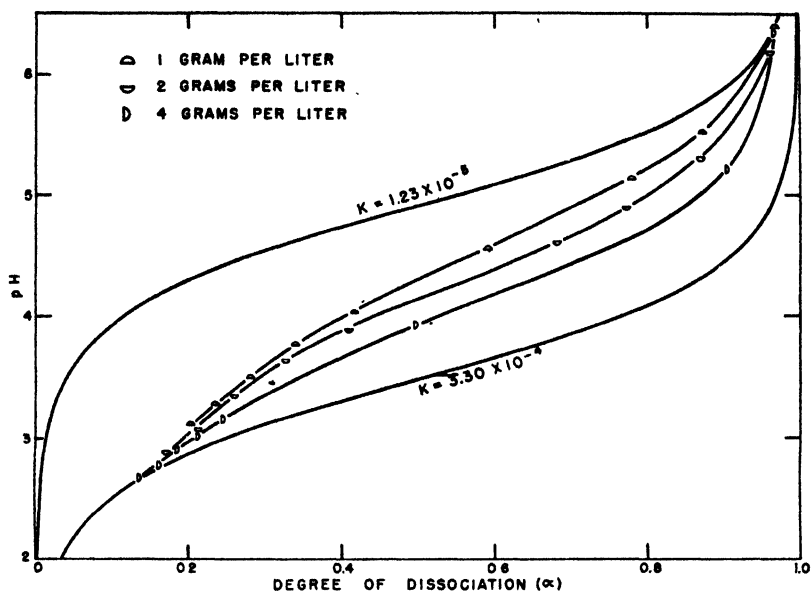
FIG. 4. Titration curves of pectinic acid H-91E at different concentrations, with two theoretical curves for monobasic acids with dissociation constants 1 23 × 10⁻⁵ and 3.30 × 10⁻¹.
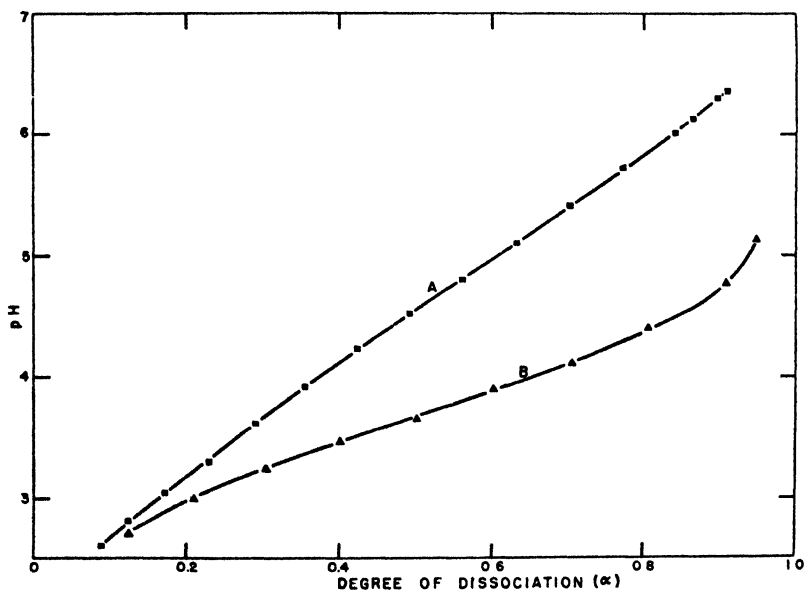
FIG. 5. Titration curves of (A) citric acid at 0.031 equivalent per liter (data obtained in this laboratory), and (B) saccharic acid at 0.0485 equivalent per liter (data of Levene and Simms (23)).

Titration constants calculated for the pectinic acids are shown in tables 2, 3, 4, and 5 and in figure 6. The titration constants follow the same general trends as the pH, and the curves bear the same positions relative to one another as do the pH curves. This is further evidence that pectinic acid is not equivalent to a monobasic acid, since the titration constant would then be independent of α and of concentration. The sharp rise in pG for α greater than 0.9 is probably not real, since, as mentioned above, the errors and spurious trends become highly magnified in this region.

The titration constant of d-galacturonic acid is independent of α and of concentration over the range studied, as shown in table 6 and figure 6. This means
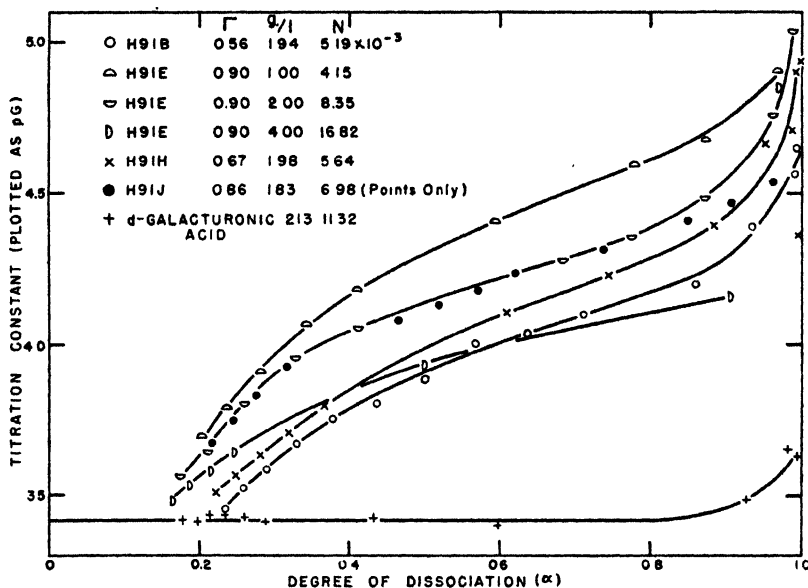
FIG. 6. Titration constants of pectinic and galacturonic acids

that d-galacturonic acid follows the equation for a theoretical monobasic acid and that the titration constant can be identified with the dissociation constant K. pK for d-galacturonic acid as determined in this work is 3.42 ± 0.01 at 27°C. ($K = 3.81 \times 10^{-4}$). Karrer and Schwarzenbach (20) found a pK value of 3.49 at 23.6°C. Measurements were made to determine whether the pH of partially neutralized α-d-galacturonic acid solutions changed upon standing for periods of 1 min., 5 hr., and 34 hr. Although the specific rotation of the solutions changed, their pH remained constant. The pH of pectinic acid solutions also remained constant when the solutions stood for similar periods.

DISCUSSION

Theories of polybasic acids have been worked out by Simms (37), Weber (42), von Muralt (41), Wyman (43), and Maxwell and Partington (24). . The basic

assumption in these theories is that all the polybasic molecules in the system are alike or at least can be divided into groups in each of which all the molecules are alike. Pectinic acid is, on the other hand, a case of exceeding complexity, with not only a variety of molecular weights but also an astronomical number of different distributions of the methyl ester groups along the chain.

For a pectinic acid molecule having p galacturonide residues and n carboxyl groups, there are

$$\frac{p!}{n!(p-n)!} \qquad (4)$$

statistically possible structures, none of which are identical since the molecule is asymmetric. If the methyl groups are removed at random, all structures will be produced with approximately equal probability, and once the deësterification reaction has been stopped, the different structures will not be in dynamic equilibrium with each other but will remain fixed. For an average sample of pectinic acid, the number of structures calculated from equation 4 is many times the magnitude of Avogadro's number, which makes it highly improbable that a given sample could contain two identical molecules or even a random sampling of distributions. Therefore, each sample of pectinic acid must be considered a special case in itself, different from all other samples. In acid deësterification, the methyl groups are probably removed at random, and the above calculation applies. In enzyme deësterification, the methyl groups may not be removed entirely at random, and the different structures may not be produced with equal probability. However, the fact that the acid behaviors of acid- and enzyme-deësterified pectinic acids are indistinguishable indicates that the difference in distribution of structures is not great or else does not involve the parts of the molecule affecting acid behavior.

In order to apply standard statistical theories to a finite sample of a high-polymeric system like pectinic acid, it is therefore necessary to assume that the actual microscopic configuration of the molecules does not have much effect on the macroscopic properties and that the behavior of an individual group is substantially affected only by the configuration and structure of groups within a limited distance along the chain. In this case, the distribution of molecular weights can be replaced by an average molecular weight, and the distributions in p and n by an average p and an average n. With these assumptions, the theory of polybasic acids can be applied to pectin.

The general dissociation theory is algebraically unworkable for substances having several hundred acid groups per molecule, because of the complexity of the equations involved. The special case of no interaction between carboxyl groups, in which all have the same microscopic dissociation constant, has been treated by Maxwell and Partington (24), who have shown that this leads to the following distribution in the K_i dissociation constants of an n-basic acid:

$$K_i = \frac{n-i+1}{i} K_0 \qquad (i = 1, 2, 3, \cdots, n) \qquad (5)$$

where K_0 is the intrinsic dissociation constant for the carboxyl group. Simms (37), Weber (42), and von Muralt (41) showed that this particular distribution in dissociation constants gives an over-all acid behavior having a single buffer range and a constant value of G that is identical with K_0:

$$G = K_0 = \frac{(H^+)\alpha}{1 - \alpha}$$

Tables 2, 3, 4, and 5 and figure 6 show that for pectinic acid G is not a constant but ranges from 3.5×10^{-4} to 9.0×10^{-6}, dependent on both concentration and degree of neutralization. Hence it is evident that the carboxyl groups in pectinic acid are not entirely free from mutual interaction.

Empirically, we have found that the experimental points follow a straight line when plotted as pG *versus* log α or as pG *versus* $\sqrt{(COO^-)}$, but the theoretical reasons for this behavior are not clear. Since log α is not a linear function of $\sqrt{(COO^-)}$, the behavior of pectin cannot follow both empirical relations exactly. However, the accuracy of our experimental data is not sufficient to permit a choice between the two.

Linearity of pG versus log α means that the dissociation follows an equilibrium of the form

$$k = \frac{(H^+)\alpha^\beta}{1 - \alpha} \tag{6}$$

where β and k are constants throughout a given titration but vary with concentration. β is always greater than unity. When pG is plotted against $\sqrt{(COO^-)}$, the points not only follow straight lines, but all of these lines extrapolate to the same intercept for zero dissociation, $pG_0 = 2.7 \pm 0.1$, as is shown in figure 7.

The fact that pG depends more simply on $\sqrt{(COO^-)}$ than on (COO^-) suggests that the variation in pG might be due to changes in the ionic concentration, since the Debye–Hückel theory (8) predicts that certain ionic atmosphere effects should be functions of the square root of the ionic concentration, rather than functions of the concentration itself. If pG depends only on the ionic atmosphere, it should be possible to make pG constant throughout a titration by adding a sufficient amount of a strong electrolyte to make the ionic strength constant. Measurements on pectinic acid in the presence of sodium chloride revealed, however, that pG was always less than in the absence of excess electrolyte. Since more added electrolyte would be required at low α's than at high α's to make the ionic strength constant, it follows that a titration at constant ionic strength would show greater variation of pG throughout a titration, rather than making pG constant. Hence the ionic strength is not the controlling factor when pG is plotted against $\sqrt{(COO^-)}$.

The fact that all the plots of pG versus $\sqrt{(COO^-)}$ pass through the same intercept for zero dissociation suggests that the common value of $G_0 = 2.0 \times 10^{-3}$ might perhaps be the fundamental dissociation constant for a single carboxyl group in a pectinic acid molecule when none of the nearby carboxyls has dissociated. That this is considerably higher than the dissociation constant for

galacturonic acid is probably due to the proximity of many more polar groups in the environment of the dissociating carboxyl group in the pectinic acid than in the galacturonic acid.

For comparison, figure 7 also contains the data of Briggs (4) for arabic acid, which likewise gives a straight line when pG is plotted against $\sqrt{(COO^-)}$. It is significant that the plots for two different concentrations of arabic acid extrapolate to the same intercept obtained for various pectinic acids at $\alpha = 0$. Except for the orientation of the hydroxyls, glucuronic acid (the carboxyl-bearing group in arabic acid (5, 7, 12, 16)) is similar in structure to galacturonic acid. It is not surprising therefore that the dissociation constant for the first carboxyl of the arabic acid is equal to that of pectinic acid.
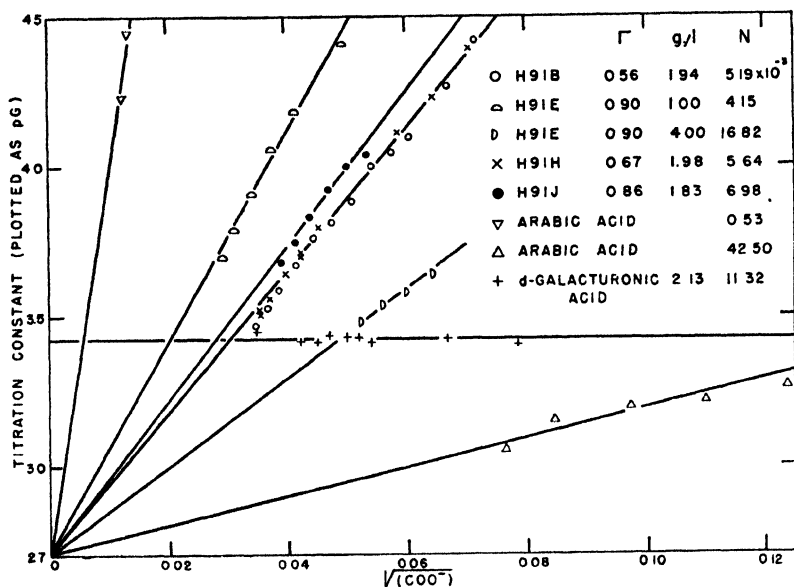
FIG. 7. Titration constants of pectinic, arabic, and galacturonic acids, plotted as pG versus $\sqrt{(COO^-)}$.

Polyacrylic acid, when plotted similarly from the data of Kern (21), likewise follows a straight line whose intercept ($pG_0 = 4.1$, $G_0 = 8 \times 10^{-5}$) is not the same as for pectinic and arabic acids; this is to be expected, since the structure of polyacrylic acid is entirely different from that of the polyuronic acids. Since polyacrylic acid may contain head-to-head, head-to-tail, and tail-to-tail combinations of the monomer, short sections of the chain may resemble isobutyric acid ($K = 1.1 \times 10^{-5}$) (21), succinic acid ($K_1 = 7.4 \times 10^{-5}$) (11), glutaric acid ($K_1 = 4.6 \times 10^{-5}$) (11), and adipic acid ($K_1 = 3.9 \times 10^{-5}$) (11), all of which have K's of the same order of magnitude as the extrapolated G_0 for polyacrylic acid.

The basis of the interpretations used in these studies is that pectinic acid is a high-polymeric material. The properties of a high polymer can be divided into two classes: (1) those which depend on the fact that its molecular weight is high,

and (*2*) those which depend on the specific nature of the active groups on the monomer units. The behavior of an active group on a high polymer may be substantially the same as on the monomer or it may be considerably modified by participating in coöperative phenomena with other active groups along the chain. In the case of acid behavior, the question is whether dissociation is purely an individual phenomenon or one involving large segments of the molecule as a whole.

Low-molecular-weight polybasic acids, such as succinic, malonic, saccharic, and citric, can be treated satisfactorily by standard mass-law methods. On the other hand, high-polymeric acids, such as pectinic, arabic, and polyacrylic, cannot be adequately treated by existing theories. The polymeric acids do, however, give straight lines when pG is plotted against log α or against $\sqrt{(COO^-)}$ and the lines for similar materials extrapolate to the same intercept when pG is plotted against $\sqrt{(COO^-)}$. This suggests that some form of coöperative action is at work in the dissociation of poly acids of these types.

Although our results have shown that acid- and enzyme-deësterified pectinic acids are nearly identical in their acid behavior, the experimental data and knowledge of empirical relations obtained by this study are not only useful but are essential for interpreting jelly properties, viscosity, osmotic pressure, solubility, and electrophoretic properties of pectinic acids, which will be reported in other papers.

The data discussed in this paper were obtained on pectinic acids derived from apple pomace. It is believed, however, that the conclusions drawn are applicable to pectinic acids from other sources.

SUMMARY

The pH as a function of degree of neutralization has been measured for several pectinic acid samples of different methyl ester contents, deësterified by acid and by enzyme treatment. Pectinic acid has a single buffer range, but does not behave as a monobasic acid. For a given pH, the degree of dissociation increases with increasing concentration and with increasing degree of methyl esterification.

pH as a function of degree of neutralization has also been measured for *d*-galacturonic acid, which can be considered the monomer of pectinic acid. This acid behaves as a typical monobasic acid, the degree of dissociation at a given pH being independent of the concentration.

Comparison of the acid behavior with that predicted from published theoretical relations shows that the carboxyl groups of pectinic acid are not free from mutual interactions.

Empirically, it has been found that the logarithm of the titration constant for pectinic acid is, within the experimental accuracy, either a linear function of the logarithm of the degree of neutralization or a linear function of the square root of the concentration of ionized carboxyls. Furthermore, for the latter case, the experimental lines for all the pectinic acid samples extrapolate to the same intercept for zero degree of dissociation. From published data it has been calculated that arabic acid and polyacrylic acid behave similarly.

We wish to acknowledge the valuable assistance of Mrs. Evelyn E. Karr of this laboratory in making many of the electrometric titrations.

REFERENCES

(1) BAKER, G. L., AND GOODWIN, M. W.: Delaware Agr. Expt. Sta. Bull. **234** (1941).
(2) BAUER, L., AND LINK, K. P.: J. Biol. Chem. **109**, 293 (1935).
(3) BEAVEN, G. H., AND JONES, J. K. N.: Chemistry & Industry **1939**, 363.
(4) BRIGGS, D. R.: J. Phys. Chem. **38**, 867 (1934).
(5) CHALLINOR, S. W., HAWORTH, W. N., AND HIRST, E. L.: J. Chem. Soc. **1931**, 258.
(6) CLARK, E. P.: J. Assoc. Official Agr. Chem. **22**, 100, 622 (1939).
(7) CRETCHER, L. H., AND BUTLER, C. L.: Science **68**, 116 (1928).
(8) DEBYE, P., AND HÜCKEL, E.: Physik. Z. **24**, 185 (1923).
(9) EHRLICH, F.: Abderhalden's *Handbuch der biologischen Arbeitsmethoden*, Abt. 1, Teil 11. Urban and Schwarzenberg, Berlin (1936).
(10) EHRLICH, F., AND SCHUBERT, F.: Ber. **62B**, 1974 (1929).
(11) GANE, R., AND INGOLD, K.: J. Chem. Soc. **1928**, 1594.
(12) HEIDELBERGER, M., AND KENDALL, F. E.: J. Biol. Chem. **84**, 639 (1929).
(13) HILLS, C. H., OGG, C. L., AND SPEISER, R.: Ind. Eng. Chem., Anal. Ed., in press.
(14) HILLS, C. H., WHITE, J. W., JR., AND BAKER, G. L.: Proc. Inst. Food Tech. **1942**, 47.
(15) HINTON, C. L.: Biochem. J. **34**, 1211 (1940).
(16) HIRST, E. L.: J. Chem. Soc. **1942**, 70.
(17) HIRST, E. L., AND JONES, J. K. N.: J. Chem. Soc. **1939**, 452.
(18) HIRST, E. L., AND JONES, J. K. N.: J. Chem. Soc. **1939**, 454.
(19) ISBELL, H. S., AND FRUSH, H. L.: Natl. Bur. Standards J. Research **31**, 33 (1943).
(20) KARRER, P., AND SCHWARZENBACH, G.: Helv. Chim. Acta **17**, 58 (1934).
(21) KERN, W.: Z. physik. Chem. **A181**, 249 (1938).
(22) KERTESZ, Z. I., *et al.*: Chem. Eng. News **22**, 105 (1944).
(23) LEVENE, P. A., AND SIMMS, H. S.: J. Biol. Chem. **63**, 351 (1925).
(24) MAXWELL, W. R., AND PARTINGTON, J. R.: Trans. Faraday Soc. **33**, 670 (1937).
(25) MORELL, S., BAUER, L., AND LINK, K. P.: J. Biol. Chem. **105**, 1 (1934).
(26) MORELL, S., BAUER, L., AND LINK, K. P.: J. Biol. Chem. **105**, 15 (1934).
(27) MORELL, S., AND LINK, K. P.: J. Biol. Chem. **104**, 183 (1934).
(28) NANJI, D. R., PATON, F. J., AND LING, A. R.: J. Soc. Chem. Ind. **44**, 253T (1925).
(29) NORRIS, F. W., AND RESCH, C. E.: Biochem. J. **31**, 1945 (1937).
(30) OLSEN, A. G.: J. Phys. Chem. **38**, 919 (1934).
(31) PIGMAN, W. W.: Natl. Bur. Standards J. Research **25**, 301 (1940).
(32) Reviews in English on the constitution and structure of pectinic acid can be found in reference 16 and the following:
NORMAN, A. G.: *The Biochemistry of Cellulose, the Polyuronides, Lignin, etc.*, p. 76. Oxford University Press, London (1937).
NORMAN, A. G.: Ann. Rev. Biochem. **10**, 76 (1941).
MEYER, K. H.: *Natural and Synthetic High Polymers*, p. 364. Interscience Publishers. New York (1942).
(33) SÄVERBORN, S.: Kolloid-Z. **90**, 41 (1940).
(34) SCHNEIDER, G. G., AND BOCK, H.: Ber. **70B**, 1617 (1937).
(35) SCHNEIDER, G. G., AND FRITSCHI, U.: Ber. **69B**, 2537 (1936).
(36) SCHNEIDER, G. G., AND FRITSCHI, U.: Ber. **70B**, 1611 (1937).
(37) SIMMS, H. S.: J. Am. Chem. Soc. **48**, 1239 (1926).
(38) SMITH, F.: Chemistry & Industry **1939**, 363.
(39) TARR, L. W.: Delaware Agr. Expt. Sta. Bull. **142** (1926).
(40) VAN ITERSON, G.: Chem. Weekblad **30**, 2 (1933).
(41) VON MURALT, A. L.: J. Am. Chem. Soc. **52**, 3518 (1930).
(42) WEBER, H. H.: Biochem. Z. **189**, 381 (1927).
(43) WYMAN, J.: Quoted by E. J. Cohn and J. T. Edsall in *Proteins, Amino Acids, and Peptides as Ions and Dipolar Ions*, p. 451. Reinhold Publishing Corporation, New York (1943).

THE FORMATION OF THE SULFOALUMINATES AND SULFOFERRITES OF CALCIUM IN THE PORTLAND CEMENT–WATER SYSTEM

F. E. JONES

Building Research Station, Garston, Watford, Herts, England

The purpose of this paper is to discuss the present state of knowledge of the aqueous equilibria in the system Portland cement–water which are involved in the formation of sulfoaluminates and sulfoferrites of calcium, to indicate the research program which is still needed to complete that knowledge, and to discuss the application of phase-rule studies to the cement–water system.

Essentially we are concerned with the various aqueous equilibria, stable, metastable, and unstable, which it is possible to set up with the oxide components CaO, Al_2O_3, SiO_2, Fe_2O_3, K_2O, Na_2O, SO_3 of Portland cement. Neglecting for the time being the presence of silica, and the possibility of the formation of hydrated calcium aluminosilicates, the most complex system which need be considered is that exemplified by the quinary system $CaO–Al_2O_3–K_2O–SO_3–H_2O$. There are three other similar systems to be considered also: namely, those where Al_2O_3 is replaced by Fe_2O_3 and K_2O by Na_2O. As regards Fe_2O_3, it is the writer's view that the part played by this component in the aqueous equilibria Portland cement–water has hitherto been undeservedly neglected. Studies of such quinary systems involve, at any rate in part, studies of the quaternary systems which can be formed, and of these the most important are $CaO–Al_2O_3–SO_3–H_2O$ and $CaO–Fe_2O_3–SO_3–H_2O$. Finally, the study of the quaternary systems involves a study of the possible ternary systems, in particular of $CaO–Al_2O_3–H_2O$ and $CaO–Fe_2O_3–H_2O$. A restricted list of systems requiring investigation would thus be, in order of increasing complexity:

(1) $CaO–Al_2O_3–H_2O$
(2) $CaO–Fe_2O_3–H_2O$
(3) $CaO–Al_2O_3–CaSO_4–H_2O$
(4) $CaO–Fe_2O_3–CaSO_4–H_2O$
(5) $CaO–Al_2O_3–CaSO_4–K_2O–H_2O$
(6) $CaO–Fe_2O_3–CaSO_4–K_2O–H_2O$
(7) $CaO–Al_2O_3–CaSO_4–Na_2O–H_2O$
(8) $CaO–Fe_2O_3–CaSO_4–Na_2O–H_2O$

Prior to work carried out by the writer during recent years, investigations reported in the literature have been almost wholly restricted to a consideration of the $CaO–Al_2O_3–H_2O$ system. Much work has been carried out on this system by many authors over a long period of years, though without complete definition of the system. A small amount of work which bears on the systems $CaO–Fe_2O_3–H_2O$, $CaO–Al_2O_3–CaSO_4–H_2O$, and $CaO–Fe_2O_3–CaSO_4–H_2O$ has also been done,

but no comprehensive investigation has been reported apart from the writer's own work on the systems $CaO–Al_2O_3–CaSO_4–H_2O$ (17, 18), $CaO–Al_2O_3–CaSO_4–K_2O–H_2O$ (1 per cent KOH) (19), and $CaO–Al_2O_3–CaSO_4–Na_2O–H_2O$ (1 per cent NaOH) (20) at 25°C.

In a recent investigation (17) the importance has been stressed of defining as rigidly as possible the nature of the calcium hydroxide and hydrated alumina solid phases involved in the equilibria. Thus we may work with crystalline $Ca(OH)_2$ as obtained by crystallization from a lime solution, or with a more or less amorphous form very finely divided and of appreciably greater solubility. In the case of hydrated alumina the possibilities include γ-$Al_2O_3 \cdot H_2O$ (böhmite), α-$Al_2O_3 \cdot 3H_2O$ (bayerite), and γ-$Al_2O_3 \cdot 3H_2O$ (gibbsite or hydrargillite) both as comparatively large crystals giving a sharp x-ray pattern, and as gel consisting of highly hydrous masses of crystals so small that no x-ray pattern is obtained, though electron-diffraction studies yield typical patterns. Thus Weiser and Milligan (28) have shown that the gel precipitated from aluminum sulfate solution at 25°C. gives the electron-diffraction pattern of γ-$Al_2O_3 \cdot H_2O$, though with x-rays only a very broad band pattern is obtained. When aged in the cold the γ-$Al_2O_3 \cdot H_2O$ gradually changes over and yields an electron-diffraction pattern of α-$Al_2O_3 \cdot 3H_2O$. Reference may also be made to the work of Hüttig and Kostelitz (16). From the results of isobaric dehydration and x-ray examination of samples of hydrated alumina, prepared and aged in various ways, these authors concluded that aging consists in the gradual change of an amorphous böhmite showing a continuous loss of water, to a crystalline hydrargillite showing a typical step in the dehydration curve. The α-$Al_2O_3 \cdot 3H_2O$ is formed initially. In the case of ferric oxide there is again the possibility of working either with a gel consisting of a highly hydrous mass of tiny crystals of α-Fe_2O_3 (hematite), the size of which will vary according to the aging treatment to which the gel has been subjected, or with crystalline $Fe_2O_3 \cdot H_2O$. In the systems listed therefore, we have to consider equilibria with coarsely crystalline and finely crystalline $Ca(OH)_2$, crystalline $Al_2O_3 \cdot 3H_2O$ and alumina gel, crystalline hydrated ferric oxide, and ferric oxide gel. In the case of lime, the essential difference between the forms is one of size of crystal, while in the case of alumina and of ferric oxide, there is not only a difference of crystal size, but of crystal structure also.

THE SYSTEM $CaO–Al_2O_3–H_2O$

Although much work has been carried out on this system (see, for example, the survey by Bessey (2)), the gel form of alumina has been considered almost exclusively. This, which when fresh is essentially a highly hydrous mass of tiny crystals of γ-$Al_2O_3 \cdot H_2O$, is the most soluble form of alumina, but the crystals not only tend to grow in size as the gel ages, but also to change, first to α-$Al_2O_3 \cdot 3H_2O$ and then finally to γ-$Al_2O_3 \cdot 3H_2O$. The equilibrium with alumina gel is unstable with respect to crystalline γ-$Al_2O_3 \cdot 3H_2O$. Assarsson (1) has reported the separation of hydrated alumina in varying degrees of crystallization from calcium aluminate solutions at various temperatures from 5° to 90°C. Some investiga-

tion has been made recently by the writer (18) in the course of other work, of the equilibria with crystalline γ-$Al_2O_3 \cdot 3H_2O$, and the fundamentally stable curves have been defined.

THE SYSTEM CaO–Fe_2O_3–H_2O

Nothing but the most tentative work seems to have been done on this system. Yet there appears to be no reason why somewhat similar equilibria to those found for the system CaO–Al_2O_3–H_2O should not exist, though the possibilities of compound and solid-solution formation may be much more limited. Eiger (9) found that ferric oxide gel when shaken with a saturated calcium hydroxide solution yields a cubic compound $3CaO \cdot Fe_2O_3 \cdot 6H_2O$ analogous to the cubic $3CaO \cdot Al_2O_3 \cdot 6H_2O$, and it seems reasonable to suppose that similar curves for gel, crystalline hydrated oxide, and the cubic hexahydrate exist for Fe_2O_3 as for Al_2O_3, though there appears to be no $Fe_2O_3 \cdot 3H_2O$ analogous to $Al_2O_3 \cdot 3H_2O$. As regards metastable equilibria there is also evidence (e.g., Hoffmann (15), MacIntire and Shaw (23)) for the existence of hexagonal forms of hydrated calcium ferrites (or solid solutions) analogous to those found with Al_2O_3.

THE SYSTEM CaO–Al_2O_3–$CaSO_4$–H_2O

This system has been thoroughly investigated at 25°C. (17, 18) in recent years. The method of treatment has been to consider the system as being formed by reciprocal salt pairs as expressed in the equation

$$(Ca(OH)_2)_3 + Al_2(SO_4)_3aq. = Al_2O_3aq. + (CaSO_4)_3aq.$$
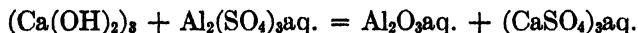
For a list of the various equilibria determined, a previous paper (18) should be consulted. It may be here recalled that the only stable quaternary compound formed is $C_3A \cdot 3CaSO_4 \cdot 32H_2O$. Metastable equilibria however readily arise, and solid solutions of general composition $xCaO \cdot yAl_2O_3 \cdot zCaSO_4 \cdot aq.$ are formed. The so-called low-sulfate form of calcium sulfoaluminate prepared originally by Lerch, Ashton, and Bogue (22) belongs to this series. A solid-solution surface has been defined within the quaternary system.

THE SYSTEM CaO–Fe_2O_3–$CaSO_4$–H_2O

Very little work has appeared which has a bearing on this system. MacIntire and Shaw (23) in 1925 deduced the existence of an iron compound analogous to the high-sulfate form of calcium sulfoaluminate, but were not able to prepare it in a pure state for analysis. Bogue and Lerch (3) placed dicalcium ferrite, $2CaO \cdot Fe_2O_3$, in calcium sulfate solution for a year and found a crystalline phase consisting of short broad hexagonal colorless prisms of refractive index $\alpha = 1.486$ ± 0.003, $\gamma = 1.492 \pm 0.003$, parallel extinction, positive elongation, and uniaxial positive. They suggest that these are identical with the crystals obtained by MacIntire and Shaw (23), but were not able to get them sufficiently pure for analysis. Malquori and Cirilli (25) have recently examined the effect of the addition of calcium sulfate to the products of hydration of $4CaO \cdot Al_2O_3 \cdot Fe_2O_3$ in the presence of lime and found that the calcium sulfate reacted to an extent

nearly equal to that required theoretically for formation of $3CaO \cdot Al_2O_3 \cdot 3CaSO_4 \cdot$ aq. and $3CaO \cdot Fe_2O_3 \cdot 3CaSO_4 \cdot aq$. The final product was white in color. Cirilli (7) later (brief abstract only seen) has found that anhydrous cements absorb calcium sulfate from a saturated solution, the molar ratio $SO_3/Al_2O_3 + Fe_2O_3$ becoming gradually near 3. The writer has prepared the compound $3CaO \cdot Fe_2O_3 \cdot 3CaSO_4 \cdot 32H_2O$ in a pure state by shaking at 25°C. a solution of iron alum, $(NH_4)_2SO_4 \cdot Fe_2(SO_4)_3 \cdot 24H_2O$, with lime in suitable proportions for 2 days. The preparation consisted of very small short needles, birefringence too slight to observe elongation, refractive index 1.490 ± 0.003. Analysis gave CaO = 25.65 per cent, Fe_2O_3 = 12.1 per cent, SO_3 = 18.1 per cent. (Theory for $3CaO \cdot Fe_2O_3 \cdot 3CaSO_4 \cdot 32H_2O$: CaO = 25.65 per cent, Fe_2O_3 = 12.15 per cent, SO_3 = 18.3 per cent.) It has not yet been found possible to carry out sufficient work to determine whether there exists a solid-solution series involving a low sulfate composition as in the case of the corresponding system with Al_2O_3, though it seems highly probable. Malquori and Caruso (24) have in fact (according to a brief abstract) described the preparation of $3CaO \cdot Fe_2O_3 \cdot CaSO_4 \cdot H_2O$ as well as corresponding calcium chloride and calcium nitrate compounds, but no details are known. It is, however, clear that the formation of the high-sulfate compound is probable in a hydrated Portland cement, and that the Fe_2O_3 content must be considered as probably equivalent to Al_2O_3, subject of course to differences in the regions of stability for the analogous compounds or solid solutions formed. The system $CaO–Fe_2O_3–CaSO_4–H_2O$ merits study on similar lines to those used in the corresponding Al_2O_3 system.

THE SYSTEM $CaO–Al_2O_3–CaSO_4–K_2O–H_2O$

The work of a number of authors has shown that when Portland cement is mixed with a limited amount of water, as is the case in practice, the liquid phase contains a high proportion of alkalies. It is, in fact, mainly a mixed solution of alkali sulfate and alkali hydroxide. A table showing the concentrations in the liquid phase reported by various authors is given in a previous paper (19). Both potassium and sodium sulfate and the corresponding hydroxides are present, though the potassium compounds largely predominate. The total alkali concentration expressed as the KOH equivalent may amount to as high as 2.1 per cent or 1.5 per cent NaOH.

No work appears to have been carried out on this system except that reported recently (19) dealing with the system at a constant total alkali concentration equivalent to 1 per cent KOH. Hein (13) carried out some tests on the reaction of potassium hydroxide solutions with gypsum, by shaking potassium hydroxide solutions of varying concentrations with gypsum and lime hydrate at 17°C. Above a concentration of 0.353 equivalent K_2O per liter (corresponding to 1.98 per cent KOH) he found that the alkali concentration of the equilibrium solution remained constant, indicating that an alkali double salt was precipitated. This is evidently the compound $CaSO_4 \cdot K_2SO_4 \cdot H_2O$, which occurs at 25°C. in both the ternary system $CaSO_4–K_2SO_4–H_2O$ (Cameron and Breazeale (6)) and the quaternary system $CaO–CaSO_4–K_2SO_4–H_2O$ (D'Ans and Schreiner (8)). It is

noteworthy that the maximum concentration of alkali which has been found in practice in the liquid phase of normal Portland cement mixes corresponds approximately to the point at which Hein found precipitation of double salt, and to the composition of the invariant point $Ca(OH)_2-CaSO_4 \cdot 2H_2O-CaSO_4 \cdot K_2SO_4 \cdot H_2O$ given by D'Ans and Schreiner. This suggests that in Portland cements of sufficiently high alkali content, the alkali double salt may well be precipitated. It seems desirable therefore to carry out a further examination of the $CaO-Al_2O_3-CaSO_4-K_2O-H_2O$ system, at least in part, using an alkali concentration equivalent to between 2 per cent and 5 per cent KOH. A Portland cement containing sufficient alkali to yield the equivalent of 5 per cent KOH in solution would be exceptional, as table 1 (4) shows. This gives for seven Portland cements both the total alkali content, and the amounts dissolved after shaking 15 g. of cement with 150 ml. of water for 48 hr. Only a small increase occurs between 16 and 48 hr. The work so far carried out on the 1 per cent KOH system has shown that in spite of the considerable modification of the

TABLE 1

Alkali contents of Portland cements

Cement...	1	2	3	4	5	6	7
Total $K_2O + Na_2O$, per cent...	0.70	0.90	1.00	1.22	1.24	1.01	1.30
Dissolved $K_2O + Na_2O$, per cent	0.14	0.35	0.39	0.49	0.63	0.71	1.11

quaternary equilibria in the system $CaO-Al_2O_3-CaSO_4-H_2O$ as regards solution compositions which the much increased solubility of alumina and decreased solubility of lime in alkali entails, the same sequence in the changing equilibria is to be expected. This involves the setting up of an invariant point equilibrium $Ca(OH)_2-CaSO_4 \cdot H_2O-C_3A \cdot 3CaSO_4 \cdot 32H_2O$ (point F in both quaternary (17, 18) and quinary (19, 20) equilibria), followed by change along the boundary curve $Ca(OH)_2-C_3A \cdot 3CaSO_4 \cdot 32H_2O$ towards the invariant point G, and into the metastable solid-solution region (figure 1).

THE SYSTEM $CaO-Al_2O_3-CaSO_4-Na_2O-H_2O$

This system has also been investigated by the writer at 25°C. for the alkali concentration equivalent to 1 per cent NaOH. The equilibria are similar in form to those found for the corresponding K_2O system. The system $CaSO_4-Na_2SO_4-H_2O$ differs from that for $CaSO_4-K_2SO_4-H_2O$ in that no stable double salt of the two sulfates is formed at 25°C., no matter what the concentration of sodium sulfate. Hill and Wills (14) give for a metastable isothermal invariant point $CaSO_4 \cdot 2H_2O-CaSO_4 \cdot Na_2SO_4$ at 25°C. the solution composition (weight per cent) $Na_2SO_4 = 25.9$, $CaSO_4 = 0.17$. At 35°C. the invariant point is stable, with solution composition $Na_2SO_4 = 22.65$ and $CaSO_4 = 0.21$. The system invariant point $CaSO_4 \cdot 2H_2O-Na_2SO_4 \cdot 10H_2O-CaSO_4 \cdot Na_2SO_4$ is reported as 27.5°C. with the Na_2SO_4 concentration 25.0 weight per cent. At 50° and 75°C., the

stable invariant point $CaSO_4$–$CaSO_4 \cdot Na_2SO_4$ is reported by the same authors, with the solution compositions $Na_2SO_4 = 19.7$, $CaSO_4 = 0.21$ and $Na_2SO_4 = 18.9$, $CaSO_4 = 0.13$, respectively. These data appear to rule out the possibility of any double sulfate of $CaSO_4$ and Na_2SO_4 arising, no matter what the temperature rise in the setting cement may be owing to the high sodium sulfate concentrations required.

THE SYSTEMS CaO–Fe_2O_3–$CaSO_4$–$K_2O(Na_2O)$–H_2O

No work appears to have been carried out on the Fe_2O_3 systems. Both systems may well be as important as the corresponding Al_2O_3 systems. Both alu-
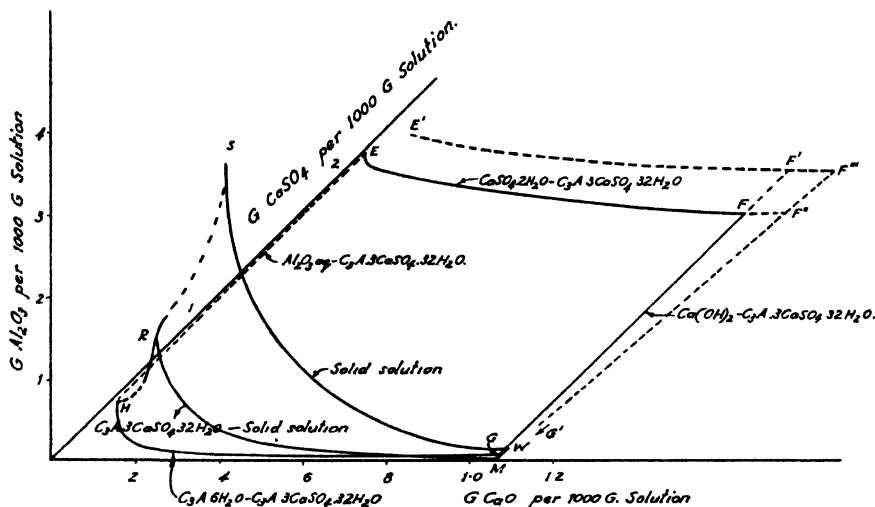
FIG. 1. Equilibria in the system CaO–Al_2O_3–$CaSO_4$–H_2O at 25°C.

minum and ferric iron form similar double sulfates with potassium sulfate, though in the case of sodium sulfate, a sodium iron alum salt does not appear to be formed. Information in the literature on aqueous equilibria involving the sulfates of sodium, potassium, and ferric iron is too scanty to permit of any conclusions being drawn as to behavior in the quinary systems.

THE FORMATION OF MIXED CRYSTALS OF CORRESPONDING Al_2O_3 AND Fe_2O_3 COMPOUNDS

The fact of the existence of corresponding compounds $3CaO \cdot Al_2O_3 \cdot 6H_2O$ and $3CaO \cdot Fe_2O_3 \cdot 6H_2O$, $3CaO \cdot Al_2O_3 \cdot 3CaSO_4 \cdot 32H_2O$ and $3CaO \cdot Fe_2O_3 \cdot 3CaSO_4 \cdot 32H_2O$, and of solid solutions involving CaO, Al_2O_3, $CaSO_4$, and CaO, Fe_2O_3, $CaSO_4$, respectively, suggests the possibility of the formation of mixed crystals involving the replacement of Al_2O_3 by Fe_2O_3. Recently Flint, McMurdie, and Wells (10) have shown that $3CaO \cdot Al_2O_3 \cdot 6H_2O$ and $3CaO \cdot Fe_2O_3 \cdot 6H_2O$ are capable of forming mixed crystals. These were prepared by heating glasses in the system CaO–$2CaO \cdot SiO_2$–$5CaO \cdot 3Al_2O_3$–$4CaO \cdot Al_2O_3 \cdot Fe_2O_3$ with water at

about 200°C. for about a week, and also by the very slow addition of dilute acidified iron and aluminum chlorides to a large volume of boiling lime solution. While these experiments were made at 200°C. and 100°C., respectively, it seems quite probable that $3CaO \cdot Al_2O_3 \cdot 6H_2O$ and $3CaO \cdot Fe_2O_3 \cdot 6H_2O$ are capable of forming mixed crystals at room temperatures. No experiments to test the formation of mixed crystals of the corresponding sulfate compounds or the formation of solid solutions involving CaO, Al_2O_3, Fe_2O_3, $CaSO_4$ appear as yet to have been made.

THE ROLE OF SiO_2

While the main purpose of this paper is to discuss the equilibria directly concerned with the production of calcium sulfoaluminates and calcium sulfoferrites, some consideration must be given to the part played by silica. A general survey of the work hitherto carried out on the system $CaO-SiO_2-H_2O$ has been given by Bessey (2), and an equilibrium diagram suggested. Further work is required before any definite conclusions can be reached. Very little work appears to have been carried out on the systems $CaO-Al_2O_3-SiO_2-H_2O$ or $CaO-Fe_2O_3-SiO_2-H_2O$. It has been shown, however, by Flint, McMurdie and Wells (10) that mixed-crystal formation may occur not only between $3CaO \cdot Al_2O_3 \cdot 6H_2O$ and $3CaO \cdot Fe_2O_3 \cdot 6H_2O$, but that these form mixed crystals with the compounds $3CaO \cdot Al_2O_3 \cdot 3SiO_2$ and $3CaO \cdot Fe_2O_3 \cdot 3SiO_2$. Various compositions have been prepared by these authors, using the methods mentioned previously, in the solid-solution series $3CaO \cdot Al_2O_3(Fe_2O_3) \cdot 6H_2O-3CaO \cdot Al_2O_3(Fe_2O_3) \cdot 3SiO_2$. It was, in fact, found difficult to prepare $3CaO \cdot Al_2O_3 \cdot 6H_2O-3CaO \cdot Fe_2O_3 \cdot 6H_2O$ solid solutions free from SiO_2, the SiO_2-free solid solutions being relatively unstable. Furthermore, 1 part of SiO_2 appears to substitute for 2 parts H_2O. The existence of such SiO_2-containing solid solutions raises the question as to whether these are formed in the reaction of Portland cement with water. Strätling (27), whose work is commented on by Büssem (5), found on shaking burnt kaolin (600°C.) with lime solution at 20°C. that after some months lime had been taken up by kaolin to give a gross composition of $3CaO \cdot Al_2O_3 \cdot 2SiO_2 \cdot aq$. The same product was obtained by mixing $3CaO \cdot Al_2O_3$ and $3CaO \cdot SiO_2$ with water in the ratio $2SiO_2 : 1Al_2O_3$. The product was considered by Büssem and Strätling to be a mixture of $3CaO \cdot 2SiO_2 \cdot aq$. and $2CaO \cdot Al_2O_3 \cdot SiO_2 \cdot aq$., though Strätling, from experiments with mixes of $3CaO \cdot Al_2O_3$, SiO_2 sol, and lime arrives at a calculated composition of $2.7CaO \cdot Al_2O_3 \cdot SiO_2 \cdot aq$. for the quaternary product. It is clear that compound or solid-solution formation involving CaO, Al_2O_3, Fe_2O_3, and SiO_2 may occur in the reaction of cement with water. In the presence of calcium sulfate therefore, the possibility exists of a compound or solid solution involving $CaSO_4$ in addition.

THE FORMATION OF PROTECTIVE COATINGS

The formation of protective coatings which interfere with or effectively prevent the attainment of equilibrium is important. Forsén (12) has drawn attention to such behavior and cites for example the retardation of the slaking of lime

in a magnesium sulfate solution, apparently as a result of the formation of a protective coating of magnesium hydroxide, and the behavior of aluminous cement concrete and also of slag mixes where prolonged mixing appears to result in the removal by attrition of an initially formed protective coating. The same author observed the formation of semipermeable membranes by allowing calcium aluminate solutions to come into contact with saturated lime and lime–gypsum solutions through a porous glass plate. The film formed in the lime solution had the composition $3.9CaO:1Al_2O_3$, and that in the lime–gypsum solution the composition $3.7CaO:1Al_2O_3:0.3CaSO_4$. The latter may be written as $12.33CaO:3.33Al_2O_3:1CaSO_4$, equivalent to 2.33 moles of $3CaO\cdot Al_2O_3\cdot Ca(OH)_2\cdot 12H_2O$ plus 1 mole $3CaO\cdot Al_2O_3\cdot CaSO_4\cdot 12H_2O$, so that a solid solution of the type found in the writer's work on the system $CaO–Al_2O_3–CaSO_4–H_2O$ appears to be formed rather than a mixture of $7(CaO\cdot Al_2O_3\cdot aq.)$ plus $3(3CaO\cdot Al_2O_3\cdot CaSO_4\cdot aq.)$, as Forsén suggested. In the writer's investigations on the quaternary system, the formation of coatings of newly formed compounds on crystal surfaces has also entered. This has been shown particularly in the work involving crystalline $Al_2O_3\cdot 3H_2O$ (18), where difficulties in the attainment of the equilibria desired arose from this cause. In the ternary system $CaO–Al_2O_3–H_2O$, reaction of crystalline $Al_2O_3\cdot 3H_2O$ in solution of high CaO concentration yields a coating of cubic $3CaO\cdot Al_2O_3\cdot 6H_2O$ over the $Al_2O_3\cdot 3H_2O$. In the quaternary system $CaO–Al_2O_3–CaSO_4–H_2O$, attainment of the stable equilibria $Al_2O_3\cdot 3H_2O–3CaO\cdot Al_2O_3\cdot 3CaSO_4\cdot 32H_2O$ with mixes of $Al_2O_3\cdot 3H_2O$ and lime–calcium sulfate solutions has been shown to be inhibited unless excessive formation of $3CaO\cdot Al_2O_3\cdot 3CaSO_4\cdot 32H_2O$ is avoided, and it must be concluded that a coating, probably of $3CaO\cdot Al_2O_3\cdot 3CaSO_4\cdot 32H_2O$, is formed on the $Al_2O_3\cdot 3H_2O$ surface. The formation of such a coating in the case of crystalline $Al_2O_3\cdot 3H_2O$ is of interest in view of difficulties experienced in the attainment of equilibrium with cubic $3CaO\cdot Al_2O_3\cdot 6H_2O$. Certain anomalous results with mixes of $3CaO\cdot Al_2O_3\cdot 6H_2O$ and calcium sulfate solutions have previously been explained as possibly due to the formation of a thin coating of $Al_2O_3\cdot aq.$ around the grains of $3CaO\cdot Al_2O_3\cdot 6H_2O$. The results with $Al_2O_3\cdot 3H_2O$ suggest that the inhibiting coating may be $3CaO\cdot Al_2O_3\cdot 3CaSO_4\cdot 32H_2O$.

In the system Portland cement–water, the formation of protective coatings is of particular importance, since it is to such coatings that the action of gypsum and other compounds in retarding the rate of set of Portland cement is to be ascribed. Forsén considers that in the presence of gypsum as retarder, the supposed compound $3CaO\cdot Al_2O_3\cdot CaSO_4\cdot 12H_2O$ is formed around the cement grains and not the high-sulfate form $3CaO\cdot Al_2O_3\cdot 3CaSO_4\cdot 32H_2O$. This will be discussed later. In an alkali-free cement, lime alone acts as retarder, and here a protective coating of $3CaO\cdot Al_2O_3\cdot Ca(OH)_2\cdot 12H_2O$ is considered to be deposited around the cement grains. Whatever the protective coating which is formed initially, its effect is to slow up the rate of hydration of the cement constituents and to delay the attainment of equilibrium.

The formation of protective coatings may also play an important part in conferring sulfate resistance on a set Portland cement. Flint and Wells (11) have

carried out tests on a limited number of preparations in the solid-solution series $3CaO \cdot Al_2O_3(Fe_2O_3) \cdot 6H_2O$–$3CaO \cdot Al_2O_3(Fe_2O_3)$–$3SiO_2$, which indicate that while $3CaO \cdot Al_2O_3 \cdot 6H_2O$ itself is readily converted to $3CaO \cdot Al_2O_3 \cdot 3CaSO_4 \cdot 32H_2O$ in contact with a sodium sulfate solution (10 per cent Na_2SO_4), the introduction of SiO_2 or Fe_2O_3 or both into the crystal rapidly increases resistance to the conversion, 10–15 per cent or more of either SiO_2 or Fe_2O_3 conferring a very high resistance. It seems possible that the reason for the efficacy of Fe_2O_3 in the crystal is that the sulfoferrite forms a protective coating more readily than the corresponding sulfoaluminate. This is supported by the work of Malquori and Cirilli (25), who found that the compound $4CaO \cdot Fe_2O_3 \cdot aq.$ reacts much less readily than any of the hydrated aluminate compounds with calcium sulfate. The inhibition of the reaction of both hydrated aluminates and $4CaO \cdot Fe_2O_3 \cdot aq.$ with calcium sulfate is ascribed by these authors to the formation of protective coatings.

APPLICATION OF PHASE-RULE STUDIES TO THE CEMENT–WATER SYSTEM

In 1938, a symposium on the chemistry of cements was held in Stockholm. The papers contributed, with the discussions thereon, provide a convenient expression of present-day knowledge. Much of the views held on behavior in the system cement–water, including the action of various compounds in modifying the rate of set, lack such light as may be afforded by the study from the phase-rule aspect of the various equilibria which are possible. It is of value to consider the application of the equilibria already worked out by the writer to some of the statements and views expressed.

For this purpose we may consider those portions of the quaternary system CaO–Al_2O_3–$CaSO_4$–H_2O at 25°C. and the quinary system CaO–Al_2O_3–$CaSO_4$–K_2O–H_2O (1 per cent KOH) at 25°C. which are of direct interest in the reactions occurring when cement is mixed with water to give a mix of normal consistence. Here we are primarily concerned with the boundary curves $CaSO_4 \cdot 2H_2O$–$3CaO \cdot Al_2O_3 \cdot 3CaSO_4 \cdot 32H_2O$, $Ca(OH)_2$–$3CaO \cdot Al_2O_3 \cdot 3CaSO_4 \cdot 32H_2O$ and the metastable solid-solution equilibria. In the case of the quaternary system, the essential equilibria are shown schematically in figure 1, using rectangular coordinates. Metastable solid-solution equilibria are given in the plane enclosed by the CaO and Al_2O_3 axes. For simplicity the lower boundary curves MR and the upper limit WS of the solid-solution surface (not a boundary curve) are alone indicated. The plane enclosed by the CaO and $CaSO_4$ axes, and close to which the boundary curves for $CaSO_4 \cdot 2H_2O$–$3CaO \cdot Al_2O_3 \cdot 3CaSO_4 \cdot 32H_2O$ and $Ca(OH)_2$–$3CaO \cdot Al_2O_3 \cdot 3CaSO_4 \cdot 32H_2O$ lie, is at right angles to the former plane. Only certain of the equilibrium curves determined are shown in the figure. The lettering has the same significance as in previous papers.

Besides gypsum, it is necessary to consider the behavior of the so-called semi-hydrate $CaSO_4 \cdot \frac{1}{2}H_2O$, which initially shows a much higher solubility than gypsum (about four times the $CaSO_4$ concentration in water) though the concentration falls quickly as the conversion $CaSO_4 \cdot \frac{1}{2}H_2O + 1\frac{1}{2}H_2O \rightarrow CaSO_4 \cdot 2H_2O$ takes place. There is too the possible formation of $Ca(OH)_2$ in such a fine state

of subdivision as to yield higher solubilities. The possible metastable equilibria are shown by the broken lines in the figure. E'F''' represents a theoretical metastable equilibrium with $CaSO_4 \cdot \frac{1}{2}H_2O$ and G'F''' that with a more soluble form of $Ca(OH)_2$. The significance of the metastable invariant points represented by F', F'', and F''' is apparent. It is clear that whatever form of hydrated calcium sulfate or of $Ca(OH)_2$ we consider, there is no fundamental difference in the equilibria set up, though the relative concentrations of salts in solution will be different. Thus for the equilibrium F''', the salt concentrations will be much higher than for the equilibrium F. At F', compared with F, there will be a marked increase in the $CaSO_4$ and K_2SO_4 concentrations, with a decrease in $Ca(OH)_2$ and KOH concentrations, and at F''' an increase in the $Ca(OH)_2$ and KOH concentrations with a decrease in the $CaSO_4$ and K_2SO_4 concentrations.

Considering in the first instance an alkali- and iron-free Portland cement, mixed with sufficient water to give normal consistence, it is apparent that the rapid saturation with respect to $Ca(OH)_2$ and $CaSO_4 \cdot 2H_2O$ which occurs must yield at 25°C. the equilibrium point F, or one which rapidly approaches F. In any case the compound $3CaO \cdot Al_2O_3 \cdot 3CaSO_4 \cdot 32H_2O$ is the stable sulfate-containing phase at 25°C. at this stage. As reaction of the calcium aluminates of the cement with gypsum proceeds (to give further $3CaO \cdot Al_2O_3 \cdot 3CaSO_4 \cdot 32H_2O$), the solution concentrations will remain at F until no more $CaSO_4 \cdot 2H_2O$ is left as solid phase. The equilibrium will then move along the boundary curve $Ca(OH)_2$–$3CaO \cdot Al_2O_3 \cdot 3CaSO_4$–$32H_2O$ towards G, the invariant point $C_3A \cdot 6H_2O$–$Ca(OH)_2$–$3CaO \cdot Al_2O_3 \cdot 3CaSO_4 \cdot 32H_2O \cdot$ At G, for stable equilibrium, $3CaO \cdot Al_2O_3 \cdot 6H_2O$ should be formed, and the solution concentration should show no further change. Probably, however, this compound is not formed at this stage. Instead the equilibrium probably proceeds to the metastable invariant point M, very close to G, and on the continuation of FG, where a third solid phase is formed consisting of a solid solution of CaO, Al_2O_3, SO_3, H_2O of high CaO and low SO_3 content. As stated in a previous paper (18), it appears probable that the $C_3A \cdot 3CaSO_4 \cdot 32H_2O$ may eventually change over completely to the solid solution. This equilibrium would in any case tend slowly to change over to that for the invariant point G.

The picture thus drawn may be oversimplified if saturation with $Ca(OH)_2$ and $CaSO_4 \cdot 2H_2O$ does not occur rapidly enough. Thus in the immediate neighborhood of a hydrating C_3A particle, local concentrations of CaO, Al_2O_3, and $CaSO_4$ may initially be such that a metastable solid solution is formed first, corresponding to some point on the solid-solution surface. As, however, CaO and $CaSO_4$ concentrations rise, conversion to $C_3A \cdot 3CaSO_4 \cdot 32H_2O$ should occur and the equilibrium of F reached, followed by the sequence of changes described.

For an alkali-containing cement, we have to consider the corresponding alkali systems. The solid-solution equilibria have not yet been examined, but it is possible to follow the equilibria up to the corresponding stable invariant point G. A similar method of representation may be adopted as for the quaternary system, but because of the additional alkali component, sulfate will be present both

as alkali sulfate and calcium sulfate. Along the third axis, therefore, the concentration of SO_3 is plotted instead of $CaSO_4$. Figure 2 gives a partial representation of the 1 per cent KOH system. The lime concentrations shown give the total lime present both as calcium hydroxide and as calcium sulfate. The point O' represents a pure solution of K_2SO_4 (equivalent to 1 per cent KOH). The same sequence of equilibria apply for the alkali system up to the invariant point G, as has already been discussed for the quaternary system. It seems probable that similar solid-solution equilibria to those found in the quaternary system will then appear.

We are now in a position to discuss some examples of the views held on behavior in the system cement–water.

FIG. 2. Equilibria in the system $CaO–Al_2O_3–CaSO_4–K_2O–H_2O$ (1 per cent KOH) at 25°C.

Forsén states that a technical quick-setting cement (i.e., quick-setting before gypsum addition) was rendered normal setting with dihydrate and with a mixture of dihydrate and semihydrate (3:1), but was quick setting with 1–15 per cent of semihydrate alone. He considers therefore that gypsum acts on cement quite differently if it is present as di- or as semi-hydrate, and that this is due to the fact that the difference in solubility gives rise to different reactions with the aluminates. It is suggested that with much $CaSO_4$ present (from the semihydrate) the compound $3CaO \cdot Al_2O_3 \cdot 3CaSO_4 \cdot 31\frac{1}{2}H_2O$ is formed, but that with $CaSO_4 \cdot 2H_2O$ as retarder the so-called low-sulfate compound $3CaO \cdot Al_2O_3 \cdot CaSO_4 \cdot 12H_2O$ must be formed. The phase-rule studies show that at 25°C. it is the compound $3CaO \cdot Al_2O_3 \cdot 3CaSO_4 \cdot 32H_2O$ which is in equilibrium with solutions saturated with respect to a $CaSO_4$ solid phase (whether $CaSO_4 \cdot 2H_2O$ or

$CaSO_4 \cdot \frac{1}{2}H_2O$) and $Ca(OH)_2$, and indeed throughout a range of solutions of increasing CaO but decreasing $CaSO_4$ concentrations, down to a very small $CaSO_4$ value. It must be concluded therefore that this compound is formed unless there is interference with the attainment of the expected equilibrium. It may, however, be as previously indicated that the hexagonal solid solution is formed initially around the grains of hydrating $3CaO \cdot Al_2O_3$. Forsén states that when crystals of $3CaO \cdot Al_2O_3$ were placed in a solution of $CaSO_4 \cdot 2H_2O$, they were immediately surrounded by a border of finely crystalline "$3CaO \cdot Al_2O_3 \cdot CaSO_4 \cdot 12H_2O$". The refractive indices given are $\alpha = 1.499$, $\gamma = 1.515$. From the work carried out by the writer on the formation of metastable solid solutions in the system $CaO–Al_2O_3–CaSO_4–H_2O$, the indices quoted suggest that the crystals formed constitute a solid solution involving CaO, Al_2O_3, and SO_3. It is not stated what were the relative amounts of $3CaO \cdot Al_2O_3$ crystals and gypsum employed but if, as is probable, there was sufficient gypsum for the formation of $3CaO \cdot Al_2O_3 \cdot 3CaSO_4 \cdot 32H_2O$ at equilibrium at 25°C., an explanation must be found for the solid-solution formation. Apart from the initial setting up of local concentration conditions leading to initial formation of solid solution, an alternative explanation has already been suggested by the writer in a previous paper in discussion of Schläpfer's (26) similar results: namely, that the heat of hydration of the $3CaO \cdot Al_2O_3$ crystals may raise the temperature at the surface of the grains to a value where the solid solution and not the $3CaO \cdot Al_2O_3 \cdot 3CaSO_4 \cdot 32H_2O$ is stable. In this connection a study of the system $CaO–Al_2O_3–CaSO_4–H_2O$ at temperatures greater than 25°C. is desirable.

It may well be that the retardation of the $3CaO \cdot Al_2O_3$ hydration and therefore of set does depend on the initial formation of such a solid-solution deposit, and that with the high initial $CaSO_4$ concentration obtained with the semihydrate, this solid-solution phase is no longer formed even at the higher temperatures which presumably exist at the surface of the hydrating $3CaO \cdot Al_2O_3$. It is clear, however, that eventually the equilibrium of normal temperatures must prevail, so that even if a solid solution is formed initially as a protective coating around the $3CaO \cdot Al_2O_3$ grains whether as the result of a temperature effect or transitory local concentration conditions, since it is in contact with a calcium sulfate solution it must gradually be converted to the high-sulfate form, probably followed by reversion to the solid solution.

It is now possible to arrive at a more comprehensive picture than has hitherto been available of the equilibrium relations in a setting cement, and the parts played by the various components. This picture will be clear from the foregoing discussion without recapitulation. It may be added that in the case of a cement possessing an exceptionally high content of K_2O (in excess of the equivalent of 2 per cent KOH), the double salt $CaSO_4 \cdot K_2SO_4 \cdot H_2O$ may be formed initially. No essential difference in the course of the reactions in the setting cement is, however, to be expected.

Reference may be made to the attack of gypsum and alkali sulfate waters on concrete. Some discussion has been given in a previous paper (17) of attack by calcium sulfate waters. The further work carried out since by the writer throws additional light on this matter, and on attacks by alkali sulfates. It seems clear

that in a set Portland cement the final equilibrium is that for the invariant point M or G, i.e., either $Ca(OH)_2$–$3CaO \cdot Al_2O_3 \cdot 3CaSO_4 \cdot 32H_2O$–solid solution or $Ca(OH)_2$–$3CaO$–$Al_2O_3 \cdot 3CaSO_4 \cdot 32H_2O$–$3CaO \cdot Al_2O_3 \cdot 6H_2O$ or possibly $Ca(OH)_2$–solid solution alone, not only for an alkali-free but probably also for an alkali-containing cement. The expected similar behavior with the Fe_2O_3 component is here neglected. In contact with such sulfate waters, therefore, the solid solution (or $3CaO \cdot Al_2O_3 \cdot 6H_2O$) will gradually be converted to $3CaO \cdot Al_2O_3 \cdot 3CaSO_4 \cdot 32H_2O$. In the quaternary system CaO–Al_2O_3–$CaSO_4$–H_2O at 25°C. the minimum concentration of calcium sulfate required for this conversion is 0.004 g. $CaSO_4$ per liter (invariant point M) and 0.025 g. $CaSO_4$ per liter (invariant point G). In the alkali systems the SO_3 concentrations at the invariant point G are respectively: 1 per cent KOH, 0.050 g. SO_3 per liter; 1 per cent NaOH, 0.075 g. SO_3 per liter. It is probable that at the invariant point M these concentrations would be much reduced. It is apparent that to obtain a concrete resistant to sulfate waters, some means must be found of either preventing formation of the solid solution (or $3CaO \cdot Al_2O_3 \cdot 6H_2O$) or protecting it when formed from the further action of sulfate, or ensuring its complete conversion to $3CaO \cdot Al_2O_3 \cdot 3CaSO_4 \cdot 32H_2O$ during the hardening period and while the concrete is still in a relatively plastic state. The introduction of SiO_2 or Fe_2O_3 into the crystal, as in the work described by Flint and Wells (11) on the solid-solution series $3CaO \cdot Al_2O_3(Fe_2O_3) \cdot 6H_2O$–$3CaO \cdot Al_2O_3(Fe_2O_3) \cdot 3SiO_2$ may be regarded as a method of protection, but this work is related only to solid solutions crystallizing in the cubic system. Flint and Wells found that a hexagonal hydrated calcium silicoaluminate preparation, prepared as described by Strätling (27), was completely converted to $3CaO \cdot Al_2O_3 \cdot 3CaSO_4 \cdot 32H_2O$ after 3 weeks in a 10 per cent sodium sulfate solution. Thus in hexagonal crystals, silica appears to be much less efficacious. It is a possibility, however, that even in the hexagonal system the presence of silica is advantageous. The readiness with which protective coatings appear to be formed in the case of the hexagonal $4CaO \cdot Fe_2O_3 \cdot aq.$ has already been referred to in connection with the work of Malquori and Cirilli (25). The use of pozzolanic materials to increase sulfate resistance has long been known, though the mechanism of the action has remained obscure. It is well known that such materials remove lime from solution. The action is slow and so presumably takes place mainly after the equilibrium of the invariant point G or M would be reached. It appears unlikely therefore that there would be any interference with the initial course of the reactions in a setting cement. Lea (21) states that from tests on pozzolana mortars and concretes up to one or two years complete removal of free lime has not been found, so that it would appear that equilibrium in the region of G or M must persist. This suggests that the purely physical protective effect of the pozzolana–lime product is of major importance in increasing sulfate resistance, and not any modification of the equilibria resulting from removal of lime. It is also possible that the lime–pozzolana product provides a reserve of material with which sulfate must first react to give solid solution. It is not until such formation is complete that formation is complete that formation of the high-sulfate form and consequent

disintegration is to be expected.   However this may be, more knowledge of the aqueous equilibria on the lines indicated is needed before the mechanism of behavior can be satisfactorily cleared up.

SUMMARY

The present state of knowledge of the aqueous equilibria in the system Portland cement–water which are involved in the formation of sulfoaluminates and sulfoferrites of calcium is discussed.   The further phase-rule studies which are needed to complete this knowledge are indicated, and the application of those already made by the writer to the cement–water system considered.   The formation and nature of protective coatings to which retardation of set is ascribed, and the attack of sulfate waters on concrete are also discussed.

The work described in this paper was carried out at the Building Research Station of the Department of Scientific and Industrial Research, and the paper is published by permission of the Director of Building Research.

REFERENCES

(1) ASSARSSON, G.: Sveriges Geol. Undersokn., Arsbok 1936, Ser. C. 30 (6), No. 399.
(2) BESSEY, G. E.: Symposium on the Chemistry of Cements, Stockholm, 1938, p. 178.
(3) BOGUE, R. H., AND LERCH, W.: Ind. Eng. Chem. **26**, 837 (1934).
(4) BUILDING RESEARCH BOARD: Annual Report **1931**, p. 34.
(5) BUSSEM, W.: Symposium on the Chemistry of Cements, Stockholm, 1938, p 163.
(6) CAMERON, F. K., AND BREAZEALE, J. F.: J. Phys Chem. **8**, 335 (1904).
(7) CIRILLI, V.: Ricerca sci. **11**, 973-7 (1940), Chem. Abstracts **35**, 3409 (1941).
(8) D'ANS AND SCHREINER: Z. anorg. Chem. **67**, 437 (1910).
(9) EIGER, A.: Rev. matériaux construction trav. publics **33**, 141 (1937).
(10) FLINT, E. P., McMURDIE, H. F., AND WELLS, L. S.: J. Research Natl. Bur. Standards **26**, 13 (1941).
(11) FLINT, E. P., AND WELLS, L. S.: J. Research Natl. Bur. Standards **27**, 171 (1941).
(12) FORSÉN, L.: Symposium on the Chemistry of Cements, Stockholm, 1938, p. 298.
(13) HEIN, H.: Tonind.-Ztg. **56**, 203 (1932).
(14) HILL, A. E., AND WILLS, J. H.: J. Am. Chem. Soc. **60**, 1647 (1938).
(15) HOFFMANN, H.: Zement **25**, 113, 130, 675, 693, 711 (1936).
(16) HÜTTIG, G. F., AND KOSTELITZ, O.: Z. anorg. allgem. Chem. **187**(1), 1 (1930).
(17) JONES, F. E.: Trans. Faraday Soc. **35**, 1484 (1939).
(18) JONES, F. E.: J. Phys. Chem. **48**, 311 (1944).
(19) JONES, F. E.. J. Phys. Chem. **48**, 356 (1944).
(20) JONES, F. E.: J. Phys. Chem. **48**, 379 (1944).
(21) LEA, F. M.: Private communication.
(22) LERCH, W., ASHTON, F. W., AND BOGUE, R. H.: J. Research Natl. Bur. Standards **2**, 715 (1929).
(23) MACINTIRE, W. H., AND SHAW, W. M : Soil Sci. **19**, 125 (1925).
(24) MALQUORI, G., AND CARUSO, E.: Atti X° congr. intern chim. **2**, 713-18 (1938); Chem. Abstracts **33**, 8134 (1939).
(25) MALQUORI, G., AND CIRILLI, V.: Ricerca sci. **11**, 244 (1940).
(26) SCHLÄPFER, P.: Symposium on the Chemistry of Cements, Stockholm, 1938, p. 270.
(27) STRÄTLING, W.: Dissertation, Braunschweig, 1937 (STRÄTLING, W., AND ZUR STRASSEN, H.: Z. anorg. Chem. **245**, 257-78 (1940)).
(28) WEISER, H. B., AND MILLIGAN, W. O.: J. Phys. Chem. **44**, 1081 (1940).

LIQUID–LIQUID EQUILIBRIUM DATA

C. G. DENZLER

Department of Chemical Engineering, University of Cincinnati, Cincinnati, Ohio

In the course of a research problem, it became necessary to have data on the liquid–liquid equilibria and refractive indices of the ternary systems benzene–1-propanol–water and carbon tetrachloride–1-propanol–water, and refractive index data for the binary system carbon tetrachloride–1-propanol. A search of the literature up to the present yielded insufficient data (2, 5). Therefore determinations were made on these systems at 20°C.
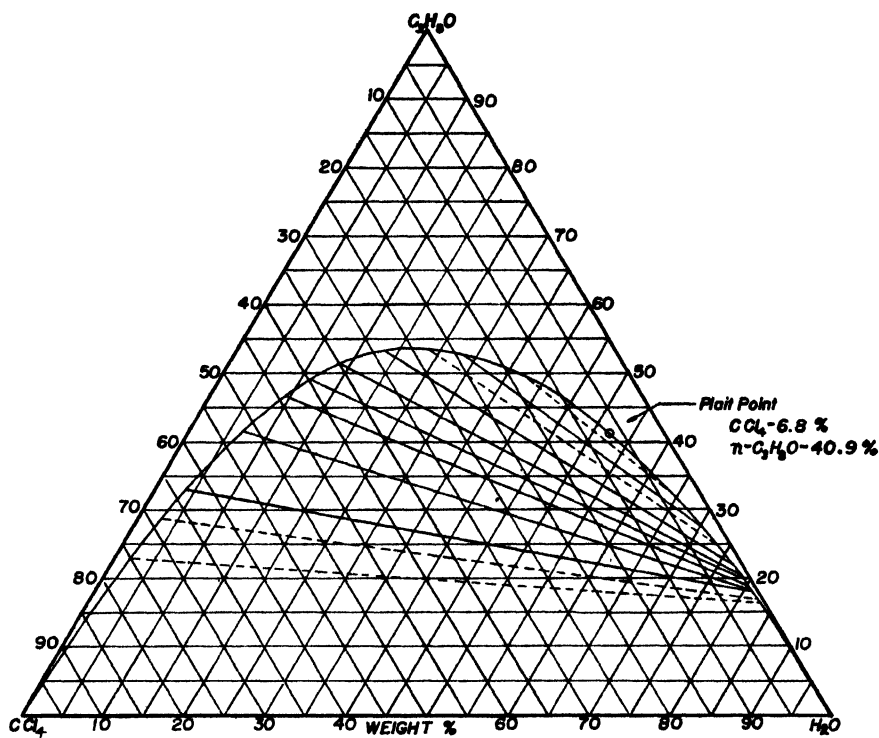
Fig. 1. Binodal curve for the ternary system carbon tetrachloride-1-propanol–water at 20°C. and atmospheric pressure.

Both of the ternary systems contain a single pair of non-consolute liquids whose mutual solubilities increase upon addition of a third component, and therefore their binodal curves (figures 1 and 2) show the characteristic "hump". Tables 1 and 2 present the data from which the binodal curves were drawn. The binary system was one of complete mutual solubility.

The liquid–liquid equilibrium curves have been supplemented with tie lines to increase the usefulness of the data.
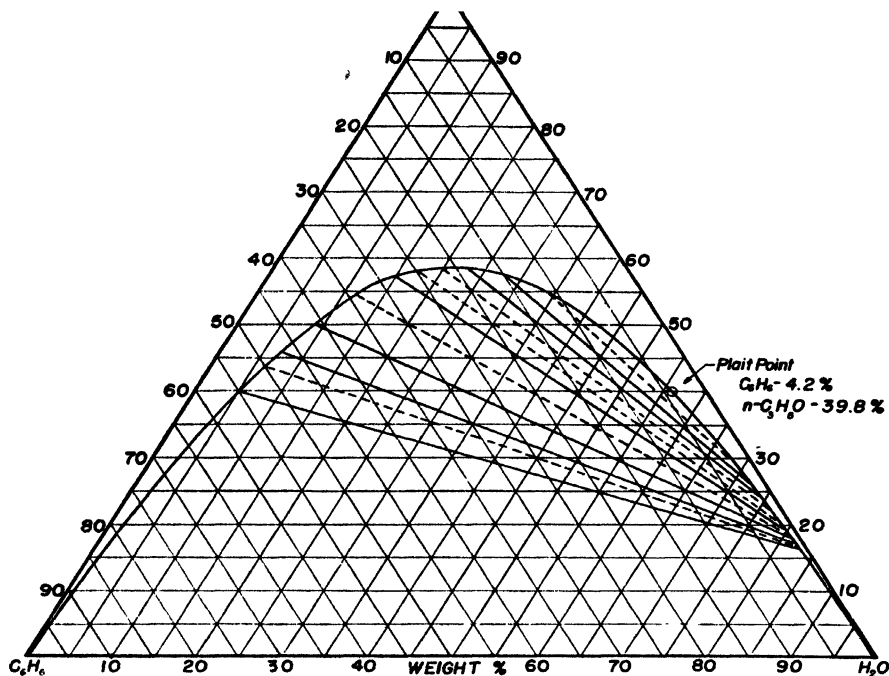
Fig. 2. Binodal curve for the ternary system benzene–1-propanol–water at 20°C. and atmospheric pressure.

TABLE 1

Ternary system carbon tetrachloride–1-propanol–water at 20°C.

CARBON TETRACHLORIDE	1-PROPANOL	REFRACTIVE INDEX (25°C.)	CARBON TETRACHLORIDE	1-PROPANOL	REFRACTIVE INDEX (25°C.)
weight per cent	*weight per cent*		*weight per cent*	*weight per cent*	
0.51	21.1	1.3509	37.3	50.1	1.3969
1.6	26.7	1.3552	40.3	48.6	1.3991
2.4	30.0	1.3578	42.8	47.2	1.4013
6.0	39.6	1.3656	44.5	45.6	1.4022
11.7	48.4	1.3743	52.9	40.8	1.4089
17.6	53.0	1.3810	59.2	35.1	1.4130
23.8	54.0	1.3866	75.4	22.5	1.4275
28.7	53.7	1.3903	89.3	10.1	1.4411
32.0	52.3	1.3928	96.2	3.7	1.4512

TABLE 2

Ternary system benzene–1-propanol–water at 20°C.

BENZENE	1-PROPANOL	REFRACTIVE INDEX (25°C.)	BENZENE	1-PROPANOL	REFRACTIVE INDEX (25°C.)
weight per cent	*weight per cent*		*weight per cent*	*weight per cent*	
0.35	19.3	1.3501	30.3	56.5	1.4124
1.6	28.9	1.3569	45.6	46.1	1.4300
4.2	39.1	1.3678	47.3	45.1	1.4321
8.5	50.7	1.3794	51.0	42.1	1.4364
12.2	56.3	1.3872	60.5	34.9	1.4474
15.1	57.7	1.3928	66.6	29.8	1.4547
18.5	59.0	1.3970	75.6	22.2	1.4654
25.3	58.6	1.4058	83.0	15.8	1.4747
27.4	57.8	1.4085			

All materials used were C.P. purified chemicals. The 1-propanol was dried for one week over calcium chloride and then subjected to three redistillations, a three-ball fractionating column being used. The first and last portions of each distillation were discarded.

The values of the refractive indices of the materials at 20°C. were as follows: benzene, 1.5010; carbon tetrachloride, 1.4604; 1-propanol, 1.3860; water, 1.3330. Refractive indices were taken with an Abbe refractometer with the temperature regulated to within ±0.1°C.

A 2-liter beaker, about two-thirds filled with water, was used as a constant-temperature bath during end-point titrations. A small-sized bath of this type has the advantage of permitting close observation of the sample being titrated. It also allows the sample to be viewed from any desired angle, thus eliminating the necessity of looking directly into the source of illumination. The temperature during titration was controlled to ±0.1°C.

The buret used for titrations was modified by attaching to the tip of it, by means of rubber tubing, a piece of 5-mm. glass tubing about 4–5 in. long. The one end of the glass tubing was drawn to a fine capillary. This attachment allowed constant shaking during titration and gave better control of the titration, since smaller drops formed from the capillary than from the buret. It was found that a small piece of rubber tubing, ¼-in. in length, formed an air-tight stopper for the 2-ounce glass-stoppered bottles which were used in titrating the samples. This piece of tubing was placed just above the capillary which extended into the bottles.

PROCEDURE

In determining a point on the binodal curve, two of the components of a system, one of the non-consolutes and the homogenizer liquid, were mixed in definite weighed amounts. The third component was then added from a buret until the mixture reached the state where the beginning of the formation of two liquid phases was indicated. The quantity of the third component added was then determined gravimetrically. After titration was finished the average sample weighed almost 20 g.

The titrations were carried out at 20°C. Since the samples were not clear at this temperature, they were allowed to warm up and the refractive index was then taken at 25°C.

After the binodal curves were obtained, it was possible to obtain the tie lines by simply making up known mixtures in the two-phase region, allowing them to come to equilibrium at 20°C., and then measuring the refractive index of the top layer. This gave the composition of one layer which, coupled with the overall composition of the mixture, fixed a tie line. From the several tie lines determined experimentally for the systems (table 4), Bachman charts (figure 4) were constructed and more lines were added by interpolation.

For the binary system, appropriate portions of the components were weighed
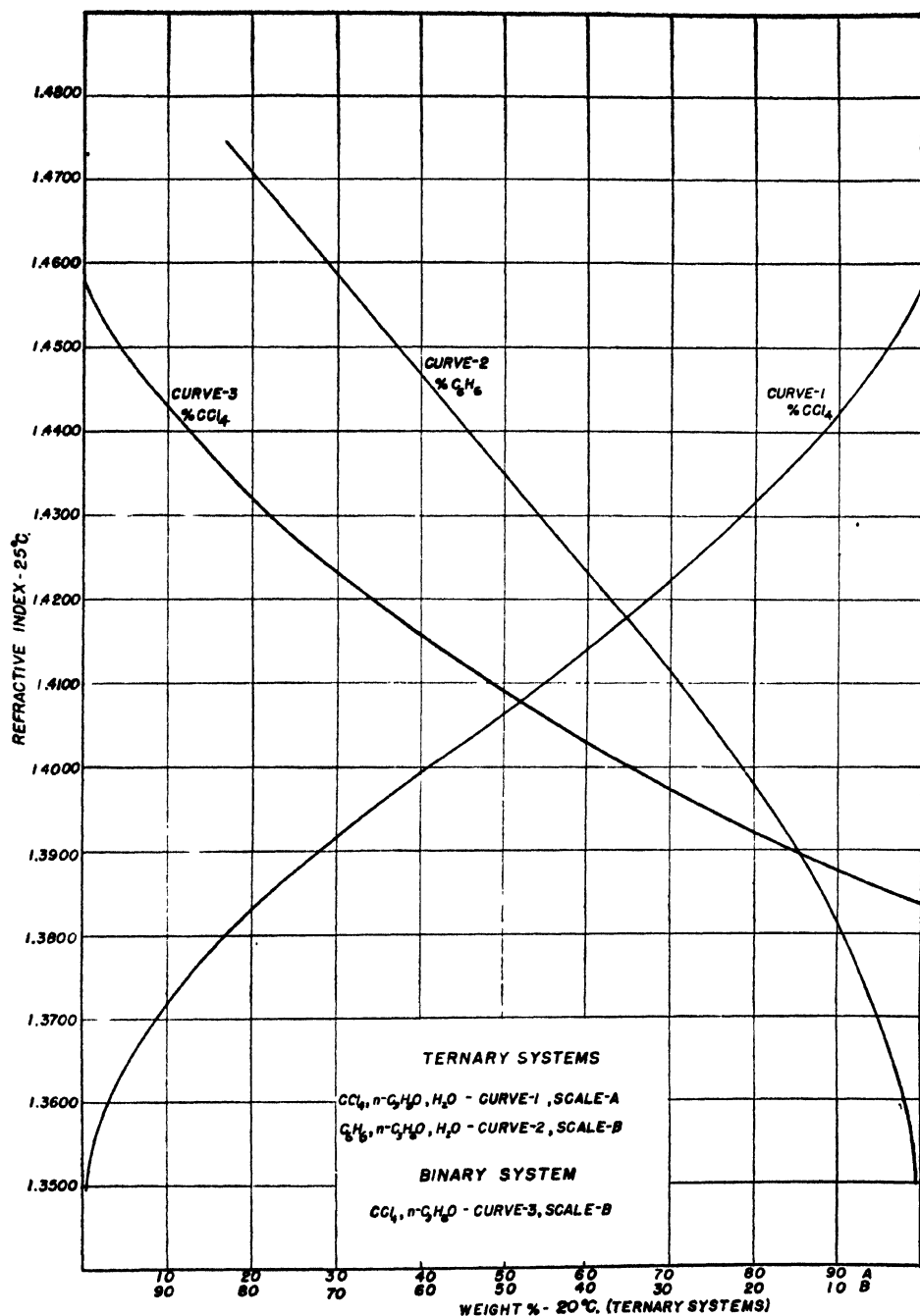
FIG. 3. Graphical representation of refractive-index data. The composition of one of the components of each system is plotted against refractive index. Carbon tetrachloride and benzene are the components for the ternary systems.

361
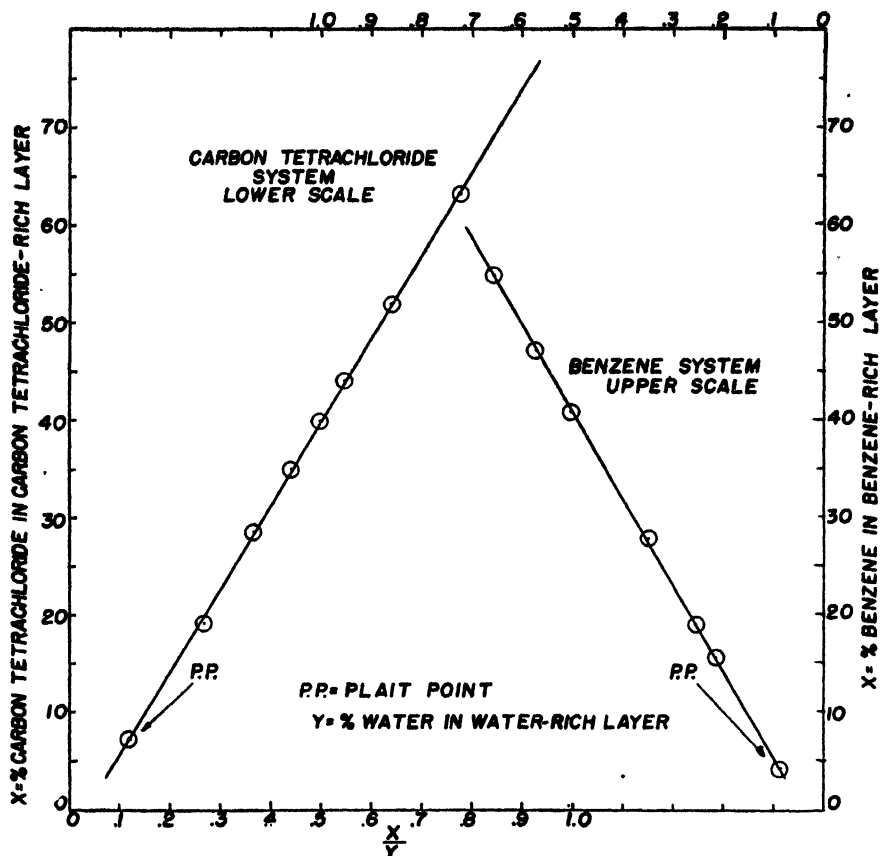
FIG. 4. Bachman diagram for interpolation of tie lines

TABLE 3
Binary system carbon tetrachloride–1-propanol

CARBON TETRACHLORIDE	REFRACTIVE INDEX (25°C.)	CARBON TETRACHLORIDE	REFRACTIVE INDEX (25°C.)
weight per cent		*weight per cent*	
0.0	1.3839	55.8	1.4126
6.0	1.3859	60.2	1.4160
10.1	1.3879	65.6	1.4199
16.3	1.3906	70.4	1.4237
20.9	1.3926	75.1	1.4275
26.0	1.3953	80.0	1.4325
32.6	1.3988	84.9	1.4375
34.8	1.4004	89.7	1.4433
40.8	1.4033	94.6	1.4490
47.9	1.4076	100.0	1.4574
51.8	1.4101		

and mixed and the refractive index measured at 25°C. The total weight of a sample was about 10 g. Table 3 gives the data for this system.

END-POINT CHARACTERISTICS

Since the "cloud point" method was used in the determination of the liquid–liquid equilibrium data, accurate attainment of this end point became of primary importance. There is little material in the literature on the appearance of this point. Bonner (2), Cline and Dunn (3), and Curtis and Titus (4) describe it as the appearance of a haze which becomes opaque on further titration and then separates into two layers. For the two systems investigated in this case, the end point was not found to be such. The appearance of the end point varied with concentration. For small concentrations of one of the non-consolutes (concentration here referring to the final value) up to approximately 1 per cent, the end point was a blue haze which appeared slowly. In spite of the gradual appearance, the end point could still be obtained accurately since, as the end point was approached, a drop of titrant became cloudy immediately upon striking the solution. Therefore it was possible to titrate rapidly until the titrant began to cloud upon entering the solution. It follows that each additional drop cleared more slowly, and when the complete dispersion of a drop became very slow, the end point was near and the blue haze was watched for closely.

As the concentration of one of the non-consolutes increased over the range 1–10 per cent, or it might be said as the concentrations of the non-consolutes approached each other, the appearance of the end point gradually changed to that of a grey mist. The mist appeared much more sharply than did the haze and little indication was given of its approach. For this type of end point, titration could be made rapidly only after familiarity with the end point had been attained. This point, however, was more easily identified than the first.

Above the 10 per cent concentration of one of the non-consolutes, neither the blue haze nor the grey mist appeared. The end point was indicated by a suspension of fine globules of a second layer in the solution. The point was taken at the first permanent, but not dense, suspension. This end point had to be identified with care since, as it was approached, the suspension of globules formed by each additional drop disappeared more slowly and sometimes a suspension which seemed to be permanent actually disappeared after a while. Here again, familiarity with the end point is required to make rapid titrations.

All three kinds of end point actually consisted of a suspension of a second layer, the particles of each type of suspension differing in size. The blue haze was a suspension of extremely fine particles, undetectable with the eye. The grey mist was also a fine suspension but detectable with the eye if observed closely enough. The particles of the third type of suspension were of such a size that reflected light made them plainly visible to the eye.

Further titration past the end point rendered the first and second types opaque. The second formed two layers and eventually cleared, while the first merely remained opaque. The third type formed two layers immediately upon further titration and could be rendered opaque only by agitation.

PLAIT POINTS

The plait points or critical points of the two ternary systems were determined by extrapolation of the lines on the Bachman charts to intersect with the equilibrium curve. The actual procedure is one of trial and error. Its application depends upon the accuracy of the data and how closely the data run to the

TABLE 4

Tie-line data for the system carbon tetrachloride-1-propanol-water at 20°C.

UPPER LAYER		LOWER LAYER	
CCl₄	C₃H₇OH	CCl₄	C₃H₇OH
weight per cent	*weight per cent*	*weight per cent*	*weight per cent*
12.7	49.4	3.6	32.6
19.2*	53.7	2.2	27.6
1.7	24.9	23.0	53.4
0.72*	21.5	28.5	53.6
0.43*	20.2	35.0	51.4
0.38*	19.5	39.8	49.0
0.30*	19.0	44.1	46.4
0.28*	18.7	51.8	41.3
0.26*	18.5	63.2	32.9
0.2	16.9	68.2	28.8
0.2	16.4	75.0	23.0

Tie-line data for the system benzene-1-propanol-water at 20°C.

UPPER LAYER		LOWER LAYER	
C₆H₆	C₃H₇OH	C₆H₆	C₃H₇OH
weight per cent	*weight per cent*	*weight per cent*	*weight per cent*
11.0	55.0	1.9	28.1
15.6*	57.8	1.7	25.3
19.0*	58.6	1.4	23.6
21.6	58.6	1.2	21.2
25.0	58.2	1.1	20.0
27.9*	57.3	1.0	19.2
34.0	54.4	0.9	18.3
40.8*	50.1	0.8	18.1
47.2*	46.3	0.7	17.2
50.0	43.6	0.6	16.7
54.8*	39.8	0.4	16.3

* Experimentally determined values.

plait point. If the data do not fit a straight line closely or are taken over a range removed from the plait point, large errors would probably result in the values at the plait point.

In this case, the data are satisfactory for the use of the method. The procedure is the same as that for obtaining an interpolated tie line, with the special condition in mind that the composition of the two phases must be the

same. Since the approximate location of the point is known from the phase diagram, usually not more than three or four trials are required.

The values obtained here for the ternary systems investigated are as follows:

	per cent by weight			*per cent by weight*
Water.................	56.0		Water.................	52.3
1-Propanol............	39.8		1-Propanol............	40.9
Benzene..............	4.2		Carbon tetrachloride.........	6.8

RESULTS

The carbon tetrachloride ternary system exhibited an interesting characteristic, in that, during the determination of the tie lines, there was a reversal of phase relationships. Table 4 shows that for lower percentages of carbon tetrachloride, the carbon tetrachloride-rich layer is the upper layer while at higher percentages it becomes the lower layer.

With regard to the accuracy of the data, considering the binary system, a composition value is accurate to 0.3 per cent. This figure takes into account the limiting refractive index values of the system (table 3), and also the fact that the Abbe refractometer is readable to ±0.0002. Upon analysis of the ternary systems in the same way, the accuracy of a single composition figure becomes 0.14 per cent and 0.12 per cent as applied to the carbon tetrachloride and the benzene, respectively. These latter figures are average values and include the difference in accuracy of the readings over different ranges of composition. Figure 3 bears out the variation of accuracy in the ternary systems.

SUMMARY

The binodal curves for the two ternary systems benzene–1-propanol–water and carbon tetrachloride–1-propanol–water have been determined at 20°C. Refractive-index data for these systems and for the binary system carbon tetrachloride–1-propanol are presented in tabular form.

Characteristics of end points in "cloud point" titrations are described and a method for determining plait points by the use of Bachman charts is explained.

REFERENCES
(1) BACHMAN, I.: Ind. Eng. Chem., Anal. Ed. **12**, 38 (1940).
(2) BONNER, W. D.: J. Phys. Chem. **14**, 738 (1910).
(3) CLINE, C., AND DUNN, J. W.: Thesis (p. 13), University of Cincinnati, 1933.
(4) CURTIS, H. A., AND TITUS, E. V.: J. Phys. Chem. **19**, 739 (1915).
(5) SMITH, J. C.: Ind. Eng. Chem. **34**, 234 (1943).

PHASE RELATIONSHIPS IN THE SYSTEM AMMONIA–WATER–SODIUM HYDROXIDE

FRED D. AYRES[1]

Research Laboratory, Columbia Chemical Division, Pittsburgh Plate Glass Company, Barberton, Ohio

INTRODUCTION

In purely inorganic ternary systems the formation of two coexistent liquid phases is a phenomenon of relatively rare occurrence. Examples of such layer formation have been found in mixtures of ammonia and water with each of the following salts and alkali hydroxides: potassium carbonate (8, 10), rubidium carbonate (9), cesium carbonate (9), sodium hydroxide (11), potassium hydroxide (11), zinc sulfate (1), potassium phosphate (5), sodium silicate (10), and potassium vanadate (5). Apparently, no other substances thus far have been observed to cause separation of two layers in ammonia–water mixtures, although others probably exist. Of the systems listed above, only those involving the following compounds appear to have been studied quantitatively from the point of view of the phase rule: potassium carbonate (2), potassium phosphate (6), zinc sulfate (3), and potassium hydroxide (7). In the present investigation isotherms of the system ammonia–water–sodium hydroxide were determined in part at 60°, 50°, and 40°C. Attention was centered on the liquid–liquid area at each temperature, and tie lines were determined by analysis of samples of the various conjugate solutions. These phase-rule studies were undertaken in this laboratory as a part of the research program attending the development of a process for the purification of electrolytic caustic liquors by extraction with liquid ammonia.

APPARATUS

Because of the volatility of the ammonia, a closed system was necessary for the equilibrium mixtures. For this purpose a Pyrex bomb[2], capable of withstanding an internal pressure of about 600 pounds per square inch, was used as a containing vessel. The glass provided easy visibility of the mixtures at all times, a feature which more than compensated for its fragility. Before use a globe was always tested hydrostatically to 600 pounds pressure. During the progress of some experiments at 80°C., which were discontinued, two globes actually failed in service, one at a pressure of 720 pounds, the other at a somewhat lower pressure. However, the explosions were expected; no serious damage was done in either case and the apparatus was designed so that the globes could be replaced easily and quickly. In the experiments at 60°C. or below, where the pressures never exceeded 400 pounds per square inch, no breakages occurred.

The apparatus was constructed essentially as shown in the schematic dia-

---

[1] Present address: Reed College, Portland, Oregon.
[2] A standard Crouse-Hinds EV-10 explosion-resisting globe of about 750 ml. capacity.
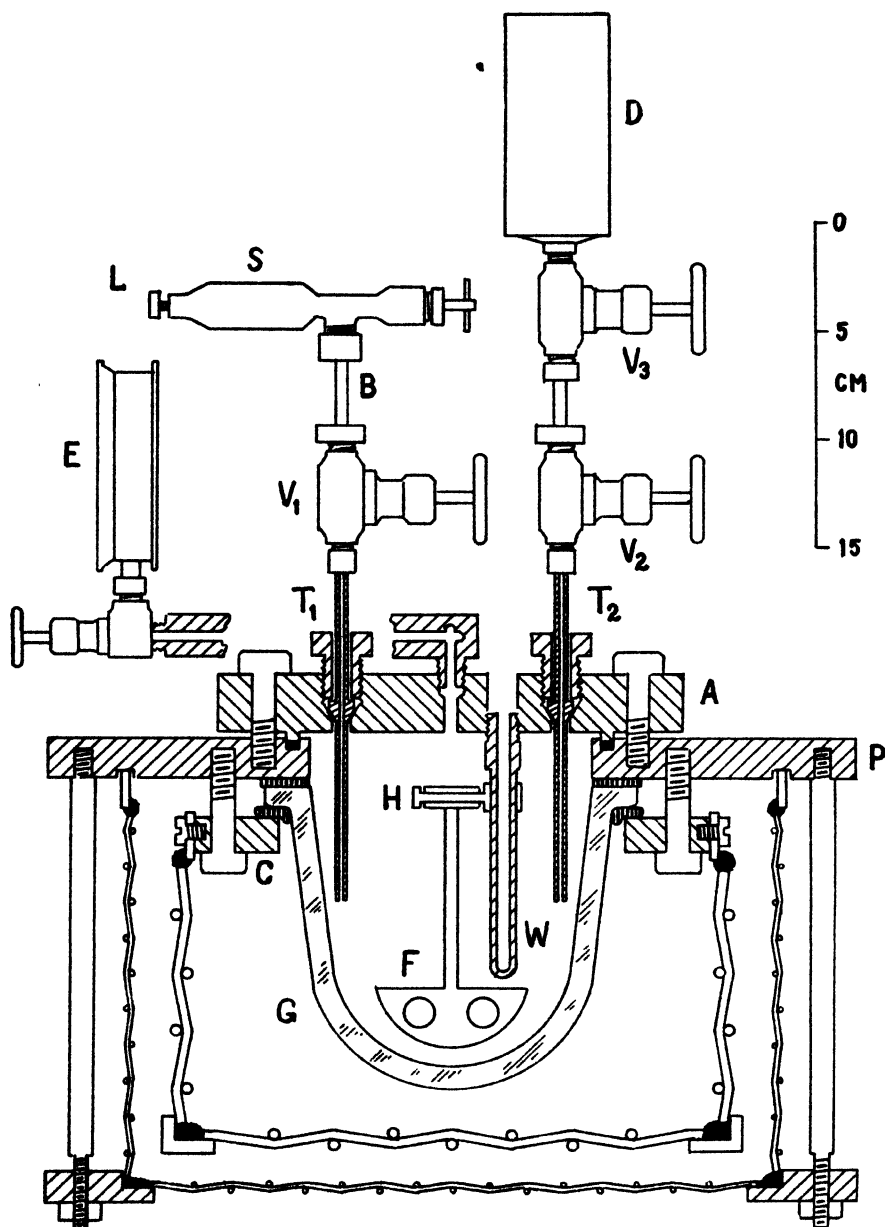
FIG. 1. Schematic diagram showing the Pyrex globe and its attachments. The scale at the right gives a rough idea of the size of the apparatus. In general the horizontal dimensions are exaggerated by about 25 per cent.

gram (figure 1). Mild steel was used throughout unless otherwise indicated. The Pyrex globe, G, was permanently clamped to the circular plate, P. The gasket between the globe and the plate was cut from a sheet of Garlock No. 907 packing, $\frac{1}{32}$ in. thick. To help protect the glass from excessive strains, three thicknesses of gasket material were interposed between the flange of the globe and the clamping ring, C. The cover plate, A, provided access to the interior of the bomb. A recessed lead gasket prevented leakage of ammonia. To reduce the hazard of flying glass, the bomb was surrounded by two protective wire screens as shown. Samples of the liquid phases were removed through tubes T_1 and T_2, which were seated in the lid, A, by means of cone joints. Valves V_1 and V_2 were attached permanently to the sampling tubes. They were standard $\frac{1}{4}$-in., iron, No. 1728 Lunkenheimer needle valves which were modified on the low-pressure side to receive the lower ends of the sample bomb connectors. In each case this modification consisted in first boring out the $\frac{1}{8}$-in. pipe threads and then machining and threading the resulting hole to form a seat for a cone joint similar to the ones in the lid. The upper ends of the connectors were attached, again by means of cone joints, to the sample bombs themselves. One of these two bombs is shown attached by means of its connector, B, to the valve V_1. (The second sample bomb is not shown but is replaced by the cylinder, D, which was used for adding liquid ammonia to the bomb. This procedure is described later.) The pressure gage, E, was of steel construction with a scale reading to 1000 pounds per square inch (±3 pounds). Temperatures were read to 0.1°C. by means of a thermometer inserted into the well, W.

The entire bomb assembly was suspended in a cradle by means of two stub shafts (not shown), which were fastened to the edges of the plate, P, at diametrically opposite positions. The common axis of these two shafts was perpendicular to the plane of the paper in figure 1. Stirring was accomplished by means of a motor-driven mechanism which swung the bomb mount back and forth in its cradle through an arc of about 30 degrees. Agitation was made more effective by the heavy steel pendulum, F, which was mounted on the thermometer well, W. In the figure, both the pendulum and the thermometer well are represented out of their correct relative positions in order to show their construction more clearly. Actually, the thermometer well should be visualized as being located below the plane of the figure and on the line of sight through the vertical axis of the Pyrex globe. So visualized, the pendulum support, H, would project perpendicularly upward through the plane of the paper. In other words, the pendulum was mounted so that its axis, H, was parallel to the common axis of the two stub shafts of the bomb support. As the bomb swung back and forth the pendulum, because of its inertia, swept through the mixtures, producing a vigorous stirring action. Short lengths of thin spring steel attached to each side of the pendulum bob prevented it from striking the glass at the ends of its · swings.

The capacity of each of the sample bombs was approximately 10 ml. The inlet needle valves were of conventional design. A mixture of shredded lead and graphite was used for packing. There seemed to be little trouble from contami-

nation of one sample by portions of a previous sample lodged in the threads of the needle valves.   This was evident from the fact that the initial weight of an empty bomb seldom differed from the final weight after filling, emptying, rinsing, and drying by more than 3 to 5 mg.   The bombs weighed about 175 g. each when empty.

The bomb assembly was mounted in an air thermostat whose temperature was automatically controlled to within 0.2 to 0.3°C. of the desired value.   The front and sides of the thermostat were provided with safety-glass windows.   The entire top was constructed from layers of thin asbestos sheet.   This purposely flimsy construction of the top allowed the force of an explosion to dissipate itself ceilingward rather than out through the safety-glass sides.   Sliding panels in the front of the thermostat allowed access to openings through which the arms of the operator could be inserted during the sampling operations (with adequate protection).

MATERIALS

In all the experiments commercial anhydrous liquid ammonia was used without further purification.   Save for a few experiments, the sodium hydroxide was added in the form of a 50 per cent solution and was siphoned as needed from a stock supply protected from the air by a soda lime tube.   This solution contained the following in amounts greater than 0.1 per cent: sodium hydroxide, 50.2 per cent; sodium carbonate, 0.35 per cent; sodium chloride, 0.25 per cent.   In a few runs, where mixtures containing a relatively high percentage of sodium hydroxide were necessary, solid sodium hydroxide was used.   The solid contained 98.6 per cent sodium hydroxide and the following impurities in amounts greater than 0.1 per cent: sodium carbonate, 0.5 per cent; sodium chloride, 0.4 per cent.

EXPERIMENTAL

Preparation of the equilibrium mixtures

After introduction of weighed amounts of sodium hydroxide (usually as 50 per cent solution) and water, the major portion of the air was removed from the bomb by attaching to an aspirator pump for a few seconds.   Then anhydrous ammonia was added as liquid from a small steel cylinder (D, figure 1) specially constructed for the purpose.[3]   Previously the necessary quantity of ammonia and no more had been transferred to the small cylinder from the stock supply in the commercial cylinder.   To introduce this ammonia into the bomb, the cylinder D was attached as shown in figure 1.   The sampling valve, V_2, was next opened a fraction of a turn; then the valve, V_3, on the ammonia cylinder was opened cautiously.   The nearly closed lower valve served to slow down the initial rush of ammonia into the bomb.   The last portions of liquid were driven from the cylinder by warming it gently.   The cylinder valve was next closed and, with

---

[3] This cylinder was constructed by welding two ends into a length of seamless steel tubing and attaching a ½-in. stainless-steel needle valve.   The cylinder could be fitted to either of the two sampling valves by means of a cone-joint connector.   Its capacity was approximately 110 g. of ammonia, although it never was filled completely with *liquid*.

the lower valve still open, the two valves, the connection between them, and the region of the cone-joint seat in the lid all were warmed to about 60–70°C. with a burner in order to volatilize and drive into the bomb any liquid remaining inside the sampling system. Finally V_2 was closed and the cylinder removed. The difference in the weights of the cylinder before and after gave the weight of the ammonia introduced save for the amount of vapor lost to the air from the space between the two valves when the cylinder was disconnected and removed. The volume of this space was known and a sufficiently accurate correction could be applied for the ammonia so lost (about 0.05 g.). It was found desirable to have the bomb and its contents preheated to about 40–50°C. before the anhydrous ammonia was added, particularly if the sodium hydroxide solution in the bomb contained a relatively high percentage of sodium hydroxide. Otherwise large masses of solid formed which were extremely difficult to dissolve. (It might be mentioned that ammonia was transferred from the stock supply to the small cylinder by a procedure much like that described above. Chilling the small cylinder caused liquid to flow into it very readily.) Whenever it was necessary to calculate the overall composition of the complex (condensed phases only), a correction was applied for the weight of ammonia in the vapor phase in the Pyrex globe. The volume of the vapor phase was determined by noting the position of the surface of the liquid with reference to calibration marks on the outside of the globe. It was assumed that the partial pressure of the ammonia was equal to the total pressure (gage reading plus atmospheric pressure). The specific volume of ammonia at the given temperature and pressure was obtained from standard tables.

As might be expected, leaks occurred during several of the runs. A piece of moist litmus paper placed inside the thermostat provided a simple and sensitive test. If leakage was serious and could not be stopped immediately, the run was abandoned and the source corrected. Leakage past the gasket between the globe and the plate, P, caused practically no trouble, which was somewhat contrary to expectations. However, it was evident that traces of ammonia were escaping from the bomb almost continually, because the litmus nearly always would show at least a faint blue color after some 30 sec. in the thermostat.

Agitation was continued at equilibrium temperature (±0.3°C.) for at least 2 hr. if only liquid phases were present, or longer if solids were present. Experiment showed that about 4 hr. constituted a sufficient length of time in the latter case. The stirring was such that no liquid or solid material was splashed up onto the lid or sides of the bomb. No liquid was observed to condense on the lid or its attachments. At no time before the sampling operations did the lower ends of the sampling tubes come into contact with the mixture in the lower part of the bomb. Many of the equilibrium mixtures consisted of two liquid phases and a solid phase ($NaOH \cdot H_2O$). In these cases the composition of the complex was chosen so that, starting with no solid present at a temperature somewhat above the desired equilibrium temperature and cooling slowly, crystals began to separate about 1°C. before this temperature was reached. The amount of solid present at equilibrium was thus quite small and did not interfere with the re-

moval of liquid samples. Under these conditions the crystals slowly separated out as very thin and slightly iridescent plates up to 2 mm. across and were kept swirling through the mixture by the stirring action of the pendulum. There seemed to be little tendency for supercooling to occur. .

Removal and analysis of samples

The sampling manipulations were accomplished by reaching in through the small opened panels in the front of the thermostat. This entailed loss of some warm air through the opening, but during the complete process, which required about 5 min., the temperature in the bomb did not change by more than 0.3–0.4°C. First, the evacuated and weighed sample bombs were attached to the sampling valves by means of their connectors. Then the bomb assembly was tilted in its bearings and clamped in such a position that the lower end of the forward sampling tube was submerged to a depth of 3 or 4 mm. below the surface of the upper liquid layer. The inlet valve on the sample bomb was opened, then the ⅛-in. valve on the main bomb. The pressure of the ammonia vapor immediately forced liquid up into the sample bomb. The latter filled more readily if the portion below the letter S had been chilled slightly with a wet cold cloth immediately before opening the valves. Finally both valves were closed. The bomb was then tilted in the opposite direction until the lower end of the rear sampling tube was well below the interface between the two layers, and a sample of the lower liquid layer was removed in the manner just described. In cases where only one liquid phase was present, two samples of this phase could be taken for check, one in each bomb. After removal of the sample bombs, the side neck of each was washed out thoroughly with water, alcohol, and ether, and then dried with a stream of compressed air. Each bomb could be detached from its connector at the joint shown just above the letter B in figure 1.

After one of the bombs had been weighed, a 15-cm. length of rubber tubing was attached to its side neck and the contents were allowed to bubble slowly into 200.0 ml. (±0.05 ml.) of standard 2 N hydrochloric acid solution. Then the needle screw, L, was removed from the sample bomb and 10-ml. portions of water washed through the latter and into the acid solution until the rinsings did not affect litmus. The resulting solution was made up to 500 ml. in a volumetric flask and aliquot portions removed for analysis. Ammonia was determined by distillation after adding an excess of sodium hydroxide to one of the portions. With another portion, total alkalinity was determined by titration of the acid solution with standard base. The percentage of sodium hydroxide was then calculated by difference. The effect on the analysis of the sodium carbonate present in the mixtures was smaller than the unavoidable errors of the sampling process and was neglected.

After completion of a run, the Pyrex bomb was conveniently emptied by tilting it nearly horizontally and conducting off the liquid contents through a length of small copper tubing attached to the forward sampling valve. The outer end of this tubing was fitted with a needle valve and an extension which dipped into a liter or two of a mixture of cracked ice and water. Only about 5 ml. of liquid

then remained in the bomb, and the ammonia could be allowed to evaporate from this without chilling the Pyrex bomb excessively. To prevent corrosion,

TABLE 1

Equilibrium mixtures involving two liquid phases

COMPOSITIONS OF SAMPLES (WEIGHT PER CENT)				PRESSURE (POUNDS PER SQUARE INCH)	PHASES PRESENT
Upper layer		Lower layer			
NH₃	NaOH	NH₃	NaOH		
60°C.					
79.4	1.4	7.5	51.5	318	Vapor, two liquids, NaOH·H₂O
78.7	1.4	7.9	50.8	318	
78.9	1.5	8.4	50.5	317	
79.4	1.1	7.2	51.2	317	
77.5	1.7	8.0	50.0	310	
73.3	2.3	9.5	47.2	298	
67.0	4.3	12.3	42.9	290	
61.8	6.8	15.0	39.4	275	
54.0	10.7	19.8	35.2	265	Vapor, two liquids
46.9	14.4	24.2	30.9	263	
43.4	17.1	26.2	29.2	261	
40.5	18.9	28.2	27.6	262	
40.9	18.6	28.7	27.5	262	
50°C.					
70.1	3.5	11.2	44.9	234	Vapor, two liquids, NaOH·H₂O
70.0	3.1	11.8	44.7	236	
69.7	4.0	11.1	44.9	237	
69.8	3.1	11.3	44.7	236	
70.2	3.5	11.6	44.9	235	
70.0	3.3	11.3	44.9	230	
67.2	4.5	12.3	42.9	233	
59.4	7.5	15.8	38.7	220	
54.1	10.2	19.2	35.5	212	Vapor, two liquids
45.4	15.6	24.8	30.2	207	
41.9	18.0	29.2	27.3	205	
40°C.					
59.4	7.9	15.9	38.4	165	Vapor, two liquids, NaOH·H₂O
56.6	9.5	18.6	35.4	166	
49.2	13.0	21.8	32.6	155	Vapor, two liquids
40.8	19.1	28.5	27.2	153	
35°C.					
50.9	13.0	20.7	35.3	138	Vapor, two liquids, NaOH·H₂O

the bomb and its attachments were cleaned and dried after each run. The sampling valves particularly were washed with hot water and the interiors steamed out and dried with a stream of compressed air.

RESULTS

The experimental results are collected in tables 1, 2, and 3. All those mixtures in which two liquid phases occurred are represented in table 1; those in table 2 produced only one liquid phase. The pressure values are included to give an idea of the pressures withstood by the Pyrex globe. In table 2, the blanks

TABLE 2

Equilibrium mixtures involving only one liquid phase

COMPOSITION OF COMPLEX (WEIGHT PER CENT)		COMPOSITIONS OF SAMPLES (WEIGHT PER CENT)						PRESSURE (POUNDS PER SQUARE INCH)	PHASES PRESENT
		Sample No. 1		Sample No. 2		Average			
NH₃	NaOH	NH₃	NaOH	NH₃	NaOH	NH₃	NaOH		

NH₃	NaOH	NH₃	NaOH	NH₃	NaOH	NH₃	NaOH		
				60°C.					
71.2	18.2	93.3	0.2	92.9	0.6	93.1	0.4	367	Vapor, one liquid, NaOH·H₂O
75.0	20.1			96.9	0.0	96.9	0.0	372	Vapor, liquid, NaOH, NaOH·H₂O
74.1	21.1	97.0	0.1			97.0	0.1	375	
55.0	34.8	96.3	0.0			96.3	0.0	373	
				50°C.					
72.2	22.2	96.3	0.0	96.4	0.0	96.4	0.0	301	Vapor, liquid, NaOH, NaOH·H₂O
71.7	14.2	90.1	0.0	90.0	0.0	90.1	0.0	277	Vapor, liquid, NaOH·H₂O

TABLE 3

Liquid–solid equilibria at 25°C.

LIQUID PHASE (WEIGHT PER CENT)		SOLID PHASE (WEIGHT PER CENT)[*]	
NH₃	NaOH	NaOH	Na₂CO₃
60.5	6.6	60.4	0.2
56.7	8.3	65.7	1.2
45.1	15.0	63.1	2.7
24.5	29.1	63.9	0.6
3.9	48.4	64.1	1.2

[*] By direct analysis.

occurring at the 60°C. temperature represent samples accidentally lost. The phase diagram (figure 2) is plotted from the data at 60°C. The diagrams for 50°C. and 40°C. are similar but are not shown. Only the liquid–liquid area in figure 2 was determined in any detail. The probable appearance of the remainder of the diagram is represented by dotted lines. The solubility of sodium hydroxide in pure ammonia was less than could be detected and was assumed to be substantially zero. The value for the solubility of sodium hydroxide in water at 60°C. (point *D*) was taken from the literature (4). Table 3 shows the results of a series of runs made at 25°C., where the region of two liquid phases

apparently had disappeared completely. No trace of a second liquid phase was observed in any of the mixtures. In each of these experiments, anhydrous ammonia was added *slowly* to a sodium hydroxide solution of given concentration at 25°C., the addition being stopped as soon as crystals barely began to appear. These crystals had the same appearance as those obtained at the higher temperatures in equilibrium with two liquid phases. After about 5 hr. at 25°C. a sample of the liquid phase was taken. Then, after removal of the remainder of the liquid phase from the bomb in the manner described in the section above, an attempt was made to determine the composition of the crystals by direct anal-
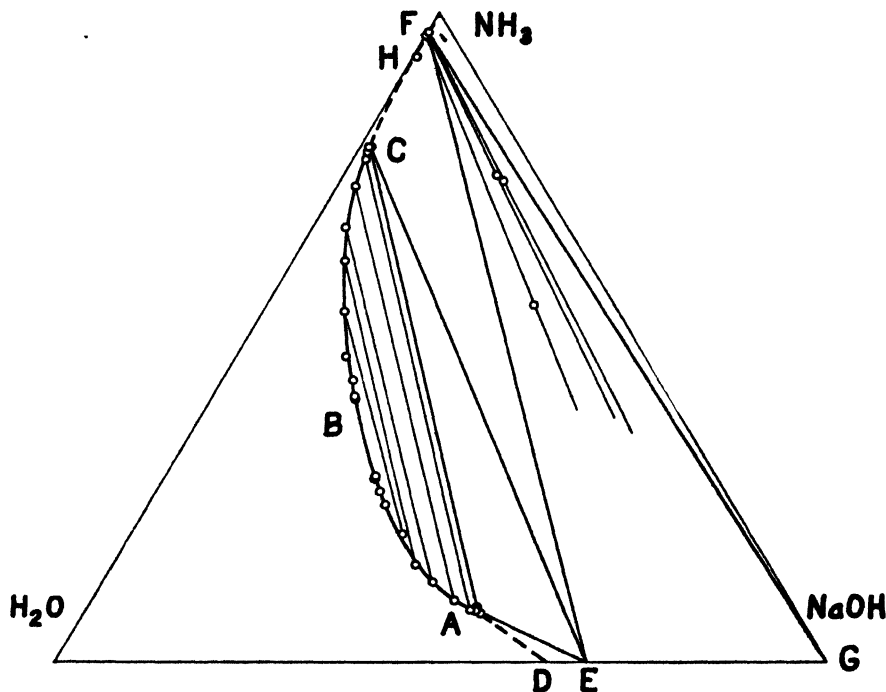
FIG. 2. Isotherm at 60°C.

ysis. Such a procedure admittedly was subject to large error, principally because of the difficulty of separating the solid completely from adhering solution. However, the Schreinemakers method was not applicable in this case because the quantity of solid was far too small. The point representing the composition of the complex would have been very nearly coincident with that for the liquid phase and extrapolation would have been impossible. By working with all possible speed, practically all the crystalline solid (about 1 to 2 g.) was removed from the bomb as soon as the lid was taken off. This sample was pressed between several successive pads of fresh filter paper, the final sandwich being pounded vigorously with a hammer. The resulting fairly dry powder was quickly placed in a stoppered weighing bottle. Table 3 shows the percentages of sodium hydroxide and sodium carbonate found in each of these samples.

DISCUSSION

The phase diagram (figure 2) shows a liquid–liquid area, ABC, adjacent to the region ACE, the latter representing monohydrate and vapor in equilibrium with the two solutions of constant compositions A and C. Points on curve CHF represent ammonia-rich solutions in equilibrium with monohydrate and vapor, while DA is a similar curve for solutions containing relatively high percentages of sodium hydroxide. Any mixture whose overall composition falls within the triangle EFG separates into anhydrous sodium hydroxide, monohydrate, vapor, and a liquid phase of constant composition, F. It should be noted that the point F cannot fall on the H_2O–NH_3 line, although it appears to in the diagram because the solubility of sodium hydroxide in the F phase was too small to be determined. The portion of the curve extending from F to the apex of the triangle represents ammonia-rich solutions in equilibrium with anhydrous sodium hydroxide and vapor. The position of the binodal curve changes little as the temperature decreases but it rapidly becomes shorter as the two isothermally invariant points at its extremities approach each other. The area of the liquid–liquid region correspondingly decreases. Table 3 shows that, by the time the temperature has fallen to 25°C., this area has disappeared completely, being replaced by one in which a single liquid phase is in equilibrium with a solid phase, presumably $NaOH \cdot H_2O$. Although the solid phase data of this table are only approximate, it is at least clear that the solid can be no higher hydrate than the monohydrate. The dihydrate contains only 52.7 per cent sodium hydroxide. In the liquid–liquid region, the tie lines for one isotherm are very nearly parallel to each other and to those of the other isotherms, a fact which is more apparent if the data for the other temperatures are plotted for comparison.

For the experiment represented by point H a mixture was prepared by adding anhydrous sodium hydroxide, water, and anhydrous ammonia to the bomb in the order named. A lumpy mixture resulted and it is doubtful whether the liquid phase ever attained complete equilibrium with all the solid. Consequently no tie line is drawn in figure 2 for this experiment, although point H itself is retained because this point would still lie somewhere on the solubility curve. In a similar experiment at 50°C.[4], the necessity for any large-scale conversion of one solid phase into another in reaching equilibrium was obviated by introducing solid monohydrate into the bomb initially and then adding a mixture of 90 per cent ammonia and 10 per cent water from the small ammonia cylinder. In this experiment at 50°C., the Schreinemakers procedure definitely indicated that the solid phase was monohydrate. Since the monohydrate is stable over the range 50–60°C., the location of the point E in figure 2 is, then, based partly on the data at 50°C. It was intended to make additional runs at each of the various temperatures, but the pressing nature of other work made this impossible.

It is believed that, save for one or two points, the experimental errors were not serious enough to shift the points by more than two units of percentage from their true positions on the diagram. The sampling operations probably were

[4] The second row under 50°C. in table 2.

the most fruitful source of errors. At best, the removal of samples from a system such as this is beset with difficulties. The method chosen was actually a compromise between several factors and involved at least the following errors: (1) Ammonia vapor was initially present in the sampling tubes and was swept into the bomb where it appeared as part of the liquid sample. (2) In the case of lower-layer samples a very small quantity of the upper layer always entered the lower end of the sampling tube before the latter passed through the interface and into the lower layer. This quantity was subsequently carried into the sample bomb along with the sample of the lower layer. (3) When the first sample was withdrawn the total volume of the vapor phase increased by about 10 ml. and ammonia vapor escaped from the liquid phases to occupy this space, thus affecting the composition of the second sample. To minimize this error, upper-layer samples were always removed first. (4) When the first portions of liquid entered one of the sample tubes a certain amount of ammonia must have flashed off into the evacuated sample bomb from this liquid. The effect of any one of the first three errors was calculated to be not greater than 0.3 per cent in any case. No such estimation was possible in the case of the fourth, but it was assumed that the main portion of liquid flowing into the sample bomb would wash in any initial portion whose composition was altered by the initial flash-off of ammonia. At any rate, serious errors of this type would be expected to cause a scattering of the experimental points much worse than was actually observed. Occasionally one or both the sample bombs failed to fill properly, either because of development of back pressure or through formation of plugs by crystallization of solids in the tubes. The latter effect was, no doubt, induced by flash-off of ammonia and the sudden cooling resulting. Lower-layer samples, with their high sodium hydroxide content, were particularly apt to cause plugging. Such occurrences could be detected by large deficiencies in the weights of the samples. These runs were discarded.

SUMMARY

A Pyrex apparatus suitable for phase-rule investigations up to about 400 pounds per square inch has been constructed. The major portions of the isotherms at 60° and 50°C. have been determined for the system ammonia–water–sodium hydroxide. Less complete data are given for 40°, 35°, and 25°C.

The writer is indebted to Dr. Irving E. Muskat for the adaptation of the Pyrex globe to the present experiments and for the design of much of the apparatus. Dr. W. F. Waldeck offered numerous useful suggestions regarding the sampling technique. Credit also should be given to Mr. Leavitt Gard of the Analytical Department of this laboratory for his work in analyzing all the samples.

REFERENCES

(1) ANDRÉ, G.: Compt. rend. **100**, 241 (1885).
(2) APPLEBY, M. P., AND LEISHMAN, MARGARET: J. Chem. Soc. **1932**, 1603.
(3) APPLEBY, M. P., AND WINDRIDGE, MARK E. D.: J. Chem. Soc. **1932**, 1608.
(4) *International Critical Tables*, 1st edition, Vol. IV, p. 235. McGraw-Hill Book Co., Inc., New York (1928).

(5) JÄNECKE, ERNST: Z. Elektrochem. **33**, 518 (1927).
(6) JÄNECKE, ERNST: Z. physik. Chem. **127**, 80 (1927).
(7) JÄNECKE, ERNST: Z. Elektrochem. **39**, 682 (1933).
(8) NEWTH, G. S.: J. Chem. Soc. **77**, 775 (1900).
(9) PAULY, H.: Ber. **56B**, 1454 (1923).
(10) PROCTOR, B. S.: Chem. News **9**, 25 (1864).
(11) WEITZ, ERNST, AND HEUBAUM, U.: Ber. **66B**, 790 (1933).

THE CHANGE OF SURFACE TENSION WITH TIME. II

THE SURFACE TENSION OF SAPONIN SOLUTIONS

SYDNEY ROSS[1]

Department of Chemistry, Stanford University, California

INTRODUCTION

The final (static) surface tension of a pure liquid is reached in less than 0.005 sec. and quite probably in 10^{-9} sec. (4). This minute period of time is required for reorientation of the surface molecules to reduce the surface free energy to its minimum value. For solutions the time required for the surface tension of a new stationary surface of solution to pass 68 per cent of its way from the water or dynamic value to the static value has been calculated on the basis of the diffusion of the solute molecules (4) and found to be generally less than 1 sec.

Experimental observations indicate that even for simple organic molecules the actual times taken are greater than predicted from considerations of diffusion alone (11). For colloidal substances the surface-tension values continue to diminish with time (1, 3, 13, 14, 15, 17) over an interval which is one thousand times or more that required by diffusion alone (6, 16). This extreme difference is more than the probable error of the calculations (though they are necessarily approximate) and argues the operation of some other mechanism. A qualitative explanation has been proposed (16) for sodium cetyl sulfate and sodium lauryl sulfate. The slow rate of fall of the surface tension is considered as due principally to an electric double layer, formed by the solute molecules at the surface, which retards the further diffusion of ions into the surface. This explanation cannot be extended, however, to cover a similar slow rate of fall of surface tension observed in saponin solutions (5), which are regarded as non-electrolytic (8, page 657).

In the present paper an explanation is attempted for saponin solutions, based on a treatment of data that are already available. While no generality is claimed for the present hypothesis, it may be significant that even in those *ionic* solutions where abnormal periods of time are required for the attainment of static surface

tension, a pellicle is formed upon the surface (12) when it is compressed. A pellicle has been shown to form upon dilute solutions of lauryl sulfonic acid where time effects are prominent, whereas *both* are absent in more concentrated solutions (13). The formation of solid surface films in saponin solutions is a well-known phenomenon. Inasmuch as the present hypothesis postulates a surface reaction in saponin solutions as the cause of the abnormal surface tension, the presence of the solid surface films is well explained. If the same hypothesis is capable of extension to ionic solutions, then the existence of a pellicle would be an argument in favor of its validity.

TIME REQUIRED FOR DIFFUSION

Two theories of diffusion to the surface permit the calculation of the time required to reach a static value of surface tension. Few substances illustrate better the dichotomy of those theories than does saponin.

On the basis of the equation of Doss (6), the time necessary to saturate half the surface with saponin is 2 sec. for a solution of concentration 0.05 g. per liter.

Before the equation of Bond and Puls (4) can be used, the variation of static surface tension with bulk concentration, as expressed for example by an equation of the type first proposed by Szyszkowski (19), must be known. When Szyszkowski's equation is applied to data for saponin, an approximate fit—and only for the more dilute solutions—is obtained. That is sufficient, however, as only an order of magnitude is expected in the answer. With this *caveat* the Szyszkowski equation for the data of Boutaric and Berthier (5) on saponin solutions is given:

$$\gamma_{H_2O} - \bar{\gamma} = 0.161\gamma_{H_2O} \log\left(1 + \frac{\bar{c}}{2.5 \times 10^{-4}}\right) \quad (1)$$

where $\bar{\gamma}$ is the static surface tension and $\bar{c}$ is the bulk concentration.

In the derivation of this equation the molecular weight of saponin is taken as 732.5, the value given by Tschesche (20) for the commonest saponin, gysophila saponin.

The agreement of equation 1 with the observed data is ±6 per cent, as shown by the following comparison:

$\bar{c}$ (in grams per liter)....	0.050	0.125	0.275	0.300	0.375
$\bar{\gamma}$ (calculated).........	55.8	51.2	47.3	46.8	45.7
$\bar{\gamma}$ (observed)	52.3	50.4	48.1	47.4	47.0

When the constants in Szyszkowski's equation and a value for the diffusion constant of saponin of 2.93×10^{-6} cm.^{2} per second are used, the equation of Bond and Puls gives a result of $3\frac{1}{2}$ hr. for the surface tension of a new, stationary surface of a saponin solution to pass 68 per cent of its way from its dynamic value to its final static surface tension.

It has been pointed out, however, in the first paper of this series (18) that the agreement, in order of magnitude, between the actual time required and that predicted by the equation of Bond and Puls is not necessarily a proof that diffu-

sion to the surface is the functioning mechanism. The arguments there advanced cast the greater share of probability on the value of a few seconds as correct for the time required for saponin to diffuse to the surface.

DYNAMIC SURFACE TENSION

The data of Boutaric and Berthier (5) are employed in the development of the present argument. A du Noüy tensiometer was used to measure the variation of surface tension with time for different concentrations of saponin at a pH of 4.16. The use of the ring method has been criticized (3) because of the local disturbance of the surface by the removal of the ring; however, the tests of Nutting, Long, and Harkins (16) on aged surfaces indicate that the most violent motion of the ring on the surface does not introduce a variation of more than 1 per cent.

The time required for a single determination by the ring method, although only a matter of seconds, is still too long to permit the observation of a dynamic surface tension. It has already been indicated that diffusion and adsorption of saponin at the surface take place within a few seconds and the true dynamic surface tension exists only instantaneously. This is borne out experimentally by measurements of dynamic surface tension (2, 9, 17). At zero age of surface the surface contains no higher concentration than does the bulk. For low concentrations of the bulk liquid, the tension at such a surface may be presumed to differ only slightly from that of pure water. For a certain solution of saponin Lord Rayleigh (17) obtained data by the vibrating jet method; his data were later calculated by Freundlich (8, page 534) with the following results: dynamic surface tension = 71 dynes per centimeter; static surface tension = 51 dynes per centimeter.

By extrapolation of an empirical equation Boutaric and Berthier (5) obtain the surface-tension value "at zero time". The values thus obtained (table 1, below) are about 10 dynes per centimeter less than the value for pure water and hence cannot be true dynamic surface tensions. It is no mere graphical error in the extrapolation that reduces the zero time value by this amount; the abscissae of the graph would have to have a value for time as low as −20 min. for γ = 72 dynes per centimeter. This is too great to make it reasonable that the same process operates continuously in lowering the surface tension from its true dynamic value. It is necessary to assume that two mechanisms are at work: the first, taking place instantaneously after the formation of the surface, lowers the surface tension as a result of diffusion and adsorption at the surface; the second proceeds at a much slower rate and continues to cause a lowering of the surface tension over a long time interval. In figure 1 the curve AB (exaggerated on the time scale) represents the first process and the curve BC of greatly smaller slope represents the succeeding one. The extrapolation of the curve BC meets the vertical axis at the zero time value (γ_0) recorded by Boutaric and Berthier. This value is perhaps best termed a semi-dynamic surface tension.

It is supposed that the initial rapid change of the surface tension (portion

AB of figure 1) is due to adsorption. The conditions under which surface forces act at any boundary are always similar; it is, therefore, permissible to apply the classical parabolic adsorption isotherm in this place, to obtain a value
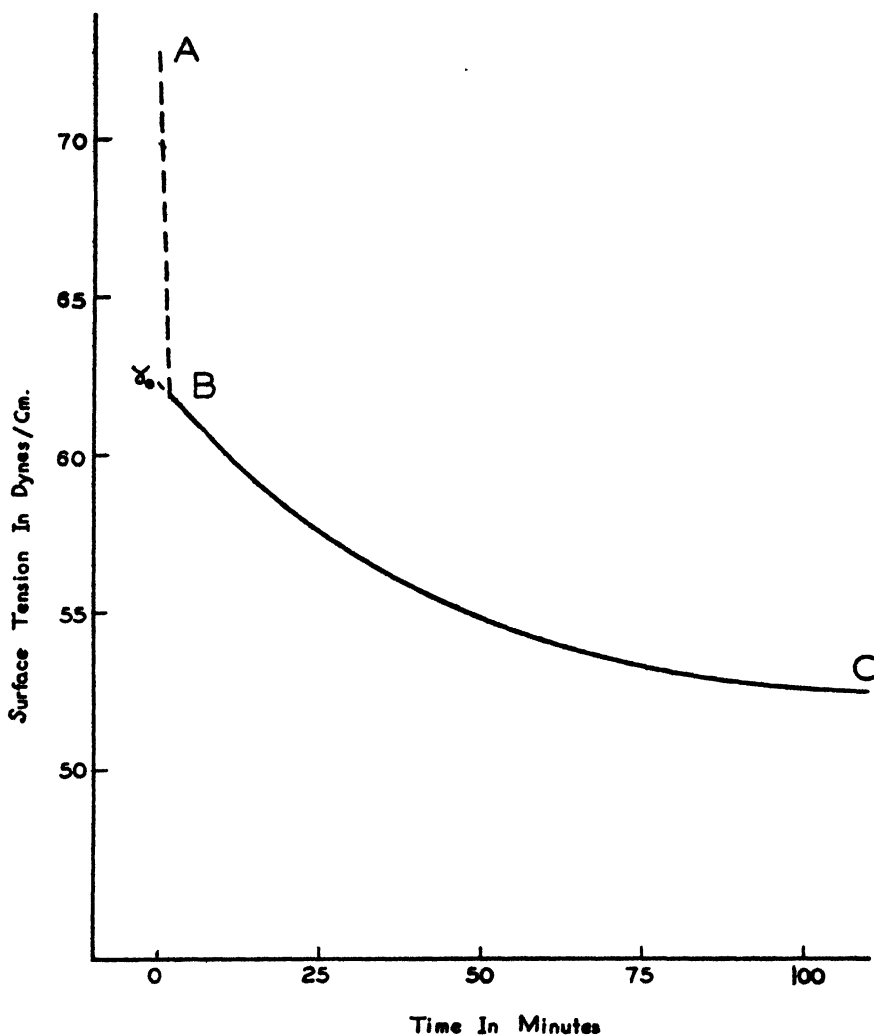
FIG. 1. Decrease of the surface tension of saponin solution with time, showing two processes in sequence.

for the surface concentration when the process *AB* is completed, but the process *BC* has not yet commenced. The surface tension at that state is the semi-dynamic value, γ_0, obtained by Boutaric and Berthier.

ADSORPTION AND SURFACE CONCENTRATION

Boutaric and Berthier (5) do not attempt to express their results for γ_0 as a function of the concentration in the bulk liquid. Their data, however, fit the

empirical equation:

$$\log C_b = 0.29\Delta - 3.9 \tag{2}$$

where C_b is the concentration in the bulk liquid in grams per liter, and Δ is the lowering of the surface tension extrapolated to zero time ($\gamma_{H_2O} - \gamma_0$). A comparison of results calculated by equation 2 and those found by Boutaric and Berthier is given in table 1. The empirical equation 2 expresses the results, within the concentration range investigated, with an accuracy of ± 1 per cent.

The values of γ_0 are the extrapolated values to zero time of the slower reaction; they are, therefore, very close to the surface-tension value at the end of the initial

TABLE 1

Comparison of results for semi-dynamic surface tension of saponin solutions

C_b	γ_0 (REFERENCE 5)	γ_0 (EQUATION 1)
grams per liter	*dynes per centimeter*	*dynes per centimeter*
0.05	62.3	62.9
0.125	61.5	61.5
0.275	60.7	60.3
0.300	60.6	60.2
0.375	59.8	59.9
0.500	59.0	59.4
1	58.4	58.4

adsorption. If we now suppose that the initial rapid adsorption is related to the concentration of the bulk liquid by an expression similar to the adsorption isotherm, then:

$$C_s = \alpha C_b^{1/n} \tag{3}$$

where C_s is the surface concentration, C_b is the bulk concentration, and α and $1/n$ are constants. Equations 2 and 3 can be related to express the surface tension as a function of the concentration in the surface, as follows:

From equation 3

$$\log C_b = n \log C_s - n \log \alpha$$

Substituting in equation 2 gives:

$$\log C_s = \frac{0.29}{n}\Delta - \left[\frac{3.9 - n \log \alpha}{n}\right] \tag{4}$$

Equation 4 is of the same form as equation 2, with a different slope and intercept on the vertical axis.

By means of equation 4 it is possible to calculate the variation of surface concentration with time, from the data on the variation of surface tension with time. The assumption underlying such a calculation is that changes in surface concentration are alone responsible for changes in surface tension; hence any value of γ depends on the value of C_s and is independent of the concentration in the bulk liquid. For this reason the symbol Δ, correctly defined for equation

2 as $(\gamma_{H_2O} - \gamma_0)$, is redefined for equation 4 as $(\gamma_{H_2O} - \gamma)$, where γ is the surface tension when the surface concentration is C_s, *independent of the value of the bulk concentration* C_b.
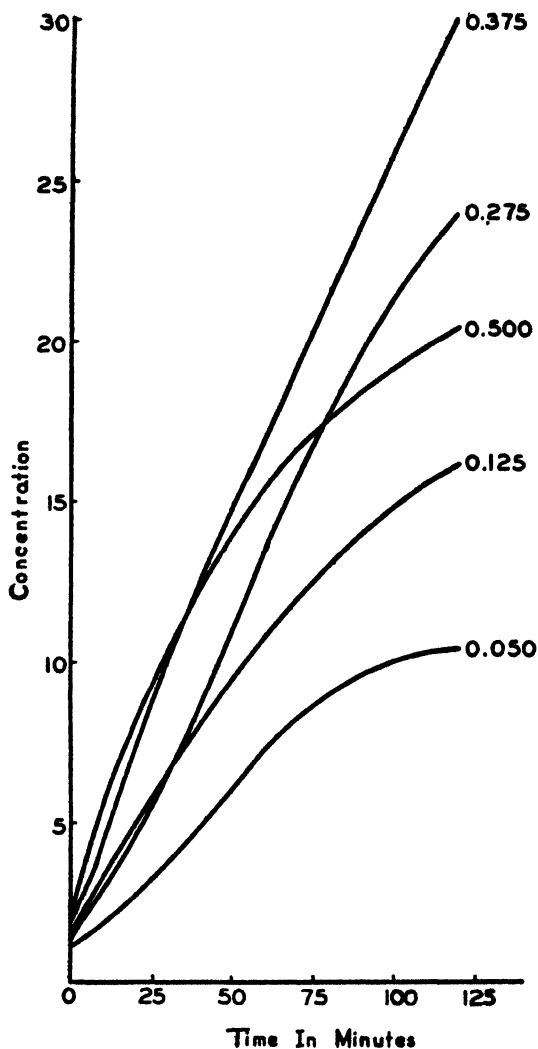
FIG. 2. Variation of surface concentration (arbitrary units) with time for saponin solutions of different bulk concentrations (grams per liter).

To perform the calculation accurately the values of the constants α and $1/n$ should be known. Arbitrary values being assumed for the constants ($\alpha = 2$; $1/n = 3$), figure 2 depicts the course of the variation of surface concentration with time, calculated from the data of Boutaric and Berthier. The shape of these curves suggests an autocatalytic process, causing an accelerating increase in the concentration at the surface.

HYDROLYSIS OF SAPONIN

When possible reactions of saponin at the surface are considered, the question of its hydrolysis is the first one that is raised. Hydrolysis of saponin is inhibited in basic and even in neutral solution. The variation of the surface tension of saponin with pH is not a general phenomenon, as certain kinds of saponin alter in one direction, while other kinds alter in the opposite direction (10).

Experiments of the same type as those of Boutaric and Berthier were conducted in this laboratory, using a Cenco-du Noüy tensiometer and a special vessel (designed by Dr. J. V. Robinson) to prevent evaporation of the solutions on standing for extended periods of time. The variation of surface tension with time was measured for buffered saponin solutions of pH = 4.0, 7.0, and 8.8. In each case the phenomenon of a drop in surface tension over a long time interval was observed. Only the data for the neutral solution can be fitted to an equation of the type given by Boutaric and Berthier (5); in the other cases the data conform to an equation of the type given by Bond and Puls (4):

$$\gamma = \bar{\gamma} + (\gamma_0 - \bar{\gamma})e^{-\frac{2}{\pi}\sqrt{\frac{t}{\tau}}}$$

Whatever may be the reason for the change in the form of the time function, the drop of surface tension with time continues to take place even when the hydrolysis of the saponin is non-existent. The phenomenon is therefore not to be ascribed to a hydrolysis reaction at the surface.

ORDER OF THE REACTION AT THE SURFACE

Changes in surface concentration can be treated by the methods of chemical kinetics to determine the order of the reaction. Two empirical equations are available; equation 4 relating surface concentration and surface tension, and the exponential equation of Boutaric and Berthier relating surface tension and time,

$$\gamma = \bar{\gamma} + (\gamma_0 - \bar{\gamma})e^{-at} \tag{5}$$

where γ is the surface tension at time t and $\bar{\gamma}$ is the surface tension at the end of infinite time. By manipulating these equations an expression for reaction rate can be obtained, but it requires some approximating before it can be reduced to a familiar form. The manipulation of interpolation equations, however, gives at best only inconclusive evidence. A more direct method is the use of the original data.

When the curves of figure 2 are plotted with the surface concentration on a logarithmic scale, the first part of the curve in each case is a straight line. The linear nature of the relation is maintained independently of whatever arbitrary values are assumed for the constants in equation 3. The straight lines obtained for different concentrations of the bulk liquid are shown in figure 3. The slopes of the straight lines vary only slightly. For values of the time greater than 15 min., the points begin to deviate more and more from the straight line. The use of equation 4 is no longer permissible when the lowering of the surface ten-

sion becomes greater than the extent of the data reported in table 1. When extrapolated, equation 4 calls for an unlimited increase in surface concentration, whereas there must be an upper limit in any practical case.
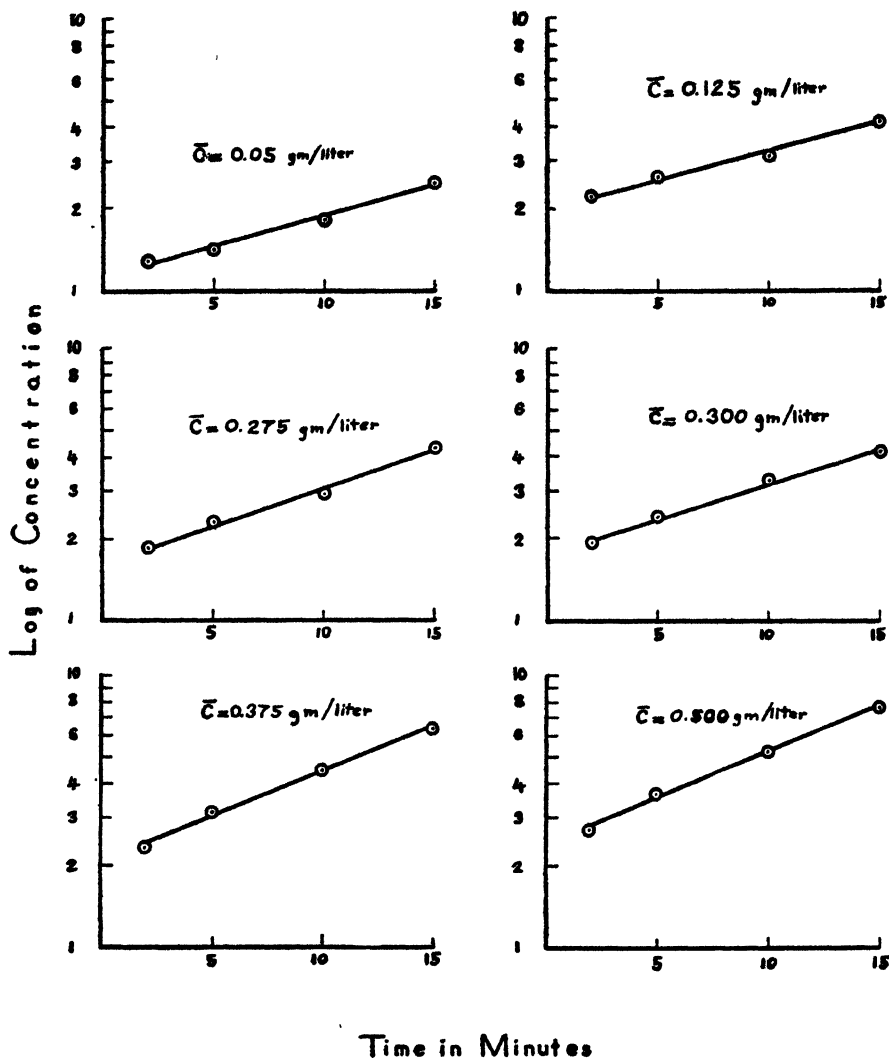
FIG. 3. Logarithm of the surface concentration of saponin solutions plotted against time, showing linear relation and nearly the same slope for different bulk concentrations.

An examination of figure 3 indicates the operation of a simple reaction mechanism. Let A represent the formula of a molecule of solute and A_s represent the formula of the same molecule after it has undergone a change, such as re-orientation (incipient crystallization), denaturation, or any other surface reaction that makes it differ in some quality from solute molecules of the bulk. The follow-

ing autocatalytic reaction is postulated:

$$A + A_s \rightarrow 2A_s$$

The velocity of reaction is given by:

$$d(A_s)/dt = k(A_s)(A)$$

In order to transform this equation into one conformable with figure 3, (A) must be constant. Then:

$$d(A_s)/dt = K'(A_s)$$

Integrating,   (6)

$$\log (A_s) = K' t + I$$

where I has the value $\dfrac{1}{n} \log \alpha(A)$ (from equation 3).

Equation 6 now has the form expected from the lines of figure 3, except that the slopes, as they depend on the value of (A), would be expected to show greater variation. There is visible only a slight tendency for the slopes to assume higher values with increase in the concentration of the bulk liquid, and even that tendency is reversed by the most concentrated solution. The physical meaning is that not only is (A) constant during the course of the reaction, but also (A) is virtually independent of the concentration in the bulk liquid. The value (A), therefore, cannot refer to concentrations in the bulk liquid. This suggests the possibility of an adsorption of A molecules on the A_s layer or skin. The adsorption of the second layer, although proceeding from bulk solutions of very different concentrations, could nevertheless remain virtually independent of the bulk concentration, if an application of the adsorption isotherm is valid.

The foregoing hypothesis for aqueous saponin solutions is strengthened by the well-known phenomenon of solid surface films and denaturation in such solutions. Nevertheless, the hypothesis of an autocatalytic surface reaction is not confined in its application to solutions where surface denaturation is known to occur. Soluble films have been shown to exist on aged surfaces of solutions of caprylic acid, hydrocinnamic acid, and phenol, whereas the surfaces of freshly swept solutions seem more nearly to resemble water (7). The existence of a semi-soluble pellicle in some solutions and a concomitant time effect in attaining final static surface tension (7, 12) could also be explained by a similar hypothesis, where the autocatalytic process refers to association or crystallization rather than denaturation. A slow attainment of a static value for interfacial tensions has been reported recently (21) and may also be due to a similar cause.

SUMMARY

Data for the change of surface tension with time in aqueous saponin solutions are interpreted on the basis of an autocatalytic reaction between molecules already sorbed upon the surface and molecules captured by them from a layer just underneath. The data are found to be in general conformity with such an explanation.

The author is indebted to Professor J. W. McBain for his careful reading of the first draft of this paper and for constructive discussions arising therefrom. He also wishes to thank Professors C. R. Noller and R. A. Ogg for specific information.

REFERENCES

(1) ADAM, N. K., AND SHUTE, H. L.: Trans. Faraday Soc. **34**, 758 (1938).
(2) ADDISON, C. C.: J. Chem. Soc. **1943**, 535; **1944**, 252.
(3) BIGELOW, S. L., AND WASHBURN, E. R.: J. Phys. Chem. **32**, 321 (1928).
(4) BOND, W. N., AND PULS, H. O.: Phil. Mag. **24**, 864 (1937).
(5) BOUTARIC, A., AND BERTHIER, P.: J. chim. phys. **36**, 1 (1939).
(6) DOSS, K. S. G.: Kolloid-Z. **86**, 205 (1939).
(7) FORD, T. F., AND WILSON, D. A.: J. Phys. Chem. **42**, 1051 (1938).
(8) FREUNDLICH, H.: *Colloid and Capillary Chemistry*, translated from the 3rd German edition by H. S. Hatfield. E. P. Dutton and Company, New York (1926).
(9) HISS, R.: "Über die zeitliche Änderung der Spannung reiner Flüssigkeitsoberflächen," Dissertation, Heidelberg, 1913.
(10) KOFLER, L.: *Die Saponine.* J. Springer, Vienna (1927).
(11) McBAIN, J. W., FORD, T. F., AND MILLS, G. F.: J. Am. Chem. Soc. **62**, 1319 (1940).
(12) McBAIN, J. W., AND SPENCER, W. V.: J. Am. Chem. Soc. **62**, 239 (1940).
   McBAIN, J. W., AND SHARP, E. R.: J. Am. Chem. Soc. **63**, 1422 (1941).
(13) McBAIN, J. W., AND WOOD, L. A.: Proc. Roy. Soc. (London) **A174**, 286 (1940).
(14) MILNER, S. R.: Phil. Mag. [6]**13**, 96 (1907).
(15) DU NOÜY, L.: *Equilibres superficiels des solutions colloïdales.* Masson et Cie., Paris (1929).
(16) NUTTING, G. C., LONG, F. A., AND HARKINS, W. D.: J. Am. Chem. Soc. **62**, 1496 (1940).
(17) RAYLEIGH, LORD: Proc. Roy. Soc. (London) **47**, 281 (1890).
(18) ROSS, SYDNEY: J. Am. Chem. Soc. **67**, 990 (1945).
(19) SZYSZKOWSKI, B. V.: Z. physik. Chem. **64**, 385 (1908).
(20) TSCHESCHE, R.: Angew. Chem. **48**, 569 (1935).
(21) WARD, A. F. H., AND TORDAI, L.: Nature **154**, 146 (1944).

POLAROGRAPHIC BEHAVIOR OF ALKALINE EARTH METALS.   II

THE POLAROGRAPHIC DETERMINATION OF CALCIUM ALONE AND IN THE PRESENCE OF OTHER ALKALINE EARTH METALS

I. ZLOTOWSKI AND I. M. KOLTHOFF

School of Chemistry, Institute of Technology, University of Minnesota, Minneapolis, Minnesota

In a previous paper (7) the polarography of barium and strontium has been discussed. The polarographic behavior of calcium has been studied by Kimura (2) in the presence of tetraethylammonium salts as supporting electrolytes. He found that the calcium waves start at about -2.2 volts (*vs.* the saturated calomel electrode = S.C.E.). The waves displayed pronounced maxima which could

not be suppressed. Consequently, calcium could not be determined polarographically. In the present paper we have investigated the polarographic behavior of calcium in water and in water–ethanol mixtures. A procedure has been developed for the polarographic determination of calcium, and also of the simultaneous determination of barium, strontium, and calcium when present together. For experimental details reference is made to the previous paper (7).
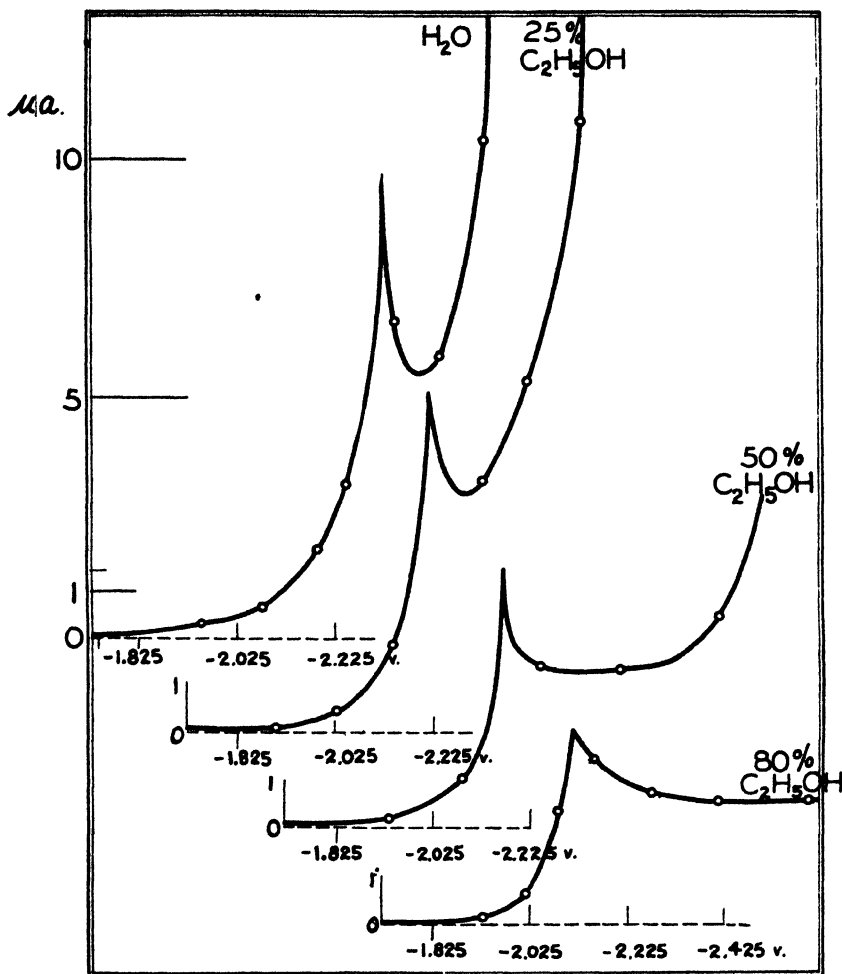
FIG. 1. Calcium-ion maxima in water and in water–ethanol mixtures. Tetraethylammonium iodide as supporting electrolyte. 0.0012 N calcium. Initial drop time. 3.0 sec.

CALCIUM WAVES IN SIMPLE CALCIUM-ION SOLUTIONS

The current–voltage curves of calcum show very pronounced maxima in water solutions. The usual maximum suppressors do not eliminate this maximum. In the present work it was found that in ethanol–water mixtures the maxima of calcium waves are considerably suppressed. The shape of the waves as well as

the height of the calcium-ion maxima was found to be dependent greatly on the alcohol concentration. In aqueous medium the waves show very acute peaks which change to smoothly rounded curves in media containing over 50 per cent ethanol. The height becomes smaller, the higher the alcohol concentration (figure 1).
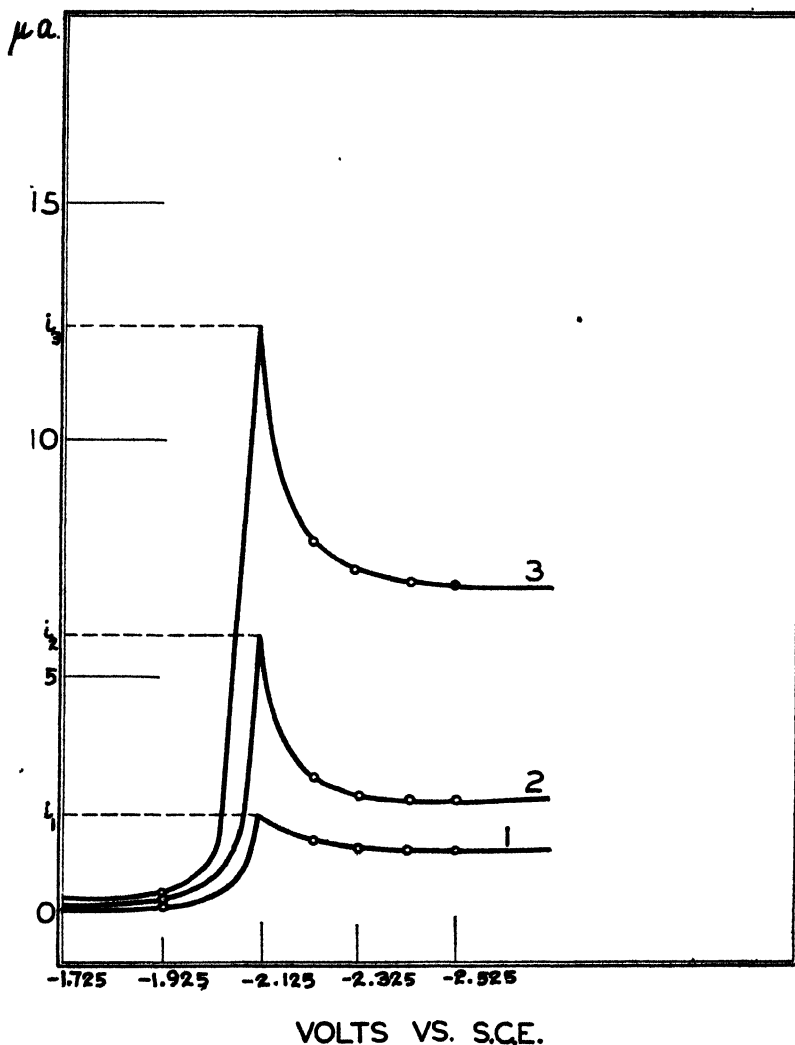
FIG. 2. Polarograms of calcium in 80 per cent ethanol. Curve 1, 0.00060 N calcium; curve 2, 0.00107 N calcium; curve 3, 0.0031 N calcium. $C_{Ca_1} : C_{Ca_2} : C_{Ca_3} = 1:1.8:5.2$. $i_1 : i_2 : i_3 = 1:2.8:7.0$.

It is to be emphasized that the height of the observed maxma increases with the amount of calcium in the solution. However, there is no linear proportionality between the current at the potential at which the peak of the curve is

reached and the calcium-ion concentration. As a rule an increase of the latter causes a manifold greater increase in the peak current (see figure 2.) However, even in 80 per cent ethanol the maxima still occur and cannot be eliminated by further increase of alcohol concentration. From the curves in figure 1 it is evident that it is hardly possible to measure the diffusion current of calcium in water or in 25 per cent ethanol. After the maximum, the current decreases to a fairly acute minimum, after which the current increases by the discharge of hydrogen. On the other hand, in 50 per cent and especially in 80 per cent ethanol a practically horizontal plateau is found, corresponding to the diffusion current of calcium.

From the data in table 1 it is seen that the diffusion current constant decreases with increasing alcohol concentration. From figure 1 it is seen that a maximum occurs even in 80 per cent ethanol. We found that the elimination of maxima in calcium-ion solutions containing 50 per cent or more ethanol can be

TABLE 1

Diffusion current constant of calcium in water and in water–ethanol mixtures with tetraethylammonium iodide as supporting electrolyte

Medium...................	H₂O	25 per cent C₂H₅OH	50 per cent C₂H₅OH	80 per cent C₂H₅OH
Diffusion current constant of Ca⁺⁺, in μa* per mole per liter .. .	9.17	8.50	5.65	4.33

* Microamperes.

accomplished easily by the addition of barium ions to the mixture. Actually, a concentration of barium ions of 3.5×10^{-5} M was ample to eliminate the maximum in a millimolar solution of calcium chloride in 50 per cent ethanol (figure 3). The fact that a further increase of the barium-ion concentration (table 2) does not affect the diffusion current constant of calcium is evidence of complete elimination of the maximum. In order to get a regular S-shaped wave, it is necessary to keep the barium-to-calcium concentration ratio in the solution above a certain limiting value. According to the experimental data shown in table 2, a barum-ion concentration of about 4 per cent of that of calcium present in the solution is needed in order to eliminate the maximum. In an extensive investigation we found that this 4 per cent limiting ratio is adequate over a relatively wide range of calcium-ion concentrations (0.5 to 5 millinormal). It should be noted that in aqueous solutions barium ions are not as effective as in alcohol–water solutions. Although the maxima are practically eliminated, the calcium waves obtained have an abnormal shape which makes the measurement of the diffusion current very uncertain.

Since the calcium maximum is a negative one (i.e., it occurs on the negative side of the electrode capillary curve), it is to be expected that trivalent cations should be more effective than barium in eliminating the calcium maximum. These expectations have been confirmed fully by the use of lanthanum solutions as suppressors of calcium maxima. We found (table 3; figure 4) that about a 5×10^{-5} M concentration of lanthanum chloride completely eliminates the

maximum, giving a regular diffusion wave in a 10^{-3} M aqueous solution of calcium chloride, while a 10^{-4} M concentration of barium chloride in the same cal-
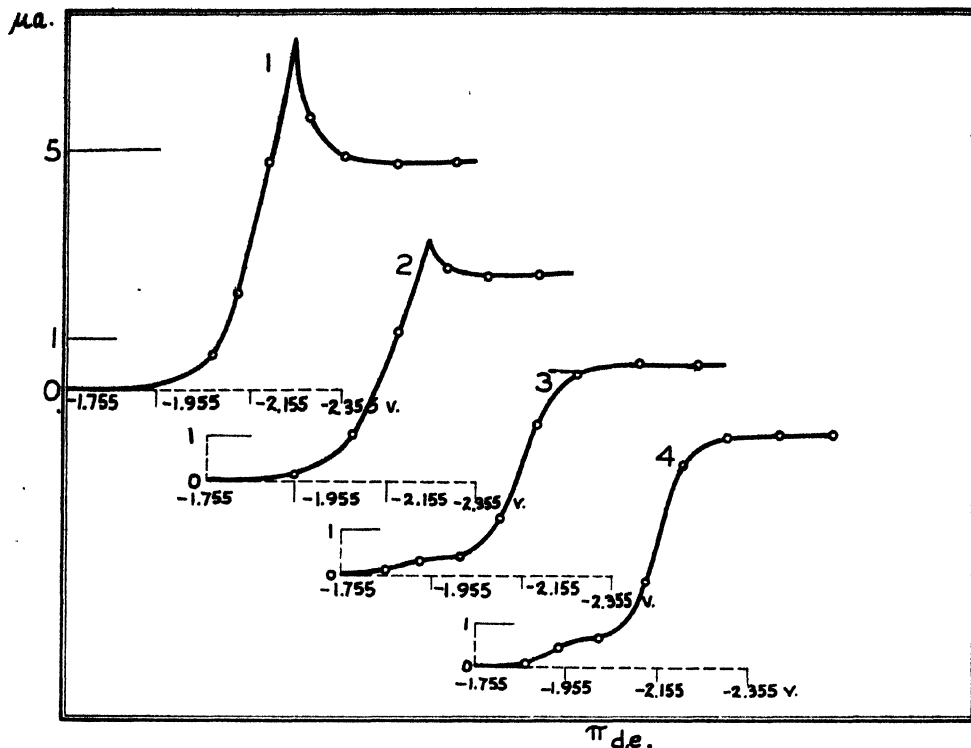
FIG. 3. Suppression of calcium maximum in 50 per cent ethanol. $C_{Ca^{++}} = 0.00172$ N. Drop time at $\pi = 0$ is 2.9 sec. Tetraethylammonium iodide as supporting electrolyte. Curve 1, no barium; curve 2, $C_{Ba^{++}} = 1.8 \times 10^{-5}M$; curve 3, $C_{Ba^{++}} = 3.15 \times 10^{-5}M$; curve 4, $C_{Ba^{++}} = 7.4 \times 10^{-5}M$.

TABLE 2

The elimination of the calcium wave maxima by means of barium chloride

$C_{Ca^{++}} = 0.00086$ M (C_1); medium, 50 per cent ethanol

BARIUM-ION CONCENTRATION (C_2)	C_2/C_1	DIFFUSION CURRENT CONSTANT
moles per liter		*μa per millimole per liter*
0		5.65
1.8×10^{-5}	2.1×10^{-2}	5.25
3.6×10^{-5}	4.1×10^{-2}	5.10
7.4×10^{-5}	8.3×10^{-2}	5.00
1.4×10^{-4}	1.6×10^{-1}	5.05

cium solution still gives a wave which is abnormal in appearance. Therefore, from the analytical point of view, lanthanum appears to have a great advantage over barium as a suppressor of calcium maxima in aqueous medium. It is appar-

ent from the figures in table 3 that the calcium diffusion current (corrected for the residual current of the supporting electrolyte and the diffusion current of

TABLE 3

The elimination of the calcium wave maxima by means of lanthanum chloride

$$C_{Ca^{i+}} = 0.00088 \ M \ (C_1); \text{ medium, water}$$

LANTHANUM-ION CONCENTRATION (C$_2$)	C$_2$/C$_1$	DIFFUSION CURRENT CONSTANT
moles per liter		*μa per millimole per liter*
0		(~10.20)
7.0×10^{-6}	8.0×10^{-3}	(~9.50)
5.0×10^{-5}	5.7×10^{-2}	5.85
1.1×10^{-4}	1.3×10^{-1}	5.90
3.0×10^{-4}	3.4×10^{-1}	5.90
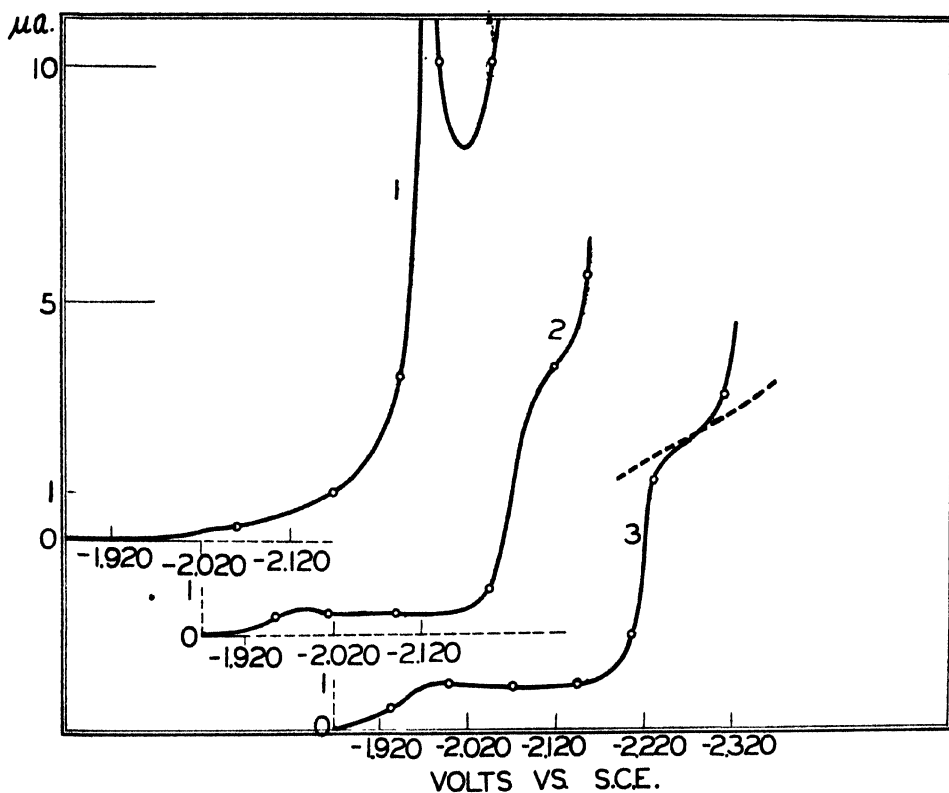
FIG. 4. Suppression of calcium maximum by lanthanum in water. Drop time at $\tau = 0$ is 3.05 sec. 0.15 N tetraethylammonium iodide as supporting electrolyte. Curve 1, $C_{La^{+++}} = 7 \times 10^{-6}M$; curve 2, $C_{La^{+++}} = 5 \times 10^{-5}M$; curve 3, $C_{La^{+++}} = 1.1 \times 10^{-4}M$.

added lanthanum) is practically constant when the concentration ratio of lanthanum to calcium ion is 5 per cent or more. It will be noted that the accepted

TABLE 4

Comparison of barium and lanthanum as maximum suppressors of 0.001 M calcium in water and water-ethanol mixtures

Medium	H_2O	25 per cent C_2H_5OH	50 per cent C_2H_5OH	80 per cent C_2H_5OH
$C_{Ba^{++}}$ in moles per liter	∼10^{-4}	5×10^{-5}	3×10^{-5}	1×10^{-5}
$C_{La^{+++}}$ in moles per liter	5×10^{-5}	3×10^{-5}		
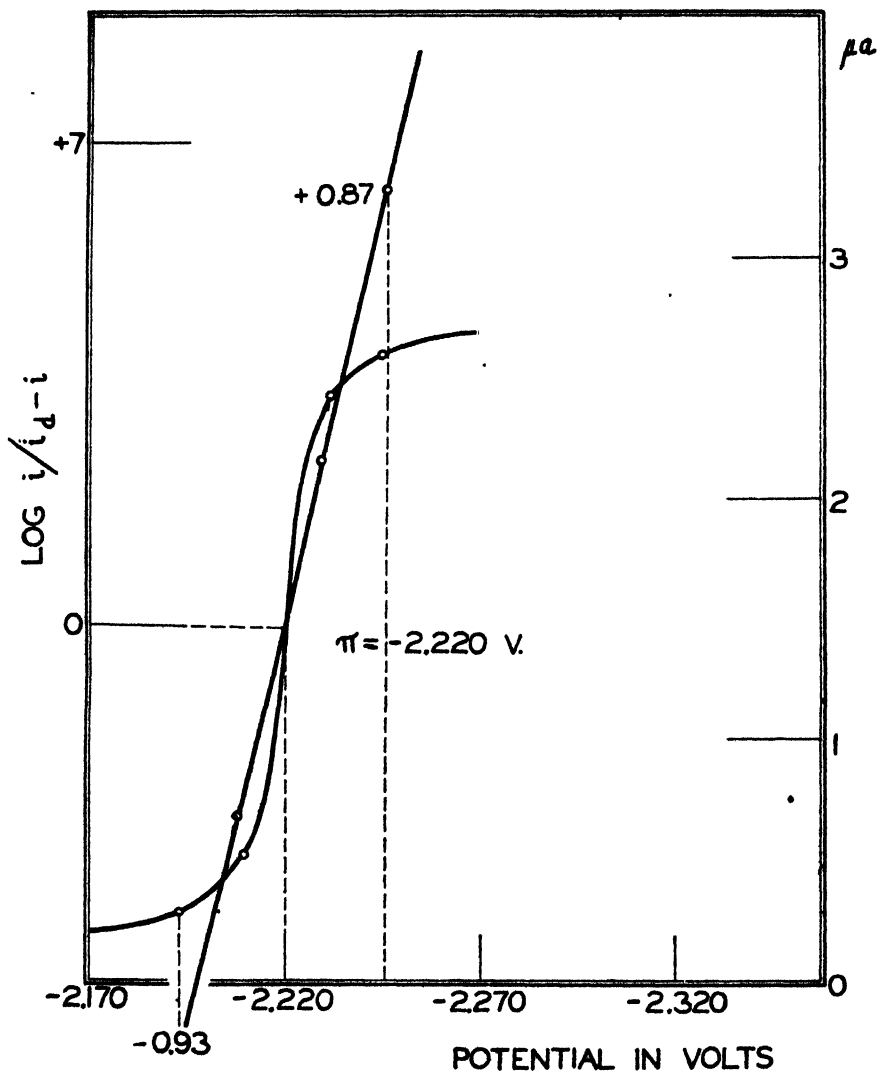
FIG. 5. The wave and the log $i/i_d - i$ plot of $1.2 \times 10^{-3}N$ calcium in water. 0.08 N tetraethylammonium iodide as supporting electrolyte. 0.001 M lanthanum as maximum suppressor. Slope = 0.050/1.80 = 0.028.

values of the diffusion current correspond to the ordinates of the inflection points of the polarograms obtained.

The use of lanthanum is less suitable in alcohol–water solutions because lanthanum ions themselves give a slight maximum in solutions containing more than 25 per cent ethanol, thus making the determination of calcium diffusion currents less accurate. Therefore, barium is recommended as a maximum-eliminating agent in alcoholic solutions.

The minimum concentrations of either barium or lanthanum chloride sufficient for a complete elimination of maxima in 10^{-3} M solutions of calcium chloride in water and in various alcohol–water mixtures are given in table 4.
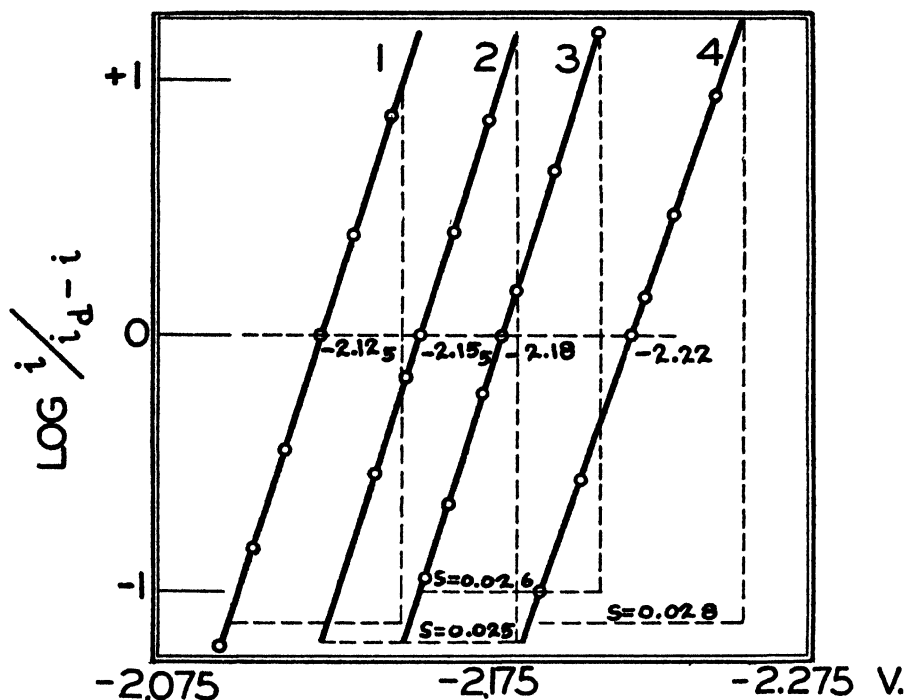
FIG. 6. Log plots of calcium waves in water–ethanol mixtures. Curve 1, in 80 per cent ethanol; curve 2, in 50 per cent ethanol; curve 3, in 25 per cent ethanol; curve 4, in water.

In neutral aqueous or ethanol–water solutions which, in addition to the required amount of supporting electrolyte, also contain enough barium or lanthanum ions to eliminate calcium maxima, the reduction of calcium appears to be reversible. The equation of the wave is given by the Heyrovsky–Ilkovič equation for a divalent ion. Several polarograms have been analyzed by plotting log $(i/i_d - i)$ vs. the cathode potential. An example of such an analysis is given in figure 5, in which both the polarographic wave and the log plot of the diffusion current of calcium in aqueous solution are given. The log plot yields a straight line with a slope of 0.028, while according to the Heyrovsky–Ilkovič equation the theoretical slope is 0.029 at 25°C. Some log plots obtained in

ethanol–water mixtures are given in figure 6. In all cases straight lines are obtained with slopes conforming within the experimental error to the Heyrovsky-Ilkovič equation. Finally, the data summarized in table 5 and graphically presented in figure 7 show the dependence of the calcium half-wave potential upon

TABLE 5

The dependence of the half-wave potential of Ca^{++} upon the ethanol concentration

Medium...............	H_2O	25 per cent C_2H_5OH	50 per cent C_2H_5OH	80 per cent C_2H_5OH	90 per cent C_2H_5OH	C_2H_5OH
Half-wave potential vs. S.C.E...............	−2.220*	−2.180†	−2.155†	−2.125†	−2.115†	(∼2.10)‡

* Maximum eliminated by addition of La^{+++} ions.
† Maximum eliminated by addition of Ba^{++} ions.
‡ Extrapolated value.

TABLE 6

Proportionality between diffusion current and calcium-ion concentration
(All maxima eliminated)

$t_0 = 2.9$ sec.; $\pi_{d-e.} = -2.26$ volts			$t_0 = 2.9$ sec.; $\pi_{d.e.} = -2.30$ volts		
H_2O 5×10^{-4} to 10×10^{-4} M La^{+++}			25 per cent C_2H_5OH 5×10^{-4} to 8×10^{-4} M Ba^{++}		
$c_{Ca^{++}}$	i_d	i_d/C	$c_{Ca^{++}}$	i_d	i_d/C
millimoles per liter	*μa*	*μa per millimole per liter*	*millimoles per liter*	*μa*	*μa per millimole per liter*
0.375	2.17	5.79	0.315	1.73	5.49
0.505	2.95	5.85	1.06	5.97	5.63
0.885	5.22	5.90	1.88	10.73	5.72
2.06	12.48	6.06			

$t_0 = 2.9$ sec.; $\pi_{d.e.} = -2.40$ volts			$t_0 = 3.0$ sec.; $\pi_{d.e.} = -2.30$ volts		
50 per cent C_2H_5OH 5×10^{-4} to 8×10^{-4} M Ba^{++}			80 per cent C_2H_5OH 5×10^{-4} to 8×10^{-4} M Ba^{++}		
$c_{Ca^{++}}$	i_d	i_d/C	$c_{Ca^{++}}$	i_d	i_d/C
millimoles per liter	*μa*	*μa per millimole per liter*	*millimoles per liter*	*μa*	*μa per millimole per liter*
0.22	1.08	4.91	0.43	1.81	4.21
0.50	2.36	4.72	0.83	3.57	4.30
0.88	4.40	5.00	1.525	6.33	4.15
1.57	7.99	5.08	2.045	8.18	3.99
2.75	13.28	4.83			

the alcohol concentration. As was found with the other two alkaline earth metals (7), the half-wave potential of calcium is practically a linear function of the alcohol concentration.

From the experimental data presented in table 6 it is seen that in both aqueous and ethanol–water media there is a satisfactory proportionality between calcium

diffusion currents and calcium-ion concentrations provided that the maxima are eliminated by means of barium or lanthanum salt solutions.   It should be mentioned, however, that in order to keep this proportionality within 1 to 2 per cent, the concentration of calcium ions in water should be kept between 0.00025 to 0.001 M and in alcohol–water mixtures below 0.0025 M.
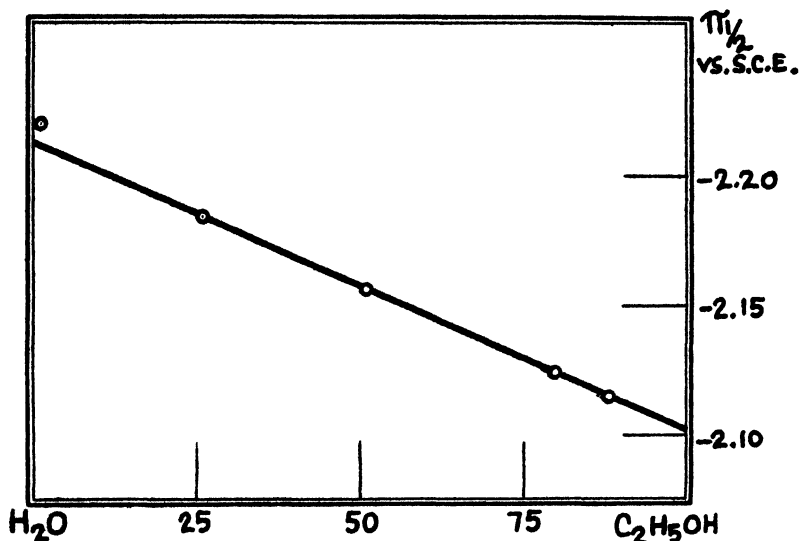
FIG. 7. Half-wave potential of calcium ($vs.$ S.C.E.) as function of alcohol concentration

TABLE 7

The dependence of the calcium diffusion current upon alcohol concentration

$(C_2H_5)_4NI$ as supporting electrolyte; $C_{Ca^{++}}$ varied between 0.00025 and 0.001 M; concentration of supporting electrolyte $= 0.05$ to $0.2 M$

Medium...............	H_2O	25 per cent C_2H_5OH	50 per cent C_2H_5OH	80 per cent C_2H_5OH	90 per cent C_2H_5OH	C_2H_5OH
Diffusion current constant in μa per millimole per liter.. ..	5.90*	5.50†	5.00†	4.30†	4.40‡	(4.55)§

* Maximum eliminated by addition of La^{+++} ions.
† Maximum eliminated by addition of Ba^{++} ions.
‡ Practically the same values with and without suppression of maximum by Ba^{++} ions.
§ Extrapolated value.

The alcohol concentration dependence of the calcium diffusion current is evident from the data given in table 7.   Accepting the value of calcium-ion mobility in water as given in the literature, it is possible to compare the experimental diffusion current constant in water solution with that calculated from the Ilkovič equation (4).   The mobility of calcium ion at 18°C. reported by Fergusson and Vogel (1) is 52.18 cm.² per ohm equivalent.   Taking the temperature coefficient

equal to 0.024 as given by Kohlrausch (3), the mobility at 25°C. should be 61.0 cm.^{2} per ohm equivalent. The diffusion coefficient of calcium ions as calculated by means of the Nernst formula is:

$$D_{Ca^{++}} = 2.67 \times 10^{-7} \times 61.0 \times \tfrac{1}{2} = 8.14 \times 10^{-6} \text{ cm.}^2 \text{ per second}$$

Hence, the diffusion current constant

$$K_{(H_2O)} = 605 \times 2 \times (8.14 \times 10^{-6})^{\frac{1}{2}} \times 1.74 = 6.05 \text{ microamperes per mole per liter}$$

as compared with the experimental value of 5.90. This agreement indicates that when the maximum is eliminated satisfactorily and correction is made for the

TABLE 8

Diffusion coefficient of Ca^{++} *in ethanol–water mixtures (calculated by means of the Ilkovič equation)*

Medium.	H$_2$O	25 per cent C$_2$H$_5$OH	50 per cent C$_2$H$_5$OH	80 per cent C$_2$H$_5$OH	90 per cent C$_2$H$_5$OH	C$_2$H$_5$OH
$D \times 10^6$ cm.^{2} per second.	7.86	6.83	5.64	4.17	4.37	(4.65)*

* Extrapolated value.
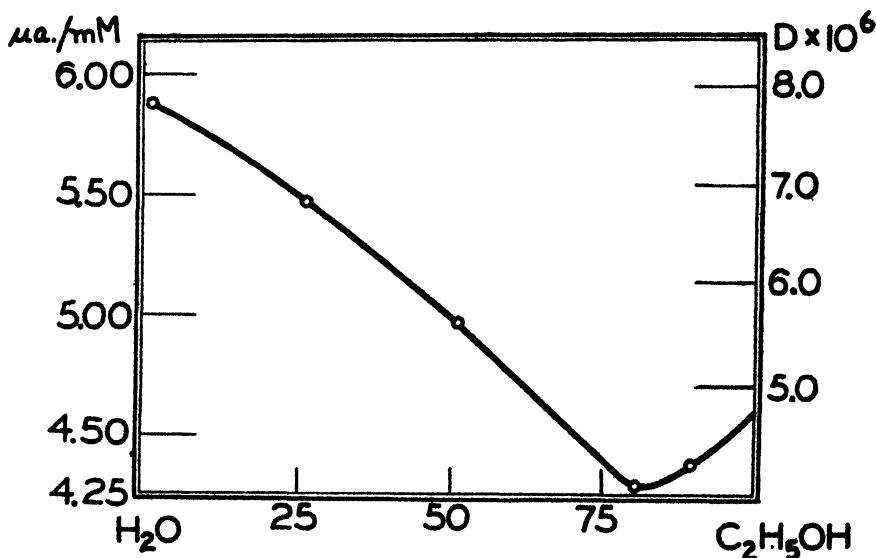
FIG. 8. Diffusion coefficient D and diffusion current constant of calcium as function of ethanol concentration.

residual current, the Ilkovič equation is obeyed within 2.5 per cent over a concentration range from 2.5×10^{-4} to 1×10^{-3} M.

Assuming the validity of the Ilkovič equation in alcohol–water mixtures, it is possible to compute the diffusion coefficients of calcium ions in water–ethanol

mixtures of various concentrations. The data obtained have been summarized in table 8 and plotted in figure 8. It is interesting to note that the curve in fig-

TABLE 9

Calculated equivalent conductances at infinite dilution of Ba^{++}, Sr^{++}, Ca^{++} *at 25°C. in sq. cm. per ohm equivalent*

ION MEDIUM	Ba++		Sr++		Ca++	
	Absolute values	Relative values	Absolute values	Relative values	Relative values	Absolute values
Water ...	64.21	1.00	60.3	1.00	61.0	1.00
50% ethanol	44 0	0.68	42.1	0.70	42.1	0.69
80% ethanol	35.0	0.54	32.6	0.54	31.1	0.51
90% ethanol.		0.58		0.55		0.56
100% ethanol.		0 62*		0.60*		0.59*

* Extrapolated.
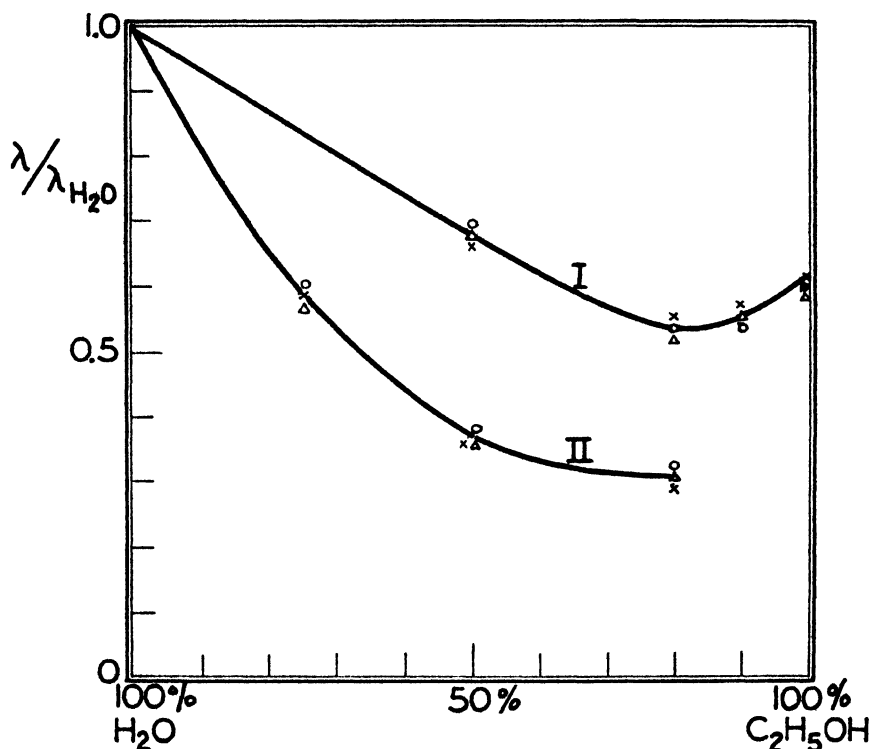
FIG. 9. Relative equivalent conductances at infinite dilution of alkali and alkaline earth ions in water–ethanol mixtures. Curve I: ×, barium ion; Δ, calcium ion; o, strontium ion. Curve II: ×, potassium ion; Δ, sodium ion; o, lithium ion.

ure 8 shows a well-pronounced minimum in about 85 per cent ethanol. With the aid of both the Nernst formula and the Ilkovič equation, we have calculated from the experimentally determined diffusion current constants the equivalent

conductances of all three alkaline earth metals (see reference 1) at infinite dilu-
tion in various alcohol–water mixtures. The results of our computation are
given in table 9. From the data, the conclusion may be drawn that the relative
decrease of the observed equivalent conductances with increasing alcohol con-
centration is practically the same for barium, strontium, and calcium.

It is interesting to compare the change of the relative mobility of the alkaline
earth ions with that of the alkali ions in water–ethanol mixtures of varying com-
position. This is done in figure 9. It is seen that the relative change of the
equivalent conductance of the alkali ions[1] with increasing ethanol concentration
is the same for potassium, sodium, and lithium, and much greater for the alkali
ions than for the alkaline earth ions. Thus, the relative change of the mobility
of these cations in going from water to alcohol as a solvent is independent of the
ionic size (or degree of hydration). Apparently, it is the valence of these cations
which determines the effect of ethanol upon their relative mobilities. The mag-

TABLE 10

Barium and calcium diffusion current constants in mixtures of Ba^{++} *and* Ca^{++}

(No other maximum eliminators added; K = diffusion current constant; medium,
50 per cent ethanol)

COMPOSITION OF SOLUTION	$\dfrac{c_{Ca^{++}}}{c_{Ba^{++}}}$	$K_{Ba^{++}}$ DETERMINED AT $\pi_{d.e.}$ = −2.00 VOLTS			$K_{Ca^{++}}$ DETERMINED AT $\pi_{d.e.}$ = −2.20 VOLTS		
		In solution with calcium (a_1)	In solution without calcium (b_1)	$\Delta = \dfrac{a_1 - b_1}{b_1} 100$	In solution with barium (a_2)	Just enough barium to eliminate the maximum (b_2)	$\Delta = \dfrac{a_2 - b_2}{b_2} 100$
millimoles per liter							*per cent*
0.15 Ba^{++} + 1.5 Ca^{++}. ..	10.0	5.16	5.10	+1.2	4.95	5.00	−1.0
2.12 Ba^{++} + 0.32 Ca^{++}.....	0.15	5.02	5.10	−1.6	5.14	5.00	+2.8

nitude of this effect decreases with increasing charge of the ions. We intend to
make a more systematic study of this interesting subject and reserve further con-
clusions for future work.

SIMULTANEOUS DETERMINATION OF BARIUM, STRONTIUM, AND CALCIUM

Since barium is an excellent agent for eliminating the maxima of the calcium
wave, it is reasonable to expect that in a mixture of calcium and barium it should
be possible to determine both metals with the ordinary accuracy of 2 to 3 per
cent. These expectations have been confirmed by a series of measurements
carried out in both water and alcohol–water media with mixtures of barium and
calcium in the presence and absence of strontium. It is interesting to point out
that strontium ions affect the calcium maxima very slightly, if at all. The re-
sults summarized in table 10 show that the polarographic analysis of mixtures of

[1] The values have been calculated from polarographic data given by I. Zlotowski and I.
M. Kolthoff: J. Am. Chem. Soc. **64**, 1297 (1942).

barium and calcium yields very satisfactory results.   A complete description of the procedure employed in the calculation of the concentration of two or more metallic ions from the measured diffusion currents, in a mixed solution, is given
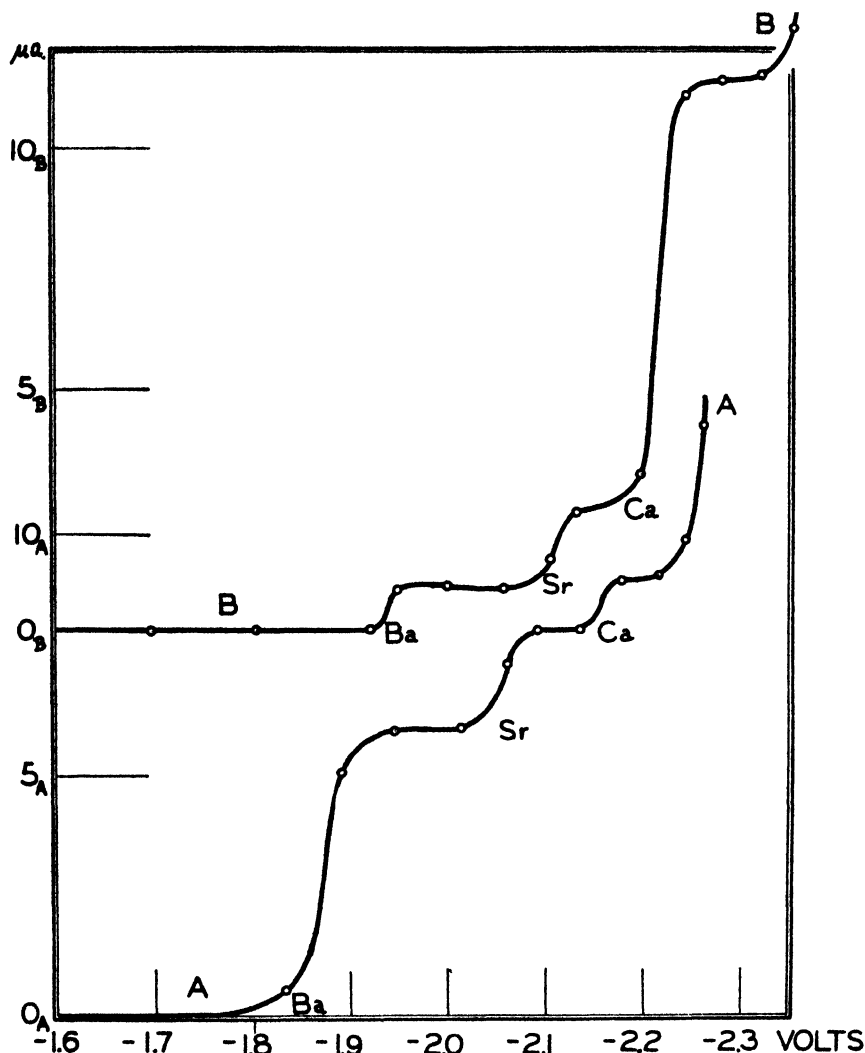
FIG. 10. Polarograms of mixtures of barium, strontium, and calcium.   Curve A: 0.3 N tetraethylammonium iodide in 50 per cent ethanol; $C_{Ba^{++}} = 23.2 \times 10^{-4}N$; $C_{Sr^{++}} = 8.2 \times 10^{-4}N$; $C_{Ca^{++}} = 4.4 \times 10^{-4}N$.   Curve B: 0.25 N tetraethylammonium iodide in water; $C_{Ba^{++}} = 2.8 \times 10^{-4}N$; $C_{Sr^{++}} = 5.4 \times 10^{-4}N$; $C_{Ca^{++}} = 30.5 \times 10^{-4}N$.

below in connection with the analysis of a ternary mixture of salts of alkaline earth metals.

We found that in both water and alcohol–water media all three alkaline earth

metals can be determined simultaneously with the ordinary polarographic accuracy. This is also illustrated by the two polarograms shown in figure 10, as well as the summary of numerical data presented in table 11. By means of the

TABLE 11

Barium + strontium + calcium: diffusion currents in mixtures of Ba^{++}, Sr^{++}, *and* Ca^{++}
(No other maximum eliminators added)

A. Medium: 50 per cent C_2H_5OH

COMPOSITION OF SOLUTION	$\pi_{d.e.} = -1.95$ volts; $m^{2/3}\mu^{1/6} = 1.80$				$\pi_{d.e.} = -2.12$ volts; $m^{2/3}\mu^{1/6} = 1.77$					$\pi_{d.e.} = -2.18$ volts; $m^{2/3}\mu^{1/6} = 1.75$			
	Diffusion current (measured) i_1	Diffusion current (calculated) i_1'	Δ_{Ba} $\dfrac{i_1 - i_1'}{i_1}$	$i_1 \times \left(\dfrac{1.77}{1.80}\right)$	Diffusion current (measured) I_2	$I_2 - i_1$ $\left(\dfrac{1.77}{1.80}\right)$ (i_2)	Strontium diffusion current (calculated) i_2'	Δ_{Sr} $\dfrac{i_2 - i_2'}{i_2'}$	$I_2 \times \left(\dfrac{1.75}{1.77}\right)$	Diffusion current (measured) I_3	$I_3 - I_2$ $\left(\dfrac{1.75}{1.77}\right)$ (i_3)	Calcium diffusion current (calculated) i_3'	Δ_{Ca} $\dfrac{i_3 - i_3'}{i_3'}$
millimoles per liter	μa	μa	*per cent*		μa			*per cent*		μa			*per cent*
1.16 Ba^{++}	5.93	6.12	−2.3	5.88									
+													
0.41 Sr^{++}													
+					8.00	2.12	2.08	+1.9	7.91				
0.22 Ca^{++}										9.05	1.14	1.11	+2.7

B. Medium: H_2O

COMPOSITION OF SOLUTION	$\pi_{d.e.} = -2.0$ volts; $m^{2/3}\mu^{1/6} = 1.78$				$\pi_{d.e.} = -2.15$ volts; $m^{2/3}\mu^{1/6} = 1.76$					$\pi_{d.e.} = -2.30$ volts; $m^{2/3}\mu^{1/6} = 1.73$			
	Diffusion current (measured) i_1	Diffusion current (calculated) i_1'	Δ_{Ba} $\dfrac{i_1 - i_1'}{i_1'}$	$i_1 \times \left(\dfrac{1.76}{1.78}\right)$	Diffusion current (measured) I_2	$I_2 - i_1$ $\left(\dfrac{1.76}{1.78}\right)$ (i_2)	Strontium diffusion current (calculated) i_2'	Δ_{Sr} $\dfrac{i_2 - i_2'}{i_2'}$	$I_2 \times \left(\dfrac{1.73}{1.76}\right)$	Diffusion current (measured) I_3	$I_3 - I_2$ $\left(\dfrac{1.73}{1.76}\right)$ (i_3)	Calcium diffusion current (calculated) i_3'	Δ_{Ca} $\dfrac{i_3 - i_3'}{i_3'}$
millimoles per liter	μa	μa	*per cent*		μa			*per cent*		μa			*per cent*
0.14 Ba^{++}	0.93	0.90	+3.3	0.92									
+													
0.27 Sr^{++}					2.52	1.60	1.64	−2.4	2.48				
+													
1.52 Ca^{++}										11.46	8.98	9.00	−0.2

method described in a previous paper (6), the diffusion current of barium is first determined and corrected for the residual current of the supporting electrolyte. The results agree within 3 per cent with the values calculated from the diffusion current constants determined for simple barium solutions in water and in 50 per

cent ethanol at the same potential (7). The diffusion current of strontium is obtained by subtracting from the measured sum of both strontium and barium
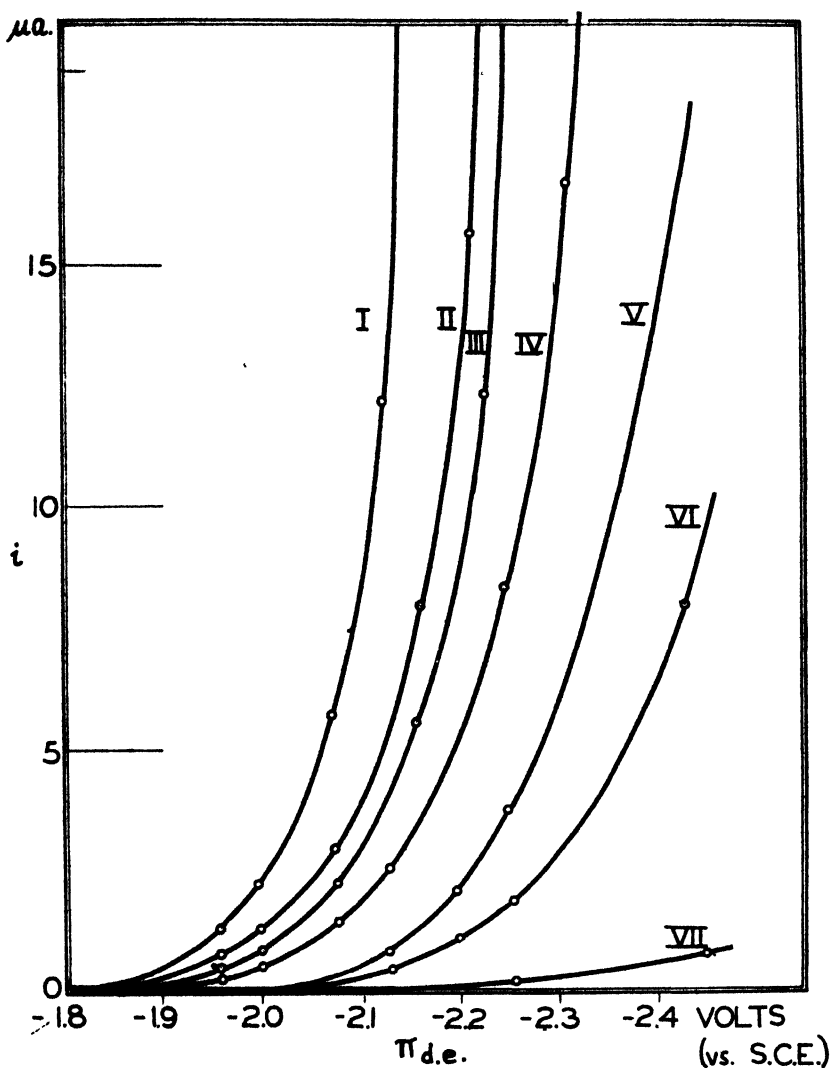
Fig. 11. Current-voltage curves with magnesium chloride in water. Tetraethylammonium iodide as supporting electrolyte. Curve I, $3.46 \times 10^{-3}N$ magnesium; curve II, $1.54 \times 10^{-3}N$ magnesium; curve III, $9.6 \times 10^{-4}N$ magnesium; curve IV, $5.0 \times 10^{-4}N$ magnesium; curve V, $1.83 \times 10^{-4}N$ magnesium; curve VI, $9.2 \times 10^{-5}N$ magnesium; curve VII, $8.3 \times 10^{-6}N$ magnesium.

diffusion currents (corrected for "i_v"), the value of the diffusion current of barium recalculated at the strontium diffusion current cathode potential. Similarly, the actual diffusion current of calcium is equal to the difference between the

measured sum of all three diffusion currents at the calcium diffusion current potential and the recalculated $(m^{\frac{2}{3}}t^{\frac{1}{6}})$ sum of both barium and strontium diffusion currents taken from preceding branches of the same polarogram. The accuracy of both strontium and calcium determinations is quite satisfactory, the differences between the measured values and those computed by means of the diffusion current constants being of the order of 2 to 3 per cent. The accuracy, of course, depends on the ratio of concentrations of the various constituents.

WAVES OF CALCIUM IN THE PRESENCE OF MAGNESIUM IONS

Experiments conducted by Kimura (2) and Müller (5) indicate that magnesium yields very poorly defined waves in aqueous solutions of tetraethylammonium salts at a potential about -2.2 volts vs. S.C.E. The main characteristics of the polarograms obtained were a very pronounced maximum and an abnormally large apparent diffusion current. We found that when tetraethylammonium iodide is used as supporting electrolyte in water, the polarograms of magnesium

TABLE 12

Proportionality between current and magnesium-ion concentration at potentials between -2.125 and -2.425 volts

$(C_2H_5)_4NI$ as supporting electrolyte in water

MgCl$_2$ CONCENTRATION,	$\pi_{d.e.} = -2.125$ volts vs. S.C.E.		$\pi_{d.e.} = -2.225$ volts vs. S.C.E.		$\pi_{d.e.} = -2.325$ volts vs. S.C.E.		$\pi_{d.e.} = -2.425$ volts vs. S.C.E.	
	i	i/c	i	i/c	i	i/c	i	i/c
M	μa	μa per millimole per liter	μa	μa per millimole per liter	μa	μa per millimole per liter	μa	μa per millimole per liter
4.15×10^{-6}	0.04	(9.6)	0.14	(34)	0.36	(87)	0.70	169
4.6×10^{-5}	0.40	8.7	1.37	30	3.70	81	7.50	163
9.15×10^{-5}	0.81	8.85	3.05	33.4	7.75	85	15.7	172
2.5×10^{-4}	2.35	9.4	8.05	32.2	20.3	81.2		
4.8×10^{-4}	3.90	8.13	13.1	27.3	32.6	68.0		
7.7×10^{-4}	5.40	7.02	18.9	24.6	50.8	66.0		
1.73×10^{-3}	13.00	7.52	42.6	24.6				

ions present curves with steadily increasing slopes and without diffusion current portion (figure 11). From the data given in table 12 it may be seen readily that the measured currents at potentials between -2.12 and -2.42 volts within 10 per cent remain proportional to the concentration of magnesium ions provided the latter does not exceed 2.5×10^{-4} moles per liter. At higher concentrations, the ratio i_d/c becomes smaller. In general, it is not safe to use current–voltage curves for analytical estimation of the magnesium concentration.

It is evident that the abnormally large currents obtained with magnesium cannot be due solely to reduction of magnesum ions to magnesium amalgam. By far the largest part of the current must be attributed to a simultaneous discharge of hydronium ions with magnesium ions. Apparently, the discharge of magnesium ions catalyzes the discharge of hydronium ions at the dropping mercury electrode.

In view of the fact that calcium ions are often accompanied by magnesium, it seemed worth while to study the effect of the latter upon the polarogram of calcium.
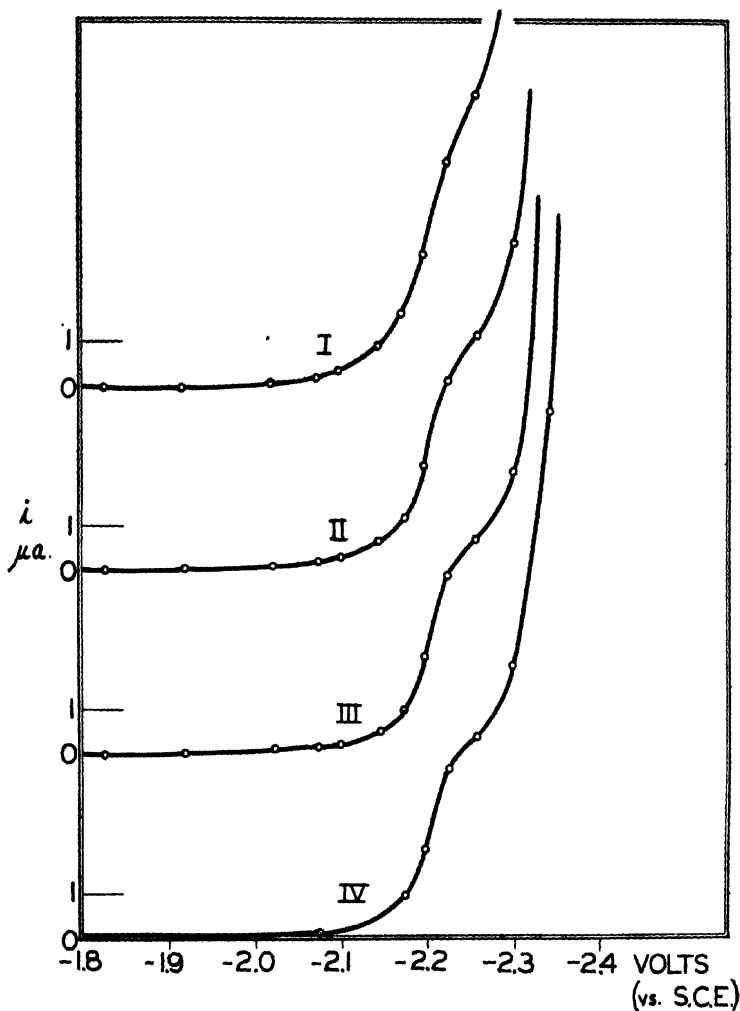
Fig. 12. Interference of magnesium in polarographic determination of calcium. Polarograms in water; 0.00158 N calcium; 6.3 $\times$ 10^{-5} N lanthanum; 0.15 N tetraethylammonium iodide as supporting electrolyte. Curve I, $C_{Mg^{++}} = 6 \times 10^{-5}N$; curve II, $C_{Mg^{++}} = 1.6 \times 10^{-5}N$; curve III, $C_{Mg^{++}} = 1.0 \times 10^{-5}N$; curve IV, $C_{Mg^{++}} = 6.5 \times 10^{-6}N$.

It was found (figure 12) that in water the calcium diffusion current regions practically disappear if the concentration of magnesium ions is greater than 4 $\times$ 10^{-5} N. In the presence of less than 2 $\times$ 10^{-5} N concentration of magnesium the

calcium waves are well defined. In order to read an accurate value for the diffusion current of calcium, the concentration of calcium ions should be about 100 times as large as that of magnesium. A few illustrative results are summarized in table 13. Finally, in alcohol–water media, the limiting concentrations of magnesium ions in 0.00099 M calcium solutions were found to be as follows:

MEDIUM	MAGNESIUM-ION CONCENTRATION
	moles per liter
25 per cent C_2H_5OH	2.5×10^{-5}
50 per cent C_2H_5OH	3.0×10^{-5}
80 per cent C_2H_5OH	5.0×10^{-5}

A large number of "unknowns" containing calcium in the presence of traces of magnesium have been analyzed. All experimental results obtained both in water and in ethanol–water mixtures agreed within 3 per cent or better with the actual concentration of calcium in the solution, provided the amount of magnesium

TABLE 13

Diffusion currents of calcium in the presence of magnesium in aqueous medium

CONCENTRATION OF $CaCl_2$ C_1	CONCENTRATION OF $MgCl_2$ C_2	C_1/C_2	DIFFUSION CURRENT CONSTANT (MEASURED) K_m *	DIFFUSION CURRENT CONSTANT WITHOUT Mg K_e *	$\Delta = \dfrac{K_m - K_e}{K_e} \times 100$
M	M		*μa per millimole*	*μa per millimole*	*per cent*
0.79×10^{-3}	1.05×10^{-6}	750	5.86	5.90	-0.7
0.79×10^{-3}	3.3×10^{-6}	240	5.82	5.90	-1.4
0.79×10^{-3}	5×10^{-6}	160	5.99	5.90	$+1.5$
0.39×10^{-3}	5×10^{-6}	78	6.12	5.90	$+3.8$
0.18×10^{-3}	8×10^{-6}	22.5	6.65	5.90	$+12.7$

* For $(m^{2/3} t^{1/6}) = 1.74$ mg.$^{2/3}$ sec.$^{-1/2}$

was kept below the indicated limiting values. In general, however, a separation of calcium from magnesium will be necessary.

SUMMARY

1. With tetraethylammonium iodide as supporting electrolyte in water the calcium wave gives a pronounced maximum and no diffusion current is found. In 50 per cent and especially 80 per cent ethanol the diffusion current can be measured.

2. Lanthanum is a good suppressor of the calcium wave maximum in water. In water–ethanol mixtures barium is more suitable as an eliminator of the maximum.

3. The half-wave potential of calcium in water (maximum eliminated) is independent of the concentration and is equal to -2.220 volts *vs*. S.C.E. In 90 per cent ethanol the half-wave potential is -2.115 volts. After elimination of the maximum, the diffusion current in water and water–ethanol mixtures is

proportional to the calcium concentration. The Ilkovič equation is found to describe the calcium wave.

4. Barium, strontium, and calcium in a mixture can be determined polarographically without separation.

5. The discharge of magnesium ions at the dropping electrode promotes the discharge of hydronium ion. More than traces of magnesium interfere with the polarographic determination of calcium.

6. The relative change of the mobility with increasing ethanol concentration is the same for potassium, sodium, and lithium. It is also the same for barium, strontium, and calcium. The change is much greater for the alkali ions than for the alkaline earth ions.

Acknowledgement is made to the Carnegie Corporation of New York for a grant which enabled us to carry out the work.

REFERENCES

(1) FERGUSSON, A., AND VOGEL, I.: Phil. Mag. **4**, 240 (1927).
(2) KIMURA, G.: Coll. Czechoslov. Chem. Commun. **4**, 492 (1932).
(3) KOHLRAUSCH, F.: Z. Elektrochem. **14**, 129 (1908).
(4) Cf. KOLTHOFF, I. M., AND LINGANE, J. J.: Chem. Rev. **24**, 1 (1939).
(5) MÜLLER, O. H.: Coll. Czechoslov. Chem. Commun. **7**, 321 (1935).
(6) ZLOTOWSKI, I., AND KOLTHOFF, I. M.: Ind. Eng. Chem., Anal. Ed. **14**, 473 (1942).
(7) ZLOTOWSKI, I., AND KOLTHOFF, I. M.: J. Am. Chem. Soc. **66**, 1431 (1944).

COMMUNICATION TO THE EDITOR[1]

ON REPORTS BY F. E. JONES IN THE NOVEMBER, 1944, ISSUE OF THE JOURNAL OF PHYSICAL CHEMISTRY ON STUDIES OF SYSTEMS INVOLVING $CaO-Al_2O_3-SO_3-K_2O-Na_2O-H_2O$ AS CONSTITUENTS

F. E. Jones merits highest praise for an outstanding contribution to the chemistry of cements as presented in his reports on the system $CaO-Al_2O_3-CaSO_4-H_2O$ at 25°C. (J. Phys. Chem. **48**, 34 (1944)) and the two related quinary systems with 1 per cent of potassium hydroxide (J. Phys. Chem. **48**, 356 (1944)) and 1 per cent of sodium hydroxide (J. Phys. Chem. **48**, 395 (1944)), respectively, as fifth components.

In the report on the system $CaO-Al_2O_3-CaSO_4-Na_2O-H_2O$ (loc. cit.) reference is made by Jones to a statement in a discussion (G. L. Kalousek: Am. Concrete Inst. 12 (Proceedings **37**), 692 (1941)) based on results given in a dissertation by the present writer (G. L. Kalousek: Dissertation, University of Maryland, 1941). It is stated in this later discussion that the work "indicated that the stable sulfate-bearing compounds in the presence of NaOH are members of a solid solution

series having $3CaO \cdot Al_2O_3 \cdot CaSO_4 \cdot 12H_2O$ and $3CaO \cdot Al_2O_3 \cdot Ca(OH)_2 \cdot 12H_2O$ as end members." Jones concludes in his report that at a sodium hydroxide or potassium hydroxide concentration of 1 per cent the compound $3CaO \cdot Al_2O_3 \cdot 3CaSO_4 \cdot 32H_2O$ (trisulfate) is the only stable sulfate phase and suggests that solid solutions will occur as a metastable phase as in the quaternary system $CaO-Al_2O_3-CaSO_4-H_2O$. Inasmuch as the difference in conclusion may be traced to a difference of choice regarding criteria for stable equilibrium, the following comments appear pertinent.

In discussing the quaternary system Jones states, "...it thus appears probable that $3CaO \cdot Al_2O_3 \cdot 3CaSO_4 \cdot 32H_2O$ initially formed may eventually change over completely to solid solution." Either of two implications is contained in this statement: (1) the trisulfate is metastable; or (2) the third solid phase, $3CaO \cdot Al_2O_3 \cdot 6H_2O$, besides $Ca(OH)_2$ that is required for invariance, does not appear. In the latter case the solid solution formed would be metastable with respect to $3CaO \cdot Al_2O_3 \cdot 6H_2O$.

Jones's interpretation is given later in the discussion of the quinary system $CaO-Al_2O_3-CaSO_4-K_2O-H_2O$ at 25°C., in which he states, "...at G, for stable equilibrium, formation of $3CaO \cdot Al_2O_3 \cdot 6H_2O$ should occur. From analogy with behavior in the quaternary system $CaO-Al_2O_3-CaSO_4-H_2O$, however, it seems probable that the fundamentally stable phase $(3CaO \cdot Al_2O_3 \cdot 6H_2O)$ will not appear, at any rate for considerable time, and that equilibria will pass into a metastable region where formation of a solid solution of general formula $xCaO \cdot yAl_2O_3 \cdot zCaSO_4 \cdot aq$ commences, and an appropriate metastable equilibrium is set up." The same summary holds true for the findings in the quinary system $CaO-Al_2O_3-CaSO_4-Na_2O-H_2O$ at 25°C. It is seen, therefore, that if $3CaO \cdot Al_2O_3 \cdot 6H_2O$ appears and is the stable phase in the presence of calcium hydroxide in the quinary system, the trisulfate is likewise a stable phase. The composition of the solid solution would be variable as expressed by Jones, and x in the general formula given is not restricted to a value of 3, y being assigned a value of 1.

The determination of the boundary $Ca(OH)_2$-trisulfate (or monosulfate, $3CaO \cdot Al_2O_3 \cdot CaSO_4 \cdot 12H_2O$)-"lime aluminate hydrate" in the system $CaO-Al_2O_3-SO_3-Na_2O-H_2O$ at 25°C. was undertaken by the writer (G. L. Kalousek: Dissertation, University of Maryland, 1941). The sodium hydroxide concentration was varied between 0.0 and about 0.5 N (0.0–20 g. per liter), and the solid phases were precipitated in all tests by mixing aliquots of aqueous solutions of the constituents. In addition to the two known sulfate-bearing compounds, another sulfate phase (solid solution $3CaO \cdot Al_2O_3 \cdot CaSO_4 \cdot 12H_2O-3CaO \cdot Al_2O_3 \cdot Ca(OH)_2 \cdot 12H_2O$, which was isolated and identified) had to be considered. The results of mixtures agitated occasionally and allowed seven to nine weeks to age showed that in the range of sodium hydroxide concentration of about 0.2 to 0.5 N the three phases for the boundary were $Ca(OH)_2$-trisulfate–solid solution. In not a single preparation in this range was there found any of the compound $3CaO \cdot Al_2O_3 \cdot 6H_2O$. Companion mixtures in the same sodium hydroxide range were prepared and set aside. After eighteen months they were examined for $3CaO \cdot Al_2O_3 \cdot 6H_2O$, but none was found. The

other phases (solid solution and trisulfate), except for slight carbonation, appeared to be about the same as in the seven- to nine-week tests. In the range of sodium hydroxide concentration of 0.0 to about 0.15 N, hydrous alumina appeared as a third phase but, since the time of seven to nine weeks seemed short for attainment of equilibrium for a gelatinous phase, no conclusions were drawn. Long-time tests were not carried out in this range. The absence of $3CaO \cdot Al_2O_3 \cdot 6H_2O$ in the prolonged tests indicates either that equilibrium was reached, and therefore, the solid solution is actually a stable phase, or that the compound in question forms very slowly indeed.

Jones's conclusion that $3CaO \cdot Al_2O_3 \cdot 6H_2O$ is the stable phase in the quinary system was actually based on analogy to findings in the quaternary system. In view of the evidence just given, the question arises whether possibly the hexagonal structure is not stabilized by the sulfate ion in the presence of the stated concentrations of sodium hydroxide and that in reality it is the stable structure (i.e., the solid solution is the stable phase). Further experimental work concerned with long-time tests appears to be necessary before a summary conclusion can be made as to which is the stable phase.

Jones's deduction that the trisulfate is formed initially in hydrating cements was not borne out by tests carried out by the writer and reported in detail in the dissertation (loc. cit.). The platy, hexagonal forms instead were precipitated initially from aqueous solutions, simulating in composition those in hydrating cements. These phases persisted as such for periods of 1 to 40 days before starting to convert to the trisulfate. However, only trisulfate precipitated from similar mixtures of solutions designed to yield 1000 g. of the trisulfate, when these solutions were seeded with as little as 0.002 g. of this compound.

The writer is now a member of the staff of the Toledo Calsipore Laboratory of the Research Department of the Owens-Illinois Glass Company, and permission for publication of this communication is granted by the Director of Research. His investigations on these subjects, however, were performed at the National Bureau of Standards in Washington, D. C.

GEORGE L. KALOUSEK.

Owens-Illinois Glass Company
Toledo, Ohio

NEW BOOKS

Outline of the Amino Acids and Proteins. MELVILLE SAHYUN, *Editor.* 251 pp. New York: Reinhold Publishing Corporation, 1944. Price: $4.00.

This comparatively small volume contains a surprising amount of information and is highly recommended as an introduction to or a brief survey of the field. Eleven people, in addition to the editor, have contributed material, and each speaks with authority in his particular field. The purpose of the book is to outline briefly the essentials of the chemistry and the biochemistry of the proteins and the amino acids. The authors have skillfully

refrained "from becoming too deeply involved in the theoretical and the argumentative aspects of the various hypotheses dealing with the chemical structure of proteins, of the relations of proteins to immunological reactions, of theories of denaturation and detoxication, as well as certain thermodynamic considerations." Ample references for further reading are given to the current publications and to the larger treatises.

The book describes the isolation from protein hydrolysates of the accepted amino acids, their syntheses, and methods of analysis. About one-third of the text deals with the metabolism and the nutritive value of the proteins and their constituent amino acids. This portion treats of the rôle of amino acids in detoxication, the metabolism of the amino acids including the intermediates involved, and a consideration of the evidence that certain of the acids are indispensable in the diets of man and the higher animals. The remaining one-third of the text treats of the structure and the denaturation of proteins and includes a brief summary of the proteins as antigens.

Throughout the text the applications to clinical chemistry are indicated and given the major emphasis. The most current viewpoints and techniques are described; for example, the very recent method of assay for amino acids by the use of microörganisms is mentioned. The appendix contains a list of patents issued in the United States on amino acids and related compounds, most of which date from 1930.

W. M. SANDSTROM.

Allgemeine Funktionentheorie—Elliptische Funktionen—Geometrische Funktionentheorie. By A. HURWITZ AND R. COURANT. 534 pp. Berlin, 1929. Published and distributed by Interscience Publishers, Inc., New York. Price: $7.50.

This book is divided into two parts and presents the theory of analytic functions from two different standpoints. The first part, written by Hurwitz, develops the subject almost entirely from the arithmetical point of view in the spirit of Weierstrass. In the second part of the book, by Courant, the main emphasis is placed on the geometrical aspects of the subject which have grown out of the original concepts and discoveries of Riemann. In this third edition no changes have been made in the first part aside from minor improvements in details. The second part, however, has been extended and rearranged in many places so as to take account of recent contributions to the subject, and the introduction has been expanded so that now either one of the two parts may be read independently of the other.

FULTON KOEHLER.

Chemical Engineering Thermodynamics. By BARNETT F. DODGE. 664 pp. New York: The McGraw-Hill Book Company, Inc., 1944. Price: $6.00.

Though this book was written for use by graduate students, it is also very useful for undergraduates because it is based on the fundamental training that chemical engineering students should receive in the first three years of their course. The first two chapters develop the fundamental concepts and definitions underlying the laws of thermodynamics. These are followed by a chapter on the mathematical approach to simple systems and one on the more complex systems. Chapters V and VI set up differential equations and their integrations of the thermodynamic properties. Thus the foundations of the applications of the operations and processes of chemical engineering have been laid. These are presented in separate chapters on compression and expansion of fluids, heat transfer, refrigeration, chemical reaction equilibrium, vaporization and condensation equilibria, distillation processes.

The subject material of this book is presented in a clear manner. Though mathematics is used freely, this supposedly dry subject is made interesting and understandable. The applications are well selected though limited in number. However, if the first six chapters have been mastered, the student should be able to extend the applications in other direc-

tions. This is indeed a sound and excellent textbook of chemical engineering thermodynamics.

<div align="right">CHARLES A. MANN.</div>

Valency, Classical and Modern. By W. G. PALMER. 12×22 cm.; x + 242 pp. Cambridge (England): Cambridge University Press, 1944. Price: 10/6.

There is undoubtedly scope at the present time for another book on valency. The substantial advances which have been made in the last ten years already have an important bearing on many branches of chemistry, and, although the subject has by no means reached a "stationary state"—it is, of course, still developing steadily—many chemists, industrial and academic, undergraduate and postgraduate, will welcome the opportunity of taking stock of the present state of knowledge.

Dr. Palmer's monograph, which is of medium size, will therefore meet a wide demand. It differs from the well-known pioneering textbooks of Sidgwick and Pauling on the one hand and from elementary introductions such as Speakman's small book on the other, in being essentially a concise review of the whole field of valency theory at its present stage.

The treatment is original. The first two chapters deal with the early history of the valency concept and the development of the periodic classification. Chapter III, which occupies nearly a third of the entire book, consists of a summary of the valency behavior of the elements as revealed by direct chemical and physical evidence. In this section no theories are used except the simple "classical" ideas of single and double bonds, steric arrangement, and ionic and covalent binding, but the full weight of modern experimental methods (x-ray crystallography, electron diffraction, dipole moments, spectroscopy, etc.) is brought to bear on the problem. The chapter is therefore a notable survey of recent developments in pure inorganic chemistry, and would be valuable on that account alone.

Chapter IV introduces—unfortunately, in a rather superficial manner—the electronic spin theory of valency, the idea of resonance hybrids, and the isoelectronic principle. With this basis, the probable valency structure of a number of compounds formed between first-row elements is then deduced, and the chapter concludes with a short section on the stereochemistry of the light elements.

Chapters V and VI are of an advanced standard. In the former the spin theory is extended to the Periodic Table generally, and the latter deals briefly with some special topics including coördination compounds, the method of molecular orbitals, aromatic substitution, single-electron bonds, and "proton" bonds.

The book thus provides a very useful, though somewhat uncritical, summary of the modern developments. It would form an excellent outline for a postgraduate course, but is not very suitable for a beginner who needs a lucid exposition of the subject, because it is too highly concentrated in style and matter to be either easy to read, or, by itself, wholly comprehensible. To quote but one example: the concept of resonance hybrids, which is such a characteristic and significant feature of the newer electronic theory as contrasted to the old, is explained sketchily in little more than two short pages—surely too brief a treatment to give the student any real understanding of resonance. In fact, the book needs supplementing at every stage by wide reading. Perhaps this was the author's intention, as he has provided ample references to textbooks and original papers throughout. Nevertheless, in the reviewer's opinion, the book would be vastly improved if, in a future edition when paper shortage is past, the supersaturated text could be diluted with an equal volume of explanatory matter.

The successful production of a textbook of this kind under difficult war-time conditions is a remarkable achievement on the part of both the author and the publishers. The quality is very good for the present time and the price reasonably low.

<div align="right">J. A. KITCHENER.</div>

·EQUILIBRIA OF TWO-DIMENSIONAL SYSTEMS. II[1]

W. B. INNES[2] AND H. H. ROWLEY[3]

Division of Physical Chemistry, State University of Iowa, Iowa City, Iowa

A method of approach in dealing with equilibria between two- and three-dimensional phases has previously been outlined, and this method has been applied to equilibria between a three-dimensional gas or vapor phase and an insoluble surface phase for a single-component system (2). The present study proposes to apply the method to two-component systems.

EQUILIBRIA BETWEEN A THREE-DIMENSIONAL GAS OR VAPOR PHASE AND A TWO-DIMENSIONAL SINGLE-PHASE INSOLUBLE FILM[4] FOR A TWO-COMPONENT SYSTEM AT CONSTANT TEMPERATURE

This system, according to the "modified phase rule" ($V = C - P + 3$) which should be employed when surface phases are present (2), possesses two degrees of freedom, since there are two components and two phases and the temperature is fixed. Utilizing the equilibrium criteria (2) for the two- and three-dimensional systems, respectively:

$$n_1^s \, d\mu_1^s + n_2^s \, d\mu_2^s = A dF \qquad (1)$$

$$n_1 \, d\mu_1 + n_2 \, d\mu_2 = V dp \qquad (2)$$

The superscript s refers to a surface phase; the subscript i refers to the ith component.

A = area occupied by the surface phases,

V = volume occupied by the three-dimensional phases,

F = spreading or surface pressure,

n_i = moles of component i in the three-dimensional phase,

n_i^s = moles of component i in the surface phase,

$$\mu_i = \left(\frac{\delta E}{\delta n_i} \right)_{V,S,n_i}$$

$$\mu_i^s = \left(\frac{\delta E}{\delta n_i^s} \right)_{A,S,n_i^s}$$

E = total energy of the system, and

S = total entropy of the system.

Since:

$$\mu_1 = \mu_1^* \ ; \quad \mu_2 = \mu_2^*$$

$$d\mu_1 = d\mu_1^* \ ; \quad d\mu_2 = d\mu_2^*$$

Hence:

$$n_1^* \, d\mu_1 + n_2^* \, d\mu_2 = A dF \tag{3}$$

$$n_1 \, d\mu_1 + n_2 \, d\mu_2 = V dp \tag{4}$$

Eliminating $d\mu_2$ between equations 3 and 4 and collecting terms:

$$(n_1 n_2^* - n_2 n_1^*) d\mu_1 + n_2 \, A dF = n_2^* \, V dp \tag{5}$$

As there are two independent variables, several relationships are possible. If the chemical potential μ_1 is held constant:

$$n_2 A dF = n_2^* \, V \, dp$$

$$\left(\frac{\partial F}{\partial p} \right)_{\mu_1} = \frac{n_2^* \, V}{n_2 \, A} \tag{6}$$

If the perfect gas law is applied to the three-dimensional phase:

$$V = \frac{nRT}{p}$$

and

$$\left(\frac{\partial F}{\partial p} \right)_{\mu_1} = \frac{n_2^* nRT}{n_2 A p} \tag{7}$$

or

$$\frac{A}{RT} \left(\frac{\partial F}{\partial \ln p} \right)_{\mu_1} = n_2^* \frac{n}{n_2} \tag{8}$$

where n = total moles of gas in the three-dimensional phase and n^* = total moles of gas in the two-dimensional phase.
Letting:

$$X_1 = \frac{n_1}{n} \quad \text{and} \quad X_2 = \frac{n_2}{n}$$

$$X_1^* = \frac{n_1^*}{n^*} \quad \text{and} \quad X_2^* = \frac{n_2^*}{n^*}$$

---

and neglects any contribution of the solid component to the vapor phase. Since the adsorbent adds one component and one phase to the system if it is a pure chemical compound, it can be neglected in applying the phase rule. If it were not a pure substance and were a solid solution, for example, the same would be true if it could be assumed that the adsorbent composition remained constant.

Substituting in equation 8 and rearranging:

$$\frac{A}{RT}\left(\frac{\partial F}{\partial \ln p}\right)_{\mu_1} = n^{\bullet}\frac{X_2^{\bullet}}{X_2} \tag{9}$$

If the pressure is constant, according to equation 5:

$$(n_1 n_2^{\bullet} - n_2 n_1^{\bullet})\, d\mu_1 + n_2\, A dF = 0 \tag{10}$$

Dividing equation 10 by $n^{\bullet}n$;

$$(X_1 X_2^{\bullet} - X_2 X_1^{\bullet})\, d\mu_1 + \frac{X_2}{n^{\bullet}}\, A dF = 0 \tag{11}$$

Remembering:

$$X_2^{\bullet} = 1 - X_1^{\bullet} \quad \text{and} \quad X_2 = 1 - X_1$$

the following relationship is obtained on substitution in equation 11 and simplifying:

$$A\left(\frac{\partial F}{d\mu_1}\right)_{p,T} = \frac{n^{\bullet}(X_1^{\bullet} - X_1)}{X_2} \tag{12}$$

In an analogous fashion to that used in deriving equation 12 the following relation may be obtained:

$$V\left(\frac{\partial p}{d\mu_1}\right)_{F,T} = \frac{n^{\bullet}(X_1 - X_1^{\bullet})}{X_2^{\bullet}} \tag{13}$$

The variations in equation 5 may be carried out while holding constant dependent variables which are completely determined by p and F, such as $X_1^{\bullet}$, $n_1^{\bullet}$, $n^{\bullet}$, and θ, the fraction of the surface covered defined as $n^{\bullet}/\phi$, where ϕ is the number of moles of the same composition required for a complete monolayer. If any of these dependent variables are held constant, according to equation 5, where q represents the dependent variable in question:

$$(n_1 n_2^{\bullet} - n_2 n_1^{\bullet}) + n_2 A\left(\frac{\partial F}{\partial \mu_1}\right)_q = n_2^{\bullet} V\left(\frac{\partial p}{\partial \mu_1}\right)_q$$

Upon dividing through by $n^{\bullet}n$ and assuming that $V = nRT/p$, the following relation is obtained on simplification:

$$A\left(\frac{\partial F}{\partial \mu_1}\right)_q - \frac{n^{\bullet}X_2^{\bullet}}{X_2} RT\left(\frac{\partial \ln p}{\partial \mu_1}\right)_q = \frac{n^{\bullet}(X_1^{\bullet} - X_1)}{X_2} \tag{14}$$

EVALUATION OF SPREADING PRESSURES FROM ADSORPTION DATA

If the two components of a three-dimensional gas or vapor phase can be considered as independent entities so that the total pressure is equal to the sum of the partial pressures exerted through semipermeable membranes and there is no heat effect involved in mixing, then the first and second laws of thermodynamics can be applied separately to each component as below. This statement

is justified by considering a reversible compression with a semipermeable membrane. The work done by the system will be $p_1 dV$, and the heat absorbed will be only that due to compression of the first component, since no heat effect is involved in the removal of the first component from the second component.

$$dE_1 = TdS_1 - p_1 dV + \mu_1 dn_1$$

$$dE_2 = TdS_2 - p_2 dV + \mu_2 dn_2$$

Integrating at constant values for the intensity factors and comparing with the original equations gives at constant temperature:

$$n_1 d\mu_1 = V dp_1$$

$$n_2 d\mu_2 = V dp_2$$

Let it now be assumed that this gas or vapor phase is in equilibrium with a surface phase. Substituting the above expressions for $d\mu_1$ and $d\mu_2$ into equation 3, the following relation is obtained:

$$AdF = \frac{n_1^s}{n_1} V dp_1 + \frac{n_2^s}{n_2} V dp_2 \tag{15}$$

If

$$V = \frac{n_1 RT}{p_1} = \frac{n_2 RT}{p_2}$$

the following relations follow from equation 15:

$$A\left(\frac{\partial F}{\partial p_1}\right)_{p_2} = \frac{n_1^s}{n_1} V = \frac{n_1^s RT}{p_1} \tag{16}$$

$$\left(\frac{\partial p_1}{\partial p_2}\right)_F = -\frac{n_1 n_2^s}{n_2 n_1^s} = -\frac{X_1 X_2^s}{X_2 X_1^s} \tag{17}$$

By integration of equation 15 the spreading pressure may be evaluated. Thus:

$$FA = \int_0^{p_1} \frac{n_1^s}{n_1} V dp_1 + \int_0^{p_2} \frac{n_2^s}{n_2} V dp_2 \tag{18}$$

if

$$V = \frac{n_1 RT}{p_1} = \frac{n_2 RT}{p_2}$$

$$FA = RT \int_0^{p_1} n_1^s d \ln p_1 + RT \int_0^{p_2} n_2^s d \ln p_2 \tag{19}$$

Hence, the spreading pressure may be evaluated if amounts adsorbed of each component are known functions of the partial pressures over the indicated limits. However, in general n_1^s and n_2^s are functions of both p_1 and p_2, so that the evaluation is not as simple as it might first appear.

EQUILIBRIA BETWEEN A THREE-DIMENSIONAL VAPOR PHASE, A THREE-DIMEN-
SIONAL LIQUID PHASE,[5] AND A TWO-DIMENSIONAL SURFACE PHASE AT
CONSTANT TEMPERATURE FOR A TWO-COMPONENT SYSTEM

According to the "modified phase rule" given above (2), a system of this type possesses one degree of freedom. Application of the first law of thermodynamics, integration with constant values for the intensity factors, and comparison with the original equations gives for the different phases, since $\mu_i = \mu_i^L = \mu_i^s$ and $dT = 0$:

$$n_1 \, d\mu_1 + n_2 \, d\mu_2 - V dp = 0 \tag{20}$$

$$n_1^L \, d\mu_1 + n_2^L \, d\mu_2 - V^L dp = 0 \tag{21}$$

$$n_1^s \, d\mu_1 + n_2^s \, d\mu_2 - A dF' = 0 \tag{22}$$

where the subscripts refer to the ith component, the superscript L refers to the liquid phase, the superscript s refers to the surface phase, the absence of a superscript indicates the vapor phase, A represents the surface area, and F' is the spreading or surface pressure.

There are three linear equations by means of which the two quantities $d\mu_1$ and $d\mu_2$ can be eliminated. Thus in the notation of determinants:

$$\begin{vmatrix} V & n_1 & n_2 \\ V^L & n_1^L & n_2^L \\ 0 & n_1^s & n_2^s \end{vmatrix} dp = \begin{vmatrix} 0 & n_1 & n_2 \\ 0 & n_1^L & n_2^L \\ -A & n_1^s & n_2^s \end{vmatrix} dF'$$

Evaluation then gives the following expression:

$$\left(\frac{\partial p}{\partial F'} \right)_T = \frac{-A \, (n_1 n_2^L - n_1^L n_1)}{(n_1^s n_2 - n_1 n_2^s) V^L + (n_1^L n_2^s - n_2^L n_1^s) V} \tag{23}$$

Upon dividing through by the total number of moles in the different phases so as to obtain mole fractions and simplifying, equation 23 becomes:

$$\left(\frac{\partial p}{\partial F'} \right)_T = \frac{-A n n^L (X_1 - X_1^L)}{n^s n (X_1^s - X_1) V^L + n^s n^L (X_1^L - X_1^s) V} \tag{24}$$

where the symbols X_i, X_i^L, X_i^s refer to mole fractions of the component i in the gas, liquid, and surface phases, respectively.

[5] Considerations are limited to cases where the three-dimensional liquid phase is not contiguous with the surface phase. This situation is probably realized in most cases where the contact angle is not zero, under which condition the three-dimensional liquid phase will not spontaneously distill on top of the surface phase. It also may be realized if steric reasons prevent a three-dimensional liquid phase from being in contact with the surface phase, a situation which is probably closely approximated, owing to fine pore structure, in the case of most charcoals and chabasite.

In general the following relation is a good approximation:

$$\frac{V}{n} \gg \frac{V^L}{n^L}$$

Hence:

$$Vn^L n^\bullet \gg V^L nn^\bullet$$

If $(X_1^\bullet - X_1) \ggg (X_1^L - X_1^\bullet)$, it would be a good approximation to neglect the term involving V^L in equation 24, giving on simplification:

$$\left(\frac{\partial p}{\partial F'}\right)_T = \frac{-An(X_1 - X_1^L)}{n^\bullet(X_1^L - X_1^\bullet)} \tag{25}$$

If $V = nRT/p$, then on simplifying:

$$A\left(\frac{\partial F'}{\partial \ln p}\right)_T = \frac{n^\bullet(X_1^\bullet - X_1^L)RT}{(X_1 - X_1^L)} \tag{26}$$

Equation 26 can be integrated at constant area giving:

$$A(F_2' - F_1') = RT \int_{p_1}^{p_2} \frac{n^\bullet(X_1^\bullet - X_1^L)}{(X_1 - X_1^L)} \tag{27}$$

The quantities $d\mu_2$ and dp may be eliminated between equations 20, 21, and 22, giving in the notation of determinants:

$$\begin{vmatrix} A & n_2^\bullet & 0 \\ 0 & n_2^L & -V^L \\ 0 & n_2 & -V \end{vmatrix} dF' = \begin{vmatrix} n_1^\bullet & n_2^\bullet & 0 \\ n_1^L & n_2^L & -V^L \\ n_1 & n_2 & -V \end{vmatrix} d\mu_1$$

Evaluating:

$$A\left(\frac{\partial F'}{\partial \mu_1}\right)_T = \frac{(n_1^L n_2^\bullet - n_1^\bullet n_2^L)V + (n_2 n_1^\bullet - n_1 n_2^\bullet)V^L}{(n_2 V^L - n_2^L V)} \tag{28}$$

This may be simplified as in the previous case, giving:

$$A\left(\frac{\partial F'}{\partial \mu_1}\right)_T = \frac{n^L n^\bullet(X_1^L - X_1^\bullet)V + nn^\bullet(X_1^\bullet - X_1)V^L}{(n_2 V^L - n_2^L V)} \tag{29}$$

If

$$\frac{V}{n_2} \gg \frac{V^L}{n_2^L} \quad \text{and} \quad \frac{V}{n} \gg \frac{V^L}{n^L}$$

and it is further assumed that

$$(X_1^\bullet - X_1) \ggg (X_1^L - X_1^\bullet)$$

then by neglecting terms of second-order magnitude and simplifying, the following relation is obtained:

$$A \left(\frac{\partial F'}{\partial \mu_1} \right)_T = - \frac{n^s (X_1^L - X_1^s)}{X_2^L} \tag{30}$$

The above equation is similar in form to that obtained for a two-phase system (see equation 12). The difference is that this relation imposes the conditions of equilibrium with a liquid three-dimensional phase, while the relationship for a two-phase system imposed the condition of constant pressure. No special assumptions were employed in deriving the latter.

SUMMARY

Several thermodynamic relationships involving equilibria between a three-dimensional gas or vapor phase and a two-dimensional insoluble surface phase for a two-component system have been derived. One of these makes possible the evaluation of spreading pressures from two-component adsorption data.

Equilibria between a three-dimensional liquid and vapor phase and a surface phase for a two-component system have also been treated and several relationships derived. One of these relates the selective adsorption to the change of spreading pressure with chemical potential.

REFERENCES

(1) INNES, W. B.: Ph. D. Dissertation, State University of Iowa, 1941.
(2) ROWLEY, H. H., AND INNES, W. B.: J. Phys. Chem. **46**, 537 (1942).

THE HYDRATE NATURE OF SOAP

K. W. GARDINER, M. J. BUERGER, AND L. B. SMITH

Research Department, Lever Brothers Company and the Massachusetts Institute of Technology, Cambridge, Massachusetts

I. INTRODUCTION

The degree of hydration of solid soap systems has been the subject of many physicochemical examinations, of which only a few are cited here (11, 12, 14), and much valuable information has been derived from these studies. However, there is some question whether the relation of hydration to structure was recognized in these earlier investigations. The inadequacy of the earlier experimental techniques employed became evident when Buerger *et al.* (2, 3) established the hemihydrated character of the alpha forms of sodium stearate and sodium palmitate. These investigations showed that the amount of hydrate moisture present is directly associated with the crystalline phase of the soap as

distinguished by x-ray diffraction photographs. The desirability of extending structural-hydration studies is apparent, especially in view of the many crystal phase forms now recognized (4, 7, 8).

A method combining the results obtained by controlled dehydrations and x-ray diffraction studies has been developed and successfully employed in determining the nature and amount of water present in many of the crystalline forms. The samples examined have been prepared by crystallizing pure single soaps or acid soaps from organic solvents and by intensely working concentrated soap–water systems in a small laboratory mixer. It is the purpose of this paper to describe the dehydration technique and to present some of the results that have been obtained by its use in conjunction with x-ray diffraction studies.

II. MATERIALS

All the sodium soaps used were prepared directly by neutralizing the corresponding pure methyl esters with a 25 per cent aqueous sodium hydroxide solution. The esters were obtained by a careful fractional distillation of esterified fatty acids derived from the treatment of selected natural fats and oils. Stearic acid needed for the preparation of the acid soap compound $1NaC_{18}:1HC_{18}$ was produced by the acidulation of pure sodium stearate. The resulting fatty acid was extracted, washed, and twice recrystallized from acetone at $-20°C$.

Crystals of the alpha form of neutral sodium stearate and of the alpha form of the 1:1 acid soap (1) suitable for dehydration were grown from solution in 95 per cent ethyl alcohol at room temperature. The large crystals that appeared were filtered and freed of all extraneous or occluded solution before being examined.

Samples of sodium caprate, sodium myristate, sodium palmitate, sodium stearate, and sodium oleate, representing in part the large group of discrete crystalline phases occurring in "worked" soap systems (4), were prepared at various temperatures and moisture contents in a small reciprocating piston-type mixer. Crystalline calcium palmitate produced by the method described by W. Faber (6) was kindly supplied by Dr. C. W. Sheppard of the Massachusetts Institute of Technology. The $CuSO_4 \cdot 5H_2O$ used as a reference sample was of C.P. reagent grade and was examined directly without any further treatment.

III. EXPERIMENTAL

The experimental procedure consists essentially in noting the losses in weight which occur when the sample being studied is heated to successively higher temperatures in an atmosphere of constant partial pressure of water vapor. A schematic drawing of the dehydration equipment used is shown in figure 1. In principle it is very similar to that employed by Milligan (16) and by Weiser and Milligan (17, 20, 21, 22) in studying hydrous and hydrated compounds, and more recently by Kelley, Jenney, and Brown for similar work on soil colloids (9). Small aluminum weighing pans (A) containing 3-g. to 5-g. samples of the material to be dehydrated are supported in an electrically heated oven on a circular

platform (B). The platform, which can accommodate up to seven samples, can be lifted and rotated, permitting the wire bails of each pan to be engaged in turn by the fine wire hook (C) attached to the arm of a Becker surface-
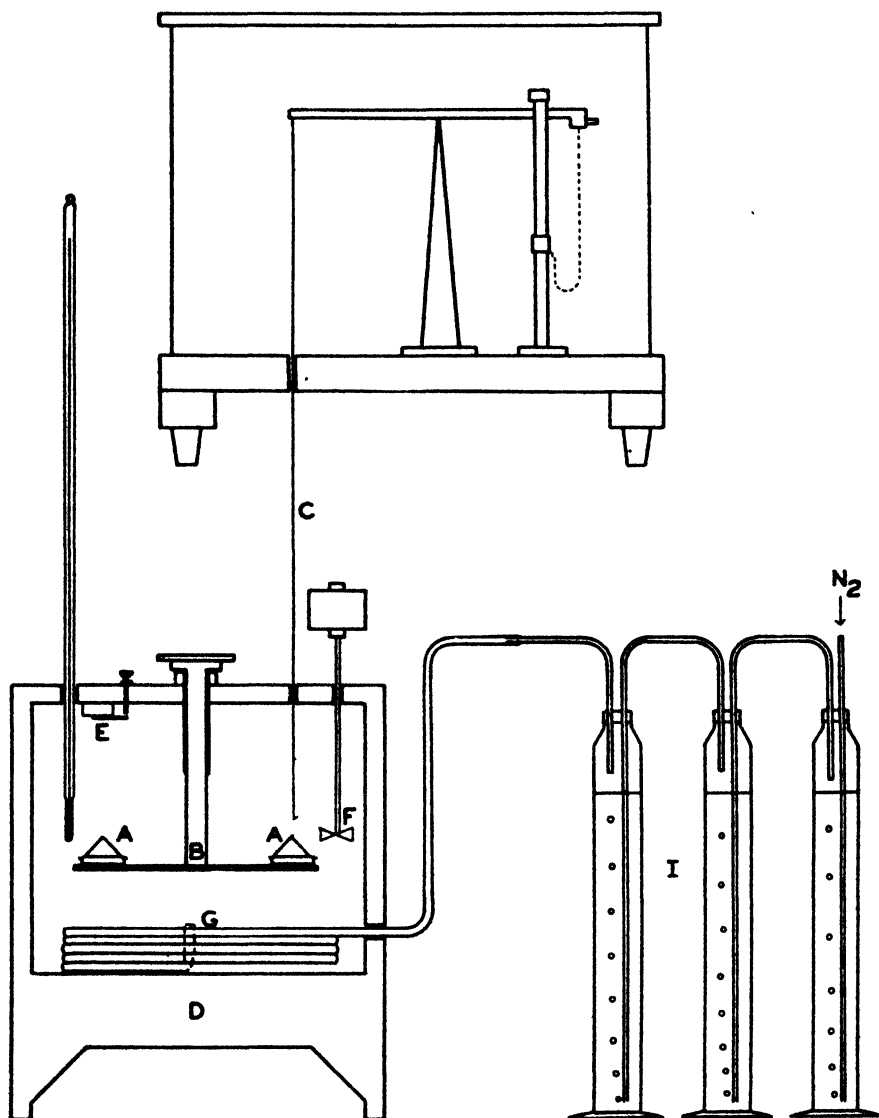
Fig. 1. Dehydration equipment

tension balance. In this manner the individual weighings of a relatively large number of specimens can be rapidly made without the necessity of removing them from the oven. All samples are run in duplicate so that small portions can be taken for x-ray powder photographs after each step of the dehydration

process. The structural significance of any detected losses in weight that may occur can thus be readily determined.

The dehydration is controlled by passing a moist stream of nitrogen of constant vapor tension through the oven and by carefully adjusting the temperature. The moisture content of the gas stream is fixed by bubbling it through a series of wash towers (I) containing saturated brine solutions. After being humidified, the nitrogen passes through a preheating coil (G) and finally enters the oven. The temperature is slowly raised by small increments and can be maintained at any desired value by means of a thermoregulator and voltage-control unit. The weight of each sample is taken after each 5°C. increase in temperature and a plot of loss in weight vs. temperature is made.

IV. DISCUSSION

The interpretation of the dehydration curves shown here (figures 2–8) is based upon the previously demonstrated principle (9, 16, 17, 21, 22) that true hydrate water is lost suddenly when a temperature is reached at which the dissociation pressure of the hydrated compound just exceeds the partial pressure of water vapor in the surrounding atmosphere. This sudden loss of moisture is represented by a sharp stepwise break in the dehydration curve, while adsorbed water is lost more or less continuously as the temperature is raised. As already mentioned, the significance of each inflection of the curve is determined by an x-ray diffraction study of the material, both before and after the loss in weight has occurred. This has been done for each of the soap samples studied. The discussion is divided into three sections: the first deals with a check on a known hydrate, the second with the dehydration of soap crystals prepared from solvent solutions, and the third with a description of the dehydration behavior of the individual phases produced in "worked" soap–water systems.

Check on a known hydrated crystal

As a check on the validity of the method, an inorganic salt of a known degree of hydration was examined simultaneously with the soap crystals. $CuSO_4 \cdot 5H_2O$ was chosen for this purpose, since the manner in which it loses its hydrate water is well known.

Figure 2 represents a plot of the loss in weight of a 5-g. sample of the copper salt when examined by the dehydration technique. The very sharp step in the curve occurring between 35°C. and 43°C. represents a loss of approximately 15 per cent in weight, or two moles of water per mole of copper sulfate pentahydrate. A second sharp rise at 45°C. to 55°C. again corresponds to the loss of about 15 per cent moisture, or two more moles of water to a mole of salt. The overall decrease in weight occurring between 35°C. and 55°C. is equal to approximately 30 per cent water, or four moles of water lost in two steps of $2H_2O$ each. The fifth molecule of water present is held quite firmly, as indicated by the flat portion of the curve after 55°C., and it has been found that a further loss in weight does not occur below 125°C. This is in very good agreement with the known dehydration behavior of this compound.

Dehydration of crystals grown from solution

As an example of a simple hydrated soap, the case of calcium palmitate, hitherto regarded as non-hydrated, is presented. Figure 3 shows the loss in weight recorded on dehydrating the sample. The sharp break in the curve noted at 90–100°C. represents the loss of 3.0 per cent of hydrate moisture, a value which is in very close agreement with the theoretical value of 3.17 per cent required for the monohydrate. X-ray powder diffraction photographs of the
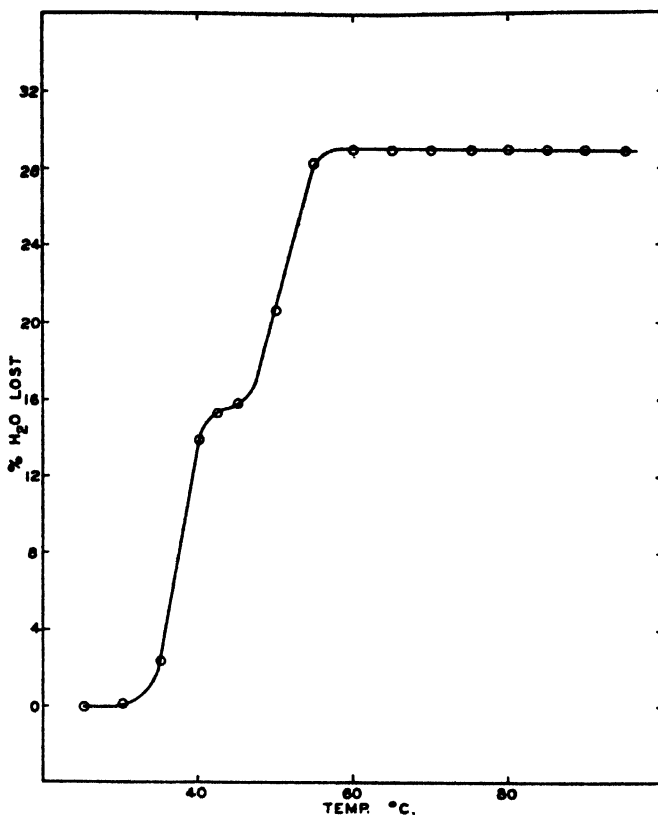
Fig. 2. Dehydration curve of copper sulfate pentahydrate

crystals before and after heating show that a definite change in the crystal structure accompanies the dehydration process.

As an example of the behavior of a non-hydrated soap, the case of alpha 1:1 acid sodium stearate is next presented. The existence of stoichiometric acid soaps of the formula 1 soap:1 fatty acid has been recognized for some time (5, 10, 13, 15, 18). Although Malkin made use of x-ray diffraction in examining several of these compounds (15), it was only recently that they were made the subject of a thorough x-ray diffraction study (1). Large crystals of the alpha form (1) of the acid soap $1NaC_{18}:1HC_{18}$, suitable for both x-ray crystal studies

and dehydration, were prepared from 95 per cent alcohol solutions. The dehydration curve for a 3-g. sample of the material is shown on figure 4, and it is
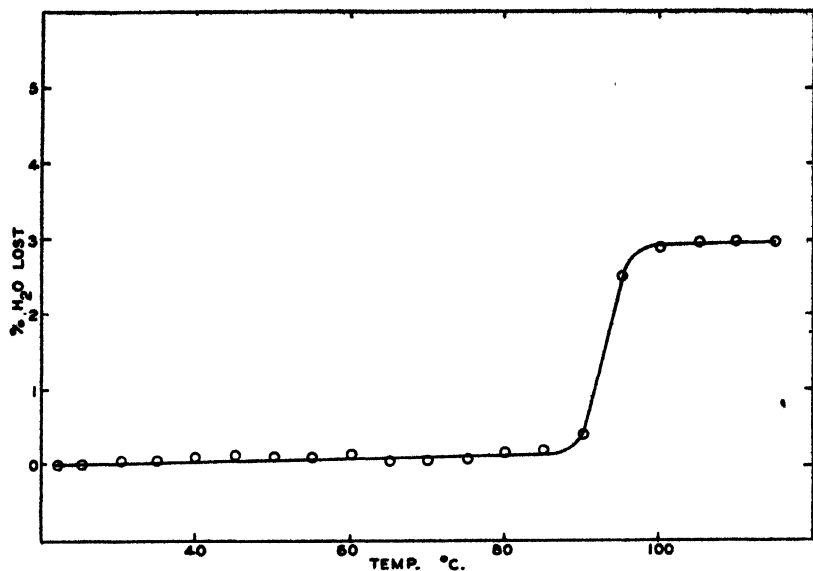
Fig. 3. Dehydration curve of calcium palmitate
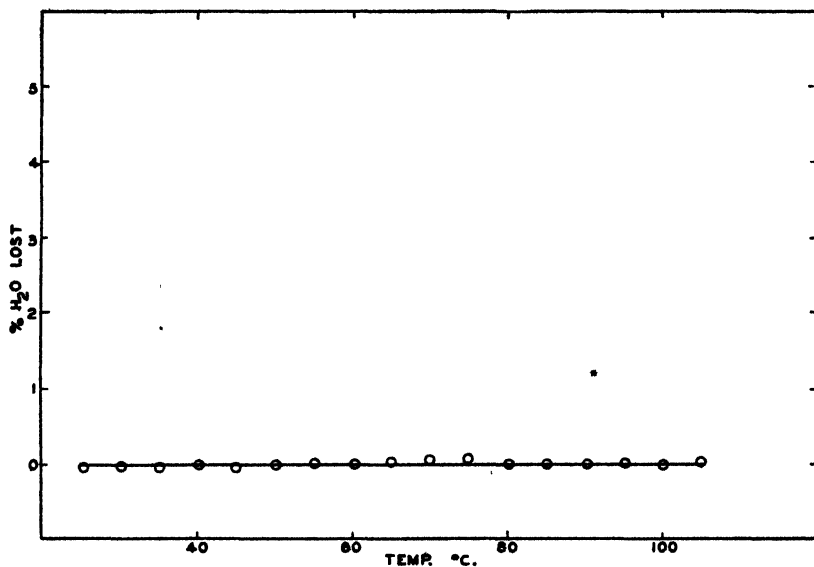
Fig. 4. Dehydration curve of alpha 1:1 acid sodium stearate

apparent that no loss in weight could be detected between room temperature and 105°C. Further heating above this point resulted in decomposition of the crystals as fatty acid slowly distilled off at elevated temperatures. From this

behavior it is evident that the alpha acid soaps are anhydrous. The x-ray powder pattern of the material remains unchanged after heating to 105°C., as would be expected if no change in hydration occurs.

Figure 5 shows the somewhat more complicated dehydration curve obtained when the starting material is composed of crystals of the alpha form of neutral sodium stearate grown from an alcoholic solution. As shown by the curve, the loss of hydrate moisture occurs in several steps. The first inflection, corresponding to a loss of 3/8 H_2O per mole of soap, occurs slightly below 50°C. and is associated with the alpha-to-beta transformation reported by Thiessen and Stauff (19). The second decrease in weight of the sample, occurring between 55°C. and the end of the experiment, represents the dehydration of Thiessen and Stauff's beta form of sodium stearate. This amount is necessarily the
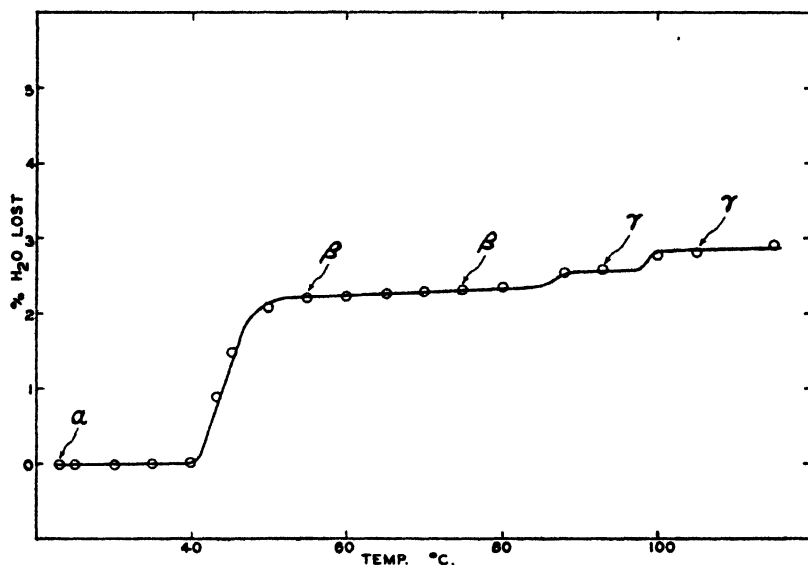
Fig. 5. Dehydration curve of alpha sodium stearate crystals

difference between the recorded total loss of 1/2 H_2O, representing the degree of hydration of the alpha form, and the amount lost on the formation of beta,— namely, 3/8 H_2O, or a net loss of 1/8 H_2O per mole of soap. X-ray powder diffraction photographs show that the inflection at about 85°C. is concomitant with a change in phase from beta to gamma. These values for hydrate water content confirm the earlier work of Buerger et al. (3) on the degree of hydration of the alpha and beta phases.

Dehydration of some typical phases occurring in worked soap–water systems

κ *sodium caprate:* A sample of the kappa phase (4) was prepared by working sodium caprate at 30 per cent water and 88°C. in a small laboratory mixer for about 30 min. The material produced was air dried and then placed in the dehydrator. Figure 6 represents a plot of the loss in weight recorded as the
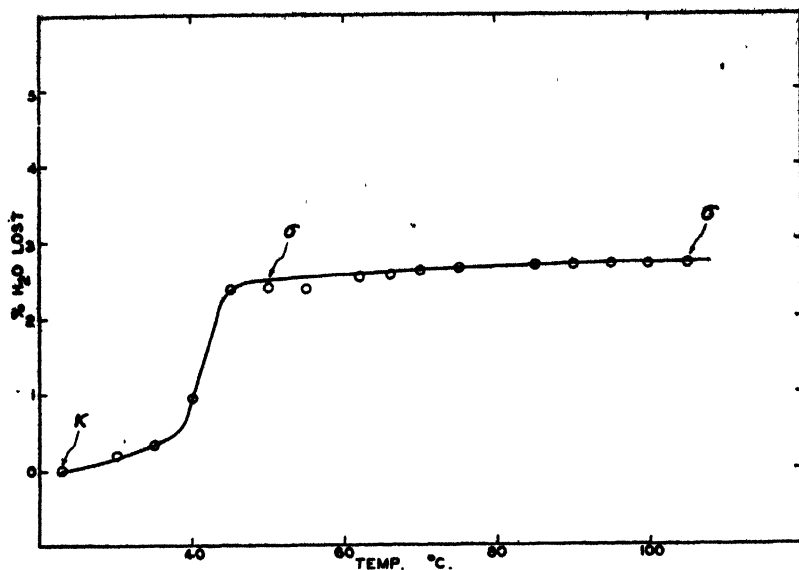
Fig. 6. Dehydration curve of kappa sodium caprate prepared at 30 per cent
water content and 88°C.
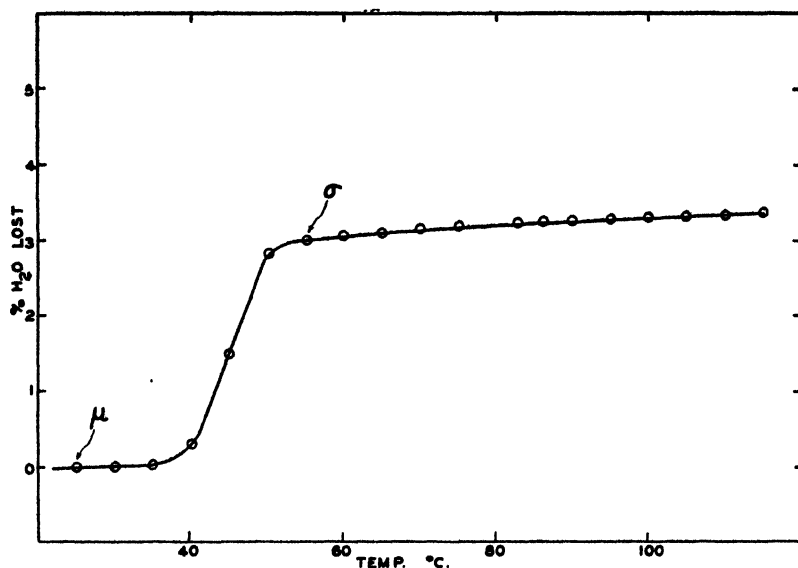
Fig. 7. Dehydration curve of mu sodium myristate prepared at 40 per cent
water content and 49°C.

temperature was slowly raised by 5°C. increments. The sharp step-like break
at 40–45°C. corresponds to the loss of approximately 2.1 per cent moisture.
This figure is in very good agreement with the theoretical value of 2.17 per cent

H₂O needed to satisfy the formula C₉H₁₉COONa·1/4H₂O. The x-ray powder photograph of the material after heating to 50°C. revealed that the decrease in moisture content resulted in a change of phase from kappa to another, believed to be sigma (4). The relative stability of this latter phase is indicated by the fact that continued heating to 105°C. produced no further change in the x-ray powder photograph.

μ sodium myristate: The hydrate nature of the mu phase (4) is shown by the curve obtained on dehydrating an air-dried sample of sodium myristate (figure 7) prepared by working the soap at 49°C. and 40 per cent water content. The curve is characterized by a sharp break at 40–50°C., representing the loss of about 3.0 per cent hydrate water which occurs simultaneously with the change
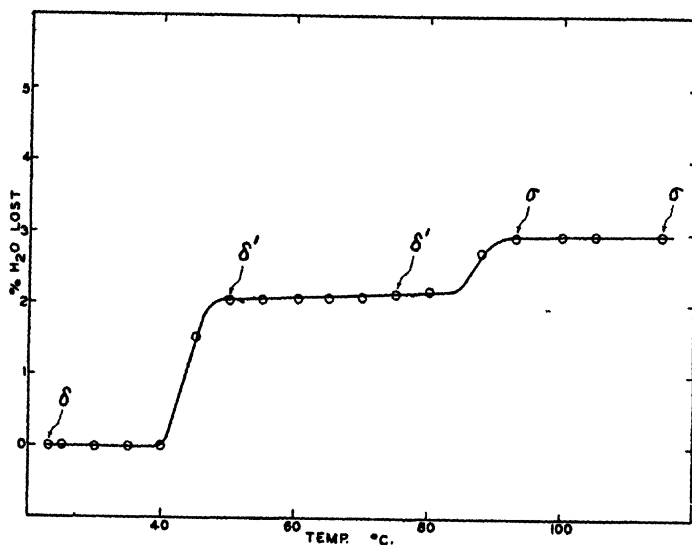
Fig. 8. Dehydration curve of delta sodium palmitate prepared at 40 per cent water content and 49°C.

in phase from mu to sigma. The theoretical amount of moisture necessary for a compound of the type C₁₃H₂₇COONa·3/8H₂O is 2.90 per cent, indicating that the mu phase is approximately a 3/8 hydrate. No further loss in weight was recorded, although the sample was heated to 150°C.

δ, ε, and ζ sodium palmitate: Delta (δ) sodium palmitate was produced by intensely working a sample of the pure soap containing 40 per cent moisture at 49°C. After being allowed to come to a constant weight in the dehydrator at room temperature, the material was then slowly heated.

Figure 8 is a plot of the loss in weight recorded as the sample was heated to 115°C. The first sharp inflection in the curve at 40–50°C. represents the loss of about 2.1 per cent of water, corresponding to the liberation of 1/3 H₂O per mole of soap. This is accompanied by a very slight but real alteration in

the powder photograph of the material. This phase resulting from partially dehydrating delta has been designated delta prime (4). A second inflection in the curve at 85°C. represents the loss of approximately 1.0 per cent of moisture, which corresponds to about 1/6 H_2O. This loss, however, is accompanied by a complete change in powder photograph from the delta prime pattern, mentioned above, to the sigma pattern. The overall loss in moisture content at 105°C. is therefore 3.1 per cent, a value which is in good agreement with the theoretical value of 3.13 per cent necessary for the hemihydrate.

A sample of the epsilon form (4) of sodium palmitate, made by working the soap with 20 per cent moisture at 77°C., has a dehydration curve very similar in character to that of the delta form. The two steps in the curve, however, represent losses of approximately 3/8 H_2O and 1/8 H_2O at 45°C. and 90°C., respectively. The overall loss of 1/2 H_2O per mole of soap indicates that epsilon sodium palmitate prepared in this manner is a hemihydrate. The powder pattern of the material is only slightly modified from epsilon to epsilon prime (4) by the first dehydration step, but there is a sharp change from epsilon prime to the sigma pattern accompanying the last loss of hydrate water.

The dehydration curve of zeta sodium palmitate, produced by working the soap with 30 per cent water at 99°C., also shows two stepwise losses of hydrate moisture. The first sharp inflection at 40–45°C. represents a decrease of 1.7 per cent in the weight of the sample. At the same time the original zeta phase transforms to the beta phase (4). The amount of moisture lost corresponds to about 1/4 H_2O per mole of soap. A further loss in weight amounting to 1/8 H_2O per mole of soap is represented by a second break in the curve at approximately 85°C. Powder photographs show that this decrease accompanies the change in phase from beta to sigma. The overall loss in moisture content at 105°C. appears to be equal to about 2.7 per cent. This amount is in fair agreement with the value of 2.37 per cent H_2O satisfying a compound of the type $NaC_{16} \cdot 3/8 H_2O$.

δ, ε, *and* ζ *sodium stearate:* The curves representing the loss in weight on dehydration for the delta, epsilon, and zeta forms of sodium stearate are similar to those described above for the corresponding forms of sodium palmitate. In each case the moisture loss associated with the first dehydration break is the same for sodium stearate and sodium palmitate. The loss of hydrate water represented by the second step in the dehydration process, however, appears to be slightly greater for the delta, epsilon, and zeta forms of sodium stearate. The values for the degree of hydration of these forms are not included here because of the incomplete nature of the data. At the present time we believe the results for sodium palmitate are the more reliable of the two.

η *sodium oleate:* The eta form (4) of sodium oleate was prepared by working the soap with 5 per cent water at 71°C. The dehydration curve of this material showed one step representing the loss of about 1.5 per cent moisture, or 1/4 H_2O, at 50–60°C. The dehydration is accompanied by a change in powder pattern from eta to eta prime (4).

In a subsequent communication we hope to present a more detailed descrip-

tion of the dehydration behavior of some of the soap phases that have been only briefly mentioned here.

SUMMARY

A method combining the use of controlled dehydrations and x-ray diffraction analysis has been employed in studying the hydrate nature of several crystalline forms of soap. Calcium palmitate, as prepared, is a monohydrate and loses moisture in one step with an accompanying change in powder pattern.

The alpha form of 1:1 acid sodium stearate, on the other hand, is shown to be a non-hydrated phase at room temperature and no change in the powder pattern occurs on heating the crystals to 105°C.

The hemihydrate composition of the neutral alpha variety of sodium stearate has been confirmed. Thiessen and Stauff's alpha-to-beta transformation is shown to be associated with the loss of 3/8 H_2O per mole of soap, while another 1/8 H_2O is lost on complete dehydration, producing the anhydrous form.

The dehydration curves for kappa sodium caprate, mu sodium myristate, and delta sodium palmitate are presented as typical of the dehydration behavior of the large class of phases which occur in "worked" soap–water systems. These phases are definite hydrates containing 1/4, 3/8, and 1/2 mole of water per mole of soap, respectively.

A study of the dehydration behavior of several other "worked" soap phases has also been made. The phases and their approximate hydrate content are as follows: epsilon sodium palmitate, 1/2 H_2O; zeta sodium palmitate, 3/8 H_2O; eta sodium oleate, 1/4 H_2O.

Phases which are partial dehydration products of other phases appear to have the following compositions: delta prime sodium palmitate, 1/6 H_2O; epsilon prime sodium palmitate, 1/8 H_2O; and beta (equivalent to zeta prime) sodium palmitate, 1/8 H_2O.

As a result of this work it is believed that all neutral sodium soap phases occurring in the central areas of the phase maps of worked soap–water systems are definite hydrates.

REFERENCES

(1) BUERGER, M. J.: Am. Mineral. **30**, 551–71 (1945).
(2) BUERGER, M. J.: Proc. Natl. Acad. Sci. U. S. **28**, 529 (1942).
(3) BUERGER, M. J., SMITH, L. B., DE BRETTEVILLE, A., AND RYER, F. V.: Proc. Natl. Acad. Sci. U. S. **28**, 526 (1942).
(4) BUERGER, M. J., SMITH, L. B., RYER, F. V., AND SPIKE, J. E.: Proc. Natl. Acad. Sci. U. S. **31**, 226–32 (1945).
(5) EKWALL, P., AND MYLIUS, W.: Ber. **62**, 1080 (1929).
(6) FABER, W.: Centr. Mineral. Geol. **1933A**, 191.
(7) FERGUSON, R. H.: Oil & Soap **21**, 6 (1944).
(8) FERGUSON, R. H., ROSEVEAR, F. B., AND STILLMAN, R. C.: Ind. Eng. Chem. **35**, 1005 (1943).
(9) KELLEY, W. P., JENNEY, H., AND BROWN, S. M.: Soil Sci. **41**, 259 (1936).
(10) McBAIN, J. W., AND FIELD, M. C.: J. Chem. Soc. **1933**, 920.
(11) McBAIN, J. W., AND LEE, W. W.: Oil & Soap **20**, 17 (1943).
(12) McBAIN, J. W., AND LEE, W. W.: Ind. Eng. Chem. **35**, 784 (1943).

(13) McBAIN, J. W., AND STEWART, A.: J. Chem. Soc. 1927, 1392.
(14) McBAIN, J. W., VOLD, R. D., AND JOHNSTON, S.: J. Am. Chem. Soc. 63, 1000 (1941).
(15) MALKIN, T.: Ber. 63, 1807 (1930).
(16) MILLIGAN, L. H.: J. Phys. Chem. 26, 247 (1922).
(17) MILLIGAN, W. O., AND WEISER, H. B.: J. Phys. Chem. 41, 1029 (1937).
(18) OUDEMANS, A. C.: J. prakt. Chem. 89, 206 (1863).
(19) THIESSEN, P. A., AND STAUFF, J.: Z. physik. Chem. A176, 397 (1936).
(20) WEISER, H. B., AND MILLIGAN, W. O.: J. Phys. Chem. 38, 513 (1934).
(21) WEISER, H. B., AND MILLIGAN, W. O.: Chem. Rev. 25, 1 (1939).
(22) WEISER, H. B., AND MILLIGAN, W. O.: J. Am. Chem. Soc. 59, 1456 (1937).

RELATIONSHIPS BETWEEN THE VELOCITY OF SOUND AND OTHER PHYSICAL PROPERTIES OF LIQUIDS

R. T. LAGEMANN AND W. S. DUNBAR

Department of Physics, Emory University, Emory University, Georgia

In the past the chief use of measurements of the velocity of sound in liquids has been in the determination of the adiabatic compressibility from which the ratio of the specific heats may be found provided the isothermal compressibility is known. At the same time certain qualitative facts relating the sound velocity to structure have become well known. These showed that the velocity of sound itself was not an additive and constitutive property, and little application of measurements of the velocity of sound to the elucidation of molecular structure seemed possible, until Rao discovered a function of the velocity which was independent of the temperature.

Rao (15, 16) showed that in any one liquid the density and the velocity of sound are connected by the relation $v^{1/3}M/d = V$, where v is the velocity of sound, d the density measured at the same temperature as the velocity, M the molecular weight, and V a constant independent of the temperature. It is the purpose of this communication to draw attention to the very simple relationships existing between the quantity V, which we choose to call the molecular sound velocity, and certain other physical properties. These relations have been applied only to the lower members of some homologous series. As more data are accumulated the relations will probably be more generally applicable.

LINEAR RELATIONSHIPS OF MOLECULAR SOUND VELOCITY

For the members of each homologous series for which data are available, it has been found that a linear relationship exists between the molecular sound velocity and the following physical properties: molecular refraction (M_D), parachor (P), Souders' viscosity constant (I), van der Waals' b (b), molecular magnetic rotation (T), and the critical volume (V_c). In a graphical plot of any of these properties against V, the slopes of the straight lines obtained for

the series of homologues are very nearly identical, but the intercepts vary. In most cases the curves for all the series are almost coincident, and to a good approximation a single line would represent the data for all compounds. To make such graphs, values of V were taken from Rao (16), values of M_D from Herz (7), Eisenlohr (5), and the Landolt-Börnstein tables (10), values of P, b, and V_c from the Landolt-Börnstein tables (10), values of I from Souders (19), and values of T from Perkin (14). The plots show a typographical error in Souders' data (19), where the value of I for ethyl alcohol should be 171, not 117.
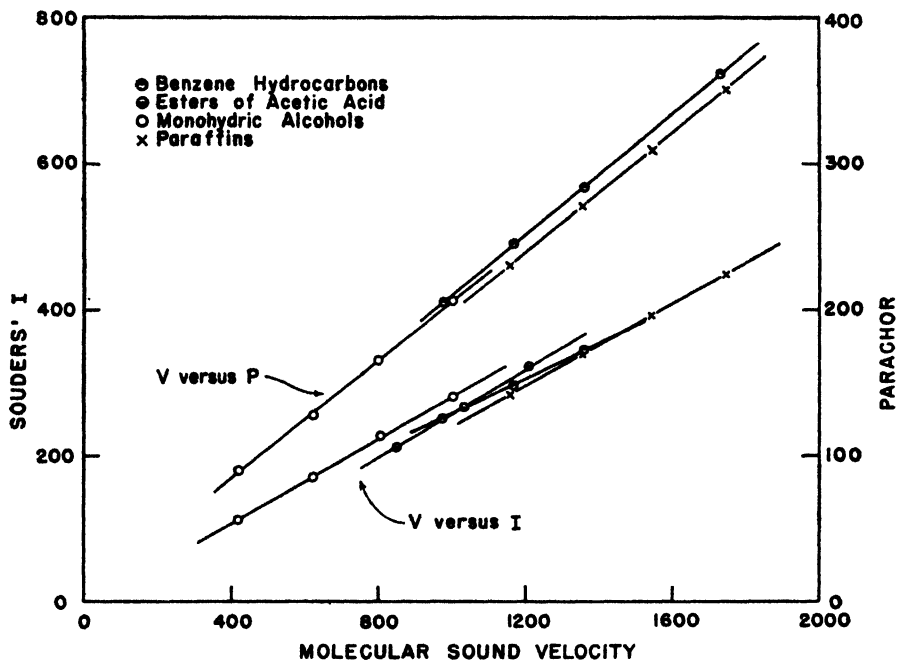
FIG. 1. Relation of molecular sound velocity to the parachor and Souders' I

Figure 1 shows the relationship between the molecular sound velocity and the parachor and Souders' I for four homologous series. Plots of V against the other properties mentioned above have a similar appearance.

On the assumption that a linear relation holds for each homologous series, the constants A and B of the relation $V = A + BX$ have been evaluated by the method of least squares and are listed in table 1. X may be any of the quantities: mole refraction, parachor, van der Waals' b, Souders' I, critical volume, or molecular magnetic rotation. Table 2 shows how well the data are fitted by these equations. Here values of the observed molecular sound velocity are listed in the third column. In column 4 appear values of the molecular sound velocity calculated from the mole refraction values of column 2 by use of the appropriate constants taken from table 1. The average error of about 0.5 per cent between the calculated and observed values of V is characteristic of

the small error involved in connecting any of the other physical properties with the molecular sound velocity.

It is obvious that the constants recorded in table 1 may be used to find values of V for higher members of the series from known values of any other of the

TABLE 1

Constants of the linear equations relating molecular sound velocity and other physical properties

SERIES	M_D		P		I		b		T	
	A	B	A	B	A	B	A	B	A	B
Paraffins......	101.4	41.89	16.67	4.935	150.3	3.550	220.6	144,400	89.7	189.8
Esters of acetic acid.....	172.2	38.61	46.87	4.551	46.17	4.555	150.7	140,100	281.3	169.4
Monohydric alcohols....	81.63	41.70	−27.38	5.072	31.57	3.454	−313.6	247,300	123.4	180.9
Benzene hydrocarbons .	−59.10	39.61	−41.31	4.939	−27.75	4.035	195.8	147,300	−1117	186.9

TABLE 2

Observed and calculated values of the molecular sound velocity

COMPOUND	M_D (OBSERVED)	V (OBSERVED)	V (CALCULATED)	PER CENT DIFFERENCE
Pentane.............................	25.26	1160	1160	0.0
Hexane........................ ..	29.91	1356	1355	−0.1
Heptane...........................	34.57	1545	1550	0.3
Octane...................	39.19	1746	1743	−0.2
Methyl acetate...........	17.65	851	854	0.3
Ethyl acetate...	22.25	1037	1031	−0.6
Propyl acetate.........	26.98	1211	1214	0.2
Methyl alcohol.........	8.23	421	425	1.0
Ethyl alcohol.............	12.78	624	615	−1.5
Propyl alcohol.........	17.52	806	812	0.8
Butyl alcohol:.............	22.13	1004	1005	0.1
Amyl alcohol.............	26.74	1198	1197	−0.08
Benzene.	26.18	979	978	−0.1
Toluene.	31.06	1170	1171	0.09
Cymene.	45.18	1731	1731	0.0

constants (and *vice versa*), assuming the linear relation to hold. This procedure would appear to be better than summing additive and constitutive factors, which may not consider such effects as exaltation as one goes to higher members.

The fact that the other quantities are linear with V means that they are linear with one another. Equations connecting two at a time can be set up from table 1. For example, since $V = 16.67 + 4.935P$ and $V = 220.6 + 144,400b$

for the paraffins, it follows that $P = 41.32 + 29,260b$. Although a few isolated examples of such linear relations are recorded in the literature (6, 8, 11, 17), it now appears that twenty-one linear relations exist among the seven properties considered here.

It should be stated that several workers (1, 4, 7, 20, 21) have indicated that the ratio of two of the above-mentioned properties yields a constant for a great number of compounds. While this may be useful as a rough working rule, it would generally be more exact to say they are linearly related. For example, Buehler (1) states that the ratio of Souders' I to the parachor is 1.22 for about twenty-five compounds (1.27 for paraffins). Use of the constants of table 1 gives $I = 1.39P - 37.6$ for paraffins; this is a more accurate statement of the facts, as can be seen from a plot of I versus P. The addition of CH_2 groups in a homologous series does not, in general, cause a constant ratio to exist between the physical properties, but instead adds constant amounts to the previous value. This leads to a linear curve which as a rule does not pass through zero.

It is interesting to note that from the equation $V = A + BP$ and from the definitions of V and P, it may be shown that

$$v^{1/3} = B\gamma^{1/4} + A \frac{d}{M}$$

a relation between velocity of sound, surface tension (γ), and density, in which A and B are constants for all compounds of a single series. Similar relations may be set up by using the refractive index, viscosity, and Verdet's constant in addition to the surface tension and sound velocity.

VELOCITY OF SOUND AND BOILING AND CRITICAL POINTS

Examination of the data on normal boiling points (T_B) and critical temperatures (T_C) reveals that they are connected with the molecular sound velocity by equations of the form $T_B = A + B \log V$ and $T_C = C + D \log V$, where A, B, C, and D are constants for each homologous series. The boiling point is plotted against the log of the molecular sound velocity for four series in figure 2. It may be seen that straight lines result for series of unassociated compounds. A similar plot can be made for T_C versus V. Lewis (11) has found that T_C and T_B are linear functions of the log of the parachor, as would be expected from the linearity between V and P. Wan (22), however, states that $T_C = k_1 M_D + k_2$, whereas the considerations above favor the relation $T_C = k_1 \log M_D + k_2$. On the basis of the data given by Wan on two series of unassociated compounds, the two equations appear to possess about equal merit. Wan's value of k_2 for paraffins, incidentally, should be 267.5, not 268.5.

ATOMIC AND BOND INCREMENTS

When considering the aforementioned physical properties as additive and constitutive, it is customary to separate the molecular constants into atomic increments and to ascribe values to double bonds, triple bonds, and other constitutive factors. Table 3 lists some of these values, along with references
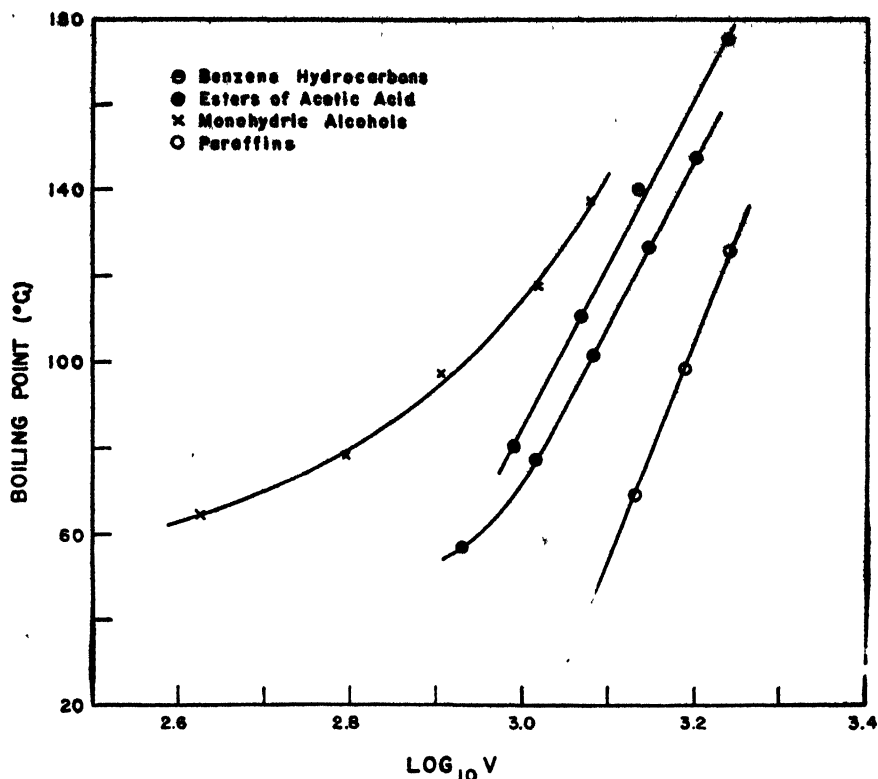
FIG. 2. Relation of the boiling point to the molecular sound velocity

TABLE 3

Atomic increments

	SOUDERS' I (19)	PARACHOR (12)	MOLE REFRACTION (5)	VELOCITY OF SOUND (16)	COVALENT RADIUS (13)
H......	2.7	15.4	1.100	92.5	0.30
C....... . .	50.2	9.2	2.418	10	0.77
N...	37	17.5			0.70
O............	29.7	20.0	1.525	74	0.66
F......		25.5	1.00		0.64
Cl.	60	55	5.967	227	0.99
Br	79	69	8.865	245	1.14
I..	110	90	13.900	304	1.33
CH₂	55.6	40.0	4.618	195	
Double bond..	−15.5	19.0	1.733	110	
Triple bond. .		38	2.398		

to the literature from which they were obtained. In a column of the Periodic Table, the atomic increments for all the properties listed increase with increase in the principal quantum number. Except for Souders' I, the contributions

of bonds increase with their multiplicity. Figure 3 is a plot of the covalent radii of the halogens *versus* their atomic increments as found from four molecular constants. A smooth curve can be drawn in each case. Likewise, for atoms of a column of the Periodic Table, a similar relation exists between the atomic increments of any two of the properties.

An alternative procedure (2, 3, 9, 18, 24) in synthesizing molecular constants is to sum bond increments. Such a scheme is particularly useful when comparison is made with interatomic distances and dissociation energies. Values for some frequently occurring bonds and also the sources of the data are compiled in table 4. To obtain the values given for the bond velocities (9) and for
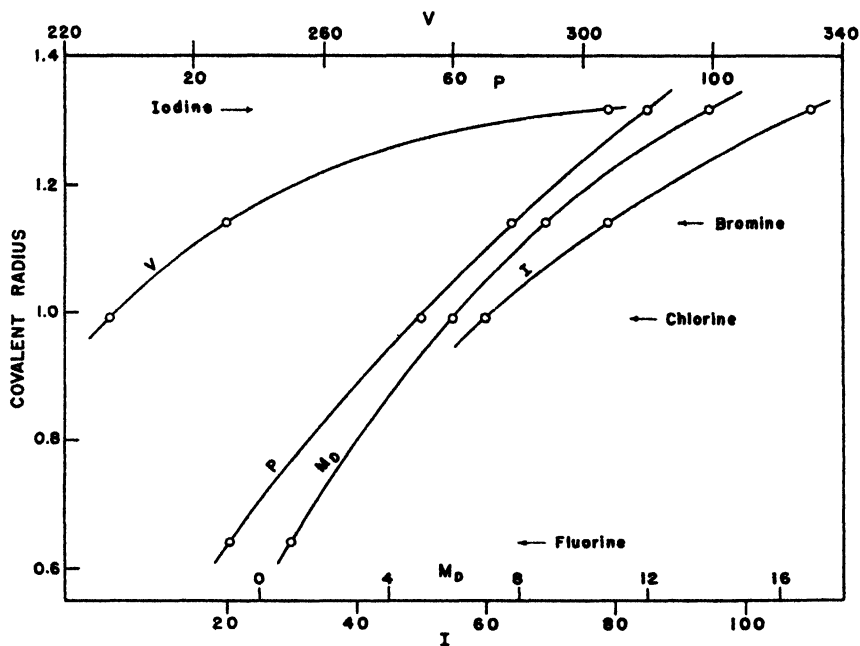
FIG. 3. Graph showing the relation between the covalent radius and atomic increments for elements from a column of the Periodic Table.

the bond parachors, the best values for the C—C and C—H bonds were obtained by least squares from the paraffins, following which, these values were used on single molecules to find other bond values. Improved values could no doubt be obtained by taking for the bond parachors and bond velocities the mean values from measurements on a number of similar molecules. From table 4 it may be seen that the bond increments, except for bond lengths, of all the atom pairs increase with increase in the bond multiplicity.

Figure 4 shows the relation of bond length to bond refraction and is representative of the curves obtained by plotting any of the columns of table 4 against any other column for bonds of the same multiplicity. For bonds of an atom with a series of atoms from a row or from a column of the Periodic Table, a

TABLE 4
Bond increments

BOND	BOND REFRACTION (3, 18)	BOND PARACHOR	BOND VELOCITY (9)	LONGITUDINAL POLARIZABILITY (23)	BOND LENGTH (13)
C—H .	1.705	17.7	95.2	7.2	1.07
C—F. .	1.60	26.0			1.41
C—Cl	6.51	54.9	230	35.3	1.76
C—Br..	9.47	68.1	247		1.91
C—I. .	14.51	92.7	305		2.10
C—S	4.59				1.81
C—N	1.54				1.47
C—O	1 425	7.0	34.5		1.43
C—C	1.209	4.6	4.25	18.2	1.54
H—H	2.08	35.2		5.55	0.60
H—Cl		67.8		31.3	1.29
H—O .	1.73	26.4	99		0.99
Cl—Cl		111.5		66.0	1.98
C=C..	4.15	28.7	129	30.2	1.33
C=S.... .	10.61	72 1	319		1.61
C=O	3.42	37.4	186		1.22
C≡N........	4.77	63.3	285		1.15
C≡C........	6.025	53 2		36 8	1.20
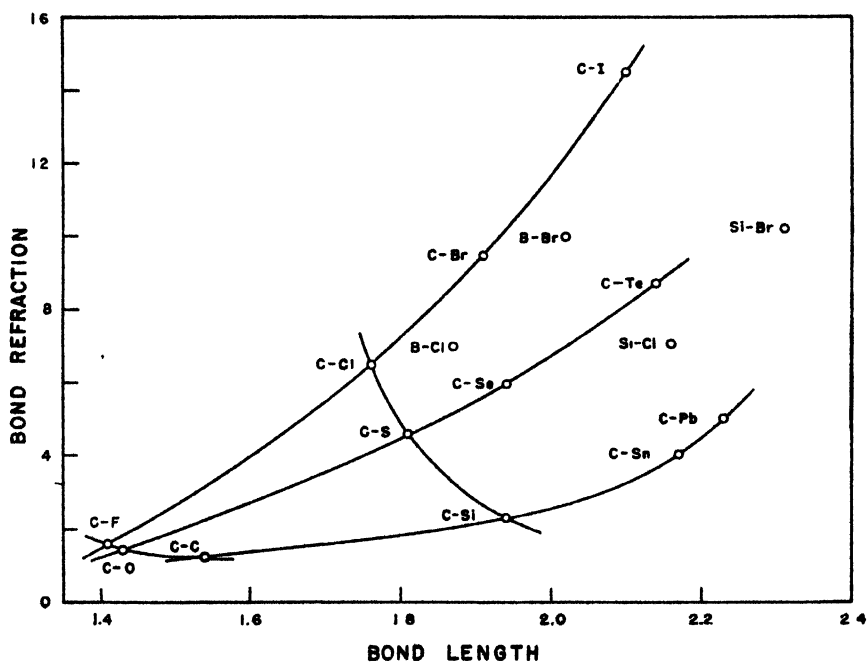
FIG 4 Relation between bond refraction and bond length

smooth curve is obtained. This graph, of course, enables one to estimate bond increments which are not as yet known. It is apparent that the bond increments for the various properties bear a close relationship to one another, provided the rows and columns of the Periodic Table are taken into account.

CONCLUSIONS

It should now be clear that measurements on the velocity of sound can supplement and replace measurements on other physical properties in studies of molecular structure. Although the sound velocity may not be so conveniently measured as the refractive index of a liquid, it is comparable in ease of measurement to the other properties discussed, with the definite drawback, however, that relatively large amounts of liquid are required with the interferometer method. At present, values are usually quoted which include four and sometimes five significant figures. This yields an accuracy at least as good as, and in some cases better than, that for any of the other physical properties except refractivity.

SUMMARY

1. A new physical constant,

$$V = \frac{M}{d} v^{1/3}$$

involving the velocity of sound in liquids, is found to be a linear function of the parachor, mole refraction, Souders' viscosity constant, molecular magnetic rotation, critical volume, and van der Waals' b for members of four homologous series. The constants of the equations are evaluated.

2. This implies that all the aforementioned properties are linear among themselves for homologous series.

3. To a good approximation the linearity may be applied to all compounds.

4. The critical temperatures and boiling points of homologous series of unassociated compounds are linear with the log of V.

5. Lists of atomic increments and the accompanying constitutive values are compiled for several of the properties, including molecular sound velocity.

6. Lists of bond increments are reported and their relationships noted.

REFERENCES

(1) BUEHLER, C. A.: J. Phys. Chem. **42**, 1207 (1938).
(2) COPLEY, G. N.: Chemistry & Industry **60**, 702 (1941).
(3) DENBIGH, K. G.: Trans. Faraday Soc. **36**, 936 (1940).
(4) DESREAUX, V.: Bull. soc. chim. Belg. **44**, 249 (1935).
(5) EISENLOHR, F.: Z. physik. Chem. **75**, 585 (1910).
(6) GARDNER, T. S.: J. Tennessee Acad. Sci. **13**, 246 (1938).
(7) HERZ, W.: Z. anorg. Chem. **159**, 316 (1927); **179**, 211 (1929).
(8) LAGEMANN, R. T.: J. Am. Chem. Soc. **67**, 498 (1945).
(9) LAGEMANN, R. T., AND CORRY, J. E.: J. Chem. Phys. **12**, 759 (1942).
(10) LANDOLT-BÖRNSTEIN: *Physikalisch-chemische Tabellen*, 5th edition. J. Springer, Berlin (1931).

(11) Lewis, D. T.: J. Chem. Soc. 1938, 1056.
(12) Mumford, S. A., and Phillips, J. W. C.: J. Chem. Soc. 1929, 2112.
(13) Pauling, L.: *The Nature of the Chemical Bond.* Cornell University Press, Ithaca, New York (1940).
(14) Perkin, W. H.: J. Chem. Soc. 69, 1026 (1896).
(15) Rao, M. R.: Indian J. Phys. 14, 109 (1940).
(16) Rao, M. R.: J. Chem. Phys. 9, 682 (1941).
(17) Samygin, M. M.: J. Phys. Chem. (U. S. S. R.) 10, 455 (1937).
(18) Smyth, C. P.: Phil. Mag. 50, 361 (1925).
(19) Souders, M., Jr.: J. Am. Chem. Soc. 60, 154 (1938).
(20) Sugden, S.: *The Parachor and Valency,* p. 31. Alfred Knopf, London (1930).
(21) Trouton: Phil. Mag. 18, 54 (1884).
(22) Wan, S. W.: J. Phys. Chem. 45, 903 (1941).
(23) Wang, S.: J. Chem. Phys. 7, 1012 (1939).
(24) von Steiger, A. L.: Ber. 54, 1381 (1921).

EFFECT OF SURFACE-ACTIVE AGENTS UPON DISPERSIONS OF SILICA IN XYLENE

V. R. DAMERELL, K. GAYER, and H. LAUDENSLAGER

Department of Chemistry, Western Reserve University, Cleveland, Ohio

This work is a continuation (1, 2) of the study of the effect of surface-active agents upon particle-size distribution in organosols. This paper describes results obtained with finely divided silica dispersed in xylene.

CHEMICALS

A purified grade of xylene was redistilled, and the fraction boiling between 137° and 138.5°C., a mixture of o- and m-xylenes, was used in the research. A sample of Kahlbaum silica was used. This contained 16 per cent of water and 0.01 per cent of material not volatilized with hydrofluoric acid. It was heated in a furnace at 900°C. for 24 hr. in a stream of dried air, then ball-milled for 45 min. and screened through a 200-mesh seive. It finally had a water content of 0.4 per cent. The surface-active agents used are shown in table 3. These were all of the purest grade obtainable.

PREPARATION OF SILICA–XYLENE SYSTEMS

To 500 ml. of xylene in a wide-mouth Dewar flask was added 0.500 g. of silica powder. The surface-active agent (about 0.001 mole) was added to this mixture, and the whole was then mixed for 45 min. at 25°C., using a stirrer with a three-blade propeller operating at 500 R.P.M. Loss of xylene was diminished by mixing in a draftless, enclosed compartment. The temperature inside the flask was held at 25°C. ± 0.5° by a glass U-tube connected to a variable-temperature water line. The U-tube also served as a baffle.

MEASUREMENT OF PARTICLE-SIZE DISTRIBUTION

Particle-size distribution was measured by sedimentation analysis. After the 45-min. stirring period, the stirrer and U-tube were quickly replaced with a balance pan, the top of which was attached at once to the left stirrup of a sedimentation balance. The balance and the method of using it have been described previously (1). In brief, the precautions observed included: (a) avoidance of hindered settling, by using only a 0.1 per cent suspension of silica; (b) correction for variation of density, and therefore buoyancy of xylene with temperature; (c) correction for evaporation losses of xylene; (d) checking of balance pan at frequent intervals for weight changes (thus the wetting agent

TABLE 1

Typical sedimentation data for the system silica, xylene, and lecithin

TIME	TEMPERATURE	WEIGHT ON PAN	WEIGHT OF SETTLED MATERIAL	WEIGHT OF SETTLED MATERIAL CORRECTED FOR TEMPERATURE
min sec.	°C.	*grams*	*grams*	*grams*
0–0	25.0	7.587		
1–21	25.2	7.607	0.015	0.014
2–17	25.2	7.610	0.023	0.022
3–42	25.2	7.620	0.033	0.032
5–48	25.2	7.629	0.042	0.041
9–45	25.2	7.638	0.051	0.050
18–05	25.2	7.648	0.061	0.060
30–30	25.0	7.655	0.068	0.068
47–09	25.0	7.658	0.071	0.071
64–00	25.0	7.660	0.073	0.073
97–00	25.0	7.662	0.075	0 075
170	24.8	7.665	0.078	0.079
287	24.5	7.671	0.084	0.086
1200	23.9	7.669	0.082	0.087
Infinity*				0.093

* Determined by running a blank, where no colloidal material remained.

copper oleate was found to react with the pan and change its weight); (e) use of a jig in centering the Dewar (when it was off center, and without the pan touching the side, an error of as much as 2 mg. in 85 mg. was possible); (f) use of only a small angle of swing (two index plate scale divisions) to insure relative constancy of pan depth.

The weights of sediment obtained were recorded as shown in table 1. These were corrected for temperature, as shown, and then plotted against time, as illustrated in figure 1. The reproducibility of results is also indicated in figure 1, where values are given for two separate sedimentation analyses with the same surface-active agent, lecithin. The curves obtained in this manner were analyzed by use of a tangentimeter, and particle-size distribution was calculated from Stokes's law, assuming that the particles were spherical. In the calculation of radius the viscosity of the xylene solution of the surface-active agent was

needed. A number of these values were determined, and were found to be nearly the same for the solution as for the pure xyelene. Thus, at 25°C. the viscosity of xylene was found to be 0.00632 poise, of the copper oleate solution 0.00633 poise, of the lecithin solution 0.00643 poise, and of the aerosol O.T.
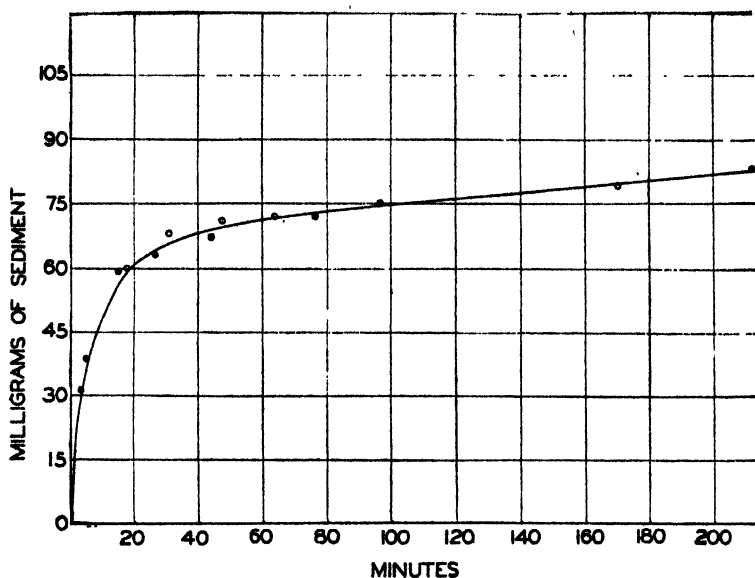
FIG. 1. Plot of weights of sediment against time

TABLE 2

Particle-size distribution obtained from figure 1

RADIUS	TIME	WEIGHT	WEIGHT PERCENTAGE
cm. $\times 10^4$	*minutes*	*grams*	
Above 14	2.7	0.008	9
12–14	3.7	0.003	3
10–12	5.3	0.007	7
8–10	8.2	0 012	13
6–8	15	0.010	11
4–6	33	0.017	18
2–4	132	0.014	15
0.6–2	1200	0.016	17
Below 0.6	Infinity*	0.006	6

* Determined by running a blank, where no colloidal material remained.

solution, 0.00628 poise. The particle-size distribution for the curve given in figure 1 is shown in table 2, and the results for all of the surface-active materials used are summarized in table 3.

The percentages given in table 3 have not been corrected for the weight of the adsorbed surface-active agents, since a method has not as yet been worked out

for calculating the distribution of this material. This correction will make the percentages of pure silica a little lower than reported for the settled material (0.6 micron and over) and a little higher than reported for the colloidal material (under 0.6 micron).

TABLE 3

The effect of surface-active agents upon silica dispersed in xylene

SURFACE-ACTIVE AGENT	QUANTITY USED	PARTICLE-SIZE DISTRIBUTION IN WEIGHT PERCENTAGE					
		Above 14 microns radius	10-14 microns radius	6-10 microns radius	2-6 microns radius	0.6-2 microns radius	Under 0.6 microns radius
	grams						
Sodium dioctyl sulfosuccinate........	0.434	0	8	36	29	2	25
Sodium dihexyl sulfosuccinate..........	0.403	1	19	28	29	17	6
Zinc dioctyl sulfosuccinate	0.511	0	20	24	31	17	8
Barium dioctyl sulfosuccinate....	0.502	0	20	48	23	4	5
Lecithin........... . . .	0.789	8	12	24	33	17	6
Lead naphthenate . .	0.726	5	17	19	31	19	9
Zinc naphthenate. . .	0.724	17	17	17	29	16	4
Cobalt naphthenate	0.714	9	20	24	35	12	0
Manganese naphthenate....	0.360	0	20	48	23	9	0
Copper oleate......... ...	0.400	1	6	17	46	27	3
Oleic acid..	0.282	23	36	19	8	14	0
Magnesium oleate. ..	0.587	4	6	30	59	0	0
Calcium oleate.	0.603	0	24	29	47	0	0
n-Octyl alcohol........ ...	0.270	1	39	30	10	10	0
Benzidine.	0.184	31	30	12	14	13	0
Aminodiphenyl.	0.400	78	9	6	1	6	0
Blank....			72*	13	15	0	0

* This is the percentage larger than 10 microns. The sedimentation curve was too steep for determination of the percentage larger than 14 microns.

EFFECT UPON THE SYSTEM OF VARYING SINGLE FACTORS

Effect of stirring time

Increase in stirring time from 45 min. to 300 min. substantially increased the percentage of intermediate-sized particles, but did not greatly affect the percentage of colloidal material. This is shown in table 4. In each case 0.434 g. of sodium dioctyl sulfosuccinate was used.

Effect of concentration of surface-active agent

The effect of varying the amount of surface-active agent was studied with zinc naphthenate. Increased amounts of this substance resulted in a greater degree of dispersion, as shown by the sedimentation curves in figure 2.

TABLE 4

Effect of length of mixing upon degree of dispersion

STIRRING TIME	PARTICLE-SIZE DISTRIBUTION IN WEIGHT PERCENTAGE					
	Above 14 microns radius	10–14 microns radius	6–10 microns radius	2–6 microns radius	0.6–2 microns radius	Under 0.6 microns radius
minutes						
45	0	8	36	29	3	24
300	0	1	9	41	21	28
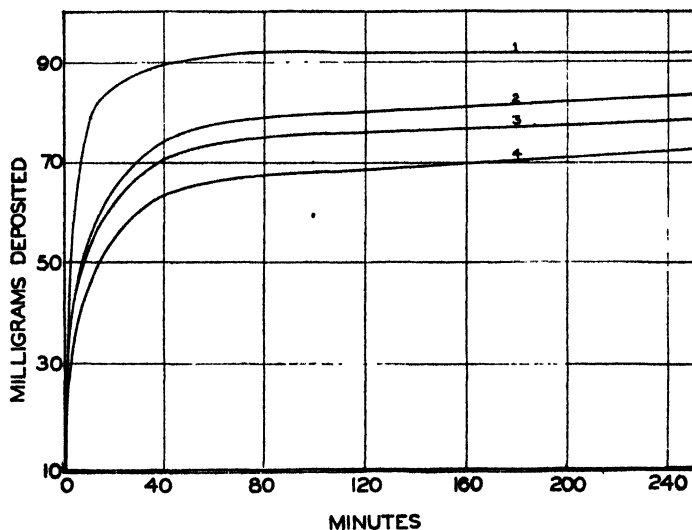
FIG. 2. Sedimentation curves: curve 1, blank; curve 2, 0.172 g. zinc naphthenate; curve 3, 0.751 g. zinc naphthenate; curve 4, 1.755 g. zinc naphthenate.

Effect of extreme dryness

Two systems were made up under extremely dry conditions, one containing sodium dioctyl sulfosuccinate and the other containing no surface-active agent. The xylene used was dried over sodium for one to two years in tightly closed bottles. The silica was air dried for 72 hr. at 105°C., and then vacuum dried for 24 hr. The sodium dioctyl sulfosuccinate was vacuum dried for 24 hr. Then all materials were dried in a dry box (described previously (1)) until fresh quantities of phosphorus pentoxide did not cake on the surface (two weeks). Mixing and stirring of the system was done in the dry box, using the technique described earlier; then a sedimentation analysis was run at once. The results

are shown in table 5 for these two systems and, for comparison, two similar systems prepared under ordinary conditions.

PHYSICAL PROPERTIES OF THE SYSTEM AND ITS COMPONENTS

The density of the finely divided silica was determined as follows: silica was weighed into a flask of known volume; the flask was evacuated, and then partially filled with xylene; the mixture was heated and stirred for 24 hr. The flask was then cooled, xylene was added to the mark, and the weight and density of the silica were determined. The density was found to be 2.094.

TABLE 5
The effect of extreme dryness upon dispersions of silica in xylene

SURFACE-ACTIVE AGENT	QUANTITY USED	PARTICLE-SIZE DISTRIBUTION IN WEIGHT PERCENTAGE					
		Above 14 microns radius	10–14 microns radius	6–10 microns radius	2–6 microns radius	0.6–2 microns radius	Under 0.6 microns radius
	grams						
Sodium dioctyl sulfosuccinate (dry).............	0.403	1	4	20	40	27	8
Sodium dioctyl sulfosuccinate (ordinary)...... .	0.403	1	19	27	29	17	7
Blank (dry)...	0	14	19	21	15	31	0
Blank (ordinary).....	0	(72)		13	15	0	0

TABLE 6
Adsorption of surface-active agents by silica

SURFACE-ACTIVE AGENT	GRAMS PER 500 ML. OF XYLENE	GRAMS ADSORBED PER GRAM OF SiO₂
Zinc naphthenate.......	0.751	0.102
Zinc naphthenate...	1.720	0.170
Lecithin......	0.400	0.128
Sodium dioctyl sulfosuccinate..	0.446	0.170
Sodium dihexyl sulfosuccinate.......	0.403	0.096

The densities of the xylene solutions of the surface-active agents, as well as the viscosities, were found to be essentially the same as that for pure xylene, i.e., 0.862 at 25°C.

The surface area of the silica was determined by the Emmett low-temperature adsorption method in the same manner as described previously for carbon and calcium carbonate (1, 2). It was found to be 118 square meters per gram.

The silica particles migrated to the cathode in a cataphoresis experiment using a 900-volt potential. The increase in concentration in the cathode compartment was small, but always present. Systems containing copper oleate, sodium dioctyl sulfosuccinate, and sodium dihexyl sulfosuccinate were so tested, as well as one in which no surface-active material was used.

The silica organosols left after settling of the larger particles were milky in

appearance, but with a variation in tint depending upon the surface-active agent used. Water had an immediate coagulating effect, and the addition of alcohol, ether, or acetone caused precipitation within a short time. The systems were also heat sensitive, and coagulation began after several minutes' heating at 70°C. The organosols quickly precpitated at the boiling point of xylene.

Adsorption of surface-active agents

The adsorption of some of the more successful surface-active agents was determined by analysis of the supernatant liquid. The results are shown in table 6.

SUMMARY

Dispersions of silica in xylene have been made in the presence of a number of surface-active materials. The particle-size distributions of these dispersions have been determined by sedimentation analysis. The most successful surface-active agents were found to be the various metal sulfosuccinates, metal naphthenates, and lecithin. These agents are thought to aid dispersion by forcing aggregates apart in the process of adsorption, since in all cases where adsorption · was determined the successful surface-active agents were found to be strongly adsorbed on the silica.

The silica had a surface of 118 square meters per gram. It was positively charged in the xylene suspension and was coagulated by the addition of water, alcohol, acetone, and ether. Heating also produced coagulation.

REFERENCES

(1) DAMERELL, V. R., AND MATTSON, R.: J. Phys. Chem **48**, 134–41 (1944).
(2) DAMERELL, V. R., AND URBANIC, A.: J. Phys. Chem **48**, 125–33 (1944).

DISTRIBUTION LAW, ADSORPTION, AND CHEMICAL REACTION

B. P. GYANI

Chemical Laboratory, Science College, Patna, India

INTRODUCTION

In this paper, the subject of adsorption has been examined on the basis of the idea that not only the planar surface of the adsorbent is important in the process, but the entire bulk of the solid and patches, active lines, and points on the surface come into operation, either individually or in superimposition with one another. On this idea, a theoretical basis of the classical adsorption equation has been indicated, and an attempt has been made to interpret in a ·simple way some general facts of adsorption, chemical reactions, and surface catalysis.

The adsorption equation

$$x/m = kC^{1/n} \tag{1}$$

is usually considered to be empirical. It is possible, however, to give a theoretical basis to this equation in terms of the distribution law. The general distribution equation

$$C_2 = kC_1^n \tag{2}$$

where n represents the association factor, may be easily derived from the kinetic theory of gases. Though k is considered to represent a purely numerical coefficient, it is possible to ascribe to it a definite physical significance. This coefficient may be considered to represent the relative degree of packing of the solute molecules distributed between the two phases. Thus, taking a system like aniline distributed between water and benzene, let us consider the two liquid layers as subdivided into small cubes such that each cube contains one molecule of aniline. The size of these cubes will be different for the two phases, being larger for the aqueous layer. k, which is defined to represent the ratio of numbers of solute molecules in equal volumes of the two phases, thus represents the inverse ratio of the sizes of these cubes. This picture of distribution may be extended to apply to cases of adsorption.

Let the benzene now be frozen to form cubes of larger dimensions. The size of these cubes is such that they contain a large number of the elementary cubes as pictured above in the case of simple distribution. Some of these elementary cubes will be so arranged that they will compose the surface layer of the larger cubes, while others will be embedded in the interior of their body. As in the case of distribution, so also in the case of adsorption, one molecule of the solute is considered to be associated with one elementary cube. During an adsorption process, however, it is not all the elementary cubes that are effective, but only such of them as are exposed on the faces of the larger cubes, for they alone can accommodate solute molecules. In the limit, the ratio of the total number of cubes to those exposed on the surface will be as $L^3:6L^2$, where $L = $ the number of elementary cubes along any edge of the larger cubes. Since the ratio volume:area varies as $L^3:L^2$ for any geometrical figure, the distribution equation (equation 2) will apply to cases of surface adsorption if expressed in the form

$$C_2 = k \cdot C_1^{2/3} \tag{3}$$

if the molecular condition of the solute remains unchanged in the two phases.

If the adsorption is not general on the surface, but is limited to the edges of the larger cubes, the number of effective elementary cubes will be further reduced. Since the radio of volume to edges for any geometrical figure varies as $L^3:L$, the adsorption equation will now take the form

$$C_2 = k \cdot C_1^{1/3} \tag{4}$$

An extreme case of adsorption would be such that the solute molecules are confined to the corners of the larger cubes only. Since the number of elementary

cubes at the corners is a fixed quantity, and in no way depends on the volume of the figure, equation 2 will assume for this case yet another form:

$$C_2 = k \cdot C_1^0 \quad \text{or} \quad C_2 = \text{Constant} \tag{5}$$

The circumstances which led to equation 1 as being considered empirical are as follows: In most cases of distribution in which one phase is a solid, the value of n in equation 2 was found to be fractional when this latter equation was applied to the data obtained over a large range of concentrations. Thus, Walker and Appleyard (36) applied this equation to the distribution of picric acid between water and silk. The value of the exponent, instead of being an integer, was found to be about $1/3$. If the mode of distribution is assumed to be similar in the two phases (bulk distribution), it must be concluded that the picric acid molecule dissociates into three components, which would mean a decomposition of the molecule; it cannot be a case of dissociation of the solute molecules polymerized in the aqueous phase, since the molecular weight of the acid in water was found to be normal. Decomposition of the acid in the silk phase could not be proved. There could thus be no physical significance of the numerical value of n in this and similar cases. The equation for this kind of distribution thus came to be written in the form of equation 1, $1/n$ signifying a fractional value and stressing its distinction from the ordinary distribution equation, well known as the classical, or Freundlich, adsorption equation (23). In McBain's words, $1/n$ "is any sort of irrational fraction, varying with circumstances between 1 and $1/10$, and is frequently in the neighbourhood of $1/3$" (23). The frequency of occurrence of $1/n$ in the neighborhood of $1/3$ is also stressed by Richardson and Robertson (29). This is evident from table 1, where some data obtained by different workers have been collected.

The frequency with which $1/n$ occurs in the vicinity of $1/3$ requires that, in most cases of adsorption from solutions, the solute should be confined to certain lines only in the solid phase. These lines may probably be identified with the exposed edges of microcrystals constituting the solid phase, or scratches and other imperfections in them. A bulk of evidence has accumulated in recent years in support of this idea. Evidence both from the field of surface catalysis and from measurements of heats of adsorption compels us to assume that the surfaces concerned are heterogeneous. This heterogeneity may be due to particularly active points, or lines, or patches on the surface. Felman and Adhikari (9) were able to prove that the reaction $Hg + I_2 = HgI_2$ occurs only on the phase boundary of mercury and mercuric iodide. The pulsating decomposition of hydrogen peroxide observed by Bredig and Stark (5) is also localized at the boundary of mercury and its peroxide. Identification of active centres with lines has been discussed in detail by Schwab and Pietsch (32). They have further shown that such a conception does not change the form of Langmuir's adsorption isotherm, which is essentially a distribution equation in which changes due to alteration of concentration in the solid phase have been taken into consideration. Smekal (34) from other considerations is led to a similar conclusion. Some recent microphotographs of etched surfaces (30)

TABLE 1

ADSORBENT	SOLVENT	SOLUTE	1/n	AUTHOR
Blood charcoal.......	Water	Formic acid	0.451	Freundlich (10)
	Water	Propionic acid	0.394	Freundlich (10)
	Water	Butyric acid	0.301	Freundlich (10)
	Water	Chloroacetic acid	0.363	Freundlich (10)
	Water	Succinic acid	0.243	Freundlich (10)
	Water	Benzoic acid	0.338	Freundlich (10)
	Water	Mandelic acid	0.140	Freundlich (10)
	Water	Sulfanilic acid	0.257	Freundlich (10)
	Water	Chlorine	0.297	Freundlich (10)
	Benzene	Picric acid	0.302	Freundlich (10)
	Ether	Benzoic acid	0.455	Freundlich (10)
	H_2SO_4	Bromine	0.351	Freundlich (10)
Animal charcoal.....	Water	Acetic acid	0.5	Schmidt (31)
	Water	Succinic acid	0.5	Schmidt (31)
Blood charcoal......	Alcohol	Iodine	0.25	Schmidt (31)
	Alcohol	Iodine	0.25	Schmidt (31)
	Benzene	Iodine	0.25	Schmidt (31)
	Water	Phenylthiourea	0.245	Freundlich and Bjercke (13)
	Water	Acetone	0.520	Michaelis and Rona (26)
	Water	Isoamyl alcohol	0.263	van Duin (8)
Animal charcoal.....	Alcohol	Iodine	0.324	Davis (7)
	Chloro-form	Iodine	0.336	Davis (7)
	Benzene	Iodine	0.311	Davis (7)
Silk................	Water	Picric acid	0.347	Walker and Appleyard (36)
	Alcohol	Picric acid	0.363	Walker and Appleyard (36)
Animal charcoal....	Water	Methyl alcohol	0.435	Richardson and Robertson (29)
	Water	Isopropyl alcohol	0.278	Richardson and Robertson (29)
	Water	n-Propyl alcohol	0.526	Richardson and Robertson (29)
	Water	Methyl acetate	0.417	Richardson and Robertson (29)
	Water	Acetone	0.385	Richardson and Robertson (29)
	Water	Sucrose	0.208	Richardson and Robertson (29)
	Water	Ether	0.435	Richardson and Robertson (29)
	Water	Ethyl acetate	0.323	Richardson and Robertson (29)
	Water	Pyridine	0.263	Richardson and Robertson (21)
	Water	Aniline	0.385	Richardson and Robertson (29)

TABLE 1—*Continued*

ADSORBENT	SOLVENT	SOLUTE	$1/n$	AUTHOR
Charcoal (norite)....	Water	Formic acid	0.435	Linner and Gortner (22)
	Water	Acetic acid	0.351	Linner and Gortner (22)
	Water	Propionic acid	0.236	Linner and Gortner (22)
	Water	Caproic acid	0.175	Linner and Gortner (22)
	Water	Isobutyric acid	0.273	Linner and Gortner (22)
	Water	Glycolic acid	0.390	Linner and Gortner (22)
	Water	Lactic acid	0.335	Linner and Gortner (22)
	Water	Glyceric acid	0.267	Linner and Gortner (22)
	Water	Glyoxalic acid	0.455	Linner and Gortner (22)
	Water	Pyruvic acid	0.273	Linner and Gortner (22)
	Water	Malonic acid	0.410	Linner and Gortner (22)
	Water	Succinic acid	0.303	Linner and Gortner (22)
	Water	Glutaric acid	0.201	Linner and Gortner (22)
	Water	Malic acid	0.252	Linner and Gortner (22)
	Water	Tartaric acid	0.275	Linner and Gortner (22)
	Water	Fumaric acid	0.248	Linner and Gortner (22)
	Water	Maleic acid	0.203	Linner and Gortner (22)
	Water	Bromosuccinic acid	0.195	Linner and Gortner (22)
	Water	Dibromosuccinic acid	0.320	Linner and Gortner (22)

and observations on latent splitting of bars undergoing lateral vibrations (27) testify to the physical existence of these lines and cracks.

An examination of published data shows that the occurrence of the values of $1/n$ in the neighborhood of 2/3, though less common, is not infrequent. In fact, it is very striking for certain systems, as appears from table 2. Thus, as far as adsorption from dilute solutions is concerned, a planar distribution of the solute on the adsorbing surface, corresponding to equation 3, is by no means rare.

Adsorption of gases on solids is often characterized by high values of $1/n$ (11), more so towards higher pressures (28, 35). Particularly interesting is the observation that the value of $1/n$ approaches 1 above a certain temperature (12). These facts are in accord with the concept that a bulk distribution of the gas molecules in the body of the adsorbent takes place—the phenomenon termed persorption by McBain (23). This process corresponds to equation 2 in its simplest form ($n = 1$), and the distinction between adsorption and ordinary distribution is lost.

Finally, the type of adsorption corresponding to equation 5 is probably of particularly frequent occurrence with adsorbents of biological origin. The adsorption of sugar by yeast, of iodine by seaweed, or of heavy metal ions by *Sacch. cerevisiae* (14) appears to present examples of this type. This case also seems to be realized in some adsorption measurements by McBain and his students (25), where drastic cleansing of the adsorbent had been undertaken. They found that the adsorption isotherm rose steeply at minute pressures.

There is no justification for the assumption that in a given case of adsorption any one of these processes should occur to complete exclusion of the others. On

the other hand, it is more reasonable to look for a diversity of phenomena in actual cases, where one or more of these processes may be operative at a given

TABLE 2

Adsorption of carbohydrates on charcoal and of electrolytes on alumina

ADSORBENT	SOLVENT	SOLUTE	$1/n$	AUTHOR
Blood charcoal.... ...	Water	Fructose	0.539	Herzog (16)
	Water	Glucose	0.474	Herzog (16)
Carbo Med., Merck.. . .	Water	Arabinose	1.054	Gyani (15)
	Water	Xylose	0.820	Gyani (15)
	Water	Dextrose	0.652	Gyani (15)
	Water	Galactose	0.613	Gyani (15)
	Water	Mannose	0.641	Gyani (15)
	Water	Fructose	0.531	Gyani (15)
	Water	Rhamnose	0.870	Gyani (15)
	Water	Maltose	0.605	Gyani (15)
	Water	Sucrose	0.605	Gyani (15)
Fibrous Al_2O_3	Water	NaCl	0.620	Ishizaka (19)
	Water	KNO_3	0.610	Ishizaka (19)
	Water	K_2SO_4	0.523	Ishizaka (19)
	Water	$K_2C_2O_4$	0.360	Ishizaka (19)
	Water	NH_4Cl	0.610	Ishizaka (19)
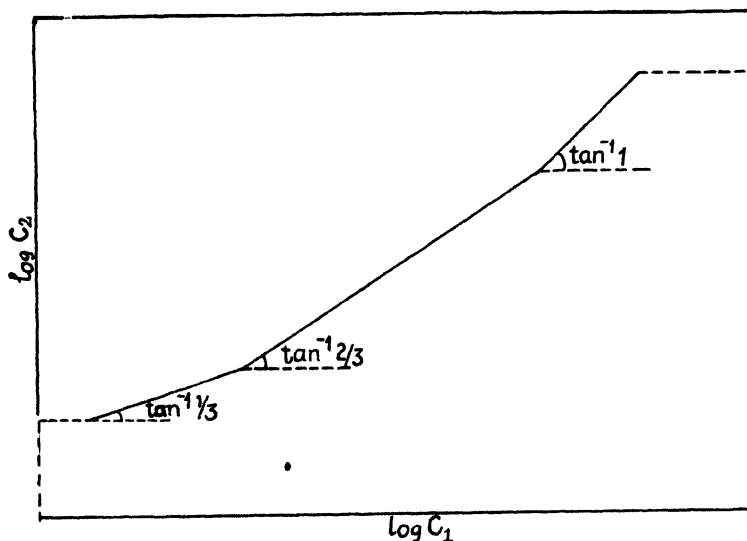
FIG. 1

stage. Experience fully bears this out. The adsorption equation (equation 1) plotted in the logarithmic form should give rise to a straight line, with a constant slope of $1/n$. In actual practice, where observations extend to a large

pressure range, such a case is rarely realized. Coolidge's form of this curve (6; actually, it is a semi-log curve) exhibits varying slopes in different portions, for which he offers no satisfactory explanation. It is possible to find an explanation for this behavior on the basis of the ideas expressed above. If the active points, lines, patches, and finally the bulk of the interior come into operation successively as the pressure in the gas phase increases, it is clear that the branches of the isotherm corresponding to these distinct stages will have varying slopes, increasing in the order 0, 1/3, 2/3, and 1. The isotherm, in which the slope will vary in this manner, will have the form shown in figure 1. This is strikingly similar to the curve proposed by Coolidge.

Some applications of the above hypothesis, which gives definite physical significance to constants of the classical adsorption equation and which visualizes adsorption as a synthesis of distinct simple operations of distribution involving points, lines, surfaces, and finally the bulk which constitute the adsorbent, will now be described.

ADSORPTION AND CHEMICAL REACTION

According to Langmuir (20) adsorption is not different from chemical reaction, inasmuch as actual chemical bonds are formed between adsorbed molecules and those on the adsorbing surface. Isothermal decomposition of calcium carbonate takes place at constant pressure, i.e., the reaction is univariant. The adsorption equation developed by him, which is based on the assumption that there is a dynamic equilibrium between the molecules evaporating from the covered surface and those condensing on the bare parts, requires that the isothermal decomposition should involve a variation of the decomposition pressure with the fraction of the surface covered. If the phase rule is applied to the system, since the number of components is two, and the degree of freedom is one, the number of phases must be three. Two solid phases, therefore, must exist. Langmuir (21) says, "In order that calcium carbonate may dissociate and form a phase of calcium oxide (instead of a solid solution), it is necessary that the reaction shall occur only at the boundary between two phases." In his opinion, such a possibility may be visualized if the escape of a carbon dioxide molecule weakens the bonds which hold the neighboring atoms on the surface. The adjoining atoms would be the next ones to be lost in the form of carbon dioxide, and the subsequent reaction will proceed at the boundary between the patches still covered with carbon dioxide and those uncovered. If the loss of the first CO_2, on the other hand, strengthens the neighboring bonds, the subsequent loss of carbon dioxide will take place from all over the surface. A solid solution of carbon dioxide in calcium oxide will thus be formed, corresponding to adsorption of the gas on the solid.

This explanation raises certain difficulties. If we picture the recombination process according to each mechanism, we get a solid-solution effect in the first case and a boundary reaction in the second. The effects are thus reversed. In other words, the isotherms corresponding to decomposition and recombination should differ, so that there would be a hysteresis phenomenon somewhat analo-

gous to condensation and evaporation of liquids in capillaries (37). The energy changes corresponding to decomposition and recombination would also differ.

Let us apply equation 2 to the present case, bearing in mind the physical significance of the constants. When C_2 (concentration of carbon dioxide in the solid phase) is plotted against C_1 (concentration of carbon dioxide in the gas phase), a line parallel to the C_2-axis is obtained. If log C_2 is plotted against log C_1, the form of the curve remains unchanged. Now, n = slope of this curve = α; and k = intercept on the C_2-axis = α. It is thus found that the degree of association of the carbon dioxide molecules in the solid phase is infinite and so is their degree of packing as compared to the same in the gas phase. Both these experiences are clearly understood if we realize that the carbon dioxide molecules form part of a crystal lattice in the solid phase. For the modern conception identifies a molecule with the entire crystal. X-ray and electron-diffraction studies of crystals demand that the familiar inorganic molecules such as NaCl, $CaCO_3$, or ZnS should have no existence in the solid state as such, but form part of a continuous lattice where their separate identity is lost.

It remains to be explained how two solid phases make their appearance as compared to only one in the case of true adsorption. The answer is given partly by Langmuir himself (21). When oxygen is adsorbed on a tungsten surface, a film of the oxide is formed. "Two primary valences of the oxygen are turned downwards, and are saturated by the tungsten. . . . The hexavalent tungsten atoms are, however, not saturated by the oxygen, so that they are held firmly to the underlying layer of tungsten atoms." We can think of another arrangement of oxygen atoms, such that they lie in the same plane as the tungsten atoms, surrounded by them, or partly by other oxygen atoms, much as they do in the actual space lattice of the oxide, WO_3. The two cases differ in the important respect that whereas the original tungsten surface remains homogeneous in the first one, it becomes heterogeneous in the second, although primary valences may be involved in both combinations. In the first case, the surface layer of oxygen is a continuation of the gas phase in the sense that it is not attached to any particular tungsten atom but is free to move from one point to another on the surface, a necessary condition for a solution effect; whereas in the second, an additional phase, the crystal lattice of WO_3 besides that of tungsten, appears, containing oxygen which has lost its mobility, a necessary condition for the "precipitation" of a solid phase. The number of phases thus increases by one, and the degree of freedom is lost by one. It is thus unnecessary to assume that the combination of carbon dioxide and calcium oxide takes place at the phase boundary of the two. The flat initial portion of the isotherm (from zero pressure to dissociation pressure) must then conform to the first mechanism whereby a feeble adsorption of carbon dioxide on the solid takes place until enough pressure is developed to force the gas molecules into the crystal lattice of calcium carbonate. The whole process can be easily compared to the taking up of hydrogen chloride by aqueous silver nitrate solution. The Langmuir mechanism leaves unexplained the absence of the phase boundary below the dissociation pressure during which stage minute quantities of carbon dioxide

must be taken up. Incidentally, this line of thought neatly explains the specific character of chemical reactions where a solid separates, which comprises most cases of complex formation; for specific chemical reactions must always be identified with specific steric considerations.

The magnitude of energy changes cannot be made the basis of distinction between true chemical reactions on the one hand and adsorption or ordinary distribution processes on the other. The distinction lies in the fact that chemical reactions always involve a distribution in spaces of zero dimension, whereas the other processes involve spaces of one, two, or three dimensions. Even this distinction is lost in that type of adsorption which is governed by equation 5. A distinction of theoretical character still persists in the relative degree of packing (k) which should, in general, be finite for cases of adsorption or ordinary distribution, but infinite for true chemical reactions where a new phase separates. This consideration requires that the lower part of the isotherm corresponding to equation 5 should coincide with the zero pressure axis. Such cases have been strikingly realized in the adsorption measurements of McBain and his students already referred to. Such behavior is certainly difficult to explain on any of the current theories of adsorption.

PERIODIC ADSORPTION

The phenomenon of linear adsorption has been suggested to be the cause of certain periodicities in adsorption, first observed by Allmand and Chaplin (1). They expressed the opinion that the primary adsorption is on certain active spots around which concentric rings are afterwards built up (2). Benton and White (3) urge the reverse mechanism, in which primary adsorption is supposed to occur along edges of microcrystals constituting the solid adsorbent, which then spreads inwards in parallel rows. Whatever the detailed mechanism may be, the concept of linear adsorption seems to be an attractive hypothesis for the explanation of this type of adsorption.

SURFACE CATALYSIS

Reactions of zero order are not infrequent, particularly in biological processes. The Langmuir theory requires that such reactions shall occur only when the catalyst surface is saturated with the reactant. The present hypothesis provides this possibility for those cases also where the surface as a whole is not fully covered, for it is enough if the active points or lines are saturated. In the case of points, it is immaterial whether all of them are covered or not, for the amount of adsorption is independent of concentration at any stage—a viewpoint particularly to be favored in biological reactions. According to Hogness and Johnson (18), the rate of decomposition of germanium hydride on metallic germanium is proportional to the cube root of the pressure. This experiment is easily understood if decomposition occurs mainly among linearly adsorbed molecules. According to Langmuir's ideas, this case requires that the GeH_4 molecule be adsorbed on three elementary spaces ($n = 3$), each prod-

uct of decomposition subsequently occupying a unit space ($m = 1$). A physical picture of this mechanism is not easily acceptable. The rate of decomposition of stibine on antimony, studied by Bodenstein and Stock (4), varies as $p^{0.6}$. This result agrees with the simple concept that decomposition occurs mainly among molecules adsorbed in a general way on the surface. Decomposition of arsine, phosphine, and formic acid on certain surfaces is apparently mono-molecular (17), i.e., the rate is proportional to the gas pressure. This result is possible in various ways. Thus, the decomposition may occur as a result of binary collisions between molecules from the gas phase and those adsorbed on certain active spots; it may also occur as a result of collision between molecules linearly adsorbed and those generally distributed on the surface; for the rate in the latter case:

$$\mathrm{d}x/\mathrm{d}t = k \, [\mathrm{AsH_3}]_{\mathrm{line}} [\mathrm{AsH_3}]_{\mathrm{surface}} = k' \cdot p^{1/3} \cdot p^{2/3} = k' \cdot p$$

For such cases, which are of frequent occurrence, the Langmuir theory requires that each decomposition product occupy the same number of elementary spaces as it did when it was a part of the original molecule.

The rate of decomposition of ammonia on platinum is proportional to its pressure and inversely proportional to the pressure of hydrogen gas (33). Corresponding to the two mechanisms for decomposition of arsine, the reaction may be written as

$$\mathrm{NH_3}_{\,\mathrm{point}} + \mathrm{NH_3}_{\,\mathrm{gas}} = \mathrm{H_2}_{\,\mathrm{point}} + \mathrm{H_2}_{\,\mathrm{gas}} + \mathrm{N_2}_{\,\mathrm{point}} + \mathrm{N_2}_{\,\mathrm{gas}} \qquad (a)$$

or

$$\mathrm{NH_3}_{\,\mathrm{line}} + \mathrm{NH_3}_{\,\mathrm{surface}} = \mathrm{H_2}_{\,\mathrm{line}} + \mathrm{H_2}_{\,\mathrm{surface}} + \mathrm{N_2}_{\,\mathrm{line}} + \mathrm{N_2}_{\,\mathrm{surface}} \qquad (b)$$
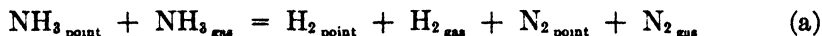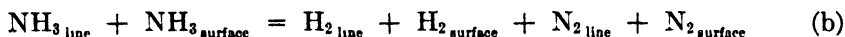
The effective concentration of ammonia molecules on the active lines will no longer be proportional to $p_{\mathrm{NH_3}}^{1/3}$, since other kinds of molecules are also present. The actual quantity $k_1 \cdot p_{\mathrm{NH_3}}^{1/3}$ must be replaced by the fractional concentration

$$\frac{k_1 \cdot p_{\mathrm{NH_3}}^{1/3}}{k_1 \, p_{\mathrm{NH_3}}^{1/3} + k_2 \, p_{\mathrm{H_2}}^{1/3} + k_3 \, p_{\mathrm{N_2}}^{1/3}} = P_{\mathrm{line}}$$

say. If the mechanism corresponding to equation b is considered probable, the rate of reaction will be given by

$$\mathrm{d}x/\mathrm{d}t = \mathrm{const} \cdot P_{\mathrm{line}} \cdot P_{\mathrm{surface}}$$

If the ammonia and nitrogen terms in the denominators may be neglected in comparison with the $\mathrm{H_2}$ terms, we finally get

$$\mathrm{d}x/\mathrm{d}t = \mathrm{Const} \cdot \frac{p_{\mathrm{NH_3}}^{1/3}}{p_{\mathrm{H_2}}^{1/3}} \cdot \frac{p_{\mathrm{NH_3}}^{2/3}}{p_{\mathrm{H_2}}^{2/3}} = \mathrm{Const} \, \frac{p_{\mathrm{NH_3}}}{p_{\mathrm{H_2}}},$$

The most general velocity equation may evidently be written as:

$$\mathrm{d}x/\mathrm{d}t = \mathrm{Const} \cdot P_{\mathrm{point}} \cdot P_{\mathrm{line}} \cdot P_{\mathrm{surface}} \cdot P_{\mathrm{gas}}$$

This consideration may probably be helpful in clarifying the hitherto unexplained rate of decomposition above a pressure of 10 mm., which is reported to be governed by

$$dx/dt = k \frac{[NH_3]}{[H_2] \cdot \{[H_2] + 6[NH_3]\}} \cdot \frac{[NH_3]}{[H_2]}$$

Finally, the idea of linear adsorption has been utilized elsewhere (32) by Schwab and Pietsch to explain the complicated oxidation of·sulfur dioxide.

SUMMARY

1. Adsorption on solids has been regarded as a distribution of molecules on isolated points, lines, patches, and the entire bulk of the adsorbent. These processes may occur singly, or in combination.

2. A simple interpretation of the classical adsorption equation has been indicated on this basis.

3. A few applications of the present hypothesis to some general facts of adsorption, chemical reactions, and surface catalysis have been discussed.

4. The distinction between chemical reaction on the one hand, and adsorption or ordinary distribution on the other, has been presented from a new point of view.

REFERENCES

(1) ALLMAND, A. J., AND CHAPLAIN, R.: Proc. Roy. Soc. (London) 129A, 257 (1930).
(2) ALLMAND, A. J., CHAPLIN, R., AND BURRAGE, L. J.: Trans. Faraday Soc. 28, 222 (1932).
(3) BENTON, A. F., AND WHITE, T. A.: J. Am. Chem. Soc. 53, 3301 (1931).
(4) BODENSTEIN, M., AND STOCK, A.: Ber. 40, 570 (1907).
(5) BREDIG, G., AND STARK, A.: Z. Physik. Chem. B2, 282 (1929).
(6) COOLIDGE, A. S.: J. Am. Chem. Soc. 48, 1796 (1926), figure 1.
(7) DAVIS, O. C. M.: J. Chem. Soc. 91, 1666 (1907).
(8) DUIN, C. F. VAN: Kolloid-Z. 17, 123 (1915).
(9) FELMAN, J., AND ADHIKARI, G.: Z. physik. Chem. 131, 347 (1928).
(10) FREUNDLICH, H.: Z. physik. Chem. 57, 444 (1906).
(11) FREUNDLICH, H.: Colloid and Capillary Chemistry, p. 120. London (1923).
(12) Reference 11, p. 122.
(13) FREUNDLICH, H., AND BJERCKE, A.: Z. physik. Chem. 91, 1 (1916).
(14) GOETZ, A., AND GOETZ, S.: Phys. Rev. 59, 219 (1941).
(15) GYANI, B. P.: J. Indian Chem. Soc. 21, 79 (1943).
(16) HERZOG, R. O.: Z. physiol. Chem. 60, 79 (1909).
(17) HINSHELWOOD, C. N., HARTLEY, H., AND TOPLEY, B.: Proc. Roy. Soc. (London) A100, 575 (1922).
(18) HOGNESS, T. R., AND JOHNSON, W. C.: J. Am. Chem. Soc. 54, 3583 (1932).
(19) ISHIZAKA, N.: Z. physik. Chem. 83, 97 (1913).
(20) LANGMUIR, I.: J. Am. Chem. Soc. 38, 2221 (1916).

(21) LANGMUIR, I.: J. Am. Chem. Soc. **39**, 1848 (1917).
(22) LINNER, E. R., AND GORTNER, R. A.: J. Phys. Chem. **39**, 35 (1935).
(23) McBAIN, J. W.: *The Sorption of Gases by Solids*, p. 5. G. Routledge and Sons, Ltd., London (1932).
(24) Reference 23, p. 13 et seq.
(25) Reference 23, p. 128 et seq.
(26) MICHAELIS, L., AND RONA, R.: Biochem. Z. **15**, 196 (1908).
(27) PROSAD, K.: Nature **127**, No. 3194, 90 (1931).
(28) RICHARDSON, J. B.: J. Am. Chem. Soc. **39**, 1842 (1917).
(29) RICHARDSON, H. L., AND ROBERTSON, P. W.: J. Chem. Soc. **127**, 553 (1925).
(30) SCHAEFFER, V. J.: Phys. Rev. **62**, 495 (1942).
(31) SCHMIDT, G. C.: Z. physik. Chem. **15**, 56 (1894).
(32) SCHWAB, G.-M., AND PIETSCH, E.: Z. physik. Chem. **B1**, 385 (1929).
(33) SCHWAB, G.-M., AND SCHMIDT, H.: Z. physik. Chem. **B3**, 337 (1929).
(34) SMEKAL, A.: Z. Elektrochem. **35**, 567 (1929).
(35) TITOFF, A.: Z. physik. Chem. **75**, 641 (1910).
(36) WALKER, J., AND APPLEYARD, R.· J. Chem. Soc. **69**, 1334 (1896).
(37) ZSIGMONDY, R.: Z. anorg. Chem. **71**, 356 (1911).

ON THE NATURE OF ALUMINO-SILICATE AND IRON-SILICATE PRECIPITATES FORMED BY THE MUTUAL COAGULATION OF SILICIC ACID AND ALUMINA AND IRON HYDROXIDE SOLS

S. P. RAYCHAUDHURI AND KHONDHAR AMIR HASAN

Chemical Laboratory, Dacca University, India

INTRODUCTION

It is well known that on mixing two hydrophobic sols of opposite signs of charge, mutual adsorption of the oppositely charged particles takes place with the lowering of the ζ-potential of the mixed particles (*cf.* Freundlich (5); Weiser and coworkers (16–18)). Weiser and coworkers have shown that the precipitating power of a positive sol for an oppositely charged colloid is determined by (*a*) the magnitude of the ζ-potential in the two sols, (*b*) mutual adsorption of oppositely charged particles, (*c*) the presence of precipitating ions as impurities in the sol, and (*d*) the interaction between stabilizing ions in the sols. It appears, however, that there is no definite information in the literature regarding the chemical composition of the mutual coagulum. Thus the precipitating colloids may lie side by side or definite chemical compounds may be formed. These alternative points of view have important bearings on the formation of clay complexes.

The alumino-silicates of rocks are broken up by hydrolysis mostly into oxides of aluminum, silica, and other oxides which, when first formed, are present in the colloidal state. The colloidal sesquioxides are positively charged, whilst colloidal silica is negatively charged; mutual coagulation takes place between

these oppositely charged colloids, leading to the formation of clay minerals. According to this picture of the formation of clay minerals, the clay complex is a composite body, the ultimate constituents of which are alumino-silicate minerals, silica, and oxides of aluminum and iron lying side by side. Mattson (7), however, thinks that the clay minerals which are formed by mutual coagulation are compounds of alumino-silicates of indefinite composition and are formed by the interaction between the oppositely charged alumina and silicic acid sols. The evidence of x-ray diagrams showing definite crystalline patterns proves that Mattson's theory, as such, cannot be true. It is now held that part of the clay complex consists of crystalline materials and part of silica and oxides of aluminum and iron. It was accordingly considered interesting to determine the percentages of free silica and free oxides of aluminum and iron in the precipitates formed by mixing negatively charged colloidal silica with positively charged colloidal oxides of aluminum and iron. Truog et al. (15) have determined experimentally the total amounts of free silica and of free alumina and iron oxide in the clay complexes (cf. also Drosdoff and Truog (4)). It was felt desirable that this method should be applied to the determination of the percentages of free constituents in the coagulum formed by mixing oppositely charged colloidal silica and alumina and iron oxides. The method has obvious limitations, since it has been shown by Truog et al. (loc. cit.) themselves that from nontronite, an iron silicate mineral, iron was extensively released (12.60 per cent Fe_2O_3) by this method; in other words, the method does not properly distinguish between free and combined iron oxides. In spite of these limitations it was felt that the method should give an approximate measure of the contents of free silica and free sesquioxides in the precipitates. Generalizations drawn from such data should therefore be recognized to be approximately applicable.

Raychaudhuri and Qudrat Ghani (12) have shown that the uptake of base is highest with alumino-silicate gel having a $SiO_2:Al_2O_3$ ratio of 8.0. Also, Raychaudhuri and Hussain Miah (11) have shown that freshly prepared aluminosilicate gels possess much less buffer capacity than aged ones, and that the buffer capacity of freshly prepared materials passes through a maximum value with increasing $SiO_2:Al_2O_3$ ratios, whilst with aged ones the buffer capacity continuously increases as the $SiO_2:Al_2O_3$ ratios of the precipitates increase, attaining a maximum value with pure silica gel. The maximum value of buffer capacity at a certain $SiO_2:Al_2O_3$ ratio of the freshly prepared gels is in agreement with the findings of Mattson (6, 7) and Wiegner (19). Chatterjee and Sen (3), working with synthetic mixtures of colloidal solutions of silicic acid and aluminum hydroxide, have given evidence of a slow interaction between colloidal silicic acid and aluminum hydroxide.

Raychaudhuri and Datta (10) have determined the properties of aluminosilicates formed under different conditions of mutual coagulation. These authors have mixed silicic acid and aluminum hydroxide sols in three molar ratios ($SiO_2:Al_2O_3 = 2, 3,$ and 4) in the following ways, and have studied the physicochemical properties of the precipitates: (1) silicic acid sol was added slowly at the rate of about 120 drops per minute to an aluminum hydroxide

sol in a beaker with continuous stirring; (2) aluminum hydroxide sol was added slowly, at a rate of about 120 drops per minute, to a silicic acid sol in a beaker, with continuous stirring; (3) silicic acid sol and aluminum hydroxide sols were taken in two bottles and were allowed to come in contact with each other drop by drop. It was found that on heating in steam autoclaves, the precipitated alumino-silicates tend to acquire more and more the properties of clay minerals. It was therefore felt desirable to investigate in greater detail the physicochemical properties of the mutual coagulum formed under different conditions, especially the percentages of free silica and free sesquioxide components (as determined by the method of Truog *et al.*) which may be present in the precipitates. It was also felt desirable to determine the distribution of sizes of particles in the precipitates. The electroösmotic charges and the $SiO_2 : Al_2O_3$ ratios have been determined. Next to alumina, iron oxide is the most important constituent of the clay fraction; hence it was also felt desirable to obtain precipitates by mixing oppositely charged colloidal solutions of silicic acid and ferric hydroxide and to determine the important physicochemical properties of these precipitates.

EXPERIMENTAL

Preparation of sols and precipitates

Silicic acid sol: Silicic acid sol was prepared by adding a 10 per cent solution of sodium silicate (Merck) to an excess of dilute hydrochloric acid, and was dialyzed in a parchment bag in running distilled water for 3 days.

Aluminum hydroxide sol: Ammonium hydroxide was added drop by drop to an 8 per cent solution of aluminum chloride. The precipitate was filtered through a Büchner funnel and was well washed with hot water. This precipitate was then transferred to a flask containing water, the actual proportion being 1 liter of water for every 3 g. of Al_2O_3. The whole was then heated and kept boiling, and 0.05 N hydrochloric acid was added from a buret. After each addition, water was added to replace that boiled off. An opalescent liquid that could be filtered unchanged was obtained. The colloidal solution of aluminum hydroxide, thus prepared, was then subjected to dialysis in a parchment bag for several days, till almost all the chloride was removed.

Ferric hydroxide sol: A 10 per cent ferric chloride solution was prepared. Of this 40 cc. was added to 2 liters of boiling water, whereupon colloidal iron hydroxide was formed. The sol was then dialyzed in parchment bags. The dialysis was continued for several days in running distilled water, till almost all the chloride was removed.

Alumino-silicate precipitates: The silicic acid and aluminum hydroxide sols were mixed (in proportions such that the mixture would contain silica and alumina in the ratios 2, 3, and 4) in different ways, such as: (*i*) Aluminum hydroxide sol was added to silicic acid sol at the rate of 60 drops per minute. (*ii*) Silicic acid sol was added to aluminum hydroxide sol at the rate of 60 drops per minute. (*iii*) The sols were mixed drop by drop with each other, and the rate of addition of drops was from 100 to 120 drops per minute. Nine precipi-

tates having $SiO_2:Al_2O_3$ ratios of 2, 3, and 4 were prepared in these three different ways.

Iron-silicate precipitates: The silicic acid and ferric hydroxide sols were mixed in the proportion $SiO_2:Fe_2O_3 = 2$ and in three different ways, as in the case of the alumino-silicates. The precipitates appeared only after dialysis for 12 to 24 hr.

Purification of the precipitates: Both the alumino-silicate and the iron-silicate precipitates formed were first washed by ordinary dialysis in parchment bags and subsequently by electrodialysis in a three-compartment apparatus, until there was no change in the conductivity of the wash water.

Determination of total silica, alumina, and iron oxide: The procedure followed was essentially that given in reference 1.

Determination of the electrical charge by electroösmosis: The electroösmotic experiments with the precipitates were carried out by the modified method of Briggs, Bennett, and Pierson (2), as recommended by Mukherjee (8).

Determination of free alumina, free silica, and free iron oxides: The percentages of free alumina, iron oxides, and silica were determined by following the method of Truog *et al.* (15).

Determination of saturation capacity: The saturation capacity was determined at pH 7.0, by the barium acetate and ammonium chloride method of Parker (9).

Determination of buffer curves: The buffer curves of the precipitates were obtained by the procedure adopted by Schofield (14).

<center>RESULTS</center>

A. Physicochemical properties of alumino-silicates

In the following tables, the symbols A_1, A_2, and A_3 denote alumino-silicate precipitates, silicic acid sol being added from buret to alumina sol in the beaker; B_1, B_2, and B_3 stand for precipitates obtained by adding alumina sol drop by drop to silicic acid sol; C_1, C_2, and C_3 were obtained by mixing silicic acid and alumina sols in drops.

Table 1 shows the $SiO_2:Al_2O_3$ mixing ratios and the percentages of moisture contents of the various precipitates.

Table 2 gives the data for the $SiO_2:Al_2O_3$ composition ratios of the different alumino-silicate precipitates, together with the electroösmotic charges.

Table 3 shows the percentages of free alumina and free silica of the alumino-silicate precipitates.

B. Physicochemical properties of iron-silicate precipitates

Tables 4 to 6 give the data on the physicochemical properties of the iron-silicates. The mixing ratio $SiO_2:Fe_2O_3$ of the sols was 2.0 in each case. The following notations were used: (*i*) D_1 stands for the precipitate obtained by adding silicic acid sol dropwise to ferric hydroxide sol; (*ii*) E_1 stands for the precipitate obtained by adding ferric hydroxide sol dropwise to silicic acid sol;

and (iii) F_1 stands for the precipitate obtained by mixing silicic acid and iron hydroxide sols drop by drop.

TABLE 1

PRECIPITATE NO.	MIXING RATIOS (SiO₂:Al₂O₃)	HYGROSCOPIC MOISTURE
		per cent
A₁	2.0	91
B₁	2.0	89
C₁	2.0	91
A₂	3.0	94
B₂	3.0	91
C₂	3.0	92
A₃	4.0	91
B₃	4.0	91
C₃	4.0	90

TABLE 2

PRECIPITATE NO.	COMPOSITION RATIO (SiO₂:Al₂O₃)	ELECTROÖSMOTIC MOVEMENT OF THE BUBBLE PER 5 MIN.
		cm.
A₁	1.6	−2.2
B₁	1.0	−0.7
C₁	1.8	−2.4
A₂	1.8	−2.3
B₂	2.6	−3.2
C₂	2.5	−3.4
A₃	3.5	−3.6
B₃	3.5	−3.2
C₃	2.1	−3.7
Silicic acid gel		−5.9
Alumina gel		+2.5

TABLE 3

PRECIPITATE NO.	FREE Al₂O₃	FREE SiO₂	FREE Al₂O₃ + FREE SiO₂
	per cent	*per cent*	*per cent*
A₁	10.7	23	33.7
B₁	8.3	13	21.3
C₁	14.5	19	33.5
A₂	8.9	21	29.9
B₂	6.0	27	33.0
C₂	4.0	33	37.0
A₃	9.9	37	46.9
B₃	4.0	43	47.0
C₃	4.6	44	48.6

Table 4 shows the percentages of hygroscopic moisture, the chemical compositions (SiO₂:Fe₂O₃), and the electroösmotic charges of the precipitates.

Table 5 shows the percentages of free SiO_2 and free Fe_2O_3 in the iron-silicates.

Table 6 gives the data on the uptake of base in milliequivalents per 100 g. of oven-dry material at different pH values. The corresponding data with SiO_2 and Fe_2O_3 gels are also included.

TABLE 4

PRECIPITATE NO.	HYGROSCOPIC MOISTURE	COMPOSITION RATIO (SiO_2:Fe_2O_3)	ELECTROÖSMOTIC MOVEMENT OF THE BUBBLE PER 5 MIN.
	per cent		*cm.*
D_1............	84.7	1.57	−0.2
E_1........	83.9	1.86	−0.9
F_1......, ...	83.1	1.81	−0.3
Silicic acid gel........			−5.2
Fe_2O_3 gel............			+2.6

TABLE 5

PRECIPITATE NO.	FREE SiO_2	FREE Fe_2O_3	FREE SiO_2 + FREE Fe_2O_3
	per cent	*per cent*	*per cent*
D_1	34.05	66.04	100.09
E_1....	36.00	64.00	100.00
F_1...........	36.20	63.81	100.01

TABLE 6

PRECIPITATE NO.	UPTAKE OF BASE IN MILLIEQUIVALENTS PER 100 G. OF OVEN-DRY MATERIAL					
	pH = 1.3	pH = 2.9	pH = 4.6	pH = 7.1	pH = 9.8	pH = 12.5
D_1	−48.0	−25.6	−10.6	+40.8	+150	+422
E_1....	−39.6	−28.5	−10.8	+39.3	+160	+473
F_1........	−47.5	−25.9	−15.0	+38.8	+170	+511
SiO_2 gel.	+2.0	+2.0	+6.9	+12.7	+107	+149
Fe_2O_3 gel............. ...	−96.7	−100.9	−30.8	+27.1	+86	+160

DISCUSSION

A. Work on alumino-silicates

Table 1 shows that the moisture contents of the precipitates are very high, approximately 90 per cent. This large amount of moisture should not have affected the results, since the data have been expressed on an oven-dry basis. Table 2 shows that the composition ratios of the precipitates are less than the mixing ratios. Similar results have been obtained by Raychaudhuri and Qudrat Ghani (12). Table 2 also shows that when silicic acid sol from the buret is added to aluminum hydroxide sol in the beaker, the SiO_2:Al_2O_3 ratios are 1.6, 1.8, and 3.5, the mixing ratios being 2, 3, and 4, respectively. It is therefore noticeable that the highest amount of silica is retained by the precipitates when the sols are mixed in the ratio SiO_2:Al_2O_3 = 4.0. The same fact is noticeable with precipitates B_1, B_2, and B_3, in that the composition ratio

(SiO_2:Al_2O_3) is highest (3.5) when the sols are mixed in the ratio SiO_2:Al_3O_3 = 4.0. With precipitates C_1, C_2, and C_3, however, the precipitate having the mixing ratio SiO_2:Al_2O_3 = 3.0 has the highest composition ratio. Table 2 also shows that the electroösmotic charges of all the alumino-silicates are negative, except that of Al_2O_4 gel which is positively charged. It is found that the higher the composition ratio (SiO_2:Al_2O_3), the higher is the electroösmotic charge. This corroborates the findings of Mattson (6), who has shown that the base-exchange properties of alumino-silicate precipitates increase with the increase in the ratio of silica to alumina. The data in table 2 show that the electroösmotic charge depends on the mode of formation of the precipitates. For the same mixing ratio, the precipitate formed by mixing the sols dropwise possesses the highest electroösmotic charge. Table 3 shows that the higher the mixing ratio

UPTAKE OF BASE IN M. EQ. PER 100 G. OVEN-DRY MATERIAL
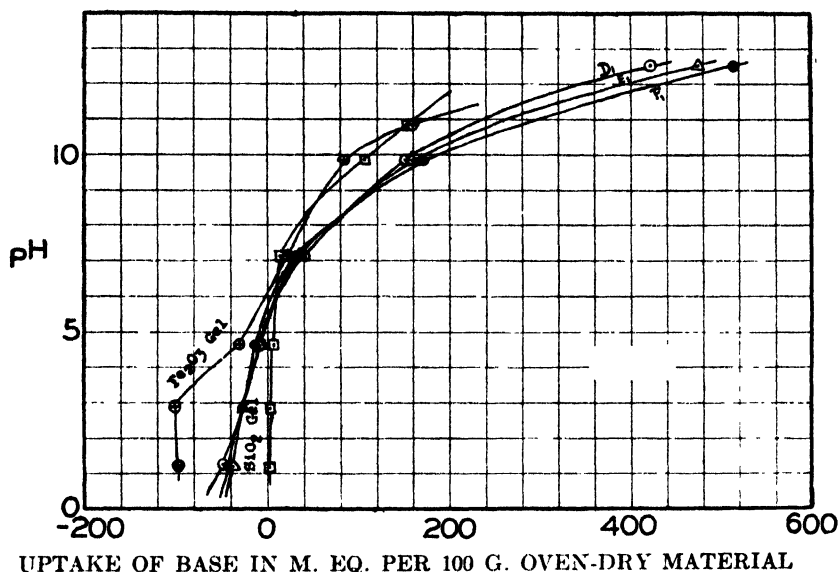
Fig. 1. Buffer curves

(SiO_2:Al_2O_3) of the precipitates, the higher is the percentage of free silica. On the whole, it appears that in the mutual coagulation of oppositely charged aluminum hydroxide and silicic acid sols, the greater portion of silica and alumina remains in the combined state, as is evidenced by the sum of the percentages of free alumina and free silica (vide table 3).[1] This may be due to the strong chemical affinity between silica and alumina.

B. Work on iron-silicates

Table 4 shows that the moisture contents of all the iron-silicate precipitates is nearly 83 to 84 per cent. Table 4 also shows that the composition ratios

---

[1] In view of the limitations of the method of Truog et al. for the determination of free silica and free sesquioxides, as pointed out above, this fact of itself does not preclude compound formation.

$(SiO_2:Fe_2O_3)$ of all the precipitates are less than the mixing ratios (2.0). The electroösmotic charge is always negative and increases as the composition ratios $(SiO_2:Fe_2O_3)$ increase. Table 5 shows the percentages of free silica and free iron oxide components in the iron-silicate precipitates. It is interesting to note that the sum of the percentages of free silica and free iron oxide components add up to 100 with all three precipitates.[1] It appears likely, therefore, that in the coagulum, D_1, E_1, and F_1, silicic acid and iron hydroxide have remained generally side by side. The fact that mineral formation has not taken place to a considerable extent is also evidenced by the low base-combining capacity of the coagulum (table 6).

Table 6 gives the data on the uptake of base, at different pH values. The corresponding buffer curves are shown in figure 1. It will be seen from the curves that up to pH 7.0 the buffer curves are steep, indicating that the buffer capacities of these materials are very low up to this pH. After pH 7.0, however, the buffer curves are flatter. The buffer curves of the freshly precipitated ferric oxide gel and of the silicic acid gel are steeper throughout than those of the iron-silicate precipitates, indicating that they possess less buffer capacities throughout the pH range. These observations suggest, therefore, that com-'ination between silicic acid and ferric oxide sols takes place more effectively above pH 7.0, whilst below pH 7.0 the precipitates contain iron oxide and silica more in the free state. That these constituents of the precipitates are generally in the uncombined state, under ordinary conditions of precipitation, has been shown in connection with the studies on the free iron oxide and free silica contents of the precipitates (table 5).

SUMMARY

Alumino-silicate gels have been prepared by mixing alumina and silicic acid sols in the ratios $SiO_2:Al_2O_3 = 2, 3,$ and 4 in three different ways. Iron-silicate gels have also been prepared by mixing iron hydroxide and silicic acid sols in the ratio $SiO_2:Fe_2O_3 = 2$ in the same three ways. The precipitates have been purified by electrodialysis, and the following properties of the purified precipitates and of electrodialyzed silica, alumina, and iron oxide gels have been studied: (a) chemical composition $(SiO_2:Al_2O_3$ ratio); (b) electroösmotic charge; (c) percentages of free silica, free alumina, and free iron oxides; (d) saturation capacity; and (e) buffer curves.

The alumino-silicate and iron-silicate precipitates are negatively charged, and the negative charges bear fair correlation with the composition ratios $(SiO_2:Al_2O_3$ or $SiO_2:Fe_2O_3)$.

In the alumino-silicates the greater part of the silica and alumina remains in the combined state, and the extent of combination depends on the pH. In the iron-silicate precipitates below pH 7.0, silicic acid and iron hydroxide remain generally in the free state.

REFERENCES

(1) Association of Official Agricultural Chemists (A. O. A. C.) *Methods of Analysis* (1938).
(2) BRIGGS, T. R., BENNETT, H. S., AND PIERSON, H. L. J. Phys Chem **22**, 256 (1918).
(3) CHATTERJEE, B., AND SEN, A. Indian J. Agr Sci **13**, 59 (1943).
(4) DROSDOFF, M., AND TRUOG, E. J. Am. Soc Agron. **27**, 312 (1935)
(5) FREUNDLICH, H. *Colloid and Capillary Chemistry* (1921)
(6) MATTSON, S. Soil Sci **25**, 289 (1928).
(7) MATTSON, S. Soil Sci **30**, 459 (1930).
(8) MUKHERJEE, J. N. Nature **110**, 732 (1922).
(9) PARKER, F. W. J. Am. Soc. Agron. **21**, 1030 (1929)
(10) RAYCHAUDHURI, S. P., AND DATTA, N. B.. J. Phys. Chem **49**, 21 (1945)
(11) RAYCHAUDHURI, S. P., AND HUSSAIN MIAH, A. J Indian Chem Soc **20**, 195 (1943)
(12) RAYCHAUDHURI, S. P., AND QUDRAT GHANI, A. K. M. J Indian Chem Soc **19**, 311 (1942).
(13) ROBINSON, G. W. *Soils* D Van Nostrand Company, New York (1932)
(14) SCHOFIELD, R. K. J Agr Sci. **23**, 252 (1933)
(15) TRUOG, E., *et al* Proc Soil Sci Soc Am. **1**, 101 (1936)
(16) WEISER, H B, AND CHAPMAN, T S J. Phys Chem **35**, 543 (1931)
(17) WEISER, H B, AND CHAPMAN, T S J Phys Chem **36**, 713 (1932)
(18) WEISER, H B, AND MILLIGAN, W. O J Phys Chem **47**, 424 (1943)
(19) WIEGNER, G J Soc Chem Ind **50**, 65T, 103T (1931)

MOLECULAR-SIZE DISTRIBUTION OF CROSS-LINKED POLYSTYRENE

I VALYI[1], A. G. JANSSEN[2], AND H. MARK

Polytechnic Institute of Brooklyn, Brooklyn, New York

Experiments on the influence of divinylbenzene on the polymerization of styrene were carried out several years ago by Staudinger *et al.* (4, 5) and similar studies were recently published by Ch. Walling (7). The principal result is that copolymers containing only a few per cent of the cross-linking agent are insoluble in benzene, toluene, ethyl methyl ketone, etc., but do swell in such liquids. The purpose of this article is to investigate the molecular-size distribution of copolymers of styrene and divinyl derivatives.

Divinylbenzene is difficult to obtain and preserve in the pure monomer state

---

because of its strong tendency to polymerize as soon as the last traces of inhibitor are removed.   It seemed, therefore, advisable to carry out the cross linking with other divinyl derivatives, which are solid around and above room temperature and therefore can be adequately purified by repeated crystallization.

Two new divinyl derivatives, divinyldiphenyl and diisopropenyldiphenyl, were prepared for this purpose.   Immediately after their preparation both substances are fusible and soluble and exhibit the sharp x-ray powder diagram of a normal crystalline organic material.   After standing at room temperature for a few hours, however, divinyldiphenyl loses its sharp melting point, becomes insoluble in all solvents, and its x-ray powder ceases to exhibit sharp rings. Figures 1a and 1b show the powder diagrams of divinyldiphenyl and diisopropenyldiphenyl 8 days after their preparation.   The first pattern shows only a
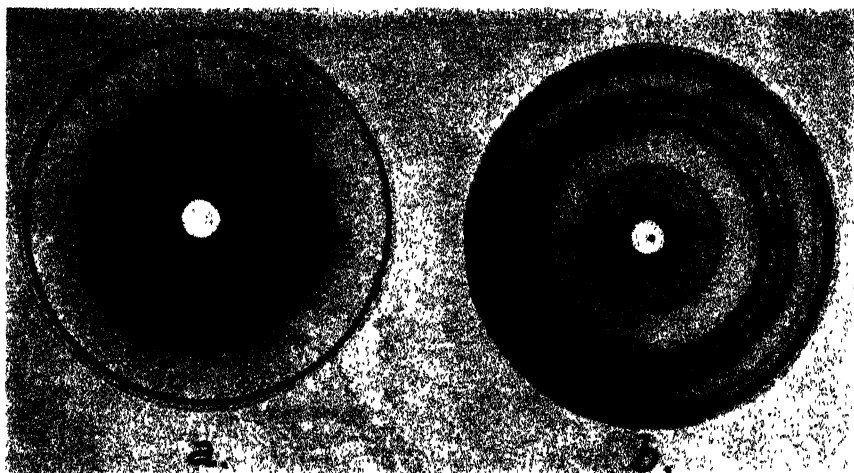
FIG. 1a. Powder diagram of divinyldiphenyl after it had polymerized in the solid state
    FIG. 1b. Powder diagram of diisopropenyldiphenyl showing that this substance has not polymerized.

few diffuse halos, characteristic of most crystalline polymers.   The second corresponds to the sharp powder diagram of a normal organic chemical substance. This indicates that divinyldiphenyl polymerizes at room temperature in the solid state, without changing the external form of the needle-shaped crystals. Diisopropenyldiphenyl remains fusible and soluble for several months, but ultimately it also polymerizes.   It can be stored indefinitely in an ice box and therefore was used for all cross-linking experiments.

PREPARATION OF DIVINYL DERIVATIVES

Twenty-five grams of diacetyldiphenyl (m.p. 185–187°C.) was added to a Grignard solution prepared in ether from 16.7 g. of magnesium and 39 ml. of methyl iodide at room temperature.   Then 250 ml. of dry toluene was added, the ether was distilled off, and the remaining mixture was refluxed for 6 hr.

The reaction product was decomposed with a mixture of ice and ammonium chloride, and the residue from the toluene solution was dissolved in acetal and repeatedly crystallized therefrom. The dicarbinol can be obtained in two forms: white silky needles, f.p. 154°C., C = 78.5 per cent, H = 8.2 per cent; and white platelets, f.p. 149–150°C., C = 80.2 per cent, H = 7.9 per cent, molecular weight = 267.3. The theoretical values for p,p'-di(hydroxyisopropyl)diphenyl are C = 80.0 per cent, H = 8.1 per cent, molecular weight = 270. Both forms give the same divinyl derivative upon dehydration. Eighteen grams of the dicarbinol was obtained from 25 g. of diacetyldiphenyl.

Nine grams of the dicarbinol was boiled with 15 ml. of acetic anhydride for 6 hr. The original material first dissolved completely, but later a white precipitate appeared, which was separated from the mother liquor on a suction filter. By addition of water, more of this material could be obtained from the mother liquor. After repeated recrystallizations from isobutyl alcohol, the material still exhibited an unsharp melting point around 165°C. and was not very stable. Drying *in vacuo*, even at room temperature, resulted in a yellow resinous material before the last traces of solvent could be eliminated. To purify the product and obtain a material that is stable for at least half a year, a sublimation in high vacuum (1.5 mm.) at 170°C. has to be carried out. Beautiful crystals were obtained: m.p. 173–177°C. (closed capillary); analysis, C = 92.1 per cent, H = 7.8 per cent. The calculated values for the divinyl derivative are C = 92.3 per cent, H = 7.7 per cent. The yields of the dehydration and sublimation steps were almost quantitative.

The p,p'-divinyldiphenyl was prepared from p,p'-diacetyldiphenyl; the diketone was reduced by the use of aluminum triisopropoxide in the presence of isopropyl alcohol, and the p,p'-di(β-hydroxyethyl)diphenyl so obtained was then dehydrated with activated alumina. It was so much less stable than the homologous isopropyl compound that it was not used in the present copolymerization experiments.

COPOLYMERIZATION OF STYRENE WITH DIISOPROPENYLDIPHENYL

Commercial (inhibited) monostyrene was purified by washing six times in a separatory funnel with 10 per cent sodium hydroxide solution and then with six portions of distilled water. It was then dried for 3 days at 0°C. with calcium chloride. The styrene so prepared was fractionally distilled at reduced pressure until it was characterized by the following data: b.p. = 146°C.; d = 0.907; n = 1.5434.

Bulk polymerization was carried out with the following materials in glass ampoules: 15 g. purified styrene, 0.05 mole per cent benzoyl peroxide catalyst, and diisopropenyldiphenyl as cross-linking agent varying from 10 to 1000 parts per million. A blank was run containing no cross-linking agent. The polymerization took place in a thermostatically controlled water bath at 70°C. for 3 days, and gave approximately 95 per cent conversion to polystyrene.

The polymer containing the highest amount of cross-linking agent (1000 ppm.) was insoluble in toluene. It did, however, swell to several hundred per

cent of its original volume. A qualitative representation of this swelling is shown in figure 2. Here, a disc of the polymer is shown in its original size and shape (figure 2a), after it has swelled in toluene for several days (figure 2b), and after it has been allowed to return slowly to its original dimensions out of contact with the swelling agent (figure 2c).

The polymers containing up to 100 ppm. of cross-linking agent, as well as the blank, were completely soluble in toluene. They were freed from residual monomer by precipitation with an excess of methanol. These polymers were further purified by redissolving several times in ethyl methyl ketone and precipitating with methanol.
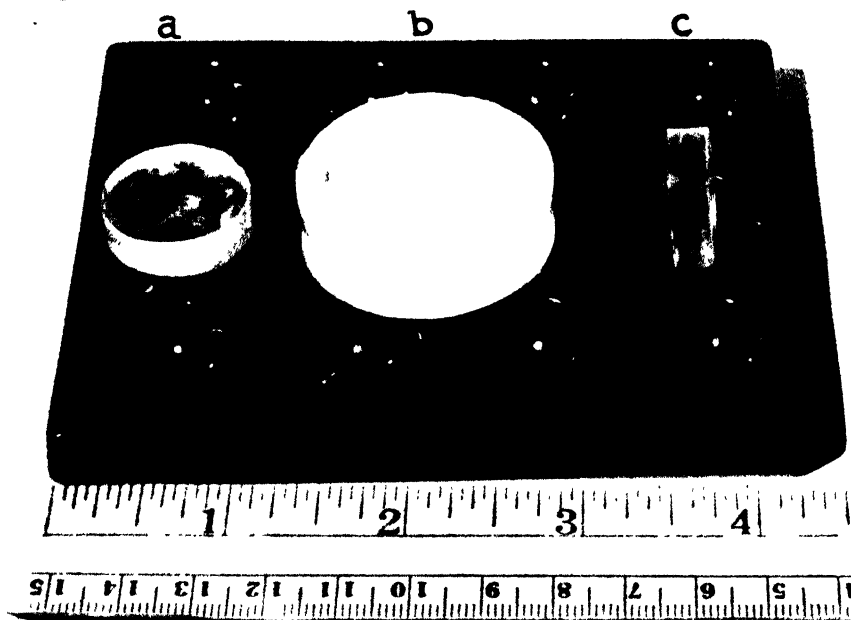
Fig. 2a. Disc of polystyrene containing 100 ppm. diisopropenyldiphenyl
Fig. 2b. Same disc after swelling in toluene at room temperature
Fig 2c. Same disc after evaporation of the swelling agent

FRACTIONATION OF THE SOLUBLE POLYMERS

Polystyrene without any divinyl derivative and the samples containing 10, 25, and 100 ppm. of the cross-linking agent were dissolved in ethyl methyl ketone (2 per cent polymer) and fractionally precipitated. This was achieved by first cooling the solution to 0°C. and adding methanol drop by drop until a slight turbidity resulted. The solution was then warmed to 20°C., whereupon the turbidity completely disappeared. Upon cooling the system very slowly (16–18 hr.) to 0°C., it split into two layers which could be separated by decantation. The same procedure was then repeatedly applied to each layer and a number of fractions were obtained in this way. All fractions were reprecipitated from ethyl methyl ketone, thoroughly washed, and dried to constant weight at room temperature *in vacuo*. In the case of the polymer containing 10 ppm.

twenty fractions were obtained, in all other cases six (compare table 1). Solutions of the fractions in dust-free toluene were used for viscosity measurements. The concentrations ranged from 0.2 to 1 per cent. Viscosities were measured

TABLE 1

Fractions of the various copolymers of styrene and diisopropenyldiphenyl with their intrinsic viscosities, molecular weights, and degrees of polymerization

A. *Sample containing no cross-linking agent*

$f = 2.000000; \alpha = 0.99965$

NUMBER OF FRACTION	WEIGHT OF FRACTION	INTRINSIC VISCOSITY	MOLECULAR WEIGHT	DEGREE OF POLY-MERIZATION
	grams			
1	0.30	0.20	38,000	380
2	0.57	0.43	110,000	1100
3	1.35	0.74	240,000	2400
4	6.85	1.38	560,000	5600
5	6.60	1.72	750,000	7500

Total initial weight of sample................... .... 16.00 g.
Total weight of all fractions... 15.67 g.
Viscosity average *DP*.................................... 5800

B. *Sample containing 10 ppm. of cross-linking agent*

$f = 2.000018 \leftrightharpoons 2.00002; DP$ (calculated) $= 6100$

NUMBER OF FRACTION	WEIGHT OF FRACTION	INTRINSIC VISCOSITY	MOLECULAR WEIGHT	DEGREE OF POLY-MERIZATION
	grams			
1	0.09	0.23	45,000	450
2	0.08	0.46	115,000	1150
3	0.24	0.56	163,000	1630
4	1.15	0.66	206,000	2060
5	1.35	0.73	232,000	2320
6	0.54	0.90	302,000	3020
7	1.55	1.04	376,000	3760
8	0.59	1.12	410,000	4100
9	0.13	1.15	426,000	4260
10	0.85	1.18	447,000	4470
11	0.49	1.23	485,000	4850
12	0.27	1.28	500,000	5000
13	0.75	1.33	535,000	5350
14	0.73	1.50	631,000	6310
15	0.38	1.52	658,000	6580
16	1.26	1.58	680,000	680
17	1.11	1.98	923,000	9230
18	0.69	2.03	950,000	9500
19	1.23	2.15	1,060,000	10,600
20	2.19	3.00	1,660,000	16,600

Total initial weight of sample.. 16.00 g.
Total weight of fractions.. 15.67 g.
Viscosity average *DP* 6900

TABLE 1—*Continued*

C. *Sample containing 25 ppm. of cross-linking agent*

$f = 2.000045 \leftrightharpoons 2.00005$; DP (calculated) = 6700

NUMBER OF FRACTION	WEIGHT OF FRACTION	INTRINSIC VISCOSITY	MOLECULAR WEIGHT	DEGREE OF POLY-MERIZATION
	grams			
1	0.45	0.13	21,000	210
2	0.60	0.25	54,000	540
3	1.60	0.75	250,000	2500
4	2.25	0.94	333,000	3300
5	3.65	1.23	480,000	4800
6·	6.30	2.20	1,070,000	10,700

Total initial weight of sample.... .... 15.00 g.

Total weight of all fractions....... .. .. 14.85 g.

Viscosity average DP.............. · ... · 6600

D. *Sample containing 100 ppm. of cross-linking agent*

$f = 2.00018 \leftrightharpoons 2.0002$; DP (calculated) = 13,300

NUMBER OF FRACTION	WEIGHT OF FRACTION	INTRINSIC VISCOSITY	MOLECULAR WEIGHT	DEGREE OF POLY-MERIZATION
	grams			
1	0.20	0.50	140,000	1400
2	1.10	0.81	280,000	2800
3	2.35	0.90	310,000	3100
4	4.80	1.60	690,000	6900
5	6.40	2.90	1,600,000	16,000

Total initial weight of sample................... .. .. 15.00 g.

Total weight of all fractions....................... . .. . 14.85 g.

Viscosity average DP................................... 9900

at 35°C. in an Ostwald viscosimeter. The capillary was 10 cm. long and 0.4 mm. in diameter, and had an efflux time for the pure solvent of 80–90 sec. Specific viscosities were calculated in the usual way. η_{sp}/c was plotted against the concentration c, expressed in grams of solute per 100 cc. of solution, and the intrinsic viscosities of the various fractions were obtained by extrapolation. In all cases sufficiently straight lines were indicated by the experimental points to justify this standard procedure. The molecular weights of the fractions were then calculated by formula 1[3]:

$$[\eta] = KM^a \tag{1}$$

[3] It should be pointed out here that the application of this formula is strictly justified only for the uncross-linked material, because both K and a very probably depend upon the structural details of the chain molecules, and hence upon the degree of branching or cross linking. However, the concentration of the divinyl derivative in the polymer is so small that even in the case of 100 ppm. the distance between two branches or cross links along a chain corresponds on the average to 10,000 monomer units. It seems therefore not un-reasonable to use the same constants in equation 1 to convert intrinsic viscosities of the fractions in DP's.
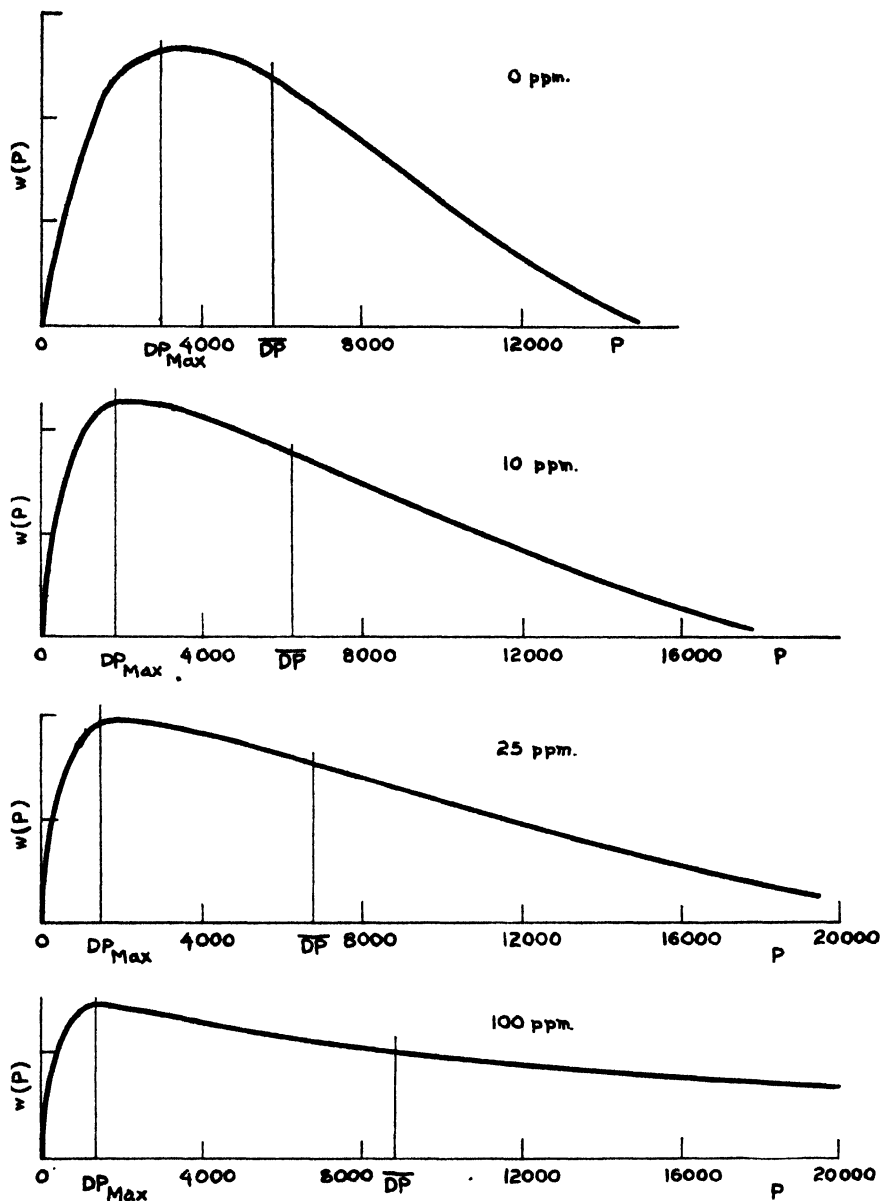
Fig. 3. Differential weight distribution curves of polystyrene containing different amounts of diisopropenyldiphenyl. The average degree of polymerization, $\bar{DP}$, moves to higher values as cross linking increases; the maximum of the distribution curve, DP_{max}, however, moves to lower values of DP.

where $K = 1.0 \times 10^{-4}$, $a = 0.72$, and $[\eta]$ = intrinsic viscosity. The molecular weights were found to range from 40,000 to 750,000 for the uncross-linked material up to 1,500,000 for 100 ppm. of diisopropenyldiphenyl. A few of the

fractions were also subjected to light-scattering measurements, and it was found that the molecular weights obtained were in reasonable agreement with the values calculated from the viscosity data using equation 1[3].

RESULTS AND DISCUSSION

Table 1 contains the results of the fractionation of an uncross-linked sample and of three polymers containing 10, 25, and 100 ppm. of diisopropenyldiphenyl. The first column shows the number of the individual fraction, the second its weight, the third its intrinsic viscosity, and the fourth and fifth its molecular weight and degree of polymerization (DP) computed according to equation 1. From these data integral and differential molecular weight distribution curves were constructed in the conventional way (3). Figure 3 represents the four distribution curves of polymers with 0, 10, 25, and 100 ppm. It can be clearly seen that even as little as 10 ppm. of a divinyl derivative exhibits a considerable influence on the shape of the molecular weight distribution curve long before it causes insolubility of the polymer. Such slightly cross-linked polymers have a

TABLE 2

A few data characterizing the distribution curves of vinyl-divinyl copolymers

CONCENTRATION OF DIISOPROPENYL-DIPHENYL	$\overline{DP}_w$ (OBSERVED)	$\overline{DP}_w$ (COMPUTED)	DP_w (MAX) (OBSERVED)	DP_w (MAX) (COMPUTED)	$\Delta(DP_w)$ (OBSERVED)
ppm.					
0	5800	(5800)	2600	2900	8000
10	6500	6100	1600	2100	9000
25	6600	6700	1400	1500	11500
100	9900	13300	1200	600	14000
300	gel	∞			
1000	gel	∞			

higher average molecular weight than the normal polymer prepared under the same conditions, and their distribution curve has a greater spread than that of the normal polymer. Table 2 shows the weight average molecular weight $\overline{M}_w$, and the width $\Delta(DP)_w$ of the distribution curve at half of its maximum height, of a normal polymer and of the three cross-linked samples. It can be seen that both quantities increase with increasing amount of cross-linking agent. Qualitatively this appears as a consequence of the fact that, for statistical reasons, the number of tetrafunctional monomers in a chain will be approximately proportional to its length. Larger molecules therefore contain more double bonds distributed along their chains and have a greater tendency to develop a branch or a cross link than short ones. This results in a distortion of the molecular weight distribution curve towards higher DP's, as shown in figure 3.

Quantitatively, the theory of cross linking and gelation has been worked out by Flory (2) and Stockmayer (6) for polymerization processes involving the presence of several-functional monomers. The conditions on which their computations are based are not entirely identical with those holding for a radical-

type polymerization as investigated in this paper, but their equations contain the general tendency of cross-linking agents to shift the average DP to higher values and to increase the width of the distribution curve. According to Stockmayer[4] the weight average DP of a cross-linked polymer is given by

$$\overline{DP}_w = \frac{1 + \alpha}{1 - (f - 1)\alpha} \qquad (2)$$

where α is the reacted fraction of functional groups and f represents the average functionality of the polymerizing mixture. For linear polymers equation 2 reduces to

$$\overline{DP}_w = \frac{1 + \alpha}{1 - \alpha} \qquad (3)$$

Because of the small amount of divinyl derivative used in our experiments, $(f - 1)$ is only very slightly larger than unity, and $\alpha(f - 1)$ is smaller than 1. This is the range in which still soluble polymers are obtained, the average DP of which increases with the amount of divinyl derivative employed.

To compare our results with the degrees of polymerization as expected by the theory, we have first determined α from the $\overline{DP}$[5] of the uncross-linked polymer ($\overline{DP}$ = 5800) with the aid of equation 3. One obtains $\alpha = 0.99965$. Using this value and the values for f as they result from the proportion of styrene–divinyl derivative (compare table 1), we have then computed from equation 2 the weight average degrees of polymerization for the cross-linked samples. Table 2 contains in its first column the amount of cross-linking agent employed, in the second column the observed $\overline{DP}_w$, and in the third column the $\overline{DP}_w$ computed from equation 2. It can be seen that both columns indicate an increase of the average DP and that the numerical values for the 10-ppm. and 25-ppm. samples agree fairly closely. The larger theoretical value of 13,300 for the 100-ppm. sample as compared with the experimental value of 9900 may be explained by the fact that, as often in copolymerization, the amount of divinyl derivative in the polymer was not simply proportional to its concentration in the monomer mixture. It may also be caused by the fact that the constants K and a of equation 1 do not hold any more for polymers with as much branching as was produced by 100 ppm. of divinyl derivative. Equation 3 can also be used to predict the gel point of the copolymer; it is reached as soon as

$$f = \frac{1 + \alpha}{\alpha} \qquad (4)$$

---

[4] Reference 6: equation 16 on page 48.

[5] The average DP as obtained from viscosity measurements with the aid of equation 1 is the viscosity average, while Stockmayer's equations hold for the weight average. If the exponent in equation 1 is not too far from unity (above 0.70), the difference amounts to about 15–20 per cent. In using the viscosity average instead of the weight average, we are thereby introducing an error of the above magnitude. We presume, however, that because of the relatively small number of fractions (five and six) in the case of three of the samples, none of the conclusions of this paper can be made with an accuracy better than 25 or 30 per cent.

because equation 4 makes the $\overline{DP}_w$ of equation 3 infinitely large; for the conditions prevailing in our experiments this should happen at about 250 ppm. of divinyl derivative. This is in fair accord with a previous observation of Staudinger and Heuer (4). Evaluating their figures according to equation 4, one arrives at a gel point at 225 ppm. of divinylbenzene in styrene. It also is confirmed by our own observations that all copolymers containing more than 300 ppm. of diisopropenyldiphenyl are practically insoluble.

Another interesting phenomenon is revealed by the distribution curves of figure 3. The average DP increases with increasing amount of cross-linking agent, but the maximum of the distribution curve moves to lower DP values. This is actually predicted in the theories of Flory (2) and Stockmayer (6). Considering that in our case f is very close to 2, equation 14 on page 47 in Stockmayer's paper (6) leads to the following approximate expression for the DP_w-(max) which is most abundantly present in the polymolecular mixture:

$$DP_w \text{ (max)} = -\frac{1}{\ln \alpha + (f - 2) \ln (1 - \alpha)} \tag{5}$$

Using the above values for α and f (compare table 1), one obtains for DP_w (max) the values which are given in column 5 of table 2. On comparing them with the observed figures in column 4, it appears that the observed shift of the maximum of the distribution curve towards lower DP's is in reasonable agreement with the theoretical expectation for 10 and 25 ppm. For 100 ppm. of divinyl derivative, however, the observed and calculated values for DP_w (max) differ to a considerable degree. They behave just as the corresponding $\overline{DP}_w$ did, and it may be that one of the explanations offered for them can also be applied for the maximum values.

SUMMARY

1. p,p'-Divinyldiphenyl and p,p'-diisopropenyldiphenyl have been prepared. They are crystalline at room temperature, but polymerize rapidly upon melting. Diisopropenyldiphenyl is stable at room temperature for a long time, while divinyldiphenyl polymerizes in the crystalline state within a few days.

2. Copolymers of styrene with 10, 25, 100, and 1000 ppm. of diisopropenyldiphenyl were made, and it was found that samples containing more than 300 ppm. are practically insoluble.

3. Molecular weight distribution curves for the soluble polymers were worked out. It was found that with increasing amount of cross-linking agent the weight average DP shifts to larger values, the most frequent DP shifts to smaller values, and the distribution curve flattens out.

REFERENCES

(1) ALFREY, T., BARTOVICS, A., AND MARK, H.: J. Am. Chem. Soc. **65**, 2319 (1943).
(2) FLORY, P. J.: J. Am. Chem. Soc. **63**, 3083, 3091, 3096 (1941).

(3) *Cf.* MARK, H., AND RAFF, R.: *High Polymeric Reactions*, p. 47. Interscience Publishers, Inc., New York (1941).
(4) STAUDINGER, H., AND HEUER, W.: Ber. **67**, 1164 (1934).
(5) STAUDINGER, H., AND HUSEMANN, E.: Ber. **68**, 1618 (1935).
(6) STOCKMAYER, W. H.: J. Chem. Phys. **11**, 45 (1943).
(7) WALLING, CH.: J. Am. Chem. Soc. **67**, 441 (1945).

SEPARATION OF METAL IONS BY CATION EXCHANGE

R. KOZAK AND H. F. WALTON

Department of Chemistry, Northwestern University, Evanston, Illinois

It is a well-known fact that metal ions are taken up preferentially from solution by materials capable of cation exchange. It should, therefore, be possible to separate a mixture of cations of varying ionic size by passage through an exchanger. This principle has been used by Russell and Pearce (1) in an attempt to fractionate the rare earths. Tests have here been made with a number of different mixtures—copper and nickel, cadmium and zinc, silver and copper—to determine whether a practical quantitative separation could be attained by cation exchange.

EXPERIMENTAL

The cation exchanger used was the sulfonated coal known as Zeo-Karb, which was first washed with concentrated hydrochloric acid to remove metallic cations and small amounts of iron oxide and then rinsed with water. All experiments but the last one cited were performed in a 2-ft. column of 20-mm. glass tubing, containing 70 g. of Zeo-Karb. In the last experiment, a 6-ft. column, containing 244 g. Zeo-Karb, was used. In most cases, the solution containing a mixture of two salts was passed through the exchanger at a rate of about 10 ml. per minute until one of the metal ions began to appear in the effluent. The metals were then regenerated with acid, 100-ml. fractions being collected and analyzed. Both ammoniacal and slightly acid solutions of varying concentrations were tried. Some typical results are given in table 1.

CONCLUSION

The fractionation of metal ions by cation exchange does not give a quantitative separation. The method could be improved by using a much longer column, but the process would then not be as practical as chemical separation.

REFERENCE

(1) RUSSELL AND PEARCE: J. Am. Chem. Soc. **65**, 595–600 (1943).

TABLE 1

Separation of metal ions by cation exchange

INFLUENT	REGENERANT	EFFLUENT FRACTION	ANALYSIS	
3115 ml. CuSO₄ (0.1 *M*) + NiSO₄ (0.1 *M*) + NH₃	2 *M* H₂SO₄	*ml.*	Cu and Ni analyzed electrolytically	
			millimoles Cu	millimoles Ni
		0–100	13.4	12.4
		100–200	33.4	26.0
		200–500	12.7	7.0
			——	——
			59.5	45.4
3076 ml. CdSO₄ (0.1 *M*) + ZnSO₄ (0.1 *M*) + NH₃	2 *M* H₂SO₄		Cd and Zn determined polarographically	
			millimoles Cd	millimoles Zn
		0–100	14.2	9.5
		100–200	33.8	18.2
		200–500	4.1	1.5
			——	——
			52.1	29.2
500 ml. ZnSO₄ (0.01 *M*) + CdSO₄ (0.01 *M*); stopped when metal ion first appeared in effluent	2 *M* H₂SO₄		millimoles Cd	millimoles Zn
		0–100	1.0	1.2
		100–200	3.1	3.4
		200–400	0.5	0.5
			——	——
			4.6	5.1
2 liters Ag₂SO₄ (0.01 *M*) + CuSO₄ (0.01 *M*); stopped when Cu first appeared in effluent	2 *M* H₂SO₄		Ag and Cu determined together electrolytically; Ag determined by precipitation as AgCl, Cu obtained by difference	
			millimoles Ag	millimoles Cu
		0–100	1.0	4.8
		100–200	6.8	12.9
		200–300	5.4	0.8
		300–800	16.6	0.2
			——	——
			29.8	18.7
2 liters Ag₂SO₄ (0.01 *M*) + CuSO₄ (0.01 *M*); stopped when Cu first appeared in effluent	2 *M* H₂SO₄		millimoles Ag	millimoles Cu
		0–100	0.6	14.6
		500–600	3.4	1.3
		600–700	5.1	0.5
		700–1300	21.7	0.1
			——	——
			30.8	16.5

SIMPLE KINETIC THEORY OF IONIC EXCHANGE FOR IONS OF UNEQUAL CHARGE

LANNES E. DAVIS

Division of Soils, University of California College of Agriculture, Davis, California

Received March 20, 1945

INTRODUCTION

A theoretical discussion of ionic exchange equilibria may be approached either from a consideration of the thermodynamics or statistics of a system at equilibrium or by developing the kinetics of the exchange process. Kinetic theories have been presented by Vageler and Woltersdorf (8), Gapon (2), and Jenny (5).

Vageler and Woltersdorf attempted to apply Langmuir's adsorption theory to the case of ionic exchange. Gapon assumed that ionic exchange is a reversible process, leading to the formation of two complexes, formed by adsorption of each kind of exchangeable ion. At equilibrium the rates of adsorption of each kind of ion must be equal. It is assumed that the rate of each adsorption is proportional to the concentration in the liquid phase of the ion which is being adsorbed, to the number of the other kind of ion on the colloidal surface, and to a constant.

These two theories apparently are based upon the assumption that the adsorption is a simple process involving a monomolecular layer on the colloidal surface. Ions are present in the system in one or the other of two discrete states,—an adsorbed state and a completely free state. This idea is not entirely consistent with the concept of a diffuse double layer.

THE OSCILLATION VOLUME THEORY

Jenny's theory represents the ions as present in a diffuse double layer. Each ion required to neutralize the charge on the particle is oscillating in an oscillation cell adjacent to a charged area on the particle surface. Other ions from the added electrolyte may enter the oscillation cells, or may remain in the external phase. A condensed statement of this theory, with minor changes in terminology, is presented.

Ions of equal charge

The two ionic species in an exchange process are labeled w and b. The rate of adsorption of w ions and release of b ions from a surface containing b ions may be considered. Each adsorbed b ion is oscillating in the neighborhood of one or more active spots, of unit electronic charge, on the surface of the colloid particle. The number of active spots per oscillation cell will be equal to the charge number of the b ion. The volume of the oscillation cell is v_b. The total volume of the system is V. The numbers of wandering w and b ions present in the system are N_w and N_b, respectively.

Wandering members of both ionic species w and b may be present in the os-

cillation cell of an adsorbed b ion. The numbers of each, n and m, respectively, may vary from time to time. The probabilities, W_n and B_m, of each number being present, and the probability, $W_n B_m$, of both being present simultaneously may vary. The fraction, $\alpha_{n,m}$, of the number, n, of w ions present in the oscillation cell of a b ion which will be adsorbed will vary with n and m, so that the probability of adsorption will be $\alpha_{n,m} W_n B_m$, for an oscillation cell containing n and m ions, respectively, of the species w and b. The total probability of adsorption will then be

$$P_w = \sum_{n,m} \alpha_{n,m} W_n B_m = (\alpha_0 W_0 B_0) + (\alpha_1 W_1 B_0 + \beta_1 W_0 B_1)$$

$$+ (\alpha_2 W_2 B_0 + \beta_2 W_1 B_1 + \gamma_2 W_0 B_2) + \cdots \quad (1)$$

where the various coefficients refer to the general term $\alpha_{n,m}$.

The individual probability terms, W_n and B_m, are functions of the numbers n and m of ions actually present at any moment and of the average numbers, μ_w and μ_b, present in the oscillation cells of the b ions. The terms μ_w and μ_b are proportional to the number of wandering ions per unit volume of the system and to the volume of the oscillation cell. That is,

$$\mu_w = \frac{v_b}{V} N_w \quad \text{and} \quad \mu_b = \frac{v_b}{V} N_b$$

The probability terms are then

$$W_n(v_b) = \frac{(\mu_w)^n}{n!} e^{-\mu_w} \quad \text{and} \quad B_m(v_b) = \frac{(\mu_b)^m}{m!} e^{-\mu_b}$$

Equation 1 then becomes

$$P_w = e^{-(v_b/V)(N_w + N_b)} \left[\alpha_0 + \frac{v_b}{V} (\alpha_1 N_w + \beta_1 N_b) \right.$$

$$\left. + \left(\frac{v_b}{V} \right)^2 \left(\alpha_2 \frac{N_w^2}{2} + \beta_2 N_w N_b + \gamma_2 \frac{N_b^2}{2} \right) + \cdots \right] \quad (2)$$

The rate of adsorption of w ions by the colloid is proportional to P, the probability of adsorption for each cell; to z_b, the number of cells; and to $f(u)$, a function of the velocity of the ions. Thus, we have

$$\frac{\Delta w}{\Delta t} = z_b P_w f(u)_b \quad (3)$$

We may now consider a surface containing w ions. Since the number of active spots per oscillation cell is the same for the two kinds of ions if they have the same charges, an expression similar to equation 3 will hold for the adsorption of b ions in the oscillation cells of w ions. At equilibrium

$$\frac{\Delta w}{\Delta t} = \frac{\Delta b}{\Delta t}$$

or

$$\frac{z_b}{z_w} = \frac{P_b}{P_w} \cdot \frac{f(u)_b}{f(u)_w} \quad (4)$$

Comparing equations 1 and 2, we note that α_0, β_1, and γ_2 equal zero. Furthermore, since v_b and v_w are very small compared with V, the higher terms in equation 2 may be quite small. To a first approximation they may be neglected, *particularly since they occur to the same power in both numerator and denominator of the expansion of the right member of equation 4.* The ratio of the exponentials is approximately unity. We may, therefore, write

$$\frac{z_b N_w}{z_w N_b} = \frac{v_w \alpha_{1(b)} f(u)_b}{v_b \alpha_{1(w)} f(u)_w} = K \tag{5}$$

Jenny has assumed that the ratios v_w/v_b, $\alpha_{1(b)}/\alpha_{1(w)}$, and $f(u)_b/f(u)_w$ are constants, the latter two equal to unity, so that K is a constant.

Although, by elimination of the higher terms in equation 2, a result identical with Gapon's equation is finally obtained, Jenny's theory is probably to be preferred. The approximate character of the final result is explicitly indicated. The value K may be expected to vary somewhat with variation in N_w and N_b. The direction, and possibly the approximate magnitude, of this variation might be predicted in favorable cases. Gapon's theory leaves us no such opportunities. Furthermore, as has been stated, Jenny's theory explicitly recognizes the diffuse character of the double layers.

Ions of unequal charge

Hofmann and Giese (4) state that in accordance with an investigation by Jenny they have attempted to derive an equation for ions of unequal charge on the basis of the law of mass action. The method of derivation is not presented and it is by no means certain that they utilized Jenny's method. However, they employ the terms v_{Ca} and v_{NH_4} to symbolize the volumes which are available to the calcium or ammonium ions bound to the clay, i.e., the "oscillation volumes," according to Jenny. It seems probable that they merely set up an equation analogous to those which may be derived from the law of mass action considered as a chemical reaction, but applied the law of mass action to a partition between the external system and the oscillation volumes. Translated into the terms used by Jenny, their equation becomes

$$\frac{z_b N_w^2}{z_w^2 N_b} = k \left(\frac{v_b}{V}\right) \Big/ \left(\frac{v_w}{V}\right)^2 \tag{6}$$

By utilizing the statistical method developed by Jenny, with no reference to the concept of mass action, an entirely different expression can be derived. Let us consider an exchange involving ions whose charge number equals 1, labelled w ions, and ions whose charge number equals 2, labelled b ions. The criteria for the equilibrium state cannot be that the rate of adsorption of w ions is equal to the rate of adsorption of b ions in the case of unequal charge. We may set up the simple criterion that the rate of adsorption of w ions is equal to the rate of release of w ions at equilibrium.

Let us start with a colloid saturated with b ions and consider the rate of adsorption of w ions. The oscillation cell of a doubly charged b ion occupies a space adjacent to two active spots. The wandering w ions enter the oscillation

cells of the b ions. One w ion is adsorbed when it gets between one b ion and one of the active spots on the colloid, that is, when it breaks one of the bonds of the b ion. The w ion will be completely adsorbed but the b ion will not be completely released. The probability of adsorption is identical with equation 2 for the case of ions of equal charge.

We shall now consider a colloid saturated with w ions which occupy spaces adjacent to single active spots. Wandering b ions may enter the oscillation cells of the w ions and release the latter. The rate of release of the w ions will be equal to the rate at which the b ions break the bonds of the w ions and become bound to a single active spot with one of the two available bonds.

In developing the probability of these events, we have to take into consideration additional events which could not occur with ions with equal charge numbers. One or more b ions may enter the double oscillation cell of two adjacent w ions, and one b ion may simultaneously break both bonds of the two w ions or, in other words, get in between both w ions and the particle surface. The terms W_0, W_1, W_2, etc., may represent the probabilities that a double oscillation cell shall contain none, one, two, respectively, wandering w ions, and likewise the terms B_0, B_1, B_2, etc., refer to wandering b ions. Then for the probability equations we have

$$P_b' = (\alpha_0'W_0B_0) + (\alpha_1'W_1B_0 + \beta_1'W_0B_1)$$
$$+ (\alpha_2'W_2B_0 + \beta_2'W_1B_1 + \gamma_2'W_0B_2) \cdots \quad (7)$$

The coefficients are primed to indicate that the fractions of ions adsorbed in the double cells with wandering b's may be different from those for the case of the w's entering single oscillation cells of b ions. (The chances of one b ion getting in between the two w ions and the two active spots may be different from the chances of one w ion getting between one b ion and one active spot.)

Application of the Poisson series leads to the expression (eliminating the exponential term):

$$P_b' = \alpha_0' + \frac{2v_w}{V}(\alpha_1'N_w + \beta_1'N_b)$$
$$+ \left(\frac{2v_w}{V}\right)^2\left(\frac{1}{2}\alpha_2'N_w^2 + \beta_2'N_wN_b + \frac{1}{2}\gamma_2'N_b^2\right) + \cdots \quad (8)$$

By definition α_0', α_1', and α_2' are zero. This expression gives us the probability that one b ion will release two adjacent w ions.

When one b ion is present in the double oscillation cell of two w ions, it may replace either one or the other alone (and with equal likelihood for each), as well as both simultaneously. When one w ion has been replaced, this event will not influence the probability of the subsequent replacement of the other w ion. The two events are independent. Therefore, the probability of both occurring simultaneously is equal to the product (i.e., the square) of the probabilities of each occurring alone. The probability of one event occurring alone will equal the square root of the probability of both occurring simultaneously. Thus,

the probability of one w ion being released when one b ion is present in the double oscillation cell of two w ions will be

$$\left(\frac{2v_w}{V}\, \beta_1' N_b\right)^{1/2}$$

Similar considerations will hold for those cases in which varied numbers of w and b ions are present in the double oscillation cell of two w ions. The total probability of release of w ions, one at a time, becomes

$$P_b = \left(\frac{2v_w}{V}\, \beta_1' N_b\right)^{1/2} + \frac{2v_w}{V}\, (\beta_2' N_w N_b)^{1/2} + \frac{2v_w}{V}\, N_b \left(\frac{\gamma_2'}{2}\right)^{1/2} + \cdots \qquad (9)$$

It may be noted that, after transformation of the coefficients $2\left(\dfrac{\gamma_2'}{2}\right)^{1/2}$, the third term in equation 9 represents the first term of the series which would have been obtained if we had considered simply the probability of a single b ion entering the single oscillation volume of a w ion and neglected the other possible events. Mathematically, the terms of higher order will be negligible in comparison with the first term. Physically, the first term represents an event of greater probability than the remaining terms, because the probability of one b ion being present somewhere in a double oscillation cell is greater than that for a single oscillation cell. The chance of the b ion getting in between the particle surface and one or the other of the two w ions in a double cell cannot be significantly different from the chance of so releasing the w ion from a single oscillation cell.

An alternative criterion for equilibrium would be that the rate of adsorption of b ions must equal the rate of release of b ions. Equation 8 represents the probability of complete adsorption of a b ion. In this case we would neglect events of higher probability. Likewise, to obtain the rate of release of b ions, equivalent to the rate of adsorption of two w ions simultaneously, we should have to square the terms in equation 2, also leading to the neglect of the terms with higher probability. The proper kinetics involve, for the first approximation, a process analogous to a reaction of the first order in ordinary chemical kinetics.

The higher terms in equations 2 and 8 may be neglected to a first approximation. However, *it should be noted that the corresponding higher terms do not have the same power in this case.* This lack of symmetry may be expected to render the simplified equation less nearly exact than in the case of ions of equal charge.

The simplified equation will be

$$\frac{z_w (N_b)^{1/2}}{z_b\, N_w} = \frac{\alpha_1 (v_b/V) f(u)_b}{\beta_1 (2v_w/V)^{1/2} f(u)_w} = K \qquad (10)$$

The effect of dilution

It should be noted that there is a volume factor in this expression. The expression may be modified by transferring the volume factor, V, to the left side. In this case it would appear that K is a constant when the concentrations,

N_b/V and N_w/V, rather than the total numbers, N_b and N_w, of the external ions are employed in the calculations. However, Wiegner and Müller (9) found in an experimental study that the equilibria were conditioned by the total number of ions rather than by the concentrations. Dilution of a mixture of colloidal substrate and ordinary electrolyte did not alter the numbers of ions of each ionic species on the colloid and in the external liquid. On the other hand, Eaton and Sokoloff (1) and Kelley (6) have presented evidence to indicate that dilution of a sodium–calcium soil system affects the base-exchange equilibria markedly. The total amount of sodium in the external liquid increased with dilution.

Jenny has suggested that when the exchanging ions are not very dissimilar, the ratio v_w/v_b may not be affected by the number of migrating ions. As he points out, the individual oscillation volumes will increase with dilution because the thickness of the double layer on a colloidal particle varies with the electrolyte concentration. But the *ratio* of the oscillation volumes may remain nearly constant. Since no volume factor is explicitly present in the case of ions of equal charge, as indicated by equation 5, the value of K should not be markedly affected by dilution except for differences due to hydrolysis.

Since a volume factor is explicitly present in the case of ions of unequal charge, we should expect K to vary with dilution in general, when total amounts of ions in the external liquid are employed in the calculations. The rate of variation with dilution would depend upon the relative rates of variation of v_b and v_w with changes in the total volume V. Debye and Hückel found that for dilute solutions of simple electrolytes, the "thickness" of the ionic atmosphere varied with the square root of the dilution. However, as Hartley (3) has shown, colloidal electrolytes cannot be expected to obey the limiting law of Debye and Hückel. Furthermore, we are not concerned here with the "thickness" of the double layer, composed of two ionic species, but with the relative oscillation volumes of the two ionic species. It is quite probable that the relative variation of v_b and v_w with V would depend upon the characteristics of the colloidal substrate and the exchangeable ions. In actual cases, a differential degree of hydrolysis would be a complicating factor.

Equation 10 is identical with the equation presented by Gapon (2) for the case of a calcium–ammonium exchange. The method of derivation of equation 10 indicates explicitly the probability that K will not be a constant in general over a wide range of variation of colloidal substrate or added electrolyte. The simple assumptions made by Gapon do not provide for this possibility.

A review of the experimental literature indicates that equation 10 generally yields more nearly constant values of K than several other equations which have been proposed by various authors. Some of the available comparisons have been prepared by the author for another paper which is now in the process of publication. It is not necessary to repeat these tabulations here. For similar comparisons the reader may be referred to a paper by Magistad, Fireman, and Mabry (7). In this paper, the columns headed "Gapon" in the tables refer to an equation identical with equation 10 rather than to the equation 6 of these authors. In the latter equation, there is apparently a typographical

error. The term Ca^{++} should be taken to the one-half power rather than to the first power.

The derivation of equations involving ions of other charge numbers than 1 and 2 should follow the general procedure given in this paper. It does not seem necessary to present such derivations, particularly since the common ions of charge numbers greater than 2, iron and aluminum, frequently appear to enter into exchanges which are incompletely reversible.

CONCLUSIONS

The statistical method devised by Jenny for ionic exchange involving ions of equal charge can be extended to ions of unequal charge, provided the criteria for exchange equilibria are carefully considered. The simple equations have a considerable utility and lead to more nearly constant values of the "equilibrium constant" than do many other equations which have been proposed.

In conclusion it should be emphasized that Jenny's kinetic theory implies that ionic exchange is essentially a complex redistribution of ions both between an external phase and the ion swarm, and also within the ion swarm. The nature of this redistribution depends upon several factors. The process cannot be considered as a simple metathesis precisely defined by a simple equation of the mass-action type. The equations having the form of simple mass-action equations, i.e., equations 5 and 10, must be considered solely as approximations, from which there may be considerable variation in "unfavorable" cases.

SUMMARY

1. The kinetic ionic exchange theories of Vageler and Woltersdorf and of Gapon are briefly discussed.

2. The oscillation volume theory of Jenny is described in more detail and the advantages of this theory are discussed.

3. The oscillation volume theory is extended to the case of ions of unequal charge and a simple approximate equation is derived.

4. It is shown that the oscillation volume theory implies that ionic exchange is a complex ionic redistribution in the colloidal suspension. The redistribution exchange cannot be described rigorously by simple mass-action expressions. The simplified equations presented are approximations having considerable utility in "favorable" cases.

REFERENCES

(1) EATON, F. M., AND SOKOLOFF, V. P.: Soil Sci. **40**, 237 (1935).
(2) GAPON, E. N.: J. Gen. Chem. (U. S. S. R.) **3**, 144 (1933).
(3) HARTLEY, G. S.: Trans. Faraday Soc. **31**, 31 (1935).
(4) HOFMANN, U., AND GIESE, K.: Kolloid-Z. **87**, 21 (1939).
(5) JENNY, H.: J. Phys. Chem. **40**, 501 (1936).
(6) KELLEY, W. P.: Soil Sci. **47**, 367 (1939).
(7) MAGISTAD, O. C., FIREMAN, M., AND MABRY, BETTY: Soil Sci. **57**, 371 (1944).
(8) VAGELER, P., AND WOLTERSDORF, J.: Z. Pflanzenernähr. Düngung Bodenk. **A15**, 329 (1930).
(9) WIEGNER, G., AND MÜLLER, K. W.: Z. Pflanzenernähr. Düngung Bodenk. **A14**, 321 (1929).

CONDUCTANCE AND VISCOSITY OF CONCENTRATED SOLUTIONS OF CALCIUM AND ZINC CHLORIDES

DARWIN J. MEAD AND RAYMOND M. FUOSS

Research Laboratory of the General Electric Company, Schenectady, New York

Although a number of mixed salt systems have been studied in the moderately low concentration range, very few data are available for highly concentrated solutions. We present herewith some exploratory data on the system $CaCl_2$–$ZnCl_2$–H_2O. No attempt was made to obtain high precision.

Stock solutions of technical-grade calcium chloride and zinc chloride were prepared, and centrifuged to remove suspended impurities. Chloride was determined by titration of weighed samples, and then the solutions were adjusted to 12.0 N by weighing in the required amount of water. Densities given in the *International Critical Tables* were used to calculate volume concentrations. Mixtures were then made up, all 12 N in chloride, in which the Ca:Zn ratios were 3:1, 1:1, and 1:3. Next the stock solutions were diluted to 9 N, the concentration checked by titration, and another set of mixed solutions prepared. Similarly, 6 N and 4 N solutions were made. Possible volume changes on mixing were neglected in calculating the weights of stock solutions taken for the mixtures.

Conductance measurements were made in 4-mm. diameter U-type conductance cells, standardized by 1.0 demal potassium chloride solution at 25°C. The cell constants (specific conductance of standard solution times cell resistance) were 112 and 108. A simple direct-reading Wheatstone bridge was used; 2000-ohm I.R.C. precision wire-wound resistors were the fixed ratio arms, and the cell resistance was matched on a General Radio decade box; to compensate cell capacity, the circuit included an air capacitor parallel to the decade box. The conductances were measured at 1000 cycles; preliminary experiments showed that the results were independent of frequency in the range 500–5000 cycles. Temperatures were controlled manually; the 25°C. bath was a large beaker of water, the 0°C. bath a beaker of ice and water, and the low-temperature bath a Dewar flask containing alcohol chilled by controlled addition of solid carbon dioxide.

The viscometers were 30-cc. pipets to which 10-cm. lengths of capillary were sealed (diameters 0.5 and 1.0 mm.). The viscometer was mounted in a water jacket held at 25°C. It was calibrated by determining the flow time for water, and viscosities of the solutions were calculated as

$$\eta = \eta_0 \, dt/d_0 t_0$$

where η is viscosity in centipoises, d is density, t is time of flow, and the subscript zero refers to water. No kinetic energy correction was made; since the relative viscosities varied by better than a decade, the error in neglecting it is undoubtedly large.
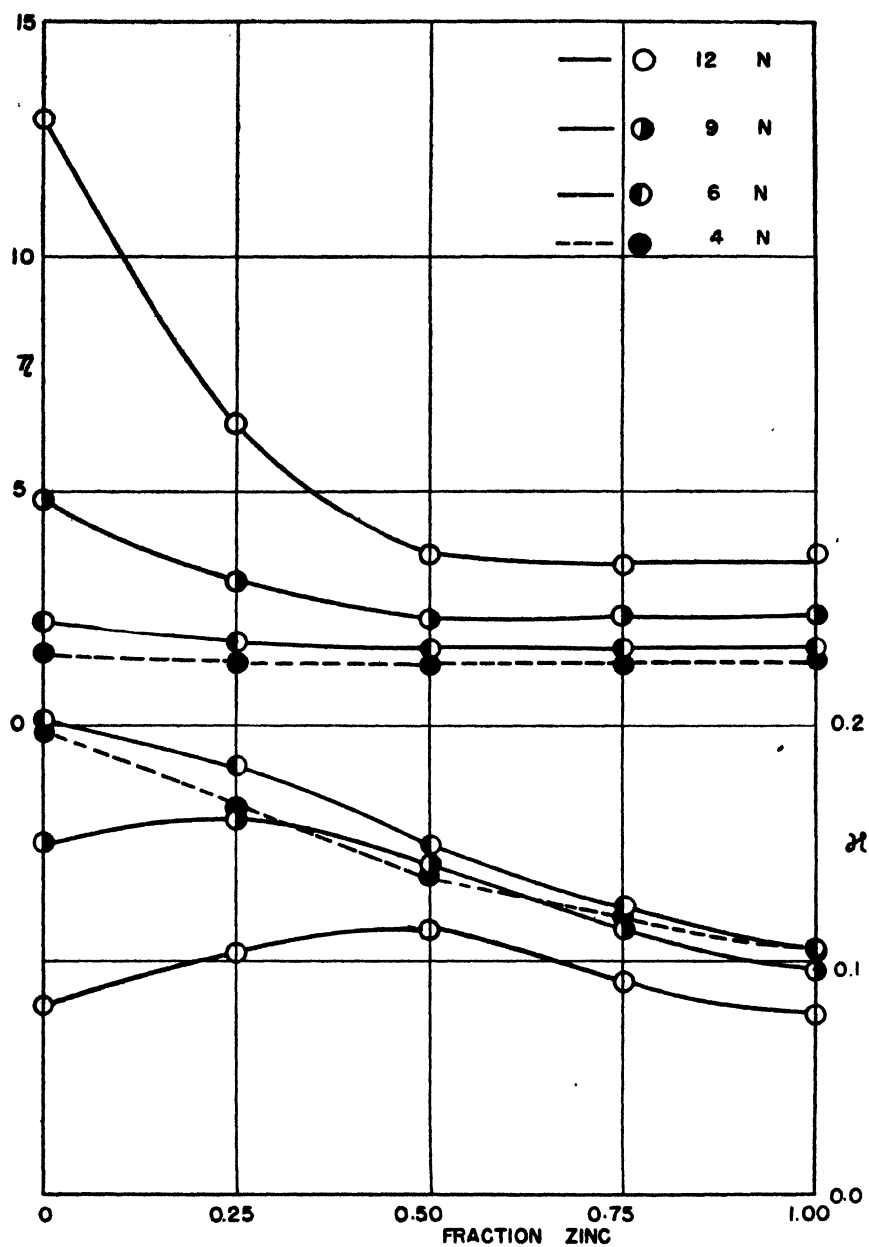
FIG. 1. Plot of conductance and viscosity against fraction of zinc in the mixture

The results are summarized in table 1, where concentrations are given both as (calculated) normality and as (observed) weight percentage. The symbol F indicates that the solution froze. Densities used are also given; for the pure components, they are figures from *International Critical Tables* and for the mixtures, calculated values assuming no volume change, as already mentioned. The last column gives viscosity (η) at 25°C. in centipoises, and the preceding four give the specific conductance (κ) at the various temperatures.

Figure 1 shows the results at 25°C., where conductance and viscosity are plotted against fraction of zinc in the mixture. Decrease of equivalent conduc-

TABLE 1

Conductances and viscosities of solutions of CaCl$_2$ and ZnCl$_2$

EQUIVALENTS PER LITER		WEIGHT PER CENT		d AT 25°C.	κ				η AT 25°C.
Ca	Zn	CaCl$_2$	ZnCl$_2$		25°C.	0°C.	−20°C.	−40°C.	
12.0	0.0	45.5	0.0	1.465	0.0808	F			13.0
9.0	3.0	33.4	13.6	1.494	0.1025	0.0518	F		6.49
6.0	6.0	21.6	26.8	1.524	0.1132	0.0629	0.0329	0.0130	3.69
3.0	9.0	10.7	39.5	1.554	0.0909	0.0508	0.0246	0.0085	3.42
0.0	12.0	0.0	51.6	1.585	0.0774	0.0415	0.0197	0.0055	3.68
9.0	0.0	36.9	0.0	1.354	0.1488	0.0803	F		4.88
6.75	2.25	27.3	11.1	1.376	0.1598	0.0902	0.0489	0.0181	3.07
4.5	4.5	18.2	22.2	1.398	0.1411	0.0834	0.0446	0.0168	2.28
2.25	6.75	8.9	32.4	1.420	0.1141	0.0685	0.0363	0.0126	2.33
0.0	9.0	0.0	42.5	1.442	0.0963	0.0579	0.0287	0.0100	2.38
6.0	0.0	26.8	0.0	1.244	0.2020	0.1183	0.0670	0.0235	2.22
4.5	1.5	19.8	8.2	1.259	0.1828	0.1078	0.0593	F	1.80
3.0	3.0	13.1	16.2	1.274	0.1485	0.0906	0.0506	F	1.61
1.5	4.5	6.5	24.0	1.289	0.1235	0.0771	0.0426	F	1.61
0.0	6.0	0.0	31.6	1.304	0.1062	0.0649	0.0341	F	1.67
4.0	0.0	19.1	0.0	1.165	0.1980	0.1166	0.0639	F	1.54
3.0	1.0	14.1	5.8	1.175	0.1654	0.0988	F		1.39
2.0	2.0	9.4	11.5	1.186	0.1377	0.0847	F		1.37
1.0	3.0	4.7	17.0	1.196	1.1188	0.0755	F		1.35
0.0	4.0	0.0	22.6	1.207	0.1050	0.0658	F		1.41

tance with increasing concentration is familiar; here, the effect of high concentration is so marked that the *specific* conductance decreases. The maximum in the κ–c curve comes at about 5 N. One very interesting fact appears at the highest concentrations: replacement of calcium by zinc causes a very sharp initial decrease in viscosity but the conductance does not rise correspondingly; only a slight maximum in the conductance–mixing ratio plot appears. Evidently zinc chloride is a much poorer conductor than calcium chloride in this range of concentrations, although the two salts do not differ greatly at low concentrations.

SOLUBILITY IN SILVER AMALGAMS AND DEVIATIONS FROM RAOULT'S LAW

DOUGLAS RENNIE HUDSON

Heriot-Watt College, Edinburgh, Scotland

I. SURVEY OF EXISTING DATA

The power possessed by mercury of "licking up" gold and silver has been utilized to extract enormous tonnages of these metals in Central and South America and South Africa. Pliny refers in his *Historia Naturalis* to wringing gold amalgam through a canvas or leather bag "whereby the mercury exudes like a sweat," a treatment still in use at the beginning of this century.

At lower temperatures numerous results for the solubility of silver have been reported, but above 200°C. one single value appears; this is about the temperature where the volatility becomes troublesome.

Joyner (20) in 1911 published six values for the range 14–163°C., preliminary to his investigation of dental alloys. From seven very careful determinations in the interval 80–200°C., Sunier and Hess (44) found the solubility to be given very closely by

$$\log_{10} N = -1074 \ (T)^{-1} + 0.501$$

Using the same apparatus but with greater care in analysis Reed (37) obtained slightly lower values for three temperatures near 200°C.

De Right (7) paid special attention to attainment of equilibrium, starting from silver foil, filings, and the intermetallic compound with identical results. For the range 18–80°C. he proposed an expression very similar to the above:

$$\log_{10} N = -1105.8 \ (T)^{-1} + 0.5894$$

He filtered off the excess solid phase by means of a filter of glass wool plus a capillary tube, a combination found to be very satisfactory; values obtained with wash-leather filtration were always higher, in accordance with the results of Russell (41) for base metal amalgams. Discussing the concept of solubility in terms of particle "aggregates," de Right suggested that some optical property might be used to define solubility in view of the opacity of mercury, and concluded that greater weight should be given to *lower* results, provided that equilibrium was established. Maurer (26), using a sintered-glass filter, extended this formula to the range 5–20°C., but was unable to confirm the existence of aggregates of various sizes in solution below 40°C.

II. THEORETICAL CONSIDERATIONS

Two methods of solubility determination are possible.

(a) *Analysis:* A small sample of the saturated solution is removed at the

---

[1] Lecturer in Metallurgy, Heriot-Watt College.

TABLE 1

Values of the solubility of silver in mercury previously recorded

OBSERVER	TEMPERATURE IN °C.	$(T)^{-1}$ ABSOLUTE	ATOMIC PER CENT Ag	SOLUBILITY GRAMS Ag PER 100 G. Hg	ESTIMATION
Joyner (1911)	14	0.003484	0.07	0.038	Analysis by vapouri-
	25	0.003356	0.082	0.044	zation of mercury
	30	0.003300	0.086	0.046	
	63	0.002976	0.19	0.102	
	90	0.002755	0.34	0.183	
	163	0.002294	1.13	0.611	
Sunier and Hess (1928)	80.2	0.002831	0.286	0.144	Analysis by precipi-
	98.2	0.002694	0.411	0.221	tation of silver as
	121.9	0.002535	0.612	0.330	silver chloride
	144.5	0.002395	0.849	0.458	
	160.6	0.002306	1.057	0.571	
	177.9	0.002217	1.346	0.728	
	198.9	0.002118	1.746	0.946	
Reed (1928)	181.8	0.002206	1.365	0.738	Analysis by precipi-
	193.3	0.002144	1.573	0.852	tation of silver as
	212.7	0.002059	1.953	0.059	silver chloride; special care taken in the assay
De Right (1933)	8.92	0.003547	0.0641	0.0344	Solid phase sepa-
	18.17	0.003434	0.0643	0.0346	rated by glass wool
	19.01	0.003425	0.0636	0.0342	plus capillary; an-
	25.28	0.003352	0.0766	0.0412	alysis by vapour-
	25.60	0.003349	0.0792	0.0426	ization of mem-
	29.93	0.003301	0.0881	0.0474	cury; special care
	30.15	0.003309	0.0965	0.0519	given to attain-
	40.11	0.003194	0.1139	0.0612	ment of equilib-
	50.02	0.003096	0.1450	0.0780	rium, starting
	60.26	0.003001	0.1901	0.1022	from foil, filings,
	70.54	0.002911	0.2402	0.1292	and compound
	80.94	0.002825	0.2892	0.1557	
Maurer (1938)	5.72	0.003588	0.0421*	0.0226	Solid phase sepa-
	9.71	0.003537	0.0474	0.0255	rated by sintered-
	12.39	0.003504	0.0519	0.0279	glass filter; analy-
	18.98	0.003425	0.0625	0.0336	sis by vapouriza-
	16.12	0.003459	0.0586	0.0315	tion
	19.24	0.003422	0.0652	0.0351	

* The value at 5.72° C. is recalculated from data for the run as given in the memoir referred to; in Maurer's summary of results the figure is incorrectly stated as 0.0403 atomic per cent.

temperature in question, cooled, and analysed. In theory this method is perfect but in practice it has some disadvantages. At high temperature, sampling must be mechanical to be efficient; this is complicated, and if inversion of a

fashioned or constricted tube is used, there is danger from hammer, which is serious with such a dense metal as mercury, despite the increased toughness of the refractory when hot. Further, unless the sample is sealed off at once, there is a risk that the composition may change by distillation if any temperature gradient exists, and sealing may set up this very evil through local heating. Hume-Rothery and coworkers have recently (16) called attention to *serious changes in composition in aluminium–silver alloys on annealing at 600–700°C.; despite the very high boiling points of 2270° and 2150°C.* marked sublimation had occurred. The vapour pressure of silver is 1 mm. Hg at 1218°C. and 0.0001 mm. at 837°C.

(b) *Direct:* The metals are maintained in contact and the solubility is calculated from observations made after cooling. This method is not so well based in theory. By a well-known principle of physical chemistry, when two components are maintained in contact, the fields attained at equilibrium are those which the isotherm cuts on the binary constitution diagram. The depth of the layers (provided it exceed a few million molecules) does not matter; in practice it is governed by the rate of solution or diffusion, whichever be the slower. The diffusion of silver in mercury is very rapid in the liquid phase (Humphreys (18)) and slow in the solid phase (Daniell (5)), so that saturation of the liquid can occur long before any large quantity of mercury has entered the solid silver. This was confirmed during the investigation, and it was found possible to obtain a core into which little diffusion had taken place, coated with a thin layer of silver-rich solid solution in equilibrium with the saturated solution of silver in liquid mercury.

According to the binary diagram (figure 1), based mainly on the observations of Murphy (30) and of Preston (35), the solution above 276°C. is in equilibrium directly with the silver lattice carrying up to 45 per cent by weight of mercury atoms in substituent solid solution. With falling temperature the figure changes little, but liquid solubility falls rapidly owing to precipitation of a solid phase. Down to 276°C. this is identical with the α coating, but at this point a reaction occurs between α and the mercury-rich liquor, to yield a new phase containing about 40 per cent silver. [γ was known to the alchemists as the intermetallic compound *Arbor Dianae*.] As the system continues to cool, impoverishment of the liquor in silver continues by deposition of this (β) phase. At 127°C. a second peritectic between it and the liquor yields the γ phase, which has the structure of γ-brass, possibly imperfect. For sufficiently slow cooling therefore the cross-section would consist of

$$\text{Ag-rich } \alpha \mid \alpha + \beta \mid \beta \mid \beta + \gamma \mid \gamma \mid \gamma + \text{ Hg-rich liquid}$$
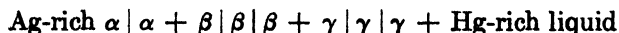
In view of the two peritectic reactions at low temperatures, one involving the complex γ-brass structure of fifty-two atoms in the unit cell, the probability of metastability is very high. Murphy has pointed out, "It appears therefore that the reaction between β and liquid, as well as between α and liquid, is completely suppressed with the rates of cooling employed in cooling-curve observa-

tions." From consideration of his facts one may deduce that formation of γ is about one-tenth complete in about 3 hr. and about nine-tenths complete in about 3 days at 100°C.

The following possible errors are therefore inherent in the direct method: (1) That some peritectic β or γ may remain attached to the core of unchanged silver. (2) That some α formed by diffusion may be removed during separation of the components at room temperature. These would give too low and too
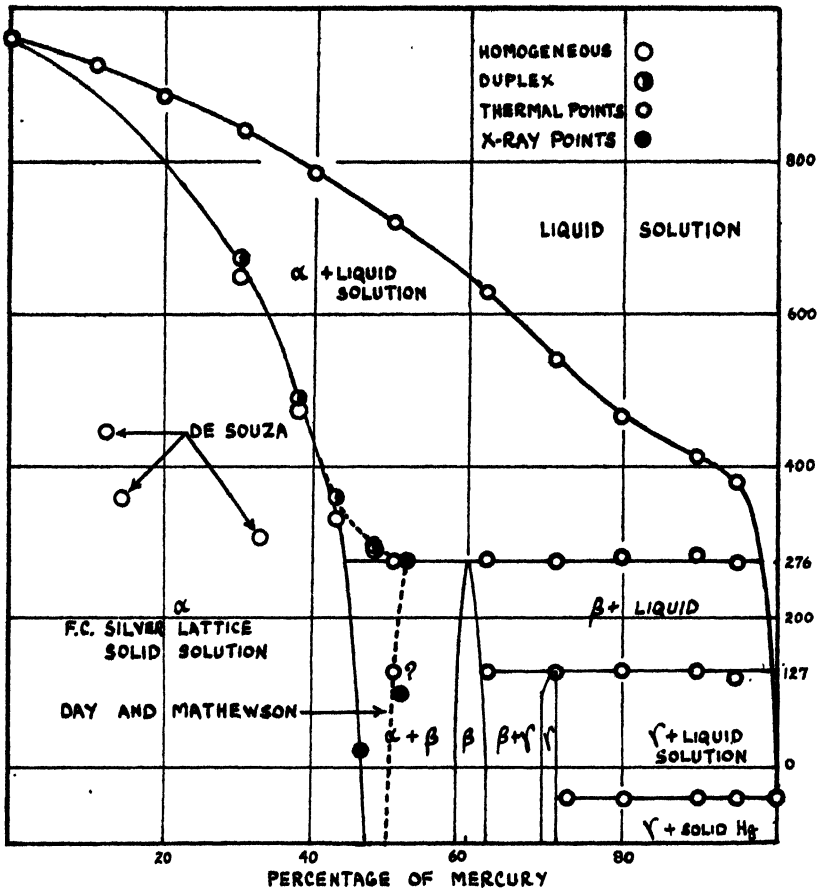
FIG. 1. Constitution of synthesized silver amalgams

high values, respectively, and would be self-destructive to some extent. (3) That diffusion within the solid might form a deep layer of α, virtually removing this element from the system. This has been shown to be too slow to have this effect.

During the experiments a very clean separation of amalgam from core was invariably obtained, and it is considered that the above factors cannot greatly have vitiated the results. This is confirmed indirectly by de Right's observa-

tion that the same solubility was obtained whether from the element or from the intermetallic compound.

III. EFFECT OF USING A SEALED VESSEL

The bugbear of solubility determination is the volatility of mercury. Minute under ordinary conditions, its vapour pressure increases rapidly with rising temperature, approximately following the exponential law.

Temperature	0°C.	20°C.	100°C.	200°C.	300°C.	400°C	500°C.
Vapour pressure...	1.186×10^{-5} cm.	1.2×10^{-4} cm.	2.6×10^{-1} cm.	1.7 cm.	25 cm.	155 cm.	315 cm.

An obvious solution is to carry out the determination in a sealed vessel. This has the advantage of precluding contamination, but at higher temperatures (and this is precisely where the artifice is most necessary) two marked disadvantages are evident.

(1) The pressure at which solubility is measured greatly exceeds normal. We can estimate the error introduced here by use of the Clausius–Clapeyron relation

$$\frac{\mathrm{d}T}{\mathrm{d}P} = \frac{T(V_2 - V_1)}{H_f}$$

where H_f is the thermal energy involved, in this case the latent heat of fusion.

At the melting point of 1234°K., H_f for silver is 26 calories per gram (Wüst, Meuthen, and Durrer (46)). V_1 is 9.46 g. per milliliter (19), and the change in density on melting is 4.99 per cent (Losana (25)). From these values $\mathrm{d}T/\mathrm{d}P$ = 0.006°C. per atmosphere, since 1 gram-calorie is equivalent to 41.4 ml. atm. At the boiling point of sulphur, for example, the vapour pressure of pure mercury is about 3 atm., and the solubility of silver sufficient to give a mole fraction of about 0.27. If Raoult's law is obeyed, the vapour pressure above the alloy would amount to $2\frac{1}{4}$ atm. and even though it be not, is likely to lie between this and the 3 atm. of pure mercury. One may assume it to be $2\frac{1}{2}$ atm. and the air pressure within the bulb $1\frac{1}{2}$ atm. In comparison, the vapour pressure of the silver may be neglected. An excess pressure of 3 atm. would thus raise the melting point of silver (if in fact this could ever be depressed to 444.5°C.) by 0.018°C. The mean atomic volumes of the intermediate phases do not differ much from those of the constituent elements—16.9 A.^{3} for silver and 25.4 Å.^{3} for mercury against 18.4 for Ag_5Hg_4 and 19.3 for Ag_5Hg_8 (Preston (35)). The heat of synthesis of Ag_5Hg_8 is very small,—2973 calories according to the physicochemical determination of Ogg (31), and 7336 according to his later determination (32). It appears unlikely, therefore, that the use of sealed tubes can introduce an error even approaching the experimental error.

(2) The second disadvantage is that it is not easy to obtain a vessel which at the working temperature is (a) refractory, (b) non-porous, (c) strong enough

to withstand the high internal pressure, (d) not liable to attack or alloy with the metals, and is in addition endowed with a coefficient of expansion low enough to withstand the thermal shock of rapid sealing-off while cold, and also reasonably workable without too much deterioration.

IV. EXPERIMENTAL

After trial of a number of materials, refractory borosilicate tubing used for organic nitrogen determinations was found to be suitable. Following many
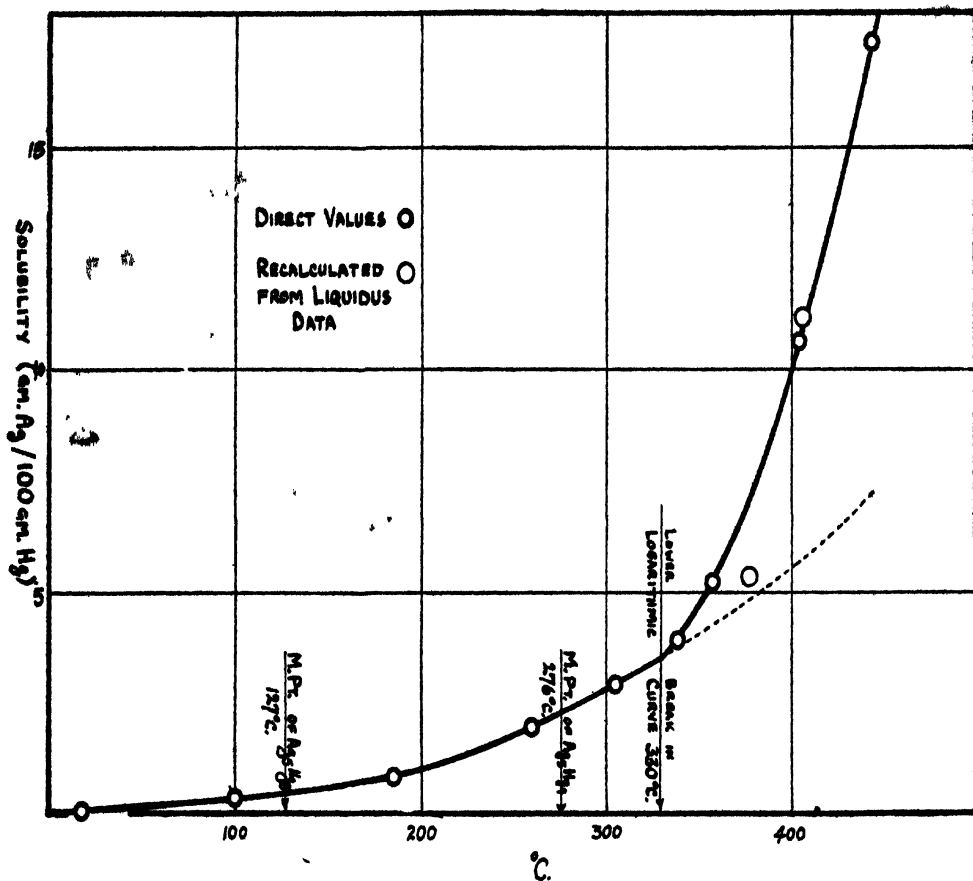
FIG. 2 Solubility of silver in mercury

failures a satisfactory technique was devised; it was necessary to attend closely to a number of apparently trivial points in order to obtain success. Subsequently thick-walled "Carius" tubing for halide estimation was found to be even better, provided it was new; an attempt to use old tubes which had been stored for about twenty years proved to be a very costly economy. Later, the cracking within the wall which occurred in these old tubes was found to be due partly, but not wholly, to a very tenacious layer of adsorbed moisture. All

manipulations were carried out by orthodox glass-blowing methods, but in the oxygen–coal gas blowpipe.

(1) The Carius tube was sealed, rounded, blackened, and cooled. Insertion of the silver directly into the hot tube, even after preheating, invariably caused fracture. This is probably due to the difficulty of equalizing the temperatures of metal and glass, combined with the high thermal conductivity of silver.

(2) A silver cube, about 0.5 g. in excess of that required for saturation at the particular temperature, was amalgamated and the mercury removed by heating

Fig 3. Bulb showing uniform wall thickness

Fig. 4. Filled bulb (unannealed) showing transverse cracks

it on asbestos gauze to about 900°C. in a Méker burner with a fierce flame, cooled in a desiccator, and weighed (m_1). After this treatment the metal showed a brilliant surface like white blotting paper.

(3) The cube was introduced and the tube constricted by surface tension alone to give a vessel of 2.5–3.5 ml. It was found essential to maintain wall thickness equal to the original, neither thicker nor thinner (see figure 3).

(4) After cooling just to rigidity, the wall of the bulb was heated almost to its melting point in the same flame at higher temperature, blackened, and slowly

cooled. This process was introduced to prevent the sharp cracks which other-
wise formed sharply across the bulb, whether filled or empty, in 2 to 3
days (see figure 4). The difference induced can be clearly seen in radiographs
of treated and untreated bulbs taken between Polaroid plates in crossed-Nicols
position (figures 5 and 6). Before insertion of the bulb the ground is completely
dark and the whitening is a measure of the internal stress in the wall.

(5) The vessel was filled to about four-fifths its height by the thermometer
method, i.e., by pouring mercury into the cone above the constriction and
coaxing it beyond by alternately heating and cooling the bulb, using the palm
of the hand. To allow for thermal expansion a small cushion of air had to be
left. It was not necessary to know the mass of mercury at this stage.
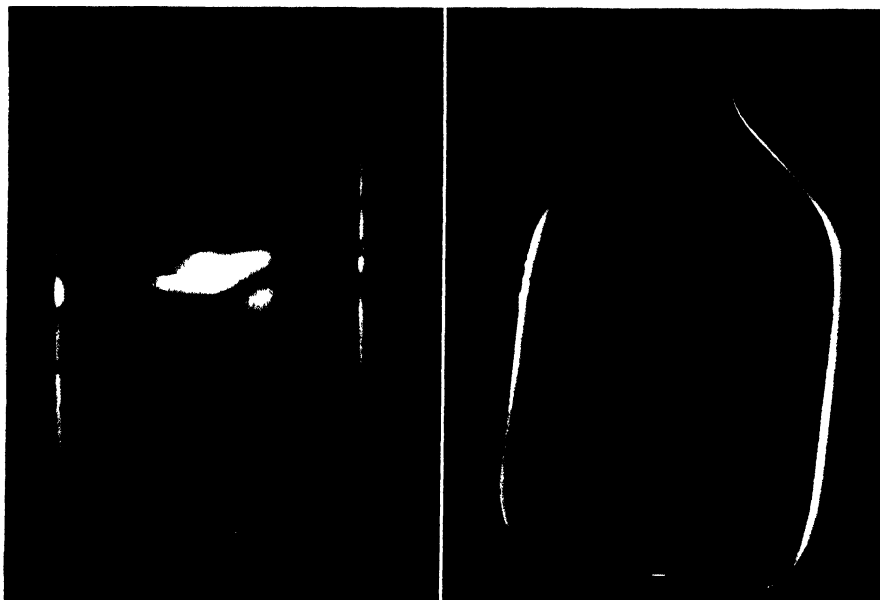
FIG. 5. Before tempering   FIG. 6. After tempering
          Radiographs showing removal of strain on tempering

(6) Sealing was carried out in a small and very hot flame. By careful and
rapid working it could be completed without danger of cracking and with only
a few degrees rise in temperature, so that the filled bulb could be held in the
hand meanwhile. It was in this operation that the suitability of the glass
became apparent. Owing to the great risk of cracking, neither blackening nor
annealing could be attempted, so the filled vessel was transferred to the vapour
bath and heating begun forthwith.

(7) After the desired time of contact (2 hr. at the boiling point of sulphur;
about six weeks at room temperature) the bulb was allowed to cool *in situ*.
It was then wrapped in a clean cloth and cracked by squeezing gently in a vice.
After determinations at higher temperatures the amalgam was rigid enough to
retain the shape of the bulb, but where the amount of dissolved silver was less,

some free mercury escaped and was caught by the cloth.   The total mass of the contents was then determined (m_2).

(7) The small core was separated from the mush and bounced several times in a tray to remove the final globule of mercury adhering; it then showed a bright liquid surface and was greasy to the touch.   In a supplementary experiment it was found that as little as 3.6 mg. per cm.[2] was sufficient for amalgamation; this corresponds to a thickness of less than 3×10^{-4} cm., and although removal of the adherent mercury is unlikely to be as efficient as this, it is obvious that the quantity remaining is small.   The silver core was brought back to its original state by vaporization of the adherent mercury as in (2) and then weighed (m_3).   The solubility in grams of silver per 100 g. of mercury is then given by $100(m_1 - m_3)/(m_2 - m_1)$.

Constant-temperature bath

Constant temperatures were obtained by use of pure liquids boiling under reflux in a simple vapour bath arranged so that the tube containing the experimental vessel was, so far as possible, surrounded by vapour.   A wide (bacteriological) hard-glass tube was inserted almost to its mouth into a cork also carrying an air or water condenser and fitted into a tall 400-ml. beaker heated on a wire gauze.   This simple apparatus gave very consistent temperatures, reproducible to $\frac{1}{4}$°C. or better, after sufficient time had been allowed to attain constancy.   The variations of the barometer were found to have only a small effect on the various boiling points, contrary to expectation, except in the case of steam and aniline.

"Commercially pure" substances were found to be quite suitable without subsequent laboratory purification.   The temperature was measured on short-range Anchütz pattern thermometers, Reichsanstalt calibrated, which proved excellent in every way.   The boiling points quoted are those actually observed, not always identical with those in reference books.   Eugenol was at first tried as a vapour bath but was replaced by amyl benzoate, owing to its blunt boiling point.   All other substances were satisfactory and remained constant during use.

Materials

Fine silver of nominal purity 99.95 per cent (an assay of 99.96 per cent has subsequently been reported) and A. R. grade mercury with the following limits of impurity, were used: non-volatile matter, 0.002 per cent; acid-insoluble matter, nil; other metals, no reaction.   The chief impurity in the silver is said to be oxygen.

Both the silver and the mercury are standard commercial products despite their high purity.   Kathode silver of even greater purity is available as a mercantile article, but its great fineness cannot survive melting and rolling processes.

V. RESULTS

The solubility values are tabulated in table 2, and plotted in figure 2.   Deviation from theoretical uniformity is difficult to appreciate on this curve, es-

pecially at the low solubilities below 100°C. Physical intuition, however, suggests that above, say, 400°C. one might expect the curve to run more on the line of that shown dotted in the diagram.

For a solution obeying Raoult's law the following expression can be derived thermodynamically (Hildebrand (13)):

$$\log_e N = \frac{H_f}{R}\left(\frac{1}{T_m} - \frac{1}{T}\right) + \frac{(C_L - C_S)}{R}\left(\frac{T_m}{T} - 1\right) - \frac{(C_L - C_S)}{R}\log_e \frac{T_m}{T}$$

where N is the mole fraction of the solute, H_f its latent heat of fusion at T_m, its melting point at standard pressure, and C_L and C_S its molar specific heats at constant pressure in the liquid and solid states, respectively. If $C_L = C_S$, as is true to a first approximation, the thermal energy involved in fusion is independent of temperature, i.e., the heat of fusion is equal to that of solution, provided that no exothermic or endothermic compound is formed and that

TABLE 2

Values of solubility (grams of silver per 100 g. mercury), mole fractions, and reciprocals of the absolute temperatures

SUBSTANCE	°C.	T°K.	T^{-1}	s	N	$\log_{10} N$		$\log_e N$
Room temperature............	16.2	289.2	0.003458	0.030	0.000558	$\bar{4}$.74663	−3.25337	−7.491
Water...........	99.6	372.6	0.002684	0.222	0.004121	$\bar{3}$.6150	−2.3850	−5.492
Aniline..........	184.4	457.4	0.002187	0.768	0.014192	$\bar{2}$.1520	−1.8480	−4.255
Amylbenzoate....	260.	533.	0.001876	1.885	0.03450	$\bar{2}$.5378	−1.4622	−3.367
Diphenylamine...	306ι	579.	0.001727	2.823	0.05251	$\bar{2}$.7098	−1.2902	−2.971
Anthracene......	338.	611.	0.001637	3.816	0.06872	$\bar{2}$.7610	−1.2390	−2.853
Mercury.........	356.7	629.7	0.001588	5.22	0.09294	$\bar{2}$.9682	−1.0318	−2.376
Benzidine........	405.	678.	0.001475	10.59	0.18053	$\bar{1}$.2566	−0.7434	−1.712
Sulphur..........	444.5	717.5	0.001394	17.35	0.28081	$\bar{1}$.4484	−0.5516	−1.270

heat involved in solvation, if such should occur, is zero. The second and third terms then vanish, leaving the well-known text-book expressions in which log N is a linear function of T^{-1}.

$$\log_e N = \frac{H_f}{R}\left(\frac{1}{T_m} - \frac{1}{T}\right) \quad \text{i.e.,} \quad \log_{10} N = \frac{H_f}{R}\left(\frac{1}{T_m} - \frac{1}{T}\right)\bigg/ 2.3026$$

According to these relations the plot of log N is a straight line of slope H_f/R or $H_f/2.026R$, according to which logarithmic base is used, intersecting the horizontal axis at T_m^{-1} at which $N = 1$ and log $N = 0$. With the more exact relation that takes into account the difference between the heats of liquefaction and fusion, the theoretical solubility is greater; the two plots for solubilities calculated under these two assumptions are shown in figure 7. Owing to the linear relation between the specific heat of solid silver and temperature (19), the divergence increases with falling temperature. These curves are *independent of the second metal, provided the solution obeys Raoult's law.*

Where the solvent is appreciably soluble in the *solid* solute, the left-hand term must be modified to allow for this. The equation then becomes

$$\log_e (N_L/N_S) = \log_e N_L - \log_e N_S = \frac{H_f}{R}\left(\frac{1}{T_m} - \frac{1}{T}\right)$$
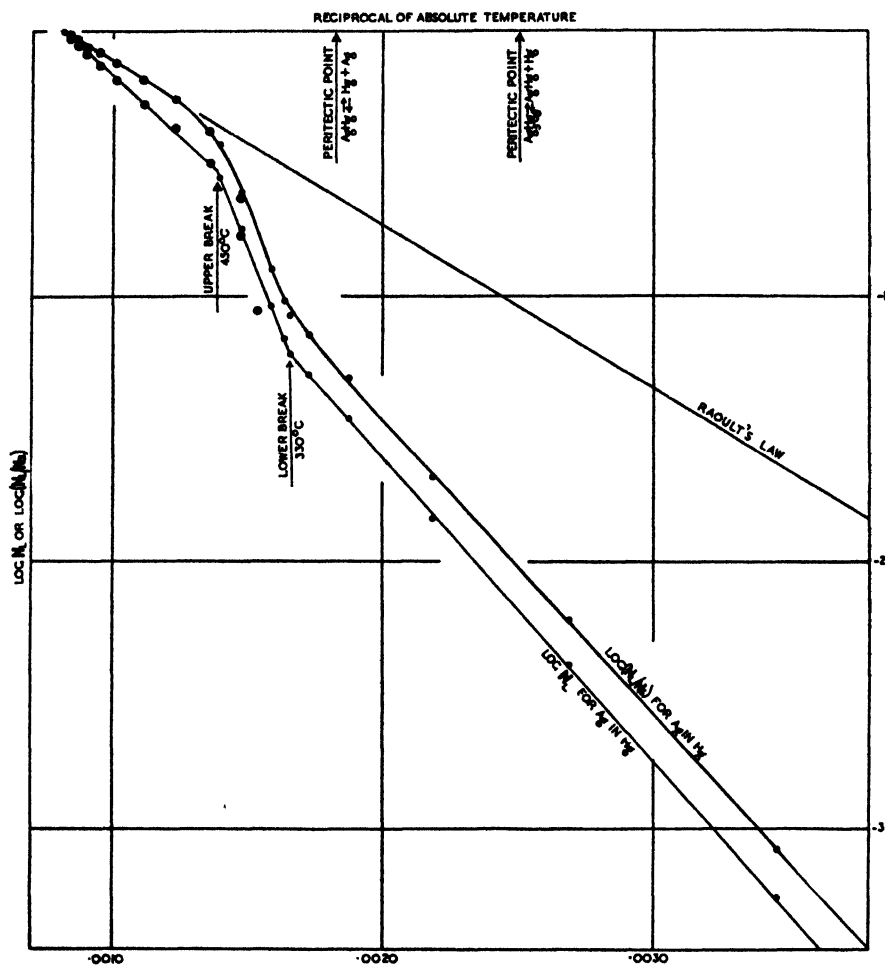
FIG. 7. Plot of log N_L and log (N_L/N_S) against T^{-1}, showing correction for solid solubility.

where suffixes denote liquid and solid states, respectively. In the present pair the mercury atom can replace silver in its close-packed cubic lattice to a maximum of a little over 50 per cent by weight at 276°C., as shown by the data in table 3.

For temperatures higher than those covered by this work, estimates of solu-

bility may be made from data published for the liquidus of the binary system, although one cannot expect the accuracy of a direct determination. Smith (43) has pointed out how far errors of thermocouple calibration, measurement, temperature fluctuation within the furnace, etc. may vitiate the true result. Hume-Rothery and coworkers (17) estimate the possible error as high as 5° for each 100° depression from the freezing point, stating somewhat pessimistically "... in the most careful work yet available, observations may differ by 10°C. from the smoothed curve." More recently (1), however, this school, in

TABLE 3

Solid solubility of mercury in silver

TEMPERATURE	MERCURY	OBSERVER	METHOD
°C.	*weight per cent*		
655	30	Murphy (30)	Microscopical
485	37.5	Murphy (30)	Microscopical
345	42.5	Murphy (30)	Microscopical
276	52.4	Day and Mathewson (6)	X-ray photography
100	51.6	Day and Mathewson (6)	X-ray photography
R.T.	46.2	Preston (35)	X-ray photography

TABLE 4

Mole fractions and reciprocals of absolute temperature calculated from liquidus determinations

Ag	°C.	T°K.	T	N	$log_{10}N$		$log_e N$
per cent							
5.00	378	651	0.001536	0.08916	$\overline{2}.9502$	−1.0498	−2.4174
10.03	407	680	0.001471	0.1718	$\overline{1}.2250$	−0.7750	−1.7846
20.08	465	738	0.001355	0.3185	$\overline{1}.5031$	−0.4969	−1.1441
28.86	541	814	0.001228	0.4300	$\overline{1}.6335$	−0.3665	−0.8438
37.72	630	903	0.001107	0.5298	$\overline{1}.7241$	−0.2759	−0.6353
49.96	721	994	0.001006	0.6500	$\overline{1}.8129$	−0.1871	−0.4308
60.23	786	1059	0.000944	0.7380	$\overline{1}.8681$	−0.1319	−0.3038
69.60	843	1116	0.000896	0.8098	$\overline{1}.9084$	−0.0916	−0.2110
80.08	886	1159	0.000863	0.8802	$\overline{1}.9445$	−0.0555	−0.1278
88.97	928	1201	0.000833	0.9375	$\overline{1}.9720$	−0.0280	−0.0645
100.	961	1234	0.000810	1.0000	0.0		0.0

treatment of pioneer work by Heycock and Neville (12), seems to have abrogated this tenet.

VI. DISCUSSION

The results obtained agree well with those of Sunier and Hess (44) and of de Right (7). The author's result is rather lower at room temperature than a corresponding one by Maurer (26), although a prolongation of the line passes exactly through the latter's point at 5.72°C. The earlier results of Joyner (20) are much more erratic, although some lie exactly on the curve. Reed's (37)

three values around 200°C., for which great care was used in analysis, are in good agreement with the author's curve. Values recalculated from metallographic work by Murphy (30) dovetail very well into the present results. So far as comparison is possible (the two series of values overlap only between the
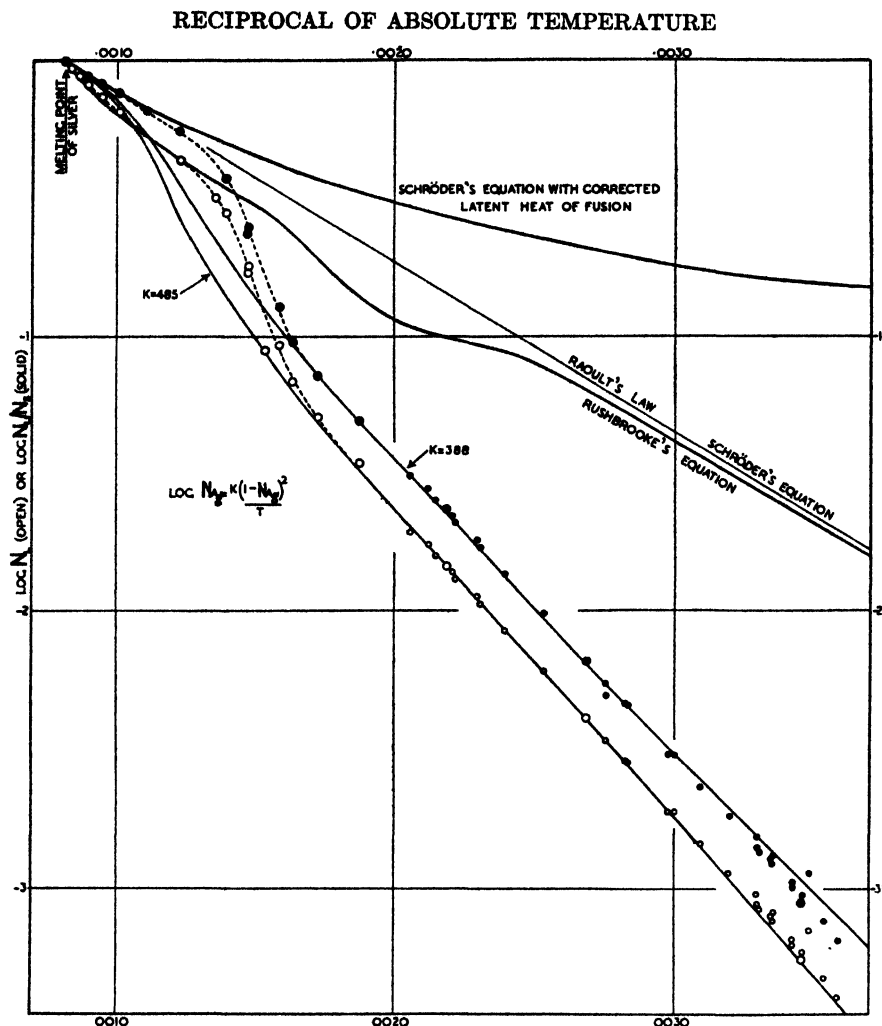
Fig. 8. Plot of logarithmic solubility of silver in mercury, including previously reported values, for comparison with those deduced from various theoretical equations.

temperatures of 445° and 357°C.—a comparatively short range), they show excellent agreement.

Empirical formulae

The author's results, together with those of Murphy (30), comprising in all a series from room temperature to the melting point of silver at 961°C., can be

represented very successfully by three straight lines, intersecting at or very near 330° and 450°C. The equations for these are

$$\log_{10} N = 0.67035 - 1134.7 T^{-1} \ldots \text{up to } 330°C.$$
$$\log_{10} N = 2.9065 - 2481.8 T^{-1} \ldots 330° \text{ to } 450°C.$$
$$\log_{10} N = 0.7441 - 918.2 T^{-1} \ldots 450° \text{ to the melting point of silver}$$
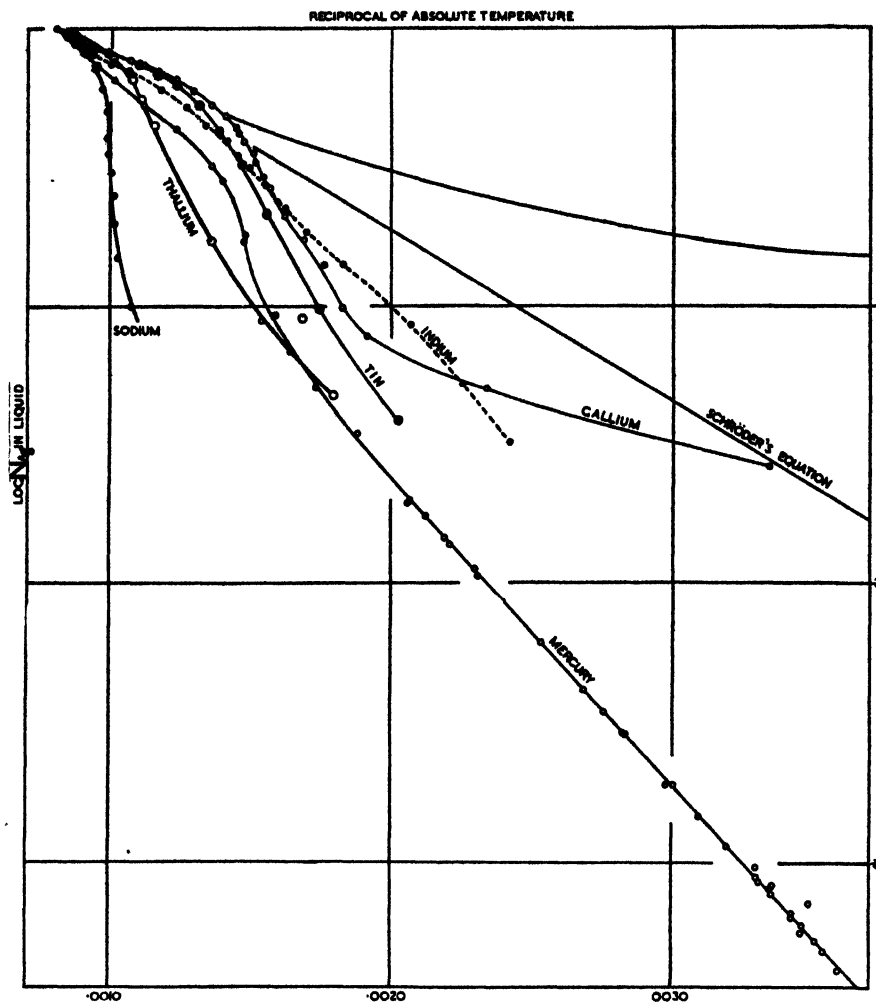
FIG. 9. Comparison of the solubility of silver in metals of low melting point, recalculated from liquidus determination, without correction for solid solubility.

It appeared an attractive possibility to correlate these breaks, at the time believed to be definite, with the peritectic dissociation points of β and γ at 276° and 127°C., respectively. A careful check showed, however, that this would not hold and there is no ground for questioning the accuracy of the peritectics. It is now believed that the results can more properly be represented by a re-

versed-S curve, this being fairly typical for pairs which show wide deviation from ideal solubility. In the short range of temperature available for the investigation of the organic systems which have hitherto been studied, non-development of such curves is quite understandable; nevertheless, Mortimer (28) has reported one pair in which the reversed-S shape is attained,—namely, acetanilide–toluene. Figure 9, on the same scale as figures 7 and 8, shows clearly the shape of this curve and the shortness of the temperature range.

In the metallographic investigation, no thermal points were observed in the alloys at or near the temperatures of 330° and 450°C., although the peritectic melting points were reproducible accurately over a range of composition of the silver–mercury alloys.

It is noteworthy that a similar reversed-S curve holds for the solubility of silver in molten tin (figure 8).

Effect of the intermetallic compounds

Obviously the peritectic reactions at 276° and 127°C. possess quite definite heats of reaction; otherwise the thermal points would not be so well marked and reproducible. One would therefore expect a definite, though perhaps small, change in the *slope* of the logarithmic curve at these temperatures. To test this possibility a curve was re-plotted including the solubilities reported by *all* observers (figure 8). This also shows no departure from a straight line other than a slight but consistent concavity. From considerations of statistical mechanics Guggenheim (11) has suggested that in *dilute* solution solvation does not necessarily "affect thermodynamic behaviour." Surely compound formation must be regarded as solvation *par excellence*.

Mortimer's rule

From figure 8 it is evident that the rule propounded by Mortimer (28), that to a first approximation the logarithmic plot of the mole fraction is a linear function of the reciprocal of the absolute temperature, is valid for this system. The approximation does not, however, represent the experimental results as accurately as one might wish.

Effect of solid solubility of "solute" in "solvent"

The plot of log (N_L/N_S), virtually the original curve corrected for the solid solubility of silver atoms in the silver lattice, is given in figure 7; it does not differ in essentials from the former, with which it runs almost parallel; at higher temperatures, however, its course is substantially identical with the theoretical Raoult's law curve, from which the simple plot diverges.

Raoult's law

Ramsay (36) reported that an amalgam containing 3.22 atoms of silver per 100 atoms of mercury yielded an atomic weight of 112.4 for silver against the actual value of 107.9. Beckmann and Liesche (2) found that the boiling-point elevation agreed with the assumption that silver was monatomic in its amalgam.

On the other hand, Eastman and Hildebrand (8) found a rather large positive deviation in a 1.27 per cent solution at 318°C.

At 16.2°C. the actual solubility of 0.03 per cent is minute, and the value of N at 0.00056 is about one-fortieth of that calculated by the approximate equation or one-hundredth of that given by the more exact equation in which H_f is corrected for temperature change. Possible causes of this discrepancy are:

RECIPROCAL OF ABSOLUTE TEMPERATURE
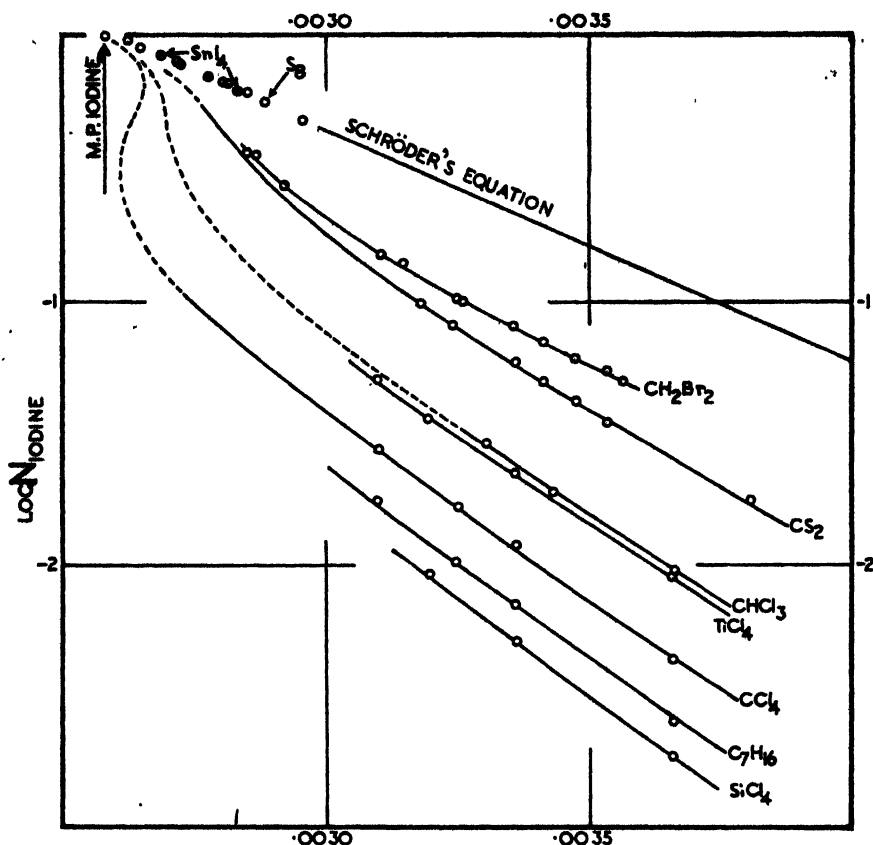
FIG. 10. Logarithmic plot of the solubility of iodine in inorganic and organic solvents, showing degradation from the ideal as the difference in the internal pressure (energy density) of solvent and solute increases (plotted from Hildebrand's published data).

(1) If the actual value of the latent heat of fusion were twice that used in the calculations, values of N much nearer those determined experimentally would result. In fact, the latent heats of fusion by different workers agree much better than might be expected in view of the experimental difficulties of determining it. Le Verrier (21) has indeed reported an anomaly in the specific heat of silver, which, he suggested, rises suddenly from 0.565 to 0.075 at about 260°C. Such a discontinuity would affect the second and third correcting terms in the

more exact equation for solubility. His results have not been confirmed, however.

(*2*) The upper and lower portions of the logarithmic curve have roughly the same slope, while that of the middle part is distinctly greater. The existence

RECIPROCAL OF ABSOLUTE TEMPERATURE
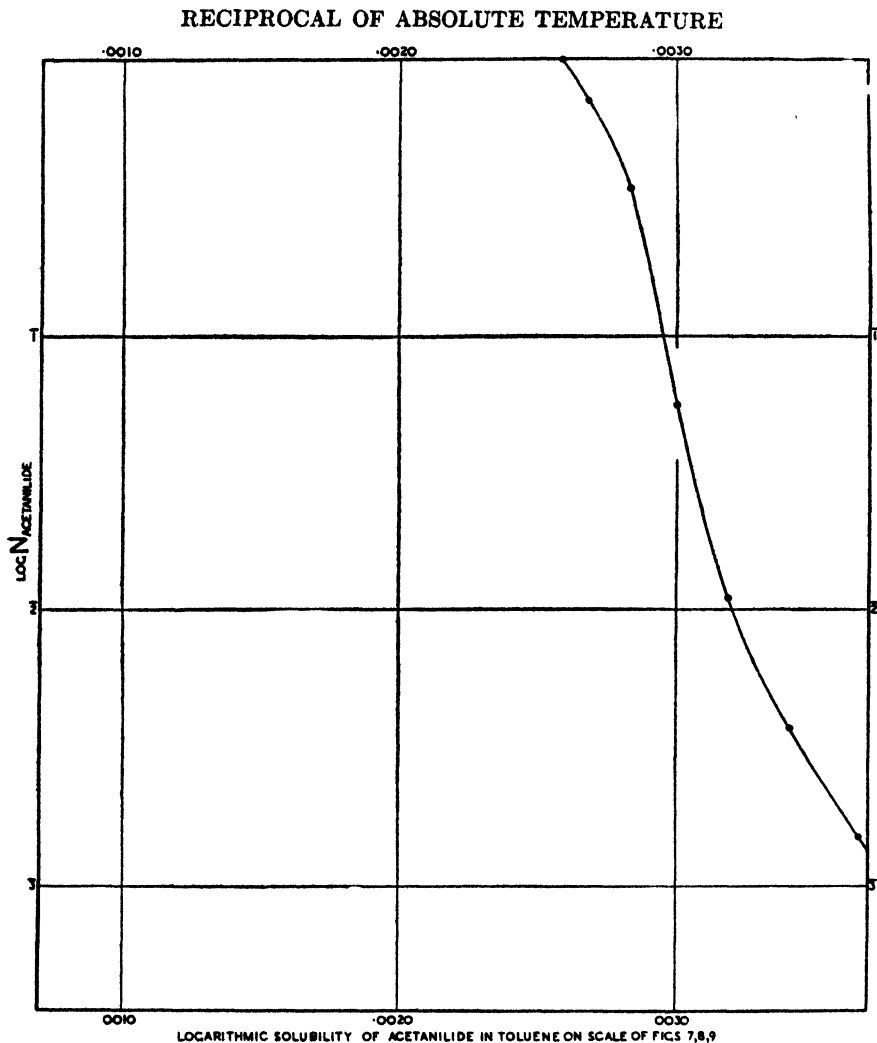
Fig. 11. Logarithmic solubility plot for acetanilide in toluene, from data published by Mortimer. So far as the present author is aware, this is the only set of data hitherto published which exhibits the reversed-*S* curve. Note the small temperature interval in comparison with the metallic systems.

of a crystal lattice stable only between 330° and 450°C. would account closely for such behavior. A similar phenomenon—the gamma loop—is well known in iron, but the evidence that it occurs in silver is very slight. Petersen (33) in 1891 from a difference in heats of oxidation deduced a heat of transformation of

13.7 kilojoules per mole for silver (octahedral) to silver (cubic). Rice (39) in 1940 has also stated that possibly silver may exist in an allotropic form, but without quoting an authority. Mellor (27) has surveyed lucidly the voluminous if unconvincing *chemical* evidence of allotropy.

(*3*) The solid solubility of substituent mercury atoms in the silver lattice is high, over half by weight, and an order–disorder transformation might take place within the solid solution. It seems unlikely that such a change could affect the liquid solubility, especially in view of the metastability so readily set up in this system. Certainly no thermal point has been observed, but in general the energy change in the internal rearrangement is small, so that a blunt and attenuated point might easily be missed.

None of the above suggestions appears very plausible and one is forced to the conclusion that the equations are derived from incomplete premises. Now the theoretical reasoning is purely thermodynamical and takes no account of any difference between the atoms concerned, assuming them to be identical apart from label. The obvious possible differences are *polarity, constitution*, and *volume.*

Polarity: There is little difference between the two ions, standard electrode potentials being 0.799 volt for $Hg:Hg_2^{\cdot}$ and 0.798 volt for $Ag:Ag^{\cdot}$ (Butler (3)).

Constitution: The constitution of the silver and mercury atoms is, respectively:

Shells	K	L		M			N				O			P			TERM SYMBOL
Sub-shells ..	1s	2s	2p	3s	3p	3d	4s	4p	4d	4f	5s	5p	5d	6s	6p	6d	
Ag 47	2	2	6	2	6	10	2	6	10		1						$^2S_{1/2}$
Hg 80	2	2	6	2	6	10	2	6	10	14	2	6	10	2			$^1S_0$

It must be admitted that these are not wholly dissimilar, the main difference being the inclusion of an extra thirty-two electrons in the latter. Now the silver atom is very similar to its successor in the periodic classification, gold (No. 79), which immediately precedes mercury. In lattice parameter, melting points, and thermal and electrical properties, silver and gold show the close similarity which one would expect from their atomic orbitals. The great difference which does exist in internal bonding between the atoms of mercury on the one hand, and silver and gold on the other, is shown by (*a*) the interval between the melting points, 1000°C. for silver–mercury, and 1102°C. for gold–mercury; (*b*) the heats of vaporization, 249 and 368 kilojoules per mole for silver and gold, respectively, against 59.3 for mercury; (*c*) the ratio of electrical conductivities in the solid and liquid states, 1.9 for silver, 2.3 for gold, 3.2 and 4.9 for the anisotropic mercury (Grüneisen and Sckell (10)).

 Volume: Silver is a much closer packed metal than mercury, the respective atomic volumes being 10.27 and 14.14 for the solid state, although the inter-atomic distances are not so different at 2.883 Å. and 2.999 Å., owing to the unusual (simple rhombohedral) structure of mercury (Mott and Jones (29)).

VII. THEORY FOR DISSIMILAR ATOMS

The much more complicated question of dissimilar atoms has been studied by Van Laar (45), Scatchard (42), and Hildebrand and coworkers (14, 15), who have deduced analogous but not identical expressions; these, however, have been severely criticized by Guggenheim in 1935 (11) on the ground that they conflict with conclusions obtained by statistical mechanics. Using probability functions and assuming (1) negligible repulsion, (2) spherical symmetry, (3) attraction forces between unlike molecules to be the geometric mean of those between like molecules, Hildebrand (13) has derived the expression

$$RT \log_e \left(\frac{a_1}{N_1} \right) = V_1 \left(\frac{N_2 V_2}{N_2 V_2 + N_1 V_1} \right)^2 [P_1^{1/2} - P_2^{1/2}]^2$$

in which V is the atomic volume, a_1 is the "ideal" solubility of N_1, i.e., the "activity" of component 1 as if it obeyed Raoult's law, and P is the "internal pressure" or "energy density." Butler and Harrower (4), using Langmuir's principle of independent surface action, have deduced a similar expression involving "cohesive energy." This equation satisfies the condition of symmetry emphasized by Porter (34). Where the molar volumes are equal it reduces to

$$RT \log_e \left(\frac{a_1}{N_1} \right) = V_1 N_2^2 [P_1^{1/2} - P_2^{1/2}]^2$$

i.e.,

$$\log_{10} \left(\frac{a_1}{N_1} \right) = K N_2^2 T^{-1} = K (1 - N_1)^2 (T)^{-1}$$

which can in any case be used as an approximation. The curve obtained in this way, using a value of $K = 465$, derived from the experimental data at the steam point, agrees very well with the experimental results in the range 0–340°C. but deviates above the boiling point of mercury. It is very encouraging to note that this approximate equation, despite the deviation, does in fact show the same remarkable reversed-S shape as the experimentally determined curve, and that roughly in a parallel position.

Calculation of internal pressures

The quantity within the square bracket is the difference between the square roots of the "internal pressures" (Hildebrand) or "energy densities" (Scatchard) of the components. Calculation of this is doubtful, usually introducing small physical coefficients of none too high accuracy. It is not surprising therefore, that the values yielded by different methods show a marked variation; notwithstanding this, the order of magnitude is remarkably consistent. One may reasonably expect therefore that a difference term, in which the method is to some extent eliminated, would show greater concordance.

The following measurements can be used, results being expressed in calories per milliliter.

(1) *Surface tension:* The function $\gamma/V^{1/3}$, or more strictly the free surface energy $\left[\gamma - T\left(\dfrac{d\gamma}{dT}\right)\right]V^{-1/3}$, gives comparative values; by comparison with other methods it may be deduced that a factor of about 15 is necessary to convert these to calories per milliliter.

For silver, $\gamma = 800$ (average, the values show wide variation) and $V = 11.47$, since $\Delta = 9.4$. Then $\gamma/V^{1/3} = 400$ and $P = 6000$ with a factor of 15. For mercury $\gamma = 473$ (data again conflicting, there being an apparent flat peak about 20°C.) and $V = 14.79$, since $\Delta = 13.56$. Then $\gamma/V = 192$ and $P = 2880$ with a factor of 15.

$$[P_{Ag}^{1/2} - P_{Hg}^{1/2}] \text{ is then } 23.8$$

(2) *Heat of vapourization:* $P = \left(\dfrac{H_v - RT}{V}\right)$

For silver $H_v = 61,800$ and $V = 11.47$, so that $P = 5173$ calories per milliliter. For mercury $H_v = 14,670$ and $V = 14.79$, so that $P = 958$ calories per milliliter.

$$[P_{Ag}^{1/2} - P_{Hg}^{1/2}] \text{ is then } 40.9$$

(3) *From coefficients of expansion and compressibility:*

$P = T\,(dV/dT)/(dV/dP) = T(\alpha/\beta)$, where α is the coefficient of expansion and β that of compressibility. For silver $\alpha = 57 \times 10^{-6}$ and $\beta = 1.01 \times 10^{-6}$, so that $P = 56.4 \times T = 17,340$. For mercury $\alpha = 90 \times 10^{-6}$ and $\beta = 3.67 \times 10^{-6}$, so that $P = 24.5 \times T = 7180$.

$$[P_{Ag}^{1/2} - P_{Hg}^{1/2}] \text{ is then } 47.3$$

but this must be taken as qualitative only, since the data refer to the solid state. For liquid mercury corresponding values are much more accurately known: $\alpha = 182 \times 10^{-6}$ and $\beta = 4.08 \times 10^{-6}$, so that $P = 44.6 \times T$. Moreover an independent value of 13,200 megabars has been quoted for mercury.

(4) *From the coefficient of expansion:*

$$P = \frac{R}{V}\left(\frac{1}{\alpha} + 2T\right)$$

For silver $\alpha = 110 \times 10^{-6}$ in the range 960–1200°C., so that $P = 2200$ calories per milliliter near its melting point. For mercury $\alpha = 182 \times 10^{-6}$ in the range 0–50°C., so that $P = 825$ calories per milliliter at room temperature.

$$[P_{Ag}^{1/2} - P_{Hg}^{1/2}] \text{ is then } 18.2$$

(5) *From van der Waals value of a:* This cannot be applied for the present pair, owing to lack of data for silver.

(6) *Calculation from van der Waals "reduced" equation:* By consideration of

compressibility data Richards (40) has deduced the internal pressures for silver to be 4960 and for mercury 980 calories per milliliter.

$$[P_{Ag}^{1/2} - P_{Hg}^{1/2}] \text{ is then } 39.1$$

The value of this quantity obviously shows great variation and it is clearly not yet possible to eliminate the effect of the method.

If the same quantity is calculated from the value of solubility at 16.2°C. the figure of 14 is obtained, and that at the steam point is not much different. The conclusion would seem to be that *in the present system the attraction between unlike molecules is greater than the geometric mean of those between pairs of like molecules*, considered separately. It is noteworthy that the *deviation from ideal behaviour is only one half to one third what would be expected from consideration of the differences in the internal pressures* of the constituent elements. *This is in sharp contrast to the behaviour shown by a large majority of the pairs of organic molecules hitherto studied. It is however quite consistent with the formation of the definite chemical species Ag_5Hg_4 and Ag_5Hg_8* (London (23, 24)). In such intermetallic compounds the metallic cohesive forces are presumably intermediate in character between van der Waals forces on the one hand, and Coulomb forces existing in a lattice composed of oppositely charged ions as in an alkali halide. "It is impossible to escape the conclusion that the outer electron structures of the metallic atoms exert highly specific effects upon the intermolecular forces" (Hildebrand (*loc. cit.*)).

VIII. EFFECT OF THE INTERMETALLIC COMPOUNDS ON SOLUBILITY

The theoretical deviations from Raoult's law solubility of Hildebrand (13) and of Butler and Harrower (4) quoted in Section VII presume separation of a pure solute. Where solid solution of the solvent occurs, and this is frequent in metallic systems, a relatively simple correction must be applied, log N_L being replaced by log (N_L/N_S). In the system now investigated, in which two peritectic intermetallic species are formed, it is not easy to decide what value of N_S should be used below the peritectic point. The compounds are relatively definite in composition, the range of stability probably not exceeding ± 0.5 per cent. If N_S be taken as the value in the compound, the correction for solid solubility would entail a sharp change in direction of the corrected theoretical curve at 276° and 127°C.; but the observed values show no trace of such kinks.

After very careful deliberation it seems probable that the evidence is in favor of N_S for the solid solution of mercury in solid silver. This decision is greatly strengthened by the results of de Right (7) in the interval 9–81°C. He gave special attention to attainment of equilibrium and obtained identical results by starting from foil, filings, and the intermetallic compound. It seems clear that the liquid mercury–silver solution can be regarded as in virtual (metastable) equilibrium with the solid silver–mercury solution. This is in accord with the well-known reluctance of the compounds to crystallize from the melt; metastability is very marked and previous formation of Ag_5Hg_4 (or AgHg) is necessary for formation of Ag_5Hg_8 (Ag_3Hg_4) by the peritectic reaction.

Applying this correction, one obtains a value for K at the steam point of 388, the corresponding figure for $[P_{Ag}^{1/2} - P_{Hg}^{1/2}]$ being 12.8. To avoid congestion, the curve plotted for this has not been included in figure 8. Its agreement with observed values of log (N_L/N_S) is somewhat better than the corresponding agreement of log N_L points with the plotted curve ($K = 465$), but it shows no distinctive new feature.

Heat of formation of Arbor Dianae

Clearly, the heat of formation of an intermetallic compound will have the effect of a virtual increase in the latent heat of solution of the silver. Conflicting values have been reported. Littleton (22) found a heat of formation of 3432 calories for a supposed "compound" $AgHg_4$. Using the physicochemical constants of the displacement reaction at three different temperatures, Ogg (32) found 7336 calories per mole of Ag_2Hg_4, compared with his earlier value of 2937 in 1897 (31). These quantities are equivalent to 2445, 991, and 3424 calories per gram-atom of silver, compared with the well-established figure of 2800 for H_f. It is difficult to assess what weight should be given to data which show such wide variation.

IX. SUMMARY

The validity of direct determination of the solubility of silver in mercury is established from theoretical and practical considerations, and error due to using a sealed vessel is shown to be negligible. Values of solubility from room temperature up to 450°C., i.e., well above the boiling point of mercury at normal pressure, are reported. From liquidus data it is shown that solubility right up to the melting point of silver can be represented very closely by three straight lines:

$$\log_{10}N = 0.67035 - 1134.7T^{-1} \ldots \text{up to } 330°C.$$
$$\log_{10}N = 2.9065 - 2481.8T^{-1} \ldots 330° \text{ to } 450°C.$$
$$\log_{10}N = 0.7441 - 918.2T^{-1} \ldots 450°C. \text{ to the melting point of silver}$$

Their intersections, however, have no relation to the peritectic formation temperatures of Ag_5Hg_4 at 276°C. and Ag_5Hg_8 at 127°C., and these points do not appear at all on the logarithmic curve.

At low temperatures the solubility is about one-fortieth of that calculated from the elementary equation established by Schröder in 1893:

$$\log_{10} N = \frac{H_f}{R}\left(\frac{1}{T_m} - \frac{1}{T}\right)$$

or about one-hundredth if H_f is corrected for temperature variation. Possible explanations for this are unconvincing.

The approximate expression derived from consideration of unlike atoms

$$RT \log_{10} (a_1/N_1) = KN_2^2$$

(a being the Schröder solubility) fits the experimental curve very well up to 340°C. if $K = 465$, as calculated from solubility at the steam point; and even

after its departure gives an analogous reversed-S curve. A roughly parallel curve holds for the solubility of silver in liquid tin.

In the more exact expression

$$RT \log_{10}\left(\frac{a_1}{N_1}\right) = V_1\left(\frac{N_2 V_2}{N_2 V_2 + N_1 V_1}\right)^2 [P_1^{1/2} - P_2^{1/2}]^2$$

the observed solubilities lead to a figure of 14 for $[P_1^{1/2} - P_2^{1/2}]$ compared with approximate values of 23.8, 40.9, 47.3, 18.2, 39.1, derived from diverse physical properties. The deviation from theoretical solubility is thus only a half or a third of what might be expected from consideration of the internal pressures of the two metals. It is concluded that the mutual attraction within a pair of unlike atoms is greater than the geometric mean of corresponding attractions within pairs of like atoms, in sharp contrast to the behaviour of most organic molecules and to previous conjectures, on theoretical grounds.

A convenient method is described for determining strain in glass vessels after blowpipe manipulation, by use of polarized light.

REFERENCES

(1) ANDREWS, DAVIES, HUME-ROTHERY, AND OSWIN: Proc. Roy. Soc. (London) **A177**, 153 (1941).

(2) BECKMANN AND LIESCHE: Z. anorg. Chem. **89**, 171 (1914).

(3) BUTLER: *The Fundamentals of Chemical Thermodynamics.* Macmillan and Company, London (1935).

(4) BUTLER AND HARROWER: Trans. Faraday Soc. **33**, 171 (1937).

(5) DANIELL: J. Royal Institution **1**, 1 (1930).

(6) DAY AND MATHEWSON: Am. Inst. Mining Met. Engrs., Tech. Pub. No. **884** (1931).

(7) DE RIGHT: J. Phys. Chem. **37**, 405-16 (1933).

(8) EASTMAN AND HILDEBRAND: J. Am. Chem. Soc. **36**, 2020 (1914).

(9) GOUY: J. phys. **4**, 320 (1895).

(10) GRÜNEISEN AND SCKELL: Ann. Physik **19**, 387 (1934).

(11) GUGGENHEIM: Proc. Roy. Soc. (London) **A148**, 304 (1935).

(12) HEYCOCK AND NEVILLE: Phil. Trans. **A189**, 25 (1897).

(13) HILDEBRAND: *Solubility of Non-Electrolytes.* Reinhold Publishing Corporation, New York (1936).

(14) HILDEBRAND: Trans. Faraday Soc. **33**, 144 (1937).

(15) HILDEBRAND AND COWORKERS: J. Chem. Phys. **1**, 817 (1933).

(16) HUME-ROTHERY AND COWORKERS: J. Inst. Metals **66**, 209 (1940).

(17) HUME-ROTHERY, MABBOTT, AND CHANNELL-EVANS: Phil. Trans. **A233**, 1 (1934).

(18) HUMPHREYS: J. Chem. Soc. **69**, 243 (1896).

(19) *International Critical Tables*, Vol. V, p. 92. McGraw-Hill Book Company, Inc., New York (1929).

(20) JOYNER: J. Chem. Soc. **99**, 195 (1911).

(21) LE VERRIER: Compt. rend. **144**, 907 (1892).

(22) LITTLETON: J. Chem. Soc. **67**, 239 (1895).

(23) LONDON: Z. Physik **60**, 491 (1930); **63**, 245 (1930).

(24) LONDON: Z. physik. Chem. **11**, 222 (1930).

(25) LOSANA: Gazz. chim. ital. **68**, 863 (1938).

(26) MAURER: J. Phys. Chem. **42**, 515-19 (1938).

(27) MELLOR: *Comprehensive Treatise on Inorganic and Theoretical Chemistry*, Vol. III, p. 568. Longmans, Green and Company, London (1923).

(28) MORTIMER: J. Am. Chem. Soc. **45**, 633 (1923).
(29) MOTT AND JONES: *The Theory of the Properties of Metals and Alloys.* The University Press, Oxford (1936).
(30) MURPHY: J. Inst. Metals **46**, 507 (1931).
(31) OGG: Z. physik. Chem. **22**, 536 (1897).
(32) OGG: Z. physik. Chem. **27**, 285 (1898).
(33) PETERSEN: Z. physik. Chem. **8**, 601 (1891).
(34) PORTER: Trans. Faraday Soc. **24**, 343 (1928).
(35) PRESTON: J. Inst. Metals **46**, 507 (1931).
(36) RAMSAY: J. Chem. Soc. **55**, 532 (1889).
(37) REED: J. Am. Chem. Soc. **50**, 662 (1928).
(38) REINDERS: Z. physik. Chem. **54**, 609 (1905).
(39) RICE: *Electronic Structure and Chemical Binding.* McGraw-Hill Book Company, Inc., London (1940).
(40) RICHARDS: J. Am. Chem. Soc. **48**, 3063 (1926).
(41) RUSSELL AND COWORKERS: J. Chem. Soc. **32**, 835 (1932).
(42) SCATCHARD: Chem. Rev. **8**, 321 (1931).
(43) SMITH: J. Inst. Metals **40**, 359 (1928).
(44) SUNIER AND HESS: J. Am. Chem. Soc. **50**, 662 (1928).
(45) VAN LAAR: Z. physik. Chem. **137A**, 421 (1928).
(46) WÜST, MEUTHEN, AND DURRER: Forsch. Gebiete Ingenieursw. No. 240 (1918).

COMMUNICATION TO THE EDITOR

In a recently published communication (David M. Gans: J. Phys. Chem. **49**, 165-6 (1945)) it is contended that a zero contact angle is a rare and fortuitous event. The writer there states, "In the borderline case where γ_{AB} precisely equals the difference between γ_{AS} and γ_{BS}, γ_{AB} will ally itself fully with either γ_{AS} or γ_{BS}, whichever is the smaller, and a contact angle of 0° in A or in B will exist. It must be expected that only fortuitously will the energy relations at three independent interfaces balance so nicely as to result in a contact angle of 0°. In many instances either γ_{AS} or γ_{BS} exceeds the sum of its two associates, and the one liquid spreads over the solid to the exclusion of the other." In this instance "the spread layer does not form a contact angle of 0° with the solid— in fact, it forms no contact angle at all, since no equilibrium line of contact can under these conditions be maintained .... This holds for two liquids against air as well as for two fluids against a solid.... Water on clean glass shows no contact angle. 'No contact angle' and 'zero contact angle' are not synonymous."

Unfortunately, Gans has confined his deductions exclusively to the situation where the continuous surface (such as a solid surface) is horizontal. In practical applications the surfaces to be wet are rarely strictly horizontal. If the continuous surface be inclined, or vertical, it is obvious that an equilibrium line of contact can be maintained even though γ_{AS} or γ_{BS} exceeds the sum of its two associates. It should suffice to mention, as well-known examples, the phenomenon of water or benzene rising to a definite height in a capillary tube, or

between plane parallel plates. We have it on good authority that the contact angle between liquids and clean glass is generally zero (N. K. Adam: *The Physics and Chemistry of Surfaces*, 3rd edition, pp. 10, 186, The Clarendon Press, Oxford (1941)). Whether or not "no contact angle" and "zero contact angle" are synonymous would seem to be largely a matter of intent, possibly solvable by methods outside the realm of the physical sciences.

United States Department of Agriculture H. L. CUPPLES.
Agricultural Research Administration
Bureau of Entomology and Plant Quarantine
Beltsville, Maryland
June 13, 1945.

NEW BOOKS

Plastics. By H. RONALD FLECK. 305 pp.; 76 illustrations. New York: Chemical Publishing Co., Inc., 1945. Price: $6.50.

It is surprising how thoroughly and completely the author has covered the scientific and technological phases of the extensive field of plastics. A short history of plastics, the raw materials, theoretical principles of polymerization, chemistry of plastics materials, the manufacture of plastic materials and synthetic elastomers are presented concisely but clearly. This is followed by two chapters on the physical properties of thermoplastic and thermosetting materials. Three following chapters are on synthetic resins, synthetic fibres and textiles, and adhesives, plywood, and impregnated wood. Included in this book are chapters on the manufacture of dies and moulds, and the manufacture of plastic articles, the chemical, physical, and electrical testing and the chemical analysis of raw materials.

The many illustrations, numerous tables, and references makes this a very useful book for chemists, manufacturers, and students. The arrangement of the material is sometimes confusing, but this has permitted grouping the abundant information available on plastics into a compact space. The type is rather small but this was probably controlled by Federal regulation to allow so much information to be included in about three hundred pages.

This is an excellent book, which is written in clear and interesting style. It covers the subject completely, and such details as have been omitted can be found in the many references.

CHARLES A. MANN.

The Chemical Process Industries. By R. NORRIS SHREVE. 930 pp. New York: The McGraw-Hill Book Company, Inc., 1945.

This is the first book that appears under the title "Chemical Process Industries." It is more than the ordinary industrial chemistry book, in that the approach to the subject is from the standpoint of the unit operations, unit processes, physical chemistry, economics and energy and power and their impact on the industries considered.

The many flow sheets, statistical tables, and excellent chapter references make this a very useful book. Both the inorganic and the organic industries are presented and in addition about forty-five pages of introductory material on classification of unit operations and processes, materials of construction, process instrumentation, chemical control, containers, safety and fire protection, patents, research, waste disposal, and other topics. The book makes a rather good general reference volume, but it is too inclusive for a student text unless a limited number of chapters are selected for this purpose. A close tie-up

between the unit operations and the technology would improve certain chapters. The make-up of the book is excellent. It is well arranged; the printing is clear and on good paper. The flow sheets are too small and somewhat difficult to follow through.

The author must be complimented upon a big job well done. *The Chemical Process Industries* is a fine contribution, which will be valuable to practicing chemists, chemical engineers, and students.

<div align="right">CHARLES A. MANN.</div>

Fundamental Principles of Physical Chemistry. By CARL F. PRUTTON AND SAMUEL H. MARON. 779 pp. New York: The Macmillan Company, 1944. Price: $4.50.

There are at least three types of students of physical chemistry. A few who are particularly interested and specially qualified study the subject intensively for its own sake. Many college students take it as a "required course," in the rather vague hope that they will thereby acquire (as painlessly as possible) a general impression of the subject which may later serve as a partial background for some more "practical" specialty, such as medicine. Probably the largest group of students who attempt to master the elements of physical chemistry intend to use it as a tool in some other field of chemistry or in chemical engineering. Prutton and Maron's text is apparently written with the needs and interests of this third group of students in mind.

The authors use the thermodynamic rather than the statistical or kinetic approach to the subject. The fundamental laws are presented concisely and in an orderly way, and some attempt is made to show their applications and their relation to the experimental aspects of the subject. The average student will be delighted to discover that in this book derivations are either given in complete algebraic detail or not at all. The last three chapters, which are devoted to atomic and molecular structure and to the relation between physical properties and molecular structure, are presented in the purely descriptive or survey-course manner.

Students who are seriously interested in the fundamental aspects of the subject may find certain characteristics of the book rather annoying. In a number of places the authors sacrifice rigor for the sake of simplicity. The problems are mostly of the simple substitution-in-formula type, and at least in a few instances the algebraic detail is complete to the point of being painful. On the other hand, the students who desire a survey course and who have been brought up on chatty texts filled with predigested descriptive material and profusely illustrated with cartoons and photographs, will find the thermodynamic approach, the rather prosaic style, and the simple line drawings of this book distinctly discouraging.

On the whole, the authors have presented a highly satisfactory if not exactly inspired text. It is well adapted to the needs of the average student of chemical engineering.

<div align="right">ROBERT LIVINGSTON.</div>

Synthetic Rubber from Alcohol. A Survey based on the Russian Literature. By ANSELM TALALAY AND MICHEL MAGAT. 6 x 9 in.; 312 pp.; 64 illustrations. New York: Interscience Publishers, Inc., 1945. Price: $5.00.

This book is divided into four major parts. The first part is devoted to the Lebedev process of converting alcohol to butadiene. A comprehensive discussion is given of the probable reaction mechanisms and the various chemical and physical factors influencing the Lebedev catalysis. The second part gives, in considerable detail, a discussion of the technology of the production of synthetic rubber according to the Lebedev process (sodium polymerization), on the laboratory, pilot-plant, and full plant scales. It will be noted that the majority of the literature references in this section are to 1937 or earlier years. This is due, of course, to the fact that publication of recent synthetic rubber research and production has been subject to secrecy restrictions for military reasons. Many of the problems discussed in this section of the book arose from the relatively low purity of the butadiene which was commercially available seven or eight years ago, and therefore these problems have disappeared now that high-purity butadiene is being produced as a routine

matter on an enormous scale. Nevertheless, in spite of the impossibility of obtaining exact knowledge of current Russian synthetic rubber practice, this section probably enables one to form a reasonable estimate of the present situation. The third part is devoted to polymerization in general, including theoretical and experimental discussions of thermopolymerization, emulsion polymerization, as practiced in the United States, England, and Germany, and sodium polycondensation, as used in the U.S.S.R. The fourth part deals with the physicochemical properties of the polymer, including polymer structure and methods for its investigation, chemical properties, and an excellent survey of the theoretical and practical aspects of the properties of high-polymer solutions.

Although the book contains nearly six hundred references, it is by no means a mere literature compilation. The authors have presented a careful evaluation of an enormous amount of material, most of which is not readily available to the average chemist. Actually the book has a much wider scope than is indicated by its title, which hardly does justice to the subject matter. It can be recommended strongly to all chemists and engineers interested in polymerization in general, or in butadiene production.

Only one error was noted by the reviewer: the statement on page 215, that a number-average molecular weight is given by light-scattering measurements, is incorrect.

E. J. MEEHAN.

The Theory of the Photographic Process. By C. E. KENNETH MEES. 1124 pp. New York: The Macmillan Company, 1944. Price: $12.00.

In its more than one thousand pages, this book contains a wealth of interesting and stimulating facts. Rather than being an intensive exposition of the theories of the basic photographic reactions, as its title suggests, this book is nearly an encyclopedia of the facts and related theories of the photographic industry. As a result it touches on such unrelated subjects as the physics of crystals, the synthesis of dyes, statistical analysis of skewed distributions, and the dietary habits of rabbits. To the reviewer, it appears that the technological and organochemical aspects of the subject are treated somewhat more comprehensively than its theoretical (physical and physicochemical) phases. In general the approach to the several theoretical fields is historical rather than critical. This, the historical approach, adds somewhat to the complexity of an inherently complicated subject. In a few cases some minor faults might be found with the interpretation of facts, but in an encyclopedic work of this sort one marvels at the general accuracy rather than being surprised at a few slips.

It is somewhat surprising that the general subject of color photography is not treated in this book (except for an incidental mention of the Kodachrome process on pages 393–8). Photographic processes which do not use silver halides are not mentioned. The use of photographic emulsions for recording x-rays or radioactive rays is not discussed. In the preface, the author apologizes for omitting a detailed treatment of emulsion-making, on the grounds that the greater part of such information is still confidential.

The author's style is in general simple and direct. The value of the book is increased by numerous references to the original literature. The book is clearly printed on opaque, glazed paper and is well illustrated in the diagrams and reproductions of photographs.

ROBERT LIVINGSTON.

MONOLAYERS OF OXIDIZED AND HEAT-BODIED LINSEED OIL

D. C. LICHTENWALNER[1], H. E. ADAMS, AND P. O. POWERS

Armstrong Cork Company, Lancaster, Pennsylvania

Linseed oil readily spreads on water into a monomolecular film whose surface pressure–area (*f–A*) curve is typical of unsaturated long-chain fatty acids. The film is in the expanded state at low pressures and changes into a condensed form at higher pressures. This change in state of the film is evident from a definite break in the slope of the force–area curve.

Since linseed oil contains a high proportion of unsaturated fatty acids (14) —namely, oleic, linoleic, and linolenic acid present as glycerides—its monomolecular films are very susceptible to oxidation. However, the rate of oxidation of monolayers of the esters of unsaturated fatty acids varies with the pressure exerted on the film (8). To eliminate this difficulty the oil in this study was oxidized in bulk, and monolayers of the oxidized oil were studied. Long *et al.* (13) have made a similar study.

Many investigators have studied the film properties of the individual fatty acids or their various esters (1–4, 7, 9–11, 15). These naturally fall into two classes: the saturated fatty acids which form a condensed film at room temperature with practically the same limiting area (A_0) of 20.5 sq.Å., and the unsaturated fatty acids which form an expanded film at room temperature. However, this behavior is a function of the surface pressure and temperature, as the expanded films change into a condensed film at high pressures and the condensed films change into the expanded state at high temperatures. The expanded films tend to a definite area at low compressions of about twice the size of condensed films (11).

EXPERIMENTAL PROCEDURE

In this study of monolayers of blown and heat-bodied linseed oil, the Cenco Hydrophil balance was used. After cleaning, the metal trough was coated with paraffin. A dilute solution of paraffin in benzene was used to coat the floating mica barrier and the attached platinum strips. The trough was filled with water and the scale on the torsion head was calibrated over the entire range, using known weights from a Westphal balance. The values in dynes per degree were calculated by using the ratio of the two arms. An average value of 3.23 dynes per degree was obtained from a total of eighteen readings over a wide range of weights. The width of the trough was 14.0 cm.; however, the value 14.1 cm. was used in calculating the area of the film in order to compensate for the curvature of the water surface. Likewise, the value 13.0 cm. was used in calculating the pressures in dynes per centimeter length of the float in place of 12.0 cm., the length of the float. This was done to correct for the effect of the platinum strips at the ends of the float.

[1] Present address: Drexel Institute, Philadelphia, Pennsylvania.

After some preliminary work it seemed desirable to use concentrations of linseed oil in benzene of about 0.1 per cent. Samples of about 0.1 g. were weighed, dissolved in benzene, and diluted to 100 cc. at 26°C., which was the approximate room temperature. The benzene solution was at first added to the water surface from a pipet on a volume basis, but it was soon found that
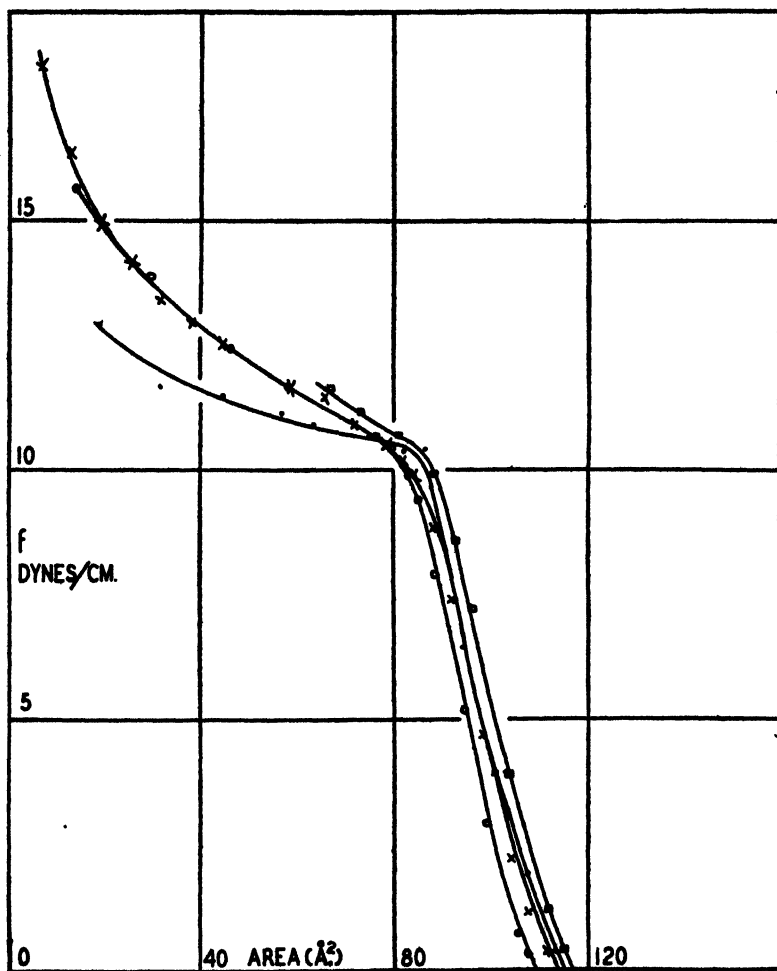
Fig. 1. Plot of pressure–area data for heat-bodied linseed oil. Hours at 305°C.: •, 0.0; ○, 2.0; □, 3.0; ×, 6.0.

there was a considerable variation in drop size, so the method was abandoned. A small weighing bottle with a ground-glass stopper and attached dropper being used, the sample of three drops was added as quickly as possible and the weight of the sample was determined by difference. With this procedure, duplicate determinations checked quite closely. The barrier was then moved

up in definite increments and the areas determined at varying pressures. This procedure was also carried out as rapidly as possible, as the area tends to increase, owing to oxidation by the air of the thin film, if it is allowed to stand for some time.
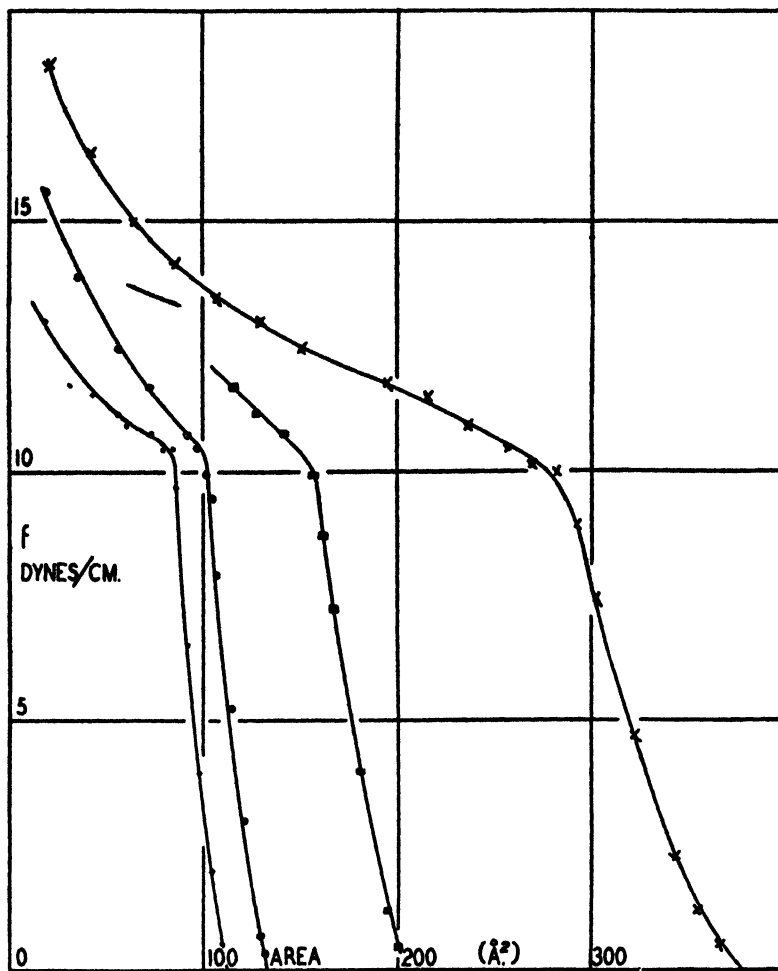
FIG. 2. Plot of pressure–area data for heat-bodied linseed oil. Hours at 305°C.: •, 0.0; ○, 2.0; □, 3.0; ×, 6.0.

The preparation of the heat-bodied linseed oil is described by Adams and Powers (6) as sample I. The various samples were bodied at 305°C. under vacuum for the designated times. Other properties of the oil samples are given in the paper referred to. The pressure–area data are plotted in figures 1 and 2. The areas (A) plotted in figure 1 are cross-sectional areas per linseed oil monomer (725 mol. wt.), while figure 2 shows the areas (Ap) calculated from

the experimentally determined molecular weights. This takes into account the increase in area due to polymerization.

In preparing the oxidized samples, linseed oil containing 1.1 per cent lead as lead resinate and 0.0015 per cent manganese as manganese resinate was oxidized at 60°C. by blowing air through it. The oil gelled at the end of 29½ hr. Samples
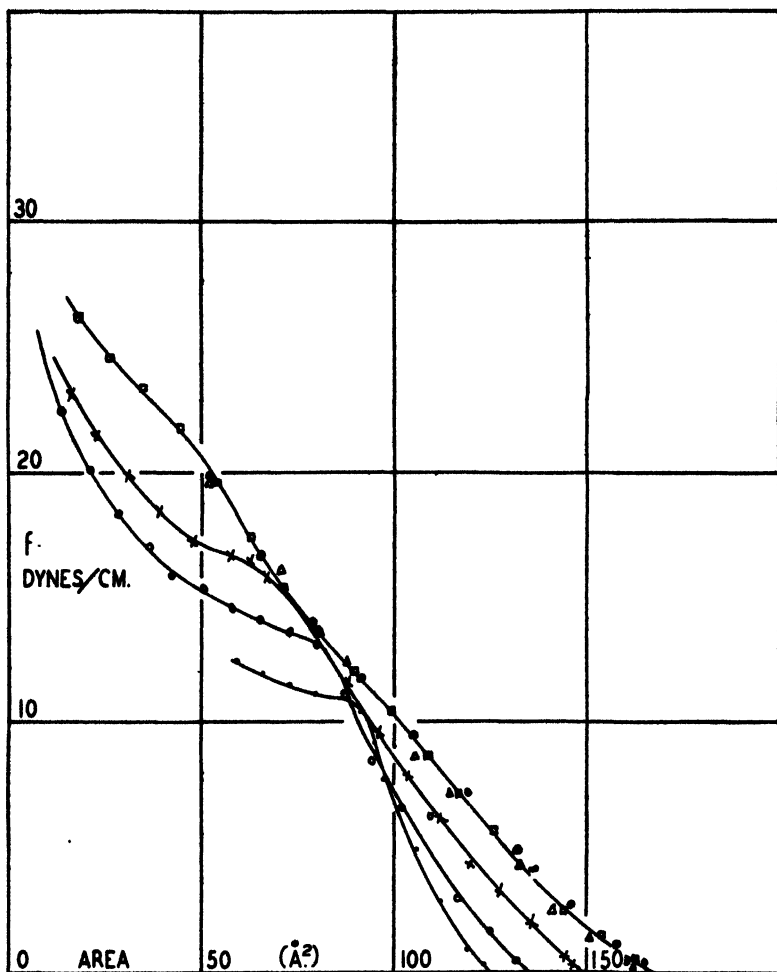
FIG. 3. Effect of varying degrees of oxidation on the pressure–area curves. Hours at 60.0°C.: •, 0.0; ○, 4.0; ✕, 8.0; □, 12.0; △, 16.0; ●, 20.1.

were taken at various times. Figure 3 contains the pressure–area curves and shows the effect of varying degrees of oxidation. In calculating the cross-sectional area per molecule the molecular weight of the monomer was used, and this molecular weight was corrected for the amount of oxygen absorbed to calculate the area of the oxidized samples.

All of the curves obtained are composed of three distinct parts. At low pressures the films are in the expanded state; then at some definite pressure a sharp break occurs and the curves continue nearly parallel to the area axis; finally they gradually change into the steep curve indicative of the condensed state.

Langmuir (11, 12) has developed a theory for the expanded state by considering the monolayer as a "duplex film". He noted the similarity between the expanded films and the spreading force of a large thin layer of a hydrocarbon oil placed on water with a monomolecular film of some substance such as a long-chain fatty acid at the oil–water interface. He considers the upper part of the monomolecular expanded film, consisting of the hydrocarbon part of the molecule, as the liquid phase and the lower interface against the water as containing a number of water-soluble groups per square centimeter equal to the number of molecules. He derives the following equation

$$(F - F_0)(a - a_0) = kT$$

where F, a, and T are the pressure, area, and temperature, respectively, k is the gas constant, and F_0 and a_0 are two constants. F_0 is the spreading coefficient of the hydrocarbon end of the molecule, and a_0 is a constant related to the area actually covered by the water-soluble groups. This is the equation for a rectangular hyperbola with asymptotes $F = F_0$ and $a = a_0$. Qualitatively, this equation fits the data obtained in this study for the films in the expanded state. For the equation to fit the data for the original linseed oil, F_0 must have a value of -11.0 and a_0 a value of 35. These are to be compared with the constants for oleic acid (5), $F_0 = -11.2$ and $a_0 = 19.9$.

It is apparent from figure 1 that the process of heat bodying does not introduce any radically new polar groups into the molecule or materially change the points of anchorage of the film. This is evident from the almost identical nature of the force–area curves obtained when the area per molecule is calculated on the basis of the starting monomer or molecular weight of the linseed oil. The slight spread of the curves is probably indicative of the accuracy of the experimental results. However, there does seem to be a difference between the curves for the polymerized and unpolymerized oil at the higher pressures that cannot be explained by experimental error. The transition from the expanded state to the condensed state takes place over a wider range of pressures in the case of the polymerized oil. Thus polymerization has a tendency to inhibit the mechanism of this transition. This is not a true phase transition, as it does not take place at constant pressure.

If the increase in molecular weight due to polymerization is taken into account, as is done in figure 2, several points become evident. First, the curves extrapolate to increasingly larger limiting areas as the molecular weight increases, a result which is self-explanatory. Secondly, the points (f_c, A_c) at which the curves experience a sharp change in slope occur at slightly smaller pressures with increasing molecular weights. Thus, it takes a slightly smaller force to

start the film to change into the condensed state as the oil polymerizes. This is probably due to the disappearance of the unsaturation and consequently a slight weakening of the force of attraction between the oil and water. The third point is that apparently all of the films are compressed to the same area at high pressures, irrespective of the molecular weight.

The various constants for the heat-bodied curves are plotted in figure 4 as a function of the iodine number. The slight effect on fc of the change in unsaturation is shown. On the basis of the monomer, Ac and A_0 remain constant, while
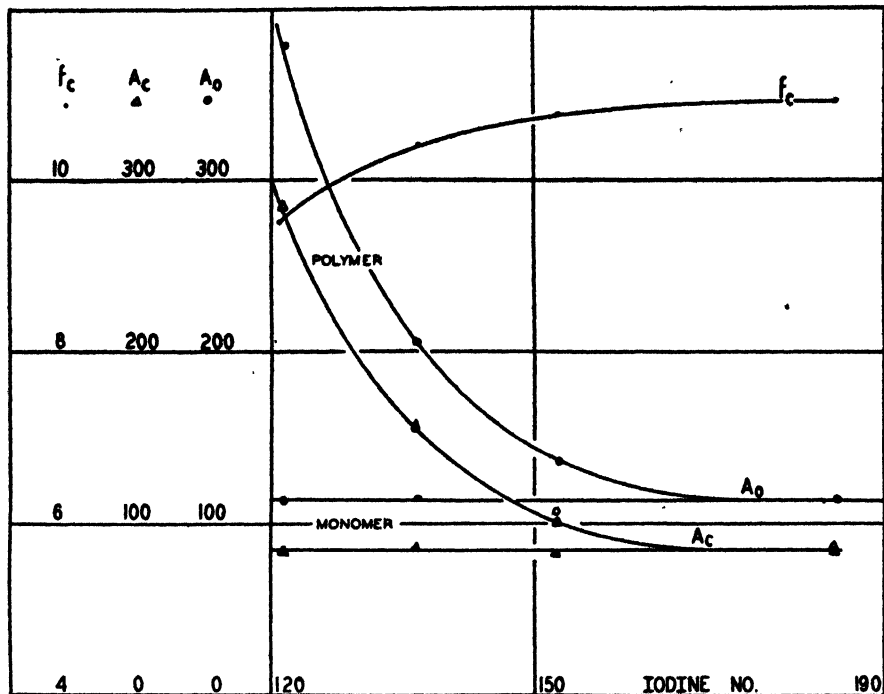
FIG. 4. Influence of unsaturation. Plot of the various constants for the heat-bodied oil curves as a function of the iodine number.

on the basis of the polymer Ac and A_0 reflect the change of the molecular weight with iodine number.

In the process of oxidizing linseed oil, polar oxygen groups are continually being added to the unsaturation of the fatty acids; consequently the film properties of the oxidized material should be highly dependent upon the amount of oxygen added. That this is true is evident from figure 3. The same qualitative facts are true here that were true for the heat-bodied samples. On the introduction of polar groups to the unsaturation, it takes progressively higher pressures to start to change the film from the expanded state to the condensed state. These facts substantiate the early observation of Langmuir (4) that the presence of double bonds in the middle of a fatty acid chain causes the films to

expand much more readily than films with saturated chains of similar length. Here again, the curves tend to a common area under very high compressions.

The various constants of the oxidized oil curves are plotted in figure 5 as a function of the atoms of oxygen added. With the addition of three atoms of oxygen per glyceride molecule, fc, the pressure necessary to condense the film, practically doubles. Long (3) reports that fc changes from 11.0 dynes per
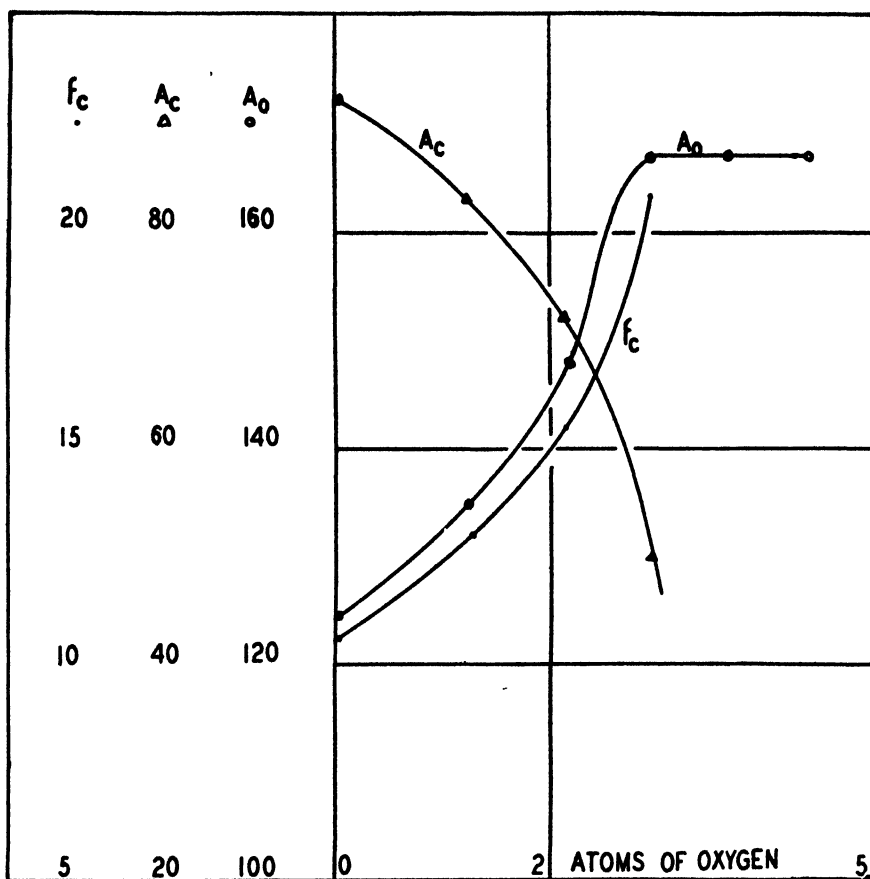
Fig. 5. Influence of oxygen. Plot of the various constants of the oxidized oil curves as a function of the atoms of oxygen added.

centimeter to 19.5 dynes per centimeter upon oxidation for 185 hr. at 23°C., a result which agrees with our results of a change in fc from 10.6 dynes per centimeter to 20.8 dynes per centimeter upon oxidation at 60°C. for 12 hr. The area (Ac) corresponding to this pressure (fc) continually decreases, while the limiting area (A_0) increases with the addition of oxygen. This effect is too large to be caused by the mere change in bulk density. This increase in limiting area must be due to the greater attraction of the oxygen groups for the water,

causing the film to flatten out and occupy a larger area. Strangely enough, the addition of more than three oxygen atoms per glyceride molecule causes no further increase in area. Also, the further addition of oxygen above three atoms does not cause the pressure–area curves to differ appreciably from one another. Apparently, on the average it is only necessary to have one oxygen
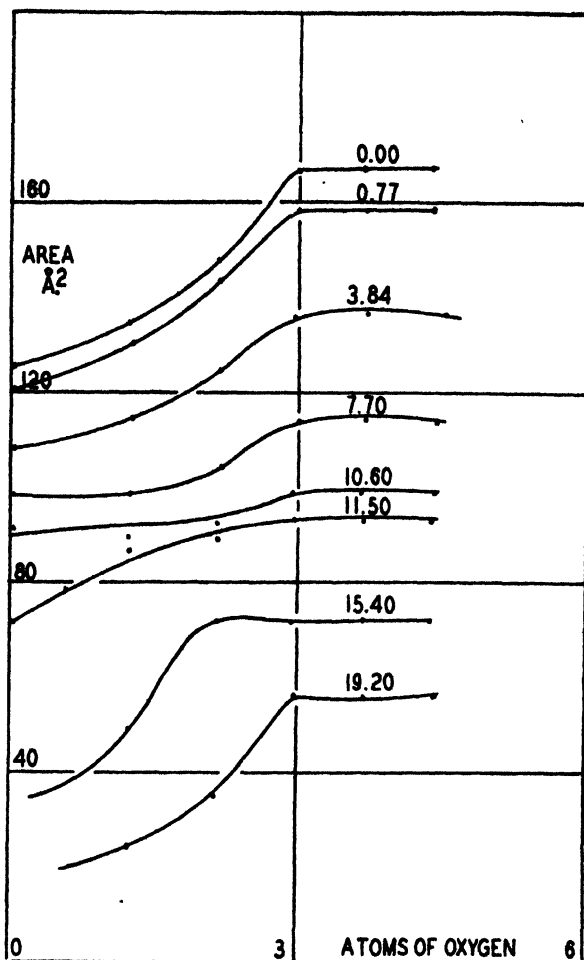
Fig. 6. Variation of the area with increasing amounts of oxygen at various constant surface pressures.

atom per fatty acid chain to get the maximum area and maximum force of attraction between the oil and water.

Figure 6 shows the variation of the area with increasing amounts of oxygen at various constant surface pressures. This indicates that if the measurement of the area at constant pressure were used as a measure of the oxidation, little change would be experienced at the higher amounts of oxygen. Also, it should

be noted that oxygen has little or no effect upon the area at the constant pressure of 10.6 dynes per centimeter, the value of fc for the original linseed oil.

SUMMARY

These results show that under low compressions the individual glyceride molecules of linseed oil in a monomolecular film are lying almost flat on the water surface. The chief points of attraction between the oil and water are the carboxyl groups, but the double bonds in the unsaturated fatty acids are also attracted to the water and thus cause the molecule to spread and occupy a much larger area. The addition of oxygen increases this attraction and causes the molecules to flatten further. A limiting area of 167 sq.Å. is reached with the addition of three atoms of oxygen per glyceride molecule. Polymerization has very little effect on the pressure–area curves, as shown by the heat-bodying data. Consequently, it is impossible to isolate the polymerization reaction taking place in the oxidation of monolayers of linseed oil.

REFERENCES

(1) ADAM, N. K.: Trans. Faraday Soc. **29**, 104 (1933).
(2) ADAM, N. K.: Proc. Roy. Soc. (London) **A101**, 516 (1922).
(3) ADAM, N. K., AND DYER, J. W. W.: Proc. Roy. Soc. (London) **A106**, 694 (1924).
(4) ADAM, N. K., AND JESSOP, G.: Proc. Roy. Soc. (London) **A110**, 423 (1926); **A112**, 516 (1926).
(5) ADAM, N. K., AND JESSOP, G.: Proc. Roy Soc. (London) **A120**, 473 (1928).
(6) ADAMS, H. E., AND POWERS, P. O.: Ind. Eng. Chem. **36**, 1124 (1944).
(7) GEE, G.: Proc. Roy. Soc. (London) **A153**, 129 (1935).
(8) GEE, G., AND RIDEAL, E. K.: Proc. Roy. Soc. (London) **A153**, 116 (1935).
(9) HUGHES, A. H., AND RIDEAL, E. K.: Proc. Roy. Soc. (London) **A140**, 253 (1933).
(10) LABROUSTE, H.: Ann. phys. **14**, 164 (1920).
(11) LANGMUIR, I.: J. Am. Chem. Soc. **39**, 1848 (1917).
(12) LANGMUIR, I.: J. Chem. Phys. **1**, 756 (1933).
(13) LONG, J. S., KITTELBERGER, W. W., SCOTT, L. K., AND EGGE, W. S.: Ind. Eng. Chem. **21**, 950 (1929).
(14) MITCHELL, J. H., KRAYBILL, H. R., AND ZSCHEILE, F. P.: Ind. Eng. Chem., Anal. Ed. **15**, 1 (1943).
(15) NUTTING, G. C., AND HARKINS, W. D.: J. Am. Chem. Soc. **61**, 2040 (1939).

THE EFFECT OF SODIUM SILICATES ON IRON OXIDE SURFACES[1]

FRED HAZEL

Department of Chemistry and Chemical Engineering, University of Pennsylvania, Philadelphia, Pennsylvania

Addition of strongly adsorbable negative ions (5, 7) and negative colloids (8) to iron oxide sols converts the surfaces of the particles from the positive to the negative form. At low concentrations of the added substances coagulation occurs, while at somewhat higher concentrations, the hydrous oxide is changed into a stable negative colloid. Solutions of the alkali silicates, because of the presence therein of hydroxyl ions, polyvalent negative ions, and/or negative ionic micelles, should be capable of producing these effects. Strength is given to this supposition by the fact that the silicates are used technically in water treatment as floc-producing aids (1, 2, 4). In addition they are employed in corrosion control (10), a fact which may be associated (5) with their ability to recharge iron oxide surfaces.

The present investigation was undertaken to study the effect of silicate composition in relation to the colloidal behavior of the systems. Colloidal ferric oxide was used as the reference system. Mobility and stability measurements were made in experiments conducted at different hydrogen-ion activities. The silicates employed varied in sodium oxide–silica ratio from 1:1 to 1:4.

EXPERIMENTAL

The ferric oxide sol was prepared by dropwise addition of ferric chloride solution to boiling distilled water. Purification was effected by dialysis for 1 week at room temperature with Visking casing. The sol was diluted before use to a concentration of 0.2 g. of ferric oxide per liter.

The silicates employed in the study were furnished by the Philadelphia Quartz Company. The compositions of the samples are given below in terms of molecular ratio of sodium oxide to silica.

COMMERCIAL BRAND	RATIO Na$_2$O:SiO$_2$	PERCENTAGE SOLIDS
Metso Crystals......................	1:1.00	57.57
C brand............................	1:2.02	53.65
N brand............................	1:3.30	37.77
S brand............................	1:3.98	30.95

Solutions containing 2000 p.p.m. of silica were prepared fresh daily by weighing and dissolving the calculated amount of samples. These solutions were diluted, at once, to a silica concentration of 200 p.p.m., using distilled water and/or 0.02 N hydrochloric acid. After preparation of the solutions, hydrogen-ion activity measurements were started without delay, and continued until constant

[1] Prepared for the 1945 Meeting-in-print, Division of Colloid Chemistry, American Chemical Society.

readings were obtained. Equilibrium was established in a few minutes with these dilute solutions. The pH data are given in the following table:

DILUENT	SILICA RATIO							
	1:1.00		1:2.02		1:3.30		1:3.98	
	Fresh	24 hr. old	Fresh	24 hr. old	Fresh	24 hr. old	Fresh	24 hr. old
Distilled H₂O...............	11.2	11.2	10.3	10.3	9.8	9.8	9.6	9.6
Dilute HCl.................	9.1	9.1	9.1	9.0	9.1	9.0	9.2	9.2
Dilute HCl......	7.2	7.2	7.3	7.1	7.0	6.9	7.0	6.9
Dilute HCl................					4.7	4.6	4.7	4.7

In the preparation of the silicate–iron oxide samples to be investigated, measured volumes of the stock solutions containing 200 p.p.m. of silica were diluted to 15 cc. with distilled water and mixed with 10 cc. of the iron oxide sol. Mobility and pH determinations were made after the samples had stood undisturbed for 30 to 60 min. Evidence of coagulation also was observed.

The pH values were measured with a Leeds and Northrup pH meter. Mobility determinations were made by a method described previously (12). All experiments were conducted at room temperature.

RESULTS

Tables 1–4 give mobility, pH, and flocculation data for iron oxide sols with the four silicates used as electrolytes. Results are given for freshly prepared silicate solutions and for solutions which had aged 24 hr. Mobility values are expressed in μ per second per volt per centimeter. Partial coagulation is indicated with a single asterisk and complete coagulation with two asterisks.

The data in table 1 were obtained with stock solutions of different ratios prepared by diluting the commercial samples with distilled water to a silica concentration of 200 p.p.m. The results show that the more alkaline silicates were the most effective in discharging the iron oxide surfaces. Aging the solutions for 24 hr., under the conditions of these experiments, may be seen to have had little effect. In this respect the behavior of the most silicious of the samples was exceptional, especially at low silica concentrations where a decrease in activity accompanied the aging.

Mobility data from table 1, for the freshly prepared silicate solutions, are plotted in figure 1. The relationship of the mobility of the iron oxide particles to their stability is shown in this figure. The positive critical mobility region, above which the particles were positive and stable, and the negative critical mobility region, below which the particles were negative and stable, were constructed from coagulation data. It may be seen that the courses of the mobility curves through the coagulation zone are very steep for the two most alkaline silicates. In addition, inspection of the figure shows that the most alkaline of the samples recharged the system at the lowest silica concentration. In this case the mobility curve crosses the isoelectric zone at a silica concentration of approximately 4.4 p.p.m.

TABLE 1

SILICA RATIO

SILICA	1:3.98 Fresh		1:3.98 24 hr. old		1:3.30 Fresh		1:3.30 24 hr. old		1:2.02 Fresh		1:2.02 24 hr. old		1:1.00 Fresh		1:1.00 24 hr. old	
p.p.m.	pH	Mobility	pH	Mobility	pH	Mobility	pH	Mobility	pH	Mobility	pH	Mobility	pH	Mobility	pH	Mobility
0	5.9	+3.4			5.9	+3.4			5.9	+3.4			5.9	+3.4		±0.0**
4	6.7	+2.6	6.5	+2.4	6.65	+2.1	6.55	+2.2	7.0	+2.2		+2.4	8.15	+0.5**		
8	7.65	+0.2**	7.1	+1.6**	8.25	−1.1**	7.55	−1.05**	8.7	−2.4*		−2.1	9.5	−2.7		
12	8.45	−2.45*	8.25	−1.85*	8.85	−2.3*	8.6	−2.3*								
16	8.7	−3.1	8.7	−2.65	9.05	−3.0	8.9	−2.7								
20	8.9	−3.3	8.9	−3.2	9.2	−3.2	9.05	−3.0	9.4	−3.25			10.1	−3.15		
40	9.25	−3.6	9.2	−3.6	9.5	−3.25	9.3	−3.2	9.75	−3.4			10.4	−3.35		
80	9.45	−3.8	9.4	−3.7	9.6	−3.5	9.6	−3.2	10.0	−3.65			10.8	−3.1		

* Partial coagulation.
** Complete coagulation.

The data in table 2 were obtained with silicate stock solutions containing 200 p.p.m. of silica and adjusted to a pH of 9.1–9.2. The results show the effects of partial neutralization of the silicates and the elimination of pH as a variable. It is revealed, under these conditions, that the effectiveness of the silicates decreases with decrease in the silica ratio, and that aging modifies the behavior only with the most silicious of the samples. Mobility values from table 2, for the freshly prepared samples, are plotted in figure 2. Comparison of the mobility curves with those of figure 1 shows that their passage through the coagulation zone was shifted to higher silica concentrations. The decrease in effectiveness caused by the reduced pH was greatest for the least silicious of the samples. It may be observed also that the recharging concentrations were shifted to
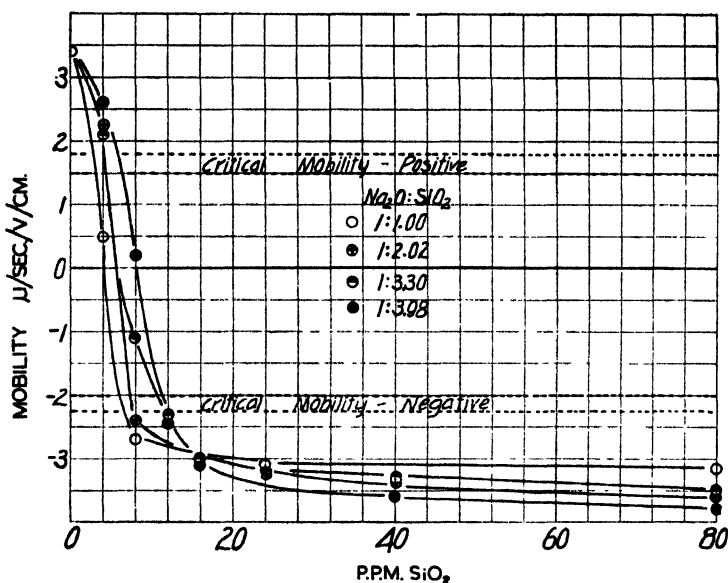
FIG. 1. Effect of silicates at their normal hydrogen-ion activities

higher values and that coagulation extended over a wider range of silica concentrations.

The data in table 3 and figure 3 obtained with silicates neutralized to a pH of 7.0–7.3 show the effects of the elimination of excess hydroxyl ions.

The behavior of the compositions corresponding to $Na_2O,3.98SiO_2$ and $Na_2O, 3.30SiO_2$, adjusted to pH 4.6–4.7, is shown in table 4 and figure 4. The broken curve corresponds to values determined after the sol–electrolyte mixtures had stood for 24 hr.

The mobility curves in figures 5–8 summarize the modifying effects of pH on each of the silicates when employed as electrolytes with iron oxide.

In an experiment designed to evaluate the effect of calcium-ion concentration on the mobility behavior of iron oxide with the silicates, 66.6 p.p.m. of calcium chloride was added to the sol–electrolyte samples. The results are shown in

TABLE 2

SILICA RATIO

SILICA (p.p.m.)	1:3.98				1:3.30				1:2.02				1:1.00			
	Fresh		24 hr. old		Fresh		24 hr. old		Fresh		24 hr. old		Fresh		24 hr. old	
	pH	Mobility	pH	Mobility	pH	Mobility	pH	Mobility	pH	Mobility	pH	Mobility	pH	Mobility	pH	Mobility
0	5.9	+3.4			5.9	+3.4			5.9	+3.4			5.9	+3.4		
4	6.25	+2.8	6.25	+2.6	6.2	+2.7	6.3	+2.9		+2.9		+3.05	6.15	+2.9		+2.7
8	6.55	+2.2	6.55	+2.1	6.5	+2.5	6.55	+2.5	6.6	+2.7		+2.9		+2.8		
12	6.8	+1.55**	6.8	+2.0	6.7	+1.8	6.8	+1.9		+2.25*		+2.3		+2.35		
16	7.0	+0.65**	7.05	+1.55**	7.05	+1.3**	7.0	+1.6**	6.9	+1.8**		+1.8**	6.8	+2.05**		
20	7.5	−1.15**			7.3	−0.2**	7.35	−0.3**		+0.5**				+1.1**		
24	8.05	−2.35	7.7	−1.4**	7.85	−1.9*	7.8	−1.8**	7.6	−0.7**		−0.9	7.7	−1.6**		+0.7**
32	8.5	−3.15	8.15	−2.5	8.3	−3.0	8.3	−2.9		−2.6*		−2.5*		−2.5**		
40	8.65	−3.3	8.5	−3.3	8.5	−3.1		−3.3	8.5	−2.6			8.3	−3.1		−2.4**
60			8.65	−3.35												
80	8.95	−3.6	8.95	−3.7	8.8	−3.3		−3.4	8.9	−3.2			8.8	−2.9		

* Partial coagulation.

** Complete coagulation.

figure 9. The silicate stock solutions were prepared by diluting the commercial products with distilled water. The data in figure 9 may be·compared with those in figure 1, which also were obtained at the normal hydrogen-ion activities of the electrolytes. It is seen that the presence of calcium chloride caused an upward displacement of the mobility curves from the region of negative stability to the coagulation zone. This behavior may be attributed to the adsorption· of calcium ions, which decreased the negative charge on the (recharged) particles and thus opposed the recharging effect of the silicates.[2]
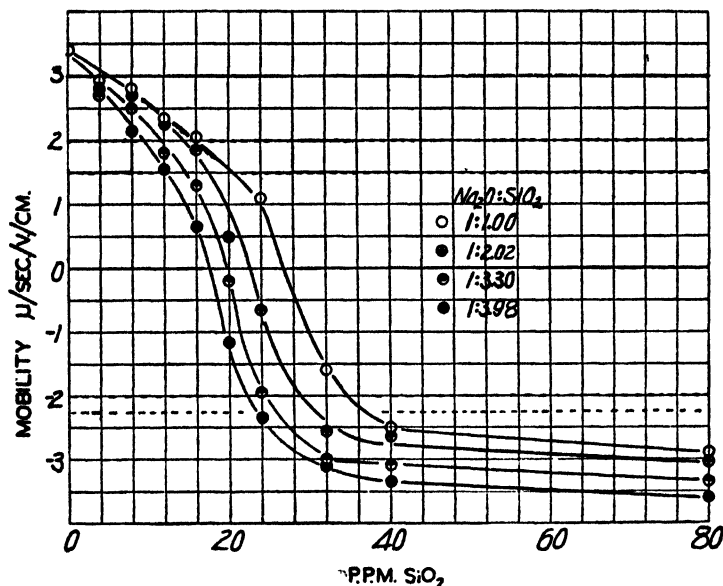
FIG. 2. Effect of partial neutralization of silicates

DISCUSSION

A comparison of the present data with those obtained previously (6) in a pH study with a dilute iron oxide sol shows that the silica in alkali silicates was active from the electrokinetic point of view. For example, alteration of the

[2] The presence of calcium chloride extended the coagulation range of the silicates in much the same way, although more so, as a moderate reduction in pH of the samples. (The effectiveness of silicates, in practice, as floc-producing aids is enhanced by partial neutralization (2) and by the addition of polyvalent metal ions (1).) However, in the experiment described, i.e., employing the silicates at their normal hydrogen-ion activities, the concentration of silicates required to initiate coagulation was not increased (as judged from the mobility curves). This fact is of interest since colloidal silicious particles, if present in the samples, would have had their negative charge reduced by adsorption of calcium ions, and thus the samples would have been made less effective in reducing the stability of the iron oxide particles. Time was not available for extending the investigation to the study of the effect of calcium chloride on the behavior of partially neutralized silicates.

TABLE 3

SILICA RATIO

SILICA	1:3.98				1:3.30				1:2.02				1:1.00			
	Fresh		36 hr. old		Fresh		24 hr. old		Fresh		24 hr. old		Fresh		24 hr. old	
	pH	Mobility	pH	Mobility	pH	Mobility	pH	Mobility	pH	Mobility	pH	Mobility	pH	Mobility	pH	Mobility
p.p.m.																
0	5.9	+3.4			5.9	+3.4			5.9	+3.4			5.9	+3.4		
8	6.3	+2.55		+2.8	6.1	+3.1		+3.0	6.2	3.1				+3.0		
20	6.3	+2.3		+2.5	6.2	+2.55										
24					6.25	+2.25		+2.2		+2.6		+2.6		+2.5		+2.7
32		+0.8**		+1.55**	6.3	+1.7**		+1.6								
40	6.4	−1.0**		+0.9**	6.3	+0.5**		+0.8**	6.4	+2.0**		+2.1**		+2.0**		
60		−1.5		−1.1**	6.4	−1.5		−1.3**		+1.0**		+1.0**		+1.5**		
80	6.6	−1.85		−1.9	6.5	−2.0		−2.0	6.6	−0.6**		−0.5**		+0.8**		+1.4**

* Partial coagulation.

** Complete coagulation.

hydrogen-ion activity of a positive iron oxide sol with hydrochloric acid or sodium hydroxide has been shown to produce the following effects (6):

(1) An increase in pH from 5.9 to 6.6 decreased the mobility from 3.7 to 3.2 μ/sec./v./cm.

(2) At pH 8.6 the particles were isoelectric.

(3) At pH 11.0 the particles displayed a mobilty of about -1.3 μ/sec./v./cm. The system was flocculated under these conditions, however, and it was not stabilized even in the presence of increased amounts of sodium hydroxide.

On the other hand, data in table 1 reveal that alkali silicates may convey a sufficient negative charge to iron oxide particles to cause them to be stable at pH 8.7. Table 2 discloses that iron oxide particles may be made isoelectric at a pH between 7.0 and 7.3 by the addition of silicates[3], while table 3 shows that
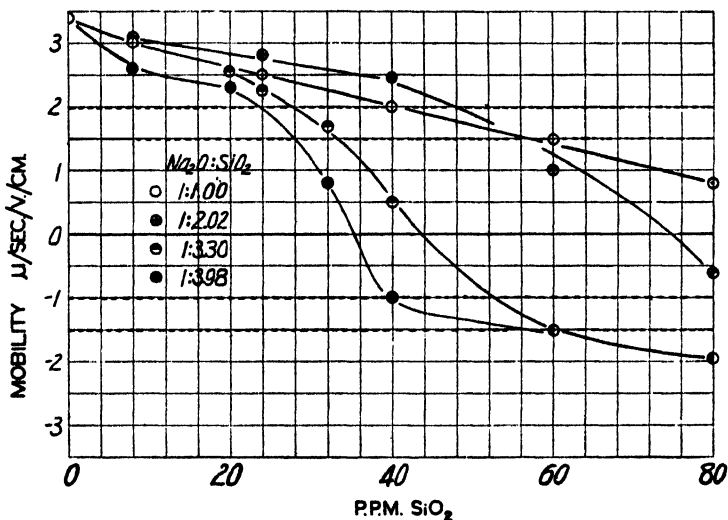
FIG. 3. Effect of elimination of excess hydroxyl ions

all the phenomena accompanying the recharging of the iron oxide system to the stable negative form may occur in the pH interval 5.9 to 6.6.

The stabilizing action of silica for iron oxide is enhanced at high pH values. This conclusion is supported by the data in table 1 and figure 1, where it is shown that when used at their normal hydrogen-ion activities, the silicates were least effective as coagulators for the hydrous oxide. Coagulation extended over narrow concentration ranges under these conditions. Decreasing the pH of the solutions shifted their recharging concentrations to higher values. This fact is portrayed in figures 5–8 and in table 5.[4]

[3] The shifting of the isoelectric point from 8.6 to lower pH values by strongly adsorbable negative ions has been encountered before (5, 7).

[4] The data in table 5 also may be used to estimate the coagulation ranges of the silicates at various hydrogen-ion activities. These data were approximated from figures 1, 2, and 3. Concentrations are expressed in parts per million of silica, the first number corresponding

TABLE 4

SILICA	SILICA RATIO							
	1:3.98				1:3.30			
	Fresh		24 hr. old		Fresh		24 hr. old	
	pH	Mobility	pH	Mobility	pH	Mobility	pH	Mobility
p.p.m.								
0	5.9	+3.4			5.9	+3.4		
8	5.9	+3.1		+2.8	5.9	+3.2		
20		+2.6		+2.4		+3.15		
32	5.8	+1.2*†		+1.2*	5.8	+3.1		
40	5.7	+0.7*†		+0.6**	5.7	+3.0		
60	5.5	±0.0(−0.2)‡		±0.0(−0.2)‡	5.5	+2.8		
80	5.3	±0.0(−0.8)‡		±0.0(−0.7)‡		+2.9		+2.7

* Partial coagulation.

** Complete coagulation.

† These samples, which were only partially flocculated at the time of the mobility measurements, were observed after the lapse of 24 hr. and found to be completely coagulated.

‡ The values in parentheses were determined after the samples had stood for 24 hr. These systems were *stable*, and the faint opalescence which had developed during their preparation had not increased.
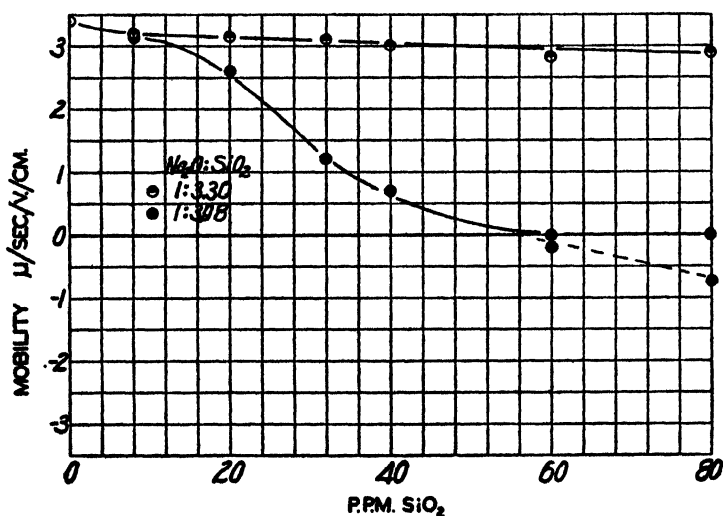
FIG. 4. Effect of silicious silicates at pH 4.6–4.7

As indicated earlier, the present work compared different silicates at the same silica concentrations and, except for the series of experiments reported in figure

to the flocculation value, the second designating the deflocculating concentration. The differences between the numbers measures the coagulation ranges for a given silicate. These may be seen to be greater the lower the pH of the systems.

1 and table 1, at the same hydrogen-ion activities. The results obtained (see tables 2, 3, 4, and 5 and figures 2, 3, and 4) force the conclusion that at a given
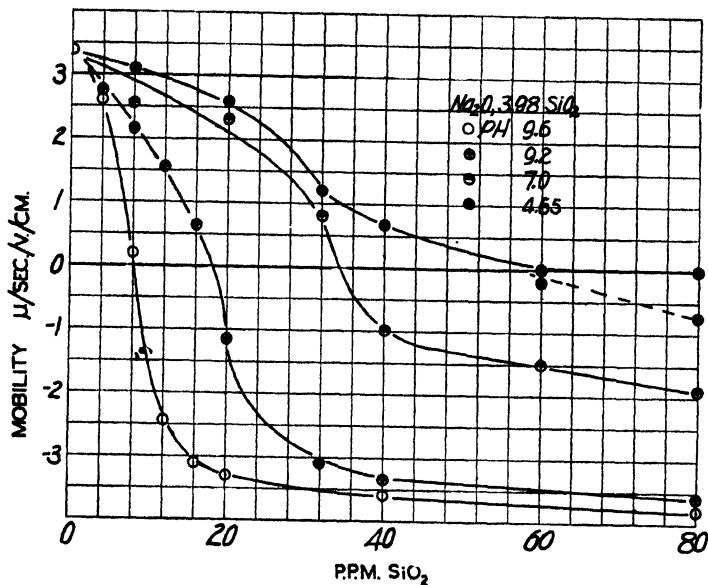
FIG. 5. Effect of pH on the behavior of composition $Na_2O,3.98SiO_2$
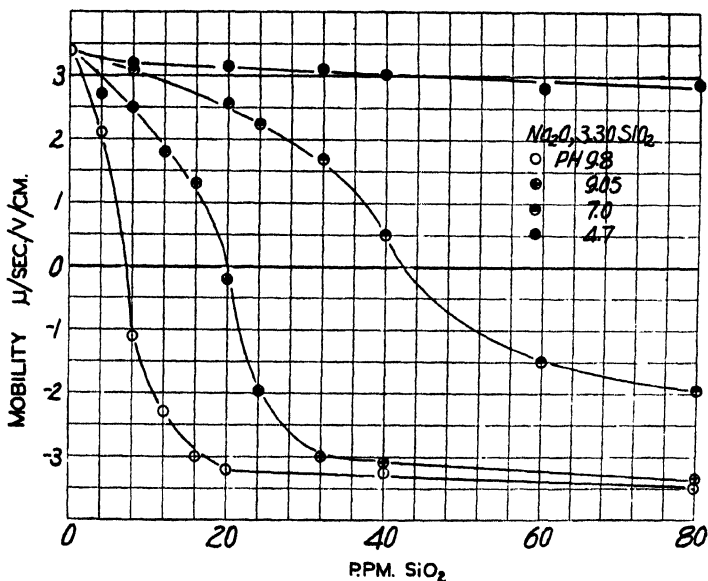
FIG. 6. Effect of pH on the behavior of composition $Na_2O,3.30SiO_2$

silica concentration and a given hydrogen-ion activity the effectiveness of the silica in the solutions depended upon the silica ratio of the source material.

This fact is illustrated further by table 6, which gives the silica concentration in parts per million required to reduce the mobility of the iron oxide particles to
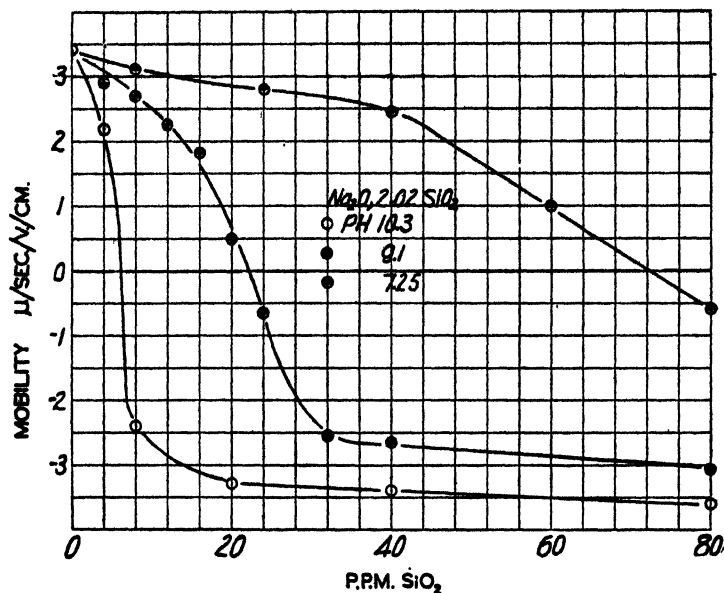
FIG. 7. Effect of pH on the behavior of composition $Na_2O,2.02SiO_2$
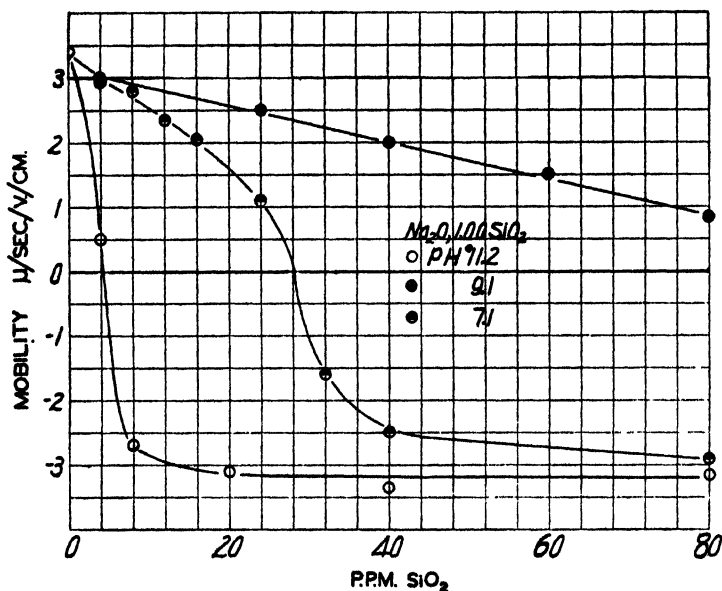
FIG. 8. Effect of pH on the behavior of composition $Na_2O,1.00SiO_2$

the isoelectric condition. The pH values recorded in table 6 are for the stock solutions of the different silicates, each containing 200 p.p.m. of silica.

Addition of hydrochloric acid to the silicates resulted in the formation of different amounts of sodium chloride and a constant amount of hydrous silica. The largest amount of sodium chloride was formed with the sample having the smallest silica ratio. The same sample showed the greatest decrease in activity on the addition of acid. In seeking a possible connection between these facts it may be pointed out that 1–1 type electrolytes have little effect on the mobility
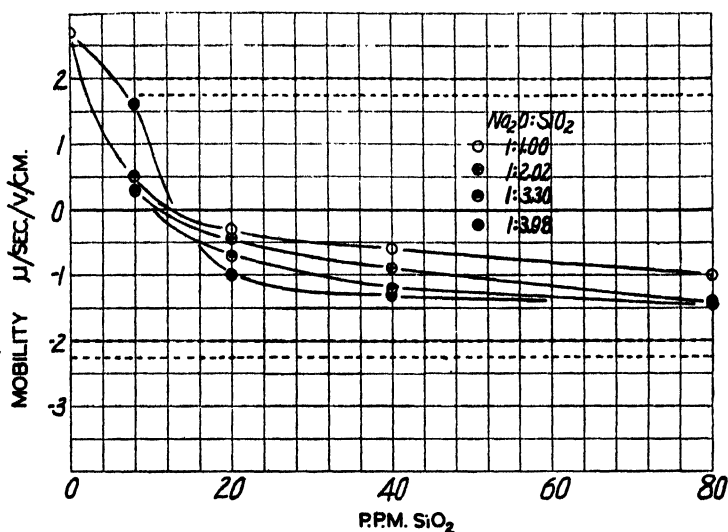
FIG. 9. Effect of 66.6 p.p.m. of calcium chloride on the behavior of silicates at their normal hydrogen-ion activities

TABLE 5

Coagulation ranges of silicates

SILICA RATIO							
1:3.98		1:3.30		1:2.02		1:1.00	
pH	p.p.m.	pH	p.p.m.	pH	p.p.m.	pH	p.p.m.
9.6	6–12	9.8	4–11	10.3	4–7	11.2	3–6
9.2	10–23	9.1	12–26	9.1	14–30	9.1	16–37
7.0	23–56	7.0	28–60	7.3	48–>80	7.2	40->80

and stability of iron oxide (6) even at concentrations much higher than those encountered in the present work. However, when applied to its effect on colloidal silica, which undoubtedly was present to a greater or less extent in the various samples, the part played by sodium chloride is not so evident. Available data were obtained with an aged, dialyzed silica sol (5a) and show that sodium chloride decreased the negative character of silica substantially at concentrations

of the order encountered here. This factor may have contributed to the observed differences of the silica in the various samples of the present work.[5]

It has been recognized for some time that the colloidal nature of silicates increases with silica ratio (11). This was verified for the samples used in the present study by several experiments involving dialysis and based on the premise that retention by a membrane was a measure of colloid concentration. Solutions containing 2000 p.p.m. of silica were prepared by diluting the original samples with distilled water. The freshly prepared solutions (the metasilicate solution was 14 days old) were placed in Visking casing and dialyzed 5 days. At the end of this period the pH values of the solutions ranged between 5.8 and 6.1. Silica determinations were made, with the results tabulated below:

SILICA RATIO	SiO₂ IN DIALYSATE
	p.p.m.
1:3.98	200
1:3.30	68
1:2.02	<4
1:1.00	8

TABLE 6

Isoelectric concentrations of silicates

pH	SILICA RATIO			
	1:3.98	1:3.30	1:2.02	1:1.00
9.1–9.2	17.5	19.5	22.5	27
7.0–7.3	35	43.5	75	>80
4.6–4.7	60	>80	>80	>80

The above data, while showing that a high colloid content was associated with a high silica ratio and thus might serve as a basis for rationalizing the

[5] The coagulation behavior of the composition corresponding to $Na_2O, 3.98SiO_2$ requires special consideration at pH 4.7. The silica in the sample at this pH apparently was largely in the form of negatively charged, highly hydrated aggregates. When added to iron oxide the silica was adsorbed and lowered the mobility of the particles. The decrease in charge of the iron oxide lowered its stability. At the same time, however, the adsorbed silica conveyed a hydrophilic surface to the iron oxide particles, thus increasing their stability. At low concentrations of the silica mutual coagulation occurred, but as the concentration of the silica was increased, and the surface of the iron oxide became more completely covered, the silica functioned as a protective colloid. As a result the system was stabilized even though the electric charge was eliminated.

Baylis (2) has observed that silicates reduced to a pH in the acid range offer small aid to coagulation. It has been shown with dialyzed and aged silica sols (5a), however, that the silica coagulates iron oxide at a high critical potential.

The change in mobility of the particles on standing, noted in table 4 and figure 4, may have been due to a rearrangement of the adsorbed silica, possibly by syneresis, in such a manner that more of it was accommodated on the iron oxide surfaces.

results which have been presented, did not distinguish between the colloidal particles originally present in the starting solutions and those formed during the reduction of pH by dialysis. In an effort to gain information on this point as well as to check the above results, the compositions corresponding to the molecular ratios $Na_2O,3.98SiO_2$ and $Na_2O,3.30SiO_2$ were dialyzed. The original samples were employed in this study, the results being given in some detail below.

About 175 ml. of each of the samples was introduced into Visking casing and the latter placed in 1-liter beakers filled with distilled water. After standing 24 hr., during which time it was stirred at intervals, the diffusate (outside liquid) was replaced with water. The water was not changed again until 48 hr. had elapsed. It was changed again after a second 48-hr. period. The three diffusates from each sample were retained for study. Qualitative tests showed that the silica from the sample with the lower silica ratio diffused at the faster rate. A strong gel formed immediately upon neutralization of the 24-hr. diffusate with hydrochloric acid, while a weak gel formed at once upon neutralization of the first 48-hr. diffusate. There was no immediate gel formation upon neutralization of the second 48-hr. diffusate. Similar tests under like conditions with the more silicious sample resulted in the formation of a weak gel from the 24-hr. diffusate and no gels from the 48-hr. diffusates.

During the first several days of dialysis there was evidence of considerable osmotic phenomena. Water flowed into the bags to such an extent that the solutions were diluted about threefold. There also was evidence of some sedimentation with deposition of silicious material in the bottom of the bags. The deposit was greater with the sample that had the greater original turbidity $(Na_2O,3.98SiO_2)$ and may have been due to the settling of coarse particles of silica.[6]

After the second 48-hr. period and over an interval of 15 days, the water was changed twenty-nine times, the diffusates being discarded. The Visking casings containing the partially dialyzed silicates then were placed in approximately 2 liters of distilled water in separate beakers and permitted to rest with daily stirring for 80 hr. At the end of this period the hydrogen-ion activities of the diffusates and the dialysates (solutions inside the membrane) were determined. In order to verify the results, the experiment was repeated, discarding the diffusate and replacing it with water. Twenty-four hours later the water again was changed and the systems permitted to come to equilibrium for 144 hr. The results of the hydrogen-ion activity determinations are shown in table 7 in terms of pH. It may be noted in both experiments and with both silicates that the liquids outside the membrane were more alkaline than those inside. These findings were a result of "membrane hydrolysis" and were a demonstration of the fact that the silicates retained by the membrane were in the form of colloidal

[6] By coarse particles is meant those above the colloidal size range. The presence of these being postulated, it is possible to ascribe their stability in the original samples to the "suspending action" (9) of the electrolytes therein. As the originally high concentration of the electrolytes was reduced by dialysis and dilution, the particles settled owing to gravity.

electrolytes. Sodium ions, but not colloidal silicate ions, diffused through the membrane, and, in order to meet the requirements of the Donnan membrane equilibrium, hydrogen ions diffused into the inner compartment.

TABLE 7

NUMBER OF WATER CHANGES	EQUILIBRIUM TIME	SILICA RATIO			
		1:3.98		1:3.30	
		Diffusate	Dialysate	Diffusate	Dialysate
29	80	7.6	7.0	6.83	6.5
31	144	7.2	6.6	6.8	6.43

Dialysis was discontinued after 10 more days, during which period the water was changed twelve times. Silica concentrations and pH values of the sols were determined. The results are tabulated below:

RATIO	pH	PERCENTAGE SILICA
1:3.98	5.3	1.24
1:3.30	5.5	0.35

The above data show that a high percentage of the silica from both samples had diffused through the membrane and, accordingly, was non-colloidal from this standpoint.

The diffusates collected at the end of the first 24 hr. were analyzed for silica and then placed in Visking casing. They were dialyzed for 19 days, during which time the water was changed twenty times.[7] The sols were analyzed for silica and their pH values determined. The results are shown below:

RATIO	pH	PERCENTAGE SILICA
1:3.98	4.72	0.5
1:3.30	4.75	0.32

Table 8 summarizes the results of the dialysis experiments. The data in the table refer to the silica concentrations in terms of percentage and are given for the original silicates and the sols obtained from these. Similar data are given for the diffusates collected at the end of the first 24 hr. of the dialysis of the original samples and for the sols resulting from the dialysis of the diffusates. These data demonstrate that the tendency to assume the colloidal state increases with increase in silica ratio of the starting material. This is illustrated not only

[7] At the end of the twelfth day and after the thirteenth water change the systems were permitted to approach equilibrium for 96 hr. The pH values of the liquids on the opposite sides of the membrane were determined, and it was found that membrane hydrolysis had occurred as in the previous dialysis. In this case the pH values of the inside liquids were lower by about 0.7 of a unit.

by a comparison of the silica concentrations of the sols but also by a comparison of the concentration of the sol precursors, particularly the diffusates.

The conclusions of Harman (3) concerning the constitution of silicates of different ratios are consistent, in general, with that portion of the results of the present work which bears on this subject. In concentrated solutions at high alkalinities the silica in the silicates of ratio 1:1 and 1:2 exists predominantly as small hydrated particles approaching, or of, ionic size. On the other hand, the silica in concentrated solutions of the silicates of ratios 1:3.30 and 1:3.98 is polydisperse with respect to size. In the latter case it is present as aggregates which range in size from ionic to colloidal dimensions. Increase in silica ratio increases the size and number of these aggregates. The ability of the aggregates to function as nuclei for condensation increases with size.[8]

The results in table 8 can be explained on the above basis: the silica in the sample with the highest silica ratio was present to the greatest extent as aggregates of such a size as to be capable of nuclear action under the conditions of the experiment.[9]

TABLE 8

RATIO	ORIGINAL SAMPLE	SOL[*]	DIFFUSATE	SOL[†]
1:3.98	24.56	1.24	3.48	0.5
1:3.30	28.78	0.35	5.97	0.32

* The volumes of these sols were about three times the volumes of the original samples.
† The volumes of these sols were about one and one-half times those of the "diffusates."

The present work yielded no defininite evidence as to the presence of simple silicate ions in the solutions, nor was a sharp differentiation between the aggregates (or nuclei) and ionic micelles, in relation to their effect on iron oxide surfaces, accomplished. However, it is plausible to assume that at high pH values and with silicates of low silica ratios the discharging action was due to hydroxyl ions and to very small aggregates or ions. At lower pH values and with silicates of high silica ratios the discharging action predominantly was due to larger, but diffusible, aggregates[10] and to ionic micelles.

[8] While it is reasonably certain that a reduction of pH favors the formation of nuclei, the effect of the reverse change, i.e., the effect of increase in pH on the number and the size of nuclei, was not investigated.

[9] The silica sols obtained by dialysis of the original samples appeared to be identical, as measured by the effect of their silica on iron oxide sols. However, the experiments in this connection were conducted at only two silica concentrations and at one hydrogen-ion activity.

[10] Evidence of a negative charge on the aggregates was furnished by dialysis experiments with solutions of the composition corresponding to $Na_2O,3.98SiO_2$. Dilutions containing 200 p.p.m. of silica were made and adjusted to pH values of 7.0 and 4.65, respectively. Dialysis for 1 week resulted in a decrease of the discharging activity of the solutions by about 60 per cent. It was assumed that simple silicate ions did not exist in the solutions of the above hydrogen-ion activities and that the residual activity, after dialysis, was due to ionic micelles. Sodium chloride, of course, was removed by the dialysis, but being a

Particle growth by condensation requires time. It is well known that silica sols prepared by acidifying silicate solutions must be permitted to age before dialysis. If this is not done, an appreciable loss of silica occurs by diffusion. The dilute solutions employed in the present work did not present favorable systems for age studies. Only small changes in effectiveness were noted during the 24-hr. observation period under the experimental conditions described. Baylis (2), in connection with studies of the application of partially neutralized silicate solutions as coagulation aids in water purification, has shown that age has little effect on the properties of the solutions when the concentration of silica is less than 0.5 per cent. However, with solutions containing between 1.0 and 1.5 per cent silica prepared from a highly silicious sample, Baylis found that the solutions changed in activity depending on the time of standing and the alkalinity.

In a preliminary experiment with the silicate of ratio 1:3.30 diluted to a concentration of 1.5 per cent silica and adjusted to a pH of 10.2 with hydrochloric acid, it was found that changes in the properties of the solution (including pH changes) occurred with age and that they could be followed by the techniques applied to the dilute solutions already described. It is hoped that these will be investigated in the future, using different silicates under different conditions.

SUMMARY

1. It has been shown that silicates, varying in sodium oxide–silica ratio from 1:1 to 1:4, display a behavior toward iron oxide resembling that of electrolytes which contain strongly adsorbable, polyvalent negative ions.

2. It has been found, in silicate solutions with unadjusted hydrogen-ion activities, that flocculation was initiated at low silica concentrations, while at somewhat higher concentrations the iron oxide was recharged to the stable negative form.

3. Neutralization of the silicates to varying degrees has been observed to increase the amounts required for flocculation and for recharging the iron oxide. Although a decrease in pH reduced the effectiveness of the silicates in these respects, the same factor increased the concentration range over which coagulation occurred.

4. Calcium chloride, at a concentration of 66.6 p.p.m., was found to extend the concentration range over which the silica produced coagulation without, in samples at their normal hydrogen-ion activities, increasing the silica requirements for initiating coagulation.

5. It has been shown that, at a given hydrogen-ion activity and a given silica

1-1 type electrolyte and present in only a low concentration, its effect on the mobility was negligible.

Since this salt was formed in all solutions to which hydrochloric acid was added and for which coagulation data have been given, it should be pointed out that sodium chloride decreases the stability of iron oxide particles. This effect is proportional to its concentration and presumably is caused by a decrease in thickness of the double layer with an attendant elevation (or depression for the negative sol) of the critical mobility (5c).

concentration, the effectiveness of the silica in discharging and recharging iron oxide surfaces increased with the silica ratio of the original samples.

6. The tendency of sodium silicates to form colloidal suspensions has been found to increase with increase in silica ratio.

7. Evidence has been presented which supports the belief that silica sols are colloidal. electrolytes.

REFERENCES

(1) BAKER AND DEDRICK: U. S. patent 2,310,009 (February 2, 1943).
(2) BAYLIS: Water Works & Sewerage **84**, 221 (1937).
(3) HARMAN: J. Phys. Chem. **32**, 44 (1928).
(4) HAY: J. Am. Water Works Assoc. **36**, 626 (1944).
(5) HAZEL: J. Phys. Chem. **46**, 516 (1942); (a) J. Phys. Chem. **42**, 409 (1938); (b) J. Phys. Chem. **45**, 731 (1941).
(6) HAZEL AND AYRES: J. Phys. Chem. **35**, 2930 (1931).
(7) HAZEL AND AYRES: J. Phys. Chem. **35**, 3148 (1931).
(8) HAZEL AND McQUEEN: J. Phys. Chem. **37**, 553 (1933).
(9) See McBain's discussion in Kraemer's *Advances in Colloid Science*. Interscience Publishers, Inc., New York (1942).
(10) STERICKER: Ind. Eng. Chem. **30**, 348 (1938).
(11) VAIL: *Soluble Silicates in Industry*. The Chemical Catalog Company, Inc., New York (1928).
(12) WILLEY AND HAZEL: J. Phys. Chem. **41**, 699 (1937).

HIGH-TEMPERATURE CRYSTAL CHEMISTRY OF A_mBX_n COMPOUNDS WITH PARTICULAR REFERENCE TO CALCIUM ORTHOSILICATE

M. A. BREDIG

Applied Chemicals Division, Vanadium Corporation of America, 420 Lexington Avenue, New York, New York

I. INTRODUCTION

Recently, an attempt has been made to apply the results of crystal-structure determinations of silicates and aluminates occurring in cement to an interpretation of their chemical behavior, such as the hardening by reaction with water (10). Brandenberger (2) has tried to explain in terms of crystal structure the greater reactivity of the high-temperature modifications of compounds such as calcium orthosilicate (α and β) as compared with the inertness of the low-temperature (γ) form of this compound. A tendency of the calcium cation at room temperature to surround itself with a larger number of negative ions, such as O^{2-}, than at higher temperatures was assumed. Specifically, it was suggested that the coördination number of calcium for oxygen in the reactive β-form

which is metastable below 675°C. might be 4, that is, less than the corresponding figure (6) for the inactive low-temperature (γ) form, the crystal structure of which has lately been shown by O'Daniel and Tscheischwili (28) to be of the type of olivine. By all these authors a CaO_4 group was assumed to have a greater tendency to add water molecules and thus to produce a normal, high oxygen coördination of 6 or 8 around calcium than a CaO_6 group such as the one occurring in the olivine structure of the low-temperature form.

No actual experimental determination of the atomic arrangement in the reactive high-temperature forms of calcium orthosilicate was available to support the assumption of CaO_4 groups in stabilized β-calcium orthosilicate. On the contrary, the writer (4, 7) has shown that the crystal structures of the two forms of calcium orthosilicate above 1420°C. most likely are the same as those of the two forms of potassium sulfate. In the low-temperature (β) form of potassium sulfate, potassium has nine to ten nearest neighbors, oxygen atoms belonging to tetrahedral SO_4 anions (33). In high-temperature α-K_2SO_4, shown (4) to have the structure of glaserite (18), the number of nearest neighbors of potassium is similar. Because of the isotypy of α- and α'-calcium orthosilicates, the forms stable above 1420°C., with these two forms of potassium sulfate, calcium must necessarily have the same number of nearest neighbors in these two crystal modifications of Ca_2SiO_4, that is, nine to ten. With the corresponding coördination number having been shown to be only 6 in the low-temperature (γ) form of Ca_2SiO_4, we note that the tendency of calcium in regard to its coördination with oxygen as a function of temperature appears to be just the reverse of that assumed in Brandenberger's theory. The coördination around calcium actually is lowest at low temperatures and highest at high temperatures.

Before a more detailed and at the same time more general discussion of this problem will be presented, some additional experimental evidence is examined in the following, which demonstrates the existence in calcium orthosilicate, at high temperatures, of an atomic arrangement in which the coördination around calcium is 10 rather than 4.

II. THE STRUCTURE OF MERWINITE, A SOLID SOLUTION OF Mg_2SiO_4 IN α'-Ca_2SiO_4

The effect of additions, to calcium orthosilicate, of small amounts of phosphate or potassium silicate was considered to represent the stabilization of a heretofore unknown crystal phase of Ca_2SiO_4, designated the α'-form by the writer, and isotypic with β-K_2SO_4 (4, 7). It now appears that magnesium orthosilicate also belongs to the agents able to stabilize the orthorhombic, second-highest-temperature form (α'). Merwinite, "$3CaO \cdot MgO \cdot 2SiO_2$," which occurs as a natural mineral (24) as well as an occasional constituent of slags (32), and which has also been recommended as a refractory material (25), is believed by the writer to be nothing but the α'-form of Ca_2SiO_4, stabilized by and containing in solid solution a maximum of approximately one-third of one mole of Mg_2SiO_4 per mole of Ca_2SiO_4.

In table 1, d values of an orthorhombic crystal lattice with the constants $a_0 = 5.20$, $b_0 = 9.20$, and $c_0 = 6.78$ Å. ($a:b:c = 0.565:1:0.737$), isotypic with

β-K$_2$SO$_4$, are compared with the experimental d values reported by Phemister (32). The agreement is considered rather satisfactory. The lattice constants, and also in general the intensities of the x-ray reflections, are quite similar to those of β-CaNaPO$_4$ with $a_0 = 5.215$, $b_0 = 9.32$, and $c_0 = 6.83$ Å.

TABLE 1

Interpretation of powder x-ray pattern of merwinite, α'-(Ca$_2$SiO$_4 \cdot \frac{1}{3}$Mg$_2$SiO$_4$)

$a_0 = 5.20$, $b_0 = 9.20$, $c_0 = 6.78$Å.; $z = 4$; specific gravity (x-ray) = 3.34*

INTENSITY	$d_{experimental}$ (Phemister (32))	$d_{calculated}$ (Bredig)	INDICES hkl
	Å.	Å.	
w.	2.94	(2.94)	(130 K$_\beta$)
w.	2.83	2.845	102
m.	2.73	$\begin{cases}2.72\\2.73\end{cases}$	$\left.\begin{array}{l}112\\022\end{array}\right\}$
s.	2.65	2.65	130
v.w.	2.41	2.42	122
w.	2.30	2.30	040
w.	2.20	2.20	013
w.	2.16	2.15	221
w.	2.03	$\begin{cases}2.025\\2.03\end{cases}$	$\left.\begin{array}{l}113\\023\end{array}\right\}$
m.	1.90	$\begin{cases}1.905\\1.905\\1.89\end{cases}$	$\left.\begin{array}{l}231\\042\\123\end{array}\right\}$
m.w.	1.87	1.88	222
v.w.	1.75	1.74	150
v.w.	1.69	$\begin{cases}1.70\\1.68\\1.68\end{cases}$	$\left.\begin{array}{l}004\\213\\151\end{array}\right\}$
	etc.		

Reflections $h0l$, $l = 2n + 1$, and $hk0$, $h + k = 2n + 1$ are not observed; space group = D_{2h}^{16}.

* In the mineral merwinite, Larsen and Foshag (24) have found 3.15. Spurrite and gehlenite of considerably lower specific gravity were reported to have been closely associated with merwinite in the sample.

$(a:b:c = 0.560:1:0.733)$, space group D_{2h}^{16}, which is also isotypic (4) with β-K$_2$SO$_4$, $a_0 = 5.76$, $b_0 = 10.05$, $c_0 = 7.46$ Å. $(a:b:c = 0.573:1:0.742)$. The orthohexagonal lattice constants of solid solutions of the highest-temperature (α) form of Ca$_2$SiO$_4$ (4) are, for comparison, $a_0 = 5.40$, $b_0 = a_0\sqrt{3} = 9.35$, $c_0 = 6.996$ (19) $(a:b:c = 0.577:1:0.749)$.

In a brief discussion of the structure, H. J. Goldschmidt and Rait (16) re-

cently suggested that merwinite was isotypic with perovskite, $CaTiO_3$. Such an isotypy seems extremely improbable. It would require the same arrangement of the oxygen ions in relation to the metal ions. In perovskite titanium is surrounded by six oxygen atoms. It is not clear how the authors propose to reconcile with this fact the assumption of SiO_4 tetrahedra.

Just as in the cases of phosphate and potassium silicate additions to calcium orthosilicate, where formulas for ternary compounds such as "$Ca_7(PO_4)_2(SiO_4)_2$" or "$Ca_{22}K_2(SiO_4)_{12}$" could be discarded (4, 7), present experimental facts do not warrant considering merwinite as a ternary compound, "$3CaO \cdot MgO \cdot 2SiO_2$." This is true even though Osborn (30) and Parker and Nurse (31) have found merwinite to exist in equilibrium with the liquid, where it had not been observed originally in the first comprehensive study of the ternary equilibrium diagram by Ferguson and Merwin (14) and by Greig (20). In none of these studies was any evidence presented which would exclude complete solubility in the solid state, in the temperature range between 1420°C. and, say, 1550°C., between Ca_2SiO_4 (α'-form) and the composition of the alleged "Compound $3CaO \cdot MgO \cdot 2SiO_2$." According to the more recent investigations cited above (30, 31), the phase called merwinite melts incongruently at 1580°C., decomposing into melt and Ca_2SiO_4. At this temperature, pure Ca_2SiO_4 is most likely to be present in its hexagonal glaserite-type form (α). On quenching, it will, however, be found in the β-modification, owing to successive transformation into the α'- and β-forms because of the absence of a sufficient quantity of stabilizers in solid solution.

In a previously published representation of the equilibria of calcium orthosilicate with orthophosphate (7) the transition point $\alpha' \rightleftharpoons \alpha$ in pure Ca_2SiO_4 had been placed tentatively near 1800°C., halfway between the long known transition point at 1420°C. and the melting point. The latest data by Osborn and by Parker and Nurse, however, make it necessary (8) to place the transition $\alpha' \rightleftharpoons \alpha$ at a temperature between 1420° and 1580°C., if the assumption of the identity of merwinite as a solid solution of Mg_2SiO_4 in α'-Ca_2SiO_4, proposed by the writer, is to be maintained. These relations are indicated schematically in the diagram of figure 1, representing a pseudo-binary join from Ca_2SiO_4 towards $CaMgSiO_4$ (monticellite) and Mg_2SiO_4 (forsterite), in the ternary system $CaO-MgO-SiO_2$. They will have to be tested experimentally in the region close to Ca_2SiO_4.

If a careful interpretation of x-ray intensities should show that magnesium is not randomly placed on the cation positions of the α'-Ca_2SiO_4 crystal lattice, but occupies only one type of these, it would be necessary to revert to the concept of merwinite as a ternary compound in spite of complete isomorphism with α'-Ca_2SiO_4. Such a condition has been assumed to exist in monticellite, $CaMgSiO_4$, of Mg_2SiO_4 (olivine) structure (9), which forms an uninterrupted series of solid solutions with Mg_2SiO_4.

Some observations on merwinite are in disagreement with the orthorhombic symmetry assumed here for α'-Ca_2SiO_4. If these observations are considered indicative of lower crystal lattice symmetry, it might be necessary to modify

the assumption of the identity of the merwinite specimens examined optically at room temperature with the actual α'-Ca_2SiO_4 solid-solution phase at high temperatures: A transformation may have occurred on cooling which may have diminished the crystal symmetry from that of the orthorhombic β-potassium sulfate structure of α'-Ca_2SiO_4 to that (monoclinic, triclinic) reported by Phemister and others for merwinite. In fact, the polysynthetic twinning reported by these authors seems to point to such a possibility, just as did the twinning in
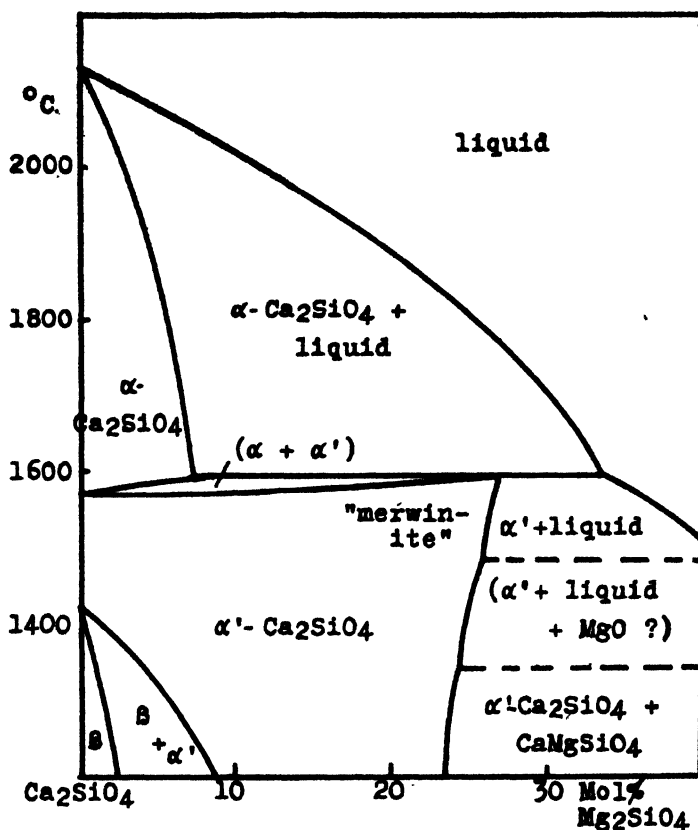
Fig. 1. Probable phase relations of the system CaO–MgO–SiO$_2$ in the vicinity of Ca$_2$SiO$_4$ (schematic).

so-called α-Ca_2SiO_4, which was actually β-Ca_2SiO_4 (Hansen (21); Insley (22)). The conclusions drawn both from the occurrence of the β-potassium sulfate structure in Ca_2SiO_4 containing phosphate or potassium silicate and from the striking similarity of Phemister's x-ray pattern of merwinite with that of β-potassium sulfate, even though merwinite might actually be of lower symmetry, would remain valid regardless of the existence of such a transition. (The formation of a highly asymmetric monoclinic or triclinic structure from melts of simple orthosilicates at high temperatures seems rather unlikely.)

III. DISCUSSION

The oxygen coördination of 9 to 10 around calcium in the potassium sulfate-type, high-temperature, α', crystal structure of Ca_2SiO_4 represents a considerable increase from the CaO_6 coördination of the olivine-type, lowest-temperature γ-form. It is precisely this increase, rather than a decrease to CaO_4 presumed by O'Daniel and Tscheischwili and others, that must actually be expected from theoretical considerations.

The authors just mentioned pointed to the following rule pronounced by V. M. Goldschmidt (17) in 1926: At high temperatures that crystal structure (of an A_mBX_n compound) is stable which could be also obtained, through a morphotropic change in structure, by substituting a lower homologue for the cation (A) by which the BX_n radical ion is "contrapolarized."

The term "contrapolarization" was introduced by Goldschmidt (17) in reference to the theory of the—mutual—deformation (polarization) of the electronic shells of ions, advanced and extensively developed by Fajans (11–13). "Contrapolarization," according to Goldschmidt, is the electrostatic influence (loosening) which A cations such as Ca^{2+}, surrounding, in a crystal lattice, the BX_n radical anions composed of strongly polarizing central B ions and strongly polarized (deformed) X ions (Si^{4+} and O^{2-}, respectively, in SiO_4^{4-}) exert upon the state of polarization of the X ions, upon their distance from the central B ion, and, thus, upon the strength of the B—X bond.

Applied to calcium orthosilicate, the above rule seemed to O'Daniel and Tscheischwili, Brandenberger, or Büssem, and others, to mean that the—presumedly—increased "contrapolarization" or expansion of the SiO_4 ion at high temperatures would lead to a relatively more active rôle of the calcium ion in the crystal lattice, and to a decrease from a coördination CaO_6 to CaO_4, somewhat similar to the change brought about by substituting for calcium the much smaller and stronger contrapolarizing beryllium (BeO_4 in phenacite, Be_2SiO_4).

V. M. Goldschmidt had been careful to limit the rule to those cases in which the transformation would actually be effected by no other of several possible causes but an increase in contrapolarization of the BX_n radical ion by the cation A at increasing temperature. It can be shown, however, that such cases must be quite rare, if not entirely lacking, and that in the examples given by Goldschmidt an increase in contrapolarization with increasing temperature does not occur, and therefore cannot be the cause of the polymorphous transition.

On the contrary, it is both plausible and borne out by actual observation, that with increasing temperature the weakest binding (A—X, e.g., Ca—O) in A_mBX_n compounds (e.g., Ca_2SiO_4) will be further weakened to a considerable degree long before the stronger bonds (B—X, e.g., Si—O) are materially affected by the thermal energy. This, however, means that the contrapolarization of the BX_n radical ion (e.g., of SiO_4^{4-}) by the cation A (e.g., Ca^{2+}) must be expected to decrease with increasing temperature rather than to increase. The average distance between calcium and oxygen must be increased gradually and in steps (polymorphous transitions) until at the melting point "dissociation" into cal-

cium cations and SiO_4 anions takes place, with the Si—O bonds still largely intact. It is a fallacy to ascribe the increase in the amplitude of thermal oscillations almost entirely to the oxygen ions (O'Daniel and Tscheischwili) and to postulate a virtual decrease in the effective radius ratio $R_{Ca}:R_O$ with increasing temperature.

At a larger average distance from the center of the calcium ion, a larger number of oxygen ions may be thought to be located. Thus an increase in the coördination around A ions may be generally expected in compounds A_mBX_n with increasing temperature. Under these circumstances, let us examine in greater detail the evidence upon which the older rule was based.

Of three examples of the effect, upon the crystal structure, of a loosening of the B—X bond by increasing temperature, the group of the alkali metal sulfates (K_2SO_4, Rb_2SO_4, and Cs_2SO_4) was assumed to take on phenacite structure with AX_4 beside BX_4 coördination above their transition points at 588°, 650°, and 660°C., respectively. However, the phenacite structure with an extremely improbable KO_4 coördination—RbO_4 and CsO_4 would be even less plausible—does not occur in potassium sulfate, but what is formed is the glaserite structure (4) with a rather high coördination around potassium, such as KO_{10}. In addition, it is even quite probable that rotation of the anion SO_4 as a whole sets in above the transition points (6). This represents an even greater degree of differentiation in the relation of the oxygen atoms to the A cations as compared with their close and intense connection with the central, S, atom.

In a second example, the spinel structure is said to be formed at higher temperatures in a group of lithium compounds (Li_2SO_4, Li_2BeF_4, Li_2MoO_4, and Li_2WO_4) from a low-temperature phenacite-type lattice. This transformation does not include the dissolution, or even a pronounced expansion, of the BX_4 radical ions SO_4, BeF_4, MoO_4, and WO_4, but it does represent the transition from the lower (LiO_4) coördination to the higher one (LiO_6). A relative loosening rather than a relative strengthening of the A—X (Li—O or Li—F) binding was, then, observed here at increased temperature, quite in agreement with the newly proposed theory.

The third example, the morphotropic and polymorphous relationships in the alkali metal nitrates and alkaline earth metal carbonates, of the general type ABX_3, may seem without consideration of the new principle to bear out the old rule: "Stronger contrapolarizing" A cations such as Li^+ in $LiNO_3$ and Zn^{2+} in $ZnCO_3$ seem to produce the high-temperature structures of calcite and potassium nitrate even at room temperature, while larger and less "contrapolarizing" ions, such as Sr^{2+} and Ba^{2+} in the carbonates, and Rb^+ in the nitrates, seem to prevent entirely the formation of the "contrapolarized" calcite structure even at higher temperatures.

However, in using the old concept of an increased contrapolarization with increased temperature, that is, of a loosening of the B—X bond in the radical ion BX_3, as an explanation, it is difficult to understand why a crystal structure of *lower* symmetry, such as the low-temperature aragonite form should be produced by a *decrease* in contrapolarization, that is with undeformed, highly sym-

metrical anions BX$_3$. One may further ask why the simultaneous replacement of Sr^{2+} and C^{4+} in SrCO$_3$ by the less strongly "contrapolarizing" Na$^+$ and the stronger center ion N^{5+} as in NaNO$_3$ should lead from the aragonite structure of SrCO$_3$, with allegedly less "contrapolarized" BX$_3$ anion, to the calcite structure of NaNO$_3$ with allegedly more strongly contrapolarized BX$_3$ anion. Actually, replacement of Sr^{2+} by Na$^+$ introduces a weaker binding A—X, and replacement of C^{4+} by N^{5+} a stronger bond, B—X.

A more plausible explanation for the structural relationships in these nitrates and carbonates seems to be the following: No use is made of the assumption of "contrapolarization" of the anion BX$_3$. The changes—through substitution or temperature variation—in the strength of the A—X binding, although necessarily accompanied by some minor influence upon the B—X bond, are thought to be the principal cause for the calcite–aragonite transformation. The relationship between A and X in these crystal lattices is believed to depend mainly on the size and polarizability of the A cation, that is, its deformation, in the negative field of the anion.

The assumption of this deformation of the cation by the anion forms an integral part of the Fajans theory of chemical binding (11–13). In the course of personal discussions with the writer, Professor Fajans suggested it as the specific cause for the rise of the transition temperatures in the alkali metal sulfates, dealt with further below. It is thought by the writer to produce the lower symmetry of the aragonite structure of those of the ABX$_3$ compounds, such as KNO$_3$, CaCO$_3$, SrCO$_3$, BaCO$_3$, and PbCO$_3$, that contain the larger and therefore more easily polarized cations. In the first two of these substances, the influence of the deformation of the cation is overcome at elevated temperatures, under transformation into the higher symmetric form of calcite, while at least up to the present no such inversion has been reported for the other compounds, containing the still more readily polarizable cations strontium, barium, and lead. However, it seems not unlikely that at elevated temperatures, possibly under higher carbon dioxide pressure, the calcite structure might be formed even in the latter three compounds. It is interesting to note that aragonite, CaCO$_3$, has been reported to be an entirely metastable form, as indicated by its higher solubility compared with that of calcite. Apparently the deformation of the still relatively rigid Ca^{2+} cation by the anion is slight at room temperature, but might at subnormal temperatures be sufficient to make aragonite an actually stable form.

The polarizability of the cation in the field of the anion must also be responsible for the increase in the temperature of the transition from orthorhombic to hexagonal structures in the alkali metal sulfates A$_2$BX$_4$, mentioned above (Na$_2$SO$_4$, 238°C.; K$_2$SO$_4$, 590°C.; Rb$_2$SO$_4$, 650°C.; Cs$_2$SO$_4$, 660°C.). Beyond sodium sulfate, in which the mutual deformation of the A and X ions is at a minimum, lithium sulfate has again at a higher temperature (575°C.) a transition of a somewhat different nature, that is, from hexagonal (17) or monoclinic (1) (LiO$_4$) to cubic (LiO$_6$) (17). This special behavior of the lithium sulfate is due to the polarizing, or deforming, effect, in the low-temperature form, of the small

lithium cation upon the anion,—that is, to "contrapolarization," if one wishes. Either influence, the polarization of the cation by the anion or of the anion by the cation, extends the temperature range of the lower-symmetric forms to higher temperatures, by adding a certain amount to the strength of the A—X binding.

The influence of the deformation of the cation A in the field of the anion may be illustrated by a comparison of the transitions in alkali metal sulfates and perchlorates. In the perchlorates, a transformation occurs from a low-temperature, orthorhombic crystal lattice with the coördination AO_{12} (except for $NaClO_4$, where it is NaO_8 (36)) into a cubic structure (34) probably containing rotating ClO_4 anions (15)), that is, with an obviously weak A—X coördination. Significantly, the temperature of this transition *drops* from 309°C. in $NaClO_4$, over 300°C. in $KClO_4$, and 279°C. in $RbClO_4$ to 219°C. in $CsClO_4$.

This is the behavior one must expect in crystals of an A_mBX_n compound in which the A—X binding is a comparatively very weak one, such as in these orthorhombic low-temperature structures with AO_{12} (or AO_8 in $NaClO_4$) coördinations. If we consider these perchlorates, for instance, at an intermediate temperature of 285°C., we find $NaClO_4$ to be orthorhombic with NaO_8 coördination, and $KClO_4$ also orthorhombic with KO_{12} coördination. An increase in temperature in either compound produces the same effect as a substitution of the cation A by one of larger size, such as rubidium in $RbClO_4$ or cesium in $CsClO_4$. In both cases, that is, substitution or temperature increase, the cubic structure is formed in which the coördination around A, that is, the binding A—X, is further weakened to such a degree that rotation of the ClO_4 anions could be shown to occur at least in the cases of $NaClO_4$ and $KClO_4$.

In the sulfates of the alkali metals we find the reverse behavior: The temperature of a transition from orthorhombic to hexagonal—the latter probably also characterized by rotating SO_4 ions (6)—*rises* from 240°C. in Na_2SO_4 to 590°C. in K_2SO_4, 650°C. in Rb_2SO_4, and 660°C. in Cs_2SO_4.

A logical explanation seems to be the following: The polarization of the increasingly larger cations in the negative field of the BX_4 anions, which produces orthorhombic symmetry, must be of a considerably higher order in the case of the SO_4 ions with double charges than in the case of the ClO_4 ions with single negative charges. The behavior of the perchlorates is one to be expected when a minimum of polarization exists in the A—X binding (the oxygen ions, of course, being strongly deformed in the field of the central Cl^{7+} ion). In the sulfates, on the other hand, the influence of the polarization of the A cations in the field of the SO_4 ions stabilizes the lower-symmetric, low-temperature structures up to comparatively high temperatures. To explain the antithetic behavior of the alkali metal sulfates and perchlorates by "contrapolarization," that is, by a loosening of the strong B—X bonds of the BX_4 ions, seems both impossible and unnecessary.

The examination of the experimental evidence for the influence of increased "contrapolarization" at increased temperature on the type of phenomena discussed to which the transitions in calcium orthosilicate also belong, shows, then,

that no such evidence exists, and that the loosening of the A—X binding must be considered responsible for the changes in crystal structure at elevated temperatures to a far greater degree than the minor changes in the strength of the B—X bond under the influence of temperature. Some degree of "contrapolarization" must naturally be present at any temperature, but preferentially at low ones, where under the influence of the closely approaching A cation the B—X bond is loosened to an extent depending on the nature of the ions involved. No reason exists to consider the newly advanced evidence for the occurrence of high coördinations such as CaO_9 and CaO_{10} in the high-temperature (α') form of calcium orthosilicate as being in disagreement with any evidence pointing to preferential formation of low coördinations around A cations in A_mBX_n compounds at elevated temperatures.

In considering, besides calcium orthosilicate, the orthosilicates of other divalent metals, especially of the alkaline earth metals, it may be noted that thus far none seems to have been observed to occur in more than one crystal modification. This is in sharp contrast to the occurrence of four polymorphous forms in the calcium compound, and is of significance in more than one regard.

Firstly, if increased "contrapolarization" were an important factor in producing polymorphous forms at elevated temperature, and if CaO_4 coördinations really occurred in any of the high-temperature forms of Ca_2SiO_4, it would be very hard to understand why a corresponding MgO_4 coördination should not be found in Mg_2SiO_4, with the smaller and therefore much stronger "contrapolarizing" magnesium ion (radius: 0.78 cm.$^{-8}$) even at a lower temperature than in Ca_2SiO_4 (radius of calcium ion: 1.06 cm.$^{-8}$). In fact, magnesium orthosilicate has been found to occur only in the form of forsterite, of olivine structure, with MgO_6 coördination. This stability of the MgO_6 coördination even at high temperatures makes Mg_2SiO_4 a valuable refractory material because of the absence of discontinuous volume changes in heating or cooling. The absence of polymorphism in Mg_2SiO_4 can be easily understood, if the apparent insensitivity of the olivine-type structure against an increase in the radius ratio $R_A:R_O$, as evidenced recently by the finding of the olivine structure in γ-Ca_2SiO_4 (28) with the considerably larger calcium cation, is recalled.

Secondly, the absence of polymorphous transformations in the orthosilicates of elements of Group II of the Periodic System other than calcium, that is, beryllium orthosilicate (phenacite, BeO_4 coördination), magnesium orthosilicate (forsterite, MgO_6), strontium and barium orthosilicates (β-potassium sulfate structure, AO_{9-10} coördination), to which may be added the orthosilicates of zinc,[1] cadmium, iron (Fe^{2+}), and manganese (Mn^{2+}), is believed to indicate a general trend also to be found in other groups of compounds such as sulfates, nitrates, carbonates, and others (23). Polymorphous forms seem to be most

---

[1] Zn_2SiO_4 may actually occur not only in the phenacite structure as willemite (ZnO_4), but, in addition, in a high-temperature form in which the zinc is partly in higher coördination (probably ZnO_6), according to experimental facts reviewed by Linwood and Weyl (26). Here again one finds a preferential loosening of the A—X binding at higher temperature.

numerous in those of the compounds A_mBX_n in which the cation A is of a medium size, and where therefore mutual polarization (deformation), of the anion by the A cation and of the A cation by the anion, is at a minimum (figure 2).

The following is an attempt to understand this behavior. Besides the number of atoms in the molecular formula, two other major factors determine, according to V. M. Goldschmidt (17), the structural type of a crystal: the relative size and the deformation (polarization) of the electron shells of the ions.[2]
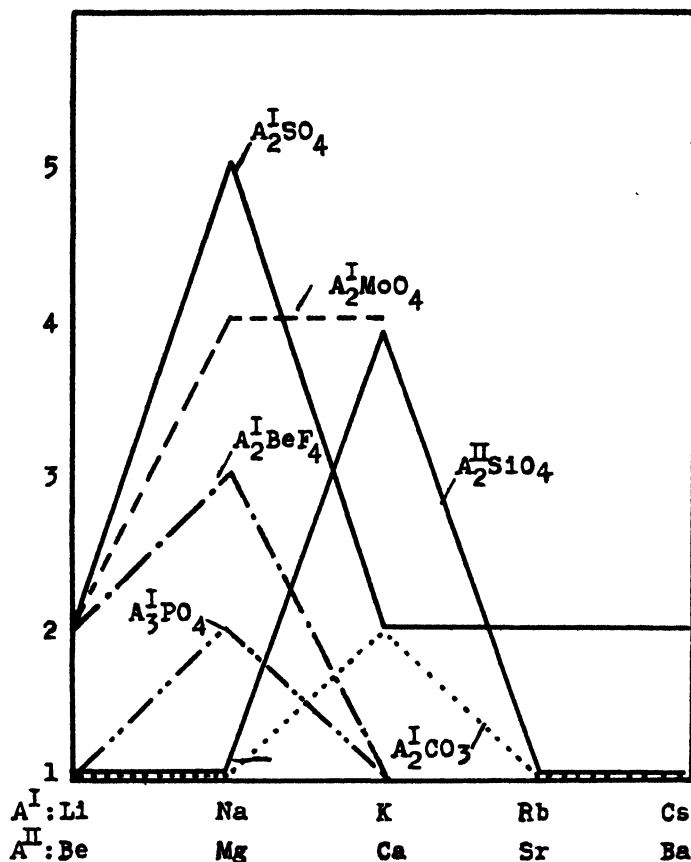
FIG. 2. Frequency of polymorphism in A_mBX_n compounds

In contrast to treatments by others of the theory of polymorphism, the most important effect of increasing temperature in a compound A_mBX_n must be considered the loosening of the A—X binding, which may be more or less equivalent to an increase in the radius ratio $R_{cation}:R_{anion}$ ($R_A:R_{BX_4}$). To a change

[2] Goldschmidt's discussion of a deformation of a cation by an anion was limited to complex cations such as NH_4^+. In compounds containing K^+, Rb^+, Cs^+, and others, the loosening of the electron shell of the cation in the negative field of the anion was first demonstrated by K. Fajans through its effect upon the optical properties.

of this sort crystal structures of A_mBX_n compounds seem particularly sensitive, because of the variety of geometric possibilities of binding BX_n radical ions by A cations, with comparatively small variations in energy. However, where a sufficient degree of polarization of either of the two types mentioned exists in the A—X binding, there will be an additional amount of energy involved beyond the mere electrostatic attraction of rigid spheres, and an increased resistance to a change with rising temperatures will be encountered. This will cause the extension of the ranges of stability of polymorphous forms to higher temperatures where, owing to the greater variation in the amplitudes of thermal motion, the variety of possible structures compatible with such distortions is somewhat limited, and therefore less than at lower temperatures. The total effect of ionic polarization in the A—X binding of either type is therefore a domination by low-temperature structures, due to this upward extension of their stability ranges and suppression of intermediate crystal structures. The maximum in the number of polymorphous forms seems to be most pronounced in those of the A_mBX_n compounds in which m is 2 or higher. The reason is probably the greater negative field around each A cation, which causes a greater amount of polarization of the A cations of higher atomic numbers.

In these statistics, the increased difficulty of finding polymorphous transitions at high temperatures may also have to be considered, as well as the possible influence of ion polarization upon the rate of transition at low temperatures.

In calcium orthosilicate we find the same increase in the coördination around calcium with increasing temperature that we find by increasing the size of the A cation: Strontium and barium orthosilicates (29) have the same structure as α'-Ca_2SiO_4 (7), with the coördinations AO_9 and AO_{10}, possibly even at as low a temperature as room temperature, owing to the increase in ionic size from calcium to strontium and barium. This increase in the size of the cations produces the regular increase in the coördination of the cation in the orthosilicates A_2SiO_4 from 4 in Be_2SiO_4, over 6 in Mg_2SiO_4 and γ-Ca_2SiO_4, to 9 and 10 in Sr_2SiO_4 and Ba_2SiO_4. The coördination number 8, then, has thus far not been observed in the orthosilicates. It seems most likely that it will be found in the middle-temperature (β) modification of calcium orthosilicate. In that case, we would have a regular gradual increase with increasing temperature from CaO_6 in γ, over CaO_8 in β, to CaO_9 and CaO_{10} in α', and to still higher coördination, or rotation of the SiO_4 anions, in α.

The large volume change in the $\beta \rightleftharpoons \gamma$ transition at 675°C. is indicative of a change in the coördination of calcium. The low density of the γ-form must be due to a considerable expansion of the so-called closest, pseudohexagonal packing of oxygen ions assumed in the olivine, Mg_2SiO_4 structure. This expansion must occur when instead of the small magnesium ions the comparatively large calcium ions (or the sodium ions, as in Na_2BeF_4, where a similar volume change occurs at 187°C.) find their places in the octahedral interstices of this oxygen packing. Such an expanded "closest packing" arrangement must be made possible by a slight expansion of the SiO_4 (BeF_4) radical ion. We, then, assume here "contrapolarization" to occur in A_mBX_n compounds such as calcium ortho-

silicate, but at the lower rather than at the upper end of the temperature scale of polymorphous forms, in contrast to the previous structural theory of the polymorphism of such compounds. It is at low heat contents where we must assume the weaker cation A to approach the BX_4 radical close enough to exert increased attraction upon the electron shell of the X ion, and to begin repulsing the B ion. Contrary to the assumption of Brandenberger (3), the difference in the relation of calcium and silicon to oxygen must, then, be somewhat smaller at low temperatures than at high temperatures where the independence of SiO_4, as thermal units, and of calcium cations becomes more and more pronounced.

Above the transition point at 675°C. in Ca_2SiO_4 (and at 187°C. in Na_2BeF_4), owing to the weakening of the A—X (Ca—O or Na—F) binding and to the increasing A—X distance, the deformation ("contrapolarization," if one wishes) of the SiO_4 (BeF_4) radical ion becomes too small to suit an olivine-type structure, that is, that highly expanded, pseudohexagonal "close" packing of oxygen ions. The structure changes into one in which the calcium (sodium) ions have a higher coördination appropriate to the weakening of the A—X binding. (In Na_2BeF_4 the glaserite structure is formed, possibly with rotating BeF_4 ions.) In Ca_2SiO_4 we obtain the β-modification in which we expect a coördination around calcium of hardly less than 8. Even before the structure of the β-form is actually known, it is not difficult to imagine that in it a much closer packing should be attained than in the so-called "closest"—in fact, however, unusually expanded—packing of the olivine-type γ-form.

We consider the frequency of the coördination 8 around calcium in complex minerals, mentioned by O'Daniel and Tscheischwili (28), as a further indication for the existence of this same coördination in β-Ca_2SiO_4. We believe that the crystal lattices of these complex minerals, even if they had to be considered as being in the equilibrium state at room temperature, could very well represent structures stable also at higher temperatures. It seems, namely, that in complex substances such atomic arrangements frequently become stabilized at low temperatures, which in the single components are stable only at elevated temperatures. One example is the stabilization of the high-temperature structure of Na_2SO_4 by the addition of considerable amounts of K_2SO_4 or Na_2CO_3; another is the stabilization of the high-temperature (α) form of $CaKPO_4$ by K_2CO_3, and so forth (4). This principle may also furnish the explanation for the occurrence of $CaNaPO_4$ in the structure of β-potassium sulfate, doubted by O'Daniel and Tscheischwili (29) but demonstrated by the writer (4). Here calcium and sodium are actually found in AO_{9-10} coördinations instead of their "normal" AO_6 coördination. A general reason for the stabilization, at low temperatures, of high-temperature structures in complex substances (compounds or solid solutions) may be the usually greater tolerance of such high-temperature structures to substitution.

IV. THE HYDRATION OF CALCIUM ORTHOSILICATE

Following the demonstration that the β-modification of calcium orthosilicate is most unlikely to contain coördinated CaO_4 groups, another explanation for

the high reactivity of this phase is needed, which takes the reverse stand, that is, the assumption of an increased coördination, of at least CaO_8, rather than a decreased one. The most general explanation possible would refrain from any attempt to attribute this greater reactivity to any specific mechanism, and would just point to the higher thermodynamic potential involved in any reaction of a phase metastable at the reaction temperature, such as β-Ca_2SiO_4. However, if one wants to be a little more specific, one might recall that the calcium ion, at room temperature, has the very definite tendency to establish a shell of six oxygen ions around itself, as in $Ca(OH)_2$. In γ-Ca_2SiO_4, in which it has already relinquished all coördinated oxygen ions surrounding it above 675°C., in excess of six, no or very little tendency is left to the Ca^{2+} ion to exchange partners in order to achieve this low and close coördination of six oxygens, normal for it at room temperature. With the instable coördination CaO_8 such a tendency to revert to CaO_6 must certainly be considerable, and the difference in the change of free energy may very well be sufficient to account for the activation energy of the hydration reaction. A calcium ion in metastable β-Ca_2SiO_4 may be pictured as caught in a loose, unstable "basket," CaO_8, the individual wall units of which (SiO_4 ions) are held together less strongly by the calcium ion in its center. Both the tendency to establish a coördination smaller and closer than in CaO_8 and an increased rate of an exchange for the original more loosely bound eight neighbors may help to explain the higher rate of hydration of the β-modification.

There are, however, still other possibilities: A CaO_4 coördination, such as proposed by O'Daniel and Tscheischwili and by Brandenberger for β-calcium orthosilicate, has to the writer's knowledge never been found experimentally except in one case, Na_2CaSiO_4, whose structure was believed to be that of cubic high-temperature cristobalite (α). Machatschki (27) pointed out that Ca^{2+} could not possibly be considered as an isomorphous substituent for Si^{4+}. The extremely small Ca—O distances given as 1.90 and 2.07 Å., as against those expected of at least 2.30 Å. (1.32 + 0.98, as an approximation), as well as an error in the stated coördinates of the metal ion positions in the lattice ($1/2 - u, u + 1/2, \bar{u}$, should have read $1/2 - u, \bar{u}, u + 1/2$), indicate that a revision of this structure determination is desirable. The writer expected, and found, cubic Na_2CaSiO_4 ($a_w = 7.48$) to be completely isomorphous with the cubic high-temperature form of Na_3PO_4 ($a_w = 7.45$,[3] if containing 10 per cent Na_2CO_3). The Na^+ ion can no doubt even less than the Ca^{2+} ion be considered as a possible substituent for Si^{4+}. A comparison with cristobalite therefore does not seem appropriate at all, particularly if finally a coördination NaO_4 as well as CaO_4 should be confirmed in these compounds, similar to the AgO_4 coördination in cubic Ag_3PO_4. Not the high temperature of formation, but the comparatively large number— three— of A cations in a compound of the formula A_3BX_4 makes the AX_4 coördination appear possible in any of the three substances mentioned.

For a similar reason, the coördination CaO_4 is theoretically not impossible in

---

[3] According to a personal communication which the writer owes to the courtesy of H. W. Rinn, Spectroscopy Department, The Dow Chemical Company, Midland, Michigan.

the A_3BX_6 compound Ca_3SiO_6 (2, 10), considered one of the most important and active constituents of Portland cement. The composition of a stabilized β-Ca_2SiO_4 might differ somewhat from the ideal composition Ca_2SiO_4, owing to a slight excess of CaO. "Active" calcium such as a very few CaO_4 coördinations, interspersed in solid solution with the vast majority of CaO_8 coördinations, might be another factor to be considered as a cause for both the (meta-)stabilization, below 675°C., and the high reactivity of the β-form. Addition of foreign substances such as Cr_2O_3 or B_2O_3 or P_2O_5, which stabilize the β-form (37), perhaps through slightly changing the Si:O ratio of the β phase in the direction of lower values, may, with simultaneous formation of a vitreous phase, produce an excess of calcium over 2Ca:1Si and thereby a few CaO_4 coördinations.

In still another—more macroscopical—view of the different reactivity of the β and γ phases of calcium orthosilicate, their different densities might be used together with the possible formation, in the hydration reaction of the γ phase, of a surface film inhibiting the further progress of the reaction: The difference in the specific volumes of the first reaction product of hydration and of the abnormally dense β phase may be too large to permit formation of a coherent surface film, while this difference in the case of the voluminous γ phase may be small enough to permit its formation.

In a discussion of the properties, such as crystal structure, of high-temperature phases such as the β-form of Ca_2SiO_4, which they show after quenching to room temperature, a further word of caution may be added. It is well to remember that at room temperature we may perhaps not be dealing actually with the structure present at the elevated temperature, above the transition point. The only safe procedure is to obtain data, such as x-ray patterns, directly above such transition point. An alleged β-form of Ca_2SiO_4 obtained by quenching from above 675°C. may actually have undergone an inversion different from that into the γ-form, but at a temperature so close to 675°C. that no difference in transition temperature could be noted. Such conditions have for instance been observed in calcium carbide at 450°C. (5). The writer would hesitate to exclude a similar state of affairs in Ca_2SiO_4, if, for instance, a symmetry lower than orthorhombic (monoclinic, triclinic) were suggested for the phase presently called β-Ca_2SiO_4. A phase having such low symmetry is not likely to be inserted between the orthorhombic γ and α' phases. Another, real, orthorhombic β phase might be found to exist above 675°C. In this case, the phase presently called β-Ca_2SiO_4 might, then, actually be a transition product, completely metastable at any temperature, of the true β phase. It may owe its particular reactivity to the presence of asymmetric, half-open "baskets"[4] of oxygen ions in which the calcium ion might be trapped in an eccentric reactive position, after it had actually been surrounded more symmetrically, by at least eight neighbors, in a true β structure, above 675°C., entirely unstable below that temperature and therefore never observed thus far.

There is so much room for speculation about the differences in reactivity of β- and γ-Ca_2SiO_4, because in spite of a considerable amount of work done a

---

[4] W. Büssem proposed such a coördination for calcium in highly reactive $12CaO \cdot 7Al_2O_3$.

number of crucial questions have remained unattacked. The need for further experimental work is obvious, if this difference in behavior is to be fully understood.

V. SUMMARY

1. The polymorphism of A_mBX_n compounds is shown to be determined primarily by the changes in the strength of the A—X binding as a function of temperature.

2. The preferential loosening of the A—X binding leads to higher coördinations of X around A at increasing temperatures. This conclusion is reached in contradiction to current theory.

3. Through application of the Fajans polarization theory of ionic binding it is shown that enantiotropic transition temperatures are raised through substitution of the A cation, wherever the relative strength of the A—X binding is increased by such substitution. Such increase in the strength of the binding is obtained when either the polarization of the X anion by the A cation, or that of the A cation by the anion, is increased by such substitution.

4. An increase in enantiotropic transition temperatures with increased size of the A cation is due to the strengthening of the A—X binding through increasing polarization of the A cation in the negative field of the anion (example: alkali metal sulfates, except lithium sulfate).

5. A drop in enantiotropic transition temperatures with increased size of the A cation is encountered where the weakening of the positive field around A, which is due to this increase in size, overbalances the strengthening of such binding by the increased polarization of the A cation in the negative field of the anion (example: alkali metal perchlorates).

6. The maximum in the number of polymorphous forms occurring in homologous groups of A_mBX_n compounds is attributed to the effect of polarization in the A—X binding. The drop at A cations having higher atomic numbers seems particularly pronounced in A_mBX_n compounds in which m is larger than 1, for instance 2, owing to the greater strength of the negative field around the A cations.

7. Merwinite, thus far considered a compound ($3CaO \cdot MgO \cdot 2SiO_2$), is more likely a solid solution of Mg_2SiO_4 in the second-highest-temperature (α') form of calcium orthosilicate, having a potassium sulfate-type structure and CaO_9 and CaO_{10} coördinations.

8. The formation, above 675°C., of the higher reactive β-form of calcium orthosilicate cannot be explained by a transition from the CaO_6 coördination of the low-temperature (γ) form to a CaO_4 coördination. Rather, CaO_8 coördination is expected in the β structure, similar to the CaO_8 coördination found in complex minerals.

9. Several possible explanations of the higher reactivity of the β-form of calcium orthosilicate are enumerated.

The author had a valued opportunity to consider applications of the theory of polymorphism, expounded in this paper, to the "crystal chemistry" of glass during his recent association, as a consultant, with Glass Science, Inc.

REFERENCES

(1) ALBRIGHT, J. G.: Z. Krist. **84**, 150–8 (1932).
(2) BRANDENBERGER, E.: Schweiz. Arch. angew. Wiss. Tech. **2**, 45–58 (1936).
(3) BRANDENBERGER, E.: Symposium on the Chemistry of Cements, Stockholm, 1938, p. 122.
(4) BREDIG, M. A.: J. Phys. Chem. **46**, 747–64 (1942).
(5) BREDIG, M. A.: J. Phys. Chem. **46**, 801–19 (1942).
(6) BREDIG, M. A.: J Phys. Chem. **47**, 587–90 (1943).
(7) BREDIG, M. A.: Am. Mineral. **28**, 594–601 (1943).
(8) BREDIG, M. A.: Trans. Iron and Steel Div. Am. Inst. Mining Met. Engrs. **158**, 95–6 (1944).
(9) BROWN, G. B., AND WEST, J.· Z. Krist. **66**, 154–61 (1927).
(10) BÜSSEM, W.: Symposium on the Chemistry of Cements, Stockholm, 1938, pp. 141–68.
(11) FAJANS, K., AND JOOS, G.: Z. Physik **23**, 1 (1924).
(12) FAJANS, K.: Z. physik. Chem. **B24**, 103 (1934).
(13) FAJANS, K.: J. Chem. Phys. **9**, 281–3, 378–9 (1941).
(14) FERGUSON, J. B., AND MERWIN, H. E.: Am. J. Sci. [4]**48**, 81–123, 165–89 (1919).
(15) FINBAK, C., AND HASSEL, O.: Z. physik. Chem. **B32**, 130–4 (1936).
(16) GOLDSCHMIDT, H. J., AND RAIT, J. R.: Nature **152**, 356 (1943).
(17) GOLDSCHMIDT, V. M.: *Geochemische Verteilungsgesetze*, Vol. VII, pp. 105–9. Oslo (1926).
(18) GOSSNER, B.: Neues Jahrb. Mineral. Geol., Beilage Bd. **A57**, 89–116 (1928).
(19) GREENE, K. T.: Natl. Bur. Standards (U. S.), R.P. 1570 (January, 1944).
(20) GREIG, J. W.· Am. J. Sci. [5]**13**, 1–44 (1927).
(21) HANSEN, W. C.: J. Am. Ceram. Soc. **11**, 68 (1928).
(22) INSLEY, H.: J. Research Natl. Bur. Standards **17**, 353 (1936) (R.P. 917).
(23) LANDOLT-BÖRNSTEIN: *Physikalisch-chemische Tabellen.*
(24) LARSEN, E. S., AND FOSHAG, W. F.: Am. Mineral. **6**, 143–8 (1921).
(25) LEE, H. C.: Canadian patent 358,403 (1936); Ceram. Abstracts **19**, 290 (1940).
(26) LINWOOD, S. H., AND WEYL, W. A.: J. Optical Soc. Am. **32**, 443–53 (1942).
(27) MACHATSCHKI, F.: Naturwissenschaften **26**, 74 (1938).
(28) O'DANIEL, H., AND TSCHEISCHWILI, L.: Z. Krist. **104**, 124–41 (1942).
(29) O'DANIEL, H., AND TSCHEISCHWILI, L., Z. Krist. **104**, 348–57 (1942).
(30) OSBORN, E. F.: J. Am. Ceram. Soc. **26**, 321–32 (1943).
(31) PARKER, T. W., AND NURSE, R. W.: J. Iron Steel Inst. (London) **148**, 475–88 (1943).
(32) PHEMISTER, J.: Mineralog. Mag. **26**, 225 (1942).
(33) *Strukturbericht* II, p. 87 (Z. Krist., 1936).
(34) *Strukturbericht* II, pp. 411–15 (Z. Krist., 1936).
(35) *Strukturbericht* II, p. 557 (Z. Krist., 1936).
(36) ZACHARIASEN, W. H.: Z. Krist. **73**, 141–6 (1930).
(37) ZERFOSS, S., AND DAVIS, H. M.: J. Am. Ceram. Soc. **26**, 302 (1943).

INFLUENCE OF METHOD OF DEËSTERIFICATION ON THE VISCOSITY AND ACID BEHAVIOR OF PECTINIC ACID SOLUTIONS

T. H. SCHULTZ, H. LOTZKAR, H. S. OWENS, AND W. D. MACLAY

Western Regional Research Laboratory,[1] Albany, California

Considerable interest has developed in pectinic acids (colloidal polygalacturonides, partly esterified with methyl alcohol) that have lower ester contents than those used commercially for high-solids gels. Although investigations concerning the preparation of such pectinic acids have been thorough and methods have been devloped using acid (4, 10, 15, 19, 20), alkali (17, 18), and enzymes (10, 22), little information is available on the effect of the catalyst on the properties of the products. Hills, White, and Baker (10) have reported that enzymatically deësterified pectins form weaker calcium gels and are more sensitive to precipitation by calcium than are pectinic acids deësterified by acid. Baker and Goodwin (5) and Hills, Mottern, Nutting, and Speiser (9) compared the gel-forming characteristics of several pectinic acids prepared in different ways. Speiser, Hills, and Eddy (25) have found that the acid behavior of pectinic acids prepared with acid is similar to that of pectinic acid prepared with tomato pectinesterase (pectase). These investigations comprise the only recent work in this field.

This paper is concerned with the effect of method of deësterification on the viscosity behavior of pectinic acid solutions at different pH values and with degree of dissociation of pectinic acids of varying methoxyl contents.

MATERIALS

The first pectin listed in table 1 was a commercial product, which was de-ashed in ion-exchange columns, as previously described (21). The second was a commercial product that had been deësterified by acid treatment (19). De-ashing was accomplished by precipitating a 1 per cent aqueous solution of the pectinic acid in acid–alcohol so that the resulting mixture was 0.2 M with respect to hydrochloric acid and contained about 53 per cent ethanol. The pectinic acid was filtered and repeatedly suspended in about 55 per cent ethanol until the washings were free from chloride. Subsequent samples were purified in the same way. Samples No. 3 to No. 7 were prepared from commercial citrus pectin and were deësterified by means of ammonium hydroxide at pH 10.8 and 15°C., following the method of McCready *et al.* (17). Sample No. 8 was extracted from sliced lemon peel. The pectin was extracted in 3 volumes of water containing 12 g. of hexametaphosphate per kilogram of peel for 20 min. at pH 3.5 and 90–95°C.

Samples No. 9 to No. 11 were deësterified by citrus pectinesterase acting *in situ* on lemon peel. The pH of a slurry of sliced peel dispersed in 3 volumes of water was adjusted to 8.5 or 9.0 and maintained there to achieve the desired degree of deësterification, following the procedure used previously (22). When the calculated quantity of alkali had been consumed, the slurry was adjusted to pH 3 and filtered. This treated peel was suspended in boiling water containing hexametaphosphate and extracted as described for sample No. 8.

Sample No. 12 was prepared according to the method of Baier and Wilson (2). The last (No. 13) was prepared from a commercial citrus pectin, similar to No. 1, by the use of a citrus pectinesterase product supplied by E. F. Jansen of this laboratory. The reaction was performed at pH 7 in the presence of 0.2 M sodium chloride.

TABLE 1

Analytical data on the pectinic acids used

SAMPLE NO.	SOURCE OF PEC-TINIC ACID	METHOD OF DEËSTERIFICATION	ASH	METHOXYL	ANHYDRO-GALACTU-RONIC ACID	EQUIVALENT WEIGHT
			per cent	*per cent*	*per cent*	
1	Citrus		0.2	10.7	85	720
2... ..	Apple	Acid	0.2	6.6	86	360
3..	Citrus	Alkali	1.3	7.8	86	430
4 ...	Citrus	Alkali	1.3	6.6	86	370
5 . .	Citrus	Alkali	0.4	5.6	86	320
6 ..	Citrus	Alkali	0.4	3.5	88	265
7.. .	Citrus	Alkali	1.2	0.0	90	195
8. ..	Citrus		0.6	10.7	83	760
9 .	Citrus	Esterase *in situ*	0.3	7.9	81	480
10	Citrus	Esterase *in situ*	0.4	5.8	81	360
11	Citrus	Esterase *in situ*	0.4	3.6	83	280
12.. . ..	Citrus	Esterase *in situ*	0.4	0.7	82	225
13... ...	Citrus	Esterase *in vitro*	0.2	5.2	87	300

PROCEDURE OF MEASUREMENTS

Methoxyl content was determined by means of Hinton's method (11). The methoxyl contents of Nos. 8, 10, and 12 (table 1) were also determined by means of Clark's modification (6) of the Zeisel method after the samples had been humidified to remove the adsorbed alcohol (14) and redried. Differences between the two methods averaged less than 0.2 per cent. Contents of uronic acid anhydride were calculated from the equivalent weights and methoxyl contents. Samples Nos. 1, 2, 7, and 12 were analyzed by a modified Lefevre–Tollens method (16) for uronic anhydride content, with results checking within 1 per cent of the calculated value. This agreement between results of the various methods eliminates the possibility that the non-galacturonide material is united with carboxyl groups of the galacturonide chain by frequent ester links. If the non-galacturonide material were attached by ester links, its molecular weight

would be fairly high. The analytical data are summarized in table 1. All values were corrected for ash content and adsorbed alcohol.

Viscosity measurements were made in Ostwald–Cannon–Fenske pipets at 25°C. ± 0.05° with an electric timer measuring to 0.1 sec. Precautions noted earlier (21) were taken and the data are reliable to ± 0.5 per cent of the relative viscosity. The pectinic acid solutions were adjusted to the desired pH values with sodium hydroxide or hydrochloric acid. It was observed earlier (21) that aggregation tended to be a direct function of both the concentration and the intrinsic viscosity of the pectinic acid. To make this factor nearly constant for the samples used, it appeared desirable to perform the viscosity measurements at concentrations that yielded viscosities relative to water of 3 to 6. In doing this the pectinic acids with the higher intrinsic viscosity values were run at the lower concentrations, while those with the lower values for the intrinsic viscosity were run at the higher concentrations.

The equivalent-weight determinations were made by titrating 0.5 per cent pectinic acid solutions with standard alkali, using a Beckman pH meter. Alkali was added slowly to prevent localized deësterification. The inflection point of the titration curve is at pH 7.5. The values were corrected for titratable alkali present in the ash of the pectinic acid and for ammonia in samples de-esterified by alkali.

The pH values for figure 4 were taken from the titration curves. The maximum deviation of these values was ± 0.03 unit.

<center>RESULTS</center>

Figure 1 shows the viscosity–pH curves for some of the pectinic acids. There is a maximum in the curves in the range of pH values centering near 6, as might be expected from previous work (3, 21), but only the low-methoxyl pectinic acids exhibit minima near pH 4, resembling pectic acid in this respect. The methoxyl content at which the minimum becomes evident depends upon the catalyst used, being above 8 per cent for the enzymatically prepared pectinic acids and about 6 per cent for those prepared with alkali. If conditions are changed so that aggregation tendencies are different, the values for the methoxyl contents in the transition range may be altered. Increasing the concentration of sample No. 4 (6.6 per cent methoxyl) from 0.3 to 0.5 per cent changed the type of curve to that obtained with pectic acid. Higher concentrations were not examined completely because the results were not closely reproducible. Decreasing the concentration of sample No. 5 (5.6 per cent methoxyl) from 0.5 to 0.2 per cent changed the curve from one with a minimum to one similar to those obtained with high-methoxyl pectinic acids as shown in figure 2. Increase in temperature to 50°C. also changed the type of the curve. Despite these changes with sample No. 5, it is apparent that the difference between the enzymatically prepared and the alkali-prepared samples is real. The former were measured in the more dilute solutions, yet they showed pectic acid characteristics when they had higher percentages of methoxyl groups.

Figure 3 indicates that pectinic acids with 6.6 per cent methoxyl content have similar viscosity characteristics whether prepared by acid or by alkaline methods. A comparison of results with those by Baker and Goodwin (4) shows
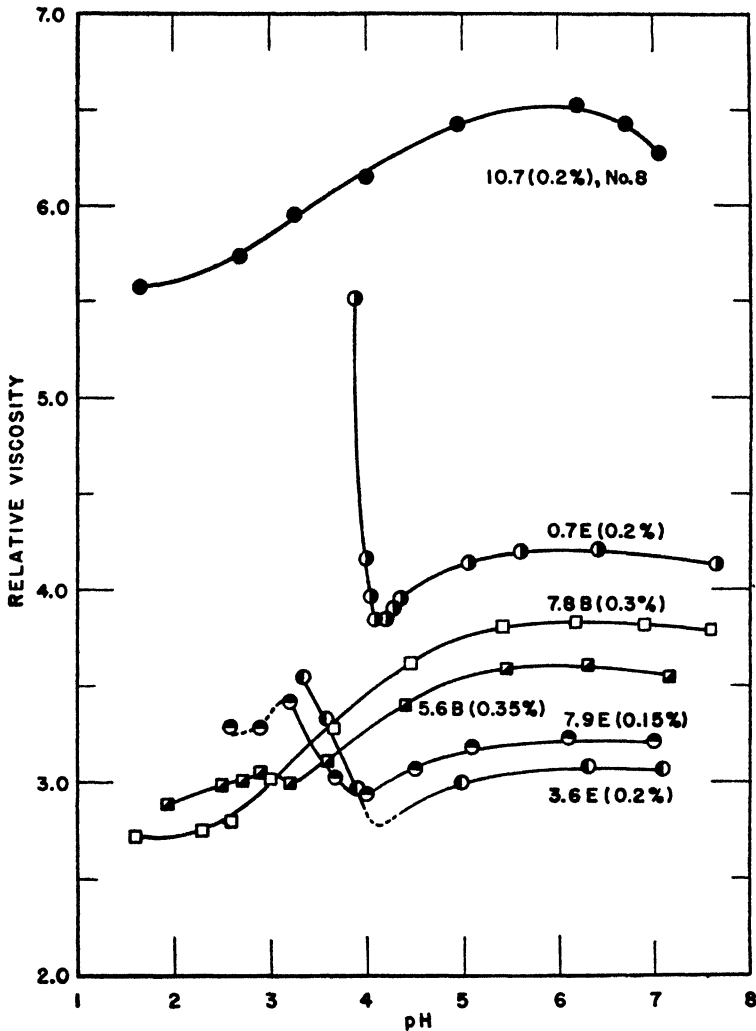
FIG. 1. Effect of pH on viscosities of pectinic acid solutions. The first number inserted refers to the methoxyl content in per cent, the letter to the type of catalyst used (E = enzyme, B = alkali, A = acid), and the second number to the concentration in weight per cent.

that the transition for pectinic acids deësterified by acid also occurs at a methoxyl content near 6 per cent. Similarity between the viscosity characteristics of pectinic acids deësterified by citrus pectinesterase *in vitro* and *in situ* is also shown.

The apparent ionization constant of pectinic acids decreases with pH (7, 23) and increases with concentration (7, 12, 21, 23, 25, 26) and methoxyl content (7, 25). That it is also influenced by the method of deësterification is illustrated
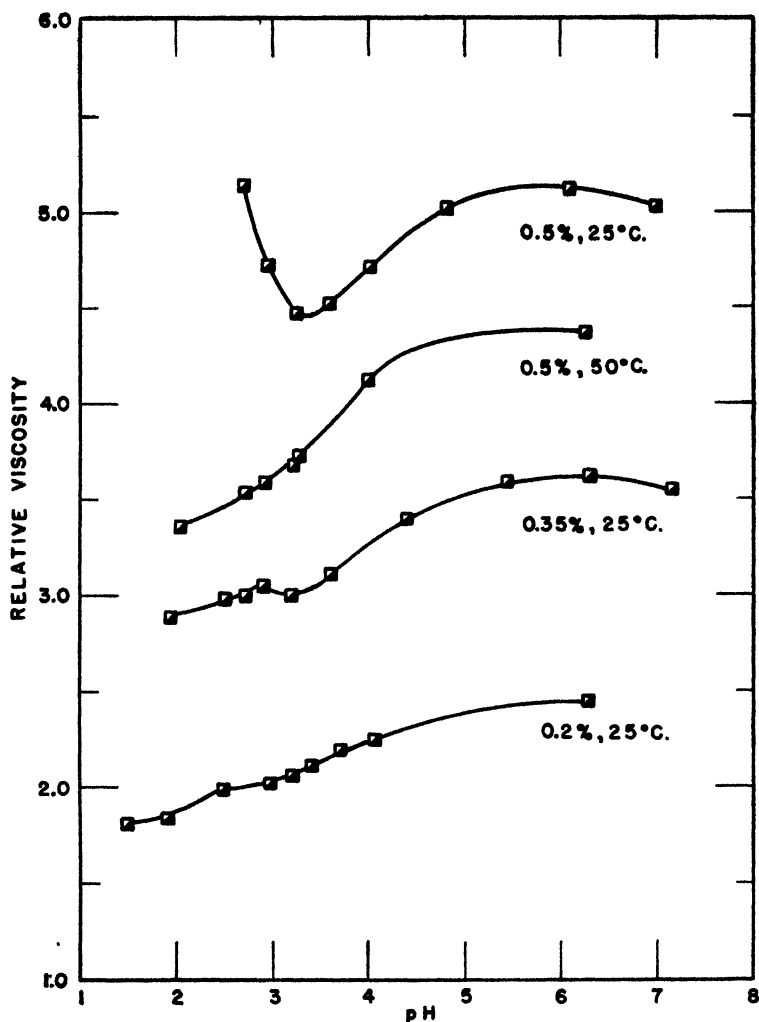
FIG. 2. Influence of temperature and concentration on the pH–viscosity curves of pectinic acid sample No. 5 (5.6 per cent methoxyl).

in figure 4, where the pH at half-neutralization is plotted against the methoxyl content of various pectinic acids.

The esterase appears to produce acids of similar dissociation characteristics whether it acts *in vitro* or *in situ*. It is significant that the enzymatically prepared pectinic acids are weaker acids and resemble pectic acid more closely than those prepared by alkali.
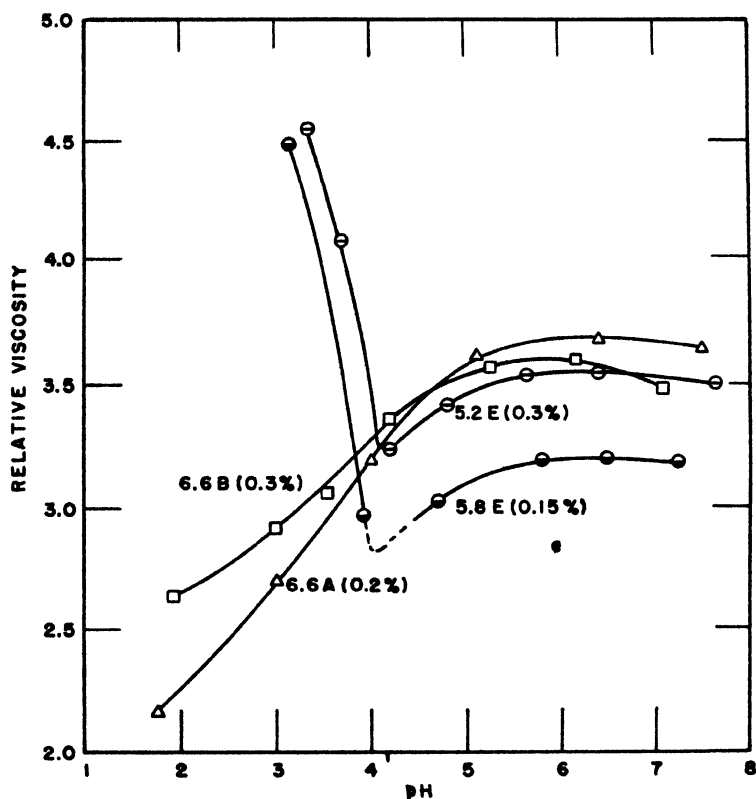
FIG. 3. Comparison of effect of method of deësterification on the pH–viscosity curves of some pectinic acids.
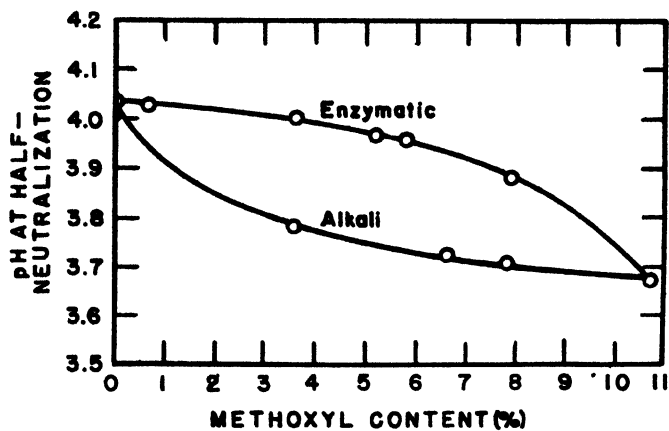
FIG. 4. pH at half-neutralization *vs.* methoxyl content

The viscosity–pH curves for pectin solutions follow the curve usually obtained with proteins and many similar colloidal electrolytes in the anionic form. An hypothesis to explain the increase in viscosity as the pectinic acid is neutralized was offered in a previous paper (21).

The change from the type of curve which is characteristic of high-methoxyl pectinic acids to that characteristic of low-methoxyl pectinic acids is not unexpected. Pectinic acids are carboxylic acids and probably undergo hydrogen bonding in the same way that similar weak acids do. Increasing the proportion of free carboxyl groups by removing methyl ester groups increases the probability of hydrogen bonding between chains and the formation of the type of aggregate which increases the viscosity at pH values below 4. These aggregates are readily dispersed by small increases in temperature and by dilution, thus indicating the weak type of forces which hold them together.

The decrease in viscosity of some solutions of low-methoxyl pectinic acids, which has been observed at pH values below 2 (4, 25), may result from the effect of the added anion. Perhaps the added anion interferes with bonding between pectinic acid molecules, thus reducing aggregation and viscosity.

The observation that at the same methoxyl content enzymatically deësterified pectinic acids act more like pectic acid is interesting. Possibly the enzyme proceeds along the galacturonide chain, splitting off successive methoxyl groups, producing characteristics of pectic acid.[2] Such a progressive reaction would increase the heterogeneity of the pectinic acid sample by removing all of the ester groups from some portions of the chains while leaving others practically untouched. Electrophoretic data obtained at this laboratory show that the distribution of pectinic acids having different methoxyl contents is greater with the enzymatically prepared samples than with those prepared with alkali. Hills et al. (9) obtained similar information with their acid- and enzyme-prepared pectinic acids. Whenever the pectic acid-like parts of the galacturonide chains are adjacent, at low pH values, hydrogen bonding could cause aggregation of a type that would increase viscosity.

The other catalysts, acid or alkali, act in a more random manner, requiring that the proportion of free carboxyl groups be much greater before a significant number of galacturonide chains develop characteristics of pectic acid.

Many of the difficulties involved in the interpretation of the acid-dissociation behavior of pectinic acids are apparent (7, 8, 25). Ionization of pectinic acid involves the formation of a new electrostatic field and a proton shift. In addition, carboxyl groups on the same chain may be as close as 4 to 5 Å., making interaction between them possible. An insight into the acid behavior may be gained by following the suggestion of Deuel (7) that the electrokinetic potential plays an important rôle. It may be assumed that pectinic acids act like proteins on the alkaline side of their isoelectric points. Thus it would be expected that an

---

[2] Jansen and McDonnell (13) obtained evidence from work with various pectinic acids and enzymes that the esterase removes ester groups in a progressive manner.

increase in the number of free carboxyl groups by deësterification would increase the electrokinetic potential (1). Preliminary measurements of electrophoretic mobility have shown that this assumption is valid. Such an increase would cause the hydrogen ion to be attracted to the molecule more strongly, and a decrease in the ionization of the solute would be obtained. As shown in figure 4 and mentioned in the results, the data on the dissociation of pectinic acids agree with this hypothesis.

The lower degree of dissociation of pectinic acid deësterified with citrus pectinesterase can be explained on that basis. Those portions of the galacturonide chains freed of ester groups offer a high concentration of carboxyl groups which would attract hydrogen ions more strongly than if the carboxyl groups were randomly situated; thus these acids are weaker than the corresponding ones deësterified with alkali.

Speiser and coworkers (25) did not observe this difference when they used tomato enzymes or acid as catalysts. High-methoxyl pectinic acids from apples, which they used, are stronger pectinic acids than those from citrus fruits (23), thus indicating, according to the hypothesis presented, that the free carboxyl groups are more randomly distributed in the acids from apples. The randomness may influence the action of the enzymes (13) so that no effect of the method of deësterification is apparent. Another possibility depends upon the fact that tomato extracts contain a polygalacturonase as well as an esterase. Jansen and MacDonnell (13) have found that polygalacturonase acts on ester-free portions of the galacturonide chains. Therefore when a mixture of enzymes is used, the portion of the chain that is freed of ester groups by the action of the esterase would be susceptible to action of the glycosidase. Splitting the chain at the part stripped of ester groups would result in fragments less characteristic of pectic acid, because the high concentration of carboxyl groups in a single part of the molecule would be reduced. This explanation cannot account entirely for the difference between the observations of Speiser et al. and those presented here, because the number average molecular weight did not decrease markedly in their experiments (24).

The low elastic limit of calcium gels prepared from esterase-demethoxylated pectinic acids (10, 23) may be explained, in part, by the tendency of the enzyme to liberate a series of adjoining carboxyl groups. There is a wide distribution of methoxyl contents among the pectinic acid molecules, as shown by electrophoretic mobilities and by fractionation experiments under way in this laboratory. Where pectic acid portions are adjacent, the calcium ion forms cross links, but when they are not adjoining such cross-linking does not occur. As a result the gel structure is not uniform and it shears even when weak forces are applied. When the other catalysts are used, the calcium ion is distributed randomly throughout the gel and the supplementary action of the electrovalent and hydrogen-bond forces yields a coherent structure (9). Possibly the enzymatically prepared product can be improved by the use of a greater concentration of enzyme in an attempt to obtain a narrower distribution of pectinic acids around the average methoxyl content. The characteristics of gels prepared from such products and some similar to those used in this study are being investigated.

SUMMARY

The viscosity–pH curves for high-methoxyl pectinic acids exhibit maxima near pH 6, while the low-methoxyl acids exhibit maxima near pH 6 and minima near pH 4.

Under the conditions used, the transition from characteristics of high-methoxyl to those of low-methoxyl pectinic acids occurs at a methoxyl content above 8 per cent for esterase-deësterified pectinic acids and near 6 per cent for those deësterified by acid or alkali.

Pectinic acids deësterified by citrus pectinesterase are weaker than pectinic acids of the same methoxyl content prepared with alkali.

An hypothesis based on evidence that the esterase deësterifies portions of the galacturonide chain, while acid or alkali acts in a random manner, is proposed to explain the differences observed in behavior.

REFERENCES

(1) ABRAMSON, H. A., MOYER, L. S., AND GORIN, M. H.: *Electrophoresis of Proteins*, pp. 80–143. Reinhold Publishing Corporation, New York (1942).
(2) BAIER, W. E., AND WILSON, C. W.: Ind. Eng. Chem. **33**, 287 (1941).
(3) BAKER, G. L., AND GOODWIN, M. W.: Univ. Delaware Agr. Expt. Sta. Bull. No. 216 (1939).
(4) BAKER, G. L., AND GOODWIN, M. W.: Univ. Delaware Agr. Expt. Sta. Bull. No. 234 (1941).
(5) BAKER, G. L., AND GOODWIN, M. W.: Univ. Delaware Agr. Expt. Sta. Bull. No. 246 (1944).
(6) CLARK, E. P.: J. Assoc. Official Agr. Chem. **15**, 136 (1932); **22**, 100, 622 (1939).
(7) DEUEL, H.: Mitt. Lebensm. Hyg. **34**, No. 1/2, 41 (1943).
(8) HARNED, H. S., AND OWEN, B. B.: *The Physical Chemistry of Electrolytic Solutions*, pp. 42–5, 410, 411. Reinhold Publishing Corporation, New York (1943).
(9) HILLS, C. H., MOTTERN, R. H., NUTTING, G. C., AND SPEISER, R.: 108th Meeting of the American Chemical Society, New York, September, 1944.
(10) HILLS, C. H., WHITE, J. W., JR., AND BAKER, G. L.: Proc. Inst. Food Technol. **1942**, p. 47.
(11) HINTON, C. L.: *Fruit Pectins*, p. 33. Chemical Publishing Company, Inc., New York (1940).
(12) HINTON, C. L.: Biochem. J. **34**, 1211 (1940).
(13) JANSEN, E. F., AND MACDONNELL, L. R.: Arch. Biochem., in press.
(14) JANSEN, E. F., WAISBROT, S. W., AND REITZ, E.: Ind. Eng. Chem., Anal. Ed. **16**, 523 (1944).
(15) KAUFMAN, C. W., FEHLBERG, E. R., AND OLSEN, A. G.: Food Industries **14**, No. 12, 57–8, 109 (1942); **15**, No. 1, 58–60 (1943).
(16) LEFEVRE, K. V., AND TOLLENS, B.: Ber. **40**, 4513 (1907).
(17) MCCREADY, R. M., OWENS, H. S., AND MACLAY, W. D.: Food Industries **16**, No. 10, 69–71, 139–40 (1944).
(18) MCDOWELL, R. H.: British patents 541,528 (1941); 555,842 (1943).
(19) OLSEN, A. G., AND STUEWER, R.: U. S. patent 2,132, 577 (1938).
(20) OLSEN, A. G., STUEWER, R., FEHLBERG, E. R., AND BEACH, N. M.: Ind. Eng. Chem. **31**, 1015 (1939).

(21) Owens, H. S., Lotzkar, H., Merrill, R. C., and Petersen, M.: J. Am. Chem. Soc. **66**, 1178 (1944).
(22) Owens, H. S., McCready, R. M., and Maclay, W. D.: Ind. Eng. Chem. **36**, 936 (1944).
(23) Owens, H. S., and Maclay, W. D.: Unpublished results.
(24) Speiser, R.: Private communication.
(25) Speiser, R., Hills, C. H., and Eddy, C. R.: J. Phys. Chem. **49**, 328 (1945).
(26) Stuewer, R.: J. Phys. Chem. **42**, 305 (1938).

KINETICS OF DEËSTERIFICATION OF PECTIN[1]

R. SPEISER, C. R. EDDY, and C. H. HILLS

Eastern Regional Research Laboratory[2], Philadelphia 18, Pennsylvania

The kinetics of deësterification of pectin has assumed practical and scientific importance with the growth of interest in pectins of low degree of esterification. Data on rates make possible the selection of industrial operating conditions for lowest cost and highest quality of product. Activation energies derivable from rate data also throw light on unanswered questions concerning the structure of pectin.

Pectin is a complex polysaccharidic material and in any chemical process may undergo several reactions simultaneously. Demethylation of pectin may be accompanied by chain degradation, removal of ballast,[3] oxidation, and opening of pyranose or furanose rings. In this paper, kinetics of demethylation by acid catalysis and by tomato pectase is described, and a method for determining the rate of ballast removal is discussed. In a subsequent paper, degradation of pectin will be considered fully. Kinetics of demethylation by alkaline catalysis and by citrus pectase has already been described by others (21, 22, 29).

The extent of the deësterification reaction can, in general, be followed by measuring either the loss in methyl ester or the gain in free carboxyl groups. In acid deësterification, direct titration with alkali of the liberated carboxyls in the reaction mixture is not feasible, because the change in the number of carboxyls is only an extremely small fraction of the total titratable acidity of the mixture. Direct Zeisel determination of the methyl ester content of the reaction mixture is also not possible because of interference from the liberated methanol. Hence the pectin must be precipitated from the reaction mixture and washed free of acid and methanol before analytical determinations can be made.

[3] For the purposes of this paper, the word *ballast* will be defined as any non-uronide organic material in a sample of pectin whether or not attached to the polygalacturonide chain, in general agreement with Olsen (28) and Schneider (31).

Since some of the ballast material is lost during the washing process, the carboxyl and methyl ester contents of the precipitated and washed samples bear no simple relation to the concentrations of carboxyl and methyl ester in the reaction mixture. However, it can be shown that the degree of esterification (14) is proportional to the concentration of methyl ester in the reaction mixture and is independent of the quantity of ballast or other inert substance present. For these reasons, the degree of esterification was used in this work for following the extent of the demethylation reaction.

The amount of ballast associated with a given weight of polygalacturonide in a sample purified by washing is always less than that associated with the same weight of polygalacturonide before removal from the reaction mixture. However, if the removal of ballast follows a first-order law, and if each sample is purified under such conditions that the same *fraction* of the contained ballast is washed out, then it can be shown that the rate constant calculated from the ballast content of the purified samples will be equal to the rate constant that would have been obtained if the ballast content of the reaction mixtures could have been determined directly. Hence in this investigation the washing procedure was standardized, and the ballast content of the purified samples was used for following the extent of the ballast-removal reaction. By similar reasoning it can be seen that ballast lost in the purification of the original raw material will not affect the rate constants, provided the same batch of purified raw material is used for all the experiments of a given series. Because of small uncontrollable variations in the amount of ballast removed by washing, the data on ballast removal will of course have a higher probable error than that for the demethylation reaction.

<div align="center">EXPERIMENTAL</div>

<div align="center">*Preparation of starting materials*</div>

For one series of deësterifications (H84, H85, H86, H87, H88, H89, H91) pectin was extracted from a good grade of commercial apple pomace and purified by several precipitations from water solution with alcohol, in order to remove electrolytes and organic material of low molecular weight. The final precipitates were washed several times with 70 per cent alcohol, and about 80 per cent of the liquid was pressed out. The moist precipitates were used as starting materials for the deësterifications. For another series (H103, H106) commercial 200-grade apple pectin[4] was used without further purification. The pectins prepared by these methods and used as starting materials for the various deësterifications were all approximately 200-grade and analyzed in the following ranges: polygalacturonide content, 66–78 per cent; methoxyl, 7.5–9.4 per cent; degree of esterification, 0.63–0.80; ash content, 0.25–1.5 per cent; ash alkalinity, 0.027–0.44 milliequivalent per gram of pectin.

<div align="center">*Acid deësterification*</div>

Acid-catalyzed deësterifications were carried out at temperatures from 30° to 60°C., at hydrochloric acid concentrations from 0.1 to 1.0 N, and at pectin con-

---

[4] Kindly furnished by Speas Company, Kansas City, Missouri.

centrations from 0.5 to 2.5 per cent. Pectin purified as above was dissolved in water and diluted to the desired concentration. The solution was placed in a constant-temperature bath (regulated to ±0.1°C.) and allowed to come to the reaction temperature before final adjustment of volume. An amount of concentrated hydrochloric acid calculated to give the desired normality was added to the solution, and time was counted from this moment. The solution was vigorously stirred at all times. Portions of the reaction mixture were removed at intervals, immediately precipitated with twice the volume of 80 per cent alcohol, and strongly stirred to break up the lumps of gel that were formed. The precipitate was filtered and washed with 80 per cent alcohol until the filtrate showed no turbidity with silver nitrate. A uniform washing procedure was used in all cases, so that the amounts of easily removable ballast washed out would be comparable. The samples were then washed with absolute alcohol, pressed, dried for 1 day at room temperature, and then dried for 1 or 2 days at 60°C. in a mechanical convection oven. Finally, the dried samples were ground to pass a 40-mesh screen and analyzed for ash content, alkalinity of the ash, carboxyl content, and methyl ester content.

Enzyme deësterification

Enzyme-catalyzed deësterifications were carried out at temperatures from 30° to 50°C. and at a pectin concentration of 1.2 per cent. The procedure was similar to that described above, except that tomato pectase was used as catalyst instead of hydrochloric acid and that a pH of 6.00 ± 0.05 was maintained by continuous addition of $2 N$ sodium hydroxide with rapid stirring. Because of the speed of the enzyme-catalyzed reaction, a fresh reaction mixture was made up for each sample, and the reaction was stopped at the desired time by quickly lowering the pH of the whole solution to 3.0 with hydrochloric acid, at which pH the enzyme is inactive. Finally, the enzyme was destroyed by heating the solution to 65°C. for 20 min., after which the product was purified in the same manner as the acid-deësterified samples.

Preparation of the enzyme catalyst

Firm, ripe tomatoes were ground to a pulp, the pH adjusted to 6.0 (37), and the juice expressed from the pulp. Suspended material and pigment were removed by decantation and filtration. The clear, yellow solution containing the pectase was stored at 0°C. under a layer of xylene as a preservative. In the deësterifications, 44 ml. of this preparation was used for each liter of 1.2 per cent pectin solution.

Figures 1 and 2 show the variation of the activity of this enzyme preparation with pH and temperature, as determined by a method to be described in another paper (12). The relation of the enzyme activity, at the pH used for deësterification, to the maximum activity of the enzyme can be seen from figure 1. From figure 2 it can be seen that all the deësterifications were run at temperatures below that at which significant denaturation of the enzyme occurs.

Analytical methods

The methyl ester content was determined by a Zeisel procedure, modified by Clark (4), upon samples treated with water vapor at low pressure to remove adsorbed alcohol (13, 17). The carboxyl content was determined by titration with sodium hydroxide to pH 7.5 (35). Ash content was determined by ignition
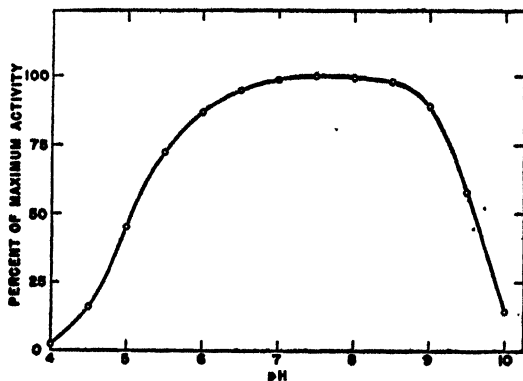
FIG. 1. Activity of tomato pectase as a function of pH. Temperature, 30°C.; total ionic strength, 0.06.
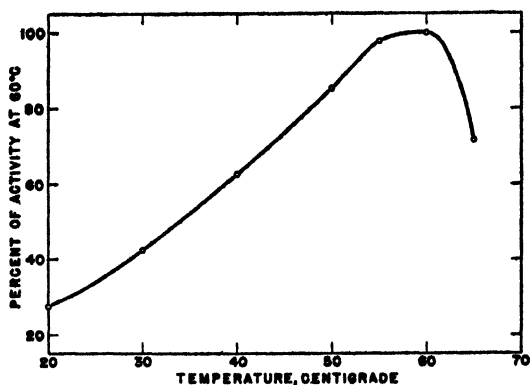
FIG. 2. Activity of tomato pectase as a function of temperature. pH, 6.5; time of reaction, 10 min.; total ionic strength, 0.06.

to constant weight at 600°C. The weights of all samples were corrected for the percentage of ash, and all carboxyl contents were corrected for the alkalinity of the ash.

Calculations

The degree of esterification (14) was calculated from its defining equation:

$$\lambda = \frac{COOCH_3}{COOH_3 + COOH} \tag{1}$$

where $COOCH_3$ and $COOH$ are the methyl ester and carboxyl contents, respectively, in moles per gram of the solid sample.[5]

The weight per cent of polygalacturonide was calculated by the expression

$$\%P = 100(176.12 \times COOH + 190.15 \times COOCH_3) \tag{2}$$

and the weight per cent of ballast material by the expression

$$\%B = 100 - \%P \tag{3}$$

as described by Hills and Speiser (14).

In acid deësterification, the hydrogen-ion and water concentrations were sufficiently high to be unaffected by the production of carboxyl groups during the reaction. · Also, because of the low concentration of the pectin, the concentration of the hydrolysis product, methanol, was always low enough for the reverse reaction to be neglected. Therefore, changes in the rate of demethylation were due solely to changes in the methyl ester concentration, and a pseudo first-order law could be assumed to describe the rate. To insure that these assumptions were applicable, rate calculations were confined to the early part of the reaction, where log λ was a linear function of time. For acid deësterification this linearity extended down to a degree of esterification of approximately 50 per cent.

The rate constant, k, was determined from the slope of log λ *versus* time by the method of weighted least squares, using the statistical methods of Birge (1). Several Zeisel values were determined for each sample, and an individual value of log λ was calculated for each Zeisel value. In this calculation, a single average value of carboxyl content was used for each sample, because the determination of carboxyl is considerably more precise than the determination of methyl ester. The several values of log λ for each sample were averaged, and the average was weighted according to the spread of the individual values, using the formulae of Birge. The probable error of k was also calculated by the method of Birge. The Arrhenius activation energy, μ, and its probable error were calculated from the slope of log k *versus* $1/T$ by the least squares procedure described above. The data for ballast removal were handled similarly.

In enzyme deësterification, calculations were made according to both the zero-order and first-order equations. Linearity of both λ and log λ *versus* time extended down to a degree of esterification of approximately 30 per cent. Otherwise, the calculation of enzyme data was performed in the same manner as for acid deësterification.

RESULTS

Figures 3 and 4 show the variation of degree of esterification and ballast content with time for a typical acid-catalyzed demethylation and a typical enzyme-catalyzed demethylation. The same starting material was used in both cases. It can be seen that in acid deësterification, ballast is lost at a rate comparable to

[5] In the acid behavior of pectin, $\Gamma = 1 - \lambda$ is the significant quantity (35).

that of demethylation, whereas in enzyme deësterification the rate of ballast removal is much less than that of demethylation.   Figure 3 also shows that the ballast content is still decreasing at an appreciable rate after 144 hr., although it has fallen to 6.14 per cent.   In other experiments continued for longer periods of time (14), ballast contents have been obtained as low as 0.9 per cent, a value which is equal to zero within the experimental error and corresponds to a pectic acid of 100 per cent polygalacturonide.
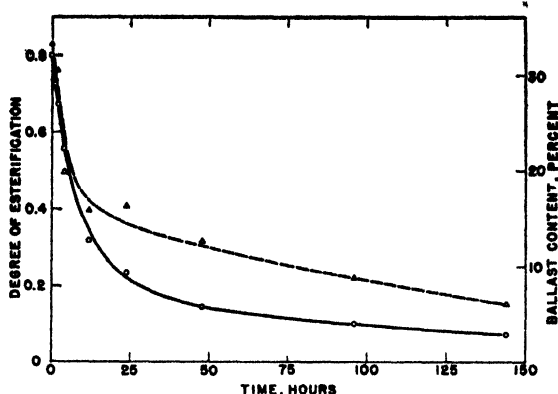
FIG. 3. Acid deësterification of pectin sample H84.   Temperature, 50°C.; pectin concentration, 1.3 per cent.   O = degree of esterification; △ = ballast content.
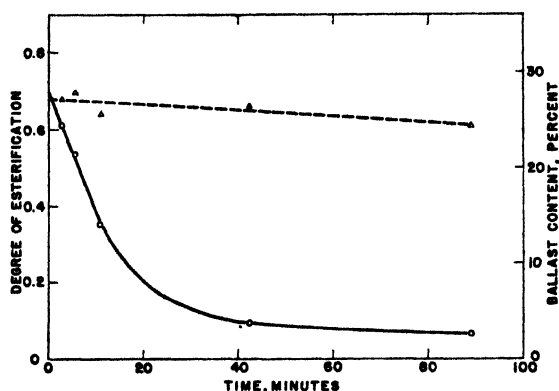
FIG. 4. Enzyme deësterification of pectin sample H87.   Temperature, 50°C.; pectin concentration, 1.2 per cent.   O = degree of esterification; △ = ballast content.

In figure 5 are plotted the logarithms of degree of esterification and of ballast content *versus* time for the same acid-deësterified samples illustrated in figure 3. The demethylation curve is linear for degree of esterification greater than about 0.5 (log λ = 0 to −0.3), showing that the rate of demethylation is first order with respect to concentration of methyl ester.   This means that the over-all reaction is pseudo first order, with concentrations of water and catalyst substantially constant.   From the linear portions of this curve and similar curves for other

series of samples, pseudo first-order rate constants were calculated and are listed in table 1.
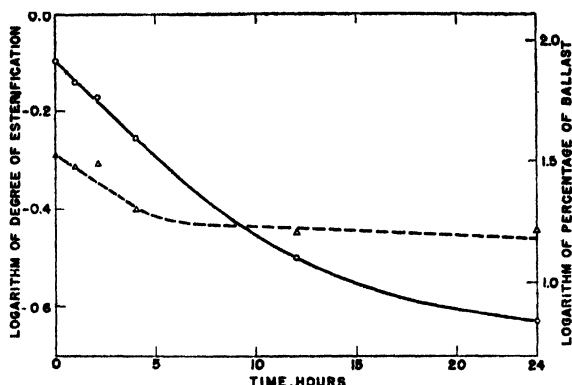
FIG. 5. Acid deësterification of pectin sample H84. Temperature, 50°C.; pectin concentration, 1.3 per cent. O = logarithm of degree of esterification; △ = logarithm of ballast content.

TABLE 1

Rate constants for demethylation of pectin as a function of temperature

Acid-catalyzed, pseudo first order; pectin concentration, 1.3 per cent; HCl, 0.87 N

TEMPERATURE	SERIES	$k \times 10^5$
°C.		sec.$^{-1}$
30	H86	0.316 ± 0.044
40	H91	1.039 ± 0.15
50	H84	2.543 ± 0.36
60	H85	4.201 ± 0.59

Enzyme-catalyzed, pseudo zero order; pectin concentration, 1.2 per cent; pH, 6.00

TEMPERATURE	SERIES	$k \times 10^4$
°C.		sec.$^{-1}$
30	H89	2.85 ± 0.10
40	H88	3.88 ± 0.04
50	H87	5.18 ± 0.23

Enzyme-catalyzed, pseudo first order; pectin concentration, 1.2 per cent; pH, 6.00

TEMPERATURE	SERIES	$k \times 10^4$
°C.		sec.$^{-1}$
30	H89	5.75 ± 0.23
40	H88	8.55 ± 0.11
50	H87	12.15 ± 0.56

The logarithms of these rate constants are plotted against the reciprocal of the absolute temperature in figure 6, and the activation energy for this series

was calculated to be 17,400 ± 1300 cal. The slight curvature of the points is within the experimental error.

In figure 7 are plotted the logarithms of degree of esterification and ballast content *versus* time for the same enzyme-deësterified samples illustrated in figure 4. Both the degree of esterification and its logarithm appear to be linear functions of time for λ greater than about 0.3 (log λ = 0 to −0.5). Thus the probable error of our points is such that the data fit both the zero and the first orders
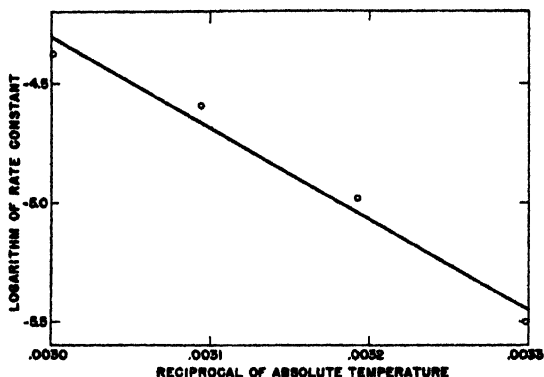
FIG. 6. Rate of acid demethylation of pectin as a function of temperature
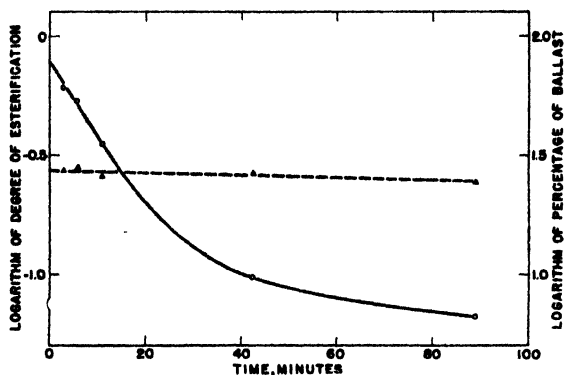
FIG. 7. Enzyme deësterification of pectin sample H87. Temperature, 50°C.; pectin concentration, 1.2 per cent. ○ = logarithm of degree of esterification; △ = logarithm of ballast content.

equally well. From the linear portions of these curves and of similar curves for other enzyme deësterifications, rate constants were calculated according to both orders and are listed in table 1.

Logarithms of these two sets of rate constants are plotted against the reciprocal of the absolute temperature in figure 8. Activation energies calculated from these data are 5790 ± 520 cal., if a pseudo zero order is assumed, and 7310 ± 590 cal. if a pseudo first order is assumed. In both cases the activation energy is constant over an interval of 20°.

The loss in ballast during enzyme demethylation is so slight that an analysis was not made of the enzyme ballast data; however, acid-catalyzed deësterification removes ballast fast enough to warrant quantitative treatment. From figure 5 it can be seen that the logarithmic curve for ballast removal is substantially linear over approximately the same range as the demethylation curve. The poorer fit of the ballast points is due to the method of calculating ballast content by difference and to the uncontrollable variations in the amount of loose ballast
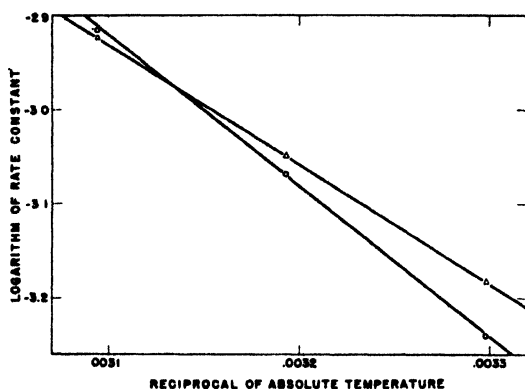
FIG. 8. Rate of enzyme demethylation of pectin as a function of temperature. O = logarithm of first-order rate constant; △ = logarithm of zero-order rate constant + 0.3622.
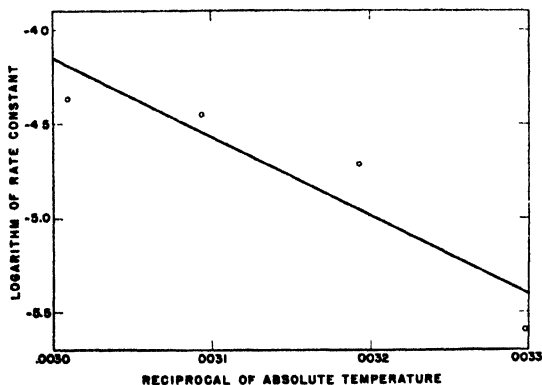
FIG. 9. Rate of ballast removal during acid deësterification, as a function of temperature

washed out in the purification process. The initial linearity of the logarithmic curve shows that ballast was removed as a chemical reaction obeying a first-order law. From the linear portion of this curve and from similar ballast curves, for the same series of samples and temperatures used in the demethylation experiments, rate constants were calculated and are shown in figure 9. From these values, the activation energy was calculated according to the method of least squares and was found to be 18,500 ± 4000 cal. Ballast not chemically attached to the galacturonide chain does not affect this calculation because of the standardized washing procedure used.

Table 2 lists pseudo first-order rate constants for acid demethylation of pectin at a fixed temperature for varying concentrations of pectin and of hydrochloric acid. The data for H103, H106E, and H106F show that the velocity constant is independent of the concentration of pectin, since each of the three rate constants differs from the weighted average by less than the experimental error. This is further evidence that the reaction is first order with respect to methyl ester concentration.

The data for varying acid concentrations are shown in figure 10. These rate constants fall on a straight line that passes through the origin, which shows that

TABLE 2

Pseudo first-order rate constants for acid demethylation of pectin as a function of pectin concentration and acid normality

(Temperature, 40°C.)

SERIES	CONCENTRATION OF PECTIN	CONCENTRATION OF ACID	$k \times 10^6$
	per cent	*N*	*sec.*$^{-1}$
H106D.........	2.5	0.1	0.963 ± 0.084
H106C........	2.5	0.2	1.655 ± 0.156
H106B..........................	2.5	0.3	2.67 ± 0.33
H103..................	2.5	0.6	6.35 ± 1.12
H106E..................	1.5	0.6	5.62 ± 0.34
H106F.............	0.5	0.6	6.25 ± 0.50
H106A..........................	2.5	1.0	9.86 ± 0.34
Weighted average of H103, H106E, H106F......		0.6	5.85 ± 0.28

the reaction is also first order with respect to acid concentration. This line was found, by least squares calculation, to follow the equation:

$$k = (9.62 \pm 0.24) \times 10^{-6} (H^+) \text{ at } 40°C. \qquad (4)$$

Using this value of k and 17,400 cal. for the activation energy, we have derived an empirical equation giving the rate of acid demethylation of pectin as a function of temperature and acid concentration:

$$- \frac{d(COOCH_3)}{dt} = (COOCH_3)(H^+) \times 1.35 \times 10^7 \exp \left(- \frac{17,400}{RT} \right) \qquad (5)$$

This should be useful in industrial practice, although it should be mentioned that, at high acid concentrations, temperatures above 70°C. may produce serious degradation of the pectin chain.

DISCUSSION

Acid deësterification

Our value for the activation energy for acid demethylation of pectin, 17,400 ± 1300 cal., is in good agreement with values appearing in the literature for

esters of low molecular weight, such as 17,100 cal. for methyl acetate (10) and 16,100 to 16,500 cal. for ethyl esters of normal fatty acids from acetate to caprylate (6, 34).

We found that at all temperatures the plots of log λ *versus* time began to deviate from linearity at a degree of esterification of approximately 0.5.   An explanation
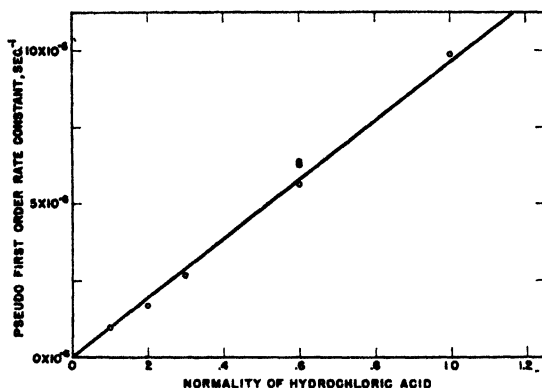
FIG. 10. Rate of acid demethylation of pectin as a function of acid concentration. Temperature, 40°C.
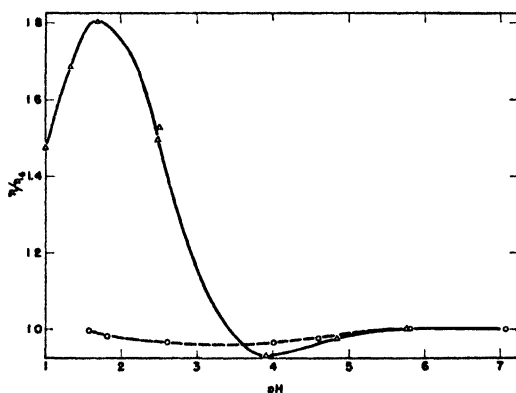
FIG. 11. Viscosity of partially deësterified pectins relative to viscosity at pH 6.0. Concentration, 0.6 per cent in aqueous solution; temperature, 30°C. O = sample H84C: degree of esterification, 0.577; ash content, 0.16 per cent. Δ = sample H84D: degree of esterification, 0.317; ash content, 0.18 per cent.

for this phenomenon can be obtained from figure 11.   In this figure, the viscosity of sample H84C (the last point on the linear portion of figure 5) is compared with the viscosity of sample H84D (the first point of figure 5 that deviated from linearity).   The striking difference in viscosity behavior as a function of pH is typical of the difference between a pectin which will not gel in acid solution in the absence of sugar and a pectin which will.   The same behavior is reflected in the formation of calcium pectinate jellies (14), where a rather sharp dividing line

occurs at $\lambda = 0.5$ between pectins which will form low-sugar calcium pectinate gels and those which will not.

This difference in the gelling behavior of samples H84C and H84D suggests that incipient gel formation in the reaction mixture is the cause of the departure from linearity of the logarithmic demethylation curves.

The deësterification of a polymethyl ester such as pectin can take place in one of two ways: (1) All the ester groups are attacked at the same rate, independent of the condition of esterification of nearby groups; or (2) the removal of a given methyl group is influenced by the condition of esterification of adjacent parts of the chain. These two types can usually be distinguished by a simple rate analysis, as it can readily be shown that Case 1 follows a pseudo first-order law, whereas Case 2 should have a more complex behavior.

The nth stage in the hydrolysis of a pectin molecule containing s main-chain residues can be symbolized as

$$A_{n-1} M_{s-n+1} \xrightarrow{k_n} A_n M_{s-n} \tag{6}$$

where A refers to acid groups and M to methyl ester groups. The rate of loss of methyl groups for this stage of hydrolysis is

$$-\frac{d(COOCH_3)}{dt} = k_n(A_{n-1} M_{s-n+1}) \tag{7}$$

If Case 1 applies, such that each of the $(s - n + 1)$ methyl ester groups hydrolyzes independently and at the same rate v, then

$$k_n = (s - n + 1)v \tag{8}$$

and it follows that the observed over-all rate of hydrolysis, due to all stages combined, will be

$$-\frac{d(COOCH_3)}{dt} = \sum_{n=1}^{s} k_n(A_{n-1} M_{s-n+1}) = v \sum_{n=1}^{s} (s - n + 1)(A_{n-1} M_{s-n+1}) \tag{9}$$

But the total concentration of methyl ester groups in the system is

$$(COOCH_3) = \sum_{n=1}^{s} (s - n + 1)(A_{n-1} M_{s-n+1}) \tag{10}$$

Therefore

$$-\frac{d(COOCH_3)}{dt} = v(COOCH_3) \tag{11}$$

which is identical with the equation for a first-order reaction. A similar result can be obtained from the equations of Ingold (16) (assuming all v's equal) and has also been derived for the special case of dicarboxylic esters by Wegscheider (36).

We have found that acid deësterification of pectin obeys a pseudo first-order law and fits the Arrhenius equation well, which suggests that the hydrolysis of a given methyl ester group is independent of the condition of the rest of the mole-

cule (Case 1). This is in contrast to the acidic dissociation of pectinic acid, which was found (35) not to be independent of the degree of dissociation of the rest of the chain. In this respect the macromolecule, pectin, shows the same behavior as low-molecular-weight esters and acids. Many esters of dibasic acids are hydrolyzed according to the assumptions of Case 1, since k_1/k_2 is experimentally found (23) to be equal to 2, as required by equation 8. This is in contrast to the wide difference in order of magnitude usually observed between the first and second acid dissociation constants of dibasic acids, instead of the simple 4 to 1 ratio expected from independent ionization (see equation 5 of reference 35). For example, Meyer (23) found $k_1/k_2 = 1.98$ (theoretical 2.00) for the hydrolysis of dimethyl succinate, whereas Gane and Ingold (8) found $K_1/K_2 = 16.4$ (theoretical 4.0) for the dissociation of succinic acid.

A possible explanation for this difference in behavior can be found in the mechanism proposed by Datta, Day, and Ingold (5) for the hydrolysis of esters. The rate-determining step of their mechanism involves no net change in the number of electrical charges, whereas acidic dissociation and recombination produce and destroy charges. It should therefore not be necessary to do electrostatic work on the surrounding ionic atmosphere in ester hydrolysis, and the influence of dipoles in nearby molecules or in adjacent parts of the same molecule should have less effect on hydrolytic reactions than on electrolytic dissociations. A similar point of view has been put forward by Brönsted (2) and checked experimentally for ester hydrolysis by Dawson and Lowson (7), who found that the rate of hydrolysis of ethyl acetate is proportional to the concentration of hydrochloric acid rather than to its thermodyamic activity. For pectin, we also find that the rate of deësterification is proportional to hydrochloric acid concentration, as shown in figure 10, although our experimental error is too great to decide definitely between concentration and activity. Therefore, it is apparent from the above discussion that pectin hydrolysis follows Case 1, whereas its acidic dissociation follows Case 2.

Enzyme deësterification

The values 5790 ± 520 cal. and 7310 ± 590 cal. for the activation energy of demethylation of apple pectin by tomato pectase may be compared with 6000 cal. found by Owens, McCready, and Maclay (29) for demethylation of citrus pectin by citrus pectase *in situ*. Both are also comparable to activation energies found for several other esterases acting on diverse substrates, such as 7600 and 8500 cal. for pancreatic lipase (33, 32) and 5700 cal. for grasshopper esterase (3).

Under the conditions used in this set of experiments, enzymic deësterification fits either the pseudo zero-order law or the pseudo first-order law equally well. Other experiments by Hills and Mottern (12) suggest that tomato pectase follows the zero-order law better than the first-order law. On the other hand, Kertesz (19) found that tobacco pectase obeyed the first-order law up to 60 per cent of reaction. This point is not definitely settled and will be considered in more detail in a later paper (12).

Preliminary calculations applying the Michaelis–Menten theory (24) to other

unpublished data on tomato pectase indicate that the substrate concentrations used in experiments H87, H88, H89 fall in the intermediate range where it cannot be predicted from the theory which of the two orders of reaction should apply. There is also some question whether the Michaelis–Menten equations in their present form should be applied to a high polymeric system such as pectin, where several groups in the same molecule may be reacting simultaneously. For these reasons, we are including calculations according to both orders.

Since the data follow regular reaction-rate laws up to 50 per cent of reaction and fit the Arrhenius equation well, enzymic deësterification appears to follow Case 1 along with acid deësterification. However, electrophoretic data and gel strengths (to be reported in a later paper) indicate that, unlike acid deësterification, the methyl ester groups are not attacked at random. Likewise, Kertesz (18) found that molecular size may be an important factor in enzyme deësterification of pectin, and Lineweaver, Jansen, Owens, et al. (20) have suggested that the action of pectase is more selective than alkaline hydrolysis. This suggests that, although the *selection* of a methyl group for enzymic removal depends on the condition of the neighboring parts of the chain, the *rate* of enzymic removal of a methyl group is not dependent on the nearby parts of the molecule. Differences in mechanism between acid and enzyme deësterification are not surprising in the light of the highly specialized character of enzyme catalysis.

Ballast removal

Hirst and Jones (15) concluded that the ballast material in pectin is not joined to the main polygalacturonide chain by covalent chemical bonds but is merely loosely associated by secondary valences, in general agreement with Schneider and Bock (31). On the other hand, Norris and Resch (27) were of the opinion that a part of the non-galacturonide material may be attached to the main chain by primary bonds, for they have stated, ". . . it is probable that the usual sample of pectin consists of a central nucleus of galacturonic acid units to which arabinose and galactose units may be chemically attached. . . . In addition to this there must be varying amounts of araban and galactan or arabogalactan which are held to the main nucleus by physical forces" (27).

Re-analysis by us of the data of Hirst and Jones (15) does not confirm their conclusion that only loose association forces are involved. Although they found that a portion of the ballast was easily washed out in 70 per cent alcohol, their data also showed that alkaline treatment sufficiently harsh to remove all the methyl ester still left 15–20 per cent of the original galactan, as shown by their final equivalent weight of 185 and uronic anhydride content (by carbon dioxide liberation) of 96.7 per cent. Similarly, Norris and Resch (27) found that treatment of hops pectin for 193 hr. with 4 per cent sodium hydroxide (which would remove most of the methyl ester) still left araban and galactan contents of 3.8 and 7.7 per cent, respectively.

Experimentally, we find that, after removal of loose ballast by the washing procedure described in the experimental section, a substantial quantity of ballast remains that requires an activation energy of 18,500 cal. for its removal, which

lends evidence to the theory that covalent bonds are involved. Polysaccharide ballast could be chemically attached to a polyuronide chain by ether, ester, anhydride, or hemiacetal linkages, assuming the necessary end groups on the ballast chain. The anhydride and hemiacetal linkages are ruled out immediately by their instability in the aqueous environment in which pectin occurs naturally. The ether linkage is also ruled out because of its high bond strength of at least 29,000 to 35,000 cal. (11, 25). The ester linkage is a possibility because its bond strength is in the neighborhood of the 18,500 value we obtain.

Our method of calculating degree of esterification and ballast content is based on the assumption that the sum of the methyl esters and free carboxyls is a true measure of the number of galacturonide units present. If some of the galacturonide units have their carboxyl groups tied up by ester linkages to ballast, the sum of methyl ester groups plus free carboxyl groups will not be equal to the number of galacturonide units. However, the molecular weights of araban and galactan are so high (6000 and higher (9, 26)) that the error introduced into the carboxyl content will be too small to detect, except by elaborate end-group analysis.

Another possible way to account for the nature of the ballast-removal curves we obtain is that all the ballast is merely physically mixed with the polygalacturonide but that a portion is of such high molecular weight that it is only difficultly soluble in the 80 per cent alcohol used in the purification process. In this case the increasing amount of ballast washed out by the alcohol after deësterification must be accounted for by degradation of the ballast. This possibility is eliminated because the activation energy for ballast removal would then be found to be of the order of magnitude of 30,000 cal., as for degradation of other polysaccharide materials (30).

There have been suggestions that the araban and galactan are part of the main chain, occurring between polygalacturonide sections. Two facts rule this out: (1) The molecular weight of the ballast is so high that its removal from the midst of the main chain would result in a very rapid falling off of viscosity, which is not observed, and (2) by the continuation of acid hydrolysis for sufficiently long periods, the ballast content can be reduced to substantially zero, as shown in figure 3. The molecular weights of samples thus treated are still at least as high as 30,000, as indicated by viscosity, gel formation, and film formation.

Hence it is our conclusion that a substantial fraction of the ballast is probably attached to the polygalacturonide chain by ester linkages. The remainder may be merely physically mixed with the polygalacturonide or attached by secondary valences such as hydrogen bonds. One is strongly tempted to say that the loosely bound material is araban and that the chemically bound material is galactan, in the light of findings of Hirst and Jones (15) that mild hydrolytic means removed practically all the araban but hardly affected the galactan. However, two facts should be noted: (1) Their washing procedure with 70 per cent alcohol removed both araban and galactan at approximately equal rates but did not completely remove either; (2) their hydrolytic treatment that

removed araban almost completely was conducted under such conditions that the araban was degraded to arabinose. Since the furanose structure of araban makes it very susceptible to hydrolysis (15), there still remains the possibility that the araban was joined to the polygalacturonide by an ester linkage and that the arabinose was produced by degradation of the araban while still attached, leaving the last arabinose residue esterified to the polygalacturonide. Because of the high molecular weight of araban, the amount of arabinose thus left with the galacturonide would be too small to be detected, except by the methods of end-group analysis.

SUMMARY

The kinetics of acid- and enzyme-catalyzed deësterification of apple pectin has been studied.

Rate constants were measured for acid demethylation at hydrochloric acid concentrations from 0.1 to 1.0 N, at temperatures from 30° to 60°C., and at pectin concentrations from 0.5 to 2.5 per cent. Under these conditions, the reaction was found to be of pseudo first order, with an activation energy of 17,400 ± 1300 cal. The rate of acid demethylation, over the intervals of temperature and concentration used, can be expressed as an empirical equation:

$$- \frac{d(COOCH_3)}{dt} = (COOCH_3)(H^+) \times 1.35 \times 10^7 \exp\left(- \frac{17,400}{RT}\right)$$

Rate constants were measured for demethylation catalyzed by tomato pectase at temperatures from 30° to 50°C. and at a pectin concentration of 1.2 per cent. The data fit the pseudo zero-order and the pseudo first-order laws equally well. Assuming zero and first orders, activation energies of 5790 ± 520 cal. and 7310 ± 590 cal., respectively, were calculated.

Analysis of the kinetics of removal of organic non-galacturonide material (ballast) during acid deësterification suggests that, in apple pectin, a substantial portion of the ballast is attached to the polygalacturonide chain by primary covalent bonds (probably ester linkages) having an activation energy of 18,500 ± 4000 cal. The remainder of the ballast is held by secondary valence forces or merely included as a physical mixture.

By extensive acid hydrolysis, ballast can be completely removed, leaving a stripped polygalacturonic acid chain that is still of high molecular weight and has an average residue weight approaching 176. In enzyme hydrolysis, very little ballast is removed.

REFERENCES

(1) BIRGE, R. T.: Phys. Rev. **40**, 207 (1932).
(2) BRÖNSTED, J. N.: Z. physik. Chem. **102**, 169 (1922).
(3) CARLSON, L. D.: Biol. Bull. **81**, 375 (1941).
(4) CLARK, E. P.: J. Assoc. Official Agr. Chem. **22**, 100, 622 (1939).
(5) DATTA, S. C., DAY, J. N. E., AND INGOLD, C. K.: J. Chem. Soc. **1939**, 838.
(6) DAVIES, G., AND EVANS, D. P.: J. Chem. Soc. **1940**, 339.
(7) DAWSON, H. M., AND LOWSON, W.: J. Chem. Soc. **1928**, 2146.

(8) GANE, R., AND INGOLD, C. K.: J. Chem. Soc. **1928**, 1594.
(9) GAPONENKOV, T. K.: J. Gen. Chem. (U.S.S.R.) **7**, 1729 (1937).
(10) HARNED, H. S., AND ROSS, A. M.: J. Am. Chem. Soc. **63**, 1993 (1941).
(11) HEIDT, L. J., AND PURVES, C. B.: J. Am. Chem. Soc. **66**, 1385 (1944).
(12) HILLS, C. H., AND MOTTERN, H. H.: Paper in preparation.
(13) HILLS, C. H., OGG, C. L., AND SPEISER, R.: Ind. Eng. Chem., Anal. Ed. **17**, 507 (1945).
(14) HILLS, C. H., AND SPEISER, R.: "Characterization of Pectin," Science, in press.
(15) HIRST, E. L., AND JONES, J. K. N.: J. Chem. Soc. **1939**, 454.
(16) INGOLD, C. K.: J. Chem. Soc. **1930**, 1375.
(17) JANSEN, E. F., WAISBROT, S. W., AND RIETZ, E.: Ind. Eng. Chem., Anal. Ed. **16**, 523 (1944).
(18) KERTESZ, Z. I.: J. Biol. Chem. **121**, 589 (1937).
(19) KERTESZ, Z. I.: Ergeb. Enzymforsch. **5**, 233 (1936).
(20) LINEWEAVER, H., JANSEN, E. F., OWENS, H. S., et al. Private communications from the Western Regional Research Laboratory.
(21) MACDONNELL, L. R., JANSEN, E. F., AND LINEWEAVER, H.: Arch. Biochem. **6**, 389 (1945).
(22) McCREADY, R. M., OWENS, H. S., AND MACLAY, W. D.. Food Industries **16**, 794 (1944).
(23) MEYER, J.. Z. physik. Chem. **66**, 81 (1909).
(24) MICHAELIS, L., AND MENTEN, M. L.: Biochem. Z. **49**, 333 (1913).
(25) MORRELL, S., AND LINK, K. P.: J. Biol. Chem. **104**, 183 (1934).
(26) MOSIMANN, H, AND SVEDBERG, T.· Kolloid-Z. **100**, 99 (1942).
(27) NORRIS, F. W., AND RESCH, C. E.. Biochem. J. **31**, 1945 (1937).
(28) OLSEN, A. G., STUEWER, R. F., FEHLBERG, E. R., AND BEACH, N. M.: Ind. Eng. Chem. **31**, 1015 (1939).
(29) OWENS, H. S., McCREADY, R. M., AND MACLAY, W. D.· Ind. Eng. Chem. **36**, 936 (1944)
(30) SAKURADA, I., AND OKAMURA, S.: Z. physik. Chem. **A187**, 289 (1940)
(31) SCHNEIDER, G. G., AND BOCK, H.. Ber. **70B**, 1617 (1937)
(32) SCHWARTZ, B.. J. Gen. Physiol. **27**, 113 (1943).
(33) SIZER, I. W.. AND JOSEPHSON, E. S.: Food Research **7**, 201 (1942).
(34) SMITH, H. A, AND MYERS, R. R.· J. Am. Chem Soc. **64**, 2362 (1942).
(35) SPEISER, R., HILLS, C. H, AND EDDY, C. R.: J. Phys. Chem. **49**, 328 (1945).
(36) WEGSCHEIDER, R.: Monatsh. **36**, 471 (1915).
(37) WILLAMAN, J. J, AND HILLS, C. H. U. S patent 2,358,129 (1944).

CORRELATION OF VISCOSITIES OF LIQUIDS WITH TEMPERATURES

M. S. TELANG

Laxminarayan Institute of Technology, Nagpur University, Nagpur, India

A simple expression correlating viscosities of liquids with temperatures can be quite useful in a number of chemical engineering operations. Although numerous mathematical expressions connecting viscosity and temperature for various liquids are to be found in the literature, there is not a single equation applicable to all liquids at all temperatures. A critical review of many of the well-known equations has been given by Srinivasan and Prasad (9) and the applicability of each equation has been discussed. These authors have come

to the same conclusion as the Committee of the Academy of Sciences at Amster-dam (3) that of all the equations so far proposed it is Andrade's equation which is to be preferred. The equation is

$$\eta = A e^{b/T}$$

where A and b are constants, η and T being the viscosity and temperature, respectively. Andrade's equation continues to attract attention as it probably has a theoretical basis. Bingham and Stookey (2) have proposed the following equation

$$\frac{\eta}{T} = a + bT + \cdots$$

where a and b are constants; the applicability as well as the limitations of this equation have been discussed by the authors. Nissan (7) has indicated that η is a simple function of $\cdot T_B/T$ and also that log η is some function of T/T_B, where T_B is the absolute boiling point. Through a series of complicated calculations employing quite a large amount of viscosity data, Nissan has proposed a reference curve common for all liquids. However, Nissan's paper has been adversely criticized by Irany (6) for some of the strange conclusions drawn.

Batschinski (1) has proposed an interesting relationship between molecular volumes of liquids and temperatures, viz.:

$$\frac{1}{\eta} = \frac{V - W}{c}$$

where V is the specific volume of the liquid measured at the same temperature as the viscosity, and c and w are constants for each liquid. Though this relationship is quite empirical, it is closely obeyed by a number of non-associated liquids over a wide range of temperatures. Sugden (10) has shown that the following equation expresses the relation between densities and temperatures of liquids:

$$D - d = D_0(1 - T_r)^{3/10}$$

where D and d represent the densities of substances in the liquid and vapor states, respectively, and D_0 is the density of the supercooled liquid at absolute zero. Neglecting d, which is usually small in comparison with D, at lower temperatures, we have

$$D = D_0 (1 - T_r)^{3/10}$$

Hence,

$$\frac{M}{D} = \frac{M}{D_0} \times \frac{1}{(1 - T_r)^{3/10}}$$

where M is the molecular weight. So,

$$V = \frac{V_0}{(1 - T_r)^{3/10}}$$

where V_0 is the zero volume, being a constant for each liquid (11). Substituting this value of V in Batschinski's equation we obtain

$$\frac{1}{\eta} = \frac{V_0}{c(1 - T_r)^{3/10}} - \frac{w}{c}$$

Thus, putting $V_0/c = m$ and $W/c = k$, which are constants for each liquid:

$$\frac{1}{\eta} = \frac{m}{(1 - T_r)^{3/10}} - k \qquad (1)$$

According to this expression, if $1/\eta$ is plotted against $\dfrac{1}{(1 - T_r)^{3/10}}$, a straight line should be obtained with a slope of m and an intercept of k. Such values were
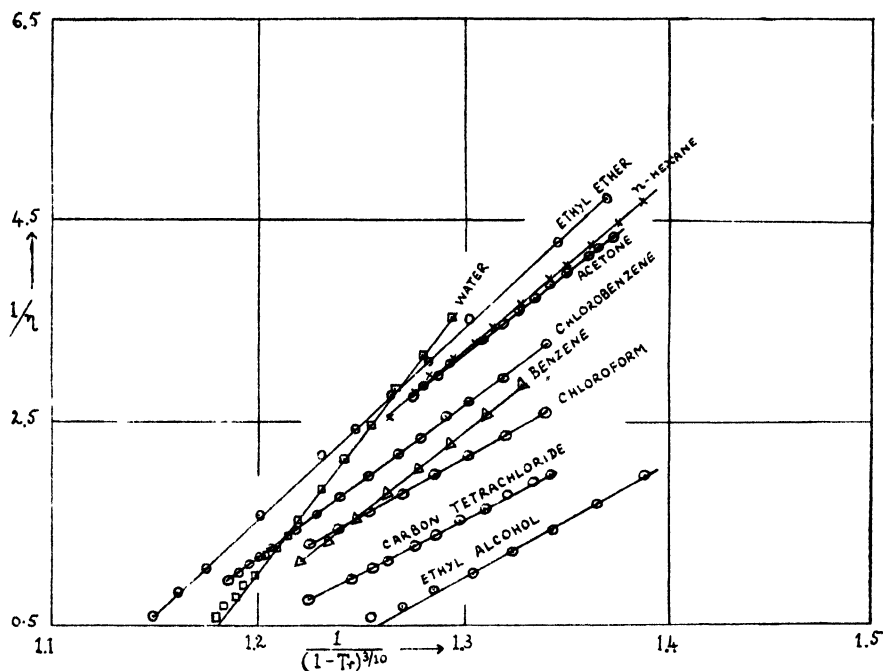
Fig. 1. Plot of $1/\eta$ against $1/1(1-T_r)^{3/10}$. η is expressed in centipoises.

plotted as shown in figure 1, and it was observed that for non-associated liquids the equation is valid at all temperatures. Positive deviations are observed for associated liquids like water and alcohol at lower temperatures. It is probable that the associated liquids at temperatures not far below their boiling points may be in less complex states and hence may tend to approach the behavior of normal liquids. From figure 1 it is further observed that the values of m and k are not the same for all liquids. However, in the case of each normal liquid all the points lie very closely on a straight line, the viscosity data being taken from the literature (5).

Batschinski (2) tested his equation for sixty-six liquids over a wide range of temperatures and found that the maximum deviations observed in the case of normal liquids were about 1 per cent or even less. Such an extensive study has not yet been made by the present writer with reference to equation 1; however, it is found that this equation is also equally applicable to a few more liquids besides those that have been mentioned in the graph. In no case was the deviation of the calculated values from the experimental more than 1 per cent. A full statistical study regarding the reliability of this equation is engaging the author's further attention and the work is in progress.

The object of the present paper is to point out that the viscosities of unassociated liquids at temperatures other than those recorded in the literature can be estimated with a fair degree of accuracy using equation 1, herein presented. It may be remarked that such values can be also had from the viscosity–temperature alignment charts given in reference tables, but the reliability of such values is not easily known, the error being in some cases as high as 10 per cent (8). Furthermore, the form of equation 1, especially because of its relation to the critical temperature, seems to indicate that it may have a theoretical basis.

The equation contains two constants, m and k, and to evaluate them the viscosities of a liquid at two temperatures as well as the value of the critical temperature must be known. For a majority of common liquids, data on critical temperatures are available in the literature, but in case they are not, the critical temperature of a liquid can be estimated from its densities at two temperatures by applying Sugden's density–temperature relationship, as illustrated by Sugden himself (10).

Nissan (7) has suggested the construction of a reference curve for temperature–viscosity relationship, but in view of the observation that the values of m and k are not the same for all liquids, it is not feasible to obtain such a curve. It is of interest to note further that instead of taking T/T_B or its reciprocal value, as done by Nissan, it may be of greater significance to take the fundamental quantity T_c, the critical temperature, which is $\frac{3}{2} T_B$ (4), into consideration in the manner of equation 1.

REFERENCES

(1) BATSCHINSKI: Z. physik. Chem. **84**, 643 (1913).
(2) BINGHAM AND STOOKEY: J. Am. Chem. Soc. **61**, 1625 (1939).
(3) Committee for the Study of Plasticity, Academy of Sciences at Amsterdam: *Second Report on Plasticity and Viscosity*, pp. 37, 57–8 (1938).
(4) GULDBERG: Z. physik. Chem. **5**, 374 (1890).
(5) *International Critical Tables*. McGraw-Hill Book Company, Inc., New York.
(6) IRANY: Phil. Mag. **33**, No. 224, 685 (1942).
(7) NISSAN: Phil. Mag. **32**, No. 215, 441 (1941).
(8) PERRY: *Chemical Engineer's Handbook*, p. 796. McGraw-Hill Book Company, Inc., New York (1942).
(9) SRINIVASAN AND PRASAD: Phil. Mag. **33**, No. 219, 258 (1942).
(10) SUGDEN: J. Chem. Soc. **1927**, 1781.
(11) TELANG: J. Indian Chem. Soc. **20**, 274 (1943).

THE DEPOLARIZATION OF LIGHT SCATTERED FROM POLYMER SOLUTIONS[1]

PAUL DOTY AND HERMAN S. KAUFMAN

Department of Chemistry, Polytechnic Institute of Brooklyn, Brooklyn 2, New York

INTRODUCTION

The size, shape, and structural anisotropy of polymer molecules is a matter of fundamental concern just as it has been in the case of small molecules. Consequently, within the last decade a number of methods have been employed in an attempt to determine the size and shape of polymer molecules. X-ray investigations have been the chief source of information on polymer molecules in the solid state, whereas in solution, studies of viscosity, flow birefringence, sedimentation, and diffusion have contributed most to our present knowledge. However, this present knowledge is not particularly impressive in its detail and certainty. For example, a commentary on our present state of knowledge can be found in the fact that there is no proof of the presence or absence of branching in most linear polymer molecules. Another case is that of the present lack of agreement on whether or not most polymer molecules in solution are larger or smaller than a random coil (Kuhn) with unsymmetrical energy barriers taken into account.

In this situation it appears that depolarization measurements on light scattered from polymer solutions may contribute to our knowledge of the geometry of these molecules, especially since this method has had considerable success in several other colloid systems. Actually, some work along these lines has been carried out earlier and summarized by Lotmar (1938) (13, 14). However, the later advances made by Krishnan suggest that more definitive results may now be obtained by applying the depolarization method to the study of polymer solutions.

In the work reported here, measurements have been made on solutions of polystyrene, cellulose acetate, and polyvinyl chloride. The results do not yield information such as exact dimensions but rather show how shape and size change with variables such as molecular weight, solvent, and concentration. This is a characteristic of the method which if properly developed may give more direct and useful results than are at present found in attempts to evaluate the dimensions of a hypothetical model.

Before proceeding to the experimental work and the discussion of the results, a concise review of the theoretical considerations is presented.

DEPOLARIZATION THEORY

A light wave passing over a loosely bound electron will in general at the expense of its own energy produce a forced vibration of the electron, and this vibration will result in the radiation of the energy received in all directions with the same wave length as the incident light. In a macroscopic medium a large amount of this radiated energy will be destroyed by destructive interference; but, owing to the fluctuations of the density of microscopic regions of the medium, the interference will be incomplete and a residual portion can be observed. This is termed scattered light. If the medium is not a pure fluid but a solution in which the components have different indices of refraction, a much larger intensity of scattered light will result because of the added effect of fluctuations of concentration on a microscopic scale.

Rayleigh (18), in his theory of the scattering of light by small particles, showed that for the case of small, spherical, isotropic particles the transversely scattered light should be completely polarized, since the incident light possessed no longitudinal components. Furthermore, for such scattering units the horizontal component of the incident light would not contribute to the light scattered at 90°, and consequently the transversely scattered light is the same for unpolarized as for vertically polarized incident light. In general, however, observations on most scattering media show that polarization of the transversely scattered light is not complete. This naturally poses the problem of relating the incompleteness of polarization with the deviations of the scattering units from small, spherical, isotropic particles, i.e., with size, shape, and anisotropy. Significant contributions to the solution of this problem have been made by Mie (15), who treated the effect of size, by Gans (8), who considered the effect of shape and anisotropy, and most recently by Krishnan (10, 11, 12), who developed and verified some extremely useful relations which permit a resolution of the effect of the above-mentioned quantities on the polarization of the scattered light.

Prior to the investigations of Krishnan, attention was focused mainly on the depolarization observed with the incident light unpolarized. The depolarization for unpolarized incident light (ρ_u) is defined as the ratio of the intensities of the horizontal and vertical components of the scattered light. For Rayleigh's small, spherical, isotropic particles, $\rho_u = 0$. Mie demonstrated that ρ_u becomes finite and is an increasing function of the particle diameter. This effect has been observed by Krishnan (11) and by Hoover, Putnam, and Wittenberg (9). Finite values of ρ_u are also observed from such small scattering units as diatomic gases. Here the cause must be in the anisotropy of the molecules. Gans evaluated this relation quantitatively for several models such as discs and ellipsoids. Thus it is clear that the measurement of ρ_u alone does not yield very definite information, since it is not the measure of any one factor alone. Gans and especially Krishnan (11, 12) have worked out a much more useful and complete theory. Reference may be made to their papers for a detailed, though sometimes obscure, development of this theory. Here an attempt is made to include in the summary of the theory qualitative, intuitive arguments which

show the physical basis for the relations between depolarization and the geometry of the scattering particles.

By using polarized and unpolarized incident light, three depolarization values may be measured:

$$\rho_u = \frac{H_v + H_h}{V_v + V_h} = \frac{H_u}{V_u} \tag{1}$$

$$\rho_v = \frac{H_v}{V_v} \tag{2}$$

$$\rho_h = \frac{V_h}{H_h} \tag{3}$$

H and V denote the intensities of the horizontal and vertical components of the scattered light, and the subscripts refer to unpolarized, vertically polarized, and

INCIDENT BEAM - WITH
HORIZONTAL VIBRATIONS

INCIDENT BEAM - WITH
VERTICAL VIBRATIONS
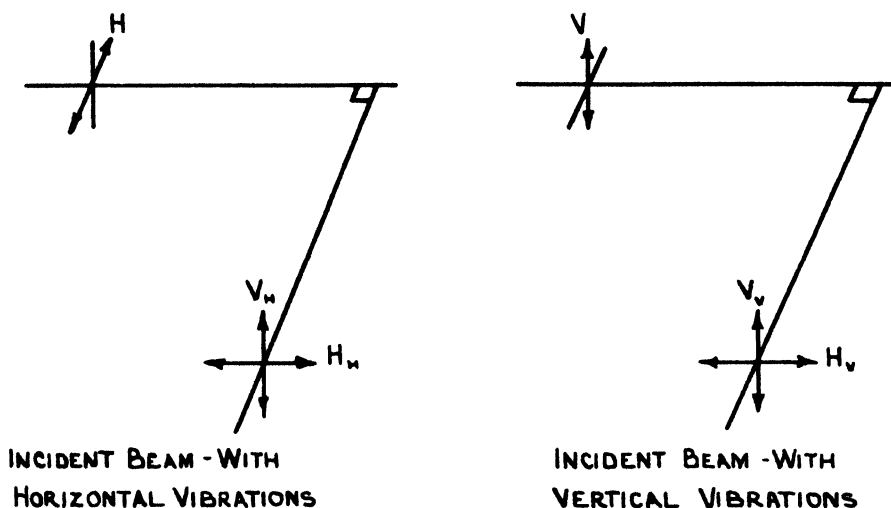
FIG. 1. Components of scattered light

horizontally polarized incident light. These relations are sketched in figure 1. It is clear that all three depolarizations may be measured experimentally.

Krishnan has shown that from the values of the three depolarizations, the scattering units may be classified on the basis of *size* and *anisotropy*. The designation of size is relative to the wave length of light. Particle diameters less than about 100 Å. are considered small. Anisotropy is used here to denote both the departure from spherical shape and the intrinsic anisotropy which signifies the presence of different properties in different directions of the particle. Now consider the possible values of H_v, V_v, H_h, and V_h for the four classes of particles: small isotropic, large isotropic, small anisotropic, large anisotropic. Reference to figure 1 will be helpful.

For all these classes of particles V_v will be finite, since the predominant effect

of the passage of vertically polarized incident light will be the forced oscillations of the dipole. In the case of small isotropic particles H_v, H_h, and V_h will be zero, because the moment induced will be colinear with the incident electric vector giving rise to only vertically polarized light.

This same consideration holds for large spherical isotropic particles except for H_h. When the particle is comparable to the wave length of light, the electric vector will vary in magnitude and size throughout the particle. This non-uniformity of field within the particle gives rise to a horizontal component and hence a finite value of H_h.

For small anisotropic particles, H_h will be finite for a different reason. The scattering units can be considered as point sources characterized by their polarizability ellipsoids. The induced moment which would for the isotropic particle be horizontal is in this case deflected approximately in the direction of the axis
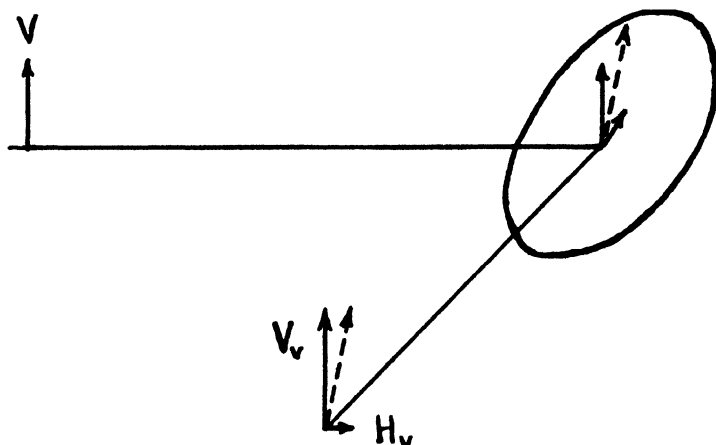
FIG. 2. Illustration of depolarization due to anisotropy

of greatest polarizability in the particle (see figure 2). Thus the induced moment will generally have an oblique orientation which gives rise to a horizontal component when the incident electric vector is horizontal. Exactly analogous reasoning applies to H_v and V_h; consequently, all these components are finite and equal.

Finally, consideration of the large anisotropic particle shows that H_v and V_h will be finite for the same reason as in the previous case. This effect holds also for H_h, but to it must be added the effect that caused H_h to be finite for a large isotropic particle. Consequently H_h is finite but larger than H_v or V_h. All these results are summarized in table 1, together with the values of the three depolarizations that result.

From table 1 an important principle is obvious: the measurement of the three depolarization values permits the classification of the scattering units with respect to both size and anisotropy. Of even more usefulness in the study of polymer solutions is the fact that these depolarization values are regular functions of size and anisotropy. This permits one to follow changes in size and

anisotropy even though during all the changes the scattering units remain within one of the above classes.

Further examination of table 1 shows another useful principle in the study of polymer solutions. When ρ_v is finite, that is, in the case of anisotropic particles, deviations of ρ_h from unity may be used as a measure of particle size. If the value of ρ_h is close to unity, then the contribution of anisotropy to the value of ρ_u is given by $2\rho_v/(1 + \rho_v)$ and the contribution of size is given by the difference $\rho_u - 2\rho_v/(1 + \rho_v)$.

For all the cases noted in table 1 the relation $H_v = V_h$ holds. This is known as the Reciprocity Theorem in optics. Its validity has been thoroughly examined by Krishnan (12) and Perrin (16), who conclude that the relation is valid, not for a single colloidal non-spherical particle with fixed orientation in space, but only for a solution containing a large number of particles which have no preferred orientation in the plane containing the incident and scattered beams. Thus, the Reciprocity Theorem can be considered to hold in the optics

TABLE 1

Depolarization values for various classes of scattering units[*]

SCATTERING UNIT	H_v	V_v	H_h	V_h	ρ_u	ρ_v	ρ_h
Small isotropic	0	+	0	0	0	0	0
Large isotropic. ..	0	+	+	0	+[a]	0	0
Small anisotropic..... . ..	+[b]	+	+	+[b]	+	+	1[c]
Large anisotropic...... . .	+[b]	+	+	+[b]	+	+	+

[*] The plus signs denote for the depolarization values positive values between 0 and 1.
[a] ρ_u increases regularly with particle diameter.
[b] $H_v = V_h$.
[c] $H_h = V_h$.

of polymer solutions. This theorem can be combined with equations 1, 2, and 3 to give the following equation, known as Krishnan's relation:

$$\rho_u = \frac{1 + \dfrac{1}{\rho_h}}{1 + \dfrac{1}{\rho_v}} \qquad (4)$$

This relation is useful, since it permits the evaluation of one of the depolarization values when the other two are known. This is particularly valuable in the case of ρ_h, which is often extremely difficult or impossible to measure accurately. When ρ_h can be measured, the relation allows a check on the experimental measurements.

<center>EXPERIMENT</center>

<center>*A. Optical apparatus and method*</center>

The visual method of Cornu was employed in measuring the depolarization values. This technique was chosen because of its directness and the short time

required for the measurements. The apparatus used was similar to that described by Hoover, Putnam, and Wittenberg (9). A schematic diagram of the optical system is shown in figure 3.

The source of light, S, was a 100-watt G.E. AH-4 mercury-vapor lamp enclosed in a water-cooled light-tight housing. The beam was made parallel by the lens, L, which had a focal length of 18 cm. It was then made monochromatic by Corning glass filters which isolated the 5461 Å. line. Next in the optical path was a polaroid, P, which could be rotated to give vertically or horizontally polarized incident light or, when desired, could be removed for measurements of ρ_u. A variable-iris diaphragm, I, was used to define the beam before entering the cell housing, H. The latter was constructed in such a manner as to permit the incident light to pass through the cell (3 x 3 x 10 cm.) and leave through the
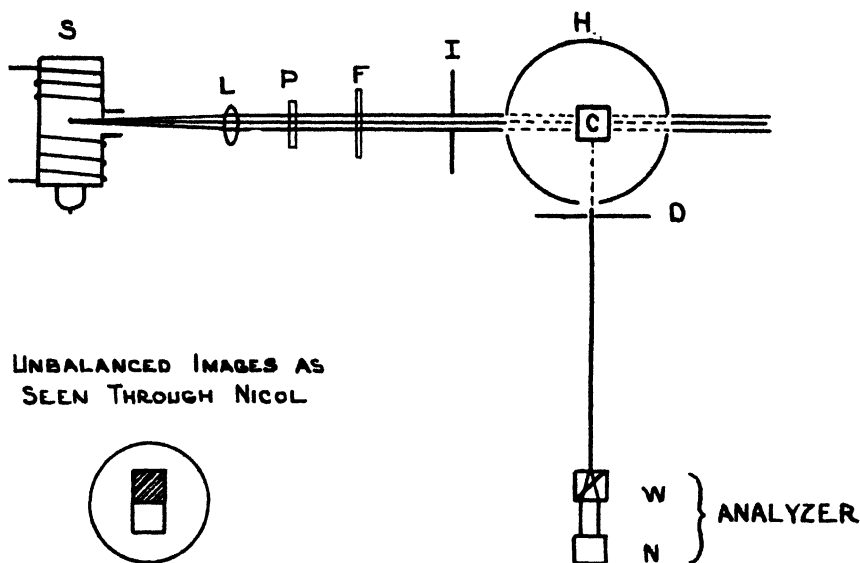
Fig. 3. Apparatus for the measurement of depolarization

exit port with a minimum of stray radiation. At right angles to the incident beam there is a port for the observation of the scattered light. The cell, C, was placed in the center of the housing through a square opening which permitted reproducibility of position by serving as a guide. The entire housing was painted dull black, providing a dark non-planar background for the observation of the scattered light.

At right angles to the plane of the incident light, in the path of the scattered light leaving the observation port, is a diaphragm, D, with an opening 0.50 cm. square. This square defines the beam before it enters the Wollaston prism, W, which separates the horizontal and vertical components. On the same axis as the Wollaston prism there is a Nicol prism, N, mounted on a divided circle read to 0.1°. The Nicol prism may be rotated through 360°.

In the optical method of observation the Wollaston prism is adjusted so that the images of the square hole (from diaphragm D) arising from the vertical and horizontal components of the scattered light are one above the other with the edges just touching (figure 3). In making a measurement, the Nicol is rotated until the two images have the same intensity. There are four such positions, corresponding to two pairs of balance positions 180° apart. In order to attain maximum accuracy it was necessary to measure points on both sides of the true equi-intensity point and average these values. In practice four readings were taken for each apparent match position. The depolarization value (the ratio of the intensities of the two beams) is given by the square of the tangent of the angle of rotation θ. In this procedure the angle θ is half the angle between match points.

In general the angle could be measured with an accuracy of $\pm 0.05°$. The precision of the depolarization values depends on the magnitude of the angle θ; consequently, the probable error is not directly related to the depolarization value. The resolution of the instrument did not permit the actual measurement of angles less than 5°. ρ_h could usually not be measured directly because the scattering was too weak.

B. Preparation of solutions

Fractions of polystyrene, polyvinyl chloride, and cellulose acetate whose molecular weights had been determined by one of the standard methods were available for investigation. Great care was exercised in purifying these fractions and in preparing optically clean solutions. From the purified fractions, solutions were made up to 1 per cent concentration and were then filtered successively through medium and fine sintered (fritted) glass. In some instances it was also necessary to filter the solutions through bacteriological filters (Selas No. 03 and/or 04). Pressure filtration was employed in all cases. The optical clarity of a solution was tested by viewing (often with the aid of a magnifying lens) the very low angle scattering, that is, a few degrees from the forward beam. In this manner dust particles or any suspended matter in the Tyndall beam is readily detected.

C. Calibration

The apparatus was checked by measuring the depolarization values of benzene and toluene. The measured values are recorded in table 2, together with the known depolarization values for these liquids. The agreement is satisfactory. The calculated values of ρ_h (equation 4) agree with the expected values of unity for such liquids.

D. Measurements

(1) *Cellulose acetate:* Three fractions and one unfractionated sample were measured in acetone solution (see table 3). The fractions were prepared and their molecular weights determined (correlated osmotic pressure and viscosity) by Badgley (1). The unfractionated material was a commercial sample whose molecular weight has been measured by osmotic pressure, viscosity, ultra-

centrifuge, and light scattering. The weight average molecular weight is recorded.

(2) *Polyvinyl chloride:* Three fractions and the unfractionated polymer from which the fractions were separated have been measured in ethyl methyl ketone solution (see table 4). Osmotic-pressure molecular weights (7) are recorded. The unfractionated material was the commercial resin Geon 101.

(3) *Polystyrene:* Three polystyrene fractions were studied both in toluene and in ethyl methyl ketone solutions and also at several concentrations (see tables 5 and 6). These fractions were prepared by only a single rough fractionation and consequently have wide distributions of molecular weight. Fraction

TABLE 2

Depolarization values for pure liquids

		BENZENE	TOLUENE
ρ_u........... ...	This work........	0.410	0.490
	Peyrot (17)..	0.420	0.480
ρ_v. .	This work	0.253	0.331
	Lotmar..........	0.267	
ρ_h..............	This work (calculated).. . . .	0.97	1.03

TABLE 3

Depolarization values of cellulose acetate in acetone

FRACTION NO.	MOLECULAR WEIGHT	1.00 PER CENT SOLUTION		0.50 PER CENT SOLUTION	
		ρ_u	ρ_v	ρ_u	ρ_v
27B.. . . .	65,000	0.045	0.006	0.045	0.006
16B	90,000	0.029	0.005	0.028	0.004
8B	158,000	0.017	0.001	0.019	0.001
Unfractionated.... . .	90,000	0.029	0.0015		

No. 70-1 was obtained from polystyrene polymerized with catalyst at 70°C. in toluene. The other two fractions were taken from polystyrene polymerized at room temperature without catalyst to 30 per cent conversion. Viscosity measurements indicated a molecular weight of 800,000. Osmotic-pressure measurements on the other two fractions showed their molecular weights to be 400,000 for 100-L and 3,200,000 for 100-H.

The measured depolarization values in toluene passed through a minimum on decreasing the concentration of the solution (see table 5). This results when the solvent scattering is comparable to the solution scattering and the depolarization values of the solvent are large, for under these conditions the solvent contributes to the observed depolarization and in an amount that increases with decreasing concentration of solute. The depolarization due to the solute alone

TABLE 4

Depolarization values of polyvinyl chloride in ethyl methyl ketone

FRACTION NO.	MOLECULAR WEIGHT	CONCENTRATION	ρ_u	ρ_v	ρ_h (CALCULATED)
		g. per 100 ml.			
20..........	76,000	1.00	0.010	0.004	0.66
14............	120,000	1.00	0.017	0.005	0.41
7............	140,000	1.00	0.024	0.004	0.25
Unfractionated........ .	120,000	1.00	0.018	<0.001	
	120,000	0.50	0.015	<0.001	
	120,000	0.25	0.014	<0.001	
	120,000	1.00	0.018	0.0006	

TABLE 5

Depolarization values for polystyrene in toluene

FRACTION NO	CONCENTRATION	UNCORRECTED		CORRECTED		CALCULATED
		ρ_u	ρ_v	ρ_u	ρ_v	ρ_h
	g. per 100 ml					
100-L	1.00	0.110	0.032	0.095	0.020	0.26
	0.58	0.088	0.026	0.064	0.008	0.06
	0.25	0.095	0.031	0.057	0.000	
100-H. . ..	1.00	0.070	0.011	0.065	0.003	0.048
	0.58	0.058	0.010	0.048	0.001	0.021
70-1.......	1.00	0.091	0.033	0.075	0.017	0.29
	0.76	0.078	0.030	0.056	0.012	0.27
	0.58	0.072	0.020	0.045	0.000	
	0.40	0.083	0.024	0.055	0.001	
	0.25	0.091	0.023	0.055	0.002	

TABLE 6

Depolarization values of polystyrene in ethyl methyl ketone

FRACTION NO.	CONCENTRATION	ρ_u	ρ_v	ρ_h (CALCULATED)
	g. per 100 ml.			
100-L...	1.00	0.015	0.0015	0.11
100-H.	1.00	0.011	0.0003	0.028
70-1.................... .	1.00	0.012	0.0003	0.0255
	0.71	0.008	0.0001	0.0126
	0.55	0.007	0.0001	
	0.38	0.007	0.0001	

is readily obtained from the following expression (13), which is derived from the assumption that the product of the observed depolarization and total intensity is equal to the sum of the corresponding products for the solute and solvent:

$$\rho_2 = \frac{\rho_{12} I_{12}(1 + \rho_1) - \rho_1 I_1(1 + \rho_{12})}{I_{12}(1 + \rho_{12}) - I_2(1 + e_{12})} \tag{5}$$

The corrected depolarization values are for the polystyrene–toluene solutions—the only case studied that required this correction. The intensities I_2 and I_{12} were obtained from the turbidities of the toluene and the solution, respectively,
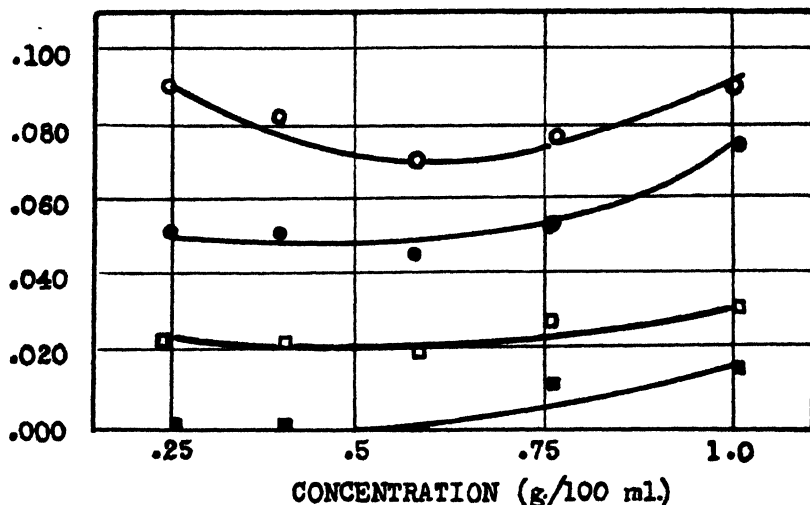
FIG. 4. Depolarization of polystyrene in toluene: O, ρ_u uncorrected; $\bullet$, ρ_u corrected; $\square$, ρ_v uncorrected; $\blacksquare$, ρ_v corrected.

as measured in a turbidimeter (20). The variation of the depolarization values with concentration and the effect of the correction for solvent depolarization are shown in figure 4 for the toluene solutions of polystyrene 70-1. Some calculated values for ρ_h are recorded for use in the discussion. These can be considered as only approximate.

<div align="center">DISCUSSION OF RESULTS</div>

<div align="center">1. Cellulose acetate</div>

In contrast to the other systems measured, the depolarization values decrease sharply with increasing molecular weight. On the basis of size alone the effect on ρ_u should have been the opposite; consequently, anisotropy must be a sensitive function of molecular weight. Since ρ_v, which is a qualitative measure of anisotropy, almost vanishes at a molecular weight of 158,000, it appears that in the range of molecular weight the cellulose acetate molecule is on the average fairly isotropic. It follows then that below 100,000 in molecular weight the

molecules must become increasingly anisotropic to a very pronounced degree. The ρ_v values corroborate this view.

The depolarization values are essentially independent of concentration regardless of molecular weight. Since acetone is far from being an indifferent solvent, this fact seems to indicate that the molecules are stiff enough to be little affected by polymer–polymer interactions. This constancy of shape and size as concentration is varied was also noted in the study of molecular size by measurements of the dissymmetry of scattered light (20).

These observations are consistent with the picture that cellulose acetate molecules are relatively quite stiff and do not tend to curl back on themselves noticeably until the molecular weight range of 100,000 is reached. Recent studies of viscosity (1) and sedimentation velocity (19) are in agreement with this view.

The ρ_u value for the unfractionated material indicates that ρ_u is a function of weight average molecular weight. The low value of ρ_v is difficult to explain. This cannot be passed by as a single anomaly, for a similar observation was made in the polyvinyl chloride system. If Krishnan's relation holds, this indicates that in going from a fraction to a wide distribution with the same weight average molecular weight, ρ_v and ρ_h both decrease. This could perhaps be possible if ρ_v depended approximately on the weight average molecular weight and ρ_h on a lower average such as the number average molecular weight. It is planned to investigate this point further.

2. Polyvinyl chloride

Here ρ_u increases regularly with increasing molecular weight, ρ_v is constant, and ρ_h (calculated) decreases. The constancy of ρ_v demonstrates that the anisotropy is essentially independent of molecular weight. The increasing departure of ρ_h from unity is solely responsible for the increase of ρ_u with molecular weight. Thus we have here a substance whose finite anisotropy is independent of molecular weight but whose size increases rapidly with molecular weight. The latter observation is consistent with the molecules being coiled in solution. The constant, finite anistropy would indicate that this is not a randomly coiled molecule, but rather that the carbon–chlorine dipoles are preferentially oriented (a coöperative phenomenon) to a degree independent of molecular weight.

Again we have the curious suppression of the ρ_v value for the unfractionated material. The last entry was a careful check on this point, using an entirely different solution. The inaccuracy of the ρ_v values prevents the determining of the cause for the gradual decrease of ρ_u with dilution.

3. Polystyrene

A number of variables have been studied in this case. The effect of molecular weight can be seen from examining the data for fractions 100-L and 100-H. In both solvents ρ_u, ρ_v, and ρ_h are larger for the compound of lower molecular weight. This indicates, of course, that the molecules of lower molecular weight are smaller and more anisotropic.

With decreasing concentration ρ_u in all cases decreases rapidly to finite values

which do not change further. Similarly, ρ_v decreases rapidly to very small values. This means that ρ_h decreases correspondingly. The picture this information presents is that upon dilution the molecules become more isotropic and also increase in size, i.e., the molecules become more swollen.

Considerable discussion has centered about the effect of polymerization conditions on branching and molecular shape. Comparing the data on fractions 100-L and 70-1, which have approximately the same molecular weight, we see that in toluene there is no significant difference in anisotropy and size. In ethyl methyl ketone, however, the data indicate that the molecules of fraction 100-L are smaller and more isotropic than those of fraction 70-1. This indication is not consistent with increasing branching at higher temperatures of polymerization (G. V. Schulz) but agrees better with the osmotic pressure-viscosity data of Alfrey, Bartovics, and Mark[2], which indicated that more extended molecules were produced at higher polymerization temperatures. *A reasonable interpretation* of this situation is given by Huggins[3] in terms of the population of the non-equivalent dispositions of hydrogen atom and styrene radical relative to the C-C plane.

It is of interest to note here the magnitude of the correction due to orientation fluctuations that must be applied to molecular weights determined by light scattering. For the systems studied here, this correction, $(6 - 6\rho_u)/(6 + 7\rho_u)$, varies from 4 to 10 per cent. Further consideration (21) shows that this quantity represents an upper limit for the correction.

SUMMARY

The theory of depolarization of scattered light is developed with particular reference to the study of polymer molecules in solution. A simple apparatus, based on the Cornu method, is described. This permits the measurement of the depolarization of the transversely scattered light, using unpolarized and vertically and horizontally polarized incident light. Measurements on fractions of cellulose acetate, polyvinyl chloride, and polystyrene as a function of molecular weight, concentration, and solvent are reported. The data are interpreted in terms of the changes in anisotropy and size as a function of the above-mentioned variables.

REFERENCES

(1) BADGLEY, W. J.: Thesis, Brooklyn Polytechnic Institute, 1945.
(2) BHAGAVANTAM, S.: *Scattering of Light and the Raman 'Effect*. Chemical Publishing Co., Inc., Brooklyn, New York (1942).
(3) CABANNES, J., AND ROCARD, Y.: *La diffusion moléculaire de la lumière*. Presses Universitaires de France, Paris (1929).

[2] T. Alfrey, A. Bartovics, and H. Mark: J. Am. Chem. Soc. **65**, 2319 (1943).
[3] M. L. Huggins: J. Am. Chem. Soc. **66**, 1991 (1944).

(4) Debye, P.: J. Applied Phys. **15**, 456 (1944).
(5) Doty, P., Zimm, B., and Mark, H.: J. Chem. Phys. **13**, 159 (1945).
(6) Doty, P., and Badgley, W. J.: Unpublished results.
(7) Gans, R.: Ann. Physik **37**, 881 (1912); **47**, 270 (1915); **62**, 330 (1920); **65**, 97 (1921).
For a general account: *Handbuch der Experimental Physik*, Vol. XIX, Akademische Verlagsgesellschaft, Leipzig (1928); Physik. Z. **37**, 19 (1936).
(8) Gehman, S. D., and Field, J. E.: Ind. Eng. Chem. **29**, 793 (1937).
(9) Hoover, C. R., Putnam, F. W., and Wittenberg, E. G.: J. Phys. Chem. **46**, 81 (1942).
(10) Krishnan, R.: Proc. Indian Acad. Sci. **1A**, 212 (1934); **1A**, 717, 782 (1935).
(11) Krishnan, R.: Proc. Indian Acad. Sci. **3A**, 211 (1936); **5A**, 94, 305, 407, 409, 551 (1937).
(12) Krishnan, R.: Proc. Indian Acad. Sci. **7A**, 21, 91, 98 (1938).
(13) Lotmar, W.: Helv. Chim. Acta **21**, 792 (1938).
(14) Lotmar, W.: Helv. Chim. Acta **21**, 953 (1938).
(15) Mie, G.: Ann. Physik **25**, 377 (1908).
(16) Perrin, F.: J. Chem. Phys. **10**, 415 (1942).
(17) Peyrot, P.: Compt. rend. **203**, 1512 (1936).
(18) Rayleigh, Lord: Phil Mag. [4] **41**, 107, 274, 477 (1871).
(19) Singer, S., and Ster, K. G.: Unpublished results, Polytechnic Institute of Brooklyn.
(20) Stein, R. S., and Doty, P.: Paper presented before the New York Section of the American Chemical Society, June 7, 1945; J. Am. Chem. Soc., in press.
(21) Zimm, B., Stein, R., and Doty, P.: Polymer Bulletin **1**, 90 (1945).

THE THERMAL DECOMPOSITION OF ETHYLENE IODIDE CATALYZED BY IODIDE IONS

T. IREDALE AND (MISS) T. RODNA STEPHAN

Physical Chemistry Laboratories, University of Sydney, Sydney, Australia

The thermal decomposition of ethylene iodide in the presence of free iodine, both in the vapor state and in solution in carbon tetrachloride, has been studied by several investigators (1, 9, 12, 15). Also, a study has been made of the influence of iodine atoms on the photodecomposition of the iodide in carbon tetrachloride solution (18, 19). In all these cases it was concluded that iodine played the part of a catalyst. The influence of iodide ions on the decomposition has not been studied very much. There is only one early paper of any importance on the subject, that by Slator (21), but he did not consider the matter from the point of view of the modern theory of reaction kinetics.

This paper presents the results of a study of the thermal decomposition of ethylene iodide in aqueous alcohol in the presence of potassium iodide at four different initial concentrations and at four different temperatures. The reaction appears to be of the second order and, within a reasonable factor, of a normal type.

EXPERIMENTAL

The ethylene iodide was prepared (20) by passing ethylene for about 3 days through a paste of iodine in absolute alcohol containing ground glass. The

ethylene iodide formed on the glass wool, and was recrystallized from aqueous alcohol. Long, needle-like crystals which melted at 82°C. were obtained. These crystals turned brown on exposure to air; if the ethylene iodide was kept in a desiccator, crystals of iodine gradually formed amidst the white solid. The substance could be kept in a pure state in an atmosphere of ethylene. Later it was discovered (12) that if the ethylene iodide was crystallized from carbon tetrachloride it remained colorless when kept in the air, but became contaminated with iodine if kept in a closed vessel, unless in an atmosphere of ethylene.

The potassium iodide was recrystallized several times from water.

All the reaction experiments were carried out in a water thermostat, the temperature of which was controlled electrically to 0.1°C.

The solvent used for all the reactions was a mixture of 75 per cent by volume of ethyl alcohol and 25 per cent water. The initial concentration of each of the reactants was the same in every case, assuming for the time being that the potassium iodide was 100 per cent dissociated.

The decomposition was measured at the temperatures 15°, 20°, 25°, and 35°C.

It was found advisable to use solutions of concentrations less than 0.04 M and greater than 0.005 M, since at low temperatures ethylene iodide reaches its solubility limit at the high concentration, and the decomposition is too slow at the low concentration. The chosen concentrations were 0.03, 0.02, 0.015, and 0.01 molar with respect to both ethylene iodide and iodide ion.

The solutions were made up in the following manner: The required amount of ethylene iodide for 100 ml. of solution was weighed out accurately, dissolved in an appropriate volume of ethyl alcohol (75 ml.), and placed in the thermostat at the temperature of the experiment. The weight of potassium iodide required for 120 ml. of solution was weighed out and dissolved in 30 ml. of distilled water, and the solution was warmed to the temperature of the experiment. Twenty-five milliliters of this potassium iodide solution was then added to the alcoholic ethylene iodide solution, the time of this addition being noted as the beginning of the reaction. Due account was taken of the slight contraction in volume which occurred, and also of the very small momentary increase in temperature. The rate of reaction was measured by withdrawing, at well-spaced intervals, 5 to 10 ml. of the solution with the aid of a calibrated pipet, chilling with a freezing mixture, and titrating the iodine formed with dilute sodium thiosulfate (0.01 N). The end point was decided by the disappearance of the yellow color of the iodine, as starch could not be used in the presence of ethylene iodide. The free iodine was titrated in neutral solution. It has been contended that titration with sodium thiosulfate is more accurate in acid (3) than in neutral solution, but equal accuracy has also been claimed for both (16, 23). A greater source of error which had to be guarded against was found, i.e., evaporation of iodine at the higher temperatures, which can reduce the accuracy of the titration (17). At the low temperatures employed in this work, iodine itself in the absence of iodide ion was not found to accelerate the decomposition of ethylene iodide to any appreciable extent, nor did strong light noticeably affect the velocity of decomposition. No oxidation process

can be involved, as replacement of the air in the reaction flask by the inert gas nitrogen does not affect the velocity. In course of time the decomposition of the ethylene iodide appeared to go to completion, determined by the iodine titrations.

TABLE 1

INITIAL CONCENTRATION a	$1/a$	$t_1/_4$	MEAN k
Temperature, 15°C.			
			liters/mole min.
0.01 M	100	640	0.051
0.015	66.6	455	
0.02	50	348	
0.03	33.3	247	
Temperature, 20°C.			
0.01 M	100	350	0.094
0.015	66.6	244	
0.02	50	195	
0.03	33.3	138	
Temperature, 25°C.			
0.01 M	100	230	0.144
0.015	66.6	158	
0.02	50	119	
0.03	33.3	83	
Temperature, 35°C.			
0.01 M	100	90	0.373
0.015	66.6	63	
0.02	50	45	
0.03	33.3	32	

DISCUSSION OF RESULTS

The results of the measurements of the velocity of decomposition are recorded in table 1. The velocity, at any rate until somewhat more than the time for half-decomposition, followed strictly the second-order equation

$$k = 1/t \, \frac{x}{a(a - x)}$$

a being the initial concentration of both ethylene iodide and potassium iodide, and x the number of moles of ethylene iodide decomposed per liter (equivalent to concentration of iodine in moles per liter) after time t (minutes). At all temperatures, a plot of the time for one-quarter of complete decomposition (t_4) against the reciprocal of the initial concentration gave a straight line (figure 1), which is a more satisfactory proof that the reaction follows the second-order kinetics.

These results are somewhat different from those of Slator (21), which seemed to show that the reaction was of the first order with respect to ethylene iodide. The important consequence of the second-order mechanism is that iodide ion is used up as well as ethylene iodide during the course of the reaction. This means that the I_3^- ion formed does not function as a catalyst. The equilibrium constant

$$K = \frac{[I_2][I^-]}{[I_3^-]}$$

is 7.2×10^{-4} at 0°C. and 14×10^{-4} at 25°C. (10), so that when $[I^-]$ is high, the greater part of the iodine goes over to I_3^-, taking the equivalent of I^- with it.
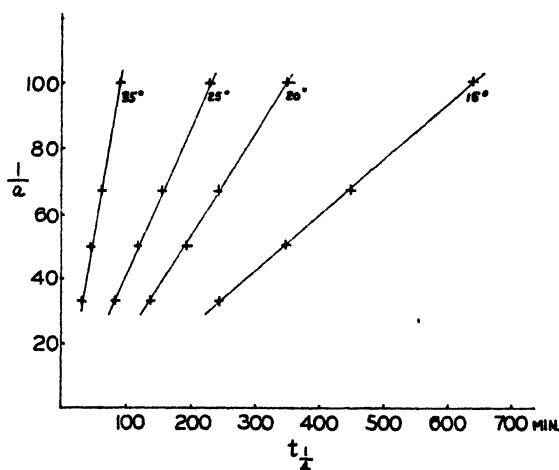
FIG. 1

The velocity of the reaction $I_2 + I^- = I_3^-$ may be assumed to be relatively very much faster than the decomposition.

But a more plausible mechanism for the decomposition is this: I^- and $C_2H_4I_2$ possessing the requisite activation energy give on collision the activated complex $C_2H_4I_3^-$. This complex may go over into C_2H_4 and I_3^- or return to the original forms $C_2H_4I_2$ and I^-. The greater probability that the former will happen requires that the entropy of activation shall have at least a positive value (6), or that the factor, P, in the equation

$$k = PZe^{\frac{-E}{RT}}$$

shall be greater than or not much less than unity (8) (Z being the collision frequency and E the experimental energy of activation).

Since Z varies as the square root of the absolute temperature, we can write

$$k = Pc\sqrt{T}e^{\frac{-E}{RT}}$$

c being a constant.   Whence

$$\log_e k = \text{const.} + \tfrac{1}{2}\log_e T - \frac{E}{RT} \qquad (22)$$

We have plotted

$$\frac{1}{2}\log_{10} T - \frac{0.4343}{T}$$

against $\log_{10}(k \times 10^2)$, a reasonably straight line being obtained (figure 2). The energy of activation was calculated to be 16,500 cal.
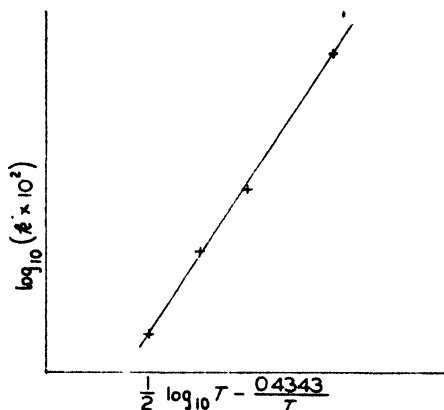
FIG. 2

In the equation

$$k = Ze^{\frac{-E}{RT}} = \sigma_{1,2}^2 \frac{N}{1000}\left(8\pi RT\left(\frac{1}{M_1} + \frac{1}{M_2}\right)\right)^{\frac{1}{2}} e^{\frac{-E}{RT}}$$

(omitting, for the time being, the probability factor, P) in which the velocity constant, k, is related to the collision frequency, Z, and the energy of activation, E, M_1 and M_2 are the molecular weights of the reactants, and $\sigma_{1,2}$, their mean effective molecular diameter, equals $\dfrac{\sigma_1 + \sigma_2}{2}$.

σ_2, the effective diameter of the iodide ion, without taking into account any solvation, may be put equal to 4.36×10^{-8} cm. (13).

σ_1, the effective diameter of the ethylene iodide molecule, is not easy to determine. Two methods have been used in arriving at an estimate of this quantity:

Method I: The cube root of the molar volume, V, of the pure liquid or solid

at low temperatures multiplied by $1.33 \times 10^{-8} = 1.33 \times 10^{-8} \sqrt[3]{V} = 6.78 \times 10^{-8}$ cm. (11).

Method II: The effective diameter is taken to be equal to twice the length of the C—I bond (2.14×10^{-8} cm.) (14) and $= 2 \times 2.14 \times 10^{-8} = 4.28 \times 10^{-8}$ cm. The results of these calculations are given in table 2. It will be seen that P, the ratio $k_{obsd.}/k_{calcd.}$, is about 5×10^{-2}, so that the reaction may be considered to be very nearly of the normal type.

The entropy of activation, ΔS_c, was calculated from the equation

$$k = e \frac{kT}{h} e^{\frac{-E}{RT}} e^{\frac{\Delta S_c}{R}} \qquad (7)$$

and came out to be $- 0.68$ E.U.

A higher order of accuracy would be obtained by evaluating k_0 from the Brønsted–Bjerrum equation: .

$$k = k_0 f_1 f_2 \qquad (2, 4)$$

where f_1 and f_2 are the activity coefficients of the reacting species, being unity at very great dilution. The activity coefficient of ethylene iodide is probably

TABLE 2

TEMPERATURE	k (obsd.) $\times 10^4$	k (calcd.) $\times 10^2$		$P \times 10^2$
		Method I	Method II	
°C.	liters/mole sec	liters/mole sec.	liters/mole sec.	
15	8.5	2.1	1.6	4.0–5.3
20	15.7	3.8	2.9	
25	24.0	6.2	4.7	
35	62.0	15.6	12.0	

very close to unity at the low concentrations employed. The activity coefficients of potassium iodide in aqueous alcohol solutions were not available to us. Gelbach (5) has found that at 25°C. in aqueous solution the coefficient varies from 0.9 at 0.01 M to 0.86 at 0.03 M, which indicates the order of the correction factor that would have to be applied to increase the accuracy of our results. We do not think that our general conclusions would be changed very much by any further refinements in the methods employed.

SUMMARY

The thermal decomposition of ethylene iodide catalyzed by iodide ion has been measured at four different temperatures.

The reaction follows second-order kinetics, the energy of activation is 16,500 cal., and the entropy of activation is $- 0.68$ E.U.

REFERENCES

(1) ARNOLD AND KISTIAKOWSKY: J. Chem. Phys. 1, 166 (1933).
(2) BJERRUM: Z. physik. Chem. 108, 82 (1924).
(3) BRAY AND MILLER: J. Am. Chem. Soc. 46, 2204 (1924).
(4) BRØNSTED: Z. physik. Chem. 115, 337 (1925).

(5) GELBACH: J. Am. Chem. Soc. **55**, 4857 (1933).

(6) GLASSTONE: *Text-book of Physical Chemistry*, p. 1082. D. Van Nostrand Company, Inc., New York (1940).

(7) GLASSTONE, LAIDLER, AND EYRING: *The Theory of Rate Processes*, p. 199.

(8) HINSHELWOOD: *The Kinetics of Chemical Change in Gaseous Systems*, p. 239. Clarendon Press, Oxford (1929).

(9) IREDALE AND MARTIN: J. Phys. Chem. **38**, 365 (1934).

(10) JONES AND KAPLAN: J. Am. Chem. Soc. **50**, 1845 (1928).

(11) MOELWYN-HUGHES: *The Kinetics of Reactions in Solution*, p. 15. Clarendon Press, Oxford (1933).

(12) MOONEY AND LUDLAM: Proc. Roy. Soc. Edinburgh **49**, 160 (1929).

(13) PAULING: *The Nature of the Chemical Bond*, 2nd edition, pp. 346, 349. Cornell University Press, Ithaca, New York (1940).

(14) Reference 13, p. 167.

(15) POLISSAR: J. Am. Chem. Soc. **52**, 956 (1930).

(16) POPOFF AND WHITMAN: J. Am. Chem. Soc. **47**, 2259 (1925).

(17) RICE, KILPATRICK, AND LEMKIN: J. Am. Chem. Soc. **45**, 1361 (1923).

(18) SCHUMACHER AND STIEGER: Z. physik. Chem. **12B**, 348 (1930).

(19) SCHUMACHER AND WIIG: Z. physik. Chem. **11B**, 45 (1930).

(20) SEMENOFF: Jahresber. Fortschritte Chem. **1864**, 483.

(21) SLATOR: J. Chem. Soc. **85**, 1697 (1904).

(22) TOLMAN: J. Am. Chem. Soc. **42**, 2506 (1920).

(23) VOSBURGH: J. Am. Chem. Soc. **44**, 2120 (1922).

RADIO-FREQUENCY DIELECTRIC PROPERTIES OF DEHYDRATED CARROTS

APPLICATION TO MOISTURE DETERMINATION BY ELECTRICAL METHODS

W. CRAWFORD DUNLAP, JR., AND BENJAMIN MAKOWER

Western Regional Research Laboratory[1], Albany, California

I. INTRODUCTION

Very few comprehensive studies have been made of the radio-frequency properties of vegetable materials containing absorbed water. Tausz and Rumm (11) have made a fairly complete study of several materials, including starch, tobacco, and slate, but their measurements were made only at low frequencies, in the neighborhood of 1000 cycles per second. Argue and Maass (1) have measured the dielectric constant of a cellulose–water system as a function of the moisture content, at one frequency, 500 kc., and one temperature, 25°C. Several investigations have been carried out on the radio-frequency properties of soils, which have dielectric properties similar to those of organic systems containing dispersed water. Smith-Rose (10) has measured the dielectric constant and the conductivity of various types of soil as a function of the moisture content and

---

[1] Bureau of Agricultural and Industrial Chemistry, Agricultural Research Administration, United States Department of Agriculture.

of the frequency (10 kc. to 10 mc.) at one temperature. Fricke and his collaborators (4, 5, 6) have made measurements on gelatin–water systems and on various other systems, such as kaolin–water and quartz–water suspensions, at frequencies from 2 kc. to 65 mc. Errera and Sack (3) have recently measured dielectric properties of animal fibers at frequencies from 8 kc. to 13 mc. No previous work has been done upon dehydrated vegetables in this field; at least there is no information available in the literature.

The work reported in the present investigation deals with the dielectric properties of dehydrated carrots, especially with the radio-frequency properties. The dielectric constant and the electrical conductivity have been measured with respect to changes of moisture content, temperature, frequency, bulk density, and particle size. Some work has also been done on the effect of electrode polarization upon the results at low frequencies. These properties are of especial importance for the measurement of moisture content by electrical methods, including d.c., low-frequency, and radio-frequency methods. Following presentation of the results a discussion is given of various electrical methods of measuring moisture content. The results reported in the present paper may also have some interest in connection with the problem of the nature of the dielectric properties of dispersed materials of biological origin containing absorbed water.

II. METHOD, APPARATUS, AND MATERIALS

The preliminary measurements of capacity were made by determination of the change of capacity required in a parallel standard condenser to restore resonance. Although the method was found to give excellent precision for capacity measurements at low moisture contents, the broadening of the resonance curve caused by the leakage conductivity of the cell at high moisture contents (above 12–14 per cent) led to abandonment of this method in favor of a radio-frequency bridge type of measurement. This bridge circuit has been discussed by Oncley (8) and T. M. Shaw (9). The frequency range obtainable by use of an all-wave receiver as detector was from 18 kc. to 5 mc. Above 5 mc. the shielding of the bridge became very poor, and balance was difficult. In the range 18 kc. to 5 mc., with this bridge and a General Radio Co. Type 722D standard condenser, and with the cell described below, capacities from 10 to 1100 $\mu\mu$f and conductivities of the order 10^{-5} to 10^{-9} mho per centimeter could be measured.[2]

[2] It is necessary in some cases to correct results obtained from a high-frequency bridge. The most commonly required correction is that for the inductance L of the leads of the cell. This inductance affects the capacity according to the following equation:

$$C_e = \frac{C}{1 - \omega^2 LC}$$

where C is the true capacity, C_e the measured value, and $\omega = 2\pi \times$ frequency of oscillation. In the present work this correction is not needed, since at high frequencies, where the correction is most likely to be needed, the capacity is small, and when the capacity is large the frequency is small. This conclusion has been checked by measurement of the inductance of the leads and calculation of the correction for several typical cases. In all these cases the correction was negligible. It has also been noticed that there were slight irregularities in ϵ when small changes of capacity were being measured, owing to lack of constancy of inductance of the standard resistor, for different resistance values.

The experiments were carried out by use of the cell represented in figure 1. The outer diameter of the inner electrode was 3.49 cm. and the inner diameter of the outer electrode was 5.60 cm. The annular region containing the sample was 5.06 cm. in length. The cell was ordinarily filled with a constant weight of 45 g. of dehydrated material. Thus the bulk density was equal to 0.760 g. per cm.³ This value for the bulk density is to be assumed in the remainder of this paper, unless otherwise specified. The outer electrode was grounded in all the measurements to avoid errors due to presence of stray capacities. Fiducial marks on each cap and on the shell enabled one to screw the caps on to the same point for each experiment and thus to reproduce accurately the end capacities. The measurements were made in a room maintained at a temperature of 22°C. ± 1.0° and a relative humidity of 50 per cent. For control of the temperature of

BRONZE

POLYSTYRENE

2 CM.
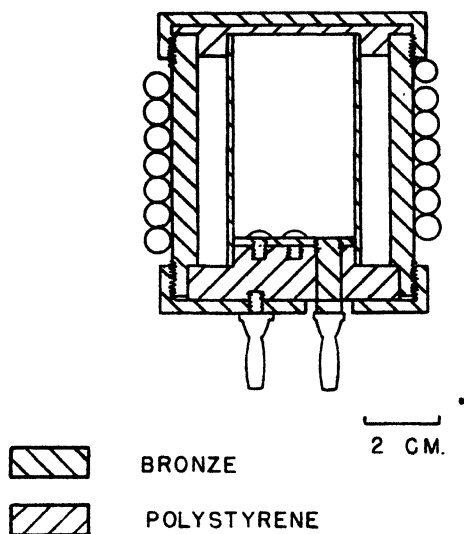
FIG. 1. Longitudinal section of cell used in the dielectric measurements

the cell, water was circulated through the coil indicated in figure 1. This coil was connected with another coil immersed in a bath whose temperature could be held constant to ±0.2°C. Circulation was obtained by use of a centrifugal pump. The temperature was read from a mercury thermometer immersed in the liquid as it returned to the bath. Since the reading on this thermometer was 0.2° or 0.3°C. different from the reading of that in the bath, the average temperature was used in tabulation of the results. All the measurements were begun after a lapse of at least 30–40 min. after beginning of circulation, which was the time required to bring the cell to constant temperature.

The preliminary experiments were carried out by use of the cell equipped with bakelite-impregnated fabric insulators. The considerable variation in the "empty" capacitance value of the cell, caused by water absorption of this insulation, led to replacement of these insulators with others made of polystyrene.

The polystyrene-insulated cell retained high insulation resistance and low power factor even at 100 per cent humidity.

It is important to know fairly accurately the value of the cell constant, C_0, which may be defined by the relation

$$C_0 = \frac{C_f - C_e}{\epsilon - 1} \qquad (1)$$

As a first approximation, C_0 is the capacity of the empty cell minus lead capacity and edge-effect capacity. C_e is the capacity of the empty cell. C_f is the capacity of the cell filled with material. ϵ is the dielectric constant of the material. C_0 can be calculated fairly accurately for an infinitely long cylindrical condenser by the formula

$$C_0 = \frac{1.11l}{2 \log \frac{b}{a}} \mu\mu\text{f}$$

where b = the inside diameter of the outer electrode, a = the outside diameter of the inner electrode, and l = the length of the cylinder in centimeters. For the present cell this value was 8.35 $\mu\mu$f, but edge effects made this value inaccurate. The value of C_0 was also determined by calibration with water, amyl alcohol, and caprylic alcohol (2-octanol). The dielectric constants of the alcohols were separately determined in a three-plate parallel-plate condenser with quartz insulation. This condenser was calibrated by use of purified acetone and benzene. Acetone and benzene could not be used in the cell of figure 1, because they dissolved the polystyrene insulation. The values of C_0 obtained by the above procedure varied from 8.35 for water to 9.04 for caprylic alcohol. It seems that changes in the end capacities caused by the presence of material of high dielectric constant caused the cell constant to decrease with increase in dielectric constant of the contents. The value for water is approximately equal to the calculated value. The value obtained by use of caprylic alcohol (C_0 = 9.04 $\mu\mu$f) was used for all ϵ from 1 to 10. When the uncorrected ϵ obtained from equation 1 with C_0 = 9.04 varied from 10 to 30, ϵ was recalculated with a value of C_0 equal to 8.90. Similarly, for uncorrected ϵ in the range of 30 to 50, C_0 = 8.70; for ϵ = 50 to 70, C_0 = 8.50; and for ϵ > 70, C_0 was taken to be 8.35 $\mu\mu$f.

No attempt was made to calibrate the cell for conductivity measurements. Instead, the calculated cell constant for conductivity was used. Thus, the specific conductivity is calculated from the observed value of the resistance, R, by means of the formula

$$\sigma = \frac{\log \frac{b}{a}}{2\pi l R}$$

The use of this equation is justified, since the observed variations in the conductivity are usually very great, often involving changes by factors of several powers of ten; hence high accuracy is not needed.

Accurate measurement and even definition of d.c. conductivity of non-conductors is in general rather difficult, because the result may vary with applied voltage, time of application of voltage, and other factors. Electrode polarization also affects the results, since for high moistures readings of resistance obtained with a d.c. ohmmeter showed immediate increase with time upon application of voltage. No special precautions have been taken in this work with respect to any of the above factors, and the results for d.c. resistance cannot be considered to be of high precision. The higher conductivities were measured with a multitester ohmmeter and the conductivities in the range 10^{-7} to 10^{-10} ohm^{-1} with an electronic ohmmeter. A ballistic galvanometer method was used for conductivities in the range 10^{-10} to 10^{-13} ohm^{-1}. Conductance of the polystyrene insulation was found to be much less than that of the sample in all cases.

The carrots used in the present work were obtained from two different sources. One type was obtained on the open market and consisted of a mixture of varieties, but was probably mostly of the Chantenay variety. The other type consisted of the Tendersweet variety. Although it has been found in other work that dielectric properties, and especially the conductivity, vary with variety, the two types used in the present work were found to have practically identical properties. The carrots were dehydrated by commercial dehydration methods by the Engineering Division of this laboratory. The samples were brought to their final moisture content by placing them in desiccators over solutions of various concentrations of sulfuric acid (7). The moisture content was determined at intervals during the work by heating for 22 hr. at 70°C. in a vacuum oven after grinding in a Wiley mill through a U. S. No. 40 sieve. Moisture content is expressed throughout this paper in terms of percentage of dry weight. Although there is some doubt as to the degree of correspondence of the "water" determined by this method and the "water" involved in a dielectric measurement, it was considered that the accuracy of the determination was satisfactory for determination of the moisture differences among the samples used.

The initial experiments consisted of measurements on loosely packed carrots (bulk density 0.76 g. per cm.³) ground to pass a U. S. No. 18 screen but not a U. S. No. 25 screen (18–25 mesh). Later a distribution of No. 18 to No. 35 was used. No significant differences in results were found for either dielectric constant or conductivity for the same density of packing for these two distributions. A discussion will be given later of the effect of using smaller particles than those present in the above distributions.

III. PRECISION OF RESULTS

An idea of the precision of the results may be obtained from the following experiment: The dielectric constant and electrical conductivity of a sample of carrots containing 6.1 per cent moisture were measured at 1.8 mc. after each of four successive fillings of the cell. The values for ϵ were 2.779, 2.777, 2.781, and 2.779. These values indicate that for materials ground to fairly narrow particle-size distribution (18–25 mesh) the dielectric constant is reproducible to better than 1 per cent. However, fluctuations in temperature and in moisture content,

and errors in the bridge itself, probably make the accuracy for the dielectric constant no better than 1–2 per cent. The results for the specific conductivity in the above experiment were: 3.43, 2.54, 4.05, and 2.17 × 10⁻⁸. It is clear that the agreement is not as good as it is with the dielectric constant, especially at

TABLE 1

Variation of the dielectric constant of dehydrated carrots with change of moisture content, temperature, and frequency

MOISTURE (PER CENT, DRY WEIGHT)	FREQUENCY IN KILOCYCLES							
	5000	1800	1000	500	180	100	50	18
(a) 1.5°C.								
1.5	2.32	2.33	2.34	2.34	2.37	2.35	2.39	2.41
4.2	2.38	2.40	2.41	2.42	2.44	2.46	2.48	2.51
6.1	2.42	2.44	2.46	2.47	2.50	2.52	2.53	2.56
8.5	2.66	2.71	2.75	2.81	2.87	2.91	2.97	3.08
9.2	2.64	2.69	2.73	2.78	2.85	2.89	2.95	3.05
10.3	2.78	2.87	2.93	3.00	3.12	3.19	3.29	3.46
16.3	4.29	4.62	4.88	5.24	5.92	6.44	7.27	8.99
18.7	5.23	5.82	6.28	6.88	8.20	9.26	10.8	13.8
20.4	6.05	6.96	7.64	8.68	10.85	11.55	14.8	19.2
(b) 20.7°C.								
1.5	2.34	2.35	2.35	2.37	2.39	2.41	2.42	2.44
3.8	2.45	2.48	2.49	2.52	2.55	2.57	2.60	2.63
4.2	2.47	2.50	2.52	2.53	2.57	2.59	2.61	2.64
6.1	2.64	2.66	2.70	2.74	2.79	2.83	2.88	2.90
8.52	3.14	3.29	3.38	3.50	3.59	3.80	4.00	4.37
8.59	3.16	3.31	3.39	3.52	3.73	3.87	4.06	4.46
16.3	5.84	6.59	7.26	8.21	10.25	11.83	14.5	19.7
18.5	7.12	8.31	9.15	10.7	13.43	15.18	18.1	24.3
(c) 35.8°C.								
1.5	2.51	2.52	2.54	2.55	2.60	2.61	2.63	2.65
2.6	2.66	2.73	2.76	2.80	2.84	2.88	2.93	3.01
4.2	2.72	2.77	2.80	2.84	2.90	2.94	3.00	3.09
6.1	2.95	3.07	3.13	3.23	3.37	3.45	3.60	3.88
8.52	3.66	3.88	3.99	4.22	4.67	5.03	5.58	6.77
10.2	4.14	4.60	4.81	5.29	6.25	7.00	8.25	10.78
15.6	7.13	8.48	9.56	11.30	13.05	16.25	19.2	24.9
16.3	7.54	9.05	10.23	12.20	16.02	19.09	24.2	35.0
18.7	8.88	10.83	12.13	14.10	18.1	21.4	26.3	37.1
20.4	9.90	12.11	14.05	16.75	23.3	28.9	38.8	64.4

the low moisture levels. Thus, whereas the maximum variations in dielectric constant are equivalent to 0.05 per cent moisture, the maximum variations for conductivity correspond to 0.15 per cent moisture. Bridge errors arising from manipulation at balance in the measurements of conductivity probably exceed those for dielectric-constant measurements.

IV. RESULTS

In tables 1 and 2 are presented values of the dielectric constant and total conductivity (a.c. and d.c.) as functions of moisture content, temperature, and

TABLE 2

Variation of the total conductivity of dehydrated carrots with change of moisture content, temperature, and frequency

Conductivities in mhos per centimeter $\times 10^7$

MOISTURE (PER CENT, DRY WEIGHT)	FREQUENCY IN KILOCYCLES							
	5000	1800	1000	500	180	100	50	18
(a) 1.5°C.								
1.5	1.45	0.545	0.280	0.124	0.046	0.031	0.016	0.016
4.2	1.70	0.482	0.295	0.124	0.039	0.0311	0.008	
6.1	1.78	0.540	0.260	0.093	0.047	0.031	0.016	
8.5	3.30	1.20	0.980	0.420	0.140	0.078	0.047	0.008
9.2	3.82	1.36	0.779	0.374	0.125	0.078	0.031	0.016
10.3	4.95	1.95	1.15	0.576	0.205	0.125	0.031	0.015
16.3	23.4	8.80	5.75	3.59	2.01	1.46	1.09	0.793
18.7	33.7	16.5	11.7	8.06	5.27	4.35	3.66	3.02
20.4	53.7	28.9	21.3	16.4	11.9	10.3	9.10	8.20
(b) 20.7°C.								
1.5	1.59	0.590	0.202	0.140	0.047	0.016	0.016	
3.8	2.22	0.794	0.420	0.185	0.062	0.016	0.031	
4.2	2.29	0.700	0.404	0.202	0.047	0.031	0.016	
6.1	3.16	1.04	0.622	0.280	0.093	0.062	0.031	0.016
8.52	7.26	2.94	1.73	0.996	0.452	0.264	0.171	0.109
8.59	7.20	2.74	1.85	1.01	0.470	0.310	0.170	0.093
16.3	45.0	25.2	18.7	14.2	10.1	8.75	7.57	6.63
18.7	82.0	50.9	41.6	33.3	29.3	27.7	26.4	25.2
(c) 35.8°C.								
1.5	2.37	0.751	0.362	0.164	0.0587	0.039	0.016	
2.6	3.10	1.07	0.624	0.327	0.109	0.062	0.031	0.031
4.2	3.70	1.24	0.747	0.327	0.125	0.110	0.047	0.023
6.1	5.51	2.15	1.23	0.717	0.327	0.187	0.125	0.062
8.52	12.7	4.27	3.27	2.08	1.16	0.904	0.607	0.374
10.3	20.6	9.92	6.87	4.66	2.76	2.06	1.52	1.04
15.6	101.0	64.4	54.1	45.2	38.5	36.2	34.8	33.8
16.3	114.	74.7	63.3	54.3	47.2	44.6	42.4	40.5
18.7	191.	141.	122.	111.	103.	100.	97.5	95.5
20.4	246.	179.	160.	146.	135.	131.	127.2	124.

frequency. By total conductivity is meant the conductivity measured by an a.c. bridge.

In figure 2 are shown curves for carrots representing the variation of the dielectric constant, ϵ, with moisture content at three temperatures, and at one frequency, 1.8 mc. Figure 3 shows the variation of ϵ with frequency for differ-
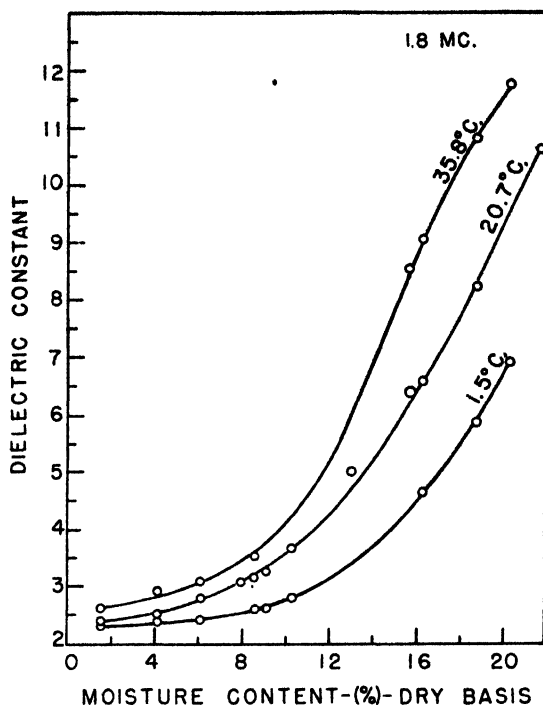
FIG. 2. Variation of ϵ of dehydrated carrots with changes in moisture content for three temperatures, at 1.8 mc. There is considerably greater variation of ϵ at low moistures at 35.8°C. than at 20.7° or 1.5°C. All moisture contents refer to dry basis.
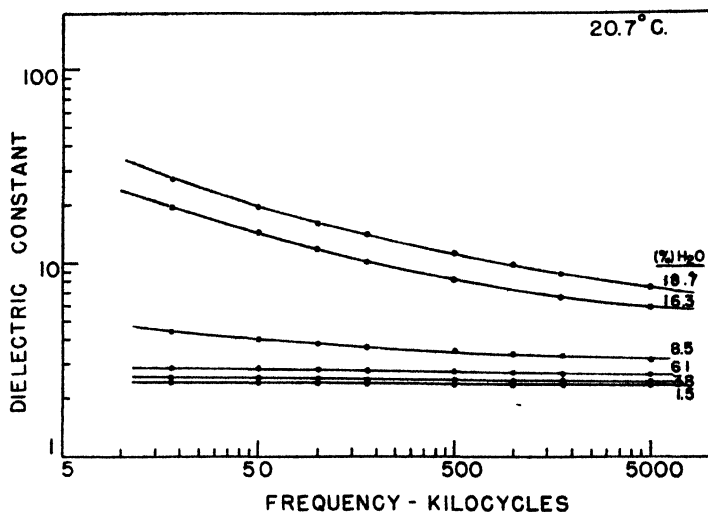
FIG. 3. Variation of the dielectric constant with frequency at various moisture contents at 20.7°C. The frequency variation of ϵ is very slight at low moisture contents, but is large for high moisture contents.

ent moisture contents at 20.7°C.   From figure 2 one notes that there is only a small increase of the dielectric constant with increasing moisture until the mois-
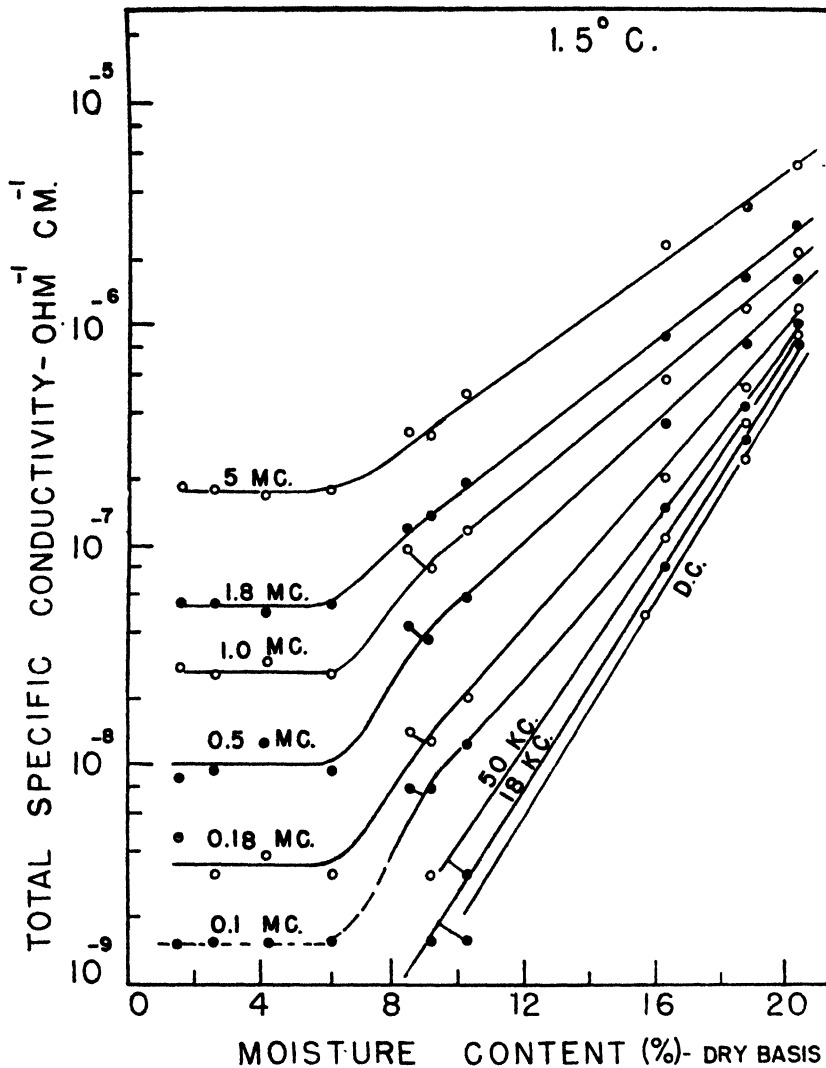
FIG. 4. Total conductivity of dehydrated carrots as a function of moisture content for various moisture contents and frequencies, at 1.5°C. As the frequency increases the conductivity also increases, but for all frequencies there is little or no change in conductivity until a moisture region of 6-8 per cent is attained. Although no work has been done upon very high moisture contents, it is probable that the curves flatten out at moistures slightly higher than the highest used in this work.

ture reaches about 8 per cent.   It is also clear that the slope of the dielectric constant–moisture curve increases with temperature.

Figure 4 shows the variation of the total conductivity of the material as a function of moisture content for various frequencies, at 1.5°C. Figure 5 shows the same curves for 20.7°C., and figure 6 the curves for 35.8°C. The three sets
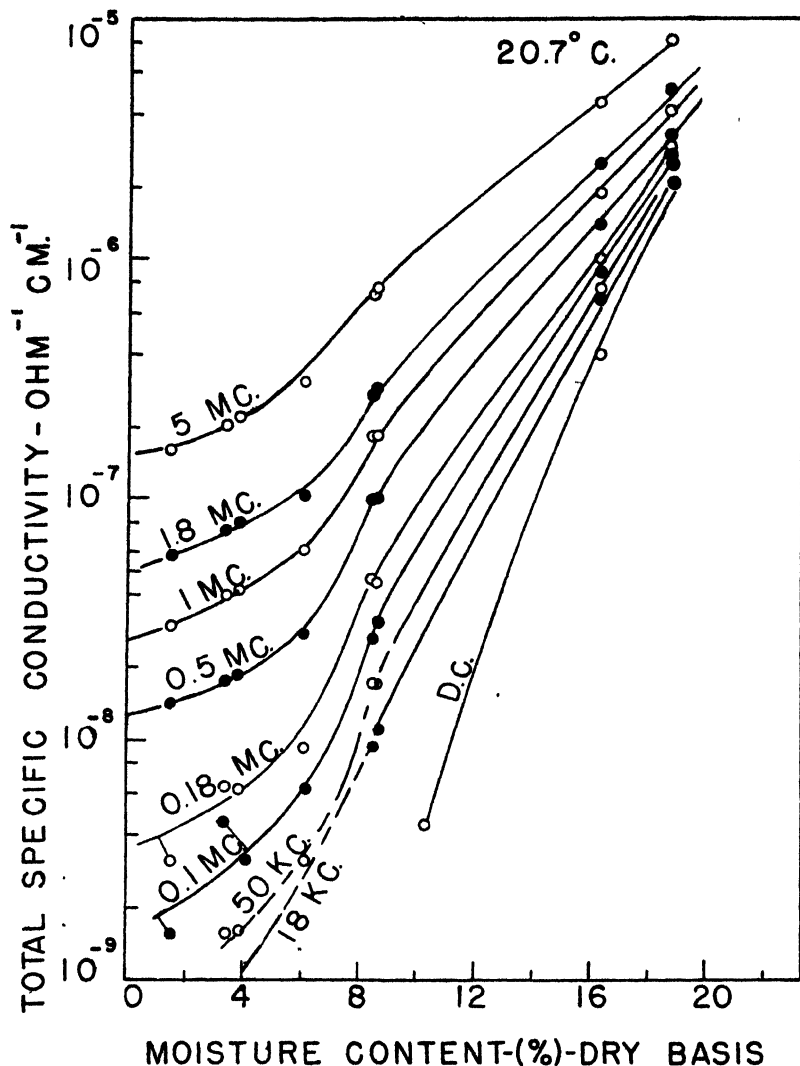
FIG. 5. Total conductivity *vs.* moisture at 20.7°C. The rapid variation at 6–8 per cent at 1.5°C. has changed into a much slower one at 20.7 and there is considerably greater variation of σ with moisture at low moisture contents.

of curves show a marked transition in conductivity at low moistures as the temperature is increased. Thus at 1.5°C., there is almost no change of conductivity with change of moisture content until the moisture content reaches 6–8 per cent, at which moisture level the conductivity begins to rise rapidly. At 20.7°C.

there is considerably greater variation of conductivity with moisture content, but there remains a definite sharp inflection in the curves. At 35.8°C. the sharp inflections have disappeared and the variation of conductivity with change of
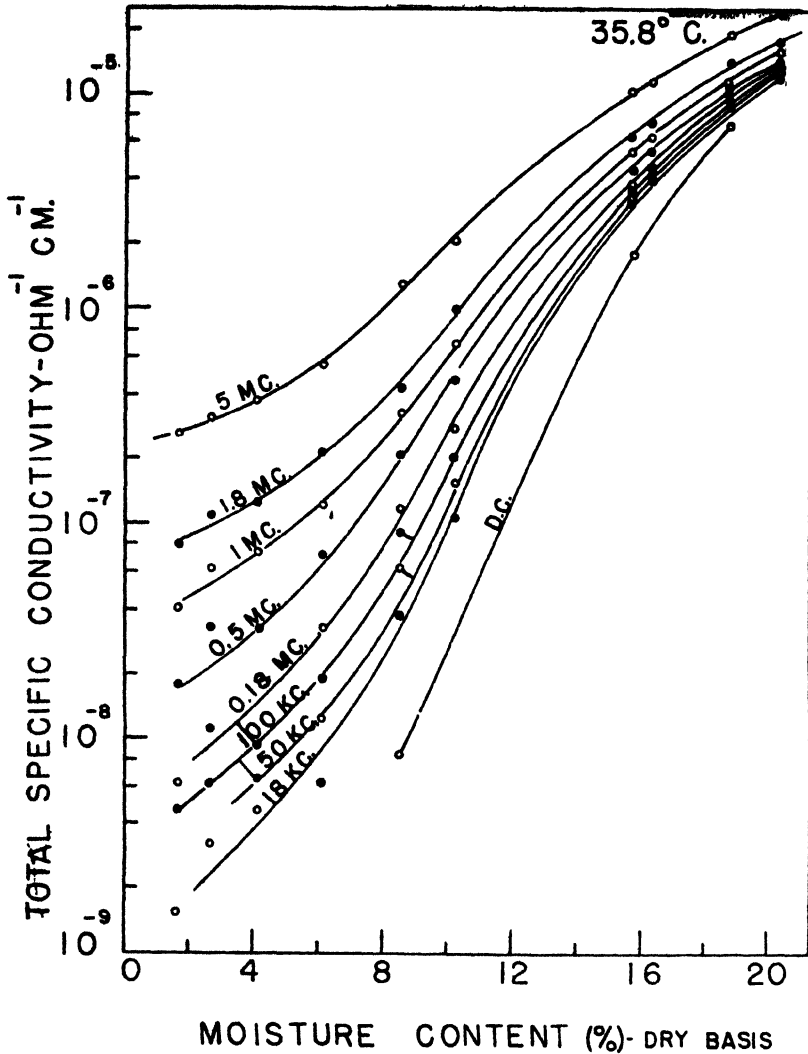
FIG. 6. Total conductivity *vs.* moisture at 35.8°C. The sharp variations of figure 5 now appear only as a mild inflection of the curves. Coincidental with this change of shape of the curves, the slope in general decreases at high moistures with increase in temperature. Change in temperature, of course, also produces a general upward shift of all the curves.

moisture is of the same order of magnitude at low and high moisture contents. In figure 7 some of the conductivity results have been replotted to show variation of conductivity with frequency at various moisture contents. It seems evident that at low moisture levels the conductivity is nearly linear with respect

to frequency change but that at high moisture levels the conductivity begins to increase markedly only above about 1000 kc.
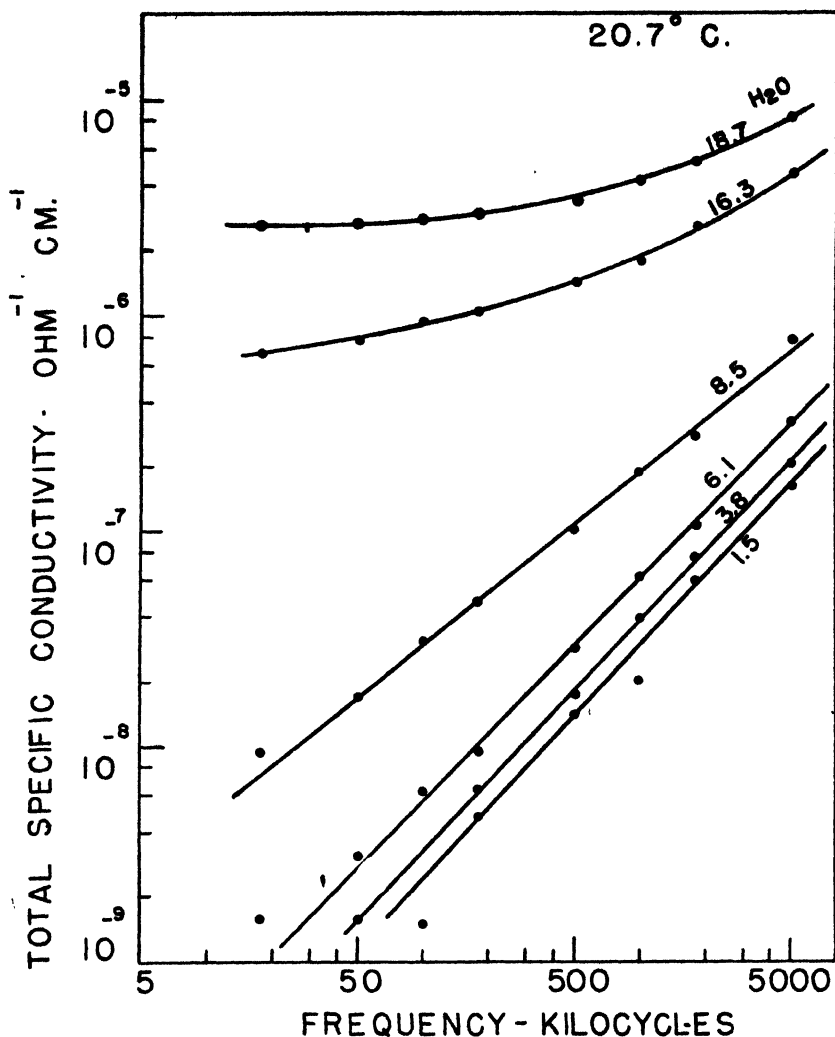
Fig. 7. Variation of total conductivity with frequency at 20.7°C. This figure is a re-plot of figure 6 to show the linear variation of σ at low-moisture conductivities upon a log–log scale. Thus the specific conductivity is proportional to frequency at low moisture contents.

Figure 8 shows the d.c. conductivity as a function of moisture content at three different temperatures. It is interesting to note that the 1.2°C. curve shows a sharp inflection similar to that for the radio-frequency curves of figures 4 and 5, but that the sharp inflections are not present in the 20.7°C. and 35.8°C. curves.

The d.c. conductivity was found to vary with the age of the sample. For this reason the curves in figure 8 are not identical with the d.c. curves in figures
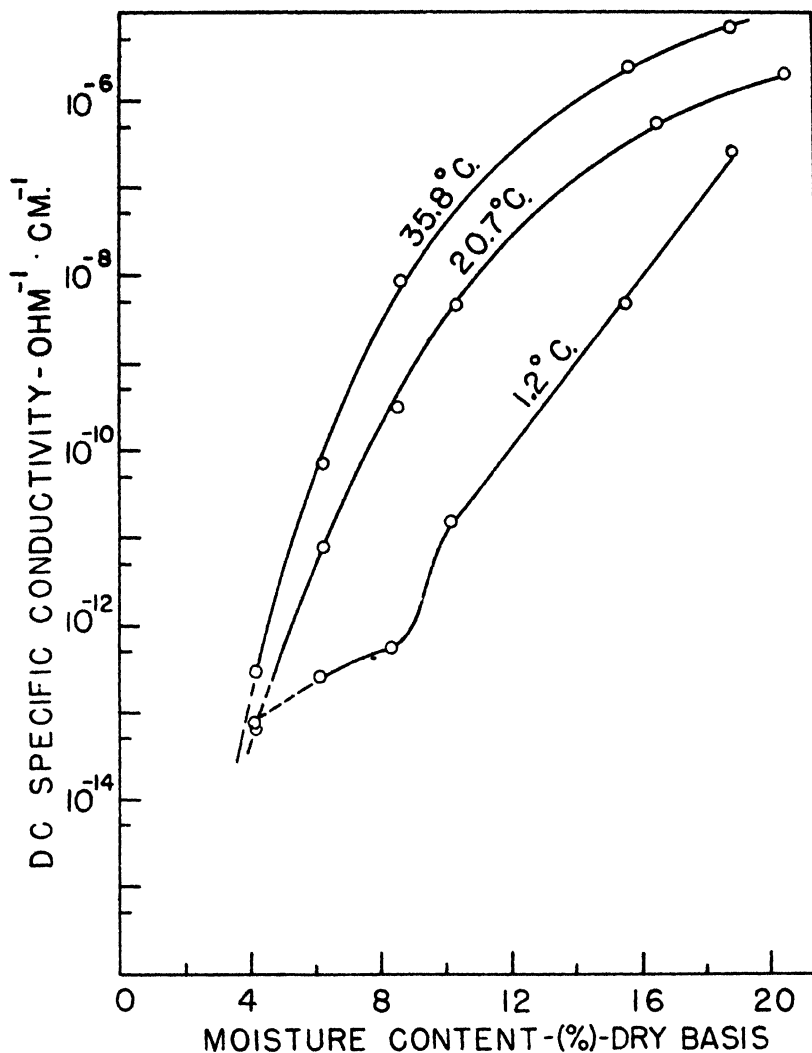
FIG. 8. D.C. conductivity of dehydrated carrots at three temperatures. No elaborate precautions have been taken in the measurement of the d.c. conductivity, so that results are not of high precision. The results are thought precise enough, however, so that the pronounced bend in the curve at 1.2°C. has some significance.

4, 5, and 6, which were obtained at an earlier date. There appeared to be an increase of conductivity with age of sample, although there was no change in moisture content. This change in conductivity can probably be attributed to deterioration of the sample. The dielectric constant appeared to be much less sensitive to aging of the sample.

To determine the effect of particle size upon the dielectric constant and conductivity, a set of experiments was carried out upon samples of 16.3 per cent and 15.5 per cent moisture and having particle-size distributions of 18–35 and <60 mesh (particles small enough to pass through a 60-mesh screen), respectively. Correcting the 18–35 mesh results (data in figures 2 and 3) for the slight difference in moisture content between the two samples (0.8 per cent), we have the results of table 3. It is seen that the two sets of figures agree quite

TABLE 3

Effect of change of particle-size distribution upon dielectric constant of dehydrated carrots of 15.5 per cent moisture content

PARTICLE-SIZE DISTRIBUTION	FREQUENCY IN KILOCYCLES							
	5000	1800	1000	500	180	100	50	18
18–35 mesh	5.50	6.20	6.68	7.50	9.10	10.60	12.60	17.00
<60 mesh........	5.35	5.96	6.47	7.26	8.90	10.33	12.73	17.35

TABLE 4

Effect of change of particle-size distribution upon specific conductivity of sample of table 1

PARTICLE-SIZE DISTRIBUTION	FREQUENCY IN KILOCYCLES					
	5000	1800	500	50	18	0
18–35 mesh........	3.9×10^{-6}	2.2×10^{-6}	1.4×10^{-6}	6.2×10^{-7}	4.2×10^{-7}	1.8×10^{-7}
<60 mesh..	3.7×10^{-6}	1.9×10^{-6}	1.0×10^{-6}	4.9×10^{-7}	4.0×10^{-7}	2.6×10^{-7}

closely, and it can be said as a first approximation that there is no pronounced difference between the dielectric constants of the 18–35 and the <60 mesh materials.

With the same procedure for the a.c. and d.c. specific conductivity for the two particle-size distributions, the results shown in table 4 were observed. The results for the specific conductivity are seen to be similar to those for the dielectric constant. The d.c. conductivity is somewhat less for the large than for the small particles. There appears to be no particularly pronounced change in either dielectric constant or conductivity with a change from 18–35 to <60 mesh distribution.

It was of interest to determine how the dielectric constant and specific conductivity vary with extent of packing of the sample. The measurements were made on 18–35 mesh material at two moisture levels, 1.5 and 16.3 per cent moisture. Curves representing the effect of compression on the variation of the dielectric constant with frequency for the 1.5 per cent moisture carrots have been plotted on a linear scale in figure 9, and for the 16.3 per cent moisture carrots on a logarithmic scale in figure 10.

The effect of compression on conductivity has also been shown for the 16.3 per cent carrots in figure 11. It may be noticed from figures 9 and 10 that
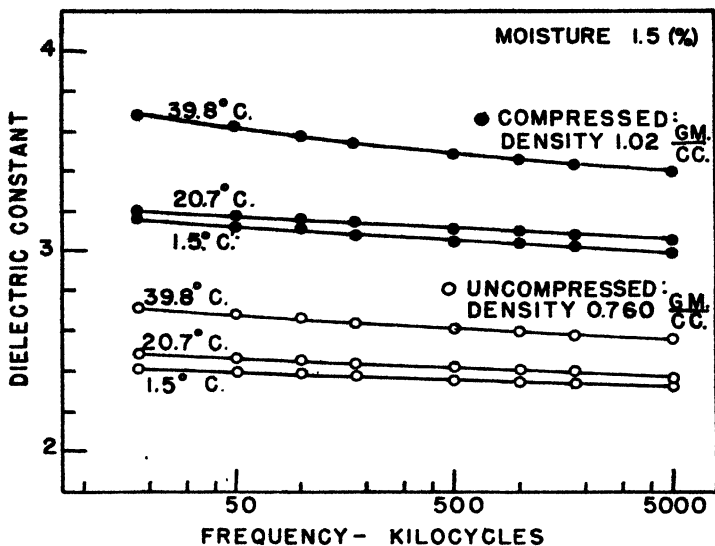
Fig. 9. Effect of compression upon the dielectric constant of dehydrated carrots of 1.5 per cent water at various frequencies. The change of temperature from 20° to 40°C. has greater relative effect upon the compressed material than upon the uncompressed.
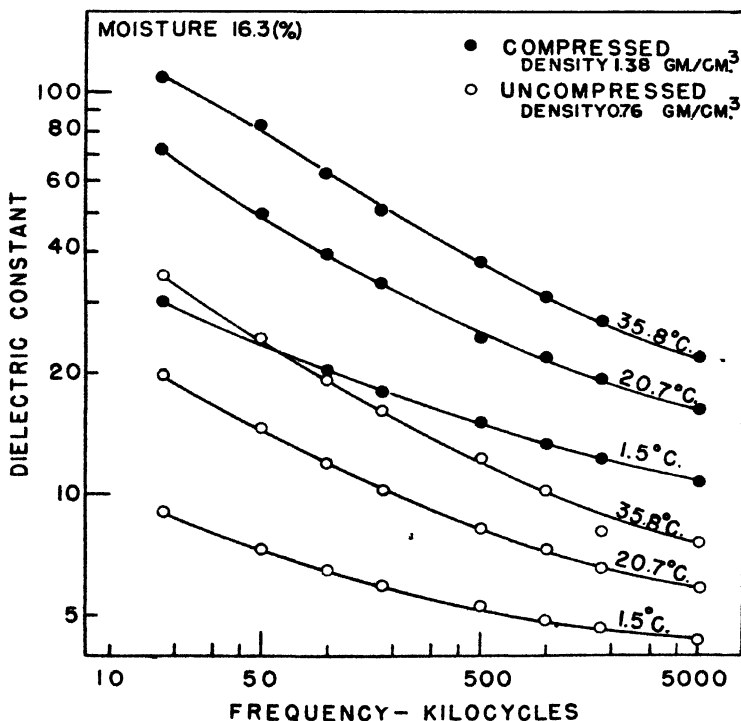
Fig. 10. Effect of compression upon the dielectric constant of a high-moisture sample at various frequencies and temperatures. The compression increases the dielectric constant almost uniformly for all frequencies. However, the temperature effect is relatively greater at low frequencies.

compression translates the frequency curve uniformly upward. However, the ε shift is for low moistures on a linear scale, and for high moistures on a logarithmic scale. Figure 11 shows that the effect of compression is to change the frequency characteristic of a.c. conductivity of 16.3 per cent moisture carrots
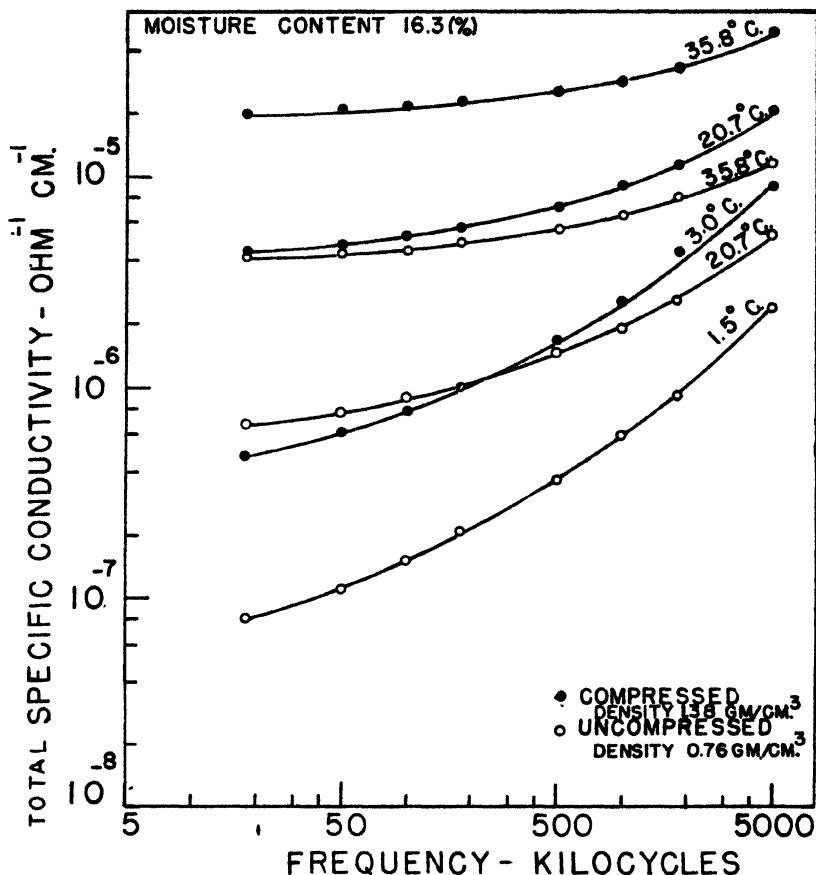
Fig. 11. Effect of compression upon the conductivity of the high-moisture sample of figure 10

in much the same way as is produced by an increase in moisture content (see figure 7); that is, both tend to decrease the frequency variation of the conductivity.

V. EFFECT OF ELECTRODE POLARIZATION

It is of some interest to determine the effect of electrode polarization upon the values for the dielectric constant. Fricke and Curtis (4) have used a variable spacing method for the elimination of error due to electrode polarization in dielectric measurements on electrolytes. In the present experiment the elec-

trode spacing was not changed. Instead, the effective electrode area was changed by insertion of a hollow brass cylinder (0.17 cm. thick and 5.62 cm. long) in the measuring cell in order to divide the cell into two individual cells of equal thickness. The two cells were thus effectively connected in series. Both halves of the cell were filled with the sample at the same density as in the experiment without the separator. The dielectric constant of a sample of about 20 per cent moisture was measured with and without the brass separator, at the lowest frequency used in this work (18 kc.) and at room temperature (21°C.). The results in the two cases were: $\epsilon = 28.5$ without separator and $\epsilon = 27.2$ with separator. It is considered that these results agree within the experimental error of this particular experiment.

It would be expected that if electrode polarization were predominant under the conditions of the experiment, the total capacity should be considerably reduced when the separator was used, since the electrode capacities of the two halves of the cell are connected in series. The fact that there was no appreciable change in apparent dielectric constant is taken to mean that the effect of electrode polarization is negligible.

It has already been mentioned (Section II) that electrode polarization has been observed to be important in the measurement of d.c. resistance. Thus there must be a frequency between 0 and 18 kc. above which the electrode polarization ceases to be of practical importance. However, no experimental work has been done to determine this frequency.

VI. DISCUSSION AND APPLICATION OF RESULTS TO MOISTURE DETERMINATION

The radio-frequency dielectric properties of dehydrated carrots discussed above may be considered as representative of a large class of materials of vegetable nature or origin. It is of interest to examine the applicability of these properties to moisture determination by radio-frequency methods, at least for measurements made directly upon the material rather than upon an extract of the water from the material, as in the "Exluan" method (2, 12).

It should be emphasized at the outset that absolute determination of moisture by electrical methods is not yet possible. Regardless of what variable is used for the measurement, one must make a calibration of the value of the variable (or of a meter reading corresponding to this value) against a standard method of measuring moisture. Since in general the calibration varies with type and variety of material, for a given instrument a separate calibration for each such material is required. The question of interest is to determine what electrical quantity is most suitable for detecting the changes in moisture content. It is also desirable that the quantity chosen show only a small (or constant) variation with change of temperature, in order to minimize the need for temperature control during measurements.

The general information of figures 2 and 3 can be applied directly to the study of electrical testing of moisture. Figure 2 shows the variation of ϵ with respect to moisture changes. It also shows variation of ϵ with temperature, which information is important in determining the degree of temperature con-

trol or correction. From figure 3 can be obtained information as to the best frequency to be used for measuring moisture. Since there is considerably greater variation of ϵ with moisture at low than at high frequencies, the lower frequencies may be best for this type of measurement. It is also true, however, that there is a greater temperature sensitivity at low frequencies. A discussion of selection of optimum conditions for moisture testing is given below.

Similar information can be had for specific conductivity or dielectric loss from the results of figures 4, 5, 6, 7, and 8. It is seen that the conductivity shows a greater variation with moisture at low than at high frequencies. Indeed, for high moisture sensitivity, the d.c. conductivity seems the best characteristic of all for moisture testing, since in the region of 3–20 per cent, the d.c. conductivity changes by a factor of 10^8 to 10^9, and most of this variation is in the first few per cent moisture. The drawback is that the d.c. conductivity is so small that it is difficult to measure accurately over a large part of this resistance range. There must also be considered the fact that temperature and packing fluctuations will have a considerable effect, and it requires further study to decide whether there is any net gain to be obtained from the use of this variable. Use of compression increases the conductivity at a given moisture content but also reduces the variation of conductivity with moisture content. Increase in frequency produces a similar effect on conductivity to that produced by compression.

Other variables besides the dielectric constant and the conductivity could be used for measurement of the moisture content. Of these we shall discuss only (1) the impedance

$$Z = \frac{R}{\sqrt{1 + \omega^2 R^2 C^2}}$$

where C is the capacity of the cell, R the associated parallel resistance, and (2) the power factor, which is equal to $\dfrac{9 \times 10^{11}\sigma}{\omega\epsilon}$ at low moistures.

Although the impedance as such is not a property of the material only, we can define what we might call the "specific impedance" for the material in a cylindrical condenser of the type used in this work. This specific impedance Z_m is given by

$$\frac{1}{\sqrt{16\pi^2\sigma^2 + \dfrac{\omega^2\epsilon^2}{81\times10^{22}}}}$$

where Z_m is in ohm-centimeters, σ in ohm^{-1} cm.$^{-1}$, and $\omega = 2\pi \times$ frequency. The impedance Z is related to Z_m by the equation

$$Z = Z_m \frac{2 \log \dfrac{b}{a}}{l}$$

At low moistures, for all radio-frequencies, Z varies very nearly as ϵ and is practically independent of σ. At higher moisture contents, Z may be equally dependent upon ϵ and σ.

As is well known, the value of the power factor is highly sensitive to the presence of water in insulating materials. Thus it can be used for measurement of the moisture content. Here we shall use the variable

$$\alpha = \frac{\sigma \times 9 \times 10^{11}}{\omega\epsilon}$$

which is equal to the power factor at low moistures. Thus α is almost entirely dependent upon σ at low moistures, because of the small variation of ϵ with moisture in this range.

Among the important properties of the variables mentioned above are (1) the range of actual values of the variable in the moisture region to be considered, (2) the relative moisture sensitivity (the percentage change in the variable per unit change in moisture content), (3) the temperature sensitivity of the variable (percentage change per unit change of temperature), and (4) the ratio of the relative moisture sensitivity to the temperature sensitivity, which is here considered to be a measure of the "net" sensitivity of the particular variable to change in moisture.

From the results already presented a series of tables giving values of the above properties has been prepared for the variables ϵ, σ, Z_m, d.c. σ, and α. Because of space limitations the tables cannot be presented *in toto*. Table 5, however, has been drawn up to summarize these results. It applies to the moisture regions of (a) 1.5–4.2 per cent, (b) 6.1–8.5 per cent, and (c) 16.3–18.7 per cent.

From the results shown in table 5 it is seen that both the relative moisture sensitivity and the "net" sensitivity are larger for d.c. conductivity than for any of the other variables. The average value of this quantity is very small in the moisture range (4–12 per cent) of greatest importance in the testing of agricultural products. Hence its usefulness is likely to be limited, because of difficulties of measurement.

In the low moisture range ϵ and Z have much smaller moisture sensitivities than the quantities (σ and α) that depend entirely or almost entirely upon σ. It is also true, however, that the temperature sensitivity is less for ϵ than for σ and α, and the "net" sensitivities are approximately the same. In the intermediate moisture region, the moisture sensitivities of ϵ and Z have increased to a greater extent than has that of σ or α, yet the ratios remain nearly the same. All, however, have nearly doubled, and it is seen that the "net" moisture sensitivity for all variables is higher in this range than in either the high-moisture or the low-moisture regions. It is significant that the values of the maximum net sensitivity are of the same order of magnitude for ϵ, Z, σ, and α, in all moisture regions used.

The power factor seems, on the basis of the results in table 5, to be the best variable for use in electrical moisture testing, on the basis of both "relative

moisture sensitivity" and "net sensitivity" in the three moisture ranges studied. However, the variations from variable to variable are not large in the case of the "net sensitivity," which is important if good temperature control is not available. If good temperature control is available, the power factor and the dielectric loss (equivalent to either a.c. or total conductivity below say 12 per

TABLE 5

Moisture and temperature sensitivity of variables that can be used for electrical moisture testinꞈ

VARIABLE	MAXIMUM RELATIVE MOISTURE SENSITIVITY	FREQUENCY FOR MAXIMUM RELATIVE SENSITIVITY	TEMPERATURE SENSITIVITY	NET SENSITIVITY	MAXIMUM NET SENSITIVITY	FREQUENCY FOR MAXIMUM NET SENSITIVITY
(a) Moisture range 1.5–4.2 per cent (dry basis)						
		kc.	*per cent*			*kc.*
z	2.14	100	0.73	2.93	3.39	500
α	24.8	100	5.76	4.3	4.42	1000
σ	24.9	100	6.24	3.99	4.19	1000
ϵ	2.34	18	0.734	3.87	3.87	18
$\sigma_{d.c.}$	900.		190.	4.7		
(b) Moisture range 6.14–8.52 per cent (dry basis)						
z	17.1	18	2.77	6.18	8.53	1800
α	50.6	50	6.36	7.96	12.82	1800
σ	56.2	180	6.59	8.38	12.8	1000
ϵ	17.0	18	2.36	7.18	9.27	1000
$\sigma_{d.c.}$	1500.		48.3	31.		
(c) Moisture range 16.3–18.7 per cent (dry basis)						
z	46.7	18	8.54	5.47	5.47	18
α	42.35	18	7.48	5.66	6.12	50
σ	48.6	18	8.32	5.84	5.84	18
ϵ	10.96	500	2.25	4.87	5.51	1800
$\sigma_{d.c.}$	270.		13.5	20.		

The relative moisture sensitivity is the percentage increase of the indicated quantity produced by unit change in percentage moisture. The temperature sensitivity is the percentage increase of the variable per degree increase in temperature (arranged over the moisture region considered). The "net sensitivity" is the ratio of the "relative moisture sensitivity" to the "temperature sensitivity." The "maximum relative moisture sensitivity" refers to the maximum value over the frequency range used. The term "maximum net sensitivity" refers to the maximum of the "net sensitivity" over the frequency range of 18 to 5000 kc.

cent moisture) appear to be the most sensitive to moisture. It must be remembered, of course, that these conclusions are made without regard to the ease or accuracy with which the variables can be measured.

It is also interesting that in general the maximum relative sensitivity and the maximum net sensitivity for all the variables discussed are at different frequencies. This is a consequence of the variation of the temperature sensitivity

with frequency. Thus for ϵ in the low-moisture region both the maximum relative moisture sensitivity and the maximum net sensitivity are at 18 kc.; in the intermediate region, 6.1–8.5 per cent moisture, the relative sensitivity remained at 18 kc.; the net sensitivity, however, was a maximum at 1000 kc. In the high-moisture region the relative sensitivity was a maximum at 500 kc., whereas the net sensitivity was a maximum at 1800 kc.

From the previous discussion it is concluded that if good temperature control is available, a low radio frequency is the most desirable for high moisture sensitivity. However, if temperature control is not available, to minimize errors from the temperature variations a high radio frequency is most suitable.

<div align="center">VII. SUMMARY</div>

As the basis for a study of electrical moisture· testing by radio-frequency methods, measurements were made of the radio-frequency dielectric properties of dehydrated carrots, a material typical of those on which such methods are used. Measurements were made of the dielectric constant ϵ and specific conductivity σ (a.c. and d.c.) as functions of moisture content (1.5–21.6 per cent), temperature (1.2–39.8°C.), frequency (18 kc. to 5 mc.), density (0.760–1.38 g. per cubic centimeter), and particle size. The value of ϵ increases little with moisture content up to 6–8 per cent; above this region ϵ increases rapidly. Increase of temperature increases both the value of ϵ and the rate of change of ϵ with moisture. At 1.5°C. there is no detectable change of total σ with increase in moisture until 6–8 per cent is reached; above this region the variation becomes exponential. At higher temperatures this apparent discontinuity disappears. Particle size has little effect upon ϵ or σ, for a given bulk density. Increase of bulk density increases ϵ and σ uniformly on a logarithmic scale for all frequencies.

Measurement of the dielectric constant with and without floating electrode in the cell indicated lack of dependence of the results upon electrode polarization in the radio-frequency range. A discussion is given of the use of various variables, including direct-current conductivity, dielectric constant, impedance, dielectric loss, and power-factor measurements, for measurement of moisture content of organic materials containing absorbed water. The conclusion is reached that, although the direct current σ is the most sensitive to moisture of the variables studied, its low average value and high sensitivity to temperature make it unsuitable for moisture determination. The power factor was found to have the greatest ratio of moisture sensitivity relative to the temperature sensitivity for all moisture ranges studied, but, in general, the variables other than direct-current σ appeared to be nearly equivalent for moisture determination. In all cases except for ϵ at low moistures, a high radio frequency is most suitable for the electrical testing of moisture.

REFERENCES

(1) ARGUE, G. H., AND MAASS, O.: Can. J. Research **13B**, 156 (1935).

(2) EBERT, L.: Angew. Chem. **47**, 305 (1934).

(3) ERRERA, J., AND SACK, H. S.: Ind. Eng. Chem. **35**, 112 (1943).

(4) FRICKE, H., AND CURTIS, H. J.: J. Phys. Chem. **41**, 729 (1937).

(5) FRICKE, H., AND JACOBSEN, L. E.: J. Phys. Chem. **43**, 78 (1939).

(6) FRICKE, H., AND PARKER, E.: J. Phys. Chem. **44**, 716 (1940).

(7) MAKOWER, B., AND DEHORITY, G. L.: Ind. Eng. Chem. **35**, 193 (1943).

(8) ONCLEY, J. L.: J. Am. Chem. Soc. **60**, 1115 (1938).

(9) SHAW, T. M.: J. Chem. Phys. **10**, 609 (1942).

(10) SMITH-ROSE, R. L.: Proc. Roy. Soc. (London) **A140**, 359 (1933).

(11) TAUSZ, J., AND RUMM, H.: Kolloid-Beihefte **39**, 58 (1933).

(12) VAN STEENBERGEN, A. B.: Het Gas **55**, 137-9 (1935).

NEW BOOKS

Fundamentals of Immunology. By WILLIAM C. BOYD. 446 pp. New York: Interscience Publishers, Inc., 1943. Price: $5.50.

This book covers the fundamental principles involved in immunological reactions, together with a brief discussion of practical applications. A chapter of the book is devoted to laboratory techniques commonly used in serological laboratories. The author states that the purpose of the book is to serve as an introduction to immunology for medical students, chemists, biologists, and others interested in an understanding of the basic principles of the science.

The introductory chapter of the book serves to introduce the reader to the science of immunity and immunology. In this chapter the author discusses the various kinds of immunity, the methods of measurement, and the mechanisms involved.

Chapter two is a somewhat detailed description of antibodies and their specificity. The subject matter in this chapter is approached from the point of view of the chemist. The author wishes to make the student familiar with the fundamental principles involved before introducing him to the theories and nomenclature inherent in older immunological literature. From the point of view of the chemist, he discusses the nature of the antibodies. the chemical behavior, methods of measurement, and purification.

Chapters three and four deal with antigens. A distinction is made between cell antigens and others, the former being taken up separately in chapter three. Here, again, the subject matter is treated from the point of view of the chemist. The author discusses in some detail the nature of the chemical groupings which are responsible for antigenic specificity.

Chapter five takes up the question of human blood groupings. This chapter is rather brief, and therefore the subject matter is not taken up in as much detail as are some of the other topics included in the book. The author discusses the basis for the four classical blood groups and treats briefly the question of other antigenic principles, in addition to the ones involved in the four basic groups.

Chapter six deals with antibody–antigen reactions. In this chapter the author has followed somewhat the scheme used by Marrack, in treating the antibody-antigen reaction as a two-stage reaction. The first stage concerns the combination of antibody with antigen, and the second stage involves those changes which make the reaction apparent to the observer, such as precipitation, agglutination, neutralization of toxin, complement fixation, etc. The author's presentation of the various theories that have been advanced concerning antibody–antigen reactions is excellent. The subject material in this chapter is developed almost entirely from the point of view of the chemist.

Chapter seven is devoted to the discussion of complement and complement fixation. The part the complement plays in antibody–antigen reactions is at best obscure, but in this chapter the author has handled the subject matter in an excellent manner.

Chapters eight and nine deal with anaphylaxis, allergy, and related phenomena. The last of these two chapters is devoted almost entirely to the question of relationship between allergy and immunity.

Chapter ten is a brief discussion of the practical applications of artificial immunity, and chapter eleven is a discussion of laboratory and clinical techniques that are commonly used in serological laboratories. This chapter is sufficiently detailed so that it can well be used as a guide for most laboratory work.

The author is to be commended for the excellent way in which he has presented the fundamental principles underlying immunology. The presentation is clear and concise. From a study of this book, a reader who is not familiar with the field will gain a good understanding of the science involved. Naturally, someone who is already familiar with the subject matter will gain more by reading the book than one who is exposed to the field for the first time. The book may be criticized, perhaps, in not making the reader more familiar with the nomenclature used in older immunological literature. One who gains his knowledge by reading this book alone may find some older literature confusing, owing to the difference in terminologies used. Many references are given throughout the book, and after each chapter there is an excellent bibliography of the more important literature.

In order to conserve space, the author has treated some subjects rather briefly, and in some cases perhaps too briefly; for example, in the last chapter he has devoted some space to the discussion of statistical principles involved in serological studies. Although the statistical principles are presented fairly clearly and briefly, I question whether a reader who is not already familiar with this subject could learn enough from this discussion to make proper use of the statistical principles. On the other hand, readers who are familiar with the field of statistics would find this discussion too brief to be of much value to them.

The author has succeeded very well in the object for which the book was intended. It is an excellent reference book for medical students, chemists, and biologists who are interested in the science of immunology. It should also be of great help to persons who are interested in research in this field.

H. O. Halvorson.

Surface Tension and the Spreading of Liquids. By R. S. BURDON. x + 85 pp. London: Cambridge University Press (New York: The Macmillan Company), 1940. Price: $1.75.

This small volume, published in the series of Cambridge Physical Tracts, reviews briefly and in a readable manner the subject matter indicated in its title. The booklet will appeal primarily to readers not familiar with the subject matter who are interested in a short, well-balanced review. The author emphasizes some points of timely interest, but he refrains from presenting an exhausting review or a critical survey of the newer literature. This, of course, limits the value of the book for a reader familiar with the field.

KARL SOLLNER.

Atomic Energy for Military Purposes By HENRY D. SMYTH 264 pp. Princeton, New Jersey: Princeton University Press, 1945. Price: $2.00 cloth bound; $1.25 paper bound.

This volume contains the full text of the official report on the development of the atomic bomb under the auspices of the United States Government during the years 1940–45. Written at the request of General L. R. Groves, it was first issued in mimeograph form. The book edition has been supplemented by including subject and name indices, photographic and line drawing illustrations, a description of the New Mexico test, and some minor changes.

In his foreword General Groves, who was in charge for the Army, warns that: "All pertinent scientific information which can be released to the public at this time without violating the needs of national security is contained in this volume. No requests for additional

information should be made to private persons or organizations associated directly or indirectly with the project. Persons disclosing or securing additional information by any means whatsoever without authorization are subject to severe penalties under the Espionage Act." Under such authorization it must have been difficult to prepare this report. Dr. Smyth has done a careful and skillful piece of tight-rope walking. If he has said more than pleased the advocates of extreme secrecy on the one hand, he has said much less than would satisfy scientists on the other.

Essentially, the account is complex in structure. The chronological element is interwoven with personnel, organization, and location to such an extent that it is difficult to follow the development of a scientific problem through to the final answer and even more difficult to find its application. This was doubtless intentional and at present is necessary and in no way justifies criticism of the author. It is to be remembered that this is a project report of work in which scientific plans were only one of the many essentials. It should be so regarded and not as an account of scientific work *per se*.

To be specific, there is an admirable discussion of the principles involved in the separation of isotopes as applicable either to deuterium or to uranium. Several methods are developed to the point where they proved either worthless or to have some value. Uncertainty remains as to which method had most potential or any final value. It is indicated that possibly one method was most useful in an early stage of investigation but was later superseded by another method more suitable for larger scale work. Such conclusions are rather left to inference. A great deal of reading between the lines is called for in many parts of the report.

It is quite clear that the separation of U^{235} proved so difficult that it was not carried on to large-scale production after it was discovered that plutonium is fissionable and can be produced on a large scale in a chain-operating neutron pile and can later be separated from uranium by chemical methods. Whether the U^{238} in the operating pile is initially enriched with U^{235} is not clear, though enriched piles do appear to have been used in some preliminary experiments.

The construction of a plant to separate and purify plutonium based on methods worked out with quantities limited to a few micrograms is indeed a triumph of nuclear chemistry. The chemistry of a previously unknown element had to be worked out and expanded in application by a few billion fold, all under the severest time limitations.

It is not clear why it was necessary to use *metallic* uranium in the pile instead of the oxide, but one is led to infer that the required purity could be attained only by electrolyzing the metal from a fused uranium fluoride bath. Also the superior heat conductivity of the metal must be a favorable factor.

The necessity for encasing uranium in a water- and gas-tight container in the pile is based on two considerations: (1) to avoid chemical attack on the uranium; (2) the necessity of preventing contamination of the air or of the cooling water by radioactive products of the fission. How well founded the fear of damage may have been cannot be judged without more complete data, but it is highly creditable that no chances were taken even under the stress of war emergency.

In early experiments an effort was made to operate a uranium neutron pile by the use of uranium oxide instead of the metal. Chain factors closely approaching unity were achieved. Just why these efforts were abandoned in favor of the metal is not made entirely clear, but aside from chemical attack and heat conductivity, metal rods present advantages in handling and in calculating the spacing and general pile pattern. The report contains little regarding the chemical effects of radiation, though they evidently are quite a factor.

Although a great deal of attention was devoted to separation of heavy water, no final use seems to have been made of it either in the plutonium pile or in the bomb itself.

At a fairly early stage of the project, interest was shifted from power utilization to the bomb. Development of useful power is therefore something for the future. This may be disappointing to those who could not imagine the expenditure of two billion dollars and the employment of 150,000 men and women over a period of five years in the production of three

bombs. But doubtless much of the undisclosed information will be valuable in the study of power production, and it is to be hoped that much more plutonium was produced than was used.

Little is said about the resources of uranium either above or in the ground or of its geographical location or distribution in either case. This is a subject of primary importance now and in the future. No doubt it has been and is being carefully studied. In the operation of the uranium pile only a small fraction of the uranium is fissioned but it becomes contaminated with fission products representing some twenty different elements, most of them radioactive and exceeding the amount of plutonium produced by perhaps ten to one hundred fold. The latter is not so stated in the report but can be inferred from some of the other data. The problem of repurifying this uranium so that it again may be used in the pile is a formidable one. It is not stated whether repurified uranium is already being used in the pile, but it is indicated that time considerations made it preferable to store the contaminated uranium temporarily and to use fresh material. This is a difficulty that will doubtless be overcome in normal operation, so that the uranium can be repeatedly used until exhausted.

No mention is made of the recovery of radium as a by-product in the treatment of virgin uranium. Presumably the radium has been saved and may be used therapeutically or otherwise at a lower cost than formerly. True, great claims are made for the substitution of some of the radioactive products of fission; but although these may be available in much larger quantities than the previously known products of artificial radioactivity, they may prove equally disappointing for therapeutic use. Radium seems likely to be preferred by radiologists for some time, especially if its cost will now be lowered. This raises also the interesting question as to whether new artificial radioactive elements other than plutonium and neptunium have been discovered. The report makes no reference to any, but the large quantities of fission products would make the detection of long-lived products much easier if any were produced.

It is greatly to be hoped that reports of the details of all the scientific work carried out in the various laboratories working on atomic power can soon be published. To enter into an era of controlled research and suppressed information is something to be deplored and resisted by all scientists of the world.

S. C. LIND.

SUBJECT INDEX

AUTHOR INDEX

629

A. Physical chemical investigations of goldenrod rubber. III. The fractionation of goldenrod and other natural rubbers, 304

See Graff, Morris M.

SMITH, L. B. *See* Gardiner, K. W.

SOLLNER, KARL. The physical chemistry of membranes with particular reference to the electrical behavior of membranes of porous character. I. The nature of physicochemical membranes—membranes as physicochemical machines; preparation and properties of membranes of highly pronounced electrical properties, 47

The physical chemistry of membranes with particular reference to the electrical behavior of membranes of porous character. II. The nature of the "dried" collodion membrane. Some current membrane theories and their limitation, 171

The physical chemistry of membranes with particular reference to the electrical behavior of membranes of porous character. III. The geometrical and electrical structure of membranes of porous character: some examples of the machine action of membranes, 265

SPEISER, R., EDDY, C. R., AND HILLS, C. H. Kinetics of deësterification of pectin, 563

HILLS, C. H., AND EDDY, C. R. The acid behavior of pectinic acids, 328

SPIEGELMAN, S. *See* Reiner, J. M.

STEPHAN, T. RODNA. *See* Iredale, T.

SULLIVAN, MARY A. *See* Skau, Evald L.

TELANG, M. S. Correlation of viscosities of liquids with temperatures, 579

TOBOLSKY, A. V. *See* Blatz, P. J.

TULLER, ELIZABETH F., AND EBLIN, LAWRENCE P. Note on the relationship between time of dialysis and the Burton–Bishop rule, 9

VALYI, I., JANSSEN, A. G., AND MARK, H. Molecular-size distribution of crosslinked polystyrene, 461

VAN KLOOSTER, H. S., AND DOUGLAS, WINSTON A. The system acetic acid–triethylamine, 67

VOLD, MARJORIE J. *See* Vold, Robert D.

VOLD, ROBERT D. The polymorphism and transitions of anhydrous and hydrous sodium stearate, 315

AND VOLD, MARJORIE J. Thermal transitions of the alkali palmitates, 32

WALTON, H. F. *See* Kozak, R.

WASHBURN, E. Roger. *See* Alberty, Robert A.

WINKLER, C. A. *See* Darwent, B. de B.

YOFFE, A. *See* Heymann, E.

ZLOTOWSKI, I., AND KOLTHOFF, I. M. Polarographic behavior of alkaline earth metals. II. The polarographic determination of calcium alone and in the presence of other alkaline earth metals, 386

INDEX TO NEW BOOKS